

# Weather & Climate



# eWeather and Climate

**Dennis I. Netoff** Professor of Geography and Geology, *Retired, Sam Houston State University*

**B. Marcus Gillespie** Associate Professor of Geography, *Sam Houston State University*

**Ava Fujimoto-Strait** Instructor of Geography, *Sam Houston State University*

**Jim Tiller** Professor of Geography, *Sam Houston State University*

The material contained herein was prepared specifically for the Sam Houston State University course entitled Geography 1401: Weather and Climate. Unauthorized usage should be reported to the copyright holder below.

Ninth Edition 2020  
Copyright 2020 by The START Group  
All Rights Reserved

The START Group  
PO Box 310895  
New Braunfels, Texas 78131-0895

# Table of Contents

Introduction .....	viii
<b>Chapter 1 The Earth's Place in Space .....</b>	<b>1</b>
<b>Cosmic Beginnings .....</b>	<b>1</b>
The Early Universe .....	1
Nebula, Stars, and Galaxies .....	4
The Solar System.....	13
Protosun and Protoplanetary Disk.....	13
The Sun .....	19
<b>Comparative Planetology .....</b>	<b>22</b>
<b>The Terrestrial Planets .....</b>	<b>22</b>
Mercury .....	24
Venus .....	30
Earth .....	35
Mars .....	42
<b>Jovian Planets and Satellites .....</b>	<b>55</b>
Jupiter .....	57
Saturn .....	62
Uranus and Neptune .....	69
Dwarf Planets, Asteroids and Comets .....	73
Exoplanets.....	83
<b>Earth's Life Support System .....</b>	<b>87</b>
Non-Variable Gases .....	89
Variable Gases .....	94
Aerosols .....	99
Vertical Zonation of the Atmosphere .....	110
Origin and Evolution of the Atmosphere .....	121
<b>Chapter 2 Air Temperature .....</b>	<b>127</b>
Solar Energy .....	130
Electromagnetic Radiation .....	135
Heat Transfer Processes .....	147
Fate of Insolation on Earth .....	157
Controls of Insolation and Absorption .....	165
<b>Earth-Sun Relationships .....</b>	<b>165</b>
Insolation: Minor and Long-Term Controls .....	165
The Intensity of Radiation and the Duration of Daylight .....	169
Rotation, Revolution, Inclination, and Polarity .....	171

Nature of the Absorbing Medium and Wavelength of Radiation .....	187
Greenhouse Gases .....	188
Temperature: Vertical Variation in the Troposphere .....	195
Temperature: Horizontal Patterns on the Earth's Surface .....	200
Land and Water Differences .....	201
Temperature Patterns and Ocean Currents .....	208
Other Temperature Controls .....	212
Temperature: Daily and Seasonal Variations .....	217
The Daily March of Temperature .....	217
The Annual March of Temperature .....	219
Global Energy Budget .....	224
Temperature Scales and Sensible Temperature .....	227
<b>Chapter 3 Air Pressure and Winds .....</b>	<b>233</b>
Temperature and Pressure .....	233
Measuring Atmospheric Pressure .....	234
Units of Barometric Pressure .....	235
Vertical Variations in Air Pressure .....	236
Horizontal Variations in Pressure .....	237
Diabatic and Adiabatic Changes in Temperature .....	240
Temperature vs Heat .....	242
Pressure and Moisture .....	244
Wind Direction and Velocity .....	245
The Pressure Gradient Force .....	245
Isobaric Maps .....	247
The Coriolis Force .....	249
Frictional Drag .....	256
Cyclones and Anticyclones .....	260
Global Pressure and Wind Belts .....	262
Surface Wind Belts .....	265
Local Winds .....	277
Upper-Level Winds .....	303
<b>Chapter 4 Atmospheric Moisture .....</b>	<b>318</b>
Special Properties of Water .....	320
Phase Changes .....	323
Solids, Liquids and Gases .....	323
Energy of Phase Changes .....	326
The Hydrologic Cycle .....	335
Factors that Control Evapotranspiration .....	337
Relative Humidity .....	339
Humidity Measurement: the Sling Psychrometer .....	343
More on Relative Humidity .....	347

Mechanisms of Cooling.....	350
Mechanisms That Can Cause Uplift .....	354
Forms of Condensation and Deposition.....	361
Dew and Frost .....	361
Fog .....	366
Clouds .....	382
Types of Clouds .....	383
Cloud Classification .....	387
Precipitation.....	417
Types of Precipitation .....	420
Global Precipitation Patterns .....	431
Observations from Precipitation Maps .....	431
Causal Mechanisms.....	434
<b>Chapter 5 Air Masses, Fronts and Frontal Cyclones .....</b>	<b>440</b>
Air Masses .....	440
Air Mass Characteristics .....	440
Air Mass Classification .....	444
Air Mass Modifications .....	445
North American Air Masses .....	449
Continental Tropical Sonoran Air Masses (cTs) .....	449
Maritime Polar Pacific Air Masses (mPp) .....	453
Continental Polar Canadian Air Masses (cPc) .....	462
Maritime Polar Atlantic Air Masses (mPa) .....	469
Maritime Tropical Pacific Air Masses (mTp) .....	477
Maritime Tropical Air Masses from the Gulf of Mexico (mTg) and Atlantic (mTa) .....	485
Fronts.....	492
Types of Fronts.....	493
Cyclones and Anticyclones .....	498
Anticyclones .....	499
Cyclones .....	501
Development of Frontal Cyclones .....	504
Cold Fronts .....	506
Warm Fronts .....	513
Occluded Fronts .....	517
Stationary Fronts .....	521
The Dry Line .....	524
Tracks of Extratropical Storms in the United States .....	527
The Alberta Clipper .....	529
The Colorado Low.....	529
The Gulf of Alaska Low .....	530
The Gulf Low .....	532
The Panhandle Hook.....	534

Pacific Lows .....	538
Impact of El Niño on Storm Tracks .....	544
<b>Chapter 6 Severe Weather .....</b>	<b>550</b>
<b>Thunderstorms .....</b>	<b>556</b>
Origin of Thunderstorms .....	556
Types of Thunderstorms Based on Uplift Triggers .....	563
Air Mass Thunderstorms .....	564
Orographic Thunderstorms .....	565
Frontal Thunderstorms .....	566
Types of Thunderstorms Based on Size, Duration, and Severity .....	568
Stages of Thunderstorm Development .....	571
Cumulus Stage .....	571
The Mature Stage .....	575
The Dissipating Stage .....	578
Severe Thunderstorms and Tornadoes .....	581
Thunderstorm Hazards .....	608
Strong Updrafts, Downdrafts and Surface Winds .....	608
Lightning .....	614
Hail .....	625
Floods .....	636
Tornadoes .....	642
<b>Hurricanes .....</b>	<b>692</b>
Hurricane Formation .....	693
Hurricane Structure .....	701
<b>Chapter 7 Climate and Ecosystems .....</b>	<b>728</b>
<b>Climate Classification .....</b>	<b>728</b>
<b>Basic Climate Patterns .....</b>	<b>734</b>
<b>Climograms .....</b>	<b>735</b>
<b>Koepfen Climate Classification .....</b>	<b>737</b>
<b>Tropical Climates (A Climates) .....</b>	<b>738</b>
Tropical Humid (Tropical Wet) Climates (Af) .....	739
Tropical Monsoon Climates (Am) .....	750
Tropical Wet and Dry Climates (Aw) .....	751
Arid (BW) and Semi-arid (BS) Climates .....	757
Deserts (BWh and BWk) .....	761
Steppe Climates (BSh and BSk) .....	772
<b>C Climates .....</b>	<b>776</b>
Humid Subtropical Climates (Cfa) .....	776
Mediterranean Climates (Csa or Csb) .....	783
Marine West Coast Climates (Cfb or Cfc) .....	791
<b>Humid Continental and Continental Subarctic (D) Climates .....</b>	<b>796</b>
Humid Continental Climates (Dfa and Dfb) .....	797

Continental Subarctic Climates (Dfc, Dwc, Dfd, Dwd) .....	800
Polar (E) Climates .....	804
Tundra Climates (ET) .....	804
Ice Cap Climates (EF).....	807
Highland Climates (H) .....	809
<b>Chapter 8 Climate Change .....</b>	<b>818</b>
Evidence of Past Climatic Change .....	820
Theories of Climate Change .....	823
Variations in Solar Output .....	823
Orbital and Axial Variations .....	828
Galactic Dust.....	837
Plate Tectonics and Continental Drift.....	840
Atmospheric Composition.....	844
Impacts (Comets, Meteors and Asteroids) .....	849
Anthropogenic .....	852
Current and Future Trends and Impacts of Global Climate Change .....	861
Climate Modeling .....	861
Temperature .....	863
Land .....	863
Oceans.....	868
Extreme Weather Events .....	871
Precipitation .....	882
Cryosphere .....	896
Sea Ice and Snow Cover .....	896
Permafrost .....	901
Sea-Floor Methane Hydrates .....	904
Glaciers and Ice Caps .....	905
Sea Level .....	909
Mitigation .....	919
Regional Trends and Impacts on Climate Change in the United States .....	920
Great Plains .....	921
Observations and Speculations about Climate Trends in the Great Plains .....	921
Southwest .....	926
Some Interesting Observations and Speculations about Climate Trends .....	926
Northwest .....	933
Some Interesting Observations and Speculations about Climate Trends .....	933
<b>Appendixes .....</b>	<b>938</b>
Appendix 1 World Climate Regions .....	939
Appendix 2 Selected Useful Websites .....	940

## Introduction

When you awoke this morning, chances are that you looked out the window to “see what the weather was doing,” or checked the weather app on your phone to see the day’s forecast. Most of us do this because we have a vested interest in the weather. It affects the choice of clothes we wear, the amount of money we spend on heating and cooling, the time it takes to commute to work or to school, the type of sports we play and even our health. Those that make a living outdoors, such as farmers and construction workers, are especially interested in the weather because it directly affects their livelihood. Too much rain, and crops rot; too little rain, and crops dry up and die. If it’s raining or snowing, or temperatures are too cold, construction workers are unable to excavate at construction sites, pour concrete or frame new homes. Highway crews can’t work on new roads if the ground is wet, and if it’s extremely dry the workers may have to spray water on the dirt to keep dust levels down. Major weather events, such as hailstorms and blizzards, can close roads, cause flight delays and damage infrastructure such as power lines and phone lines. And, we all know how devastating the impacts of tornadoes and hurricanes can be on the people and places that fall victim to them. Weather most certainly affects all of us, and that is why so many people are interested in it.

Of course, it’s also fun to know something about the weather and to be able to predict what’s going to happen based on basic principles that we can all understand. This knowledge is rewarding in and of itself; but, if we understand weather, that knowledge can also help keep us safe, and that most certainly makes it worthwhile to learn about weather.

Climate also is of profound importance because it affects many events that occur on the surface of the Earth. For example, it controls rates of chemical reactions in the soil, and that affects soil fertility. It determines the amount of rain that falls onto soil, and both soil fertility and soil moisture affect plant growth, including the crops which we depend upon for food. Soil moisture and soil fertility control the number and type of plants that live in an environment, and this, in turn, affects the number and type of animals present. The animals themselves are also directly affected by temperature and moisture because each species is adapted to a specific range of temperature and moisture conditions. In short, climate influences life on Earth and many aspects of human activity. Because of its profound



importance to life on Earth, it has been said that climate is the *Master of the Earth*. Given this, it is clear that any changes in the Earth's climate will affect everything to some degree — sometimes for the better, other times adversely.

The Earth is truly an amazing place that is full of both wonders and dangers. The crystal blue sky that follows a cold front, a fiery reddish-orange sunset along a beach and the flash of lightning in the night sky are all beautiful sights to see. But, the same atmosphere that brings us these scenes also brings us ice storms, flashfloods, tornadoes and hurricanes, all of which pose a danger to us. By studying weather and climate, you will develop a greater appreciation for the forces of nature that shape our lives in very fundamental ways.

Weather is defined as the condition of the atmosphere at a specific time and place. The weather that occurs at any point in time is a function of the composition and structure of the atmosphere, the amount of energy received from the Sun, temperature, wind and moisture — as well as a host of interacting physical processes. The study of weather, which is known as **meteorology**, requires an understanding of these things. And, because **climate** is simply the long-term average of weather conditions, the study of climate begins with the study of weather. This book follows this sequence, beginning with a discussion of basic facts and principles concerning the atmosphere, followed by an integration of that information into an understanding of weather, and then climate.

The authors of this ebook have attempted to tailor the material contained herein to the specific course requirements of students at Sam Houston State University. In developing this material, we focused on those concepts that we consider to be the most important for our students to know; accordingly, we have eliminated what we feel to be extraneous material which often impedes student learning. In essence, the material in this ebook represents the essentials of weather and climate.

We hope you will find the material contained herein to be both informative and useful.

Dennis Netoff

Marcus Gillespie

Ava Fujimoto-Strait

Jim Tiller

# Chapter 1

## The Earth's Place in Space

### Cosmic Beginnings

#### The Early Universe

A question that has inspired and stimulated the intellects of humans for centuries is whether or not life exists beyond our planet. It has been the theme of novels, movies, television series, comic characters, and a 1938 radio broadcast, *War of the Worlds*, that shook the Earth. It remains as hot a topic today as it was in the heyday of science fiction movies in the 1950s, and is a topic of debate among scientists and theologians. At present, the answer to the question is unresolved.

Over the past half-century, humans have stepped up the research effort to resolve some of the age-old questions about how things have evolved through time. For the first time in human history, scientists are beginning to solve the riddles of how the Earth began and how the life-support system evolved. A parallel question that is a natural outgrowth of this quest has to do with life elsewhere in the universe. Technological breakthroughs in telescopes, computers, radio astronomy, satellites, and cosmic exploration by robotic spacecraft have begun to give humans the ability to put the Earth properly in its place in space, which is the main theme of chapter one in this book.

The modern universe, according to the *Expanding Universe Theory*, had its beginning some 14 billion years ago. All of the matter and energy in the universe at that time was concentrated in a pinpoint in space. The matter became unstable and cataclysmically exploded, sending subatomic particles in all directions at warp speed and astronomical temperatures. What occurred before that time, and what will happen to our universe in the future, is a matter of scientific speculation. As 2006 Nobel Prize winner John Mather said in a recent address to Southern Illinois University:

“There isn’t a beginning that we can see,  
and there isn’t an end that we know about.”

There is, however, considerable evidence for today’s expanding universe, including:

- All of the known galaxies seem to be moving away from each other. The expanding universe was discovered by Edwin Hubble (the Hubble Space Telescope was named after him) in 1929. Oddly, the galaxies farthest away seem to be moving outward at a greater rate than the closer ones, as though some force other than gravity is causing repulsion. This force has been dubbed dark energy, even though very little is understood of its exact nature.
- The abundance of light elements such as hydrogen and helium support the idea that most of the matter in the first seconds after the supposed Big Bang was in the form of 10-billion degree subatomic particles, such as protons, neutrons, electrons, positrons, neutrinos and dark matter.
- The cosmic microwave background radiation that has been recently imaged by NASA is thought to be residual from the earliest (oldest) phases of the expanding universe (Figure 1.01).

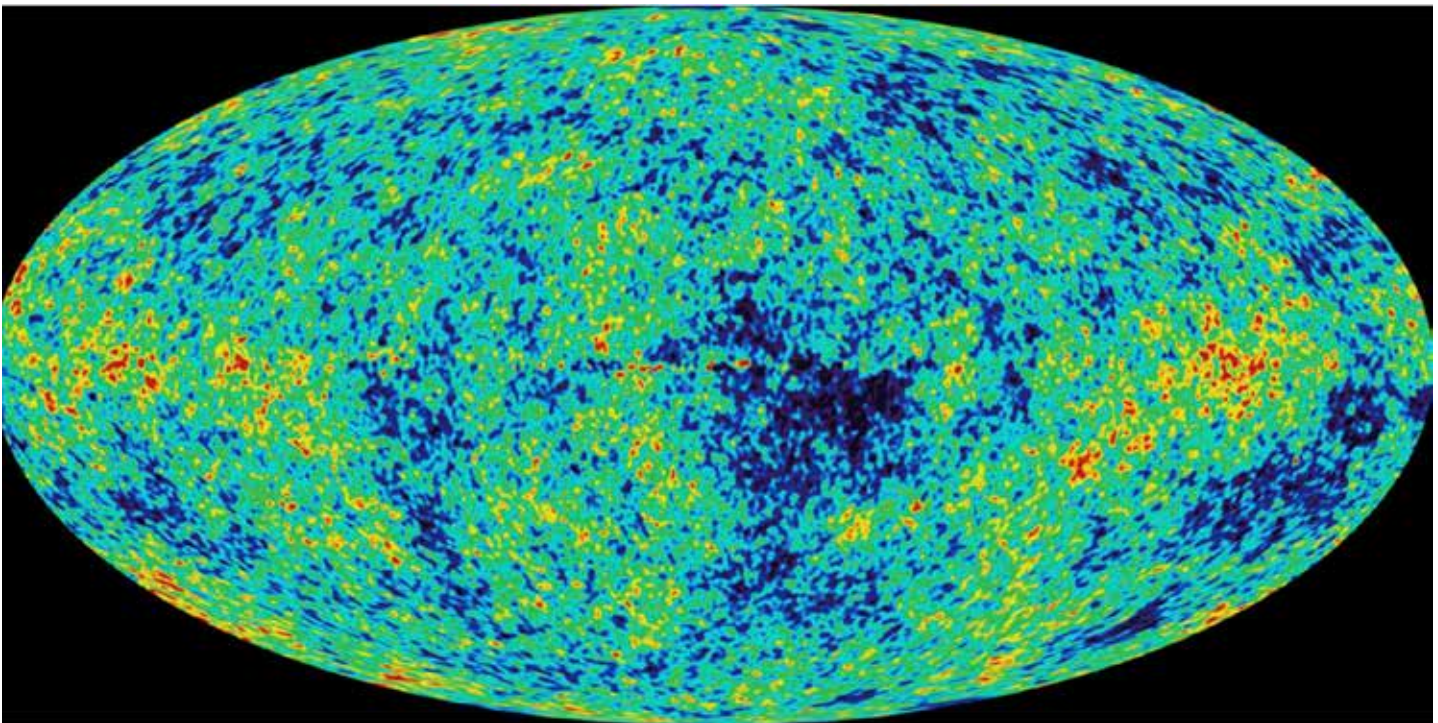


Figure 1.01. A microwave image of the first detailed, full-sky map of what is interpreted as some of the oldest light in the universe, some perhaps dating back to the **Big Bang**. The map of the **cosmic microwave background** taken from the Wilkinson Microwave Anisotropy Probe in 2003 shows the infant universe as color variations that represent 13+ billion-year-old temperature differences (Source/Credit: NASA).

Everything in the universe seems to have a life cycle: galaxies, stars, planets, and actual life forms. In the early days of the expanding universe, things happened incredibly fast. When the universe was only a fraction of a second old, changes took place that paved the way for the evolution of stars and galaxies. This *inflation* period proposes that a ball of matter that was subatomic in size, representing the fundamental building blocks of the infant universe, grew to the size of a baseball at super-light speeds. A fraction of a second later, the seething-hot primordial soup, consisted of quarks, electrons and other subatomic particles. Milliseconds later, quarks merged to form protons and neutrons, the material that forms the nucleus of all atoms. A second had eclipsed, and the proto-universe was still too hot for the formation of atoms.

Within a few minutes, the universe had expanded and cooled but charged electrons and protons prevented light from shining. The universe was uniformly opaque in a superheated fog. The *dark era* had begun. Finally, the universe expanded and cooled to perhaps 10,000°C (18,000°F), allowing protons, neutrons and electrons to combine in the form of the lightest atoms, the hydrogen and helium that still makes up the bulk of the modern universe. Opaqueness gives way to a mostly transparent universe. As unbelievable and speculative as the statements above may seem, they are the underpinnings of modern astrophysics and are supported by both theory and astronomical observations. No doubt many of these theories will be modified in the future and some discarded for new ones. Such is science.

## Nebula, Stars, and Galaxies

The early expanding universe was thought to be homogenous. There were no stars, no galaxies, and no structure. As the 400-million-year-old universe continued to expand and cool, now perhaps at minus 200°C (minus 328°F), clumps of dark matter and interstellar gases began to come together in oddly shaped masses called *nebula* (Figure 1.02). Further gravitational collapse formed massive areas of more concentrated matter. These more massive areas had a progressively stronger gravitational field and became more and more efficient in attracting additional interstellar matter (Figure 1.03). Eventually, the interior of these masses became sufficiently hot and dense to cause fusion of hydrogen atoms into helium, releasing large amounts of electromagnetic energy, including their own light. These would become infant stars, beginning a multi-billion year cycle of burning their thermonuclear fuel (Figure 1.04).



Figure 1.02. The early expanding universe was thought to be homogenous. There were no stars, no galaxies, and no structure. As the early universe cooled, clumps of dark matter and interstellar gases began to come together in oddly shaped masses called nebula. Further gravitational collapse formed massive areas of more concentrated matter, eventually leading to the breeding ground of countless new stars. This Hubble Space Telescope image taken in 2006 shows scores of giant bright blue infant stars and less massive red-orange stars forming at the expense of the surrounding nebula. The bluish haze of the nebula is largely glowing hydrogen, irradiated by the strong stellar winds of the nearby giant stars. The image is in a star-forming region of the Large Magellanic Cloud, a nearby galaxy that orbits the Milky Way galaxy some 160,000 light years away (Source/Credit: NASA).



Figure 1.03. The Great Nebula of Orion, the most famous and most photographed nebula in the universe. Orion is composed of interstellar dust and gases (mainly hydrogen), and is the breeding ground of countless stars (Source/Credit: NASA).

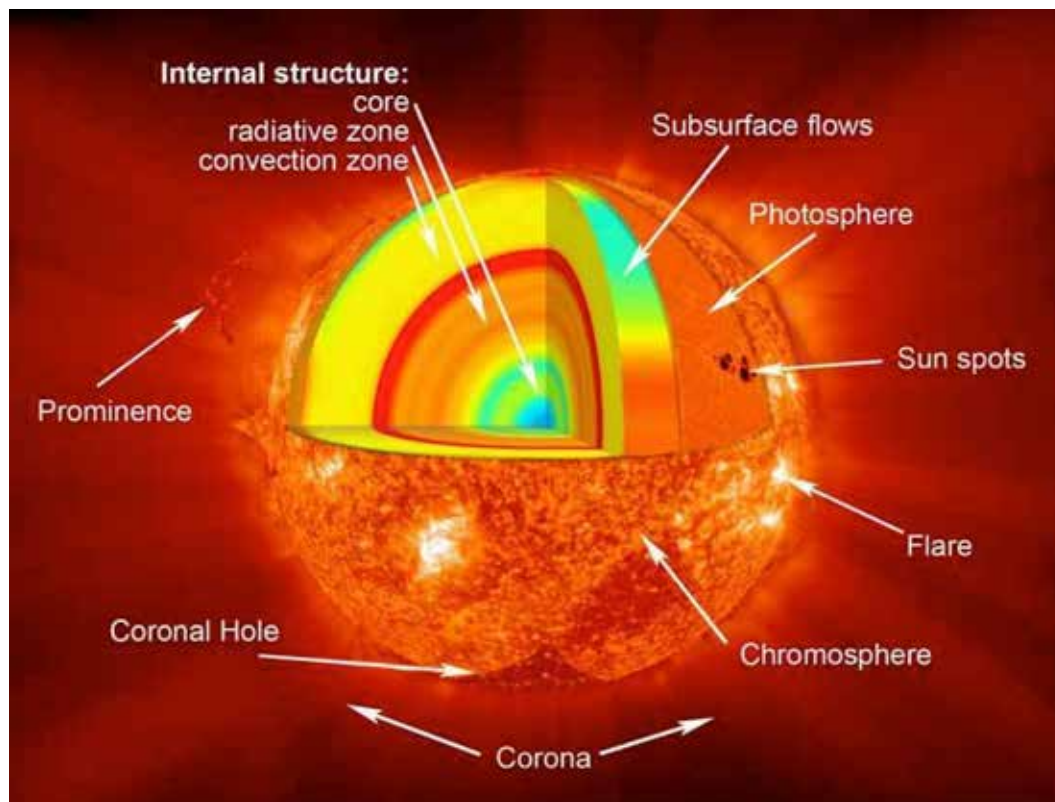


Figure 1.04. A star is born when the internal pressure and temperature are high enough to force fusion of lighter hydrogen atoms into helium atoms. The process generates massive amounts of energy, part of which is the visible light of a star (Source/Credit: NASA).

Astronomers now hypothesize that star-forming process reached their peak fairly early, perhaps only 500 million to a billion years after inception (Figure 1.05). Clusters of stars attracted other clusters of stars, and in the process huge clusters formed and began to rotate causing the initial irregular mass of stars to be transformed into a rotating disk. These became the familiar spiral galaxies, each one of which contains >100 billion stars in some cases (Figures 1.06a and 1.06b). Our closest galactic neighbor is a spiral galaxy very similar to our own, the Andromeda Galaxy (Figure 1.07).

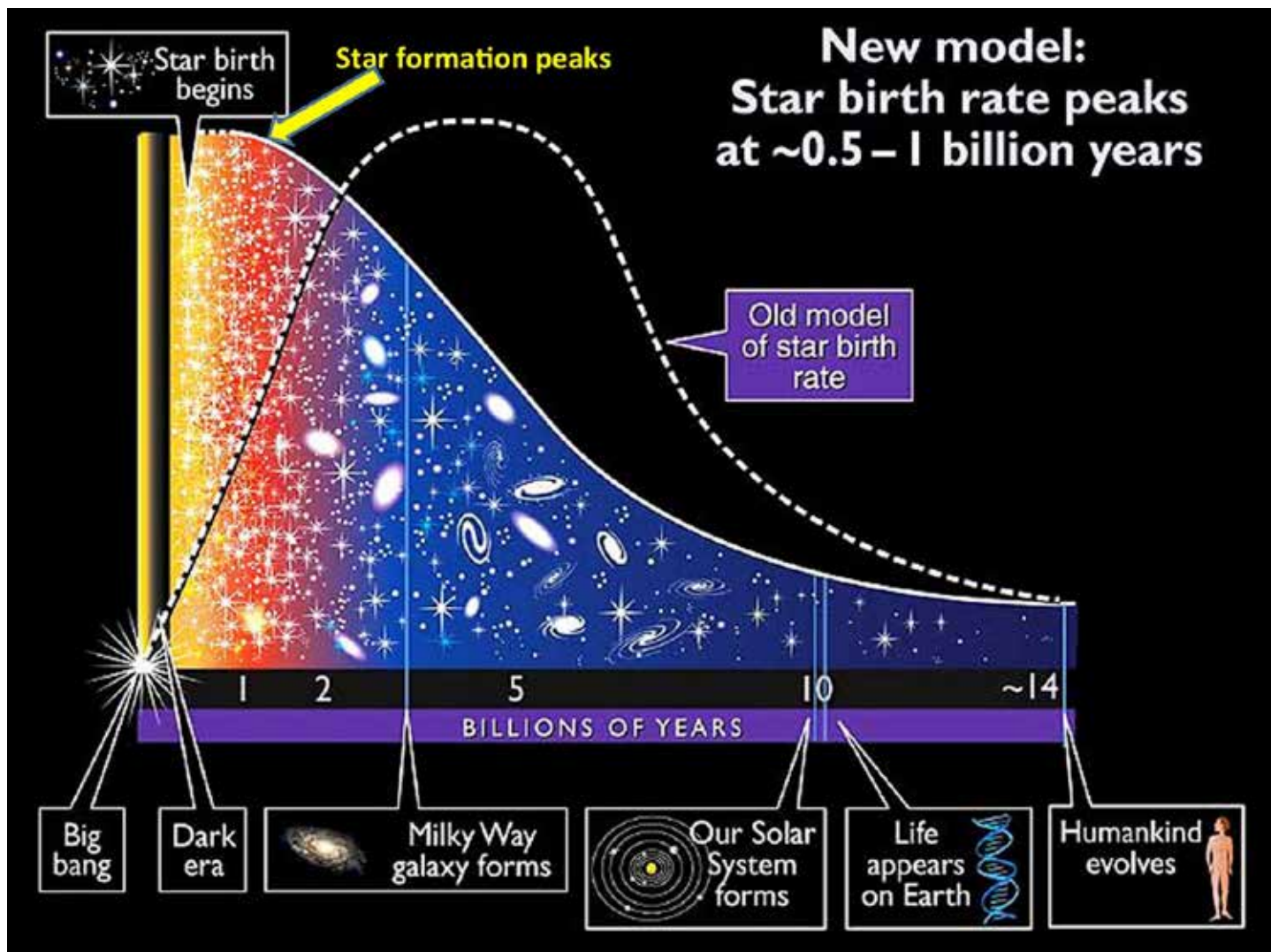


Figure 1.05. Recent observations from the Hubble Space Telescope suggest that star formation peaked very early in the expanding universe, perhaps during the first few hundred million to one billion years. The Milky Way Galaxy formed several billion years later, and our solar system another few billion years later. Life on Earth is first seen in the fossil record about 3 billion years ago (Source/Credit: NASA/Space Telescope Science Institute).

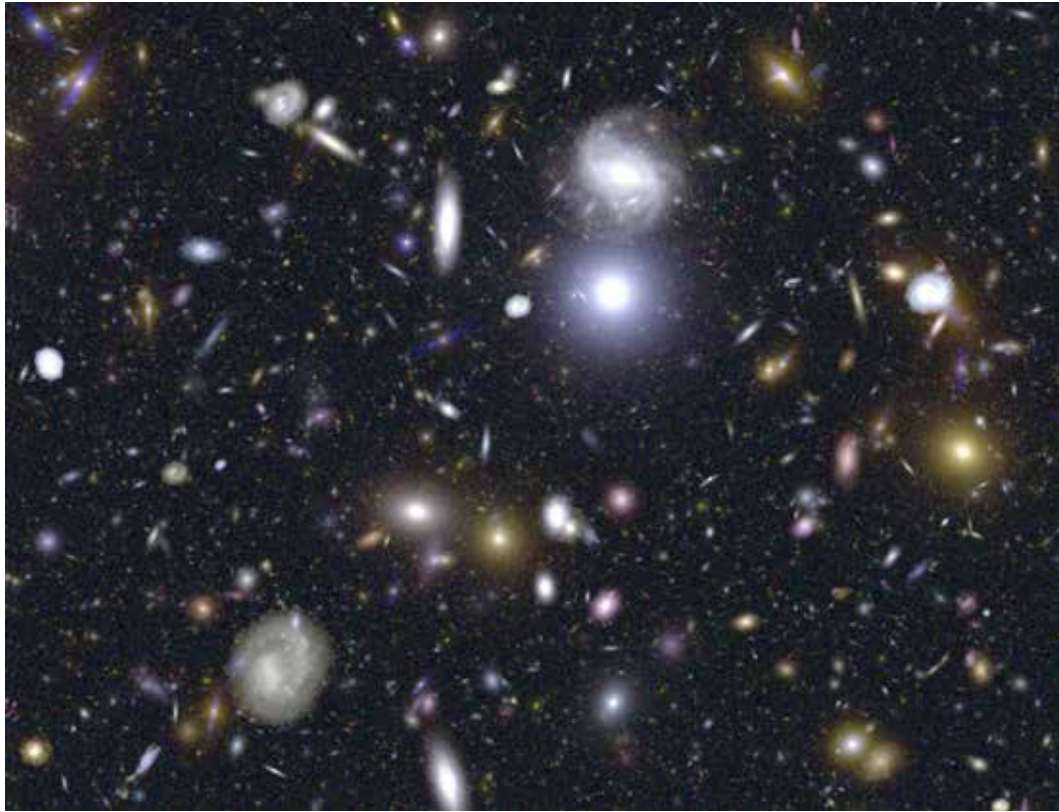


Figure 1.06a. Hundreds of galaxies imaged by the Hubble Space Telescope. There are several regions in the universe where huge clusters of galaxies can be seen in a single image (Source/Credit: NASA).

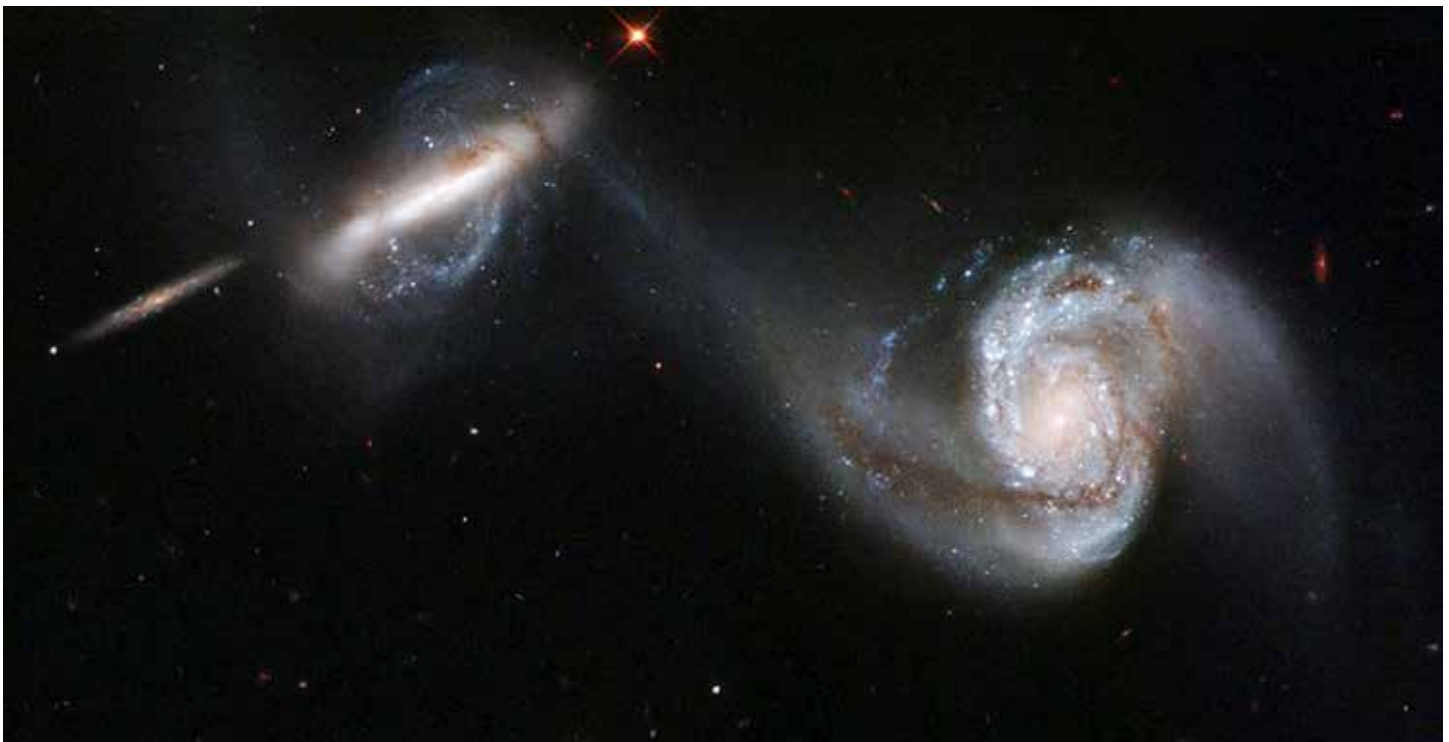


Figure 1.06b. Galaxies are attracted to other galaxies by gravity, and sometimes collide. The two galaxies involved in the cosmic spectacle are NGC3808A and NGC 3808B (Source/Credit: NASA).





*Figure 1.07. The Andromeda Galaxy is the Milky Way's largest galactic neighbor at about 2.5 million light years. Like the Milky Way, it is a spiral galaxy, but somewhat larger, at an estimated 260,000 light years across. Andromeda is so close and bright that it is only one of 10 galaxies that can be spotted from Earth with the naked eye (Source/Credit: NASA).*

Stars of different masses evolve differently and at different rates. Average-sized stars, like our Sun, go through a life cycle of perhaps 10 billion years or so before they burn up their fuel supply. When most of the hydrogen in the core is spent, the core collapses. The outer layers expand and cool to become a red giant (Figure 1.08a). Eventually, the outer layers of the red giant are expelled, forming a planetary nebula (Figure 1.08b). The core is transformed into a white dwarf, and then a black dwarf. More massive stars may end their life cycle as neutron stars or black holes (Figures 1.09a and 1.09b).



Figure 1.08a. (left) Artist's conception of stellar evolution of a medium-sized star such as our Sun. Average-sized stars go through a life cycle of perhaps 10 billion years or so before they burn up their fuel supply. When most of the hydrogen in the core is spent, the core collapses. The outer layers expand and cool to become a red giant, depicted in the image by the larger red-orange circles. Eventually, the outer layers of the red giant are expelled, forming a planetary nebula (blue-cored image on far right). The core is transformed into a white dwarf, and then a black dwarf (Source/Credit: Wikipedia, European Southern Observatory, Steinhöfel).

Figure 1.08b. (right) Spitzer Space Telescope image of the Helix Nebula (NGC 7293). The nebula is a mere 700 light years away, and is about two light years in diameter. The dust and gas cloud surrounds a spherical object, which is a white dwarf. This is considered an excellent example of the final stages in the life cycle of a medium-sized star like our Sun (Source/Credit: NASA, JPL-Caltech, Kate Su Steward Observatory, University of Arizona).



Figure 1.09a. Stars that are several times more massive than the Sun destroy themselves as supernovas. The Crab Nebula represents the remnants of a supernova explosion that was witnessed on Earth by Chinese astronomers in 1054 AD. Now 1000 years after the explosion, it still produces 100,000 times more energy than the Sun. The Crab Nebula is about 11 light years across and 6500 light years from the Earth. At the center is a neutron star only 18 miles (30 km) in diameter, spinning 30 times each second (Source/Credit: NASA).

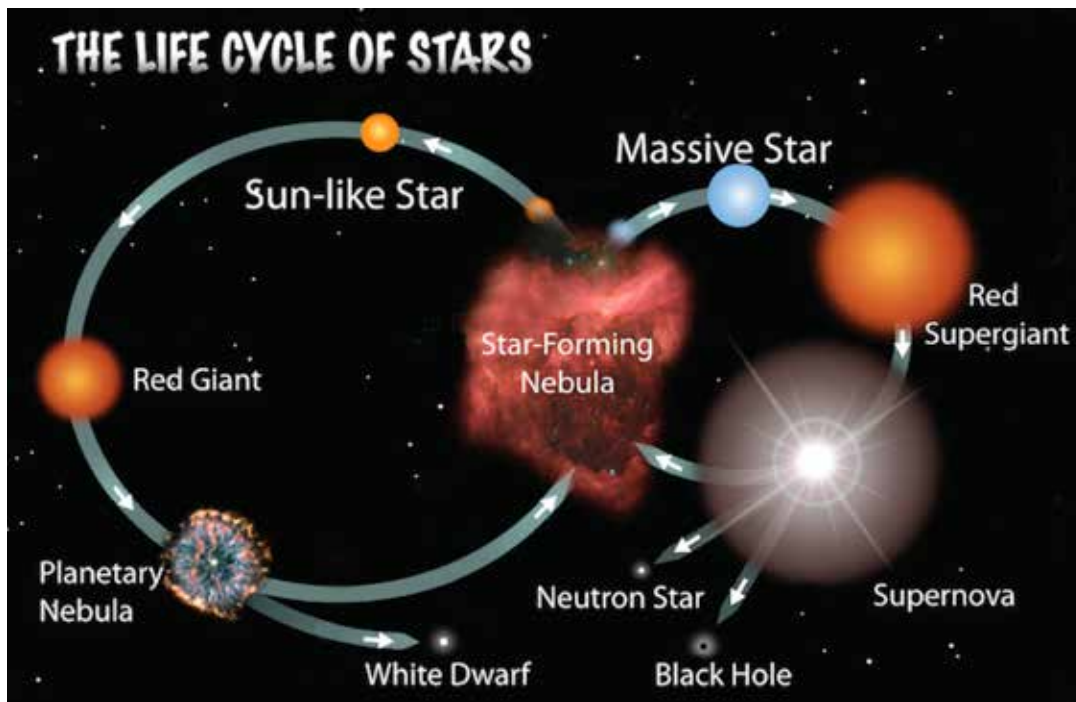


Figure 1.09b. The life cycle of a medium-sized versus a more massive star. Medium-sized stars begin as nebula and end as nebula, only to furnish the seeds of future stars (Source/Credit: adapted from NASA).

The Milky Way galaxy contains some 100-400 billion stars, including the Sun. It evolved perhaps 12 billion years ago at a time when star and galaxy formation peaked. The diameter of the galaxy, excluding the halo of dark matter, is approximately 100,000 light years. The Milky Way Galaxy is a type of spiral galaxy similar to the nearby Andromeda Galaxy. An edgewise view of it shows a lenticular (lens) shape with a central bulge. There is believed to be a supermassive black hole at the heart of the core of the galaxy. In plan view, it has several spiral arms (Figure 1.10). The solar system lies in one of the spiral arms. On a clear night, Earth-bound observers see a broad haziness in the sky representing one of the spiral arms (Figure 1.11). The entire galaxy revolves around the central bulge. The solar system, travelling at 515,000 miles per hour (828,000 km/hr), makes one complete revolution every 230 million years.

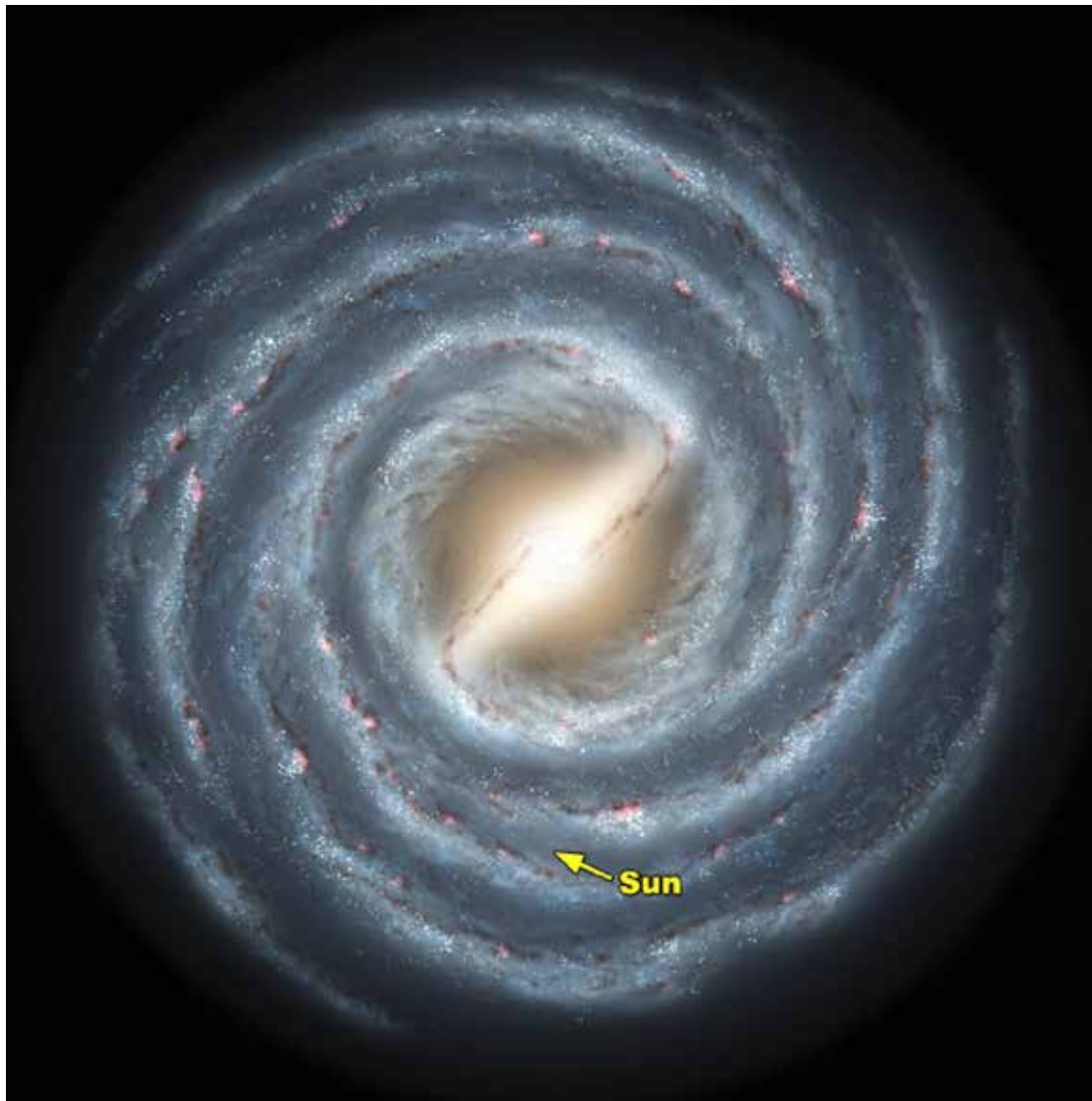


Figure 1.10. Artistic rendition of the Milky Way Galaxy, a type of spiral galaxy similar to the nearby Andromeda Galaxy. An edgewise view of it shows a lenticular shape with a central bulge. There is believed to be a supermassive black hole at the heart of the core of the galaxy. In plan view, it has several spiral arms. The solar system lies in one of the spiral arms. On a clear night, Earth-bound observers see a broad haziness in the sky representing one of the spiral arms. The entire galaxy revolves, and the solar system makes one complete revolution every 230 million years (Source/Credit: NASA Caltech).



Figure 1.11. The arch of the spiral arm of the Milky Way galaxy is seen stretching across the heavens in this panoramic view taken from central Chile. The lights of Antofagasta appear on the right horizon. The bright object above the Milky Way is Jupiter (Source/Credit: European Southern Observatory).

## The Solar System

### Protosun and Protoplanetary Disk

The age of our solar system is probably around 5 billion years. By 4.5 billion years ago, most of the main players in the system had evolved. They include the Sun, eight major planets, a host of dwarf planets, dozens of satellites (moons), several comets, and countless asteroids.

The solar system formed in a manner similar to that of a miniature galaxy. A vast mass of gases and dust, much of it probably the remains of nebula from former stars, responded to the pull of gravity and began to contract. As it contracted, it began to rotate, causing the irregular mass to take on the appearance of a spinning disk with most of the mass concentrated in the center. This was the protosun and planetary disk from which the solar system would evolve (Figure 1.12).

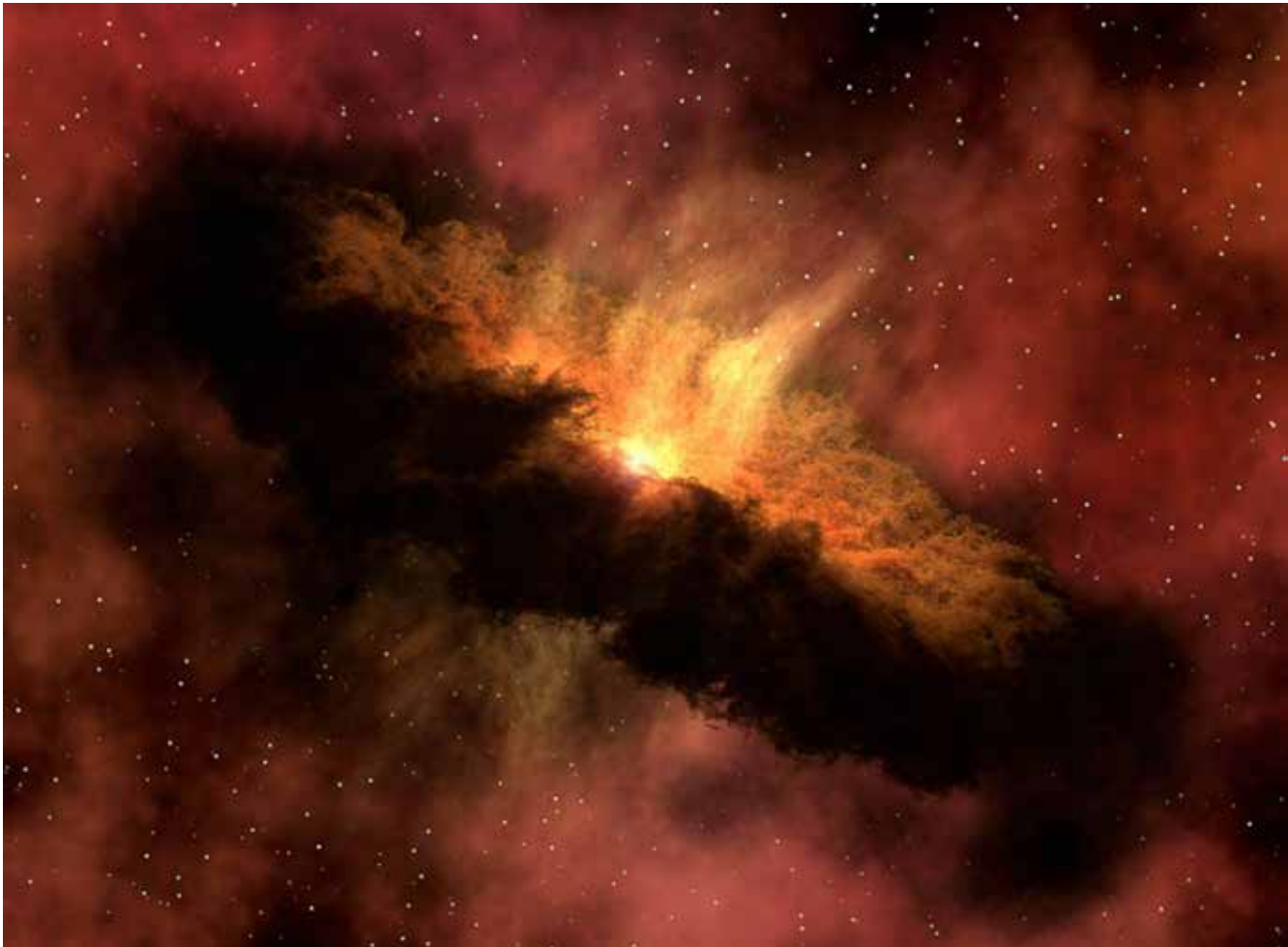


Figure 1.12. Stage 1. **Protosun and protoplanetary disk.** As the material began to assemble into a massive, rotating giant mass in the center of the proto-solar system, the protoplanetary disk formed. The disk contained gases and dust remaining from the collapse of the nebula from which all stars form. Initially, the rotating debris was composed of gases and solid particles ranging from microscopic size to perhaps pea size (Source/Credit: NASA).

As the protoplanetary disk evolved, most of the debris and gases outside of the disk became drawn into the rotating disk. The protoplanetary disk took on a cleaner, more streamlined lenticular form in cross section (Figure 1.13). Within the disk, tiny bits of dust responded to electrostatic forces representing the initial accretion process. As these bits of dust became larger, gravitational forces came into play to accelerate growth. Astronomers study the oldest meteorites to interpret the environment of their formation. These analyses indicate that some of the accreted grains, dating back 4.58 billion years, formed in a cold environment, yet others in a very hot (near-Sun) environment.



Figure 1.13. Stage 2. As the protoplanetary disk evolved, most of the debris and gases outside of the disk became drawn into the disk. The protoplanetary disk took on a cleaner, more streamlined form. Within the disk, tiny bits of dust responded to electrostatic forces representing the initial accretion process. Astronomers study the oldest meteorites to interpret the environment of their formation. These analyses indicate that some of the accreted grains, dating back 4.58 billion years, formed in a cold environment, yet others in a very hot (near-Sun) environment (Source/Credit: NASA).

As more material assembled into the protoplanetary disk, the central portion of the disk, already having more mass and gravity than the rest of the disk, began to develop a massive bulge analogous to a galactic core. This would soon become the Sun. The remaining disk contained gases and dust from the collapse of the nebula from which all stars form. Initially, the rotating debris was composed of gases and solid particles ranging from microscopic size to perhaps pea size.



The protosun has become massive enough so that the temperature and pressure required for fusion has been initiated (Figure 1.14). Material in the protoplanetary disk now accreted more rapidly as *gravitational forces* dominated electrostatic forces to form larger and larger bodies. These *planetesimals* ranged from a few hundred yards in diameter to perhaps a half dozen miles. As these bodies grew in size and mass, their gravitational pull increased, making them progressively more efficient in cleaning the smaller material in the disk and hence accelerating their own growth by accretion. Accretion became the dominant process in the formation of the planets and their satellites (Figure 1.15). Planetesimals grew in size to embryonic planets, some tens to hundreds of miles in diameter. The asteroid Vesta (Figure 1.16), with a diameter of 326 miles (525 km) represents one of these embryonic planets that never achieved planetary status.

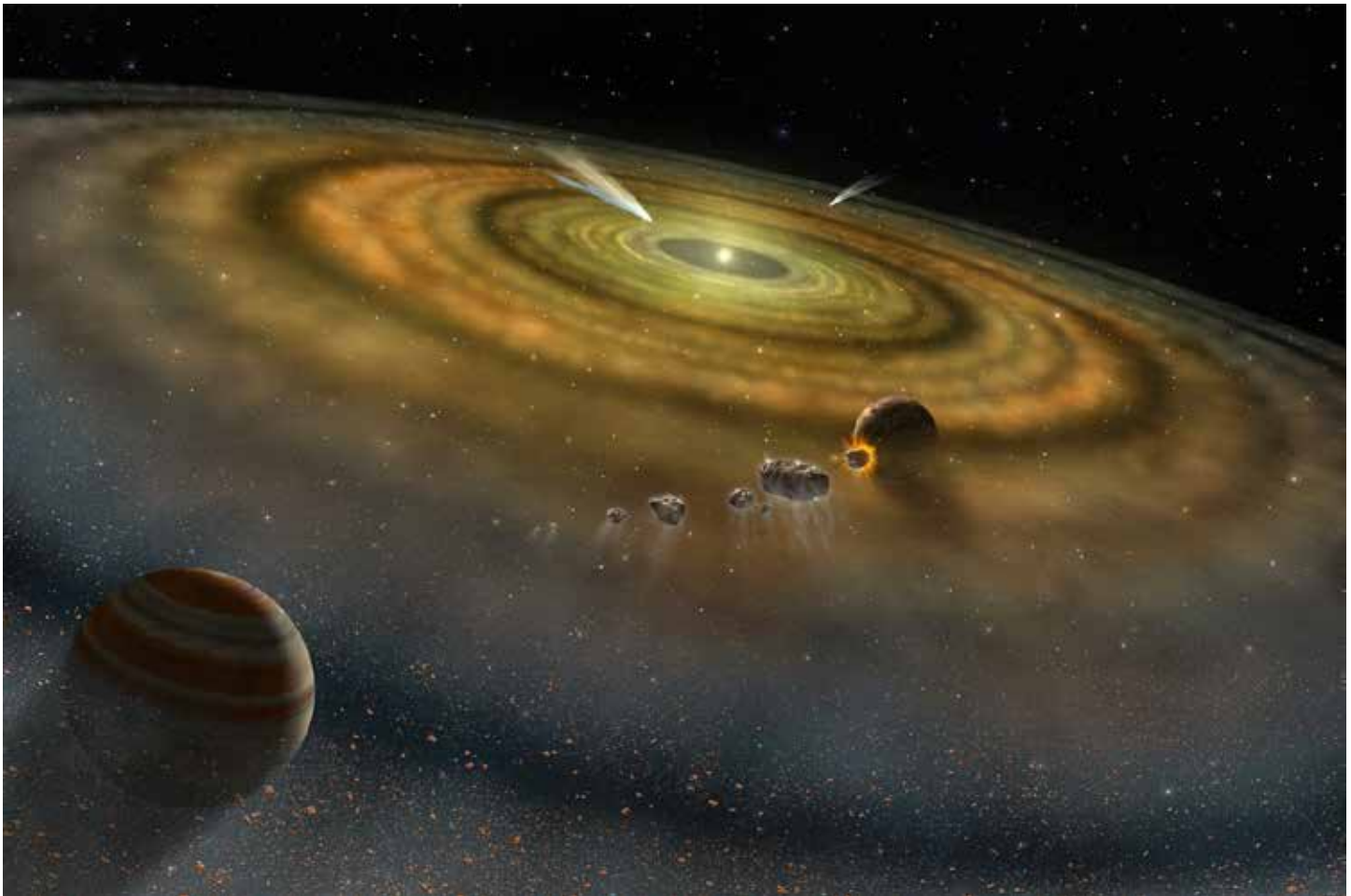


Figure 1.14. Stage 3. The protosun has become massive enough so that the temperature and pressure required for fusion has been initiated. Material in the protoplanetary disk is now accreting more rapidly, as gravitational forces combine with electrostatic forces to form larger and larger bodies. These **planetesimals** ranged from a few hundred yards in diameter to perhaps a half dozen miles. As these bodies grew in size and mass, their gravitational pull increased, making them progressively more efficient in cleaning the smaller debris in the disk and hence accelerating their own growth. Planetesimals grew in size to embryonic planets, some tens to hundreds of miles in diameter (Source/Credit: NASA).



Figure 1.15. **Accretion** became the dominate process in the formation of planets and satellites, perhaps 4.3-4.6 billion years ago (Source/Credit: NASA).

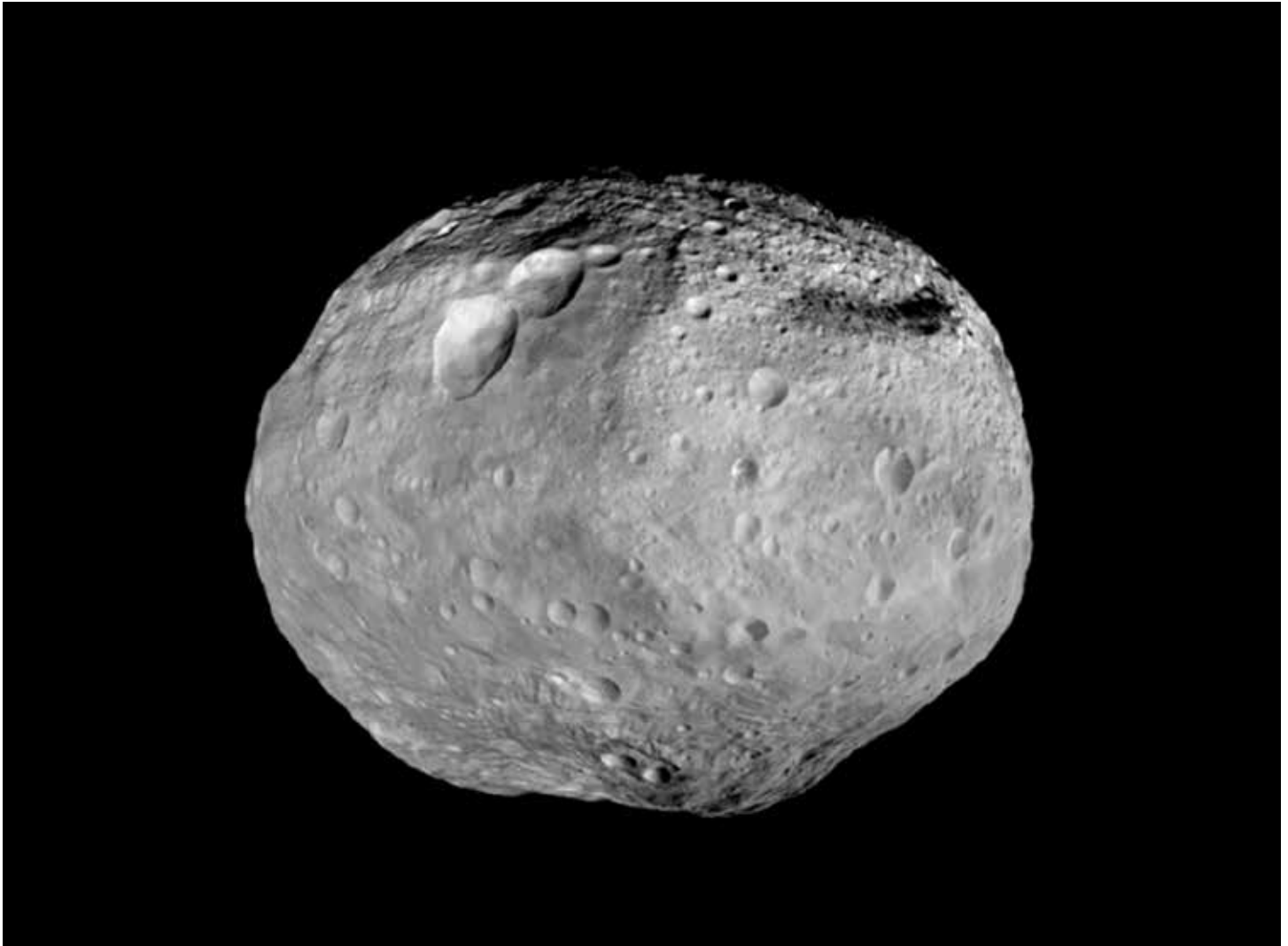


Figure 1.16. The asteroid Vesta, with a diameter of 326 miles (525 km), represents an embryonic planet that never reached true planet stature. Real planets are massive enough to acquire a spherical shape as well as to have enough gravity to sweep the surrounding space clean by accretion. Note the pockmarked surface of Vesta, revealing multiple impacts during the early stages of the evolution of the solar system (Source/Credit: NASA).

## The Sun

The Sun is the largest, most massive object in the solar system (Figure 1.17). Even though much of it is made of light elements, it nonetheless contains about 99.86% of the total mass in the solar system. It is slightly larger than the average-sized star, and yet its diameter of 865,000 miles (1,391,000 km) is over 11 times that of the largest planet, Jupiter, and 109 times that of the Earth. The overall composition of the Sun is about 98% hydrogen and helium, although a host of heavier elements are being generated in its core. Although only about 1.7% of the Sun's mass consists of heavier elements, they equal about 5600 times the mass of the Earth.

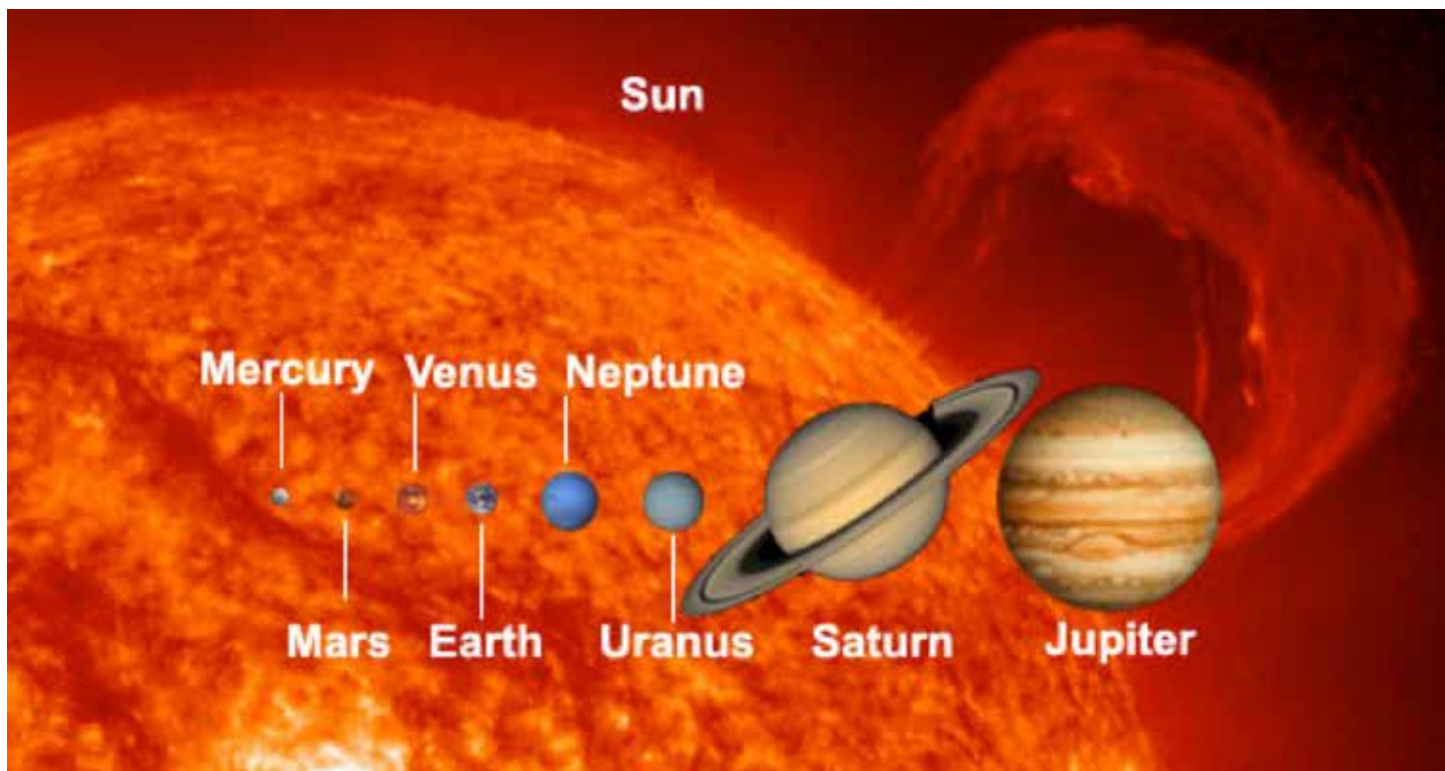


Figure 1.17. The Sun is the largest, most massive object in the solar system. Even though much of it is made of light elements, it nonetheless contains about 99.86% of the total mass in the solar system. The Sun's diameter (865,000 miles, 1,391,000 km) is over 11 times that of the largest planet, Jupiter, and 109 times that of the Earth. This image shows the relative size of the Sun and planets approximately to scale. If the Earth's diameter was about the size of a large sand grain (1/12 inch, 2 mm), the Sun would be about the size of a basketball (Source/Credit: NASA).

The Sun is the only object in the solar system capable of thermonuclear reactions (Figure 1.18).

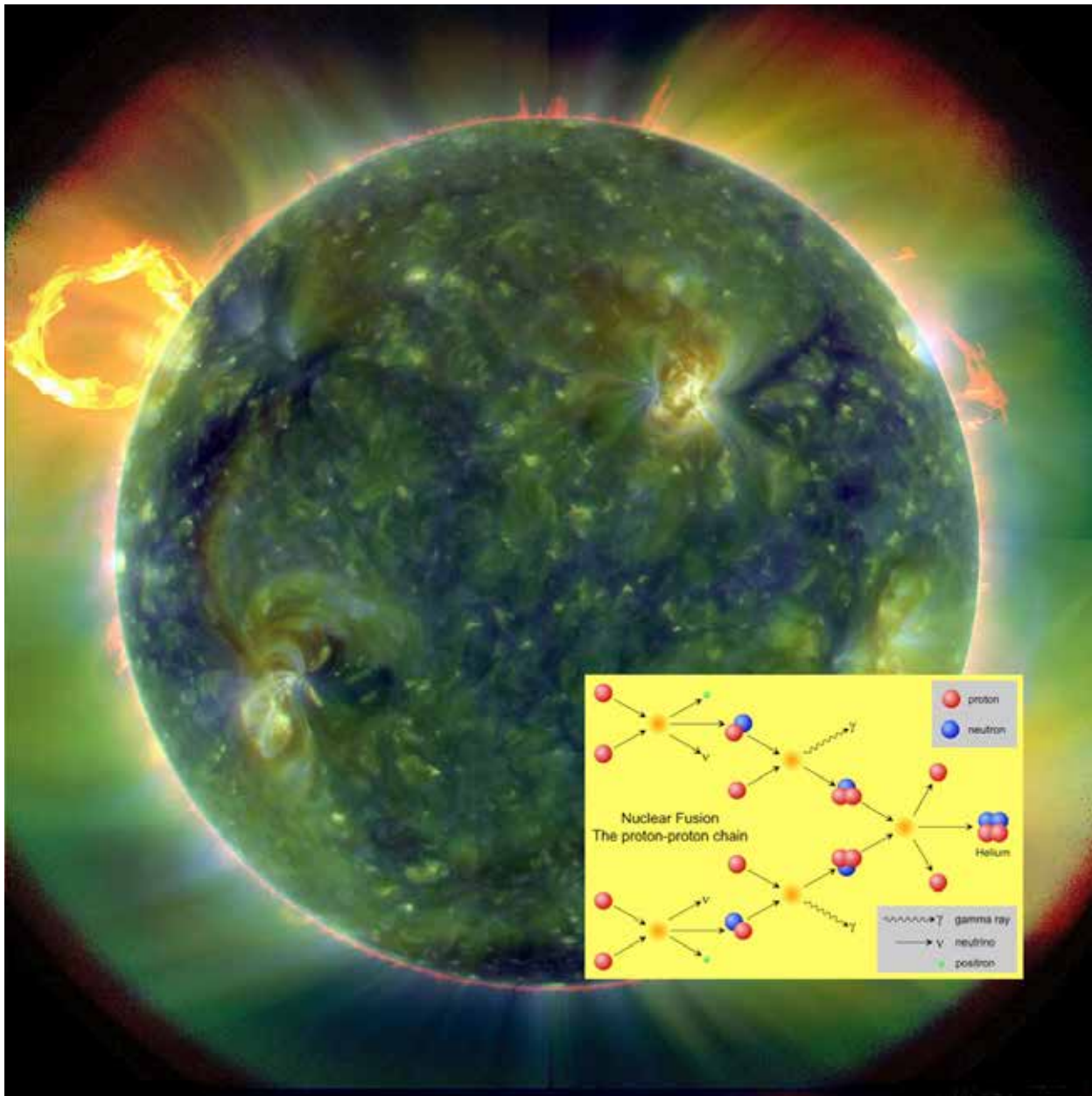


Figure 1.18. The overall composition of the Sun is about 98% hydrogen and helium, although a host of heavier elements are being generated in its core. Although only about 1.7% of the Sun's mass consists of heavier elements, they equal about 5600 times the mass of the Earth. The Sun is the only object in the solar system capable of thermonuclear reactions. Each second, millions of tons of hydrogen are converted into helium (inset), along with tremendous amounts of energy, largely in the form of radiation (Source/Credit: NASA, Randy Russell).

The Sun rotates on its axis, but different latitudes rotate at different speeds, ranging from 25 days at the Equator to 36 days near the poles. Temperatures increase from about 9900°F (5500°C) on its visible photosphere to over 27 million°F (15 million°C) in the core, where fusion occurs. The Sun is the source of most of the thermal energy in the atmospheres of the inner planets, including Earth.

The Sun is divided into several layers based on their physical characteristics (Figures 1.19a and 1.19b). The *fusion core* is the area of highest temperature and pressure where fusion generates electromagnetic radiation. The *radiation shell* is the layer where energy is slowly transported outward by radiation flow. The *convection shell* is the layer where energy is transported rapidly by massive convection cells. The *photosphere* is the visible surface of the Sun where photons are emitted. The *chromosphere* is the Sun's atmosphere. The *corona* is an extremely hot zone where solar winds originate.

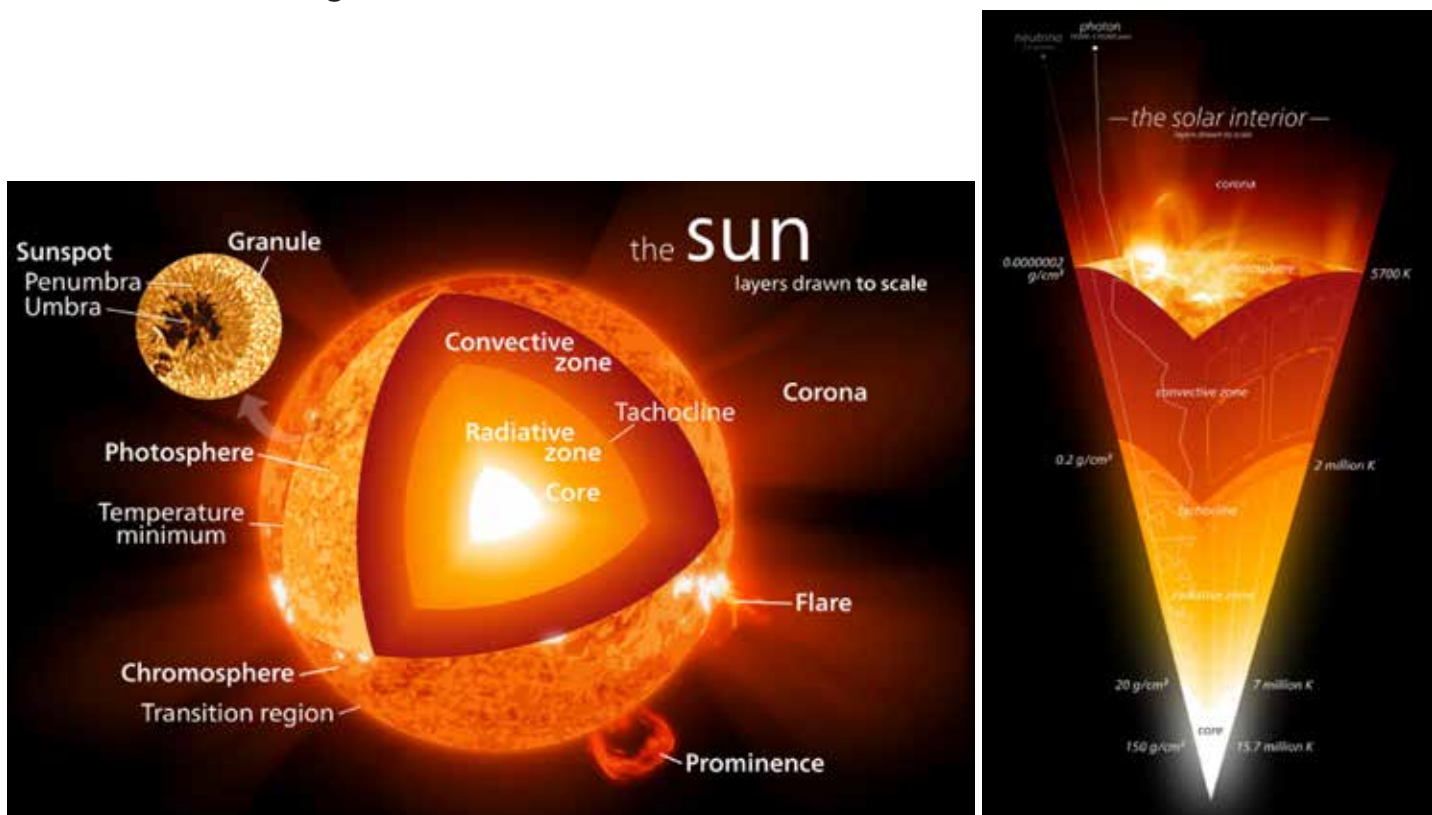


Figure 1.19a. (left) Temperature increases from about 9900°F (5500°C) on the Sun's visible photosphere to over 27 million°F (15 million°C) in the core where fusion occurs. The Sun is the source of most of the thermal energy in the atmospheres of the inner planets, including Earth. The Sun is divided into several layers based on their physical characteristics. The inset (upper left) is a sunspot, an irregularly-shaped, cool, dark spot on the Sun. Sunspots tend to increase and decrease in relative abundance in 11-year cycles (Source/Credit: <http://commons.wikimedia.org/wiki/User:Kelvinsong>).

Figure 1.19b. (right) The Sun is divided into several layers based on their physical characteristics. The **fusion core**, where fusion generated electromagnetic radiation, is the area of highest temperature and pressure. The **radiation shell** is the layer where energy is slowly transported outward by radiation flow. The **convection shell** is the layer where energy is transported rapidly by massive convection cells. The **photosphere** is the visible surface of the Sun where photons are emitted. The **chromosphere** is the Sun's atmosphere. The **corona** is an extremely hot zone where the solar winds originate (Source/Credit: <http://commons.wikimedia.org/wiki/User:Kelvinsong>).

Various dating techniques of meteorites and lunar rocks generate ages as old as about 4.6 billion years. It seems plausible that the Sun formed slightly prior to that, perhaps somewhere around 5 billion or so years ago. The planets probably began to evolve shortly after the formation of Sun.

## Comparative Planetology

### The Terrestrial Planets

The process of accretion is thought to account for the formation of the planets and most of their satellites within a few hundred million years after the Sun began burning its hydrogen fuel. Although many questions exist regarding the exact timing and formative processes, there is theoretical evidence that the gas giants evolved somewhat before the rocky planets. The outer planets, or gas giants, all have characteristics similar in many respects to Jupiter, and are often referred to as **Jovian planets**. They include Jupiter, Saturn, Uranus, and Neptune (Figure 1.20). All are large, have thick gaseous envelopes surrounding them, and are low density, owing to their makeup of lightweight gases. Pluto was once classed as a planet, but is now considered a dwarf planet.

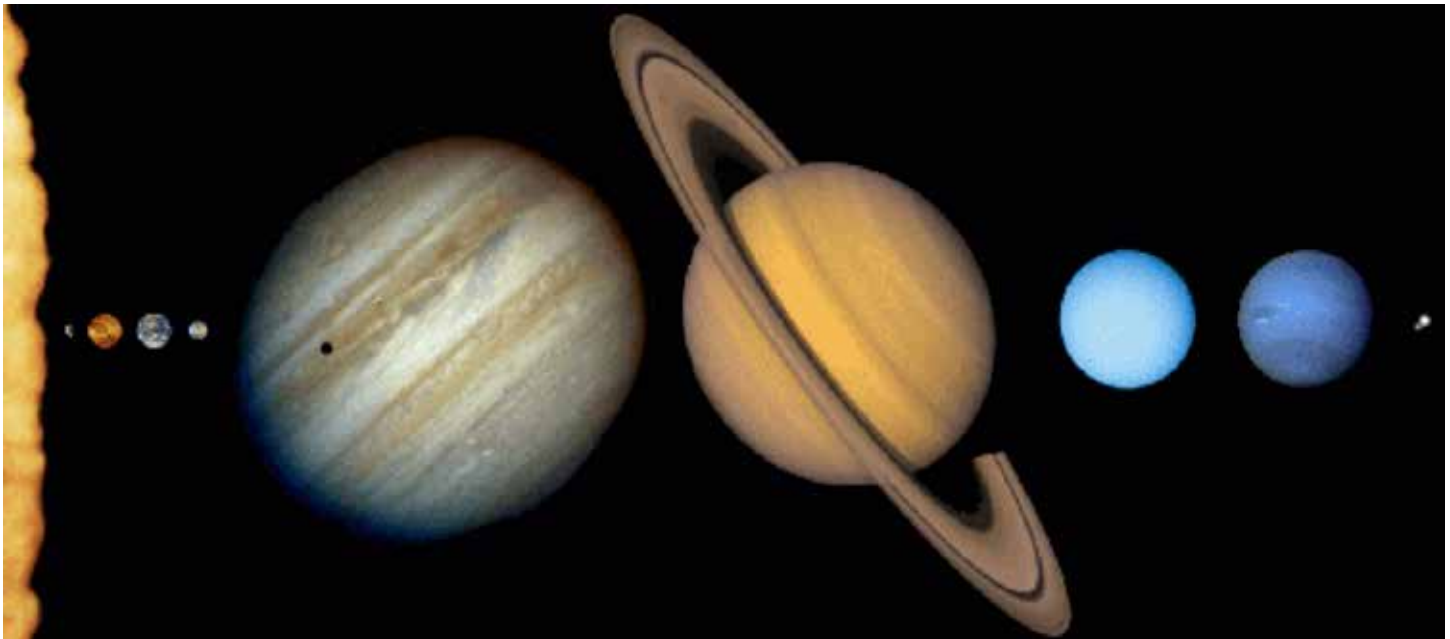


Figure 1.20. An arc of the Sun, the **Terrestrial planets** (Mercury, Venus, Earth, Mars) and the **Jovian planets** (Jupiter, Saturn, Uranus, and Neptune). Diameters are roughly to scale, distances from the Sun are not. An obvious pairing of three sets of planets is obvious; Jupiter-Saturn, Uranus-Neptune, and Earth-Venus (Source/Credit: NASA).

The inner planets all have characteristics similar to that of the Earth and are referred to as the **terrestrial planets**. They include Mercury, Venus, Earth and Mars. Compared to the Jovian planets, terrestrial planets are small, dense, and made principally of rocky and metallic material. Other objects in orbit around the Sun include comets, asteroids, and material in the Kuiper Belt and Oort Cloud (Figure 1.21).

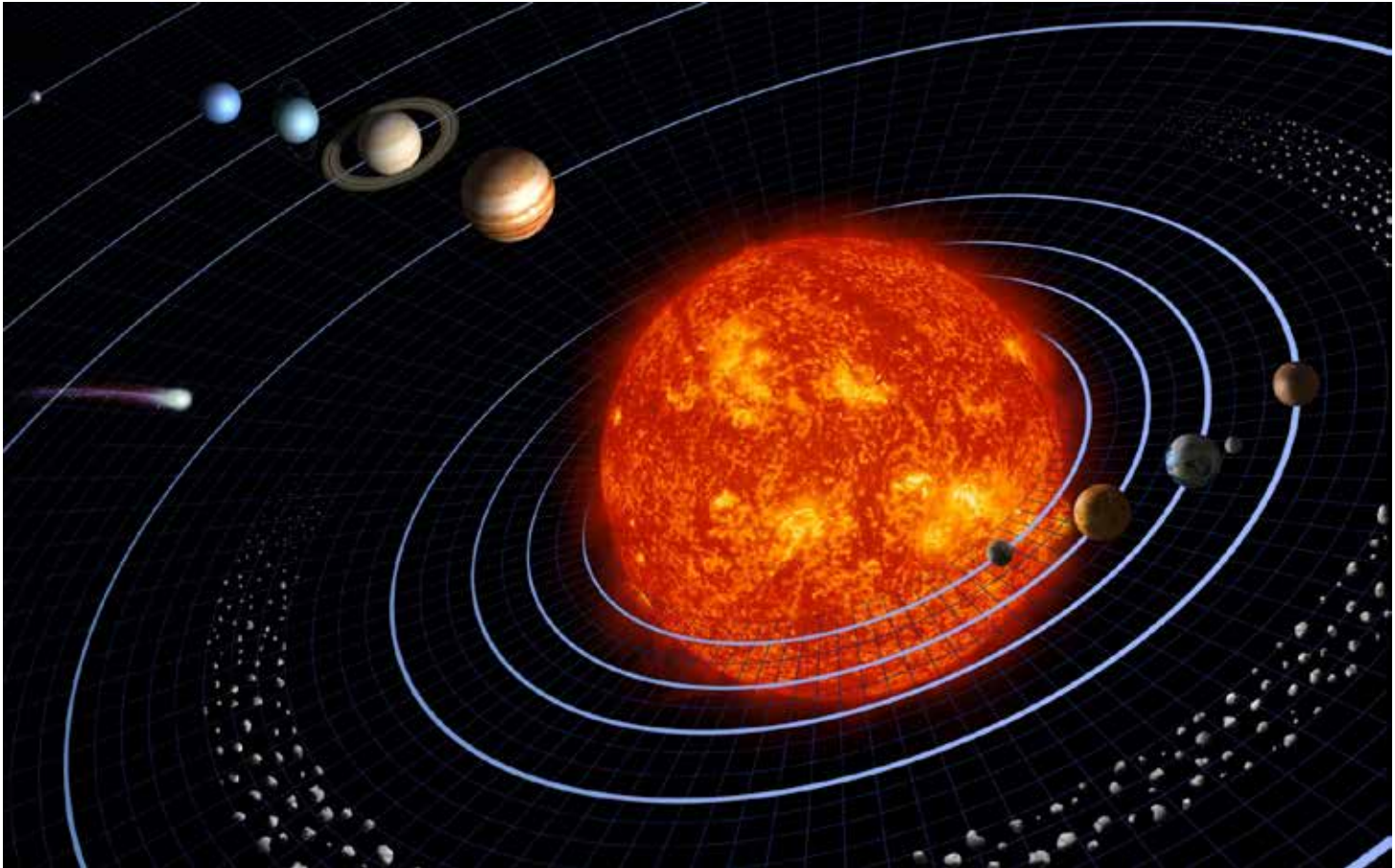


Figure 1.21. Artistic comparison of the major players in the solar system. The Sun is the dominant player, both in terms of its huge size and mass as well as the fact that all smaller objects are in orbit around the Sun. The **Terrestrial planets** (Mercury, Venus, Earth, Mars) are shown to the right of the Sun and the **Jovian planets** (Jupiter, Saturn, Uranus, and Neptune) to the upper left. Diameters and distance from the Sun are not to scale. The **asteroid belt** lies between the orbits of Mars and Jupiter. A **comet** with a long tail is shown near Jupiter. The **Kuiper belt** and the **Oort Cloud** are not shown. All are in orbit around the Sun and most of them are roughly in the same orbital plane (Source/Credit: NASA).



## Mercury

**Mercury** is the innermost planet and the smallest of the terrestrial planets (Figure 1.22). Mercury is similar in many respects to Earth's Moon (Figure 1.23). Both bodies are about the same size, have rocky silicate surfaces, dense cores, and are pockmarked with impact craters (Figure 1.24). In the early stages of planetary accretion, all of the planets were heavily bombarded by impact, the very process by which they grew to planet size. All of the terrestrial planets underwent subsequent partial or complete **resurfacing**, a process whereby old crustal features are removed and replaced by newer terrain (Figure 1.25).

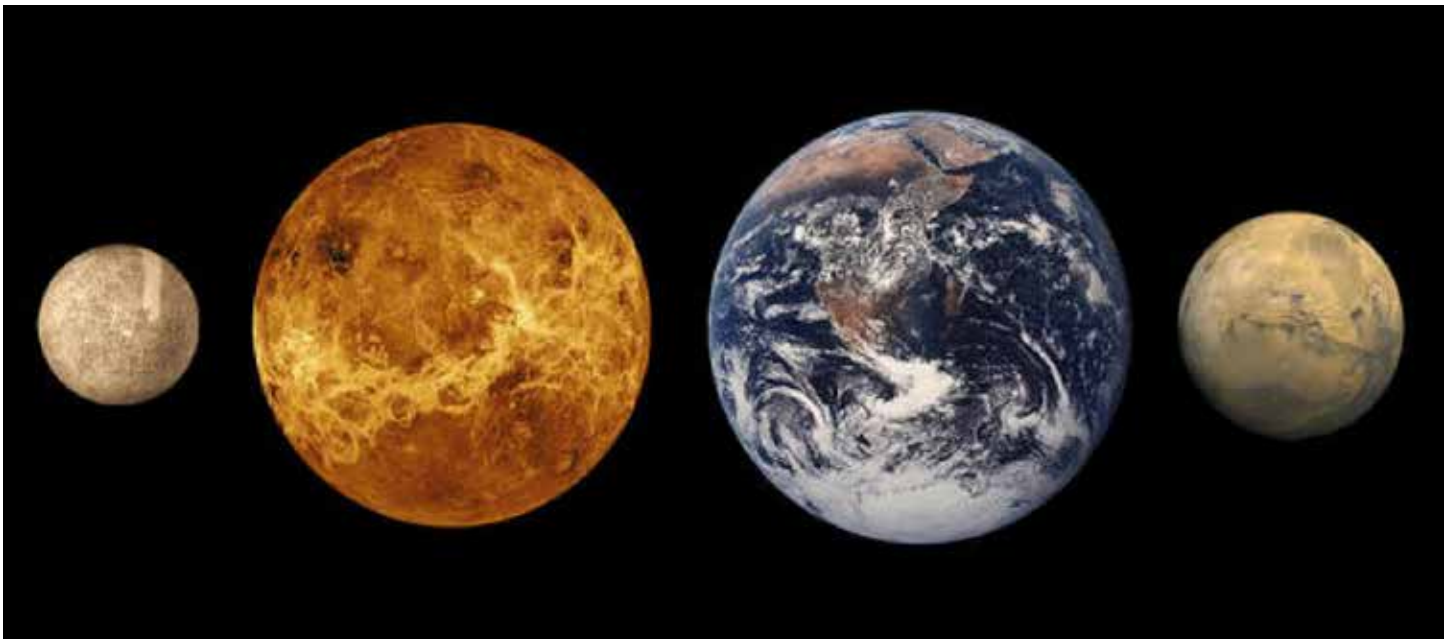


Figure 1.22. Size comparison of the terrestrial planets. Mercury is the smallest planet, since distant Pluto is now considered a dwarf planet. All of the terrestrial planets have silicate crusts and mantles and metallic cores (Source/Credit: NASA).

Mercury

Earth's Moon

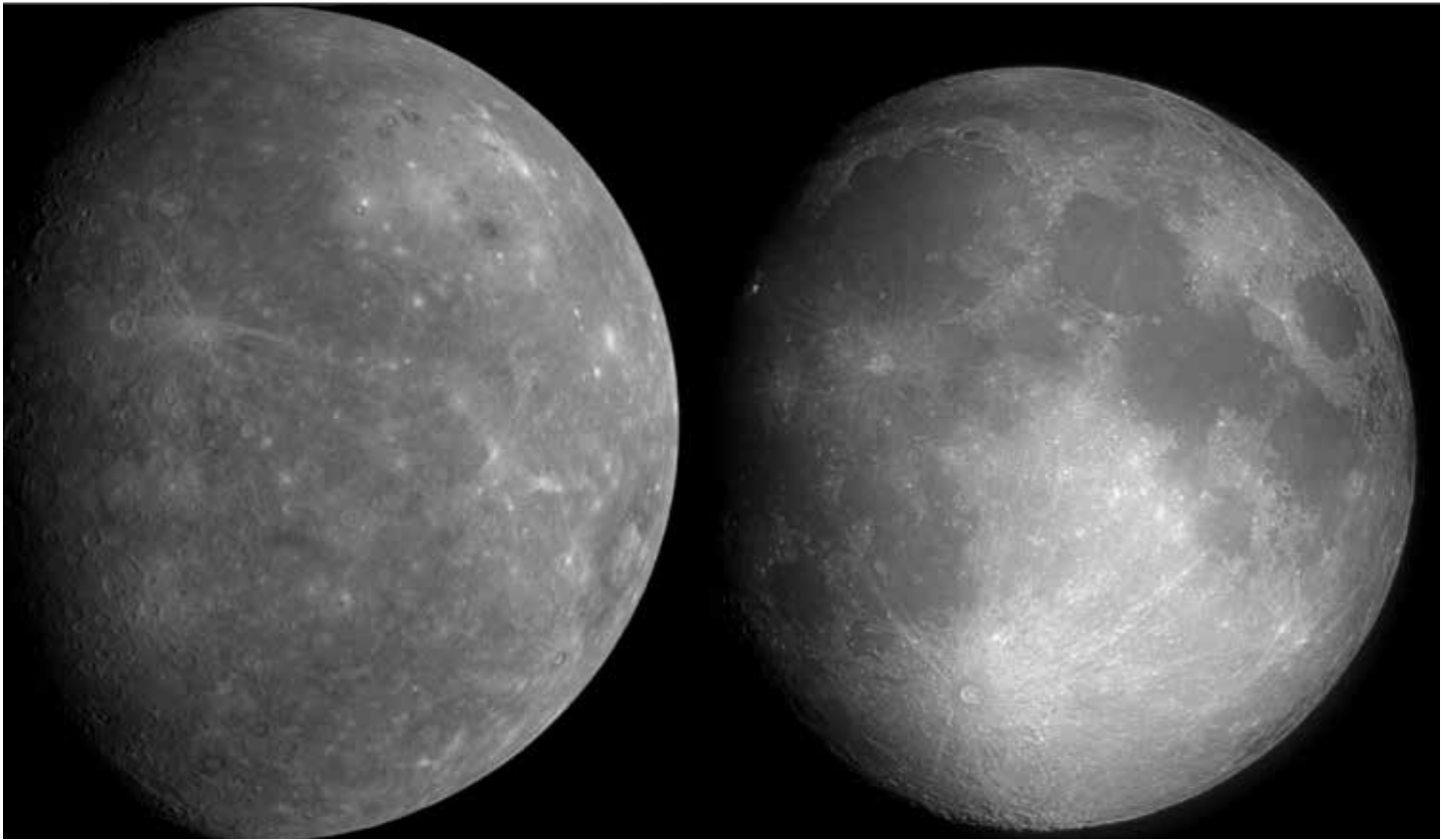


Figure 1.23. Mercury looks like and is like Earth's Moon. Both (1) are densely scarred with impact craters; (2) have been partially resurfaced with basaltic volcanism, back-filling the large, oval impact craters; (3) are virtually without atmospheres, so their surface features are very old; (4) have similar densities (Moon's specific gravity is 3.34; Mercury's is 5.42), and therefore similar composition; (5) have layered interiors, with metallic cores; and (6) are about the same diameter; Mercury at 3022 miles (4863 km); Moon at 2160 miles (3476 km) (Source/Credit: NASA).

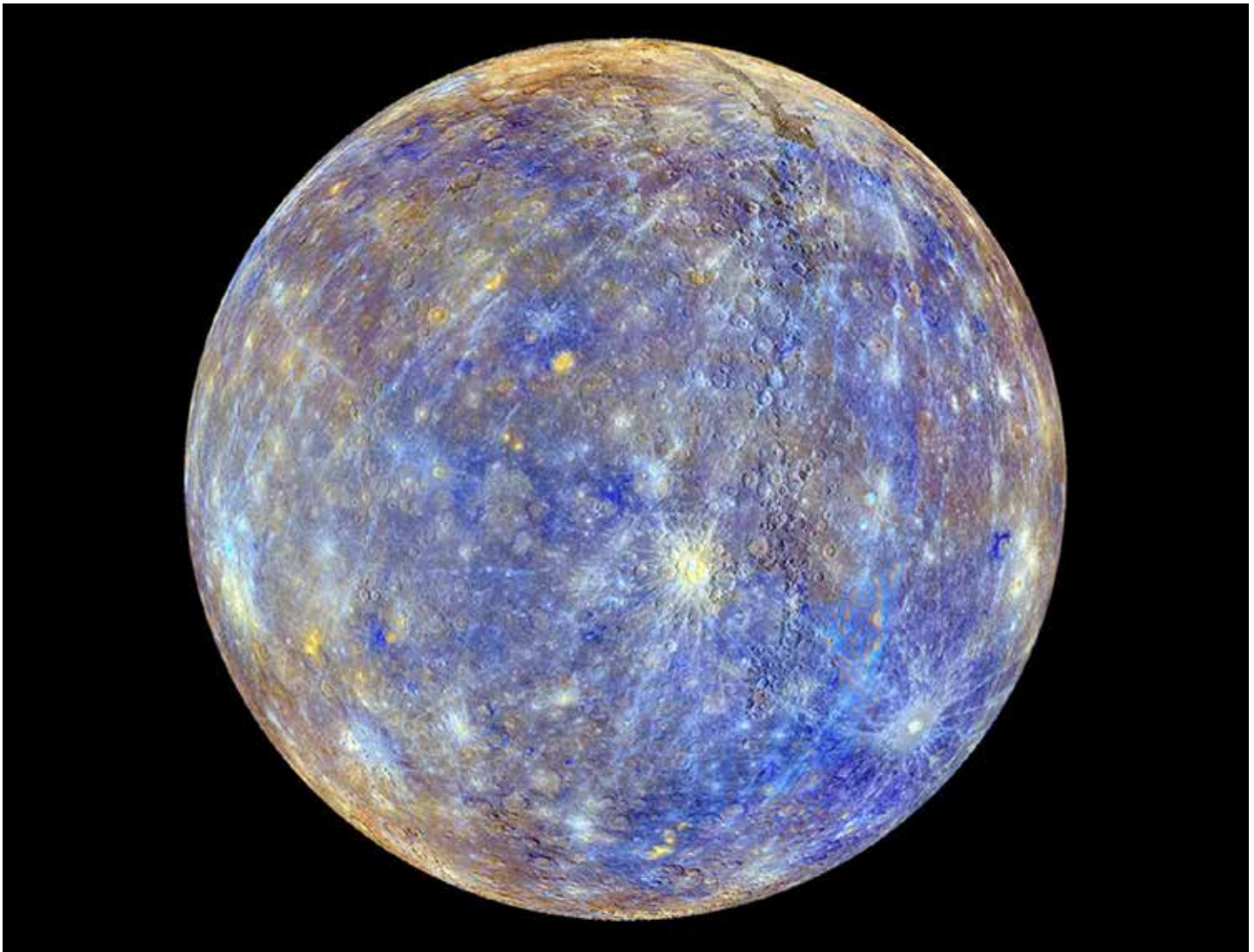


Figure 1.24. Most of Mercury's surface has been mapped recently by NASA's Messenger space craft. This false-color image illustrates the densely-cratered surface of Mercury, much the same as our own Moon. Two of the largest impact craters show a system of radial whitish splays radiating from the main crater. These rays represent **ejecta**, or material thrown outward from the force of the impact (Source/Credit: NASA).



Figure 1.25. False-color image of the Caloris Basin on Mercury from a January 2008 flyby. The 960 mile-wide (~1500 km) depression was caused by an asteroid impact early in Mercury's history. Mercury has no atmosphere. There is no rain to weather and erode the surface, and therefore the craters on its surface have remained sharp and distinct for billions of years. Mercury cannot retain an atmosphere because of its small size, which results in a weak gravitational field that cannot hold an atmosphere. The lack of atmosphere results in extreme temperature variations from day to night and from sunlit areas to shaded areas (Source/Credit: NASA).

Both Mercury and Earth's Moon had thermal events early in their history. The source of the heat was most likely from impact and internal radioactive decay. Interior temperatures were high enough to melt large volumes of rock, some of which surfaced and flowed over large distances, similar to the basalt flows on Earth. These ancient flows form the oval-shaped darker regions on the surface of Mercury and the Moon. In both cases, the basaltic plains are now heavily cratered, indicating great antiquity. Very little resurfacing has taken place in the past few billion years aside from the occasional impact crater. These thermal events are of considerable interest in comparative planetology because where there is volcanism there is **outgassing**. Outgassing ejects a host of potential atmosphere-forming gases and liquids.

The NASA spacecraft *Messenger*, the first to orbit Mercury, has taken over 200,000 images since 2011 and is revealing details of the planet's surface and interior for the first time. *Messenger* has detected small but significant amounts of water in Mercury's thin atmosphere, the *exosphere*. Geophysical data from *Messenger* suggest a molten core (Figure 1.26). There are also many enigmatic features such as clusters of irregular depressions of unknown origin (Figure 1.27).

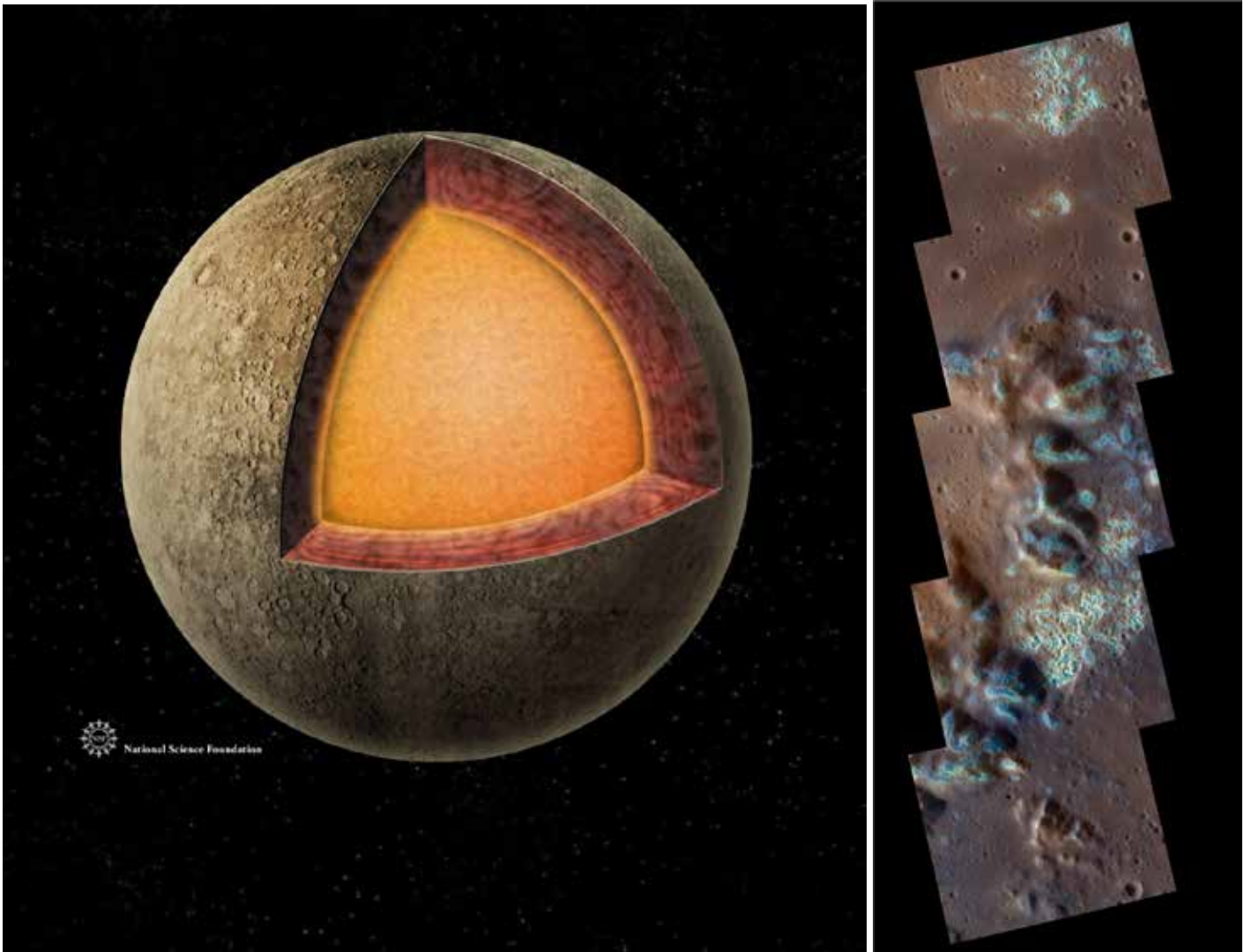


Figure 1.26. (left) Mercury has a cratered rocky crust similar to Earth's Moon. A thin, silicate mantle lies beneath the crust. A huge metallic core, the outer part perhaps molten, dominates the interior of the planet (Source/Credit: NSF).

Figure 1.27. (right) *Messenger* image of strange depressions scattered on surface of unknown origin (Source/Credit: NASA).

**Mercury's atmosphere:** Mercury's orbit is only 36 million miles (58 million km) from the Sun. The planet's small size generates only a weak gravitational field. Both of these characteristics make it ill-suited to retain an atmosphere, and Mercury is not a likely candidate for any kind of surface life support system. Surface temperatures on the dark versus daylight side of Mercury range from minus 180°C (minus 290°F) to 800°F (430°C). Even though Mercury underwent

early volcanism that could have provided an atmosphere, the lighter gases would have been quickly swept away by the intense **solar wind**, a stream of high-energy particles continuously released by nuclear fusion in the solar interior.

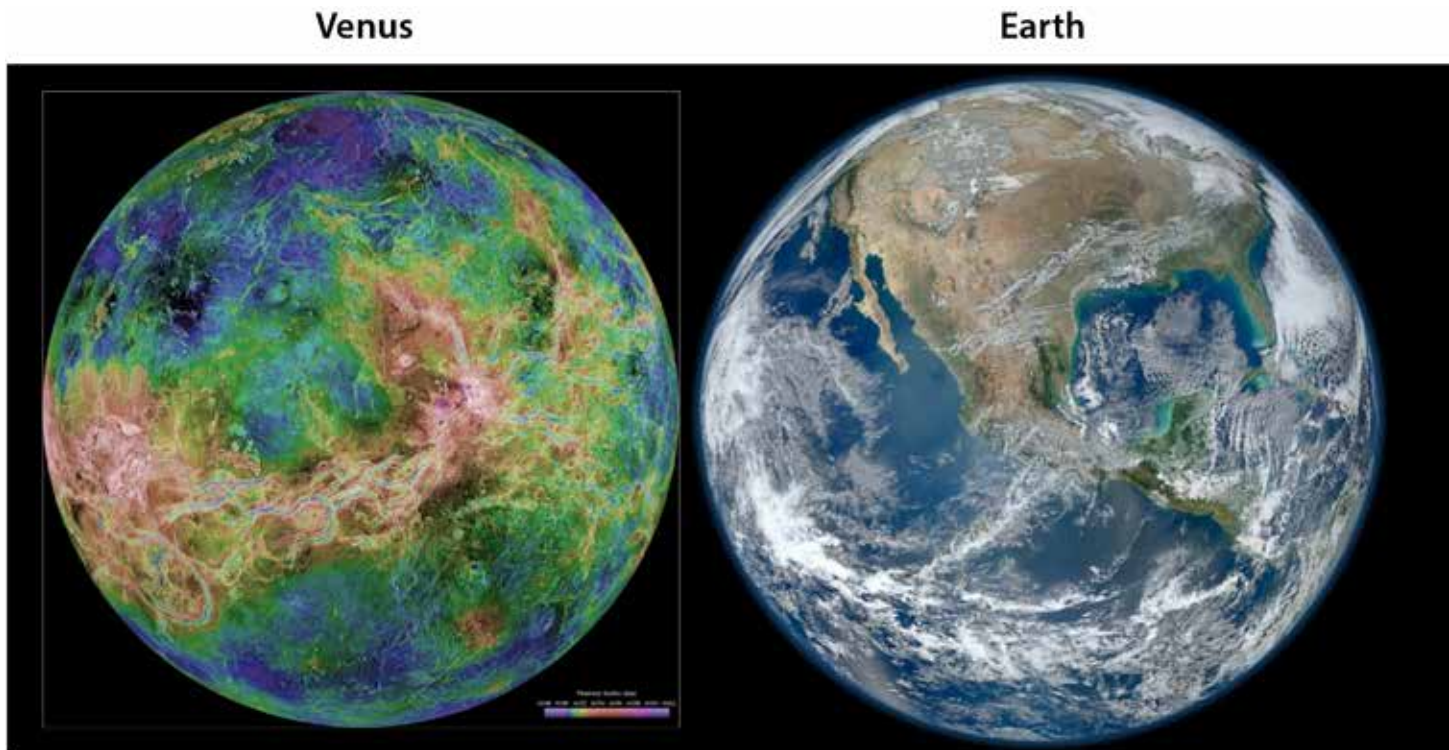
Mercury's atmosphere has only been studied by remote sensing, so numbers are poorly constrained. Evidence from the *Messenger* spacecraft (2009-2014+) suggests that the so-called exosphere is composed of hydrogen (both H and H<sub>2</sub>), helium, oxygen (O and O<sub>2</sub>), sodium, potassium, calcium argon, and even small amounts of water vapor. The origin of these constituents comes from two sources, the solar wind (e.g., hydrogen and helium), and the planetary crust. A comparison of the atmospheric pressure of Earth (~1013 millibars) and Mercury (~0.0000000001 millibars) illustrates why it is commonly said that Mercury has no atmosphere.

### Some interesting aspects of Mercury:

- Mercury is the closest planet to the Sun
- Mercury is the smallest planet
- Mercury closely resembles our own Moon in size and surface appearance
- Mercury has a weak magnetic field, a sign of a molten metallic core
- Mercury's year is 88 Earth days
- Mercury has a super-thin atmosphere; the thinnest of any planet
- Mercury has no moons
- Daytime temperatures on Mercury reach 800°F (430°C), whereas the dark side of Mercury is frigid (minus 290°F or minus 180°C )
- Mercury had early basaltic volcanism and perhaps, therefore, an early atmosphere
- The surface of Mercury is antique, with very subtle modification in billions of years
- Mercury has the most densely impact-cratered surface of any planet

## Venus

Venus is sometimes referred to as the Earth's sister planet (Figure 1.28). It is about the same size, mass, density, composition, has a cloud-shrouded atmosphere, a silicate crust and layered interior (Figure 1.29). The details of the surface of Venus were completely unknown from Earth-based observatories because of the dense cloud cover until the late 1960s and early 1970s when the Soviets launched the *Venera* (Venus) probes.



Characteristic	Venus	Earth
Equatorial radius	6052 km (3761 miles)	6378 km (3963 miles)
Overall specific gravity	5.24	5.51
Surface gravity	8.9 m/s <sup>2</sup> (29.2 ft/s <sup>2</sup> )	9.8 m/s <sup>2</sup> (32 ft/s <sup>2</sup> )
High-low elevation	15 km (49,200 ft)	20 km (65,617 ft)
Surface pressure	92,000 mb	1013 mb
Surface temperature	464°C (867°F)	14°C (57°F)

Figure 1.28. Venus might be considered Earth's sister planet. Similarities include diameter, specific gravity (~density), surface gravity, and relief (high-low elevation). Major differences include surface temperature and pressure (Source/Credit: NASA).

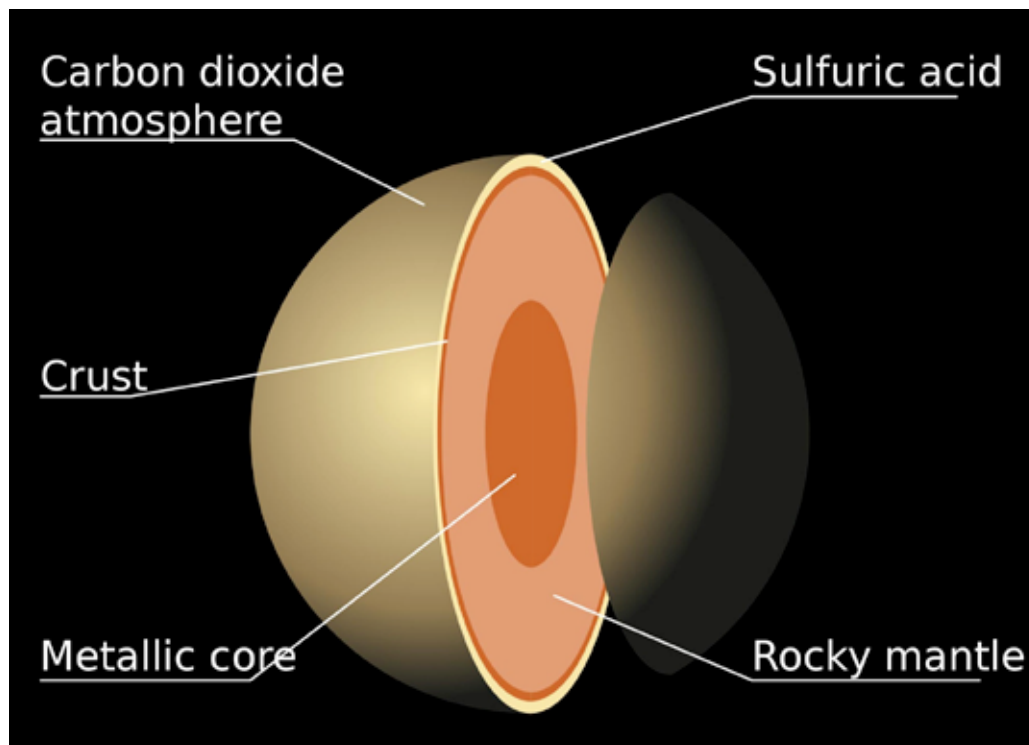


Figure 1.29. The interior structure of Venus is similar to the other terrestrial planets. There is a rocky, silicate crust and mantle and a core of partially-molten iron. The extreme slow rotation of Venus precludes a magnetic field (Source/Credit: NASA).

Ten *Venera* probes landed on the surface of Venus, and the first images were transmitted back to Earth in 1975 (Figure 1.30). Among many surprises from *Venera* probes were that the planet's sulfuric acid clouds, the dense atmosphere dominated by CO<sub>2</sub>, and broken rocks at the surface appeared to be of volcanic origin. Surface temperatures were a toasty 864°F (462°C).

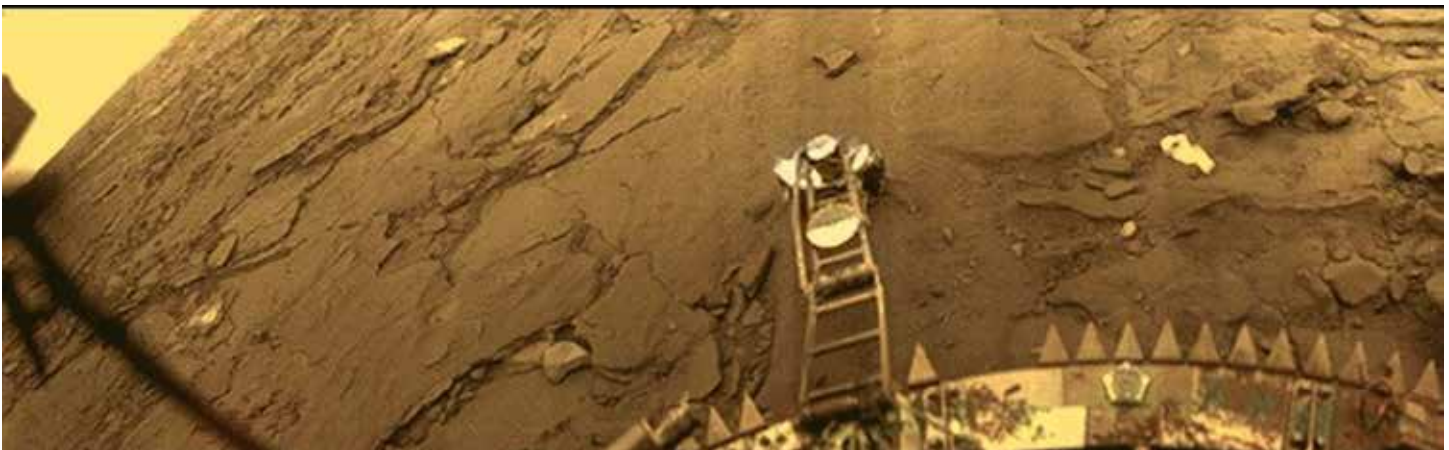


Figure 1.30. For three decades, beginning in the late 1960s, the Soviet *Venera* (Russian **Venus**) missions orbited Venus and deployed 10 probes to the surface. Because of the intense heat and pressure, most of the soft landers only transmitted information for a few tens of minutes. In 1982, *Venera 13* survived over two hours and transmitted color images of the surface. This image was taken by *Venera 14* and reprocessed in 2007 by Ted Stryk. The image shows a rocky plain of basaltic volcanic material. Venus, like Earth, has a wide spectrum of volcanic landforms and rocks on its surface (Source/Credit: Russian Academy of Sciences).



In the early 1990s, NASA's *Magellan* spacecraft began a multi-year orbital mapping job of nearly the entire surface of Venus. The spectacular imagery revealed that Venus has one of the most complicated and diverse surfaces of any in the solar system. On a planetary scale there are vast elevated, continent-like regions (Figure 1.31). Lowland regions, similar to the ocean floor of the Earth, flank the highlands. Several types of volcanoes have been mapped, equaling the volcanic diversity of the Earth.

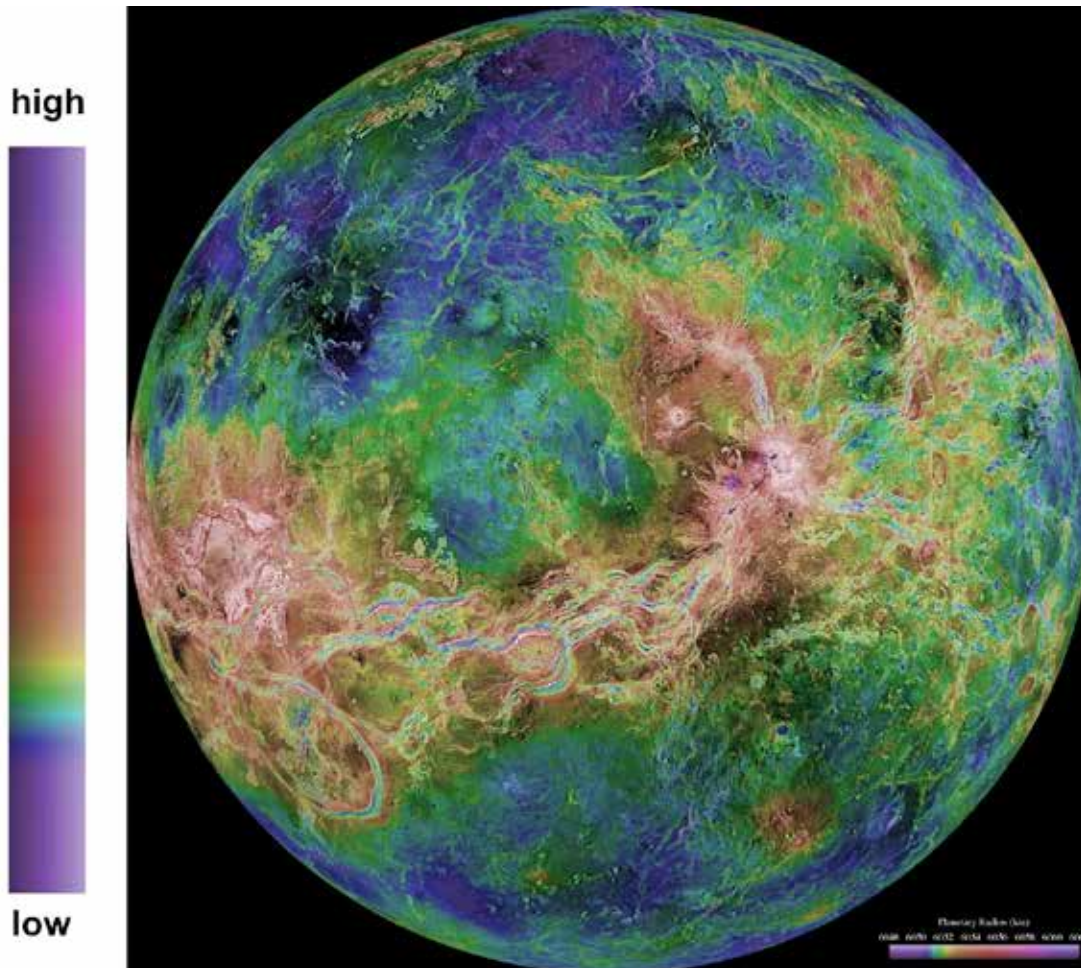


Figure 1.31. The topographic map of Venus illustrates elevational differences by color. The bar graph on the right indicates low elevations in purple and blue, and higher elevations (top) in red, magenta, and indigo. The total difference in elevation between the lowest and highest points on the planet are in excess of 45,000 feet (~14,000 m). Topography is based on the Magellan mission of the early 1990s that mapped over 90% of the Venesian surface. Some of the circular features are impact craters, whereas others are volcanoes (Source/Credit: NASA).

Interestingly, although there is an iron-rich core, Venus has no magnetic field, probably because Venus rotates so slowly (one complete rotation takes 243 Earth days). The lack of a protective magnetic field becomes an important factor when considering Venus as a candidate for a life support system. Another oddity of Venus is that it rotates in the opposite direction relative to the other planets, either because of tidal forces or because of an early impact.

Wrinkled zones and elongated escarpments are reminiscent of folded and faulted terrain on Earth, suggesting considerable internal unrest. Impact craters are abundant, but not of the density seen on Mercury or the Moon, indicating that part or the entire planet experienced resurfacing. Surface winds are strong enough to erode, transport and deposit sandy material; dunal topography is common. Unlike Earth, there is no surface water due to greatly elevated atmospheric temperatures.

**Venus' atmosphere:** Venus is farther from the Sun than Mercury, has a much larger size and gravitational pull, a long history of volcanism and outgassing, and therefore has the potential for retaining a diverse atmosphere. The atmosphere of Venus is 92 times denser than the Earth's and consists almost entirely (96%) of carbon dioxide. Carbon dioxide is a heat-trapping greenhouse gas. Although further from the Sun than Mercury, its thick carbon dioxide atmosphere traps so much heat that its surface temperature is as high as 890°F (477°C), which makes it even hotter than Mercury. Because the dense atmosphere and strong planetary winds distribute heat energy, there are very small temperature differences between areas in the light and those in the dark.

Venus may once have been much cooler prior to massive volcanic outgassing. Carbon dioxide accumulated in the atmosphere because of early volcanic outgassing, and the temperatures rose in a runaway greenhouse effect. Liquid water would have been quickly lost as would the environment for a life-support system.

The original atmospheres of the planets, the **primary atmospheres**, were largely a product of accretion from the protoplanetary disk. They were composed of the light gases, predominantly hydrogen and helium, most likely in ratios not far from the present-day Sun (94.2% H; 5.7% He; all others, 0.1%). The terrestrial planets have lost most of their primary atmospheres because of their low mass (and gravity) and nearness to the Sun. Light atoms have a low escape velocity, and the Sun's radiation can easily heat them, cause them to travel faster, and achieve escape velocity, and be lost to outer space. The outer, colder, more massive planets have retained much of their primary atmospheres.

- **Secondary atmospheres** and solid surface material are acquired by several processes, including volcanic outgassing, meteors and comets, chemical reactions, and living organisms (e.g., photosynthesis, organic decay). Secondary constituents include rocky, silicate minerals as well as icy matter (water, carbon dioxide, oxygen, methane, ammonia, sulfur compounds). Volcanic outgassing releases compounds in approximately the following proportions: water 58%, carbon dioxide 23%, sulfur oxides 13%, and molecular nitrogen 5%. The terrestrial planets have largely secondary atmospheres. Sunlight can react with ammonia and methane to produce nitrogen, hydrogen gas, and hydrocarbons. Venus and Earth acquired huge amounts of water vapor and carbon dioxide from outgassing, but on Earth much of

the carbon dioxide has been stored in carbonate rocks on the continents and carbonate sediment on the sea floor. Venus has neither oceans (too hot) nor storage of carbon dioxide in rocks, so the carbon dioxide content has sky-rocketed.

### Some interesting aspects of Venus:

- Venus has many similarities with the Earth (size, mass, density, composition, gravity, surface features, clouds, wind)
- Venus has been studied by dozens of spacecraft; the Soviet *Venera* missions landed 10 probes on the surface
- Venus has a very thick, CO<sub>2</sub>-rich atmosphere
- Portions of Venus have undergone resurfacing by volcanism and wind
- Venus' rotational period (day) is longer than its revolutionary period (year)
- Venus has experienced widespread and diverse volcanism and an evolving atmosphere
- Venus, thanks to its runaway greenhouse effect, has the warmest atmosphere, averaging 900°F (480°C) at the surface
- Venus rotates backwards compared to most of the other planets
- Venus has highlands and lowlands similar to the Earth's continents and ocean basins
- As seen from Earth, Venus is the brightest planet in the sky
- Although Venus has a large iron core, similar to the Earth, it has no magnetic field because of the super-slow rotation on its axis

## Earth

The Earth is the third planet from the Sun and is the namesake for the *terrestrial planets*. Several things are noteworthy about the Earth that separate it from its planetary neighbors. It has a strong magnetic field and long history of volcanism thanks to partially molten layers in its interior (Figure 1.32). The magnetic field protects Earth from lethal penetration of the solar wind. It has an abundance of ozone (O<sub>3</sub>) in its stratosphere, a protective layer that screens out lethal dosages of ultraviolet radiation. Its lower atmosphere has abundant O<sub>2</sub> and H<sub>2</sub>O (Figure 1.33). Water can co-exist in the atmosphere and on the surface in all three physical states (Figure 1.34). The surface of the Earth is brand new compared to its terrestrial neighbors; it bears very few scars from early impacts. It has been resurfaced continually for most of its 4.6 billion-year history. It is host to a 3+-billion-year-old life-support system.

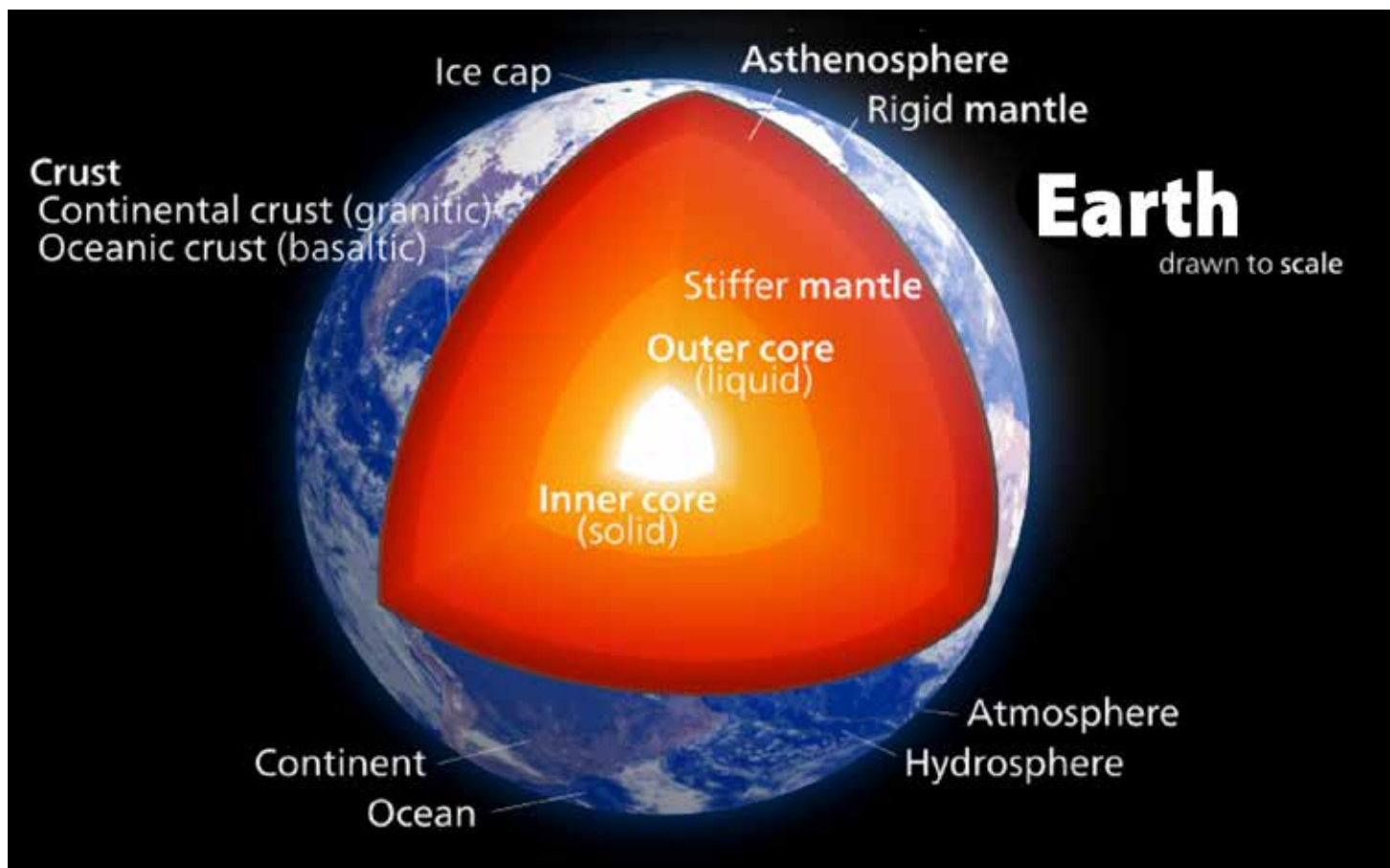


Figure 1.32. The Earth's internal structure consists of a crust, mantle, and core, like the other terrestrial planets. It differs from the other planets in that it has a soft, plastic layer in the upper mantle (labeled asthenosphere) that drives tectonic plates, and resurfaces the entire Earth every couple hundred million years (Source/Credit: modified from <http://commons.wikimedia.org/wiki/User:Kelvinsong>).



Figure 1.33. The Earth's thin atmosphere is an essential ingredient to its life-support system. The lower-most layer (orange) contains most of the mass, water vapor, clouds, and storm systems in the atmosphere. The lower atmosphere is dominated by nitrogen ( $N_2$  78%) and oxygen ( $O_2$  21%). Although it is typically depicted in drawings as a thick layer, it is paper-thin. If drawn to scale with the Earth depicted as the size of a basketball, the lower layer of the atmosphere would be the thickness of a coat of paint (Source/Credit: NASA).



Figure 1.34. Earth is the third planet from the Sun. The Earth is at the right distance from the Sun and has the right type and abundance of greenhouse gases to allow water to co-exist as a solid, liquid and gas at ambient temperatures. Over two-thirds of the Earth's surface is covered with ocean water which helps maintain fairly uniform temperatures over long periods of time (Source/Credit: NASA).

The Earth's atmosphere and life support system will be a separate topic of discussion later in this chapter.

### Some interesting aspects of the Earth

- It is the only known planet in the universe with an advanced and long-lived life support system
- It is a water planet; 70% of the surface is covered with ocean water
- Water co-exists in all 3 physical states on the surface and atmosphere (solid, liquid, gas)
- Earth's interior is differentiated into a core, mantle, and crust: portions of the core and mantle are partially molten
- Volcanism has been active for practically all of Earth history
- Earth's atmosphere is dominated by  $N_2$  and  $O_2$
- Earth's surface is continually being modified (volcanism, running water, wind, ocean waves, glaciers)
- Earth's upper mantle and crust is dynamic, consisting of moving tectonic plates
- Earth is the only terrestrial planet with a sizable Moon
- Of all the planets, only the Earth and Mars have surface features that are known to have been carved by running water

**The Moon:** The Earth is the only terrestrial planet with a sizeable Moon, the fifth largest in the solar system. The Moon is also the only other celestial body that humans have walked on (Figure 1.35). Radiometric dating of lunar rocks supports the long-suspected idea that the Moon is nearly as old as the Earth, about 4.6 billion years. The most densely-cratered lunar highlands (lighter areas when viewed from Earth) represent the oldest features on the Moon. The dark oval areas, thought by the ancients to be seas, are vast basaltic plains; resurfaced following large impacts (Figure 1.36). The Moon is similar in many respects to Mercury (Figure 1.37).



*Figure 1.35. The highly successful Apollo missions placed humans on the Moon for the first time in 1969. The image from Apollo 17 of scientist-astronaut Harrison Schmitt was taken at the Taurus-Littrow landing site on December 13, 1972. During the Apollo missions, astronauts brought back 842 pounds of lunar rock for examination of age and composition. Most of the surface of the Moon is mantled with a mixture of coarse and fine rock debris which has rained down from meteoric impacts for the 4.5 billion year history of the Moon (Source/Credit NASA).*

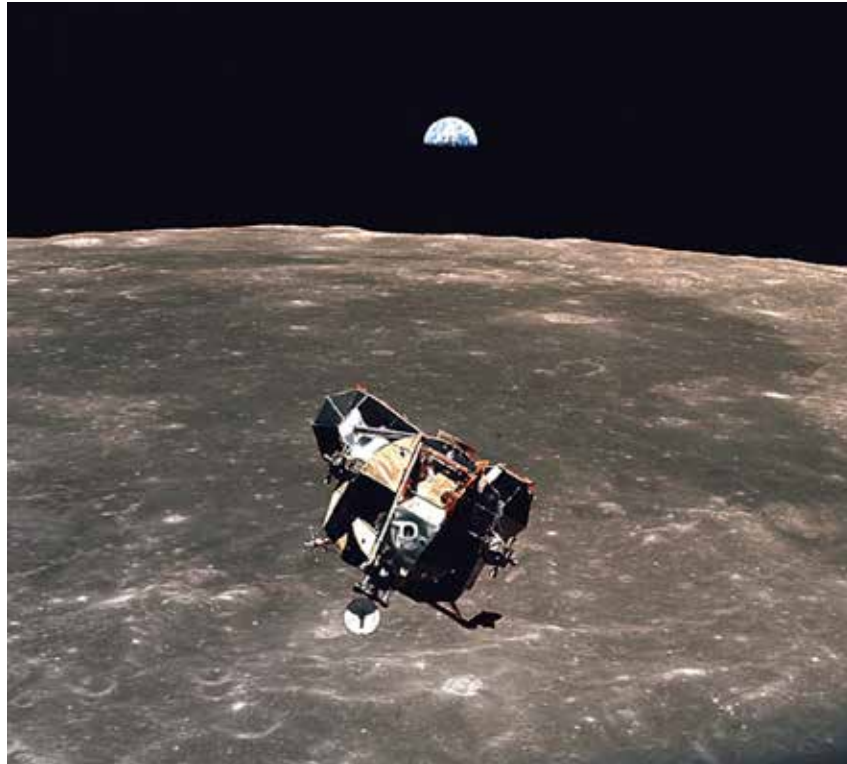


Figure 1.36. The image of the Apollo 11 lunar module “Eagle” was filmed by command module pilot Michael Collins on July 21, 1969. The relatively smooth, dark area is one of many huge impact craters that was back-filled by basaltic volcanic rock. The crescent Earth looms above the horizon (Source/Credit: NASA).



Figure 1.37. The heavily-cratered light-toned areas are the ancient lunar highlands. The dark, scantly-cratered areas are impact craters that were back-filled with a basaltic volcanic rock. Samples returned to the Earth from the Apollo astronauts have obtained radiometric dates on highland material as old as 4.5 billion years. The basaltic plains are younger, but even the youngest of them may date back to 1.2 billion years (Source/Credit: NASA).



Basaltic volcanism on the Moon could have generated an early atmosphere. The last volcanic activity, however, was over a billion years ago, and with only 1/6 the gravity of the Earth, was lost to space. Interestingly, there is some evidence of water ice on the floor of some high-latitude craters that never experience direct sunlight (Figure 1.38).

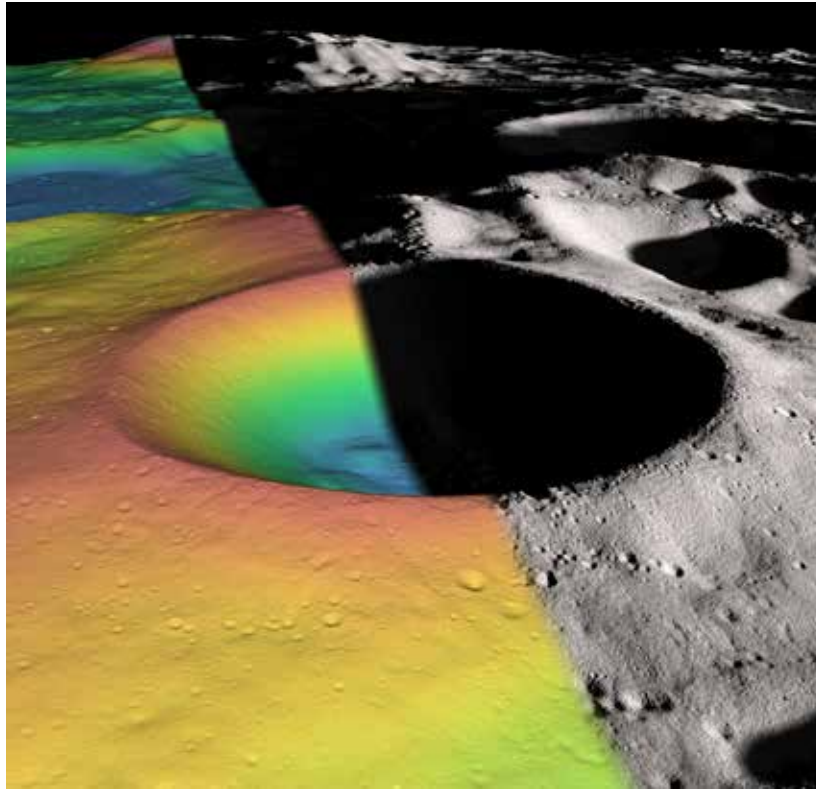


Figure 1.38. Data gathered in 2012 from NASA's Lunar Reconnaissance Orbiter indicates that the floor of Shackleton Crater, at the South Pole, may contain as much as 22% water ice. The crater is two miles deep and 12 miles wide. The colored image indicates elevation, with blue the lowest and red the highest (Source/Credit: NASA).

### Some interesting aspects of the Moon:

- July 20, 1969 Neil Armstrong is first human to set foot on any extraterrestrial object
- Moon's gravity is about 1/6<sup>th</sup> of Earth's
- Moon is virtually without an atmosphere
- The impact-scarred surface is very similar to that of the planet Mercury
- The oldest lunar rocks are ~4.5 billion years
- The Moon's rotational and revolutionary periods are the same; the Moon always shows us the same face
- The Moon had several early thermal events in which volcanic material poured onto the surface forming the *lunar maria*

- 12 humans have walked on the Moon
- The Moon has a very weak magnetic field
- The Moon is the only satellite of the inner three planets
- The Moon is the 5th largest satellite in the solar system
- Apollo astronauts brought back 842 pounds of lunar rock
- The Moon has experienced several episodes of resurfacing, each one apparently due to large meteoric impacts followed by backfilling of the impact crater by outpourings of the black volcanic rock basalt

## Mars

Mars is the last of the terrestrial planets and the most distant from the Sun. Mars has a layered interior consisting of a crust, mantle and core similar to the other terrestrial planets. Mars is thought to have undergone multiple episodes of volcanism, and some geophysicists think that it has the potential to go through another thermal event in its future. Mars has been intensely studied by Earth-based sensors and telescopes, orbiting spacecraft, soft landers, and rovers. **Mars has always been the premier candidate in the solar system, outside the Earth, for a present or past life-support system.** It has also been the object of many science fiction novels and movies.

Mars is dotted with massive volcanic mountains (Figure 1.39). One of them, *Olympus Mons*, is the largest volcano in the solar system (Figure 1.40). It is 79,000 feet (24,079 m) high and its base is so wide that it would stretch from Beaumont to Austin if placed in East Texas. The gently flanks and large summit calderas suggest that they are similar in composition to the volcanoes that make up the Hawaiian Islands, composed of dark volcanic rock basalt. Large-scale basaltic volcanism could have easily built an early atmosphere on Mars. Exactly when the last phase of Martian volcanism occurred is not known.

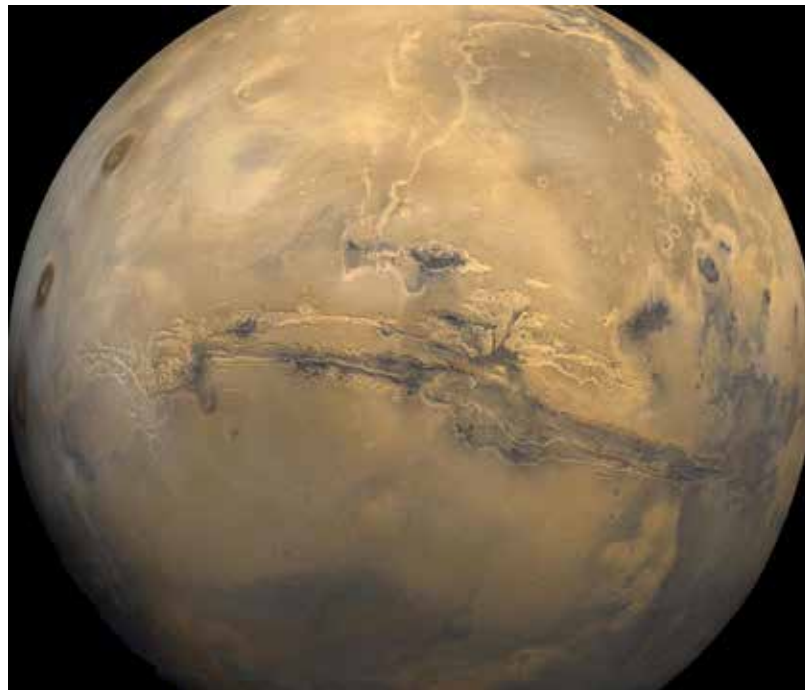


Figure 1.39. The dramatic surface of Mars is clearly visible through its thin atmosphere of carbon dioxide. Although Mars is only half the size of the Earth, it has geological features that dwarf those on our world. One of those features, the Valles Marineris, is shown in the center of this image. It is 4.5 miles (7.5 km) deep, 2800 miles (4500 km) long, and more than 370 miles (600 km) wide in some areas. This makes it more than 13 times the length of the Grand Canyon, and it would stretch from New York to California if placed on Earth. Giant volcanoes are also visible as dark ovals on the upper-left side of the image. The largest volcano on Mars, and in the solar system, is Olympus Mons. It is 79,000 feet (24,079 m) high and its base is so wide that it would stretch from Beaumont to Austin if placed in East Texas (Source/Credit: NASA).

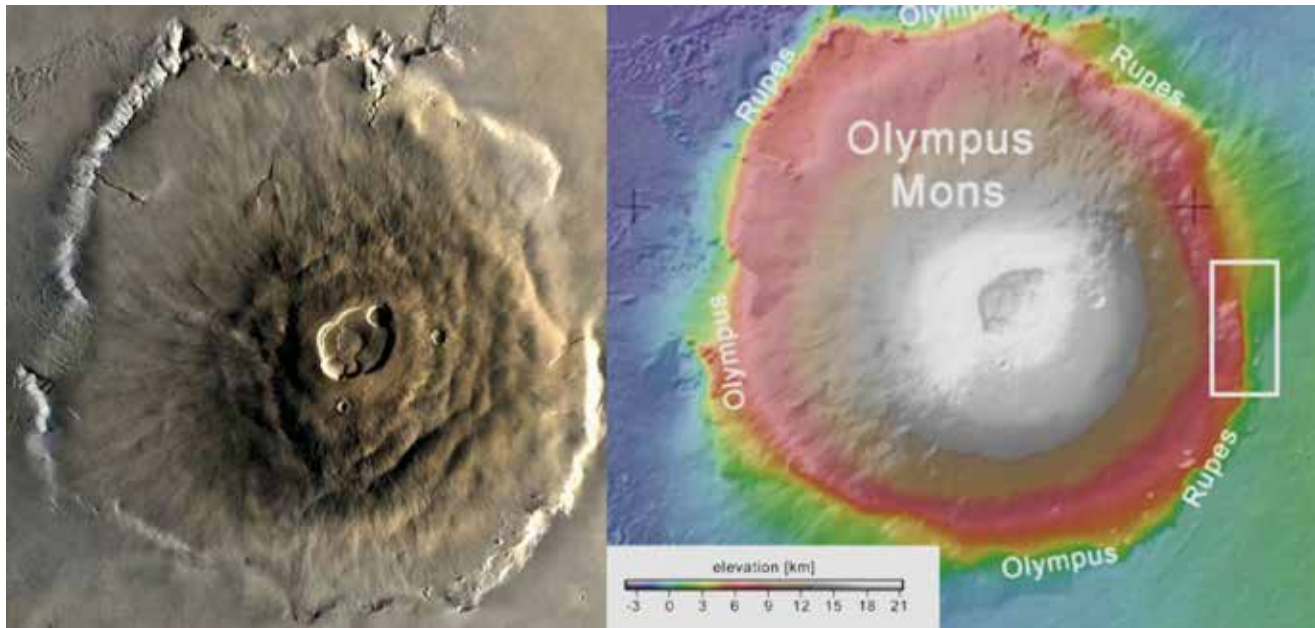


Figure 1.40. Photographic image (left) and topographic map of Olympus Mons, the largest volcano in the solar system. Olympus Mons is 79,000 feet (24,079 m) high and its base is so wide that it would stretch from Beaumont to Austin if placed in East Texas (Source/Credit: NASA).

Mars is also home to the longest fault-valley in the solar system. The *Valles Marineris* is 4.5 miles (7.5 km) deep, 2800 miles (4500 km) long, and more than 370 miles (600 km) wide in some areas (Figure 1.41). This makes it more than 13 times the length of the Grand Canyon, and it would stretch from New York to California if placed on Earth. Massive landslide scars along the steep sides of the canyon have revealed whitish areas that some scientists think represents water ice.

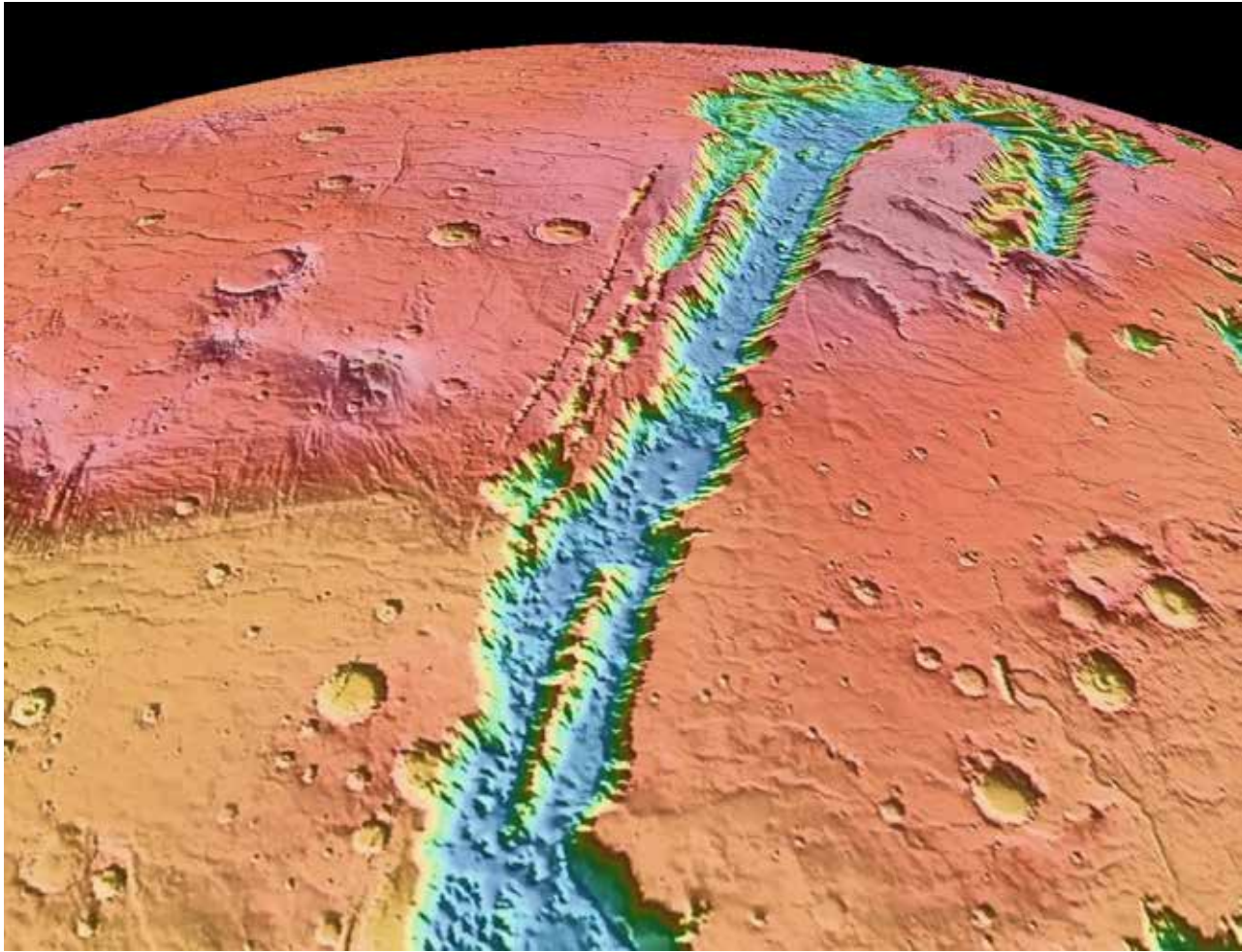


Figure 1.41. Mars boasts many planetary superlatives, one of which is having the longest fault valley in the solar system. The *Valles Marineris* dominates this image. It is 4.5 miles (7.5 km) deep, 2800 miles (4500 km) long, and more than 370 miles (600 km) wide in some areas. This makes it more than 13 times the length of the Grand Canyon, and it would stretch from New York to California if placed on Earth. Lowest elevations are in blue, highest in red. Note the low-density cratering of the plains and plateaus on either side of the fault valley (Source/Credit: NASA).

Mars' surface is pockmarked with impact craters in some areas, but in other areas they are noticeably sparse or absent. Mars may have had multiple resurfacing episodes, some undoubtedly due to volcanism, others by running water, and others by sedimentation at the bottom of large lakes or oceans. NASA surface rovers *Spirit*, *Opportunity*, and *Curiosity* (two of which are still active), have photographed sedimentary layers in several diverse locations (Figure 1.42).



Figure 1.42. The photomosaic is viewed from the landing site of NASA's *Curiosity* rover, taken on August 8, 2012. The view is near the base of Mt. Sharp, which *Curiosity* ascended, imaging hundreds of feet of layered sediment en route. The darker area in the foreground apparently represents hydrated mineral layers formed in the presence of water. The landscape is reminiscent of Glen Canyon National Recreation Area, Utah (Source/Credit: NASA/JPL-Caltech/MSSS).

Mars bears abundant evidence of past liquid water on the surface and underground. Most convincing are the Martian channels and delta-like features (Figures 1.43a and 1.43b). Recent images from the NASA rover *Curiosity* are of a rock outcrop in the Gale Crater that is a stream-laid conglomerate (Figure 1.44). The Martian bedrock surface and wind-deposited dunes are reddish-orange in color due to widespread oxidation of iron-bearing minerals, probably from a past oxygen and water-rich atmosphere. Remote sensing from one of the European satellites reveals layers of sulfate-rich minerals as well as clay minerals, both known to form by chemical reactions with water. In several areas, there are features that are very similar to the ancient, wave-cut shorelines of arid West, implying vast lakes or oceans (Figure 1.45). The recent discovery and spectral analysis of the Martian blueberries and their Earth analogue Moki marbles provides strong evidence of long-lived groundwater (Figures 1.46a and 1.46b).

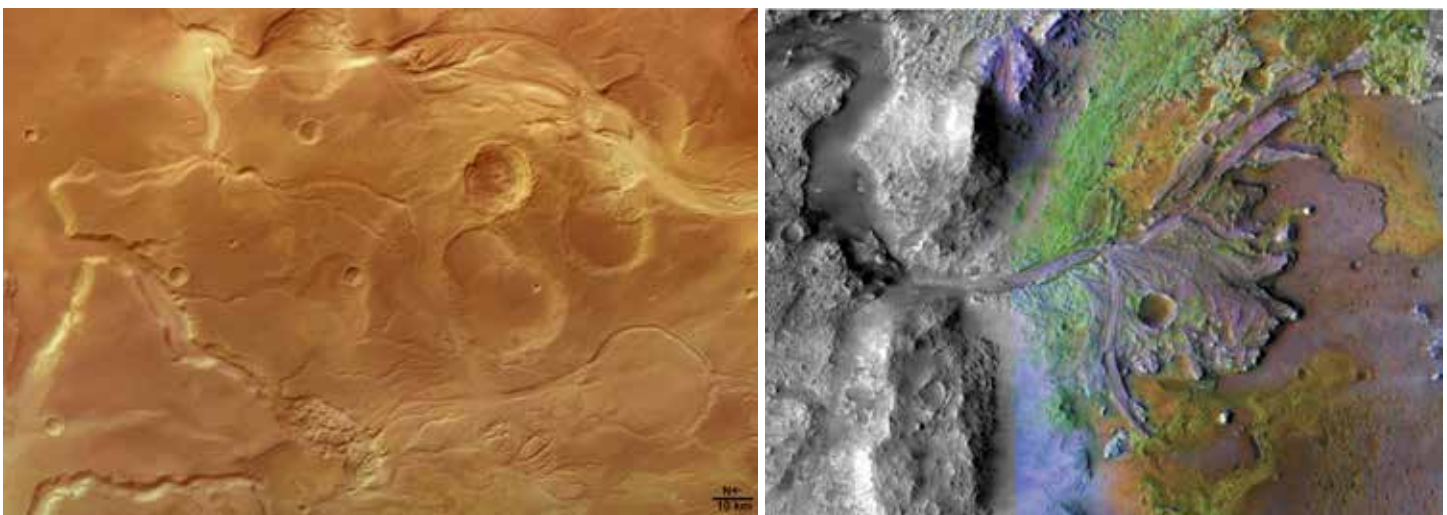


Figure 1.43a. (left) Although there is no liquid surface water on Mars today, the channels seen in this image strongly indicate that water once flowed on its surface. Recent observations by the NASA rovers *Spirit* and *Opportunity* indicate that liquid water once formed lakes on Mars. The presence of liquid water indicates that the planet was once much warmer and wetter. Mars has subsequently lost much of its atmosphere and most of its surface water. There is a possibility that water still exists below the surface, either in frozen or liquid form (Source/Credit: Mars Express Spacecraft ESA/DLR/FU [G. Neukum] June 2004).

Figure 1.43b. (right) The multi-colored feature in the center of the image has the same morphology as a bird's-foot delta on Earth where rivers empty into a standing body of water. The channel that fed the delta can be traced up-valley to the left, then upward into the nearby highlands. The green colors are thought to represent clay minerals that form in the presence of water and would be an excellent place to search for fossil life forms. Image is in the Jezero Crater (Source/Credit: NASA).

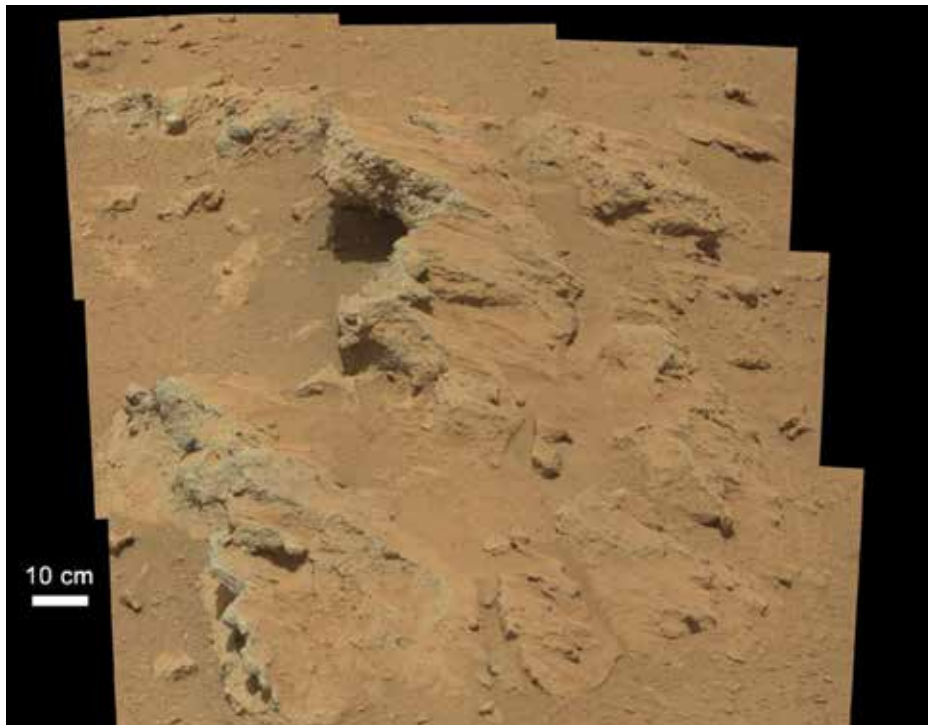


Figure 1.44. This image was taken by NASA's Curiosity rover on September 14, 2012, at the Gale Crater site. The sedimentary deposit ("Hottah" rock) is a **conglomerate**, most likely laid down by running water in an old stream bed (Source/Credit: NASA).



Figure 1.45. Artists conception of what a watery Mars may have looked like early in its history. The hypothetical sea level is 6500 feet (2000 m) below the average surface elevation. The 2500-mile-long Valles Marineris is occupied by running water that empties into the nearby ocean (Source/Credit: Wikipedia, author Daein Ballard).



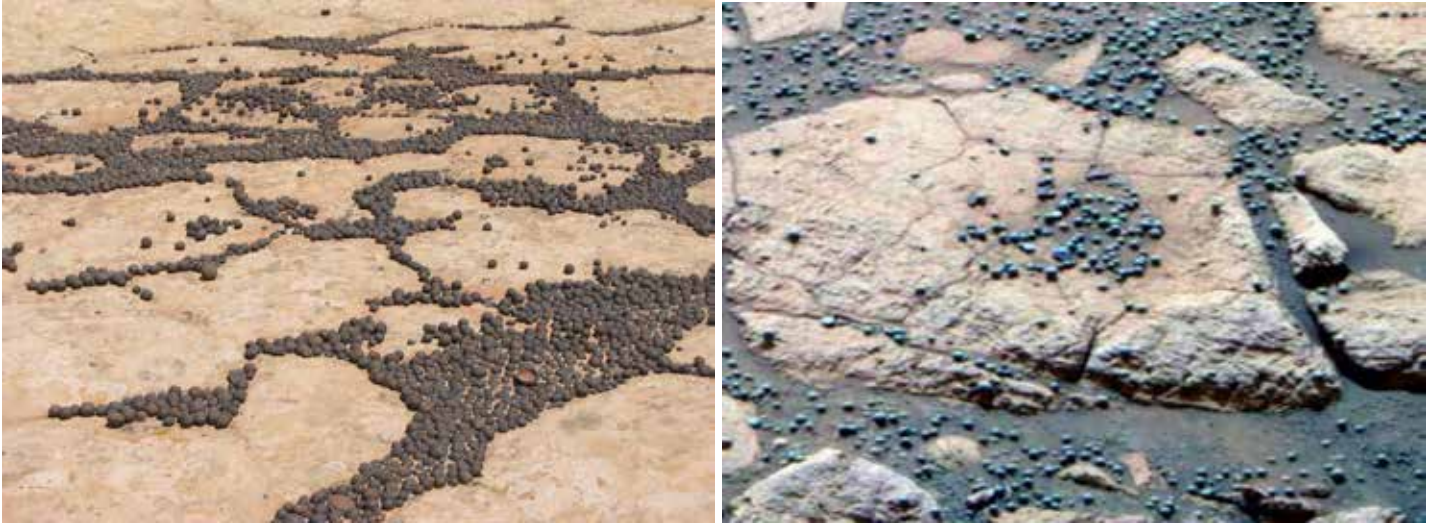


Figure 1.46a. These **Moki marbles** are iron concretions that bind together quartz grains of the Navajo Sandstone of Jurassic age at Big Spencer Flats in Utah. They formed in a groundwater environment, where iron-rich compounds in solution were precipitated as iron oxide between mineral grains making a very tough cement. Subsequent erosion by streams and wind has removed the weaker sandstone, and left behind a lag deposit of the spherical Mokis (Source/Credit: Dennis I. Netoff).

Figure 1.46b. These **Martian blueberries** are also iron concretions that are similar to the Moki marbles found on Earth in the Navajo Sandstone. They also formed in a groundwater environment suggesting long-lived groundwater movement in the Martian past (Source/Credit: NASA).

Widespread dune fields and dust storms provide evidence of strong winds on Mars (Figures 1.47; 1.48a and 1.48b). Regional and planet-wide dust storms have been observed on several occasions (Figure 1.49) and seem to be triggered by the change of seasons rather than by local and regional controls such as on Earth.

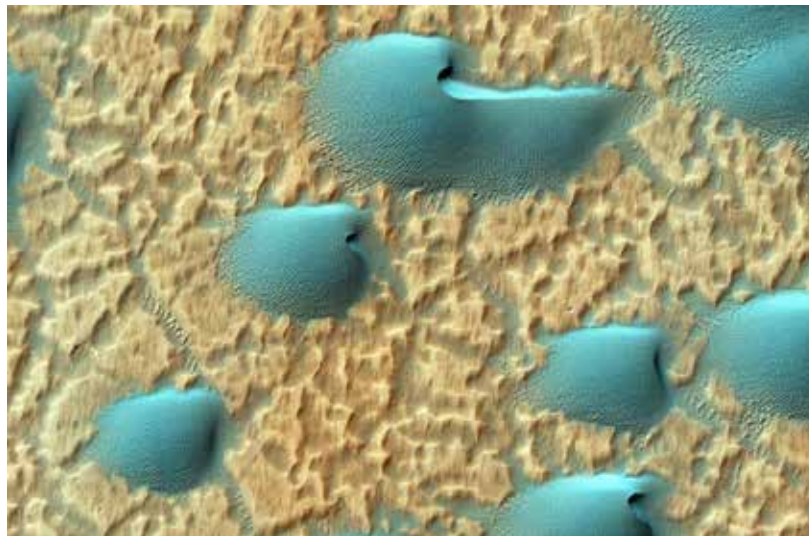


Figure 1.47. Mars has a wide spectrum of wind-eroded and wind-deposited landforms. Several types of dunes exist, depending on the supply of loose material and wind regime. The false-color imagery above highlights a series of individual **barchan dunes**, smooth and gentle on their upwind side and steep on their lee side. The barchans appear to be superimposed on an older dune field suggesting two different dune-forming environments. Image courtesy of the High Resolution Imaging Science Experiment camera onboard NASA's Mars Reconnaissance Orbiter (Source/Credit: NASA/JPL-Caltech/University of Arizona).



Figure 1.48a. (left) Self-portrait of NASA's Curiosity rover, taken on October 31, 2012. The small, dark scars on the ground in front of the rover are where Curiosity's robotic arm sampled the Martian sand dune. In the distance on the right is Mount Sharp, a target for near-future exploration by Curiosity (Source/Credit: NASA/JPL-Caltech).

Figure 1.48b. (right) The tracks of the Mars rover Curiosity in February 2014 are etched into the soft surficial dust, largely wind-deposited, and a small (3 ft.; ~1 m high) sand dune. The darker, wind-polished rocks on the slopes are most likely the volcanic rock basalt (Source/Credit: NASA/JPL-Caltech/MSSS).



Figure 1.49. Although Mars' average surface pressure is only 6 millibars (mb) (Earth's is 1013 mb), strong temperature and pressure gradients can create dust-moving winds, enough to periodically cause planet-wide dust storms. The low density of the Martian atmosphere requires winds of nearly 50 mph to entrain sand and dust grains compared to about 10 mph on Earth. Temperature variations on Mars are extreme, varying from a high of about 70°F (20°C) at the Martian Equator during the summer, to a low of about minus 225°F (minus 153°C) at the poles. Day-night temperature variations in the mid-latitudes may fluctuate 140°F (60°C). Dust storms and dust devils are common on Mars (Source/Credit: NASA).

**Martian atmosphere:** Early volcanism on Mars established a thick atmosphere rich in water vapor and oxygen. Much of that early atmosphere has been lost due to the fairly weak gravity of Mars, and some of the “ices” may be temporarily stored in the subsurface as permafrost waiting for another thermal event to release them to the atmosphere. Considerable quantities of carbon dioxide and water ice are stored in the seasonal ice caps on Mars (Figure 1.50).

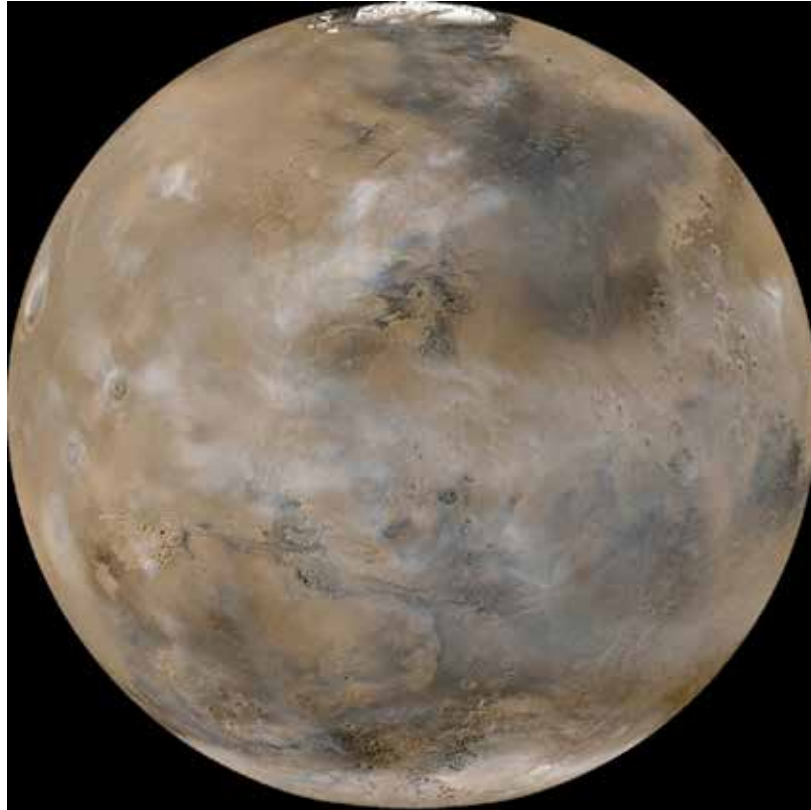


Figure 1.50. Martian icecaps (white) and clouds (wispy and semi-transparent). The southern polar ice cap on Mars is approximately 85% carbon dioxide ice and 15% water ice (Source/Credit: NASA).

The modern thin Martian atmosphere is largely carbon dioxide (96.0%, with minor amounts of argon (2.1%)), nitrogen (1.9%), oxygen (0.145%), and carbon monoxide (0.06%). Water vapor is sparse, but very low nighttime temperatures and localized uplift can bring the humidity to 100% causing occasional clouds and even fog to form (Figure 1.51). Many of these constituents would be more abundant in the Martian atmosphere if vast lakes had not existed in the distant past. Large water bodies can chemically react with certain gases causing them to precipitate out as sediment.

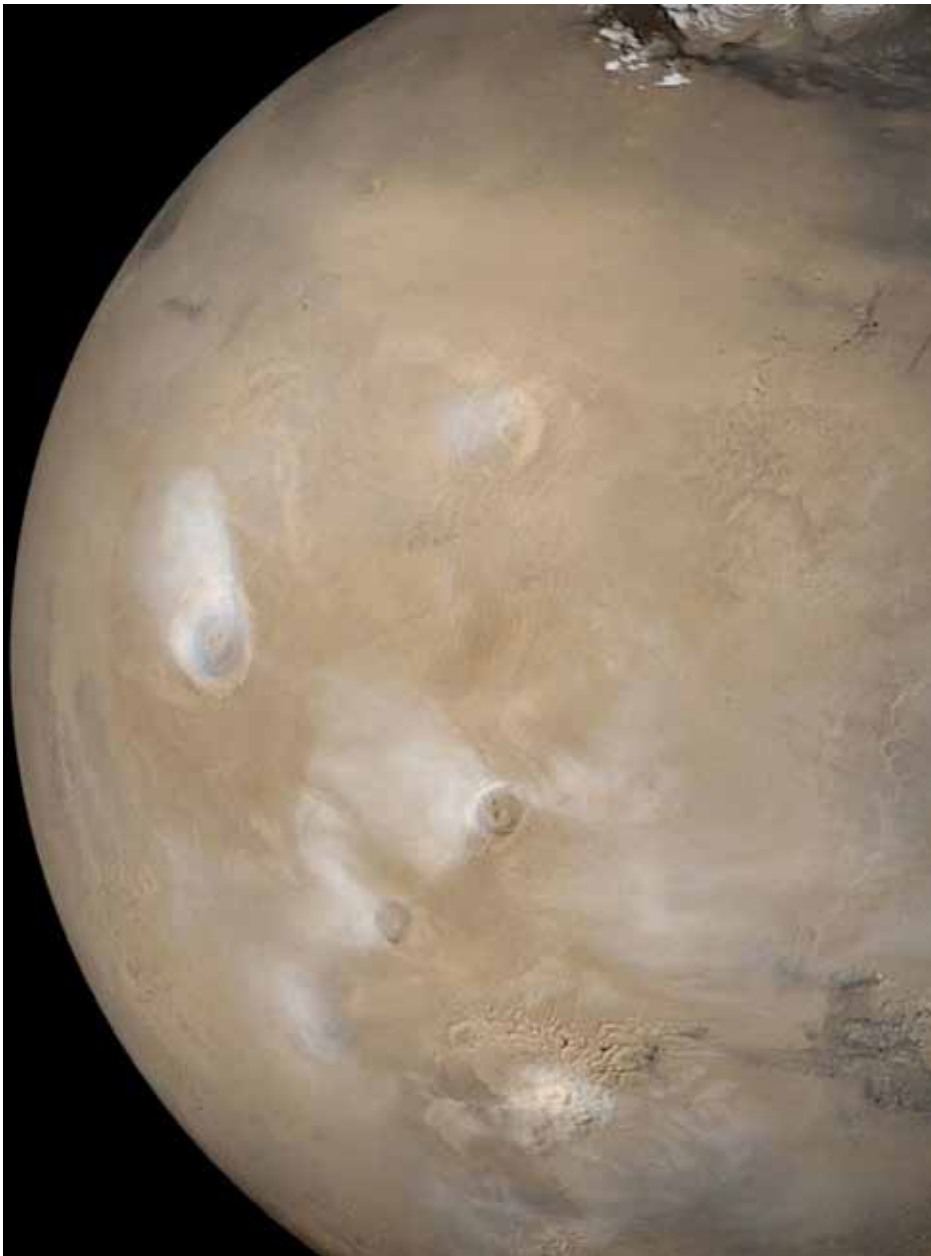


Figure 1.51. The thin Martian atmosphere is largely carbon dioxide (96.0%, with minor amounts of argon (2.1%)), nitrogen (1.9%), oxygen (0.145%), and carbon monoxide (0.06%). Although water vapor is sparse, very low nighttime temperatures and local uplift can bring the relative humidity down to 100% causing condensation in the form of occasional clouds (whitish areas on image) and even fog to form. Several of the cloud decks in this image are associated with air passing over large volcanoes, causing the air to cool by expansion and condense (Source/Credit: NASA).

Mars' average surface pressure is 6 millibars (mb), compared to Earth's 1013 mb, or about 1/169<sup>th</sup> Earth's pressure. On the top of *Olympus Mons*, Mars' highest peak, the pressure is only 0.3 mb. Temperature variations on Mars are extreme, varying from a high of about 70°F (20°C) at the Martian Equator during the summer to a low of about minus 225°F (minus 153°C) at the poles. Day-night temperature variations in the mid-latitudes may fluctuate 140°F (60°C). Winds on Mars are strong enough to create dust storms and dust devils (Figure 1.52). Winds in excess of 60 mph are fairly common.



Figure 1.52. Dust devils are relatively common on Mars. Most are generated by daytime heating of the air, causing temporary vertical instability. The dust devil in this image had a vertical plume of about 12 miles (19 km). Dust in the Martian atmosphere tends to linger for a longer time than in the Earth's atmosphere due to a lack of moisture (clouds, rain) to cleanse the air. The image was recorded by a camera on an orbiting spacecraft (Source/Credit: NASA/JPL/University of Arizona).

The thin atmosphere of Mars allows many more meteors to penetrate the atmosphere compared to Earth and Venus. The timing of one impact crater was constrained by before-and-after photography to sometime between 2010 and 2012 (Figure 1.53). Mars is large enough to attract many stray meteors, many of them probably stolen from the nearby asteroid belt.



Figure 1.53. Image of a brand-new impact crater on Mars, taken from NASA's Mars Reconnaissance orbiter on November 19, 2013. The 100-foot-wide (30 m) crater and the surrounding ejecta rays were made sometime between July 2010 and May 2012 (Source/Credit: NASA/JPL).

### Some interesting aspects of Mars:

- Mars is known as the red planet due to the abundance of oxidized iron on its surface
- Mars underwent one or more periods of past volcanism generating a water-rich atmosphere
- Of all the planets, only the Earth and Mars have surface features that are known to have been carved by running water
- Mars has the largest volcanoes in the solar system
- Mars' atmosphere is thin and consists mainly of CO<sub>2</sub>
- Mars currently is the leading candidate for having a present or past life support system
- Mars occasionally has planetary dust storms
- Mars has a wide variety of wind-laid dune forms
- Mars contains the longest canyon in the solar system, the *Valles Marineris*
- Mars has seasonally-fluctuating polar ice caps, largely CO<sub>2</sub> with lesser amounts of H<sub>2</sub>O
- Mars has two small moons, Deimos and Phobos

## Jovian Planets and Satellites

The outer planets are all much bigger than the inner planets and they all have thick atmospheres composed largely of hydrogen, helium, methane, and ammonia. They are able to retain thick atmospheres because of their huge size and strong gravity. However, because they are at great distances from the Sun, their atmospheres are intensely cold, some approaching more than 400°F below zero (minus 240°C). Unlike the inner planets, which have a solid rock surface, the gas giants have no such surface. The gaseous atmospheres gradually change into a vast ocean of liquid hydrogen at depth under very high pressure, and perhaps to metallic hydrogen at even greater depths (Figure 1.54). These gas giant planets are truly alien in nature and very inhospitable to life as we know it.

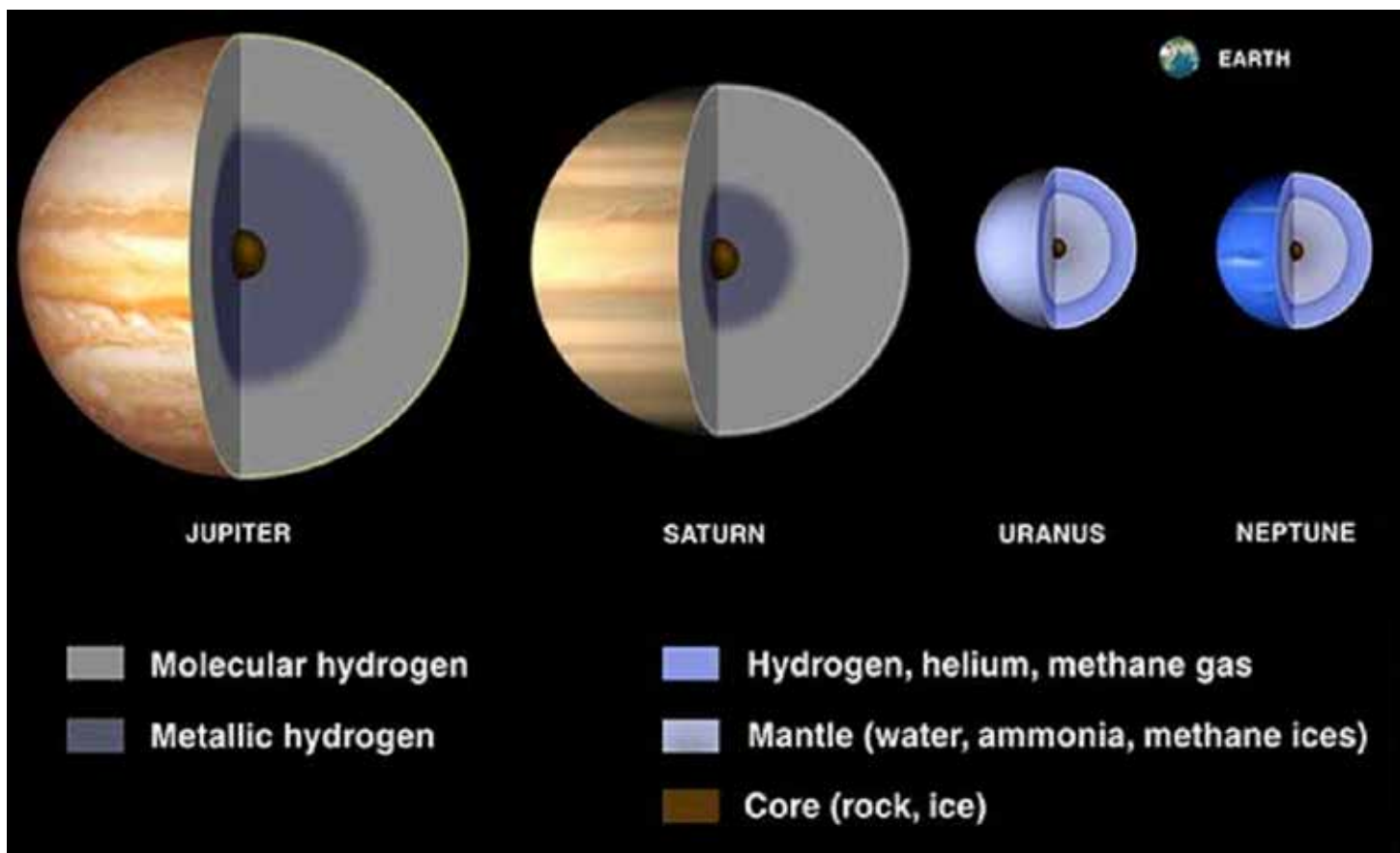


Figure 1.54. Jupiter's interior is largely hydrogen with lesser amounts of helium and perhaps a rocky core. The outer layer is mostly molecular hydrogen ( $H_2$ ), but with increasing depth temperature-pressure conditions ( $\sim 400$  GPa and 10,000K, 17,540°F, higher temperature and pressure than the Earth's core) are thought to be high enough to strip away electrons from the hydrogen atoms and convert it to a conducting liquid, or metallic hydrogen. The rotating sea of metallic hydrogen gives Jupiter a strong magnetic field. Saturn is also believed to have a thick layer of metallic hydrogen, whereas Neptune and Uranus lack sufficient mass (Source/Credit: NASA).



The gas giants have retained much of their primary atmospheres and remain dominated by hydrogen and helium. Both of these elements readily combine with other gases to form light-weight molecules such as methane (CH<sub>4</sub>) and ammonia (NH<sub>3</sub>). As a general rule, Jovian atmospheres get cooler with increasing distance from the Sun.

Clouds form through condensation, just like they do in Earth's atmosphere. On Saturn and Jupiter, there are different layers of clouds at different elevations reflecting the temperatures that each constituent condenses at. Ammonia clouds form at about 150K (minus 190°F), ammonium sulfide at 200K (minus 100°F), and water at 270K (26°F).

## Jupiter

Jupiter was most likely the first planet to form in the solar system. Jupiter is believed to have a rocky core many times more massive than the entire Earth (Jupiter is the largest of the gas giants, and by far the most massive). Jupiter has 2.5 times the mass of all the other planets combined. It also has a very faint ring system.

Jupiter's clouds form through condensation, just like they do in Earth's atmosphere. On Saturn and Jupiter there are different layers of clouds at different elevations reflecting the temperatures at which each constituent condenses. Ammonia clouds form at about 150K (minus 190°F), ammonium sulfide at 200K (minus 100°F), and water at 270K (26°F). The upper ammonia clouds are arranged into a dozen fairly simple east-west bands of varying colors. These are Jupiter's most striking visible feature (Figure 1.55). The banded appearance probably results from large, cylindrical circulation cells, similar to those that form roll clouds on Earth. Darker bands are called *belts* that represent zones of subsidence (sinking air). Lighter bands are *zones* of upwelling of gases and clouds. Their lighter color may be due to the appearance of ammonia ice.

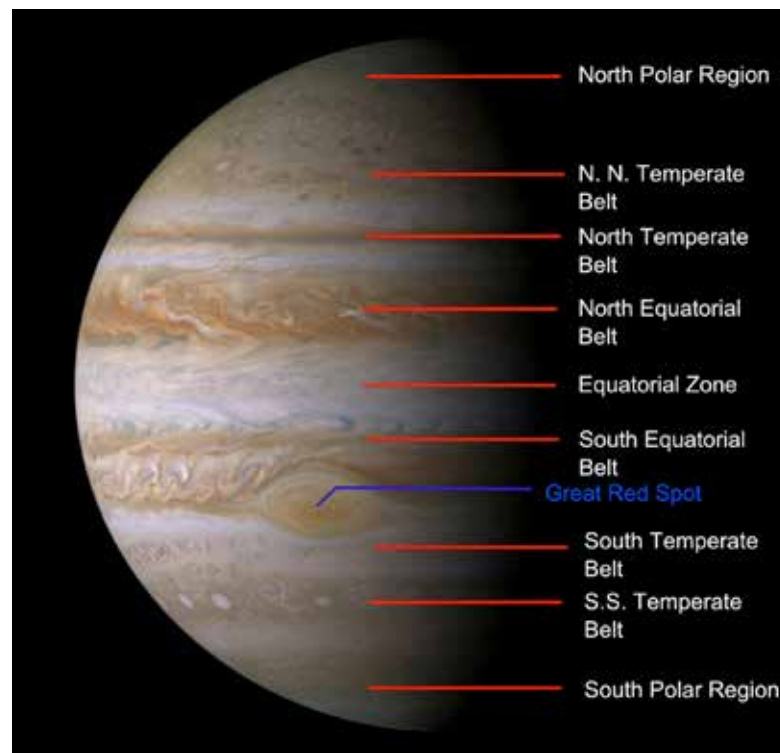
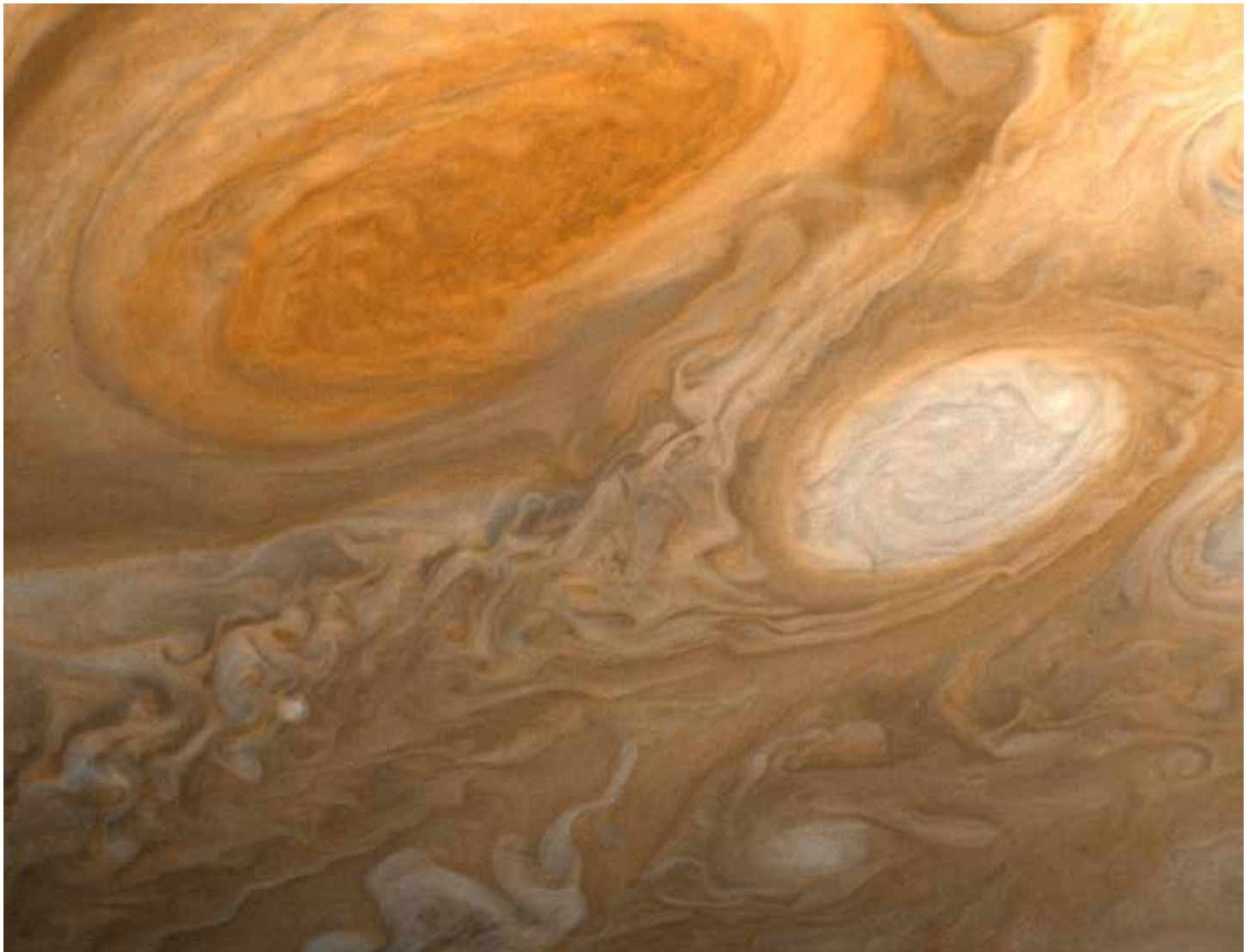


Figure 1.55. Jupiter's clouds form through condensation, just like they do in Earth's atmosphere. Different layers of clouds form at different elevations in response to the temperatures at which each constituent condenses. Ammonia clouds form the highest, coldest cloud layers, (~150K; minus 190°F), followed by lower clouds of ammonium sulfide (~200K; minus 100°F), and water at 270K (26°F). The upper ammonia clouds are arranged into a dozen fairly simple east-west bands of varying colors. These are Jupiter's most striking visible feature. The banded appearance probably results from large, cylindrical circulation cells. Darker bands are called **belts** that represent zones of subsidence (sinking air). Lighter bands are **zones** of upwelling of gases and clouds. Their lighter color may be due to the appearance of ammonia ice (Source/Credit: NASA).

Closer examination of the seemingly simple circulation pattern shows dozens of spinning vortices of different size, color, and longevity. The largest and most famous of these is the Great Red Spot (Figure 1.56), first noticed by Galileo over four centuries ago. The Great Red Spot is an anticyclonic vortex and is the largest and oldest in the solar system. Two Earths could be placed in it with room to spare. Their clockwise and counterclockwise spin is somewhat analogous to cyclonic and anticyclonic systems on Earth. Smaller vortices have been observed to form and disappear in just a few years.



*Figure 1.56. Jupiter's Great Red Spot has been visible continuously since the first telescopes were made just over 400 years ago. It has a divergent, counterclockwise spin similar to an anticyclonic system on Earth. The close-up image also shows a much more turbulent and complex circulation pattern surrounding the Great Red Spot than is observed at lower resolution (Source/Credit: NASA).*

Powerful winds, some over 400 mph, called jets form at the interface between bands. Intense storms with lightning sometimes form within the bands. Jupiter's interior changes from gas

to liquid hydrogen with increasing depth and pressure. Metallic hydrogen probably exists at even greater depths (Figure 1.54). Jupiter may have a rocky core.

The gas giants are **not strong candidates for a life support system**. The lack of a solid surface (crust), bitter-cold temperatures, atmospheric composition, and brutal gravity make them inhospitable. The satellites of Jupiter and Saturn, however, show a great diversity in shape, composition, and volcanic activity. Jupiter alone has 67 moons and counting. A few of these may be targets for future astrobiological study.

Jupiter's moon Io is one of the more fascinating satellites in the solar system. The initial NASA fly-by in the 1980s revealed a pock-marked surface of active volcanoes (Figure 1.57). Some have been observed during eruption. It is the most volcanically-active object in the solar system. Small, distant satellites such as Io were long-thought to be cold worlds. The source of internal heat is still under debate. Jupiter's moon Europa appears to have a vast outer layer of water ice, most likely underlain by an ocean of liquid water (Figures 1.58a and 1.58b). If NASA fails to find evidence of life on Mars, Europa may be a promising next choice.

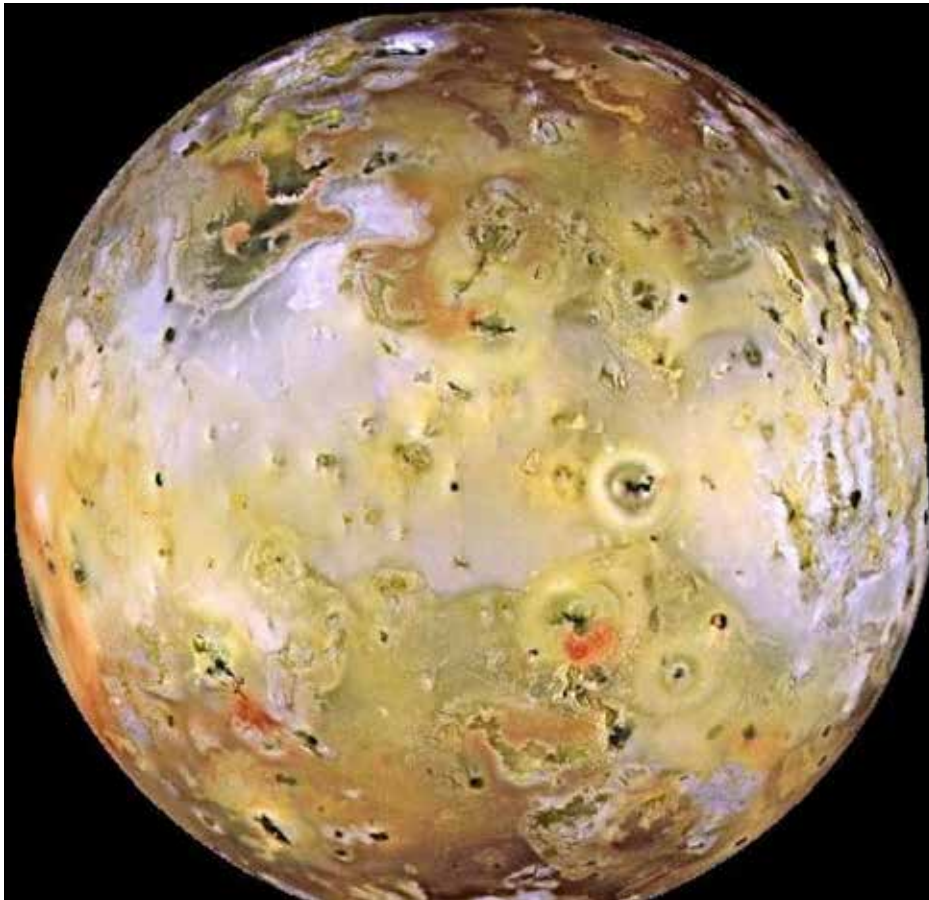


Figure 1.57. Jupiter's moon Io is one of several very interesting moons of Jupiter and Saturn. Io is the fourth largest moon in the solar system and is volcanically the most active body in the solar system. There are more than 400 active volcanoes, many of which have been imaged during eruption. The yellowish color of the surface is due to the sulfur-rich volcanic flows and deposits (Source/Credit: NASA/JPL-Caltech/University of Arizona).



Figure 1.58a. Jupiter's moon Europa is one of several icy satellites of the Jovian planets. The crisscrossed marks are similar in form to places on the floating Arctic icecap on Earth. If so, there may be a vast, ocean of liquid water (salt water?) that forms convection cells causing the ice flows to break up and fuse together multiple times. Satellites such as these may become prime targets for future astrobiological research (Source/Credit: NASA).

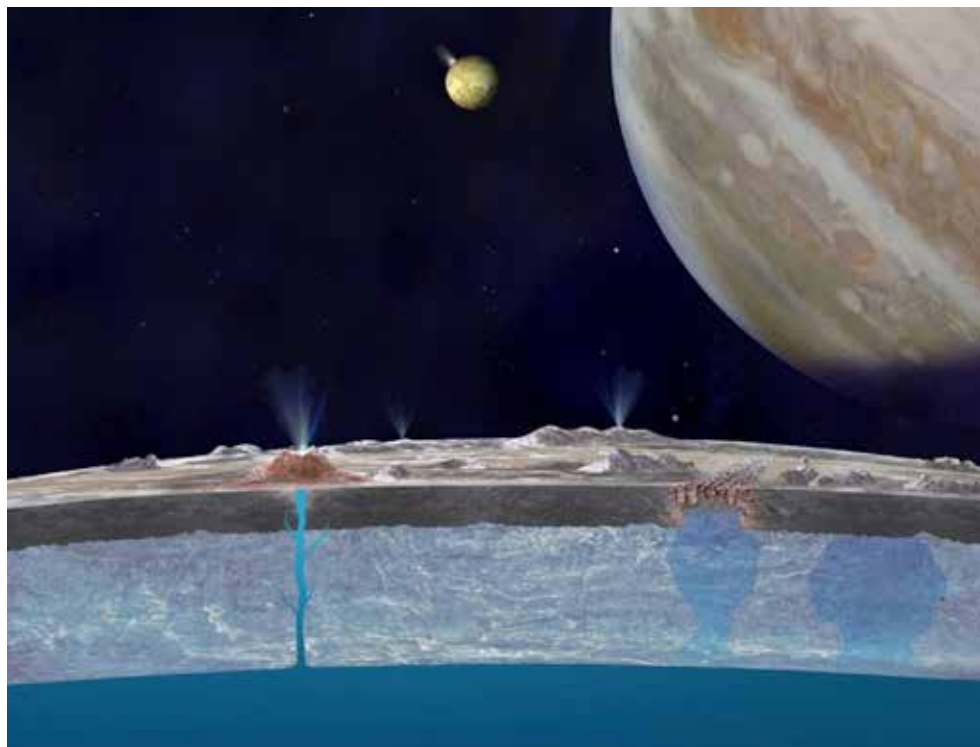


Figure 1.58b. Artist's conception of the watery surface and crust of the Jovian moon Europa. There is significant evidence that liquid water, probably salt water, periodically erupts and re-surfaces portions of the moon. Nearby yellowish moon Io, the most volcanically active Europa object in the solar system, contributes sulfur ices and gases to Europa's surface (Source/Credit: NASA/JPL-Caltech).

### Some interesting aspects of Jupiter:

- It is the largest, most massive planet
- Jupiter contains 2.5 times of the mass of all other planets combined
- Jupiter rotates rapidly, once every 10 hours
- The banded appearance of Jupiter is due to a rather simple, planet-wide atmospheric circulation
- Embedded in the banded circulation of the atmosphere are dozens of both short- and long-lived 'spots', which rotate both clockwise and counterclockwise
- Jupiter is the namesake for the outer Jovian planets, also known as the gas giants
- Jupiter has many moons, 50 confirmed and 17 awaiting confirmation at last count in 2014
- Although Jupiter has no visible solid surface, it is thought to have a solid core the size of the Earth
- Jupiter's atmosphere is mostly hydrogen and helium, probably only slightly altered in composition from its primitive ancestor
- In Jupiter's interior, pressure-temperature conditions may be right for liquid hydrogen to exist giving it the claim- to-fame of having the largest oceans in the solar system
- Jupiter has a powerful magnetic field
- Jupiter's moon Io is the most volcanically active body in the solar system

## Saturn

Saturn is second to Jupiter in size and bears many similarities to the gas giant. It has a similar composition, dominated by hydrogen and helium. It has a banded atmosphere consisting of various cloud layers of ammonia, ammonium sulfide, and water. Its interior has a rocky core surrounded by a vast ocean of metallic hydrogen (Figure 1.54).

Saturn, like Jupiter, is a world of superlatives. It has the largest and most complex ring system in the Solar System (Figure 1.59). It has by far the greatest number of satellites, with ~150. Saturn's moons Enceladus and Dione are watery moons, like Jupiter's Europa (Figures 1.60a and 1.60b).

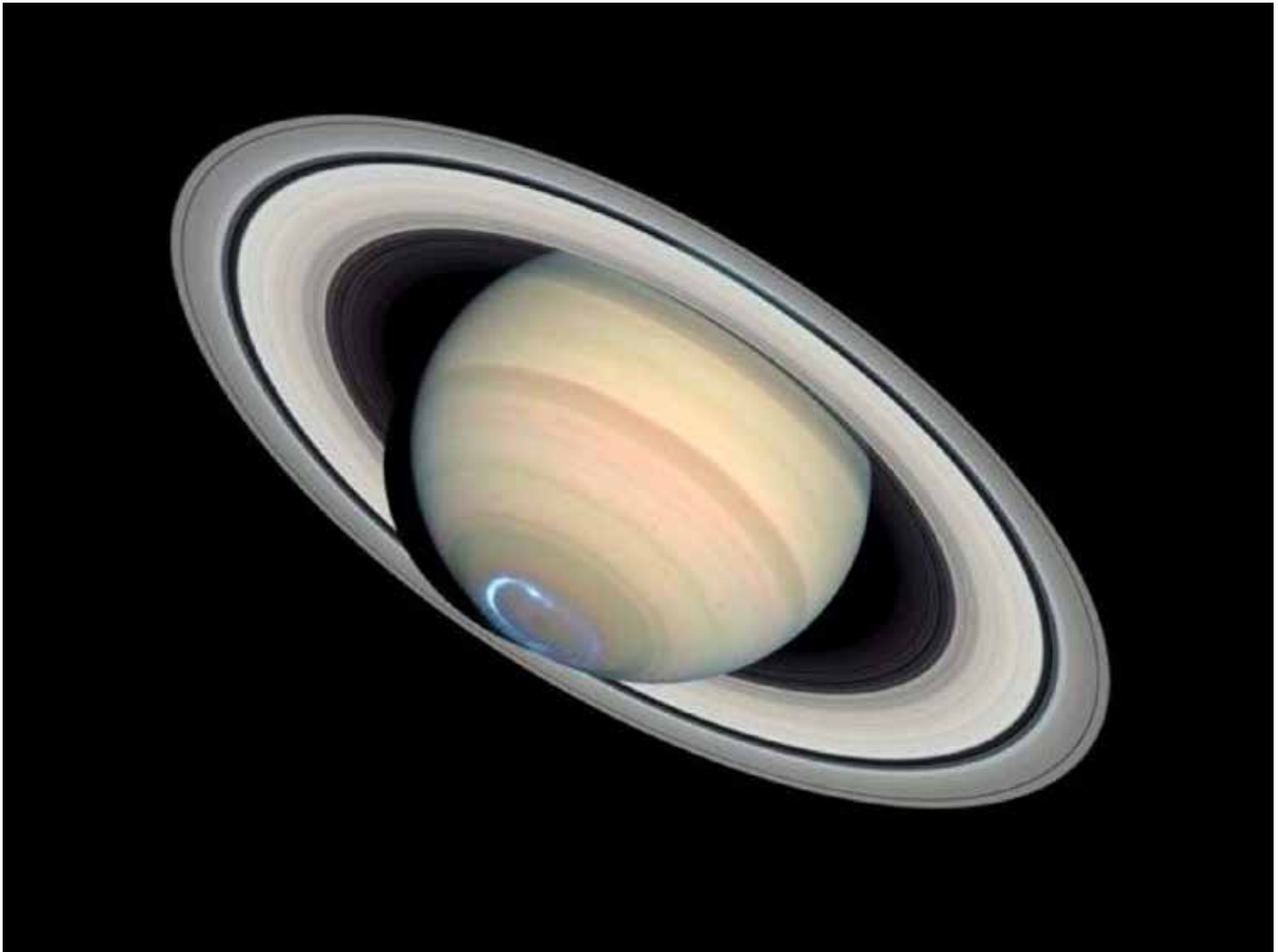


Figure 1.59. Saturn has long been known as the ringed planet. There are seven major rings and hundreds of subdivisions have been identified. Saturn's banded atmosphere is similar to that of Jupiter as is its interior. Saturn has about 150 satellites, by far the largest number of any of the planets in the solar system (Source/Credit: NASA).

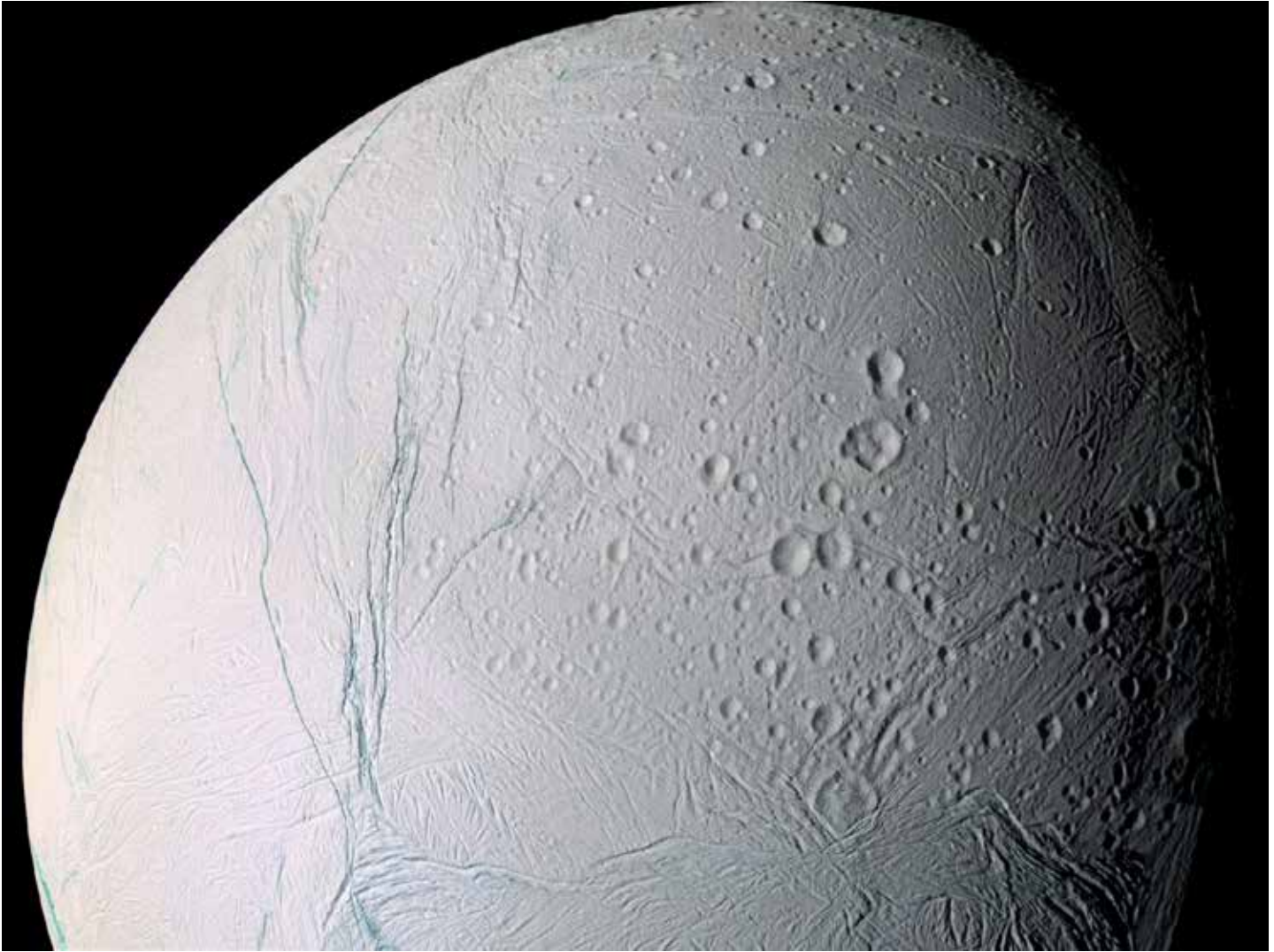


Figure 1.60a. **Enceladus** has the same surface morphology as Jupiter's moon Europa. The surface is water ice and is likely underlain by an ocean of liquid water and a silicate core. The sparsely-cratered areas suggest re-surfacing of large sections of the planet, probably through multiple episodes of ice breakup and suturing (Source/Credit: NASA).



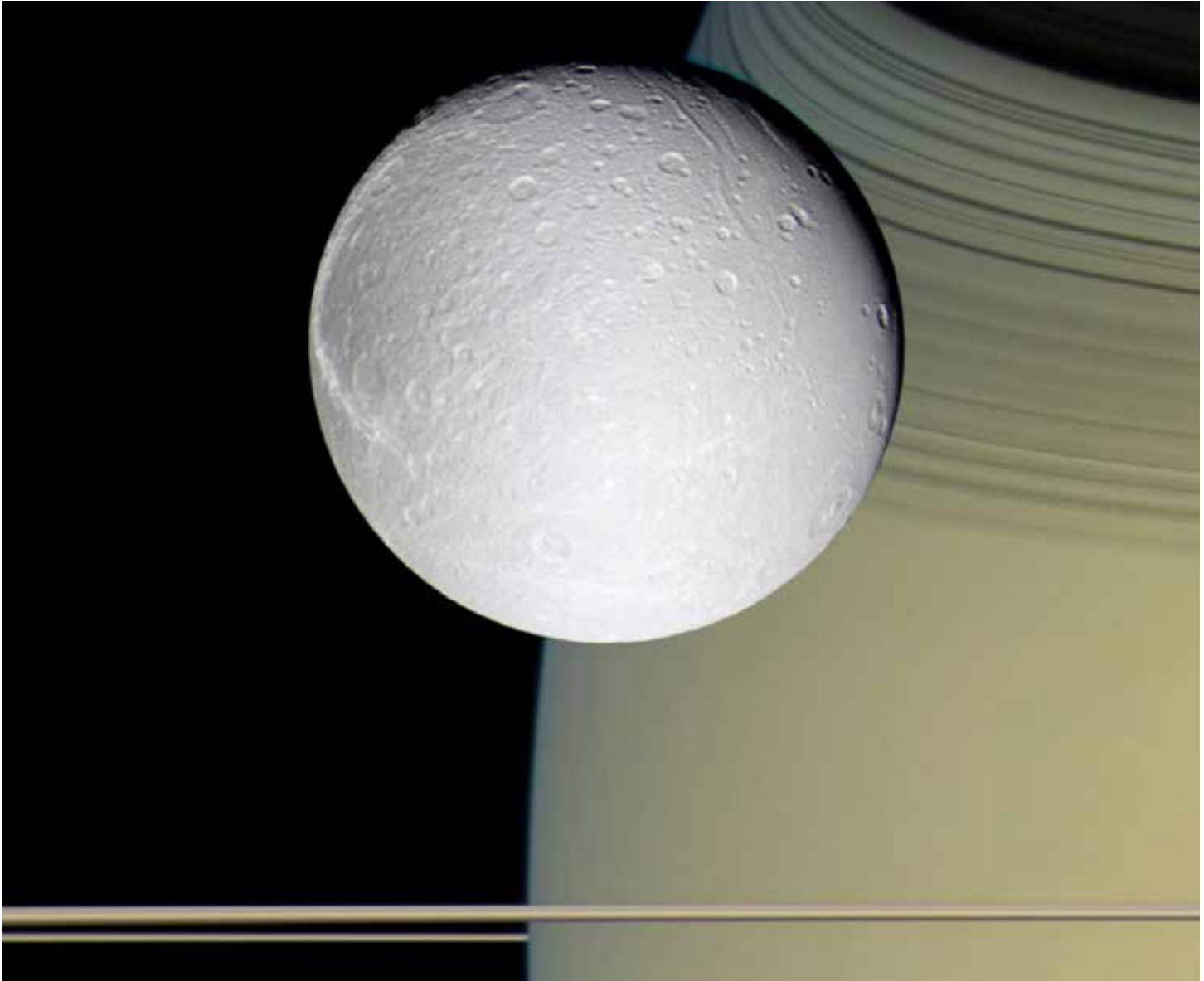


Figure 1.60b. **Dione** is one of several rocky-water-ice moons of Saturn. The surface is water ice and is likely underlain by an ocean of liquid water and a silicate core. Each of these moons may house primitive life forms. The banded atmosphere of Saturn is visible in the upper-right. The thin horizontal line under Dione is Saturn's ring system seen edge-wise. Image from the Cassini mission October 11, 2005 (Source/Credit: NASA).

Titan, the second largest satellite in the solar system (Figure 1.61), has the only significant atmosphere of any moon in the solar system. Titan may have a subsurface layer of liquid water (Figure 1.62). It is the only body in the solar system other than the Earth that has liquid lakes and rivers, and probably liquid methane (Figure 1.63). Titan's atmosphere is slightly denser than the Earth's.



Figure 1.61. Titan is second only to Jupiter's moon Ganymede in size. It is larger by volume than Mercury. Several other satellites of Saturn are indicated as well as a comparison of Earth's Moon (Source/Credit: NASA).

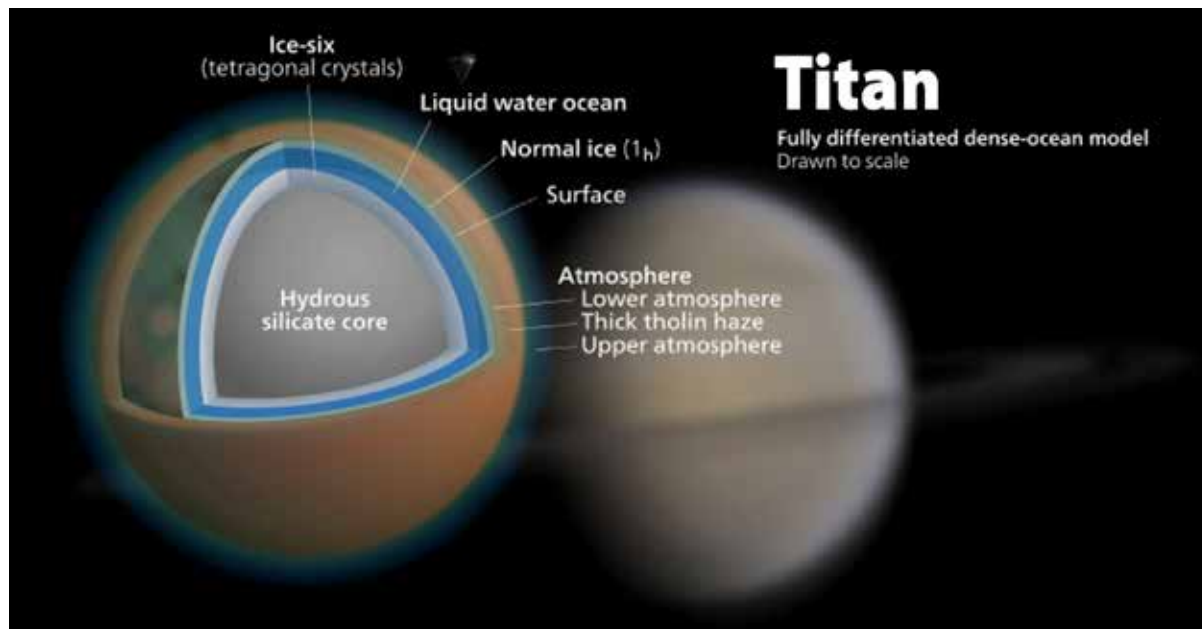


Figure 1.62. Titan is second largest satellite in the solar system and has the only significant atmosphere of any moon in the solar system. Titan may have a subsurface layer of liquid water. It is the only body in the solar system other than the Earth that has liquid lakes and rivers and probably liquid methane. Titan's atmosphere is slightly denser than the Earth's (Source/Credit: modified from <http://commons.wikimedia.org/wiki/User:Kelvinsong>).

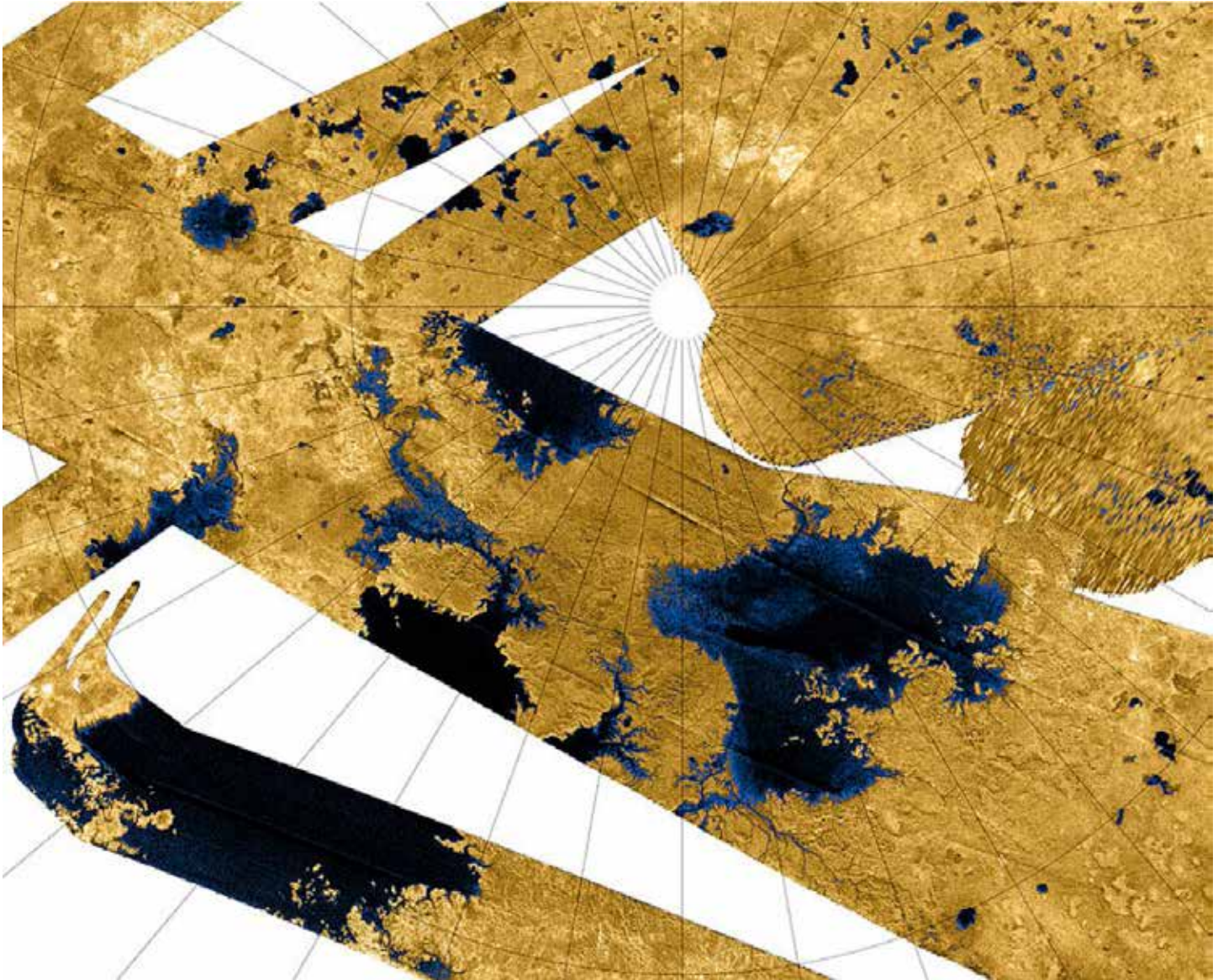


Figure 1.63. Titan is the only body in the solar system other than the Earth that has liquid lakes and rivers. A recent Cassini flyby has imaged several large lakes (dark blue), probably made of hydrocarbons such as methane and ethane. Titan's atmosphere is slightly denser than the Earth's. Rains of ethane and methane help shape the surface of Titan by constantly re-surfacing it and erasing old scars (Source/Credit: NASA).

Saturn radiates more energy than it receives from the Sun. The planet occasionally produces an aurora, similar to Earth's Northern Lights (Figure 1.64). Some polar images of Saturn capture what appears to be a roughly hexagonal circulation system of unknown origin.

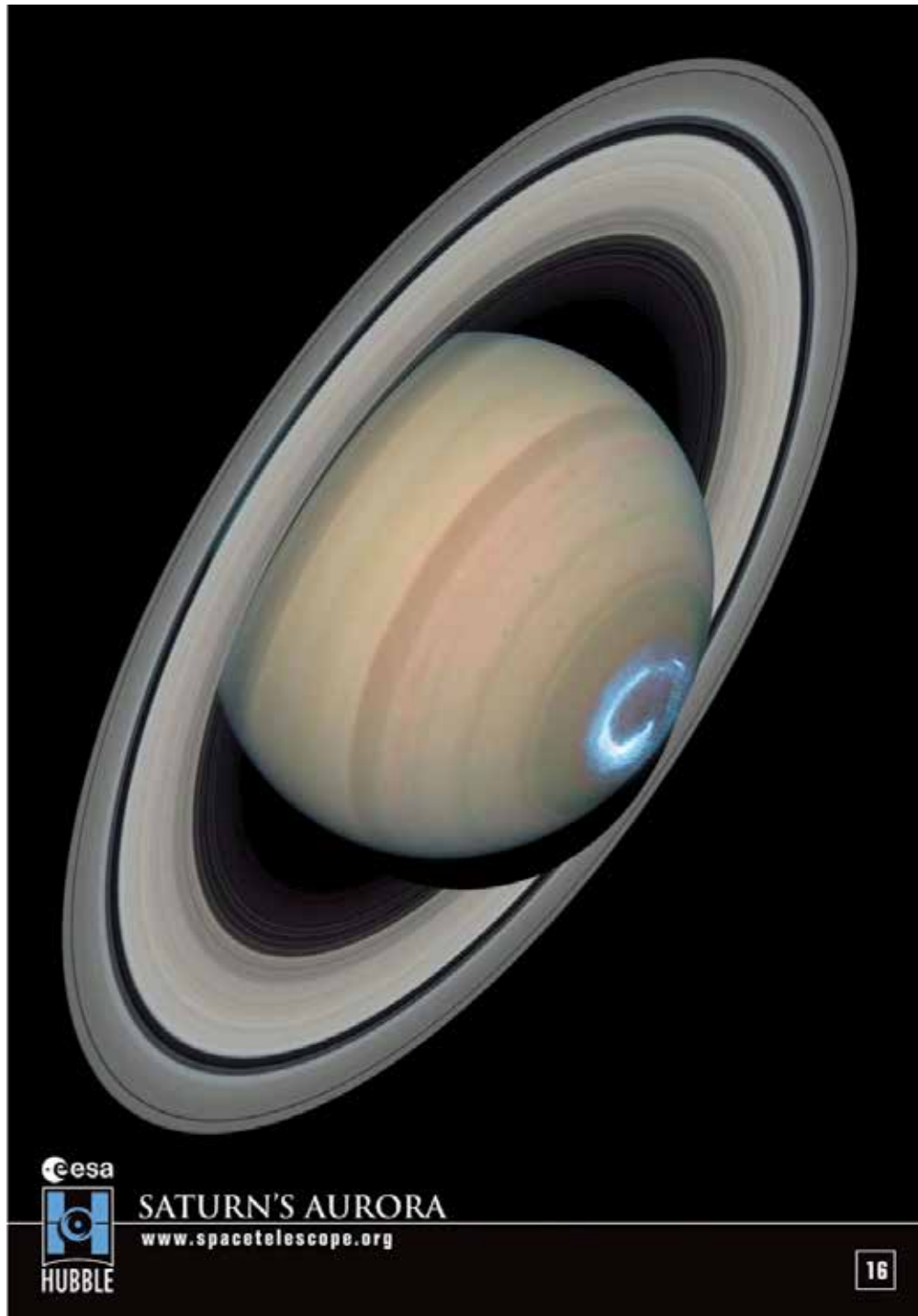


Figure 1.64. Saturn's aurora, similar to the Earth's Northern Lights, is shown in the banded atmosphere near the South Pole. Saturn's magnetic field, produced by the rotation of metallic hydrogen in its interior, collides with streams of charged particles from the Sun to generate a spectacular aurora. Gases in Saturn's upper atmosphere begin to fluoresce when irradiated by solar energy. The blue colors of the false-color image would actually appear red from a Saturn-based observer (Source/Credit: NASA/ESA, Boston University).

### Some interesting aspects of Saturn:

- It has long been known as the ringed planet; 7 major rings and hundreds of subdivisions have been identified
- Saturn's atmosphere is similar to that of Jupiter; the east-west bands are latitudinal zones of gas circulation
- Saturn is currently the front-runner in number of satellites with about 150; 53 have been named
- Saturn's internal structure is similar to Jupiter's; layers of liquid, then metallic hydrogen, perhaps with a rocky core
- Saturn is almost twice as far from the Sun as Jupiter
- Saturn spins rapidly on its axis every 10.7 hours
- Saturn's moon Enceladus likely has a surface of water ice underlain by a vast ocean of liquid or partially liquid water
- Saturn's outer atmosphere is 96.3% hydrogen and 3.25% helium
- Saturn's upper deck of clouds is largely ammonia crystals, whereas the next lower level is mostly ammonium hydrosulfide and/or water
- Saturn's moon Titan has the only significant atmosphere of any satellite in the solar system
- Most of Saturn's moons are less than 30 miles (48 km) in diameter; >40 of them could be placed in Lake Superior
- Both Saturn and Jupiter radiate more energy than they receive from the Sun

## Uranus and Neptune

Uranus and Neptune might also be considered sisters, in the same way that the Earth and Venus are (Figure 1.65). They are of similar size, composition and internal structure (Figure 1.54). They differ from Jupiter and Saturn in that they are somewhat smaller, are colder, and have an eerie blue-green color. The color is due to the presence of condensed methane. It is too warm on Jupiter and Saturn for methane to condense. Both Uranus and Neptune have several small satellites.



Figure 1.65. Sister planets Uranus and Neptune are similar in size, mass, atmospheric composition, and internal structure. They are the outermost of the **Jovian**, or **gas giant** planets and have cold atmospheres. Both planets have very faint ring systems. All remotely-sensed images of the two are of their eerie atmospheres; no one has ever seen their solid surfaces beneath. Orbital periods are long; Uranus' takes 84 and Neptune takes 165 Earth years. NASA spacecraft Voyager 2 (1986) is the only spacecraft to visit Uranus. Both planets have oval, rotating spots. The eerie blue-green color of their atmospheres is due to the presence of small amounts of methane gas. Most of the mass of the two planets is contained in an extended liquid core of icy methane, water, and ammonia. Uranus is unique among the gas giants in that it lacks a banded atmosphere, has an axial tilt that is  $98^\circ$  from the orbital plane (early impact?), and, like Venus, spins in retrograde motion (Source/Credit: NASA).

**Uranus** is unique among the Jovian planets. It is the only Jovian planet without a banded atmosphere. Its axis of rotation is tilted so much that it nearly lies on the same plane as the orbital plane (Figure 1.66). It has a retrograde rotation, the opposite spin of most of the planets, with the exception of Venus. It has a colder atmosphere (49K; minus 371°F) than Neptune, although it is closer to the Sun.



Figure 1.66. Uranus has an axial tilt that points along its orbital plane, perhaps the result of an early impact. It also has retrograde rotation, opposite that of most of the planets. Both Uranus and Neptune have very faint ring systems (Source/Credit: NASA).

**Neptune** has a banded atmosphere (Figure 1.67), a few vortices (Figure 1.68), and the strongest winds (1300 mph) of any planetary atmosphere. Neptune's orbit lies an average of 2.8 billion miles (4.5 billion km) from the Sun, or 30 times the Earth-Sun distance. Neptune has 13 confirmed moons and 6 faint rings. At times, Pluto's orbit crosses inside that of Neptune's.



Figure 1.67. A high-resolution image of banded clouds taken by NASA spacecraft Voyager 2 in 1989. Considerable vertical relief (30 miles; 48 km) can be seen in the stretched cloud streaks (Source/Credit: NASA/JPL).



Figure 1.68. Neptune's eerie-colored, banded atmosphere is apparent in this image taken by Voyager in 1989. Oval spots appear and dissipate, as they do in the atmospheres of Jupiter and Saturn. Neptune's orbit lies an average of 2.8 billion miles (4.5 billion km) from the Sun, or 30 times the Earth-Sun distance. Neptune has 13 confirmed moons and 6 faint rings. At times, Pluto's orbit crosses inside that of Neptune's (Source/Credit: NASA).



## Some interesting aspects of Uranus and Neptune:

- They are the outermost of the *Jovian*, or *gas giant* planets
- They are very similar in size, composition, and mass
- The axis of Uranus is tilted 98° from the orbital plane (early impact?)
- Both planets have very faint ring systems
- All remotely-sensed images of the two are of their atmospheres; no one has ever seen their solid surfaces beneath
- Orbital periods are long; Uranus' takes 84 Earth years; Neptune 165 years
- Uranus has 27 moons and counting; most are very small
- Uranus, like Venus, spins in retrograde motion
- Voyager 2 (1986) is the only spacecraft to visit Uranus
- Both planets have oval, rotating spots
- Uranus has an eerie blue-green color from methane gas in the atmosphere
- Most of the mass of the two planets is contained in an extended liquid core of icy methane, water, and ammonia
- Neptune's orbit lies an average of 2.8 billion miles (4.5 billion km) from the Sun, or 30 times the Earth-Sun distance
- Neptune has 13 confirmed moons and 6 faint rings
- At times, Pluto's orbit crosses inside that of Neptune's

## Dwarf Planets, Asteroids and Comets

**Dwarf planets** orbit the Sun, just like other planets. Most of them seem to originate in an orbital belt outside of Neptune's orbit called the Kuiper Belt (Figure 1.69). Others, like Ceres, inhabit the Asteroid Belt, a region of mostly smaller rocky debris between the orbits of Mars and Jupiter. Most of the known dwarf planets are smaller than Earth's Moon. (Figure 1.70) Dwarf planets range in composition from icy to rocky, silicate material. Pluto, once considered a planet, has been demoted to a dwarf; its orbit is about 40 times larger than the Earth's. Many dwarf planets (e.g., Pluto) have moons.

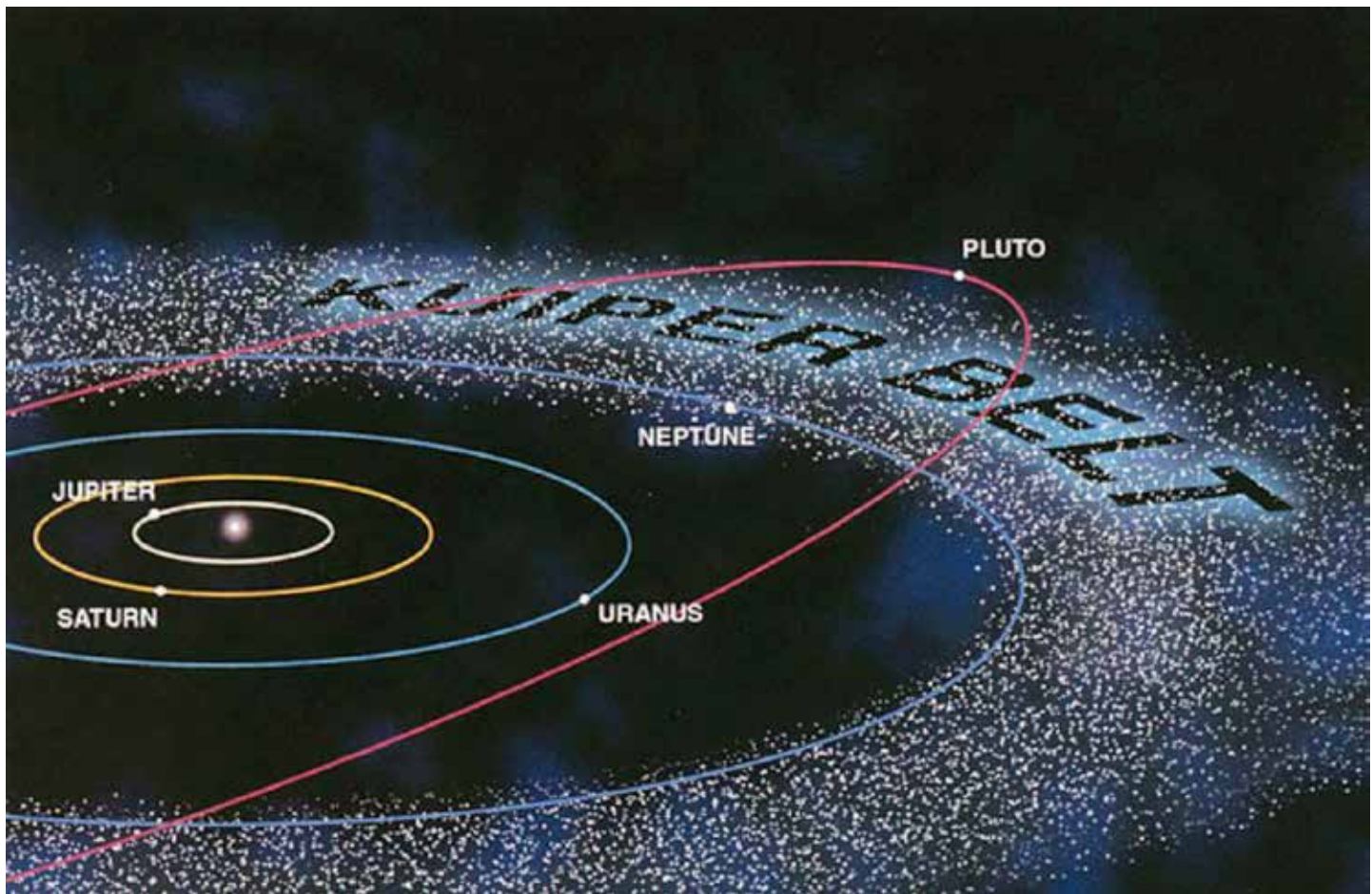


Figure 1.69. The **Kuiper Belt** was discovered officially only a couple of decades ago (1992), although one of its members, Pluto, was actually discovered in 1930. It is an ill-defined region beyond the orbit of Neptune that contains thousands of small rocky and/or icy bodies in orbit around the Sun. Over a thousand bodies, most of them between 60 and 180 miles (100-300 km) in diameter, have been discovered in the Kuiper belt since 1992. Some of these are large enough to be classified as dwarf planets. Expectations are that many more dwarf planets will be discovered in the Kuiper Belt in the next decade (Source/Credit: R. Hunt SSC Caltech/JPL/NASA).

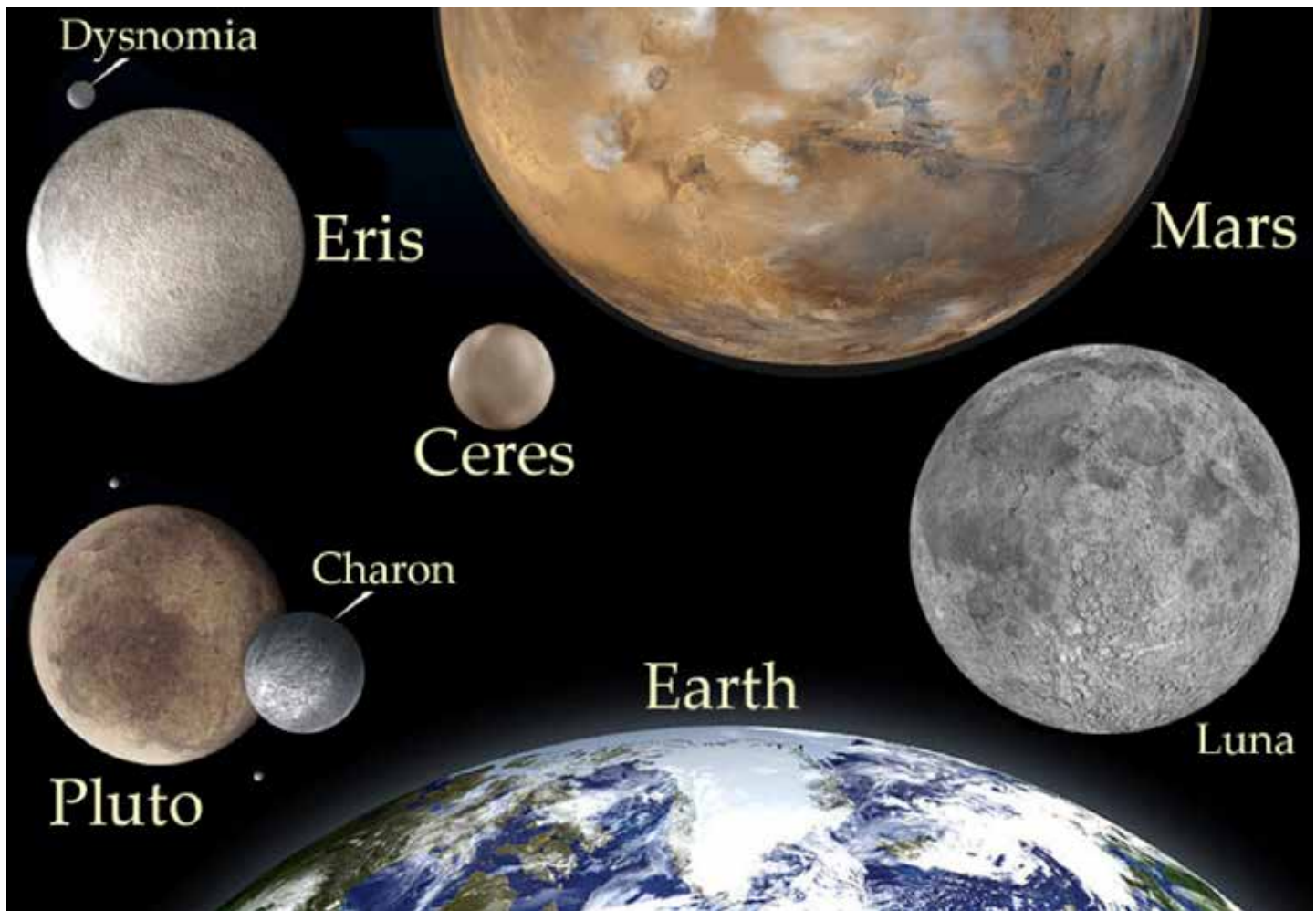


Figure 1.70. Artist's concept of size comparison of **dwarf planets** Eris, Ceres, and Pluto compared to Mars, the Earth and its Moon. Pluto's moon Charon and its two very small moons are also shown, as well as Eris' moon Dysnomia. Objects are not all to scale (Source/Credit: NASA/ESA/JPL, and A. Field, STSci).

Pluto is a small, icy-silicate planet that is only about 1500 miles (2400 km) in diameter. Its orbit is highly elliptical and inclined considerably from the orbital plane of the major planets. The distant Sun (Figure 1.71) does little to warm bodies in the Kuiper Belt; Pluto's temperature ranges from minus 387°F (-233°C) to minus 369°F (-223°C). Pluto has a relatively large companion, Charon, and several recently-discovered smaller satellites (Figure 1.72). At the 2006 meeting of the International Astronomical Union, Pluto was officially demoted to a dwarf planet. Astronomers loosely define dwarf planets as being massive enough to have their shape controlled by gravity, but not enough gravity to have cleared out nearby bodies through accretion. Although there are only a handful of recognized dwarf planets, astronomers estimate that there are more than 200 undiscovered ones in the Kuiper Belt alone.

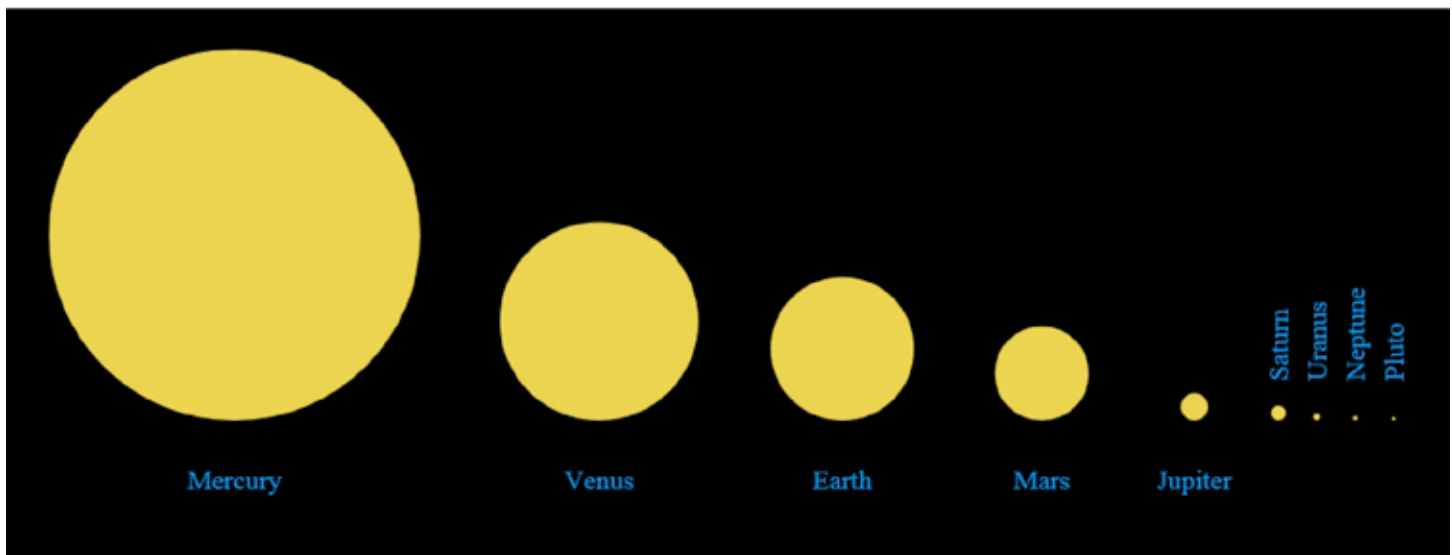


Figure 1.71. The distant Sun does little to warm bodies in the Kuiper Belt; Pluto's temperature ranges from minus 387°F (minus 233°C) to minus 369°F (minus 223°C). The image shows the relative size of the Sun as viewed from Pluto and the other planets (Source/Credit: NASA).

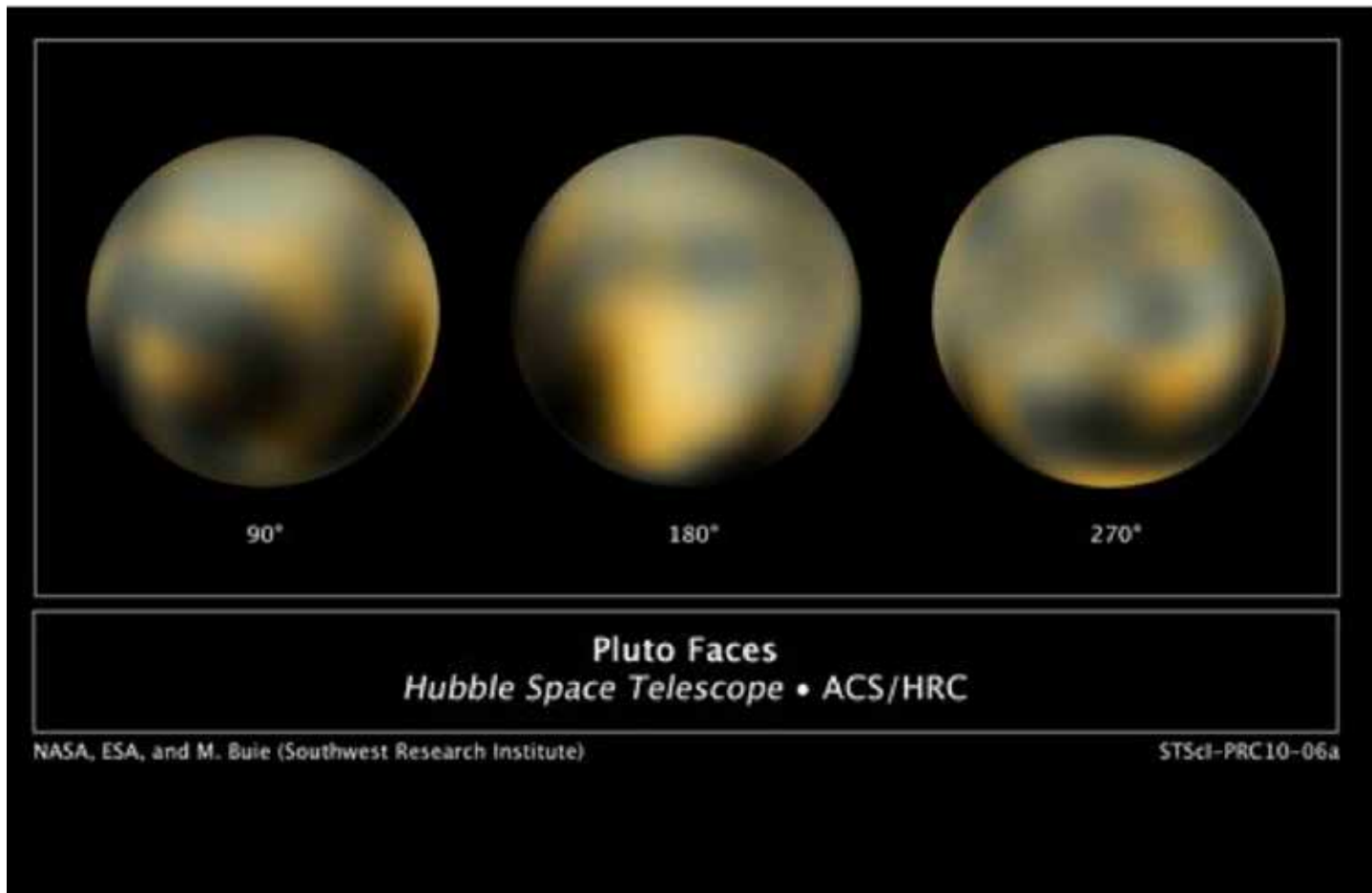


Figure 1.72. **Pluto**, once a member of the 9-planet solar system, is now considered a dwarf planet. It is a member of the **Kuiper Belt**, a region beyond the orbit of Neptune that contains thousands of icy and/or rocky bodies. Pluto is smaller than the Earth's Moon and probably consists of water and methane ices with a rocky core. Pluto's large moon, Charon, is about half Pluto's diameter and is therefore sometimes referred to as a double (dwarf) planet. Pluto has a retrograde rotation (backwards from most planets) and a steeply-tilted axis, probably the result of a close encounter with another body. The blurry images above were taken recently by the Hubble Space Telescope and are the best images of Pluto to date. The Hubble telescope found several other small companions of Pluto and Charon between 2005-2013 (Source/Credit: NASA/ESA, Southwest Research Institute).

**Asteroids** are typically smaller than dwarf planets and have irregular shapes and are typically pock-marked with ancient impact craters and scars (Figure 1.73). They are rocky silicates and have no atmosphere. Most asteroids lie within the Asteroid Belt between the orbits of Mars and Jupiter. The Dawn Mission (2011 and ongoing) is the first spacecraft to orbit an asteroid and complete a comprehensive photo gallery (Figure 1.74).



Figure 1.73. Asteroid Eros has an irregular shape and is made of rocky, silicate material. It is larger than most asteroids, measuring about 21 x 7 miles (34 x 11 km). Eros was visited and photographed twice by NASA's NEAR Shoemaker probe in 1998 and 2000, finally landing on the asteroid's surface. Eros, like most asteroids, is densely scarred from early impacts (Source/Credit: NASA).

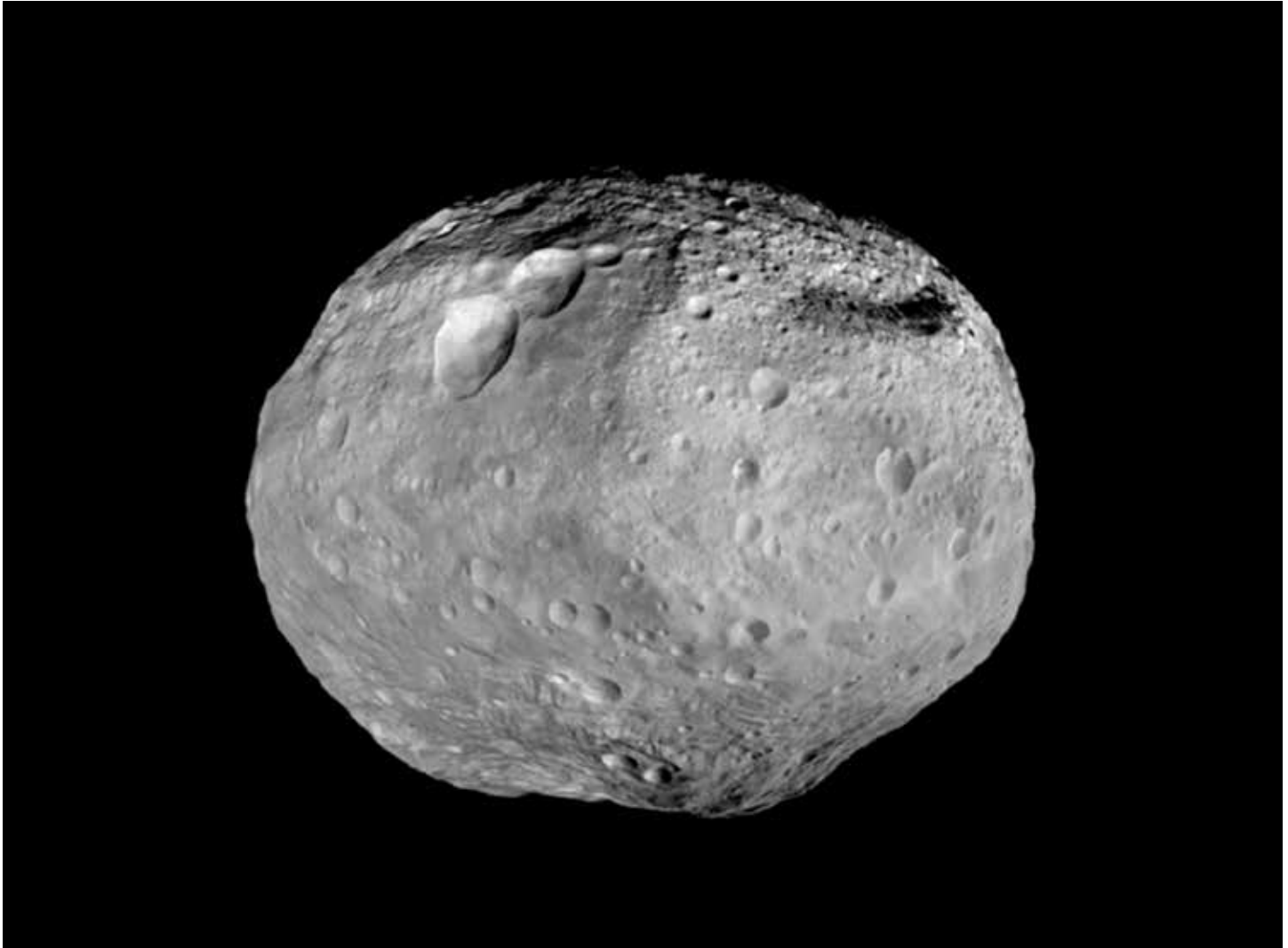
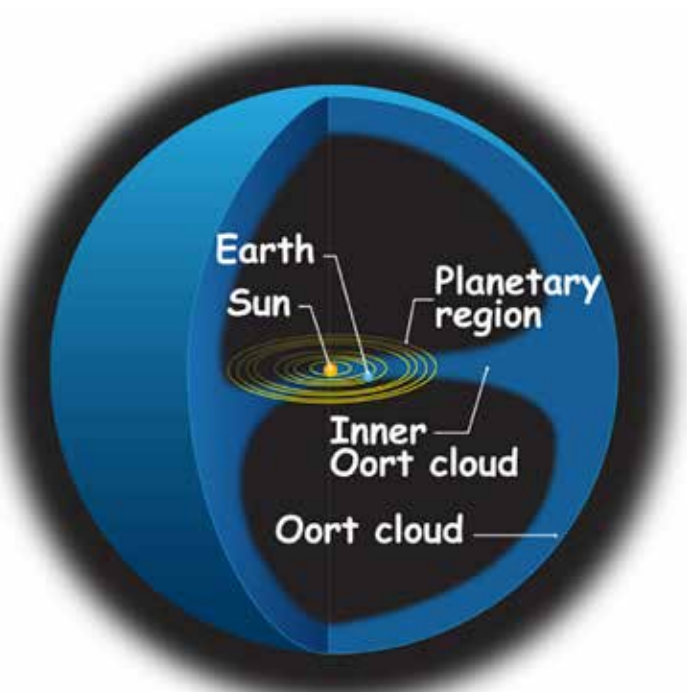


Figure 1.74. The asteroid Vesta, with a diameter of 326 miles (525 km), represents an embryonic planet that never reached true planet stature. Real planets are massive enough to acquire a spherical shape as well as to have enough gravity to sweep the surrounding space clean by accretion. Vesta is the brightest asteroid viewed from Earth. Note the pock-marked surface of Vesta, revealing multiple impacts during the early stages of the evolution of the solar system. The bulge on the underside of Vesta in this image is a mountain estimated to be twice the height of Mt. Everest. NASA's Dawn spacecraft studied Vesta from July 2011 to September 2012 (Source/Credit: NASA).

**Comets** are bodies of rock and ice that release gas or dust, particularly when their orbit brings them close to the Sun. They vary in composition, but most contain some ice, dust, ammonia, and methane. Comets orbit the Sun in very elliptical orbits that take them close to the Sun (some impact the Sun) where they are then flung out beyond the orbit of Pluto. Some, like Haley's Comet, have very well-known periods and their arrival has been predicted for centuries.

Comets are nearly invisible during most of their orbit, but when they approach the Sun, the solar wind causes many of the ices to vaporize and ionize and they develop their famous tail (Figure 1.75). The tail represents material that is lost from the comet, eventually reducing the size and mass enough to cause them to break up and dissipate. Comets may originate in the *Oort Cloud*, a vaguely-defined area beyond the orbit of Pluto (Figure 1.76).



Not to scale

Figure 1.75. (left) Comet Lovejoy appears just above the banded atmosphere of the Earth. The image was taken from the International Space Station on December 22, 2011 by NASA astronaut Dan Burbank. The long tail of comets always points away from the Sun (Source/Credit: NASA).

Figure 1.76. (right) Comets are bodies of rock and ice that release gas or dust, particularly when their orbit brings them close to the Sun. They vary in composition, but most contain some ice, dust, ammonia, and methane. Comets orbit the Sun in very elliptical orbits that take them close to the Sun (some impact the Sun) where they are then flung out beyond the orbit of Pluto. Some, like Haley's Comet, have very well-known periods and their arrival has been predicted for centuries. They are nearly invisible during most of their orbit, but when they approach the Sun the solar wind causes many of the ices to vaporize and ionize and they develop their famous tail. The tail represents material that is lost from the comet, eventually reducing the size and mass enough to cause them to break up and dissipate. Short-term comets (orbits <200 years) may originate in the Kuiper Belt whereas long-term comets probably originate in the **Oort Cloud**, a vaguely-defined area beyond the orbit of Pluto (Source/Credit: NASA).



Comets have a *solid core* consisting of ice (water ice and others) and dust coated with dark matter (hydrocarbons?). Some cores may have a rocky nucleus. As the comet approaches the Sun, some of the core ice vaporizes, forming a nebulous *coma* (Figure 1.77). Radiation from the Sun then expels some of the gas and dust particles away from the coma to form the distinctive *tail*. In some instances, a *dust tail* can be distinguished from an *ion tail*. The Earth regularly passes through the tail of some comets, causing meteor showers. Comets may have been an important source of water for the Earth and other planets in the early days of the Solar System. Comet cores range from a few hundred yards (~100s m) to about 10 miles (16 km) in diameter. Comas may reach a million miles in diameter, and some tails exceed 100 million miles (160 million km). On December 12, 2005, NASA's Deep Impact blew a 150 meter (500 foot) crater into Comet 9P/Tempel 1 (Figure 1.78), confirming that the composition was a mixture of ices and a higher proportion of dust than expected.

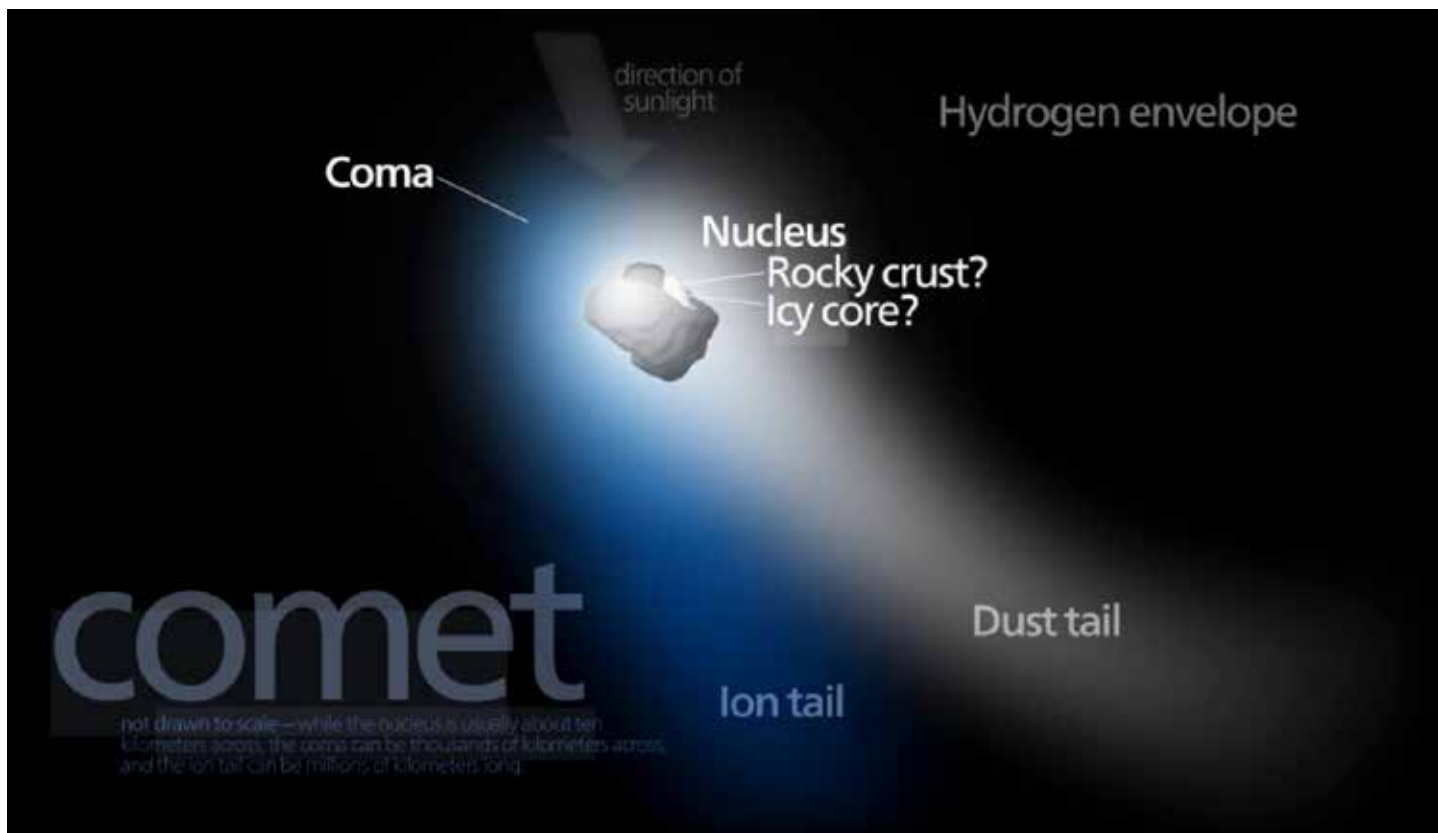


Figure 1.77. Comets have a **solid core** consisting of ice (water ice and others) and dust coated with dark matter (hydrocarbons?). Some cores may have a rocky nucleus. As the comet approaches the Sun, some of the core ice vaporizes, forming a nebulous **coma**. Radiation from the Sun then expels some of the gas and dust particles away from the coma to form the distinctive **tail**. In some instances, a **dust tail** can be distinguished from an **ion tail**. The Earth regularly passes through the tail of some comets, causing meteor showers. Comets may have been an important source of water for the Earth and other planets in the early days of the Solar System (Source/Credit: <http://commons.wikimedia.org/wiki/User:Kelvinsong>).

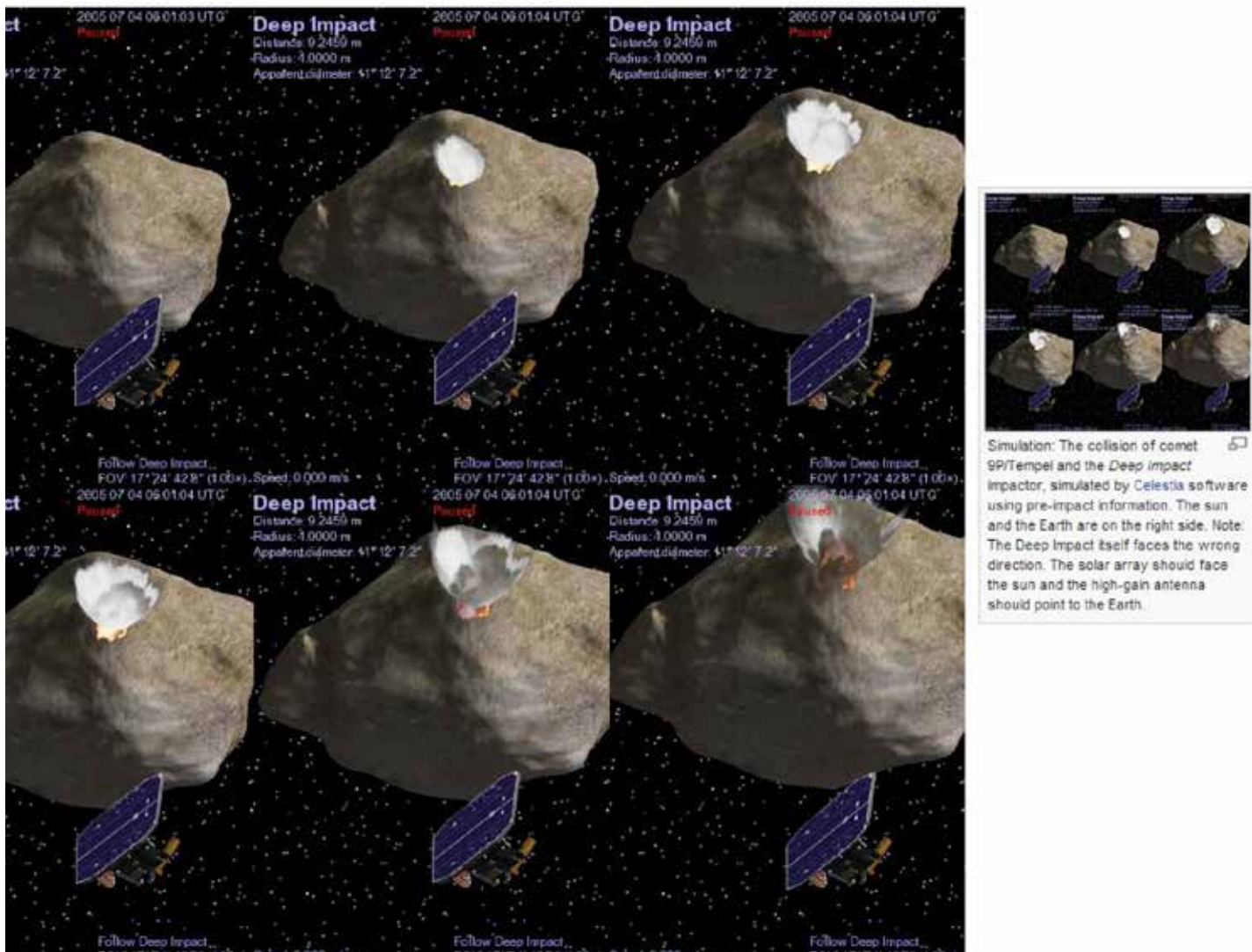


Figure 1.78. Deep Impact was a 2005 NASA mission designed to determine the internal composition of Comet 9P/Tempel 1. The image sequence above is a computer simulation time lapse, based in part on actual photo coverage. An impactor was deployed, and upon impact, was detonated. The explosion blew a hole an estimated 500 feet (150 m) in diameter. The exposed interior of the comet revealed a mixture of light-weight ices and dusty-rocky material, although less ice was found than expected (Source/Credit: NASA).

### Some interesting things about asteroids, dwarf planets, and comets:

- Dwarf planets orbit the Sun
- Most dwarf planets are located in the Kuiper Belt; some in the asteroid belt
- Pluto, once considered a planet, has been demoted to a dwarf; its orbit is about 40 times larger than the Earth's; it's composition water ice with a rocky core(?)
- Asteroids and dwarf planets are rocky and/or icy bodies
- Many dwarf planets have moons

- Pluto has a moon, Charon, about half its diameter, and probably made largely of water ice
- Asteroids are typically smaller and more rocky in composition than dwarf planets
- Comets differ from asteroids and dwarf planets in that their orbits are highly elliptical and composition rocky and/or icy; they also generate long tails as they near the Sun
- The asteroid belt lies between the orbits of Mars and Jupiter
- Asteroids are solid, rocky, irregularly-shaped bodies
- Asteroids are densely impact cratered
- The combined volume of all of the asteroids is less than that of Earth's Moon
- Large-orbit comets take them as far as 100,000 Earth-Sun distances and as close as nearly colliding with the Sun (some do)

## Exoplanets

A question that has inspired and stimulated the intellects of humans for centuries is whether or not life exists beyond our planet. It has been the theme of novels, movies, television series, comic characters, and a radio broadcast (1938's *War of the Worlds*) that shook the Earth. It remains as hot a topic today as it was in the heyday of science fiction movies in the 1950s, and is a topic of debate among scientists and theologians. The plain answer to the question at present: there is no undeniable proof of the existence of intelligent beings elsewhere in the universe.

NASA and other cooperating agencies have taken on a very ambitious task of trying to identify **exoplanets**, planets outside our solar system, some of which may have evidence of past or present life forms. The European Southern Observatory and NASA's Kepler Telescope have found hundreds of exoplanets, a few of which might be in the right planetary environment, the *habitable zone*, to provide a long-lived life-support system (Figure 1.79). The habitable zone within a planetary system is an orbital band with a certain-sized planet that is the right distance from its star to allow water to exist in liquid phase and offer a life-support system somewhat like the Earth's.

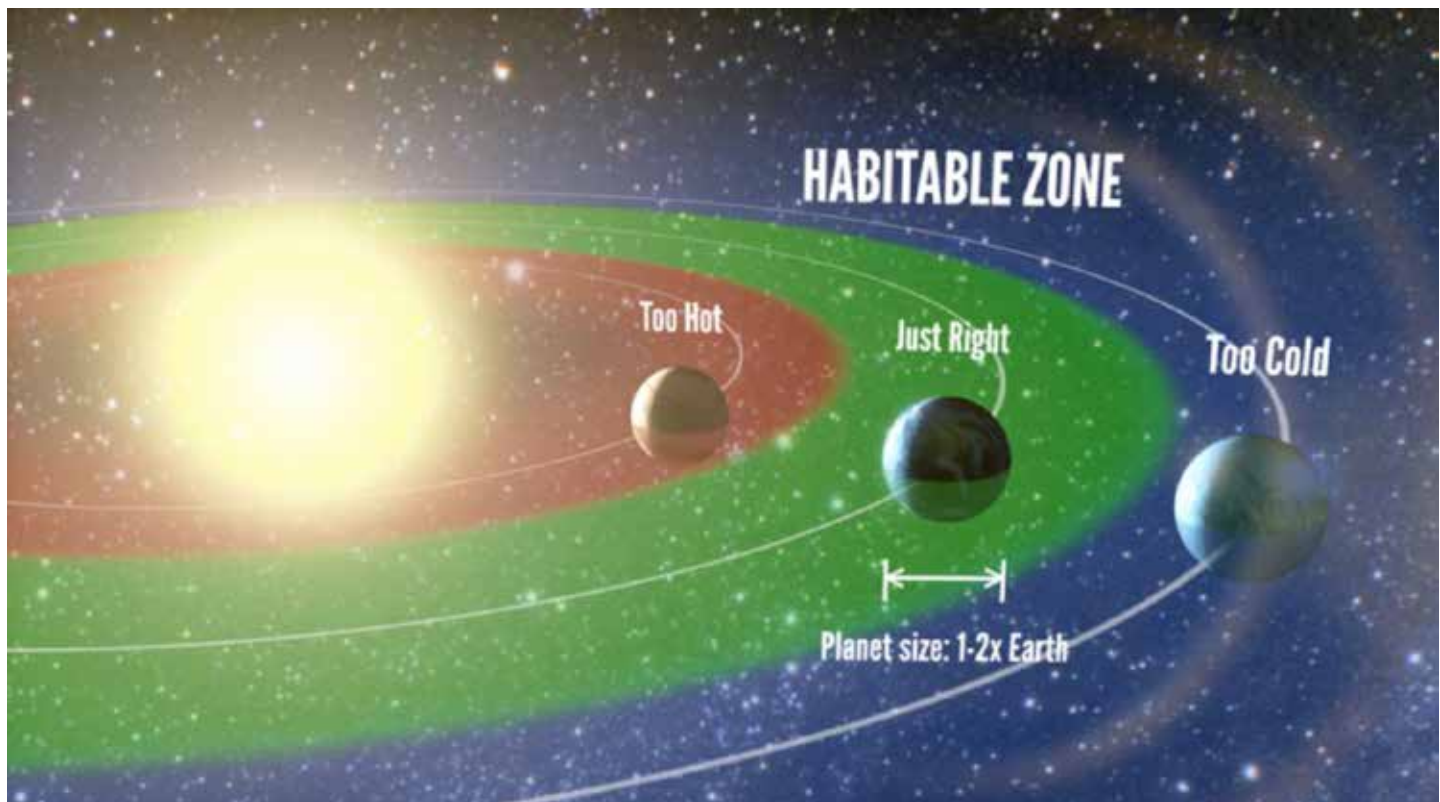


Figure 1.79. Artist's conception of the habitable zone around a star, where the temperature range allows liquid water to exist for long periods of time (Source/Credit: University of California at Berkeley).

A life-support system within the *habitable zone* includes such things as

- (1) proximity to a nearby star to heat and drive the atmospheric engine;
- (2) being the right distance from the star so that it is neither too hot or cold for life (Figure 1.80); preferably where water and other fluids could be very mobile and coexist in all three physical states (solid, liquid, gas);
- (3) suitable atmospheric composition, one with the right balance of inert gases and greenhouse gases to buffer atmospheric temperatures and sustain a chain of life forms;
- (4) the proper magnitude of magnetic field (rotating metallic core) to protect from excessive ionizing radiation from the star;
- (5) a planet that is massive enough to retain an atmosphere, but not so massive as to have a Jovian atmosphere;
- (6) having a nearby star that has a long lifetime and puts out an almost constant amount of the right kind of radiation.

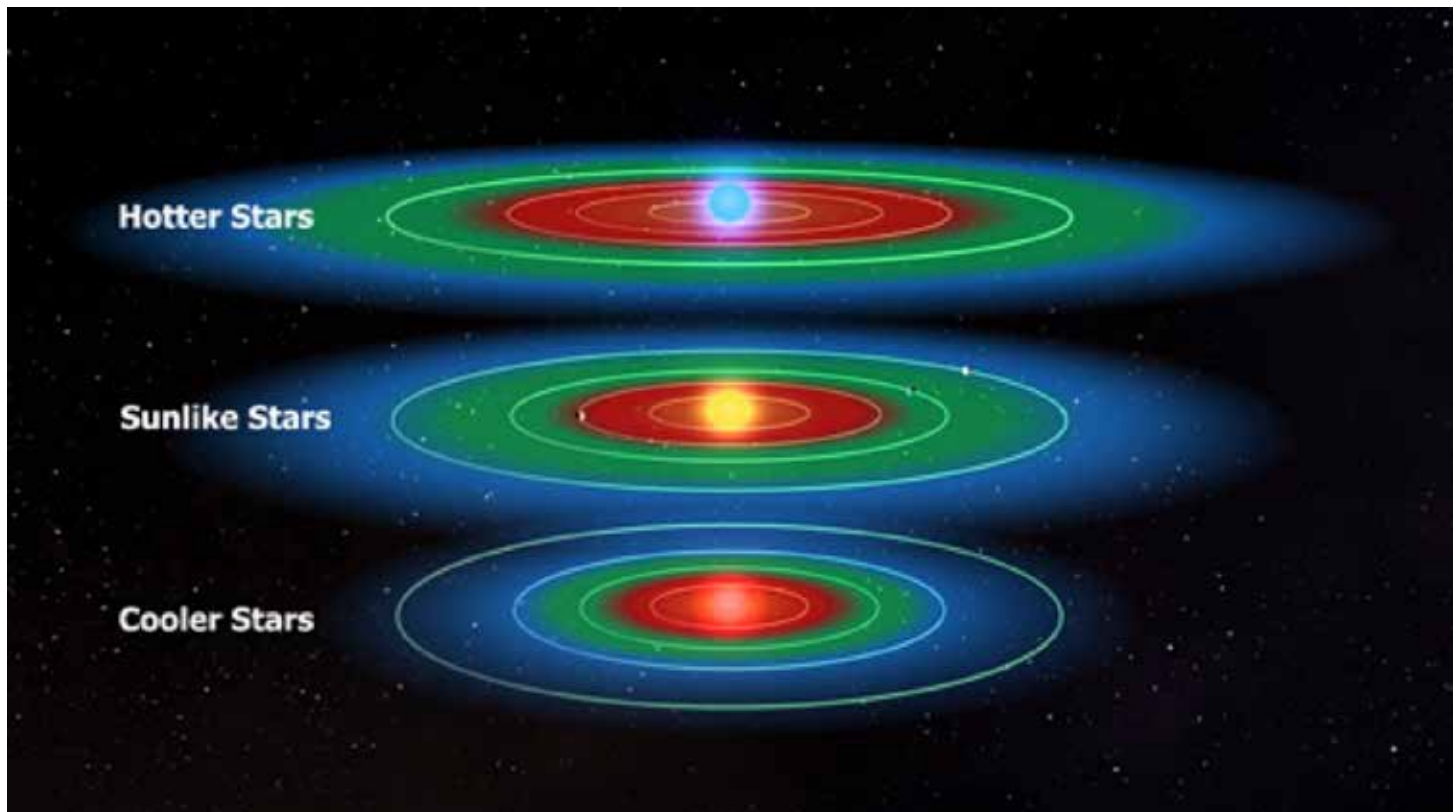


Figure 1.80. The distance from a star to the habitable zone varies with the energy output from the star. For Sun-like stars, it includes the Earth, at about 93 million miles from the Sun and, in the past, might have easily included everything from Venus to Mars. Hotter stars have a more distant habitable zone, and cooler ones a closer one (Source/Credit: NASA).

As of late February 2014, NASA had cataloged 879 planets in orbit around 678 stars. Many of them lie in a zone unusually rich in exoplanets within the Milky Way Galaxy (Figure 1.81). Astronomers now speculate as many as 400 billion exoplanets may exist in the Milky Way Galaxy. The list of exoplanet candidates soared from 200 in 2013 to over 90,000 in early 2014. Most of the exoplanets orbit too close to their star to be in the *habitable zone* (too hot), but about 0.3% are in the *habitable zone* and are not much larger than the Earth (Figure 1.82).

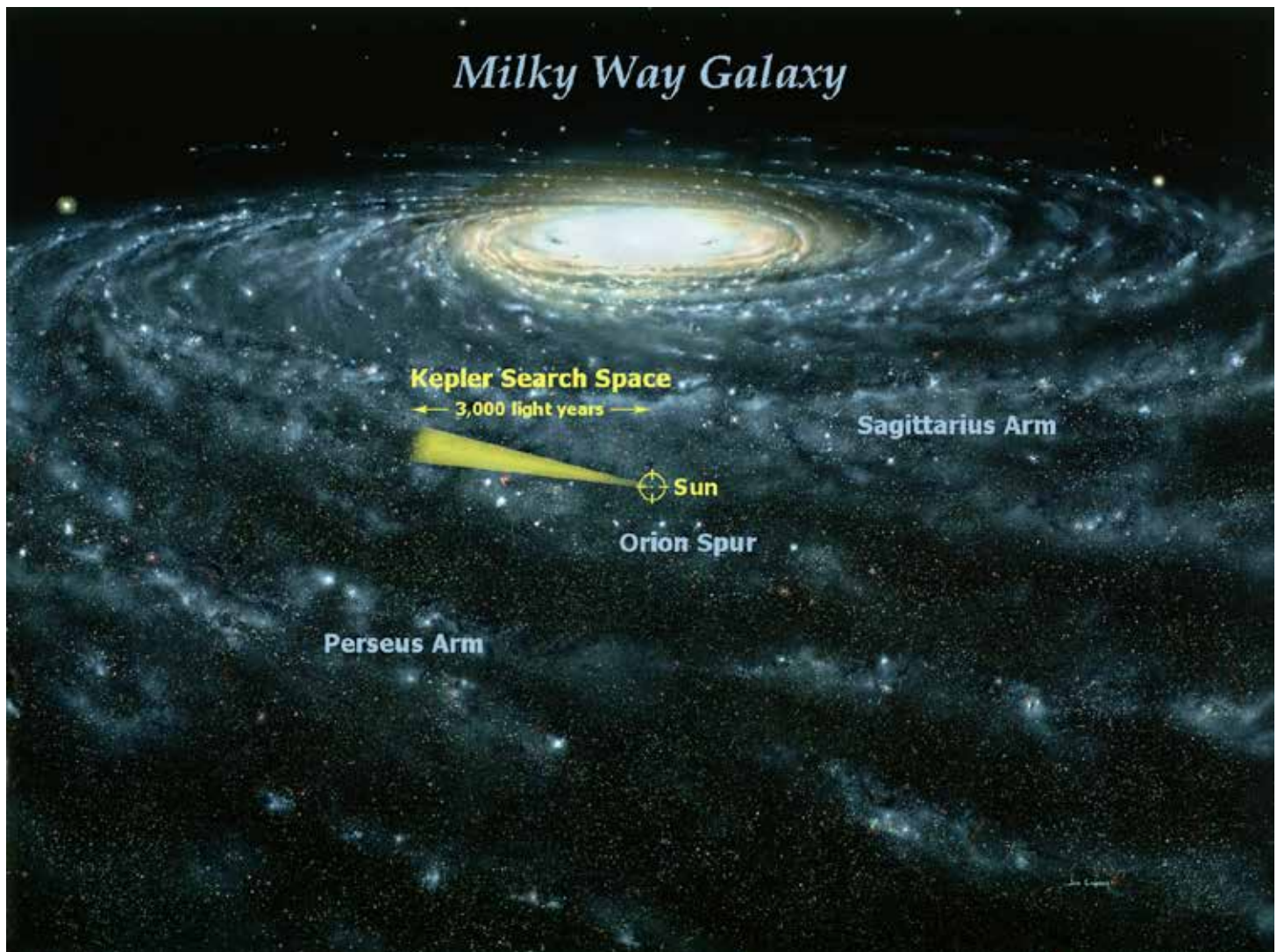


Figure 1.81. NASA's Kepler space telescope is currently focusing on a small area within the Milky Way Galaxy that has hundreds of exoplanets, some of which may have a habitable zone (Source/Credit: NASA/<http://kepler.nasa.gov/media/images/LombergA1024.jpg>).

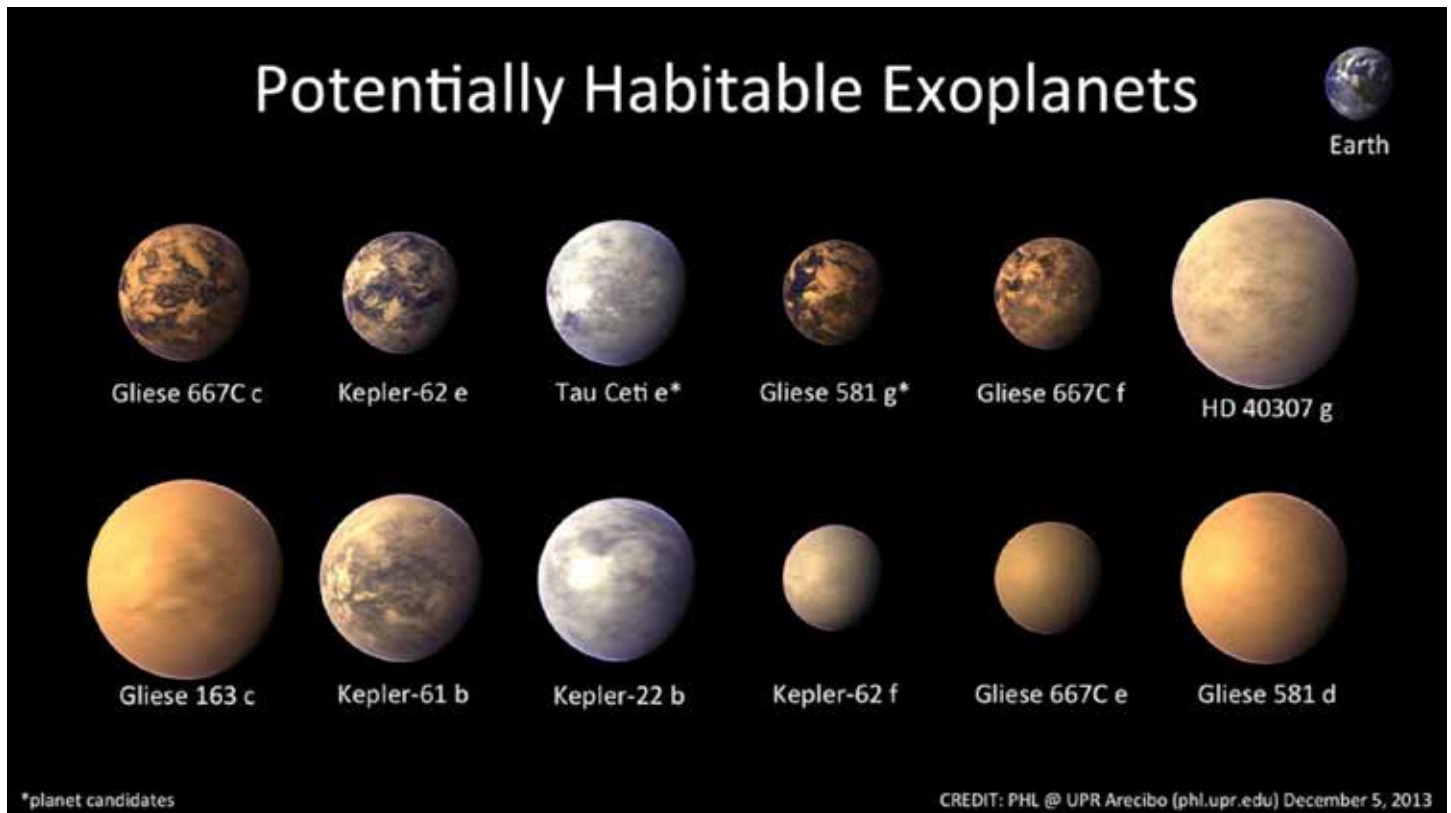


Figure 1.82. Artist's concept of some of the current candidates of potentially habitable exoplanets, as of December 2013. The number of potentially habitable exoplanets grows almost daily thanks to the Kepler telescope and the European Southern Observatory (Source/Credit: PHL@UPR Arcibo phl.upr.edu).

## Earth's Life Support System

The Earth's life-support system is truly unique. Many conditions, which collectively have a low probability of occurring, have to exist in order for a planet to have an atmosphere like the Earth's – an atmosphere that is capable of supporting life and which has a temperature range over which water can undergo phase changes from solid, to liquid to gas (Figure 1.83). For the bulk of Earth history, these conditions have kept our planet from becoming either a frozen ball or an inferno. They ensure that our atmosphere is not toxic to life.



Figure 1.83. Silhouette of the space shuttle Endeavour taken from the International Space Station on February 9, 2010. The lower layers of the atmosphere are well defined by color variations. Orange is the lowermost 10 or so miles (16 km), followed by the stratosphere in yellowish white, and transitioning into the mesosphere and thermosphere. The essential components of Earth's life-support system are largely confined to the paper-thin lower-most layer. The Shuttle and space station orbit at about 210 miles (338 km) (Source/Credit: NASA).

These conditions require that delicate balances be maintained between the atmosphere's composition, thickness and temperature. These balances are occasionally upset and result in conditions that are either colder than the current global climate, such as the Pleistocene Ice Ages, or warmer than present, such as the late Eocene climate when tropical and subtropical plants grew near the North Pole. If any of these balances were to change significantly, the life support system would be altered. **At the very least, substantial changes in the atmosphere or in the Sun's energy output would radically alter weather and climate, thereby creating substantial changes in ecosystems, agriculture, human health and civilization.**



The Earth's atmosphere is a physical mixture of gases, solids and liquids. Most gases in the lower atmosphere exist in constant proportions because of mixing by the wind. The gases that comprise the troposphere, roughly the lower-most 8-10 miles of the atmosphere, can be classified as being either variable or non-variable in terms of relative proportions.

## Non-Variable Gases

Non-variable gases occur in constant proportions in the lower atmosphere. Their relative proportions do not change significantly over years or decades or from one place on Earth to another. Over geologic time scales, the relative abundance of these gases has changed due to processes such as early impacts of meteors and comets, volcanic outgassing, sequestration of some gases by sedimentation, chemical reactions, and photosynthesis.

**Nitrogen** (N<sub>2</sub> — diatomic nitrogen). Nitrogen comprises 78%, by volume, of the atmosphere and is therefore by far the most abundant non-variable gas (Figure 1.84).

Variable and Non-Variable Constituents of the Troposphere			
Non-Variable	(%)	Variable Gases	(%)
N <sub>2</sub>	78.08	H <sub>2</sub> O	0.1 to 4.0
O <sub>2</sub>	20.95	O <sub>3</sub>	trace
A	0.93	SO <sub>x</sub>	trace
CO <sub>2</sub>	0.040	NO <sub>x</sub>	trace
Others*	<0.032	Others Aerosols (dust, ash, pollen, salt)	

\*Varies seasonally and has increased overall from 0.028% to 0.040% in the past 200 years.

Figure 1.84. The atmosphere is composed primarily of the non-variable and variable gases. For thousands of years, carbon dioxide remained in relatively constant proportion, with the exception of seasonal variations in concentration. It has long been listed as a non-variable gas. However, the use of fossil fuels, which began with the Industrial Revolution, has led to a gradual increase in the amount of carbon dioxide from 280 to 397 ppm (2014). Carbon dioxide is listed here as a non-variable gas only because of convention; it can now be listed as a variable gas. The continued use of fossil fuels is expected to double the carbon dioxide level by around 2050 (Source/Credit: modified from several sources)

Nitrogen gas is relatively inert, which means that it is not as chemically reactive as other atmospheric constituents such as water vapor or sulfur oxides. As a result, it has a longer **residence time** (average time in the atmosphere) than many other gases and aerosols in the atmosphere.

Nitrogen comprises less than 1% of living matter, but it is essential for life, especially plant life. However, because of its chemical properties, it is normally not directly available to plants from the atmosphere. This means that it must be converted into a form that can be used by plants by combining with other elements to form useful compounds. These compounds must then enter the soil or they must form in the soil in order for them to be available to plants.

Small amounts of nitrogen ( $N_2$ ) are converted to monatomic nitrogen (N) by processes such as lightning and bacterial action.

**Lightning**

The multi-thousand degree temperatures generated during a lightning strike dissociate the  $N_2$  molecule to form two nitrogen atoms. These can then combine with oxygen atoms to form nitrogen oxides. These, in turn, react with water and fall from the sky to the Earth and enter the soil where they act as a fertilizer.

**Bacterial action**

Bacteria in the soil and in symbiotic relationships with plants (such as clover, alfalfa, peas, beans, cycads and ginkgos) provide the main natural source of fixed nitrogen.

**Oxygen** ( $O_2$ ). Oxygen makes up 21% of the atmosphere and is essential to the respiratory processes of plants and animals. The amount of oxygen in the atmosphere is critical to life.

For example, the probability of a forest fire being started by a lightning flash increases by 70% for each 1% rise in oxygen concentration above the present level. An oxygen level of only a few percent above the present level would destroy much of the continental vegetation by wildfires.

The Earth's atmosphere has evolved over its 4.6 billion-year history. Several developmental stages have added, deleted, or changed many atmospheric constituents from their primordial abundance (Figures 1.85a, 1.85b and 1.85c). The amount of  $O_2$  has increased through time due to photosynthesis (Figure 1.86). Early in the Earth's history, there was very little free oxygen in the atmosphere. Once photosynthetic organisms evolved, oxygen began to accumulate and may have reached 1% of present level by 2 billion years ago. Ironically, the initial appearance of oxygen was deadly to many organisms because it reacts with organic molecules and breaks them apart (respiration). Life initially had to evolve defenses against the very gas that is now crucial to our existence! As photosynthesis continued, the amount of oxygen approached present day levels by about 500 million years ago.

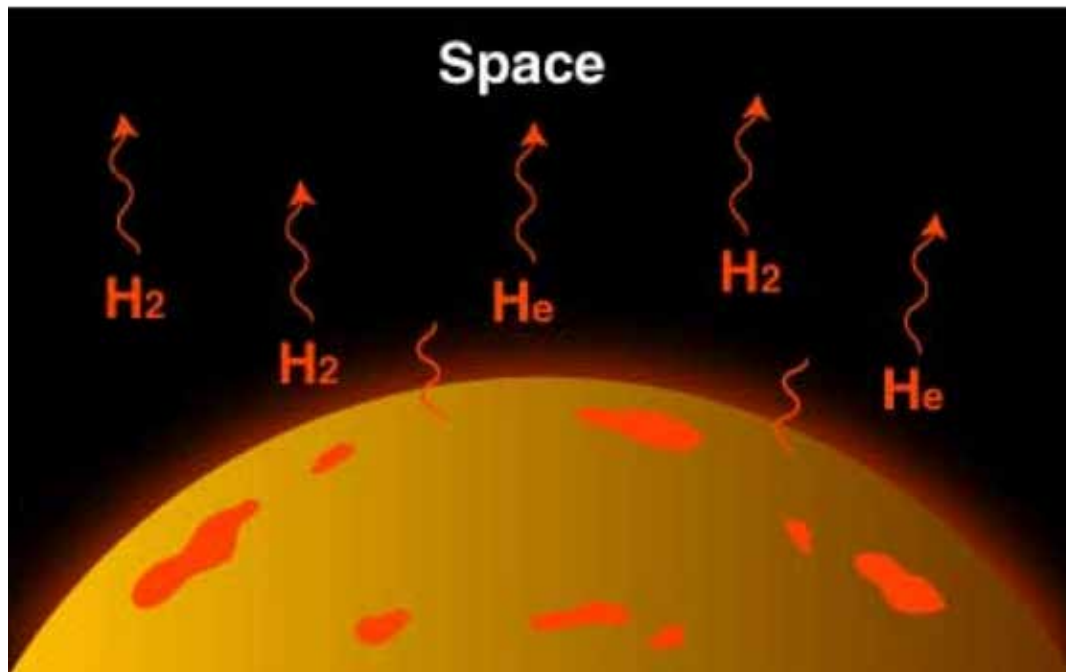


Figure 1.85a. Stage 1. The early atmosphere of the Earth was accreted from the protoplanetary disk and probably consisted mostly of hydrogen and helium. The early atmosphere was hot, and most of the lightweight gases escaped to space (Source/Credit: NASA JPL).

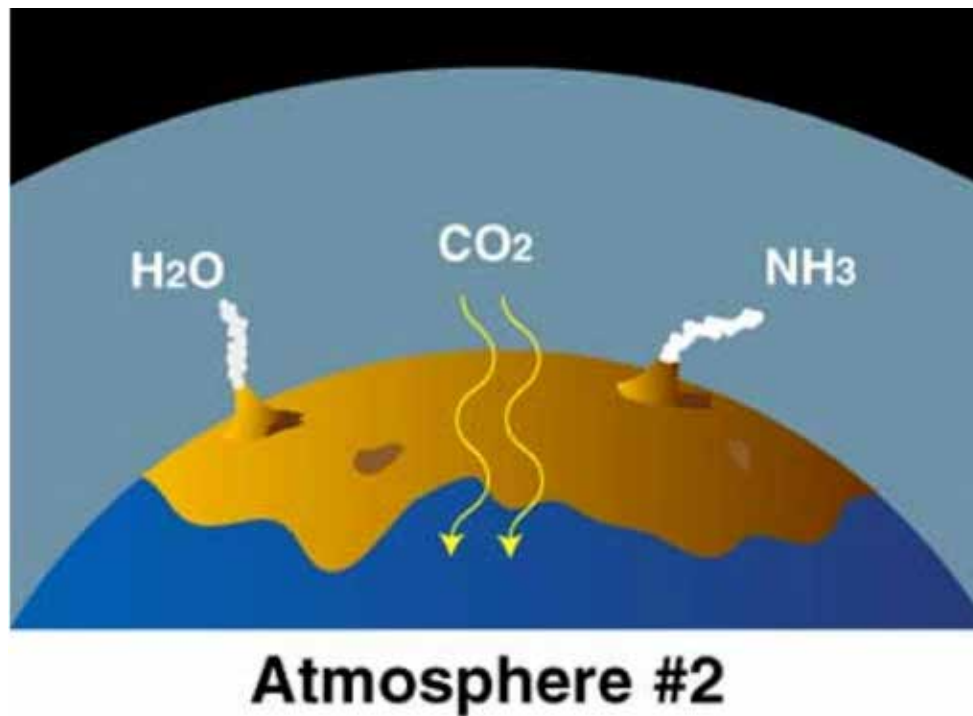


Figure 1.85b. Stage 2. Volcanic outgassing replaced the Earth's primary atmosphere by a secondary atmosphere rich in water vapor ( $\text{H}_2\text{O}$ ), carbon dioxide ( $\text{CO}_2$ ), and ammonia ( $\text{NH}_3$ ). Early oceans sequestered large amounts of carbon dioxide, preventing a runaway greenhouse such as that of Venus. The fossil record indicates the presence of marine organisms at least 3.8 billion years ago, providing a source of free oxygen to the primitive atmosphere. Some of the oxygen diffused into the stratosphere, reacted with sunlight, and began to form the protective ozone ( $\text{O}_3$ ) layer allowing other organisms to live on the surface and in the upper-most ocean water (Source/Credit: NASA JPL).

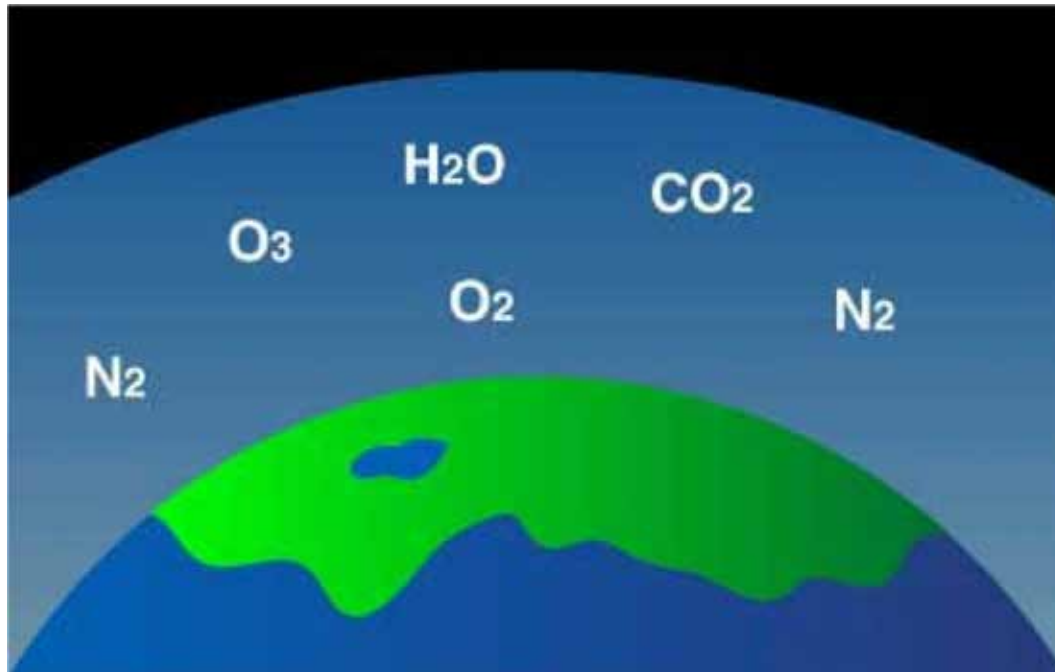


Figure 1.85c. Stage 3. Volcanic outgassing has continued throughout most of Earth history replenishing some of the compounds ( $H_2O$ ,  $CO_2$ ,  $NH_3$ ) lost to space or to sedimentation or to chemical reactions. The oceans, now teeming with life, stored vast amounts of carbon dioxide as carbonate sediment on the sea floor. About 550 million years ago, land plants became established, and add oxygen as well as taking in carbon dioxide. Photosynthesis became the dominant process in bringing oxygen levels to their present status. Some of the oxygen diffused into the stratosphere, reacted with sunlight, and began to form the protective ozone ( $O_3$ ) layer which allowed other organisms to live on the surface and in the upper-most ocean water (Source/Credit: NASA JPL).

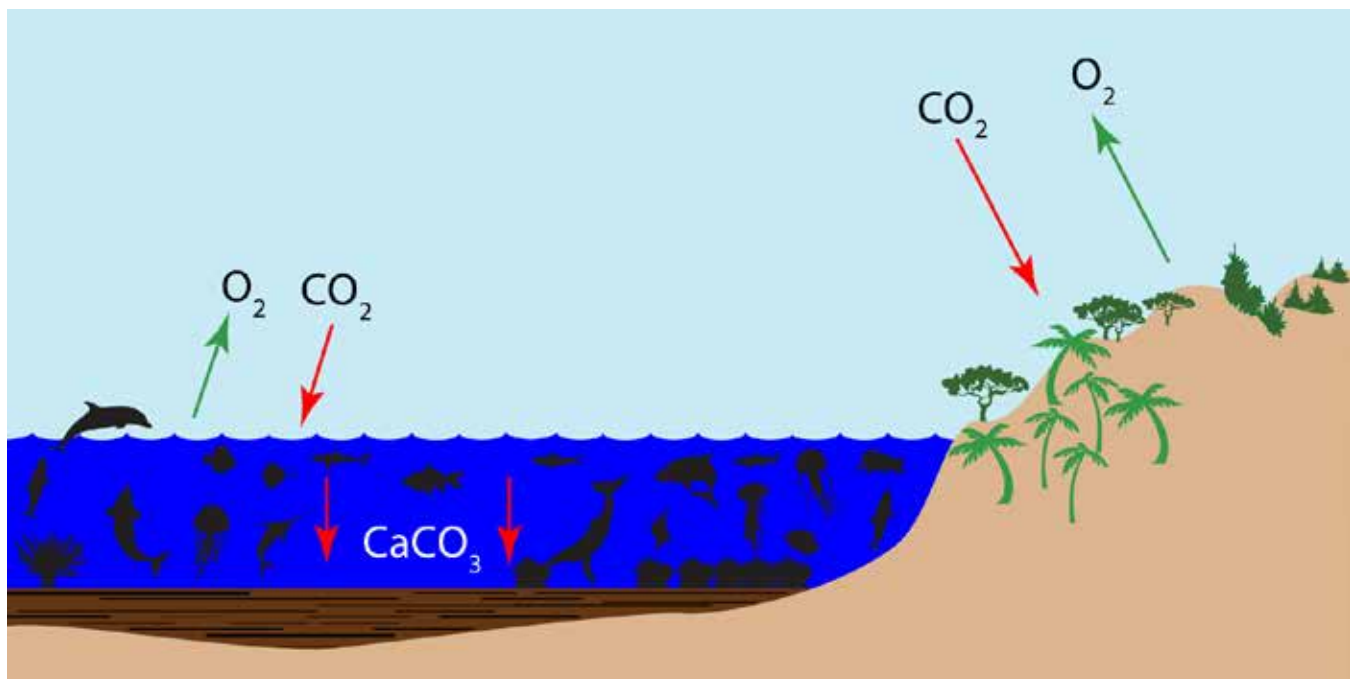


Figure 1.86. For the last 550 million years, oxygen and carbon dioxide levels have been roughly balanced by processes such as photosynthesis and sequestration of carbon dioxide by carbonate sedimentation on the ocean floor. The green plants (primary producers) of the marine and terrestrial ecosystems remove  $CO_2$  and give off  $O_2$  (Source/Credit: Dennis I. Netoff).

The presence of oxygen was also critical to the development of life on Earth because  $O_2$  reacts with oxygen to form ozone ( $O_3$ ). Ozone serves as a shield against harmful ultraviolet radiation that can cause genetic damage. Without the ozone shield, surface life in oceans and on land would have had a great deal of difficulty developing, particularly vascular land plants. In the absence of an ozone layer, only deep marine environments are protected from ultraviolet radiation because water serves as a shield. Therefore, without the ozone shield, life could not have emerged from the sea because these creatures would not have been protected from deadly ultraviolet radiation. Amphibians, reptiles, dinosaurs, birds and other creatures would probably never have evolved, including humans.

Note that just two elements, nitrogen and oxygen, comprise 99% of atmospheric gases. All of the rest make up less than 1%.

**Argon.** This gas comprises 0.93% of the atmosphere. It is formed by the radioactive decay of radon, and it is very inert. So, just three gases comprise 99.93% of the atmosphere. The remainder comprises less than 0.07%; but, as we shall soon see, a small amount does not equate with insignificance.

## Variable Gases

These gases exist in variable quantities in the atmosphere. Although they comprise a very small proportion of gases (1 to 5% collectively) they are, nonetheless, very important for the maintenance of life.

**Water Vapor** ( $\text{H}_2\text{O}$  gas). The amount of water vapor in the air varies with both availability and with temperature. Obviously, sources of water (such as oceans, lakes, streams, plants and wet soil) must be available in order to supply water to the air, and the closer the proximity to the source, the greater the amount that can potentially enter the air. Temperature controls the amount of water vapor that will actually enter the air from a source because temperature controls the rate of evaporation. The hotter the air, the greater the amount of evaporation. Thus, air over a tropical sea can contain more moisture than air over a polar sea because of the higher temperatures over the tropical sea. By way of comparison, cold air in polar regions contains as little as 0.1% water vapor, whereas warm air in the tropics contains as much a 4.5%, a 40-fold difference! The lower atmosphere averages 1.4% water vapor.

The amount of water vapor decreases in quantity rapidly with altitude for two reasons. First, as height increases the distance from potential sources, all of which are at the surface, increases. Secondly, as wet air laden with moisture rises upward into the atmosphere, it cools. As it does so, the moisture within it also cools and eventually condenses. Once it condenses, it can fall as rain or snow. In short, precipitation removes water from the air which leaves very little in the upper atmosphere. At approximately 8 to 10 miles above the Earth's surface, there is a layer of the lower atmosphere several miles thick that prevents any significant exchange of gases to the air above, so most of the moisture in the atmosphere is confined to this very thin envelope of air called the troposphere.

Water in the troposphere is not only important as the main ingredient of dew and frost, clouds, rain and snow, but it also is essential for most forms of life. Approximately three-fifths (60%) of our bodies are made of water. Water vapor also releases huge amounts of energy as it condenses and it is the principle source of energy driving severe storms. Water is a major greenhouse gas that indirectly traps heat energy from the Sun and thereby contributes to maintaining a relatively warm troposphere.

**Carbon Dioxide** (CO<sub>2</sub>). Oxygen and carbon dioxide are constantly cycled in the biosphere by photosynthesis (Figure 1.86). Unlike Venus and present day Mars, the Earth has vast ocean basins, and much of the carbon dioxide that would have otherwise accumulated in the atmosphere, has been removed and stored as carbonate rocks on the ocean floor.

The amount of carbon dioxide varies seasonally because of changes in the amount of photosynthesis that occurs over the course of the year (Figure 1.87). During summer, growing plants remove carbon dioxide during photosynthesis and this decreases the quantity of carbon dioxide. During winter, when plants become dormant, the level of carbon dioxide increases. Because there is more land and, therefore, more plants in the Northern Hemisphere, the seasons in the Northern Hemisphere play a larger role in controlling the amount of carbon dioxide in the atmosphere than do seasons in the Southern Hemisphere.

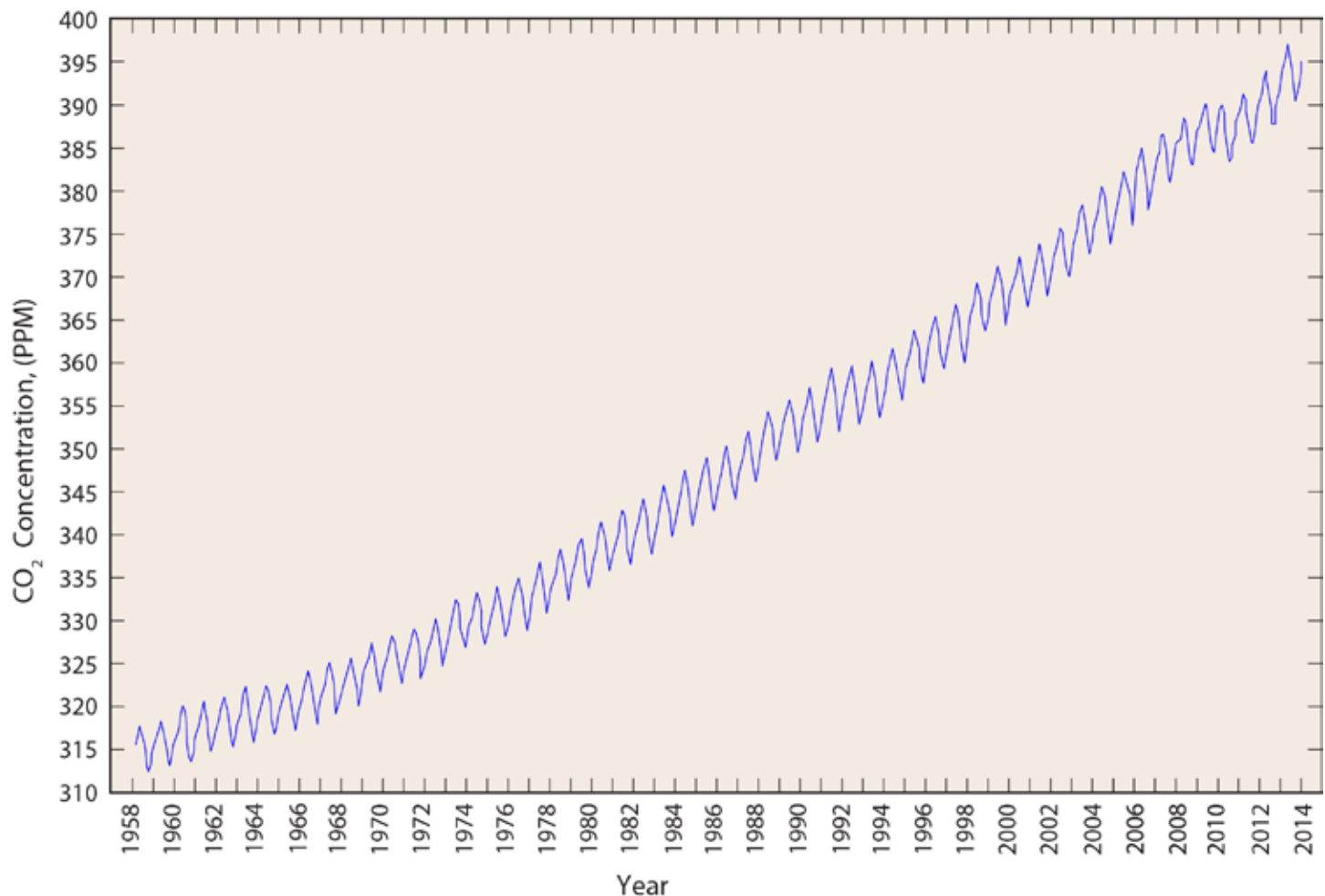


Figure 1.87. The seasonal and decadal variation of carbon dioxide in the atmosphere based mainly from readings at the Mauna Loa Observatory in Hawaii. Maximum concentration occurs during Northern Hemisphere winters when plants are dormant and are not taking in carbon dioxide. Carbon dioxide levels have risen primarily as a result of the burning of fossil fuels, the stubble in agricultural fields, and forests. In the summer of 2013, the CO<sub>2</sub> content momentarily reached 400 ppm, the highest it has been in several hundred thousand years (Source/Credit: NOAA).



Approximately half the dry weight of plant matter is composed of carbon derived from carbon dioxide in the atmosphere. This means that plants remove carbon dioxide and thereby serve as a sink for carbon dioxide. Therefore, when we cut forests we remove a carbon dioxide sink and this results in an increase in the amount of carbon dioxide in the atmosphere. Burning forests in order to convert them to agricultural land also releases the carbon stored in the plant tissues. The world's rainforests are being cut down at an rapid rate and this process will undoubtedly play an important role in global carbon dioxide levels throughout the 21<sup>st</sup> century.

Carbon dioxide and other greenhouse gases raise Earth's average temperature about 55°F. So, even though carbon dioxide comprises only about 0.040% of the atmosphere, it helps prevent our planet from becoming a frozen wasteland. Carbon dioxide is second only to water vapor as a greenhouse gas.

Trace gases such as methane also contribute to the greenhouse effect and seem to be increasing in abundance over the past few decades. Global carbon dioxide levels are rising as a result of fossil fuel combustion and the removal of trees.

Although small quantities of carbon dioxide in the atmosphere are beneficial, excessive levels may pose problems. At concentrations above 1%, carbon dioxide becomes toxic to some animals; at 8%, vertigo and dizziness may occur; and at 9% it can be fatal.

Carbon dioxide is removed from the atmosphere by the following processes:

Photosynthesis, which converts carbon dioxide into plant tissue.

Storage in plant tissues and in plant materials that become buried and converted to coal.

Solution in seawater. Once dissolved in water, it can react with calcium to form calcium carbonate which is more commonly known as limestone. Limestone strata found throughout the world are the remnants of ancient ocean floors and are huge reservoirs of carbon dioxide.

**Ozone** (triatomic oxygen —  $O_3$ ). Ozone (0.0006%) is abundant in the stratosphere at an altitude of 10 to 40 miles. It forms naturally when high-energy cosmic rays from space strike the atmosphere and cause  $O_2$  molecules to split and then recombine to form  $O_3$ .

Because ozone is unstable and readily converts to diatomic oxygen ( $O_2$ ) by losing one of its oxygen atoms, it must be continuously replenished by the process just described. The ozone concentration is variable because it decreases in winter and increases in summer as a result

of complex chemical processes that occur high in the stratosphere. These processes are more intense at lower temperatures, so the colder it is the more ozone that is destroyed.

Ozone in the stratosphere protects life by absorbing potentially lethal cosmic and ultraviolet radiation which is capable of penetrating the cells of our bodies and causing biological damage, including cancer and death (Figure 1.88).

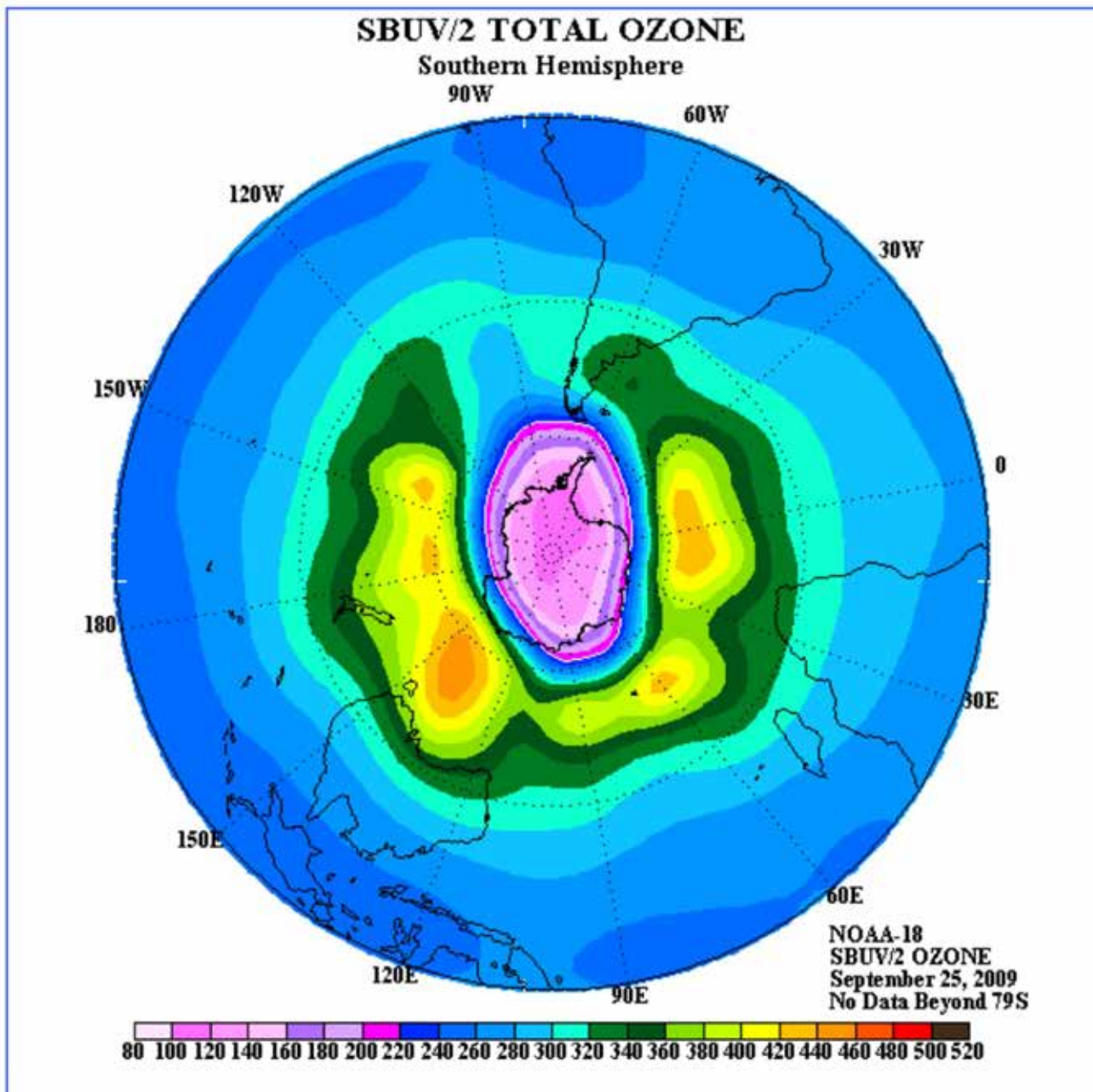


Figure 1.88 The ozone hole forms when man-made chemicals such as chlorofluorocarbons rise into the stratosphere and destroy ozone molecules. Because this process is favored by cold conditions, the stratospheric air above Antarctica experiences the largest decline in ozone resulting in the formation of an ozone 'hole.' The hole is actually a region of low ozone levels. When the hole develops, more ultraviolet radiation reaches the surface of the Earth and can have adverse impacts on organisms. The image indicates the ozone levels, in Dobson units, for September 25, 2009. The ozone levels over the South Pole have been monitored accurately since 1979 at which time the minimum levels were approximately 225 Dobson units (Source/Credit: NASA).

Tropospheric ozone (lowermost 10 miles or 16 km of the atmosphere below the stratosphere) is largely anthropogenic and is in much higher concentrations in urban and industrial regions. Tropospheric ozone, long known as an irritant, but largely ignored as a greenhouse gas in the troposphere, has been listed as the fourth most important tropospheric greenhouse gas in the most recent assessment by the Intergovernmental Panel on Climate Change (2013 IPCC), trailing only water vapor, carbon dioxide, and methane.

## Aerosols

**Aerosols** are tiny solid or liquid colloidal particles in the atmosphere. Aerosols have natural sources as well as anthropogenic sources. They are typically smaller than one micron in diameter, so may be kept aloft in the atmosphere indefinitely (Figure 1.89). Many aerosols play a role in atmospheric heating and cooling, although their exact role is poorly understood.

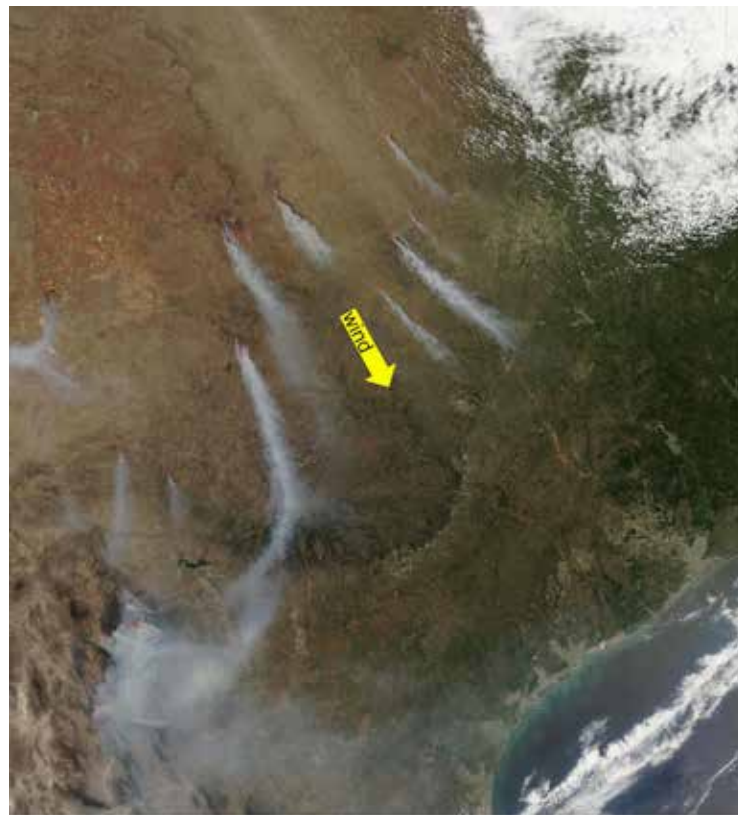


Figure 1.89. In 2011, extreme, high temperatures, and strong winds created the worst wildfire year in Texas' history. Smoke plumes extended for hundreds of miles, affecting distant locations with irritating smoke. NASA's MODIS satellite imaged these wildfires on April 15, 2011. Large dust plumes can be seen originating north of the cluster of fires. Most of the fires shown were over 10,000 acres. The long, curved smoke plume is about 300 miles (~500 km) long (Source/Credit: NASA GSFC).

Aerosols include a long list of substances, such as fine dust, volcanic ash, smoke, sulfides, fly ash, organic carbon, and sea salt. Natural sources include dust, smoke, volcanic ash and sulfuric acid droplets, and sea salt. Anthropogenic sources include hydrocarbons, fly ash, agricultural/grazing dust, acid droplets from industrial sources, and smoke. They are temporary additions to the atmosphere that are derived largely from Earth's surface, although some also come from space. They are temporary additions because they eventually settle to the ground under the influence of gravity. Particulates are variable in quantity because of both the nature of the sources from which they are derived and variations in rates at which they settle to the surface. Some of the sources of particulates are:

**Meteoric Dust.** Up to 10 tons of meteorite dust falls on the Earth each day (Figure 1.90).



Figure 1.90. The Willamette Meteorite is an iron-nickel meteorite that was discovered in Oregon. It is the largest found in North America at about 32,000 pounds. Most meteors are smaller and burn up in the atmosphere, but may still contribute dust to the Earth's surface and atmosphere (Source/Credit: American Museum of Natural History).

These pieces of rock are traveling at tens of thousands of miles per hour when they strike the atmosphere. Frictional heating occurs as they plummet through the air and most burn up and form fine particles of *ash* that eventually settles to the ground (Figure 1.91). *Shooting stars* are actually meteors that may have originated during the earliest phases of the formation of the solar system some 4.6 billion years ago. The next time you see a meteor streaking across the night sky, think about the fact that the small piece of rocky debris that is burning up before your eyes has been circling the Sun for 4.6 billion years. Its billion-year existence ends in a bright flash of light in a matter of seconds. You may be the only witness to its multibillion-year existence.



Figure 1.91. Meteors are heated to incandescence by friction as they enter the Earth's atmosphere. Without a protective atmosphere, the Earth's surface would be pelted by scores of meteors daily. Meteors and comets have added considerable mass to the Earth over the past 4.6 billion years (Source/Credit: NASA).

Larger meteorites can survive their fiery fall through the atmosphere and hit the ground as a solid mass of rock. Smaller ones barely make an imprint on the ground; but the larger ones can wreak havoc. A meteorite a mile across can cause devastation over an area the size of a continent as a result of shock waves, ejected debris and fires. One just 5 to 10 miles across could wipe out most life on Earth as has happened in the past. Fortunately for us, these large impacts are rare and astronomers are now scouting the heavens in search of these potential planet-destroyers in hopes that they can be detected and possibly diverted away from the Earth.

**Volcanic Dust.** Individual volcanic eruptions can inject millions of tons of ash and gases into the atmosphere in a short period. Fine ash can take years to settle out (Figure 1.92). Volcanic ash and some volcanic gases can affect climate by changing the amount of sunlight that reaches the Earth's surface. Very large volcanic eruptions have the potential to radically alter the Earth's climate and could significantly impact civilization if the food supply and global economy were sufficiently disrupted.



Figure 1.92. Eruption of Chile's Puyehue-Cordon Caulle Volcanic Complex in June of 2011 sent thousands of tons of ash into the atmosphere. A shift in the wind direction several hours prior to this image caused the kink (right-angle bend) in the ash plume. The total length of the plume on this satellite image is ~1000 miles (~1600 km) (Source/Credit: NASA/GSFC/Jeff Schmaltz/MODIS Land Rapid Response Team).

**Wind-Blown Surface Material.** As land on the Earth is cleared for agriculture, the amount of soil exposed to wind erosion increases. This elevates the dust concentration in the atmosphere and affects its transparency and heat-trapping properties. Some of the dust can travel oceanic distances (Figures 1.93a and 1.93b). Dust from Africa sometimes reaches the east coast of North and South America.

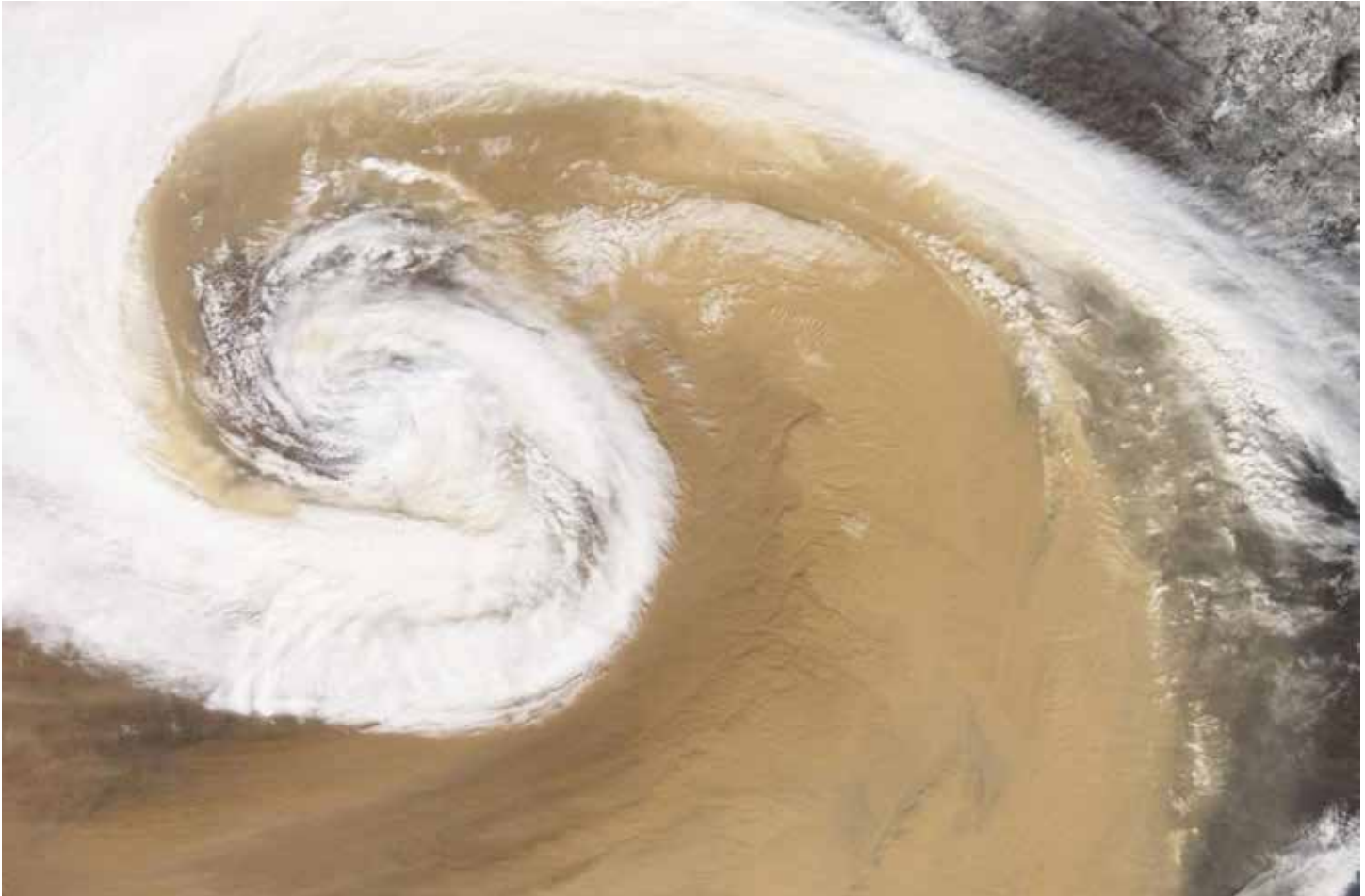


Figure 1.93a. China is famous for its dust storms, most of which originate in the drier, western part of the country. The duststorm in this image was due to the passage of a frontal cyclone in 2001. The white band of clouds is approximately 120 mi (200 km) in diameter (Source/Credit: NASA).



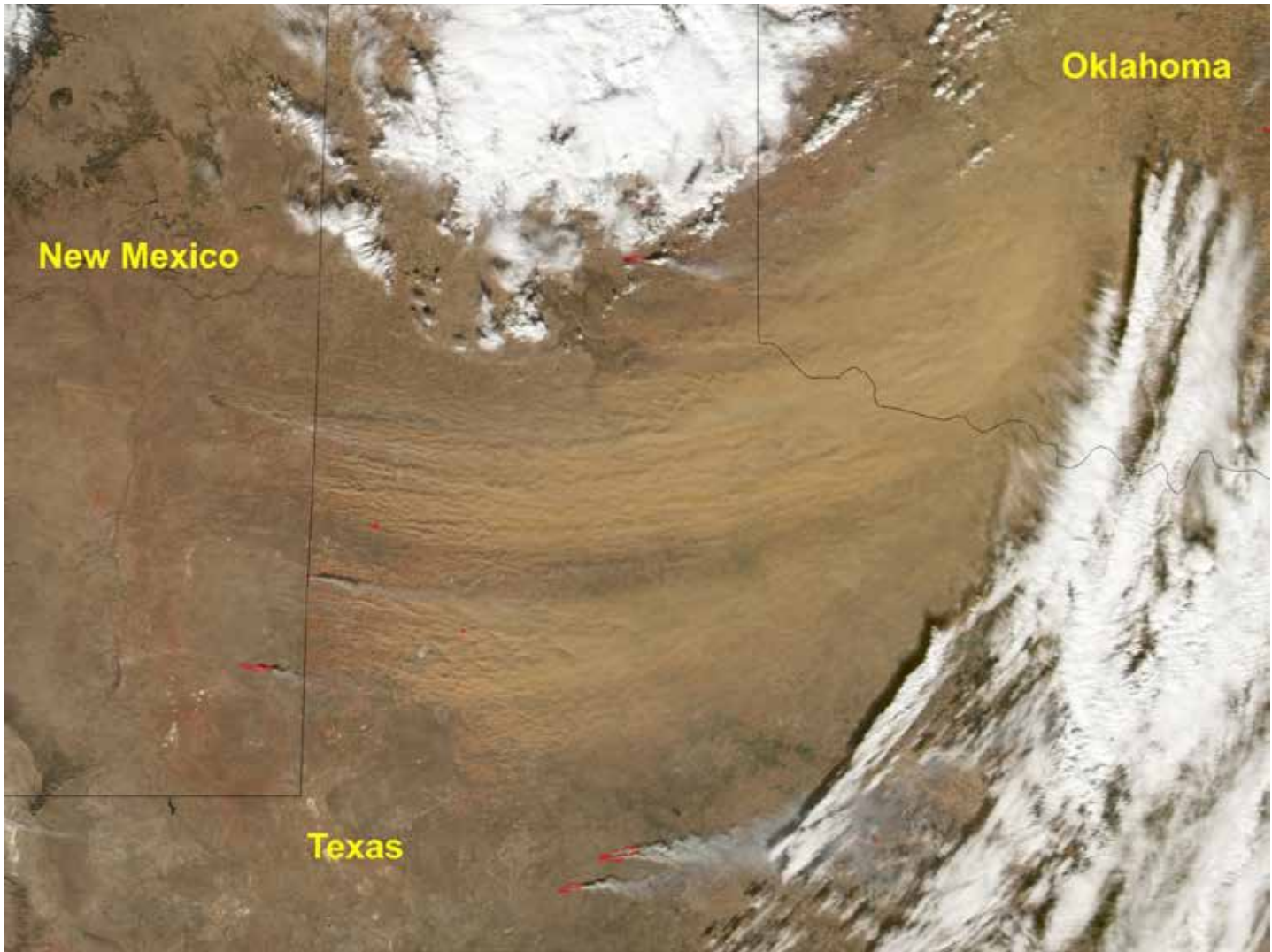


Figure 1.93b. The January 1, 2006 dust storm in New Mexico, Texas and Oklahoma was the result of very strong winds and prolonged drought. The dust plumes extend for more than 300 miles (500 km). In many places, the dust layer is so thick and dense that the ground cannot be seen. Several wildfires are adding smoke to the dust plumes (Source/Credit: USGS).

Some of this dust from Africa carries soil bacteria that can kill coral in the Caribbean. During the past four decades, North Africa has become drier, so more dust has become airborne and more of it travels to tropical seas where the microbes it carries attack coral reefs leaving many dead or weakened (Figure 1.94). On the other hand, windblown dust from Africa helps to maintain the soil fertility in the tropical rainforests of Central and South America. The atmosphere connects everything on the Earth.



Figure 1.94. The marine ecosystem is affected in many ways by human activities, including global warming, ocean pollution, pathogens in wind-blown dust, overfishing, and acidification. The United States Geological Survey is studying the impact of windblown dust and increasing CO<sub>2</sub> levels in the atmosphere here in the Virgin Islands. The ocean absorbs 22 million tons of CO<sub>2</sub> per day and that number has increased in the past few decades. More dissolved CO<sub>2</sub> means more carbonic acid (H<sub>2</sub>CO<sub>3</sub>) which can adversely affect calcium-building organisms such as coral reefs, lobsters, clams, snails, oysters, and phytoplankton (Source/Credit: USGS).

**Smoke from Fires.** Forest and grassland fires are increasing the smoke concentration in our atmosphere. Many of these fires are caused by people as they cut and burn forests to create agricultural land and burn the stubble in harvested rice paddies in order to prepare the land for the next year's planting. In the summer of 1998, the smoke from fires in Indonesia was so great that visibility was significantly impaired over tens of thousands of square miles. People became sick and an airplane crash occurred because the pilots could not see the runway.

Smoke from fires in Central America in 2000 caused visibility and health problems in the United States. Over the relatively short era of the space age, the transparency of the atmosphere has decreased because of smoke from fires, as well as other forms of pollution. In the early part of the 21<sup>st</sup> century, smoke produced from the burning of fossil fuels in China significantly affected the air quality in the western United States.

Wildfires in California during the summer and fall of 2013 scorched hundreds of thousands of acres. The Rim Fire in the central Sierra Nevada was out of control for over two months, and caused air quality problems at Lake Tahoe, Carson City and Reno multiple times (Figure 1.95).

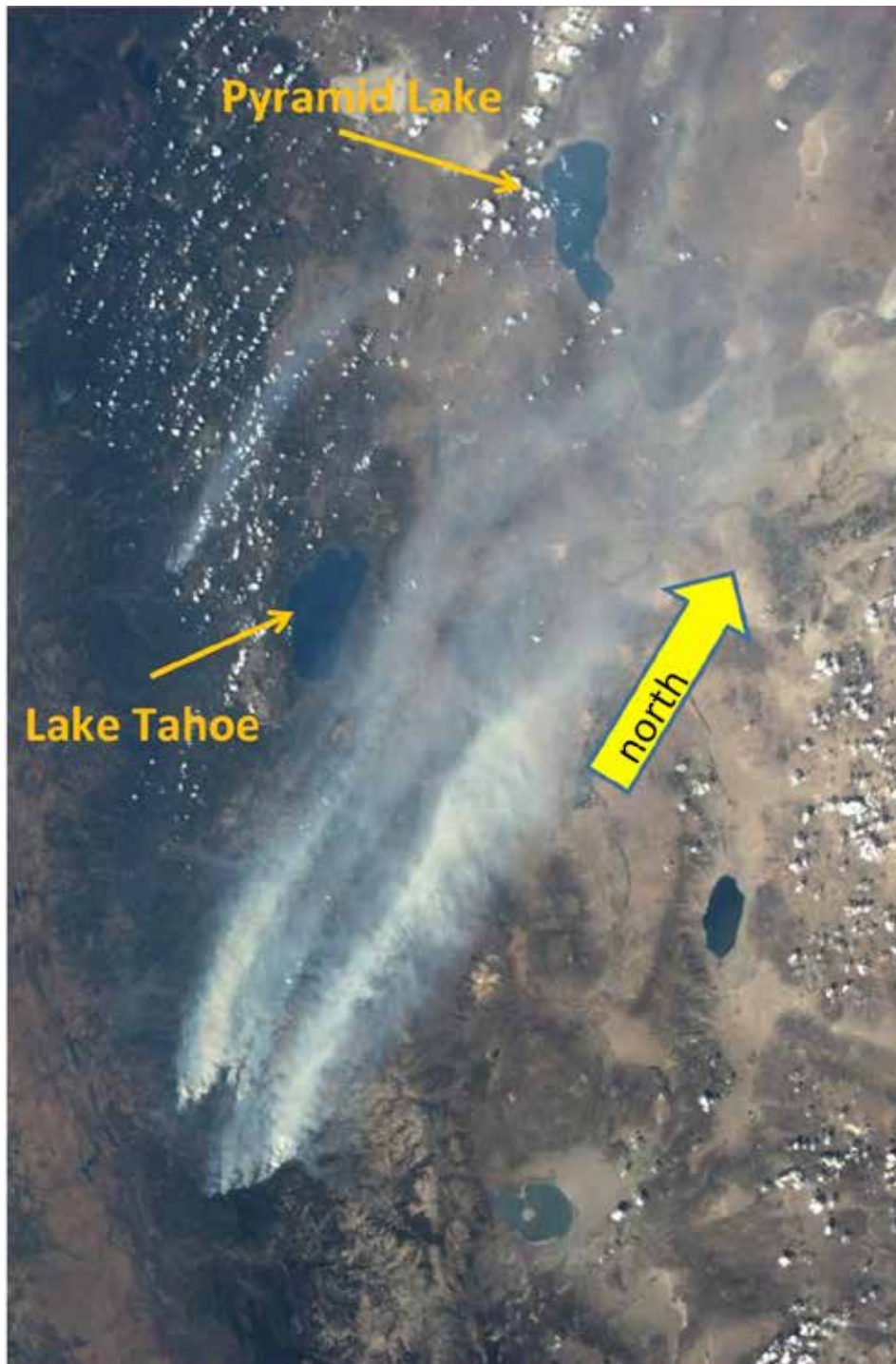


Figure 1.95. Rim Fire on August 27, 2013. Smoke plume could be traced on this photo from its source in Yosemite Valley, California northward to Pyramid Lake, Nevada, 150 miles due north. The air quality in Reno, just southwest of Pyramid Lake, went to dangerous levels several times prompting Reno schools to close down and relocate sporting events. The wildfire was the largest on record in the Sierra Nevada, burning over 400 square miles (~1000 km<sup>2</sup>). It began on August 17, 2013 and was finally declared under control on October 24 (Source/Credit: NASA).

**Salt Crystals from Sea Spray.** When sea spray is blown into the air, some of it evaporates and leaves behind salt that can remain suspended in the air (Figures 1.96a and 1.96b). This is why sunsets along the coast are so often beautiful and it is also why cars located in coastal areas rust more quickly than those in the interior do.



Figure 1.96a. Coast Guard at Morro Bay, California approaching a breaking wave near the coast. Breaking waves and white caps out at sea account for the injection of millions of tons of salt into the atmosphere every day. In the open ocean, windblown white caps also inject massive quantities of salt into the air (Source/Credit: USCG).



Figure 1.96b. Coast Guard at Morro Bay, California trying to navigate big surf during winter storm. The mast of the ship is nearly horizontal and the bow is barely visible over the crest of the wave (Source/Credit: USCG).

**Biological Materials.** Biological materials include bacteria, viruses, pollen, seeds, spores and even spiders (Figure 1.97). Some spiders can use filaments as sails that enable them to become airborne. Some arachnid flights are truly amazing, as spiders have been found floating at an altitude of 12,000 feet!

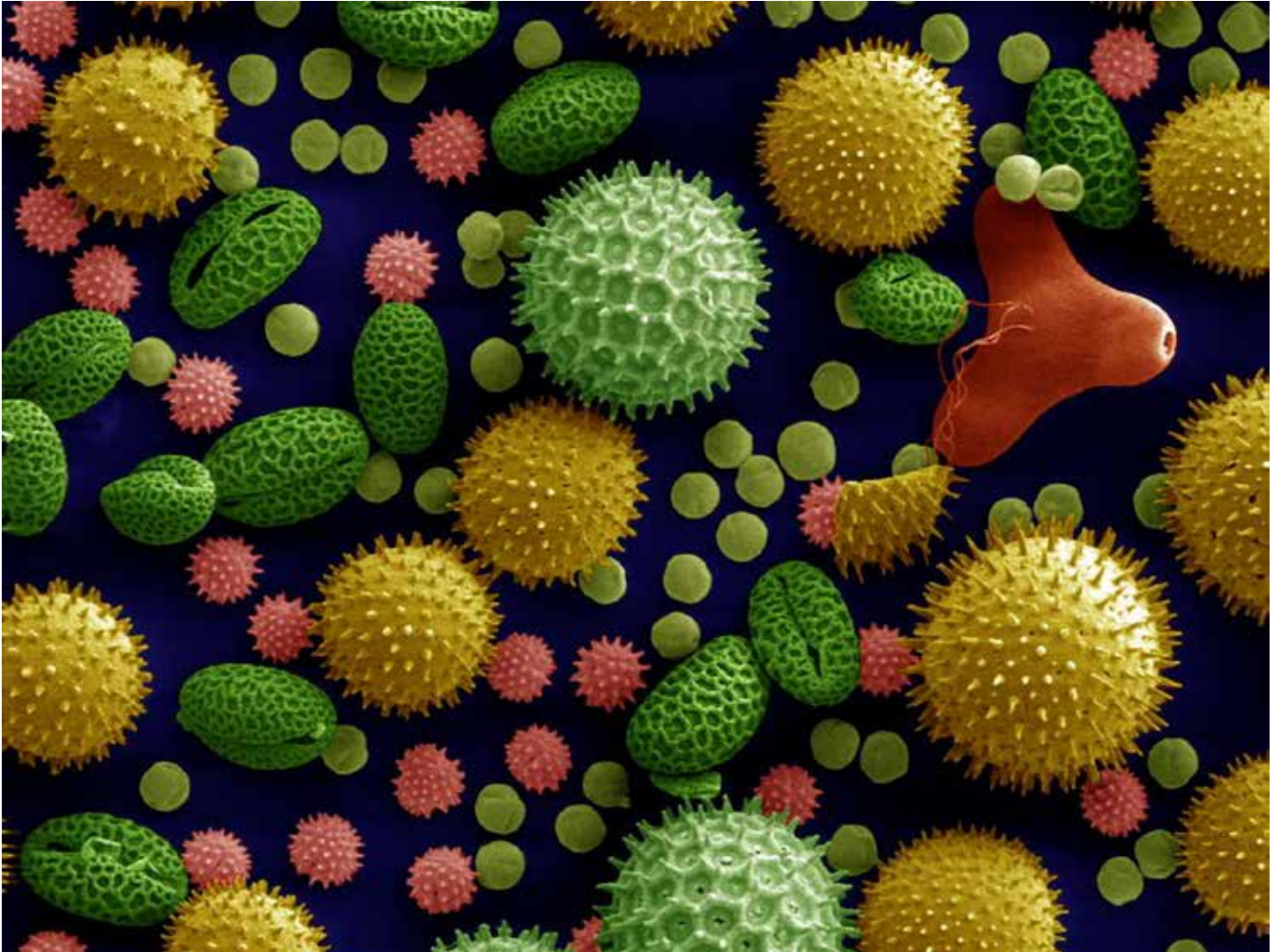


Figure 1.97. A pollen assemblage that includes common plants such as lily, sunflower, morning glory, hollyhock, primrose and castor bean. The magnification is 500x, and the oval green grain in the left corner is 50 microns long, or about twice the diameter of a human hair (Source/Credit: Dartmouth Electron Microscope Facility).

**Human Activities.** These include everything that humans are responsible for in the atmosphere, from factory and auto exhaust, to smoke from heating and cooking and smoke from fires. Indirectly, humans also contribute greatly to the amount of atmospheric dust through cultivation and overgrazing which leaves the land surface more susceptible to wind erosion.

## Vertical Zonation of the Atmosphere

The Earth's atmosphere is layered due to vertical temperature variations (Figure 1.98). These layers are known as thermal layers and the layering effect is referred to as **vertical zonation** (Figure 1.99).



Figure 1.98. The image of the sunset over the Indian Ocean taken from the International Space Station highlights the **vertical layers** of the atmosphere. The curvature of the Earth's surface is barely discernible. The **troposphere**, the lowermost layer of the atmosphere, is deep orange. It extends from the surface to an elevation of about 10 miles (16 km) in the mid-latitudes. The mottled pink and white layer above the orange layer is the **stratosphere**, extending to a height of about 30 miles (~50 km). The blue colors above the stratosphere include the **mesosphere** and **thermosphere**, gradually transitioning to the blackness of outer space (Source/Credit: NASA).

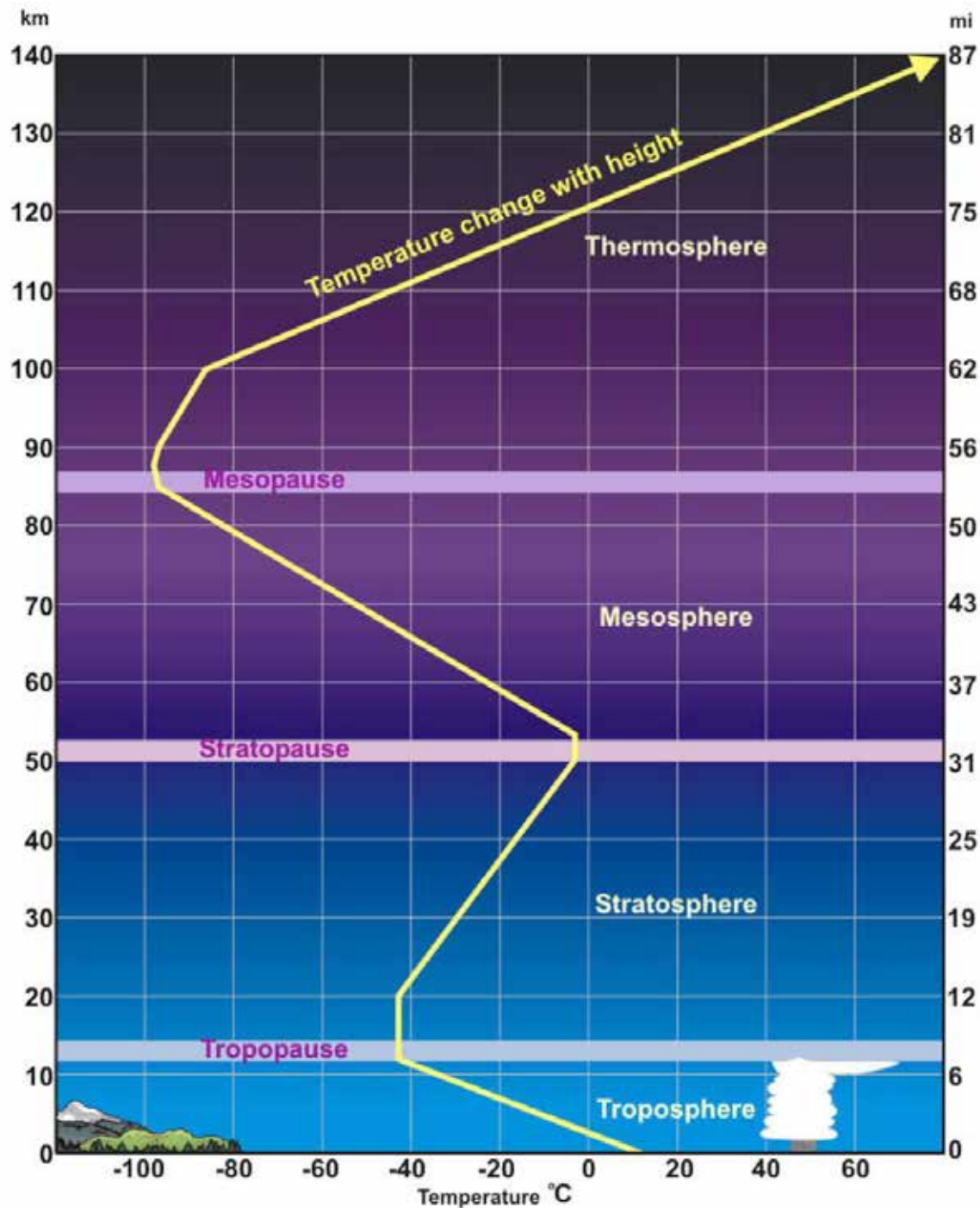


Figure 1.99. The four layers of the atmosphere, based on temperature changes (Source/Credit: NOAA).

The **troposphere** varies in thickness from about 5 miles in polar regions to 11 miles near the Equator. The altitude of the tropopause (the top of the troposphere) also varies seasonally. During the summer, heating tends to raise the tropopause whereas in winter cooling lowers it.

Before rockets and airplanes, scientists used balloons to ascend into the sky to take measurements and obtain air samples. Exploration such as this involves great danger — as the following account illustrates.



*In 1862, the British Association for the Advancement of Science sent two scientists, James Glashier and Henry Coxwell, up in a balloon to measure various properties of the troposphere. Following launch, they initially entered a thunderstorm from which they emerged at 10,000 feet. As part of their research, they released pigeons at various altitudes to determine the effects of oxygen deprivation and extreme cold on the ability of the birds to fly. Those pigeons released at 25,000 feet did not survive.*

*At 28,000 feet, Glashier and Coxwell realized that the cord to release gas from the balloon was entangled — which meant they had no way to stop going higher. As a result they, like the pigeons, began to experience severe oxygen deprivation and cold. Coxwell tried to climb out on the rigging to reach the release cord, but when he did, his hands instantly froze to the iron hoop that fastened the balloon to the gondola. Glashier then passed out around 30,000 feet (where there is only 1/3 the amount of air as at the surface). In desperation, Coxwell tried grabbing the release cord with his teeth and broke one of them. The second time he tried this approach, he caught the cord with his teeth but cut his cheek so badly that his mouth filled with blood and he became nauseated. In spite of this, he grabbed the cord with his teeth one more time and forcefully threw himself backward — freeing both the cord and his hands. Fortunately, he somersaulted into the gondola, and both men survived.*

The troposphere, although the thinnest layer, contains 80% of the total mass of the atmosphere. Half the mass of the atmosphere lies below 3.5 miles, which is lower than many mountain peaks. This is why mountain climbers attempting to reach the summits of Earth's higher mountains need to take bottled oxygen with them.

Within the troposphere, there is a rapid decrease in temperature with increasing altitude (Figure 1.100). The rate of decrease is known as the **environmental lapse rate**, and the average rate of decrease is called the normal lapse rate. The **normal lapse rate** is 3.5°F/1000 feet.

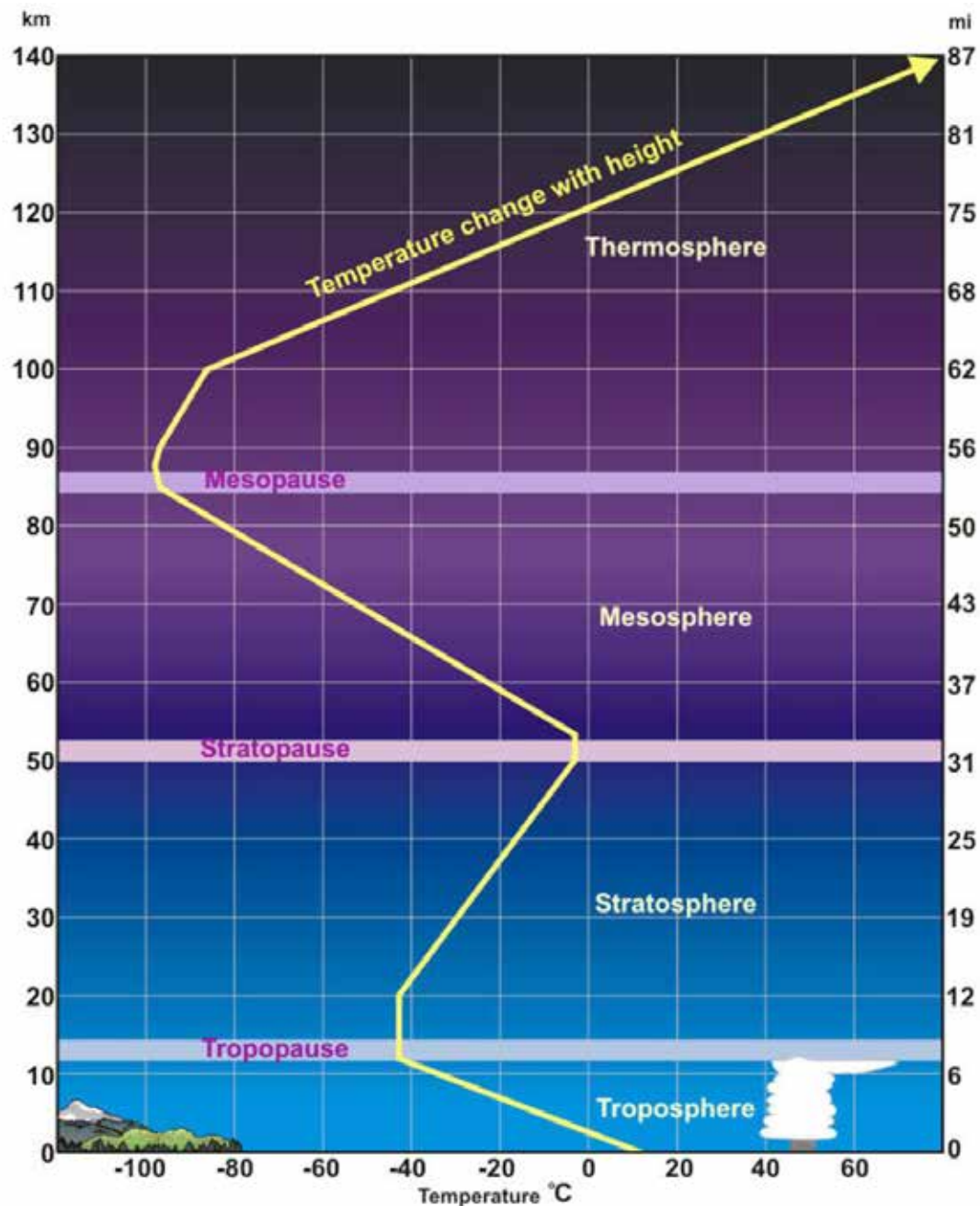


Figure 1.100. The troposphere is the lowermost layer of the atmosphere and is characterized by the vertical mixing of air which tends to promote constant composition. The vertical mixing occurs as warm air rises and cold air sinks. The altitude of the top of the layer varies both latitudinally and seasonally, and is highest when conditions are warmest; i.e., near the Equator and during summer. The altitude of the troposphere boundary shown in this diagram is an average value. Although this layer is the thinnest layer, it contains 80% of the mass of the atmosphere. All of the weather that we experience is confined to the troposphere (Source/Credit: NOAA).

Air in the troposphere is well mixed both vertically and horizontally. Horizontal temperature differences cause warm air to rise and cold air to sink and this mixes the air. As a result of this action, air also moves horizontally in the form of wind. This is because sinking air, when it moves toward the ground, must move outward in the horizontal direction. The prefix *tropo* means turning or changing. This mixing is also why the ratio of non-variable gases in the atmosphere remains constant. Most meteorological events, such as rain, snow, tornadoes and hurricanes are confined to the troposphere.

Above the troposphere lies a transition zone known as the **tropopause**. It is the transition zone between the top of the troposphere and the bottom of the stratosphere. In this zone, the temperature remains virtually the same for several miles, a zone called the **isothermal layer**. The lapse rate here is essentially zero. The temperature at the top of the troposphere ranges from minus 60°F to minus 110°F.

Immediately above the tropopause lies the **stratosphere** (Figure 1.101).

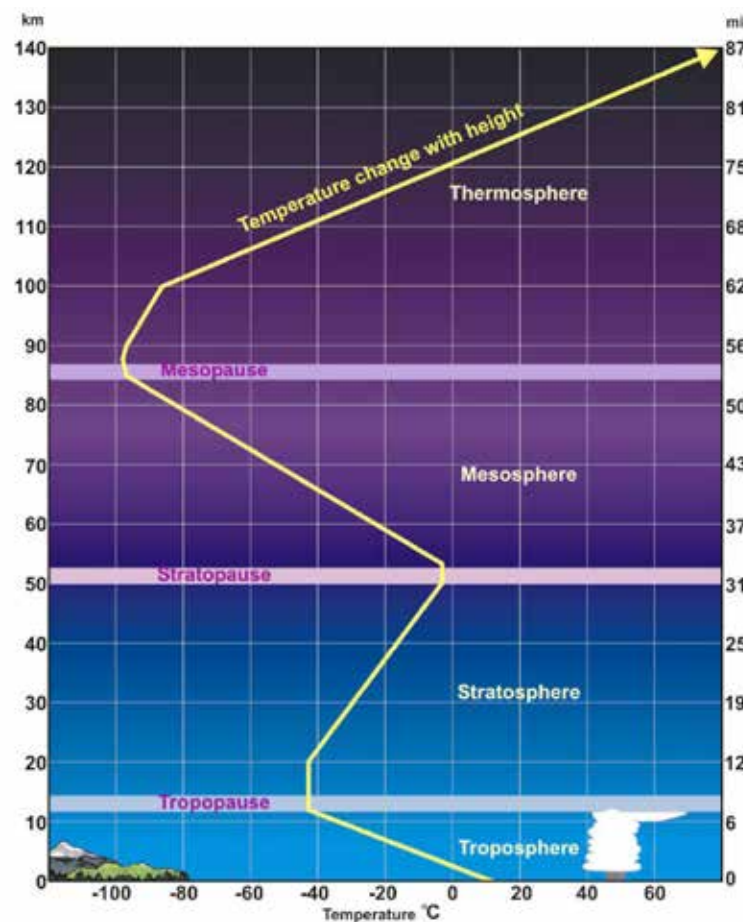


Figure 1.101. Within the stratosphere temperatures increase with increasing altitude as a result of the absorption of ultraviolet light by ozone molecules that are abundant in this layer. Because the stratosphere is warmer than the upper layer of the troposphere, air cannot readily rise into the stratosphere under normal conditions. In effect, this layer acts as a 'lid' that prevents air from the troposphere from rising to higher altitudes. As a result, the amount of water vapor in this layer is quite small and so the type of clouds that produce precipitation do not occur in this layer (Source/Credit: NOAA).

This layer extends from the tropopause to a height of 30 miles. The stratosphere is distinguished from the troposphere because within this layer temperature increases with increasing altitude. The increase in temperature is due to the abundance of ozone which absorbs much of the incoming UV radiation directly from the Sun. Because the temperature increases with altitude, the temperature at the top of stratosphere is around 5°F, not exactly *hot*, but much warmer than the minus 60 to minus 110°F temperature at the top of the troposphere 20 miles below.

Because the temperature increases with altitude, there is very little vertical mixing of air in this layer. In order for air to rise spontaneously, it must be warmer than the air above it. By way of analogy, a hot air balloon can only rise if the air inside the balloon is warmer than the air outside of it. This feature of the stratosphere also means that warm air rising from the Earth's surface upward toward the stratosphere cannot penetrate this layer. By the time this air reaches the stratosphere, it has become cooler than the overlying air in the stratosphere. This is why most weather is limited to the troposphere. Air that rises from the Earth's surface cools too much to penetrate the warmer air of the stratosphere. The stratosphere acts like a lid that stops air from rising into it, keeping the stratosphere and layers above dry and weatherless.

On hot summer days, when giant, anvil-shaped cumulonimbus clouds form, the tropopause becomes apparent. The flattened, anvil-like top of the cloud marks the boundary (Figure 1.102). Air encountering the tropopause ceases to rise. It then spreads out horizontally in the direction of the upper-level winds.



*Figure 1.102. The stratosphere's 'lid effect' is readily apparent when one observes the shape of tall cumulonimbus clouds. The top of the cloud is flat because the air in the cloud cannot rise any higher once it hits the warmer air of the stratosphere. The anvil shape results from a combination of the stratospheric boundary and upper-level winds which blow the top of the cloud downwind (Source/Credit: Bill Westphall).*

The **stratopause** is a transition zone like that of the tropopause. In this zone, the temperature stops rising, and above it the temperature begins to fall once again.

Above the stratopause lies the **mesosphere**, which occurs at an altitude of 30 miles to 50 miles (Figure 1.103). In the mesosphere, the temperature decreases to the lowest levels in atmosphere. At the upper boundary, the temperature is approximately minus 130°F (minus 90°C), but can reach a frigid minus 225°F (minus 143°C).

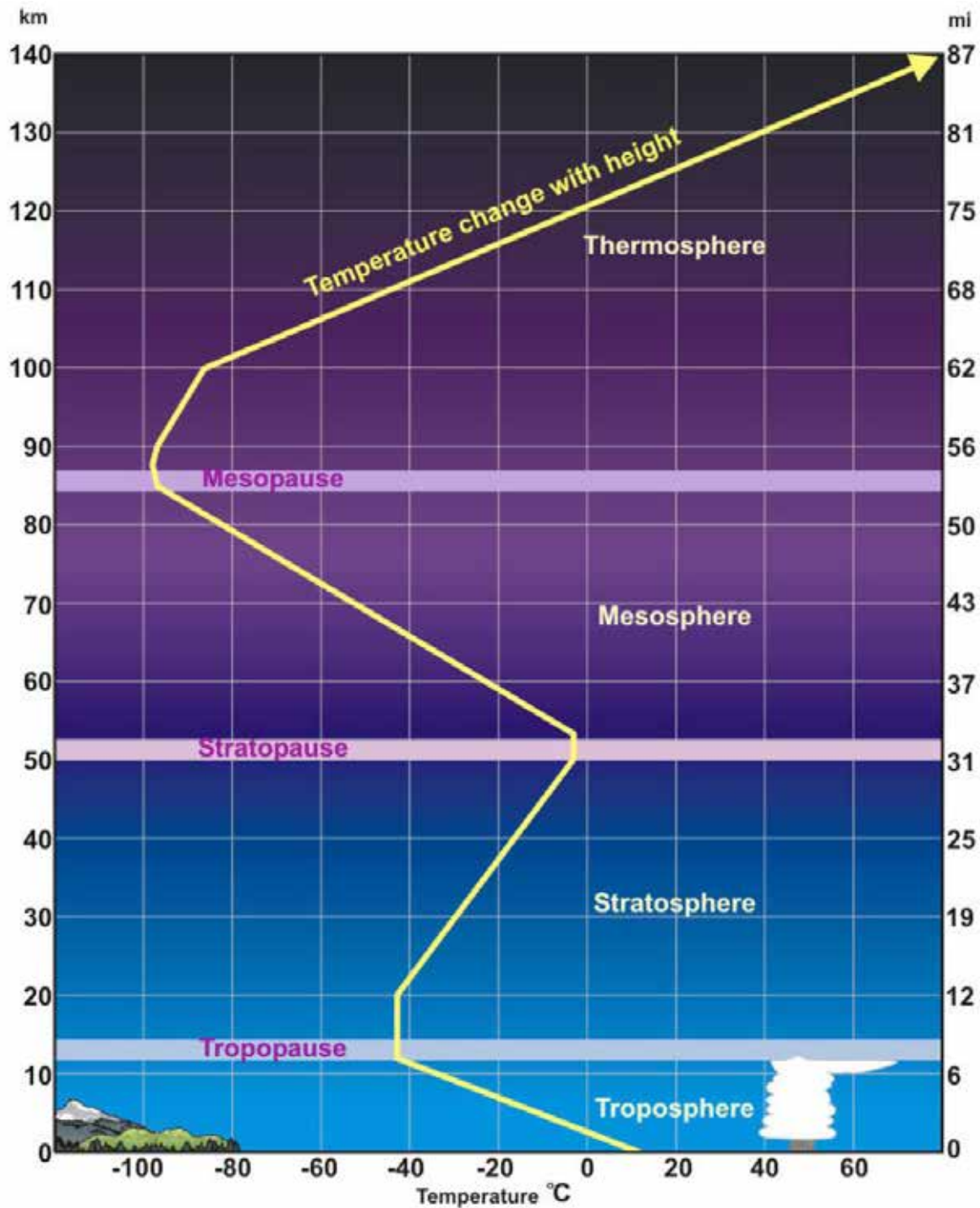


Figure 1.103. Within the mesosphere, the temperature decreases to its lowest level within the atmosphere. The low temperature results from the extremely low density of the air which means that there are very few heat-trapping gases within this layer (Source/Credit: NOAA).

The **mesopause** occurs above the mesosphere and, like the tropopause and stratopause, this layer marks a transition zone into another layer. In the mesopause, temperatures stop falling and then begin to increase in the uppermost layer of the atmosphere — the **thermosphere** (Figure 1.104).

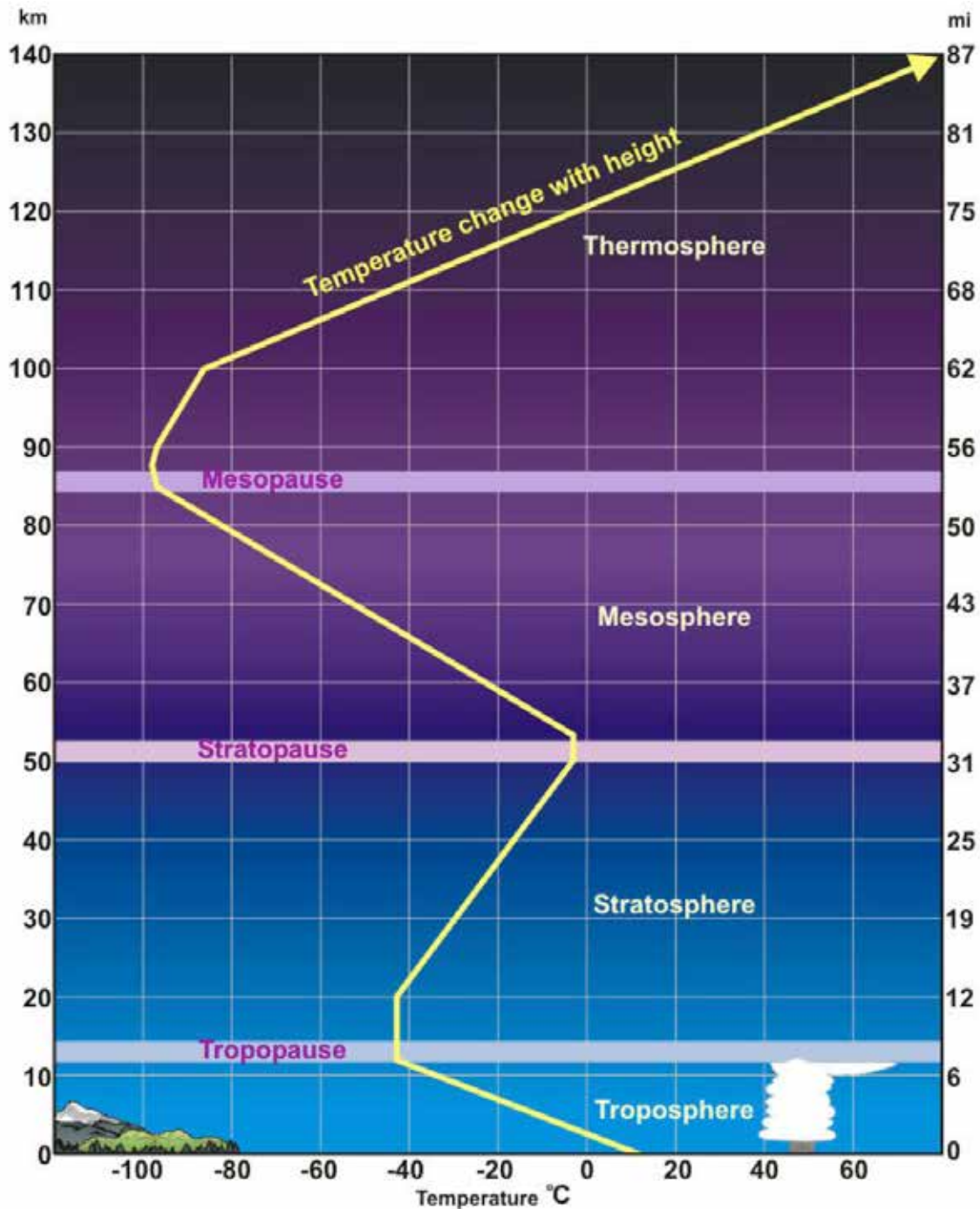


Figure 1.104. The upper-most layer of the atmosphere based on temperature is the thermosphere. Temperatures within this layer may exceed 2000°F (1093°C). Although the density of the air in this layer is even lower than that in the mesosphere, this layer is hot because it receives the most intense sunlight. The direct exposure to the intense sunlight heats the air to very high temperatures as gas molecules absorb solar energy (Source/Credit: NOAA).

The thermosphere extends from an altitude of 50 miles upward until it merges with the molecules of space. In practice, the upper boundary is generally considered to lie at an altitude of about 63 miles. Like the stratosphere, the temperature of the thermosphere increases with height although for different reasons and to a much greater degree. The temperature in this layer increases with altitude due to absorption of extreme ultraviolet radiation (EUV) from the Sun by the molecules that comprise this layer. Remember that at this altitude, the Sun's rays are undiminished by passage through the atmosphere, so they are extremely intense. Without protective space suits, this radiation would be deadly to astronauts. For those of us on the surface, the ozone layer in the stratosphere is our space suit. Although the temperature in the thermosphere may exceed 2000°F (1093°C), the air is so thin that it contains very little heat energy. This is why spacecraft and astronauts do not burn up while traveling through this layer.

Another distinguishing characteristic of the thermosphere is that the **ionosphere** occurs within this layer. Because of the intense ultraviolet radiation in this layer, atoms are stripped of their electrons and become ionized when they absorb the radiation (hence the name, ionosphere). This occurs when electrons that are hit by intense radiation and are knocked away from the atoms they were orbiting.



When the ionization above polar regions is particularly intense, this process results in the generation of the **Aurora Borealis** (Northern Lights) and the **Aurora Australis** (Southern Lights). These lights are generated when the electrons that are dislodged from atoms during the ionization process become reattached to other atoms. In the process of recombining, they release energy in the form of light. So, during these events, the sky lights up in a spectacular dance of constantly changing color (Figure 1.105). Occasionally, these events occur at lower latitudes.



*Figure 1.105. An aurora at the Poker Flat Research Range near Fairbanks, Alaska on February 28, 2011. Auroras are caused when charged particles from the Sun, known as the solar wind, become trapped by the Earth's magnetic field and are forced downward into the atmosphere above the poles. As these particles collide with nitrogen and oxygen molecules in the atmosphere, these gas molecules emit light creating a spectacular 'light show.' When the Sun emits strong solar winds, the aurora can sometimes be seen far outside of the polar regions (Source/Credit: NOAA).*

The ionization in the thermosphere makes possible long-range (over-the-horizon) radio communication. It is this layer that Ham Radio operators use to communicate with others around the world. Ham Radio operators are becoming obsolete because of modern telecommunication systems. However, in the past, these individuals played an important role in communicating important news about events in far-flung, isolated regions of the world.

## Origin and Evolution of the Atmosphere

The atmosphere that exists today and which makes life possible on this planet has constantly changed and evolved over its 4.6 billion year history. At the time of the Earth's formation and for millions of years thereafter, the Earth had an atmosphere that was literally poisonous. It was only as a result of processes that occurred over immense periods of time that the atmosphere evolved to the beneficent form we see today (Figures 1.85 and 1.86). Some of the key events and mechanisms involved in the evolution of our atmosphere include photodissociation, volcanic outgassing, photosynthesis, weathering and burial of rocks, meteoric and comet impacts, and the interaction of solar radiation with atmospheric components.

The very early atmosphere was probably composed of hydrogen, helium, methane and ammonia — a truly toxic brew. This composition is suggested by the fact that nebulae, the gas clouds in space from which solar systems form, are composed of these gases. Further support for this is that the gas giants in our own solar system (Jupiter, Saturn, Uranus, and Neptune) contain these gases. However, because the Earth was relatively low in mass, its gravitational field was too weak to retain hydrogen and so it diffused into space. Some of the remaining hydrogen combined with oxygen to form water that contributed to the growth of the primordial oceans. In addition, some of the methane ( $\text{CH}_4$ ) and ammonia ( $\text{NH}_3$ ) were broken apart by solar radiation in a process called **photodissociation** and the hydrogen released by this process escaped to space. The carbon and nitrogen, because they are heavier than hydrogen, were retained.

Subsequently, the Earth's early atmosphere was composed of water vapor, carbon dioxide, and nitrogen. There was virtually no free oxygen during this phase of evolution. The gases that came to dominate the atmosphere after the original, short-lived, nebular atmosphere dissipated are believed to have been derived from volcanic outgassing and comet strikes. **Volcanic outgassing** refers to the process by which gases that were trapped in magma are released to the atmosphere during volcanic eruptions. As the magma approaches the surface during an eruption, the pressure on it is reduced and this allows dissolved gases to come out of solution (Figure 1.106).

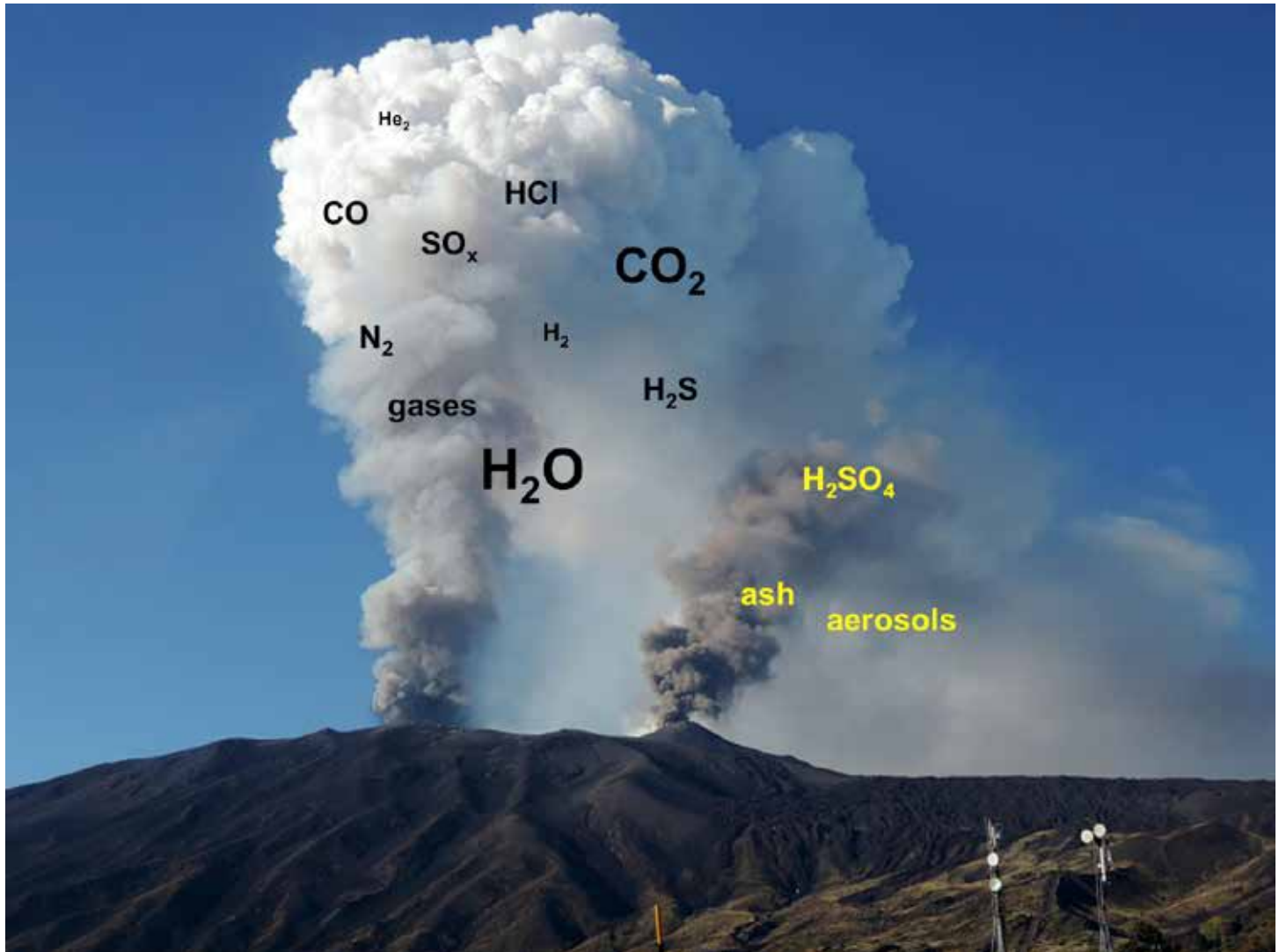


Figure 1.106. The most common gases released during volcanic eruptions include water vapor ( $H_2O$ ), carbon dioxide ( $CO_2$ ), sulfur dioxide ( $SO_2$ ), hydrogen sulfide ( $H_2S$ ), hydrogen ( $H_2$ ), helium ( $He_2$ ), nitrogen ( $N_2$ ), carbon monoxide ( $CO$ ), and hydrogen chloride ( $HCl$ ). Aerosols are also injected into the atmosphere in huge quantities. This image is of an eruption of Mt. Etna on October 26, 2013 (Source/Credit: NASA Earth Observatory).

Volcanic outgassing has been responsible for releasing most of the gases that comprise the modern atmosphere.

The evidence for the volcanic outgassing origin is based on the composition of gases emitted from modern volcanoes — 85% water, 10% carbon dioxide, and 1 or 2% nitrogen. The proportions of these gases that actually comprise our atmosphere are substantially different from these values. Currently, water vapor comprises 0.1 to 4%, carbon dioxide comprises 0.038% and nitrogen comprises 78% (Figure 1.107).

Comparison of Percentage of Gases Emitted by Volcanoes to the Percentage in the Atmosphere		
Gas	Percent Released by Volcanic Outgassing	% in Atmosphere Currently
Water	85	0.1 - 4.0
Carbon Dioxide	10	0.040
Nitrogen	1 - 2	78.08

Figure 1.107. The percentage of the gases emitted by volcanoes is quite different than that found in the atmosphere. The differences result from the fact that water vapor precipitates from the atmosphere; carbon dioxide is sequestered by plants and the oceans; and nitrogen is comparatively inert, so it accumulates (Source/Credit: modified from several sources).

Much of the discrepancy between the proportions of these gases released by volcanic eruptions versus the current amounts in the lower atmosphere can be explained by the following processes which occurred as the atmosphere evolved.

**Nitrogen** (1% --> 78%). Nitrogen is inert (does not react readily with other gases), so it accumulates with time.

**Carbon Dioxide** (10% --> 0.039%). Much of the carbon dioxide is removed from the atmosphere by a variety of carbon sinks, such as:

**Photosynthesis.** By this process, carbon dioxide is converted to sugars. Animals then eat plants, and so the carbon dioxide that was stored in the plants in the form of sugars is then stored in organisms.

**The Burial of Dead Plant Matter.** This material is then converted into peat or coal which means that the carbon it acquired in the form of carbon dioxide becomes isolated from the atmosphere for millions of years (Figure 1.108). Plants act as a **sink** for carbon dioxide because they remove it from the atmosphere and store it.



Figure 1.108. Carbon dioxide is absorbed by plants which convert it into organic matter (plant material). If dead plants are buried by sediment, such as occurs in swamps and bogs, the plant matter can be converted into coal over millions of years as a result of the heat and pressure associated with burial. This process ultimately results in the removal of carbon dioxide from the atmosphere and its storage in the ground. When the coal is mined and subsequently burned, the carbon dioxide is released back to the atmosphere. Because coal is being burned far faster than it is being formed, the concentration of atmospheric carbon dioxide is increasing and this is contributing to global warming because this gas traps heat energy (Source/Credit: Marcus Gillespie).

**The Burial of Dead Marine Organisms** (all of which contain carbon). These dead and decayed organisms, carbon dioxide sinks, can eventually be converted into petroleum-based products such as gasoline and plastics.

**Dissolution in the Ocean** (like carbon dioxide in carbonated drinks). Dissolved carbon dioxide can subsequently react with calcium or magnesium and precipitate out of solution in the form of calcium carbonate or magnesium carbonate. These precipitates form rocks that are known as limestone and dolomite.

**Water Vapor** (80% --> 0.1%-4%). Water vapor readily precipitates out of the atmosphere and forms oceans, rivers, lakes and glaciers. Much of the water also enters the ground where it is stored as groundwater. The average amount of time that a water molecule is in the air approximately 11 days.

The above processes involve a finely tuned chemical balance that enables a tremendous variety of life to thrive on Earth. Relatively slight changes in the amount of oxygen and carbon dioxide could be devastating to life, and these are only two of the many gases that maintain an atmosphere that is suitable for life.

Comets, which are objects composed largely of frozen gases and dust, also add gases and particulates to the atmosphere. Comets are often described as dirty snowballs, although these snowballs can be miles in diameter (Figure 1.109).



Figure 1.109. Comets are irregularly shaped aggregates of ice and dust left over from the formation of the solar system. Most comets are a few miles in diameter, but when they approach the Sun and their ice begins to vaporize they can produce 'tails' that are tens of millions of miles in length. In 2006, NASA smashed a space probe into Comet Tempel 1 in order to photograph the impact from the 'mother ship' that launched the probe. By analyzing the impact crater that was formed, as well the gases that were ejected, NASA hoped to learn more about the nature of comets and their role in helping to shape the atmosphere of the Earth (Source/Credit: NASA).

When a comet strikes the Earth, it is often traveling at tens of thousands of miles per hour and is vaporized in a matter of seconds by frictional and compressional heating that occurs when it enters the atmosphere. Thus the atmosphere protects us not only from ultraviolet radiation, it also protects us from small meteorites and small comet fragments.

The oxygen that now comprises a significant part of the atmosphere (21%) was produced primarily by photosynthesis which is a biological rather than a physical process. The significance of this is that the composition of our atmosphere is controlled by both physical processes and by the very life that depends on it. Without the plants and algae that produce oxygen, our planet would be a biologically impoverished planet that lacks the great diversity of life that now lives here. The atmosphere affects life — but life also affects the atmosphere.

As we noted earlier, the amount of oxygen in the atmosphere did not reach its current levels until about 500 million years ago when the Earth was about 89% of its present age. So, the atmosphere that exists now is, geologically speaking, relatively young. It has not always been the way it is; nor will it remain this way forever. Nature will change it, and so will we.

## Chapter 2

# Air Temperature

The daily weather forecast addresses several aspects of the lower atmosphere, including such things as barometric pressure, wind direction and velocity, humidity and precipitation, cloudiness, and most consistently, temperature. These descriptors of the physical state of the atmosphere at a given time are called the **weather elements**, and are important because they not only are used to describe the present weather, but also pose limitations on the types of outdoor human activities.

Temperature is the most commonly described of the weather elements, whether by a professional meteorologist on the Weather Channel, or in common casual conversation. The terms **pleasant, hot, cold, bitter cold, unseasonably warm** all refer to atmospheric temperature, and imply human response to address those conditions. In recent years, **game-day forecasts** are commonly given by meteorologists so that sports fans and players can prepare for specific adverse conditions (Figure 2.1).



Figure 2.1. Adverse weather during the NFL game between the Buffalo Bills and the Indianapolis Colts. Eight inches of snow fell during the game. Fred Jackson of the Bills (#22) stiff-arms Kevin Hayden (#26) of the Colts (Source/Credit: Rick Stewart/Getty Images, Orchard Park, NY).





In New York and Maine, snow fell on June 6 and the ground froze solid on June 9. Repeated hard freezes occurred locally in New England throughout the summer of 1816, the “year without a summer.” Many believe that the cold, dreary summer of 1816 was the inspiration for Mary Shelley’s *Frankenstein* (Figures 2.3a and 2.3b). The exact cause of this global cooling event is not completely understood, but it is likely due to a combination of lessened solar irradiance and higher-than-normal volcanic activity.

1816 Summer Temperature Anomaly

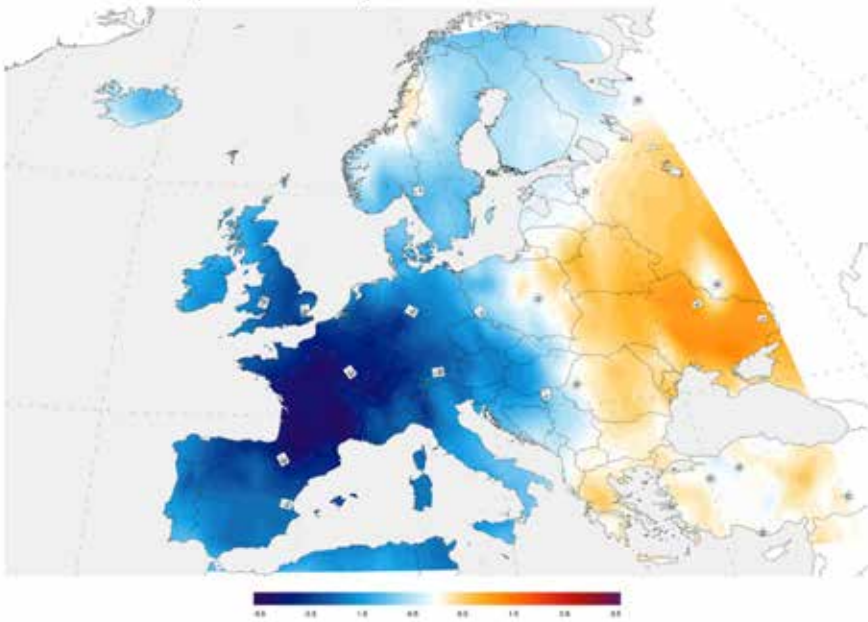


Figure 2.3a. (left) Summer temperature anomalies in western Europe in 1816 during the “year without a summer.” Similar anomalies occurred in the New England states (Source/Credit: NCDC/NOAA).

Figure 2.3b. (right) The harsh summer weather conditions in the European Alps during the summer of 1816 reputedly inspired the famous *Frankenstein* story. The story was brought to life in the movie *Frankenstein* (1931), played by Boris Karloff (Source/Credit: Wikipedia).

A third example illustrates the impact of regional temperature changes over decades to centuries. The **Medieval Warm Period**, from about AD 800-1300, saw the Norse colonization of the Americas. The ice-free seas of the North Atlantic promoted settlement of southern Greenland by the Vikings. This was apparently the warmest period in the North Atlantic in a 2000-year interval prior to the warm-up of the late 20<sup>th</sup>-21<sup>st</sup> century. Interestingly, this was followed by globally-cooler temperatures from about AD 1400-1800, often referred to as the **Little Ice Age**. Colonies in Greenland vanished and many European alpine glaciers experienced significant advance during this time.

Vertical, horizontal, and temporal (time) variations in temperature are not only tied to human activities, but are fundamental to meteorology. They initiate most of the motions in the lower atmosphere. Temperature variations affect practically every atmospheric process, and

therefore an analysis of temperature patterns is fundamental in understanding all aspects of meteorology.

## **Solar Energy**

Every object in the universe emits energy in the form of electromagnetic radiation. It can be envisioned as a wave-form of energy that is transmitted through the relative void of outer space as well as through planetary atmospheres. When electromagnetic energy is absorbed by a substance (e.g., a planet, comet, asteroid), it causes that substance to vibrate more vigorously, and that increase in vibrational energy is measured as an increase in temperature. The temperature of the Earth's surface and atmosphere is governed largely by absorption of electromagnetic radiation from many sources. Some thermal energy, called geothermal energy, is derived from the Earth's interior, but its contribution is small compared to external sources.

Solar energy is the ultimate energy source that drives the atmospheric engine. Solar energy not only controls the amount of radiation received by the Earth-atmosphere system, but it also is indirectly responsible for most of the motions in the atmosphere, including the hydrologic cycle.

The Sun and countless other stars generate tremendous quantities of energy, principally in the form of **electromagnetic radiation**. The source of most of the energy that stars generate is due to **thermonuclear reactions** that take place in their interiors. The Sun's core (Figure 2.4) is a region of extremely high temperature (~15 million °C, or 27 million °F) and pressure. Under these conditions, lighter elements such as hydrogen can be fused together to form heavier elements, beginning with the following reactions (Figure 2.5):

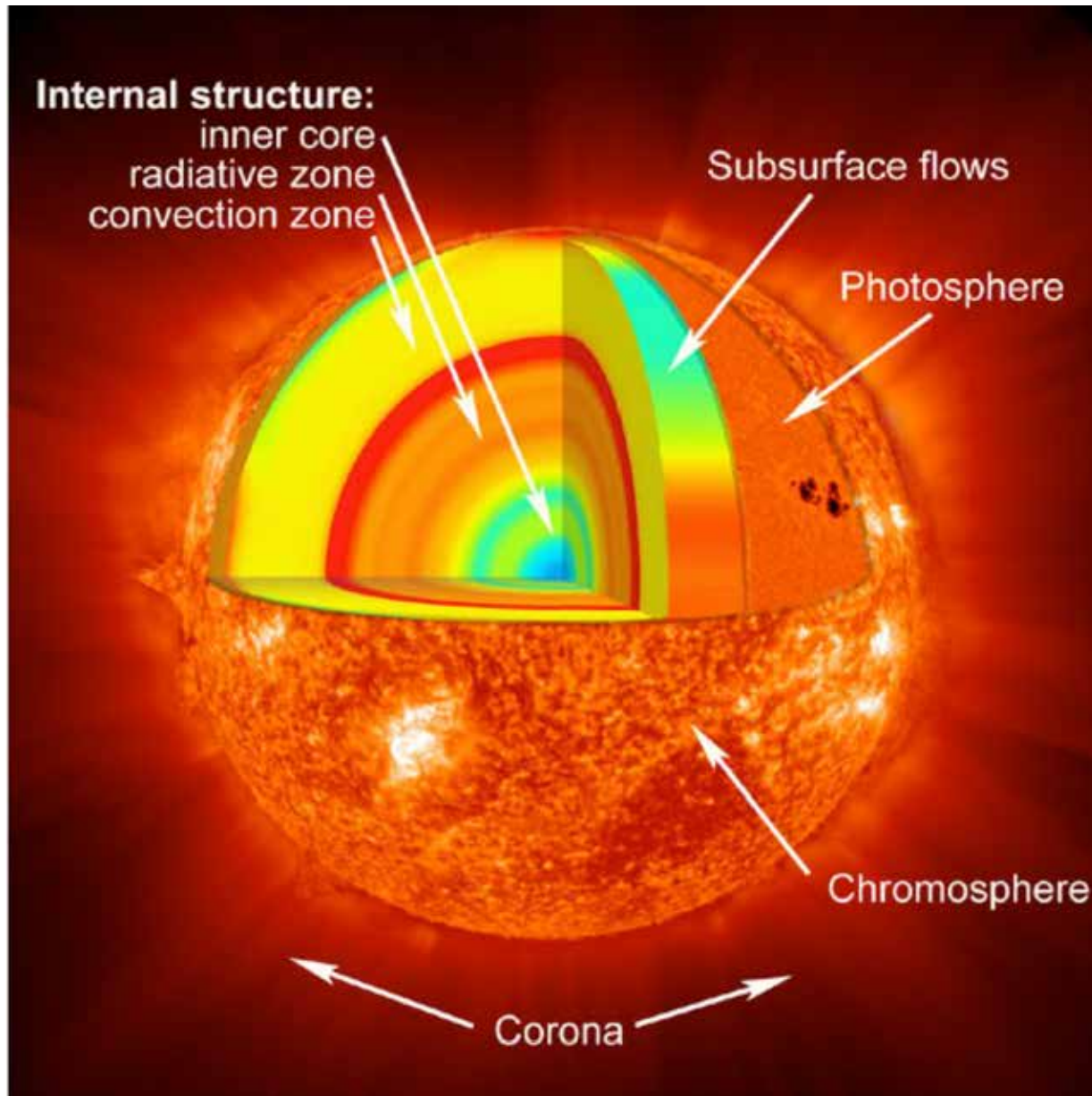


Figure 2.4. Artist's conception of the layers of the Sun. The inner layers are the core, radiative zone, and convection zone. The core is the hottest and densest layer where thermonuclear reactions occur. Outside the core is the radiative zone, where energy moves very slowly outward. The convection zone is the layer where convection currents move gases and energy more rapidly toward the surface. The outer layers are the photosphere, chromosphere, and corona. The photosphere is the deepest layer of the Sun that can be observed directly, and it often displays a granular appearance in imagery. In the chromosphere, temperatures begin to rise upwards, unlike the lower layers where temperatures increase toward the core. The corona is the outermost layer where temperatures of greater than one million °F (>555,000°C) can occur (Source/Credit: NASA).

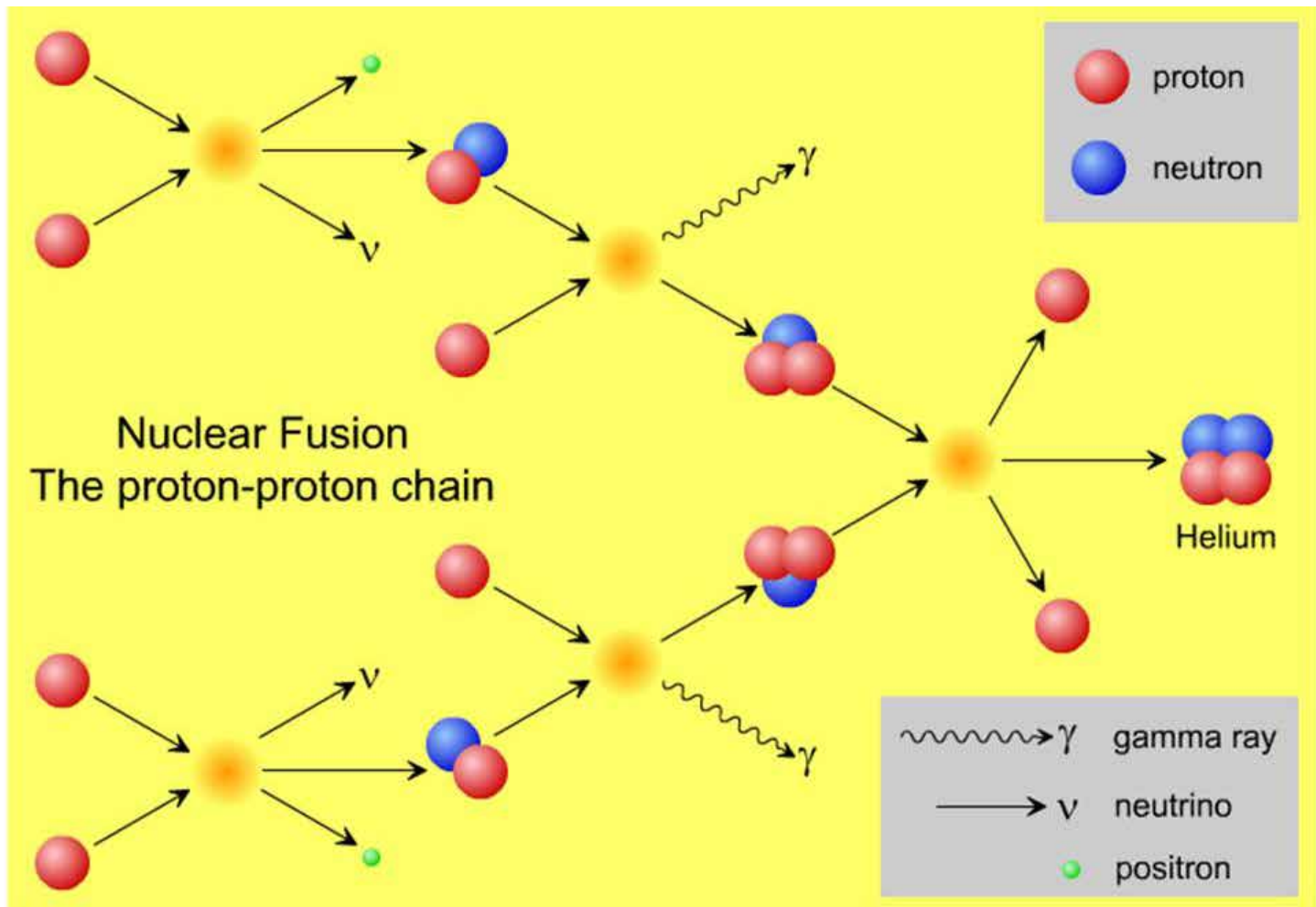


Figure 2.5. The proton-proton reaction fuses hydrogen nuclei into helium nuclei, liberating tremendous amounts of electromagnetic energy (Source/Credit: NASA/ESA/STSci).

- (1) two protons combine, forming a deuterium atom, a positron, and a neutrino
- (2) the deuterium atom then combines with another proton to form a helium-3 atom and electromagnetic radiation in the form of a gamma ray
- (3) two helium-3 atoms combine to form a helium-4 atom plus two protons
- (4) since the products of the following reactions weigh less than the original hydrogen atoms, the excess mass is converted to energy in the form of several wavelengths of electromagnetic radiation following Einstein's equation  $E = \Delta mc^2$

$E$  = energy

$c^2$  = the speed of light squared

$\Delta m$  = the difference in mass between the original protons and the resultant helium atoms

With the tremendous abundance of hydrogen in the universe, the hydrogen-helium fusion reaction would seemingly take place ubiquitously. However, in the nucleus of light atoms, there are both attractive forces (the **strong nuclear force**), and repulsive forces (the electrical repulsion of positively-charged protons; the **Coulomb force**). The huge amount of energy required to overcome the repulsive force and place the protons close enough so that the attractive force dominates is found in the interior of stars.

The fusion of hydrogen atoms described above accounts for the bulk of the energy emitted by the Sun. Most of the remaining energy released by the Sun is due to the fusion of heavier atoms, such as the conversion of helium atoms to beryllium and beryllium to lithium. Heavier elements also form in the interior of stars, but do not release large amounts of energy. Thus, the fusion of lighter elements powers the stars (Figure 2.6).



Figure 2.6. The energy that the Earth receives from the Sun drives the atmospheric engine. Although the other planets in our solar system also receive energy from the Sun, the Earth lies at just the right distance from the Sun and has just the right atmospheric composition to keep temperatures suitable for a life support system (Source/Credit: NASA).

The amount of energy released by nuclear fusion in the Sun, or any other star, is impressive (Figure 2.7). Every second the Sun releases 13 million times the amount of energy consumed annually in the United States. Every second, about 1.1 million tons of hydrogen is fused into helium. The Sun has been generating energy at approximately that rate for nearly 5 billion years, and there is enough fuel to last some 4+ billion more.



Figure 2.7. Solar prominences on the Sun in 2012. Prominences are giant masses of searing hot gas that loop thousands of miles above its surface. They attest to the tremendous amount of energy released by fusion deep inside the Sun's core. The loops are far bigger than the Earth. One of the largest ever observed arched more than 245,000 miles above the surface, which is slightly more than the average distance between the Earth and the Moon. The core temperature of the Sun is around 27 million °F (15 million °C), although the surface temperature is only 10,000°F (5538°C) (Source/Credit: NASA).

## Electromagnetic Radiation

Most of the energy that is produced by fusion in the Sun's core is in the form of **electromagnetic radiation**. All objects in the universe emit electromagnetic radiation, typically in several wavelengths. The principal wavelengths of emitted radiation depend on the nature of the radiating body. The total range of radiation emitted by all objects can be represented graphically by the **electromagnetic spectrum** (Figure 2.8).

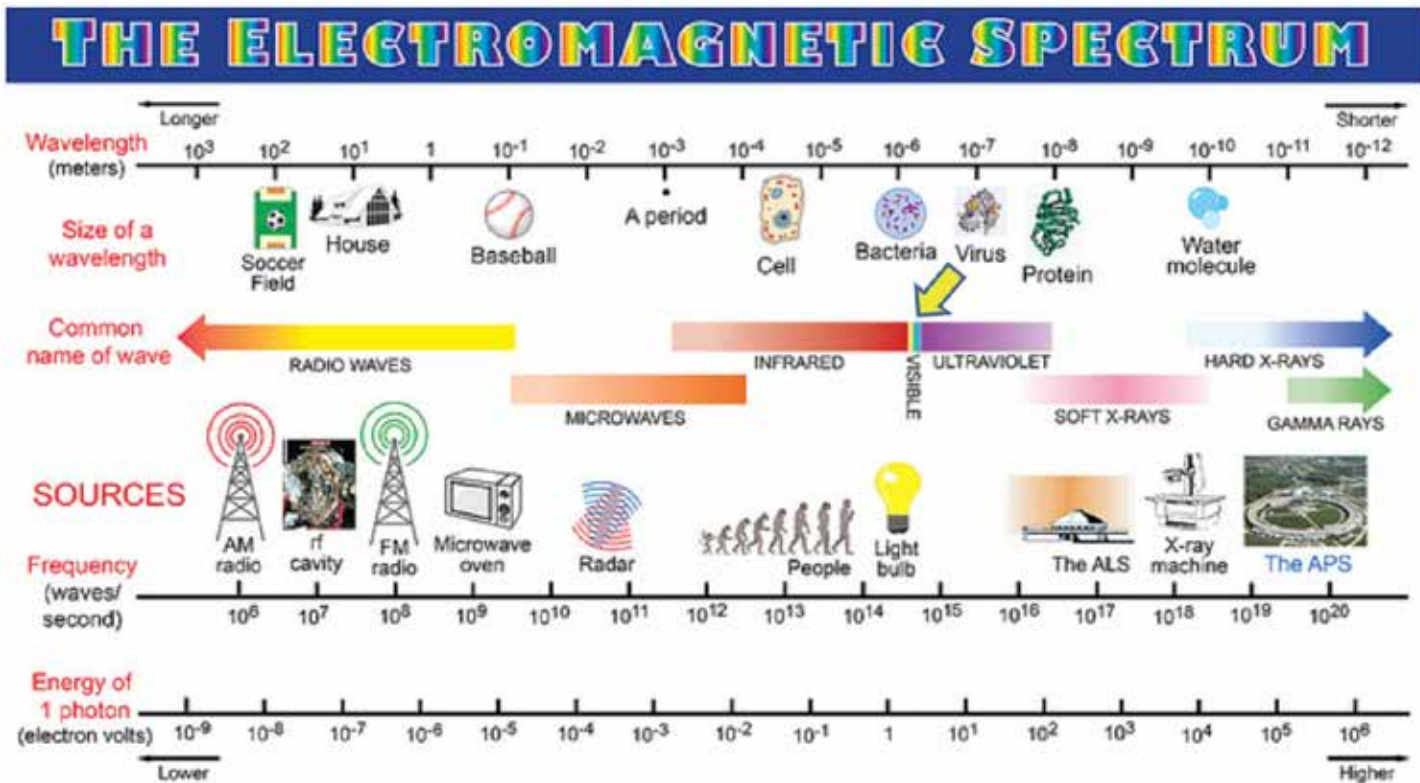


Figure 2.8. The electromagnetic spectrum encompasses the entire range of wavelengths of electromagnetic radiation. Wavelengths vary from less than one ten billionth of a meter (gamma rays) to wavelengths of more than 70 miles (100 km) (radio waves). The shorter the wavelength of radiation, the higher its energy. Only the visible part of the spectrum (yellow arrow) can be detected by the human eye (Source/Credit: Argonne National Laboratory).

Some of the characteristics of EMR are:

- It possesses both electric and magnetic properties.
- Electromagnetic radiation travels through space at a speed of approximately 186,000 miles per second. At this speed, it can travel 240,000 miles from the Earth to the Moon in a mere 1.29 seconds. Its speed is reduced somewhat as it is transmitted through planetary atmospheres.
- Unlike sound waves, electromagnetic radiation does not require a medium (such as air or water) to travel through.



- EMR transfers energy in the form of waves, and can therefore be described in terms of wavelength and frequency.
- EMR is characterized by a wide range of different wavelengths that range in length from less than one ten billionth of a yard (~ meter) to greater than 100,000 yards (~meters). The entire range of wavelengths in the universe is known as the **electromagnetic spectrum**.
- The greater the temperature of the object emitting the EMR, the shorter the wavelength of the radiation and the greater the energy produced. Thus, **wavelength is inversely related to temperature and energy. Hot objects primarily emit short wavelengths, and cool objects primarily emit long wavelengths**. Most objects emit a group of wavelengths of radiation rather than a specific wavelength. The Sun, for example, emits principally in the visible and near infrared wavelengths, but small portions of the solar spectrum occur over practically the entire electromagnetic spectrum.
- The electromagnetic spectrum can be divided into sections based on wavelength. The rationale for this is the fact that different wavelengths are associated with different energies and with differences in the ability to interact with matter.
  - **Gamma Radiation** (extremely short wavelengths). This very high energy radiation can travel through several inches of steel (Figure 2.9).

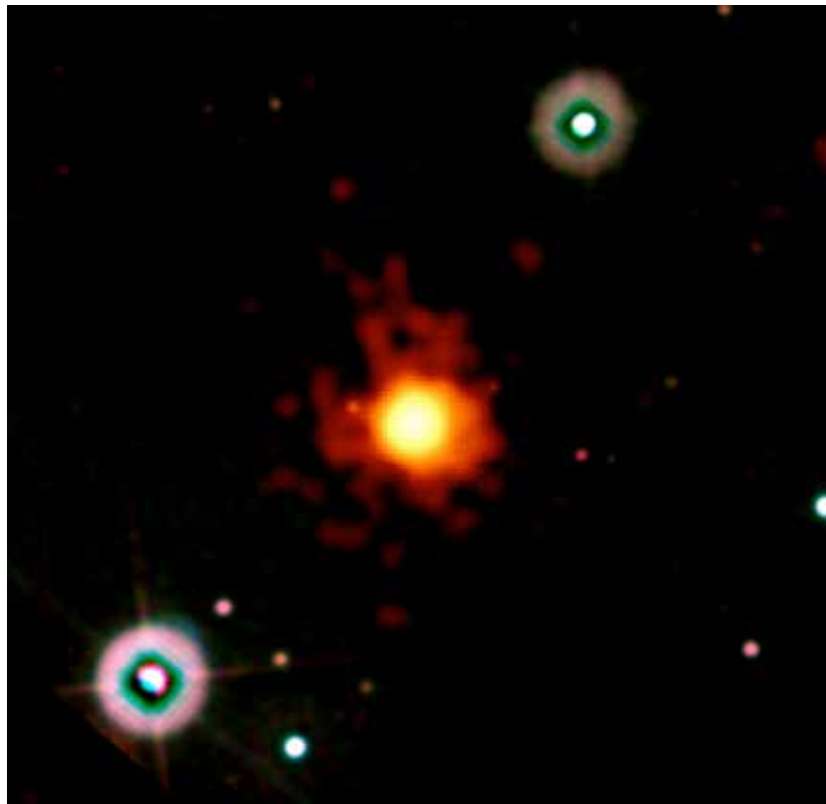


Figure 2.9. Astronomers have imaged the most distant object (to date) in the universe, a collapsing black hole and resulting gamma ray burst 13 billion light years away. This suggests that stars had formed and were dying only a billion or so years after the Big Bang (Source/Credit: NASA's Swift gamma ray satellite, April 2009).

- **X-rays** (very short wavelengths). This radiation can penetrate soft tissues. X-rays are used as diagnostic tools by doctors and dentists because of their ability to penetrate soft tissues. Special instruments use these short, energetic wavelengths to image the Sun as well as more distant celestial objects (Figure 2.10).

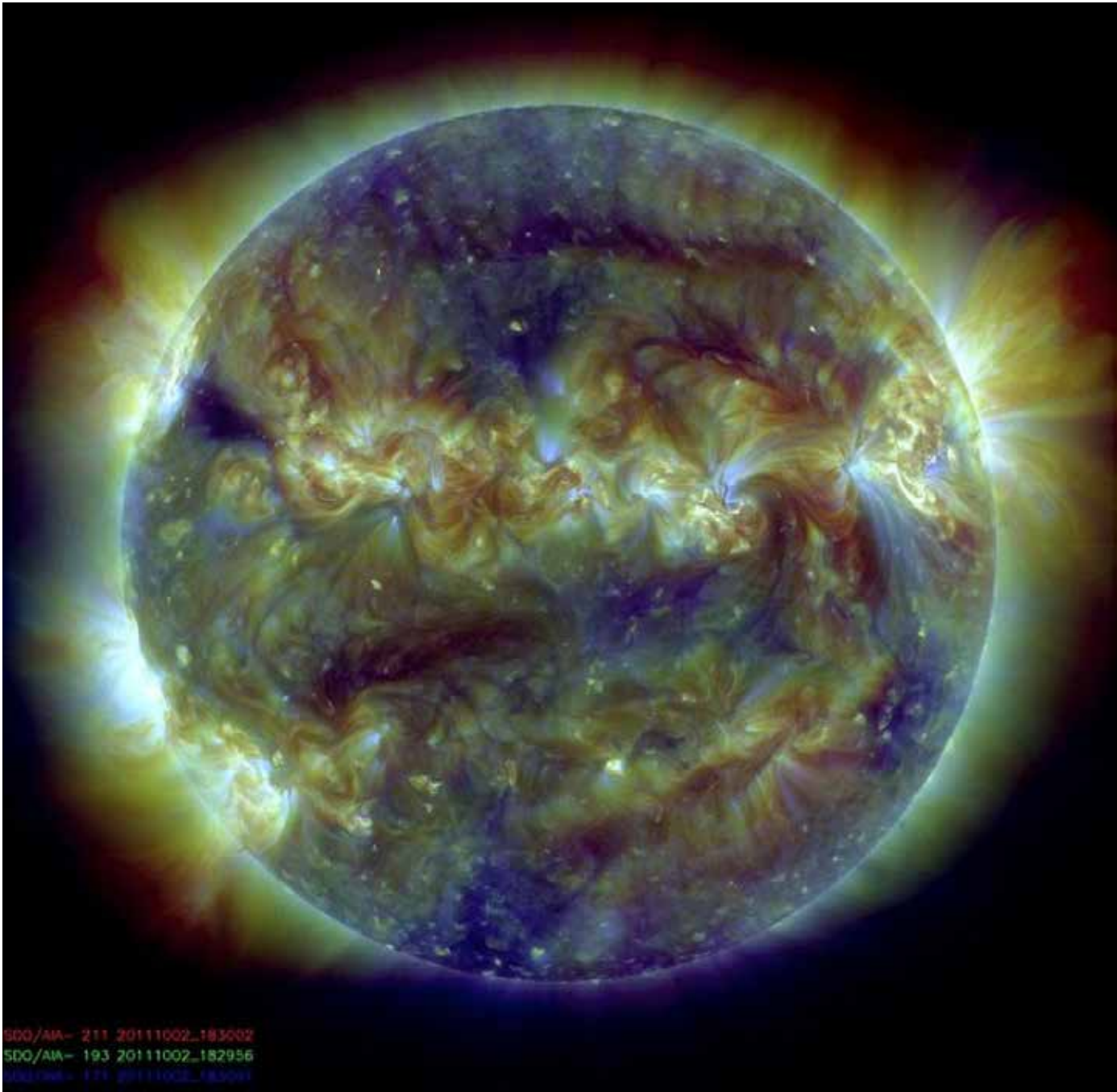


Figure 2.10. Three different wavelengths ranging from X-rays to ultraviolet are combined to enhance this image of the Sun. The bright areas are places with strong magnetic activity on the Sun's surface. The image is one of thousands sent to Earth from the Solar Dynamics Observatory, an \$855 million satellite that has been in orbit since 2010. Images such as these give us a better understanding of the connection between solar activity and the Earth's atmosphere. They also serve as a more accurate predictive tool for disturbances to communication devices as well as longer-term climate. Every day, the satellite sends out 1.5 terabytes of data, equal to 500,000 songs on an MP3 player (Source/Credit: NASA, SDO).

- **Ultraviolet** (short wavelength). Ultraviolet radiation is just outside the detection limits of the human eye. Although ultraviolet radiation is only a small component of the total solar spectrum (Figure 2.11), it is absorbed in large quantities by ozone in the stratosphere, and is the major source of stratospheric heating. The screening out of lethal dosages of ultraviolet radiation by ozone in the stratosphere is a crucial part of the Earth's life-support system. Ultraviolet is another form of high-energy radiation that NASA and other space agencies take advantage of in imaging specific characteristics of celestial objects (Figure 2.12).

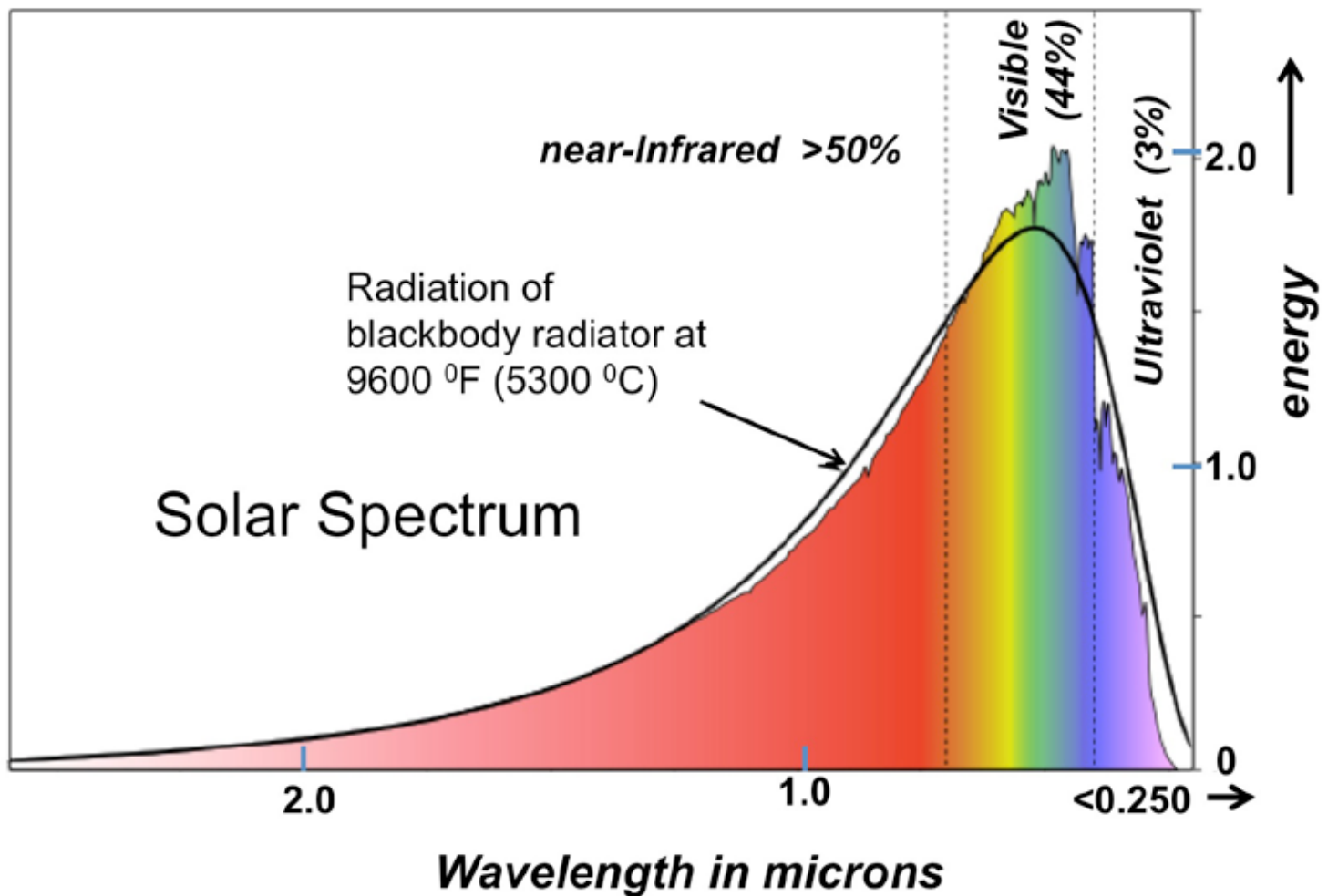


Figure 2.11. Solar spectrum outside the atmosphere. Although the Sun is a high temperature radiating body (about 9600 °F/5300°C at the surface), it emits electromagnetic radiation in a wide spectrum of wavelengths. Over 90% of the total solar spectrum is near-infrared and visible light. Ultraviolet light makes up about 3%, and wavelengths not shown on the diagram make up the remainder (far-infrared, radio waves, gamma rays, X-rays). The solar spectrum very closely approximates the theoretical blackbody spectrum of an object (black line) at the same temperature as the surface of the Sun (Source/Credit: modified from NASA, ASTM, and other sources).

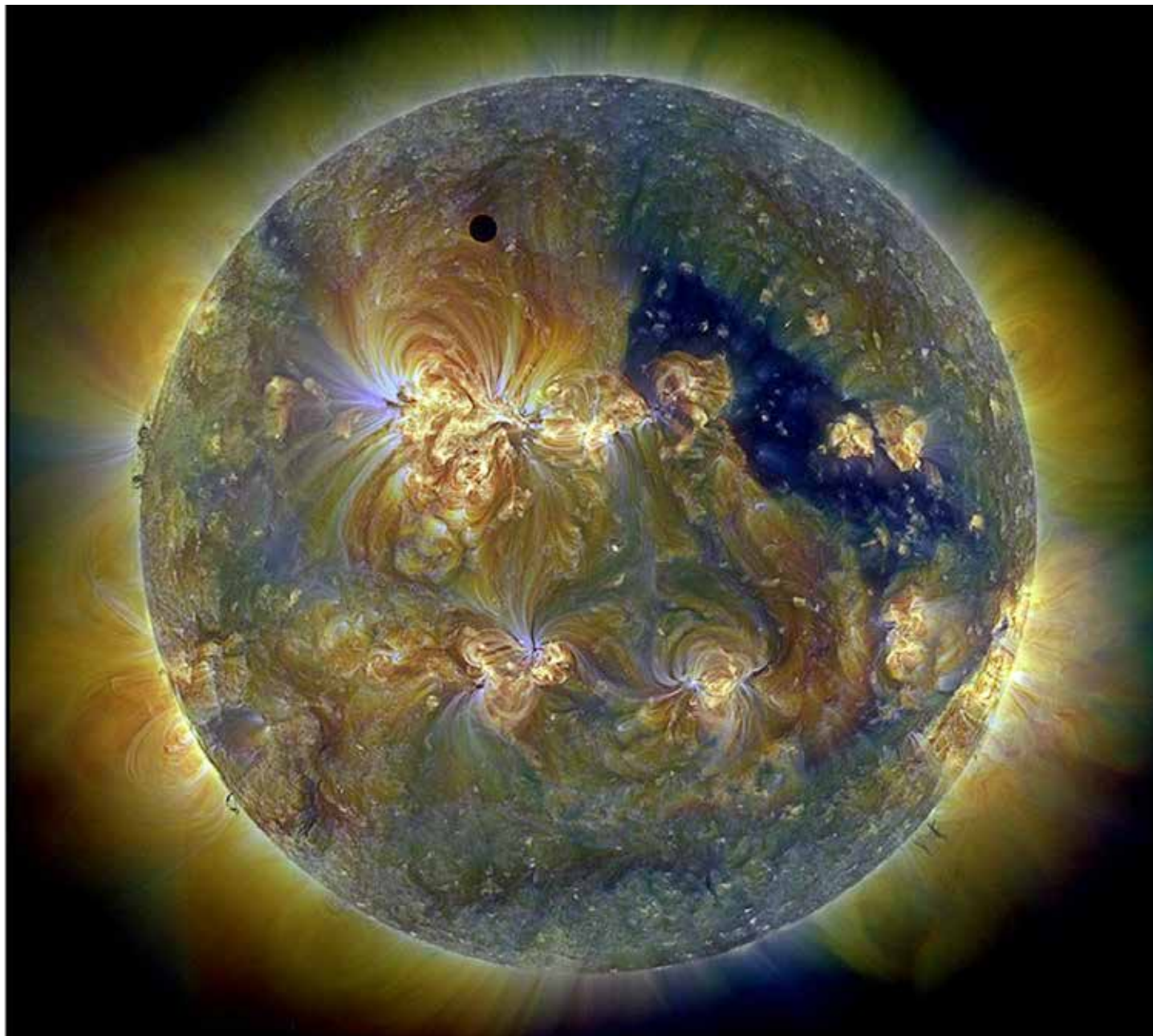


Figure 2.12. This ultraviolet image of the Sun was taken during June of 2013 by the Earth-orbiting Solar Dynamics Laboratory. The small dark spot in the central-upper portion of the image is Venus eclipsing part of the Sun's disk. The next Venesian solar eclipse will be in 2117 (Source/Credit: NASA).

- **Visible** (short wavelength). This range constitutes about 44% of the energy emitted by the Sun and consists of the colors that are visible to the human eye (Figure 2.13). When all wavelengths are combined, the color white results. Violet is the shortest visible wavelength. Shorter UV light is just a bit shorter in wavelength than the color violet. Red is the longest wavelength. Just beyond the red end of the visible portion of the spectrum lies the infrared band. Most of the energy emitted by the Sun lies within a narrow band that includes UV, visible, and near-infrared radiation (Figure 2.14).

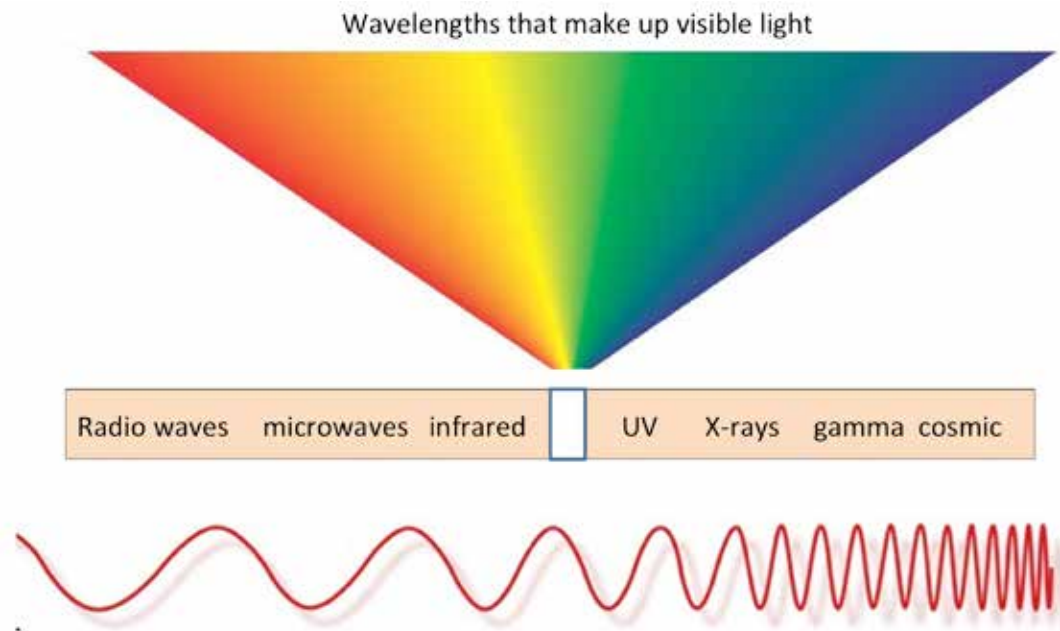


Figure 2.13. A simplified image of the electromagnetic spectrum indicating the relative position of visible light compared to longer wavelengths on the left and shorter wavelengths on the right. The small white rectangle in the middle bar graph represents **white light**, and can be broken down into the colors of the rainbow (Source/Credit: modified from several sources).

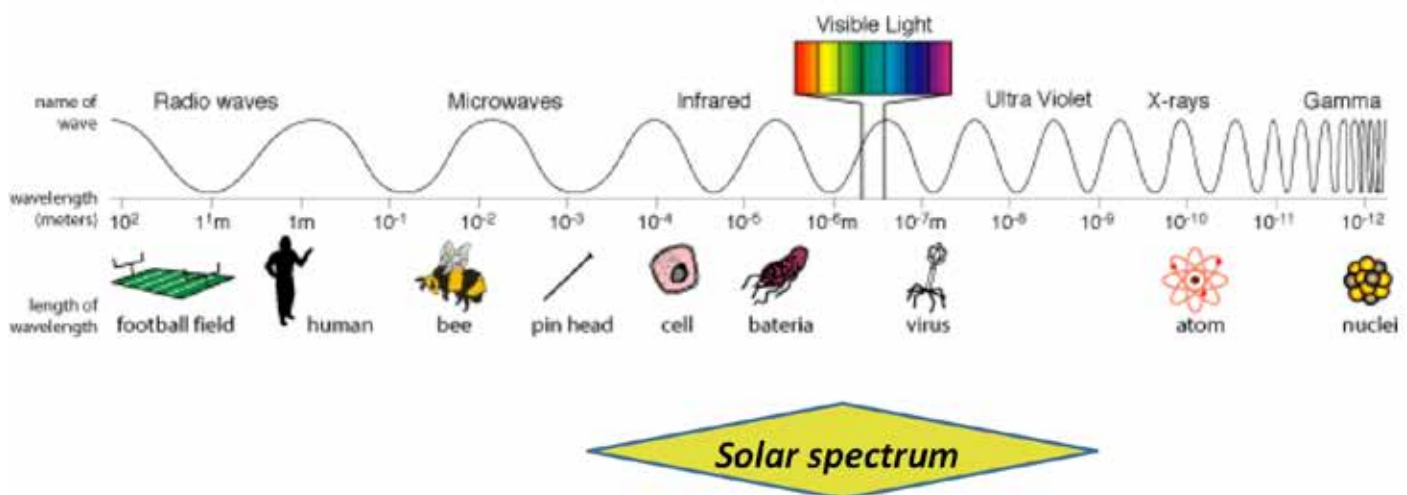


Figure 2.14. The solar spectrum is most intense in the visible, near-infrared, and UV regions (width of yellow band illustrates relative intensity of radiation). The visible portion of the spectrum is only a very small part of the solar spectrum, and an even smaller part of the total electromagnetic spectrum (Source/Credit: modified from NOAA).

- **Infrared** radiation is too long to be observed by the human eye. It includes wavelengths ranging from about one micron to 1000 microns (Figure 2.15). For comparison, the average diameter of a human hair is about 50 microns. Fine-grained sand or the average grain of table salt is a few hundred microns. The head of a pin is about 1500 microns (1.5 mm), slightly outside the range of infrared radiation.

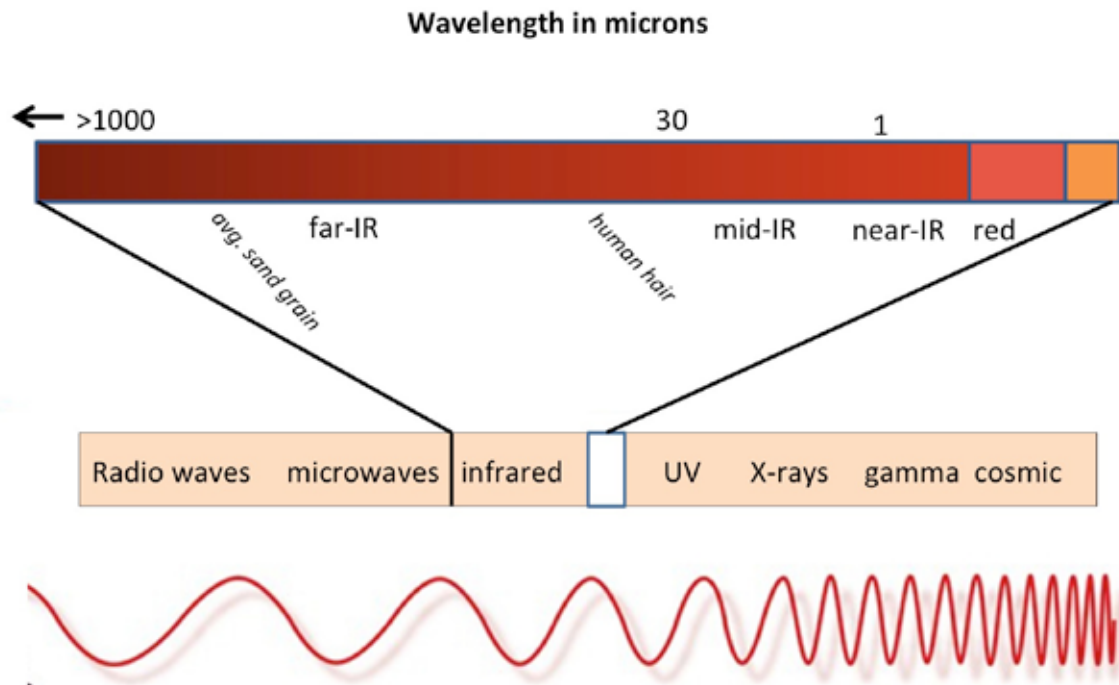
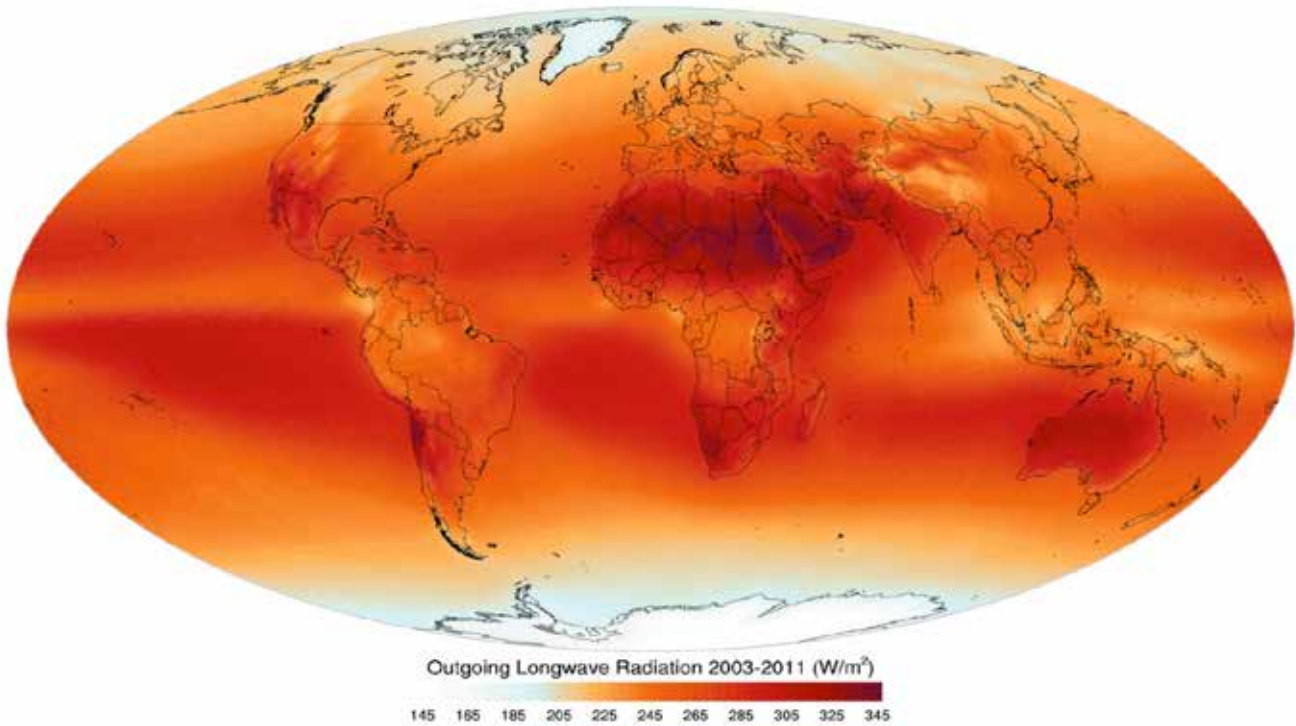


Figure 2.15. A simplified image of the electromagnetic spectrum with shorter wavelengths on the right and longer on the left. The small white rectangle in the middle bar graph represents white light. To the left of white light is infrared radiation, which is broken down in the expanded bar to far-infrared (far-IR), mid-infrared (mid-IR), and near-infrared (near-IR). Shorter wavelengths to the right of near-infrared are the beginning of the visible part of the spectrum (i.e., red) (Source/Credit: modified from NASA and other sources).

Since objects tend to emit infrared radiation across a wide spectrum of wavelengths (about 1000 times broader than the visible part of the spectrum), infrared radiation is commonly divided into several regions. The **near-infrared** ranges from just under a micron to about 5 microns. The **mid-infrared** ranges from about 5 to 30 or so microns. The **far-infrared** ranges from about 30 to nearly 1000 microns. Note that these divisions are not precise, and the spectral range varies somewhat according to the agency defining the terms. The Sun emits huge amounts of near-infrared energy (Figure 2.11). Since the Earth’s surface is a relatively cool radiating body compared to the Sun, it emits mostly mid- and far-infrared radiation. About 50% of the energy emitted from humans is in the mid-infrared range from about 8-14 microns. Much of the remotely-sensed thermal mapping of the Earth’s surface from space is in infrared wavelengths (Figure 2.16). Far-infrared astronomical imagery is capable of penetrating large amounts of galactic dust, as well as detecting very cold (<140K; minus 133°C; minus 208°F ) objects (Figures 2.17a and 2.17b).



## Annual mean outgoing longwave radiation

Figure 2.16. The Earth is a relatively low temperature radiating body, so it emits radiation primarily in the longer far-infrared wavelengths. The map shows the average annual amount of outgoing longwave radiation emitted from the Earth from 2003-2011. Although one might expect the most intense radiation in the equatorial belt, where the greatest amount of solar radiation is received during September, persistent clouds there prevent much of the radiation from escaping. Areas immediately north and south of the Equator are not only warm, but the general lack of cloud cover allows more radiation to escape (Source/Credit: NASA/CERES).



Figure 2.17a. (left) The Carina Nebula in visible light, taken in July 2009 by the Hubble Wide Field Camera 3. The Carina Nebula is about 7500 light years from the Earth in the Carina Constellation. The visible light image clearly shows the pillars and protrusions of glowing gases and dust. More distant objects are obscured (Source/Credit: NASA).

Figure 2.17b. (right) The Carina Nebula in infrared bands, taken in July 2009 by the Hubble Wide Field Camera 3. In the infrared image, the gas and dust pillars are nearly invisible. The long infrared wavelengths have penetrated through the pillars, and reveal a background of youthful stars (Source/Credit: NASA).

- **Microwave radiation** (long wavelength). Microwaves are longer than infrared radiation, but shorter than radio waves. Wavelengths range from about 1000 microns to nearly a meter (~one yard). Wavelengths of about a foot are used in microwave ovens. Microwaves are advantageous for communication devices because they can penetrate clouds, rain, snow, and smoke. Microwave astronomy is used to detect objects that emit very low levels of microwave radiation. Supporting evidence for the Big Bang Theory stems from the cosmic microwave background radiation, perhaps left over from the Big Bang event billions of years ago (Figures 2.18a and 2.18b).

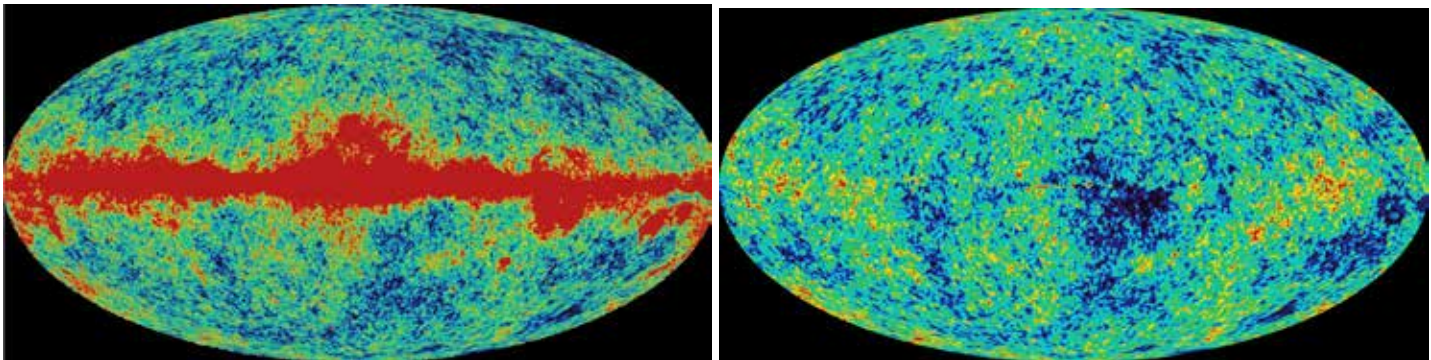


Figure 2.18a. (left) A microwave image of the first detailed, full-sky map of what is interpreted as some of the oldest light in the universe, some perhaps dating back to the Big Bang. The map of the cosmic microwave background taken from the Wilkinson Microwave Anisotropy Probe shows a red band that represents the microwave signal from our own galaxy, the Milky Way (Source/Credit: NASA).

Figure 2.18b. (right) This is essentially the same image as the one above, but the signal from the Milky Way has been removed, revealing what is interpreted as the cosmic microwave background radiation. The February 2003 image of the infant universe shows color variations that represent 13+ billion-year-old temperature differences (Source/Credit: NASA).



- **Radio waves (very long wavelength)**. Radio waves are at the far end of the electromagnetic spectrum. They cover a very broad band of wavelengths, ranging from about the size of a microwave oven to the size of the Earth. A household AM/FM radio dials in a certain frequency of radio waves, and converts them to mechanical vibrations in the speaker that we perceive as sound or music. Radio waves are emitted from many celestial objects, including most planets, the Sun, comets, distant galaxies, and nebula. Since radio waves are longer than optical waves, radio telescopes are unaffected by rain, clouds, and even visible light. One of the world's best radio telescope facilities is actually an array of 27 huge antennae in a high desert basin of New Mexico (Figures 2.19a and 2.19b).



Figure 2.19a. The Very Large Array (VLA) of giant radio telescopes in New Mexico, run by the National Radio Astronomy Observatory, is one of the most sophisticated on Earth. The 27 antennae are arranged in a Y pattern covering about 22 miles (36 km). They are linked by computers to act like a single radio telescope (Source/Credit: NASA).



Figure 2.19b. One antenna of the Very Large Array (VLA) of giant radio telescopes in New Mexico. Note the ladder in the left-center at the base of the unit for scale (Source/Credit: NASA).

Aside from being a ubiquitous energy source throughout the universe and being directly or indirectly involved in the heating of the Earth-atmosphere system, electromagnetic radiation has a vast number of residential, medical, military, scientific, and industrial applications. These include remote sensing of the Earth, Sun, planets, galaxies, and nebula. They also include communication technologies, navigation, surveillance, industrial and residential heating, and a wide spectrum of other applications (Figure 2.20).

### Uses of different wavelengths of electromagnetic radiation

Name	Wavelength	Natural Sources	Uses
Radio	1 m – 100,000 km	Celestial bodies, interstellar gases	Communications, radios, TV, cell phones, music, radiowave astronomy, radar, navigation, MRI scans, GPS technology, remote control devices, cordless phones, radio astronomy
Microwave	1 mm – 1 m	Stars, Big Bang	Microwave ovens, telecommunication, Doppler Radar, satellites, mobile phones, speed cameras
Far-infrared	30 - 1000 microns	Earth's surface, humans	Sensible heat, remote control devices, photography, heaters, weather forecasting, some lasers, saunas, thermal imaging
Mid-infrared	5 – 30 microns	Earth's surface, humans	Remote sensing, physiotherapy, thermal imaging, saunas, some lasers, guided missile technology
Near-infrared	0.7 – 5 microns	Stars	Night-vision goggles, long-distance telecommunications, homing heads of missiles, TV remote, astronomy (esp. cold-temperatures, i.e., galactic dust), video cameras, lasers
Visible	380 nm – 700 nm	Stars	Vision (sight), photography, surveillance, remote sensing
Ultraviolet	10 nm – 380 nm	Stars, UV lamps	Food irradiance, suntanning, detergents, counterfeit detection
X-ray	0.01 nm – 10 nm	Stars	Medical imaging, X-rays, CT scans, airport security, astronomy
Gamma ray	<0.01 nm	Gamma ray bursts, stars, nebula	Medicine, radiotherapy, sterilization, medical imaging

Figure 2.20. Some properties, sources, and uses of electromagnetic radiation.

## Heat Transfer Processes

Heat energy in the Earth's atmosphere can be transferred by radiation, conduction, convection, advection and the latent heat of condensation.

**Radiation.** Radiation is a heat transfer mechanism that does not require a transporting medium (liquids, solids, gases). The radiative transfer of energy from the Sun to the Earth is the initial phase in heating the Earth's atmosphere. The Earth re-radiates energy (**terrestrial radiation**), at longer wavelengths because of its low temperature compared to the Sun (Figure 2.21). Energy from Sun is called **insolation** (incoming **solar radiation**) (Figure 2.22).

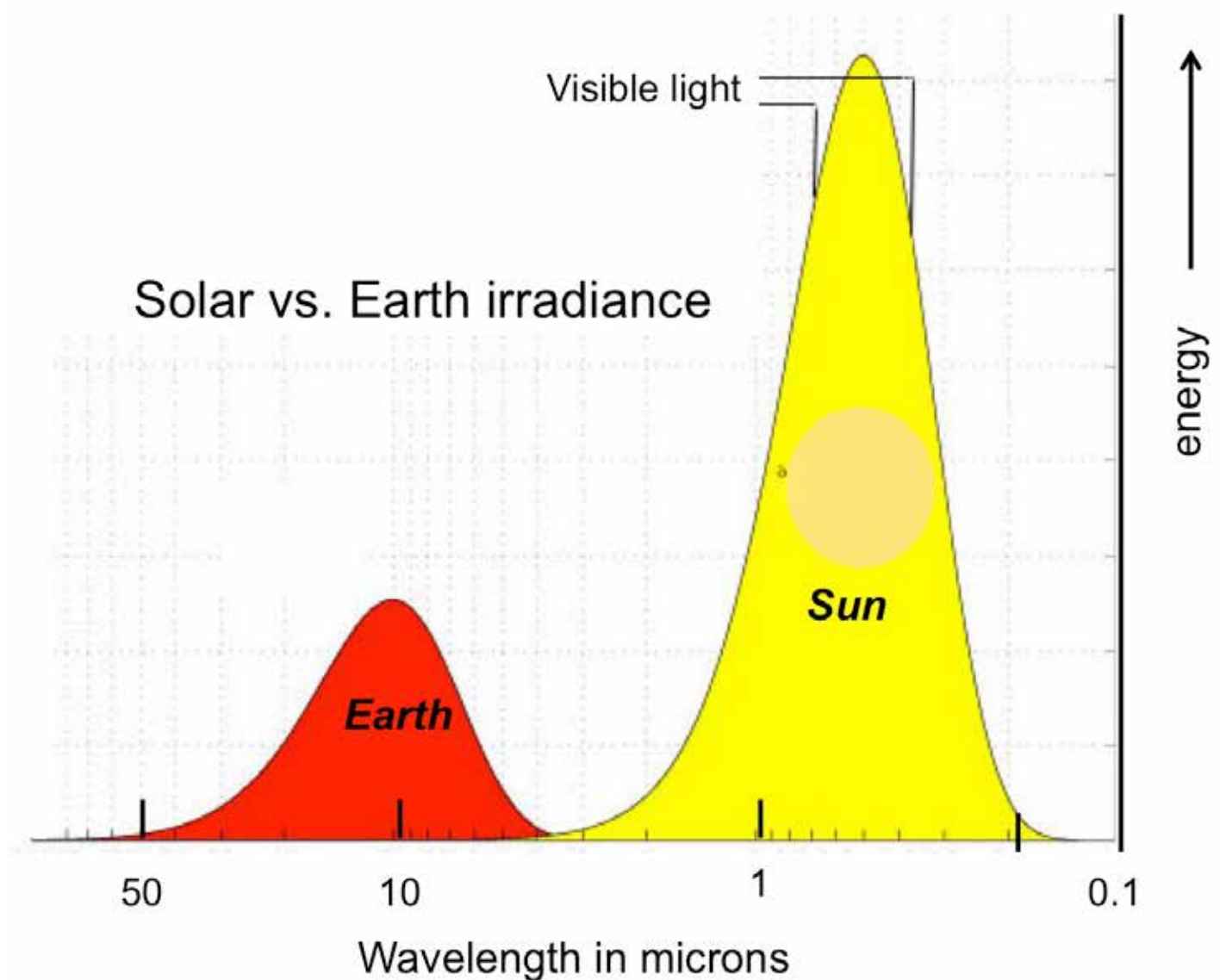


Figure 2.21. The solar spectrum is much shorter in wavelength and much more intense than Earth radiation due to the vast difference in temperature. If drawn to scale, the height (intensity) of the solar peak would be about 1,000,000 times that shown (Source/Credit: modified from several sources).

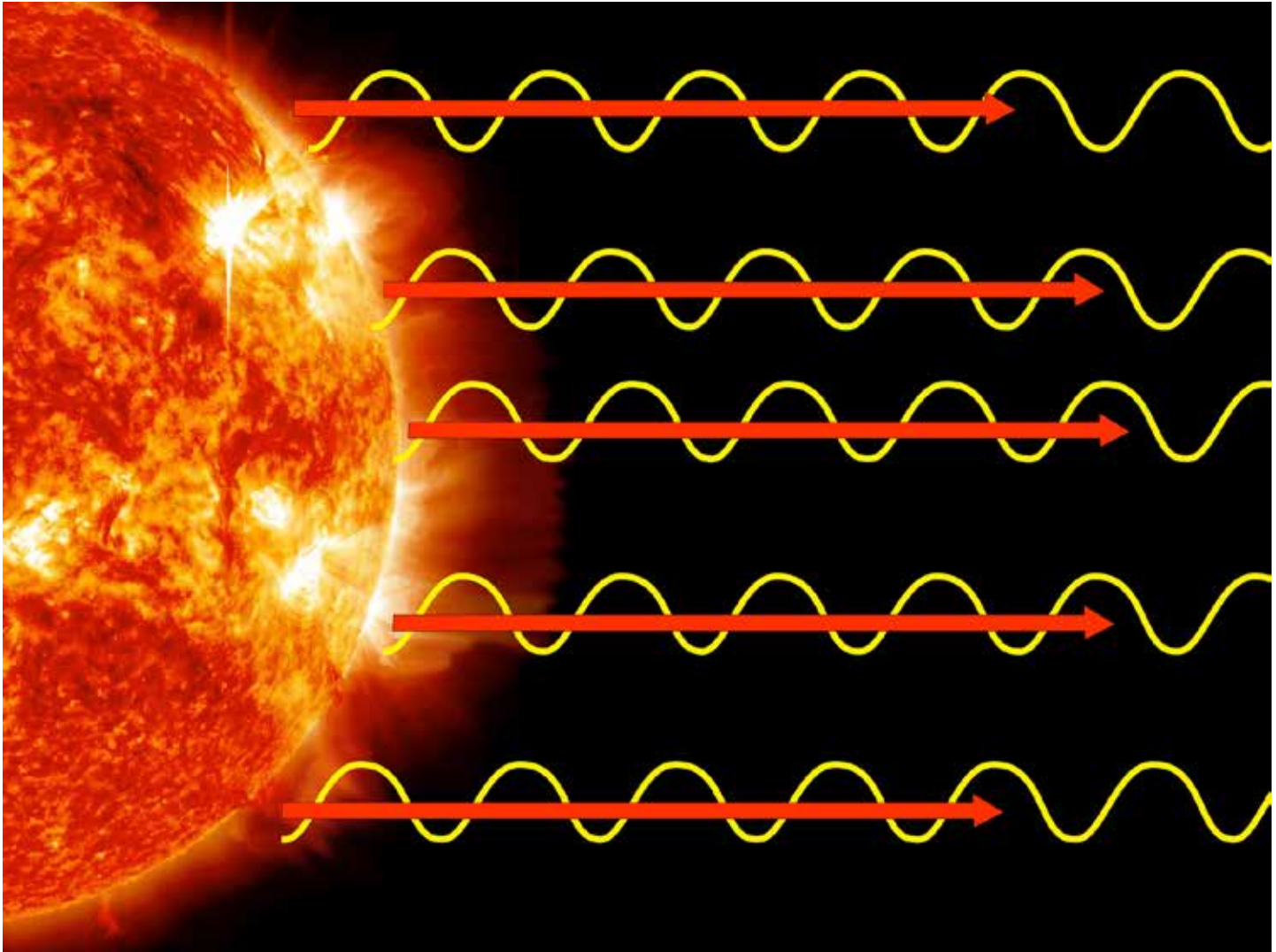


Figure 2.22. Insolation (incoming solar radiation) is generated by the Sun, and is described as a wave form of energy. Some pertinent characteristics of solar radiation include: (1) solar radiation is generated by high temperatures, so it has relatively short wavelengths; (2) most of the solar output is in the visible and near-infrared wavelengths; (3) other wavelengths are of far less abundance (ultraviolet, X-rays, radio waves, etc.), but are nonetheless very important because of their special properties (e.g., sunburn); (4) the rays do not require a medium to transport energy through, as do other types of energy transfer (e.g., conduction and advection); (5) the Sun is far enough from the Earth so that all rays are essentially parallel; (6) the rays travel through the vacuum of outer space at the speed of light (186,000 miles/second, or  $\sim 300,000$  km/sec), regardless of wavelength; and (7) they are the main source of heat energy for the atmospheres of all the inner planets (Source/Credit: Sun disk NASA).

**Conduction.** Conduction is the process of heat transfer through contact between adjacent molecules. When two adjacent molecules have different vibrational energies (i.e., different temperatures), there is a net transfer of energy from the more energetic to the less energetic molecule. Therefore, in conductive heat transfer, heat energy is always transferred from hotter objects to colder objects. When you touch the handle of a cast-iron frying pan, heat is conducted from the handle to your hand (Figure 2.23). Conversely, when you touch the handle of a cold cast-iron frying pan, heat energy is transferred from your hand to the metal, giving the sensation of coldness.

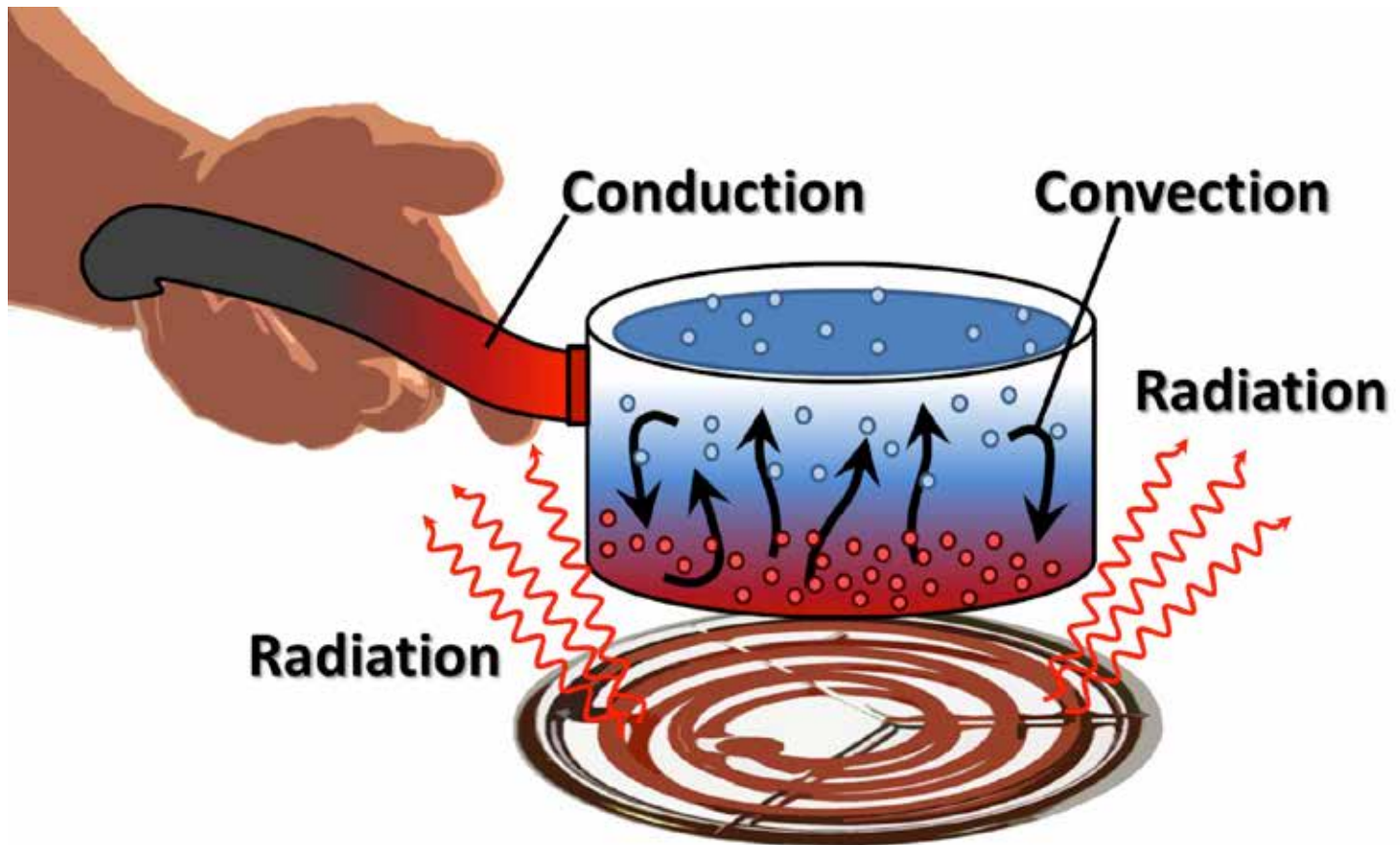


Figure 2.23. Pot illustrating conduction, convection, radiation (Source/Credit: NASA).

The rate of conductive heat transfer depends on the properties of the conductors and the difference in temperature between the objects in contact. Some solids (e.g., metals) are good heat conductors, whereas others (air, water) are not (Figure 2.24). In general, liquids and gases are less conductive than solids. The atmosphere is a poor heat conductor. As a rule of thumb, the greater the difference in temperature between two objects in contact, the higher the rate of conduction of heat.

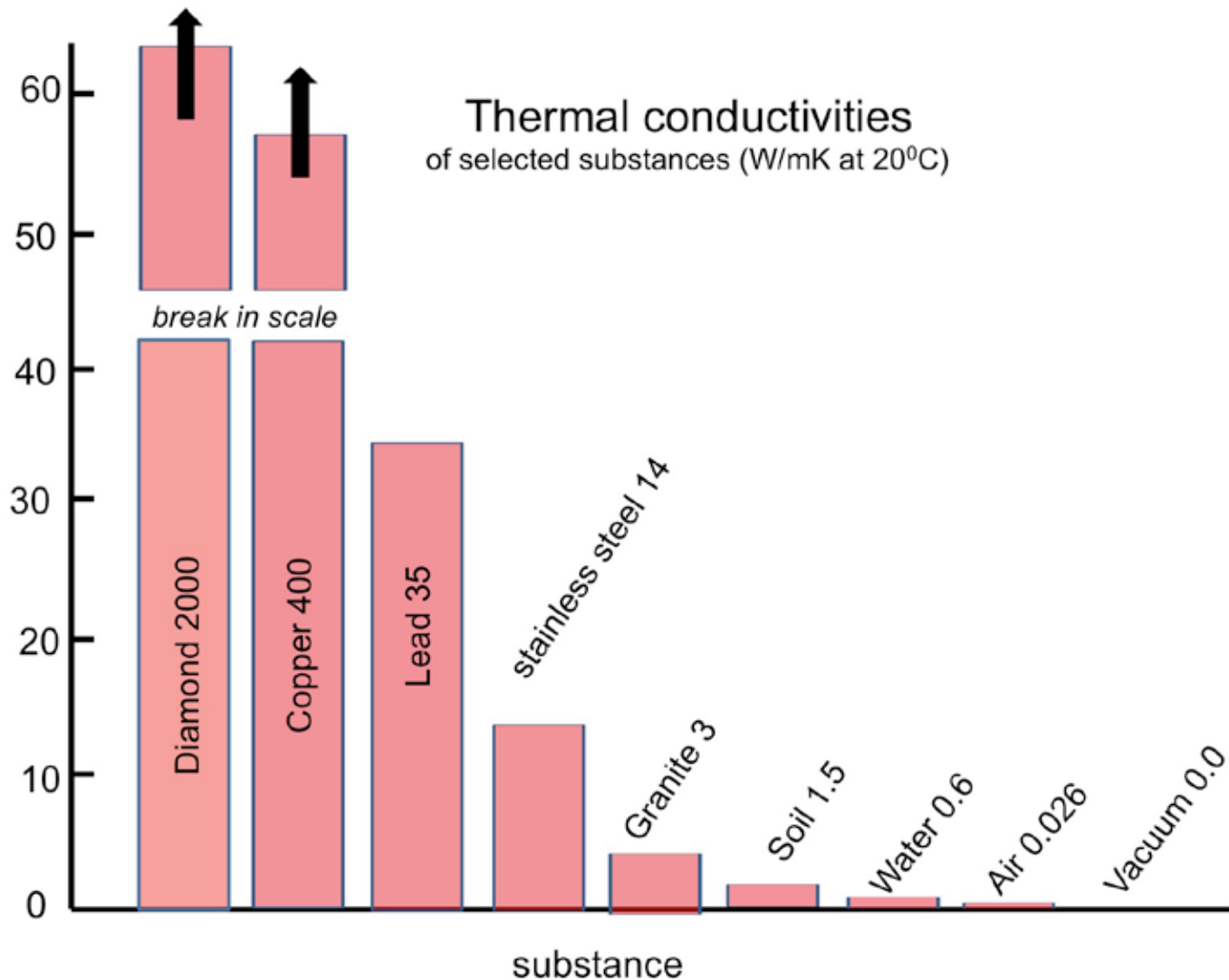


Figure 2.24. Thermal conductivities of selected substances. Solid metals are typically high, whereas fluids and gases are typically low (Source/Credit: modified from several sources).

Because air is such a poor conductor of heat, it is very difficult for conduction to heat the air to any great height. A few feet above the ground, the temperature may be much cooler or warmer than the surface. For instance, it is generally recommended that when placing a thermometer outside to measure air temperature that the instrument be placed some five feet off the ground (and in the shade). The five feet gets it away from the very warm layer right at the surface caused by conduction.

**Convection.** Convection transmits thermal energy by translocation of groups of excited (heated) molecules from one place to another in fluids and gases. In the lower atmosphere, the movement is initially vertically upward, due to the buoyancy of the heated group of molecules. This motion results from temperature-induced density differences within the medium, which causes warm air to rise and cold air to sink, often producing a circular motion in the atmosphere in the form of a *convection current* (Figures 2.25a, 2.25b and 2.25c). Hot air balloons rise when the air inside the balloon is warmed by on-board propane heaters (Figures 2.26a and 2.26b). When the balloons wish to descend, the air inside the balloon is allowed to cool, becoming denser, causing negative buoyancy.

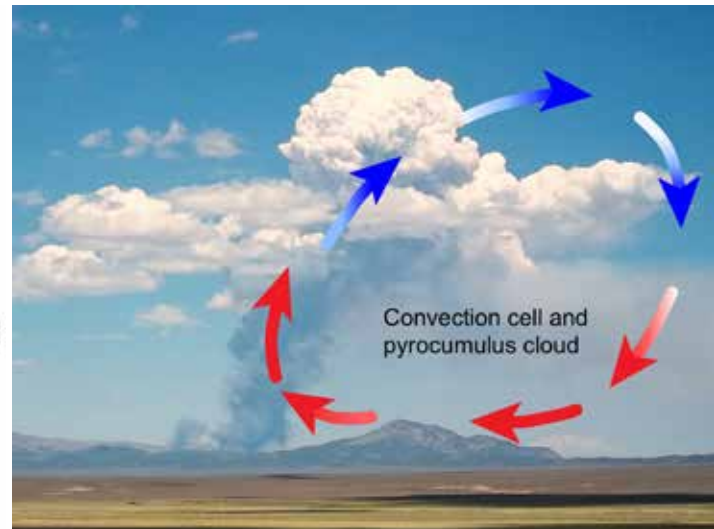
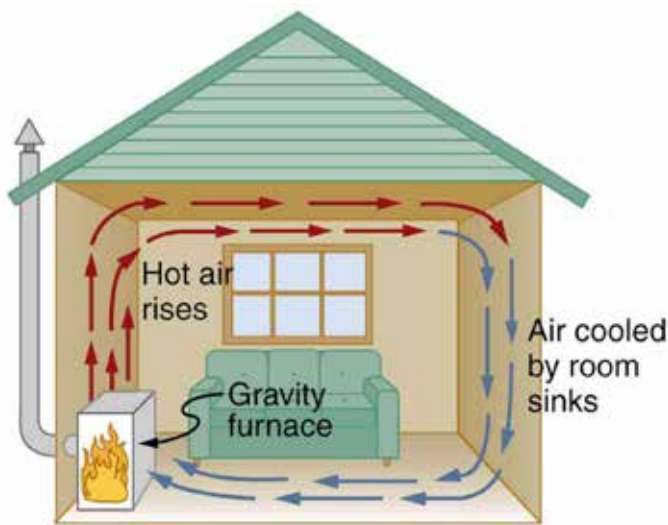


Figure 2.25a. (left) Convection currents occur on any scale. Small convection currents are initiated inside homes when air is heated by a furnace (Source/Credit: cnx.org, Rice University).

Figure 2.25b. (right) Larger convection currents occur locally in the atmosphere where there is differential heating or cooling. A forest fire in central Nevada during the summer of 2012 (rising smoke plume) heats the surface air, which then rises buoyantly and forms a pyrocumulus cloud from the local lift. Air then moves horizontally, cools, and eventually sinks. Some of the descending air reaches the surface to complete the cellular pattern of circulation (Source/Credit: Nancy Netoff).



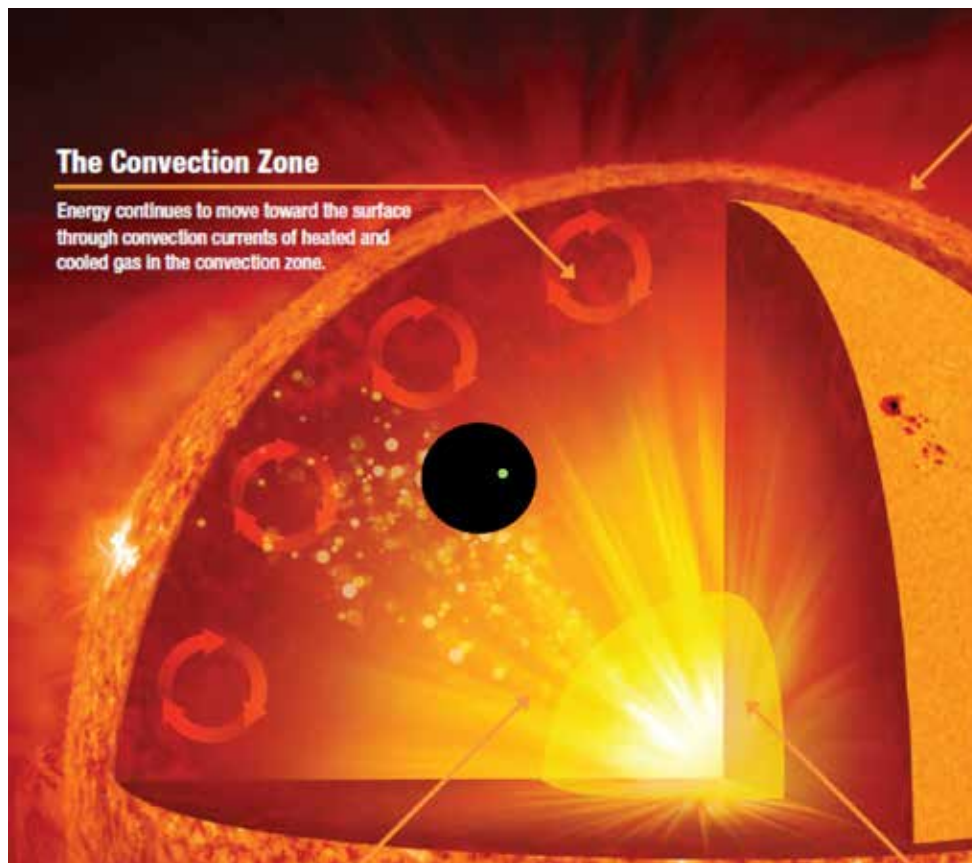


Figure 2.25c. Largest convection cells in the Solar System are depicted in this artist's conception of the Sun. In the convective zone, some 113,000 miles thick, huge convection cells bring incandescent gases from within the Sun to its surface. The black inset depicts Jupiter, the largest planet in the Solar System, and within that, a green circle representing the approximate relative size of the Earth (Source/Credit: NASA).



Figure 2.26a. (left) Hot air balloons in the annual Reno (Nevada) Hot Air Balloon Races ascending buoyantly through the lower atmosphere (Source/Credit: Tracy Netoff-Pike).



Figure 2.26b. (right) Hot air balloon in the annual Reno (Nevada) Hot Air Balloon Races on the ground being heated by a propane burner (Source/Credit: Tracy Netoff-Pike).

**Advection.** Broadly defined, advection is a transport mechanism of a substance by fluid flow due to the net transport of the substance by the fluid. In this usage, the transported substance can be a suspended mineral such as atmospheric dust, or a dissolved material in water, such as salts. As it is used here, advection is the more-or-less horizontal transfer of heat or cold by the wind. The day-to-day variations in air temperature and humidity that are caused by changes from southerly to northerly flow and vice versa are good illustrations of advection. Cool-season weather in East Texas is largely controlled by advection; southerly or southeasterly flow is accompanied by relatively warm, moist air from the Gulf, whereas cooler, drier days advect air from the interior of the continent (Figure 2.27).

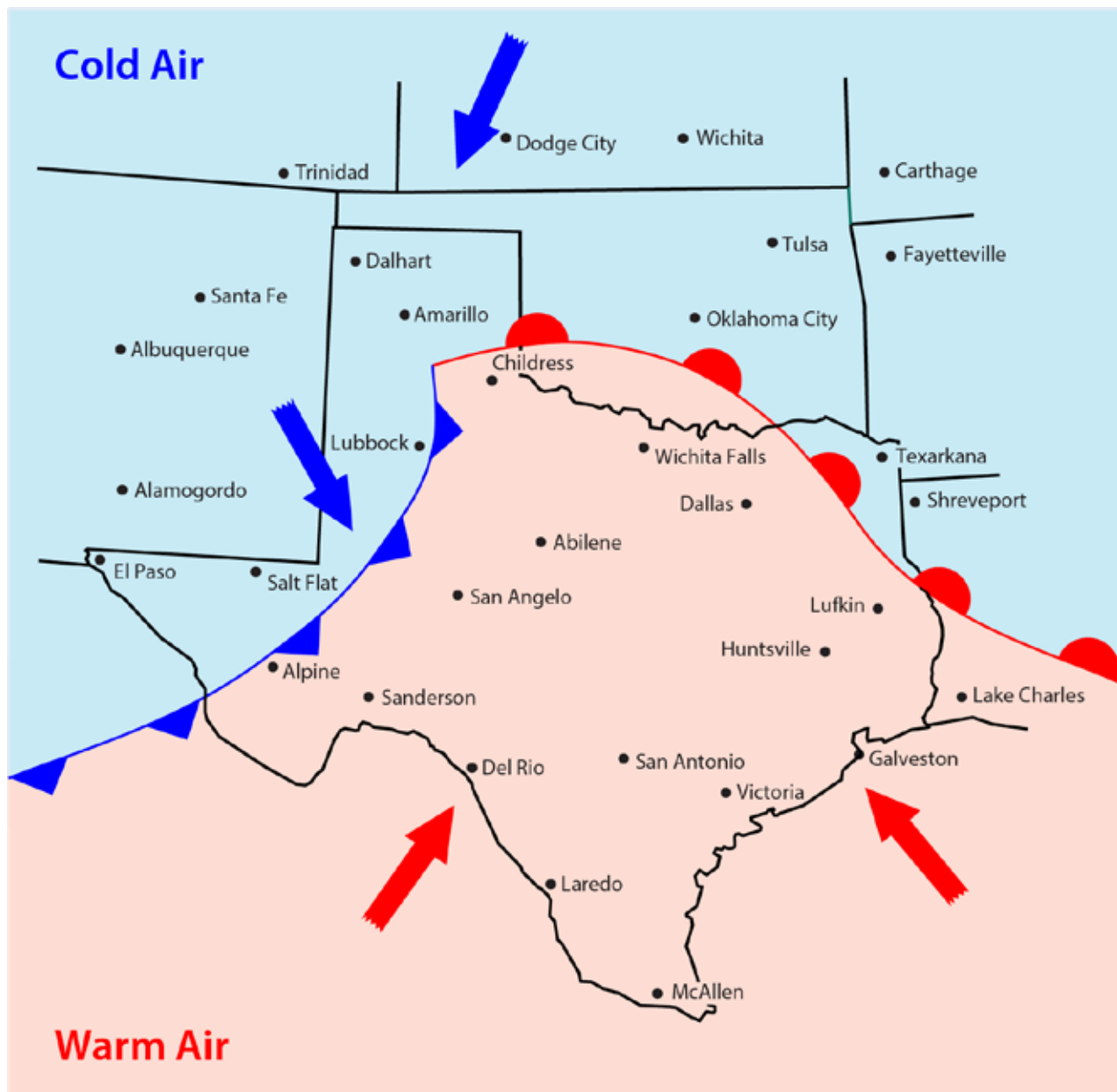


Figure 2.27. The horizontal movement of cold air southward into Texas from the north, as well as the movement of warm air from the south, is a form of heat transfer known as advection (Source/Credit: modified from Dennis I. Netoff and Ava Fujimoto-Strait, *Weather & Climate Lab Manual*).

Advection is similar to convection in that it occurs at practically any scale. Local advection of cool air from the ocean during the day is the sea breeze, which may be a component of a local convection cell (Figure 2.28). Advection in the ocean is an important mechanism of horizontal heat transport (Figure 2.29). On a sub-continental scale, the summer monsoons of the southwestern United States transport both water vapor as well as thermal energy from the tropical Pacific and Gulf of Mexico to the continental interior (Figure 2.30).

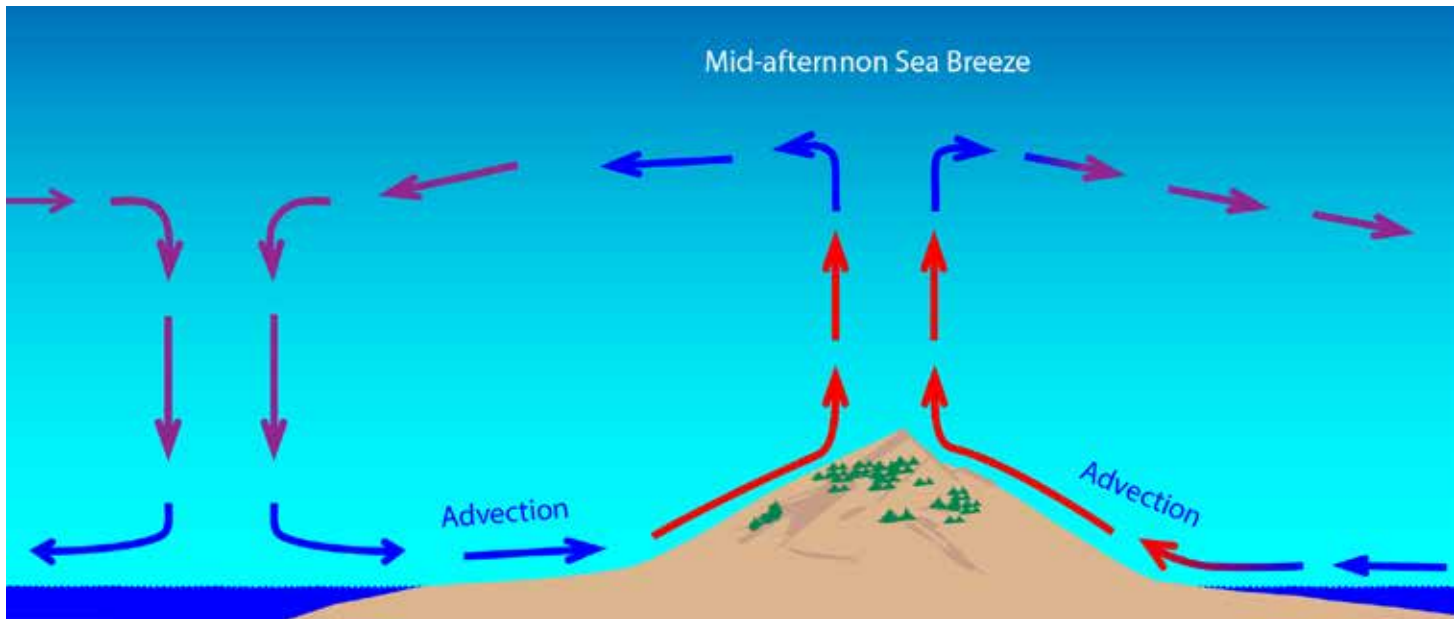


Figure 2.28. The sea breeze typically develops during the afternoon when land temperatures are substantially warmer than the adjacent water. Low pressure develops over the land, which draws welcome cool breezes in from the water and results in the sea breeze (Source/Credit: Dennis I. Netoff, based on Carmen Island, Mexico).

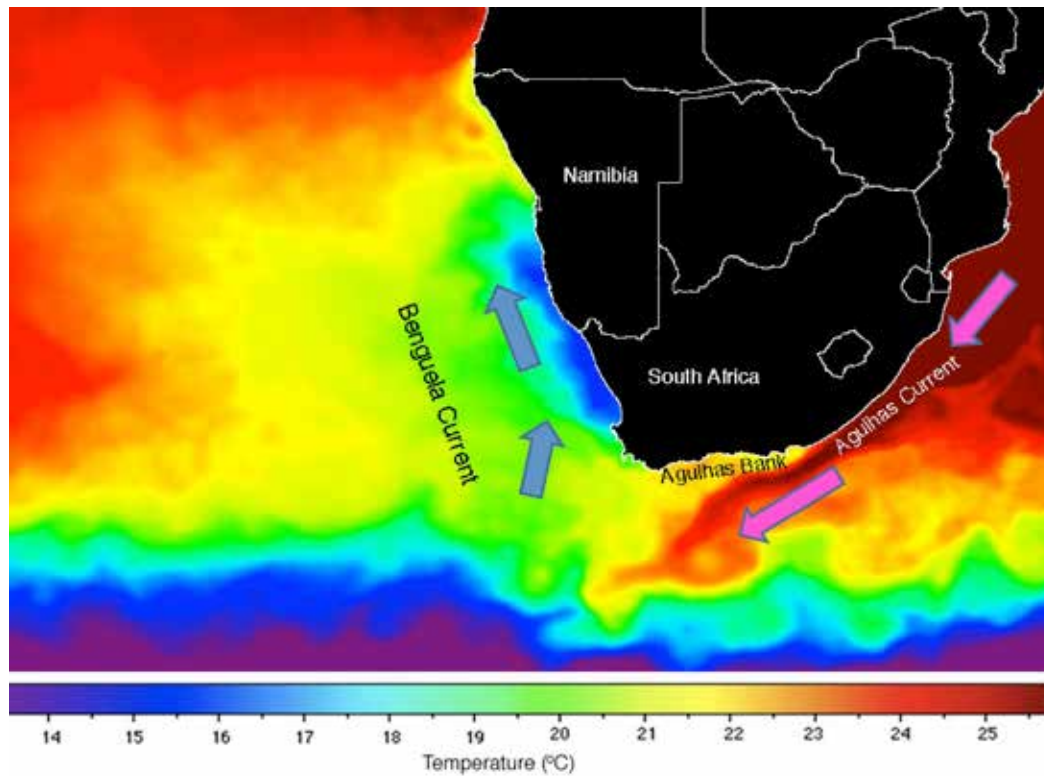


Figure 2.29. Advection of cold and warm surface ocean currents is critical in maintaining the heat balance of the Earth. The image taken on February 3, 2008 indicates sea surface temperatures along the coast of South Africa, including the warm Agulhas Current and the cold Benguela Current (Source/Credit: NOC).



Figure 2.30. During a brief period in the hot summer months, the normally bone-dry deserts of the Southwest experience a monsoon flow of moisture through advection from the tropical Gulf of Mexico and Sea of Cortez source regions. During the North America monsoons, humidities and cloud cover are much higher than normal and afternoon thunderstorms are common (Source/Credit: Accuweather.com, July 12, 2013).

**Latent Heat of Condensation.** The latent heat of condensation is another important heat transfer mechanism. Whenever water is converted from solid to liquid phase or from liquid to gaseous phase, heat energy is required in order to break chemical bonds and raise the water to a higher energy level (Figure 2.31). That same energy is returned to the atmosphere when condensation occurs. Every cloud that forms in the atmosphere adds this latent heat. The addition of latent heat aids in further cloud development, and is also an important energy source driving severe storms.

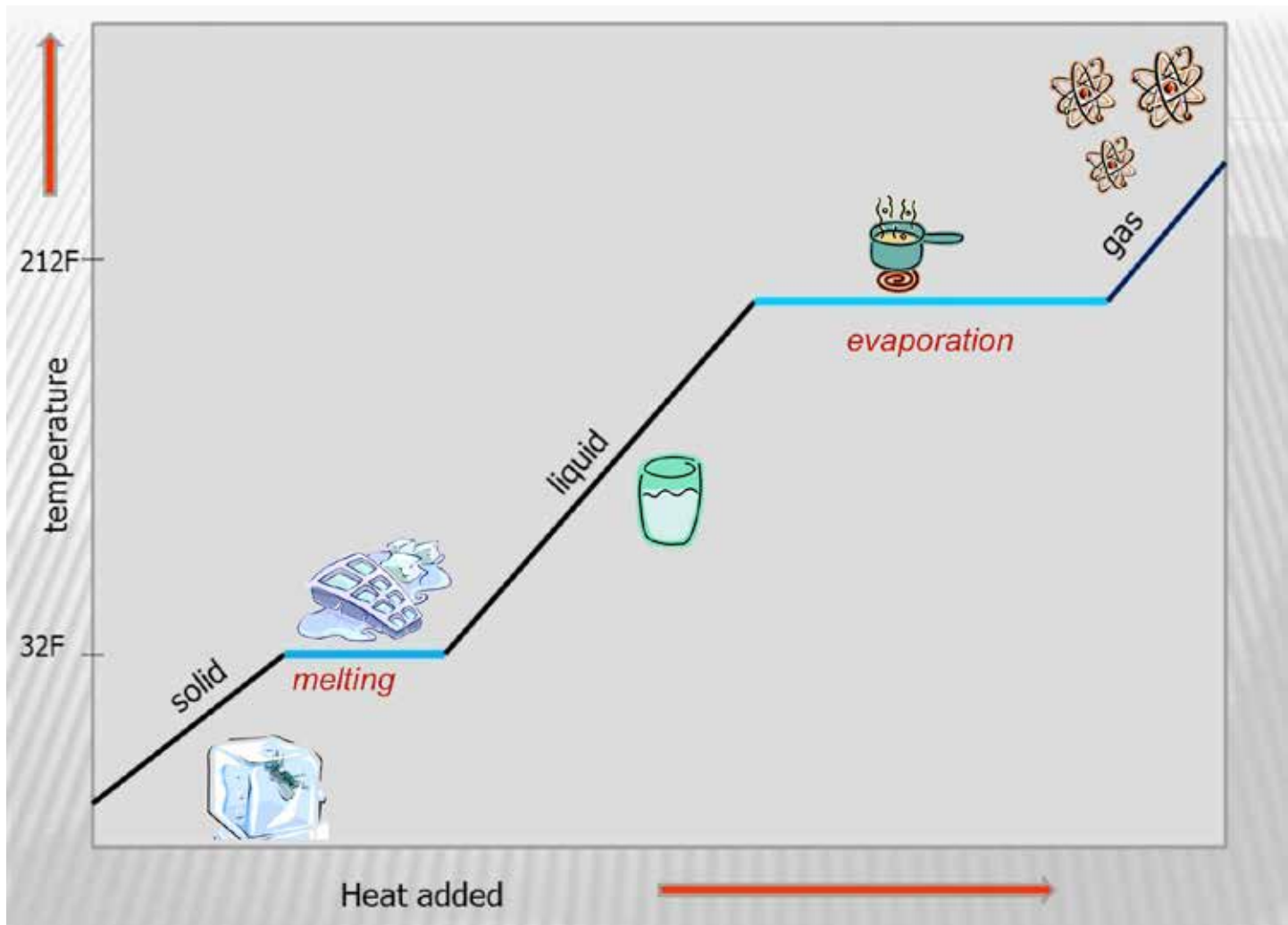


Figure 2.31. When solid ice is slowly heated at a constant rate, temperature climbs predictably until 32°F (0°C) is reached. Even though more thermal energy is being applied to the system, the temperature hovers until all of the ice has melted. Energy has been used in breaking chemical bonds, rather than increasing the temperature. A similar plateau occurs when temperatures approach 212°F (100°C), when more chemical bonds are being broken during evaporation. The same energy that was required to change state from solid to liquid or liquid to gas can be released back to the atmosphere during condensation (gas to liquid), freezing (liquid to solid) or sublimation (gas to solid) (Source/Credit: Dennis I. Netoff).

## Fate of Insolation on Earth

When sunlight reaches the Earth after traveling some 93 million miles through space, only about half of it passes through the atmosphere and strikes the surface. Approximately 30% of the insolation is reflected, which means that this energy does not result in heating of the atmosphere. Only if the energy is absorbed by the air or by the surface does heating occur. Thus, back-scattering and reflection to space represent a loss of radiative energy from the Earth that cannot be utilized in atmospheric heating (Figure 2.32).

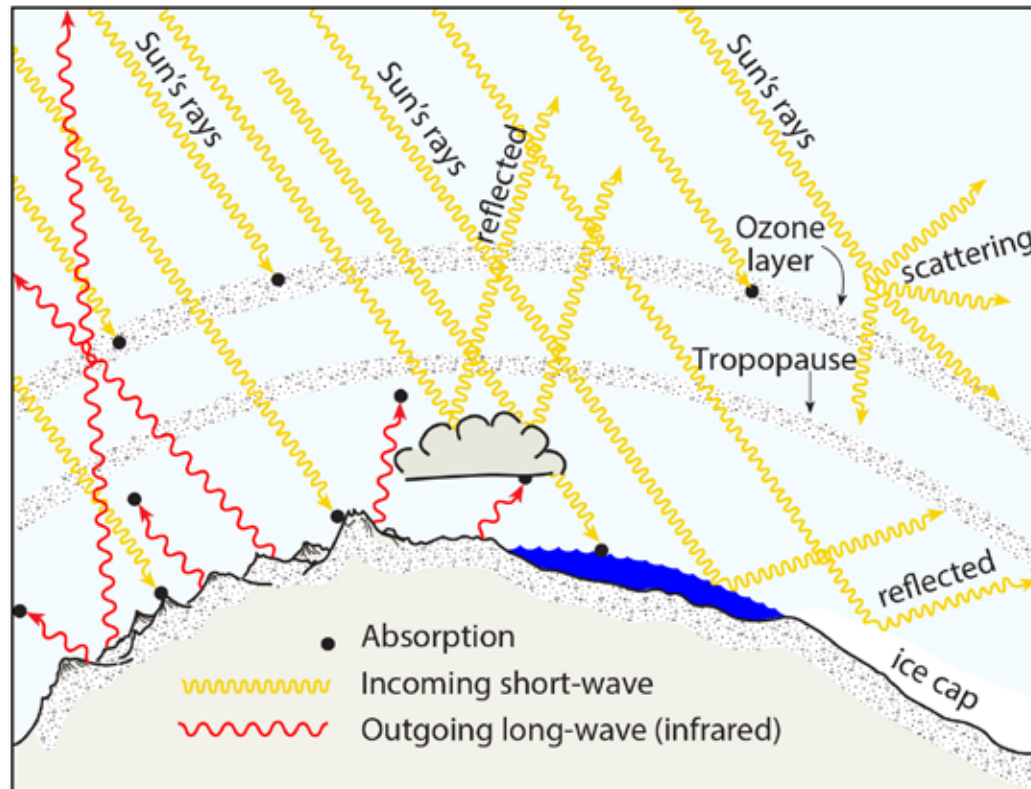


Figure 2.32. When insolation (incoming solar radiation) arrives from the Sun, approximately 30% is reflected by the atmosphere, clouds and the Earth's surface. On average, 19% is absorbed by the atmosphere, and the remainder (51%) is absorbed by the surface. Only that portion of insolation that is absorbed acts to heat the Earth.

**Scattering** is the redirection of incoming radiation in all directions by small particles such as gaseous molecules, water droplets or dust. Scattering by household dust is responsible for the shafts of incoming sunlight frequently seen around household windows. Scattering by tiny water droplets is responsible for similar shafts of light in a dimly-lit forest.

**Selective scattering** (also *Rayleigh Scattering*) is the process of scattering of certain wavelengths of radiation by certain-sized particles. Good Rayleigh scatterers are particles that have a diameter of only about 10% of the wavelength of incoming radiation. Blue skies in the Earth's atmosphere are the result of selective scattering of shorter wavelengths (blue and violet) by small  $O_2$  and  $N_2$  molecules (Figure 2.33). The light has been repeatedly scattered

throughout the atmosphere, so blue light seems to emanate from all directions. Violet light in a clean atmosphere is actually scattered more effectively than blue light, but the human eye is more sensitive to blue colors. Redder skies at sunrise or sunset are caused by the longer path through the atmosphere that incoming light takes, so more of the blues and violets are backscattered to space (Figure 2.34).

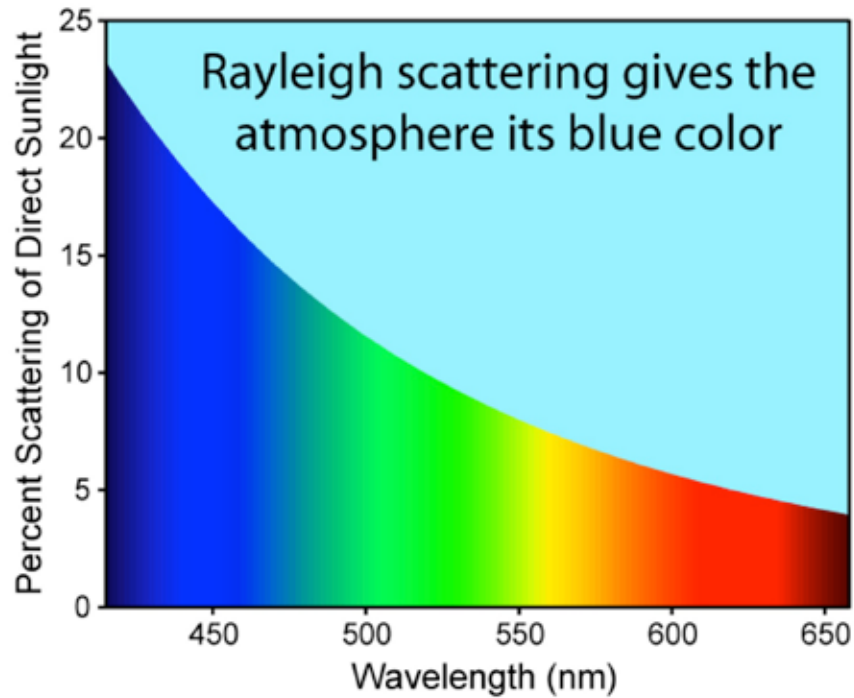


Figure 2.33. The blue color of the sky is the result of more effective scattering of blue and violet light in the atmosphere by common gases than those with longer wavelengths. The diagram approximates incoming sunlight at a high angle from the horizon and does not take into account the role of dust particles (Source/Credit: Wikipedia, [http://en.wikipedia.org/wiki/Rayleigh\\_scattering](http://en.wikipedia.org/wiki/Rayleigh_scattering)).



Figure 2.34. This image taken by an astronaut on the International Space Station shows variation in sky color as a function of the length of the path that solar radiation takes through the atmosphere. Red and orange colors close to the horizon are the result of excessive scattering and loss of blues and violets (Source/Credit: NASA/JPL, astronaut photo ISS015E10469).

**Reflection** refers to the redirection of wave energy at the interface between two different substances. The waves are reflected at the same wavelength of the incident radiation. Unlike scattering, where incoming radiation can be dispersed in any direction, reflected light is returned at the same angle that it enters relative to the perpendicular (Figure 2.35).

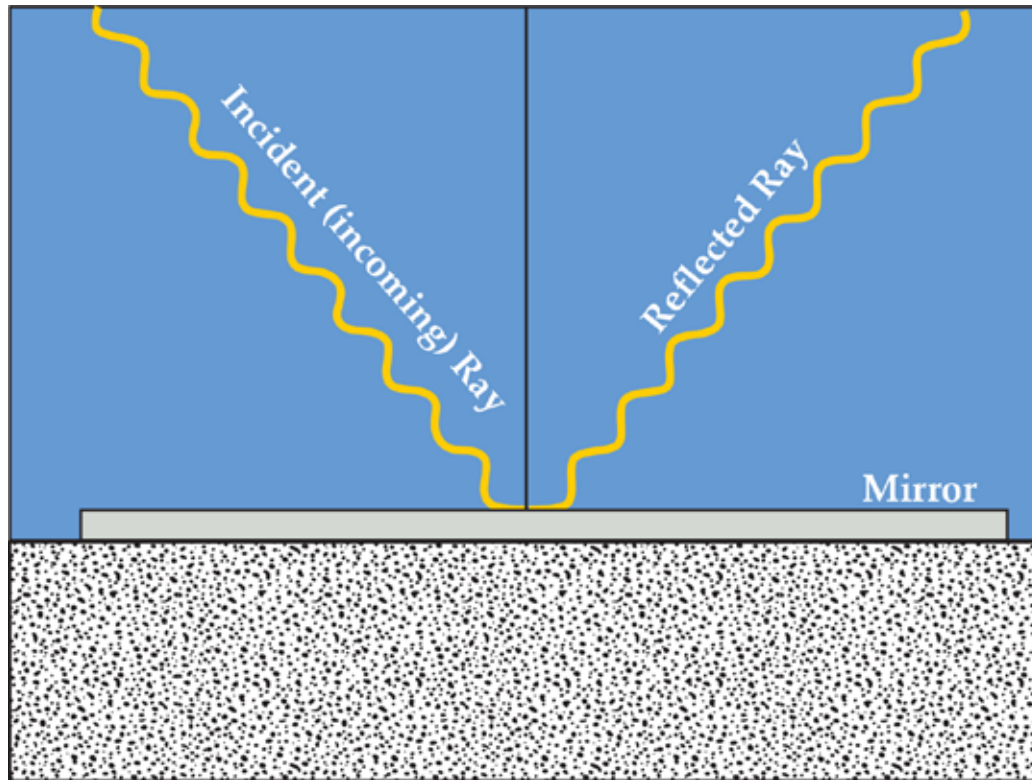


Figure 2.35. Reflected radiation from a perfect reflector will return the radiation at the same wavelength and same angle as the incident radiation (Source/Credit: Dennis I. Netoff).



Certain objects are inherently good reflectors, whereas others are not. A measure of the percentage of light that is reflected off of a surface is termed **albedo**. Albedo is indicated by the brightness of an object in reflected light (e.g., cloud tops and snow). Objects with a high albedo do not heat readily because they only absorb a small fraction of incoming radiation. Snow doesn't melt readily, even when the temperature rises above freezing, because it reflects most of the energy that strikes it, and because of the extra energy that is required to change state (latent heat).

A dark surface has a low albedo (e.g., asphalt road, dark soil). A dark color indicates that more energy is being absorbed than reflected. Absorbed energy causes an increase in molecular motion, so the temperature rises. Different surfaces on the Earth have different albedos (Figure 2.36).

Object	Albedo (%)	Comments
Earth	31	Average, all surfaces
Moon	6-8	Average, all surfaces
Asphalt	5-10	Depends on exact color, black lowest
Concrete	7-27	Depends on exact color, darker = lower
Dark roof	8-18	Depends on exact color
Soil	5	Dark and wet
Soil	40	Light and dry
Grasses	16	Long
Grasses	26	Short
Snow	80-95	Fresh, clean
Snow	40-60	Oil, dirty
Clouds	30-50	Thin
Clouds	60-90	Thick
Forest	15-20	Deciduous
Forest	10-15	Coniferous
Water	50-80+	Sun near horizon
Water	1-5	Sun overhead

Figure 2.36. Different substances consist of many different types and colors of materials which vary in their albedo. Light colored surfaces tend to reflect energy. Darker surfaces tend to have lower albedos.

Transmitted radiation is that component of incoming solar radiation that is not reflected, absorbed, or scattered. In general, of the total incoming solar radiation, Earth's surface reflects/scatters about 30% and 20% is absorbed, so only 50% of the incoming solar radiation reaches the Earth's surface (Figure 2.37).

### Insolation: top of atmosphere vs. Earth's surface

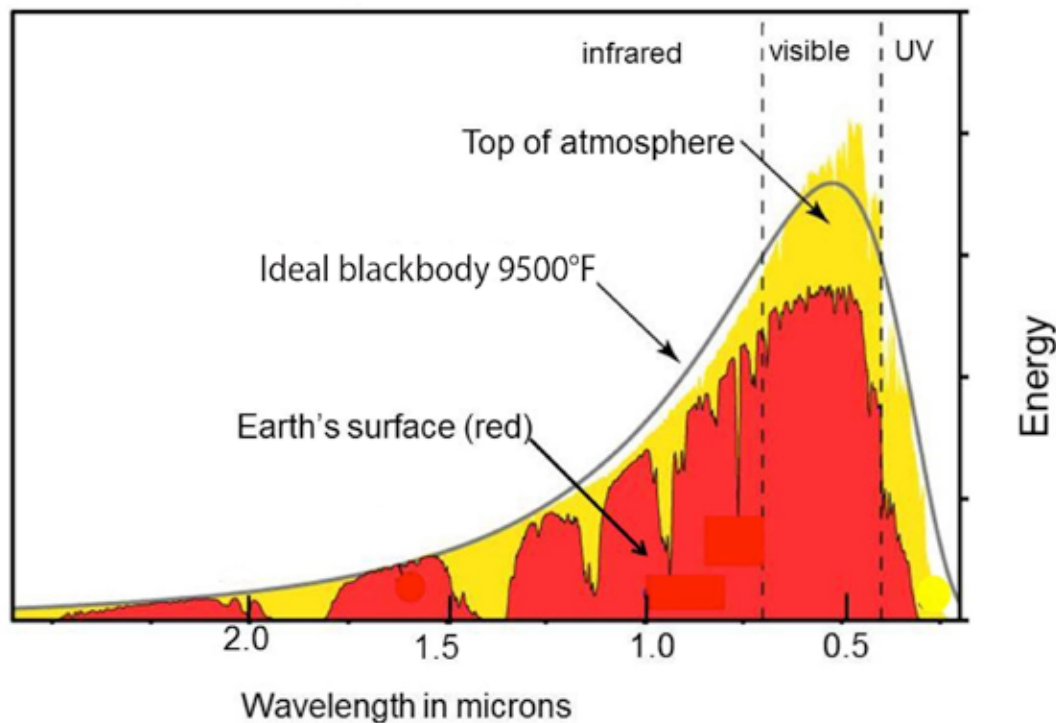


Figure 2.37. Insolation at the surface of the Earth is slightly different than that at the top of the atmosphere because of selective scattering, reflection, and absorption of certain wavelengths by ozone, carbon dioxide and water vapor (Source/Credit: modified from several sources).

**Absorption.** Approximately 19% of insolation that reaches the Earth is absorbed directly by the atmosphere. This absorption results in some heating, but this occurs mainly in the stratosphere where ozone absorbs large amounts of ultraviolet radiation.

Approximately 51% of the solar radiation that strikes the Earth-atmosphere system is absorbed by the surface. Added to the 19% absorption by the atmosphere directly, this means that 70% of the insolation is effective at heating the Earth and atmosphere.

Insolation that is absorbed by the Earth's surface is radiated back to the atmosphere at much longer wavelengths, primarily in the far-infrared. This longwave terrestrial radiation causes most of the heating of the atmosphere. This process is summarized as follows:

- Insolation arrives mostly in the visible and near-infrared portion of the spectrum, so is principally shortwave radiation.

- The Earth's surface absorbs the shortwave radiation and then re-radiates it at longer far-infrared wavelengths. This emitted energy is called **terrestrial longwave infrared radiation**, or terrestrial infrared radiation (TIR).
- Once the terrestrial infrared radiation is emitted as longwave radiation from the ground, **much of it is absorbed by greenhouse gases in the atmosphere, such as carbon dioxide, methane and water vapor. It is this process that is responsible for the majority of atmospheric heating.**

The atmosphere is therefore heated indirectly, primarily from the ground up, by the absorption of terrestrial longwave radiation by greenhouse gases, rather than from the top down by incoming solar shortwave radiation (Figure 2.38). This process of indirect heating of the atmosphere is known as the **greenhouse effect**.

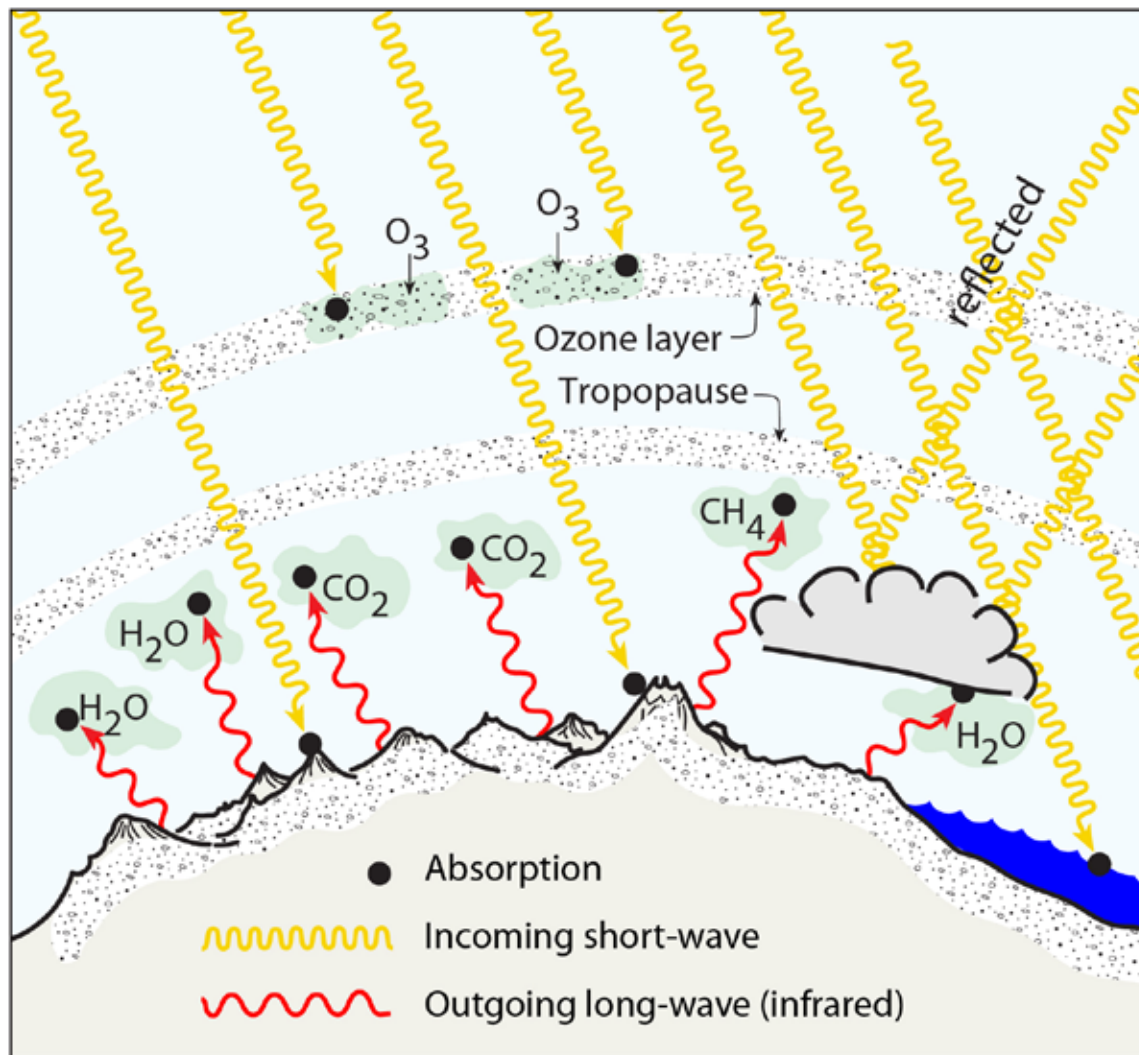


Figure 2.38. Once solar shortwave radiation is absorbed, it is then re-radiated from the surface at longer wavelengths, primarily as far-infrared radiation. Much of this longer terrestrial infrared radiation is then absorbed by greenhouse gases in the atmosphere. This process of indirect heating of the atmosphere is known as the greenhouse effect (Source/Credit: Dennis I. Netoff).

The atmosphere acts like the glass of a greenhouse. Shortwave radiation from the Sun passes through the glass and is absorbed by objects inside the greenhouse (Figure 2.39). Those objects emit far-infrared radiation which is blocked by the glass. The greenhouse temperature can rise far above the temperature of the outside air. The glass also prevents convective heat loss. The process is similar to the overheating of the inside of an automobile on a summer day.

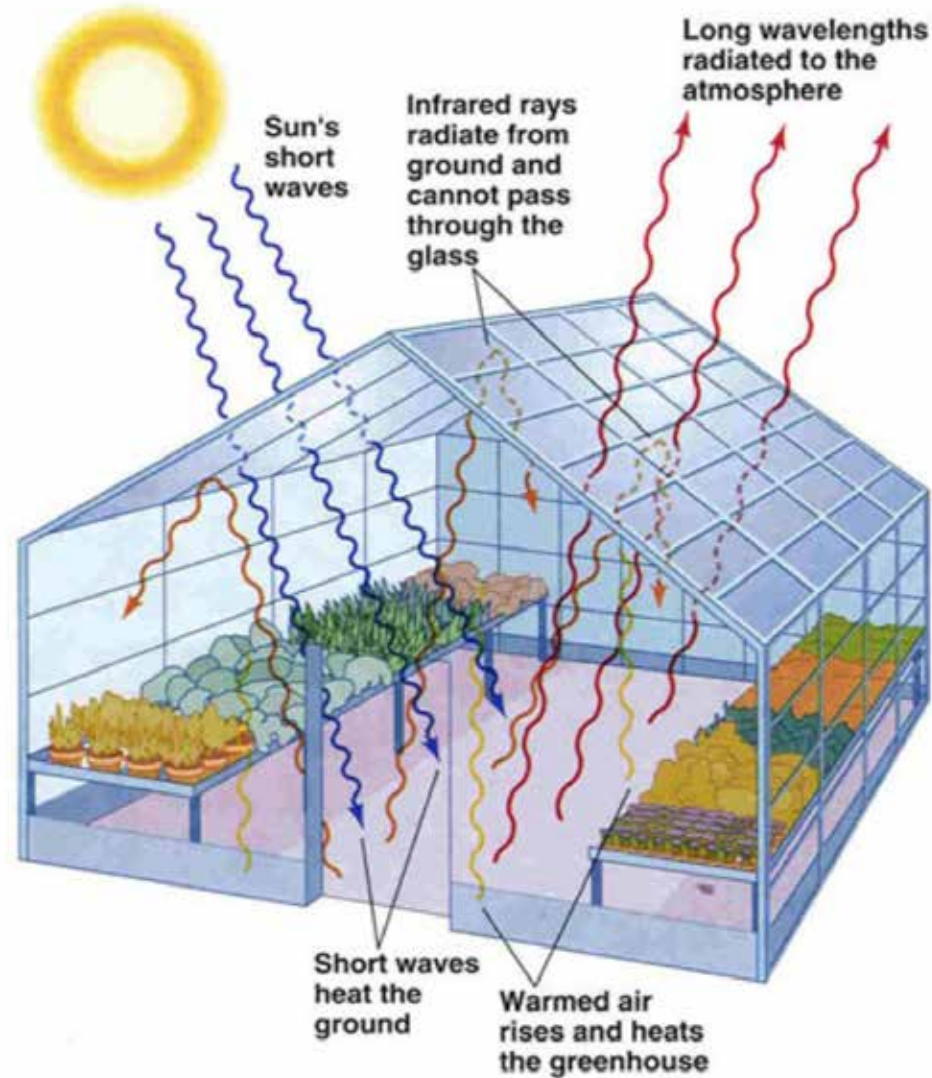


Figure 2.39. The warming of a greenhouse is somewhat analogous to the heating of the atmosphere. The greenhouse glass, like the atmosphere, permits passage of incoming short-wave radiation. Objects inside the greenhouse act the same as the Earth's surface, absorbing most of the incoming short-wave radiation and re-radiating it at longer wavelengths. The longer wavelengths are then trapped by the window glass, much in the same way as greenhouse gases prevent the escape of terrestrial radiation (Source/ Credit: OZ Climate Sense).

Clouds also affect atmospheric heating and cooling in many ways. Day-night temperature variations can be either enhanced or subdued by cloud cover. During the daytime, low, thick clouds reflect some of the incoming shortwave radiation, thereby keeping surface temperatures somewhat cooler than might be expected. However at night, those same clouds absorb some of the outgoing longwave radiation, keeping temperatures warmer. Cloudy days and nights tend to have less of a day-night temperature fluctuation than clear days and nights (Figures 2.40a and 2.40b).

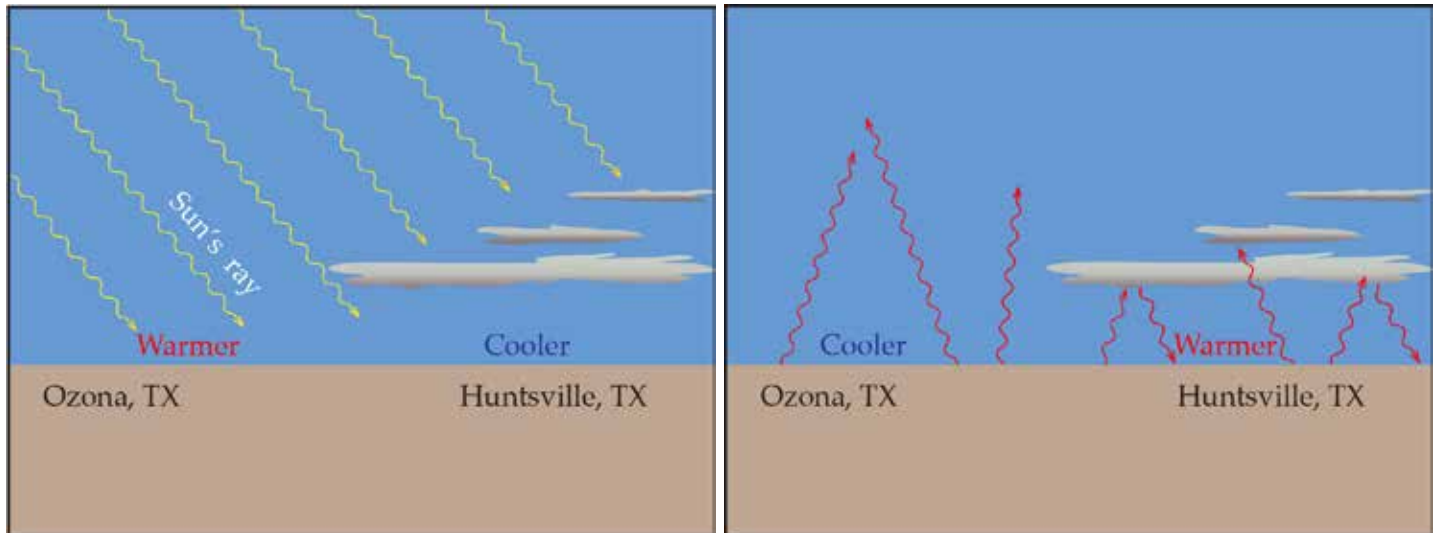


Figure 2.40a. (left) During the daytime, more of the incoming short-wave solar radiation reaches the ground under clear skies (Ozona), compared to overcast skies (Huntsville), so Ozona's daytime temperature may be higher than Huntsville's even though there is the same amount of solar radiation at the top of the atmosphere.

Figure 2.40b. (right) At night, under clear skies, much of the longwave terrestrial radiation is lost to space creating cool surface temperatures. Overcast skies tend to trap longwave terrestrial radiation and send some of the re-radiated energy back to the surface, thus maintaining warmer surface temperatures than those under clear skies.

## Controls of Insolation and Absorption

### Earth-Sun Relationships

The only energy from the Sun that is used in heating the Earth's surface and atmosphere is the radiation that is absorbed. Variations in the amount of radiation absorbed in time and space are clearly the key to understanding why some places are warmer or colder than others, as well as how a given place experiences daily and seasonal variations in temperature.

The amount of energy absorbed by a substance, and therefore its temperature, is determined in large part by **insolation**, **the nature of the absorbing medium**, and **the wavelength of radiation**. The dosage of incoming radiation, insolation, is in turn largely controlled by

- (1) **Variations in solar output**;
- (2) **Earth-Sun distance**;
- (3) **orbital and axial variations**;
- (4) **intensity of radiation**; and
- (4) **duration of daylight**.

### Insolation: Minor and Long-Term Controls

**Solar output.** All stars evolve over long periods of time as their supply of energy gradually diminishes. The Sun is a main sequence star, and over the past 4 billion years the total energy output has increased an estimated 25 percent, fairly close to predicted values assuming normal stellar evolution. The early atmosphere and surface were kept warm enough to support vast liquid water oceans, presumably by balancing this faint young Sun with a much higher concentration of greenhouse gases.

Over shorter decadal or millennial time spans, it was once thought that the Sun's total energy output was constant. The phrase **solar constant** became so deeply ingrained in the meteorological literature that it appeared in virtually all textbooks until well into the satellite era. Satellite data gathered since the early-1980s has revealed both cyclic and non-cyclic changes in solar output. The phrase solar constant is more frequently referred to today as the **total solar irradiance**. The value of the total solar irradiance is about 1361 watts/square meter, measured outside the Earth's atmosphere adjusted to an Earth-Sun distance of 93 million miles.

The most predictable decadal changes in total solar irradiance correspond to the 11-year

**sunspot cycles** (Figure 2.41). Sunspots are dark areas of intense magnetic activity on the Sun's photosphere. They appear dark because they are typically about 2000°C (3600°F) cooler than the surrounding area. They fluctuate in number and size, on cycles that last about 11 years. When there are large numbers of sunspots (sunspot maxima), the total amount of energy output from the Sun goes up about 0.1 percent (Figures 2.42a and 2.42b). Multi-decadal variations in sunspot cycles have been used as a causal mechanism for global warming, although evidence does not appear to support this (Figure 2.43). Although there is a substantial body of evidence that long-term changes in sunspot cycles may have caused minor global climatic shifts (e.g., the Little Ice Age), sunspot activity is not an important control in daily or seasonal temperature changes on Earth.

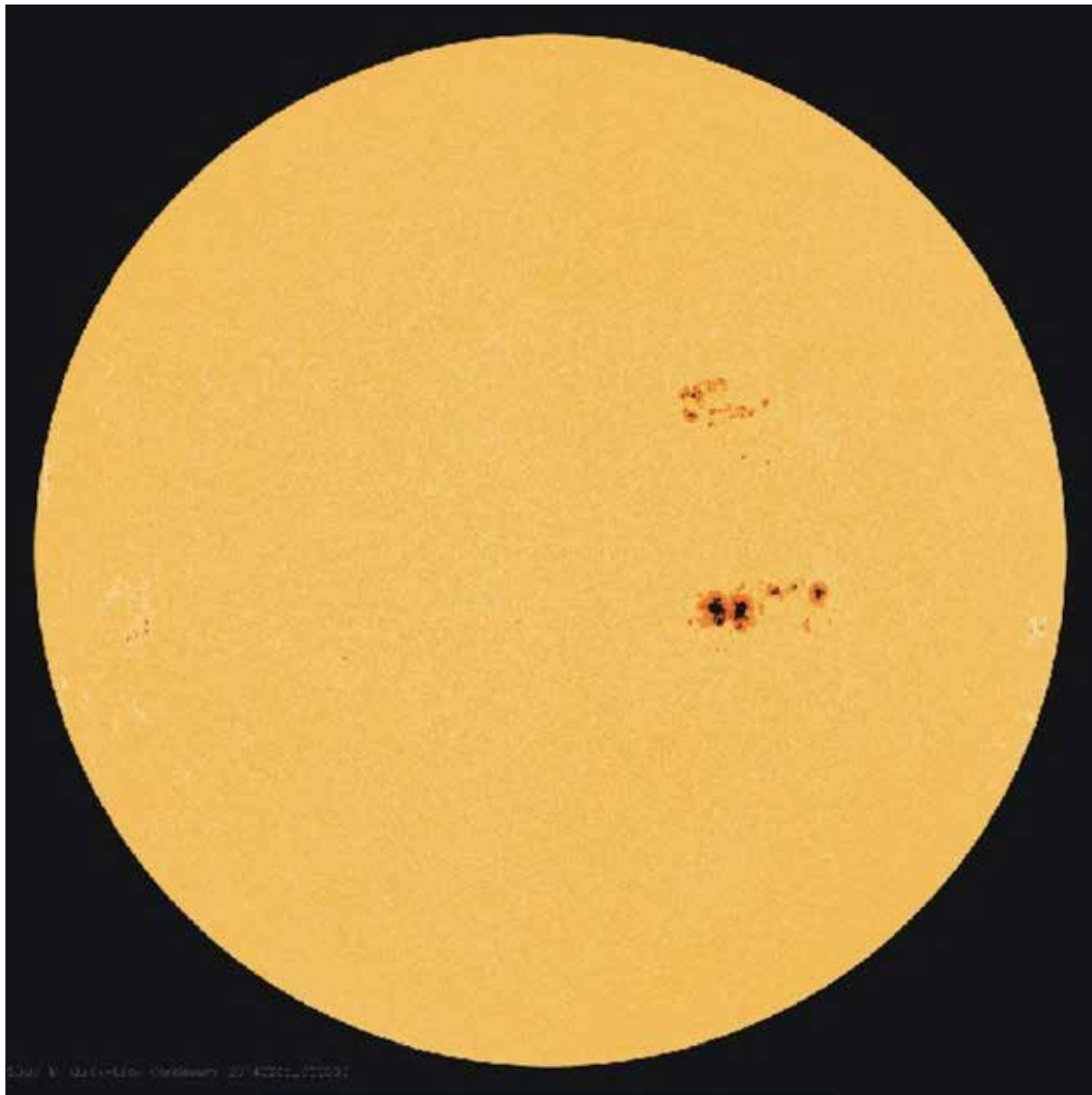


Figure 2.41. Sunspot activity on February 5, 2014. The dark blemishes on the Sun's surface are geomagnetic storms, which are areas that are actually about 2000°C (3600°F) cooler than the surrounding photosphere (Source/Credit: SOHO MDI).

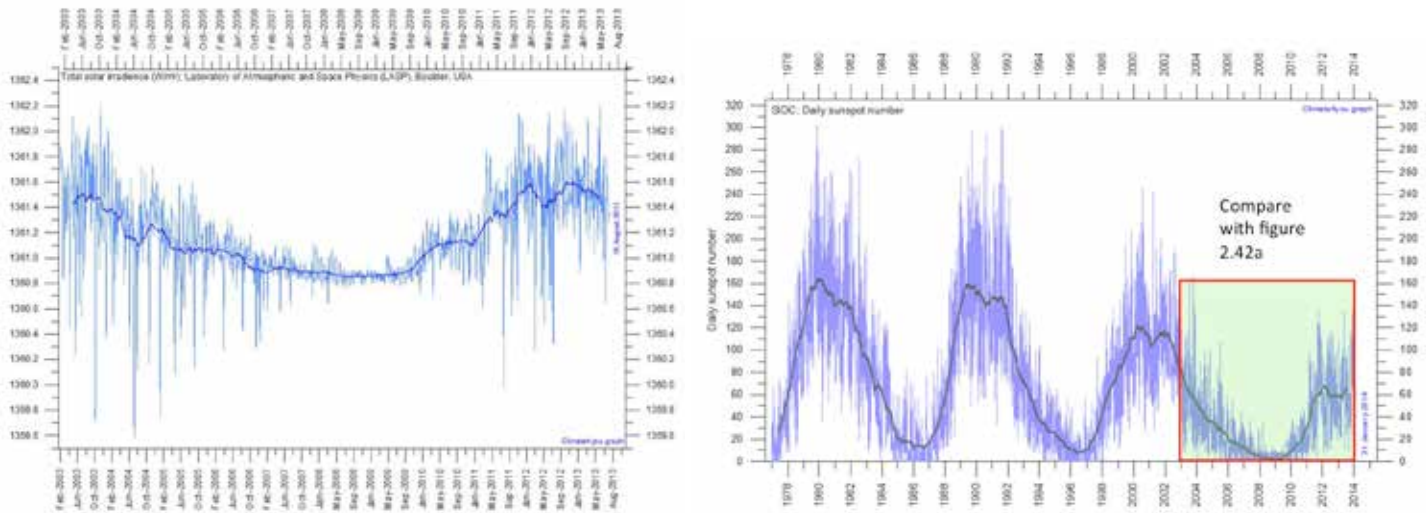


Figure 2.42a. (left) Slight variations in total solar irradiance (formerly the solar constant) from 2003 to 2013 (Source/Credit: Laboratory of Atmospheric and Space Physics, LASP).

Figure 2.42b. (right) Detailed sunspot activity over nearly four decades. The sunspot activity in the box (red outline) corresponds to the time period on Figure 2.42a. Sunspot activity and total solar irradiance show a fairly good correlation (Source/Credit: Solar Influences Data Center, SIDC).

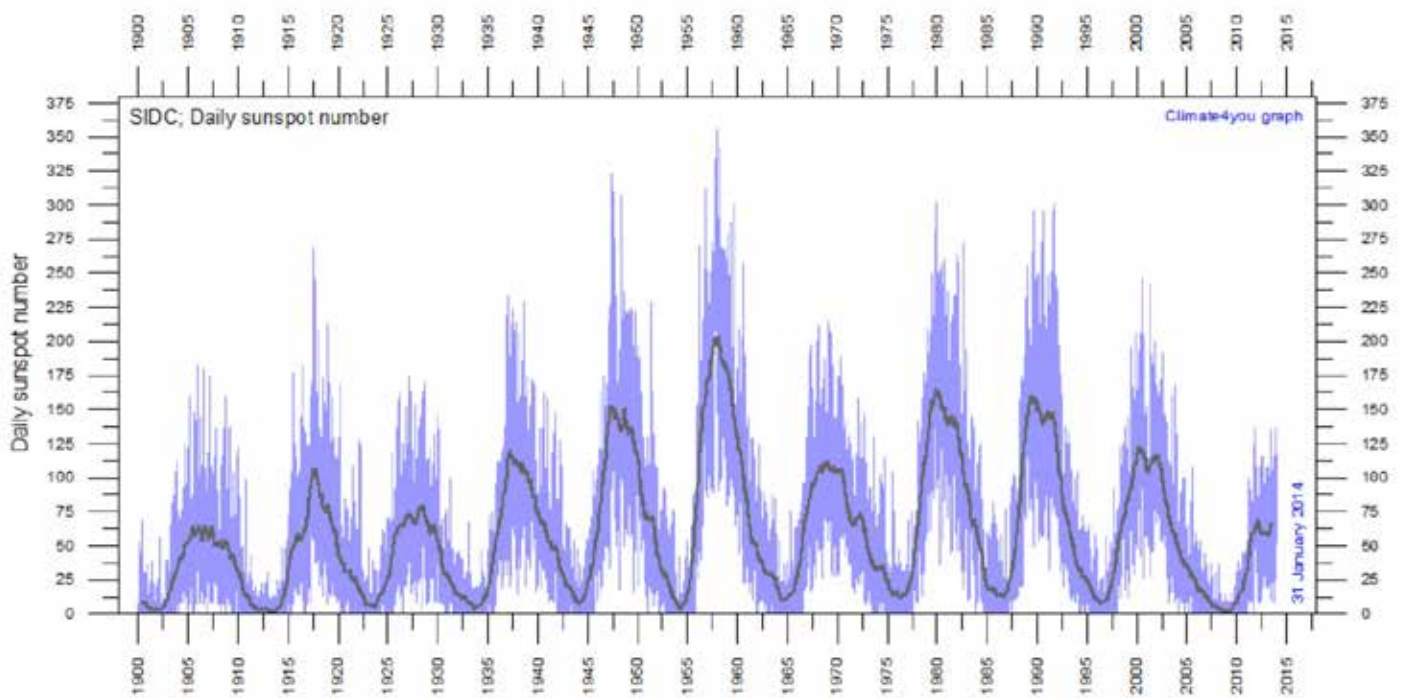


Figure 2.43. The 115-year record of sunspot cycles shows the 11-year sunspot cycles. Note that the peaks and troughs vary with each cycle, generating multi-decadal cycles. The long-term trend line (black) indicates a slight drop in recent sunspot activity, suggesting that the present trend toward global warming is not solely due to solar variability (Source/Credit: modified from SIDC).



**Earth-Sun distance.** The Earth's orbit around the Sun is elliptical. The Earth-Sun distance is minimal on or about January 3 at a distance of 91.5 million miles (*perihelion*), and is greatest on July 4 at a distance of 94.5 million miles (*aphelion*) (Figure 2.44). The average distance is close to 93 million miles. This results in a variation in insolation received at the top of the atmosphere from a minimum of 1321 watts/m<sup>2</sup> to a maximum of 1412 watts/m<sup>2</sup>, a fluctuation of about 6.9%. The timing of the seasons shows that this is only a minor factor in creating the seasons.

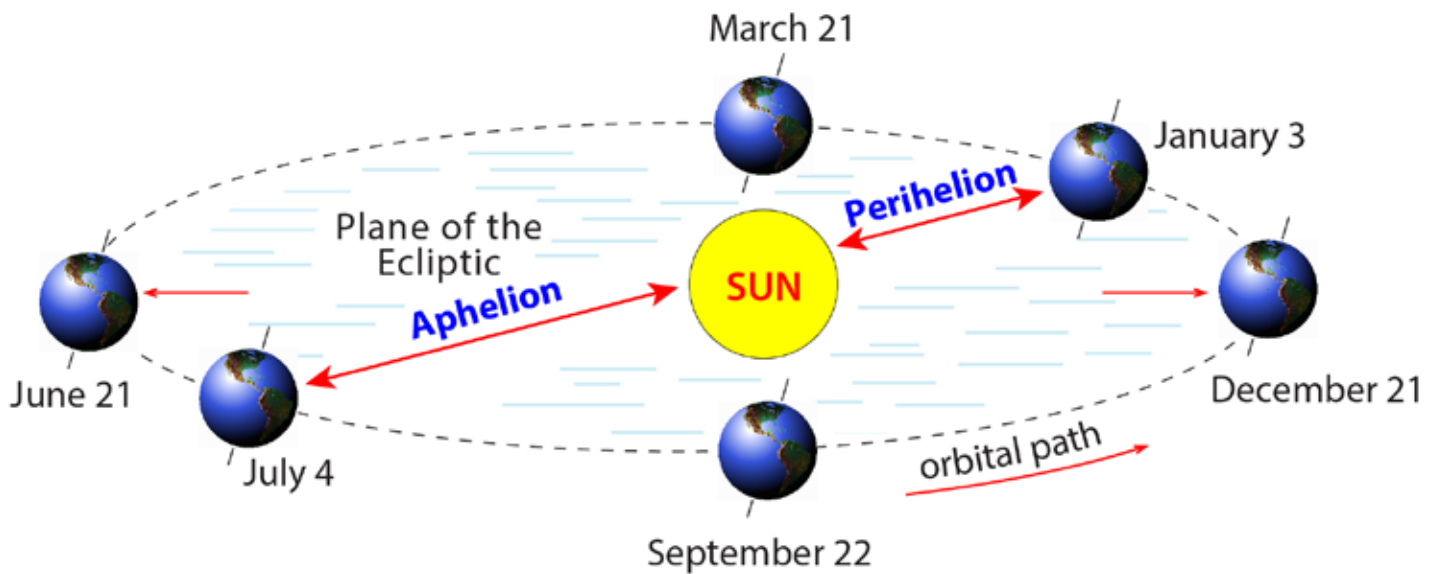


Figure 2.44. The Earth's distance from the Sun varies from 91.5 million miles at perihelion to 94.5 million miles at aphelion (Source/Credit: modified from Dennis I. Netoff and Ava Fujimoto-Strait, *Weather & Climate Lab Manual*).

**Orbital and axial variations.** Astronomers have long-known that changes occur in the shape of the Earth's orbit, in the tilt of the Earth's axis, and the timing of perihelion and aphelion. In the middle part of the 20<sup>th</sup> century, astronomer-mathematician Milutin Milankovitch calculated how these variations might affect the radiation budget of different latitudes and what the impact of changes in all three parameters might have on global meteorology and climatology. He concluded that over time periods of tens of thousands of years, orbital and axial variations played an important part in ancient glacial-interglacial cycles. They are not, however, responsible for the daily and seasonal changes in absorption and temperature. These will be dealt with in the final chapter of this book on climatic change.

## The Intensity of Radiation and the Duration of Daylight

**The intensity of radiation.** The incoming rays of the Sun are essentially parallel to each other when they reach the Earth. However, because the Earth is a sphere, the angle at which the Sun's rays strike the Earth varies with latitude. **The variation in Sun angle is important because it controls the intensity of the sunlight.** For example, if the Sun's rays are directly overhead at the Equator, the Sun angle is  $90^\circ$ , and the radiation will be intense.

Figures 2.45a and 2.45b show how the Sun angle varies with changing latitudes on a specific date. In this example, the Sun is directly overhead at the Tropic of Capricorn at solar noon, and the Sun's rays are more intense there than anywhere else on Earth. All other parallels receive the Sun's noonday rays at a lesser angle. At Huntsville, Texas, the noonday rays of the Sun are only  $31.5^\circ$  above the southern horizon. At the Antarctic Circle, the noonday rays of the Sun are  $47^\circ$  above the northern horizon on the date given.

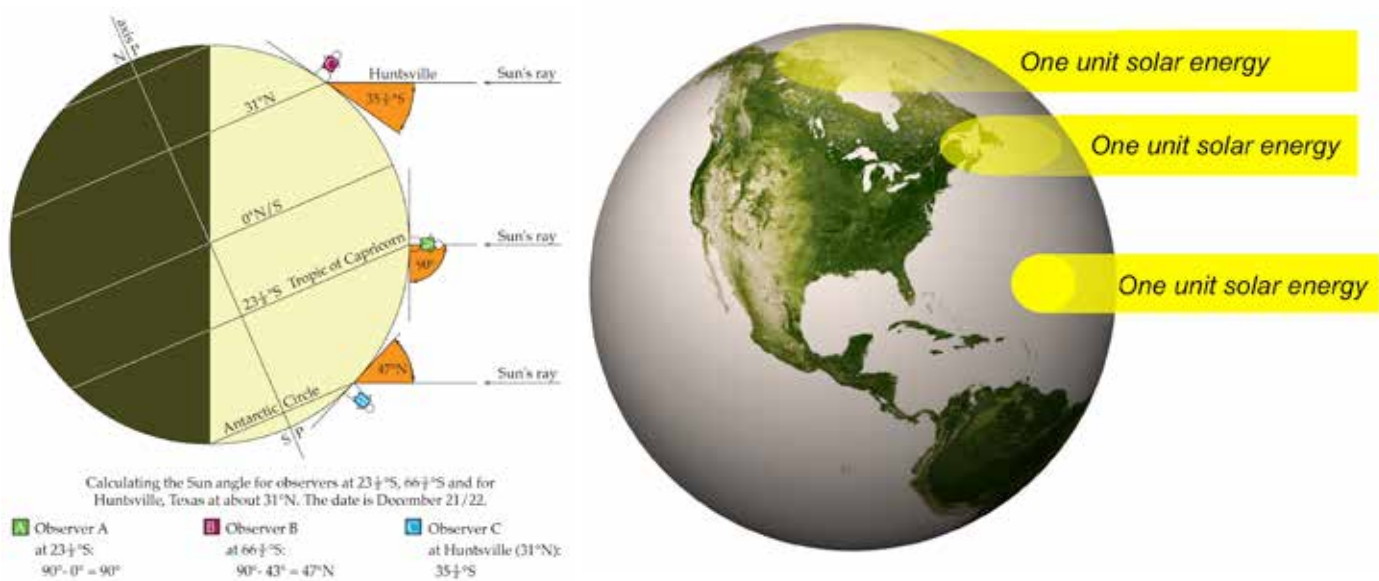


Figure 2.45a. (left) The rays of the Sun are most intense when the Sun strikes the surface at a  $90^\circ$  angle (Tropic of Capricorn). This occurs at only one parallel for any given day of the year. All other parallels receive lower angles of incoming rays relative to the Earth's surface (observers at Huntsville and the Antarctic Circle). As the Sun angle decreases, the rays of the Sun are spread over a larger area (Figure 2.45b) resulting in a decrease in the intensity of the sunlight (Source/Credit: modified from Dennis I. Netoff and Ava Fujimoto-Strait, *Weather & Climate Lab Manual*).

Figure 2.45b. (right) The rays of the Sun are most intense when the Sun strikes the surface at a  $90^\circ$  angle (smallest, brightest yellow oval). This occurs at only one parallel for any given day of the year. All other parallels receive lower angles of incoming rays relative to the Earth's surface. As the Sun angle decreases, the rays of the Sun are spread over a larger area, resulting in a decrease in the intensity of the sunlight. The more intense radiation generally results in more absorption and higher temperatures (Source/Credit: modified from several sources).

Low-Sun angles at high latitudes also increase the distance that solar rays travel through the atmosphere, further reducing the intensity of radiation at the Earth surface. Longer paths at higher latitudes increase the chance of radiation being diverted back to space by scattering and reflection (Figure 2.46).

Figure 2.46 gives the equivalent number of *atmospheres* through which insolation must travel at different latitudes. Because of increasing amounts of atmosphere that the solar radiation must pass through in order to reach the Earth's surface, the number of atmospheres increases from one (1.00) over the Equator, when the Sun's rays are directly overhead there, and increases toward the poles. Between 80° and 85°, there is a sharp and very significant increase in the thickness of the atmosphere as the Sun angle becomes very low in the sky.

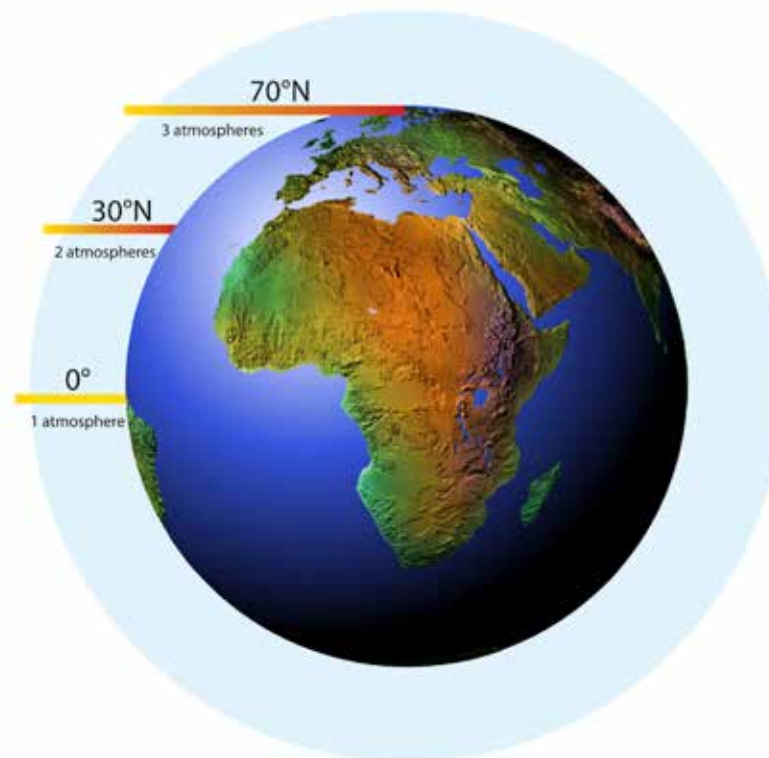


Figure 2.46. The change in Sun angle also changes the amount of atmosphere that the Sun's rays must pass through before reaching the surface. When the Sun is directly overhead, the Sun's rays pass through the least amount of atmosphere, resulting in minimal scattering and reflection. This allows more radiation to reach the surface. As the angle becomes lower, the Sun's rays pass through an increasingly thicker layer of atmosphere, resulting in more reflection and scattering. As a result, less light reaches the surface (Source/Credit: Mountain High Maps).

This effect is analogous to temperatures being lower at dawn and dusk than at midday largely because of the difference in the angle at which solar radiation strikes the surface. In the early morning and late afternoon, the Sun is lower in the sky and the Sun's rays strike the surface at a lower angle (much less than 90°). As a result, the Sun's rays are spread over a larger area, and so it is cooler.

**Rotation, Revolution, Inclination, and Polarity:**

**RRIP: rotation, revolution, inclination, and polarity (parallelism).** The geometric relationships between the Earth and Sun are fundamental in explaining daily and seasonal changes in the *intensity of radiation* as well as the *duration of daylight*. Since the Earth's surface is curved, and the incoming rays of the Sun are parallel, half of the Earth is always in shadow and the other half illuminated. The circle that separates day from night is the **Circle of Illumination** (Figure 2.47).

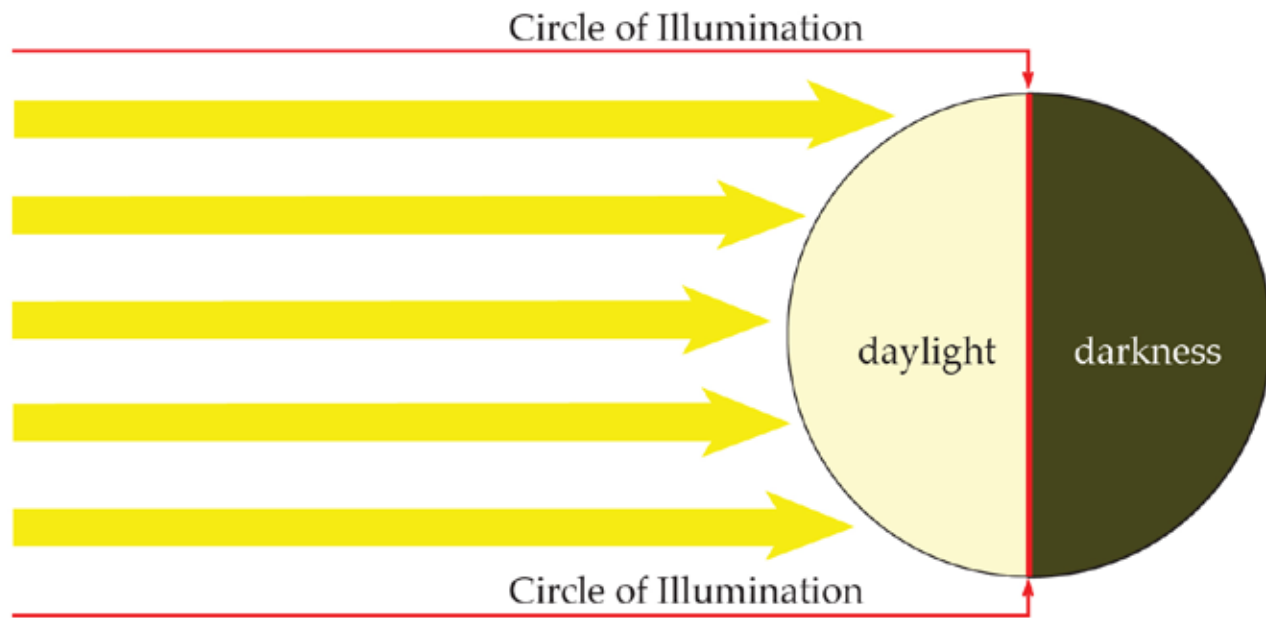


Figure 2.47. The spherical shape of the Earth combined with the parallel rays of the Sun cause daylight and darkness. The Circle of Illumination separates daylight and darkness (Source/Credit: modified from Dennis I. Netoff and Ava Fujimoto-Strait, Weather & Climate Lab Manual).

**Rotation** refers to the spin of the Earth on its axis. The Earth rotates once every 24 hours, causing most latitudes to experience some daylight and some darkness every day. The direction of rotation, when viewed from outer space toward the North Pole, is counter-clockwise (Figure 2.48).

North Polar view of the Earth, with Circle of Illumination passing through the North Pole

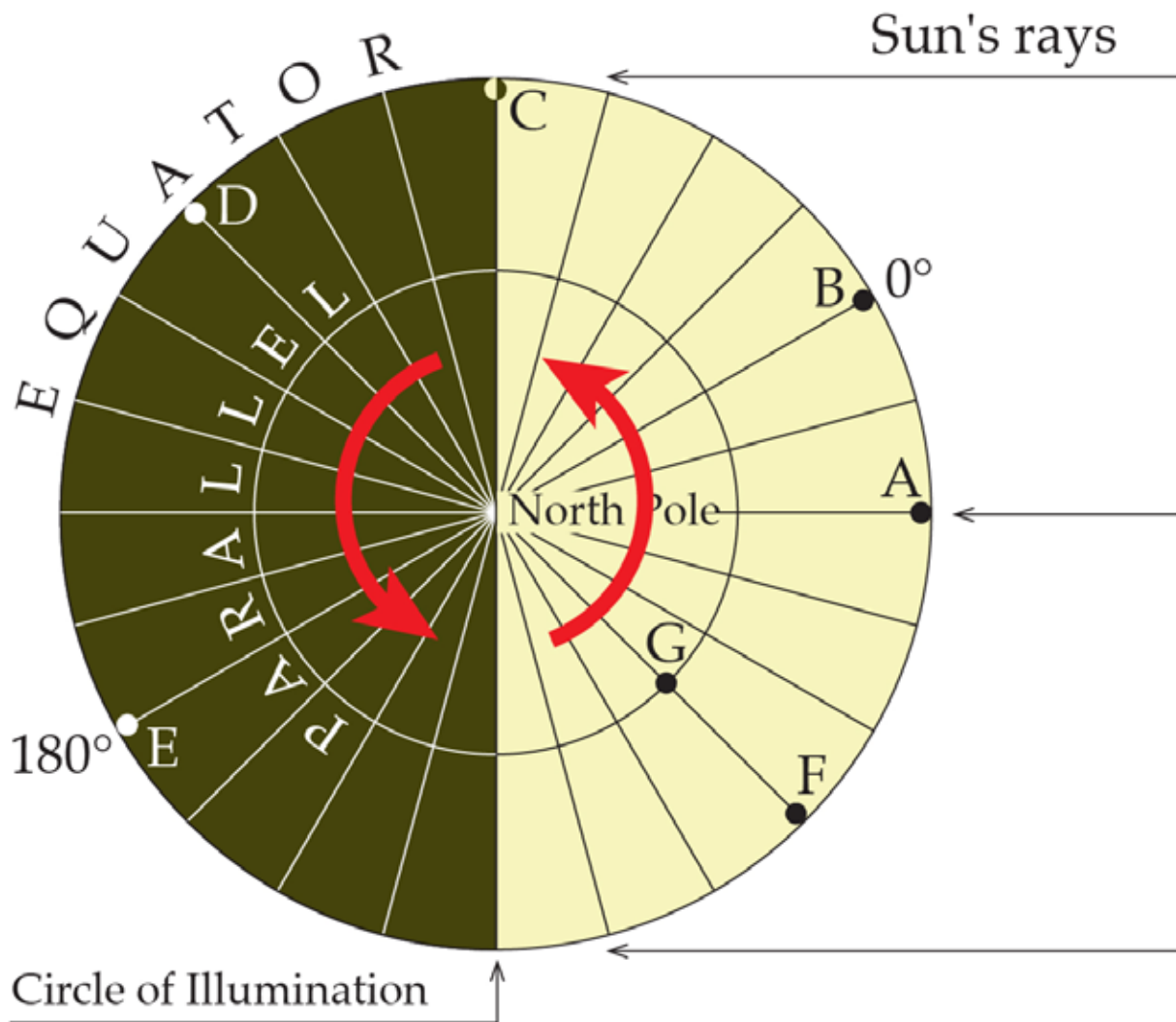


Figure 2.48. North polar view of the Earth at the time of the year when the Circle of Illumination passes through both poles. From a south polar view, the Earth would appear to rotate clockwise. One complete rotation takes 24 hours. The meridians are 15° apart, so the Earth effectively rotates 15° per hour (360°/24 hrs). An observer on the Equator would take 6 hours to rotate from point A, at solar noon, to point C, dusk. Note that for any parallel shown, there would be 12 hours of daylight and 12 hours of darkness on this date, either March 21 or September 22 (Source/Credit: modified from Dennis I. Netoff and Ava Fujimoto- Strait, Weather & Climate Lab Manual).

**Revolution** refers to the Earth's elliptical orbit around the Sun. One complete orbit takes 365.25 days, or one year. During that time, the Earth-Sun distance varies from 91.5 million miles at perihelion, on or about January 3, to 94.5 million miles at aphelion on July 4 (Figure 2.49). The direction of revolution, when viewed from outer space toward the North Pole, is counter-clockwise, similar to the direction of rotation.

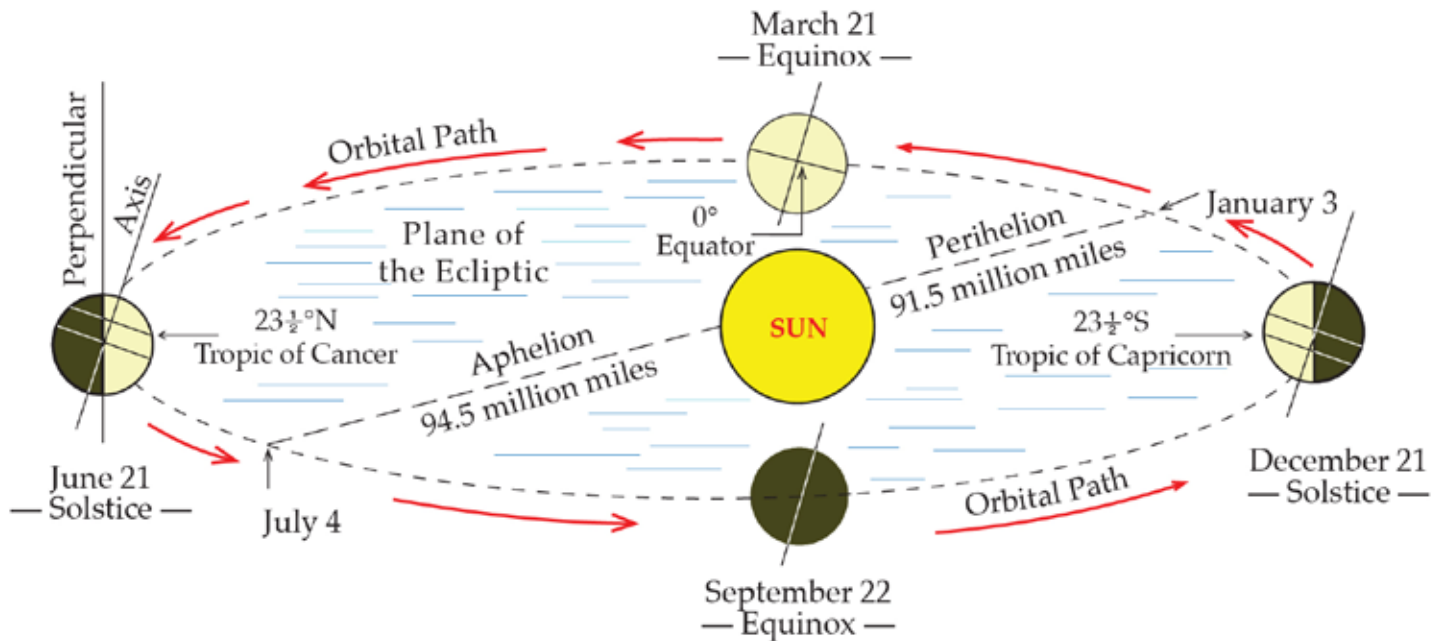


Figure 2.49. The Earth revolves around the Sun in an elliptical orbit every 365.25 days. The imaginary plane that goes through the orbit is the plane of the ecliptic. The direction of revolution is counter-clockwise, when viewed from space toward the North Pole (Source/Credit: modified from Dennis I. Netoff and Ava Fujimoto-Strait, *Weather & Climate Lab Manual*).

**Inclination** is the tilt of the Earth's axis. A line constructed perpendicular to the plane of the ecliptic serves as a reference. Inclination can then be stated as the  $23.5^\circ$  tilt of the axis of the Earth from a line constructed perpendicular to the plane of the ecliptic (Figure 2.50). The same axial tilt is maintained in every orbital position as the Earth revolves around the Sun. The axial tilt does change over cycles of tens of thousands of years, but changes are minimal over a human lifetime.

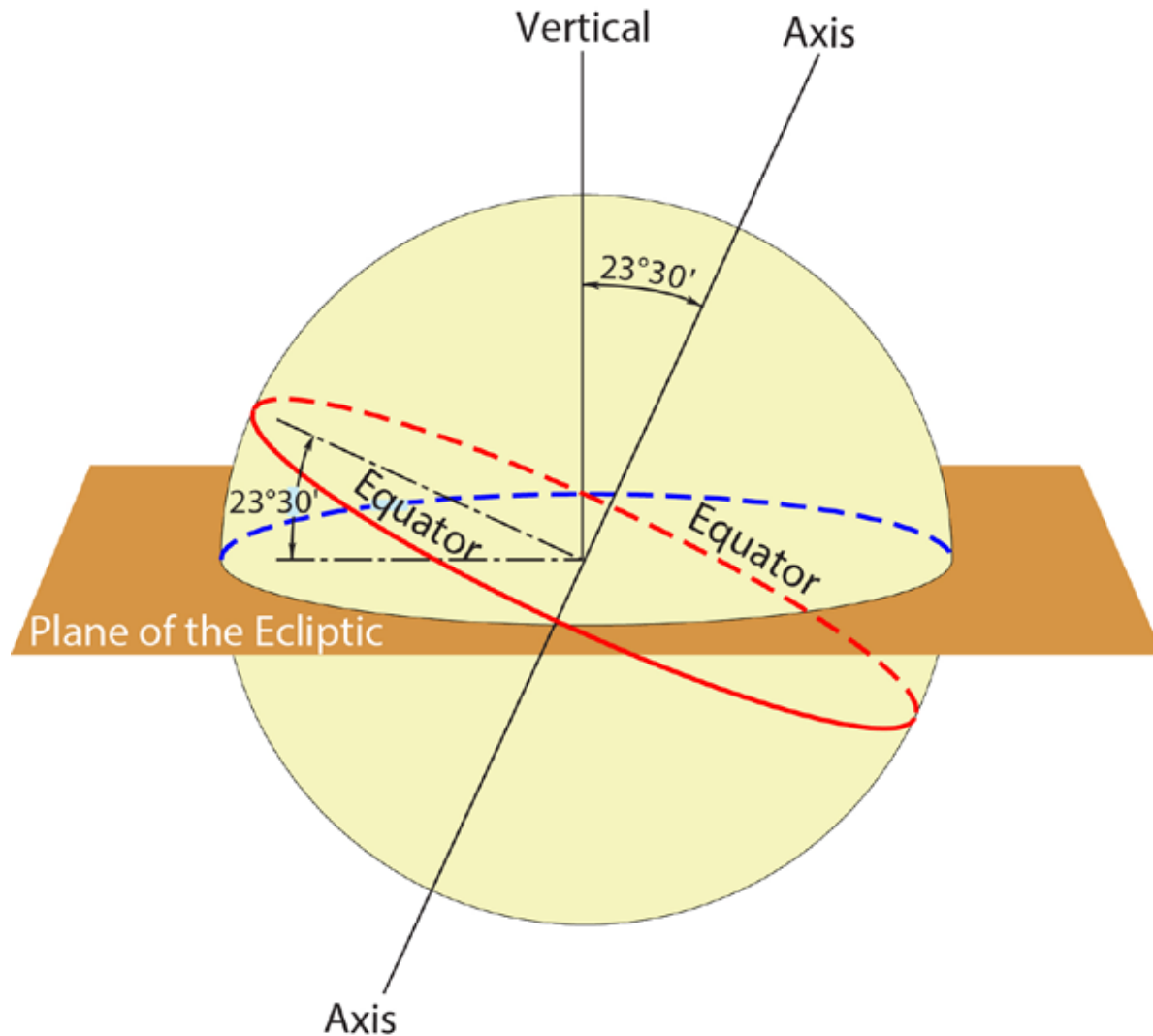


Figure 2.50. **Inclination** refers to the  $23.5^\circ$  tilt of the Earth's axis. By convention, the Earth's orbital plane, the plane of the ecliptic, is the standard reference plane. The Earth's axial tilt is  $23.5^\circ$  from a line constructed perpendicular to the plane of the ecliptic. The same axial tilt is maintained in every orbital position as the Earth revolves around the Sun.

**Polarity (Parallelism)** refers to the property that an extension into space of the north polar axis of the Earth always points in the same direction in every orbital position, very close to Polaris, the North Star (Figure 2.51). The property can also be stated as parallelism, that the axis of the Earth is parallel to itself in every orbital position (Figure 2.52). Over thousands of years, the wobble of the Earth’s axis causes this property to also change.

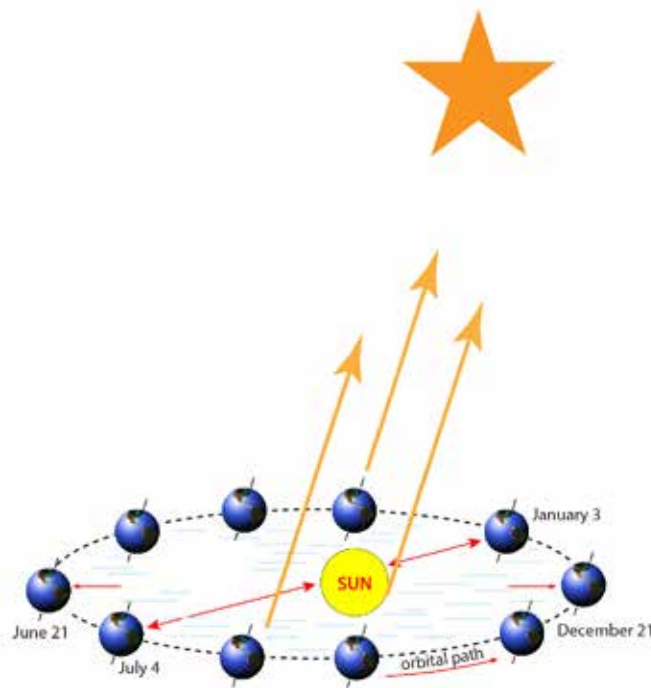


Figure 2.51. The Earth’s axis is always pointed in the same direction in outer space. The poleward extension of the north polar axis points very close to Polaris (hence **polarity**), the North Star. The axis of rotation is always parallel to itself in every orbital position (**parallelism**).

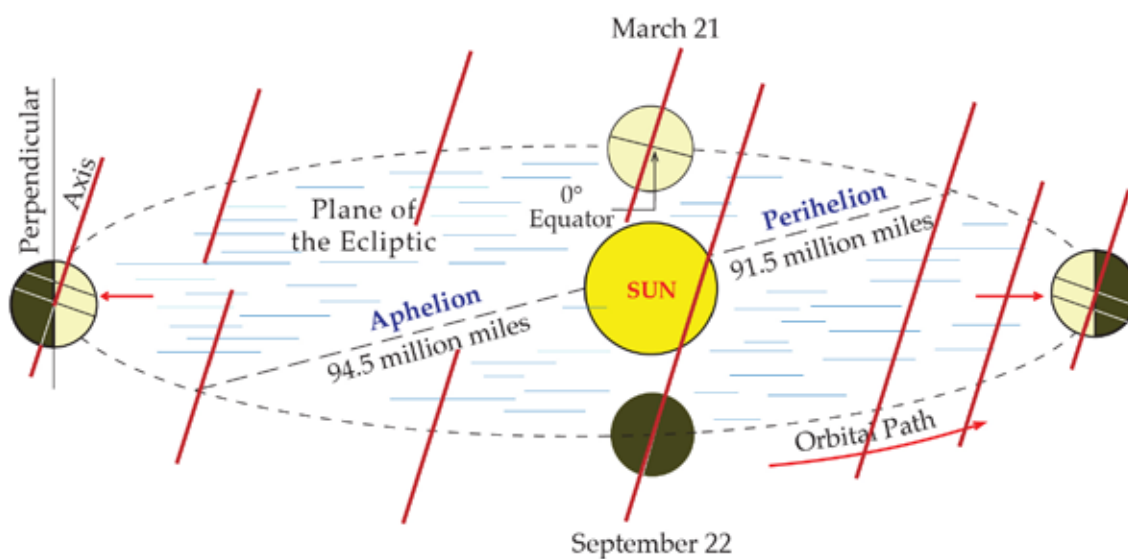


Figure 2.52. **Parallelism** refers to the fact that as the Earth orbits around the Sun, the axis is always parallel to itself in every orbital position (Source/Credit: modified from Dennis I. Netoff and Ava Fujimoto-Strait, *Weather & Climate Lab Manual*).



Rotation, revolution, inclination, and polarity (parallelism) together account for most of the **daily and seasonal variations in the intensity of incoming radiation as well as the durations of daylight**, and are the basic cause of daily and seasonal temperature variations. The intensity of incoming radiation from the Sun depends on the angle of the Sun's rays relative to the Earth's surface. The most intense rays occur where the Sun's rays are vertically overhead. Progressing toward either pole from the vertical rays of the Sun lessens the **Sun angle** and reduces the intensity of the Sun's rays.

For example, on December 21, the date of the Southern Hemisphere summer solstice, the vertical rays of the Sun, called the **declination of the Sun**, are at 23.5°S latitude. This will be the parallel that receives the most intense rays of the Sun. At solar noon, an observer at this latitude will observe the Sun directly overhead, or 90° above the horizon. The Sun angle is therefore 90° (Figure 2.53). An observer 10° farther poleward of that location will see the noonday Sun 10° lower in the sky. The Sun angle for that location will be  $90^\circ - 10^\circ = 80^\circ$ . Observers in either hemisphere 20° from the declination of the Sun will have a Sun angle of  $90^\circ - 20^\circ = 70^\circ$ . To solve for Sun angle:

- (1) find the difference in latitude between the observer and the vertical rays of the Sun (declination of the Sun),
- (2) subtract that value from 90° (Figure 2.53).

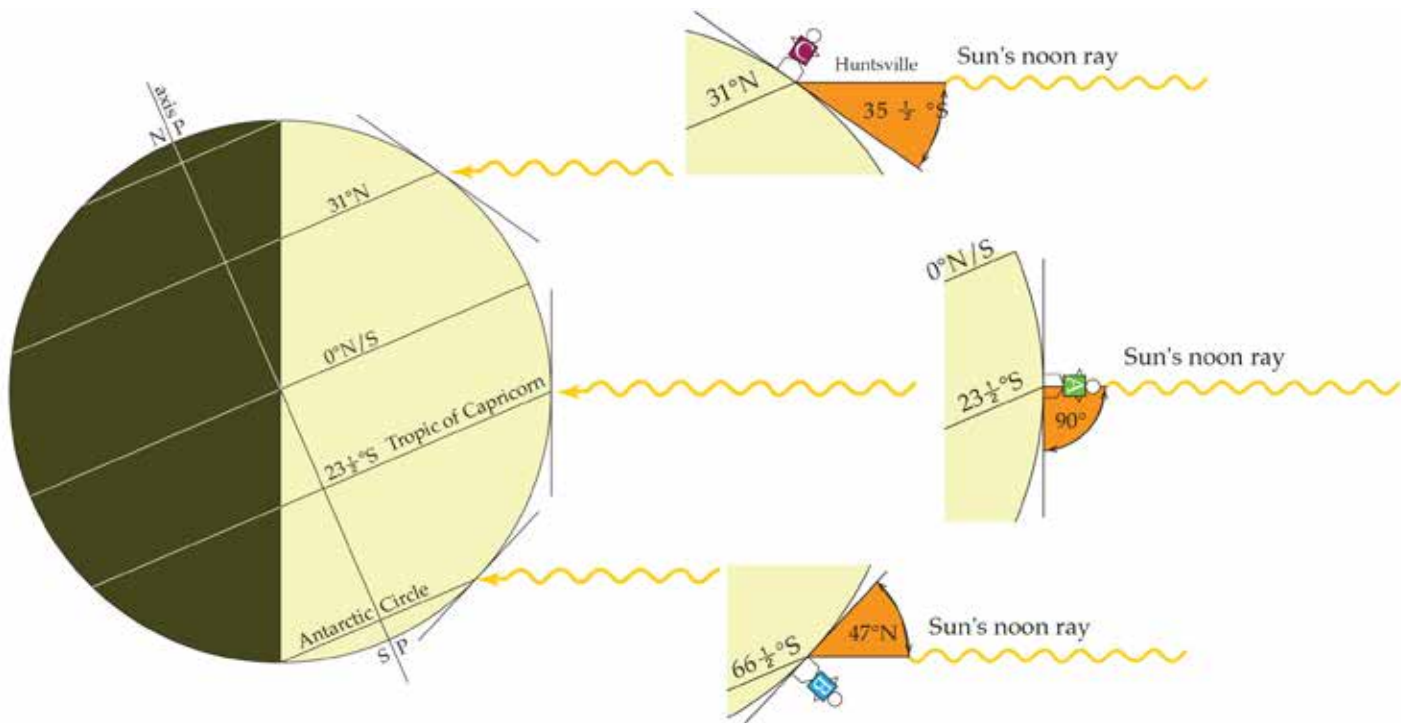


Figure 2.53. To solve for Sun angle: (1) find the difference in latitude between the observer and the vertical rays of the Sun (declination of the Sun); (2) subtract that value from 90°. Calculating the Sun angle for observers at 23°S, 66°S and for Huntsville, Texas at about 31°N. The date is December 21/22. Declination of the Sun is 23.5°S. Observer A at 23°S:  $90^\circ - 0^\circ = 90^\circ$ . Observer B at 66°S:  $90^\circ - 43^\circ = 47^\circ$ . Observer C at Huntsville (31°N):  $90^\circ - 54.5^\circ = 35.5^\circ$ .

The Sun's declination changes predictably over the course of a year. There are **four critical orbital positions**, two that mark the farthest poleward migration of the Sun's vertical rays, and two intermediate positions. These also help define specific parallels and points on the Earth, as well as the beginning dates of the seasons (Figure 2.54).

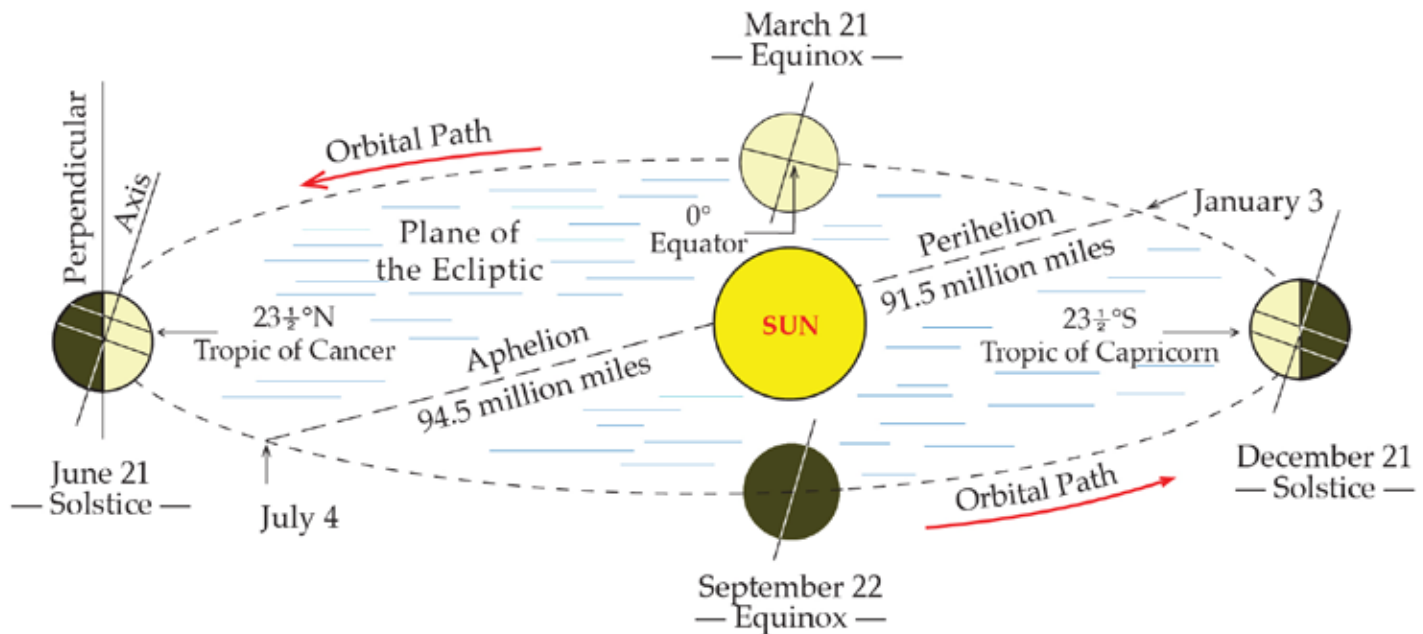


Figure 2.54. The combination of axial tilt and parallelism are responsible for the occurrence of seasons because these factors result in changes in the intensity and duration of sunlight over the course of a year as the Earth orbits the Sun. The four critical orbital dates are shown, each marking the beginning of a given season. The two solstice positions mark the beginning of summer and winter, and occur when the vertical rays of the Sun are at their farthest poleward locations, the Tropic of Cancer and the Tropic of Capricorn. The two equinox positions mark the beginning of spring and fall and occur when the vertical rays of the Sun are on the Equator (Source/Credit: modified from Dennis I. Netoff and Ava Fujimoto-Strait, *Weather & Climate Lab Manual*).

The farthest northerly latitude that the vertical rays of the Sun travel is 23.5°N, the **Tropic of Cancer**. This orbital position usually occurs on June 21-22, the date of the **summer solstice**, and marks the first day of summer for the Northern Hemisphere. Note that this same day marks the date of the winter solstice in the Southern Hemisphere. Three months later (one fourth of the rotational period of the Earth), the vertical rays of the Sun have migrated to the Equator. The date is typically September 21-23, and is called the fall or **autumnal equinox**, and marks the first day of the fall season (Figure 2.54). It marks the spring equinox in the Southern Hemisphere.

Three months beyond that, the vertical rays of the Sun have migrated to their most southerly latitude, the Tropic of Capricorn at 23.5°S. This is the date of the **winter solstice** for the Northern Hemisphere and typically occurs on December 21-22. The passage of another three months brings the vertical rays of the Sun back to the Equator, the date of the spring or **vernal equinox** on or about March 21-22. This marks the first day of the Northern Hemisphere spring

season. In three more months, the Sun's rays are back on the Tropic of Cancer, where they began.

The vertical rays of the Sun, and hence the most intense rays of the Sun, therefore migrate from the Tropic of Cancer to the Tropic of Capricorn and back during the course of one Earth year. All parallels between these two will experience the vertical rays of the Sun twice annually. Parallels poleward of  $23.5^{\circ}\text{N}$  and  $\text{S}$  will never experience the vertical rays of the Sun. Between solstices and equinoxes, the vertical rays of the Sun will be migrating from the tropical parallels to the Equator, or vice versa. The exact latitude that the vertical rays of the Sun are located on any day other than the solstices or equinoxes is indicated graphically by a device called the analemma (Figure 2.55).

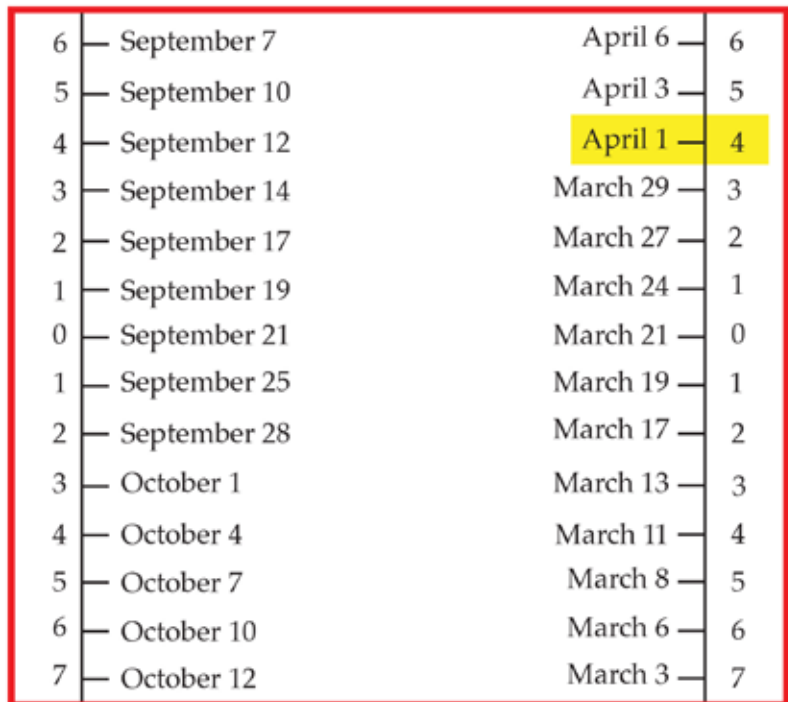
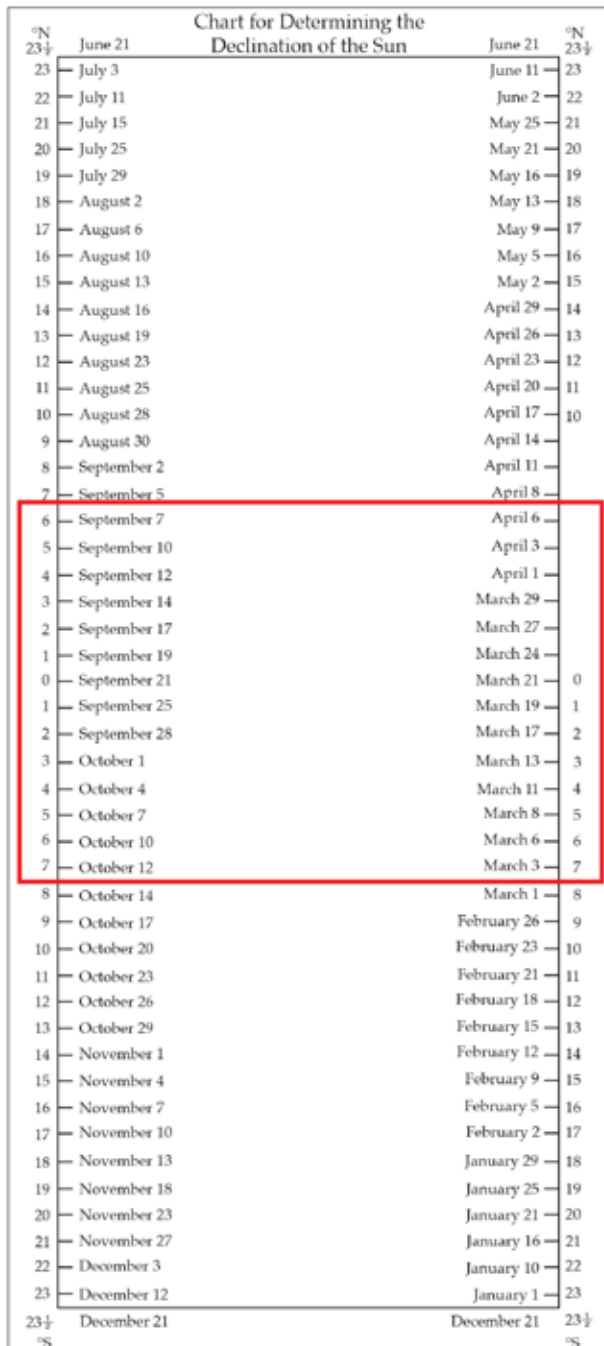


Figure 2.55. The analemma indicates the **declination of the Sun** (latitude at which the Sun’s rays are vertically overhead) on any day of the year. Predictably, the declination of the Sun on either equinox date (on or around March 21 or September 22) is 0°, whereas on either solstice date (June 21 or December 21), it is either 23.5°N or 23.5°S. On April 1, the Sun’s declination is 4°N (see inset) (Source/Credit: modified from Dennis I. Netoff and Ava Fujimoto-Strait, *Weather & Climate Lab Manual*).

**Sun angle and home design.** Proper construction and design of homes can make them more energy efficient and save money on heating and air conditioning bills. A simple application of this incorporates a knowledge of Sun angle and roof overhang (the eave). In the southern United States, the eaves of many houses, especially those built before the days of air conditioning, tend to overhang the wall a few feet. During the summer, when the

Sun in the south is high in the sky and the temperatures are very high, excessive heating of homes by solar radiation is reduced by construction design. Houses with wide overhangs are able to intercept the Sun's rays and thus reduce sunlight entering the windows. In winter, when the Sun is lower in the sky, solar energy is admitted to the home through the windows unhindered by the presence of the eave (Figure 2.56).

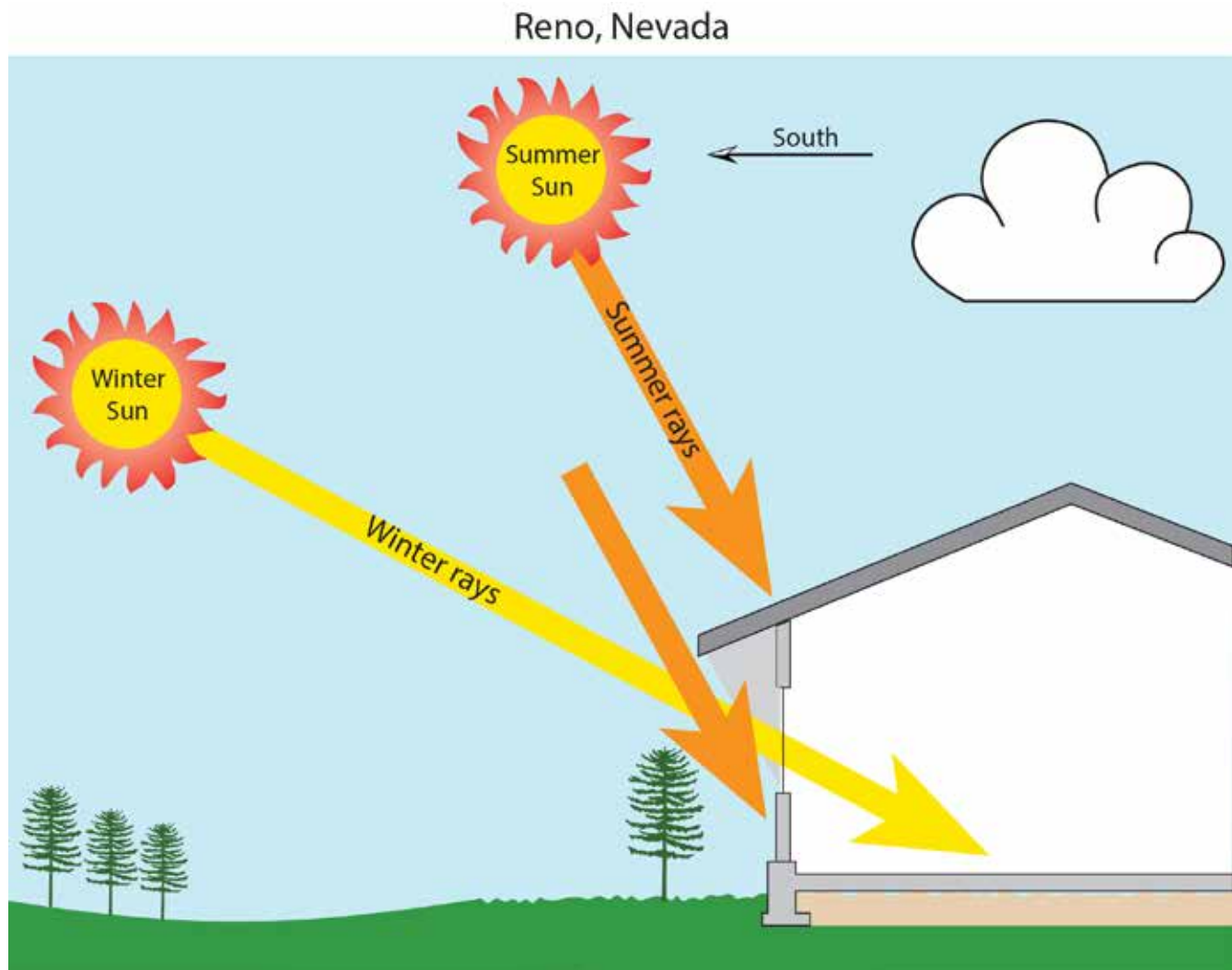


Figure 2.56. The Sun angle varies seasonally for mid-latitude locations such as Reno, Nevada at  $40^{\circ}\text{N}$ . Window placement and roof overhang on south-facing exposures can take advantage of the low-Sun angle ( $26.5^{\circ}$  on December 21) during the winter by allowing the Sun's rays to penetrate indoors and provide some room heat. Roof overhangs can be constructed to block out the intense summer rays when the Sun angle is much higher.

**The duration of daylight** is also controlled by Earth-Sun relationships (RRIP). The 24-hour rotational period of the Earth results in most places on Earth experiencing at least some daylight and darkness. The exact number of hours of daylight and darkness, however, varies with latitude and with the changing seasons. These changes are largely a function of the migration of the vertical rays of the Sun and how they control that way that the Circle of Illumination cuts any given parallel.

On an equinox date, for example, the Circle of Illumination cuts all parallels exactly in half. Since a complete rotation of any parallel takes 24 hours, all places on Earth will experience 12 hours of day and 12 hours of night (Figures 2.57a and 2.57b). An observer at either pole, however, will see the Sun on the horizon, effectively resulting in 24 consecutive hours of twilight.

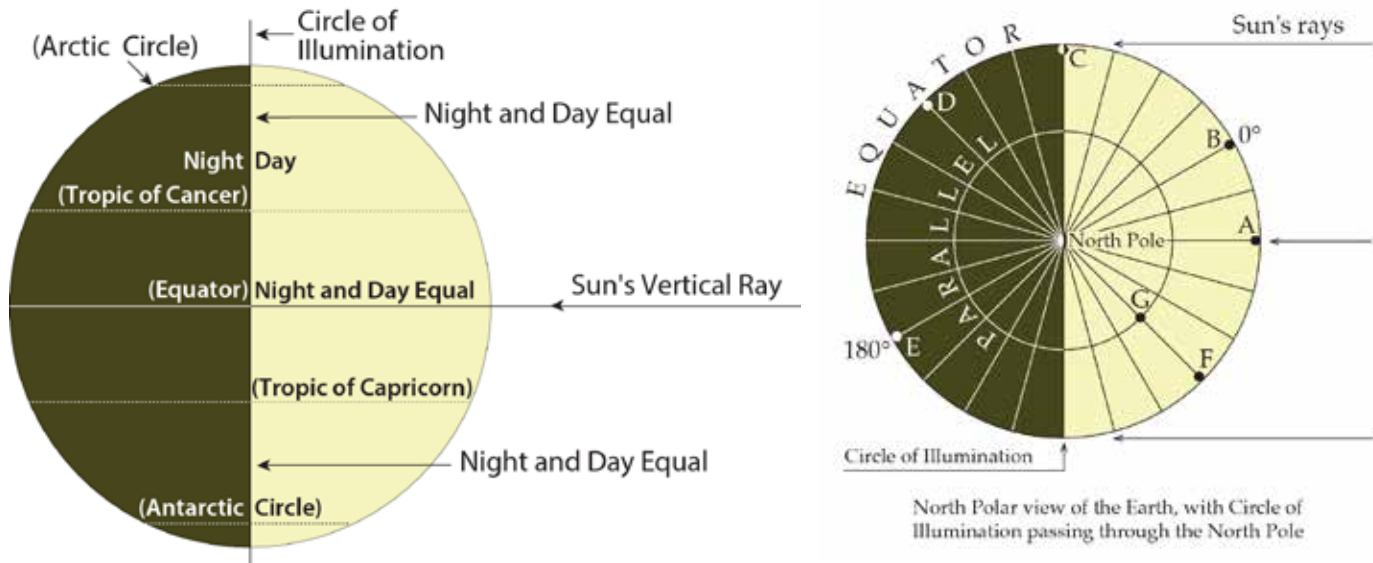


Figure 2.57a. (left) In both the Northern and Southern Hemispheres, the Circle of Illumination cuts all parallels equally on the equinox dates. Since every parallel goes through the same 360° of rotation during a 24 hour period, all places on Earth receive 12 hours of daylight and 12 hours of night. The two poles will receive 24 hours of continuous twilight (Source/Credit: modified from Dennis I. Netoff and Ava Fujimoto-Strait, Weather & Climate Lab Manual).

Figure 2.57b. (right) A view toward the North Pole illustrating how all parallels are cut exactly in half, and so receive 12 hours of day and 12 hours of night (equinox: equi = equal; nox = night; equal night duration world-wide). The two poles will receive 24 hours of continuous twilight (Source/Credit: modified from Dennis I. Netoff and Ava Fujimoto-Strait, Weather & Climate Lab Manual).

On the date of the Northern Hemisphere summer solstice (June 21-22), the vertical rays of the Sun are at  $23.5^{\circ}\text{N}$ , the Tropic of Cancer. On that orbital date, only the Equator is cut exactly in half by the Circle of Illumination, and only observers at the Equator will experience equal day and night duration (Figure 2.58). The entire area poleward of the Arctic Circle on that date is in daylight, so all places within the Arctic Circle will have between 24 hours and 6 months of continuous daylight. The length of day increases going from the Equator toward the North Pole, and decreases toward the South Pole.

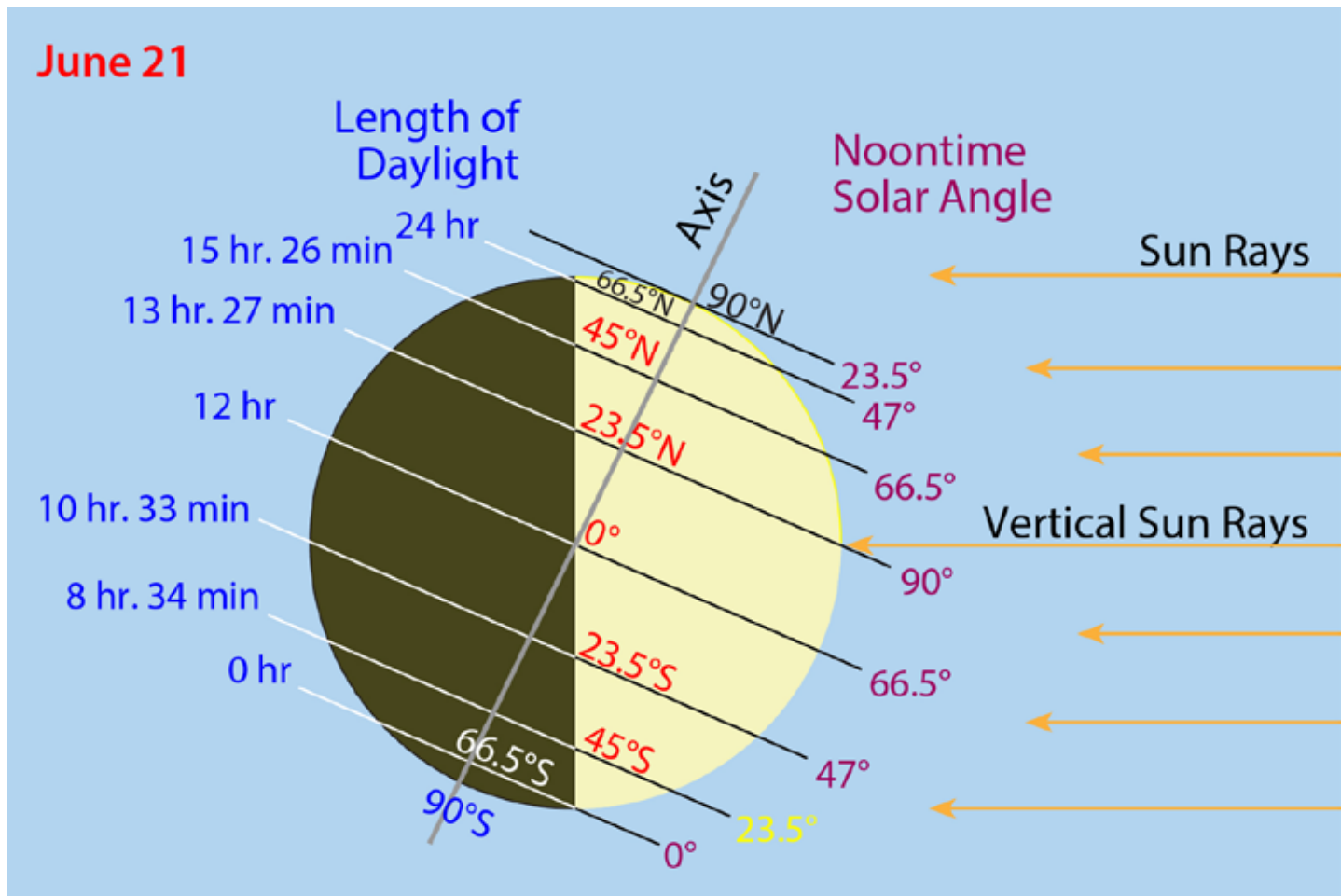


Figure 2.58. On June 21-22, the north polar axis leans toward the Sun. The vertical rays of the Sun are at the Tropic of Cancer ( $23.5^{\circ}\text{N}$ ). On this date, the number of hours of daylight increases with increasing latitude in the Northern Hemisphere, and decreases with increasing latitude in the Southern Hemisphere. All areas within the Arctic Circle are in continuous daylight, and within the Antarctic Circle continuous darkness. On this date, the Equator receives 12 hours of day and 12 hours of night, as it does every day of the year (Source/Credit: modified from Dennis I. Netoff and Ava Fujimoto-Strait, *Weather & Climate Lab Manual*).

On the date of the Northern Hemisphere winter solstice (December 21-22), the vertical rays of the Sun are at  $23.5^{\circ}\text{S}$ , the Tropic of Capricorn. On that orbital date, only the Equator is cut exactly in half by the Circle of Illumination, and only observers at the Equator will experience equal day and night duration (Figure 2.59). The entire area poleward of the Antarctic Circle on that date is in daylight, so all places within the Antarctic Circle will have between 24 hours and 6 months of continuous daylight. The length of day increases going from the Equator toward the South Pole, and decreases toward the North Pole. The important characteristics of the equinox and solstice dates are given in Figure 2.60.

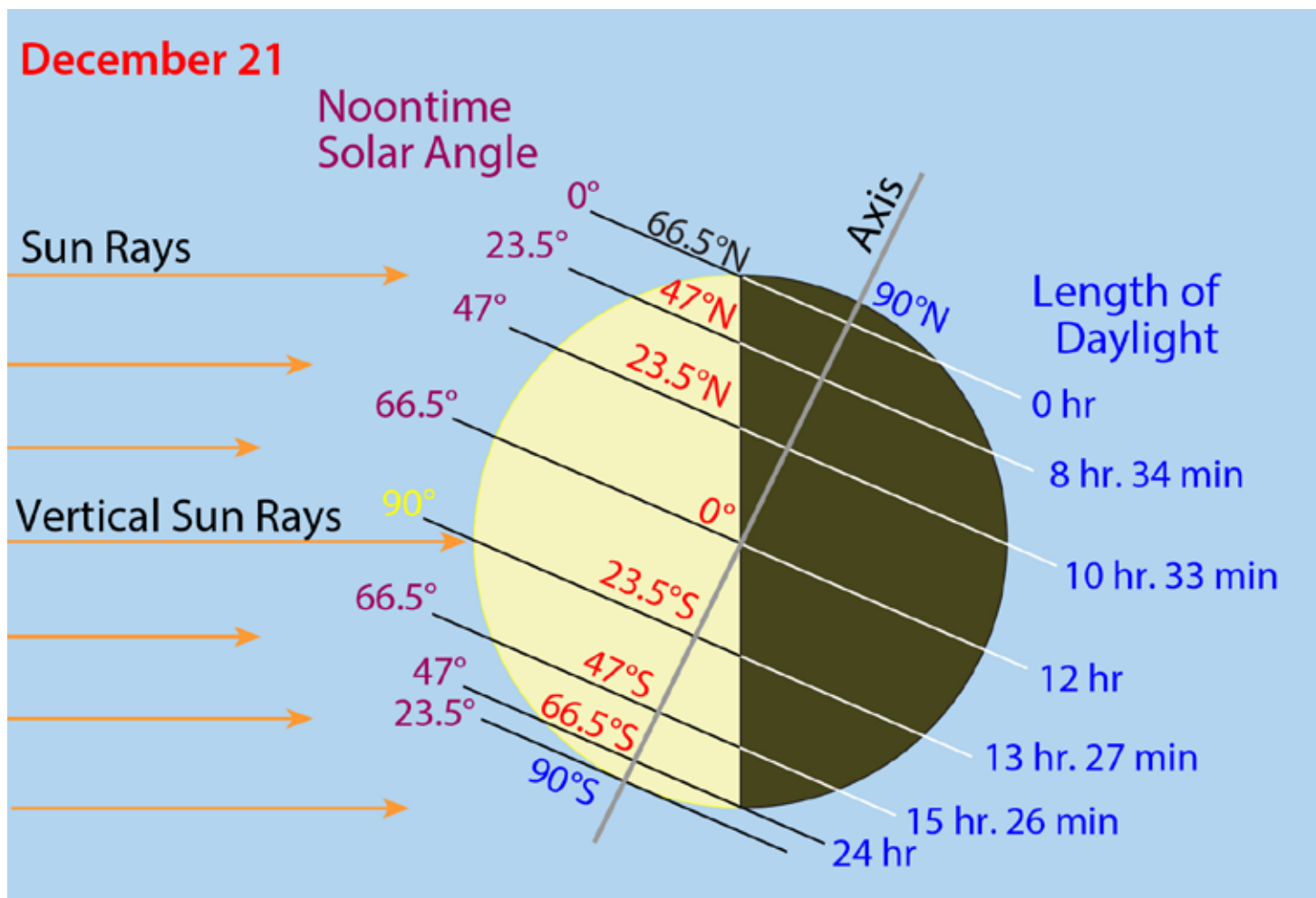
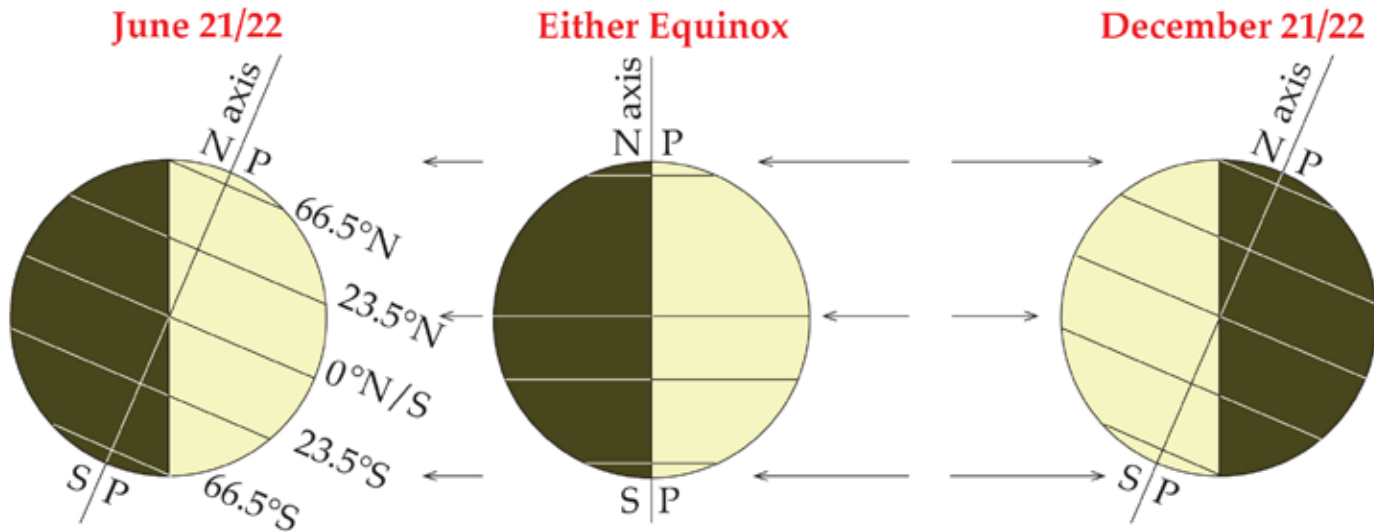


Figure 2.59. On December 21-22, the north polar axis leans away from the Sun. The vertical rays of the Sun are at the Tropic of Capricorn ( $23.5^{\circ}\text{S}$ ). On this date, the number of hours of daylight decreases with increasing latitude in the Northern Hemisphere, and increases with increasing latitude in the Southern Hemisphere. All areas within the Arctic Circle are in continuous darkness, and within the Antarctic Circle continuous light. On this date, the Equator receives 12 hours of day and 12 hours of night, as it does every day of the year (Source/Credit: modified from Dennis I. Netoff and Ava Fujimoto-Strait, *Weather & Climate Lab Manual*).



### Important Characteristics of Solstice and Equinox Dates



- vertical rays at 23.5°N
- most intense rays at 23.5°N
- 12 hour day and night at the Equator
- areas within Arctic Circle have at least 24 hours daylight
- areas within Antarctic Circle have at least 24 hours of darkness
- days get longer from the Equator to the North Pole
- days get shorter from the Equator to the South Pole
- first day of northern hemisphere summer

- vertical rays at 0°N/S
- most intense rays at 0°N/S
- 12 hour day and night at the Equator
- 12 hour day and night on all parallels
- North Pole and South Pole have 24 hours of twilight
- first day of northern hemisphere fall (September) or spring (March)

- vertical rays at 23.5°S
- most intense rays at 23.5°S
- 12 hour day and night at the Equator
- areas within Arctic Circle have at least 24 hours darkness
- areas within Antarctic Circle have at least 24 hours of daylight
- days get shorter from the Equator to the North Pole
- days get longer from the Equator to the South Pole
- first day of northern hemisphere winter

*Figure 2.60. Important characteristics of solstice and equinox dates (Source/Credit: modified from Dennis I. Netoff and Ava Fujimoto-Strait, Weather & Climate Lab Manual).*

Variations in the intensity of radiation and duration of daylight combine to make some interesting insolation and temperature comparisons (Figure 2.61). For example, Belem, Brazil (2°S), has a warmest month average temperature of 79.5°F, whereas the coldest month is 77.5°F, an annual temperature range of only 2°F. The monotony in temperature results from year-round high Sun angle and little variation in the duration of daylight. The other extreme is illustrated by Verkhoyansk, Russia (68°N), with a balmy summer averaging 59°F, and an average January temperature of minus 56°F, an annual temperature range of 115°F. Bitter cold winter temperatures are the result of very low Sun angle coupled with very short daylight hours. During the summer, however, the Sun angle is somewhat higher, and there are 24 hours of daylight.

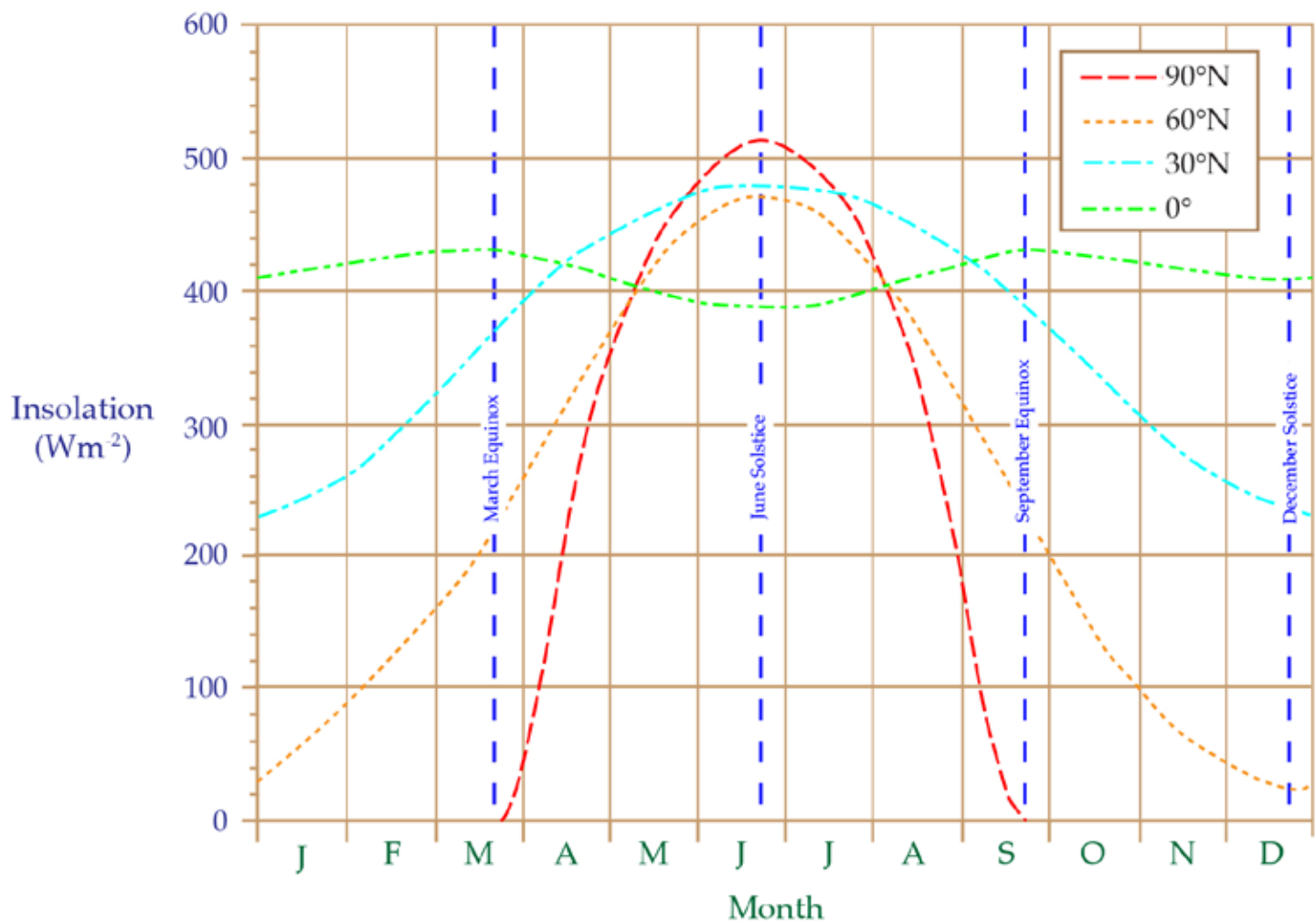


Figure 2.61. Insolation curves for the Equator, 30°N, 60°N, and the North Pole over the course of a year. Each curve represents potential insolation, which is the insolation that would be received at the Earth's surface if there was no scattering, absorption or reflection of incoming radiation by atmospheric gases and particulates. Insolation values take into account only the intensity of radiation and the duration of daylight. Using these idealized curves, an observer at the North Pole would have 6 months of total darkness, but on June 21, would actually receive more insolation than any other location because of the 24 hour daylight period (Source/Credit: NOAA).

**In summary:**

- Seasons are caused by the tilt of the Earth's axis in conjunction with its orbit around the Sun.
- Axial tilt and orbital motion control the duration of daylight and the intensity of radiation received at the surface of the Earth.
- The Tropics of Cancer and Capricorn as well as the Arctic and Antarctic Circles are determined by the axial tilt. The Sun's vertical rays are never poleward of the tropics.
- The critical orbital positions are the equinoxes and the solstices, which represent the start of the seasons in both hemispheres, and the times of the year when the vertical rays of the Sun are at their latitudinal extremes (Tropics of Cancer and Capricorn) or on the Equator.
- As latitude increases, the variation in intensity and duration of sunlight increases.

## Nature of the Absorbing Medium and Wavelength of Radiation

Certain substances are inherently good absorbers of many wavelengths of radiation. If they are also good radiators (re-radiated energy), they are called **blackbody radiators**, or simply blackbodies. Ideal blackbodies absorb all incoming radiation, regardless of wavelength or angle of incidence, and emit radiation in all directions (Figure 2.62). The hood of your automobile, particularly if it is dark in color, will become excessively hot during the day as it absorbs the Sun's energy, but that same surface in the early morning may be one of the coolest objects around. It is a good blackbody radiator. The Earth's surface, in general, is a fairly good blackbody radiator. It absorbs much of the solar radiation that strikes it during the day, and re-radiates it at longer wavelengths at night (terrestrial radiation). The atmosphere is not a good blackbody radiator.



Figure 2.62. The 2003 pahoehoe lava flow on Kilauea approximates a blackbody radiator. The flow is glowing because the temperature is high enough to be seen with naked eye. The temperature of the flow, because of its blackbody character, can be estimated from its color. This one was measured at 1000-1200°C or 1830-2190°F (Source/Credit: USGS).

## Greenhouse Gases

The troposphere is dominated by a few gases (Figure 2.63) and countless numbers of solid particles in suspension. Only one of the non-variable constituents of the troposphere, **carbon dioxide**, is a good absorber of infrared radiation. Carbon dioxide and several variable gases in the troposphere can only absorb effectively in selected wavelengths of radiation. These gases are the **selective absorbers** and they are responsible for most of the absorption of either incoming or outgoing solar radiation. The gases that absorb and emit radiation in the thermal infrared range of the electromagnetic spectrum are collectively called greenhouse gases. They include, in order of importance, **water vapor**, **carbon dioxide**, **methane**, **nitrous oxide**, and a host of **trace gases**. **Ozone** is now included in this list, although it absorbs most effectively in the ultraviolet, not in the infrared. Anthropogenically-induced (human-caused) **trace gases** such as chlorofluorocarbons, carbon tetrafluoride, sulfur hexafluoride, and hydrofluorocarbons are also greenhouse gases and will be discussed in Chapter 8 in the context of climatic change.

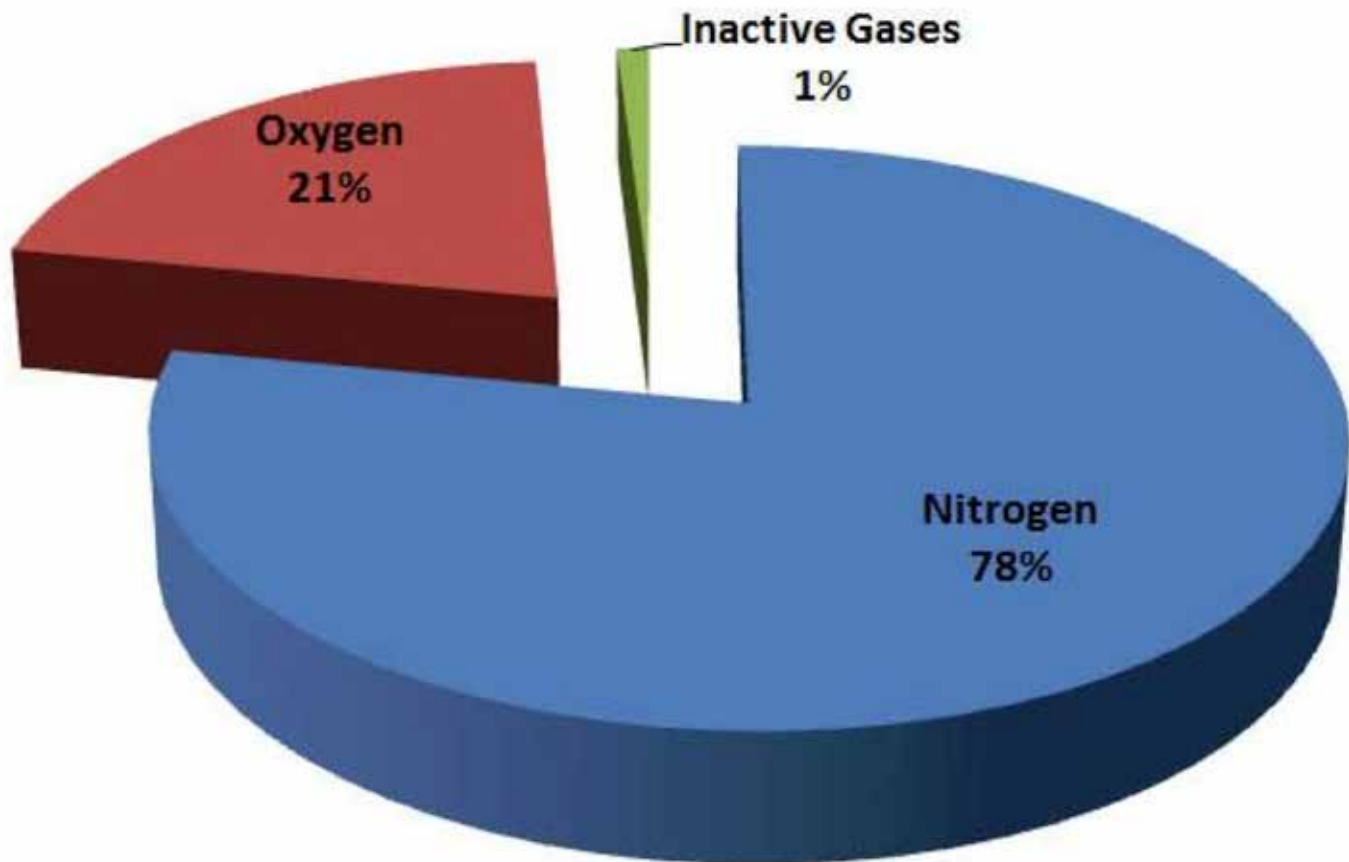


Figure 2.63. Major non-variable constituents of the troposphere. These gases play little role in the heating and cooling of the atmosphere. They are relatively transparent to incoming solar radiation, allowing much of it to be transmitted through the atmosphere and strike the Earth surface (Source/Credit: NASA).

**Ozone (O<sub>3</sub>)** is abundant in the stratosphere, at an altitude of 10 to 40 miles. Stratospheric ozone is a good selective **absorber in ultraviolet** wavelengths (Figure 2.64), and prevents lethal dosages of incoming ultraviolet radiation from reaching the surface. Absorption of incoming shortwave radiation by ozone in the stratosphere is responsible for the reversal in the temperature vs. height curve from the troposphere to the stratosphere. Tropospheric ozone is largely anthropogenic and is in much higher concentrations in urban and industrial regions. Tropospheric ozone, long ignored as a greenhouse gas in the troposphere, has been listed as the fourth most important tropospheric greenhouse gas in the most recent assessment by the Intergovernmental Panel on Climate Change (2013 IPCC), trailing only water vapor, carbon dioxide, and methane (Figure 2.65).

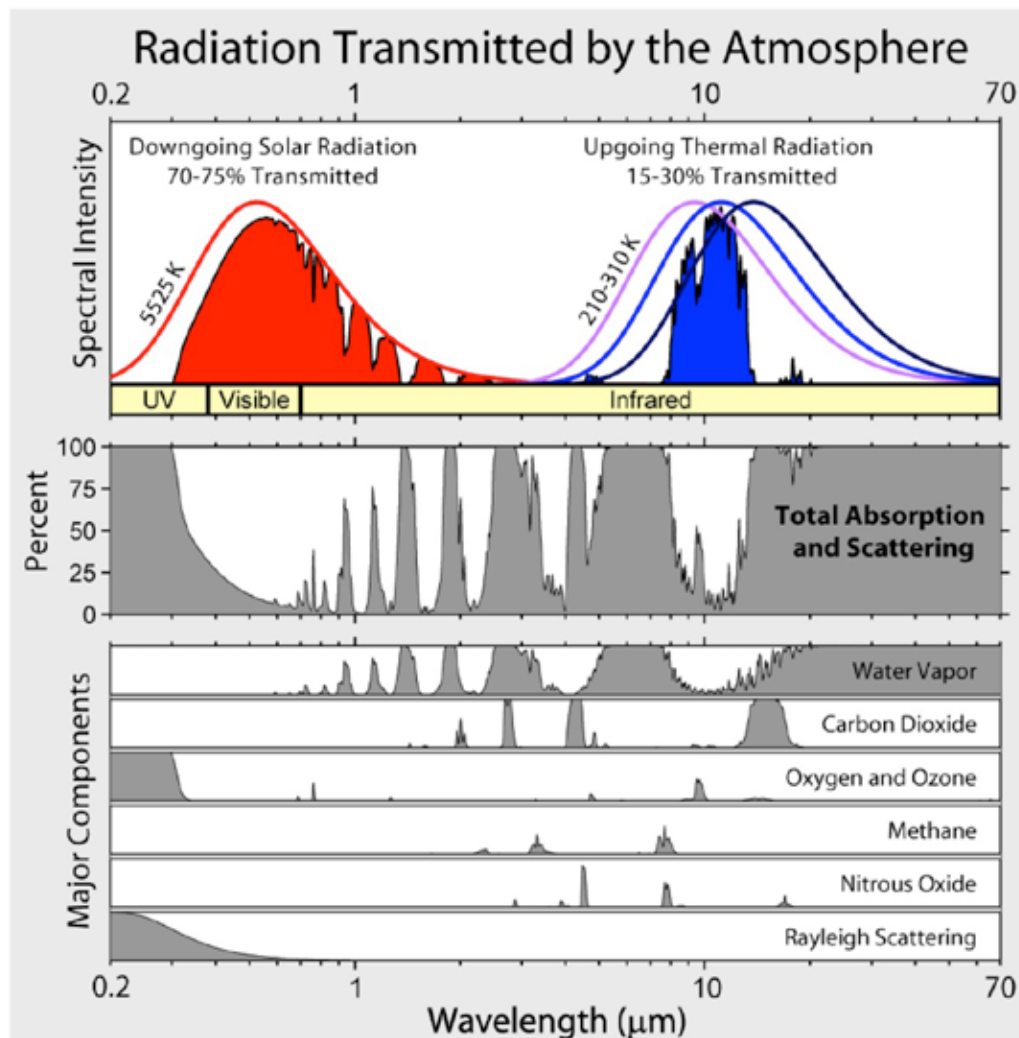


Figure 2.64. The top part of the diagram gives the spectrum for incoming solar radiation (red), 70-75% of which is transmitted, and the terrestrial spectrum (blue), which is mainly in the infrared. The gray diagrams at the bottom of this figure indicate the absorption bands of some of the principal greenhouse gases. Ozone, and to a lesser degree oxygen, are selective absorbers in the shorter ultraviolet wavelengths. Water vapor absorbs in many of the longer wavelengths, as does carbon dioxide. Methane and nitrous oxide are very selective in the wavelengths that they absorb. Together, the greenhouse gases absorb between 70 and 85% of all of the outgoing terrestrial radiation (Source/Credit: Wikipedia, Global Warming Art project, Robert A. Rhode, [http://commons.wikimedia.org/wiki/File:Atmospheric\\_Transmission.png](http://commons.wikimedia.org/wiki/File:Atmospheric_Transmission.png)).

**Water vapor (H<sub>2</sub>O)** is the principal greenhouse gas in the troposphere. It is a selective absorber in several of the infrared wavelengths (Figures 2.64 and 2.66) and is relatively abundant in the troposphere (1-5% by weight). Water vapor is ubiquitous in the troposphere, even in the air over the driest deserts and coldest ice sheets.

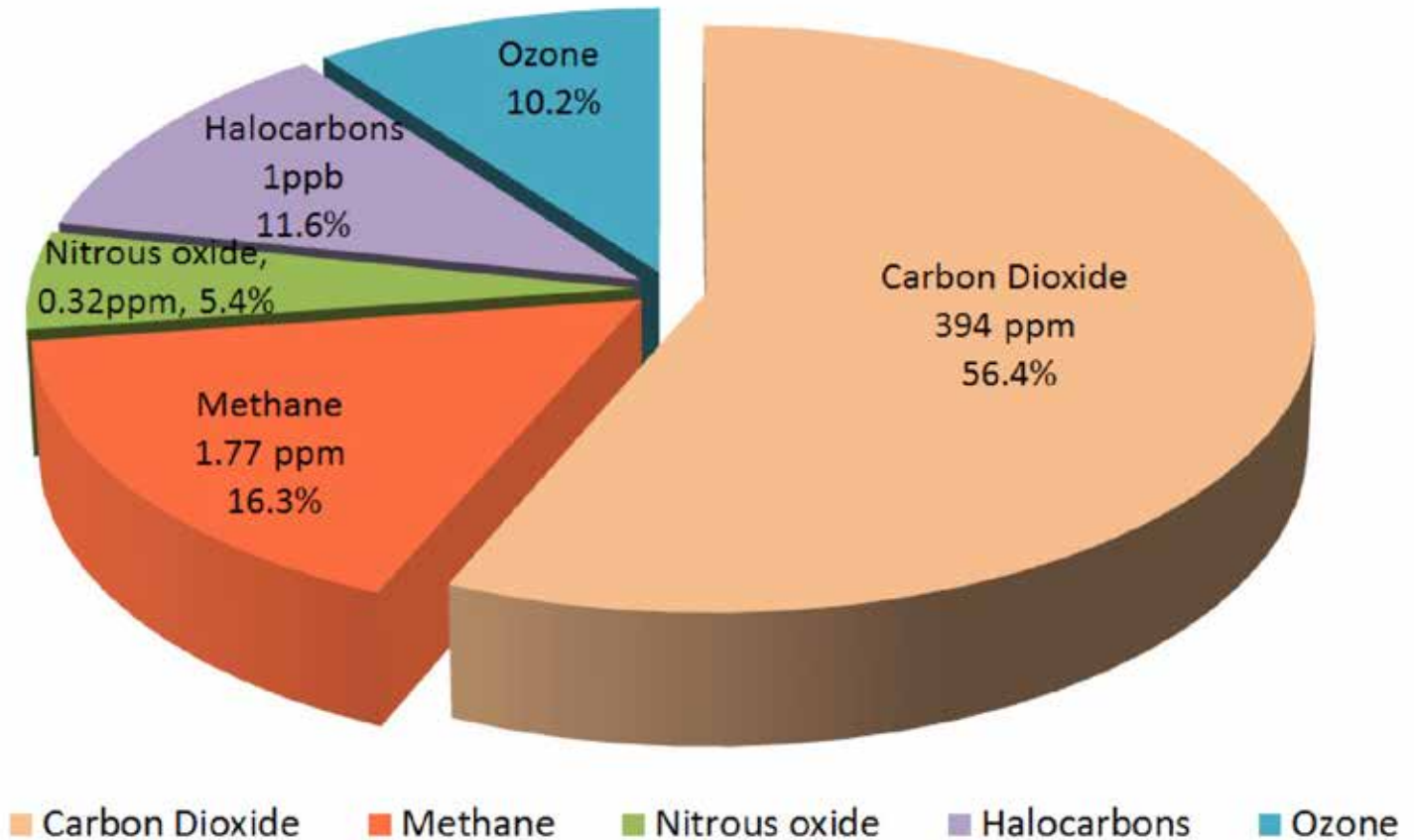


Figure 2.65. Greenhouse gas percentages following water vapor. Carbon dioxide dominates the number 2 position as a tropospheric greenhouse gas, even though some of the others are gaining in relative importance. Ozone is included in this group, even though it captures mainly incoming short-wave radiation (Source/Credit: NASA).

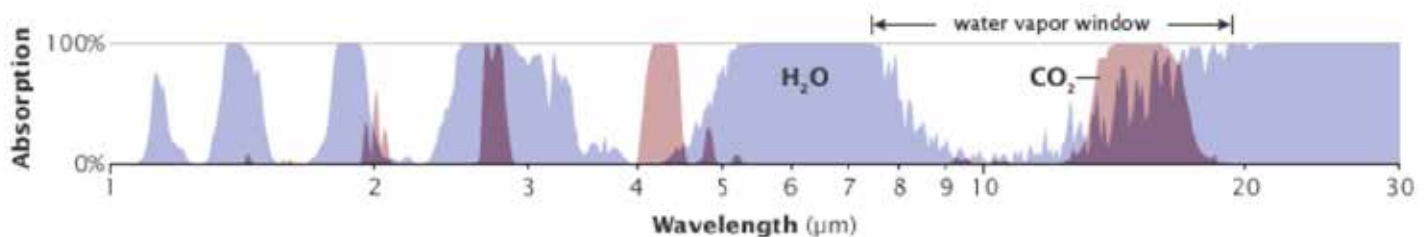


Figure 2.66. Absorption bands for water vapor and carbon dioxide, the two principal greenhouse gases. Note the gap, or water vapor window, for water vapor at wavelength of about 8-20 microns. Some of that gap is closed by carbon dioxide (Source/Credit: NASA).

**Carbon dioxide (CO<sub>2</sub>)** is the **second most important greenhouse gas in the troposphere** (Figure 2.65). It is also a selective absorber in several of the infrared wavelengths (Figure 2.66). Carbon dioxide was for decades listed as a non-variable gas by most meteorologists, but after careful monitoring over the past half-century, many now consider it a variable component (Figures 2.67a and 2.67b). The cause of much of the increase in carbon dioxide is thought to be fossil fuel combustion (Figure 2.68).

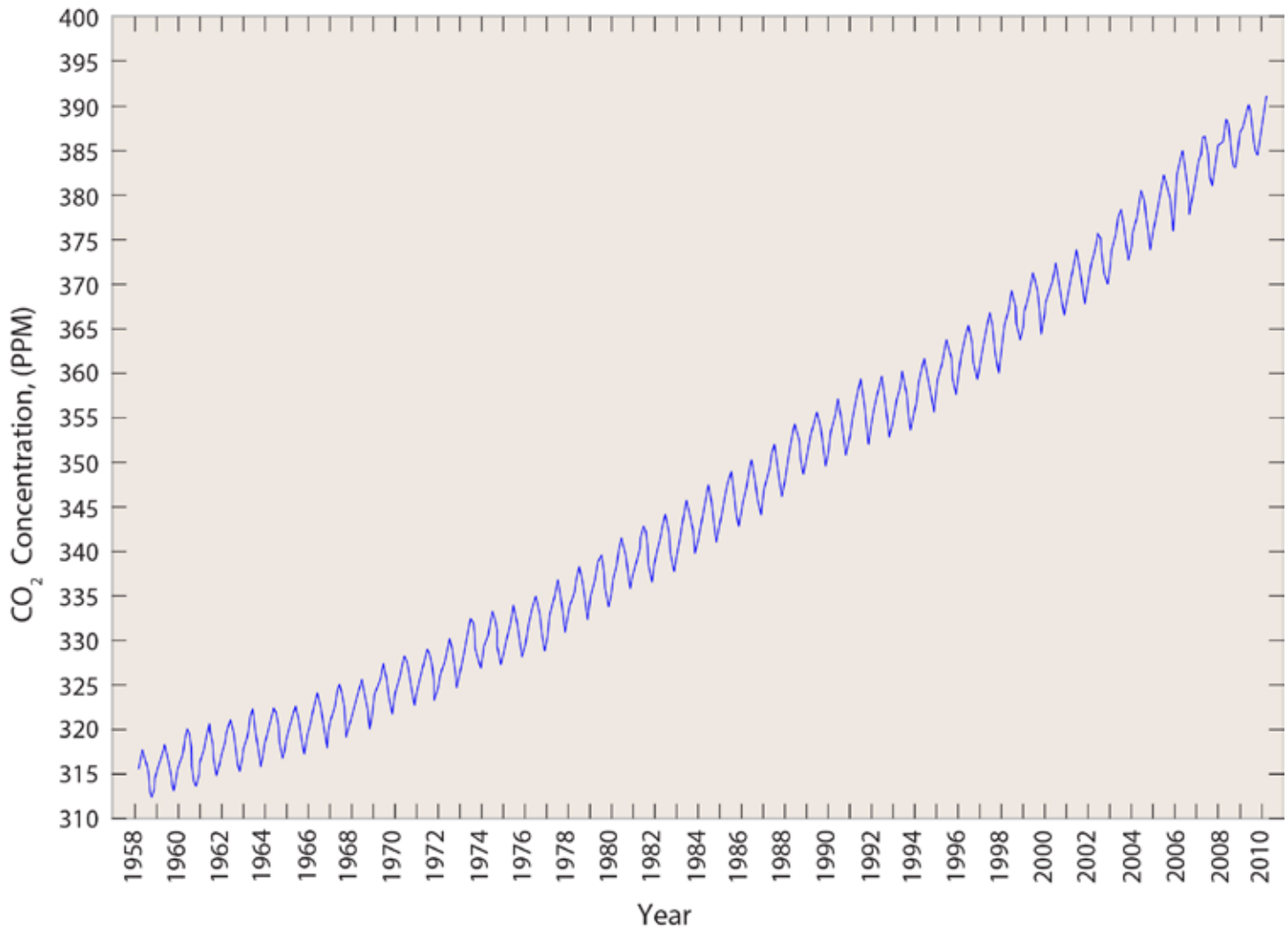


Figure 2.67a. The seasonal and decadal variation of carbon dioxide in the atmosphere based mainly from readings at the Mauna Loa Observatory in Hawaii. Maximum concentration occurs in winter (in the Northern Hemisphere which has more land than the Southern Hemisphere) when plants are dormant and are not taking in carbon dioxide. Carbon dioxide levels have risen primarily as a result of the burning of fossil fuels. The carbon dioxide concentration between 1958 and 2010 rose from about 315 ppm to nearly 390 ppm (Source/Credit: NOAA).



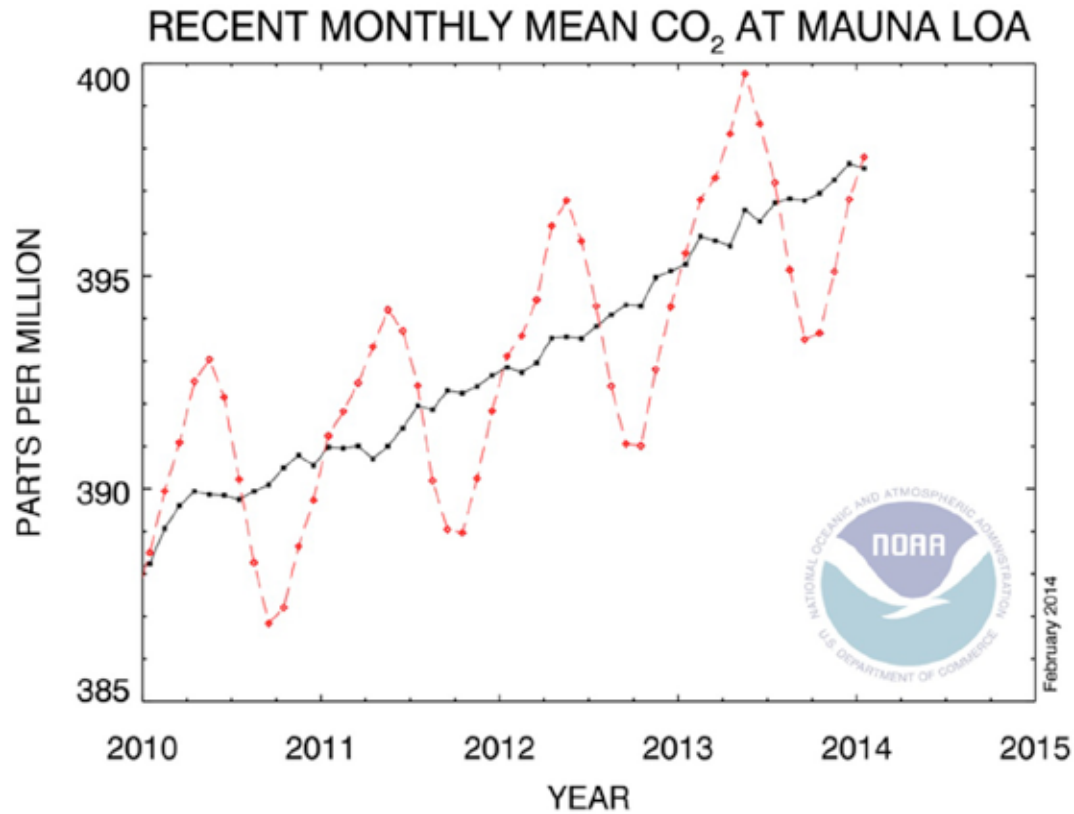


Figure 2.67b. Carbon dioxide abundance in the troposphere from 2010 to early 2014 (Source/Credit: NOAA).

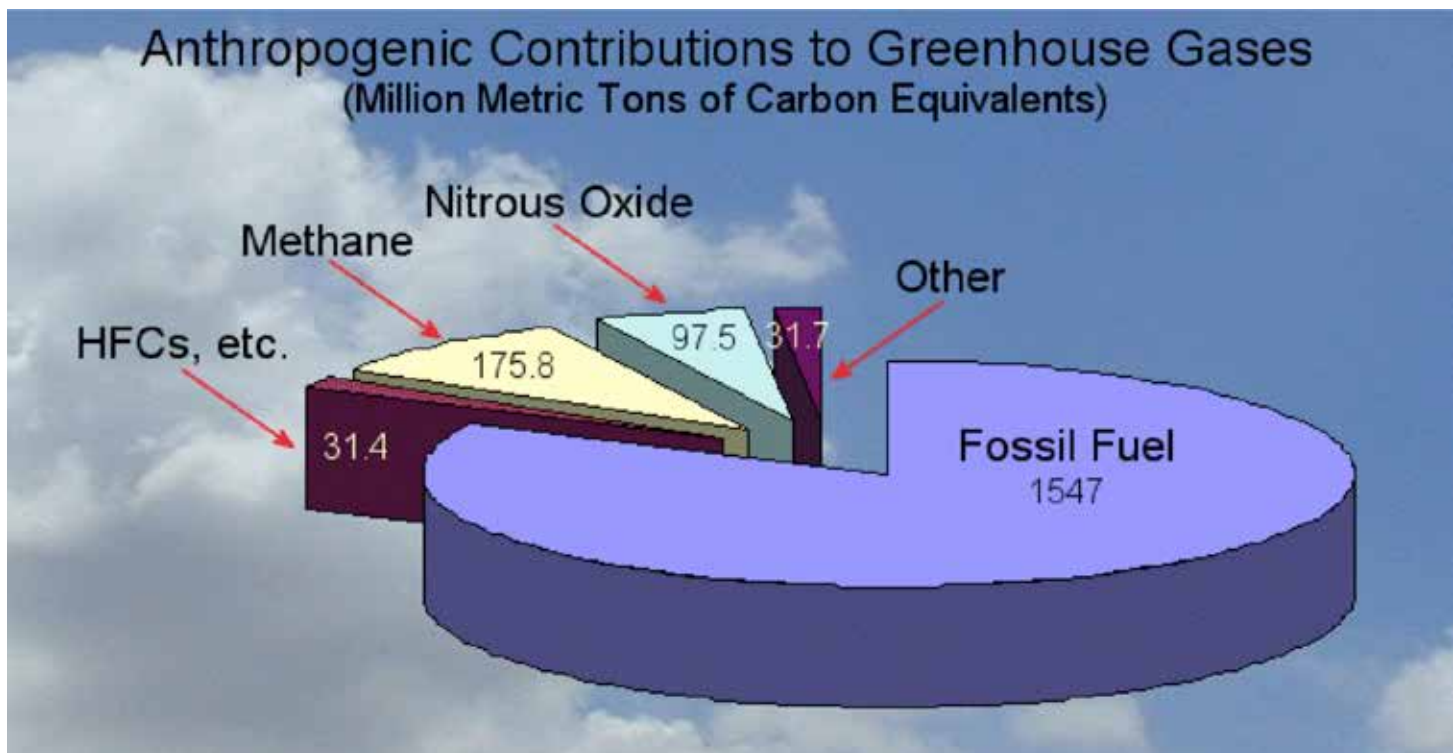


Figure 2.68. Anthropogenic contributions to greenhouse gases (Source/Credit: IPCC).

**Methane (CH<sub>4</sub>)** is the third most important greenhouse gas (Figure 2.65). Methane has natural sources as well as anthropogenic sources. Natural sources include the by-product of animals, as well as plants in low oxygen environments (e.g., swamps). Anthropogenic sources include rice fields, cattle, coal-mining, and using natural gas. Methane, along with many of the other greenhouse gases, has experienced substantial increases in tropospheric abundance since the Industrial Revolution.

**Nitrous oxide (N<sub>2</sub>O)** also has natural and anthropogenic sources. Although its contribution to tropospheric heating is relatively small (Figure 2.65), it has also been on the rise since the Industrial Revolution. Natural sources include microbial processes in water and soil. Nitrogen-based fertilizers, fossil-fuel power plants, and vehicle emissions are major sources of anthropogenic nitrous oxide.

**Chlorofluorocarbons (CFCs)** are exclusively anthropogenic. Although they are a very small component of greenhouse gases, they are very potent absorbers and have a long residence time (average length of time) in the atmosphere. Although they occur in many different chemical combinations, collectively, they are now approximately of the same importance as tropospheric ozone as a greenhouse gas (Figure 2.65). In the middle of the 20<sup>th</sup> century, they were widely used as refrigerants, spray-can propellants, and in some cleaning solutions. In the early 1970s, researchers discovered that CFCs are highly reactive with stratospheric ozone, and soon thereafter there was much speculation that CFCs were a major contributor to the *hole in the ozone layer* over the South Polar region. Their use is now banned in many countries, and CFC concentrations have been fairly constant or declining in recent decades.

**Aerosols** are tiny solid or liquid colloidal particles in the atmosphere. Aerosols have natural sources as well as anthropogenic sources. They are typically smaller than one micron in diameter, so they may remain aloft in the atmosphere indefinitely (Figures 2.69a and 2.69b). Even though they are not true greenhouse gases, many play a role in atmospheric heating and cooling, although their exact role is poorly understood.



Figure 2.69a. (left) True aerosols are small enough that they can be held in the atmosphere for great lengths of time and be transported long distances. The Rim Fire near Yosemite National Park during August and September 2013 had a visible smoke plume hundreds of miles long (Source/Credit: NASA).



Figure 2.69b. (right) Smoke from the Rim Fire in late August 2013 at Reno, Nevada nearly obscures the afternoon Sun. The Rim Fire was 125 miles to the south of Reno (Source/Credit: Nancy Netoff).

Aerosols include a long list of substances, including fine dust, volcanic ash, smoke, sulfides, fly ash, organic carbon, and sea salt. Their role in heating and cooling is generally very complex. Some scatter radiation; some are good reflectors; others are good absorbers; and many (e.g., salt and clay minerals) are **hygroscopic** (water-loving). Volcanic sulfur, for example, is injected into the atmosphere at high temperatures and may occur as elemental sulfur (not chemically combined). As it cools, it tends to combine with oxygen to become  $\text{SO}_x$  ( $x =$  variable quantities of oxygen). In the presence of water vapor, the two combine, ultimately forming sulfuric acid droplets which are good reflectors of radiation. The combined role of all aerosols is toward atmospheric cooling, according to the most recent (2013) assessment by the Intergovernmental Panel on Climate Change (IPCC).

## Temperature: Vertical Variation in the Troposphere

The **lapse rate** refers to the change in temperature per unit rise in elevation, typically given in °F/1000' elevation change. Lapse rates usually refer to decreases in temperature with increasing elevation. Temperature usually decreases with increasing elevation within the troposphere at an average rate of about 3.5°F/1000 feet (6.5°C/1000m), the normal lapse rate (Figure 2.70). Three factors are largely responsible for this condition:

- (1) the atmosphere is heated from below;
- (2) **greenhouse gases are most abundant close to the Earth's surface where the atmosphere is densest**; and
- (3) subsiding air is warmed by compression and rising air is cooled by expansion.

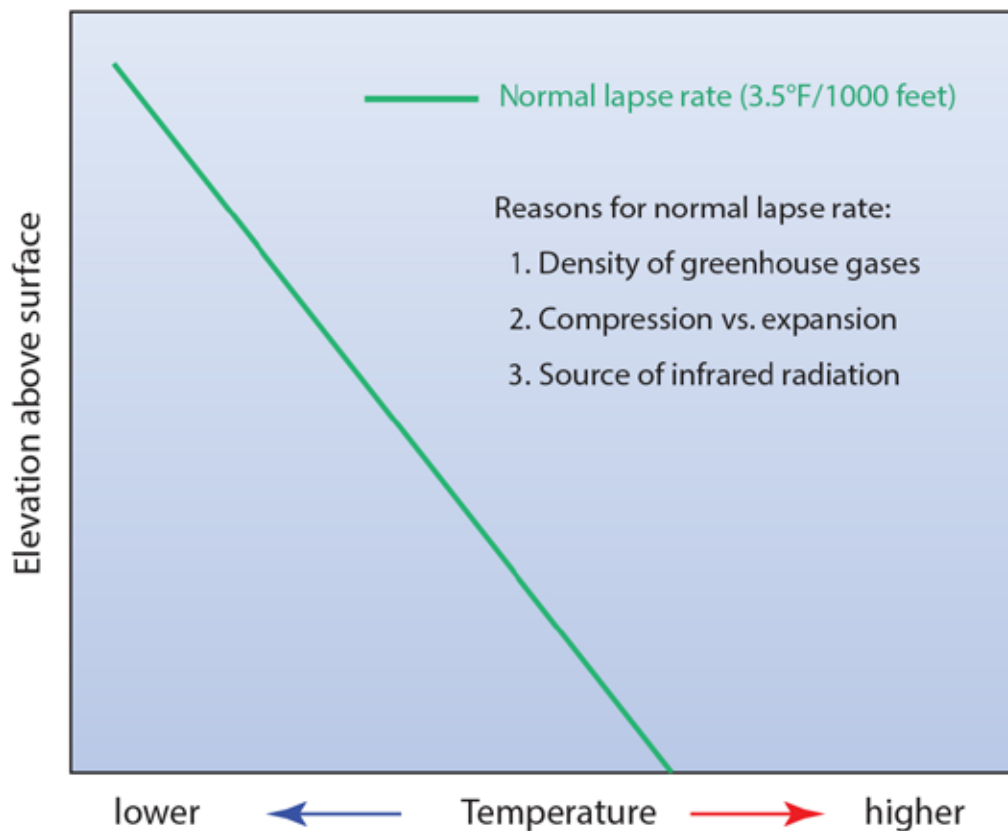


Figure 2.70. Lapse rates are shown graphically by temperature-height diagrams. Temperatures increase to the right and elevation above the surface toward the top. The normal or average lapse rate of a decrease of 3.5°F/1000 feet is a statistical average for the troposphere. The environmental lapse rate is the actual state of the atmosphere at a given time, and can deviate significantly from the normal lapse rate.

The **environmental lapse rate** is the actual state of the atmosphere at a given time, and can deviate significantly from the normal lapse rate. Local or regional factors on the surface or aloft can create higher (steeper) lapse rates, or reversed lapse rates, called temperature inversions.

For example, heating of the ground, a good blackbody radiator, on a hot summer afternoon often causes excessive heating of the overlying air by conduction and radiation. This often steepens the lapse rate to over 5.5°F/1000 feet to produce an **oversteepened lapse rate** (Figure 2.71). Oversteepened lapse rates are important in atmospheric physics because they make the air more buoyant, encouraging vertically-developed cumuliform clouds.

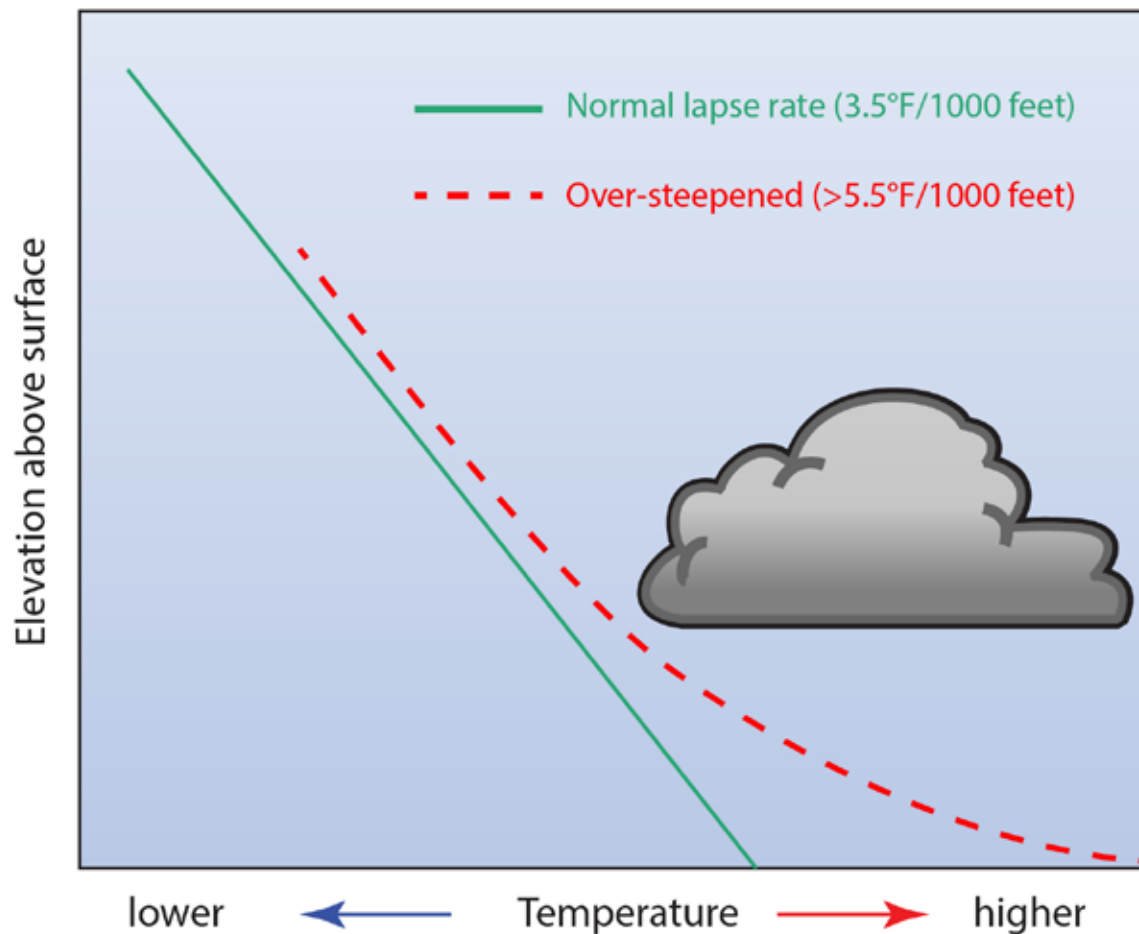


Figure 2.71. The oversteepened lapse rate occurs when there is a decrease of  $>5.5^{\circ}\text{F}/1000$  feet. This encourages buoyancy and vertical cloud development in the atmosphere. Oversteepened lapse rates can be caused by several factors, but are most typical in the mid-latitudes during the warm season on hot afternoons, particularly when the upper atmosphere is cold.

Alternatively, chilling of the ground and adjacent air on a long, cold, clear winter night may produce a temperature inversion, a condition in which temperatures increase with increasing elevation (Figure 2.72). Inversions inhibit vertical motion in the atmosphere. Clouds can form, however, but tend to be stratiform clouds, which are extensive laterally but limited vertically. Upper level inversions may occur thousands or tens of thousands of feet above the surface. They are very common under persistent high pressure systems where air sinks and is heated by compression (Figure 2.73). Inversions are important meteorologically because they make the air stable. Stable air, because it is cooler and more dense than the overlying air, resists uplift. Without uplift, cloud formation and precipitation are suppressed. Inversions are therefore associated with dry conditions.

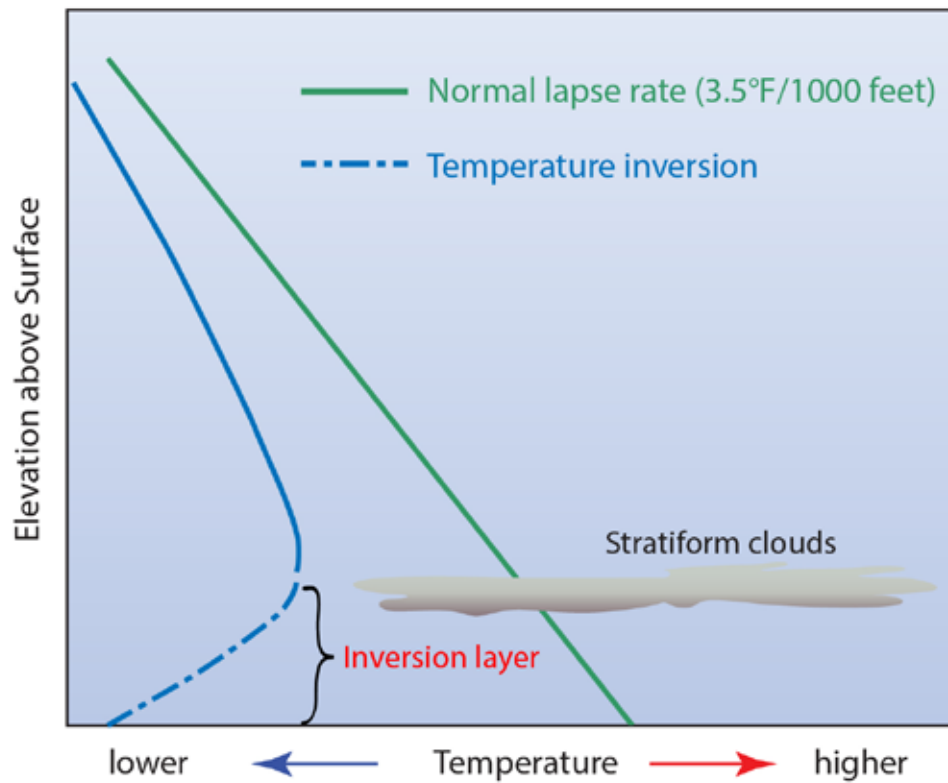


Figure 2.72. Temperature inversions occur when there is an increase in temperature with height. This discourages vertical motion in the atmosphere and often results in relatively clear skies. If conditions do cause cloud buildup (e.g., fronts or low pressure systems), they tend to be extensive laterally but restricted in vertical development.

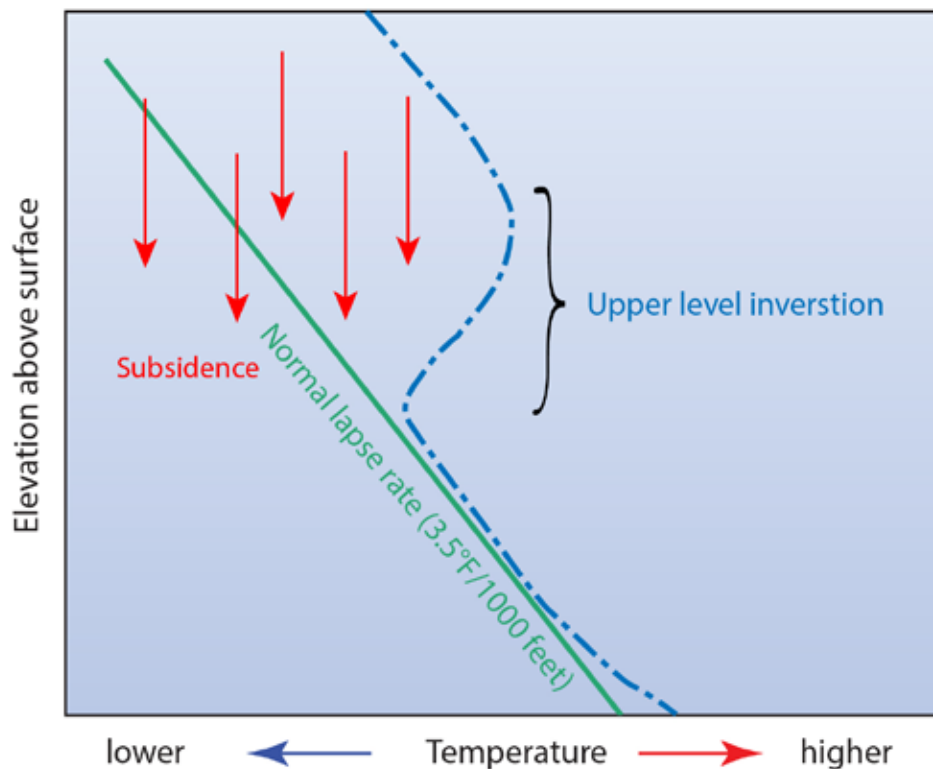


Figure 2.73. Upper-level inversions often occur under conditions of persistent high pressure which causes the upper air to heat by compression. They are quite common along west coasts of continents in the lower-mid-latitudes (e.g., Los Angeles, CA).

Temperature inversions are environmentally significant because they tend to trap low-level atmospheric pollutants. Inversions are also associated with pollution events, such as the infamous London fogs and Los Angeles smog (Figures 2.74a, 2.74b and 2.74c). By resisting uplift, the pollution from smokestacks and auto exhausts cannot rise upward and be dispersed by the wind. Instead, it becomes trapped near ground-level and remains until the inversion dissipates.



Figure 2.74a. As warm Pacific air flows over the cold, southward flowing California Current, the air is cooled. The cooling of this shallow layer of air acts to stabilize it, and this prevents it from rising and forming clouds and precipitation (Source/Credit: NASA).

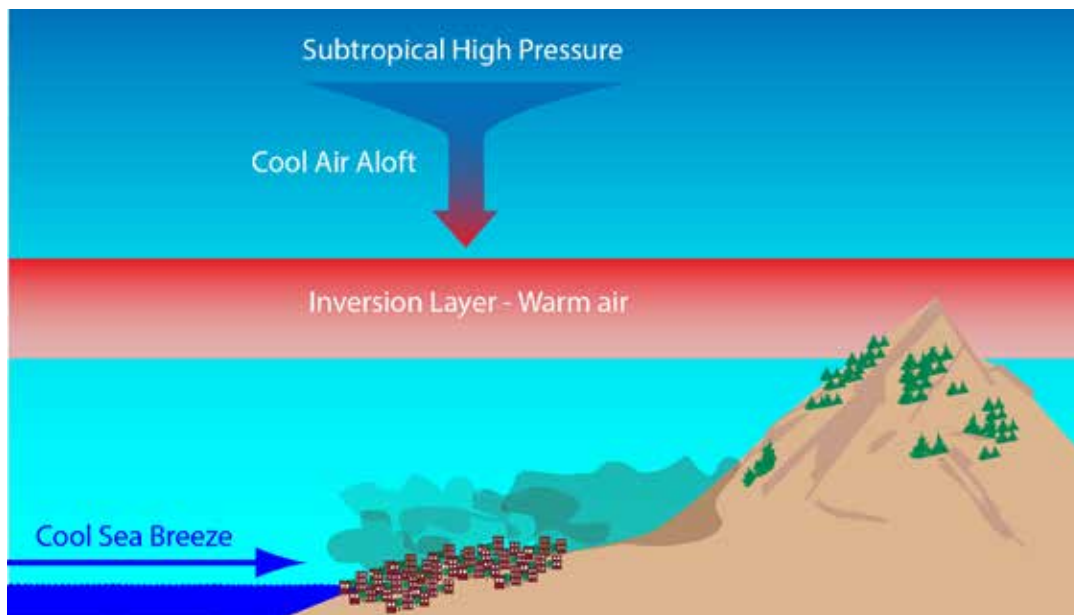


Figure 2.74b. Upper-level air above the Los Angeles Basin sinks and it warms as it descends. This creates a layer of warm air above the cooler surface layer, an inversion. This contributes to southern California's sunny skies (Source/Credit: NASA).

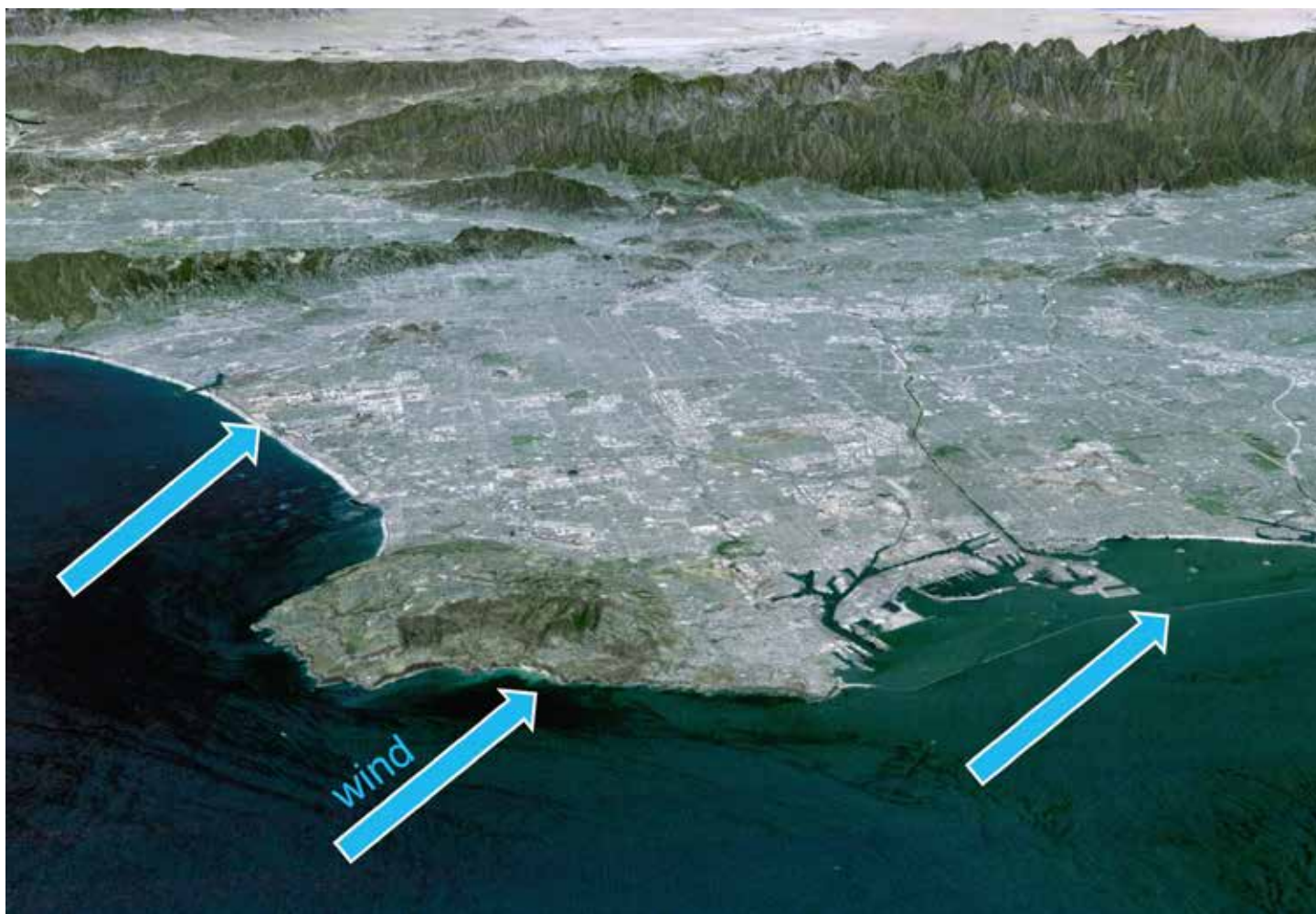


Figure 2.74c. Los Angeles smog, created by the chemical reaction of sunlight and atmospheric pollutants, and trapped by a temperature inversion and the San Bernardino Mountains (Source/Credit: iStockphoto/Daniel Stein Photography).



## Temperature: Horizontal Patterns on the Earth's Surface

Horizontal temperature patterns on the Earth's surface would be fairly simple on an idealized globe that was made of the same solid material throughout and the atmosphere was clear and clean. Temperatures would reflect the insolation patterns determined largely by the intensity of radiation and the duration of daylight. Rotation, revolution, inclination and polarity would give the Equatorial latitudes warmest temperatures, the polar latitudes coldest, and the mid-latitudes would be intermediate. Temperatures would be the same along any parallel, and one hemisphere would be a mirror image of the other (Figure 2.75). This simple pattern is unrealistic, largely because of land and water contrasts and ocean currents.

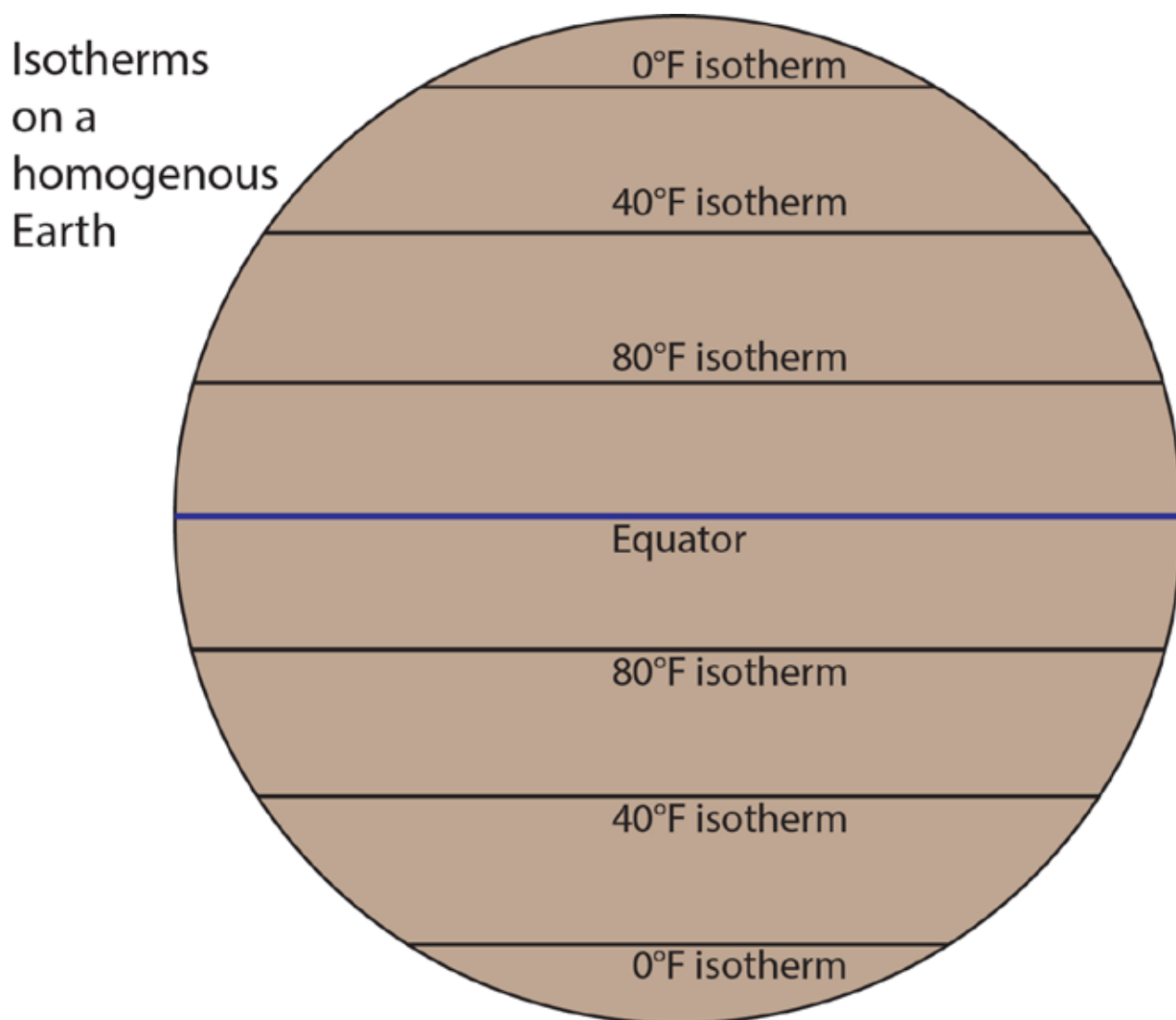


Figure 2.75. The average annual temperature on an idealized Earth can be represented by isotherms which are lines of equal temperature. This isotherm map indicates temperature changes as a simple function of latitude (Source/Credit: Dennis I. Netoff).

## Land and Water Differences

Land is much more sensitive to changes in incoming solar radiation than is water. Coastal areas that are experiencing a sea breeze during a hot summer day are cooler than inland locations (Figure 2.76).



Figure 2.76. Coastal areas experience a much smaller range of temperatures than do areas in the interiors of a continent because of differences in the thermal properties of land and water. A summer sea breeze from the cool ocean surface along the coast of the Baja Peninsula in Mexico brings 70°F air to the beach and rocky coast. Inland temperatures, unaffected by the coastal breeze, soar to nearly 100°F during the same period. Cool water temperatures are maintained year-round by the cold California Current (Source/Credit: Dennis I. Netoff).

- Those same coastal areas may be considerably warmer than inland locations during the cool season. Diving into a lake or river on a hot summer day is always refreshing because water temperatures are relatively low. On a cold winter night, those same water temperatures will be considerably warmer than the adjacent land. Observation alone indicates a basic principle in meteorology, that water bodies are slow to heat during the high-Sun season (or the heat of a summer day), and also slow to cool during the low-Sun season (or at night). Water and

land behave quite differently with respect to their ability to absorb, give off, and distribute thermal energy. The rapid heating and cooling properties of land versus water is an important principle of both meteorology and climatology; it is referred to as **continentality**. Continentality results from several different thermal properties of land and water (Figure 2.77). The effect of land and water temperature differences becomes readily apparent when we examine temperature patterns across the globe using isotherms, lines of equal temperature value (Figures 2.78).

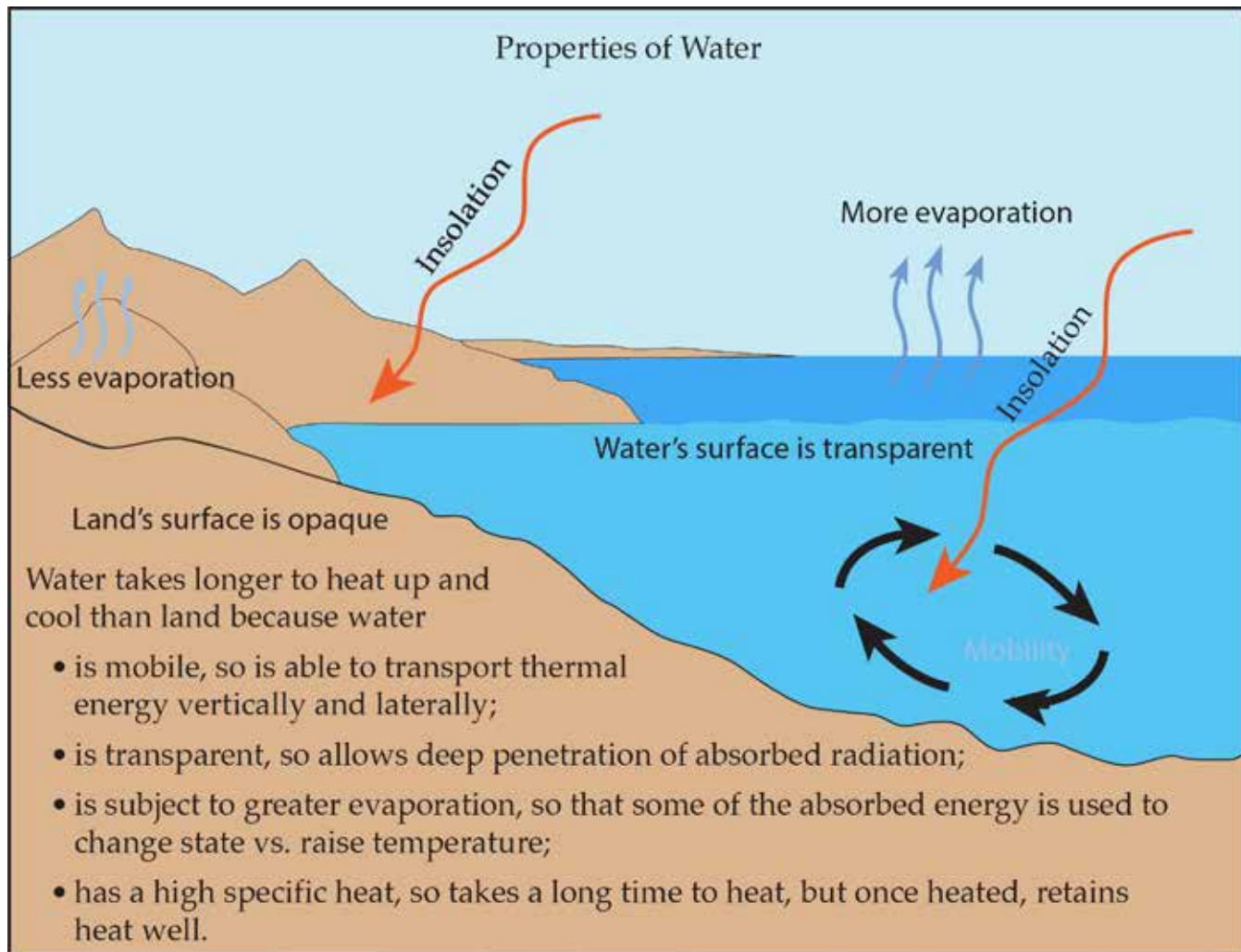


Figure 2.77. Water and land behave quite differently with respect to their ability to absorb, give off, and distribute thermal energy. Water bodies are slow to heat during the high-Sun season (or the heat of a summer day), and also slow to cool during the low-Sun season (or at night) (Source/Credit: modified from Dennis I. Netoff and Ava Fujimoto-Strait, *Weather & Climate Lab Manual*).

- In Figure 2.78, the 60°F isotherm is shown. Out over the ocean at 40°N, the air temperature is 60°F. As the isotherm is traced onto the land in summer (July), it bends poleward to maintain a 60°F temperature reading. This is because land heats up faster than water in the summer, and so it is necessary to go further north (poleward) to reach the cooler temperatures marked by the 60° isotherm. In other words, if we were to continue straight east along the

40th parallel, we may well find the temperature over the land to be 75° or 80°F or more. In order to connect with 60° temperatures over the land, the isotherm must bend towards higher latitudes.

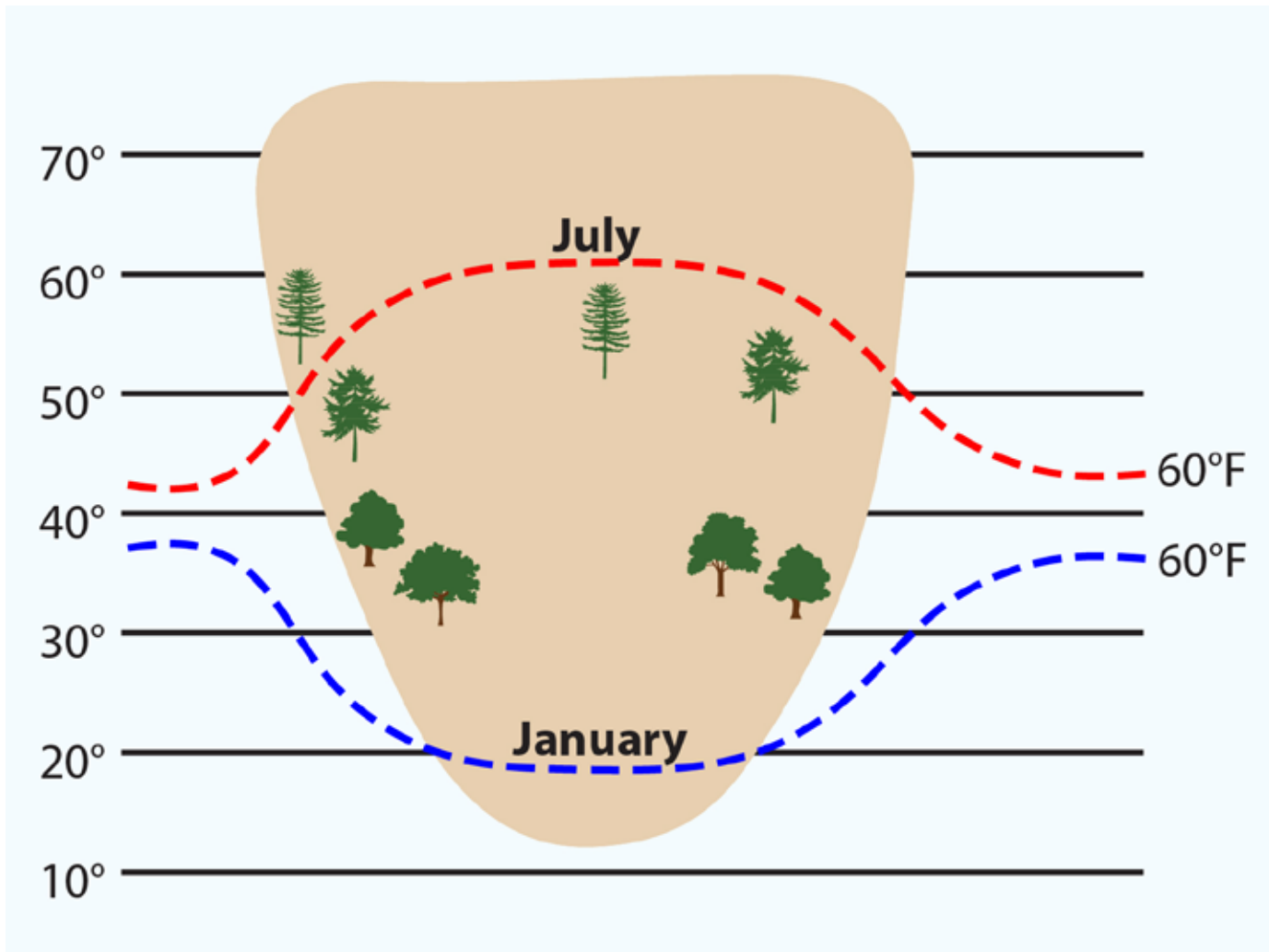


Figure 2.78. The differences in the rate at which land and water heat and cool give rise to the phenomenon known as continentality. The effects of continentality are illustrated by the pattern of the 60°F isotherm at different seasons. In the summer, the land heats more than water, so the isotherm bends northward over the warmer land. Places located south of this isotherm are warmer than 60°F. Conversely, in winter, the land cools more than the water, and so the isotherm bends to the south. Places located north of the isotherm are colder than 60°F. The location of the isotherm does not shift nearly as much over the ocean because the temperature of the ocean does not fluctuate very much over the course of the year.

- The reverse situation occurs in January, when the land is cool relative to water. Warmer temperatures are located equatorward over land, causing the isotherm to bend in that direction.
- On a seasonal scale, the **Principle of Continentality** implies that during periods of intense incoming radiation (summer), land heats faster than the water of the ocean basins, and land temperatures are therefore relatively high. During periods of little or no incoming solar radiation (winter), land cools faster than the adjacent ocean water, and land temperatures

are lower than the adjacent open ocean (Figures 2.79a and 2.79b). Consequently, the interiors of continents experience greater temperature extremes than coastal areas. This is another way of saying that **oceans moderate temperatures**. Winter temperatures along the coast in the Pacific Northwest are tens of degrees warmer than at similar latitudes inland (e.g., Idaho and Montana). **The main factors that cause land and water to heat and cool differently are differences in**

- (1) specific heat;
- (2) transparency;
- (3) evaporation, and
- (4) mobility, including ocean currents

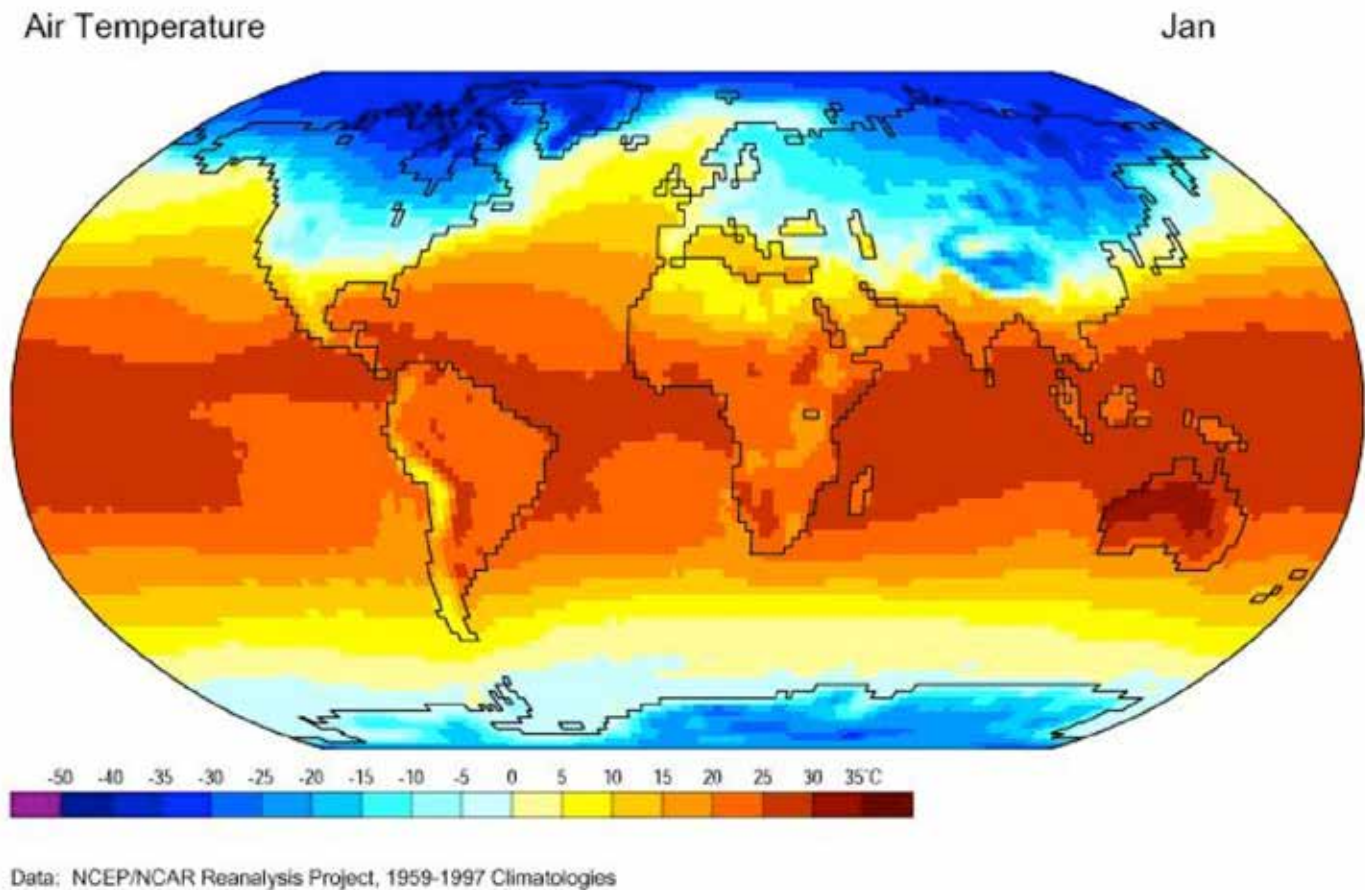
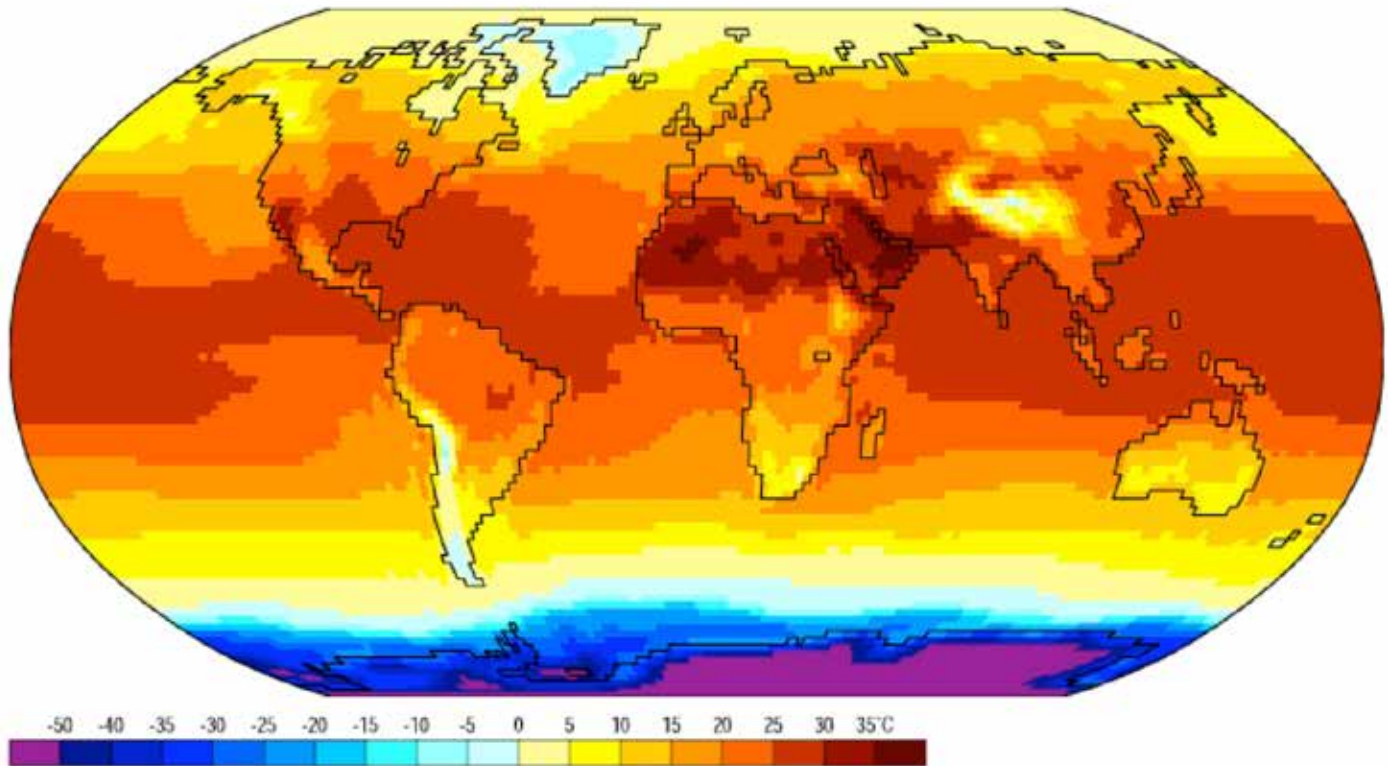


Figure 2.79a. Mean January air temperatures for the globe, based on the period 1959-1997. The warmest temperatures are on the continents at about 20-35°S, close to where the vertical rays of the Sun are located. Pockets of extremely high temperatures occur in the deserts of the Australian Outback. Southern Hemisphere temperature patterns are much simpler because of the lack of large landmasses in the middle latitudes (Source/Credit: NCEP/NOAA).

Air Temperature

Jul



Data: NCEP/NCAR Reanalysis Project, 1959-1997 Climatologies

Figure 2.79b. Mean July air temperatures for the globe, based on the period 1959-1997. The warmest temperatures are on the continents at about 20-35°N, close to where the vertical rays of the Sun are located. Pockets of extremely high temperatures occur in the deserts of the southwestern U.S., North Africa, and the Middle East. Southern Hemisphere temperature patterns are much simpler because of the lack of large landmasses in the middle latitudes (Source/Credit: NCEP/NOAA).

- **Specific Heat.** Land and water have different specific heats. Specific heat is the amount of energy required to raise the temperature of 1 gram of water by 1°C. The specific heat of water is three to five times greater than that of land, which means that it takes **three to five times** the amount of heat energy to raise the temperature of water by 1°C than to raise the temperature of land by the same amount. This is one reason why water heats more slowly than land even when both are exposed to the same intensity and duration of sunlight.

The specific heat of concrete, for example, is 0.20. If 0.20 calories of heat are applied to 1 gram of concrete the temperature of the concrete will rise 1°C. If one calorie of heat is added to the 1 gram of concrete, the temperature would rise 5°C.

Different substances have different specific heat values. Soil, for example, has a specific heat of 0.33. Limestone bedrock has a specific heat of 0.22 (Figure 2.80).

Pure Water	1.00
Sea Water	0.93
Wood	0.42
Soil	0.25
Dry Air	0.24
Concrete	0.20
Granite	0.19

*Figure 2.80. Specific heat of some common materials. The higher the specific heat of a material, the more energy required to raise its temperature.*

The high specific heat of water is why it is used in automobile radiators and other cooling systems. Even though tremendous heat is added to the water while the engine is running, its temperature does not increase enough to vaporize it, assuming the radiator is sealed.

Just as water is slow to heat up during periods of intense radiation, it is also slow to cool during periods of low intensity insolation (or none at all). It has a high capacity to retain heat, its **thermal (heat) capacity**. The larger the body of water, the slower it will warm or cool. Large, deep, open ocean basins undergo very little daily, monthly or annual temperature variations because they represent huge thermal reservoirs.

- **Transparency.** Another reason for the differential heating and cooling of land and water is that water is transparent and the ground is opaque. Virtually all of the energy that is absorbed by the ground is concentrated in the uppermost few feet. This is why there is little

to no variation in groundwater temperature throughout the year. The land surface heats intensely, but not to any significant depth.

Unlike the ground, water is translucent. Solar energy penetrates to depths within a column of water and is dispersed throughout the column, rather than being concentrated at the surface as it is with soil. This dispersal of energy slows the rate of heating at any given depth within the water column.

- **Evaporation.** Another factor responsible for land and water heating and cooling at different rates is evaporation (a cooling process). Most of the insolation absorbed at the Earth's surface is used to heat a very thin layer of the land and the air immediately above it. Thus, in addition to the relative lack of water, only a very small portion of the land's heat budget is available for evaporative cooling. Water, on the other hand, absorbs radiation to a much greater depth and has relatively less heat available at the surface for heating the air above it. Also, the vast majority of water's radiation budget is used in evaporative cooling. As a result, desert soils, with very low heat capacities and little moisture available for evaporation, tend to experience wide swings of temperature.
- **Mobility and Ocean Currents.** One of the most important differences between land and water is that **water** is a fluid, and is in constant motion, driven by such things as difference in density and the frictional effects of atmospheric winds. This allows heat energy to be dispersed both horizontally and vertically within a body of water. So, whereas solar energy shining on the ground gets trapped in the upper layer of the soil and remains there until it is radiated, heat energy that is trapped in water can be transferred from one place to another by fluid motion.



## Temperature Patterns and Ocean Currents

- Fluid movement in the oceans is affected by several factors, including density variations, atmospheric winds, astronomical tides, and Coriolis Force. The surface pattern of ocean temperatures is greatly influenced by daily and seasonal distribution of insolation (RRIP). The simple latitudinal pattern, however is altered by large, discrete bodies of surface water movement called **ocean currents**. The poleward and equatorward movement of ocean currents makes them either warmer (**warm currents**) or colder (**cold currents**) than the adjacent water. For example, Iceland is located further north than the southern tip of Greenland, but its average annual temperature is 40°F warmer than that of Greenland. The reason for this is that heat energy stored in the tropical Atlantic Ocean is carried northward in a huge warm current called the **Gulf Stream** (Figure 2.81).

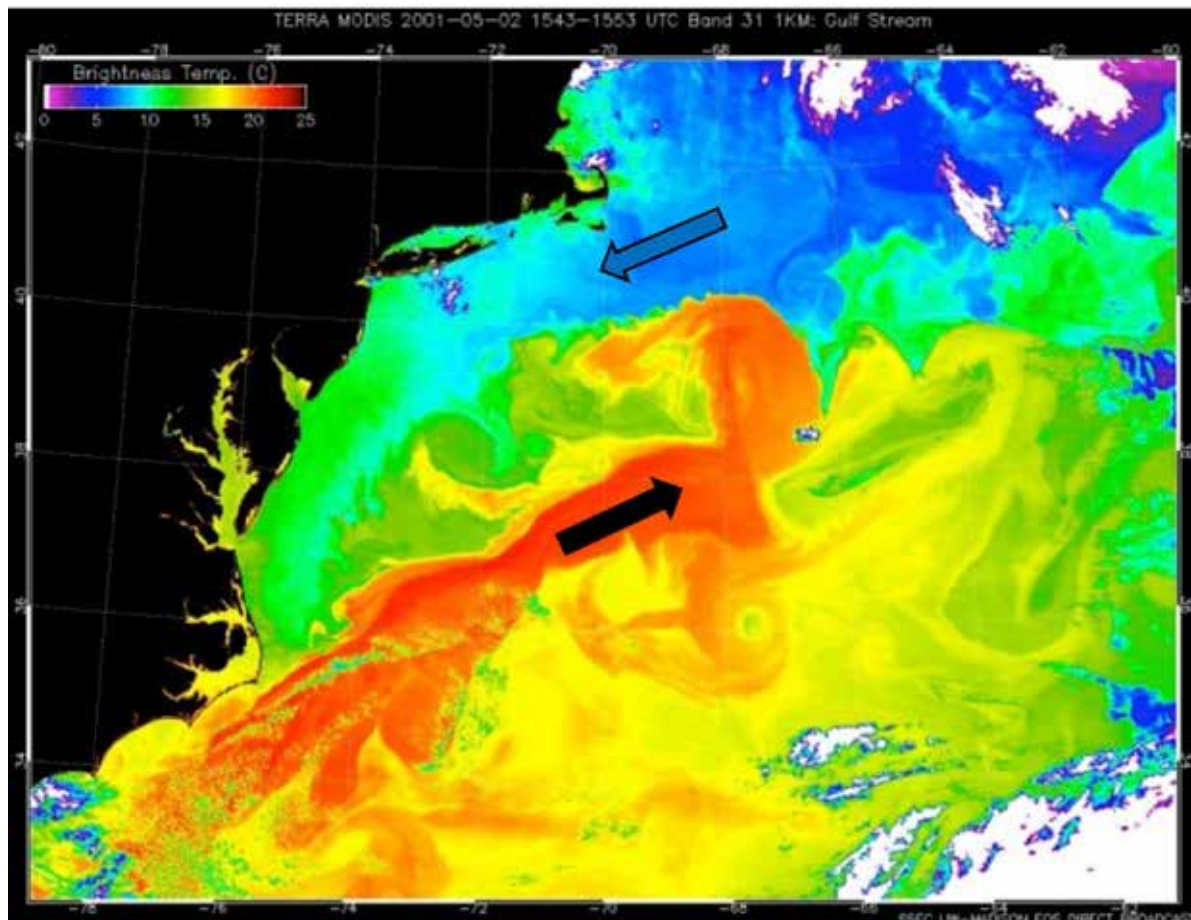


Figure 2.81. MODIS satellite infrared image of the warm Gulf Stream waters (black arrow) in contact with cooler waters of the Labrador Current (blue arrow) (Source/Credit: NASA Visible Earth).

- Heat transfer by this same current across the Atlantic Ocean gives Britain, which is located at the same latitude as Labrador and the Hudson Bay in Canada, a much warmer climate. If the poleward transport of heat energy into high latitudes of the North Atlantic were to fail, much of northern Europe could potentially cool by as much as 10 or more degrees in a very short period of time.

- The main driving force of the surface ocean currents is the planetary wind field, one of the main subjects of the following chapter. In the lower mid-latitudes in the major ocean basins, semi-permanent high pressure systems cause air to blow clockwise out of highs in the Northern Hemisphere, and counterclockwise out of highs in the Southern Hemisphere at about the same latitude. Frictional resistance of the air blowing across the surface of the oceans generates cold currents on one side of the highs and warm currents on the other (Figure 2.82).

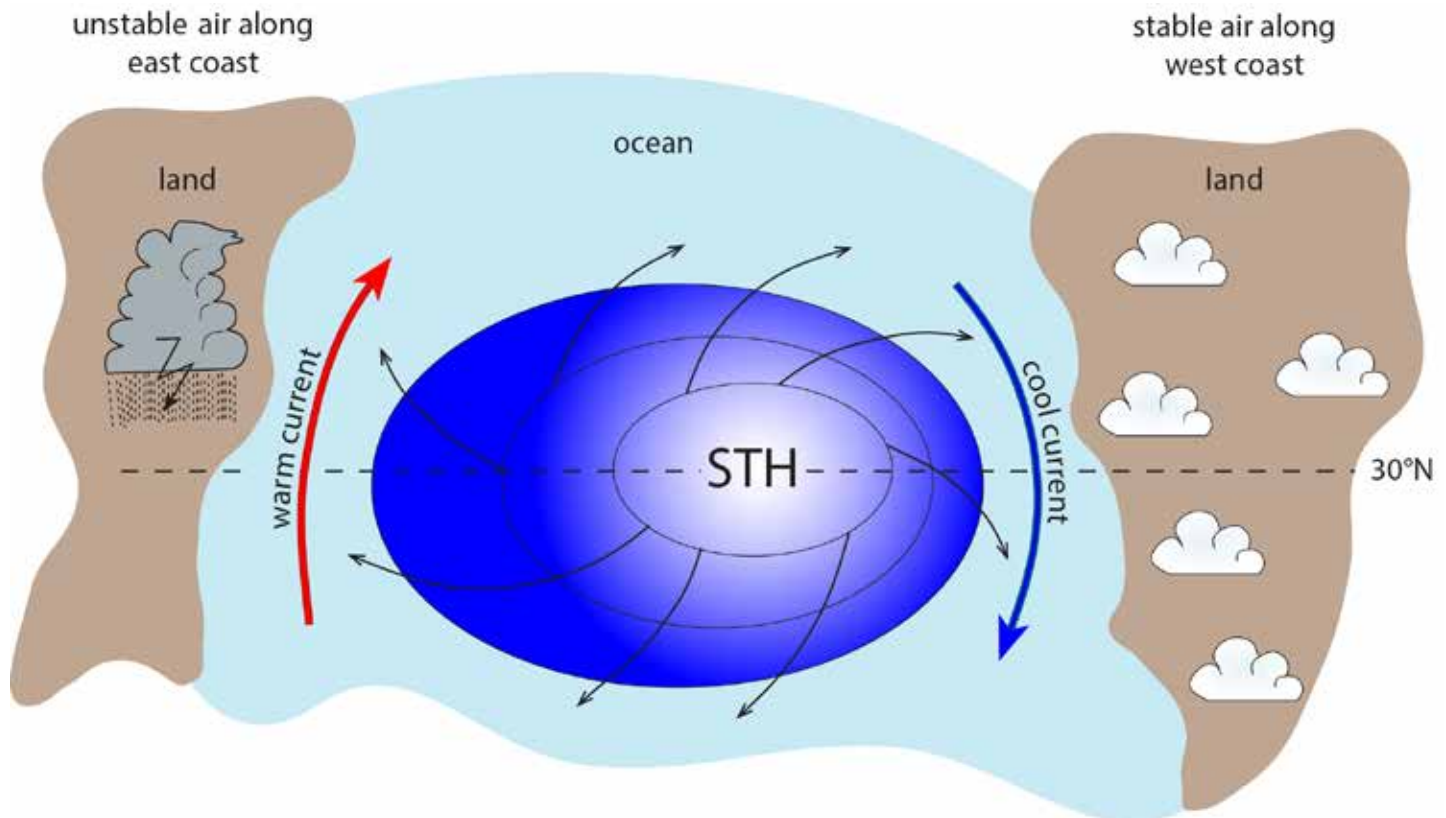


Figure 2.82. Large, semi-permanent oceanic subtropical high pressure systems (STH) are the main driving force for the lower-mid-latitude ocean currents. In both hemispheres, the western sides of continents are flanked by a cold current, the eastern sides of the continents by warm currents (Source/Credit: modified from Dennis I. Netoff and Ava Fujimoto-Strait, *Weather & Climate Lab Manual*).

- In both hemispheres, the western sides of continents are flanked by cold currents, the eastern sides of continents by warm currents. For example, the California Current off the west coast of the United States (eastern side of the Pacific) brings cold water southward from the Arctic regions (Figure 2.83). These cold ocean currents are very important because they stabilize the atmosphere and inhibit cloud development. So, the cold California Current helps keep southern California dry. The same is true for the Peru Current off the west coast of Peru and Chile (eastern Pacific). The cold Peru Current has contributed to the development of the driest desert in the world, the Atacama Desert. Some parts of this desert have received no measurable rainfall in decades.

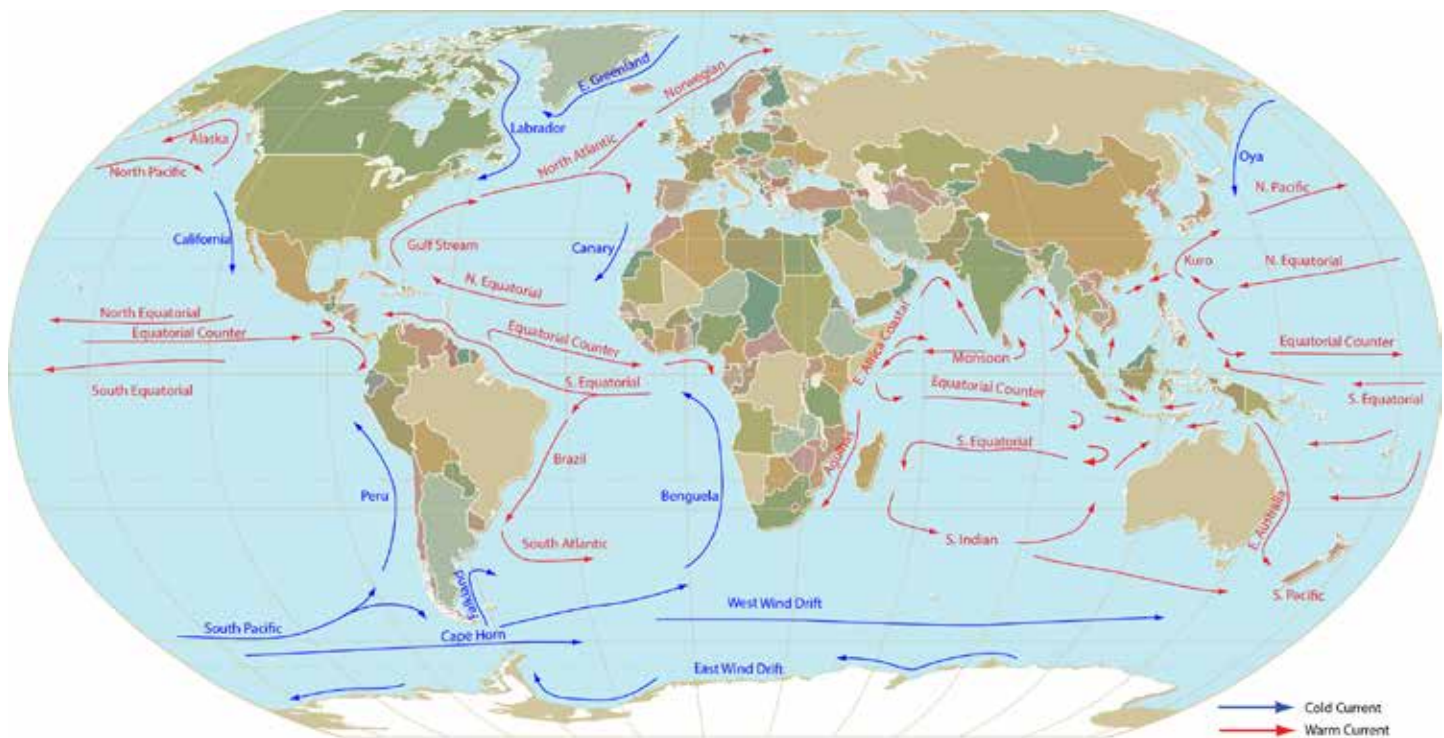


Figure 2.83. The key ocean currents in the world are indicated by the color-coding. Warm water (red arrows) is transported poleward and cold water (blue arrows) is transferred from polar regions toward the Equator. As a result of this movement, heat energy is transferred latitudinally and helps to reduce the temperature contrast between high and low latitudes. Were it not for these currents, the equatorial region would be far warmer, and the polar regions far colder than they now are. Also note that the warm water flows poleward along the east coasts of continents, and cold water flows equatorward along the west coasts of continents in the mid-latitudes. As discussed in the text, cold currents affect weather by enhancing the stability of the atmosphere, and this reduces precipitation. The ocean currents are generated by a combination of global wind currents and the Earth's rotation (Source/Credit: NOAA).

- The North Pacific Current travels eastward and collides with the North American continent at about the border between the United States and Canada. When it reaches the coast, the current splits, sending a current of warm water poleward (the Alaska Current) and a current of cold water equatorward, the California Current (Figure 2.84).

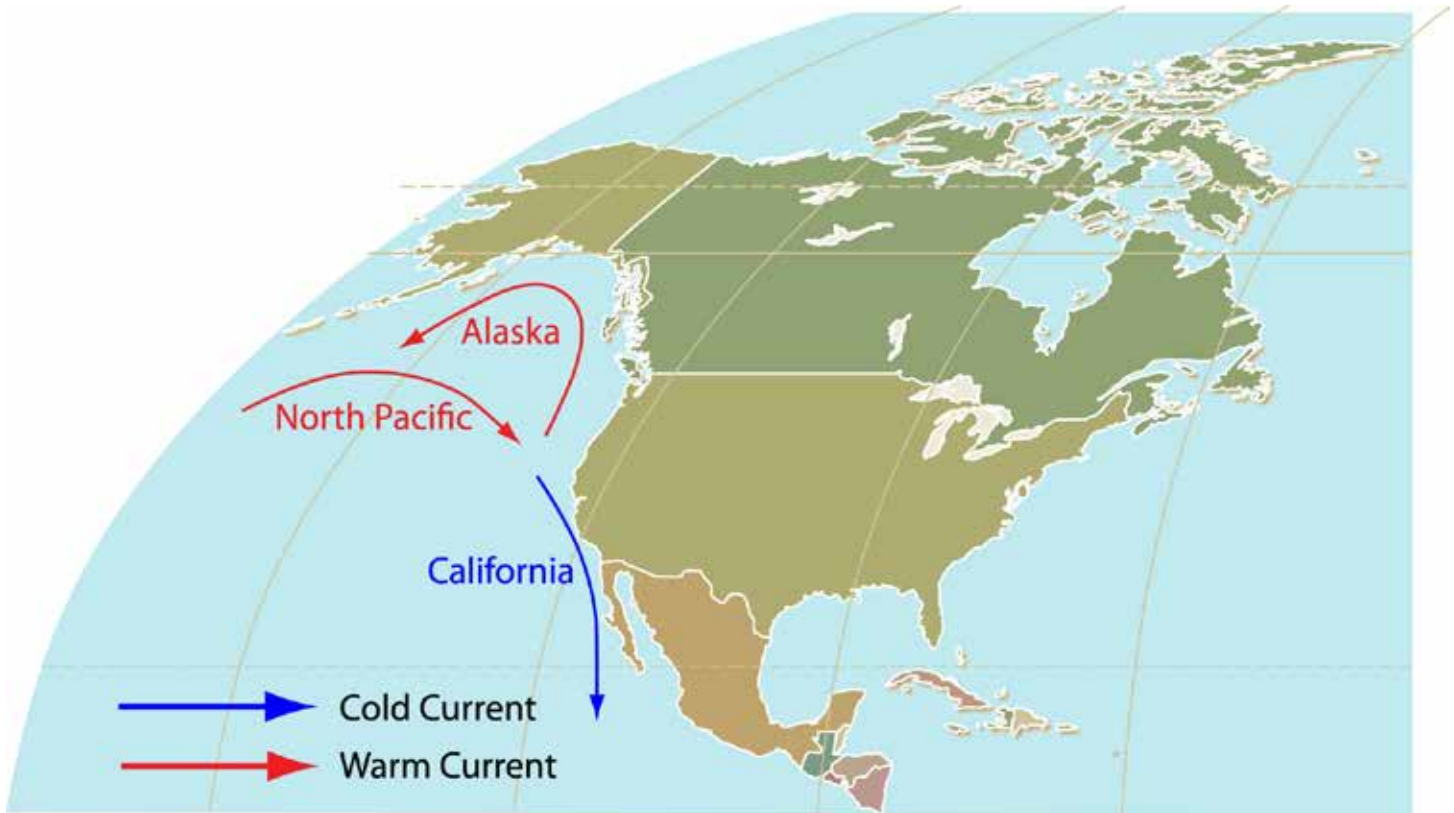


Figure 2.84. Warm and cold currents are relative terms. The portion of the North Pacific Current that flows northward as the Alaska Current is flowing into colder waters; so, relatively speaking, the current is warmer. Conversely, the portion of the current that flows southward as the California Current is colder than the water through which it flows; so, it is considered a cold current. The cold California Current is intensified by upwelling, a process whereby cold water at depth is forced to the surface by the Coriolis Force.

- The oceans cover about two-thirds of the Earth's surface, and because they are so vast and deep, they store vast massive quantities of energy and **are the primary source of heat storage in the atmosphere-hydrosphere system**. In fact, the upper 10 feet of the world's oceans contain as much heat as the entire overlying atmosphere, which is over 60 miles thick.

## Other Temperature Controls

Several other factors affect the Earth's surface temperature patterns on a local, regional, or continental scale. These include elevation, slope and orientation of the ground, the surface albedo, the type and density of vegetation, and highland barriers that impede airmass movement.

Temperatures typically decrease with **elevation**. The reasons for this were discussed previously in the section on *temperature: vertical patterns*. Mountains, high plains and plateaus are typically cooler than their low-elevation counterparts (Figure 2.85). The rate of change is fairly consistent with the normal or average lapse rate of about 3.5°F per 1000-foot change in elevation. The temperature at the top of a 5000-foot mountain will average about 17.5° cooler than at the bottom (5000) (3.5°F/1000 feet) = 17.5°F cooler.

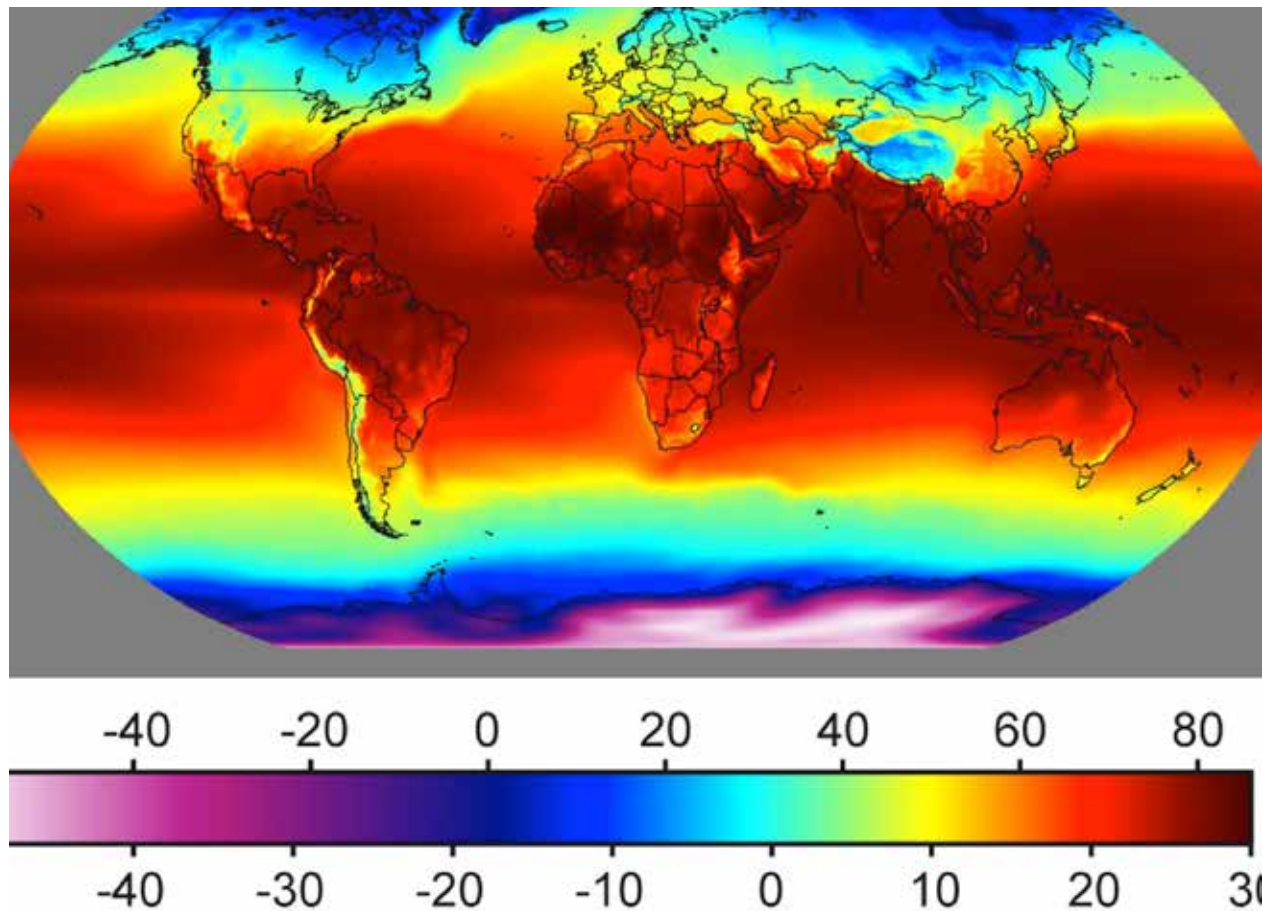


Figure 2.85. Annual near-surface mean temperature of the Earth from 1961-1990. This is similar to an isotherm map, but instead of depicting temperature by isotherms, each color band represents a range in temperatures. The transition from one color to another is similar to an isotherm. The basic pattern is latitudinal, with highest average temperatures in the Tropics, and progressively cooler temperatures toward either pole. Significant deviations from this pattern include the effects of higher elevation (e.g., the Tibetan Plateau of Asia, the Andes of South America, and the Rockies of North America). Other deviations include areas of warm and cold ocean currents, such as off the west coast of California (cold water) and Norway (warm water) (Source/Credit: NOAA, NCAR, NCEP).

Local and seasonal conditions, however, can temporarily reverse the trend of decreasing temperatures with elevation. Along west coasts of continents in the mid-latitudes, most commonly during the warm season, there is a cool layer of surface air called the marine layer. It is overlain by considerably warmer air that is heated by subsidence.

The lapse rate results in larger changes in temperature over smaller distances than any other major climate control. Mountains are known for their temperature diversity. The bases of mountains in the western United States are typically arid or semi-arid grasslands and deserts, but with a few thousand feet of rise in elevation, temperature-moisture conditions promote the growth of forests. At still higher elevations, temperatures become so cold that forests give way to alpine tundra.

The **slope of the ground** can affect local temperatures because the slope angle affects the angle of the Sun's rays. For example, in the morning, a hill slope that faces the rising Sun warms faster than the flat land around it because the Sun's rays would be more nearly perpendicular to the hillside than to the flat area. During the late afternoon, the flat land might be warmer because it is receiving more intense solar radiation (Figure 2.86).

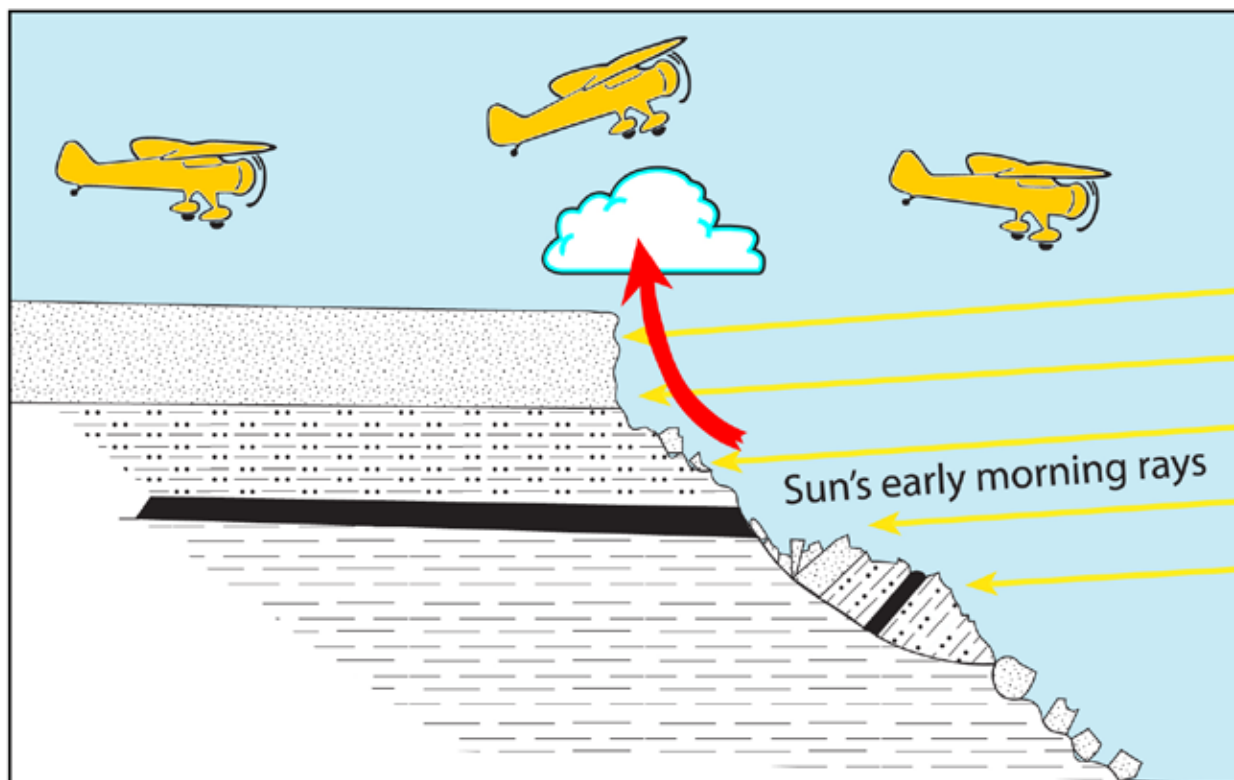


Figure 2.86. As a result of differences in slope angle, adjacent slopes may receive significantly different levels of insolation and, consequently, experience significantly different amounts of heating. In this diagram, based on an actual event that took place at approximately 9:00 AM over the Kaiparowits Plateau in Utah, the cliff is receiving more intense insolation than the plateau above it. Consequently, the cliff heats much more and generates a rising column of warm air that forces the airplane upward when it flies past the cliff. The lifting action on the aircraft can be very abrupt, producing a bumpy ride.

**Aspect** refers to the direction a slope faces. Poleward of 23.5°N, the Sun's rays are never directly overhead. The northern slopes of mountains only receive sunlight in the early morning and late afternoon. As a result of this, the north side of a mountain is cooler and retains more moisture than the south side. The soil on north slopes is more moist because of less intense radiation from the Sun, and therefore less evaporation of soil moisture. Forests are typically more dense on the north side of a mountain than on the south side (Figures 2.87a and 2.87b).

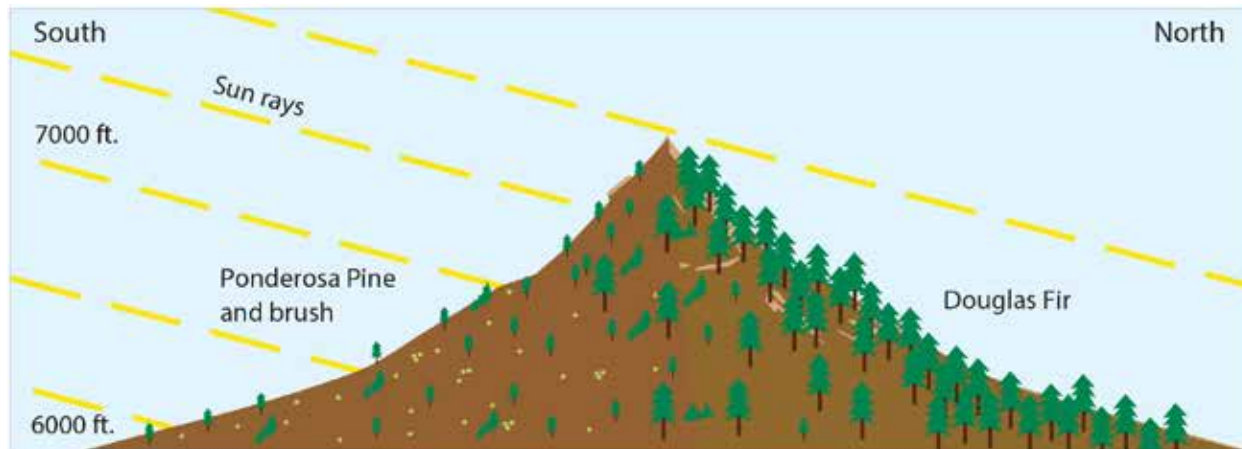


Figure 2.87a. Because the mid-day rays of the Sun never strike the north side of a mountains in areas located north of the Tropic of Cancer, north slopes receive less intense insolation than the south slopes. As a result, north slopes are significantly cooler, and this results in less evaporation of water from the soil and less sublimation of snow cover. With higher levels of soil moisture, trees can grow more readily on the north slopes than on the south slopes. At higher elevations, north slopes are far more likely to have (or have had) glaciers.



Figure 2.87b. The low, oblique aerial photograph of the Colorado Front Range illustrates the vegetation contrast due to aspect on south-facing (left side of hills) and north-facing slopes. View is toward the west. The forested north-facing slopes are mostly in shade, the ground is snow-covered, and the soil-moisture content is high. The grassy, drier south-facing slopes receive more intense solar radiation throughout most of the daylight hours (Source/credit: Dennis I. Netoff).

**Albedo** differences can affect both large regions and local areas (Figure 2.88). Dark-colored surfaces absorb more insolation and so they become warmer than light surfaces. For example, a dark-colored soil would be warmer than a light-colored soil. A dark concrete surface would be warmer than a light one. This effect is why houses in warm climates are usually painted in light colors, such as the pastel colors of Mediterranean homes. In the warm Mediterranean climate, the pastel colors provide a natural means of keeping the house cooler. It is also why many people that live in such climates prefer light-colored clothes. Large, permanent ice sheets such as Greenland and Antarctica are self-maintaining. Even during their respective summers, when long daylight hours promote large dosages of incoming radiation, most of the radiation is reflected back to space (Figure 2.89).

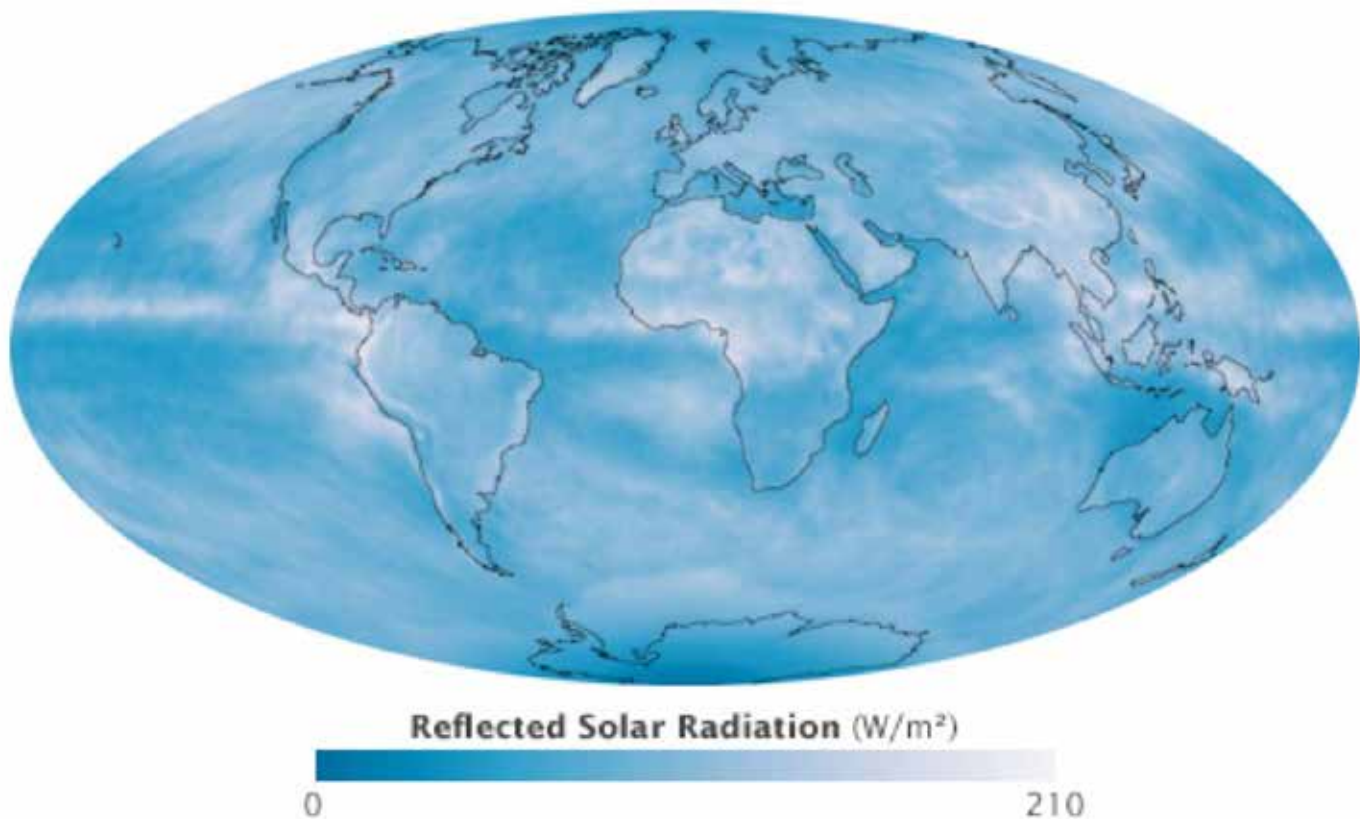


Figure 2.88. The global albedo (reflectivity) in September 2008 shows an interesting band of high albedo along the Equator due to the reflectivity of the widespread cloud cover there. The pale color of the sands and bedrock surfaces in the Sahara Desert of north Africa also show high regional albedo (Source/Credit: CERES, NASA).



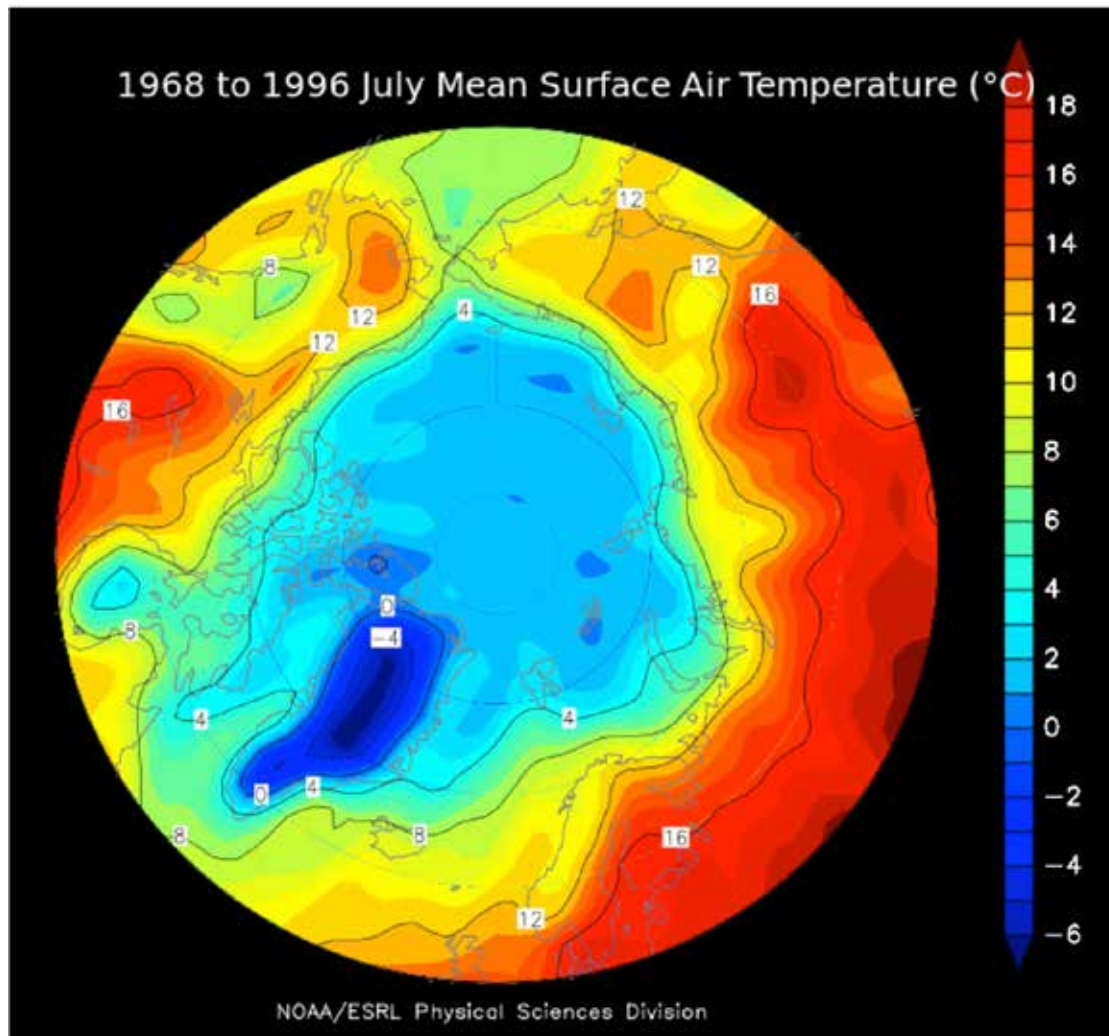


Figure 2.89. Mean surface air temperatures for the month of July are shown on this polar projection. The high albedo and high elevations of the 10,000-foot thick ice sheet keep Greenland frigid year-round (Source/Credit: NOAA and ESRL).

The presence of **vegetation** can also affect temperatures because the evaporation of water from the surface of plant leaves results in evaporative cooling, just as evaporation of moisture (sweat) from our skin results in cooling. In order for the water to evaporate, the water must absorb energy from the leaf and the surrounding air. This transfer of energy cools the air, and the leaves. So, vegetated surfaces are normally cooler than surfaces of bare soil, even when the leaves are darker than the bare soil. The evaporative cooling usually overrides the albedo effect in this instance. Vegetation cover can also significantly intercept incoming sunlight, shading the ground and providing cooler ground-level temperatures, even on the warmest days.

Because half of the mass of the atmosphere lies below 18,500 feet, tall mountain ranges can **impede the movement of air**. For example, northern India is warmer in winter than it would otherwise be because the Himalayas block much of the cold air that would otherwise move southward from the high plateau of Tibet which is located north of the Himalayan Range.

## Temperature: Daily and Seasonal Variations

### The Daily March of Temperature

In the low latitudes, the daily pattern of insolation is straight-forward, regardless of the time of the year. Daylight hours are always very close to 12 hours, and the solar angle is always high. Mid-day and early afternoon temperatures are warm, and nights are mild. The somewhat monotonous daily cycle is interrupted when afternoon thunderstorms provide momentary cooling.

Middle and high latitude insolation cycles show more variability because of the varying daylight hours and changing Sun angle. In general, the higher the latitude, the greater the insolation and temperature variability (Figure 2.90). The most predictable daily insolation cycle is on equinox dates, when there is a 12 hour insolation cycle, peaking at the time when the Sun is highest in the sky, solar noon (Figure 2.91). Predictably, the coolest part of the day is at or just after sunrise. The warmest part of the day, however, does not typically coincide with solar noon, but occurs 2-4 hours later.

Northern Hemisphere				
Latitude	March 21	June 21	Sept. 21	Dec. 21
0	12 hrs	12 h 00m	12 hrs	12h 00m
10	12 hrs	12 h 00m	12 hrs	11h 25m
20	12 hrs	13 h 12m	12 hrs	10h 48m
30	12 hrs	13 h 56m	12 hrs	10h 04m
40	12 hrs	14h 52m	12 hrs	09h 08m
50	12 hrs	16h 18m	12 hrs	07h 42m
60	12 hrs	18h 27m	12 hrs	05h 33m
70	12 hrs	24 hrs	12 hrs	0 hrs
80	12 hrs	24 hrs	12 hrs	0 hrs
90	12 hrs	24 hrs	12 hrs	0 hrs
Latitude	March 21	June 21	Sept. 21	Dec. 21

Figure 2.90. Daylight varies by latitude over the course of the year in the Northern Hemisphere. The Equator always experiences 12 hours of daylight and 12 hours of darkness; but, as distance from the Equator increases, the seasonal variation in daylight and darkness increases.

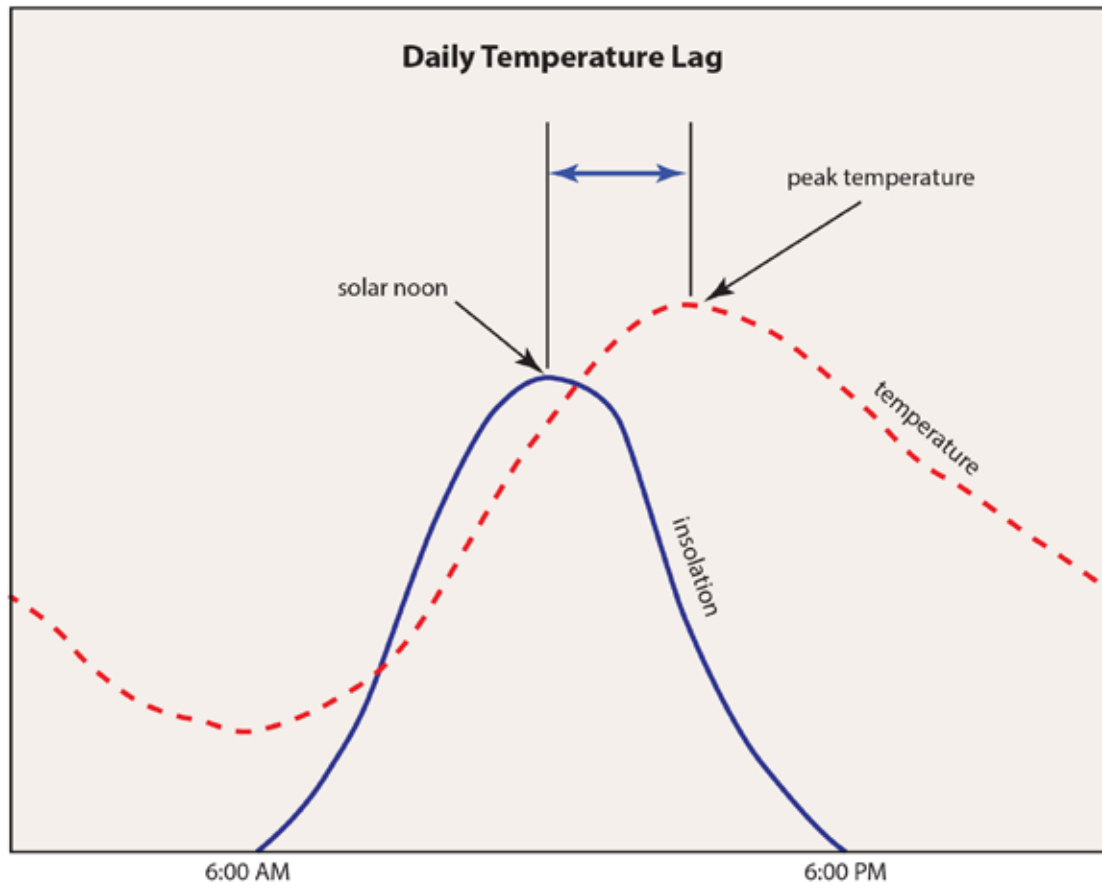


Figure 2.91. A hypothetical pattern of insolation (blue solid line) and temperature (red dashed line) for a mid-latitude location on an equinox date. On either equinox date, neglecting daylight savings, the Sun should rise at 6:00 AM and set at 6:00 PM, so there will be 12 hours of daylight and 12 of night. Lowest temperatures of the 24-hour day are generally at or just after sunrise. Highest temperatures are typically at around 3:00 in the afternoon. The difference in time between maximum insolation and maximum temperature is the daily temperature lag, usually about 3 hours.

The **daily temperature lag** is the time difference between maximum insolation and maximum temperature. The hottest time of the day is typically 2 to 4 hours past solar noon, and the coolest time of day is typically about 20 minutes or so after sunrise. The first rays of light from the Sun in the morning are relatively ineffective because the radiation is spread out and there is a long path of the atmosphere for the rays to travel through.

The delay between maximum insolation and maximum temperature results from the fact that, while the Sun is highest in the sky at solar noon, there is still more incoming energy from the Sun than is lost through terrestrial radiation, so temperatures continue to rise.

The pattern of insolation and temperature for mid-latitude locations can vary considerably from day to day, or even during the course of a day. Changes in cloud cover, wind direction, precipitation type and intensity, and airmasses may significantly alter the idealized daily pattern. The arrival of a mid-day Texas Blue Norther, for example, can drop the temperature 30-60 degrees in the course of a couple hours.

## The Annual March of Temperature

The **annual temperature pattern** of low-elevation continental locations is mainly a function of latitude. Latitude controls the changing pattern of insolation received, reflecting seasonal changes in the intensity of radiation and duration of daylight.

**Low-latitude locations** show very little seasonal change in temperature. Between the Tropic of Cancer and the Tropic of Capricorn, the Sun angle is never lower than  $66.5^\circ$  and the daylight hours are monotonously close to 12 hours year-round. Typical mid-day temperatures are in the upper 80s or low 90s and night-time lows in the low 70s. Mean monthly temperatures hover around  $80^\circ\text{F}$ , and many equatorial locations have an **annual temperature range** (difference between the warmest monthly mean and the coldest monthly mean) of only a few degrees (Figures 2.92a and 2.92b). The phrase *nighttime is the winter of the tropics* seems appropriate. Higher elevations have cooler temperatures. Coastal locations tend to have a lower day-night temperature range.

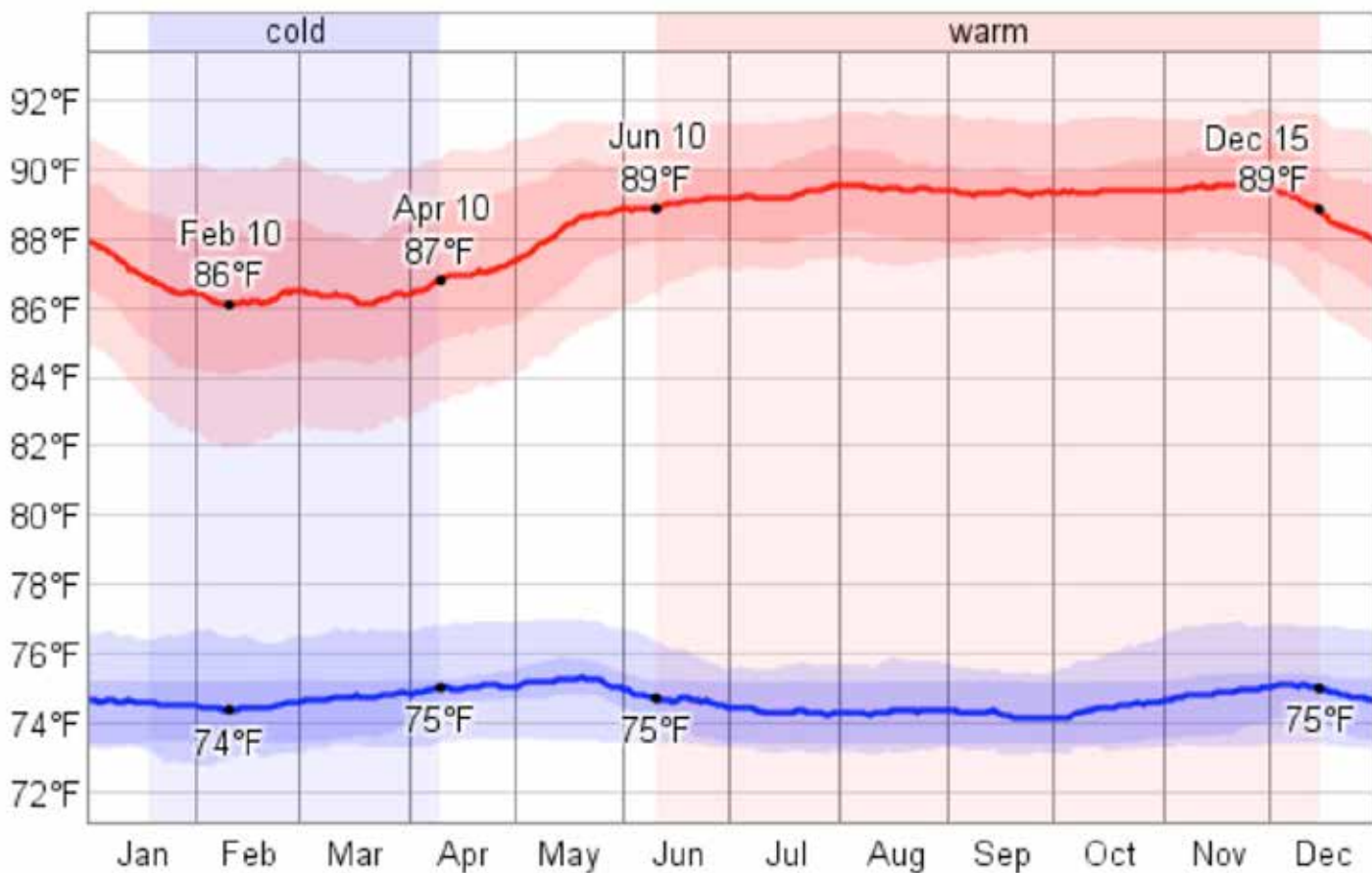


Figure 2.92a. The average high temperatures of the day at Belem ( $2^\circ\text{S}$ ) are typically in the high 80s and there is little variation throughout the year. Average nighttime lows are typically in the mid-70s, and show even less seasonal variation. The solid red and blue lines represent average highs and lows. The color bands represent statistical deviations from the averages (Source/Credit: <https://weatherspark.com/averages/33383/Belem-Para-Brazil>).

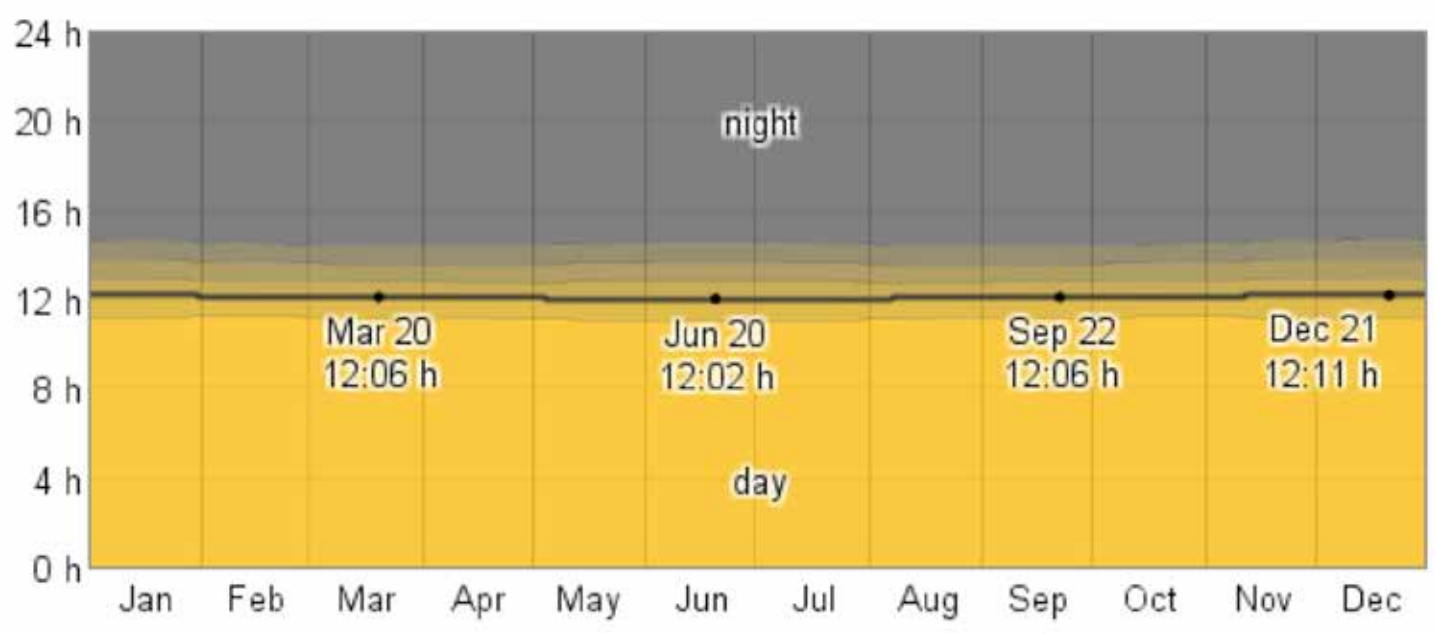


Figure 2.92b. Variations in the length of day and night for Belem, Brazil at 2°S (Source/Credit: <https://weatherspark.com/averages/33383/Belem-Para-Brazil>).

**Annual temperature lag:** Maximum and minimum average temperatures for mid-latitude locations in either hemisphere tend to occur a month or more following the actual solstice dates. Even though the Sun’s rays are slightly less intense and the daylight hours shorter than on the date of the summer solstice, there is still more energy gained by the Earth-atmosphere system in that hemisphere than is lost through re-radiation, so the temperatures continue to climb. Similarly, during the low-Sun season, energy losses by terrestrial radiation are greater than gains for about a month after the winter solstice, so temperatures continue to fall. This phenomenon is referred to as the **annual temperature lag** (Figures 2.93 and 2.94). Coastal locations may experience an annual temperature lag of more than two months because water bodies take longer to heat up and to cool down than landmasses.

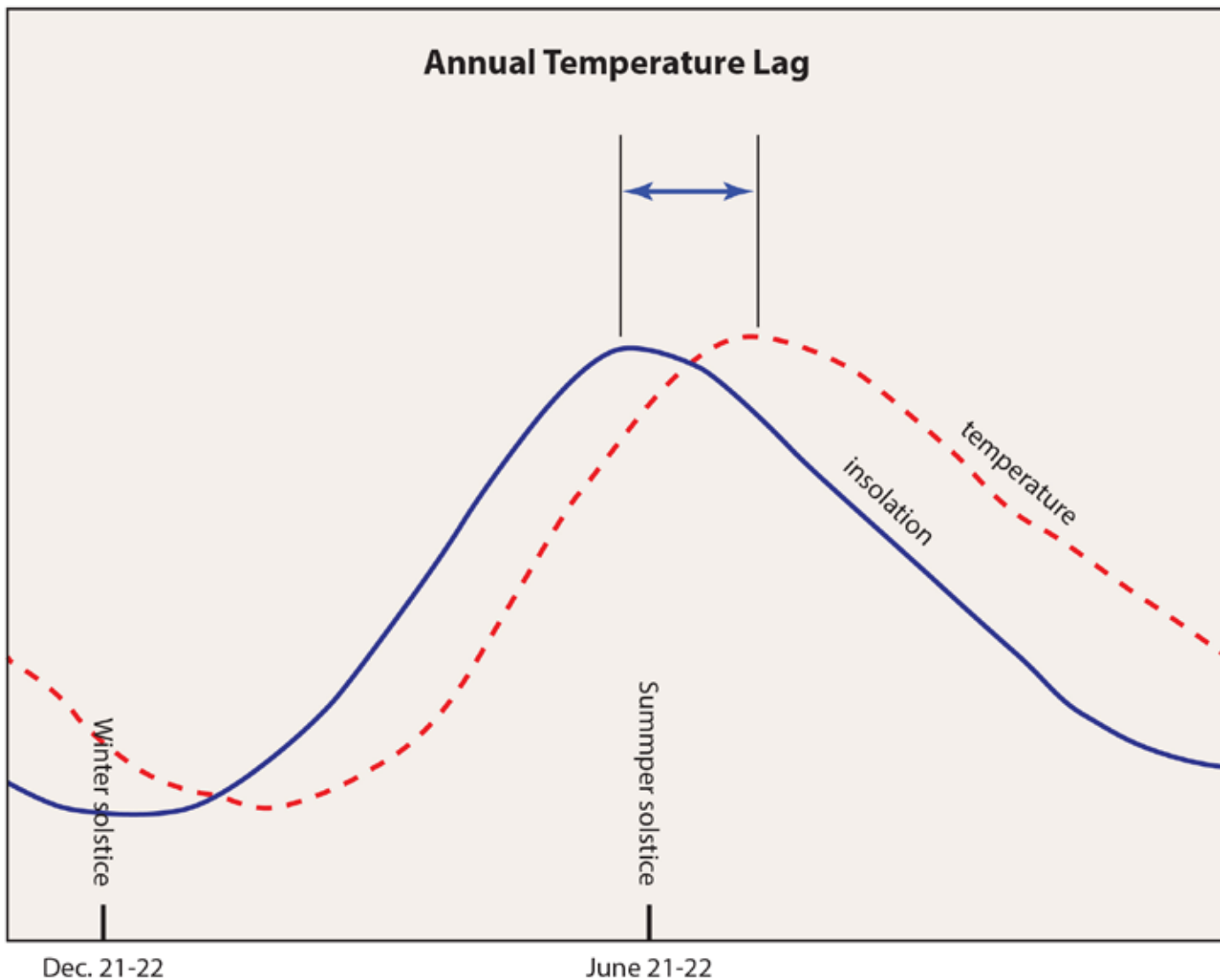


Figure 2.93. A hypothetical pattern of annual insolation (blue solid line) and temperature (red dashed line) for a mid-latitude location. Although the most intense radiation occurs on the summer solstice in late June when the Sun is highest in the sky in the Northern Hemisphere, the warmest temperatures occur one to two months later in either July or August. This delay between maximum insolation and maximum temperature is known as a temperature lag and results from the fact that there is more incoming solar radiation than outgoing terrestrial radiation, creating an energy surplus.

Seasonal Temperature Lag					
City	Latitude (°N)	June (°F)	Warmest Month (°F)	December (°F)	Coldest Month (°F)
Shanghai, China	32	73	80, July & August	49	38, January
Madison, Wisconsin	43	66	70, July	22	17, January
Edmonton, Canada	53	57	63, July	18	7, January
Yakutsk, Russia	62	59	66, July	-41	-46, January

Figure 2.94. Although maximum insolation is received in the Northern Hemisphere on the summer solstice (June 21st), the maximum temperature is usually about one month later in either July or August. This is because an energy surplus accumulates in the atmosphere and reaches a maximum value during these two months. The delay between maximum insolation and maximum temperature is known as a temperature lag.

**Middle and high-latitude locations** show progressively more seasonal change in temperature. Summer temperatures decrease gradually with increasing latitude because the reduced intensity of radiation is partially compensated for longer daylight hours (Figure 2.95). Winter temperatures decrease more rapidly because low intensity of radiation and shorter daylight hours work together to reduce total insolation (Figure 2.96). The highest annual temperature range on Earth, nearly 120°F, is not in Antarctica, but in Siberia at about 68°N. Coastal locations, particularly on the west side of the continents in the Westerly wind belt, tend to have a much lower annual temperature range.

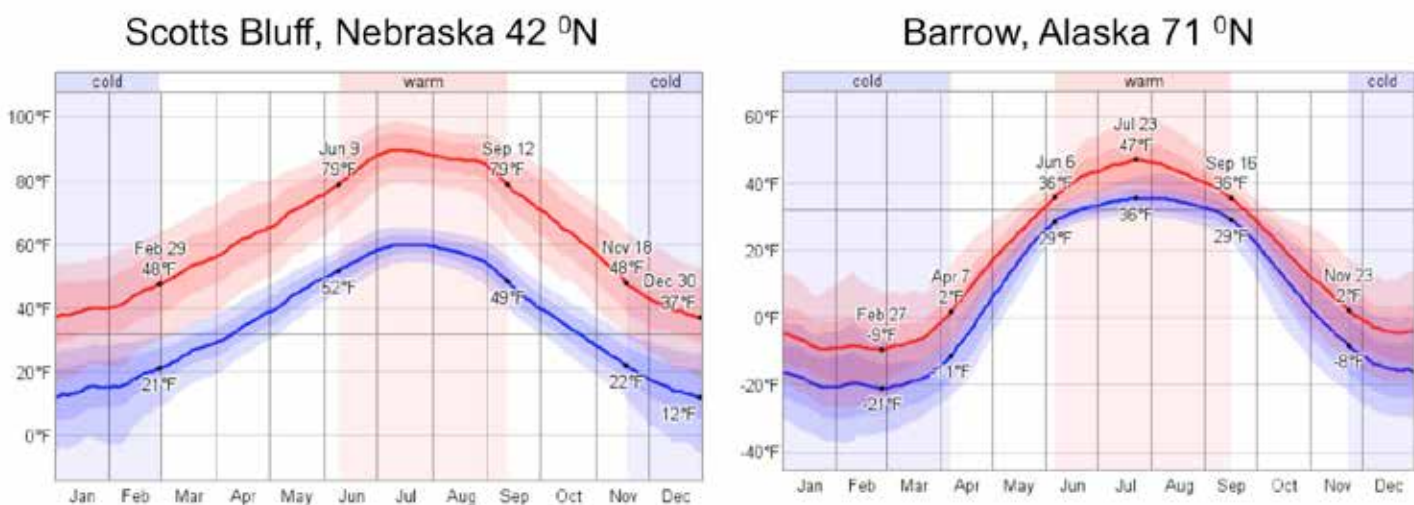
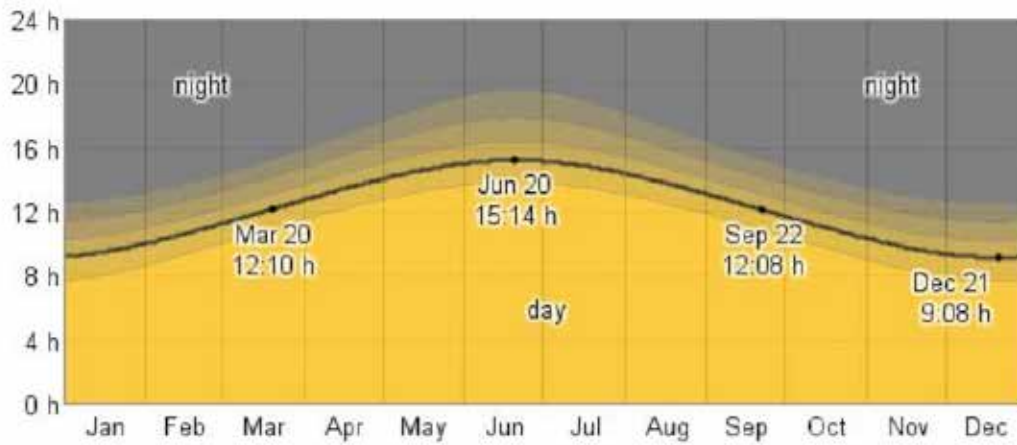
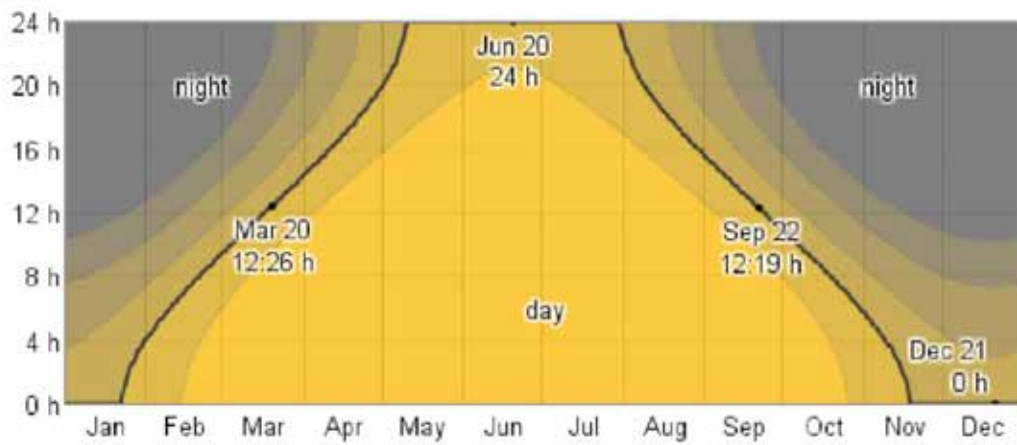


Figure 2.95. Seasonal temperature curves for a mid-latitude and high latitude location (Source/Credit: weatherspark.com).



Scotts Bluff, NE 42°N



Barrow, AK 70°N

Figure 2.96. Seasonal changes in daylight hours for a mid-latitude and high-latitude location. Barrow is beyond the Arctic Circle and has a couple summer months of continuous daylight or twilight (Source/Credit: weatherspark.com).



## Global Energy Budget

**Global heat budget.** The Earth's climate stays in thermal equilibrium if the total amount of incoming energy, mostly in the form of short-wave electromagnetic radiation from the Sun, is balanced by the total amount of outgoing energy, mainly by terrestrial radiation (Figures 2.97a and 2.97b). Imbalances result in a net gain or loss of energy, and the Earth's temperature rises or falls.

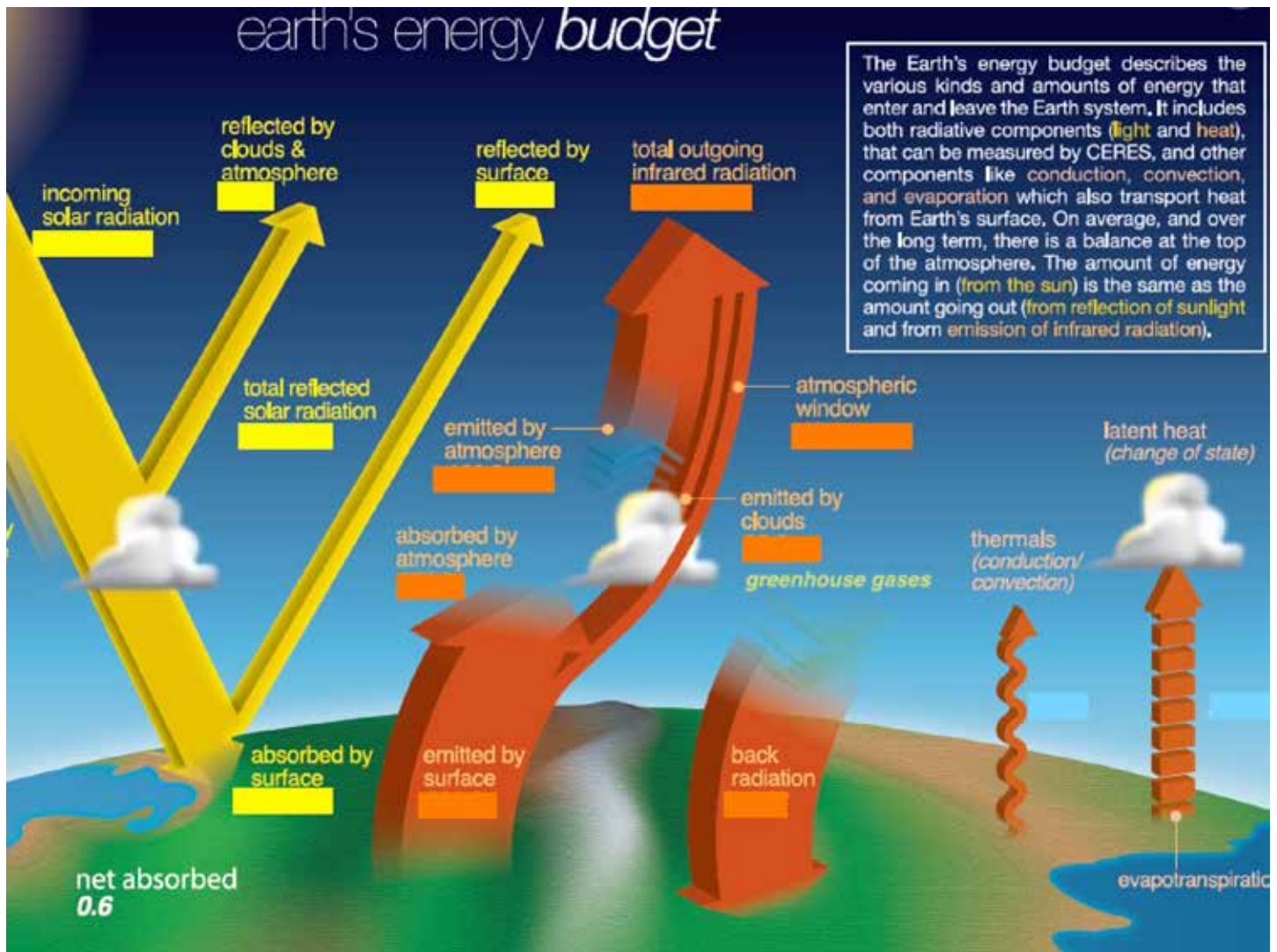


Figure 2.97a. The Earth's climate stays in approximate equilibrium if the total amount of incoming energy, mostly in the form of short-wave electromagnetic radiation from the Sun, is balanced by the total amount of outgoing energy, mainly by terrestrial radiation. Imbalances result in a net gain or loss of energy, and the Earth's temperature rises or falls (Source/Credit: NASA 2010).

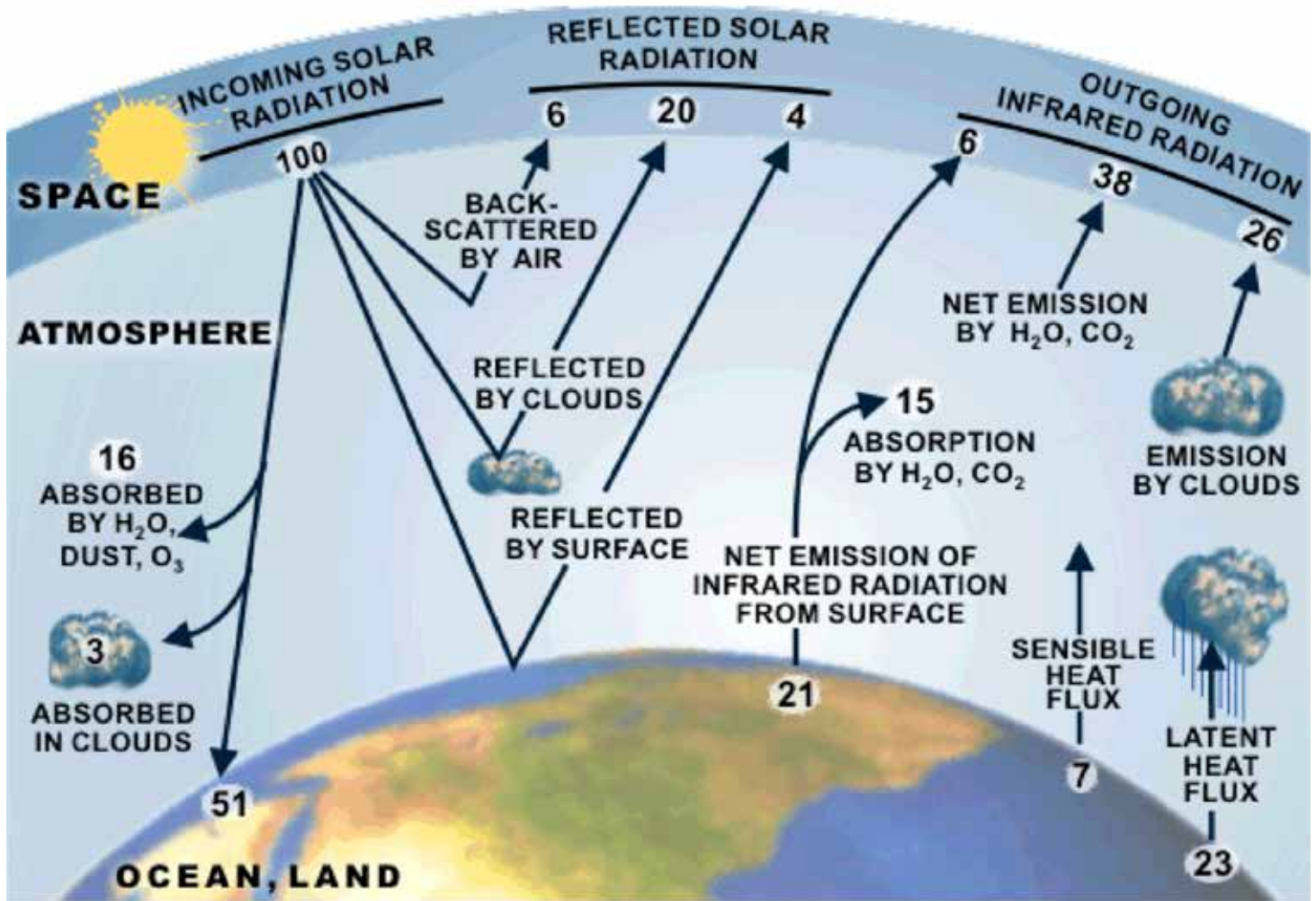


Figure 2.97b. The total incoming radiation in this image is represented by 100 units of energy, and is balanced by the energy reflected, scattered, and emitted as terrestrial radiation to space (Source/Credit: Thermopedia).

**Latitudinal energy budget.** Because the intense rays of the Sun are restricted to lower latitudes, areas located between approximately 37°N and 37°S generally experience an average annual thermal energy surplus. Areas located poleward of 37°N and 37°S tend to experience an average annual energy deficit (Figure 2.98). Without latitudinal heat transport to balance the deficits and surpluses, the lower latitudes would continue to warm year after year, and the higher latitudes would experience long-term cooling. Most of the latitudinal heat transfer is accomplished by latent heat of condensation, ocean currents, and air advection.

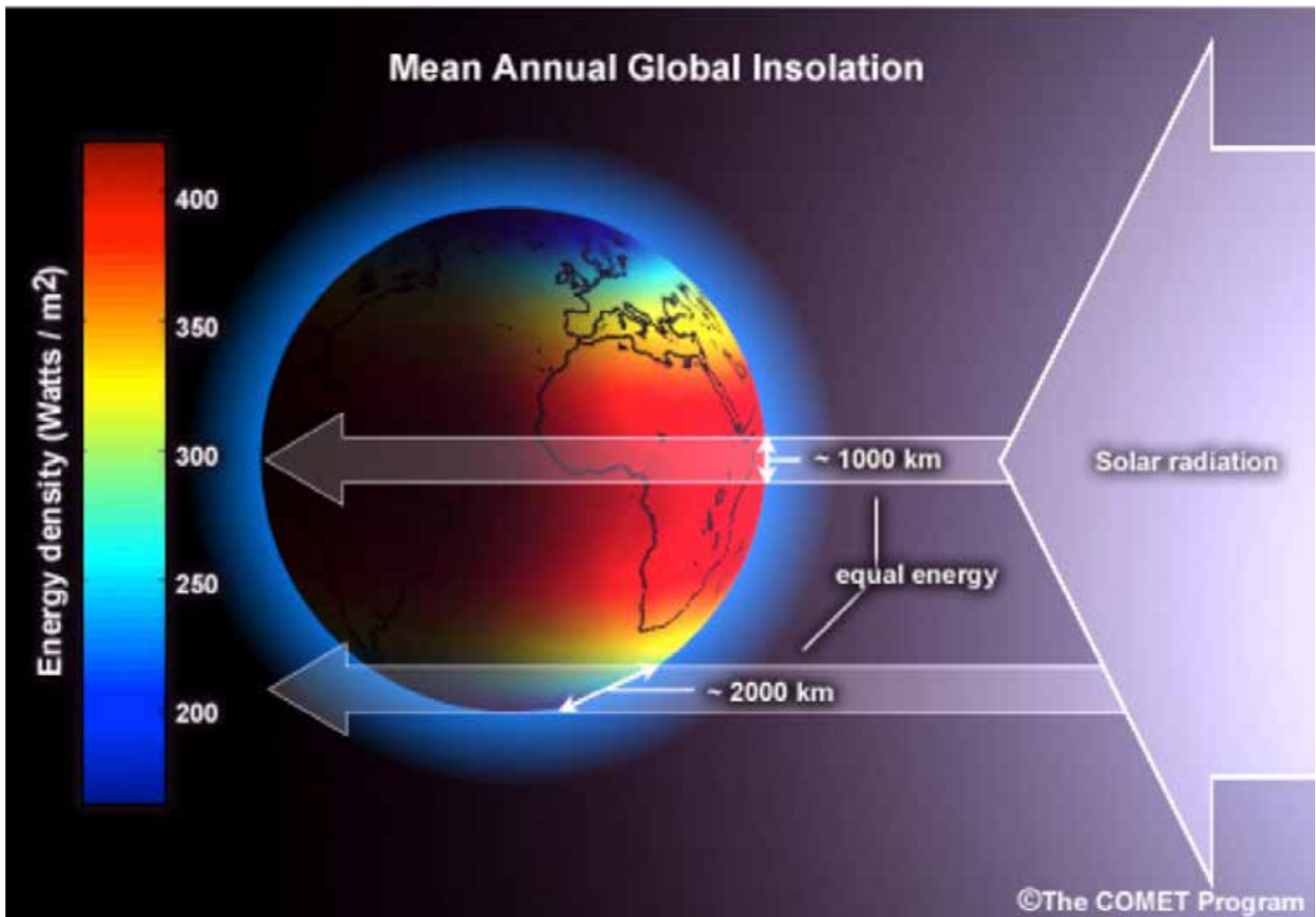


Figure 2.98. Basic Earth-Sun relationships dictate that over the course of the year, low latitudes receive far more insolation than elsewhere. These latitudes have an energy surplus over the course of the year, whereas high latitudes have an energy deficit. The latitudinal balance between the low and high latitudes is achieved mainly through heat transport by wind advection, latent heat of condensation, and ocean currents (Source/Credit: UCAR The COMET Program).

## Temperature Scales and Sensible Temperature

**Temperature** is equal to the average kinetic energy of the molecules. The faster the speed of the molecules in a material, the greater the temperature. The slower the speed of the molecules, the colder the temperature. Temperature is measured with instruments called thermometers. A number of scales have been devised and are currently in use to measure temperature.

The scale used by some scientists is the **Kelvin scale**. On this scale, the coldest temperature possible; i.e., the temperature at which all molecular motion ceases, is given a value of zero. This temperature is called **absolute zero** because it is impossible for anything to be colder than this. Because the Kelvin scale begins with absolute zero, several important properties of this temperature scale result. One of these properties is that the scale **has no negative values**. This is a very significant property because it prevents negative values from being derived when solving problems. For example, by using the Kelvin scale to solve an equation dealing with the rate of energy emission from an object, it is not possible to obtain a negative value for the rate of energy emission.

A second important characteristic of the Kelvin scale is that it is a **ratio scale**. A temperature value of 40K is really twice as hot as a temperature of 20K, a ratio of 2:1. Similarly, 100K is 5 times hotter than 20K. This property also derives from the fact that the Kelvin scale begins at absolute zero.

Two other more commonly used scales are based on the melting point of ice and the boiling point of water which means that they are clearly related to the hydrologic cycle. On the **Celsius scale** (which is used throughout most of the world), the freezing point of water is 0°C and the boiling point is 100°C. Absolute zero has a value of minus 273°C. Because this is a negative number, the Celsius scale is not a ratio scale and therefore cannot be used in many types of energy calculations.

One similarity between the Celsius and Kelvin scale is that the size of a degree is the same. One degree on the Celsius scale equals the same amount of energy as one unit on the Kelvin scale. This means that you can convert from the Celsius Scale to the Kelvin scale simply by adding 273 degrees. For example, 0°C = 273K ( $0^\circ + 273^\circ = 273\text{K}$ ). Conversely, you can convert from Kelvin to Celsius by subtracting 273 degrees. For example, 0K = -273°C ( $0\text{K} - 273^\circ = -273^\circ\text{C}$ ).

On the **Fahrenheit scale** (which is used in the United States), the freezing point of water is 32°F and the boiling point is 212°F. Again, this is not a ratio scale because absolute zero on this scale is -459°F. Notice that, on the Fahrenheit scale, there are 180 degrees between the freezing point and boiling point of water, whereas on the Kelvin scale, there are only 100 units. A Celsius degree is 1.8 times the size of a Fahrenheit degree ( $180^\circ/100^\circ = 1.8^\circ$ ). Given this, and

the fact that the freezing point of water is 32° on the Fahrenheit scale, and 0° on the Celsius scale, it is possible to convert from Fahrenheit to Celsius, or vice versa, using the following formulas. Note that the examples are based on the boiling point of water.

**Fahrenheit to Celsius:**  $(^{\circ}\text{F} - 32^{\circ}) / 1.8 = ^{\circ}\text{C}$

Example:  $(212^{\circ}\text{F} - 32^{\circ}) / 1.8 = 100^{\circ}\text{C}$

**Celsius to Fahrenheit:**  $(^{\circ}\text{C} \times 1.8) + 32^{\circ} = ^{\circ}\text{F}$

Example:  $(100^{\circ}\text{C} \times 1.8) + 32^{\circ} = 212^{\circ}\text{F}$

The relationships between the three scales are shown in [Figure 2.99](#).

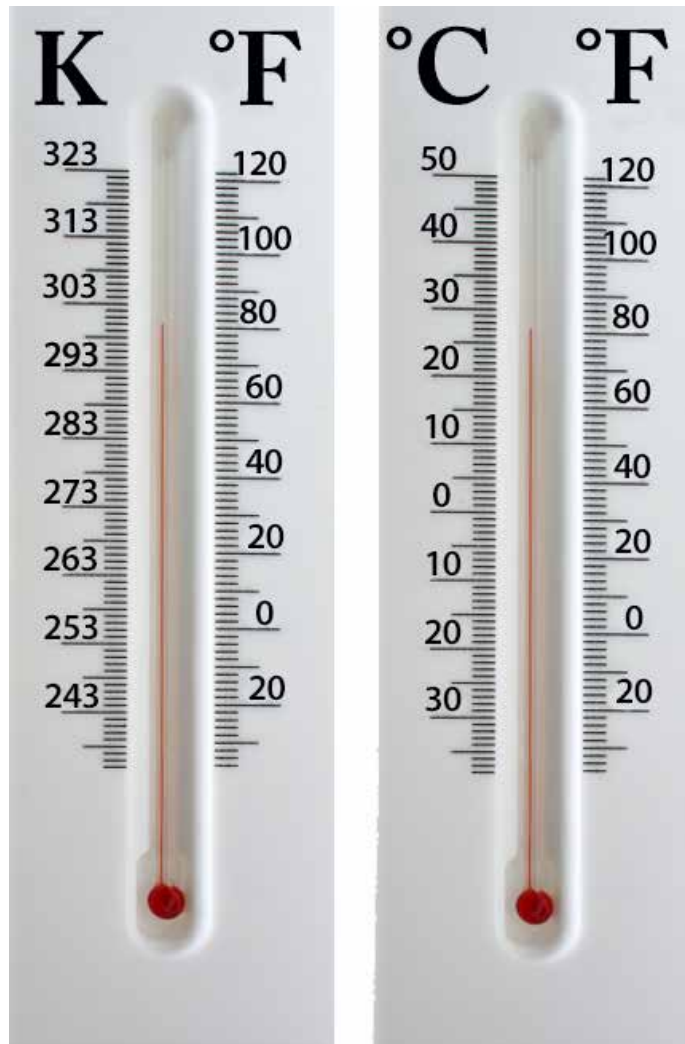


*Figure 2.99. These thermometers show the relationships between the three different temperature scales. Because the Kelvin scale begins at absolute zero, a temperature of 80°F corresponds to a much higher temperature value of 300K on the Kelvin Scale. The size of a Kelvin and Celsius degree are equal, and are 1.8 times as large as the Fahrenheit degree. Consequently, a total of 100 degrees separates the freezing point and boiling point of water on the Kelvin and Celsius scales, but 180 degrees separate these temperatures on the Fahrenheit scale.*

**Sensible temperature** is the sensation of heat energy on your skin, as contrasted with actual air temperature that is measured with a thermometer. Sensible temperature is affected by not only the air temperature, but also the relative humidity, wind speed and exposure to solar radiation.

**Wind chill** is a form of sensible temperature and is a measurement that takes into account the effect of wind speed on the rate of heat loss from the body. The temperature that we sense is related to the balance between the rate of heat gain and heat loss from our bodies. The rate of heat loss from our bodies varies as a function of many factors, such as wind speed and the moisture content of our clothes. The faster the wind blows, the more rapidly water evaporates from our bodies and, because evaporation causes cooling, windy days normally make us feel cooler. Also, because water conducts heat 20 times faster than the air, wet clothes can result in rapid loss of heat. So, even if the air temperature is not *cold*, we may feel cold and may even develop hypothermia if our clothes remain wet long enough. For example, the weather forecaster may say that the air temperature is 45°F, but the wind chill temperature is 34°F. Because of the cooling effect of the wind on exposed skin, the rate of heat loss from your body is the same as it would be if the temperature were 34°F.

The National Weather Service has developed one of many wind chill charts that have been devised to warn of the dangers of low temperatures and strong winds (Figure 2.100). The lowest wind chill equivalent temperatures on Earth occur in Antarctica where a combination of violent katabatic winds and severe low temperatures combine to make dangerous conditions (Figure 2.101).


Wind Chill Chart

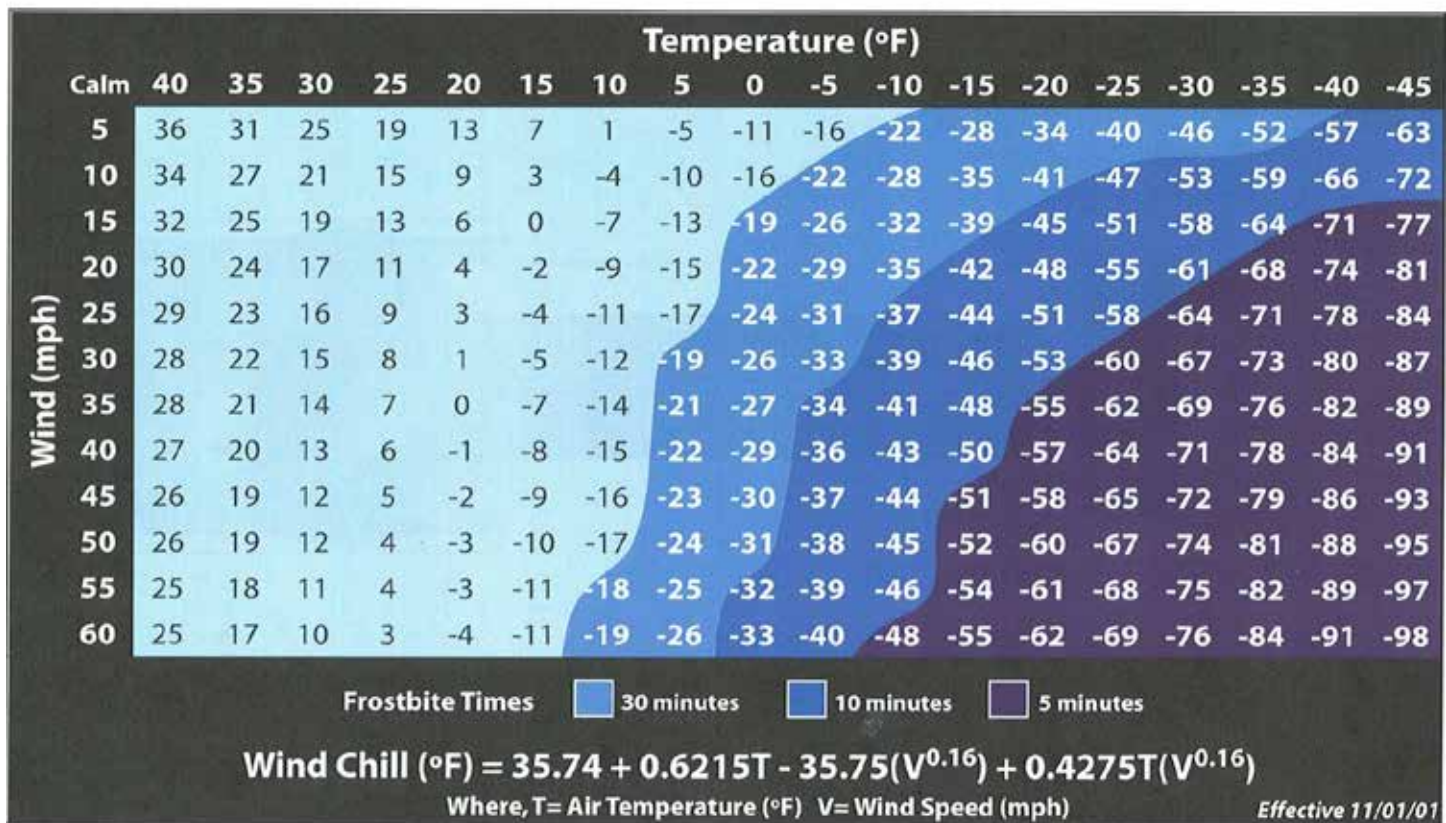



Figure 2.100. The wind chill chart combines wind speed and temperature to indicate different general warning levels for human discomfort and susceptibility to frostbite (Source/Credit: NOAA and NWS).



*Figure 2.101. Image of the eastern coast of the Antarctic Peninsula during a windstorm. Wind chill equivalent temperatures in Antarctica are the lowest on Earth, and can reach minus 200°F. For example, the wind chill equivalent temperature at an actual temperature of minus 80°F and a wind velocity of 80 mph calculates at minus 174°F. Exposed flesh will freeze in under a minute (Source/Credit: Alfred Wegner Institute, photo by W. Arntz).*

In addition to the effects of wind on the sensation of temperature, humidity also has a big effect on what we experience. Cold, wet air feels colder than cold, dry air at the same temperature. This is because water conducts heat faster than air; consequently, you lose heat energy from your body faster when the air is damp. So, if the air is damp, your clothes are wet, and it's windy, you'll be especially miserable.



**Heat stress.** Excessive heat can be just as dangerous as excessive cold, resulting in heat disorders ranging from fatigue to nausea, heat stroke, and ultimately death. High temperatures in combination with high humidities are the most hazardous. The heat stress index or simply heat index (Figure 2.102) combines relative humidity and temperature to indicate different general warning levels for human discomfort and susceptibility to heat disorders.

## NOAA's National Weather Service

### Heat Index

Temperature (°F)

		80	82	84	86	88	90	92	94	96	98	100	102	104	106	108	110	
Relative Humidity (%)	40	80	81	83	85	88	91	94	97	101	105	109	114	119	124	130	136	
	45	80	82	84	87	89	93	96	100	104	109	114	119	124	130	137		
	50	81	83	85	88	91	95	99	103	108	113	118	124	131	137			
	55	81	84	86	89	93	97	101	106	112	117	124	130	137				
	60	82	84	88	91	95	100	105	110	116	123	129	137					
	65	82	85	89	93	98	103	108	114	121	128	136						
	70	83	86	90	95	100	105	112	119	126	134							
	75	84	88	92	97	103	109	116	124	132								
	80	84	89	94	100	106	113	121	129									
	85	85	90	96	102	110	117	126	135									
	90	86	91	98	105	113	122	131										
	95	86	93	100	108	117	127											
100	87	95	103	112	121	132												

#### Likelihood of Heat Disorders with Prolonged Exposure or Strenuous Activity

- Caution     
  Extreme Caution     
  Danger     
  Extreme Danger

Figure 2.102. The heat stress index combines relative humidity and temperature to indicate different general warning levels for human discomfort and susceptibility to heat disorders (Source/Credit: NOAA).

## Chapter 3

# Air Pressure and Winds

Temperature is important not only because it affects almost every phase of everyday life, but also because it directly affects air pressure in the atmosphere, which in turn causes the wind to blow. Temperature differences are the ultimate driving force of the wind. While it is true that other factors contribute to air pressure differences, air temperature plays the most fundamental role.

### *Temperature and Pressure*

Because the atmosphere is composed of particulates and gases that all have mass and are drawn by the Earth's gravity, air has weight. At sea level, the average weight of the air is 14.7 pounds per square inch (psi). People don't feel the weight of the atmosphere because the pressure of the air is balanced by an outward-directed force of fluids in our bodies.

## Measuring Atmospheric Pressure

The instrument used to measure atmospheric pressure, the barometer, was invented in 1644 by the Italian scientist Torricelli. His work was based on earlier work by Galileo Galilei who observed that when a tube of fluid is inverted into a dish of the same fluid, the fluid level in the tube does not fall to the level of the fluid in the dish, but equilibrates at a higher level. The weight of the fluid in the tube is balanced by an equal force acting on the fluid in the dish — air pressure (Figure 3.1).

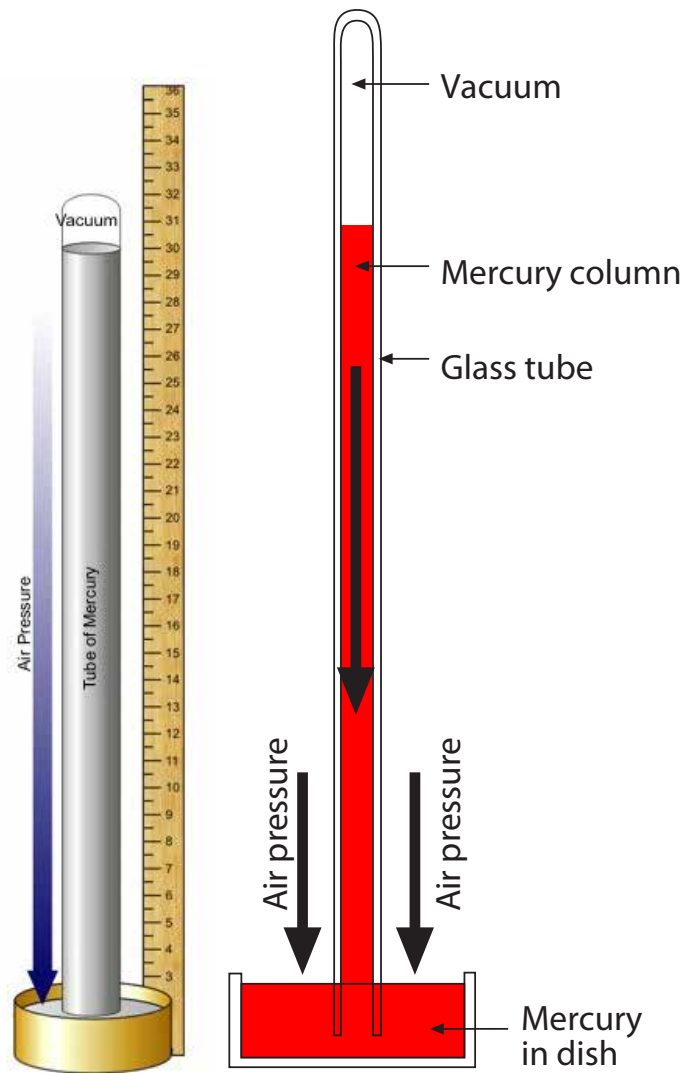


Figure 3.1. A traditional mercury barometer consists of a glass tube, the open end of which is placed in a container of mercury. The force exerted by the mercury in the tube (long arrow) is balanced by the force exerted by the atmosphere (short arrows). As the pressure changes so does the height of the column of mercury.

In some experiments, Torricelli used the dense fluid mercury (Hg) and found that at sea level, on average, the level of mercury in the tube stood about 29.92 inches above that in the dish. That instrument would become known as the **mercurial barometer**, and 29.92 inches of Hg is referred to as **standard sea level pressure**.

## Units of Barometric Pressure

Another common expression of atmospheric pressure is millibars. A **millibar** is equal to the amount of force required to raise a column of mercury 0.075 centimeters. So, **standard sea level pressure is 14.7 psi, which is equivalent to 29.92" Hg, which is equal to 1013.2 mb.**

Extreme variations in surface atmospheric pressure range from **a low of 870 mb**, which was associated with Typhoon Tip in 1979, to a **high of 1084 mb**, which occurred in Siberia during the winter of 1968. Under *normal conditions*, pressure variations are seldom outside the range of 950 to 1050 mb.

Note that the lowest pressure ever recorded was in a typhoon, which forms over warm, moist water, and the highest pressure ever recorded was in the extremely cold, dry continental interior of Siberia during winter. Clearly, there is a relationship between temperature and pressure – and between atmospheric moisture and pressure. In addition to temperature and moisture, other factors may cause variations in air pressure.

## Vertical Variations in Air Pressure

Air pressure is not constant. It varies vertically, horizontally and with time. Air pressure measured at the base and peak of a mountain on the same day shows a dramatic pressure drop with increasing elevation. Pressure decreases rapidly with elevation, so that at a mere 18,000 feet or so, about half the mass of the atmosphere lies below this elevation. Near sea level, compression of air from the cumulative weight of the overlying air causes the air molecules to be close together, and therefore dense. Therefore, as with pressure, density decreases rapidly with height (Figure 3.2). Twenty miles above the surface, air pressure is a mere one percent of its sea level value.

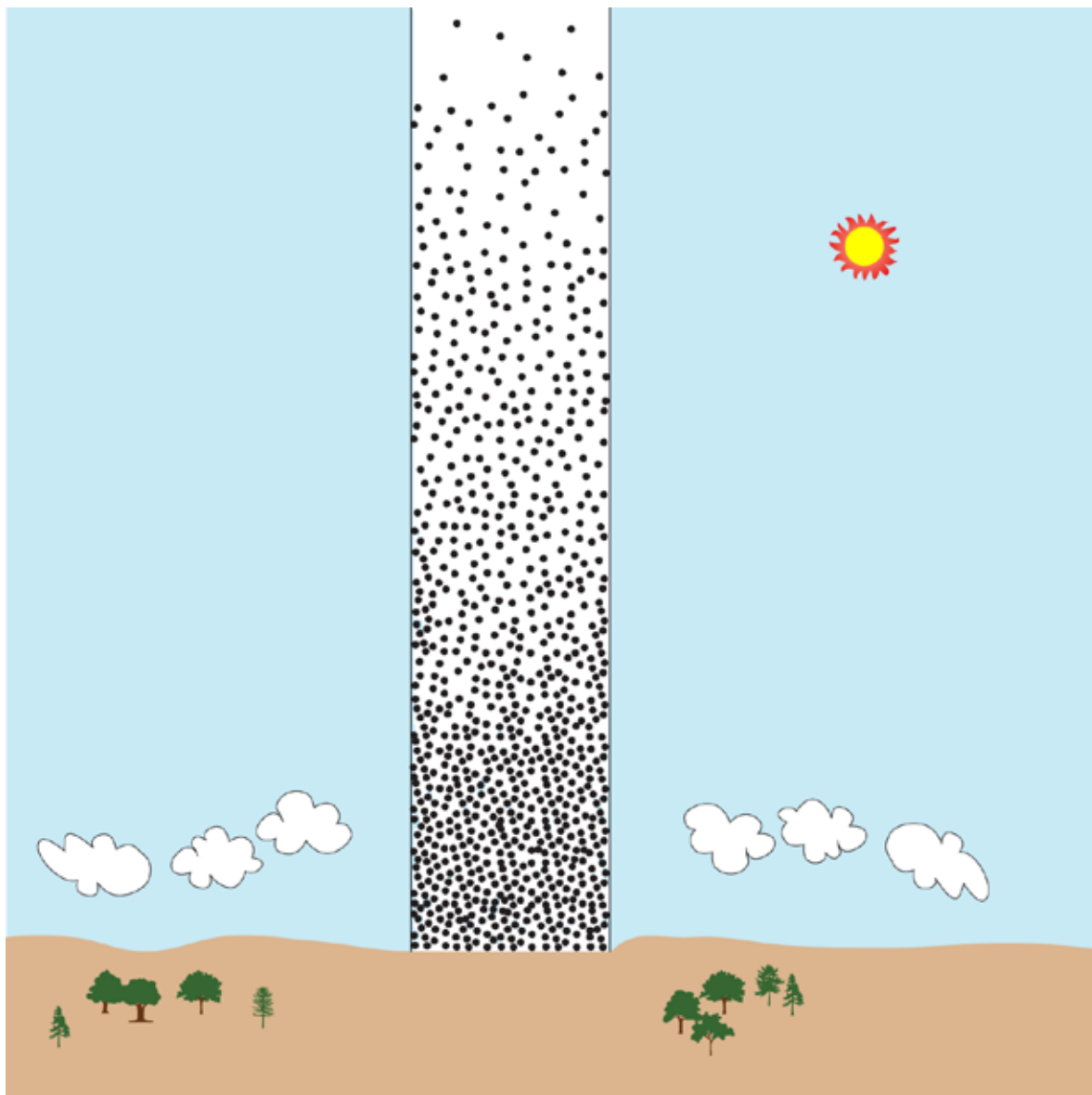


Figure 3.2. Air density decreases with altitude. In fact, it decreases by half for each 3.5-mile (5 km) increase in altitude. This rapid vertical change in pressure with altitude is vastly greater than any horizontal change in pressure that occurs horizontally at a given altitude.

## Horizontal Variations in Pressure

Horizontal variations in pressure are responsible for the horizontal movement of air — what is commonly called wind. Variations in pressure on a horizontal plane are typically due to a combination of thermal and dynamic factors. Temperature has a major effect on air pressure because it controls air density. As air temperature rises, air molecules move faster and become more widely spaced, creating lower air density and therefore lower air pressure. Conversely, as air temperature falls, the air molecules move more slowly and this allows them to become more densely packed, creating higher pressure. Pressure fields that can be demonstrated to be caused by temperature-driven density differences are said to be **thermally-induced pressure fields**.

This relationship between air temperature and air density is somewhat analogous to a volume of space occupied by thousands of ping pong balls. As the air temperature increases, the ping pong balls begin to move around faster and faster. As their speed increases, so does the force of the collision between the balls. As a result, the balls spread further apart, and this decreases their density. Conversely, as the temperature decreases, the speed of the balls decreases and so the force of collision diminishes. As a result, the balls become more closely spaced and more densely packed (Figures 3.3 and 3.4).

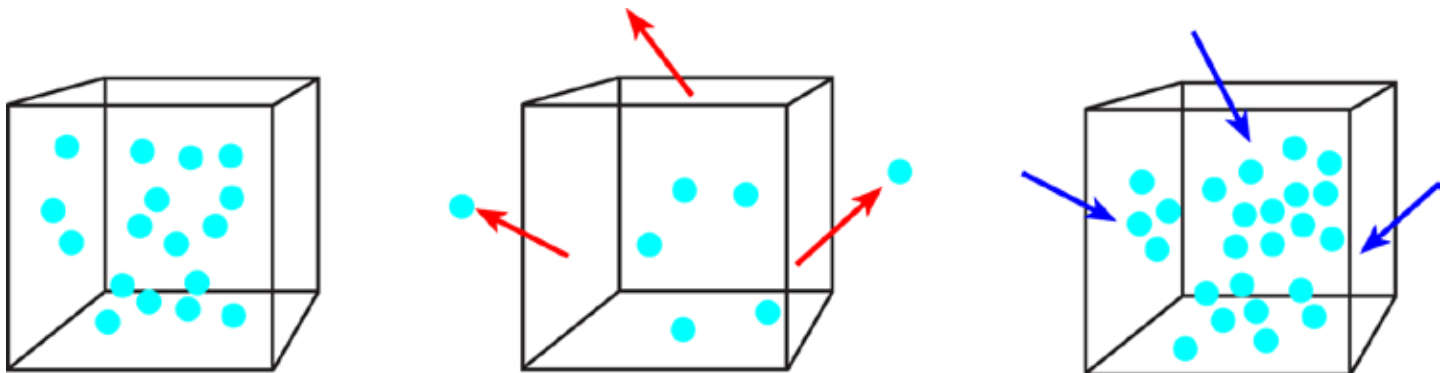


Figure 3.3. Temperature is a measure of the speed of the molecules in a substance. The faster the molecules are moving, the higher the temperature. As the temperature and speed of the molecules increases (middle box), the molecules collide with greater energy, and this forces them to move further apart. As the spacing between the molecules increases, the density decreases because there are fewer molecules in a given volume of air. Consequently, the air weighs less and the air pressure decreases. Conversely, as the temperature decreases (right box), the speed of the molecules also decreases, and so they do not collide with as much intensity. As a result, more molecules can occur in a given volume of air; therefore, the air weighs more and its pressure increases.

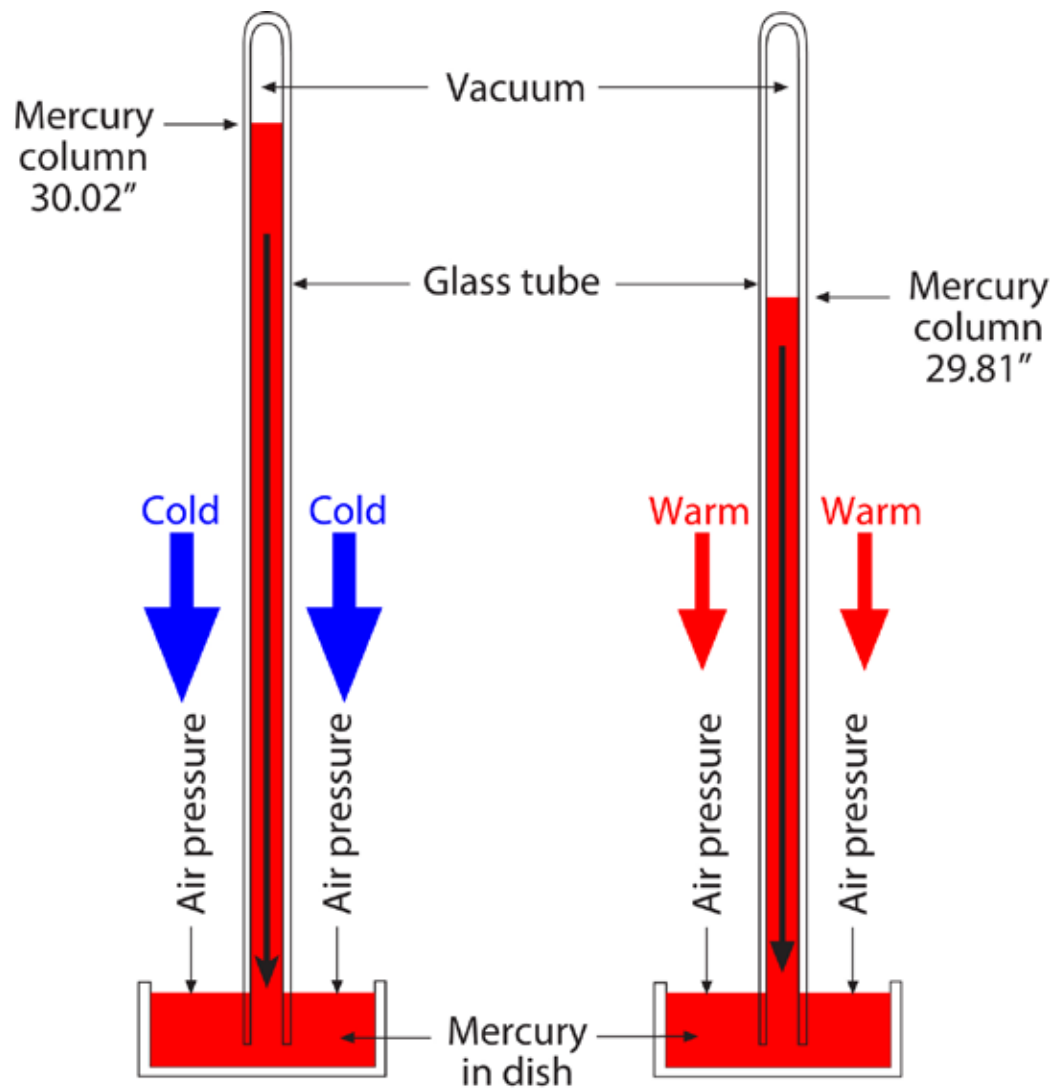


Figure 3.4. When the temperature drops, the air becomes more dense and the pressure increases. In the example shown on the left, the colder air has resulted in a pressure of 30.02 inches of mercury. In contrast, when the temperature increases, as shown on the right, the air pressures decreases. In this example, the pressure has dropped to 29.81 inches.

When a parcel of air is locally heated and becomes less dense than the adjacent air at that level, there is a buoyant upward force on the parcel, causing it to rise. Pressure variations on a horizontal plane can therefore initiate vertical air movement. Similarly, air aloft that is cooler and denser than the adjacent air at that level has negative buoyancy and subsides. The relationship between temperature and density has implications for aeronautics. The Wright brothers made their first flight at Kitty Hawk on a cold December day in 1903. Because the air was cold, it was more dense and provided much needed lift for their new, heavier-than-air flying machine. When the Wright brothers attempted a second flight later the next year when it was warmer, they were initially unsuccessful because the warmer, less dense air did not provide enough lift. Even modern planes have to deal with this fact. On hot days, planes must accelerate to higher speeds in order to get airborne.

A second mechanism for changing pressure on a horizontal plane is from either *forced uplift* or *forced subsidence*. Conditions aloft can cause air molecules to be forced closer together in a process termed **upper-level convergence**. Upper-level convergence typically causes forced subsidence of air, and if the air molecules are fed to the surface faster than they can escape, air density goes up, and the pressure rises, causing a **dynamically-induced pressure field** (Figure 3.5).

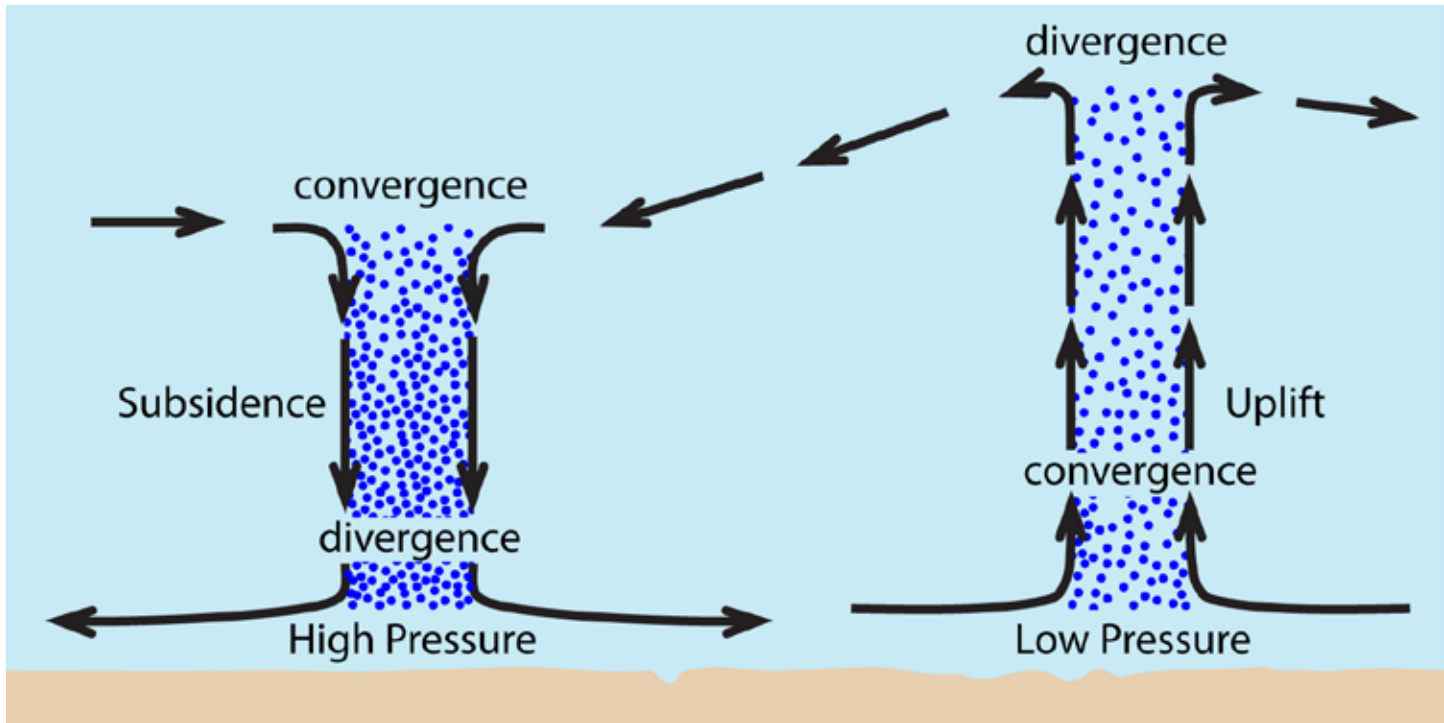


Figure 3.5. When air converges at high altitude in the troposphere (left diagram), it can increase the amount of air in a column of air extending downward to the surface below the zone of upper-level convergence, assuming that air flowing out of the base of the column occurs more slowly than air flows into the top of the column. When this happens, the air pressure at the surface increases. Conversely, when upper-level divergence occurs (right diagram), air is removed from the column extending to the surface, and this decreases the pressure, assuming that the rate of surface convergence is less than the rate of upper-level divergence. Upper-level divergence is a very important process in the formation of severe storms (Source/Credit: modified from Dennis I. Netoff and Ava Fujimoto-Strait, *Weather & Climate Lab Manual*).

Conversely, upper-level divergence favors forced uplift by removing air molecules from the surface and creating low pressure on the surface. In reality, pressure fields on the surface can be a combination of thermally and dynamically-induced causes, so that high pressure systems can be either *cold highs* or *warm highs*, and low pressure systems can be *cold lows* or *warm lows*.



## Diabatic and Adiabatic Changes in Temperature

Air temperature can be changed as a result of both diabatic and adiabatic processes. **Diabatic** processes are associated with either the addition or removal of heat energy from the air by conduction, convection, radiation and phase changes. These are the *common sense* mechanisms of temperature change because we all understand that things warm up if energy is added to them, and things cool off when they lose energy. However, air can warm and cool even if no energy is gained or lost from the air. This type of change in temperature is referred to as an **adiabatic** temperature change.

The prefix *a* in the word *adiabatic* means *without* and refers to fact that air can warm or cool without the addition or removal of heat energy by conduction, convection or radiation. This can occur because, when a gas expands, it cools, and when it is compressed, it heats. The energy associated with expansion results in a decrease in temperature – even though the gas has not lost any total energy. Some of the thermal energy has been converted to kinetic energy. Conversely, the compression of a gas causes it to warm up, even though no energy was added to it. **Compression causes heating and expansion causes cooling.**

If a parcel of air near the surface heats up and begins to rise, it will experience temperature changes due to expansion. As the parcel rises, the air pressure exerted by the surrounding (ambient) air decreases because there is less air at a higher altitude. In response to the decrease in ambient air pressure, the parcel begins to expand. However, when an air parcel expands, the air that comprises the parcel cools off. This is exactly what happens when you press the button on a can of compressed air or an aerosol spray can. As the compressed gas in the can is released, it expands and rapidly cools. **This process is responsible for cooling the temperature of rising air, forming clouds, and eventually producing most forms of precipitation.**

The rate at which an unsaturated parcel of air is cooled is known as the **dry adiabatic lapse rate** and it has a value of minus 5.5°F per 1000-foot increase in altitude (minus 5.5°F/1000 feet). In other words, for every one thousand feet the air rises, it cools 5.5°F. Note that this is greater than the normal environmental lapse rate, which applies to the *stationary, ambient air* and which averages 3.5°F per 1000 feet. Whenever unsaturated air is rising, it cools at the dry adiabatic lapse rate, regardless of the temperature of the surrounding air. When an air parcel sinks, it is compressed because the density of the surrounding air increases. As the air parcel is compressed, its temperature increases because the air molecules are forced closer together causing them to collide more frequently. As the frequency of collisions increases, so does the speed of the molecules. Recall that temperature is defined as the average speed of the molecules. The rate at which air is warmed by compression is exactly the same as the rate at which it cools by expansion, *plus* 5.5°F/1000 feet. If air subsides (sinks) 21,120 feet (just 4 miles),

it heats 116°F.

Compressional heating of subsiding air helps to explain many meteorological and climatological phenomena, such as the formation of Santa Ana and chinook wind systems and the occurrence of deserts.

## Temperature vs Heat

**Temperature** is the *average* kinetic energy of the molecules in a substance. Because kinetic energy is the energy of motion, the higher the temperature, the greater the speed of motion of molecules and the greater the average kinetic energy. **Heat**, on the other hand, is defined as the *total* kinetic energy of the molecules in a substance. To illustrate the difference, consider a cup of water at 70°F and a swimming pool at 70°F. Both have the same temperature, so they both have the same average kinetic energy. However, the swimming pool has a much greater heat content because it has far more molecules in it and therefore, far more total kinetic energy. Because it has more total energy, the pool would take much longer to cool off because it would have to lose much more heat energy in order to do so. The Earth's oceans are vast reservoirs of heat energy, and therefore play a very substantial role in regulating the temperature of the atmosphere. Because the water is so much denser than the air, it stores tremendous quantities of heat energy.

This difference between temperature and heat also explains why an astronaut can spacewalk without becoming overheated. The temperature of the thermosphere (the upper layer) is around 2000°F. However, astronauts who spacewalk for long periods at about this altitude sometimes find that their fingers become numb from the cold (Figure 3.6).



Figure 3.6. Astronauts would freeze if exposed to space, even though the temperature of the extremely rarified layer of the atmosphere and near-Earth environment may exceed 2000°F. This is because the air density is so low that it contains very little heat energy, in spite of the fact that the molecules are moving at very high speeds and therefore have a high temperature (Source/Credit: NASA).

And, in fact, the astronauts would freeze quickly in this layer if left exposed. The air at this altitude is so rarefied that the heat content is very low. But, because the atmosphere is in direct contact with solar radiation, it is also very hot. The notion that you could freeze surrounded by a medium that is heated to 2000°F seems paradoxical — but only if one doesn't distinguish temperature from heat; i.e., average kinetic energy from total kinetic energy.

## Pressure and Moisture

Atmospheric moisture also influences air pressure. This is because **moist air actually weighs less than dry air** and is therefore associated with low pressure. Intuitively, one would think that air that contains water would be heavier than dry air, but this is not the case. Air is a mixture of gases, and when the amount of water in a given volume of air increases, other gases are *displaced* from that volume. In effect, the water vapor molecules replace other molecules in the volume of air. Because the water vapor molecule ( $H_2O$ ) is dominated by the lightest of all atoms, hydrogen, the molecule weighs considerably less than the nitrogen ( $N_2$ ) or oxygen ( $O_2$ ) molecules that it replaces, so the overall density of the air is less. Air with a high water vapor content weighs less than the same volume of dry air at the same temperature. Air with high water vapor content has a tendency to rise, and air with a low water vapor content has a tendency to sink.

## Wind Direction and Velocity

Stationary objects (including air molecules) are set in motion because there is a force applied to them. The **pressure gradient force** is the fundamental driving force that causes the wind.

### The Pressure Gradient Force

Wind, like water, flows downhill; i.e., it flows from regions of high pressure (high density) to regions of low pressure (low density). This occurs because when dense air in a high pressure area sinks toward the surface it is forced to flow outward from the high pressure area toward areas of lower pressure. By default, air that sinks in a high pressure zone will flow toward regions of low pressure (low density). When it reaches the low pressure areas it then rises again (Figure 3.7).

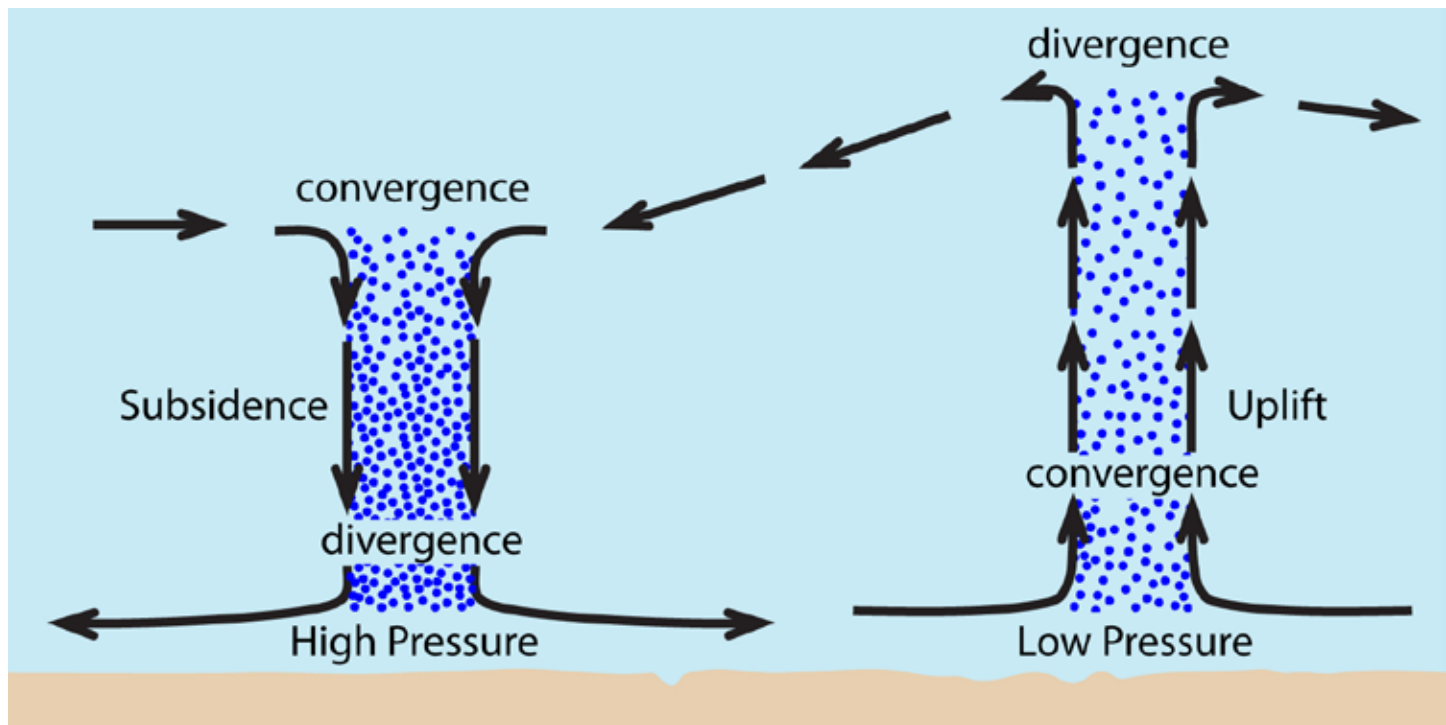


Figure 3.7. In high pressure areas (left diagram), air sinks toward the surface, at which time it is forced to flow outward, away from the center of the high pressure area. This is why air flows from areas of high pressure to areas of low pressure. In low pressure areas (right diagram), air flows toward the center of the low and then rises upward (Source/Credit: modified from Dennis I. Netoff and Ava Fujimoto-Strait, *Weather & Climate Lab Manual*).

Pressures and pressure gradients are represented on weather maps with lines of equal pressure known as **isobars** (Figure 3.8). The prefix *iso* means *equal* and *bar* refers to barometric pressure. All points along an isobar have the same pressure, just as all points on an isotherm have the same temperature. Knowing the values and spacing of the isobars enables forecasters to determine which direction the wind will blow and how fast. The pressure gradient, however, is not the only factor that affects wind direction and wind speed.

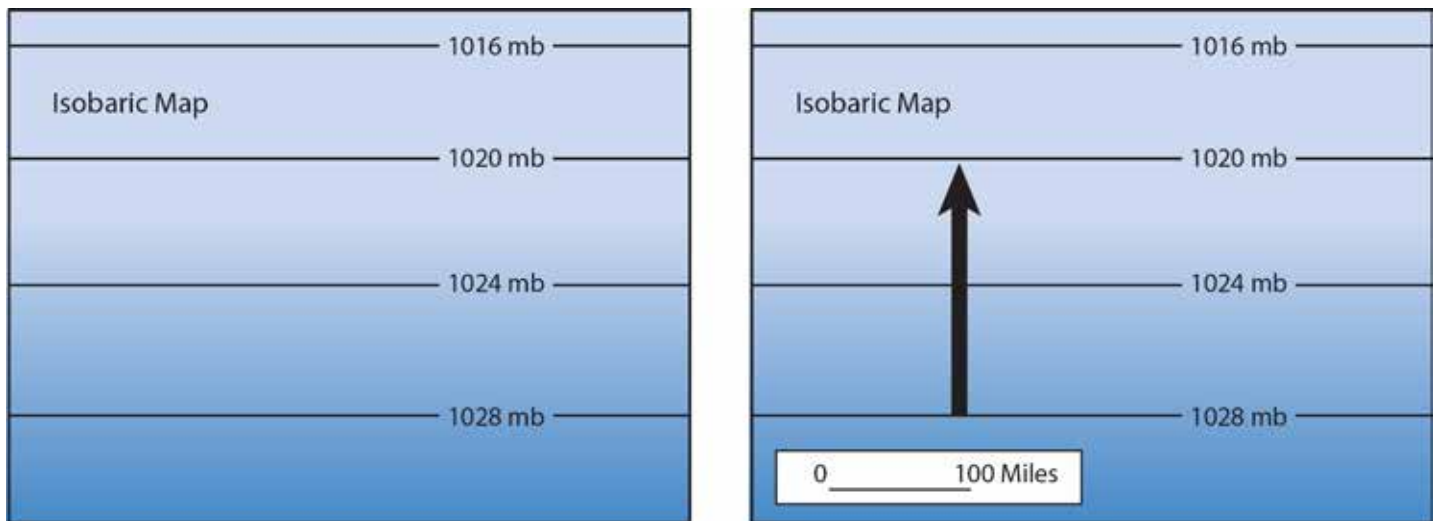


Figure 3.8. Isobaric maps depict changes in atmospheric pressure on a horizontal plane. Lines of equivalent pressure are called isobars. The spacing between adjacent isobars is typically 4 mb, the pressure interval. The simplified isobaric map sketch on the left shows an east-west pattern of isobars that are equally spaced. Pressure decreases uniformly toward the north. The net movement of air molecules will be from denser air (higher pressure) to less dense air (lower pressure). The direction of pressure change is indicated by the black arrow, the pressure gradient force. The magnitude of the force is approximately 4 mb/100 miles. If no other forces were involved in air movement, the wind would blow in the direction of the pressure gradient force at a certain velocity. If the isobars were more closely spaced, the magnitude of the pressure gradient would be greater than 4 mb/100 miles, and the wind would be of somewhat higher velocity. The more closely spaced the isobars, the steeper the pressure gradient and the faster the wind will blow.

The rate at which pressure changes from one place to another is termed the **pressure gradient**. The pressure gradient force can be given by:

$$PGF = \Delta P/s$$

Where PGF = pressure gradient force  
 $\Delta P$  = change in pressure (mb)  
 s = distance (km)

The more rapid the change in pressure, the faster the wind will blow. A rapid change in air pressure produces a *steep pressure gradient*. So, the closer the isobars, the faster the wind blows.

## Isobaric Maps

Isobaric maps depict the spatial pattern of air pressure on a horizontal plane and are the basic tool used in analyzing surface winds. Isobaric maps are known as **constant height charts** because they show what the air pressure is at a constant elevation in the atmosphere. The reference elevation for most isobaric maps is typically mean sea level.

For sea level pressure values, isobars are usually spaced at intervals of 4 mb on weather charts. For example, isobars of 996, 1000, 1004, 1008 millibars might appear adjacent to one another on a weather map. Knowing the values of the isobars and the pressure gradient, forecasters can predict both the direction and speed of the wind.

Pressure fields aloft can be used to analyze and forecast upper-level winds much in the same way as surface isobaric maps. One way to depict the pressure field aloft is to view a cross-section of the atmosphere with the use of **isobaric surfaces**. Isobaric surfaces may be horizontal, indicating to pressure gradient aloft and therefore no wind (Figure 3.9). More realistically, isobaric surfaces slope in various directions, indicating the direction of pressure gradient aloft, and the tendency for the air aloft to move (Figure 3.10).

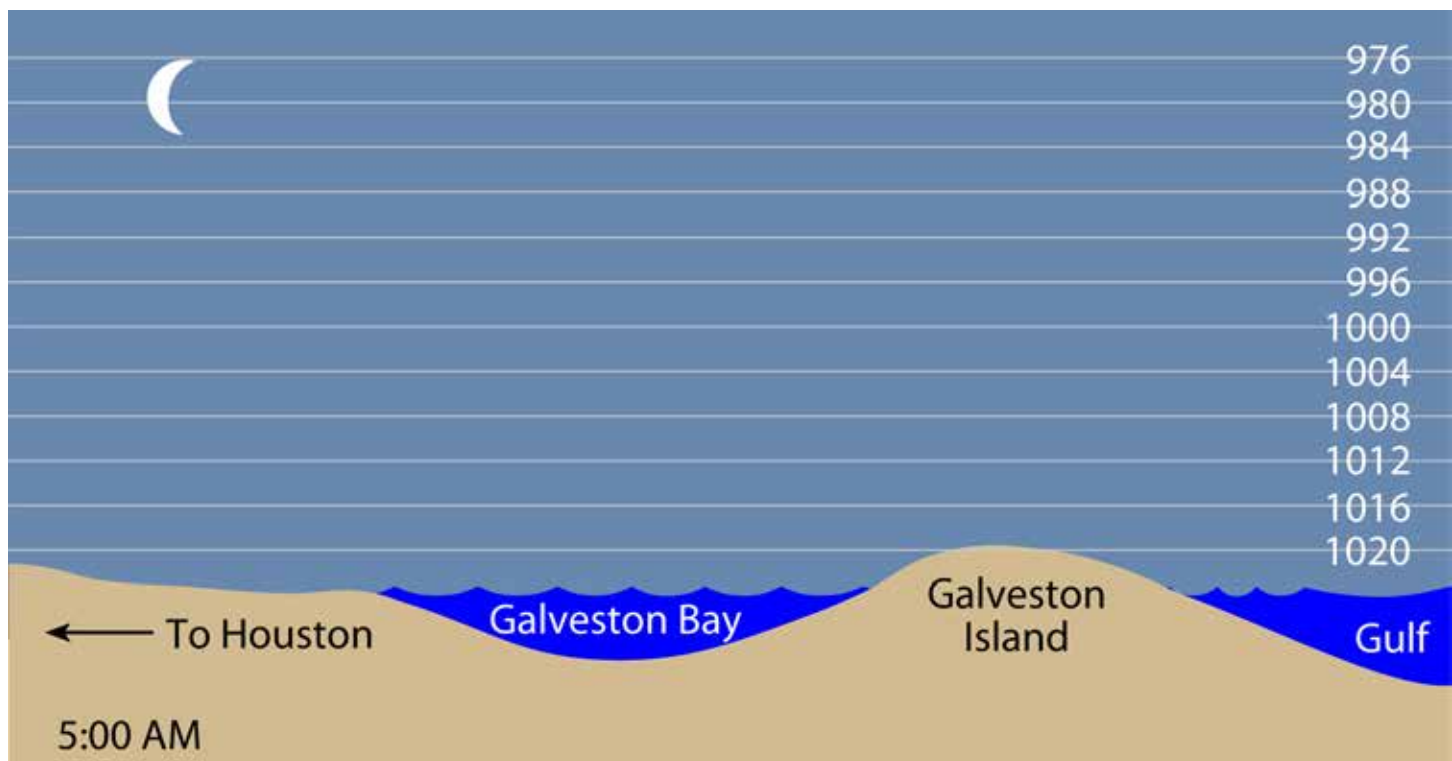


Figure 3.9. If the temperature of the atmosphere decreased uniformly with increasing altitude, the pressure also would decrease uniformly with altitude and would result in flat isobaric surfaces like those shown here. If this happened, the pressure gradient near the surface would be the same as the pressure gradient aloft, and air at all altitudes would flow in the same direction. This hypothetical situation does not normally occur, and certainly not over large areas, because the atmosphere is not heated uniformly.



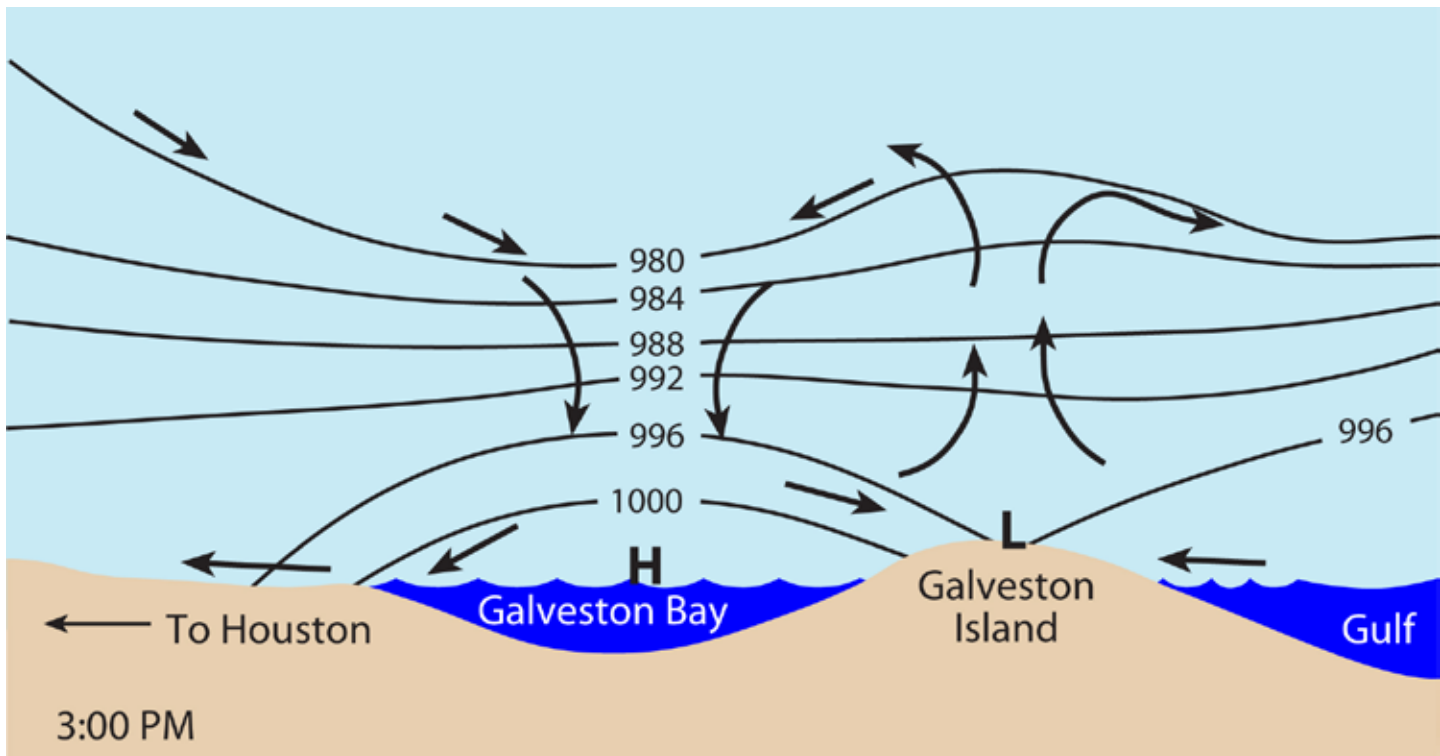


Figure 3.10. Unequal heating of the surface and atmosphere results in sloping isobaric surfaces. The less dense air over Galveston acts to raise the height of both the 984 and 980 mb surfaces relative to the height of same isobaric surfaces above the cooler waters of the Gulf and Galveston Bay. This means that the pressure gradient reverses somewhere above the altitude of the 988 mb surface. As a result, air would diverge above the 988 mb level above Galveston, but would converge toward the island near the surface because air always flows from high to low pressure. Note that the situation depicted here shows that the pressure gradient can reverse with altitude, which is the equivalent of saying that a surface low may be overlain by an upper-level high, and a surface high may be overlain by an upper-level low.

In the real world, this seldom occurs due to variations in air density caused by such things as temperature and moisture variations, as well as convergent and divergent flow. For example, because land (and the air above it) heats more quickly than water, the height of a given isobaric surface is likewise raised. Note, for example, that the 980 mb surface occurs at a higher elevation above land than above water.

Note that the *sea level* air pressure over the land is lower than that above the water. The warmer air is less dense and begins to rise. Conversely, over the cooler water, the air cools, becomes more dense and subsides. The denser column of air over the water causes the pressure to drop vertically faster than it does over the land, so that at a certain elevation aloft, the pressure gradient *reverses*, and the upper level flow pattern is *opposite* to the surface pattern. This allows for the complete circulation of a *convection cell*. In a closed convection cell, surface convergence is complimented by upper-level divergence, and surface divergence by upper-level convergence. Note that because the isobars are higher above the land, they appear to form a *hill*. This helps to visualize air movement because, just as water flows downhill, so does air flow; i.e., it flows *down* the pressure gradient.

## The Coriolis Force

The Coriolis Force was named after Gaspard Gustave de Coriolis, the man who first described this force in 1835. The **Coriolis Force** can be defined as the force that causes the apparent deflection of wind currents to the right of their original direction of motion in the Northern Hemisphere, and to the left of their original direction of motion in the Southern Hemisphere (Figure 3.11). **This apparent deflection is the result of the Earth's rotation.** The resolution of the Coriolis Force and the pressure gradient force causes the actual winds to blow across the isobars at an angle, rather than perpendicular to them (Figures 3.12 and 3.13).

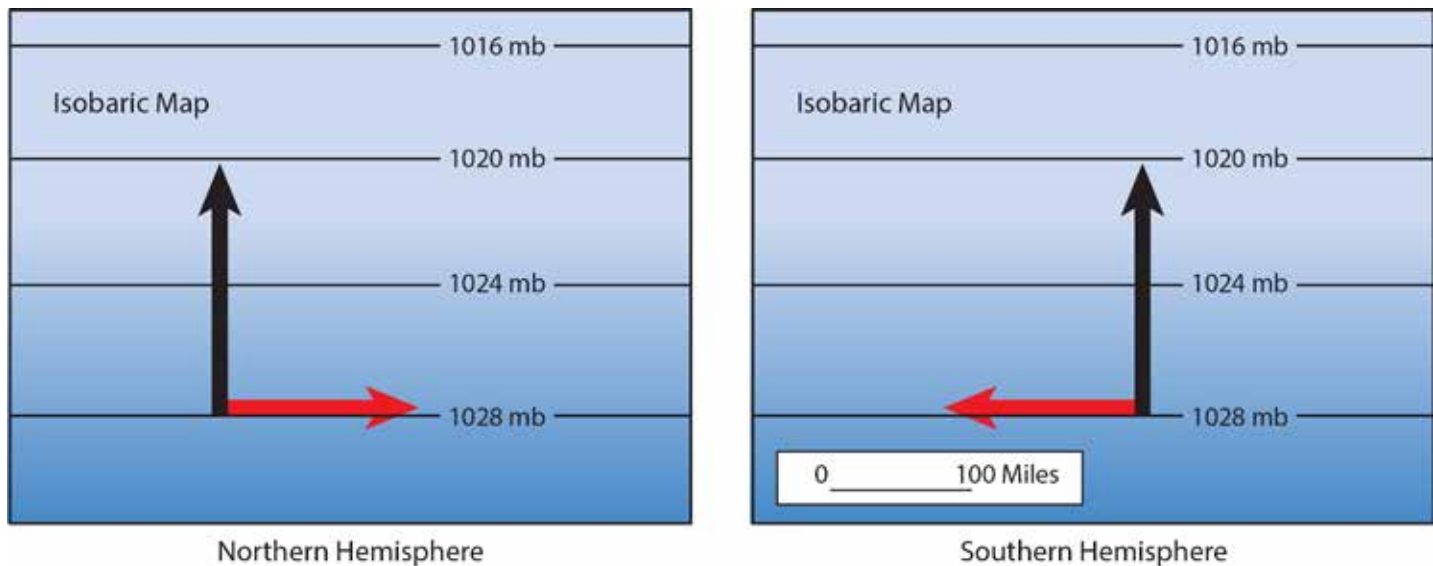


Figure 3.11. Coriolis Force deflects freely-moving objects to the right of their initial path of motion in the Northern Hemisphere and to the left in the Southern Hemisphere. As a parcel is compelled to move by the pressure gradient force (black arrow), its direction is immediately influenced by the Coriolis Force (red arrow). The magnitude of the Coriolis Force increases with increasing latitude and wind velocity.

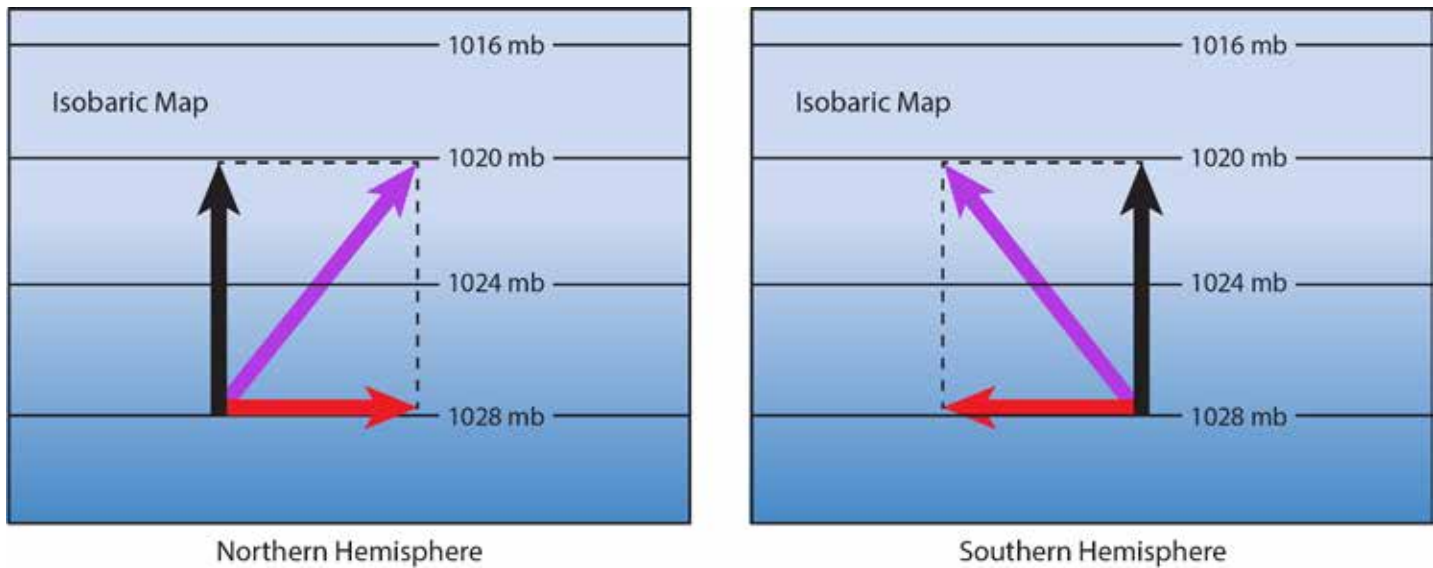


Figure 3.12. A simplistic resolution of the Coriolis Force and the pressure gradient force involves the construction of a rectangle (black dotted line) and an arrow drawn from one corner of the rectangle to the opposite representing an approximation of the actual wind (purple arrow). Most surface winds therefore lean across the isobars at an angle, either to the right of their initial path (left box) in the Northern Hemisphere, or to the left (right box) in the Southern Hemisphere.

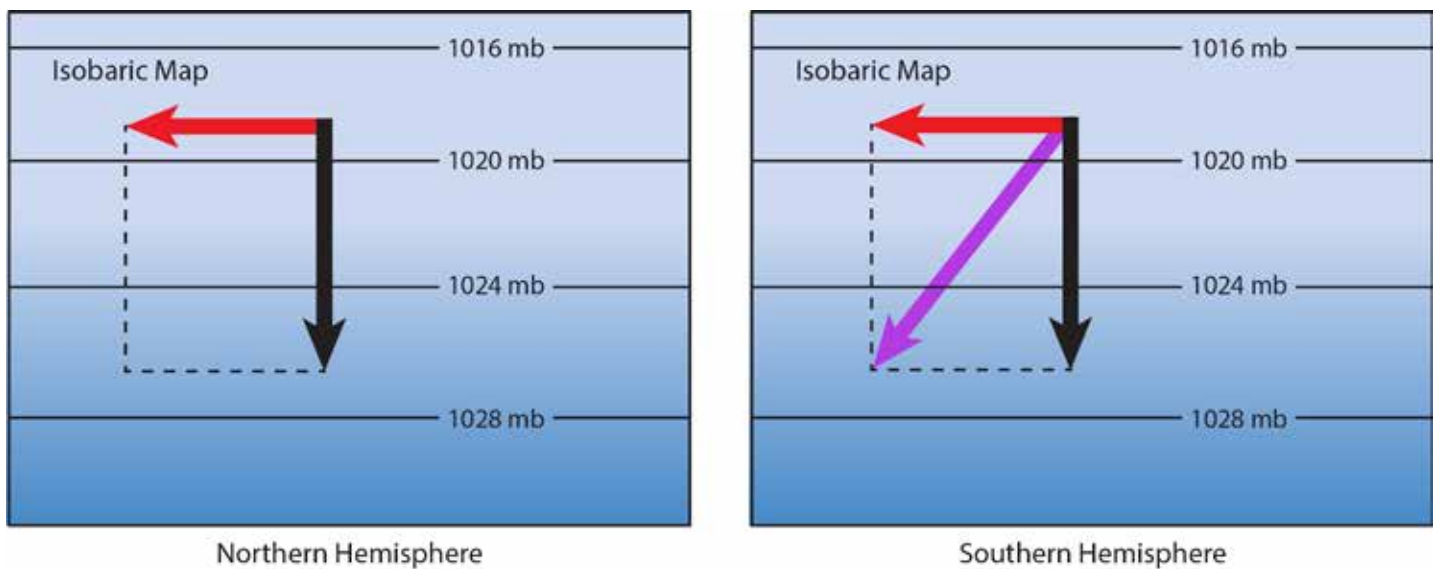


Figure 3.13. When the pressure gradient is toward the south, the resolution of the Coriolis Force and the pressure gradient force is basically the same as the previous sketches. At first glance, it appears as though the wind is moving to the left of the pressure gradient. From the perspective of viewing the pressure gradient force from the north, however, the Coriolis Force is again acting toward the right of the pressure gradient.

A good example of this concept is provided by the bombardment of Paris, France by German artillery fire in World War I. During one of the assaults on Paris, the Germans set up a large cannon north of the city that was capable of firing shells about 80 miles toward the heart of the city. However, no matter how accurately the Germans aimed their cannon at the target, the shells kept landing 0.7 mile to the west of it. Eventually, the Germans realized that the shells were missing the target because, due to the difference in rotational velocities at different latitudes, the target was moving! While the shells were in flight and headed south, the target, which was very much attached to the Earth, was traveling to the east as the Earth rotated to the east. In other words, the target rotated out from under the path of the shell while it was in flight. Relative to the flight path of the shell, it *appeared* as though the shell had been deflected to the right of its *direction of motion* (Figure 3.14).

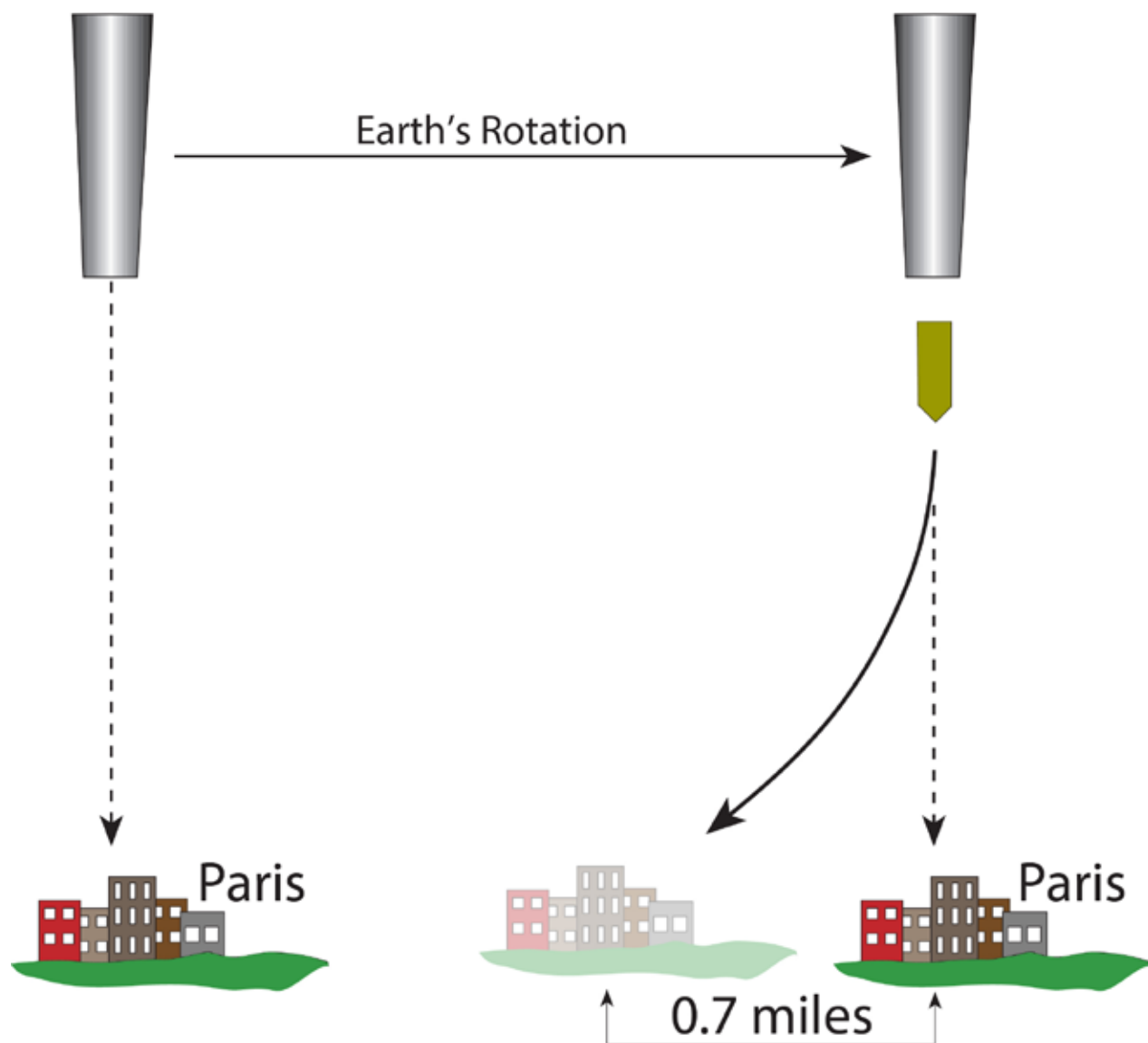


Figure 3.14. When the Germans tried to shell Paris in World War I, they kept missing their target. This occurred because the shell was in flight long enough for the target in Paris to move out from under the flight path of the shell as a result of the rotation of the Earth.

The amount of deflection associated with the Coriolis Force is related to latitude and wind speed. The higher the latitude, the greater the Coriolis Force. The Coriolis Force is zero at the Equator, which prevents hurricane formation there. The Coriolis Force increases with increasing wind speed. The faster the wind blows, the greater the amount of deflection (Figure 3.15).

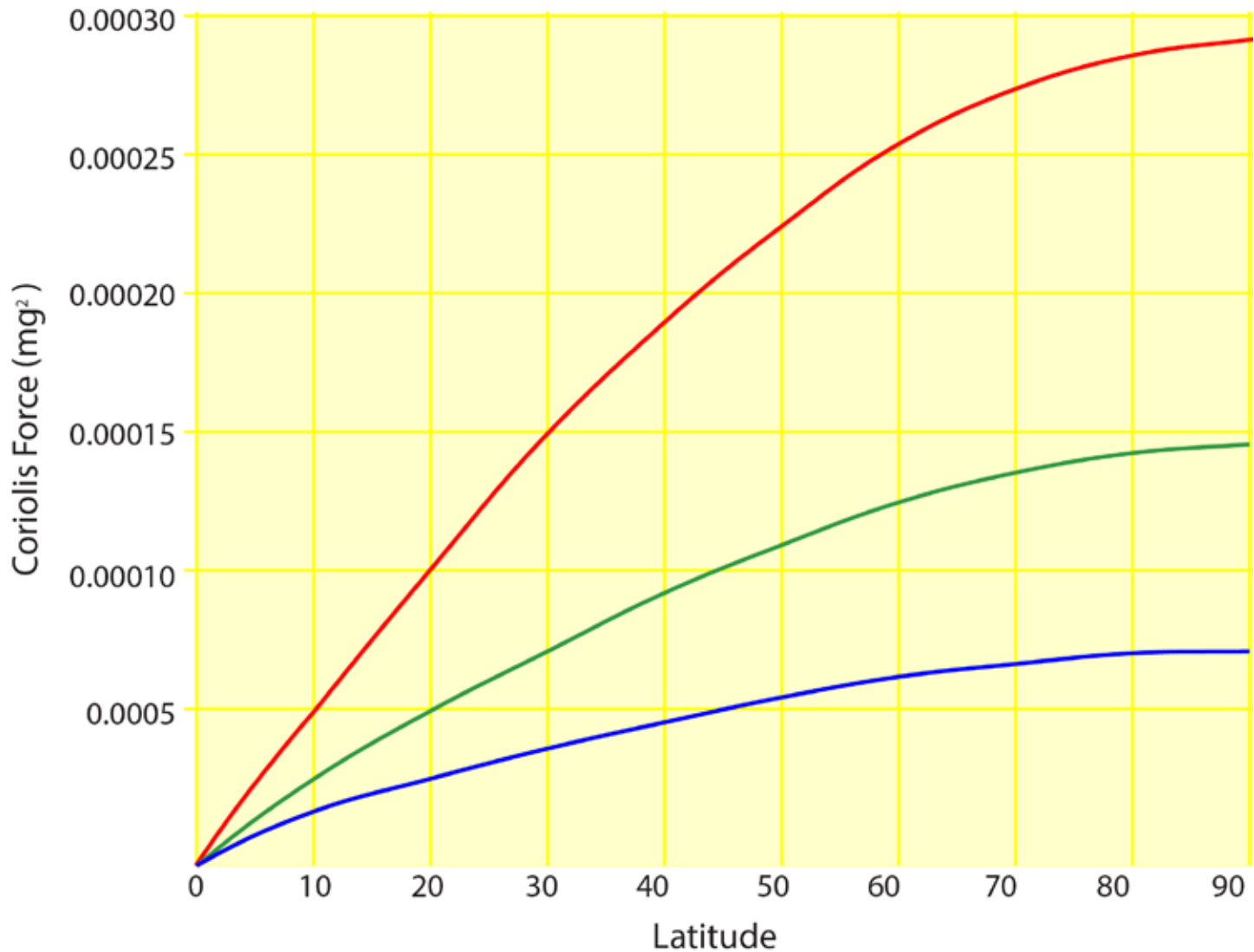


Figure 3.15. Coriolis Force increases with increasing latitude and wind velocity. Coriolis Force deflection is given on the Y-axis. The colored lines represent different wind speeds. It is zero at the Equator, but increases to a maximum value at the poles. Also, as the wind velocity increases, so does the Coriolis Force. At 90°, a 5 meter per second wind velocity (11 mph) causes a deflection of about 0.00007 meters per second squared. At the same latitude, a 20 meter per second wind (44 mph) causes a deflection of 0.00029 meters per second squared.

The pressure pattern of isobars depicted on isobaric maps almost always forms curved isobars rather than linear ones illustrated in the idealized examples above. They often loop around and close on themselves, forming a circular or oval pattern of isobars. Such a pattern of closed isobars tends to form either a **high pressure cell** or a **low pressure cell**. High pressure cells have highest pressure in their centers, and low pressure cells have the lowest. The resolution

of winds out of a high or into a low follows the same general rules that apply to linear pressure patterns. The pressure gradient forces in high pressure cells form a radial outward pattern (Figure 3.16). In the Northern Hemisphere, this results in winds that radiate outward from the center of high pressure, and that spin in a clockwise pattern (Figure 3.17). The pattern is described as divergent, clockwise flow. In the Southern Hemisphere, high pressure cells are divergent and counterclockwise (Figure 3.18). Low pressure cells in the Northern Hemisphere are convergent and counterclockwise, whereas they are convergent and clockwise in the Southern Hemisphere (Figure 3.19).

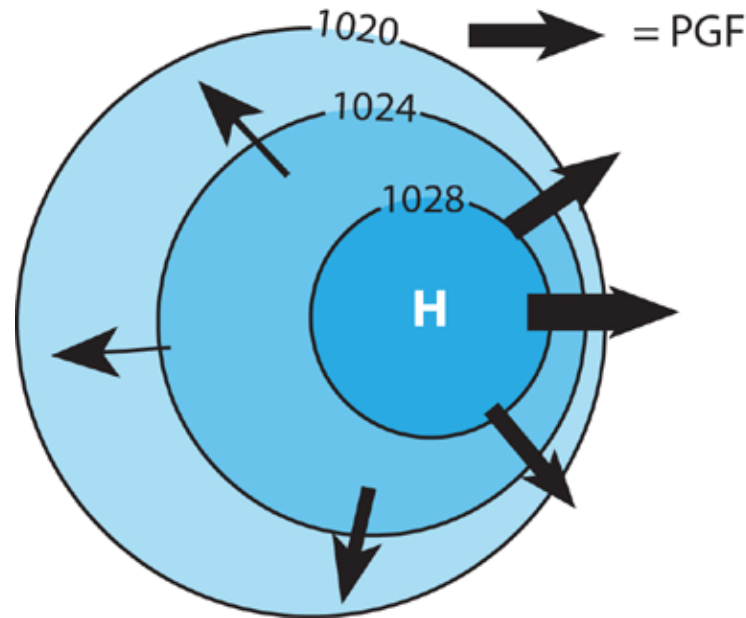


Figure 3.16. A high pressure cell has one or more closed isobars, and the highest pressure is in the center of the cell. Pressure gradient forces form a radial outward pattern, or **divergent flow**. The most closely-spaced isobars on the map just to the east of the high pressure center indicate the strongest pressure gradient force (heaviest arrow). Elsewhere, more widely-spaced isobars indicate lower pressure gradients. Neglecting frictional forces, the highest winds should correspond with highest pressure gradients.

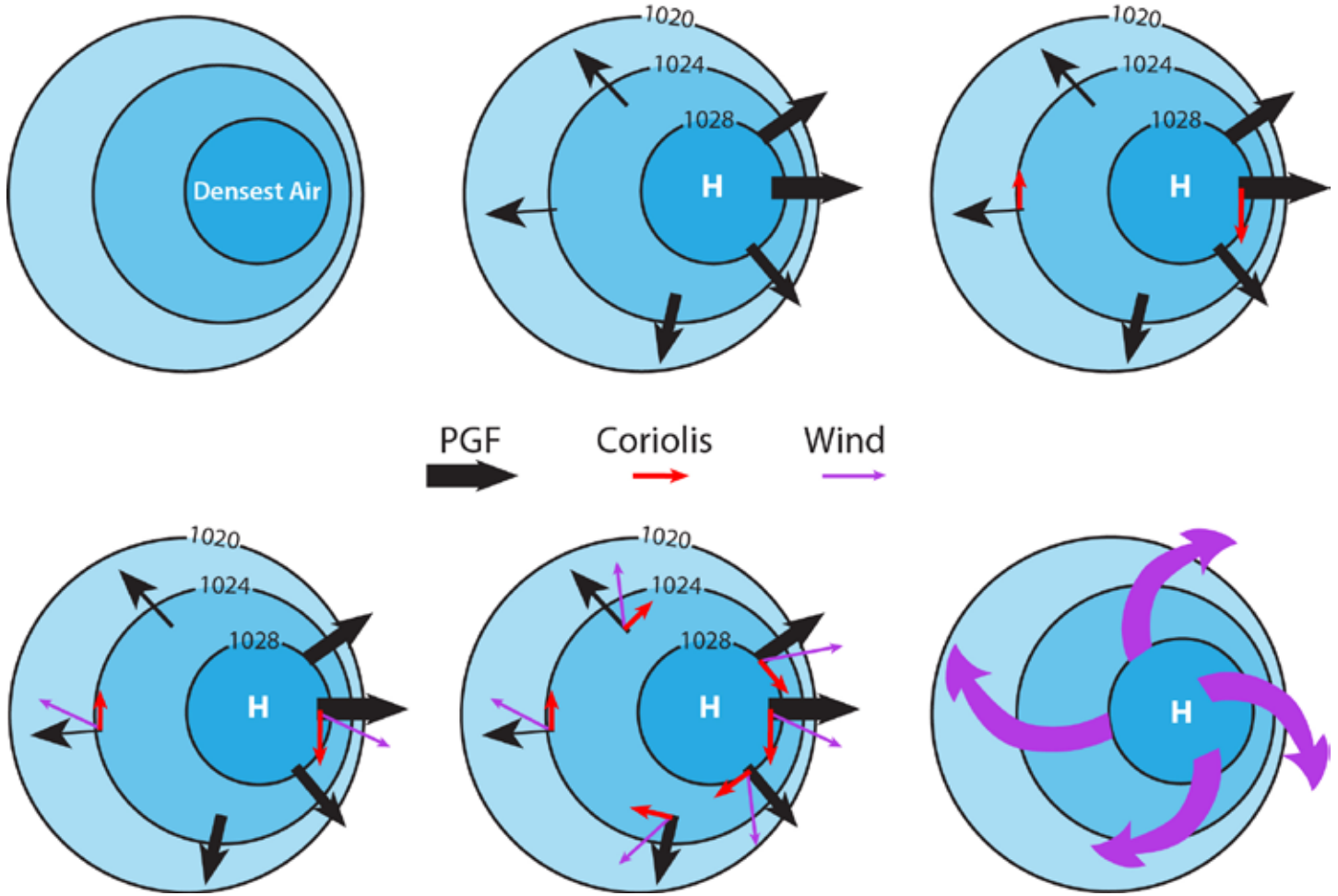


Figure 3.17. The resolution of pressure gradient forces and Coriolis Forces on a high pressure cell in the Northern Hemisphere results in surface divergence and a clockwise spin.

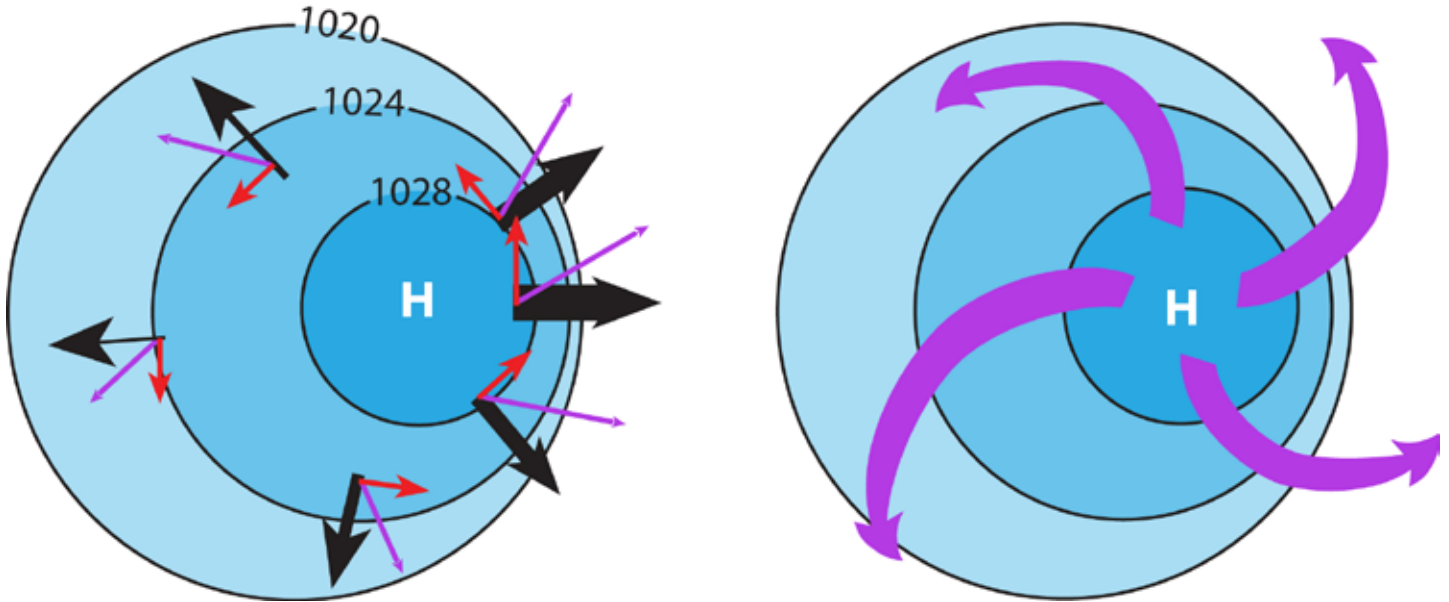


Figure 3.18. The resolution of forces in the Southern Hemisphere is similar to that of the Northern Hemisphere, except the Coriolis Force deflects the wind to the left of its initial path. The surface circulation is described as **divergent (outward flow)** and **counterclockwise**.

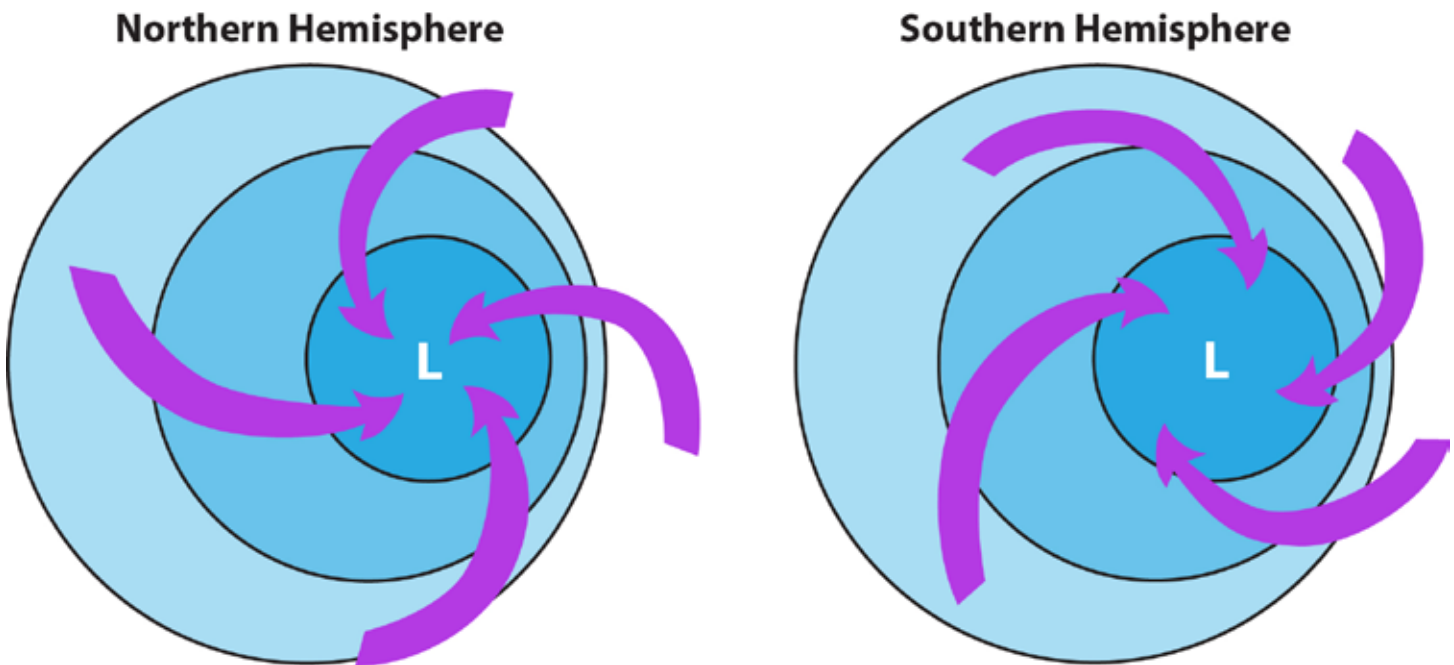


Figure 19. Low pressure cells in the Northern Hemisphere are convergent and counterclockwise (left), whereas they are **convergent and clockwise** in the Southern Hemisphere (right).



## Frictional Drag

As wind travels across the surface of the Earth, it encounters objects that interfere with its motion. These objects reduce the velocity of the wind, and in some cases, alter its direction. Much of this is of a local, small-scale nature, as when wind encounters trees and buildings (Figure 3.20). But, it can be on a much larger scale as when it encounters mountains and continents.

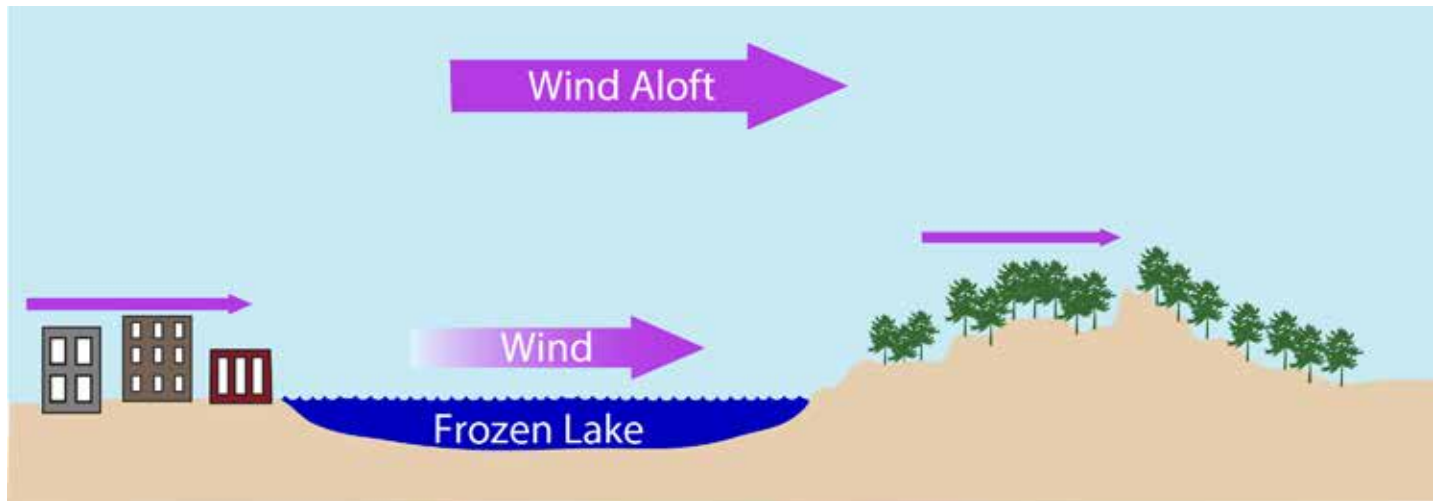


Figure 3.20. Because buildings, trees and hills project upward from the surface, they exert friction on the wind, which acts to slow it and deflect it. The frozen lake is smooth and flat and offers almost no resistance to the wind (Source/Credit: modified from Dennis I. Netoff and Ava Fujimoto-Strait, *Weather & Climate Lab Manual*).

Near the surface of the Earth, friction is greater than it is aloft. The amount of friction decreases fairly rapidly with altitude over flat areas. At elevations of 7000 feet (~3000 meters) above the ground, friction is minimal. **Reduced frictional drag aloft enables the wind to blow at a higher velocity and so increases the Coriolis Force, causing the air to flow nearly parallel to the isobars.** Upper level winds that flow parallel to isobars are known as **geostrophic winds** (Figure 3.21).

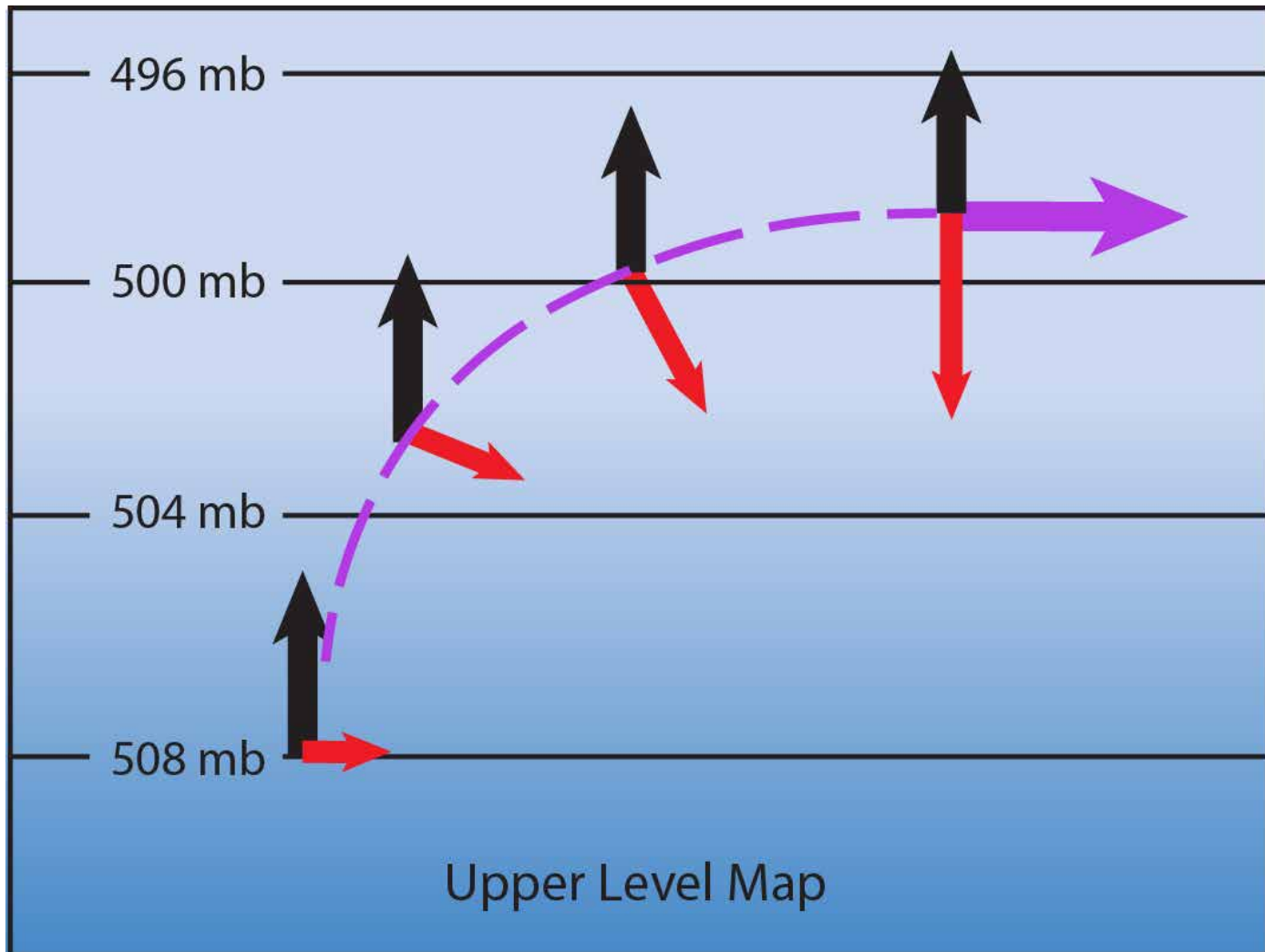


Figure 3.21. Upper level winds at about 18,000 feet (~5500 m) blow nearly parallel to the isobars. They are high-velocity winds compared to their surface counterpart, because they are nearly free of frictional resistance. The air parcel movement (dashed purple line) moves initially northward, compelled by the pressure gradient force (black arrow). The Coriolis Force (red arrow) is initially small, because the air parcel has just begun to accelerate. As the parcel moves northward, then northeastward, higher velocities increase the Coriolis deflection, causing the parcel to move progressively to the right of its initial path. Finally, the air parcel has been deflected so far to the right that it appears parallel to the isobars. These theoretical upper-level winds are called **geostrophic winds** (Source/Credit: modified from several sources).

Tall buildings are subject to tremendous *wind shear* because of the increase in wind velocity with height. Consequently, they must be designed so that they can actually bend and twist with the wind without causing structural failure.

In the Southern Hemisphere, there is a relatively large expanse of open ocean that stretches all the way around the world between Antarctica and the southern tips of South America and Africa (Figure 3.22).

## Annual 50m Wind Speed

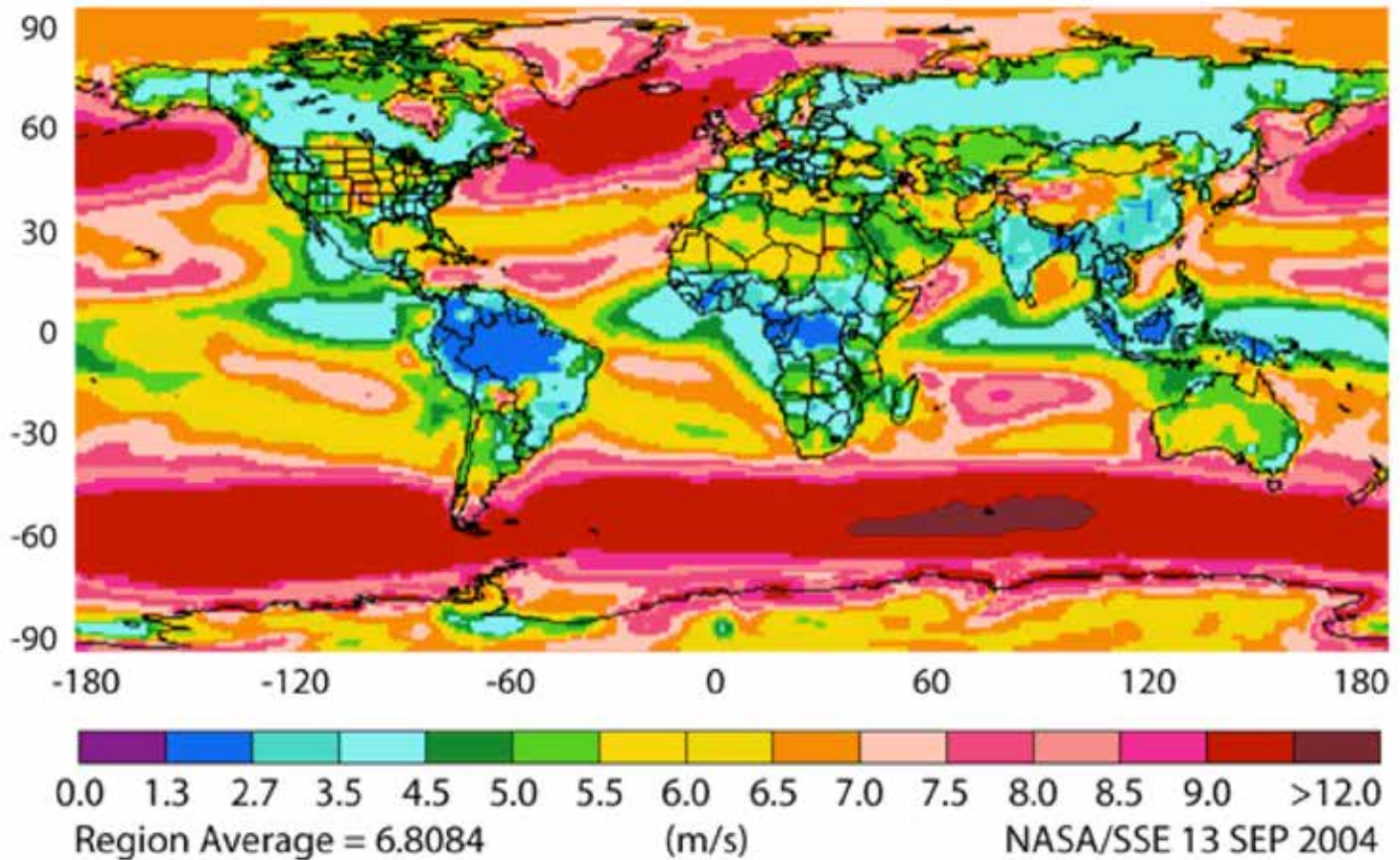


Figure 3.22. The lack of land between Antarctica and the southern tip of South America and Africa, combined with the strong high pressure system that develops over ice-covered Antarctica, leads to the formation of very strong winds in this vast stretch of open water. The only real obstruction to airflow is the roughness of the ocean surface (Source/Credit: NASA/SSE).

Because the cold air of Antarctica generates a very strong pressure gradient, and because there is no land to interrupt the flow of air in this region of the southern ocean, wind speeds can attain great velocities and this results in the generation of very large waves. In the 5000-mile open stretch of water in the South Pacific, frequent 100-mph winds create 60-foot waves with frothy tops known as graybeards. As latitude increases toward Antarctica and the pressure gradient strengthens, the winds become progressively stronger. Consequently, the latitudinal belts go by the names of the *roaring forties*, *howling fifties*, and *screeching sixties*. These high winds and waves, as well as icebergs and pack ice, delayed the discovery of Antarctica.

In summary, air flows from a high-pressure region toward a low-pressure region but is deflected

by the Coriolis Force. The amount of deflection by the Coriolis Force is limited by friction with the surface of the Earth because friction reduces the wind speed. **Most surface winds therefore cross isobars at an angle (typically 30° to 45°) rather than flowing perpendicular to the isobars down the pressure gradient. In the upper atmosphere, above the friction layer, the air flows parallel to the isobars.**

## Cyclones and Anticyclones

Regional and global surface isobaric maps typically show migratory low and high pressure cells referred to as cyclones and anticyclones. Pressure gradient force, Coriolis Force and friction all influence the flow and direction of wind moving between cells of high pressure (anticyclones) and low pressure (cyclones). An **anticyclone** is a region of high pressure that appears as a set of closed, circular or oval isobars on a weather chart. Because it is a region of high pressure, the pressure is highest in the center of the system. As the air moves away from (diverging) the center of the anticyclone, Coriolis Force causes it to be deflected to the right of its direction of motion in the Northern Hemisphere and to the left in the Southern Hemisphere (Figure 3.23). As is true with all high pressure areas, the air flow associated with this cell is descending, warming and diverging.

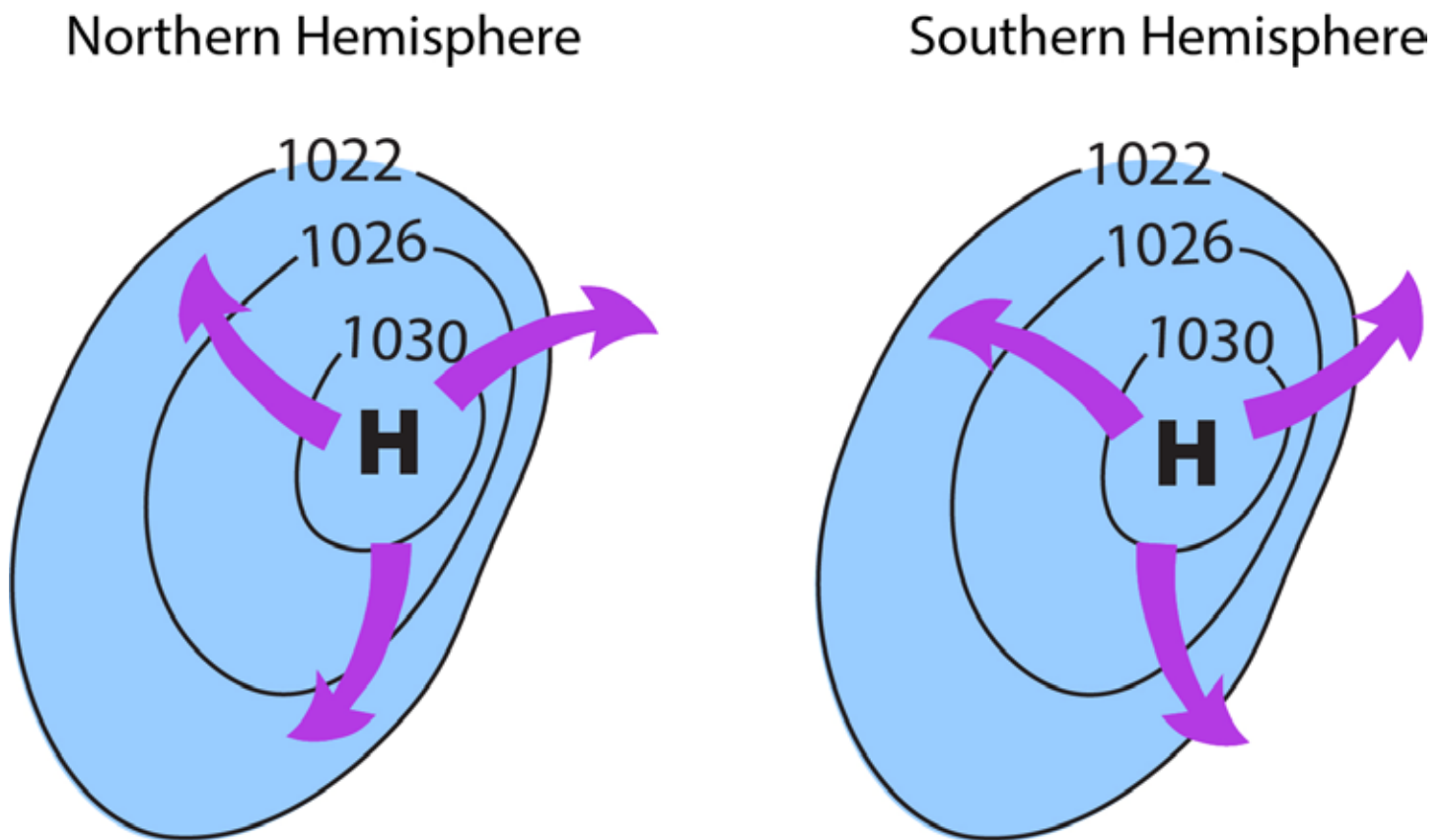
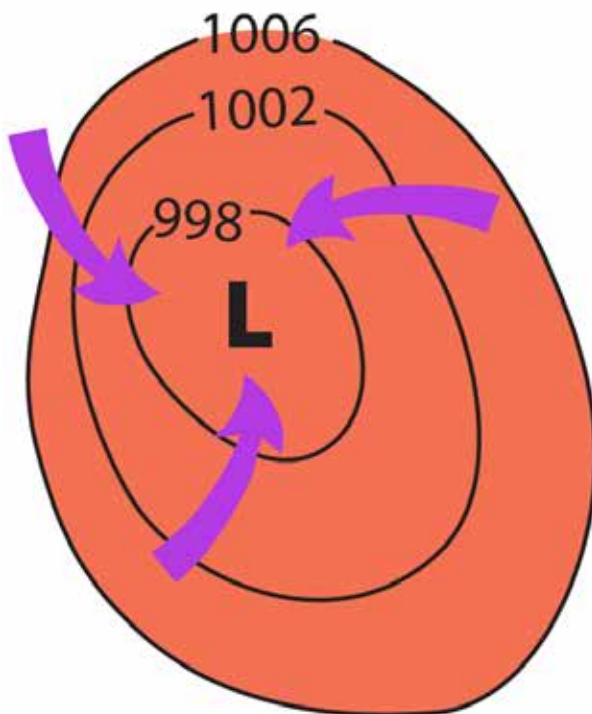


Figure 3.23. Anticyclones appear as a set of closed isobars on a weather map, with the highest pressure in the center. In the Northern Hemisphere, the air in an anticyclone flows downward, outward and clockwise. The pressure gradient sends it outward and the Coriolis Force deflects it to the right of its direction of motion, creating a clockwise, spiral pattern of airflow. In the Southern Hemisphere, it flows downward, outward and counterclockwise.

**Cyclones** are low pressure cells that appear as a set of closed isobars on a weather chart, with the lowest pressure in the center of the system. In cyclones, airflow is toward the center (converging) of the cell. In the Northern Hemisphere, this flow is in a counterclockwise direction; in the Southern Hemisphere it is in a clockwise direction. Air flow in all low pressure areas is ascending (rising), cooling, and diverging (Figure 3.24).

## Northern Hemisphere



## Southern Hemisphere

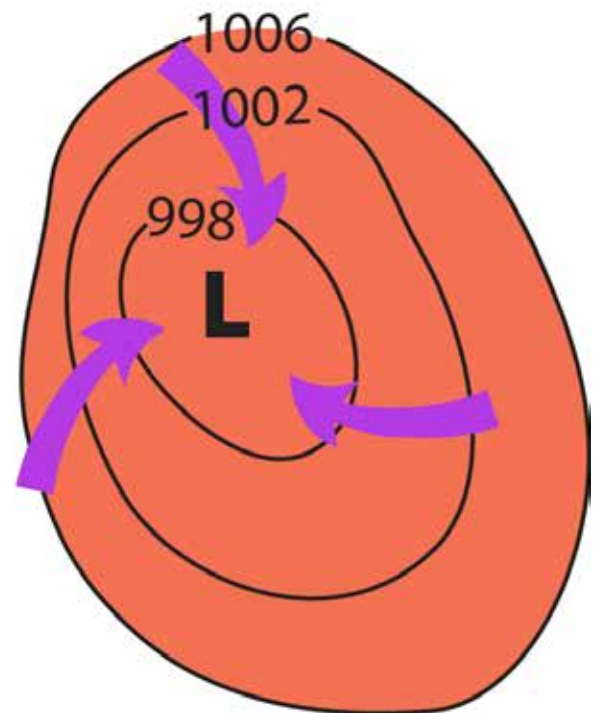


Figure 3.24. As with anticyclones, cyclones also appear on weather maps as a set of closed circular isobars, but with the lowest pressure in the center. Air that flows toward the center of cyclone is acted upon by both the pressure gradient force and Coriolis Force. The pressure gradient is stronger, but because the Coriolis Force acts to the right of the pressure gradient force (in the Northern Hemisphere), the wind spirals counterclockwise into the low. In the Southern Hemisphere, it spirals clockwise into the low.

## Global Pressure and Wind Belts

**Equatorial Low Pressure Belt (EL).** Within the equatorial regions, the Sun's rays are relatively direct all year. As a result, along either side of the Equator for some 5 to 15 degrees, there exists an area of relatively warm temperatures, moist air, ascending air and general low pressure (Figure 3.25). As the warm moist air ascends and cools, the resultant precipitation creates the vast tropical rainforests of the low latitudes.

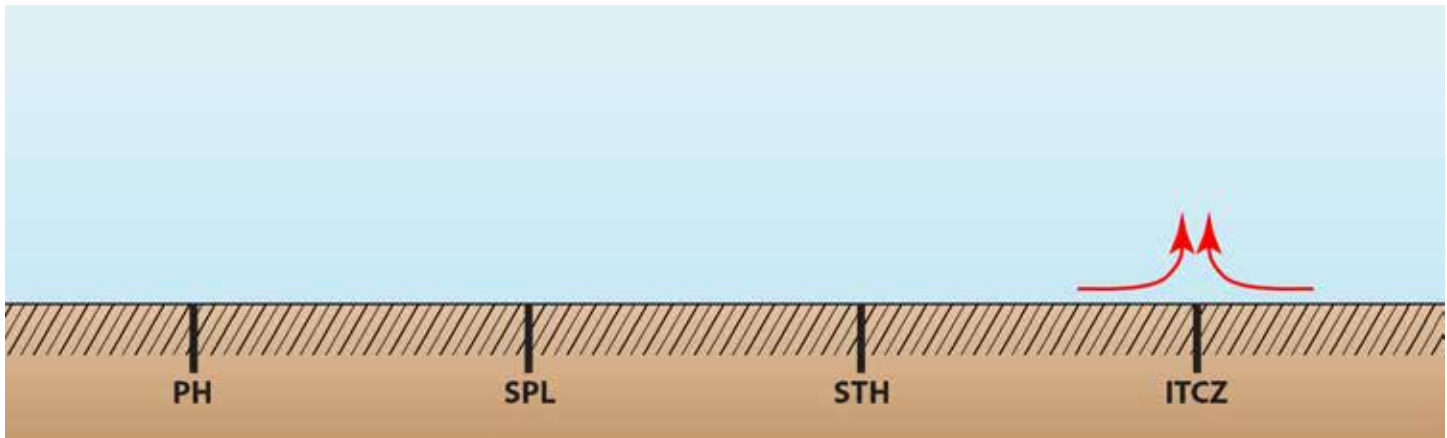


Figure 3.25. The warm, moist conditions that exist along the Equator create a low pressure belt known as the Equatorial Low. Because it is a low pressure region, air converges on the Equatorial Low and then rises. ITCZ (intertropical convergence zone at the site of the Equatorial Low). STH (Subtropical High). SPL (Subpolar Low). PH (Polar High).

The Equatorial Low shifts latitudinally over the course of the year in response to the changing position of the vertical rays of the Sun. Also, as a result of differences in temperature between land and water, the pressure belts bend either northward or southward — they are not demarcated by straight lines. For example, when it is summer in the Northern Hemisphere, the Equatorial Low will bend further northward over the continents because the land is warmer than the oceans.

**Subtropical High Pressure Belts (SH).** Air that rises at the Equator in the Equatorial Low travels north and south down the pressure gradient and then subsides at approximately 30° latitude in both hemispheres. As the air parcel descends in altitude it is compressed, density increases and the air is warmed. This causes an area of semi-permanent high pressure to develop between 25° and 40° north and south latitude (Figure 3.26).

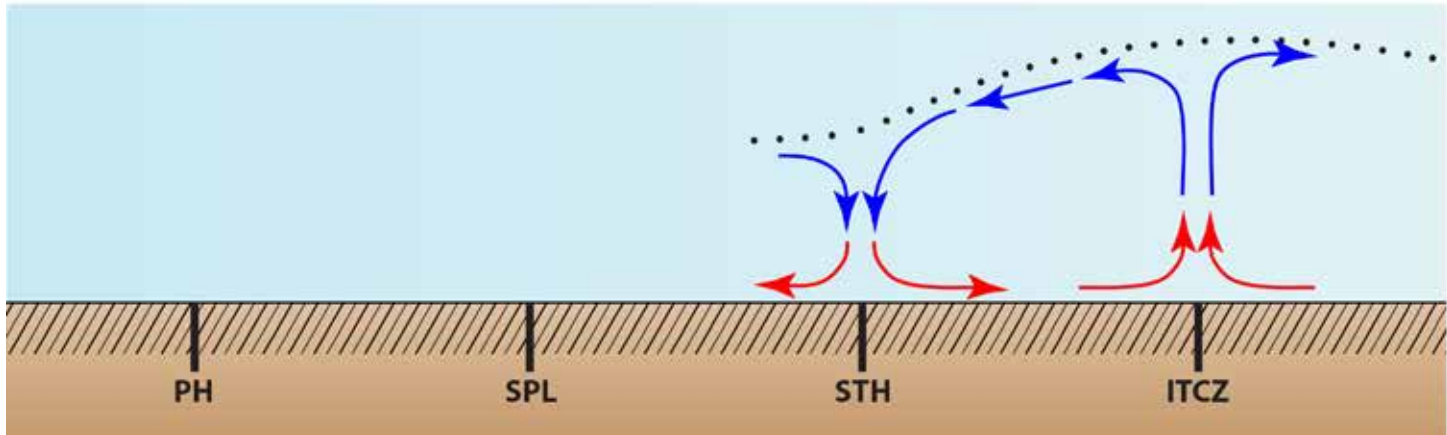


Figure 3.26. Air that rose in the Equatorial Low rises upward and cools. When it hits the tropopause, it travels poleward and then sinks at about 30° north and south latitude. It sinks because the upper level convergence that occurs here forces the air downward. This is primarily a dynamically-induced high pressure region. In addition, the fact that the upper-level air has cooled and become drier makes the air more dense and heavy, and this also enhances its tendency to sink. All of these conditions act in combination to create the Subtropical High pressure belts.

**Polar High (PH).** At the poles, the air is typically very cold and dry, and therefore very dense. The air is very dry because the temperatures are too low for significant evaporation and sublimation to occur, which would otherwise add moisture to the air. This generates a high pressure region called the Polar High around both poles (Figure 3.27). This is an area of strong subsidence — the denser the air, the more pronounced the subsidence.

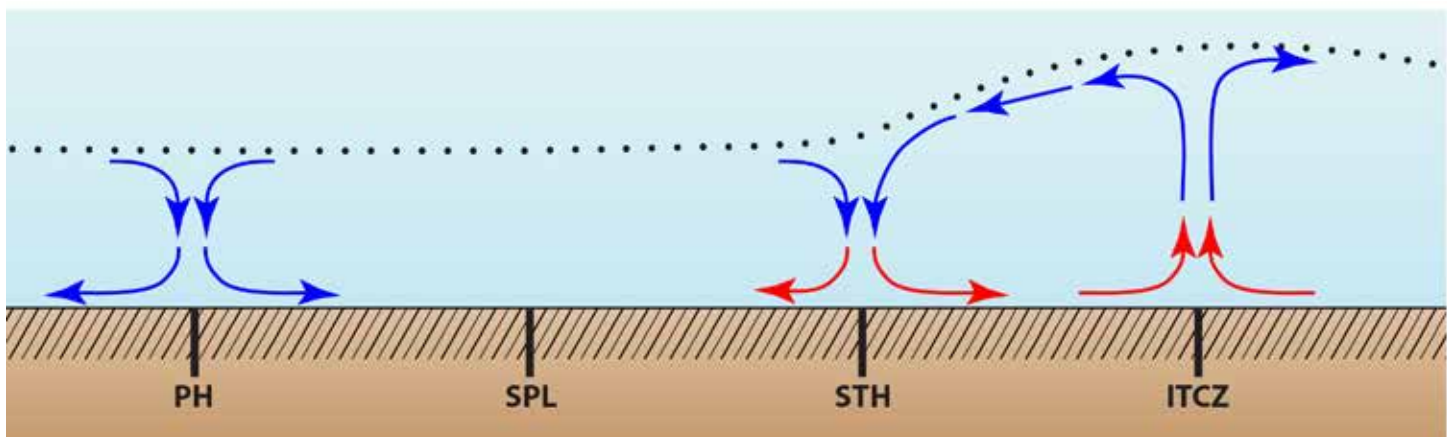


Figure 3.27. Cold, dry, dense air in the polar regions causes the thermally-induced Polar High pressure dome. The Polar High is an area of surface divergence, upper-level convergence, and vertical subsidence.



**Subpolar Low Pressure Belts (SL).** These pressure belts are located between 55° and 70° latitude in both hemispheres (Figure 3.28). This belt is created as air that flows out of the Subtropical High at the surface collides with colder air that flows out of the Polar High (discussed below). When the warmer and moister air from the mid-latitudes meets the colder and drier air from the polar regions, it is forced upward, thereby creating a belt of low pressure.

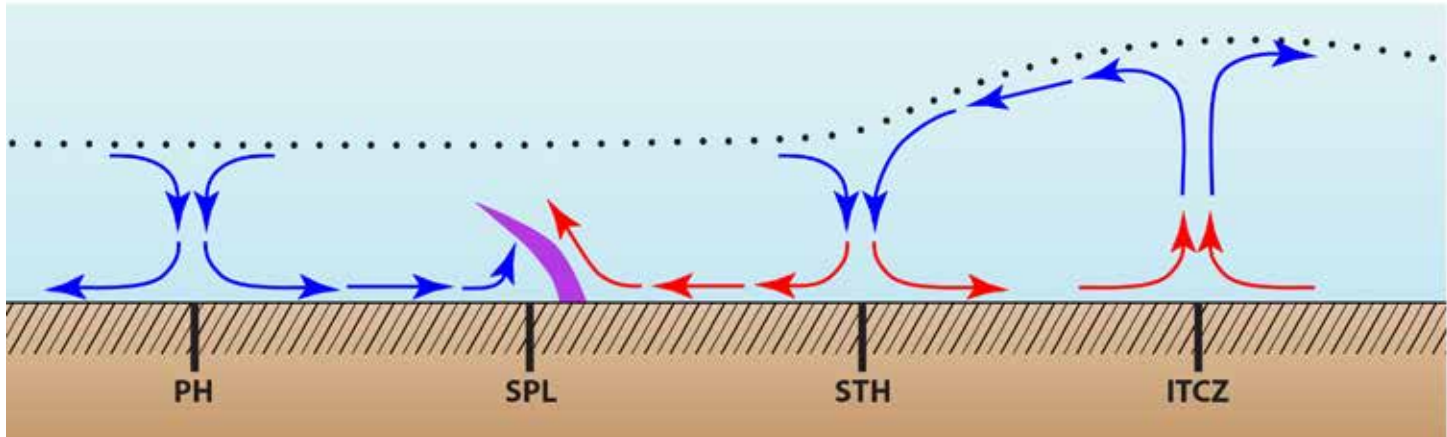


Figure 3.28. Between the Polar High and the Subtropical High is a sinuous belt of convergence and the Subpolar Low pressure system. The denser polar air acts much like a wedge (purple symbol), lifting the warmer, less dense subtropical air in the process.

## Surface Wind Belts

Air is set into motion by the large scale global pressure belts (Figure 3.29). Because these pressure belts are quasi-permanent features of the Earth's atmosphere, the wind tends to flow from the same direction within different latitudinal belts over much of the year. **Winds are named according to the direction they flow from** — not the direction toward which they are blowing. Thus a wind out of the north is called a north wind, and a wind from the west is called a west wind.

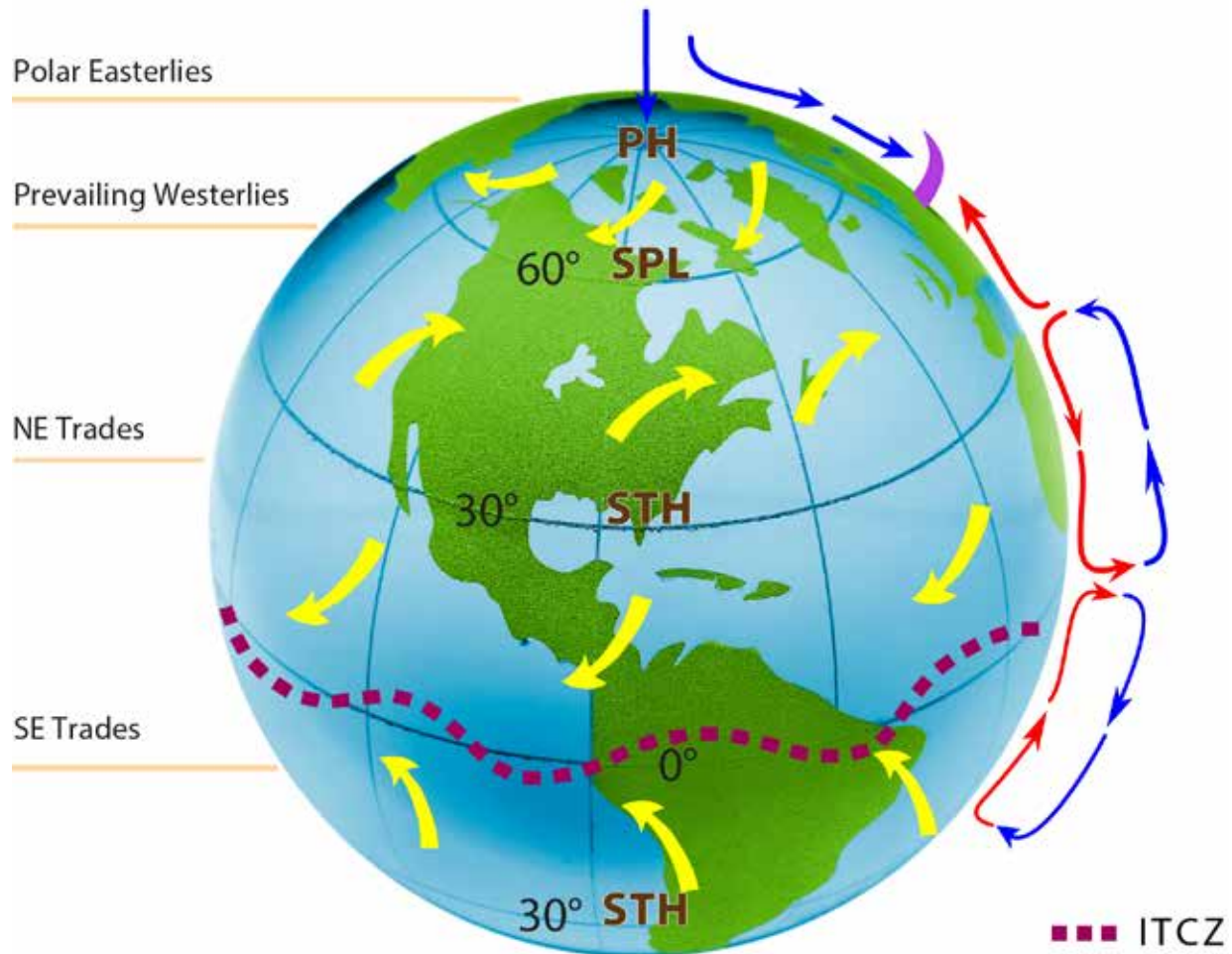


Figure 3.29. The world's wind belts are created by the interaction of the pressure gradient force and the Coriolis Force. Air flows out of high pressure belts toward low pressure belts and is deflected to the right of its direction of motion in the Northern Hemisphere, and to the left of its direction of motion in the Southern Hemisphere. Areas of surface convergence are low pressure zones (Equatorial Low [ITCZ] and Subpolar Low [SPL]), whereas areas of upper-level convergence and/or subsidence are high pressure areas (Subtropical High [STH] and Polar High [PH]).

**The Doldrums.** Close to the Equator within the Equatorial Low pressure belt is an area of weak and highly variable winds known as the Doldrums (Figure 3.30). Here is found the area of convergence of the Northeast and Southeast Trade Winds known as the **Intertropical Convergence Zone** (ITCZ). A combination of convergence and dominant upward motion of air accounts for the weak nature of the winds. In the days of sailing ships, this was a region to be somewhat feared because of the possibility of being becalmed (running out of wind) and running out of food and fresh water.

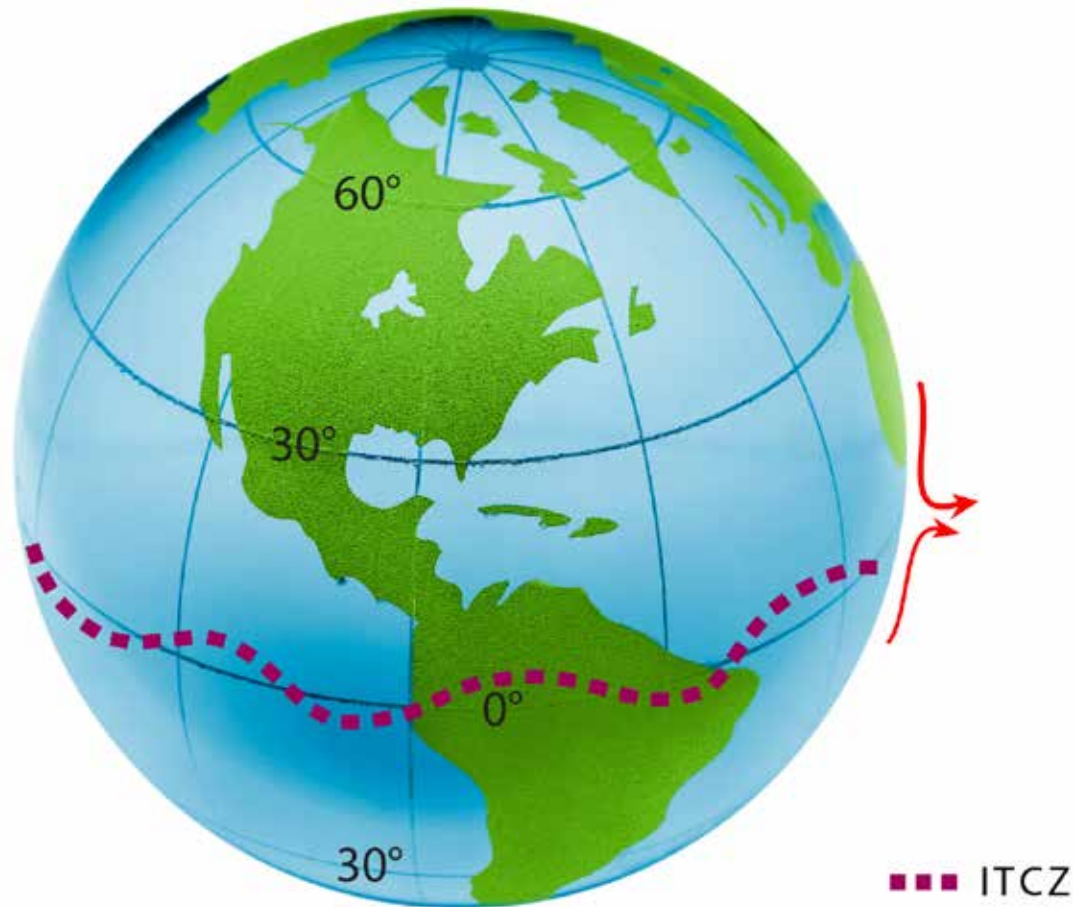


Figure 3.30. Air flows from high to low pressure and is deflected by the Coriolis Force. The Equatorial Low is a zone of surface convergence and uplift, an area known as the Intertropical Convergence Zone. The winds in this area, which are known as the Doldrums, are weak and variable. The pressure belts, including the Equatorial Low (Intertropical Convergence Zone), are not stationary. The Equatorial Low shifts northward during the Northern Hemisphere's summer when temperatures are warmer in the Northern Hemisphere. During the Northern Hemisphere's winter, the Equatorial Low shifts southward. In short, the pressure belts 'follow the Sun.'

**The Trade Winds.** The Trade Winds are located between the Equatorial Low pressure and the Subtropical High pressure belts (Figure 3.31). As the air at the surface moves from Subtropical Highs in the Northern Hemisphere toward the Equator, the Coriolis Force causes these winds to be deflected to the right, thus creating a belt of winds that tend to blow rather steadily from the northeast to the southwest — the Northeast Trades (Figure 3.32). In the Southern Hemisphere, the Coriolis Force deflects the wind at the surface to the left thus creating the Southeast Trades, where winds blow steady from southeast to northwest.

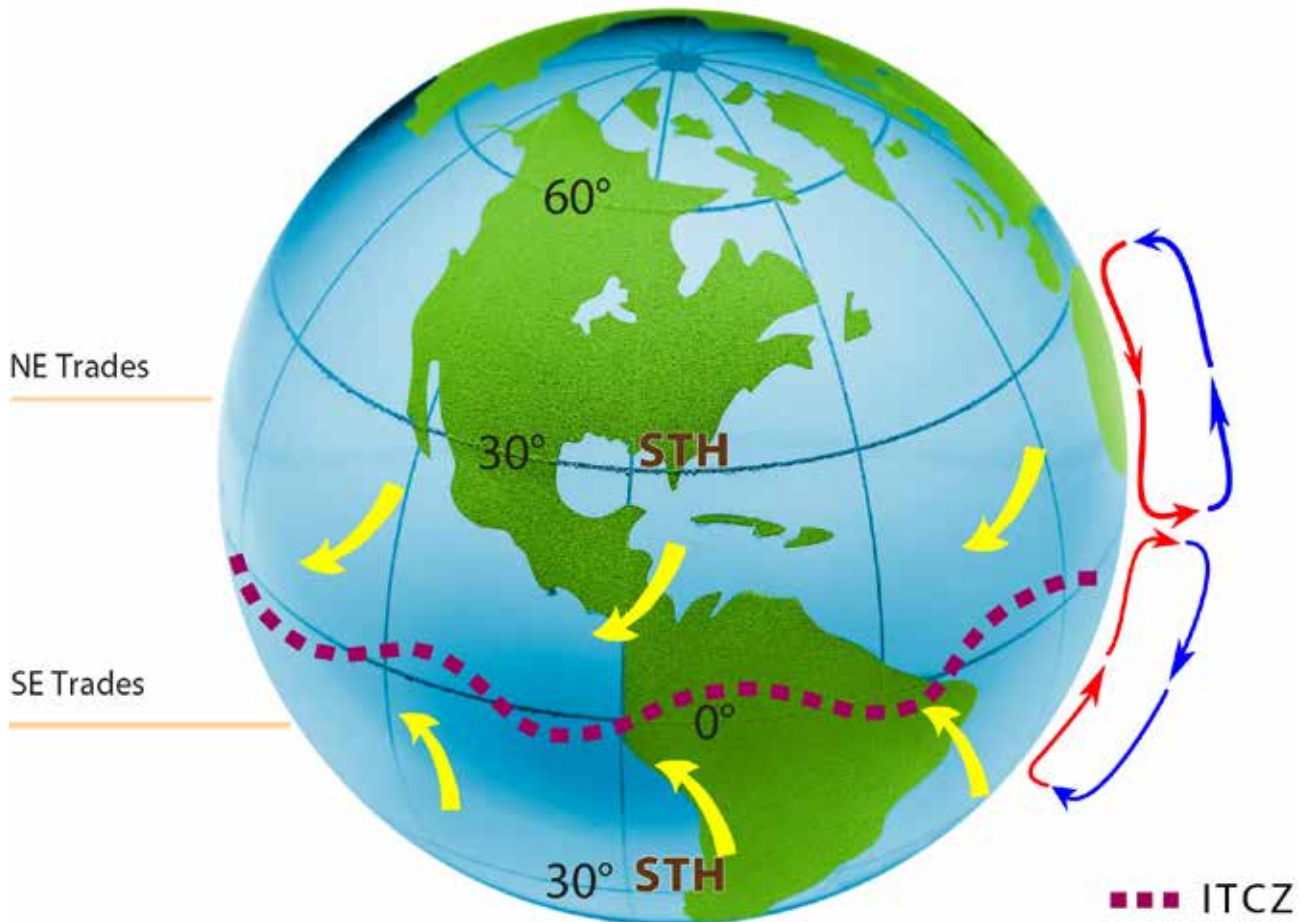


Figure 3.31. Low latitude circulation is driven largely by two large convection cells, the Hadley cells. Subsidence on the poleward margin of the Hadley cells generates the Subtropical High Pressure belt. The Trade Winds blow out of the Subtropical Highs toward the Equatorial Low. The Northeast Trade winds blow from the northeast, whereas the Southeast Trades blow from the southeast (Source/Credit: globe from iStockphoto.com).



Figure 3.32. Satellite image of the effect that the Canary Islands have on the Northeast Trade winds. The lighter-toned areas on the lee (downwind side) of the islands represent areas of quieter, more reflective water (Source/Credit: NASA).

The *Trade* portion of the name was given to this wind belt by early European sea captains headed to the New World. Five hundred years ago when wind was the primary power source for ships, those coming to the New World from Europe sailed south to points off the coast of Africa between the Equator and 30°N. Here they picked up the easterly winds that took them in a direction to the New World. These winds were generally found to be strong (Columbus made some 100 miles a day on his initial voyage), steady and highly reliable.

**The Prevailing Westerlies.** Poleward from the high pressure belt at 30°N/S, air is descending and moving poleward toward the belts of relatively low pressure at 60°N/S (Figure 3.33). As these winds move poleward, they too are deflected to the right (Northern Hemisphere) and left (Southern Hemisphere) by the Coriolis Force. As a result, the winds between 30°N and 60°N blow in a generally southwest to northeast direction. Those found between 30°S and 60°S blow in a generally northwest to southeast direction. Winds in both of these regions are known as the Prevailing Westerlies because the winds generally blow from west to east in both hemispheres.

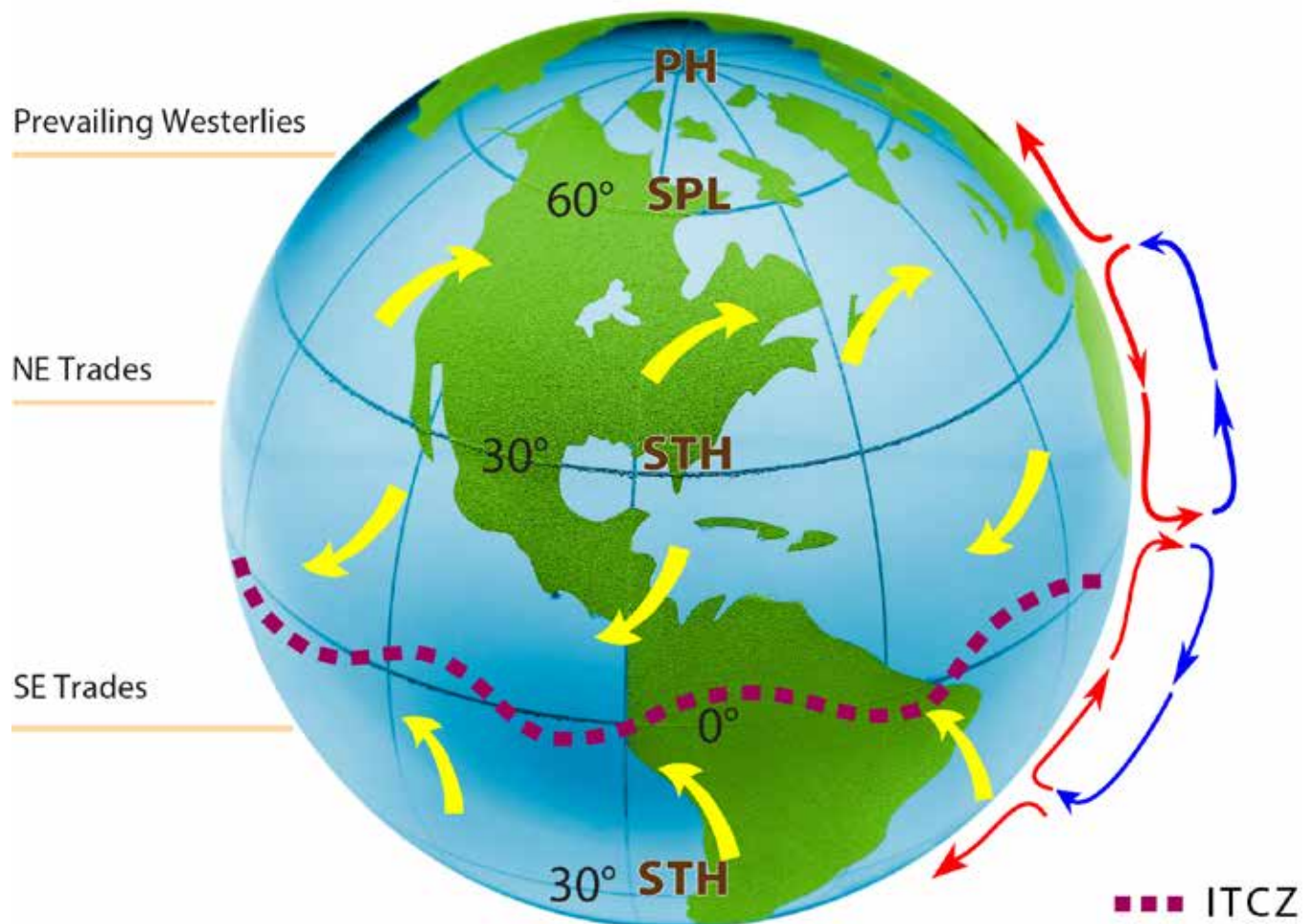


Figure 3.33. The Westerlies form on the poleward side of the Subtropical Highs in each hemisphere. The Coriolis Force deflects the wind to the right in the Northern Hemisphere and to the left in the Southern Hemisphere. The result of this deflection in both hemispheres is to send the wind from west to east. Most storms in the United States track from west to east because they are carried in this direction by the Westerlies.

Although they are discernable wind belts, the Prevailing Westerlies are less steady or persistent than the Trades. This is in large measure due to the greater temperature differences one encounters with changes in latitude, the presence of mid-latitude storms with their varying wind direction, and the monsoonal circulations around the large landmasses found in these latitudes.

While much of the year these latitudes are dominated by subtropical and tropical air masses, they are subject to invasion by much colder air from the higher latitudes. As a result, these latitudes are known for their frequent and sudden weather changes.

**The Horse Latitudes.** The Subtropical High pressure areas that give rise to the Prevailing Westerlies are sometimes referred to as the Horse Latitudes (Figure 3.34). Like the Doldrums, these are areas of variable winds, and calms were dangerous to sailors. The name is said to have had its origin with sailing ships becalmed for many days in this region. As a result, the crews often threw horses overboard to conserve water.

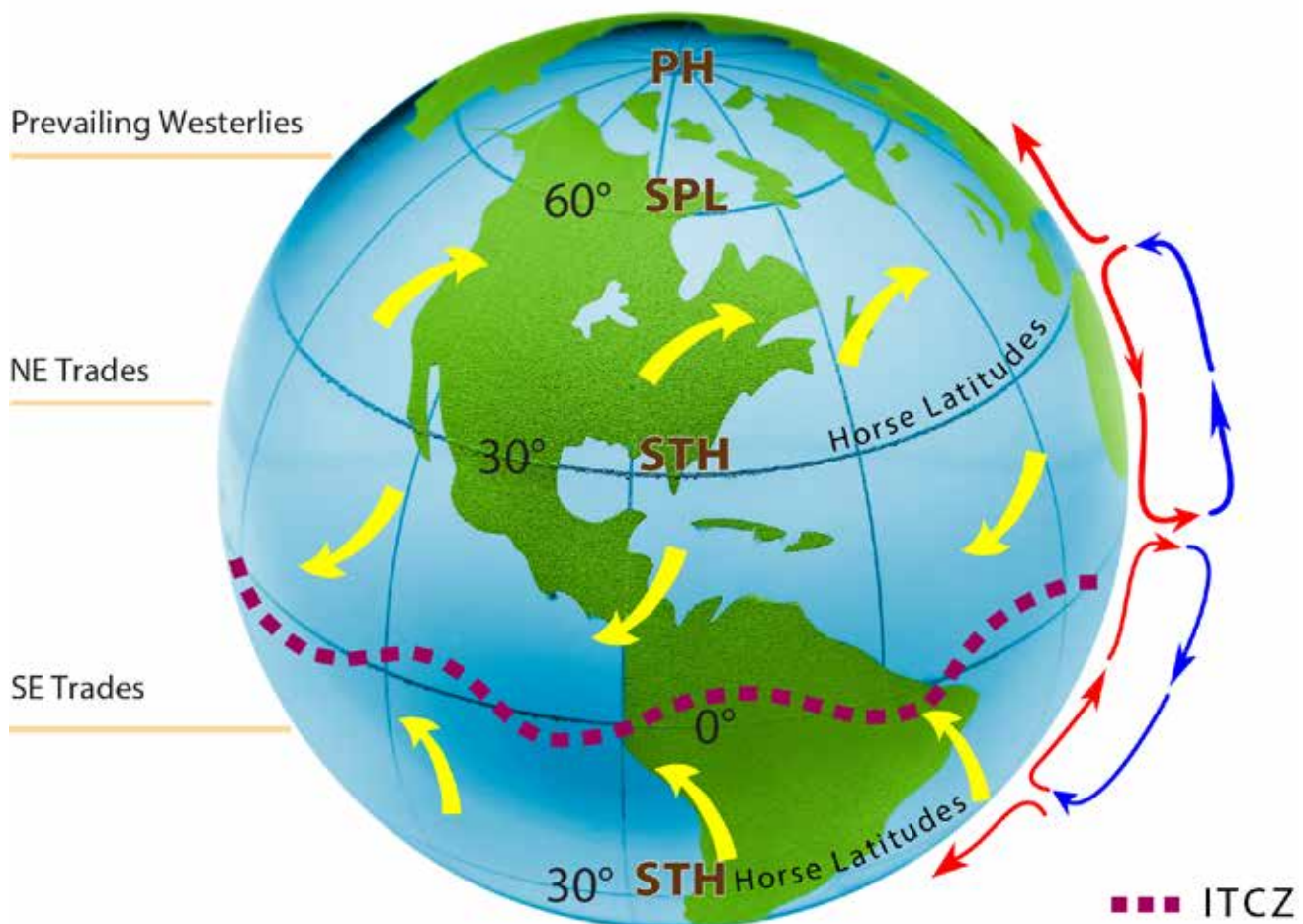


Figure 3.34. The Subtropical Highs are zones dominated by sinking air, and the winds in this area tend to be weak and variable. Legend has it that becalmed sailing ships often had to throw their horses overboard to conserve water; hence the name 'horse latitudes.'

**The Polar Easterlies.** Air flowing out of the Polar Highs is turned toward the west in both hemispheres by the Coriolis Force. Therefore, the wind generally flows from the east in the area between 60 and 90° in both hemispheres generating the Polar Easterlies (Figure 3.35). The **Polar Front Zone**, which is located between 60° and 65°N/S in the region of the Subpolar Low, is characterized by unpredictable and stormy conditions (Figure 3.36). The storms result from the rapid uplift of warmer, more moist air (carried northward by the Westerlies) that occurs when this air collides with the cold, dry Polar Easterlies.

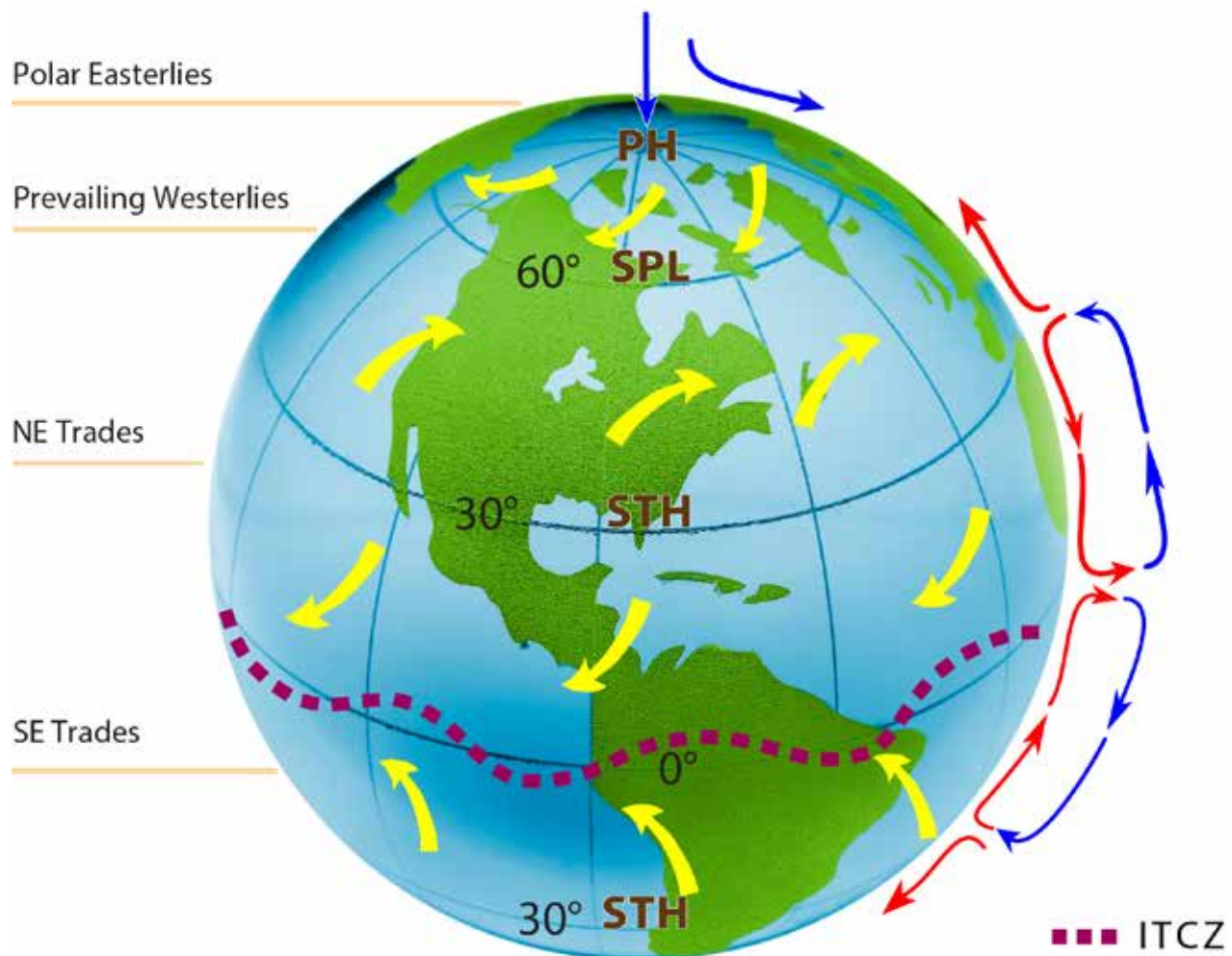


Figure 3.35. Cold, dry, dense air at either pole tends to form high pressure domes called the Polar Highs. Air diverges from the Polar Highs toward the mid-latitudes and is turned by the Coriolis Force, creating the Polar Easterlies in both hemispheres.



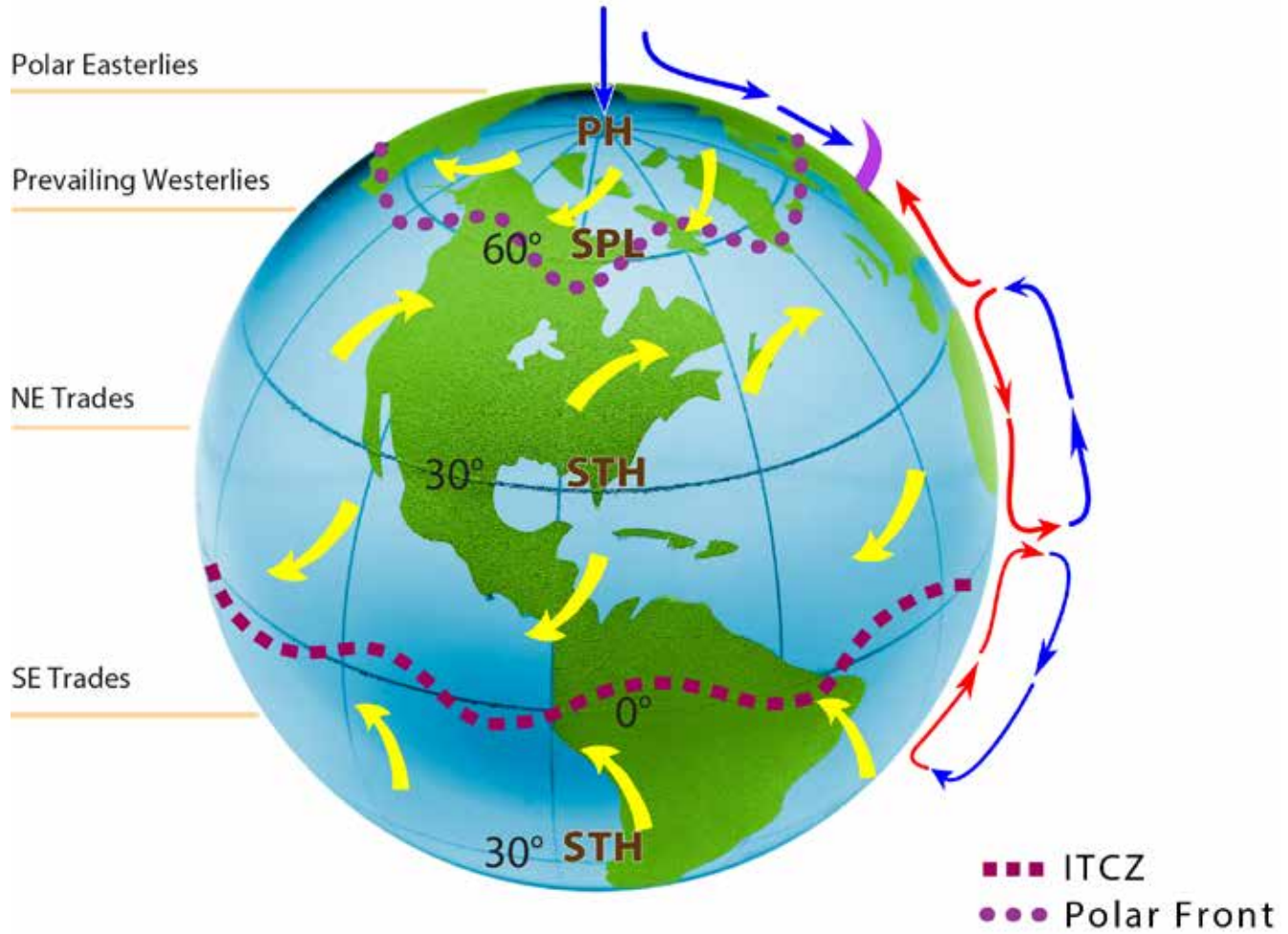


Figure 3.36. Between the Polar High and the Subtropical High is a sinuous belt of convergence known as the Subpolar Low. This is the birthplace of frontal cyclones. These migrating low pressure systems form where cold, dense air meets with warmer subtropical air, causing extensive uplift and storminess.

The idealized pattern of global pressure and wind belts is complicated somewhat by the effects of large landmasses and by seasonal changes in insolation. The continents and oceans heat and cool at different rates, and the result is that large land masses experience seasonal reversals in pressure and winds. Instead of continuous belts of pressure and winds, the pressure belts can be more accurately characterized as being composed of cells of high pressure (anticyclones) and low pressure (cyclones). Over the low-latitude ocean basins, however, the Hadley Cell circulation dominates virtually year-round, generating the quasi-permanent Subtropical Highs in all five major ocean basins (Figure 3.37, 3.38a and 3.38b).

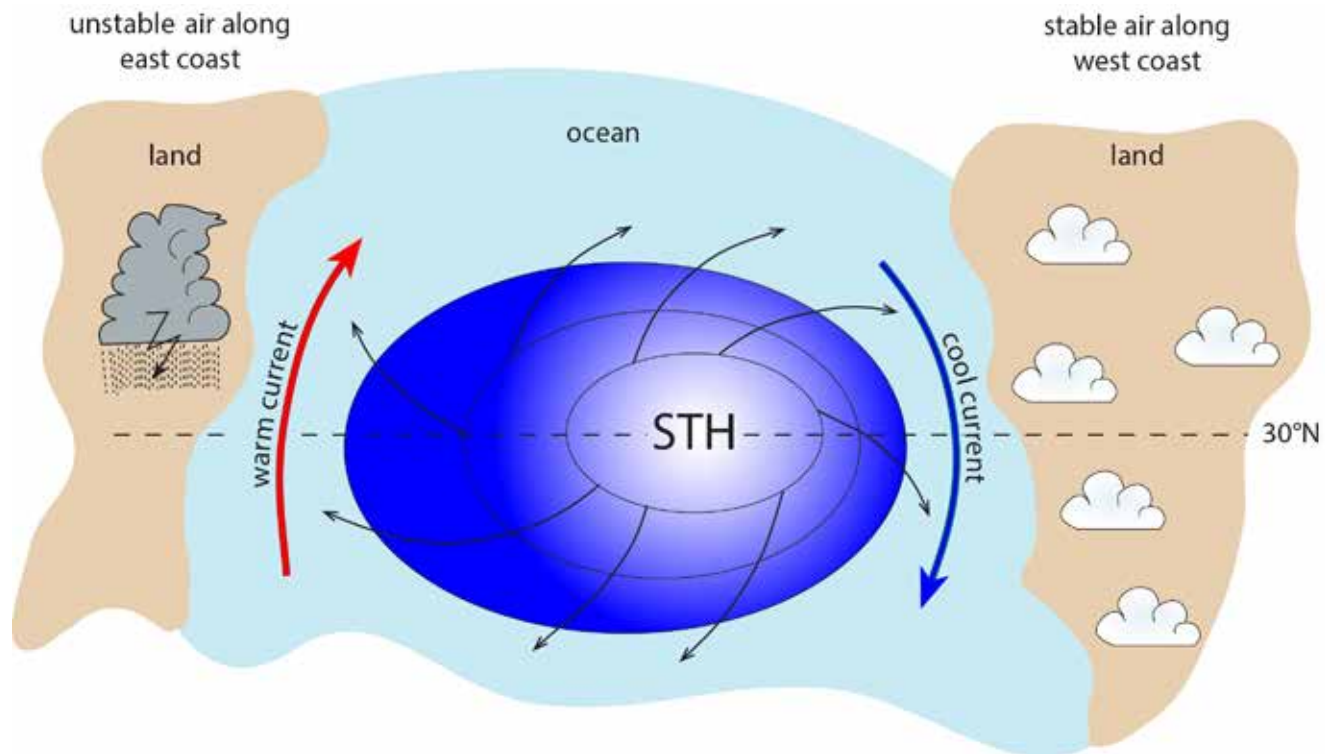


Figure 3.37. One of the more permanent features of global pressure in the existence of quasi-permanent oceanic Subtropical Highs over the major ocean basins. They dominate the ocean basins at about 30 degrees latitude in the north and south Atlantic, the north and south Pacific, and the Indian Ocean Basins. The Westerly winds blow from their poleward side and the Trades from their equatorial side in both hemispheres (Source/Credit: modified from Dennis I. Netoff and Ava Fujimoto-Strait, *Weather & Climate Lab Manual*).

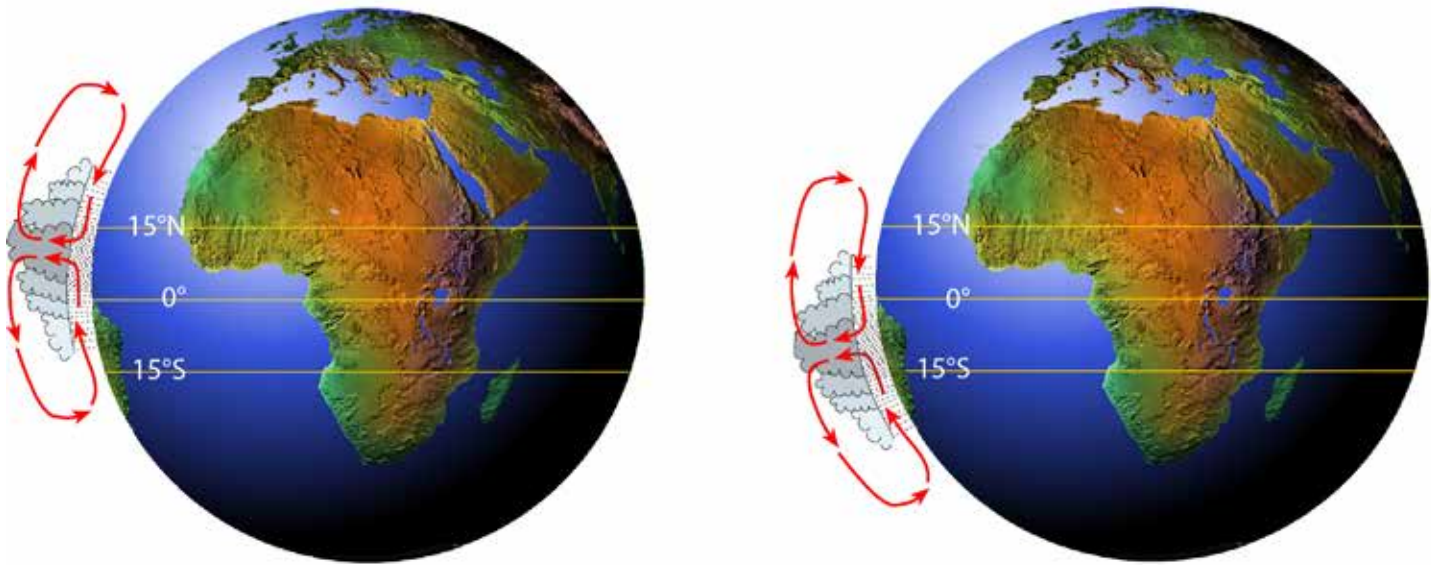


Figure 3.38a. (left) The Hadley cells migrate north and south with the change in the vertical rays of the Sun. During the Southern Hemisphere summer (above), both Hadley cells have migrated slightly toward the south, causing considerable displacement of the Subtropical Highs, the ITCZ, and the Trade Winds (Source/Credit: globe from iStockphoto.com).

Figure 3.38b. (right) The Hadley cells migrate north and south with the change in the vertical rays of the Sun. During the Northern Hemisphere summer (above), both Hadley cells have migrated slightly toward the north, causing considerable displacement of the Subtropical Highs, the ITCZ, and the Trade Winds (Source/Credit: globe from iStockphoto.com).

The **Aleutian** and **Icelandic Lows** are cyclonic systems that occur in the North Pacific and North Atlantic, respectively (Figure 3.39). They are best developed during the winter season because the ocean water at high latitudes remains significantly warmer than the land at corresponding latitudes, and also because these are preferred tracks of traveling low pressure cyclones. Airflow is convergent, counter-clockwise, and ascending, creating a broad region of foul weather. These areas are notorious for severe winter weather and prolonged periods of cloudy skies.

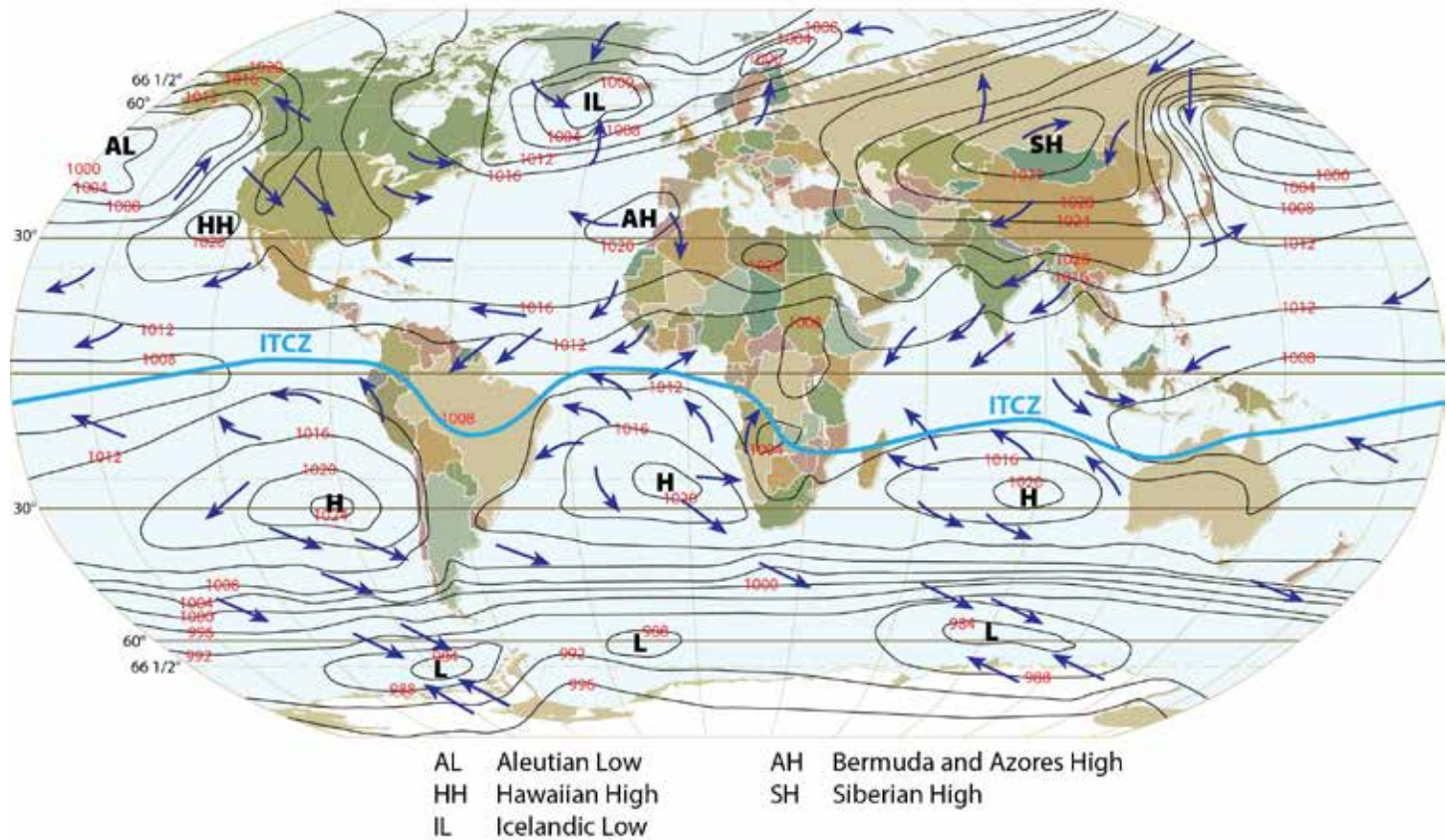


Figure 3.39. The locations of the semi-permanent cyclones and anticyclones during January. At this time of the year, the land masses in the Northern Hemisphere are colder than the oceans at high latitude. As a result, strong anticyclones (Siberian High and Canadian High) develop over the continents and strong cyclones develop over the oceans at high latitudes, the Aleutian Low and Icelandic Low. These low pressure areas are notorious for severe storms (Source/Credit: modified from NOAA).

Over the continents, where winter temperatures are cold, anticyclones develop. The **Canadian High** forms over the northern Canadian Plains. A much more dominant anticyclone, the **Siberian High**, develops over Russia. The Siberian High is particularly strong because of the sheer size of the Eurasian landmass which intensifies the effects of continentality.

During the summer, the Icelandic and Aleutian Lows diminish greatly in intensity, or disappear altogether, because the water is cool relative to the adjacent land, and frontal cyclones are less intense because of the shrinkage of the Polar High (Figure 3.40). Circulation of the Hadley Cell remains strong over the oceans, and the subtropical highs persist. They are known as the **Pacific High** (or **Hawaiian High**) and **Bermuda-Azores High**, respectively.

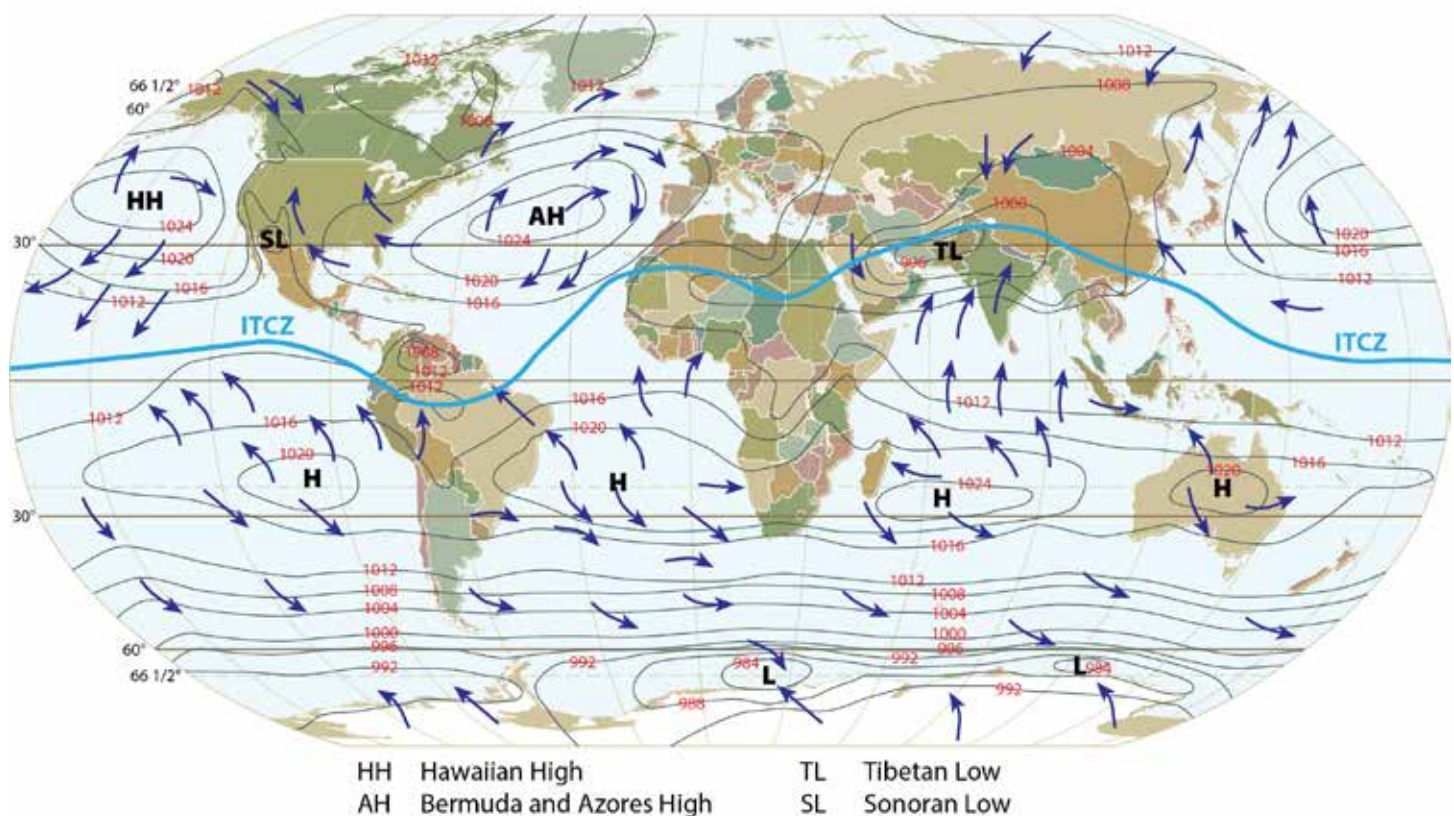


Figure 3.40. During the summer, the land becomes warmer than the oceans and low pressure systems develop over the continents. At high latitudes over the oceans, the Aleutian and Icelandic Lows weaken; but, further south, where the water is substantially cooler than the land, the Bermuda High and Pacific High pressure systems develop and intensify (Source/Credit: modified from NOAA).

In summary, the existence of the continents and ocean basins modifies the location and intensity of the pressure belts and associated wind belts. Local conditions, however, sometimes override the planetary pressure and wind systems, creating local or regional winds that are typically not as persistent or predictable as those of the planetary system.

## Local Winds

- **Land and Sea Breezes.** These are coastal breezes generated by changing temperature and pressure conditions along the coast during the day. They are caused by the differential heating and cooling of land versus water, and the pressure cells generated are often referred to as *thermal highs* and *thermal lows*. They are best developed during summer days when the skies are clear and a weak regional pressure gradient exists. During the day, the land heats faster than the adjacent water and generates low pressure over the land. This causes air to blow from the sea (higher pressure) toward the land forming a sea breeze (Figures 3.41). At night or in the early morning, the land becomes cooler than the water setting up high pressure over the land and a land breeze (Figure 3.42).

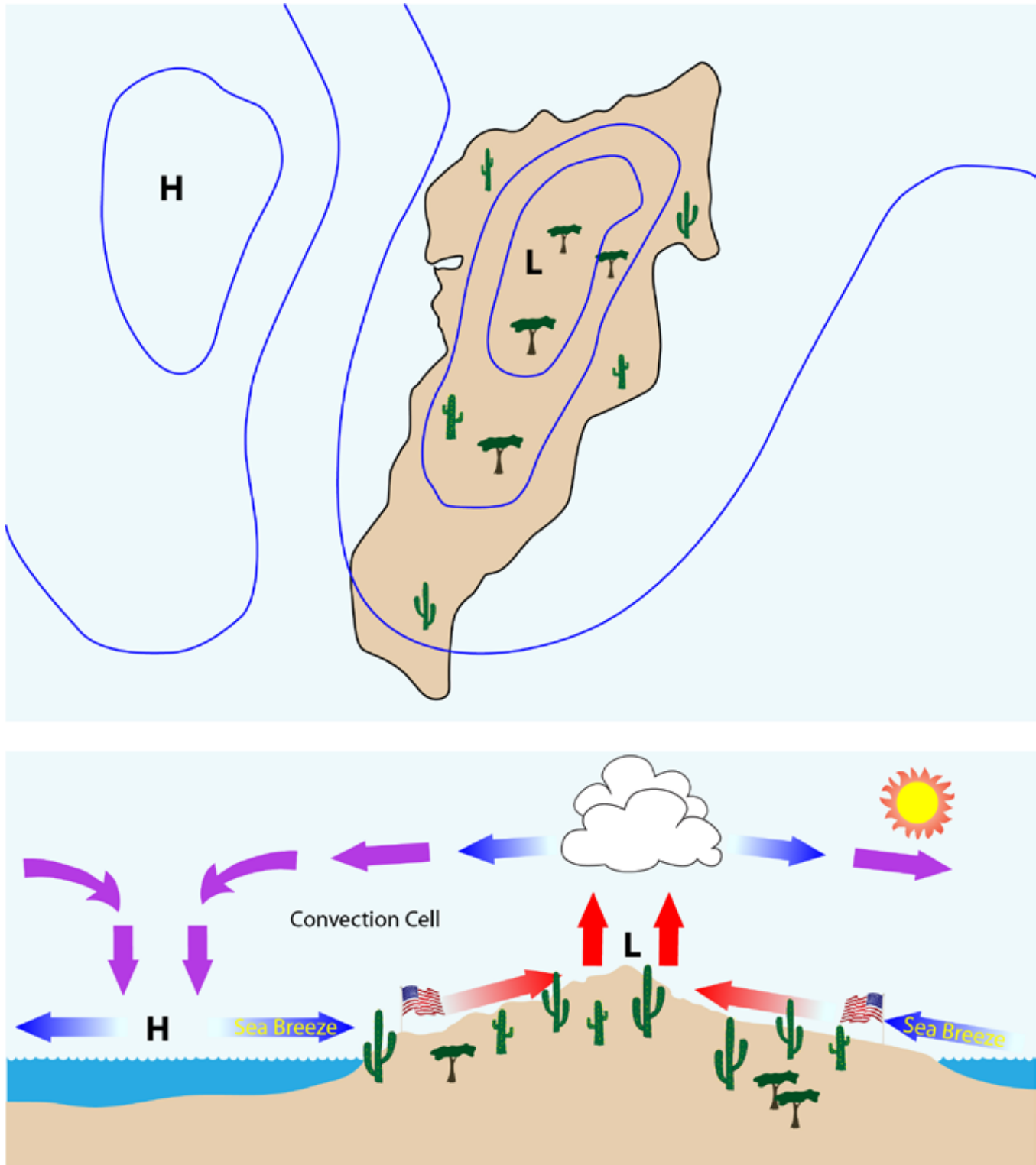


Figure 3.41. Differential heating of land and water sets up a local wind system called the land and sea breeze. During the middle of the day, land becomes warmer than the adjacent water, so the air over the land is rarefied (less dense), setting up a thermal low pressure over land (upper map sketch). The pressure gradient from water to land sets up a **sea breeze** (coming from the sea). The rarefied air over the land becomes buoyant and rises (cross-section below). Uplift may form convective clouds. At some height, the pressure gradient typically reverses, and the air aloft over the island diverges and flows away from the island. The air aloft cools during divergence, eventually becoming dense enough to subside over the sea, completing a convection cell (Source/Credit: Dennis I. Netoff).

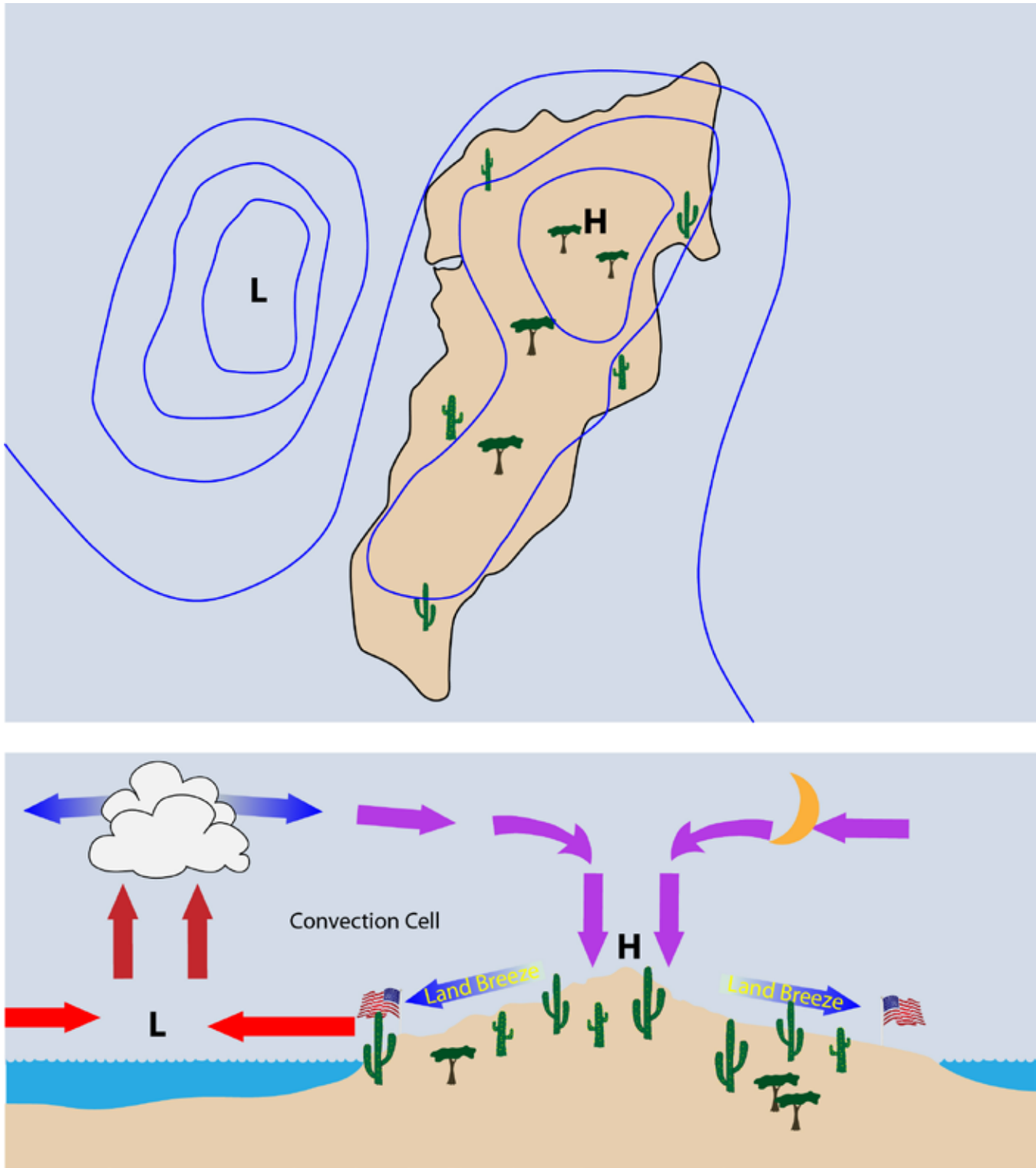


Figure 3.42. Differential heating of land and water sets up a local wind system called the land and sea breeze. During the middle of the night and early morning, land becomes colder than the adjacent water, so the air over the land becomes dense, setting up a thermal high pressure over land (upper map sketch). The pressure gradient from land to water sets up a **land breeze** (coming from the land). The rarefied air over the sea becomes buoyant and rises (lower cross-section). Uplift may form convective clouds. At some height, the pressure gradient typically reverses, and the air aloft over the sea diverges and flows toward the island. The air aloft cools during divergence, eventually becoming dense enough to subside over the land, completing a **convection cell** (Source/Credit: Dennis I. Netoff).



These breezes can develop not only along ocean coasts, but along large lake coasts as well, such as those around the Great Lakes. These winds can also have a significant effect on temperature. For example, Chicago's eastern strip has been known to cool 18°F in one hour as a result of winds blowing off Lake Michigan during the daytime.

- **Mountain and Valley Breezes.** These are winds that develop in response to differential heating of mountain slopes over the course of a day. During the morning, the eastern side of a mountain will experience the most direct rays of the Sun because of the combination of both aspect and slope angle. As a result, the sides of the mountain warm and cause low pressure to be generated. Air therefore flows toward the mountain and up its sides creating a valley breeze (Figure 3.43).



Figure 3.43. During the day, rocky mountain slopes heat rapidly, causing the air to expand and rise. The rising air on the mountain slopes draws air up-valley, forming the **valley breeze** (Source/Credit: Dennis I. Netoff).

With nightfall, the rarified mountain air quickly cools and becomes dense as it flows from the mountain summits to the valley floors creating mountain breeze (Figure 3.44).



*Figure 3.44. At night, the low-density air above the mountains cools quickly, and so the air begins to flow down the mountain producing a **mountain breeze** (Source/Credit: Dennis I. Netoff).*

As with land and sea breezes, these breezes require fair weather with weak regional pressure gradients in order to develop. Also, like any wind, they are named in the direction that they are coming from.

- **Chinook.** These winds are among the most intense winds associated with mountain ranges. In the United States, they are called *chinooks* which is a Native American word that means snow eater because of the ability of these warm winds to melt deep snows in a short period. In the Alps, the same type of wind is called a **foehn wind** (Figure 3.45).



Figure 3.45. In response to a regional pressure gradient, air will flow over mountains. As it flows down the lee side of the mountains to lower elevations, it is heated adiabatically by compression. As will be discussed in Chapter 4, this decreases the relative humidity of the air. The combination of both effects produces a hot, dry wind known as a chinook. Because the United States is located in the Westerlies, most chinooks occur on the eastern side of the mountains, such as at Denver, located on the eastern slopes of the Rockies.

Chinook winds develop in response to a regional pressure gradient that causes air to rise up and over a mountain and then flow down its side. On the way up the mountain, moisture may be lost as a result of cooling and precipitation, thereby making the air dry. Condensation of moisture on the windward side of the mountain will add heat energy to the air through the release of latent heat of condensation. Then, as the air moves down the mountain, it is heated by compression (adiabatic temperature change), thereby making it both hot and dry.

The changes in temperature and humidity as well as the wind velocities caused by these winds can be phenomenal, especially if the wind moves back and forth across the landscape during cold, winter conditions. For example, in 1943 a South Dakota chinook caused the temperature to rise 49°F in just two minutes. In Granville, North Dakota in 1918, a chinook caused the temperature to rise from minus 33°F to 50°F (83°) in just six hours. The rapid snowmelt they sometimes cause can lead to severe flooding, and the strength of the wind

can cause damage to buildings. Wind damage from chinooks costs the city of Boulder, Colorado an average of one million dollars per year. During an intense winter chinook in Boulder, the National Center for Atmospheric Research had its anemometer destroyed while measuring winds at 150 mph. Chinooks are often accompanied by wave clouds (Figures 3.46) and dust storms (Figures 3.47).



Figure 3.46. Chinook winds are often accompanied by a variety of streamlined clouds, collectively called **wave clouds**. The one shown is a **chinook arch**, and occurred during a strong chinook over Reno, Nevada in March 2014. Wave clouds form along the top of a series of standing waves in the atmosphere that are created by the flow of relatively stable air over large obstructions, such as mountain barriers (Source/Credit: Dennis I. Netoff).



*Figure 3.47. Chinook winds often kick up vast clouds of dust along the leeward base of mountains, particularly in desert environments such as here in an abandoned lake bed at Cold Springs, Nevada (Source/Credit: Dennis I. Netoff).*

- **Santa Ana.** The southern California Santa Ana is similar to the chinook in that it also creates strong, gusty winds, unseasonably high temperatures, and very low relative humidities. The principal difference between the two local winds is that the Santa Ana is warmed only by compression, whereas many chinook winds gain some heat through due to condensation. Both types of wind are considered a variety of downslope, or katabatic (Greek, to flow downhill) wind.

The setup for Santa Ana winds is a high pressure system that develops to the northeast of California, typically in the Great Basin of Nevada and Utah, and sometimes as far away as the Colorado Plateau and Southern Rockies (Figure 3.48). In order for this to occur, local influences on pressure and winds must overcome the dominant Westerlies that emanate from the oceanic Subtropical High. Strong pressure gradients in southern California may bring gusty winds to the Mojave Desert



Figure 3.48. The typical setup for the Santa Ana winds is the generation of a high pressure system in the Great Basin (as above), or as far east as the Colorado Plateau or Southern Rockies (Source/Credit: modified from NASA).

As the air flows over the San Gabriel and San Bernardino Mountains, it is accelerated by gaps in the mountains, such as Cajon Pass and Banning Pass. Winds velocities in these passes commonly reach 70 mph (113 km/hr), and occasionally top 100 mph (161 km/hr). As the air descends the southern side of the mountains, it is heated by compression at the rate of nearly 5.5°F per 1000 feet of descent (Figure 3.49). Heating not only drives up temperatures, but reduces relative humidity, which typically drops down to the teens or single digits.

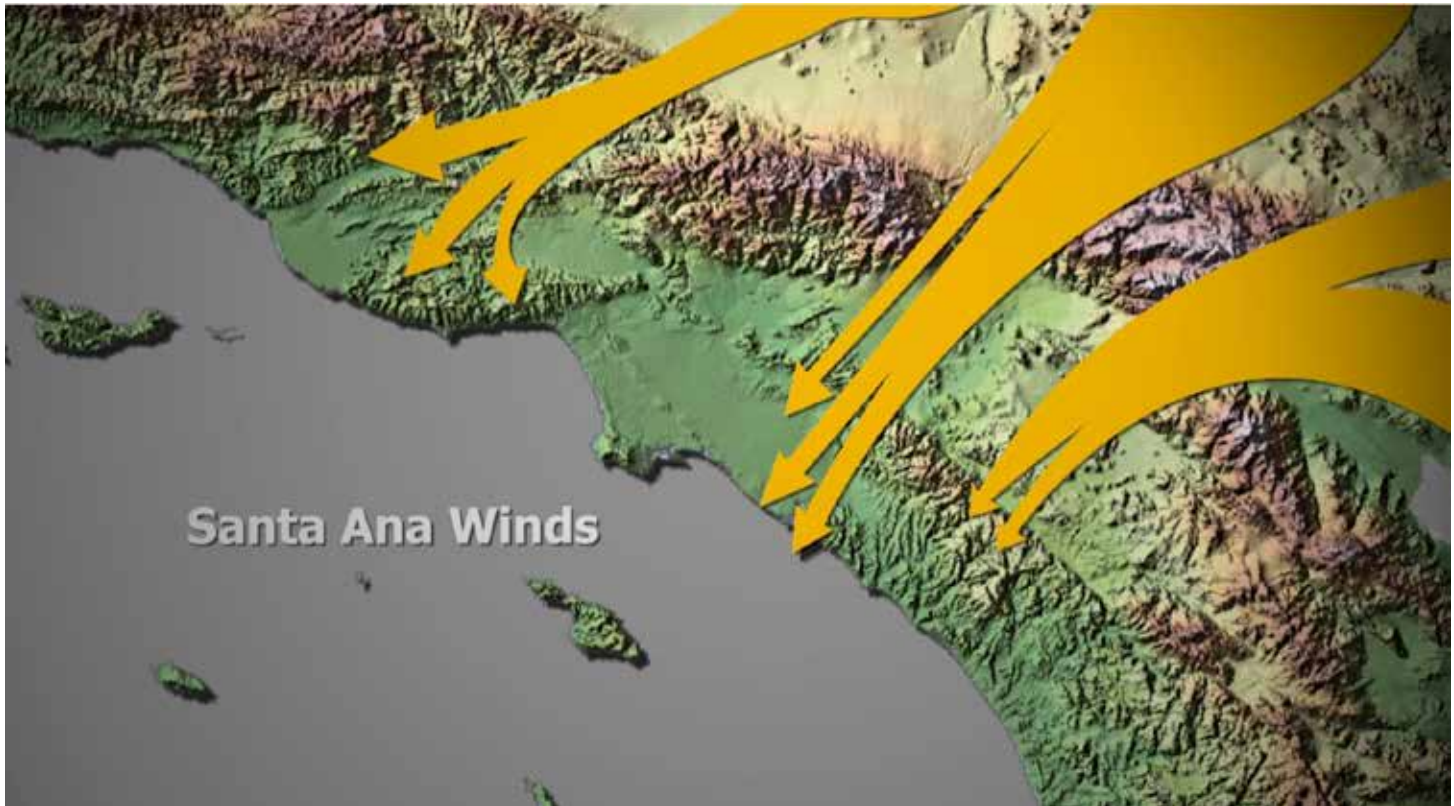


*Figure 3.49. The Santa Ana wind forms when high pressure develops over the continental interior and flows westward toward the coast bringing strong winds to cities located there, such as Los Angeles. Santa Ana winds are hot, dry winds, and because Southern California is normally dry, the combination can fan fires into major firestorms.*

Major canyons that are oriented in the same direction as the pressure gradient force, such as Carbon Canyon, San Mateo Canyon, and Santa Ana Canyon (for which the wind is named) tend to funnel the air flow, maintaining very strong wind velocities into the Los Angeles Basin and out to sea. Wintertime temperatures in places such as Los Angeles and Santa Ana, can jump to 90-100°F from their 70°F average.

The most serious hazard associated with the Santa Ana winds is wildfire (Figure 3.50). The dry summer climate and woody chaparral vegetation make the mountain slopes susceptible to wild fires, especially prior to the winter rains. A Santa Ana-fired blaze burned over 700,000 acres (~2900 sq. km.) in 2003 and 500,000 acres (~2000 sq. km.) in 2007. Dust storms also present problems during Santa Anas (Figure 3.51). Other hazards include downed power lines, debris flows, flipped 18-wheelers, smoke, and high surf. There are also benefits of the Santa Ana winds. One is that the offshore flow of air causes surface water to move seaward, which is replaced by upwelling of nutrient-rich water, providing more food for the marine food chain.



*Figure 3.50. Santa Ana winds are notorious for creating wildfire weather. The hot, dry, gusty winds often fan major wildfires, some of which last for days to weeks. The above image shows several plumes of smoke that are carried for into the Pacific Ocean by strong chinooks on October 26, 2003 (Source/Credit: NASA).*





Figure 3.51. The Santa Ana winds are the cause of major dust storms in Southern California and northern Mexico. The image shows a dust plume on October 21, 2007 that originated in the Real del Castillo agricultural valley in northern Baja Peninsula, Mexico. Warm, dry, gusty winds leave the soil susceptible to wind erosion (Source/Credit: International Space Station/NASA).

The Santa Anas have influenced the pop culture in Southern California. The Beach Boys released *Santa Ana Winds* in 1980, and mystery writer Raymond Chandler wrote *Red Wind* in 1938. Other references to the Santa Anas have been made by the Doors, Poco, Elton John, Randy Newman, and Steve Goodman.

- **Sundowner.** A local variant of the Santa Ana is the Sundowner, which is a name given to the wind by residents in and near Santa Barbara, where it commonly occurs near sundown. The setup for a Sundowner is much like that of the Santa Ana, except that the high pressure system is typically in the Pacific Ocean rather than far inland. Winds flow across the Central Valley of California, up and over the Santa Inez Mountains, and generate warm, dry, gusty conditions in places such as Santa Barbara and Goleta (Figure 3.52).

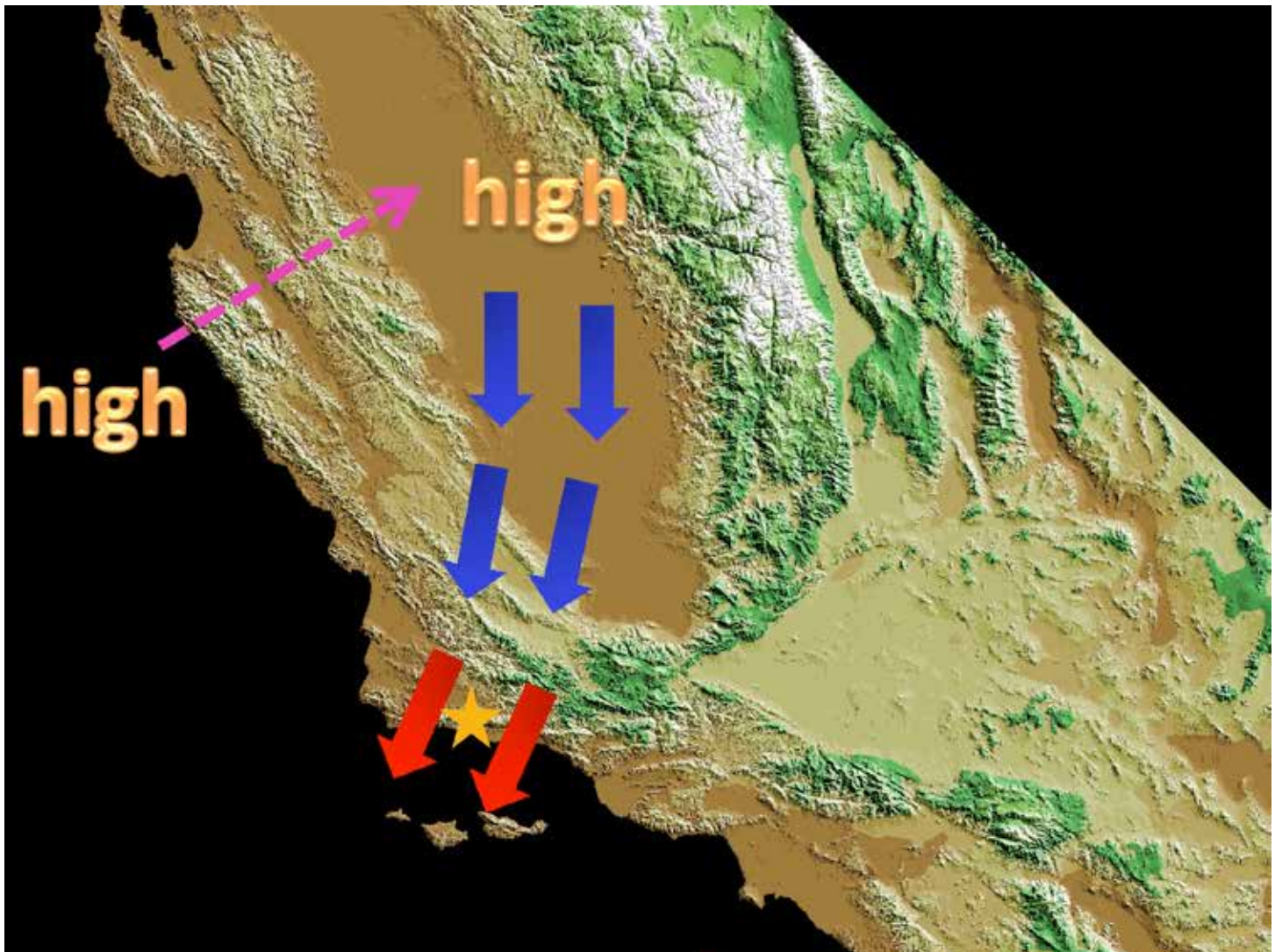
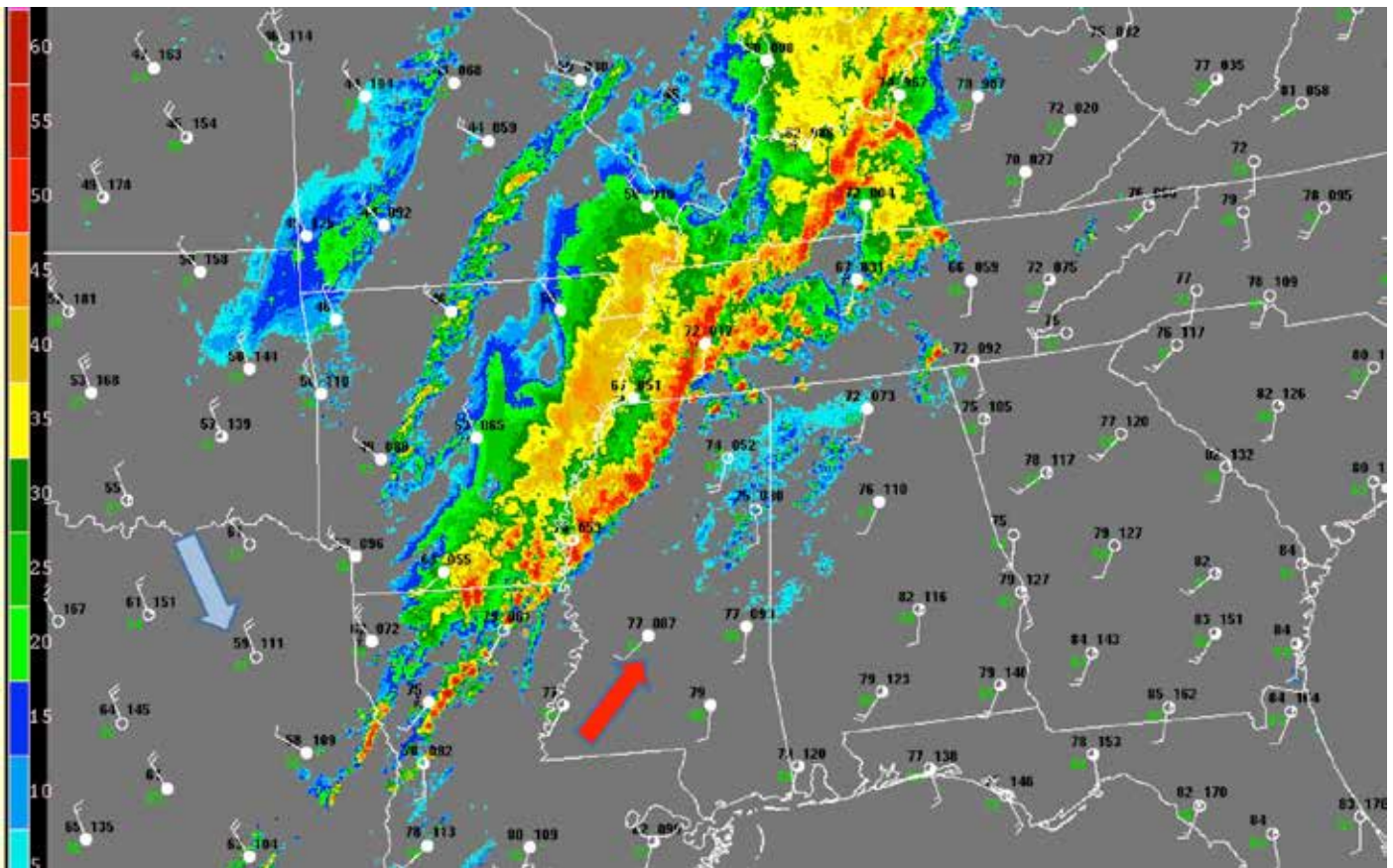
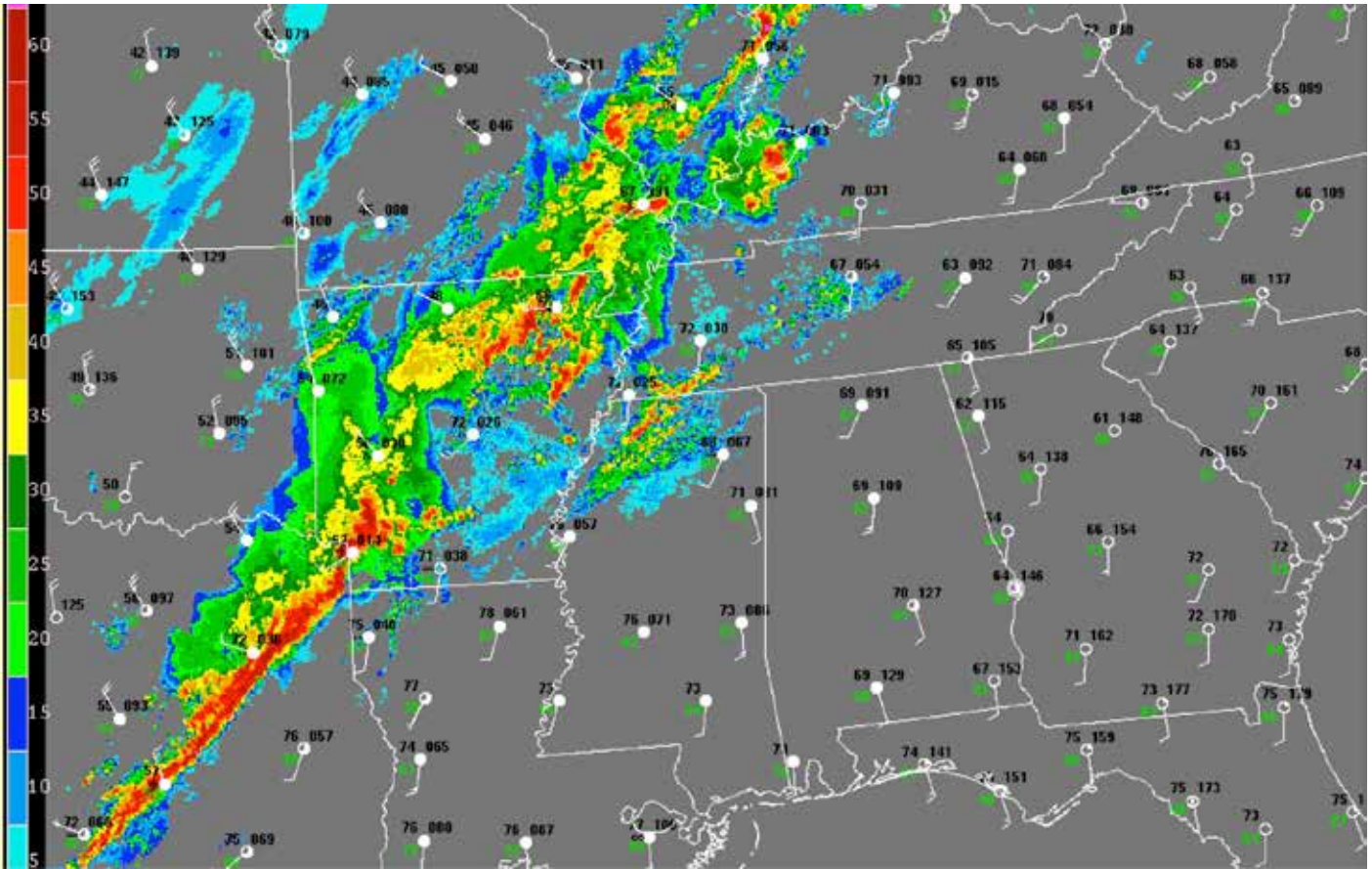


Figure 3.52. The Sundowner, which is a name given to the wind by residents in and near Santa Barbara, where it commonly occurs near sundown. The setup for a Sundowner is much like that of the Santa Ana, except that the high pressure system is typically in the Pacific Ocean rather than far inland. Winds flow across the Central Valley of California, up and over the Santa Inez Mountains, and generate warm, dry, gusty conditions in places such as Santa Barbara (Source/Credit: modified from USGS image).

A Sundowner on June 27, 1990 is responsible for setting the official modern high temperature record for Santa Barbara at 109°F (43°C). The most famous Sundowner and one of the most astonishing unofficial weather events in history occurred on June 17, 1859. Morning temperatures hovered in the mid-to upper 70s, and began to slowly increase until

about one o'clock in the early afternoon. A sudden, hot blast of air from the north sounded the arrival of the Sundowner. At two o'clock, the temperature measured on the coast and in the harbor by a Coast Guard engineering boat registered 133°F, where it hovered for nearly three hours. The burning wind knocked birds out of the sky, killed livestock, generated toxic dust clouds, burned fruit off trees, and ruined gardens. Most residents were spared as they fled to relative safety in thick-walled adobe structures. By five o'clock, the temperature dropped to 122°F, and finally by seven, cooled to a near-normal 77°F.

- **Derechos.** Derechos (Spanish, *direct/straight ahead*) are a special type of severe wind generated by a cluster of thunderstorms. Derechos form a linear or bow-shaped plan-view pattern and can continue for hours in a straight line (Figure 3.53, 4 images). They form a broad band of storms that can travel hundreds of miles maintaining a swath over 240 miles (400 km) wide. They are essentially a large, long-lived series of squall-line thunderstorms, but generate straight-line wind damage, as opposed to tornadic squall lines. They have been described as *families of downburst clusters*.



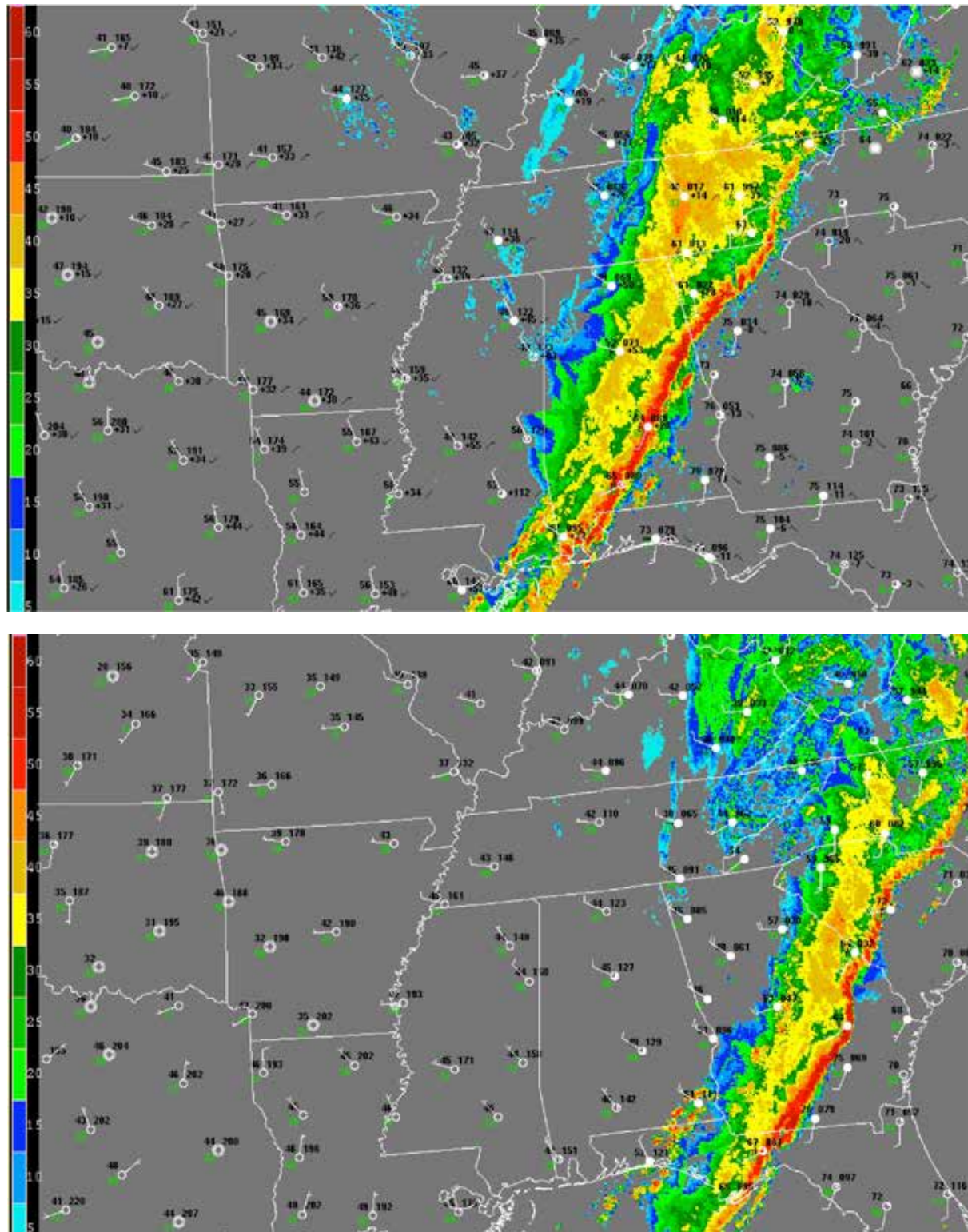


Figure 3.53. This series of radar images show the development and movement of a derecho – producing convective system and a frontal squall line on April 4-5, 2011. The time interval from the first to the last image is nearly 24 hours. Some surface data is shown by standard station model data, including wind direction and speed, temperature, and dewpoint. For example, in northeast Texas behind the derecho the temperature is 59°F, the dewpoint is 41, and winds are out of the northwest at 20 knots (~23 mph). In Mississippi, ahead of the derecho (red arrow), the temperature is 77, the dewpoint is 67, and the winds are out of the southeast at 10 knots (blue arrow) (Source/Credit: NOAA/NWS/NCEP/Storm Prediction Center).

Derechos are more common in North America than elsewhere. They most frequently occur in a belt from the southern Great Plains to the Great Lakes (Figure 3.54). Maximum activity tends to be in the late spring and summer, somewhere between maximum tornado and thunderstorm frequencies (Figure 3.55). Some derechos are associated with *mesoscale convective complexes*, a large-scale array of severe storms that is more common in the United States than elsewhere.

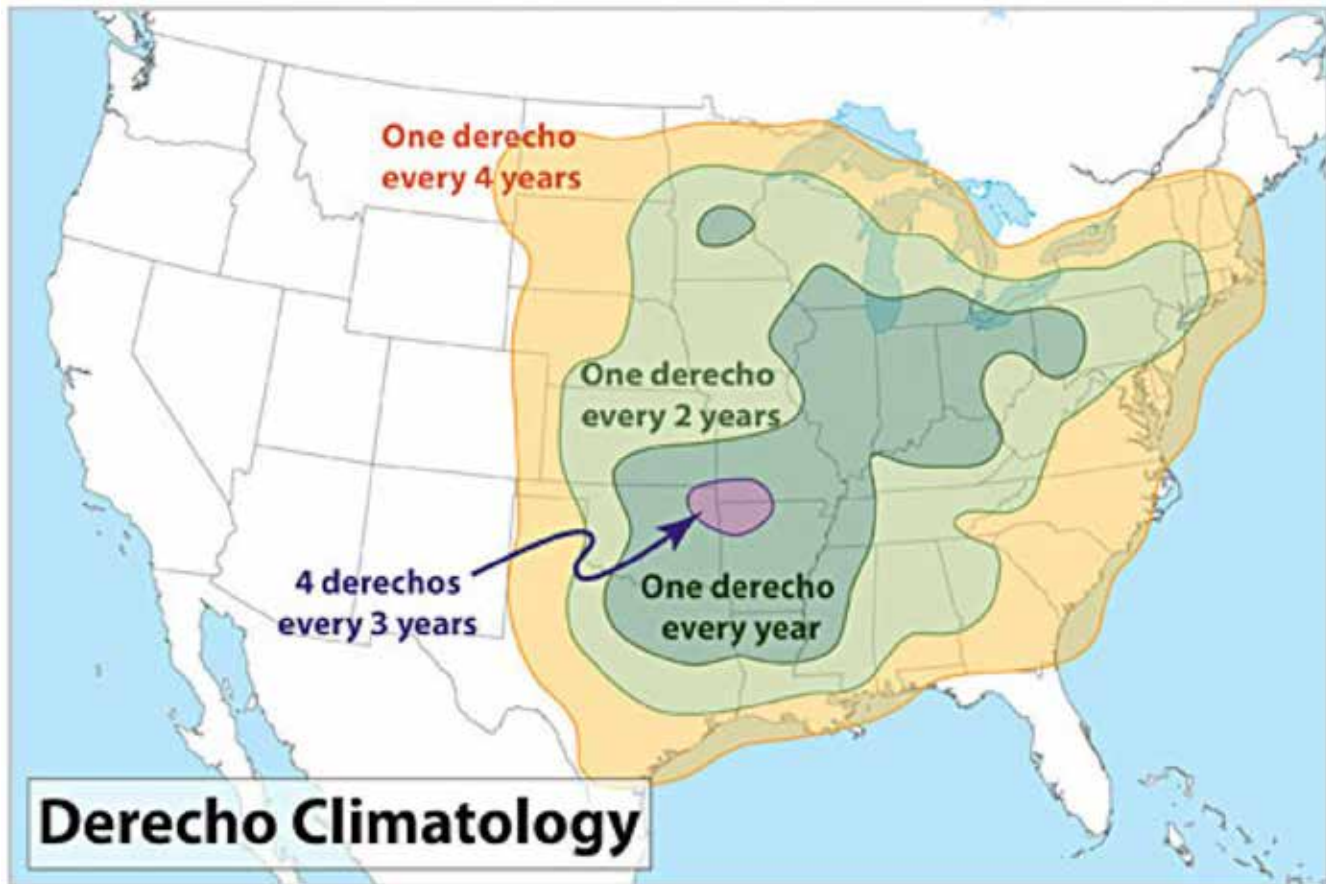


Figure 3.54. Derechos occur most frequently in a zone from the southern Great Plains of the United States to the Great Lakes. Derechos are almost unknown in the western United States (Source/Credit: NOAA/NWS/NCEP/Storm Prediction Center).

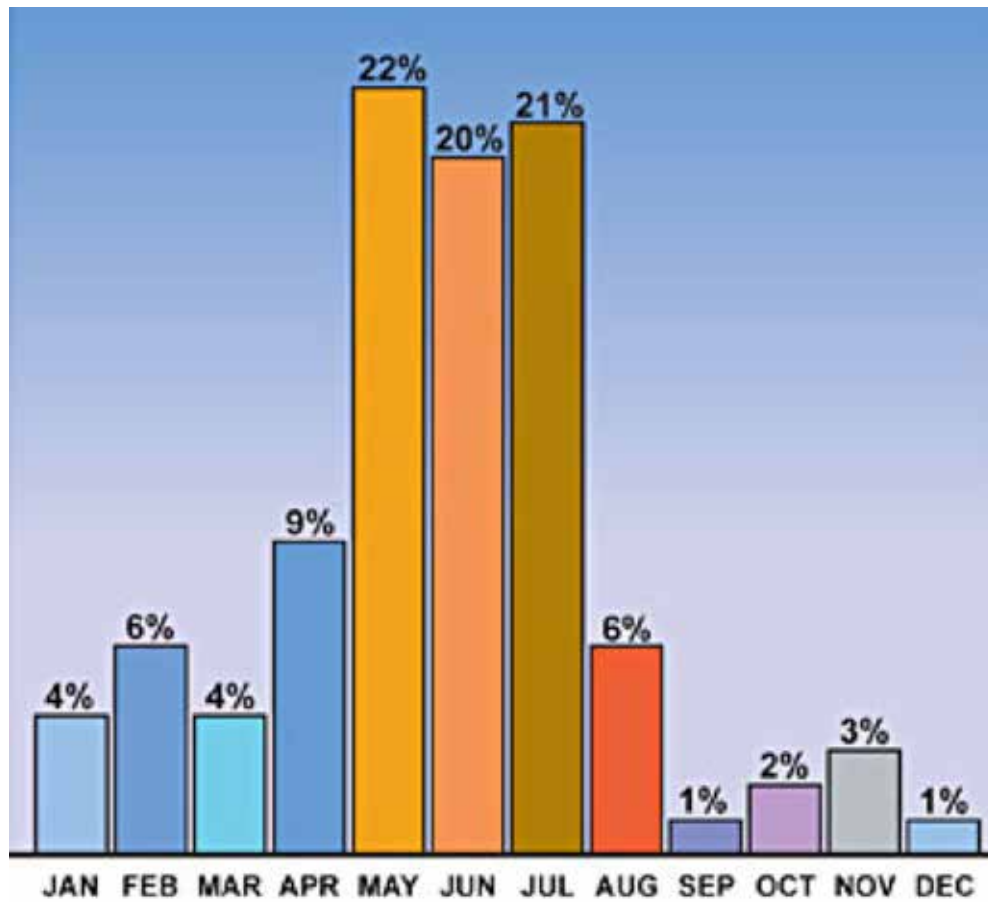


Figure 3.55. The bar graph depicts derecho frequency in the United States by month. Maximum activity occurs during the months of May, June and July, although derechos can occur in any month (Source/Credit: NOAA/NWS/NCEP/Storm Prediction Center).

- **Katabatic (drainage) Winds.** Antarctica and Greenland, both ice-covered, flat-surface plateaus, are well known for the presence of gravity or katabatic winds. Even though katabatic winds are considered local winds in much of the literature, in Greenland and Antarctica they are here considered regional winds because of their extent. These high velocity, often destructive, winds have their origins in the very cold temperatures found over the ice of these two high latitude landmasses (Figure 3.56a and 3.56b). Similar winds are found in Europe and carry such names as the **Mistral** (Rhône River valley in France) and the **Bora** (Adriatic Coast). These are another type of wind that develops in mountains, but unlike chinooks, they result from the accumulation of cold air at high elevation which then flows downhill through mountain valleys. Relative humidities sometimes drop into single digits.

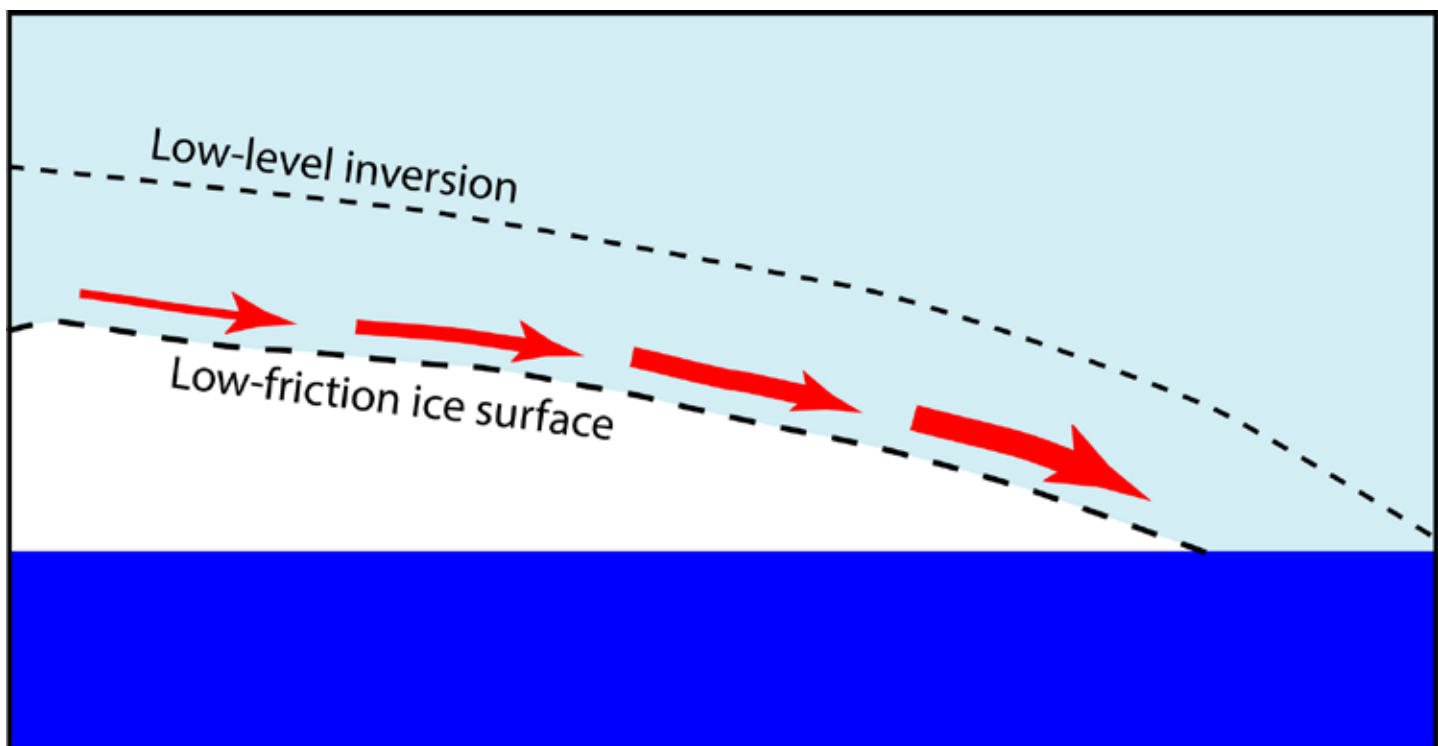


Figure 3.56a. One of the fiercest winds on Earth is the katabatic wind of Antarctica. Driven by a high pressure dome in the interior, they accelerate downslope across a near-frictionless surface to the coast. Although typical katabatic winds are a mere 15-30 mph, they are known to exceed 200 mph. Cape Dennison at Commonwealth Bay has a mean annual wind velocity of 50 mph, making it the windiest place on Earth. A low-level temperature inversion limits these winds to a very shallow layer.





Figure 3.56b. Image of the eastern coast of the Antarctic Peninsula during a windstorm. Wind chill equivalent temperatures in Antarctica are the lowest on Earth, and can reach minus 200°F. For example, the wind chill equivalent temperature at an actual temperature of minus 80°F and a wind velocity of 80 mph calculates at minus 174°F. In such conditions, exposed flesh will freeze in under a minute (Source/Credit: Alfred Wegner Institute, photo by W. Arntz).

- **Monsoon.** Monsoons can also be considered regional winds because of their geographic extent. A monsoon is a *seasonally reversing wind* that is dry during one season and wet during another. In many respects, the monsoon resembles a land-sea breeze because it operates on basically the same principles. During the summer, when India and Southeast Asia heat up, a low pressure system develops over the land (Figure 3.57a and 3.57b). This causes warm, moist air from the tropical waters of the Indian and Pacific oceans to flow inland. As it flows over the continent, it is further heated, causing uplift, cloudiness, and frequent precipitation. Uplift is enhanced by the lofty Himalayan Range, squeezing even more rainfall out of the moisture-enriched air. During winter, the situation reverses. As the land cools and a high pressure system develops over Asia, the wind begins to flow from the Asian landmass toward the ocean. Because the air originates over land in the winter, it is cold and dry. As the air flows southward it warms but it remains dry. Thus, **the winter monsoon is dry, whereas the summer monsoon is wet.**

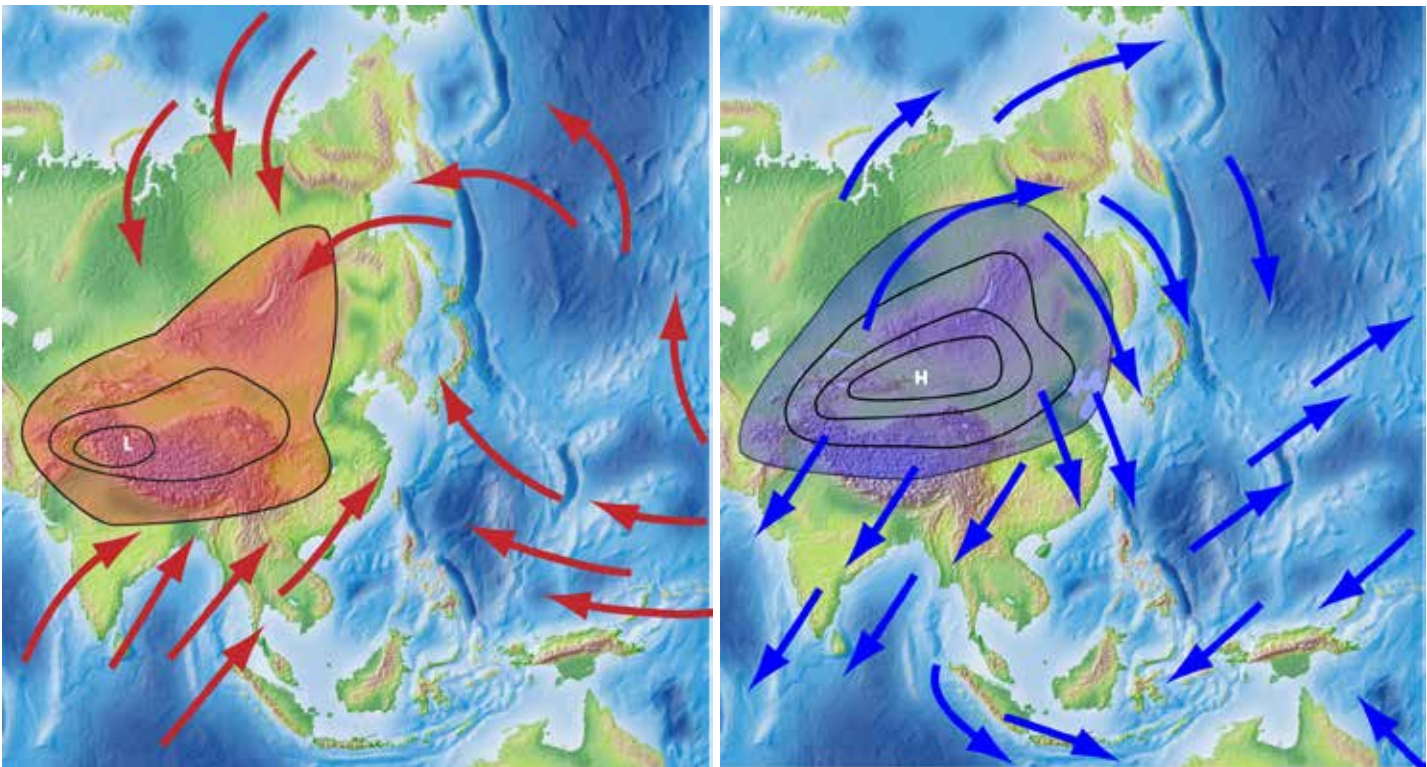


Figure 3.57a. (left) During the summer, the Asian landmass becomes warmer than the Indian and Pacific oceans. The resulting pressure difference (low over the continent and high over the oceans) causes the wind to blow from the oceans to the continents. Because the air originated over the oceans, it carries moisture which produces the summer monsoon rains.

Figure 3.57b. (right) During the winter, the situation reverses as the Siberian High develops over the Asian landmass. Air then flows from the land toward the ocean. Because the air originated as cold, dry, subsiding air in a high pressure zone, it produces a dry wind. As it flows south, it warms, but remains dry.

When the summer monsoon air-flow is combined with uplift over the Himalayas, torrential rainfall can occur. Cherrapunji, India, located on the south slopes of the Himalayas, has received as much as 30.5 *feet* of rain in one month, and 86.8 feet in a single year! By way of comparison, a typical rainfall value for the Midwest of the United States is around 30 inches (2.5 feet) per year. Areas along the Gulf Coast receive around 60 inches per year, and the Pacific Northwest, the wettest place in the contiguous United States, can experience up to 200 inches (16.6 feet) of precipitation per year.

Other regions have monsoon wind systems, or at least monsoon tendencies, although none compare to the Asian Monsoons in duration and intensity. These include northern Australia, the west coast of sub-Saharan Africa, part of Amazonia, and parts of North America. The North American monsoon affects much of northwestern Mexico and the southwestern United States. The setup for the North American Monsoon includes the development of a thermal low pressure system in northwestern Mexico or southwestern United States, and an upper-level high pressure system over the Four Corners (Figure 3.58). Moisture sources include the tropical Pacific, the Sea of Cortez, and to a lesser degree, the Gulf of Mexico. The North American Monsoon typically begins in early to mid-July, and ends at the beginning of fall. In some areas, over half of the seasonal rain totals arrive during the monsoon season. Although they bring beneficial rain, they also bring flash floods, damaging thunderstorms, and dust storms.



Figure 3.58. The setup for the North American Monsoon includes the development of a thermal low pressure system in northwestern Mexico or southwestern United States, and an upper-level high pressure system over the Four Corners. Moisture sources include the tropical Pacific, the Sea of Cortez, and to a lesser degree, the Gulf of Mexico (Source/Credit: NOAA).

There are hundreds of other local winds world-wide, each with its own characteristics, even though some of the formative elements may be similar to the winds described above. The **haboob** is a local desert dust storm, often initiated by thunderstorms in the western United States (Figure 3.59). The **Washoe Zephyr** is a local afternoon wind that blows strongly from the southwest from the eastern base of the Sierra Nevada across much of Nevada, and sometimes into Utah (Figure 3.60). The **sirocco** is a warm, dry, dusty wind that blows off the north African coastline toward Europe (Figure 3.61). The **Levante** is an interesting wind that blows from the Mediterranean Sea westward, accelerating through the Straits of Gibraltar, often generating interesting clouds (Figure 3.62).



Figure 3.59. A devastating haboob (dust storm) hit the Phoenix area in July, 2012. The wall of dust was estimated at 2000 feet (~600 m) high and 60 miles (~100 km) wide and kicked up winds in excess of 50 miles (80 km) per hour. Over 9000 people were without power (Source/Credit: Andrew Pielage Photography, with permission).



Figure 3.60. The **Washoe Zephyr** is a local afternoon wind that blows strongly from the southwest from the eastern base of the Sierra Nevada across much of Nevada and sometimes into Utah. Regional southwesterly winds can amplify the Zephyr, such as during the Rim Fire of August, 2013. The large lake just left of upper-center is Lake Tahoe, which straddles the California-Nevada line (Source/Credit: NASA/International Space Station).



Figure 3.61. The **Sirocco** is a warm, dry, dusty wind that blows from North Africa toward southern Europe across the Mediterranean Sea. The plume of wind-blown sand and silt traverses the entire Mediterranean Sea (Source/Credit: NASA).



Figure 3.62. The **Levante** (also levant, lvant, lievant) is a local wind that blows westward from the Mediterranean Sea toward the Atlantic Ocean through the Straits of Gibraltar. Winds that are accelerated by constrictions in topography are called mountain-gap winds. Strong winds and rough seas result from the accelerated flow. When conditions are right, the lift provided by the Levante wind causes a type of wave cloud to develop, the Levante cloud (Source/Credit: Wikipedia, Nol Aders).

## Upper-Level Winds

Prior to World War II, little was known about upper-level winds. What little data was available came from observations of high clouds and the periodic violent volcanic eruptions, such as Tambora in 1815 and Krakatoa in 1883. Today, there are thousands of direct observations of upper level conditions made several times per day by weather balloons (both land and ship-based) and aircraft, as well as remotely-sensed data from ground-based stations and satellites. With a more complete understanding of upper-level data has come an understanding of the complex interactions of surface and upper-level conditions. Long-range weather forecasts are in large part possible because of the ability to forecast upper-level flow patterns days and even weeks in advance.

Upper-level winds have a simpler and more persistent pattern than their surface counterpart. Their simplicity is due to (1) the near-absence of friction, which increases wind velocity and generates strong Coriolis Force, (2) upper level winds are less influenced by land and water contrasts than surface winds, and (3) upper level winds are less influenced by mountain barriers and highlands than surface winds. With the exception of seasonal easterly flow (east to west) over portions of the tropics due to thermal influences of large land masses, the upper level pattern displays a single cell per hemisphere and is typified by a wave pattern of westerly winds (Figures 3.63a and 3.63b). The Coriolis Force increases with height and wind velocity, and the deflection is so great above about 18,000 feet (~5500 m), that the wind flows **parallel to the isobars, rather than across the isobars as it does near the surface**. Thus, the wind blows at a right angle to the pressure gradient (Figure 3.64).



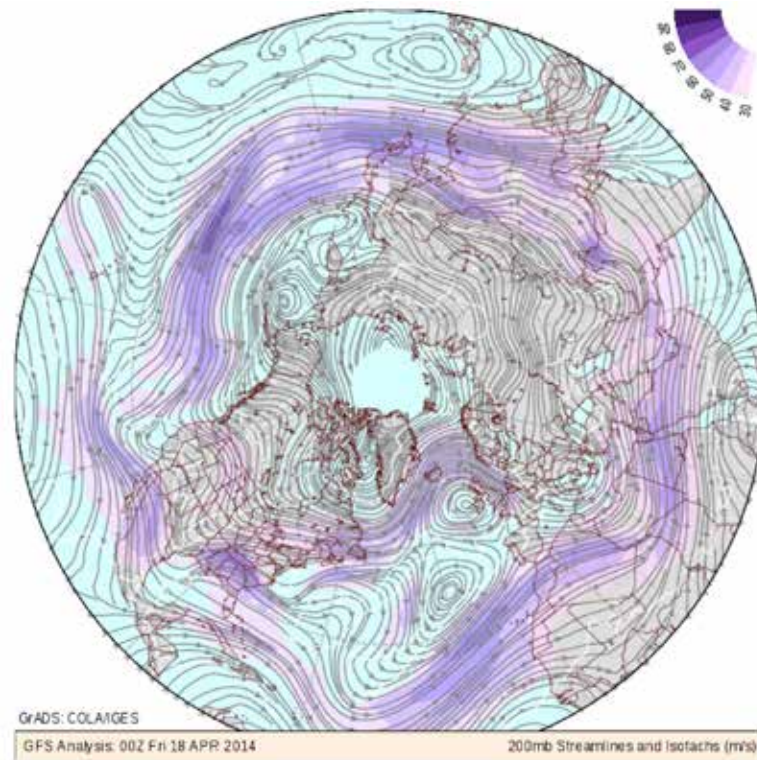


Figure 3.63a. A north polar view of wind streamlines on a 200 mb chart (about 40,000 ft; 12,200 m) indicates the typical wave-like pattern of upper-level westerly flow. Wind velocities are given in m/s for April 18, 2014 (Source/Credit: GrADS: COLA/IGES).

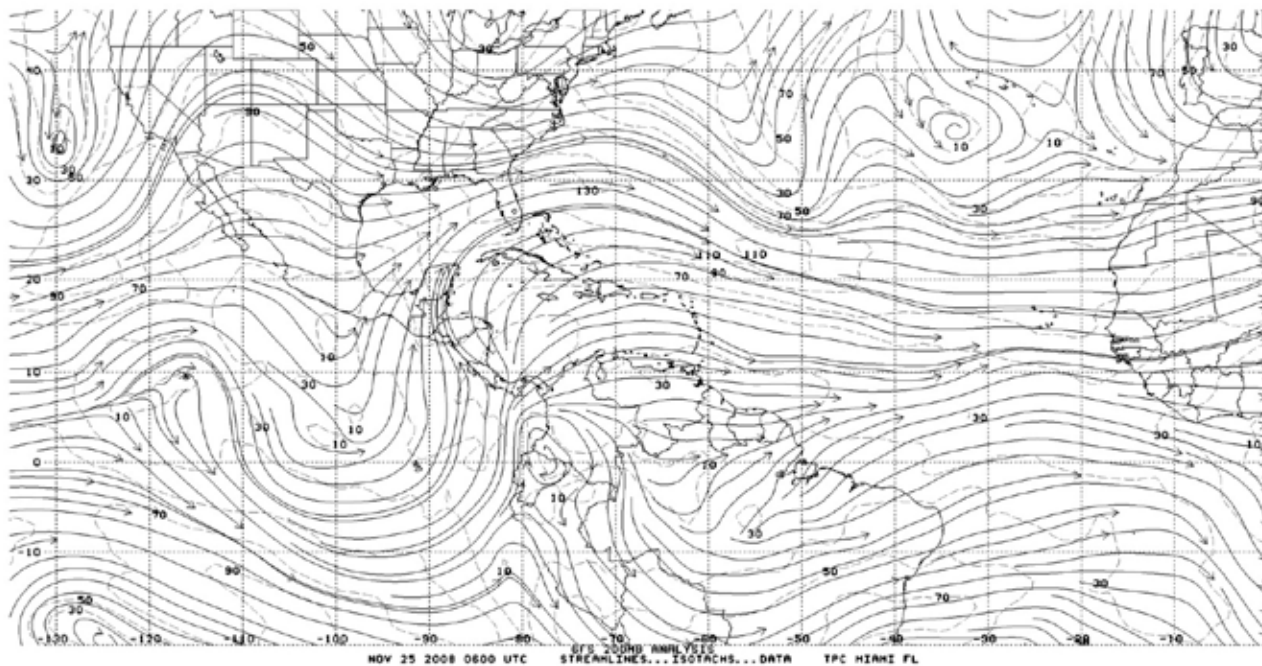


Figure 3.63b. The 200 mb chart shows low-latitude winds at approximately 40,000 feet (~12,200 m). Most of the flow in both hemispheres is westerly (west to east) in a wave-like pattern. The winds shown are for November 25, 2008. Differential heating of land and water at low latitudes will periodically cause a reversal of upper-level winds (Source/Credit: TPC Miami, Florida).

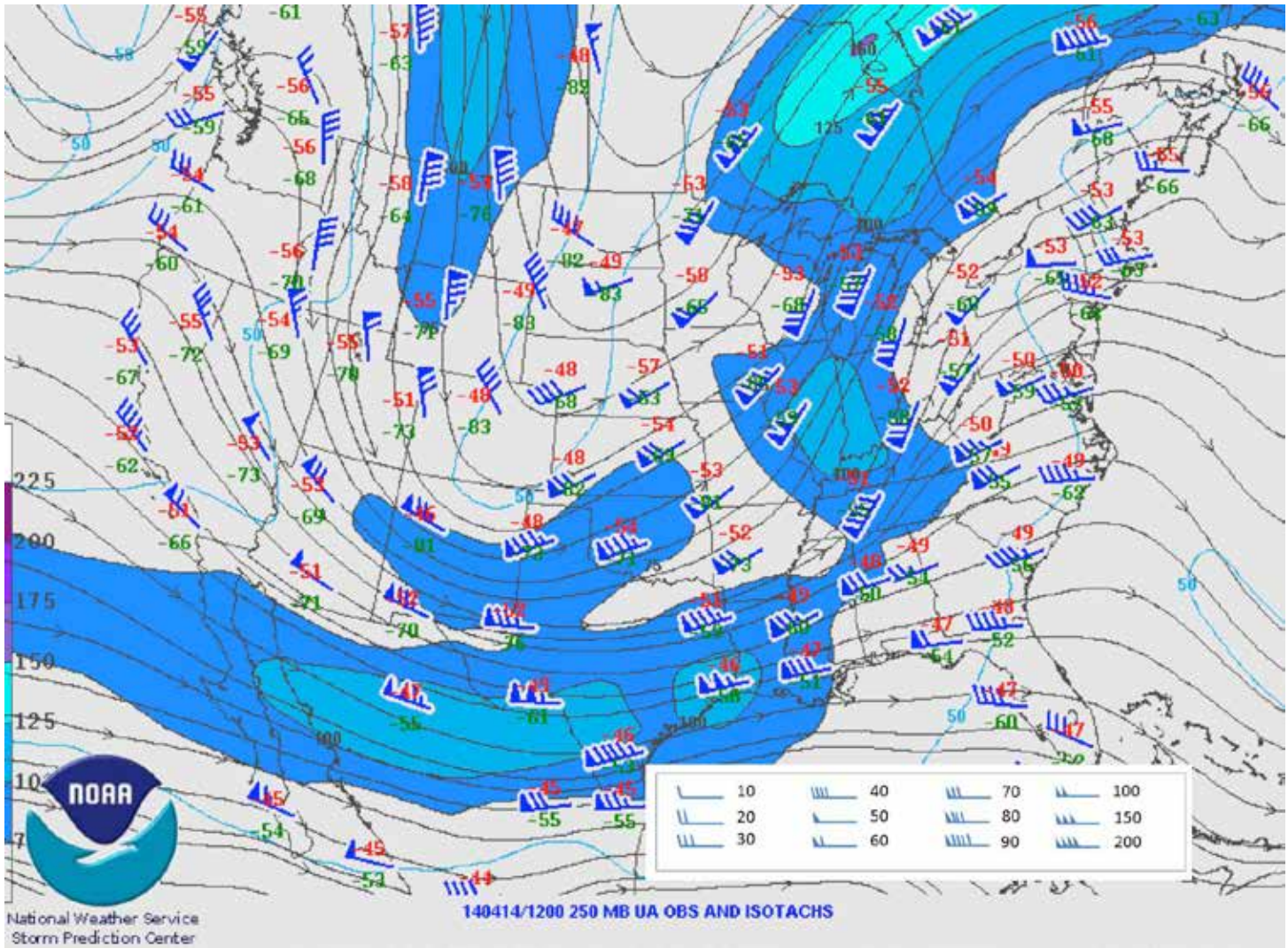


Figure 3.64. The 250 mb contours (solid lines) are given in meters above a datum, usually mean sea level. The contours show a trough (equatorward bend) over the central United States. Upper-level winds are shown by blue shafts with barbs (feathers). Winds all flow parallel to the contours. Upper level winds are generally westerly (coming out of the west), although vary from northwest to southwest, depending on position within the trough. Approximate velocities in knots (one knot = 1.15 mph) are indicated in the legend. Blue shading are highest velocities, ranging from 75 to over 100 knots (Source/Credit: NOAA, April 14, 2014, 12Z).

The most useful upper-level charts are those that depict conditions at about 18,000 feet above sea level. The type of map most-used shows the elevation at which the 500 mb pressure level occurs, the **500 mb contour map**. These are somewhat different than the sea-level-adjusted surface maps that depict a series of isobars, all at the same elevation (mean sea level). The direction of slope of the 500 mb contours indicates the pressure gradient force, and in conjunction with a known Coriolis Force, can accurately predict upper-level air flow.

Consider a simple, hypothetical situation in which vertical columns of air in the troposphere are compared from the Tropics northward toward the pole. The column closest to the Equator

will be the warmest, and therefore the tropopause and 500 mb elevations will be high relative to the other columns. The farthest poleward column will be the coldest, densest vertical column and have lowest heights of the tropopause and 500 mb levels (Figure 3.65a).

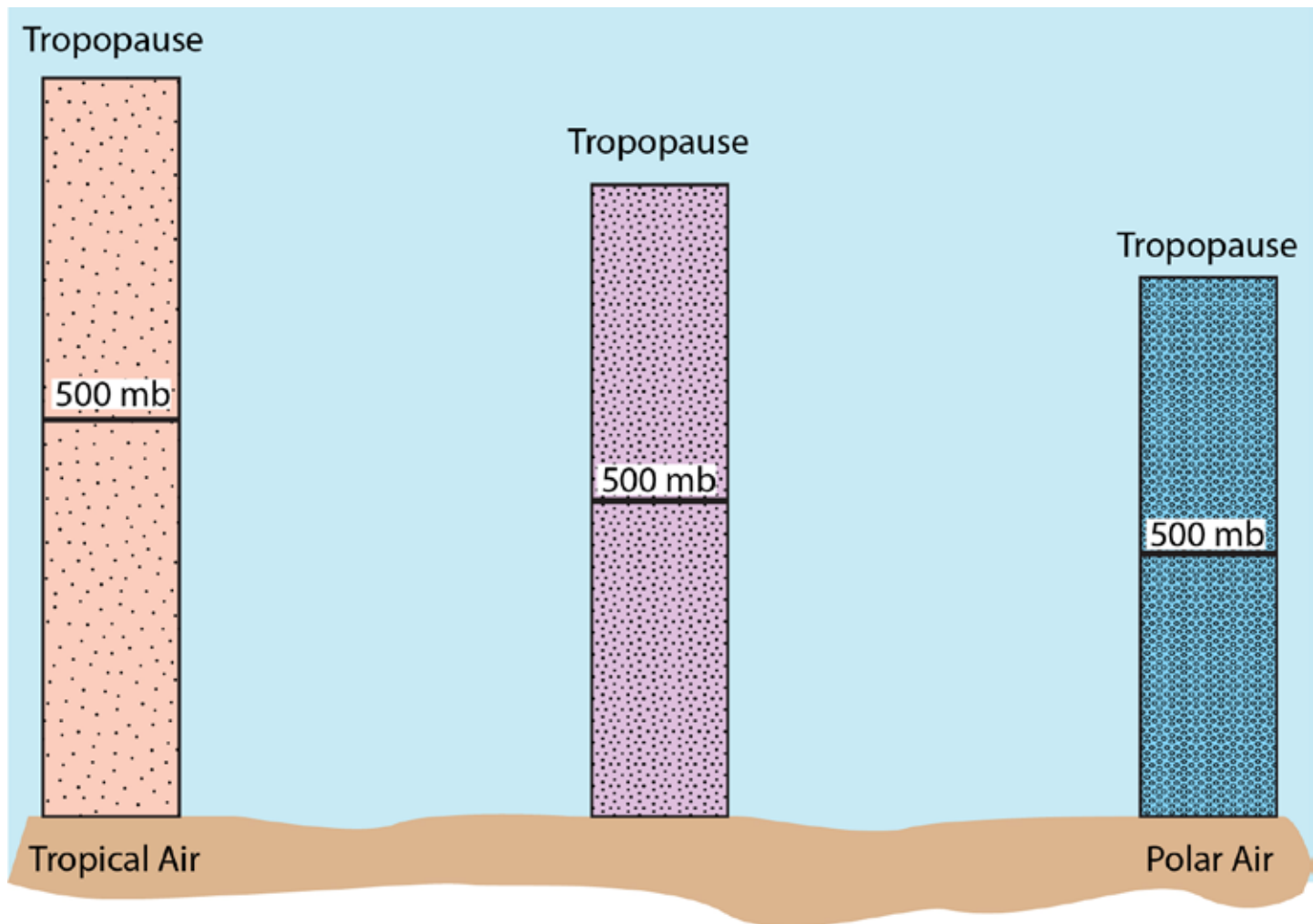


Figure 3.65a. A hypothetical cross-section of the troposphere from low to high latitude in the Northern Hemisphere. Three vertical columns of air in the troposphere are compared from the Tropics northward toward the pole. The column closest to the Equator will be the warmest, and therefore the tropopause and 500 mb elevations will be high relative to the other columns. The farthest poleward column will be the coldest, densest vertical column, and have lowest heights of the tropopause and 500 mb levels (Source/Credit: Dennis I. Netoff).

Connecting specific elevations at which the 500 mb contour occurs will generate a line that slopes poleward, which will indicate the direction and magnitude of the pressure gradient force (Figures 3.65b and 3.65c). Several lines of intersection of specified elevations at which the 500 mb contour occurs can generate a two dimensional map of the 500 mb contour map (Figure 3.66). Superimposing the Coriolis Force generates a simple map of upper-level westerly winds. These dominate global upper-level circulation in both hemispheres.

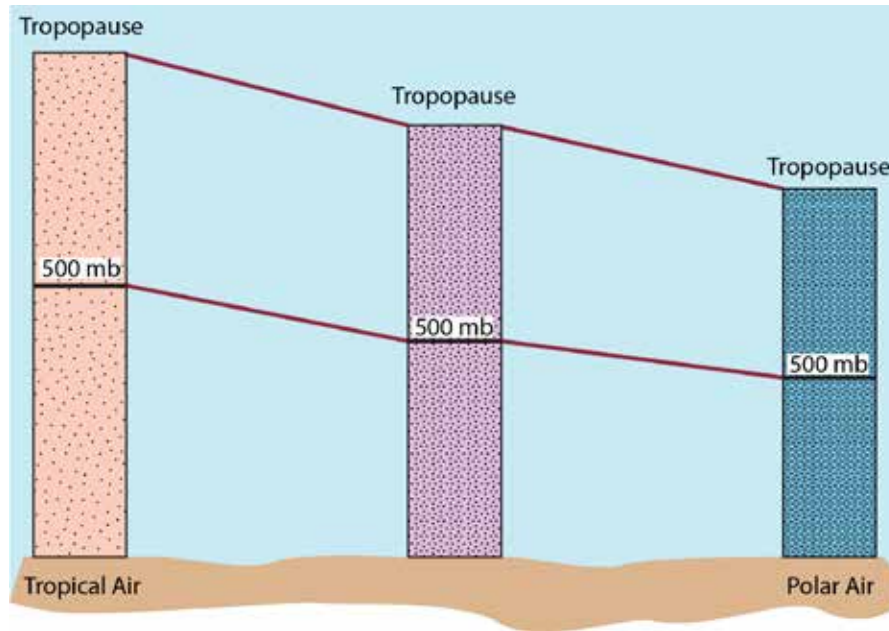


Figure 3.65b. A hypothetical cross-section of the troposphere from low to high latitude in the Northern Hemisphere. The maroon lines connect the 500 mb level and the tropopause (Source/Credit: Dennis I. Netoff).

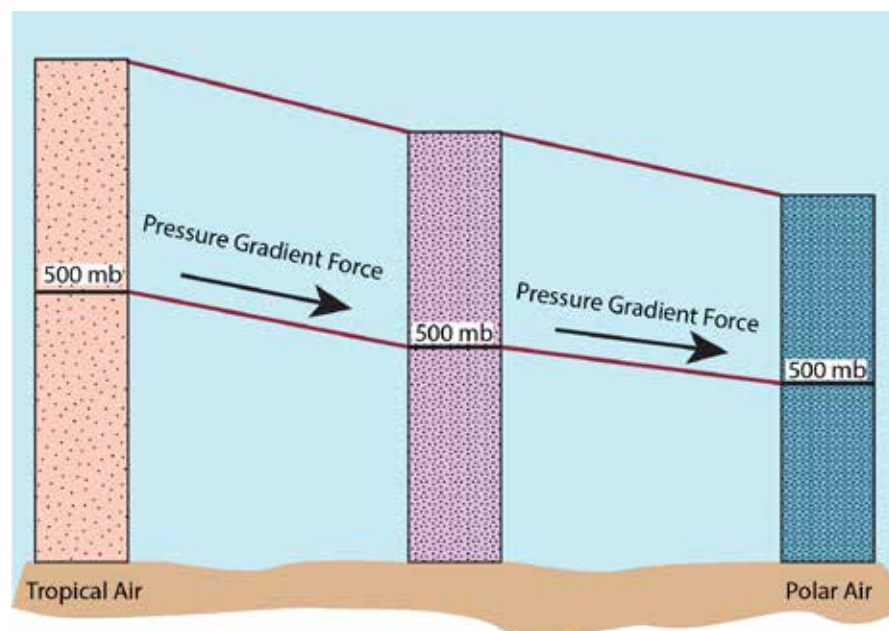


Figure 3.65c. A hypothetical cross-section of the troposphere from low to high latitude in the Northern Hemisphere. The maroon lines connect the 500 mb level and the tropopause, and indicate the direction of the pressure gradient force. Neglecting Coriolis Force, upper level winds would flow from low to high latitudes (Source/Credit: Dennis I. Netoff).

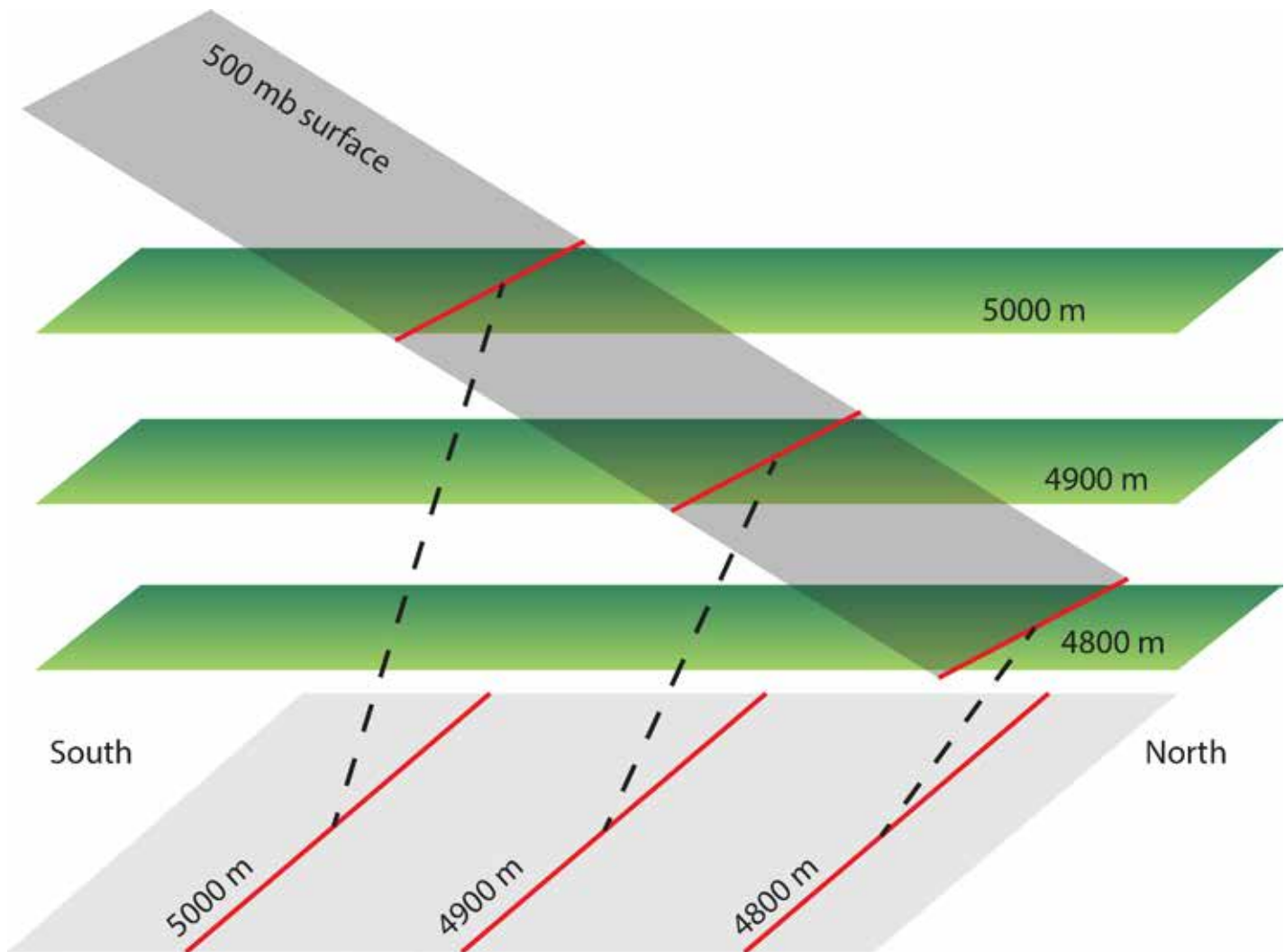


Figure 3.66. The sloping surface is a surface of constant pressure at 500 mb. Each plane that passes through it intersects the 500 mb surface, forming a line at a specific elevation above sea level (in meters). Each of those lines is a contour line. The projection of the lines of intersection onto a flat surface forms a contour map of the 500 mb surface, indicating the pressure gradient. In a typical south (left) to north (right) transect in the Northern Hemisphere, warmer columns in the south will have a higher 500 mb contour than colder air to the north, setting up a simple northward pressure gradient (Source/Credit: Dennis I. Netoff).

Now consider a slight variation of the simple scenario, where there is a more rapid temperature and density change from the Tropics to the poles. This causes a steeper slope of the 500 mb surface, and the map view of the contours indicates tighter contours (a closer spacing), and therefore a higher pressure gradient force (Figure 3.67). The westerly winds will be correspondingly stronger (Figure 3.68). The closer the spacing of the 500 mb contours (the tighter the contours), the higher the pressure gradient, the stronger the upper-level winds, and the stronger the temperature difference below 500 mb.

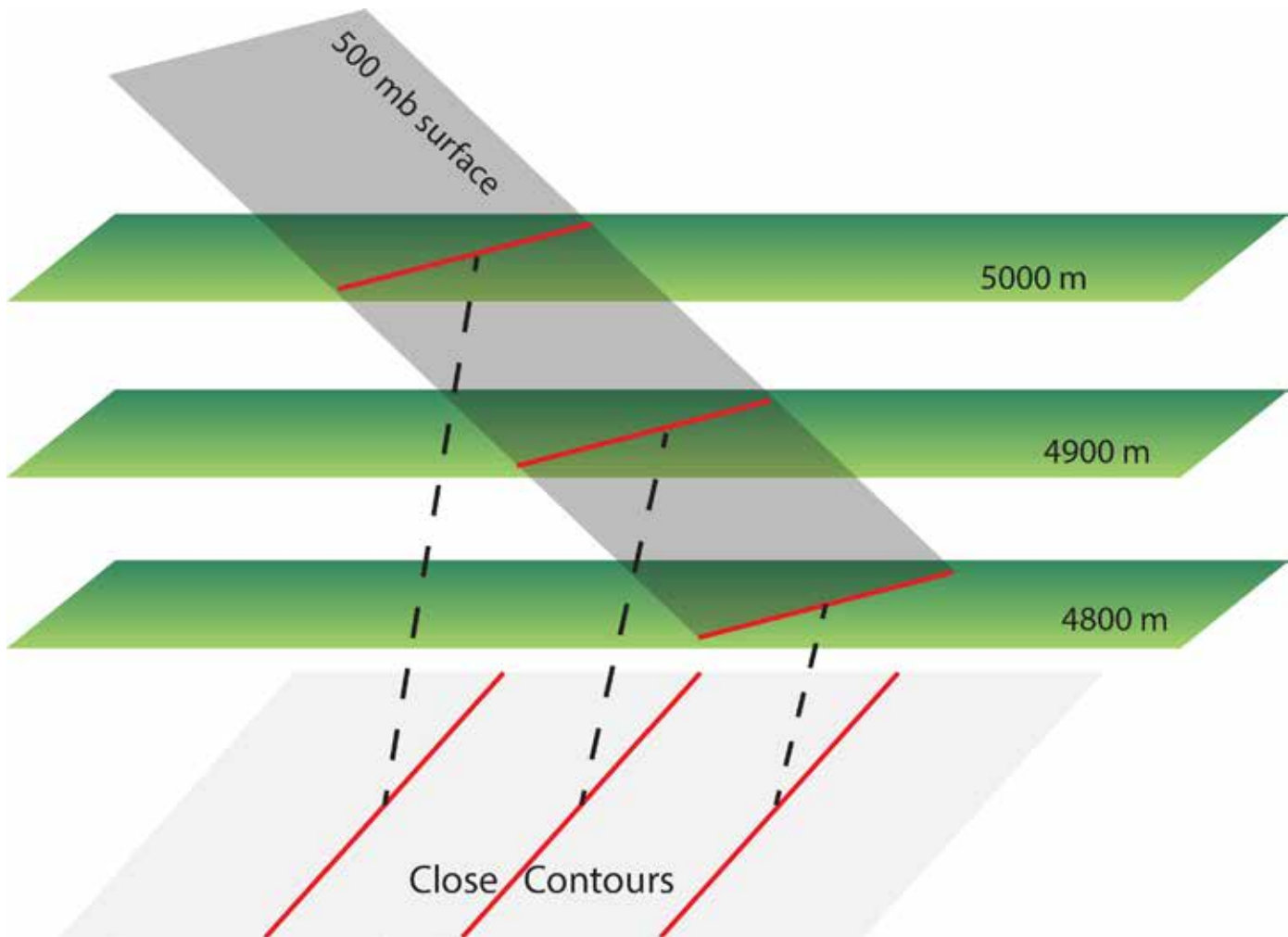


Figure 3.67. As the slope of the 500 mb surface increases, the contours on the map become tighter (more closely spaced), indicating a stronger pressure gradient force. (Source/Credit: Dennis I. Netoff).

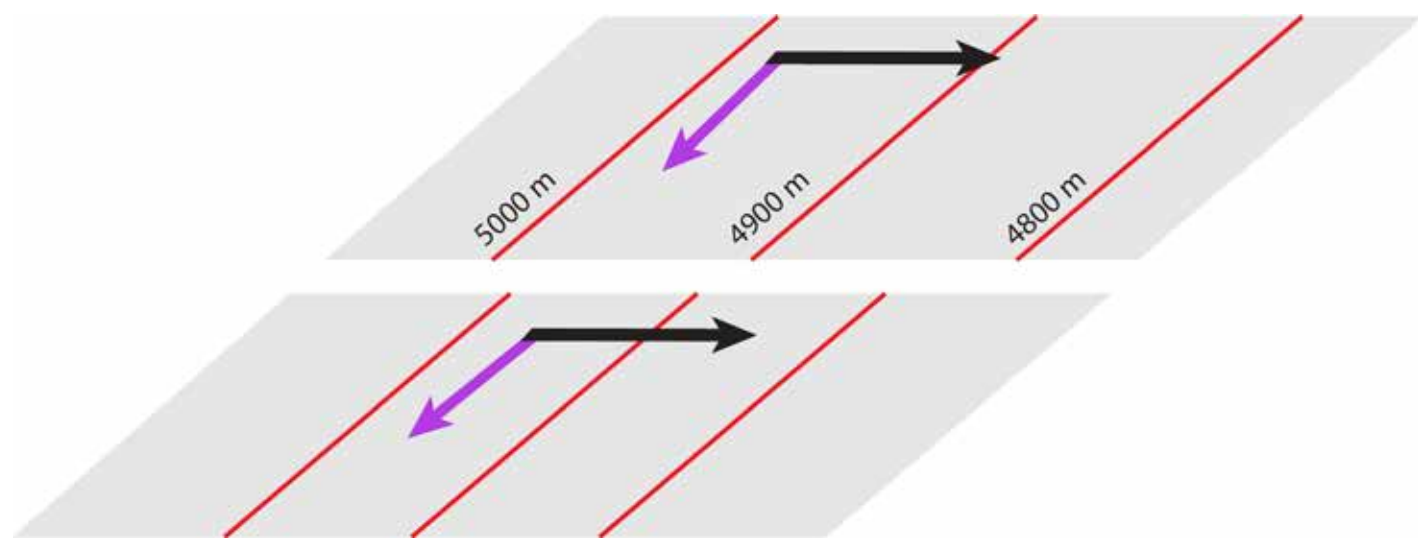


Figure 3.68. The two hypothetical maps in the previous figures will generate upper-level westerly winds. The map with the tighter contours (below) will generate stronger winds (Source/Credit: Dennis I. Netoff).

On an idealized Earth where temperatures drop uniformly from the tropics to the poles, the 500 mb maps would consist of a series of concentric circles centered on the poles, with higher latitude contours progressively lower in elevation. The winds would be westerly at all latitudes. Any local increase in tightness of contours would be indicated by stronger westerly flow (Figure 3.69).

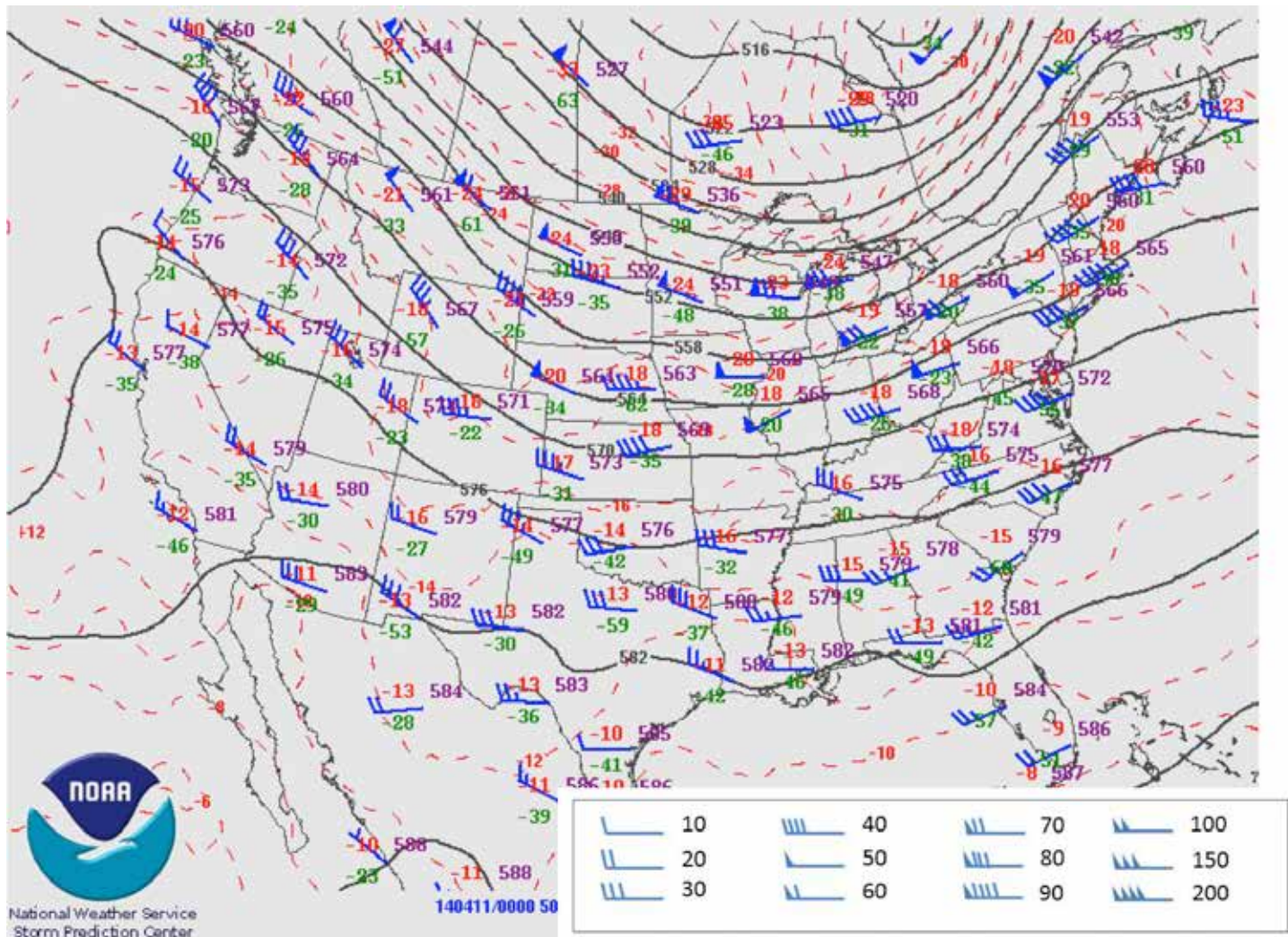


Figure 3.69. The 500 mb contours (solid lines) are given in meters above a datum, with the last digit omitted (e.g., 582 = 5820 meters). The contours show a simple east-west pattern over much of the map. Upper-level winds are shown by blue shafts with barbs (feathers). All upper level winds are **westerly** (coming out of the west). Approximate velocities in knots (one knot = 1.15 mph) are indicated in the legend. The contours get progressively tighter (more closely spaced) going northward, causing stronger upper-level winds. East-west flow patterns are referred to as **zonal flow** patterns and typically result in fairly rapid passage of surface weather disturbances from west to east (Source/Credit: NOAA, April 11, 2014, 00Z).



More typically, upper-level flow consists of a series of undulating waves within the westerly flow. These are the **Rossby Waves**, first observed and explained in 1939 by Carl-Gustaf Arvid Rossby. They occur at virtually all levels in the upper atmosphere, and are well-expressed in the 500 mb as well as the 250 mb contour maps (Figure 3.70). They can be described just like waves on water according to velocity, amplitude (height), wavelength, and movement. Waves of short wavelengths are superposed on waves with longer wavelengths. The short waves typically travel embedded in the longer ones in a general west to east fashion. The shorter waves can either dampen or amplify the ridges and troughs in the longer waves, and those changes can directly affect surface highs and lows in their intensity and movement.

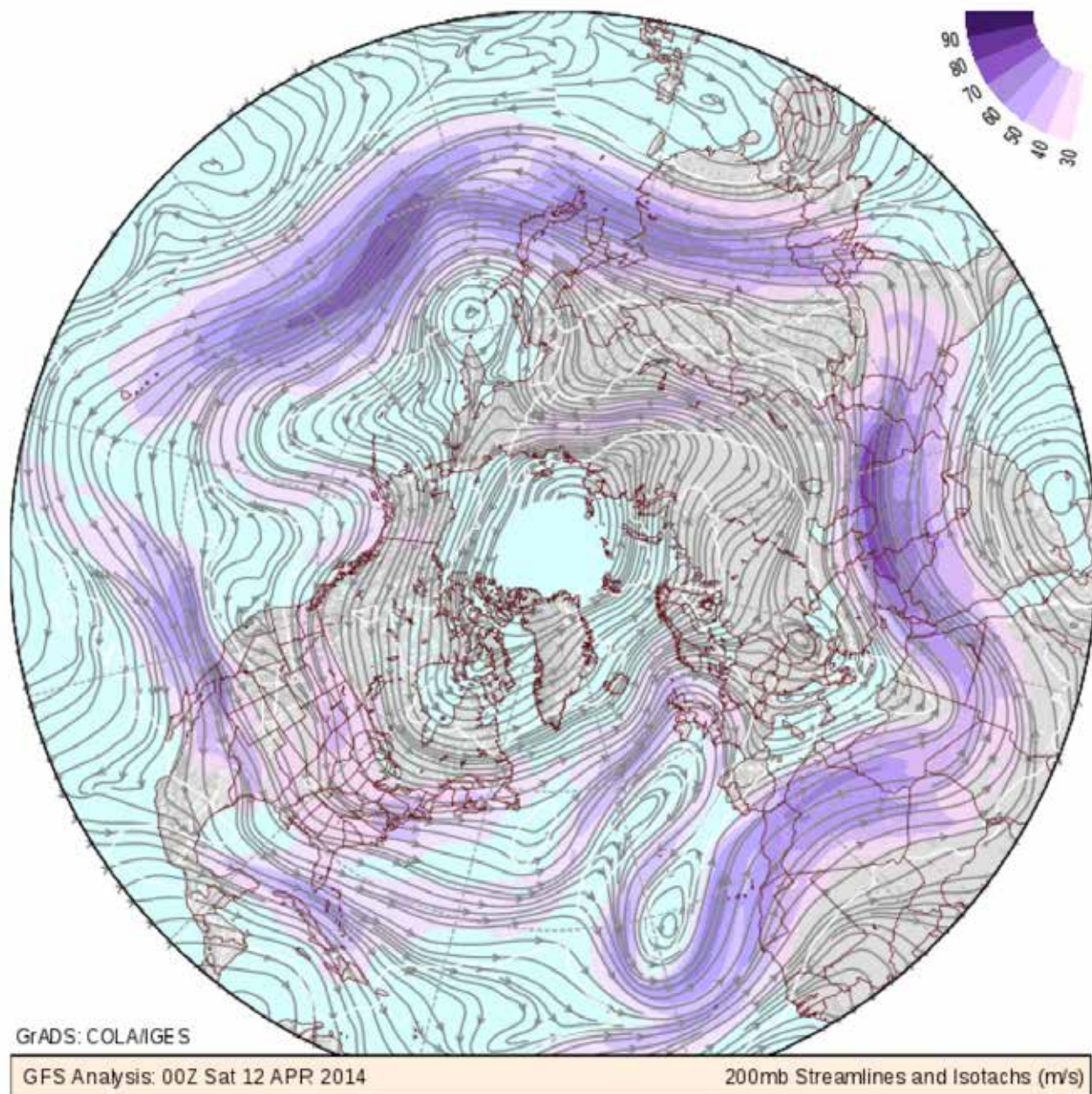


Figure 3.70. A north polar view of wind streamlines on a 200 mb chart (about 40,000 ft; 12,200 m) indicates the typical wave-like pattern of upper-level flow. Wind velocities are given in m/s for April 12, 2014 (Source/Credit: GrADS: COLA/IGES).

The Rossby Waves originate because of variations in the Coriolis Force with changes in latitude. As they develop, they result in large-scale advection of warm air poleward and cold air equatorward. Columns of alternating cold and warm air in the troposphere create variations in height of the 500 mb contour along a parallel. This causes a poleward bend in the contours where there is relatively warm air, and an equatorward bend where there is relatively cold air. In plan view, a series of ridges and troughs develop (Figure 3.71). Meridional flow occurs when the amplitude of the upper level-waves is high, accentuating the troughs and ridges. Zonal flow occurs when the amplitude of the waves is low and transport is more directly west to east, like the simplified, hypothetical case.

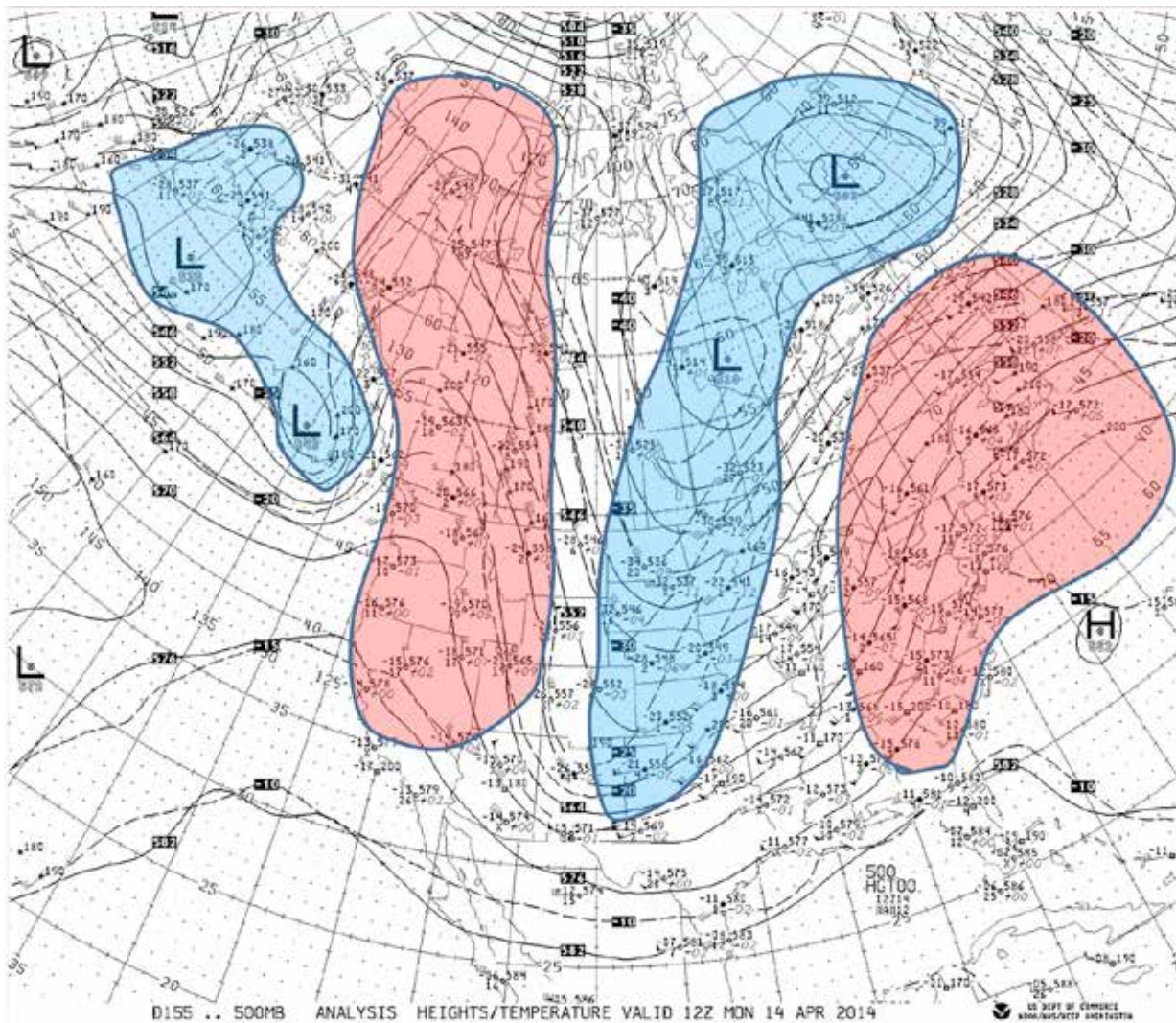


Figure 3.71. As Rossby Waves develop, they result in large-scale advection of warm air poleward (pink shaded) and cold air equatorward (blue shaded). Columns of alternating cold and warm air in the troposphere create variations in height of the 500 mb contour along a parallel. This causes a poleward bend in the contours where there is relatively warm air, and an equatorward bend where there is relatively cold air. In plan view, a series of **ridges and troughs** develop. **Meridional flow** occurs when the amplitude of the upper level-waves is high (as depicted above), accentuating the troughs and ridges. **Zonal flow** occurs when the amplitude of the waves is low and transport is more directly west to east, like the simplified, hypothetical case (Source/Credit: NOAA, April 14, 2014, 12Z).

**Jetstreams** are high velocity zones within the general upper-level westerly flow near the tropopause. Some jetstreams are continuous and can be followed around the globe. They are well-revealed in the 250 mb maps, but may actually show at several levels. The **polar jetstream**, the strongest and most continuous jetstream, tends to occur at the boundary between tropical and polar air masses (Figure 3.72). The strong contrast in temperature between the two air masses results in tight contours, and an increase in the pressure gradient force. The polar jetstream can be thought of as the cylindrical core of the upper-level Westerlies, with an average velocity of 60 to 115 mph, though winds can reach 290 mph. This tube of air occurs at altitudes of 30,000 to 45,000 feet, and can be typically 180 to 300 miles wide and up to two miles thick. On surface maps, the contact between polar and sub-tropical air masses is the polar front.

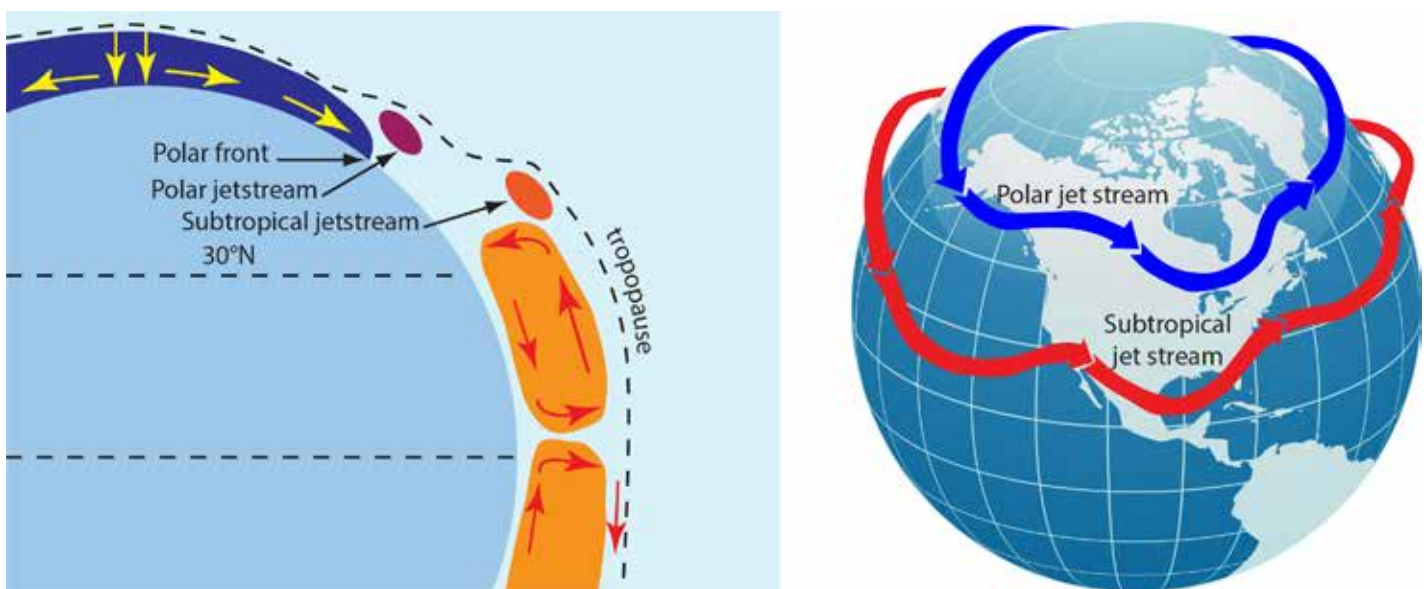


Figure 3.72. (left) Jetstreams form in the upper troposphere where warmer and colder air masses meet. The polar jetstream forms along the boundary between mid-latitude air and polar air and is strongest when the temperature difference between these bodies of air is the greatest. The subtropical jetstream forms on the poleward side of the Hadley cell and is typically weaker and not as persistent as the polar jet.

Figure 3.72. (right) Jetstreams tend to follow a wavy pattern associated with the upper level Rossby Waves. These waves vary in wavelength, wave height, and strength over time periods of weeks to months.

The position and strength of the polar jetstream varies over time. Short-term variations follow the short-term, multi-week cycles in the upper-level waves, alternating from zonal to meridional flow type. The strongest polar jetstream, often with core velocities exceeding 150 knots (173 mph), generally occurs during the late winter and early spring when temperatures between polar and tropical air are greatest. Seasonally, the cold polar begins to warm and retreat poleward during the summer, taking the polar front with it in the process. During the winter, the dome of polar air strengthens and covers a broader area, causing the average position of the polar jetstream to migrate equatorward.

A secondary **subtropical jetstream** tends to form near the poleward margin of the Hadley cell (Figure 3.72). Like the Polar Jet, it occurs at the tropopause boundary at an altitude of about 43,000 feet (13,000 m) and it also flows from west to east. This jetstream can bring upper-level disturbances into the southern tier of the United States that are capable of producing severe weather.

Upper-level patterns and surface weather. The surface weather map is a two-dimensional representation of a 3-dimensional machine. Neither dictated the pattern of the other, but they affect each other to the degree that today, upper-level observations and forecasts are essential to short and long-term surface forecasts. An example is the upper-level steering winds.

Mariners have for decades have used 500 mb charts to predict movement of surface pressure systems, particularly hazardous storm systems. The Ocean Prediction Center uses 500 mb charts to forecast both the direction as well as velocity of movement of surface systems (Figures 3.73a and 3.73b). Note how closely the forecast path of low pressure storm systems follows the trend of the 500 mb contours.

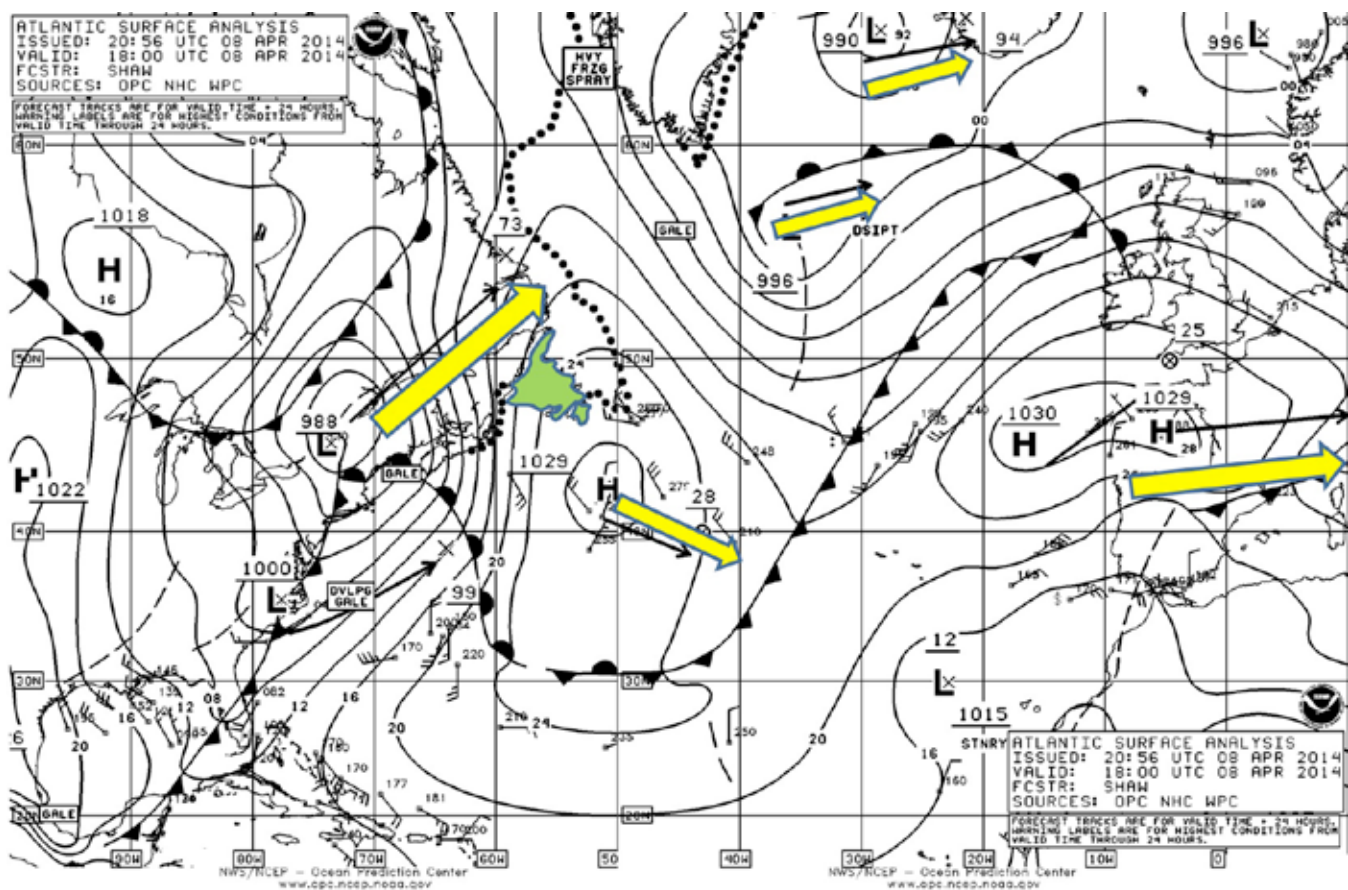


Figure 3.73a. A surface forecast map for April 8, 2014 showing high and low pressure cells and forecast tracks (yellow arrows). Compare the forecast tracks to the 500 mb contour map below. Newfoundland, Canada is shown in green for reference (Source/Credit: NOAA/OPC, issued 20:56 UTC April 8, 2014; valid 18:00 UTC April 8, 2014).

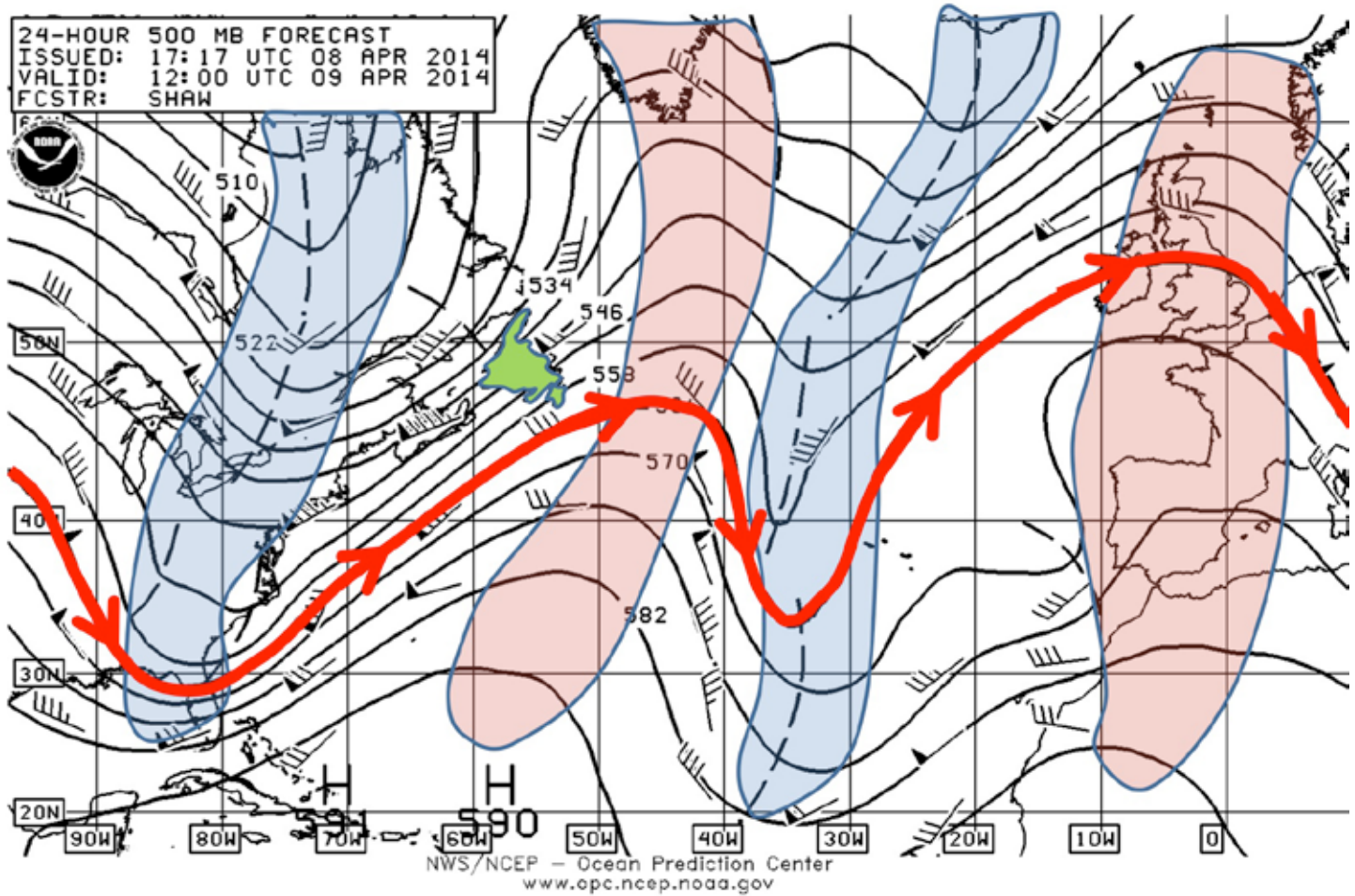


Figure 3.73b. The forecast 500 mb contour map of the North Atlantic for April 8, 2014. Troughs and ridges are shaded blue and red. Note the close correspondence of the upper-level flow to the forecast surface tracks shown in Figure 3.73a. Newfoundland, Canada is shown in green for reference (Source/Credit: NOAA/OPC, issued 17:17 UTC, April 8 2014. Valid 12:00 UTC April 9 2014).

Upper-level flow patterns also generate upper-level convergence and divergence, and that can have immediate influence on surface systems. For example, in *meridional* flow, there tends to be a preferred position of upper level convergence to the left of the axis of a large trough, whereas to the right (east) of the trough, there tends to be a zone of divergence (Figure 3.74). The upper-level flow in some cases not only helps control the path of movement of surface highs and lows, but it helps maintain (or strengthen or weaken) them.

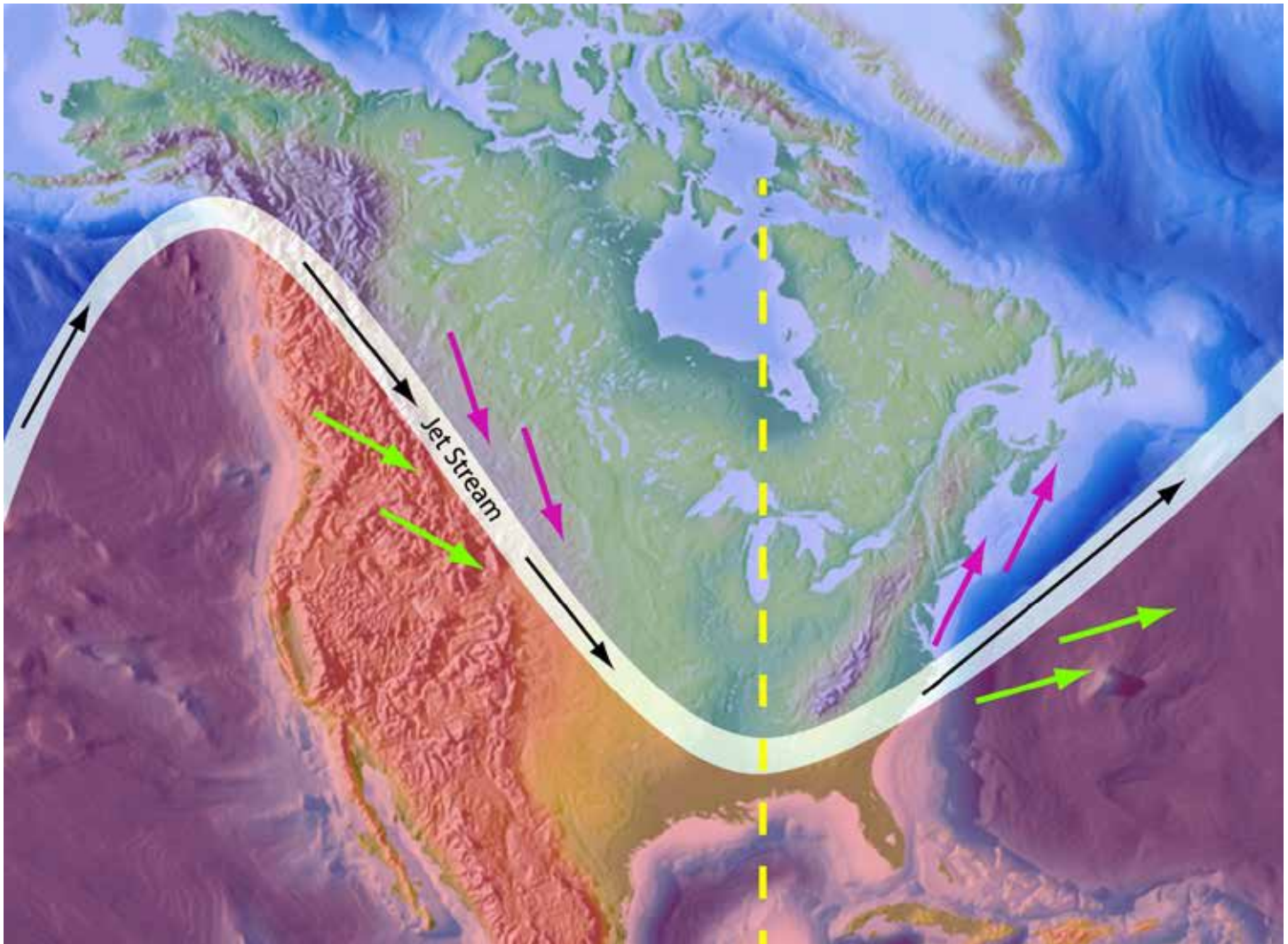


Figure 3.74. In a meridional flow regime, the area to the west of the axis (dashed yellow line) of a trough tends to develop convergent flow aloft (arrows converging). This promotes vertical subsidence, and the development of a surface high pressure system. To the east of the trough, upper-level divergence (colored arrows) favors vertical up-lift, and the development of a surface low pressure system. Upper-level convergence and divergence can not only help maintain surface pressure systems, but in some cases will strengthen them, weaken them, or cause their dissipation.

## Chapter 4

# Atmospheric Moisture

Water vapor in the atmosphere is an invisible, odorless, tasteless gas, and yet is one of the most important constituents of the atmosphere. It is the source of all forms of condensation (dew, frost, fog, clouds), and of all types of precipitation (rain, snow, sleet and hail). It is ubiquitous, and yet it is one of the most unique substances in the universe. It is essential to life itself. It plays an important role in heat transfer in the atmosphere, and through latent heat of condensation, is a major fuel for severe storms such as thunderstorms and hurricanes. It can co-exist in the atmosphere as a solid (ice), liquid or supercooled liquid, and gas within the range of common atmospheric temperatures. These properties of water, and the existence of planetary winds, allow water to continuously move from one place in the atmosphere to another, and ultimately back to its point of origin – the **hydrologic cycle**.

The hydrologic cycle is an attempt to trace the pathways that water takes as it circulates through the Earth-atmosphere system (Figure 4.1). There is no point of beginning or end to the cycle, but by convention, the cycle starts in the largest reservoir of free water in the system, the oceans. Some of the Sun's energy is used in **evaporation**, the change of state from liquid water to invisible water vapor. Some of the water vapor **condenses** to form clouds, and a few clouds release liquid or solid moisture (rain, snow) as **precipitation**. Water that falls to the surface can flow across the surface and into streams (**runoff**), return to the atmosphere through evaporation, or **infiltrate** into the ground. Infiltrated water can be held as soil moisture. Soil moisture may be taken up by plants and returned to the atmosphere by **transpiration**. Some of the infiltrated water percolates to greater depths to become **groundwater**. Groundwater, like surface water, flows downhill in response to gravity, slowly returning the water to its point of origin to start the cycle again.

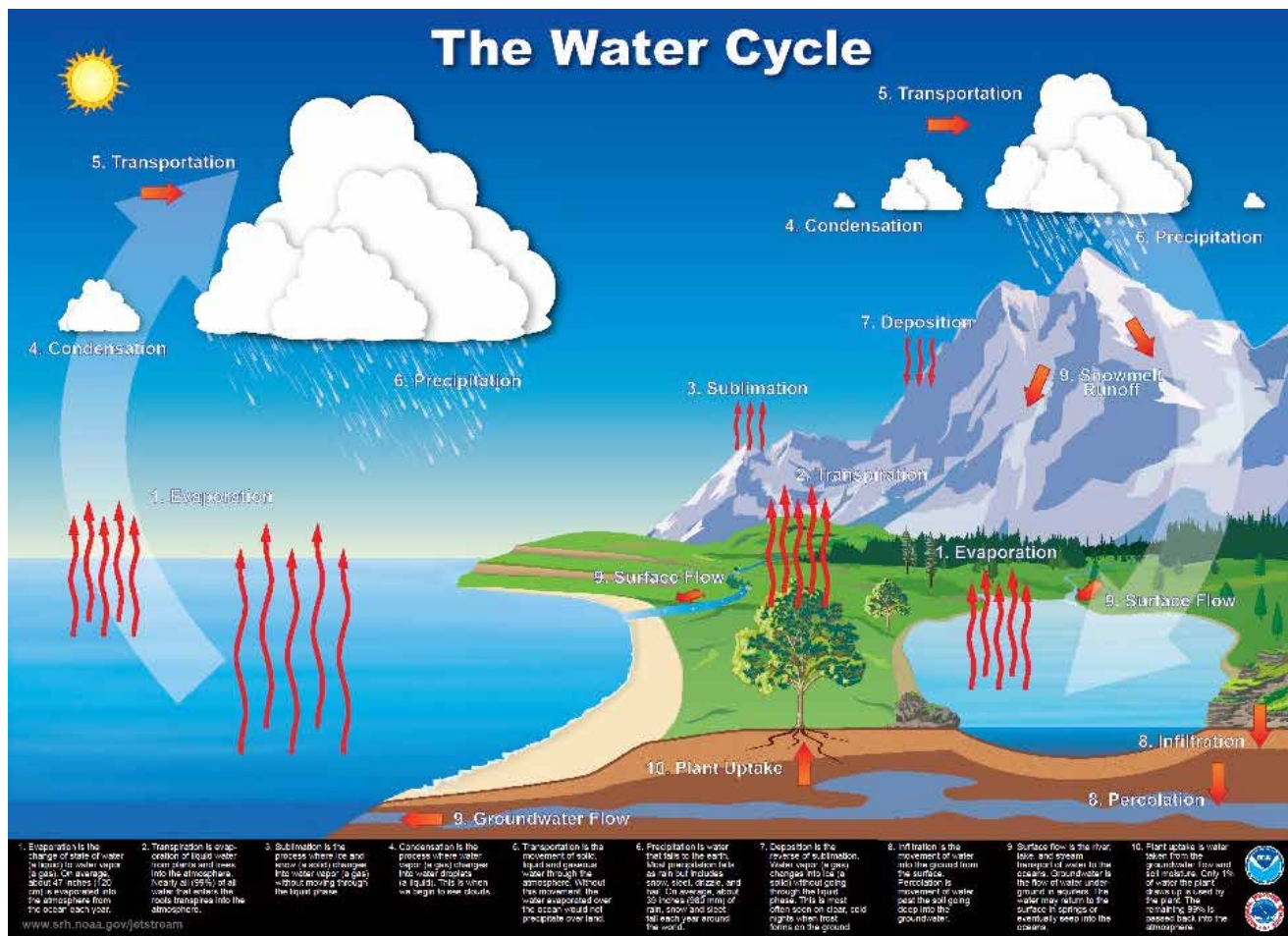


Figure 4.1. The hydrologic cycle is an attempt to trace the pathways that water takes as it circulates through the Earth-atmosphere system. By convention, the cycle starts with water **evaporating** from the oceans. Some of the water vapor condenses to form clouds, and a few clouds release liquid or solid moisture (rain, snow) as **precipitation**. Water that falls to the surface can flow across the surface and into streams (**runoff**), return to the atmosphere through evaporation, or **infiltrate** into the ground. Infiltrated water can be held as soil moisture, be taken up by plants and returned to the atmosphere by **transpiration**, or percolate deeper to become **groundwater**. Groundwater slowly returns the water to its point of origin to start the cycle again (Source/ Credit: NOAA/ National Weather Service Jetstream Project).



## Special Properties of Water

Water is one of the most abundant substances on the surface of our planet. It covers almost 75% of the surface of the Earth and makes up most of all living tissue on the planet. Some of the more unique properties of water are relevant to its role in meteorology and climatology, and are identified below:

- **Polar Nature.** Water is a polar molecule. It has an electronegative end and an electropositive end. Even though the entire molecule is neutral (the two positively-charged hydrogen ions are balanced by the negatively-charged oxygen ion), the geometric arrangement of the ions tend to separate positive and negative charges (Figure 4.2).

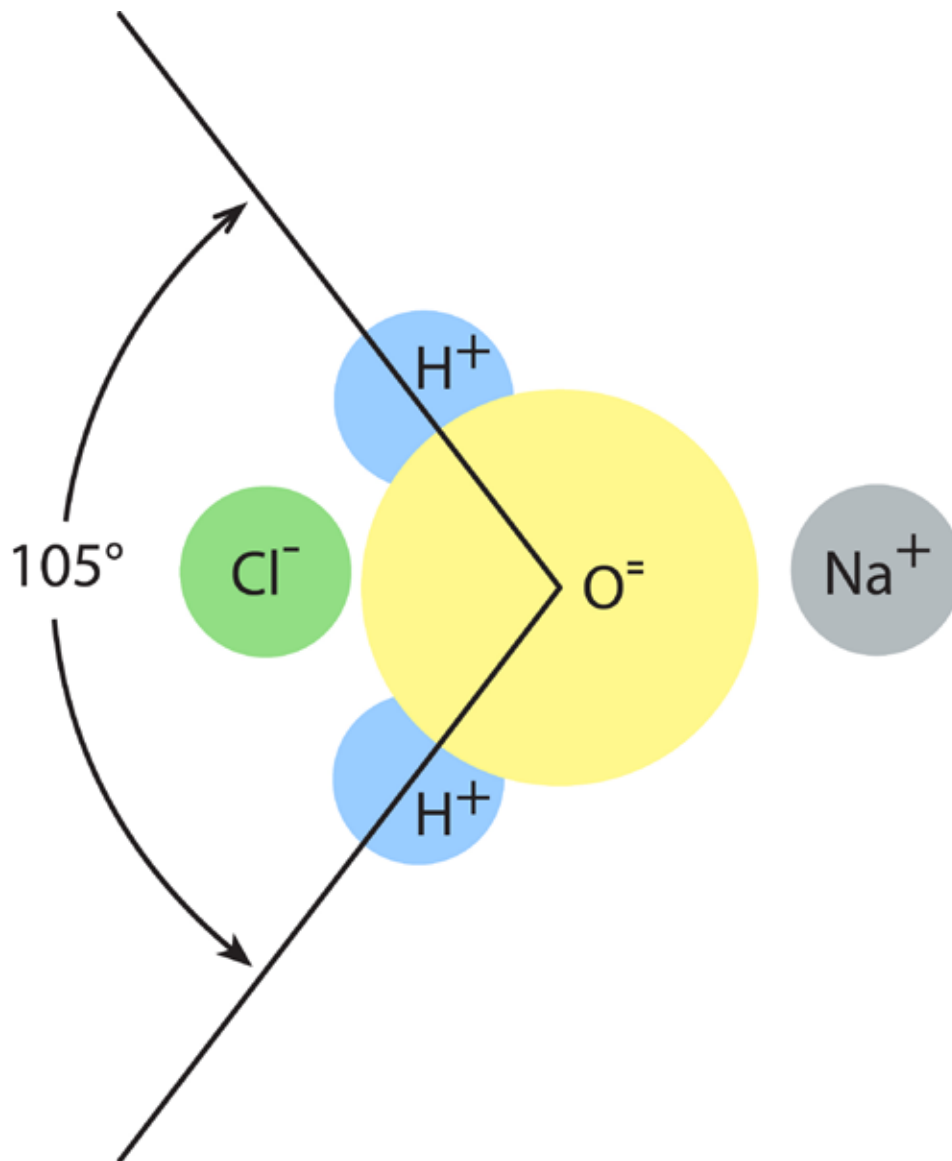


Figure 4.2. The polar nature of the water molecule stems from two hydrogen ions crowding one side of the water molecule, giving it two positive charges, and leaving the oxygen end of the molecule with a double negative charge. This charge distribution causes opposite ends of adjacent water molecules to be attracted to one another, and it also enables water to dissolve substances immersed in it, such as salt ( $NaCl$  = sodium chloride = salt).

- **Universal Solvent.** The polar nature of the water molecule makes it adhere to almost anything that is charged either positively or negatively. It even sticks to itself. This strong attraction for objects, and especially strongly charged particles like clay minerals (*dirt*), makes it a universal solvent. This is why water is used in cleaning, dishwashing, bathing and clothes washing.

For example, the positive end will attract the chlorine in a sodium chloride molecule, and the negative end will attract the sodium. Because of this, salt dissolves in water (Figure 4.2).

The electrical properties of water also enable it to bind with particles in the atmosphere, such as clay and salt. Such particles are known as condensation nuclei because they allow condensation to occur, and this is an essential step in the formation of fog, clouds and precipitation. In short, the attractive properties of water are essential to the hydrologic cycle.

- **Polar Charge.** The polar charge distribution on water molecules is also responsible for the **high boiling point of water**. The positive end of a water molecule is attracted to the negative end of another water molecule, and this leads to the formation of a **hydrogen bond**. The high boiling point of water is directly related to the strength of the chemical bond – a high amount of thermal energy is required to break the bond, and to change phase from a liquid to a gas. The amount of energy needed to evaporate every gram of liquid water is between 500 and 600 calories, **the latent heat of condensation**. This energy is a major source of energy for storms.
- **Expands When Frozen.** Unlike virtually every other substance known, water expands when it freezes. This occurs because the water molecules become organized into an open lattice structure when the water freezes. This structure is larger and less dense than the disordered liquid state of water in which water molecules are oriented randomly. The fact that water expands and becomes less dense upon freezing is meteorologically, biologically, geologically and climatologically significant.

Because ice expands when it freezes, it floats on water. The frozen layer of ice acts as insulation by slowing down the rate at which heat is lost from a water body. This property, combined with the fact that it cannot freeze unless it can expand, keeps the water bodies of the world from freezing at depth and keeps Earth from becoming an ice planet.

- **Transparency.** Unlike many liquids, **water is transparent**. If water were not transparent, then light would not penetrate the oceans, lakes, and rivers of the world, and photosynthesis would be restricted to the uppermost surficial layer. This would have radically altered the development of life on Earth because photosynthesis is the basis for almost all of the ocean's food chains. Without photosynthesis, the energy source for life would have been limited to chemosynthesis which occurs primarily in the very deep oceans near extremely hot geothermal vents.

- **Occurs in all Three Physical States.** Water is the only substance on Earth that occurs in all three physical states (solid, liquid, gas) under the narrow temperature ranges that exist at the Earth's surface. The other substances and materials that we interact with, such as the metal that makes up the chairs that we sit in, the cars we drive, and the plastics we use, do not turn into a liquid or a gas with a slight increase in temperature such as that which occurs from night to day, or from winter to summer. If they did, our reality would be quite different.
- **Mobility. Water is mobile and therefore ubiquitous:** The ability to change states over the narrow range of temperatures that occur on Earth makes the hydrologic cycle possible. Water moves from the ocean basins to the atmosphere, condenses in the atmosphere, some of it is returned to the surface as precipitation, which in turn becomes either soil moisture, groundwater, or surface runoff, and eventually the water returns to the sea from whence it came. Without this cycle, life as we know it would not be possible.

## Phase Changes

### *Solids, Liquids and Gases*

The ability of water to change states is the key to the hydrologic cycle and to an understanding of storms. Phase changes occur in response to temperature changes and temperature is a measure of the average kinetic energy of the molecules in a substance. **The reason that temperature changes produce phase changes is that the ability of atoms and molecules to bond together is a function of their temperature, or speed of motion, and the resulting effectiveness of the chemical bonds that affect them.** So, the difference between a solid, liquid, and a gas is the relative speed of motion of the molecules and the degree to which the atoms and molecules can bond together.

In the solid state, the hydrogen and oxygen atoms that make up water are held in place to form a rigid structural lattice. The atoms *vibrate* in place, but they are not free to move around because the speed of vibration is not great enough to overcome the strength of the bonds that hold the atoms in place. In a liquid, the atoms and molecules move so fast that they cannot bond together in a rigid structure; however, the effect of electrical attraction between atoms and molecules is still present. Consequently, liquids can flow and they retain their volume, but not their shape. In a gas, the motion is so fast that the forces of attraction are largely overcome and the molecules and atoms move completely independently of one another. As a result, molecules can move in any direction and so volume is no longer constant (Figure 4.3).

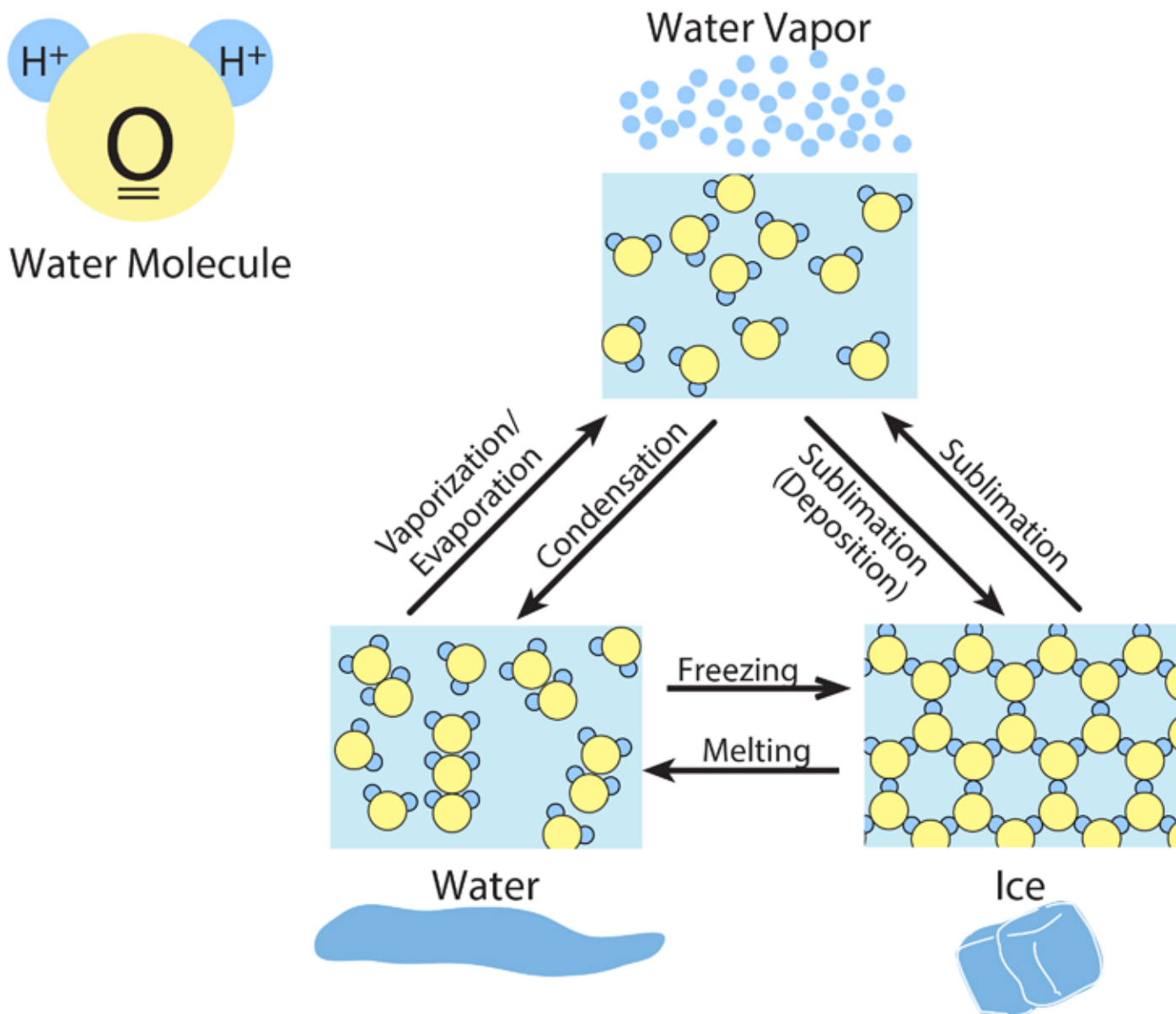


Figure 4.3. The states of matter for water. Note that in the solid state, water molecules lock together to form a crystalline structure in the form of an open lattice. Such an arrangement results in an increase in volume and a decrease in density. Once the lattice is broken apart by melting, the water molecules can pack more tightly together in the liquid state. In the gaseous state, water molecules move independently of one another.

Because temperature is defined in terms of motion, and because motion is a form of energy known as kinetic energy, kinetic energy can be used to define temperature. In physics, the calorie is a unit of kinetic energy, or heat energy. By definition, one **calorie** is equal to the amount of energy required to raise the temperature of 1 gram of liquid water 1.8°F (1°C). The amount of energy (calories) required to raise the temperature of any substance by 1°C is known as **specific heat**. Every substance has its own specific heat, and different states of matter are associated with different specific heat values. The specific heat of water is 1 calorie; but, the specific heat of ice and steam is only 0.5 calorie. The energy required to melt ice is 80 calories per gram, and the energy required to convert water into steam is 590 calories per gram.

## Energy of Phase Changes

In order to gain some sense of the amount of energy involved in phase change, imagine that 10 grams of water is heated with a constant heat source (e.g., on the stovetop) from minus 10°C to 110°C. As the ice is heated, it will change from its initial solid phase to a liquid phase, and finally to a vapor (gas phase). The temperature changes, however, occur in stages, because of the energy required to change phase (break molecular bonds).

- **Heat the Ice.** In order to raise the temperature of ice 1°C, 0.5 calorie of heat energy must be added to it. As just discussed this amount of heat energy is known as the **specific heat of ice**. The formula for calculating the amount of energy required for the change in temperature is:

$$\text{Energy, in calories} = (\text{grams ice}) (\text{specific heat of ice}) (\text{temperature change})$$

So, to raise the temperature of the ice from minus 10°C to its melting point at 0°C, 50 calories of heat energy must be added:

$$(10 \text{ grams}) (0.5 \text{ calories/gram}) (10^\circ\text{C}) = 50 \text{ calories}$$

- **Melting.** Interestingly, once the temperature reaches the melting point, **it stops rising** while the ice melts. Even though heat energy is being added, no temperature change occurs. This is because the heat energy is being used to break the bonds that hold the crystal lattice of the ice together. The amount of energy required to break these bonds is known as the **latent heat of fusion** and is equal to approximately 80 calories per gram of water. The energy is still present in the water. However, because it is not associated with a temperature change, it is said to be *hidden*. The word latent means *hidden*; so this is why the energy associated with phase changes is called latent heat.

Because **NO** change in temperature occurs during a phase change (Figures 4.4 and 4.5), the amount of energy required to melt 10 grams of ice is given by the number of grams of ice multiplied by the latent heat of fusion:

$$(10 \text{ grams}) (0.5 \text{ calories/gram}) = 800 \text{ calories}$$

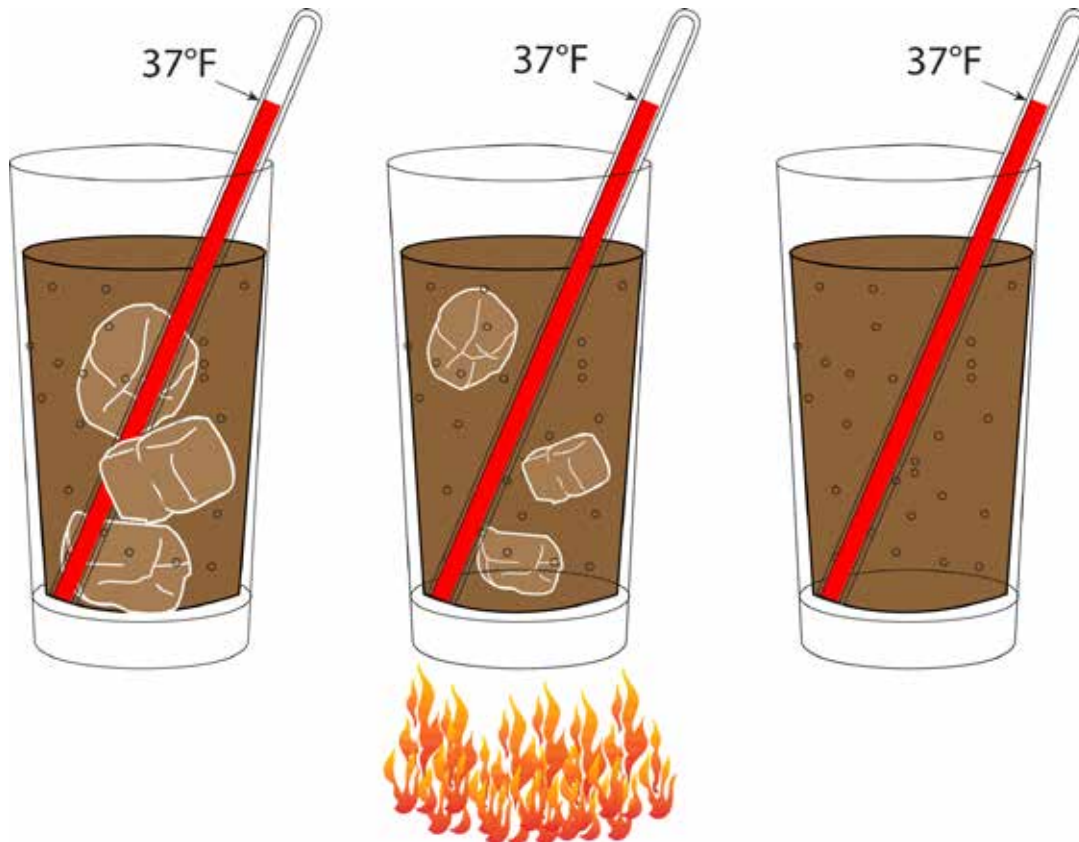


Figure 4.4. In the melting process, the solid ice is changed to liquid water. In this process, heat is absorbed from the burner below by the water molecules, and no change in temperature occurs while the ice melts.

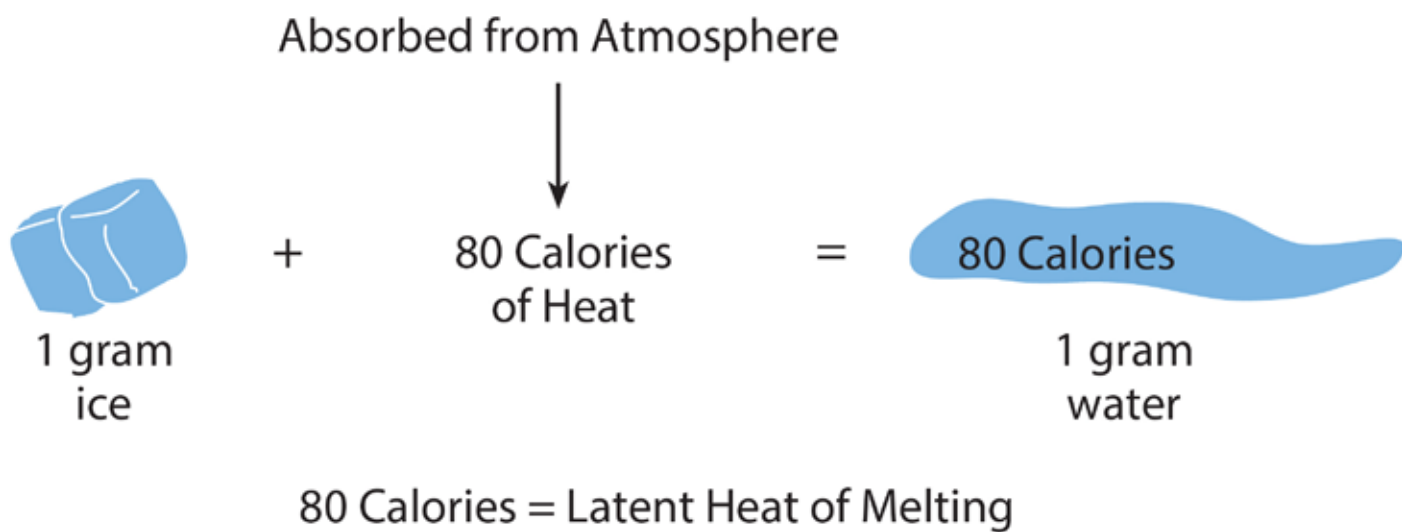


Figure 4.5. It takes approximately 80 calories of heat to melt one gram of water ice. This heat is often referred to as the latent heat of melting. The heat is retained in the water molecule to be released when the water is returned to the solid state.



When ice is melted by heat energy from the atmosphere, the atmosphere cools. This is because the energy used to melt the ice comes from the air around it (and from direct insolation). So, as the heat energy is transferred from the air to the ice, the air cools off while the ice warms and melts. This is analogous to the fact that, when ice is placed in a drink, the drink cools off as energy is transferred from the drink to the ice.

- **Freezing.** In order for water to freeze, it must **lose** heat energy. The amount of energy it gives up is the same as that required to freeze it in the first place, i.e., 80 calories per gram of water. This energy is also known as the latent heat of fusion. As with the melting of the ice, there is no change in the temperature of the water as the water undergoes a phase change from liquid to solid at 0°C (32°F). Because the water has to give up heat energy to the surrounding air in order to freeze, the freezing of water heats the air! **As the water freezes, the air is warmed** (Figure 4.6).

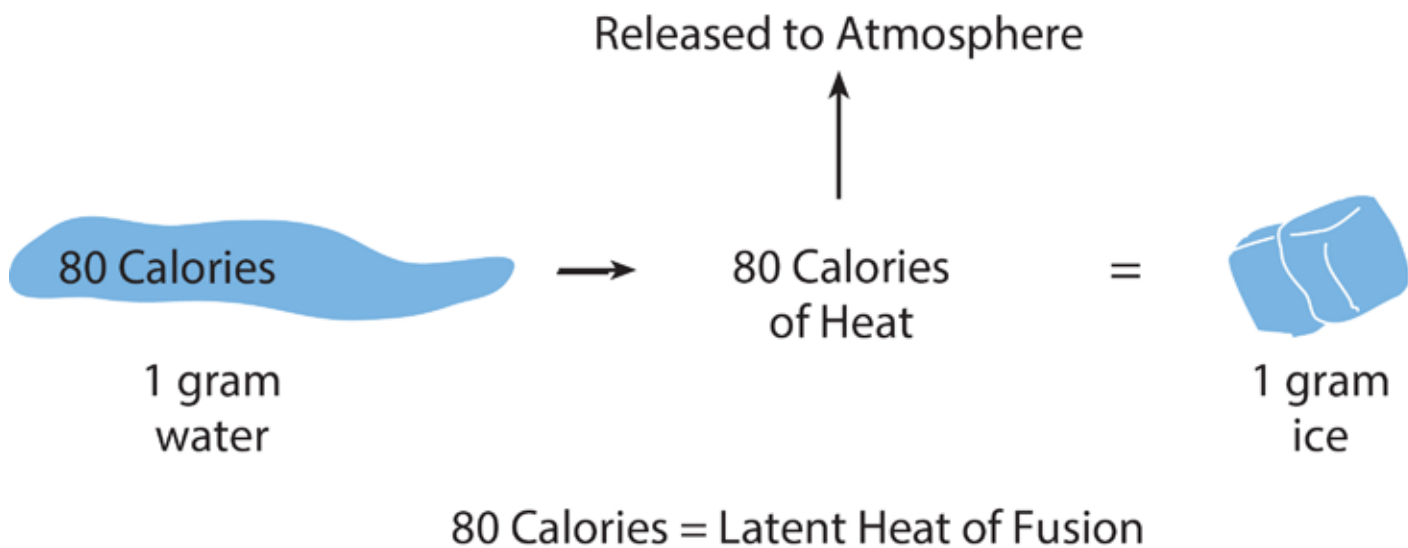


Figure 4.6. When water freezes, it must release 80 calories of energy per gram (latent heat of fusion) in order to cool. The heat energy lost by the water is transferred to the air and warms it. Therefore, the freezing of water warms the air.

- **Heat the Water.** Once the ice has melted, the continued addition of heat energy will cause its temperature to rise. The amount of heat energy required to raise the temperature of water 1°C is known as the **specific heat of water** and is equal to **1 calorie per gram**. The amount of energy required to raise the temperature of the water from 0°C to 100°C is 1000 calories.

$$(10 \text{ grams}) (1 \text{ calorie/gram}) (100^\circ\text{C}) = 1000 \text{ calories}$$

- **Evaporation.** Once the water reaches its boiling point at 100°C, it will begin to undergo a phase change from liquid to gas, and will then evaporate. As with melting, no temperature change occurs during this phase change. The amount of energy required for this phase change is known as the **latent heat of vaporization**, and is equal to approximately 590 calories per gram of water (Figure 4.7).

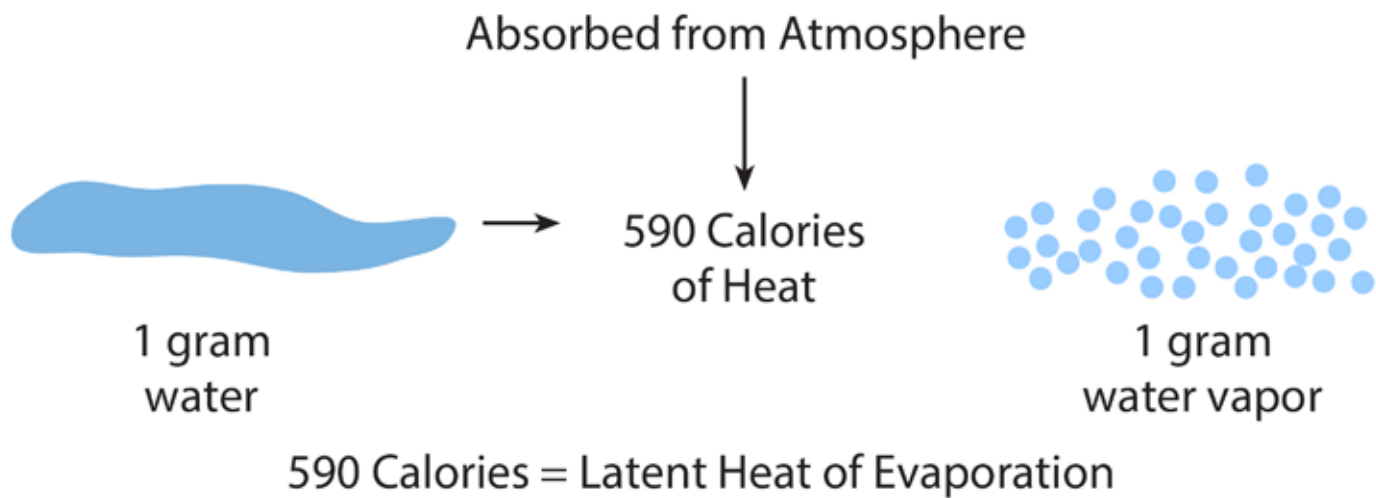


Figure 4.7. In order for water to evaporate, each gram must absorb approximately 590 calories per gram of water from the air. This cools the air; in other words, evaporation causes cooling.

For our 10-gram piece of ice, the amount of energy required is:

$$(10 \text{ grams}) (590 \text{ calories/gram}) = 5900 \text{ calories}$$

If we continue heating the water vapor from 100°C to 110°C, we will have to add 0.5 calories per gram of steam per degree Celsius. So, we will have to add 50 more calories (10 grams x 0.5 calories/gram x 10°C = 50 calories).

Thus, in this example of phase change energies involving a ten-gram piece of ice, a total of 7800 calories of heat energy was required to raise its temperature from minus 10°C to 110°C. (50 cal. + 800 cal. + 1000 cal. + 5900 cal. + 50 cal. = 7800 cal.).

*Note: The boiling point of water is equal to the temperature at which the vapor pressure of the liquid equals the external atmospheric pressure (14.7 psi at sea level). At this temperature, vapor produced in the interior of the liquid as a result of on-going phase changes results in bubble*

*formation and turbulence that is characteristic of boiling water. During the phase change, some high-speed molecules break free and leave the liquid, i.e., they evaporate. Because this represents a loss of energy, more energy must be added to keep the water boiling. This is why the temperature remains constant during the phase change: the energy that must be added to replace that which is being lost must equal that which is lost. So, the amount added equals the amount lost, and no change in temperature occurs during boiling. If you've ever boiled water at high elevation, you know that water will boil at temperatures below 100°C. This is because there is less air pressure at higher elevation.*

The evaporation of water cools both the air and the surfaces from which it evaporates. This occurs because the energy required to drive the phase change comes from the air and the surface on which the water is located. In addition, as the high-speed (high temperature) molecules evaporate and leave the surface, they leave behind lower speed (lower temperature) molecules. So, evaporation causes cooling. The cool sensation that we feel when we get out of a shower or a pool is caused by the evaporation of water from our skin.

Both liquid water and water vapor contain latent heat. Globally, 80% of incident solar radiation absorbed at the surface is used to evaporate water. **This immense amount of energy is stored in the water vapor molecules as latent heat. This latent heat is transferred in the atmosphere by convection and advection, ultimately to be released upon condensation.**

- **Condensation.** When water condenses from a gaseous state to a liquid state, energy that was stored in the water in the form of latent heat is released. The amount released is the **same** amount used to evaporate the water in the first place. However, instead of being called the latent heat of vaporization, it is now called the **latent heat of condensation**. It, too, is equal to 590 calories per gram of water (or approximately 590 calories) (Figure 4.8).

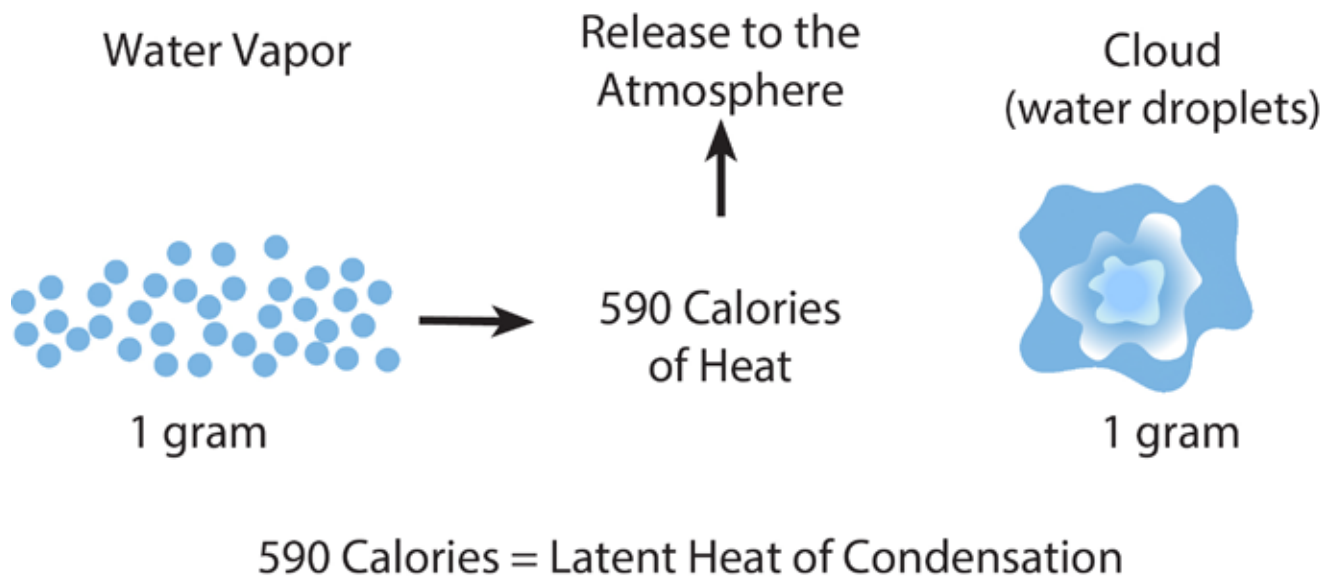


Figure 4.8. Condensation is very important in the development of storms because it releases heat energy to the air. For every gram of water that condenses in a rising parcel of air, approximately 590 calories of heat energy is released to the air parcel and this warms it. By warming the air parcel relative to the surrounding air, this increases the temperature gradient, which in turn, increases wind velocity. And, by keeping the air parcel warmer than it would be if no condensation were occurring, the air parcel will rise to a greater altitude.

Given that 80% of the insolation reaching the Earth's surface is used to evaporate water, this means that an immense amount of heat energy is released to the atmosphere when this water vapor condenses. Consequently, **the condensation of water vapor constitutes one of the major processes responsible for heat transfer in the troposphere.**

The latent heat of condensation released in cloud formation is substantial. Hurricanes, which are composed of thousands of thunderheads, can release as much energy as 100,000 one-megaton hydrogen bombs.

From the standpoint of meteorology, the energy released by condensation is extremely important because, **it is the fuel for storms. Condensation fuels storms by releasing energy to the atmosphere and heating the surrounding air.**

Because warm air is less dense than cold air, heating the air not only causes the air to rise, it also decreases the air pressure. So, **condensation causes the air pressure to drop and this increases the pressure gradient between the areas around the storm and the area of the storm. Strong horizontal and vertical winds result.** The greater the amount of condensation, the greater the pressure gradient, and the higher the wind speeds.

- **Sublimation.** Sublimation is a special type of phase change that occurs when ice goes directly to the gaseous state without first melting and becoming a liquid. The amount of energy involved is the same as that involved in **both melting and evaporation**. So, the **heat of sublimation** is equal to 670 calories per gram, i.e., the heat of fusion (80 calories per gram) plus the heat of vaporization (590 calories per gram) (Figure 4.9).

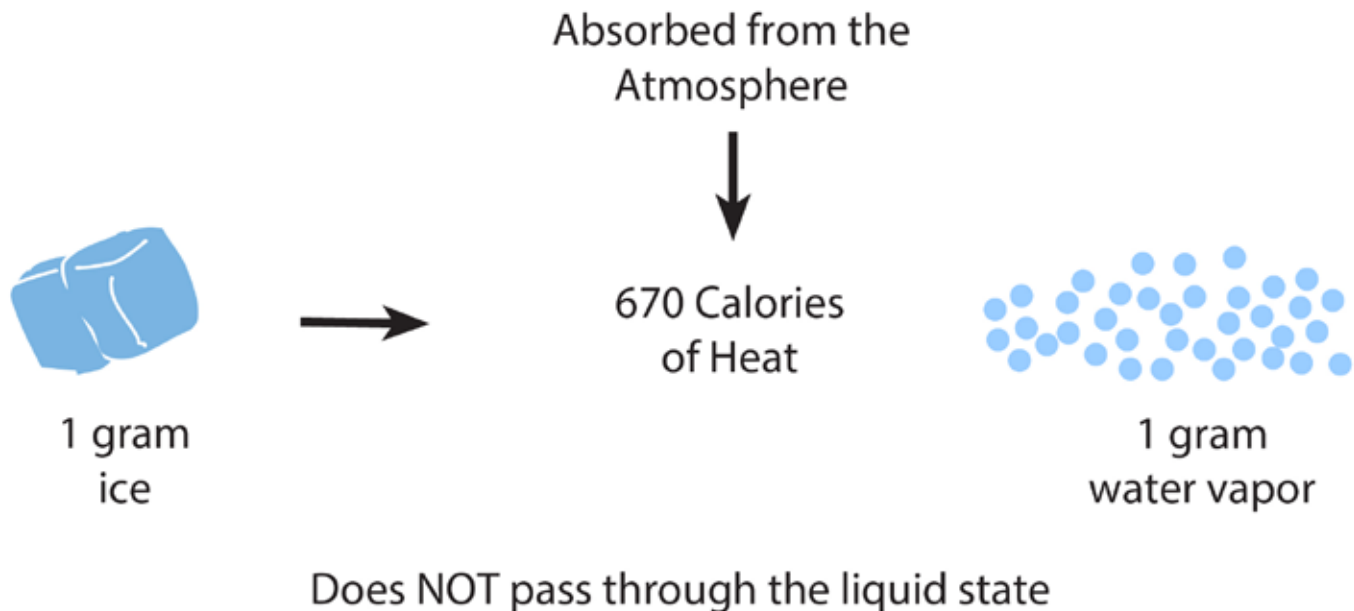


Figure 4.9. In the process of sublimation, enough energy is absorbed by ice that some molecules escape in gaseous form, skipping the liquid phase.

If water goes directly from a vapor state to the solid state, it is called **deposition** (or sublimation). The amount of energy involved is the same as that involved with sublimation (Figures 4.10 and 4.11).

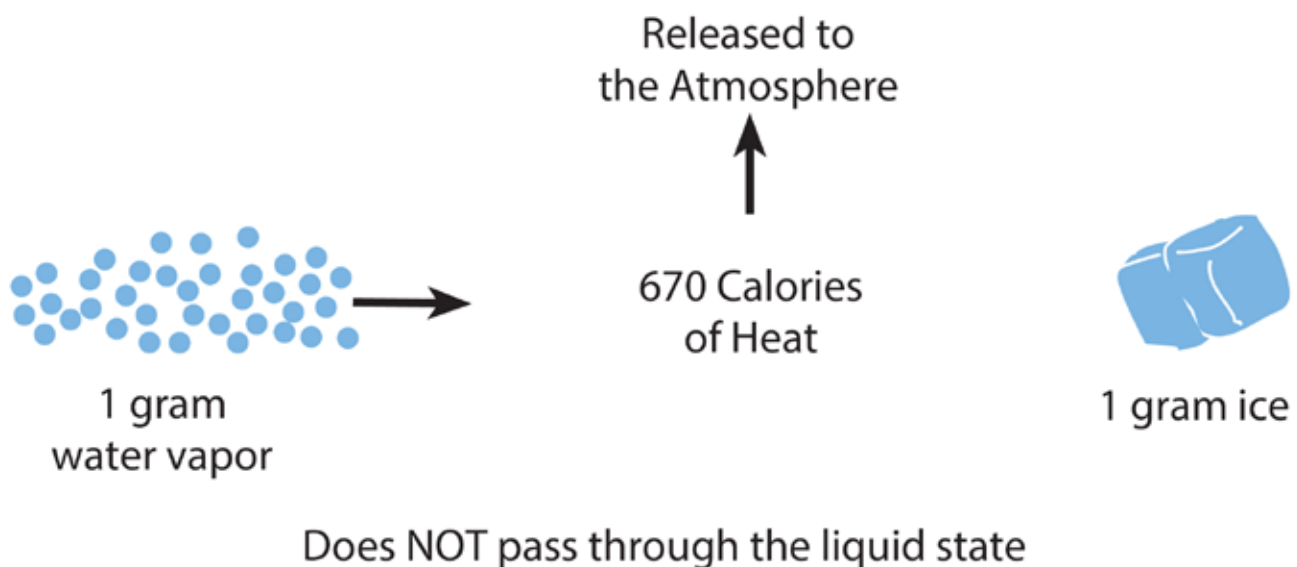


Figure 4.10. The process of deposition is the opposite of sublimation. During deposition, water molecules lose so much energy that they go directly to the solid phase without first condensing into a liquid.

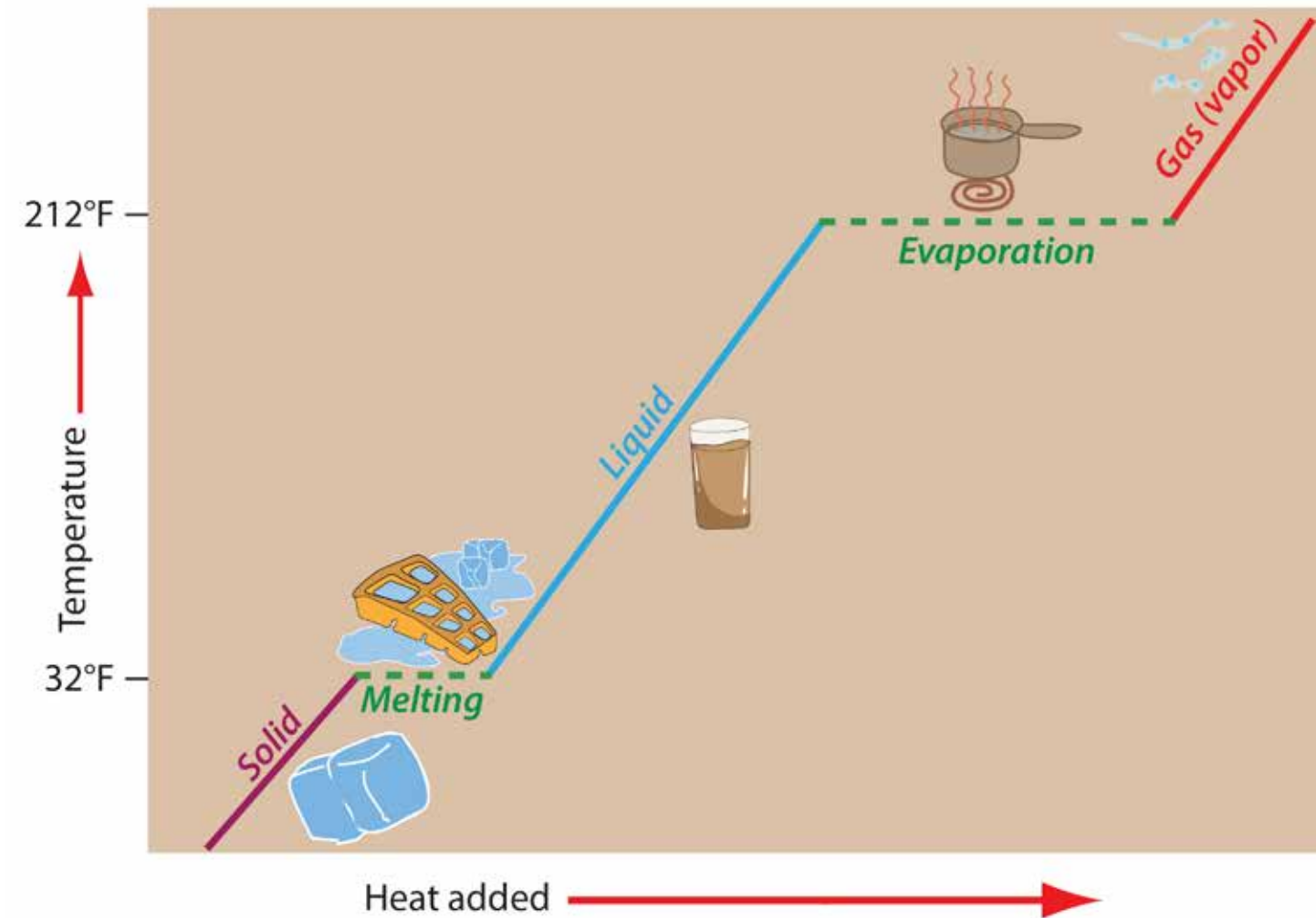


Figure 4.11. When solid ice is slowly heated at a constant rate, temperature climbs predictably, until 32°F (0°C) is reached. Even though more thermal energy is being applied to the system, the temperature hovers until all of the ice has melted. Energy has been used in breaking chemical bonds, rather than increasing the temperature. A similar plateau occurs when temperatures approach 212°F (100°C), when more chemical bonds are being broken during evaporation. The same energy that was required to change state from solid to liquid or liquid to gas can be released back to the atmosphere during condensation (gas to liquid) or deposition (gas to solid) (Credit/Source: Dennis I. Netoff).

A lot of energy is required to melt ice. This, combined with the high albedo of snow (about 90%), explains why snow can linger on the ground long after temperatures have risen above freezing. It is also interesting that sublimation dominates the phase change of snow. Because of this, much of the water that falls in the form of snow never makes it into the soil and surrounding streams because it goes directly into the atmosphere. This fact is of importance when hydrologists attempt to estimate how much water will flow in rivers following the spring snowmelt. These estimates are used to regulate water levels in reservoirs and rates of water consumption.

In summary, the process of evaporation removes energy from the Earth's surface and stores it as latent heat in water vapor. The uplift of air results in cooling of the water vapor, and ultimately condensation, which releases latent heat back to the atmosphere (Figure 4.12).

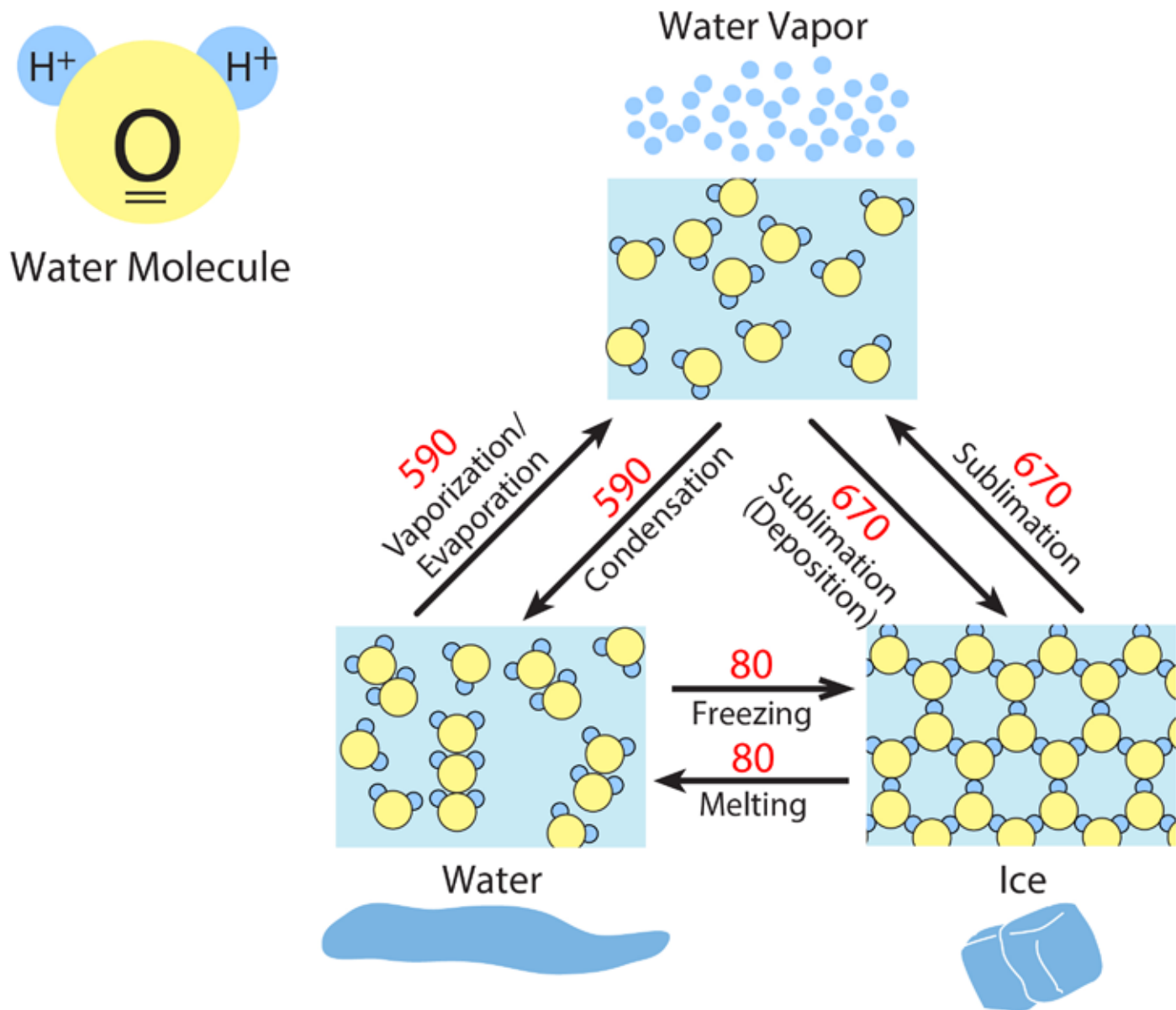


Figure 4.12. Phase changes in water require energy to convert from a lower state to a higher state (ice to water, water to water vapor). In the reverse process, energy is released.

## The Hydrologic Cycle

The Earth is essentially a closed system with regard to Earth materials, with the exception of the small input from outer space (meteorites). The amount of water on Earth through time is therefore nearly constant; the same water is recycled over and over through Earth's geologic, biologic, hydrologic, and atmospheric systems by way of the hydrologic cycle.

Water on the Earth is temporarily stored in the following *reservoirs*:

- **Oceans.** The oceans contain 96.7% of all the free water on the planet. Because the oceans cover so much of the Earth's surface, approximately 80% of all precipitation falls into the ocean.
- **Freshwater Reservoirs.** The remaining 3.3% of the world's free water is freshwater. Freshwater reservoirs include:
  - **Glaciers.** Glaciers hold approximately 75% of the available freshwater.
  - **Groundwater.** 24% of the Earth's available freshwater occurs as groundwater. Groundwater sources contain the greatest amount of **unfrozen** freshwater. Groundwater is one of the most important reservoirs of fresh water, and industrialized nations depend heavily upon it for their sustenance.
- **Rivers and Lakes.** These account for about 0.32% of the world's available freshwater. Although this is the most readily visible supply of water, it accounts for a relatively small percent of the Earth's total supply of freshwater.
- **Soil Water.** This reservoir accounts for only about 0.005% of freshwater. This small percentage, is essential to the biosphere because virtually all plants grow in soil, and plants are the basis for ecosystems.
- **Atmosphere.** The atmosphere accounts for approximately 0.04% of freshwater. If all the water in the atmosphere precipitated at once, it would cover the Earth's surface to a depth of less than 1 inch. The amount of time a water molecule remains in the air averages only 11 days.

As water absorbs heat energy from the Sun, part of this energy is utilized in either evaporation or sublimation, the initial step in the hydrologic cycle. Two forms of evaporation can be distinguished:

- **Evaporation.** This is the standard phase change from liquid to gas that occurs from bodies of water and other surfaces that contain water. In the United States, the average annual amount of evaporation varies from 16 inches/year in cool areas to potentially 100 inches/year in the arid Southwest. In other words, if you left a tub of water sitting in the open air in the American Southwest, about 100 inches would evaporate from the tub each year.



- **Transpiration.** Transpiration is evaporation of water from the leaves of plants. The source of the water lost by plants is, of course, soil water. This water was taken into roots, transported upward through plants, and then transpired from leaves. Transpiration constitutes a major mechanism by which water enters the atmosphere. For example, a single acre of corn can transpire 3542 gallons of water on a hot summer day. A single cottonwood tree can transpire approximately 100 gallons of water per day. In fact, it has been estimated that half of all the water that falls on the Amazon rainforest is transpired from the forest itself. Consequently, if the rainforest is cut down, rainfall levels will decrease. Therefore, trees help control the climate of an area by influencing rainfall levels.

In practice, it is difficult to determine whether water was evaporated from a surface or from leaves, so both processes are collectively referred to as **evapotranspiration** (abbreviated as ET). The amount of ET that can occur in an area is controlled by several factors that are discussed below.

## Factors that Control Evapotranspiration

- **Availability of Water.** This is obviously the most important factor affecting evapotranspiration. Approximately 15% of global ET occurs from land, and 85% occurs from the oceans, which cover most of the planet's surface. Temperature is a major control because the phase change from liquid to gas requires energy. As a result, the greater the temperature, the greater the potential for ET to occur. Humidity is another factor that affects the rate of ET. If the air contains a lot of vapor (i.e., if it has a high humidity), the rate of ET will decrease. This is because water molecules in the air may collide with the surface or with other water molecules, and return to the liquid state. For example, when the humidity is near 100%, almost every water molecule that evaporates from a water surface is replaced by water molecules that collide with the surface and return to the liquid state. So, losses of water molecules by ET are balanced by gains, and no net change in ET occurs (Figure 4.13). **Thus, the higher the humidity, the lower the potential for ET.**

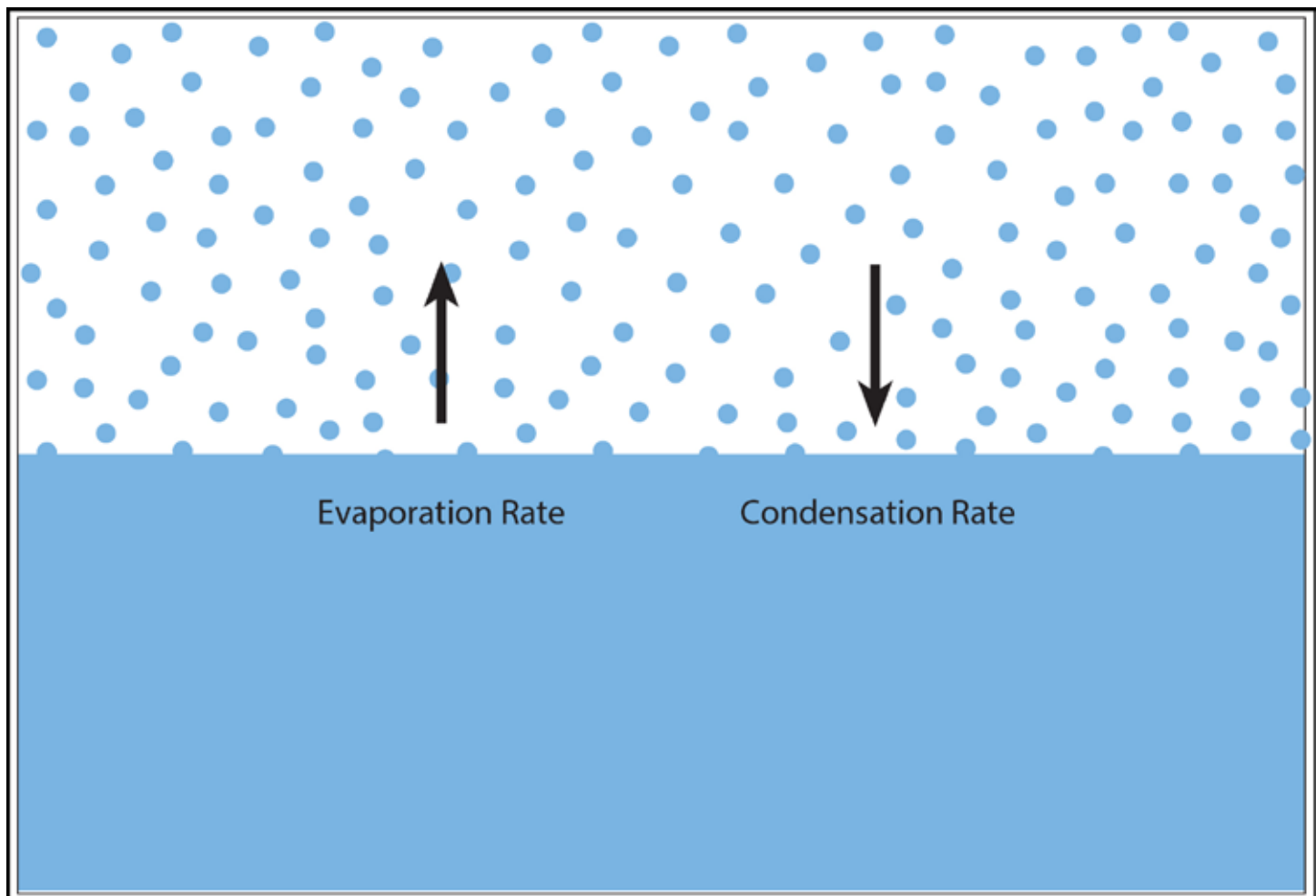


Figure 4.13. When air is saturated ( $RH = 100\%$ ) with water vapor, an equilibrium is established so that the quantity of water vapor molecules condensing equals the number that are evaporating.

- **Wind Speed.** Wind speed greatly affects the rate of ET. The greater the wind speed, the greater the rate of ET. When air is stagnant, the water vapor molecules begin to saturate the air in contact with the adjacent water surface; when the wind blows, it constantly removes these water vapor molecules, thereby making room in the air for more evaporation. The factors just discussed explain how hair dryers and clothes dryers work. Both devices generate hot air that blows across wet surfaces. This causes evaporation and drying to occur.

A distinction can be made between the amount of ET that *could* occur if water were not a limiting factor and the amount that *actually* occurs. The former is known as **potential evapotranspiration** (PET), and the latter as **actual evapotranspiration** (AET). This distinction is relevant because some areas, such as hot deserts, may have less actual ET than wetter areas because of a lack of water availability in deserts. This means that **deserts may have a higher PET, but a lower AET, than tropical rainforests.**

## Relative Humidity

Humidity refers to the water vapor content of the atmosphere. Although there are many ways to express humidity, perhaps the most common one is **relative humidity**. Relative humidity is an attempt to state how near (or far) the atmosphere is to being saturated with respect to water vapor. More precisely, it refers to the ratio of the water vapor present in the atmosphere relative to the maximum amount of water vapor that the air could hold at a specific temperature. The **mixing ratio** is the actual amount of water vapor present in a given mass of air, and the **capacity** refers to the maximum amount of water vapor that air can hold at a given temperature. Both values are expressed in grams per kilogram (g/kg) of dry air. Relative humidity can therefore be expressed by the following formula:

$$RH = \frac{MR}{C} \text{ (given in percent)}$$

Example: If the outside air on a summer afternoon in Huntsville contains 9.946 g/kg of water vapor and the capacity of the air is determined to be 30.052 g/kg at the ambient temperature of 90°F, then the RH is:

$$RH = \frac{9.946 \text{ g/kg}}{30.052 \text{ g/kg}} = 0.33096 = 33\%$$

The air above is approximately one-third saturated.

**Capacity is temperature-dependent.** At higher temperatures, air can hold more water vapor because the water vapor molecules are more energetic and are therefore less likely to drop to a lower energy level. **Figure 4.14** provides approximate values for the capacity of saturated air at various temperatures at sea level pressure. At 60°F, for example, the capacity is 10.699 g/kg, whereas at 70°F, it is 15.260 g/kg and at 80°F the capacity is 21.537 g/kg.

CAPACITY OF SATURATED AIR					
(Numbers are Approximate)					
Air Temp (°F)	Capacity (g/kg)	Air Temp (°F)	Capacity (g/kg)	Air Temp (°F)	Capacity (g/kg)
-40	.113	12	1.564	64	12.347
-39	.119	13	1.630	65	12.797
-38	.125	14	1.708	66	13.258
-37	.133	15	1.782	67	13.741
-36	.141	16	1.856	68	14.230
-35	.150	17	1.945	69	14.741
-34	.157	18	2.025	70	15.260
-33	.167	19	2.122	71	15.810
-32	.176	20	2.210	72	16.371
-31	.187	21	2.312	73	16.949
-30	.197	22	2.407	74	17.547
-29	.207	23	2.518	75	18.158
-28	.220	24	2.623	76	18.796
-27	.231	25	2.726	77	19.440
-26	.245	26	2.852	78	20.123
-25	.257	27	2.967	79	20.814
-24	.273	28	3.101	80	21.537
-23	.286	29	3.224	81	22.274
-22	.303	30	3.368	82	23.036
-21	.319	31	3.503	83	23.823
-20	.334	32	3.656	84	24.629
-19	.354	33	3.809	85	25.470
-18	.371	34	3.965	86	26.320
-17	.392	35	4.128	87	27.220
-16	.411	36	4.296	88	28.130
-15	.435	37	4.470	89	29.080
-14	.456	38	4.652	90	30.052
-13	.481	39	4.838	91	31.058
-12	.504	40	5.034	92	32.097
-11	.528	41	5.232	93	33.158
-10	.557	42	5.443	94	34.263
- 9	.583	43	5.657	95	35.380
- 8	.615	44	5.881	96	36.563
- 7	.644	45	6.112	97	37.760
- 6	.679	46	6.350	98	39.010
- 5	.710	47	6.598	99	40.596
- 4	.747	48	6.852	100	41.596
- 3	.782	49	7.119	101	42.957
- 2	.817	50	7.389	102	44.351
- 1	.861	51	7.676	103	45.803
0	.900	52	7.966	104	47.270
1	.946	53	8.271	105	48.814
2	.988	54	8.583	106	50.378
3	1.039	55	8.907	107	52.017
4	1.086	56	9.242	108	53.691
5	1.140	57	9.585	109	55.419
6	1.191	58	9.946	110	57.203
7	1.243	59	10.310	111	59.026
8	1.305	60	10.699	112	60.932
9	1.361	61	11.091	113	62.860
10	1.429	62	11.497	114	64.893
11	1.491	63	11.913	115	66.848

Figure 4.14. The capacity of the air at 90°F (a not uncommon afternoon summer temperature in southeast Texas) is 30.052 g/kg. Compare this to the capacity of air with a temperature of 50°F (a fairly typical winter day temperature); 7.389 g/kg. The

air in summer can hold over 4 times the water vapor of a typical winter day. Given this significant difference in water vapor, it is easy to see why summer storms in Texas tend to be more vigorous (more condensation taking place, thus more energy being released) and result in larger quantities of precipitation. Not only is there more water vapor in the air, but the summer storm clouds may tower 30,000 to 40,000 feet compared to winter storm clouds that are typically only a few thousand feet in vertical extent (Source/Credit: modified from Dennis I. Netoff and Ava Fujimoto-Strait, *Weather & Climate Lab Manual*).

In order for condensation to occur, the relative humidity must be at or close to 100%. It becomes obvious by analyzing the relative humidity formula that **an unsaturated parcel of air can become saturated by either (1) increasing the amount of water vapor in the parcel so that the mixing ratio is equal to the capacity, or (2) dropping the temperature of the air parcel and thereby decreasing its capacity so that it is brought to the same value as the mixing ratio** (Figure 4.15).

<p>Example #1: An unsaturated parcel of air has a RH of 60% and a temperature of 75°F. How much moisture must be added to the parcel to saturate it?</p>	<p>Example #2: An unsaturated parcel of air at 90°F has a RH of 40%. How much must the air be cooled to bring the C down to the same value as the MR (and therefore bring the RH to 100%)?</p>
<p>Solution: The MR is found by using the formula:</p> $0.60 = \frac{\text{MR}}{\text{C}}$	<p>Solution: The MR is again found by using the formula:</p> $0.40 = \frac{\text{MR}}{\text{C}}$
<p>C (from Table 1) = 18.158 g/kg</p>	<p>MR = 30.052 g/kg (0.40) = 12.021 g/kg</p>
<p>MR = 18.158 g/kg (0.60) = 10.895 g/kg</p>	<p>Refer to the capacity table to see which C most closely matches the value of this MR. The answer is 63°F. The air must therefore be cooled from 90°F to 63°F to achieve a RH of 100%.</p>
<p>18.158 g/kg - 10.895 g/kg = 7.263 g/kg</p>	

Figure 4.15. Examples of the relationship between relative humidity, mixing ratio and capacity.

Saturation of a parcel of air by the first method is generally very slow and inefficient in the atmosphere. **Cooling of air is therefore the most common way that saturation is achieved in the atmosphere.** The temperature at which a cooling parcel of air reaches saturation is called the **dew point**. The dew point for any parcel of air can be determined if the mixing ratio is known and a capacity table is accessible. But how does air cool to the dew point?

Several cooling mechanisms can drop air temperature to the dew point. Night-time **radiational cooling** commonly achieves dew point temperature in Huntsville, as is evidenced by frequent fogs, and by dew or frost on ground objects in the early morning hours. **Conductional cooling**, which occurs along the Texas Coastal Plain during the winter when

relatively warm Gulf air comes in contact with cooler land, often produces low level clouds or fog. **Mixing** of warm and moist surface air with cool air aloft will occasionally produce a layer of stratocumulus clouds over portions of East Texas. Most clouds in the atmosphere, however, are produced by **adiabatic cooling**, which is the result of the expansion of air as it rises in the atmosphere. Air may rise on its own by convection, or may be forced aloft by mountain barriers, surface convergence or along fronts.

## Humidity Measurement: the Sling Psychrometer

The sling psychrometer is one of several instruments that is used to measure relative humidity (Figure 4.16). The principles upon which it is based provide insight into the relationships between relative humidity, capacity and mixing ratio. The **sling psychrometer** consists of two thermometers attached to a metal plate which is slung around in circles, hence the name *sling* psychrometer. One of the thermometers has a piece of cloth attached to the end of the bulb and is wetted before slinging the instrument. This thermometer is known as the **wet bulb thermometer** and the temperature it records is the wet bulb temperature. The other thermometer is a standard thermometer with no cloth attached to it. Because it is not wet, it is called the **dry bulb thermometer** and it measures the *actual* air temperature.



Figure 4.16. The sling psychrometer is used to measure relative humidity. It consists of two thermometers, one with a wetted cotton pad. As the instrument is spun, evaporation from the wet bulb thermometer reduces its temperature. The greater the reduction of temperature of the wet bulb, the drier the air, and the lower the relative humidity. In the illustration, the wet bulb is 64°F and the dry bulb is 71°F; the depression is 7°F (Source/Credit: Dennis I. Netoff).



As the psychrometer is slung in circles, moisture evaporates from the wet bulb thermometer causing it to cool. Slinging the thermometer increases the rate of evaporation because this action duplicates the effect of the wind. As a result of evaporation, the wet bulb temperature is less than the dry bulb temperature, and the difference between the wet bulb and dry bulb temperatures is known as the **wet bulb depression**. The wet bulb depression and air temperature (dry bulb) are used to determine relative humidity by referring to a psychrometric table (Figure 4.17).

Relative Humidity																													
Air Temp. (°F)	Depression of the Wet Bulb Thermometer																												
	T	0.5	1.0	1.5	2.0	2.5	3.0	3.5	4.5	5.0	5.5	6.0	6.5	7.0	7.5	8.0	8.5	9.0	9.5	10	11	12	13	14	15	16	17	18	19
20	92	85	77	70	62	55	48	33	28	19	12	5	-	-	-	-	-	-	-	-	-	-	-	-	-	-	-	-	-
21	92	85	78	71	63	56	49	35	28	21	15	8	1	-	-	-	-	-	-	-	-	-	-	-	-	-	-	-	-
22	93	86	78	71	65	58	51	37	31	24	17	11	4	-	-	-	-	-	-	-	-	-	-	-	-	-	-	-	-
23	93	86	79	72	66	59	52	39	33	26	20	14	7	1	-	-	-	-	-	-	-	-	-	-	-	-	-	-	-
24	93	87	80	73	67	60	54	41	35	29	22	16	10	4	-	-	-	-	-	-	-	-	-	-	-	-	-	-	-
25	94	87	81	74	68	62	55	43	37	31	25	19	13	7	1	-	-	-	-	-	-	-	-	-	-	-	-	-	-
26	94	87	81	75	69	63	57	45	39	33	27	21	16	10	4	-	-	-	-	-	-	-	-	-	-	-	-	-	-
27	94	88	82	76	70	64	58	47	41	35	29	24	18	13	7	2	-	-	-	-	-	-	-	-	-	-	-	-	-
28	94	88	82	76	71	65	59	48	43	37	32	26	21	15	10	5	-	-	-	-	-	-	-	-	-	-	-	-	-
29	94	88	83	77	72	66	60	50	44	39	34	28	23	18	13	8	3	-	-	-	-	-	-	-	-	-	-	-	-
30	94	89	83	78	73	67	62	51	46	41	46	31	26	21	16	11	6	1	-	-	-	-	-	-	-	-	-	-	-
31	94	89	84	78	73	68	63	52	47	42	47	33	28	24	18	13	8	4	-	-	-	-	-	-	-	-	-	-	-
32	95	89	84	79	74	69	64	54	49	44	49	35	30	25	20	16	11	7	2	-	-	-	-	-	-	-	-	-	-
33	95	90	85	80	75	70	65	57	51	46	41	37	32	27	23	18	14	9	5	-	-	-	-	-	-	-	-	-	-
34	95	90	86	81	76	71	66	57	52	48	43	38	34	29	25	21	16	12	8	-	-	-	-	-	-	-	-	-	-
35	95	91	86	81	77	72	67	58	54	49	45	40	36	32	27	24	19	14	10	2	-	-	-	-	-	-	-	-	-
36	95	91	86	82	77	73	68	60	55	51	46	41	38	34	29	25	21	17	13	5	-	-	-	-	-	-	-	-	-
37	95	91	87	83	78	74	69	61	57	53	48	44	40	36	31	27	23	19	15	7	-	-	-	-	-	-	-	-	-
38	96	91	87	83	79	75	70	62	58	54	50	46	42	37	33	29	25	21	17	10	2	-	-	-	-	-	-	-	-
39	96	92	87	83	79	75	71	63	59	55	51	47	43	39	35	31	27	24	20	12	5	-	-	-	-	-	-	-	-
40	96	92	87	83	79	75	71	64	60	56	52	48	45	41	37	33	29	26	22	15	7	0	-	-	-	-	-	-	-
41	96	92	88	84	80	76	72	65	61	57	54	50	46	42	39	35	31	28	24	17	10	3	-	-	-	-	-	-	-
42	96	92	88	85	81	77	73	65	62	58	55	51	47	44	40	36	33	30	26	19	12	5	-	-	-	-	-	-	-
43	96	92	88	85	81	77	73	66	63	59	55	52	48	45	42	38	35	31	28	21	14	8	1	-	-	-	-	-	-
44	96	93	89	85	81	78	74	67	63	60	56	53	49	46	43	39	36	33	30	23	16	10	4	-	-	-	-	-	-
45	96	93	89	86	82	78	74	67	64	61	57	54	51	47	44	41	38	34	31	25	18	12	6	-	-	-	-	-	-
46	96	93	89	86	82	79	75	68	65	61	58	55	52	48	45	42	39	35	32	26	20	14	8	2	-	-	-	-	-
47	96	93	89	86	82	79	75	69	66	62	59	56	53	49	46	43	40	37	34	28	22	16	10	5	-	-	-	-	-
48	96	93	90	86	83	79	76	69	66	63	60	57	54	50	47	44	41	38	35	29	23	18	12	7	1	-	-	-	-
49	96	93	90	86	83	80	76	70	67	64	61	57	54	51	48	45	42	39	36	31	25	19	13	9	3	-	-	-	-
50	96	93	90	87	83	80	77	71	67	64	61	58	55	52	49	46	43	41	38	32	27	21	16	10	5	-	-	-	-
52	97	94	90	87	84	81	78	72	69	66	63	60	57	54	51	49	46	43	40	35	29	24	19	14	9	4	-	-	-
54	97	94	91	88	85	82	79	73	70	67	64	61	59	56	53	50	48	45	42	37	32	27	22	17	12	8	3	-	-
56	97	94	91	88	85	82	79	73	71	68	65	63	60	57	55	52	50	47	44	39	34	30	25	20	16	11	7	2	-
58	97	94	91	88	85	83	80	74	72	69	66	64	61	59	56	54	51	49	46	41	37	32	27	23	18	14	10	6	1
60	97	94	91	89	86	83	81	75	73	70	68	65	63	60	58	55	53	50	48	43	39	34	30	26	21	17	13	9	5
62	97	94	92	89	86	84	81	76	74	71	69	66	64	61	59	57	54	52	50	45	41	36	32	28	24	20	16	12	8
64	97	95	92	90	87	85	82	77	74	72	70	67	65	63	60	58	56	53	51	47	43	38	34	30	26	22	18	15	11
66	97	95	92	90	87	85	82	78	75	73	71	68	66	64	61	59	57	55	53	48	44	40	36	32	29	25	21	17	14
68	97	95	92	90	88	85	83	78	76	74	71	69	67	65	62	60	58	56	54	50	46	42	38	34	31	27	23	20	16
70	98	95	93	90	88	86	83	79	77	74	72	70	68	66	64	61	59	57	55	51	48	44	40	36	33	29	25	22	19
72	98	95	93	91	88	86	84	79	77	75	73	72	69	67	65	63	61	59	57	53	49	45	42	38	34	31	28	24	21
74	98	95	93	91	89	86	84	80	78	76	74	72	69	67	65	63	61	60	58	54	50	47	43	39	36	33	29	26	23
76	98	96	93	91	89	87	84	80	78	76	74	73	70	68	66	64	62	61	59	55	51	48	44	41	38	34	31	28	25
78	98	96	93	91	89	87	85	81	79	77	75	74	71	69	67	65	63	62	60	56	53	49	46	43	39	36	33	30	27

Figure 4.17. The psychrometric table plots depression on the horizontal axis and dry bulb temperature on the vertical axis. Figure 4.16 indicates a wet bulb reading of 64°F and a dry bulb reading of 71°F. The depression of 7 degrees is plotted on the table above by the green shading, and the dry bulb temperature by the yellow shading. The intersection of the two shaded bands gives a relative humidity of between 68% and 69%. If the wet bulb reading was 64°F and the dry bulb 78°F, then the depression would be 14°F (blue) and the relative humidity would be 46% (Source/Credit: modified from Dennis I. Netoff and Ava Fujimoto-Strait, *Weather & Climate Lab Manual*).

The amount of wet bulb depression is inversely proportional to the relative humidity of the air. If the relative humidity is low, the amount of wet bulb depression is large (big difference in temperature); conversely, if the relative humidity is high, the amount of wet bulb depression is small (little difference in temperature). This is because when the relative humidity is low, water will readily evaporate from the wet bulb causing its temperature to drop substantially thereby increasing the wet bulb depression. Conversely, if the relative humidity is high, very little moisture will evaporate from the wet bulb, and so there is very little wet bulb depression. If the relative humidity reaches 100%, no evaporative cooling will occur, and there will be no wet bulb depression. The temperature of the wet bulb and dry bulb will be the same. When this situation exists, moisture in the air condenses to form water droplets. If enough are present, clouds and/or fog result.

Other types of devices have been developed to measure relative humidity. One is the **hair hygrometer**, which is made from real hair. The hair is attached to a post at one end and a spring at the other. The spring is, in turn, attached to a recording pen that moves up and down as the relative humidity changes. As the humidity increases, the hair absorbs moisture and it expands. As humidity decreases, the hair dehydrates and shrinks.

## More on Relative Humidity

The temperature at which the air would have to be cooled (with no change in air pressure or moisture content) for saturation to occur is called **dew point**. It is the temperature at which relative humidity reaches 100% and condensation occurs. The altitude at which this occurs is readily apparent because it is the altitude at which clouds begin to form, also known as the **lifting condensation level** (LCL). The flat bases of clouds represent the dew point boundary; below the clouds, the relative humidity is less than 100%, and within the clouds, the relative humidity is 100% (Figure 4.18).

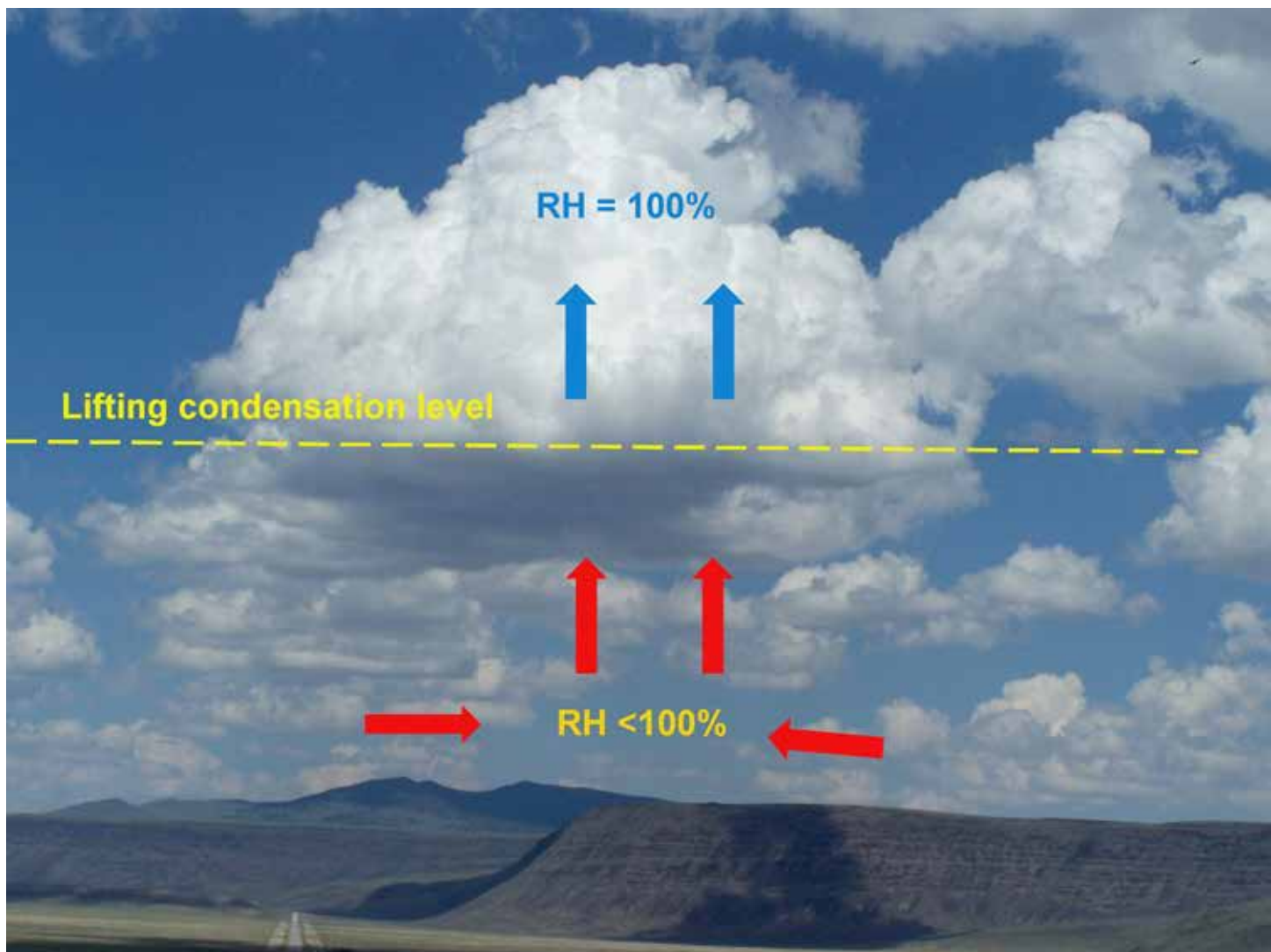


Figure 4.18. In the formation of many clouds, unsaturated air (RH less than 100%) rises, cools by expansion and becomes saturated at the lifting condensation level (LCL). The flat base of clouds marks the LCL, which is the altitude at which dew point is reached in the sky. The lower the cloud base, the higher the relative humidity. This is true because humid air does not have to rise as much as dry air before it cools enough to reach dew point (Source/Credit: Dennis I. Netoff).

The dew point is an excellent indicator of the actual amount of water vapor (the mixing ratio) in the air. Air with a high dew point will have a great deal of water vapor present; air with a low dew point will have much less. It becomes apparent that the dew point is directly tied to the amount of water vapor present. If the water vapor present in the air is reduced, the dew point drops.

When air rises and cools by expansion, the relative humidity increases. When the rising air parcel is cooled to the dew point, clouds form. Further uplift will condense progressively more moisture, and the amount of moisture condensed can be easily calculated. For example, on a warm, humid late summer day, rising air is cooled to the dew point of 75°F. The air holds 18.158 g/kg of water vapor at that point. Further cooling during continued ascent cools the air 55°F, at which point it can only hold 8.907 g/kg of water vapor (see [Figure 4.14](#)). The air condensed a total of 9.251 g/kg of moisture, some of which may have fallen as rain. A similar 20 degree drop in temperature from 50 to 30 degrees would only condense 4.021 g/kg (capacity at 50°F is 7.389 g/kg, and at 30°F it is 3.368 g/kg). Because there is more moisture condensed by warm air parcels of air, there is more water in the air available to precipitate, and so summer rains typically generate more total rainfall than winter rains of similar intensity.

**The temperature of a stagnant layer of air will typically not drop much below the initial dew point.** This is because condensation occurs when the relative humidity reaches 100% and condensation releases heat energy into the air (latent heat of condensation) and warms it. This action prevents the temperature from dropping any lower. When the air is *dry* (low mixing ratio) the temperature can drop substantially at night because: (1) there is little moisture to trap outgoing thermal infrared radiation and; (2) there will be a substantial drop in temperature before the dew point is reached. Conversely, if the air is moist, more outgoing energy is trapped and condensation may occur, thereby preventing the temperature from dropping any further. Because of this, high humidity results in less cooling than would otherwise occur. It is therefore generally true that the late afternoon's dew point is a reasonable estimate of the next morning's low temperature.

Based on this, it is clear that the dew point is a good indicator of the relative humidity. If the dew point at ground level is only a little lower than the actual air temperature, it is very likely that dew and/or fog will form at night. On the other hand, if the dew point is many degrees lower than the current air temperature, it is unlikely that dew and/or fog will form.

At saturation, the dew point is equal to the actual air temperature. This means that the wet bulb temperature on a sling psychrometer is the same as that of the dry bulb. So, at saturation, the dew point, wet bulb temperature, and actual air temperature are equal.

In summary, as air cools, its capacity to hold water vapor decreases until saturation/dew point occurs. At dew point, water droplets begin to form. In the atmosphere, the formation of water droplets is seen as fog and/or clouds. Clouds must be present before precipitation can occur. Cooling of air to the dew point is therefore an essential process in the formation of fog, clouds, and all forms of precipitation.

## Mechanisms of Cooling

One of the key concepts pertaining to cooling is that of the lapse rate. The **lapse rate** is the rate of temperature change of air as a function of its altitude above the surface or its vertical motion. The lapse rate in **stationary** air is known as a **diabatic lapse rate** (or **environmental lapse rate**, or ELR), and the lapse rate in air that is **rising** or **sinking** is known as an adiabatic lapse rate.

The diabatic lapse rate is the rate at which air temperature varies with altitude where little or no vertical motion is occurring. It is called the *environmental* lapse rate because it is the atmospheric *environment* through which a parcel of air rises or sinks. This lapse rate is the rate in stationary air, and it results from the simple fact that air high above the ground absorbs less thermal infrared energy emitted from the ground than air closer to the ground. The average environmental lapse rate (the normal lapse rate) is **3.5°F/1000 feet** (6.4°C/1000 m). For example, if it is 90°F at the surface, it is 3.5°F cooler (86.5°F) at 1000 feet. Although this is a long-term statistical average for the globe based on tens of thousands of individual measurements, local and regional conditions (such as diabatic and **adiabatic** temperature changes) can significantly alter this value.

To calculate the temperature at a given height above the surface based on the normal lapse rate, use the following procedure:

1. Calculate the change in temperature by multiplying the lapse rate by the change in elevation.
2. Subtract the product just obtained from the temperature at ground level.

For example, if the ground temperature at 1000 feet elevation is 90°F, the temperature at 10,000 feet would be about 58.5°F assuming an average lapse rate situation,

3. Change in temperature = (9000 ft.) (3.5°F x 1000 ft.) = 31.5°F
4. 90°F - 31.5°F = 58.5°F

This example illustrates why mountain climbers must dress warmly. The temperature drops substantially with elevation. It also explains why spring arrives later, and winter arrives earlier, for places located at high altitude. For example, winter in Laramie, Wyoming which is located in a high altitude basin at about 7500 feet above sea level, arrives several weeks earlier than in Fort Collins, Colorado, which is only about an hour away, but about 2000 feet lower in elevation. Spring arrives in Fort Collins several weeks before Laramie.

Adiabatic lapse rates apply to air that is being warmed by compression or cooled by expansion, with no heat energy being exchanged to/from the surrounding air or land.

Adiabatic temperature changes occur whenever parcels of air experience uplift (e.g., a low pressure system) or subsidence (a high pressure system). Adiabatic temperature changes are independent of the temperature profile of static, surrounding *environmental air* through which air parcels rise or fall (Figure 4.19).

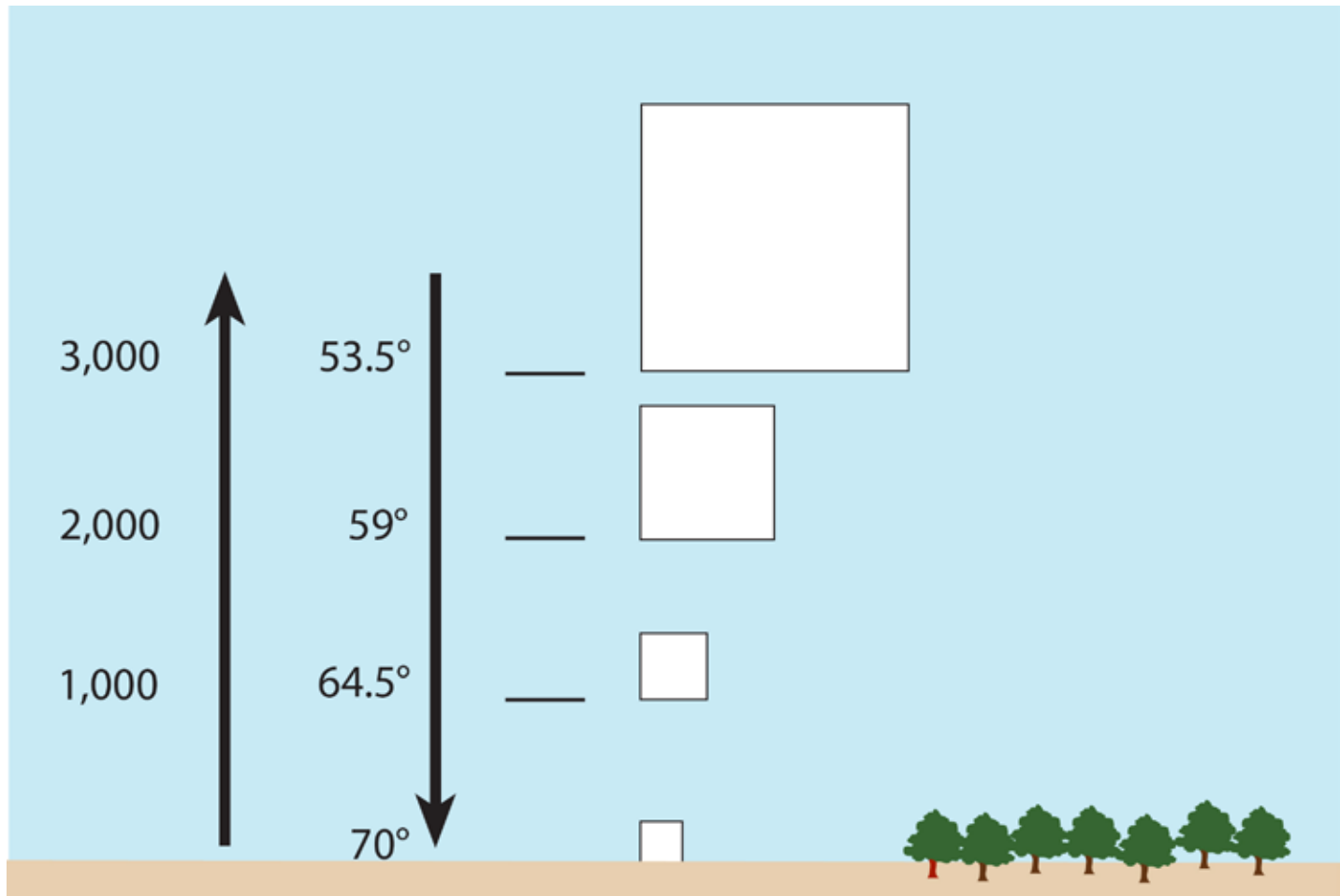


Figure 4.19. As a parcel of air rises, it expands and cools at a rate of 5.5°F/1000 feet. Cooling to the dew point induces cloud formation. As a parcel of air sinks, it warms by compression at the same rate.

The cooling effect produced by expansion is something everyone has experienced whether they realize it or not. For example, virtually everyone has used a spray can (paint spray, hair spray or shaving cream). If you noticed while using it, the material expelled from the can was cool. This is not because the material in the can is cool, but because the material is initially under pressure inside the can. When you press the nozzle on the can, the material is released into a much lower pressure-environment, and it expands and cools rapidly. That's why it feels cold.

If you've ever used a carbon dioxide fire extinguisher, you've seen a dramatic illustration of expansive cooling. The CO<sub>2</sub> is in gaseous form inside the extinguisher. However, when the gas escapes and expands, it literally turns into a white cloud of carbon dioxide ice.



Air conditioners work on this principle of cooling by expansion. The compressor in an air conditioner first compresses the air in the unit and then forces it to move into the coils. Once the air enters the coils, it rapidly expands and cools. This, in turn, cools the air moving across the coils and provides relief for all of us who would otherwise suffer on hot days.

If air that is rising has not cooled to the dew point, it will cool at the adiabatic rate of 5.5°F per 1000 feet. Because no condensation is occurring under these circumstances, this rate of cooling is known as the **dry adiabatic lapse rate** (DAR). Unlike the normal lapse rate, which varies, the DAR is always **5.5°/1000 feet** (10°C/1000 m). Temperatures at various elevations above the surface can be calculated using the same procedure as that used for the normal lapse rate; i.e., multiply the change in elevation of the air parcel by the lapse rate and subtract this value from the original temperature. For example, let's assume that a parcel of air at a temperature of 90°F rose from 1000 feet to 10,000 feet. At 10,000 feet, its temperature would be:

- Change in temperature = (9000 ft.) (5.5°F/1000 ft.) = 49.5°F
- 90°F - 49.5°F = 40.5°F

In the first example using the normal, diabatic lapse rate, the temperature at 10,000 feet was 58.5°F, but if the air is rising, its temperature at 10,000 feet is 18°F colder.

**If the air temperature cools to the dew point while the air is rising, condensation will occur and this will release heat to the air and attempt to warm it.** Two processes are competing to change the temperature of the air parcel; cooling due to expansion during uplift, and heating due to the release of latent heat of condensation. Expansional cooling is always the dominant process, so the rising air continues to cool, but at a depressed rate (always less than the DAR). Because condensation is occurring under these circumstances, this lapse rate is known as the **wet adiabatic lapse rate** (WAR) and it *averages* **3.2°/1000 feet** (6°C/1000 m). The actual value varies from just over one to nearly 5.3°F/1000 feet, depending upon the amount and rate of condensation occurring in the air parcel.

A rising parcel of air can therefore cool at the DAR until it begins to form a cloud (the lifting condensation level, LCL), but thereafter cools at the WAR). For example, assume the air temperature of a parcel is 90°F at 1000 feet and that it begins to rise. Because of its humidity, moisture begins to condense at 5000 feet. What is the parcel's temperature at 10,000 feet assuming that the wet adiabatic lapse rate is 3.3°F/1000 feet?

1. The parcel rose 4000 feet (from 1000 feet to 5000 feet) at a DAR of 5.5°F/1000 feet. So, the change in temperature is given by:

$$4000 \text{ feet} \times 5.5^\circ\text{F}/1000 \text{ feet} = 22^\circ\text{F}$$

2. The temperature at 5000 feet = 90°F - 22°F = 68°F

3. From 5000 feet to 10,000 feet, the parcel cooled at a moist adiabatic lapse rate of 3.3°F/1000 feet. So, the change in temperature is given by:

$$5000 \text{ feet} \times 3.3^\circ\text{F}/1000 \text{ feet} = 16.5^\circ\text{F}$$

4. The temperature at 10,000 feet is given by subtracting the 16.5°F from the temperature at 5000 feet:

$$68^\circ\text{F} - 16.5^\circ\text{F} = 51.5^\circ\text{F}$$

Note that you can also subtract the sum of the temperature drops from 90°F to obtain the final temperature:

$$90^\circ\text{F} - (22^\circ\text{F} + 16.5^\circ\text{F})$$

$$90^\circ\text{F} - 38.5^\circ\text{F} = 51.5^\circ\text{F}$$

Also note that this temperature is less than that of air at 10,000 feet that is not rising (example #1 = 58.5°F), but more than that for air that is rising and being cooled exclusively at the dry adiabatic lapse rate (example # 2 = 40.5°F).

**When air sinks it is heated by compression.** The rate of compressional heating is the same as the dry adiabatic lapse rate of 5.5°F/1000 feet. So, if air sinks 9000 feet, it is heated 49.5°F.

Radiational cooling is another means by which air cools. It results when air emits more infrared energy than it absorbs. Radiational cooling is facilitated by clear sky conditions when little moisture is available to stop outgoing radiation, and at higher elevations. By an increase in high elevations, relatively little heat energy is absorbed by the air from either insolation or outgoing thermal infrared radiation because of the low concentration of greenhouse gases. The low density air also has a low thermal capacity, so it cools quickly.

**Conductive cooling**, or contact cooling, occurs when the air is in contact with a cooler underlying surface (land or water). It commonly occurs when relatively warm air advects over either cold land or a cold ocean current. It is responsible for many of the world's coastal fogs.

## Mechanisms That Can Cause Uplift

Adiabatic cooling associated with uplift is responsible for cooling large bodies of air to the dew point, and the formation of clouds that can yield substantial amounts of precipitation. It is one of the most important processes in meteorology. Any mechanism that can lift the air ultimately results in a rapid cooling of the air and plays an important role in the hydrologic process. Consequently, mechanisms of uplift are essential in meteorology. There are four main mechanisms of uplift:

- **Convective Uplift.** This is the vertical movement of air in response to temperature/density differences. **Warm air is less dense than cold air, so when air is heated at ground level, it will begin to rise and, as it rises, it will cool adiabatically.** Convection is the primary cause of uplift in the tropics, and in the mid-latitudes during the summer (Figure 4.20).

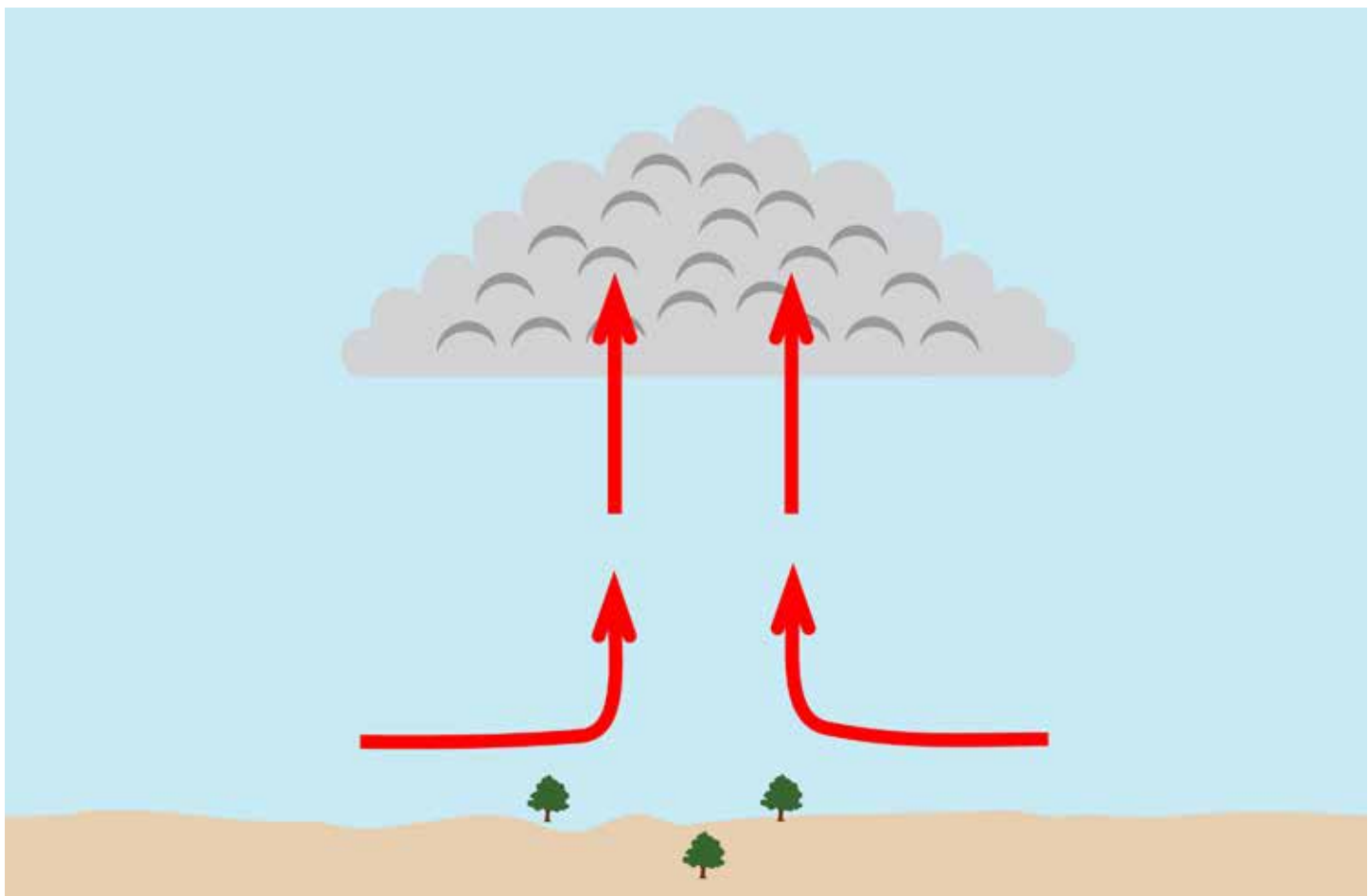


Figure 4.20. Convective uplift occurs when the atmosphere becomes unstable, and pockets of warm air rise through the surrounding air, often producing clouds.

- **Orographic Uplift** refers to uplift caused by the movement of air over mountains or highlands. In mountainous areas, this is an extremely important mechanism of uplift and results in substantial precipitation on the windward side of a mountain, i.e., on the side of the mountain facing into the wind. For example, the summits on the island of Oahu in Hawaii receive 200 inches of precipitation per year on the windward side (Figures 4.21a and 4.21b). By way of comparison, Huntsville receives around 46 inches of precipitation per year. This high level of rainfall occurs because the air near the warm ocean surface is laden with moisture. As it is forced to rise a mere 2000 feet, cooling and condensation generate substantial rainfall as the temperature drops 11°F.

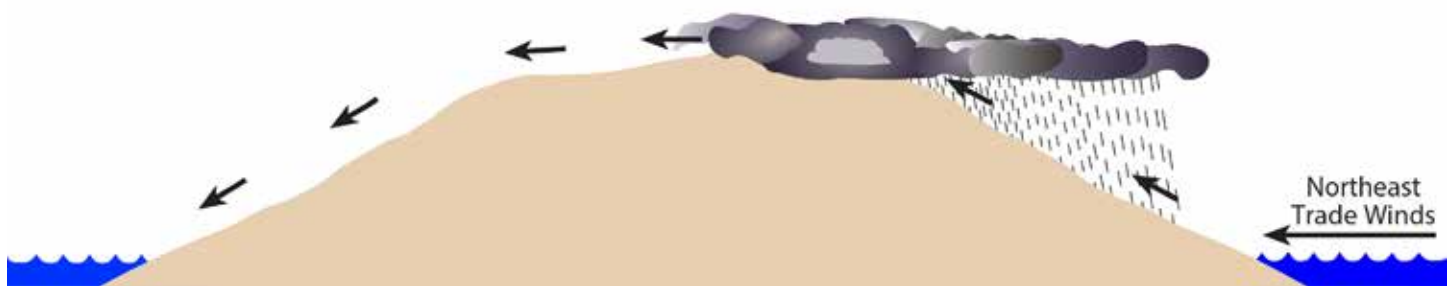


Figure 4.21a. Much of the year, the Northeast Trade winds carry tropical air over the Hawaiian Islands. The windward side of the islands is typically very wet, but the leeward side tends to be dry.



Figure 4.21b. The Hawaiian island of Oahu lies in the Northeast Trade Wind Belt. As a result, air is forced to rise along the north side of the island when it encounters the mountains. This produces frequent cloudiness and heavy rainfall on the north shore, and especially at the tops of the mountains. More than 200 inches of rainfall may occur at the summits. On the lee side of the mountains, rainfall levels drop dramatically to an average of about 20 inches per year. Honolulu is located in this area (Source/Credit: Marcus Gillespie).

On the leeward (downwind) side of the island in Honolulu, only seven miles away, less than 20 inches of rain falls per year. This is because most of the moisture that was in the air fell out as rain on the windward side, and because the air on the lee side tends to sink and warm by compression. This windward-leeward effect is of profound importance and results in dramatic differences in climate and ecosystems over short horizontal distances.

Many of the deserts in the United States result, at least in part, from this orographic effect. The United States lies in the Westerly Wind Belt, so the dominant direction of airflow is from west to east. As moist air from the Pacific Ocean rises over the Coast Ranges, the Cascades, the Sierra Nevada and other ranges as it flows across the country, more and more moisture is lost, so the interior is dry (Figure 4.22).

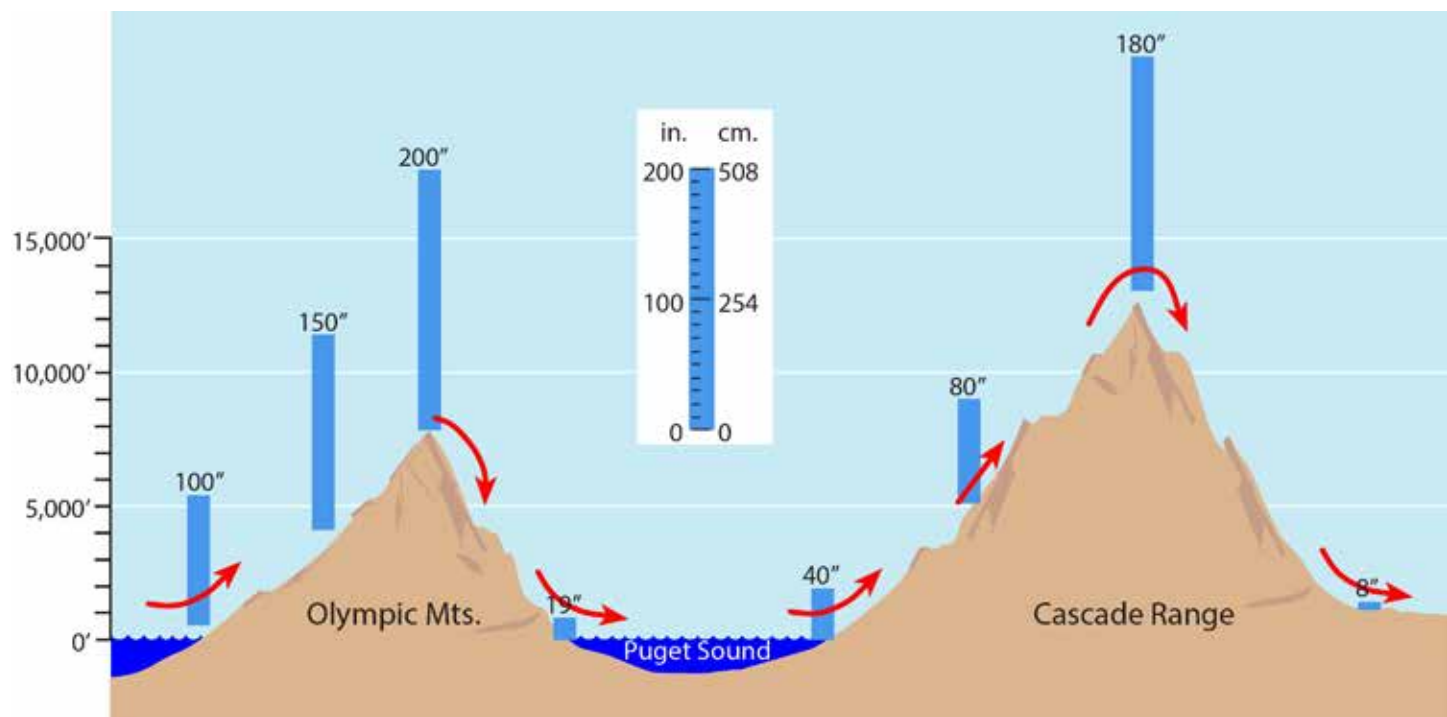


Figure 4.22. The contiguous United States is located in the Westerlies. Air typically travels from west to east across the continent. As moist air from the Pacific Ocean encounters mountain ranges, such as the Olympic Mountains and Cascade Range shown here, it loses moisture as it rises and cools. As a result, the western, windward sides of mountains receive heavy rainfall. In contrast, the lee sides of the mountains are very dry and tend to be deserts. For example, the high Cascades receive nearly 200 inches of precipitation per year, whereas Yakima, located only a few miles to the east, receives a meager 8 inches a year (Source/Credit: modified from Dennis I. Netoff and Ava Fujimoto-Strait, *Weather & Climate Lab Manual*).

As a result of a combination of orographic and convective uplift, islands often generate clouds, and are often surrounded by vast expanses of cloudless ocean. Islands can often be detected, from satellite or even when lying below the horizon, by the presence of regularly occurring clouds (Figures 4.23a and 4.23b).

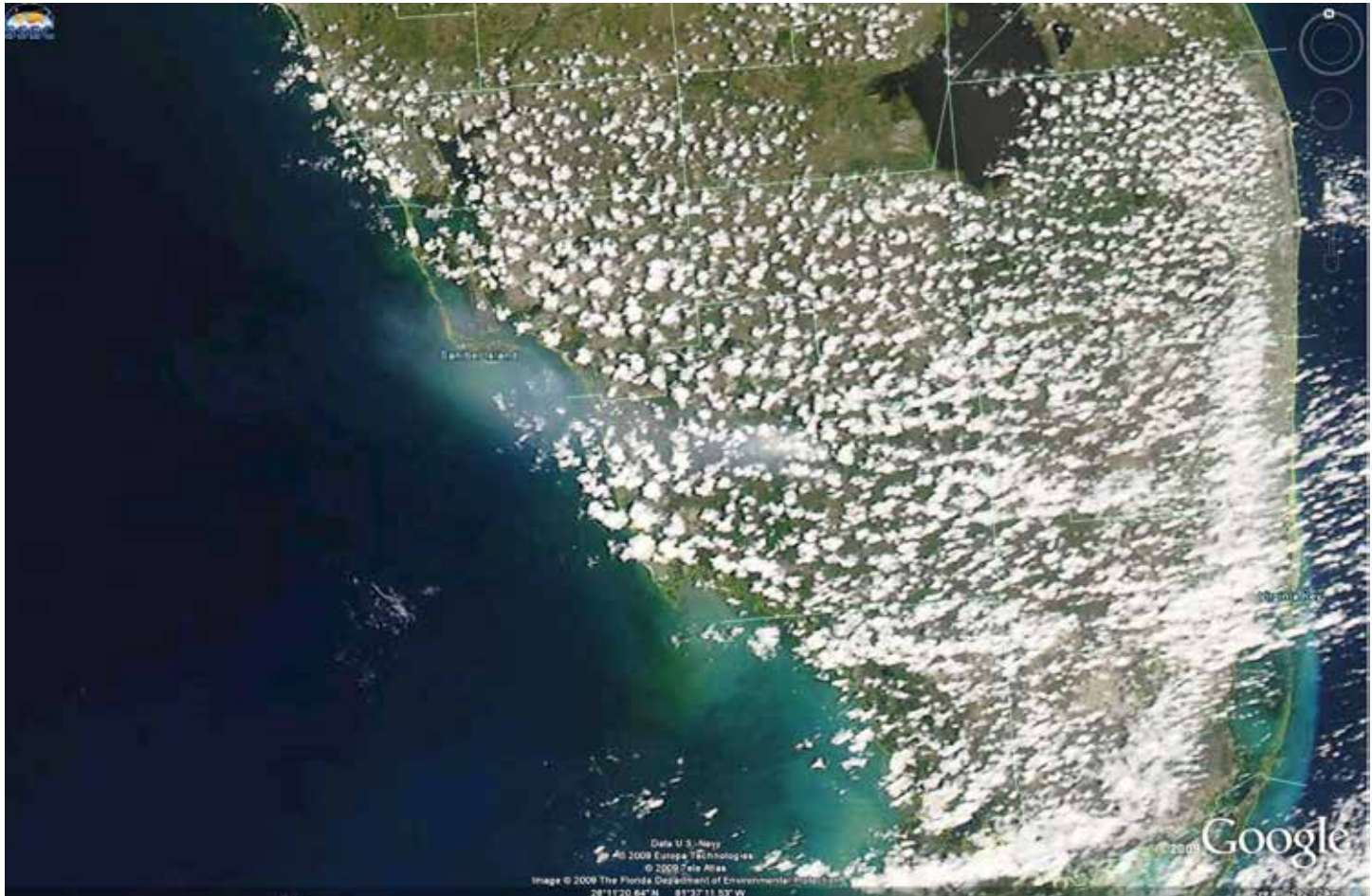


Figure 4.23a. As the Florida Peninsula warms on a summer day, a low pressure system is created that draws warm, moist air toward the land from the surrounding Atlantic Ocean and Gulf of Mexico. As this air is further heated over the land, it rises, cools and produces clouds and precipitation, much of it in the form of thunderstorms. Florida has more lightning strikes than any other state in the United States because of this effect (Source/Credit: Florida Department of Environmental Protection).



Figure 4.23b. Daytime heating of the Galapagos Islands, Ecuador. Islands produce the same effect on air flow and precipitation patterns as does the Florida Peninsula. Because land heats faster than water, daytime heating of an island causes low pressure to develop over the land. This causes moist air to flow from the cooler ocean toward the island and produces clouds. In contrast, the skies around the island may remain relatively cloud-free because of the lack of a mechanism of uplift. Because of this tendency for clouds to form above islands, it is said that, “Islands map themselves in the sky” (Source/Credit: NOAA).

New Zealand, for example, is known as the *Land of the Long White Cloud*. Early seafaring people used this phenomenon to locate islands they could not otherwise have known about. This phenomenon led to the saying that, “**Islands map themselves in the sky.**”

- **Frontal Uplift.** In the mid-latitudes, one of the primary causes of uplift is the collision of unlike masses of air along frontal boundaries. These will be discussed at greater length in the next chapter. When warmer air meets colder air, the warmer air will rise up and over the colder air because of the lower density of the warmer, more moist air. From autumn through spring, frontal uplift results in substantial cloud cover and precipitation (Figure 4.24).

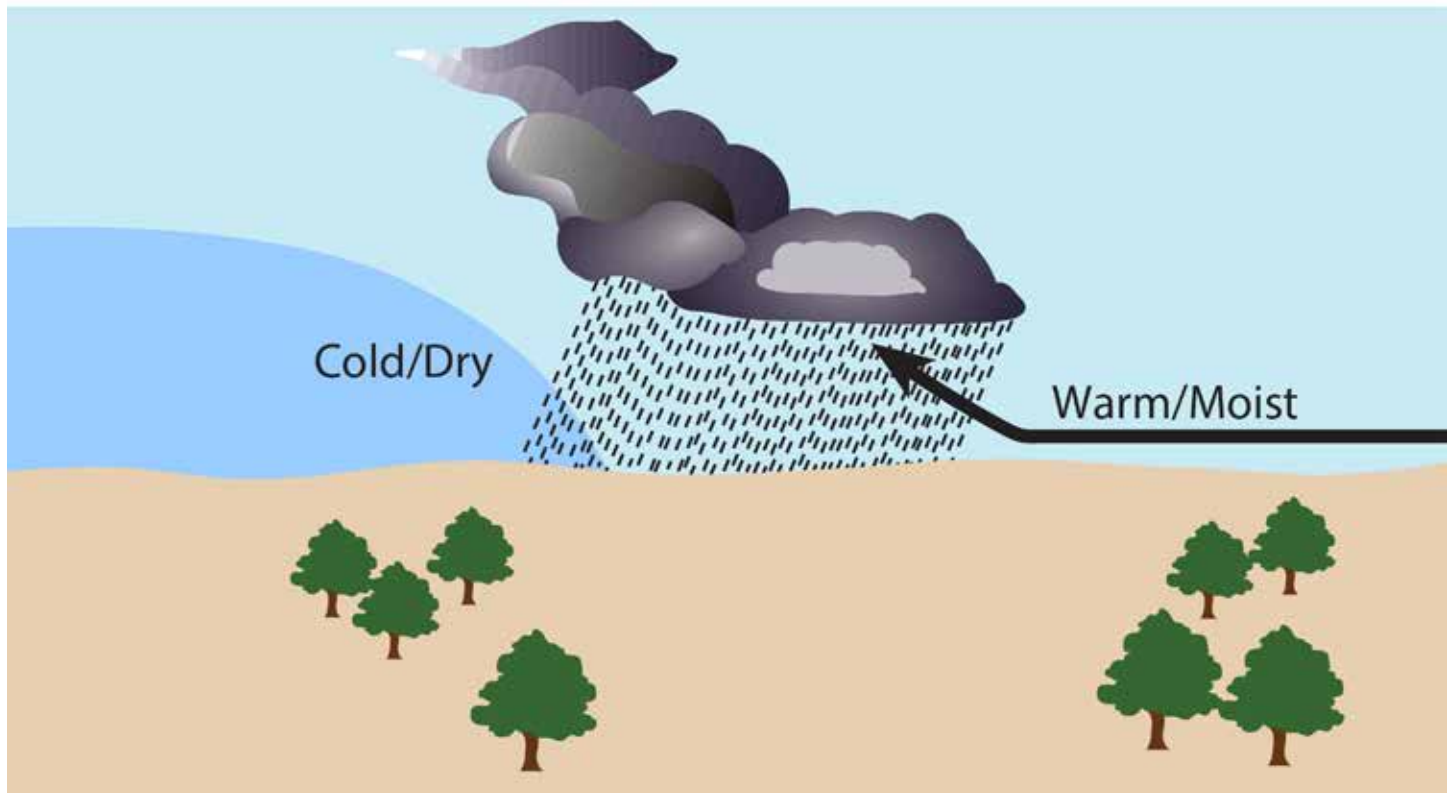


Figure 4.24. Frontal uplift is caused by a denser body of air wedging under a less dense body of air. If conditions are favorable, precipitation may occur.



- **Convergence and Cyclonic Uplift.** A cyclone is a low-pressure system in the atmosphere that causes air to flow in a spiral motion toward the center of the low and then rise upward. As the air rises, it is cooled by expansion and condensation occurs. Cyclonic uplift is sometimes associated with frontal systems, but also with non-frontal systems such as tropical storms and hurricanes (Figure 4.25).

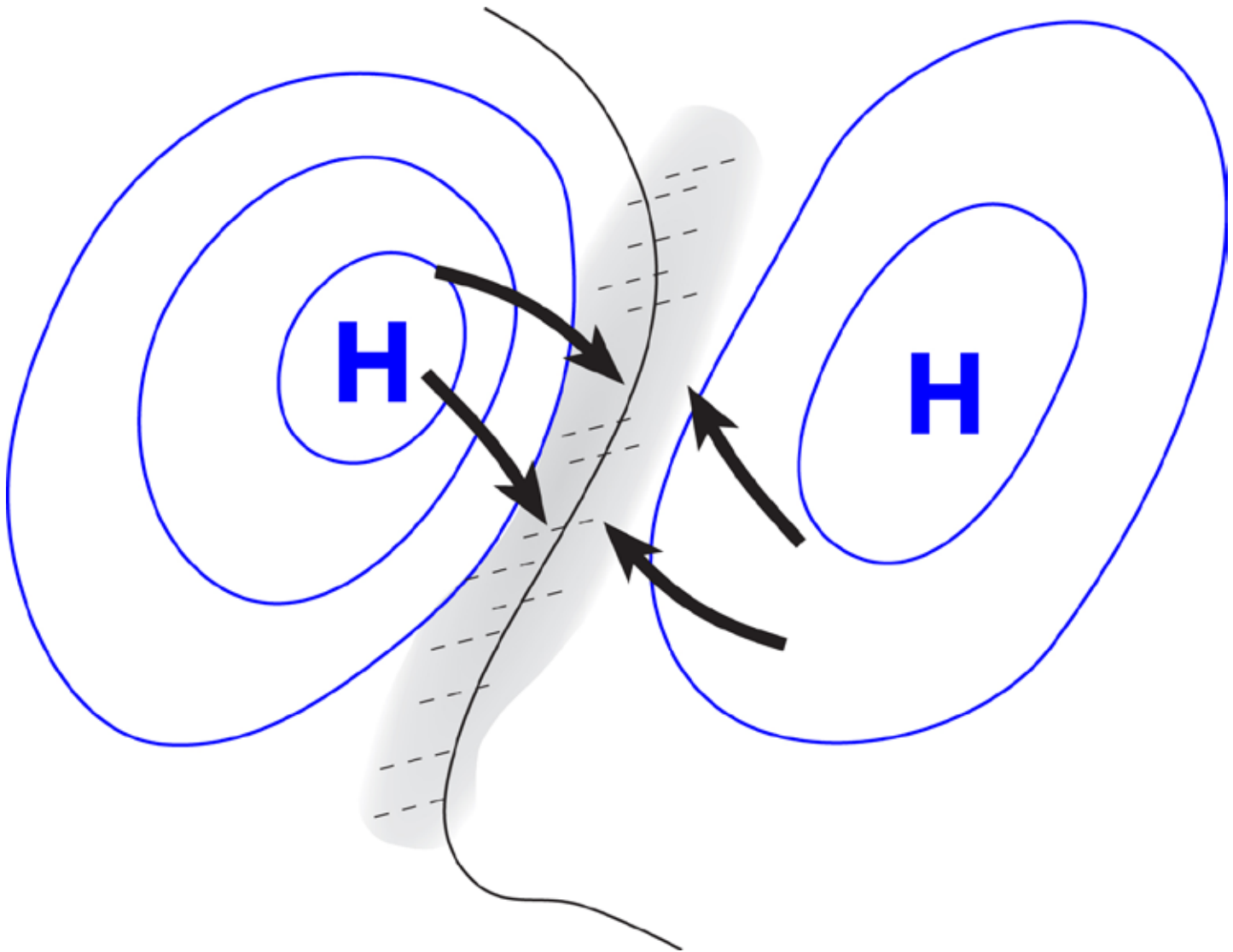


Figure 4.25. Convergence occurs when two bodies of air are forced to come together, regardless of their density differences. Surface convergence creates uplift, and may cause clouds as well as precipitation to occur (shaded area), even though no well-developed low pressure center is apparent.

## Forms of Condensation and Deposition

### Dew and Frost

When the temperature at ground level cools to the dew point or frost point, moisture condenses or deposits, respectively, onto these objects forming either *dew* or *frost*. The temperature drops because of radiant cooling. The source of moisture is from the air which is cooled by conduction to the ground. Water droplets that form on the sides of a glass of ice water also condense from the air. For instance, you are more likely to see water droplets on glasses of ice water in warm, humid areas than in warm, dry areas. Because of the high humidity in such areas, the air temperature does not have to drop very much to reach dew point. In a drier region, the relative humidity is so low that the ice usually cannot cool the air to its saturation point, and so water droplets aren't as likely to form.

Dew is most likely to occur on clear, calm nights (Figure 4.26). Such conditions encourage rapid cooling of the surface, and the ground becomes much cooler than the overlying air. Dew does not *fall* (as does rain, snow and the like), but rather it condenses upon surfaces. Dew can sometimes be very heavy, such as when a very warm, humid day (high mixing ratio and dew point), is followed by a relatively cool night. At other times, the quantity of dew is small and soon evaporates as the morning temperatures begin to rise. These conditions would be most likely when the mixing ratio is relatively low (thus a low dew point).



Figure 4.26. Dew forms when a surface such as a spider web or leaf cools to the dew point (Source/Credit: Jörg Hempel [CC-BY-SA-3.0-de (<http://creativecommons.org/licenses/by-sa/3.0/de/deed.en>)], via Wikimedia Commons).

If the dew point is below freezing, then it is referred to as the **frost point**. If the frost point is reached, water will *deposit* onto surfaces, rather than condense. When this happens, frost forms. Frost has a delicate crystalline structure which indicates that it is not a frozen dew drop (Figures 4.27 and 4.28). However, it is possible for dew to freeze and form frozen dew drops, the result is spherical droplets of transparent ice. Often, both frozen dew and frost occur together. This happens when temperatures first drop to dew point, resulting in the formation of dew, and then the temperature drops below freezing.



Figure 4.27. Frost has formed on leaves of a small plant near Colorado Springs. Frost forms when a surface cools to the frost point and water vapor deposits as ice crystals on the surface (Source/Credit: Dennis I. Netoff).



Figure 4.28. Slow-forming **window frost** on a car window takes on intricate forms, often following either micro flaws in the glass or trails of microscopic dust particles (Source/Credit: Dennis I. Netoff).

The seasonal timing and location of the formation of frost can be an important consideration in agriculture, especially as it relates to certain types of crops. For example, fruit trees are most vulnerable to frost damage during the spring months, when they are flowering. If the orchard is planted on a south-facing slope in the Northern Hemisphere, the Sun more readily warms the slope resulting in premature flowering of the trees. An orchard planted on a north-facing slope will not receive direct Sun rays, and the relatively cooler surface will result in a later flowering of the trees. This may provide a north slope orchard a week or two of protection from a late cold snap.

Planting certain types of orchards on a slope may protect them from killing frost because of inversions. Cold, dense air that forms in the mountains will generally move down slope to the bottom of a valley or out into flat lands and form a shallow layer (Figure 4.29). However, warm air above the cold layer will keep the higher slopes warmer, thereby protecting the trees that are planted there. This fact is of great economic importance because layers of cold air lay waste to millions of dollars of crops in the United States annually. By planting on slopes, more trees are spared.

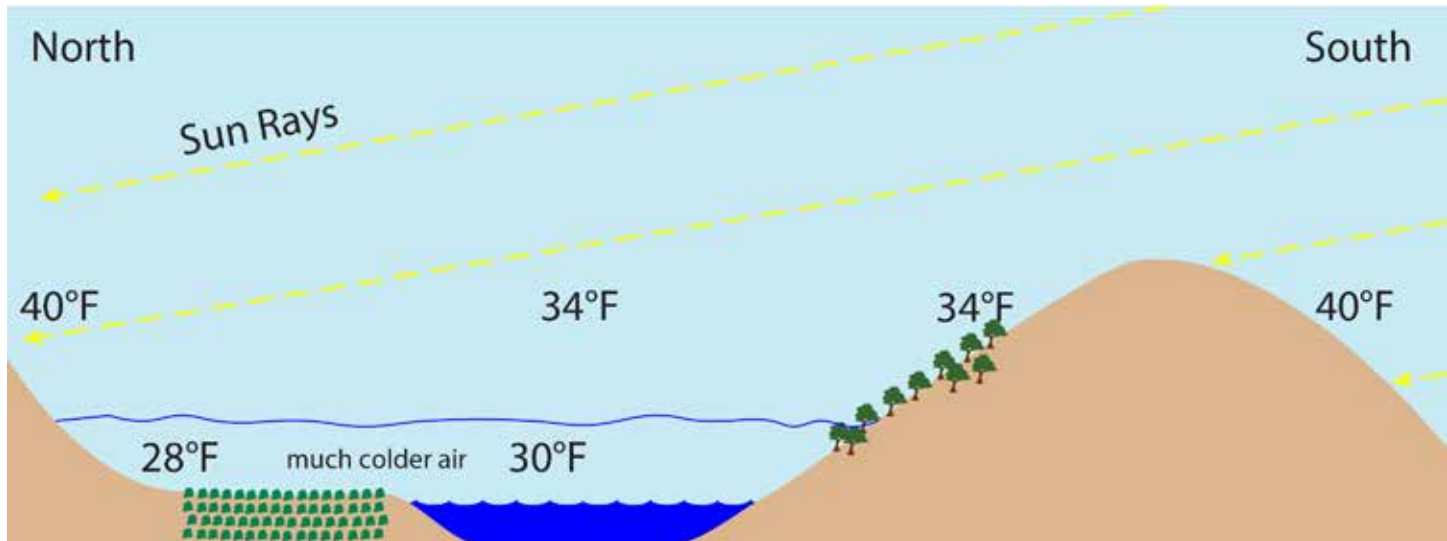


Figure 4.29. Orchard trees planted on north-facing slopes are better protected from the effects of late cold snaps because they do not flower as soon as those on south-facing slopes in the Northern Hemisphere. And, if the trees are planted higher on the slope, they will tend to lie above cold air that may sink into a valley at night. Placement near water bodies also protects them because water does not cool as much at night, and this keeps the air warmer. Frost tolerant plants are located on the north side of the lake.

Aside from planting on north-facing slopes, there are other things that can be done to inhibit frost damage. These include:

- The covering of sensitive plantings (rosebushes and the like) around homes. The covering is not there to keep the cold air off of the plant, but rather to trap warm air emanating from the Earth's surface.
- Some commercial growers that produce valuable tree crops such as citrus, avocados and the like may employ orchard heaters. The heaters serve to mix cold surface air with warmer air aloft to create an air mixture that is above freezing.
- A variant of the orchard heater would be permanently constructed wind machines (and in very rare instances the use of helicopters) to stir the air and break up the inversion.
- Spraying orchards with a light mist of water, which freezes on contact with the plants, can also save trees from killing frost, even if the fruit is lost. Covering the trees with a coat of ice (at 32°F) insulates the tree from the colder surrounding air. In addition, when the water freezes, it releases heat energy, both to the surrounding air and to the fruit, and this prevents the fruit from freezing and prevents the trees from dying. But such an activity is tricky. Too little water and the trees will be killed for lack of insulation; too much water and there is a risk of breaking the limbs and even the main trunk itself.

## Fog

Fog develops when a shallow layer of air at ground level becomes saturated and condenses. Fog and clouds are physically similar, except fog occurs at or very close to the ground, and clouds form considerably above ground. Additionally, most clouds form through adiabatic cooling, whereas most fogs form from non-adiabatic cooling and/or the addition of water vapor.

Although all fogs involve condensation, there are a variety of mechanisms by which they can develop. Therefore, fogs are typically classified according to the mechanism by which they form.

- **Advection Fog.** Advection fog derives its name from the fact that it is associated with advection; i.e., with horizontally moving air. These fogs form when a warm, moist layer of air moves across a colder surface. For example, advection fogs frequently form off the coast of California as a result of the fact that warm, moist Pacific air in the Westerlies moves across the cold waters of the California Current (Figure 4.30). As it does so, the air cools and condensation occurs producing fog along the coast. Also, the land tends to cool a lot at night, allowing the fog to penetrate inland. This process is responsible for many of the fogs that develop in coastal environments (Figures 4.31a, 4.31b, 4.31c and 4.32).

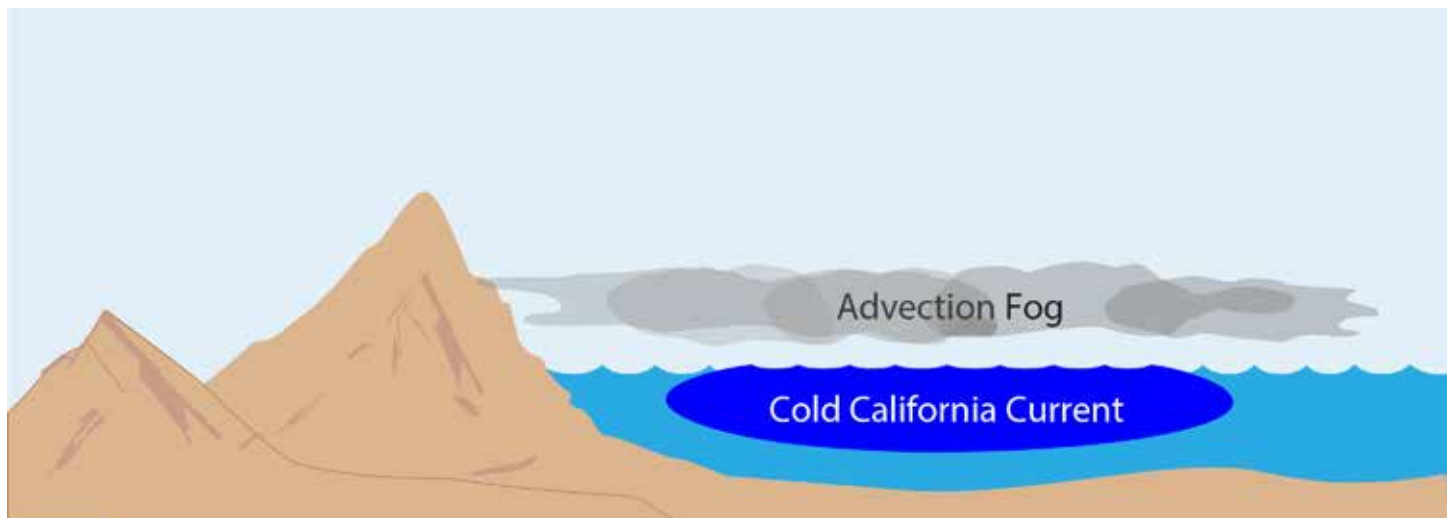


Figure 4.30. Sketch of the Northern California coastline, looking south. Advection fog forms when a thin layer of relatively warm and humid air, in this case from the Pacific Ocean, is cooled to the dew point by passage over a cold surface, in this case the Cold California Current (Source/Credit: Dennis I. Netoff).



Figure 4.31a. View southward from the Klamath River Overlook (elevation 640 ft.) along the Northern California coast near Klamath at the mouth of the Klamath River (in fog). The open Pacific Ocean is to the right (westward). In the early morning hours, when the land is about as cool as the fog, the fog may penetrate deep inland in places where it can slide through gaps in the mountains, such as the Klamath River Valley (Source/Credit: Dennis I. Netoff, Klamath CA).





Figure 4.31b. View from the Klamath River Overlook toward the south after the fog has retreated seaward or dissipated. The overlook is at ~640 feet (~195 m) above sea level (Source/Credit: Nick Strobel, <http://www.astronomynotes.com>).



Figure 4.31c. View westward from the Klamath River Overlook along the Northern California coast. The open Pacific Ocean lies directly ahead. The thickest fogs tend to develop where there is a lid on vertical circulation in the form of a temperature inversion (dashed line). Below the inversion, the temperatures can be 20 or more degrees cooler than above (Source/Credit: Dennis I. Netoff, Klamath CA).

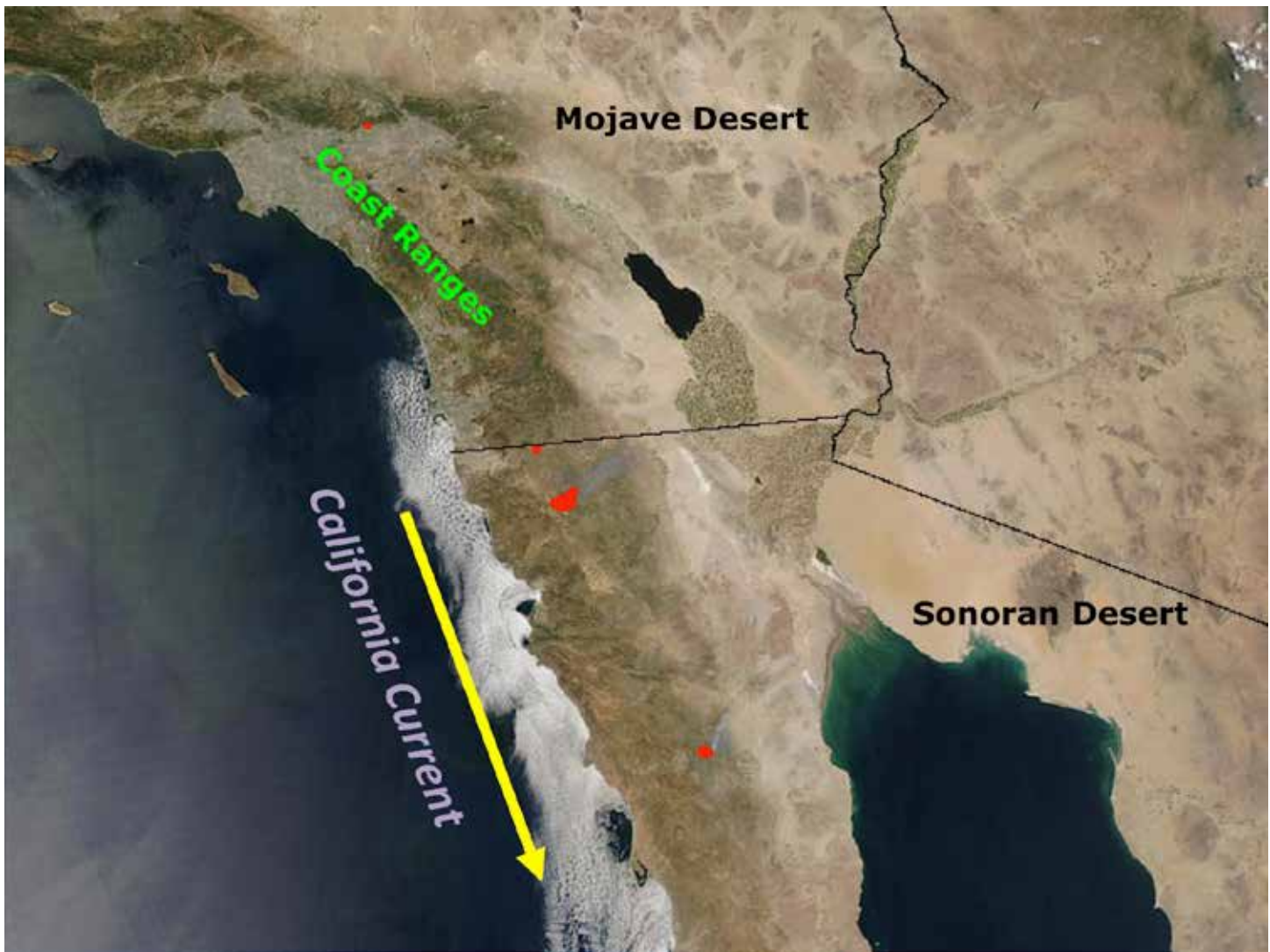


Figure 4.32. Coastal advection fogs can occur at relatively low latitudes provided that there is a cold current and onshore winds, such as on the Baja Peninsula of Mexico. They can create interesting temperature extremes, where in the summer, temperatures within the fog belt will typically be in the low 70s, whereas a few miles inland they can exceed 100°F. The international border is at about 32°N latitude (Source/Credit: NASA).

- **Steam (Evaporation) Fog.** Steam fogs involve a two-step process that begins with evaporation and ends with condensation. The fog develops best when relatively warm water bodies are overlain by cold, fairly still air (Figure 4.33). Warm water evaporates efficiently because the water molecules are moving vigorously. The cold overlying air, however, has very little **capacity** to hold water vapor, so condensation occurs. This is one of the few fogs that forms through the addition of water vapor, rather than exclusively due to the cooling of air to the dew point (Figure 4.34).

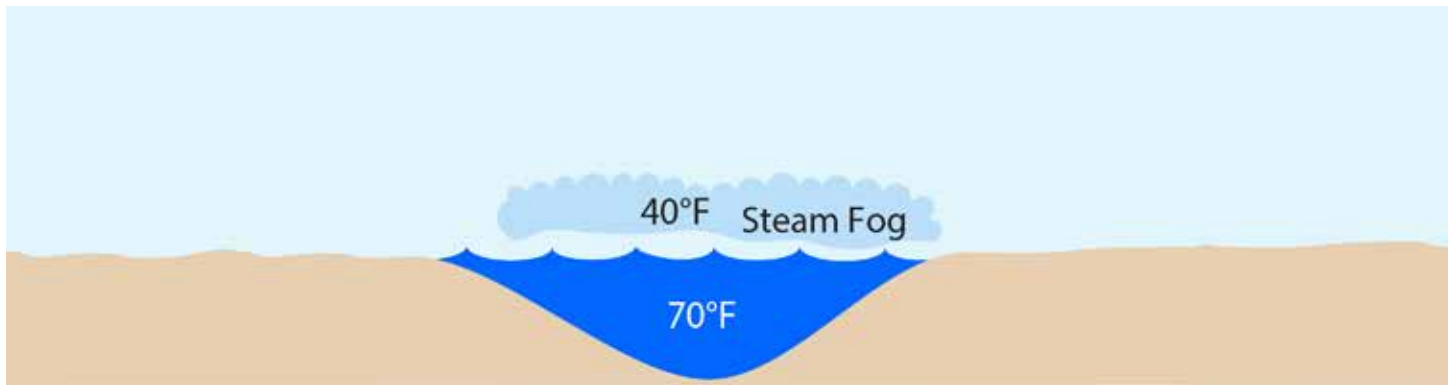


Figure 4.33. Steam fogs form when relatively warm bodies of water are overlain by cold air. Rapid movement of the molecules in the warm water cause considerable evaporation, but the cold air has a low capacity (C) for water vapor, so a thin, dense fog often forms.



*Figure 4.34. Dense steam fogs form when warm water is overlain by cool air. This is common occurrence in the fall, when lakes and rivers are still warm, and cooler air advects from the north in association with a front. This steam fog at Spring Lake, Huntsville, Texas formed at dawn with a water temperature of 70°F and air at 45°F (Source/Credit: Dennis I. Netoff).*

This type of fog also forms over warm ocean waters, such as the Gulf Stream. At high latitudes, steam/evaporation fogs are sometimes called **Arctic sea smoke**.

- **Radiation Fog/Ground Fog.** Radiation fogs form when the air at ground level cools to the dew point as a result of the loss of heat by radiation (Figures 4.35 and 4.36). Radiation fogs often look like smoke covering pastures and they are very common in the southern United States. These fogs are commonly associated with inversions, which confines the cold air to a thin surficial layer. Because air is a relatively poor conductor of heat, most radiation fogs tend to be relatively shallow events. While some such fogs may exceed 50 feet in thickness, more typical radiation fogs are seldom much more than chest-high.

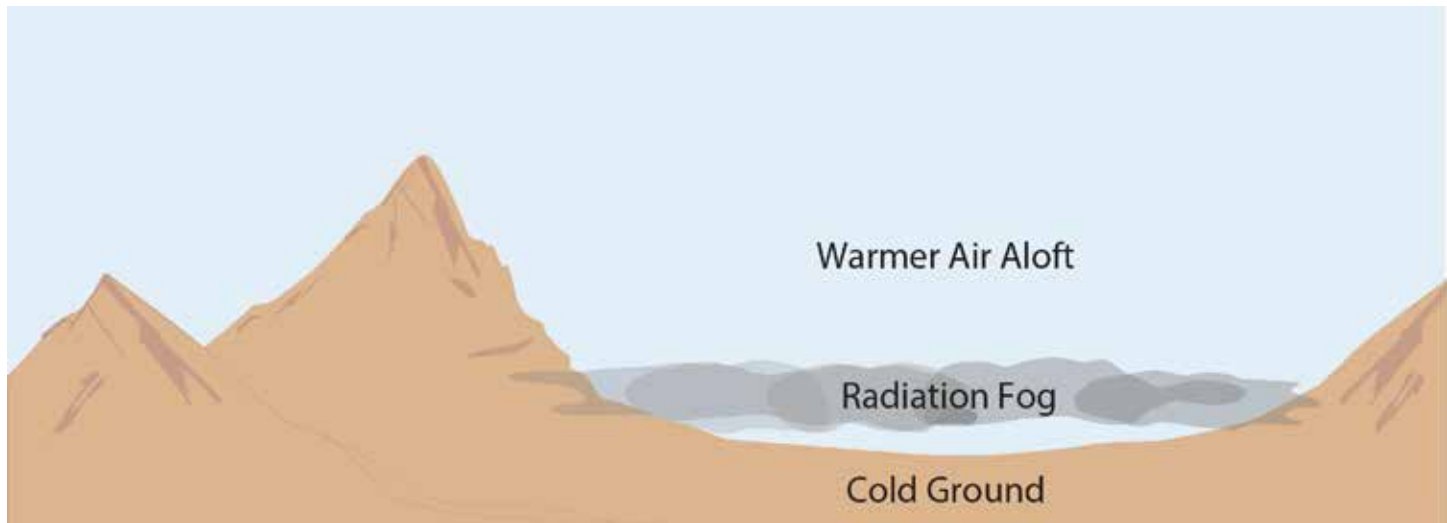


Figure 4.35. Radiation fogs are the most common fog to form over the continents. They occur when radiation cooling during the night drops the temperature to the dew point. Like other fogs, they form best when there is a low-level temperature inversion. They also tend to form first and linger longest in low places on the landscape, where cold air stagnates.



Figure 4.36. Radiation fogs tend to occur in low-lying areas such as here in the Central Valley of California. The infamous valley fog (also called tule fog) is nearly 400 miles long and 100 miles wide and poses a great hazard to ground transportation. Although most radiation fogs are short-lived and vertically thin, California's valley fog can persist for days. This fog was over 1000 feet thick in the heart of the valley (Source/Credit: NOAA).

Radiation fogs can present traffic and health hazards, especially in densely-populated regions. Extensive and relatively long-lived radiation fogs in low-lying areas of China and India are particularly notorious, because they are facilitated by condensation nuclei added by coal-fired power plants, increasing fog frequency and toxicity (Figure 4.37). In the 1950s, the phrase *pea soup fog* was introduced by Londoners because of the color imparted by coal-fired products.



Figure 4.37. Radiation fogs are fairly common in northern India during the cool season. This one nearly filled the broad valley of the Ganges River. It was confined to the north by the Himalayas. Several sources of pollution of these extensive fogs include coal-fired power plants, the burning of wood and dung, wild fires, and urban-industrial sources (Source/Credit: Jacques Desclotres, January 5, 2003, MODIS Rapid Response Team, NASA/GSFC).



London was the site of one of the most disastrous fogs in history. In December 1952 there was a long-lived **pea soup fog** that is estimated to have killed more than 10,000 people. Household coal burning during that cold December contributed to the formation, intensity, and toxicity of the fog. The superposition of an upper-level high pressure system acted as a cap or lid, not allowing the pollutants to mix vertically. Visibility on December 5<sup>th</sup> dropped to a few yards, and on the 7<sup>th</sup>, to about a foot. All vehicular traffic came to a halt. Not even ambulances could navigate the pea soup. It is now referred to as the **Big Smoke** or the **Great Smog of '52**. London today is a much less-polluted city, but is still plagued with occasional long-lasting fog. Today, some of the worst fog-related pollution disasters are in China, where recent coal-based industrialization and a large population combine to create fairly common health hazards (Figure 4.38). Some fogs form through a combination of process, such as the rather common fogs along the Gulf Coast during the cold season (Figure 4.39).

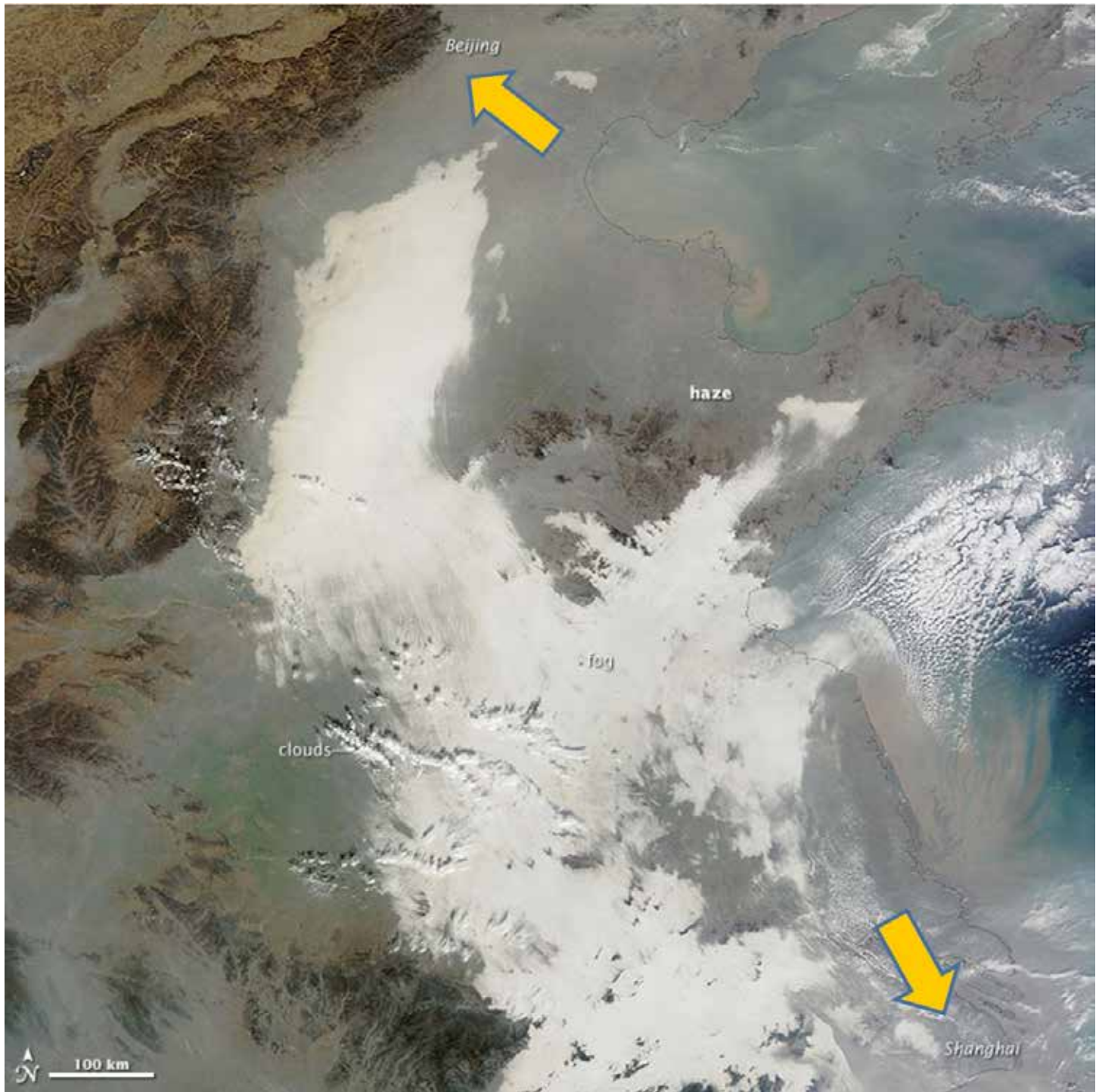


Figure 4.38. China has many of the same air pollution problems that plagued London in the 1950s. Frequent cold-season fogs are exacerbated by the soot and sulfur in the atmosphere, largely injected by the burning of coal. The December 7, 2013 image shows a thick haze stretching from Beijing to Shanghai (~750 miles; 1200km; exactly the distance from Beaumont to El Paso, Texas). Polluted air without fog or low clouds appears gray, whereas fog and/or uniform low clouds appear bright white. Textured bright white areas are higher cumuliform clouds. At the time of the image, the air quality index reached 404 in Shanghai and 487 in Beijing. An index >300 is considered hazardous to all humans. An index of <50 is considered good (Source/Credit: NASA; Moderate Resolution Imaging Spectroradiometer, Terra Satellite).



Figure 4.39. A dense radiation/advection fog surrounds the Space Shuttle Challenger on its way to the launch pad in November 1982 (Source/Credit: NASA).

Radiation fogs are less common in arid regions, but can form under specific conditions. A rare, widespread radiation fog formed in the Grand Canyon in November-December 2013 when snow melt and night-time cooling saturated the air, and an inversion plus canyon walls confined the fog to the canyon (Figures 4.40a and 4.40b).



*Figure 4.40a. A radiation fog filled the Grand Canyon between November 29 and December 2, 2013. The fog formed a few days after a winter storm had left several inches of snow on the ground. In the meantime, a strong temperature inversion over the region (note the clear skies) trapped the moisture in the Canyon. Night-time chilling of the air dropped the temperature to the dew point, and the canyon walls trapped the fog for several days (Source/Credit: NPS).*



Figure 4.40b. NASA image taken on November 30, 2013, of the radiation fog filled the Grand Canyon. The yellow arrow indicates the western margin of the Grand Canyon and the beginning of Lake Mead (Source/Credit: NASA Visible Earth).

- **Upslope Fog.** Upslope fog forms as a body of air moves upslope and cools (Figures 4.41a and 4.41b). Imagine, for example, a parcel of air moving upslope from the Gulf, through Oklahoma and into Colorado. At some point in its journey, the air will rise, expand, and may cool to its dew point. Upslope fogs can cover tens of thousands of square miles of land, and sometimes persist for two or three days.

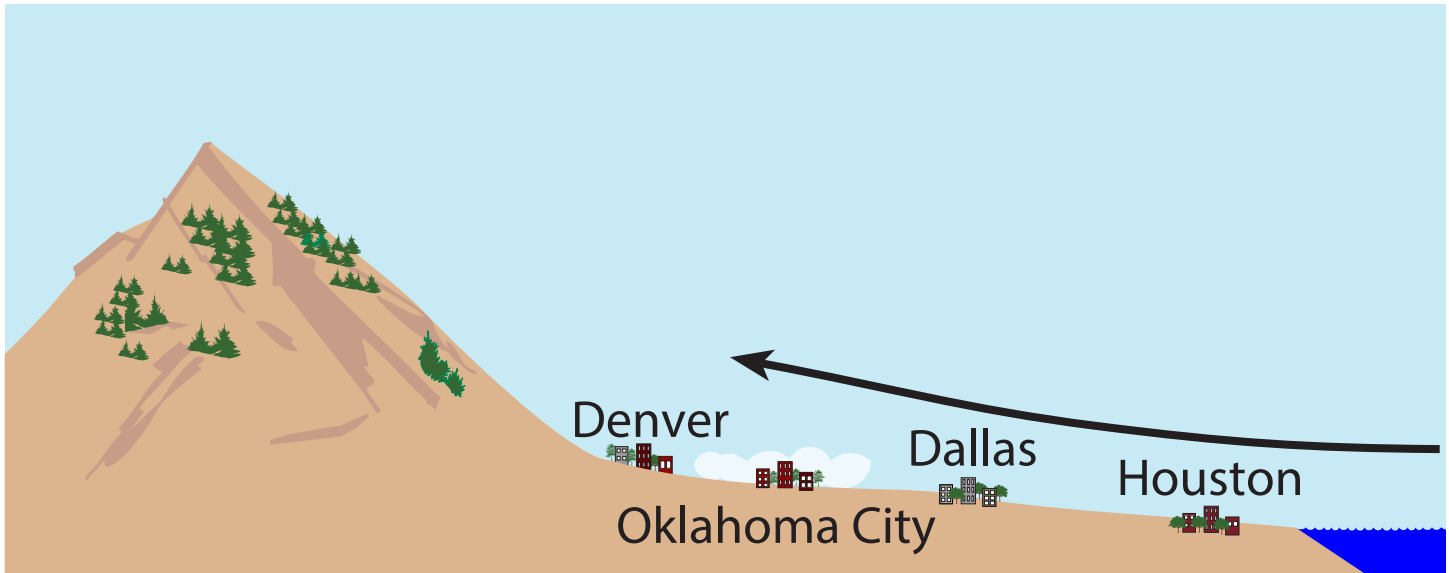


Figure 4.41a. Upslope fogs are the only fogs that form as a result of expansional cooling. Some of the most widespread and persistent upslope fogs form over the western Great Plains, when warm, moist Gulf air rises slowly over a long, inclined wedge of land to the Plains, which may be several thousand feet above sea level.



Figure 4.41b. A developing upslope fog (left-center) at the eastern base of the Wassuk Range, Nevada (Source/Credit: Dennis I. Netoff).

## Clouds

Clouds consist of water droplets and/or ice crystals that have either condensed or sublimated. In order for condensation to occur, the relative humidity needs to be very close to 100%, and there must be some type of foreign particles in the air to induce condensation; i.e., **condensation nuclei**. Typical condensation nuclei include clay minerals (soil dust), salts, ash, pollen and even bacteria. Certain types of condensation nuclei, called **hygroscopic nuclei**, are particularly effective in inducing condensation because they have a strong affinity for the water molecule. Ordinary sea salt is one of the best hygroscopic nuclei, and can cause condensation to occur at relative humidities of as low as 76%. In laboratory experiments involving super-pure air, relative humidities of 700% have been reached before condensation occurred. Fortunately, there is always an abundance of condensation nuclei in the atmosphere.

Research involving cloud seeding demonstrates the importance of condensation nuclei to precipitation. In a cloud-seeding experiment in 1946, a mere six pounds of dry ice ( $\text{CO}_2$ ) was dropped into a cloud four miles long. The result was a snowstorm!

The role of condensation nuclei in cloud formation and precipitation is also evidenced by the fact that smog in urban areas generates more cloud cover than would otherwise occur. Between 1964 and 1970, smog-generated clouds decreased the amount of sunshine received at the Earth's surface by 1.3%. This amounts to the equivalent of about 8 minutes of sunshine per day. It seems that, even without trying, humans manage to modify the atmosphere. The famous London fogs resulted from all of the soot particles and sulfuric acid droplets generated by the burning of coal.

The water droplets that condense around condensation nuclei are very small initially, only about 1/2500 inch in diameter. Because of the physical processes associated with these very small droplets, they can remain in the liquid state down to a temperature of minus 40°F (minus 40°C). Liquid droplets at temperatures below their normal freezing point are called **supercooled water droplets**.

## Types of Clouds

Clouds are named on the basis of their shape, their height and their ability or inability to produce precipitation. These defining characteristics are reflected in the names of the clouds, which are formed by a combination of root words, as well as prefixes and suffixes.

- Cloud Types Based on Appearance.
  - **Cumuliform Clouds.** The word *cumulus* means *pile* or *heap*, and such clouds have a puffy appearance (Figure 4.42). They look more or less like cotton balls and are the types of clouds often depicted in cartoons. They form as a result of convective uplift in the summer and are referred to as “fair weather” clouds, even though they do not always bring fair weather. They can also form as air is forced over a mountain or along frontal boundaries.



Figure 4.42. Cumulus clouds (*cumulus humilis*) over Cold Springs, Nevada on April 12, 2014. Cumulus clouds typically have flat bases and billowing tops (Source/Credit: Dennis I. Netoff).



- **Stratiform Clouds.** The word *stratus* means *layer*, and so stratus clouds are layer-like clouds that cover most or all of the sky (Figure 4.43). They usually form in association with fronts as a result of uplift of relatively stable air over a large area. They are not convective in nature, so they are not characterized by vertical air motion within the cloud as are cumulus clouds.



Figure 4.43. Stratus clouds associated with a weak storms system (low pressure area) moving over Peavine Peak near Reno, Nevada. Stratus clouds are low, fairly uniform, and typically dark on their base. They generally form when there is widespread uplift under stable conditions. Note the cloud base is in contact with the Peak. The valley floor is at about 5000 feet and the Peak at about 8300 feet, so the cloud deck is 3000 feet or so above the surface (Source/Credit: Dennis I. Netoff).

- **Cirroform Clouds.** Cirrus clouds are thin, wispy clouds at very high altitudes that are composed of ice crystals (Figure 4.44). They often resemble delicate brush strokes of white paint on a canvas and are sometimes called *mare's tails*. However, cirrus clouds can also form a flat layer at high altitude, in which case they are called **cirrostratus** clouds. Cirrostratus clouds are responsible for the **halos** that appear around the Sun or Moon as light is reflected into a circular pattern by the ice crystals.



Figure 4.44. Cirroform clouds are high, semi-transparent, sometimes fibrous cirrus clouds made of ice crystals. They typically form at altitudes in excess of 20,000 feet (~7000 m), although their altitude varies seasonally and according to latitude. The image looks northward over the Warner Range at Cedar Pass, California during July (Source/Credit: Dennis I. Netoff).

So, the word cirrus indicates not only the general shape of the cloud, but also implies its altitude and composition. These clouds often form in advance of large low pressure systems such as frontal cyclones.

- Cloud types based on height above the surface.
  - **Cirrus**. Cirrus clouds are very high altitude clouds above 20,000 feet.
  - **Alto**. Alto clouds typically form between 10,000 and 20,000 feet.

## Cloud Classification

- **High Clouds** (more than 20,000 feet) (Figure 4.45).

	Cloud Type	Composition	Height	Description
Ci	Cirrus	Ice	High	Thin, transparent, fibrous
Cc	Cirrocumulus	Ice	High	Repeated geometric units (small-size patches, bands)
Cs	Cirrostratus	Ice	High	Uniform "veil;" "milky" sky, may have halo around Sun/Moon
As	Altostratus	Mixed	Middle	Stratiform, lower & darker than cirrostratus, may have corona
Ac	Alto cumulus	Mixed	Middle	Larger, darker patterns, may be patches of blue sky
Sc	Stratocumulus	Liquid	Low	Larger patterns (rolls, patches) lower, darker than aotocumulus
St	Stratus	Liquid	Low	Low extensive dark, uniform deck; may merge with high fog
CuHu	Cumulus Humilis	Liquid	Low	Flat, gray bases, cumuliform top. "cottonball"
Tcu	Cumulus Congestus	Varies with height	Vertically developed	Dark, flattish base with cumuliform top
Cb	Cumulonimbus	Varies with height	Vertically developed	Lightning, thunder, dark base, precipitation, may have anvil
CbMam	Mammato cumulus	Varies with height	Vertically developed	Same as above, with mammatus on anvil or base
	Supercell	Varies with height	Vertically developed	Larger cumulonimbus with strong rotating updraft (mesocyclone)
	Lenticular	Typically mixed	Low to middle	Lens-shaped, often associated with mountain barriers, chinooks
	Virga	Varies with height	Any	Precipitation that falls from the cloud, but evaporates before reaching the ground; appear as dark streamers emanating from cloud base
	Pyrocumulus	Liquid to mixed	Vertically developed	Similar to cumulus humilis or congestus, except initiated by ground fire

Figure 4.45. A simplified cloud classification, based primarily on cloud appearance (cirroform, stratiform, etc.) and height (high, middle, etc.). Additional prefixes and suffixes describe other characteristics of clouds: nimbo/nimbus = precipitation; pyro = fire; lenticular = lens-shaped; mammatus = having bulbous pendants (Source/Credit: Dennis I. Netoff).

- **Cirrus Clouds.** As already stated, these are feathery clouds composed of ice crystals. It should be stressed that these ice crystals are not frozen water droplets; rather, they are crystals formed by deposition when water vapor (a gas) undergoes a phase change directly to a solid state (Figures 4.46a and 4.46b).



Figure 4.46a. High, transparent fibrous cirrus clouds over Huntsville, Texas 2010 (Source/Credit: Dennis I. Netoff).



*Figure 4.46b. Cirrus clouds over southern Arizona (Source/Credit: Dennis I. Netoff).*

- **Cirrostratus Clouds.** These are veil-like, semi-transparent clouds that generally cover most or all of the sky (Figure 4.47). They can generate halos around the Sun and Moon, which remain visible through these clouds (Figure 4.48).



Figure 4.47. Cirrostratus clouds are thin, transparent and uniform, typically covering much or all of the sky. They often have a milky-white appearance, and are difficult to detect as individual cloud forms (Source/Credit: Dennis I. Netoff).



Figure 4.48. Cirrostratus clouds with part of a halo, eclipsed by a jet contrail (Source/Credit: Dennis I. Netoff).



- **Cirrocumulus Clouds.** These are high-level clouds that are arranged in repeatable geometric patterns, such as patches or rolls (Figures 4.49a and 4.49b). Because of their height, individual cloudlets appear small; they have an apparent width about equal to that of the Sun. This type of cloud cover is sometimes referred to as a *mackerel sky* because the cloud has the appearance of scales on a fish. Cirrocumulus clouds generate beautiful sunrises and sunsets (Figure 4.50). When cirrus clouds give way to cirrocumulus clouds, this may indicate the approach of a low pressure system. This is the basis for an old mariner's saying, "Mackerel scales and mares' tails make lofty ships carry low sails." The strong winds that often accompany low pressure systems put the sailing ships at risk if their sails were fully deployed.



Figure 4.49a. Cirrocumulus clouds over Huntsville Texas, 2012 (Source/Credit Dennis I. Netoff).



Figure 4.49b. The larger size of the individual cloud patches indicates a lower cirrocumulus cloud deck compared to the previous image. They are still classified as cirrocumulus because of their form, height, and ice crystal composition (Source/Credit: Dennis I. Netoff).



Figure 4.50. Low cirrocumulus of a mackerel sky over Shark Bay, Australia (Source/Credit: Dennis I. Netoff).

- **Middle-Level Clouds** (10,000 – 20,000 feet).
  - **Altostratus Clouds.** These are gray puffy clouds that form at middle altitudes and are sometimes aligned in parallel waves or bands. Unlike cirrostratus clouds, which have a uniform color, altostratus clouds are varied in darkness. Altostratus clouds also appear bigger than cirrostratus clouds and are somewhat larger than the size of your thumbnail when held at arm's length (Figure 4.51).



Figure 4.51. Altostratus clouds typically have the same types of repeatable geometric patterns as cirrostratus clouds, but individual patches or rolls appear larger, and have a slightly darker underside (Source/Credit: Dennis I. Netoff).

- **Altostratus Lenticularis Clouds.** These are lens-shaped clouds that typically form either downwind or above a mountain. These clouds are stationary clouds formed when moving air is lifted to the lifting (LCL) condensation level near the mountain. As air rises over the mountain in a wave-like fashion, it cools to dew point and the cloud forms at the crest of the wave. As the air then descends, it is heated and evaporation occurs. Thus, the cloud stays in place at the apex of the atmospheric wave as air rushes through it (Figures 4.52a and 4.52b). Occasionally, lenticular clouds form when there are no obvious obstructions to air flow.



Figure 4.52a. An elongated lenticular cloud over the foothills of the Sierra Nevada near Bordertown, California (Source/Credit: Dennis I. Netoff).



Figure 4.52b. Lenticular cloud over Lake Powell, Utah (Source/Credit: Dennis I. Netoff).

- **Altostratus Clouds.** These are gray or blue-gray clouds that often cover the entire sky in a uniform layer. The Sun is usually visible through these clouds as a bright spot with no well-defined edge. Unlike cirrostratus clouds, they do not produce halos (Figure 4.53).



Figure 4.53. Altostratus clouds over Lincoln, Illinois. The Sun shows as a dim glow in the sky (the solar corona) (Source/Credit: Dennis I. Netoff).

- Low-level Clouds (below about 10,000 feet, depending on season and latitude).
  - **Cumulus Clouds.** These are clouds with a flat base and puffy top (Figures 4.54a and 4.54b). They indicate an atmosphere that is slightly convective, where parcels of air are rising freely because of their buoyancy. Local heating of the ground is commonly the cause of buoyancy, although pyrocumulus clouds become buoyant because of ground fires (Figure 4.55).



Figure 4.54a. Cumulus clouds (*cumulus humilis*) with considerable vertical development, transitioning to *cumulus congestus* (Source/Credit: Dennis I. Netoff).





Figure 4.54b. Cumulus clouds (*cumulus humilis*) can often be seen in several stages of development. In the distance, cumulus clouds are developing into *cumulus congestus* clouds. In the foreground, the fractocumulus clouds with the ragged edges indicate that those clouds are dissipating (Source/Credit: Dennis I. Netoff).



*Figure 4.55. Pyrocumulus clouds form locally because of buoyancy provided by heat from ground fires. The plume of rising smoke in this central Nevada image was caused by a distant forest fire (Source/Credit: Nancy Netoff).*

- **Cumulus Congestus Clouds.** This is a cumulus cloud whose vertical development is so great that the top of the cloud extends beyond the low altitude-level and enters the middle (alto) or higher levels. These may develop into cumulonimbus clouds (Figures 4.56a and 4.56b).



Figure 4.56a. Cumulus congestus (towering cumulus) and cirrus clouds over Boulder Mountain, Utah (Source/Credit: Dennis I. Netoff).



Figure 4.56b. *Cumulus congestus* (towering cumulus) in various stages of vertical development over Boulder Mountain, Utah (Source/Credit: Dennis I. Netoff).

- **Cumulonimbus Clouds.** These are the giants of the sky. Though their base lies within a few thousand feet of the surface, the top of the cloud can extend upward to heights of 60,000 feet. If the top of the clouds reach a strong inversion, such as the tropopause/stratosphere boundary, the cloud will spread out along this boundary. If there are strong upper-level winds, the flat top extends downwind, forming a shape like that of an anvil. The upper part of these clouds may appear fibrous as a result of the presence of ice crystals. Cumulonimbus clouds are associated with intense vertical air motion, and both updrafts and downdrafts and therefore pose a threat to aircraft. They can also produce intense rain, hail, and tornadoes. Because of their ability to generate lightning and thunder, these clouds are also known as **thunderheads** (Figures 4.57a, 4.57b and 4.57c).



Figure 4.57a. Cumulonimbus clouds have the greatest amount of vertical development of any cloud type. This one in Arizona has a base that is just a few thousand feet above the ground, and its anvil top is at the tropopause at about 50,000 feet (~15,000 m). The flat, anvil head of cumuliform clouds is the result of a cap or lid, an upper-level inversion. The ultimate lid is the tropopause, which limits all thunderstorm development, including hurricanes (Source/Credit: Bill Westphal, with permission).



Figure 4.57b. Cumulonimbus clouds produce hazardous weather, including lightning, strong winds, tornadoes, flash floods, and damaging hail (Source/Credit: NOAA).



*Figure 4.57c. Supercell cumulonimbus clouds are larger than single-cell cumulonimbus clouds, and can last much longer. This one in Modoc County, California, began as a single-cell thunderstorm over Lassen Peak at about noon, some 7 hours prior to this image. It finally dissipated in eastern Oregon in the middle of the night, after travelling over 150 miles (Source/Credit: Dennis I. Netoff).*

- **Mammatus Clouds.** These clouds resemble the bottom of an egg carton or the udder of a cow (i.e. mammary glands). They are formed at the base of a variety of clouds, most commonly cumulonimbus clouds. They form as cool, sinking air that is high in liquid water or ice content is carried below the base of their *parent* clouds. The appearance of these clouds at the base of severe thunderstorms (cumulonimbus clouds) *may* indicate that the cloud is capable of producing tornadoes (Figures 4.58a, 4.58b and 4.58c).



Figure 4.58a. Mammatus clouds, such as these near Wichita Falls, Texas, are characterized by bases that are NOT flat; rather, they have pouch-like protuberances that extend downward from their bases. These features develop in response to downdrafts of cold air within the cloud. Two tornadoes touched down within 30 minutes of the time that this photograph was taken, which indicates that these mammatus clouds formed on the underside of a cumulonimbus cloud (Source/Credit: Dennis I. Netoff).





Figure 4.58b. (left) Large, pouch-like protuberances that define mammatus clouds are clearly visible in this photograph (Source/Credit: Dennis I. Netoff).

Figure 4.58c. (right) Mammatus clouds with rainbow (Source/Credit: Dennis I. Netoff).

- **Stratus Clouds.** These are uniform, gray clouds that often cover the entire sky. They can form in association with frontal or cyclonic uplift, and when a fog lifts. They sometimes produce mist or drizzle (Figure 4.59).



Figure 4.59. Stratus clouds associated with a frontal-cyclonic storm system (low pressure area) moving over Peterson Mountain near Bordertown, Nevada on April 22, 2014. Stratus clouds are low, fairly uniform, and typically dark on their base. They generally form when there is widespread uplift under stable conditions. Note the cloud base is in contact with the flank of the mountain. The valley floor is at about 5000 feet and the mountain is truncated at about 6000 feet, so the cloud deck is 1000 feet or so above the surface (Source/Credit: Dennis I. Netoff).

- **Nimbostratus Clouds.** These are dark gray clouds that cover most or all of the sky. These clouds are associated with more or less continuously falling rain or snow. Precipitation from these clouds may be of long duration, but it is not intense, as is often the case with cumulonimbus clouds. Unlike altostratus clouds, the Sun is not visible through these clouds. Like stratus clouds, these clouds often form in association with frontal or cyclonic uplift. They often have a more irregular base than stratus clouds (Figure 4.60). Virga are similar to nimbostratus clouds, except the layer of air beneath the cloud is dry enough to cause the raindrops to evaporate without reaching the ground (Figure 4.61).



Figure 4.60. View west from Reno, Nevada of nimbostratus clouds in June 2012, during the passage of a weak storm system. Nimbostratus clouds are typically low, dark gray clouds that produce continuous precipitation. They are not associated with lightning or cumulonimbus clouds (Source/Credit: Dennis I. Netoff).



Figure 4.61. *Virga* appears as rain falling from the base of a cloud, except that it evaporates in the dry air under the cloud before reaching the ground (Source/Credit: Dennis I. Netoff).

- **Stratocumulus Clouds.** These are clouds that have characteristics of both cumuliform and stratiform clouds. They have relatively flat bases, but tend to form long rows or parallel bands. They are often associated with large low pressure systems, and hence are often associated with *foul weather*. There may be patches of blue sky between rows or bands. Individual cloud elements are about the size of your fist when held at arm's length. Shining rays of light known as crepuscular rays often emanate from between the cloud elements near sunrise and sunset (Figures 4.62a and 4.62b).



Figure 4.62a. Stratus clouds transitioning to stratocumulus over Huntsville, Texas. Stratus and stratocumulus clouds are low, fairly uniform, and typically dark on their base. They generally form when there is widespread uplift under stable conditions. Stratus clouds can easily develop into stratocumulus clouds due to the introduction of a wave-like motion in the lower atmosphere (Source/Credit: Dennis I. Netoff).



Figure 4.62b. Stratocumulus clouds with well-developed parallel banding over Ozona, west Texas (Source/Credit: Dennis I. Netoff).

There are scores of other types of clouds that are less common than the ones listed above, but nonetheless interesting because of how they form, where they form, or their appearance. The International Cloud Atlas identifies well over 2000 types. Some examples include **roll clouds**, which, as the name implies, are cylinder-shaped clouds that rotate about a horizontal axis (Figure 4.63). **Nacreous** (*mother of pearl*) **clouds** are of special interest because they form above the troposphere, where the majority of clouds occur. Nacreous clouds form in the lower stratosphere (9-16 miles) and are typically only seen in reflected light (so seen after sunset, before sunrise). They are composed of nitric and/or sulfuric acid + water ice (Figure 4.64). **Noctilucent** (*night-shining*) **clouds** have the distinction of being the highest clouds that form in the atmosphere (Figure 4.65). They typically occur from 47-53 miles (76-85km) above the surface in the mesosphere. They are ice crystal clouds that can only form at temperatures of about minus 184°F (minus 120°C). Recent studies indicate that they tend to form around dust nuclei that can be either of human origin (e.g., the Space Shuttle) or from meteoric dust. Noctilucent clouds were seen hundreds of miles from the Tunguska site in 1908, possibly the result of a comet beginning to vaporize in the mesosphere.



Figure 4.63. Roll clouds are rarely observed in association with thunderstorms, with the exception of this one from Racine, Wisconsin, taken on June 1, 2007. They are somewhat more common over the Gulf of Carpentaria in Australia, for reasons that are unclear (Source/Credit: Eazydp, courtesy Wikipedia, <http://commons.wikimedia.org/wiki/File:Roll-Cloud-Racine.jpg#filehistory>).



Figure 4.64. Nacreous (mother of pearl) clouds form in the lower stratosphere (9-16 miles) and are typically only seen in reflected light (so seen after sunset, before sunrise). They are composed of nitric and/or sulfuric acid + water ice. The stratified nature is reflected in the streamlined shape of the clouds (Source/Credit: Alan Light, Wikimedia Commons).





Figure 4.65. Image of noctilucent clouds taken from the International Space Station on July 13, 2012. Noctilucent clouds are the highest clouds that form in the atmosphere, typically from 47-53 miles (76-85km) above the surface in the mesosphere. They are ice crystal clouds that can only form at temperatures of about minus 184°F (minus 120°C). Recent studies indicate that they tend to form around dust nuclei that can be either of human origin (e.g., the Space Shuttle) or from meteoric dust (Source/Credit: NASA).

## Precipitation

Although a sizable proportion of the Earth’s atmosphere is covered with some type of cloud at any given time, only a small percentage of clouds produce precipitation, water that falls to the ground in measurable quantities. This observation indicates that something other than condensation must occur in order for precipitation to occur. The critical ingredient is a mechanism to cause **rapid growth** of incipient cloud droplets to raindrop or snowflake size. Cloud droplets are very small, only about 1/2500 of an inch (a few microns) in diameter (Figures 4.66a 4.66b and 4.66c). Because of this small size, cloud droplets are simply too light to fall to the ground because air currents keep them suspended. So, in order for them to fall, they must grow in size and mass. This can occur in two basic ways: collision-coalescence and through the Bergeron processes. **Collision-coalescence** is the process by which cloud droplets or ice crystals collide with one another and stick together to form droplets or crystals that are large enough to fall. Approximately one *million* water droplets must collide before the resulting droplet becomes big enough to precipitate.

Moisture Type	Intensity Inches/hour (cm/hour)	Median Diameter (millimeters)	Velocity of Fall Feet/second (meters/second)	Drops per Second per square foot (square meter)
Fog	0.005 (0.013)	0.01	0.01 (0.003)	6,264,000 (67,425,000)
Mist	0.002 (0.005)	0.10	0.7 (.21)	2,510 (27,000)
Drizzle	0.01 (0.0025)	0.96	13.5 (4.1)	14 (151)
Light Rain	0.04 (0.102)	1.24	15.7 (4.8)	26 (280)
Moderate Rain	0.15 (0.38)	1.60	18.7 (5.7)	46 (495)
Heavy Rain	0.60 (1.52)	2.05	22.0 (7.3)	51, est. (650) est.
Excessive Rain	1.60 (4.06)	2.40	24.0 (7.6)	76 (818)
Cloudburst	4.00 (10.2)	2.85	25.9 (7.9)	113 (1,220)

Figure 4.66a. Size and type of condensation or precipitation droplets versus fall velocity. Cloud droplets are small enough and have such a low terminal fall velocity that even the most subtle updrafts in the atmosphere can keep them suspended indefinitely. Fall velocity increases as the droplets grow (Source/Credit: H.W. Lull, USDA).

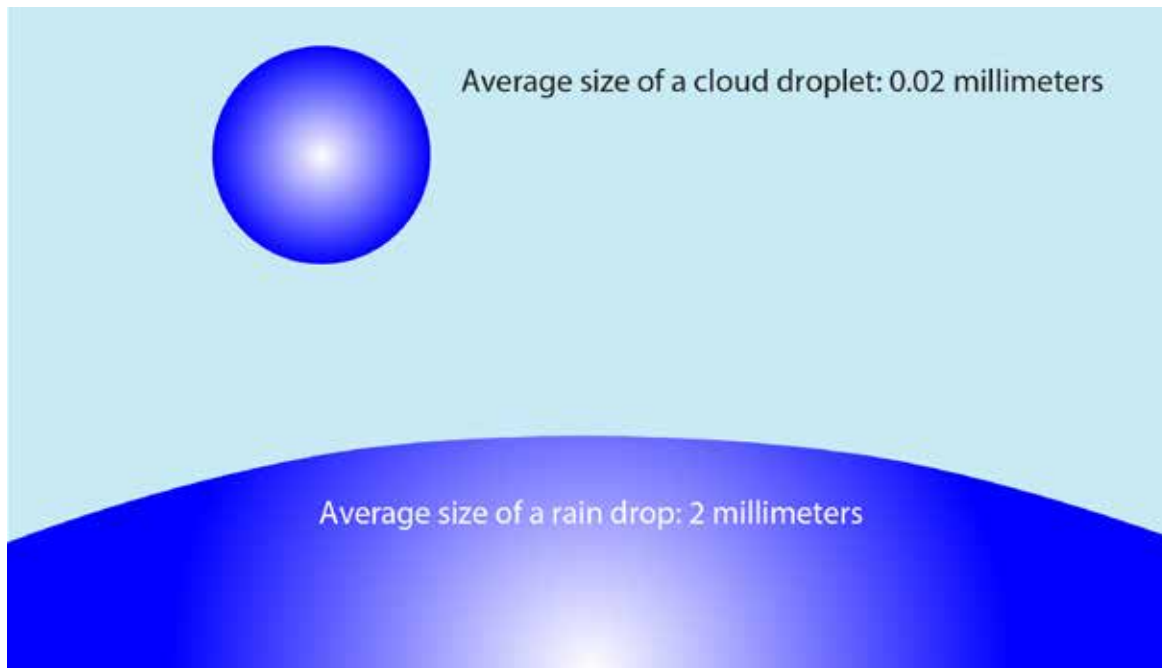


Figure 4.66b. The average raindrop is 2 to 5 mm in diameter. Droplets of this size are generally large enough to overcome the air motion in a cloud and fall to the ground. Significantly, the small droplets initially produced by condensation are too small to fall as rain. In order to form a raindrop, these tiny droplets must collide and coalesce to form bigger droplets. In fact, more than a million cloud droplets may have to coalesce in order to form a single raindrop.

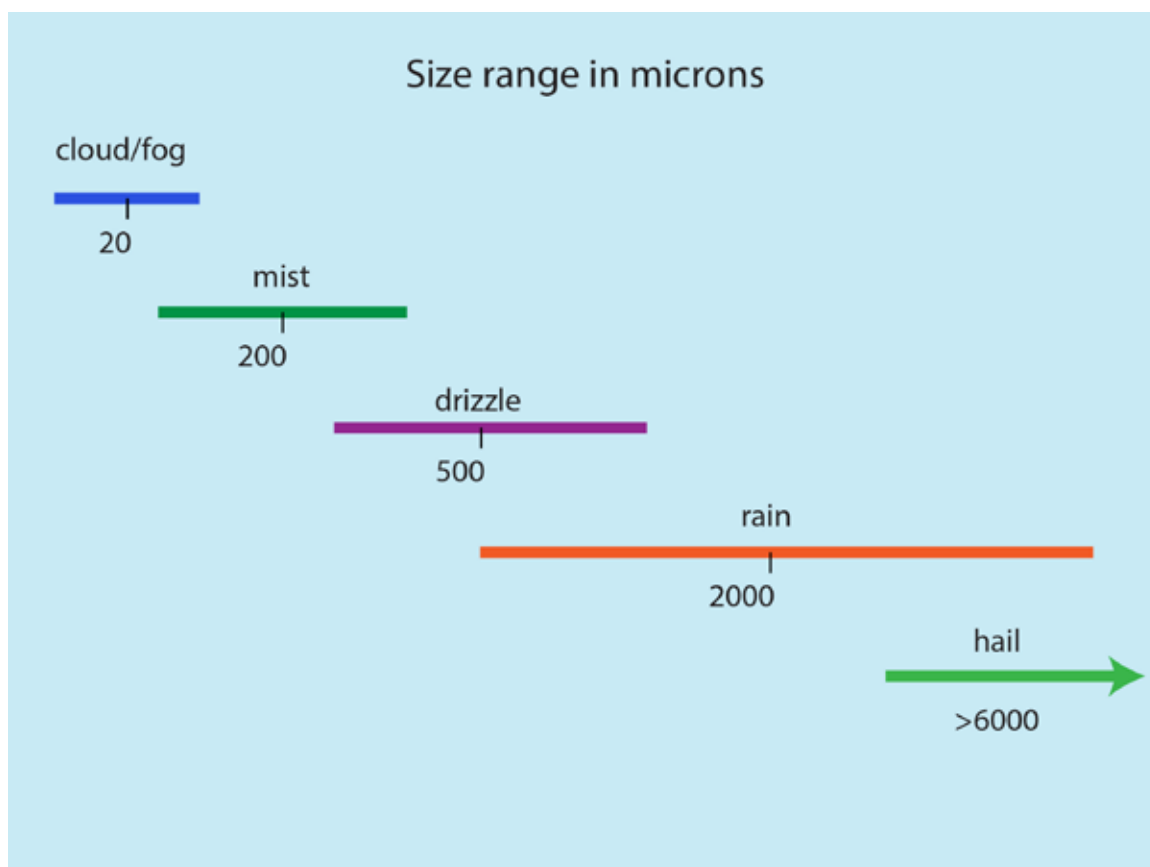


Figure 4.66c. Size comparison of various forms of condensation and precipitation. 200 microns = 2 mm or approximately 1/13 inches.

The **Bergeron Process** occurs in clouds containing both ice crystals and supercooled water droplets (i.e., a mixed water-ice cloud). One of the key concepts behind the Bergeron process has to do with vapor pressure differences. Vapor pressure refers to that portion of the total atmospheric pressure that is accounted for by the presence of water vapor. Because ice crystals are a solid, the molecules are held together more tightly than is the case with supercooled water droplets. As a result, the saturation vapor pressure tends to be higher over water droplets than over ice crystals in a cloud because more water molecules can escape from the water droplets given that the water molecules are not held as tightly in a liquid state. In effect, this creates a vapor pressure *high* around the water droplets and vapor pressure *low* around the ice crystals. As with the wind in which air moves from high to low pressure, so too do water molecules move from the water droplets (high vapor pressure) to the ice crystals (low vapor pressure). As a result of this process, the supercooled water droplets evaporate and then sublimate onto the ice crystals (Figure 4.67). So, there is a net transfer of water molecules from water droplets to ice crystals; consequently, the ice crystals enlarge at the expense of the water droplets. Eventually, the ice crystals may become large enough to fall as snow. However, the snow may melt on the way to the ground and become rain.

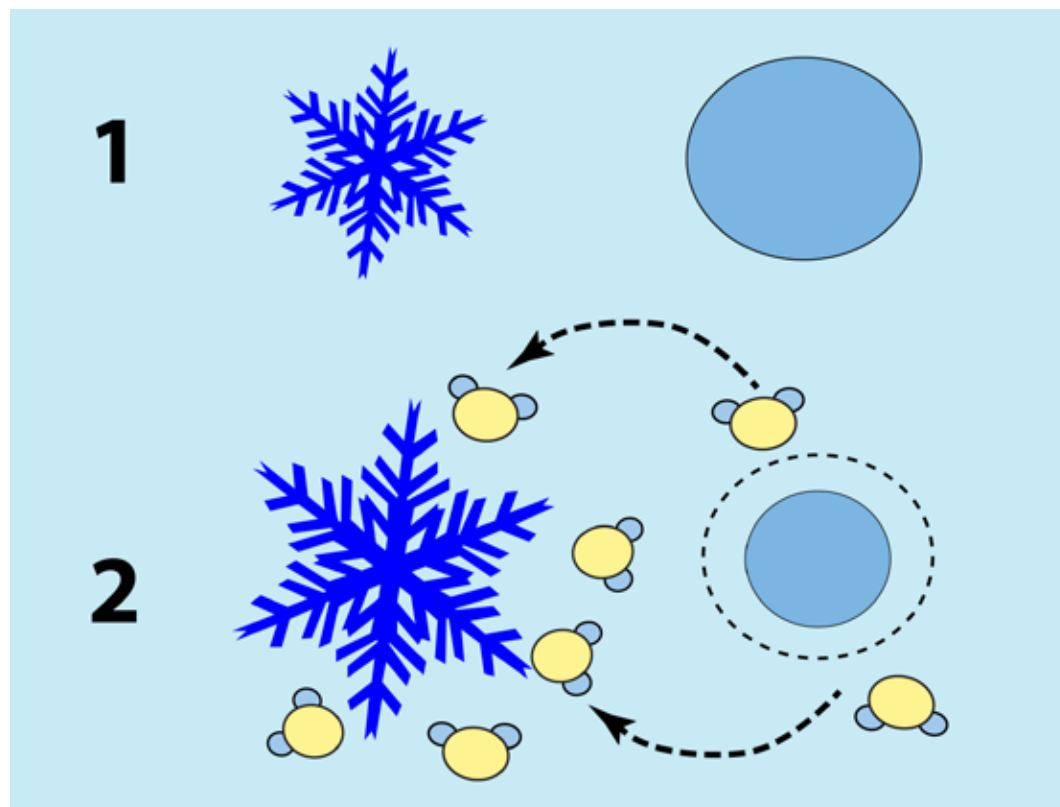


Figure 4.67. When ice crystals and supercooled liquid water droplets coexist in the same cloud, there is a natural tendency for water vapor to condense on the substance with the lower energy level (i.e., the ice crystal), allowing water to evaporate from the undersaturated air around the supercooled water droplets. The ice crystals essentially grow at the expense of the supercooled water droplets, causing a rapid increase in size and weight of the ice crystals.

## Types of Precipitation

Precipitation can be classified into two main categories, unfrozen and frozen. Unfrozen precipitation includes rain and drizzle. **Rain** consists of droplets that are larger than 0.02 inches (2000 microns) in diameter. Raindrops begin to fall in more-or-less spherical form, but flatten like pancakes as they become larger and acquire higher velocity. This is because the flow of air around the droplet flattens it as it falls to the ground. Frictional resistance of falling droplets against the surrounding air limits the fall velocity of raindrops to about 25 mph (40km/hr).

- **Drizzle.** Drizzle consists of droplets that are less than 0.02 inches (500 microns) in diameter (typically 200 to 500 microns). Because of their small size, they are readily blown about by the wind, which is why drizzle can seem to come at you from just about any direction. When drizzle-sized or small raindrops fall through a layer of drier air, they commonly evaporate before actually striking the ground, producing a type of precipitation called **virga** (Figures 4.68a and 4.68b).



Figure 4.68a. Virga is would-be precipitation that evaporates before it reaches the Earth's surface. Virga in southern Wyoming (Source/Credit: Dennis I. Netoff).



Figure 4.68b. Virga, such as this example in southern Utah, typically develops when there is a layer of very dry air close to the surface (Source/Credit: Dennis I. Netoff).

- **Freezing Rain.** There are several forms of frozen precipitation. Although rare in southeast Texas, they are quite common elsewhere in the United States at higher latitudes. Freezing rain refers to supercooled water droplets that freeze **upon contact** with the surface.
- **Sleet.** Sleet is similar to freezing rain except that it consists of small, hard pellets of ice that are formed as raindrops freeze **while falling** toward the ground. Unlike snowflakes, they are not formed by sublimation, but by freezing of liquid droplets. Freezing rain and sleet typically form when there is a **temperature inversion** (a layer of warm air rides up and over a layer of cold air along a front, usually a warm front). The sleet forms when raindrops fall through a thick layer of cold air, one that is thick enough to allow enough time for the raindrops to freeze. Freezing rain falls through a thinner layer of cold air, in this case one that is too shallow to allow time for the supercooled rain to freeze while falling (Figures 4.69a, 4.69b and 4.69c).



Figure 4.69a. Freezing rain and freezing drizzle occur when supercooled raindrops fall on a surface that is below freezing. The droplets freeze on contact and accumulate as a layer of clear ice (Source/Credit: Donna Wright, Lawton, OK January 29, 2010. iWitness Weather Photo Gallery).



Figure 4.69b. Damage from an icing storm in the American Midwest (Source/Credit: NWS).



Figure 4.69c. A thick layer of clear ice on a tree branch from a 48-hour icing storm of predominantly freezing drizzle in Lincoln, Illinois (Source/Credit: Dennis I. Netoff).



- **Snow.** Snow consists of crystalline ice formed directly by sublimation (Figure 4.70). Individual snow crystals are 6-sided, though several snow flakes may merge to form larger flakes by collision-coalescence. The largest flakes ever recorded (in Montana, January, 1887) were 15 inches (38 cm) in diameter and eight inches thick! These were most likely aggregates of smaller snowflakes that were allowed to coalesce due to temperatures being close to 32°F (0°C).



Figure 4.70. Snow forms when water vapor goes directly to a solid (called either deposition or sublimation). Most snow forms in clouds with temperatures far below 32°F (Source/Credit: Dennis I. Netoff).

When ice crystals and snowflakes fall from cirrus clouds, they sometimes sublimate as they enter warmer, drier air. In such cases, they constitute a type of virga precipitation and produce a pattern of white streaks below the cloud known as **fall streaks**. When the sunlight hits them just right, they may look like curtains of light in the sky.

- **Hail.** Hail consists of large ice particles that form inside cumulonimbus clouds (thunderheads). Inside a cumulonimbus cloud, violent updrafts and downdrafts coexist side by side. When a droplet of water gets caught in an updraft, it may be carried so high that it freezes in the cold temperatures at the top of the cloud. It may then enter a downdraft and be carried back toward the base of the cloud. While in this part of the cloud, water will adhere to the ice crystal, adding a layer of water or ice. If the ice crystal is caught in another updraft, it will be carried back up into the cloud and this new layer of water will freeze, thereby increasing the size of the hailstone. If this process is repeated, the hailstone can grow quite large and will exhibit a layered structure (Figures 4.71a and 4.71b).

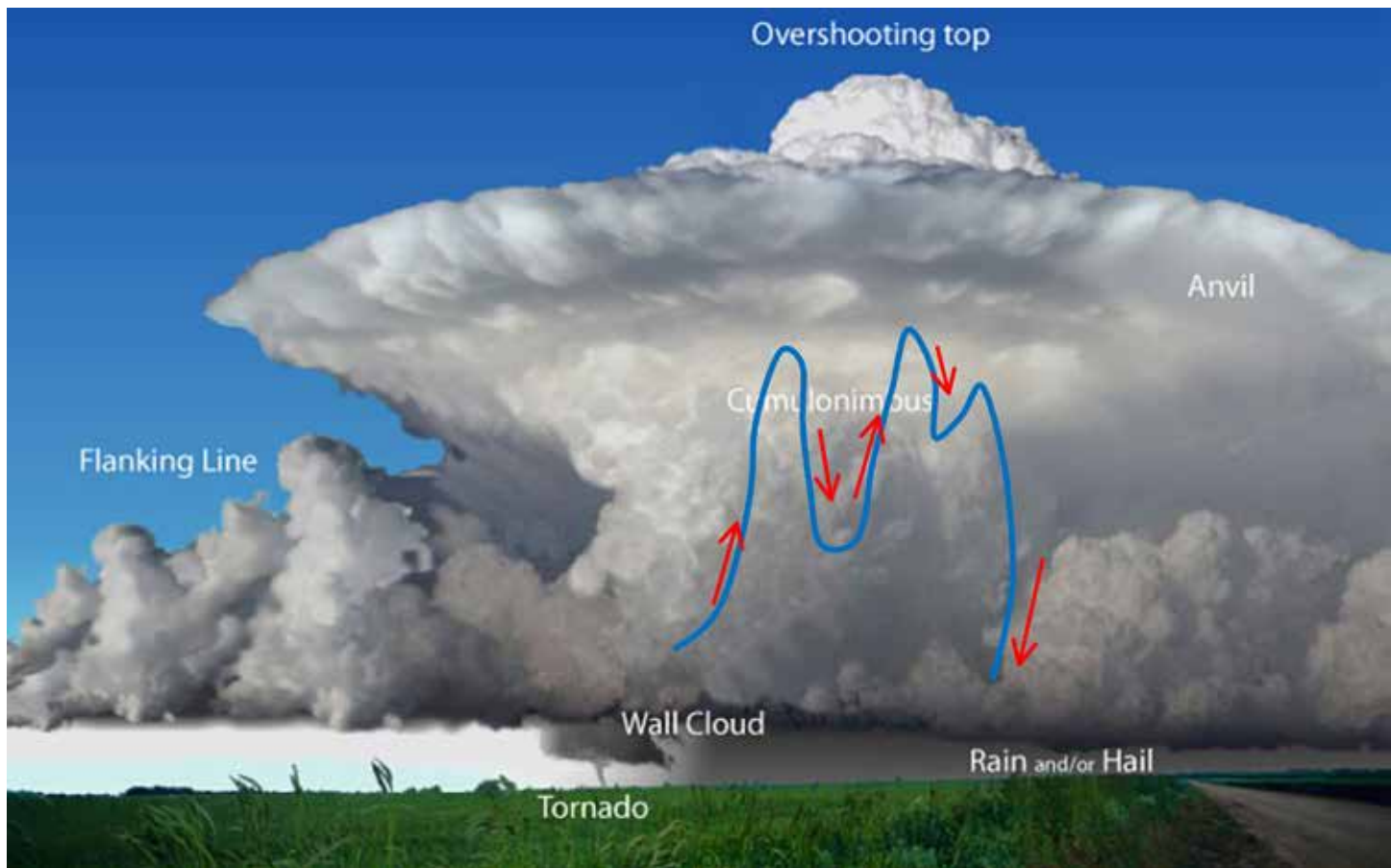


Figure 4.71a. Hail forms inside cumulonimbus clouds as water droplets are carried by updrafts and freeze. As downdrafts carry the ice pellets back to the lower part of the cloud, an additional layer of water may adhere to the frozen droplet. As the object is transported by more updrafts, it refreezes. This process adds successive layers of alternating clear and opaque ice. When the size of the ice particle can no longer be supported by updrafts within the cloud, hail falls from the cloud (Source/Credit: NOAA).



Figure 4.71b. Golf ball-to-baseball-sized hail that fell from a supercell thunderstorm over Oklahoma City on May 10, 2010 (Source/Credit: sabresiren from iWitness Weather Photo Gallery).

Aurora, Nebraska was bombarded by a hailstorm on June 22, 2003. One of the stones which struck the ground measured 7 inches (18 cm) in diameter and had a circumference of 18.75 inches (48 cm), making it the largest ever recovered in the United States (Figure 4.72). Jay Lawrimore of the National Weather Service indicated that the Aurora hailstone didn't break the record for the heaviest hailstone. Lawrimore noted, "It was hard for us to get an accurate weight for this stone because a chunk of it hit the gutter of a house and 40 percent of it was lost. We also think some of the stone's mass might have melted before it was preserved in freezing conditions."



Figure 4.72. A hailstone that fell in Queensland, Australia on October 26, 2003 measured 4 inches (10 cm) in diameter, about 60 percent the size of the Aurora, Nebraska hailstone that fell during the same year (Source/Credit: <http://australiasevereweather.com/>).

The previous 33 year record-holder fell September 3, 1970 in Coffeyville, Kansas. This hailstone was 5.7 inches (14 cm) in diameter and had a circumference of 17.5 inches (44 cm) (Figure 4.73). Updraft velocities of approximately 115 mph (185km/hr) are required to suspend hailstones of that size.



*Figure 4.73. The former United States record-size hailstone that fell on Coffeyville, Kansas. Note the chicken egg for comparison (Source/Credit: NOAA).*

In the case of hailstones, some very strange condensation nuclei have been reported. Insects, for example, have been found in hailstones, as have frogs and a 6 x 8-inch (15 to 20 cm) turtle!

Each year, hail damages crops, breaks windows in cars and homes, smashes vinyl siding, and bangs up cars. The estimated cost of this damage is more than \$750 million per year (Figures 4.74a, 4.74b and 4.74c). Ironically, this damage by ice occurs during the warmest time of the year. This is because extreme convection currents are required to produce hail, and the convection currents themselves are accelerated by surface heating.



Figure 4.74a. Hail damage to a plastic table in the Midwest (Source/Credit: NWS).



Figure 4.74b. Hail damage to automobiles, mid-western United States, 1940s (Source/Credit: NWS).



Figure 4.74c. Hail damage to corrugated plastic shelters, mid-western United States (Source/Credit: NWS).

## Global Precipitation Patterns

### Observations from Precipitation Maps

Analyses of monthly, seasonal, and annual precipitation maps for any multi-decadal period will result in some general observations. Some are readily explainable, others not so. A few of these, based on three global maps (Figures 4.75a, 4.75b, and 4.75c) reveal the following:

- there is a low latitude belt of high precipitation, both land and oceans
- the low-latitude belt of high precipitation is broadest in the western Pacific Basin
- a secondary zone of high precipitation occurs in the middle and upper-middle latitudes in both hemispheres, especially over the oceans
- there are distinctive zones of sparse precipitation at about 15-35 degrees latitude on the eastern side of all major ocean basins, extending to the west coasts of all continents at those latitudes (north Africa, south Africa, southwestern United States, northern Chile-Peru, and Australia)
- the western side of the ocean basins at those same latitudes (15-35 degrees) is wetter, extending in several cases well onto the continents
- there are distinctive coastal strips of heavy precipitation in places such as Norway, southern Chile, the Pacific Northwest, Columbia, and New Zealand
- continental interiors (Eurasia, North America, Australia) tend to be drier than regions closer to ocean basins
- highest latitudes have sparse precipitation, especially the interior ice caps of Greenland, Antarctica, and to a lesser degree, northernmost North America and Eurasia July and January maps
- equatorial latitudes (Amazon Basin, Congo Basin, Indonesia) are wet on both July and January maps
- latitudinal belts immediately poleward of the equatorial wet zone are seasonally wet-and-dry
- in the middle and high latitudes, summers are distinctly wetter than winters, except for middle-latitude west coasts (e.g., California, central Chile)
- there are many anomalies; in particular places that should be wet that are dry for their relative position, such as equatorial east Africa and eastern Brazil



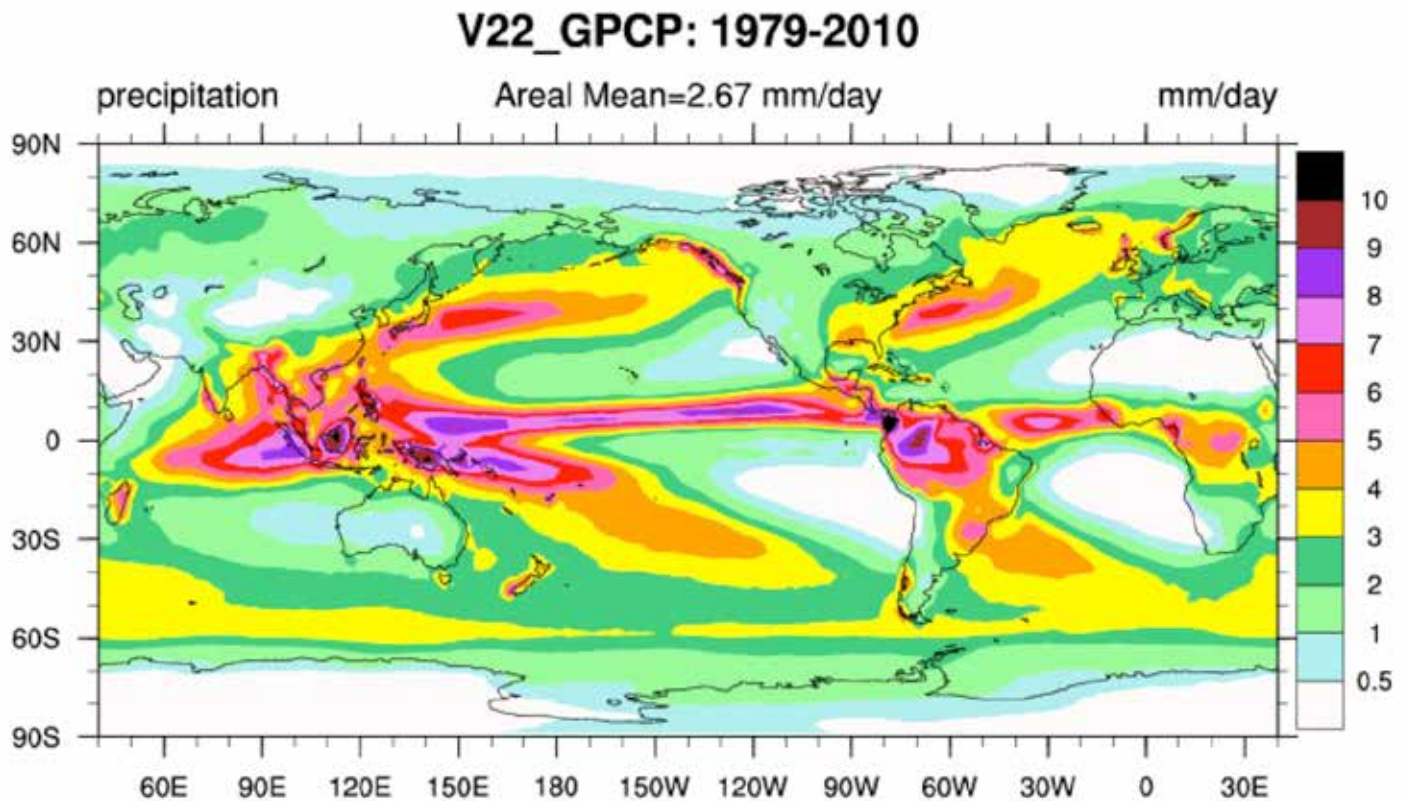


Figure 4.75a. Estimated rainfall based on data from gauge stations, satellites and sounding observations on a 2.5-degree global grid from 1979-2010. This map differs from most global precipitation maps in that it includes precipitation estimates for the world's oceans (Source/Credit: NCAR GPCP Global Precipitation Climatology Program 1979-2010).

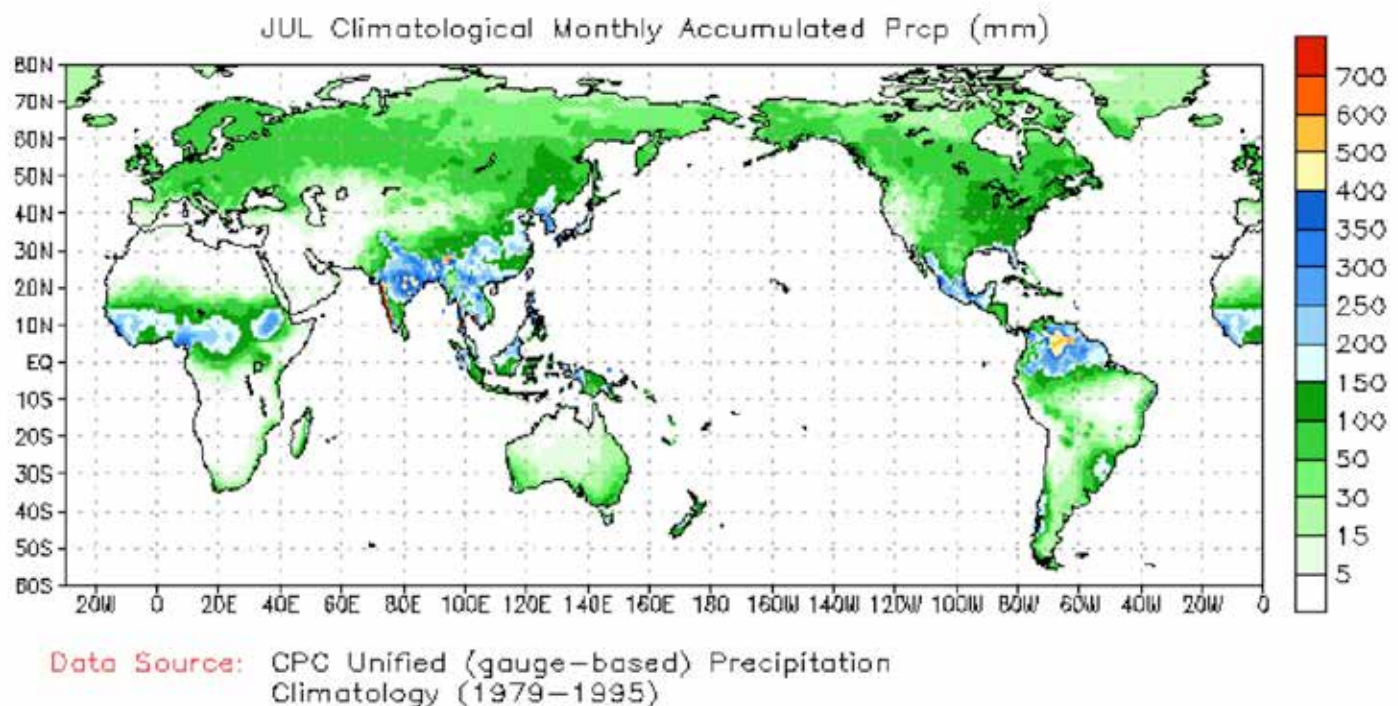


Figure 4.75b. July global precipitation over land for the period 1979-1995 (Source/Credit: NOAA/CPC).

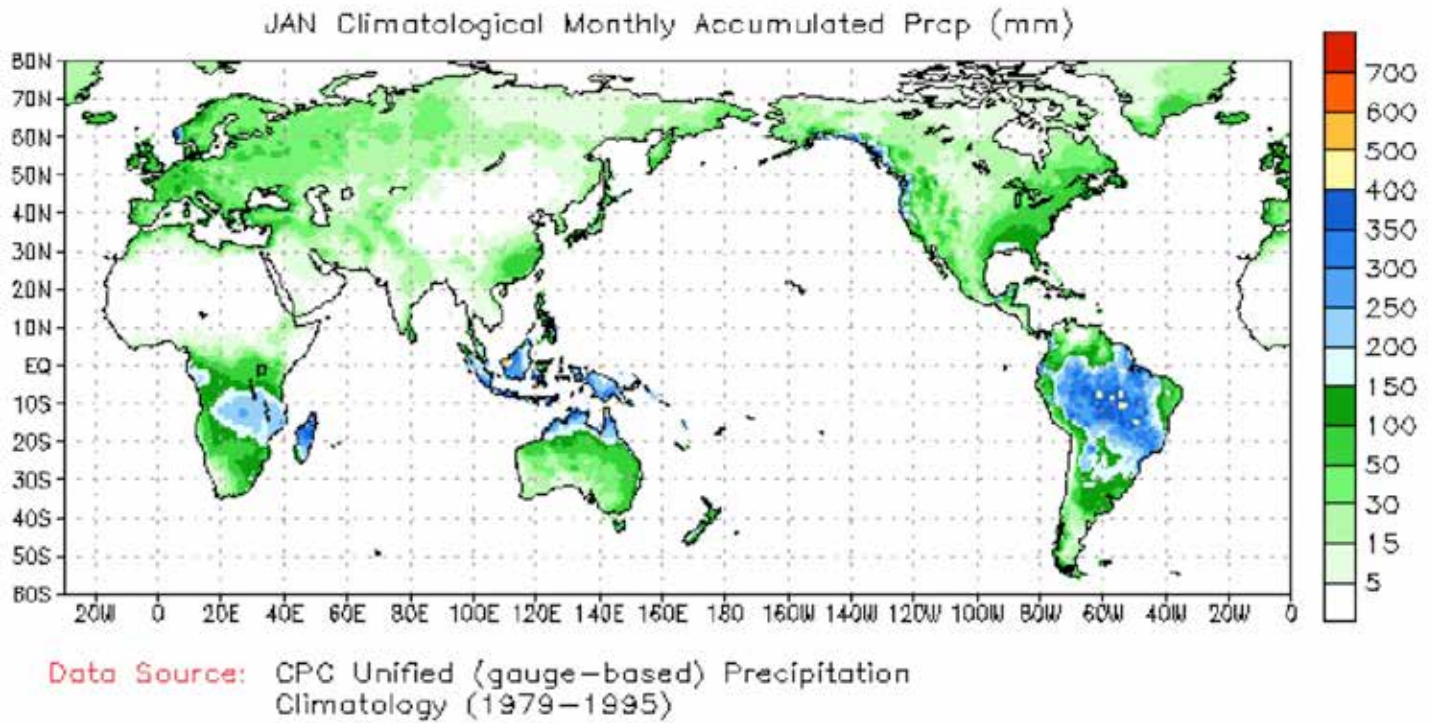


Figure 4.75c. January global precipitation over land for the period 1979-1995 (Source/Credit: NOAA/CPC).

## Causal Mechanisms

Global zones of abundant cloudiness and precipitation versus drier zones are controlled in part by planetary wind and pressure systems (Figure 4.76). The zone of heavy precipitation in the equatorial latitudes over both land and oceans is best explained by proximity to the Intertropical Convergence Zone and to vast areas of warm, moisture-laden air over warm tropical oceans. The core of the Intertropical Convergence Zone (ITCZ) is dominated by uplift, near-constant cloud cover (especially during the afternoon hours when air becomes buoyant) and frequent, abundant precipitation (Figure 4.77). Seasonal movement of the Intertropical Convergence Zone, as it attempts to follow the vertical rays of the Sun, causes areas poleward of the wet equatorial belt to be seasonally wet and dry (Figures 4.78a and 4.78b). Summers tend to be wet because of the poleward movement of the Intertropical Convergence Zone, and winters dry when the Subtropical High dominates.

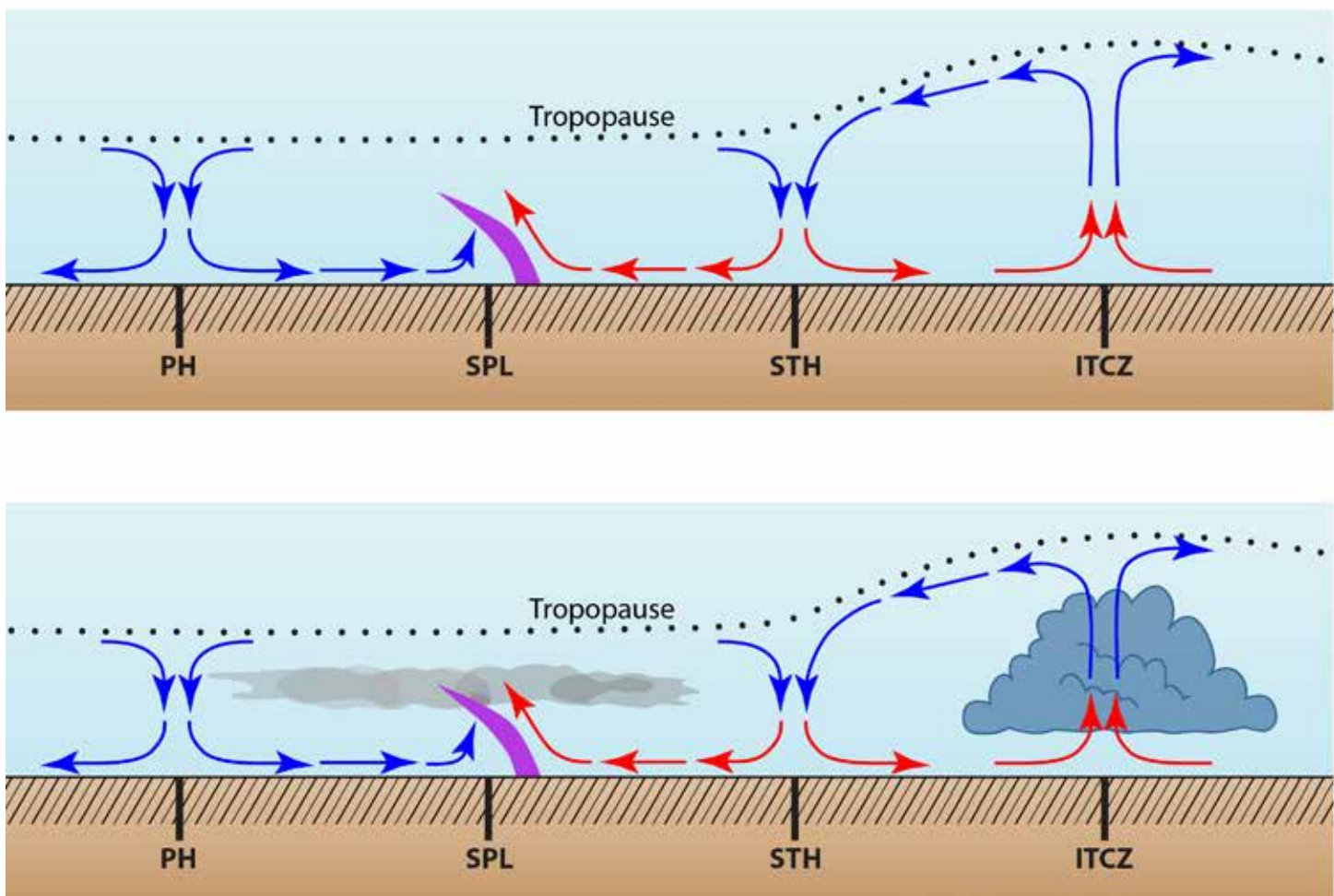


Figure 4.76. A first approximation of global precipitation is derived from an analysis of global pressure and wind systems (upper image). Areas of uplift (ITCZ near the Equator and frontal-cyclonic storms systems (SPL) are areas subject to cloudiness and precipitation (lower image). Areas dominated by subsidence (e.g., the Subtropical High STH and Polar High, PH) are areas of sparse precipitation (Source/Credit: Dennis I. Netoff).

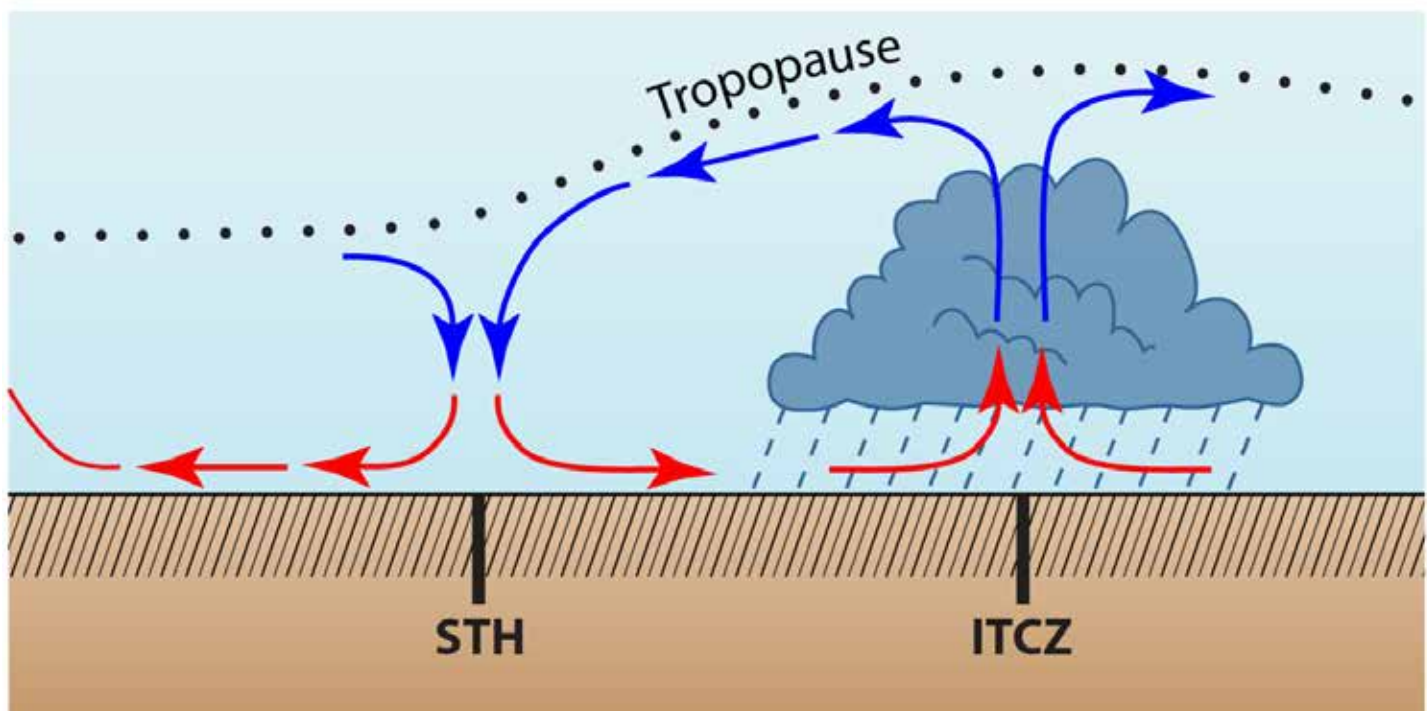


Figure 4.77. The core region of the Intertropical Convergence Zone is an area of frequent cloudiness and precipitation. Even with some seasonal movement of the Intertropical Convergence Zone, areas within a few degrees of the Equator tend to be wet year-round (Source/Credit: Dennis I. Netoff).

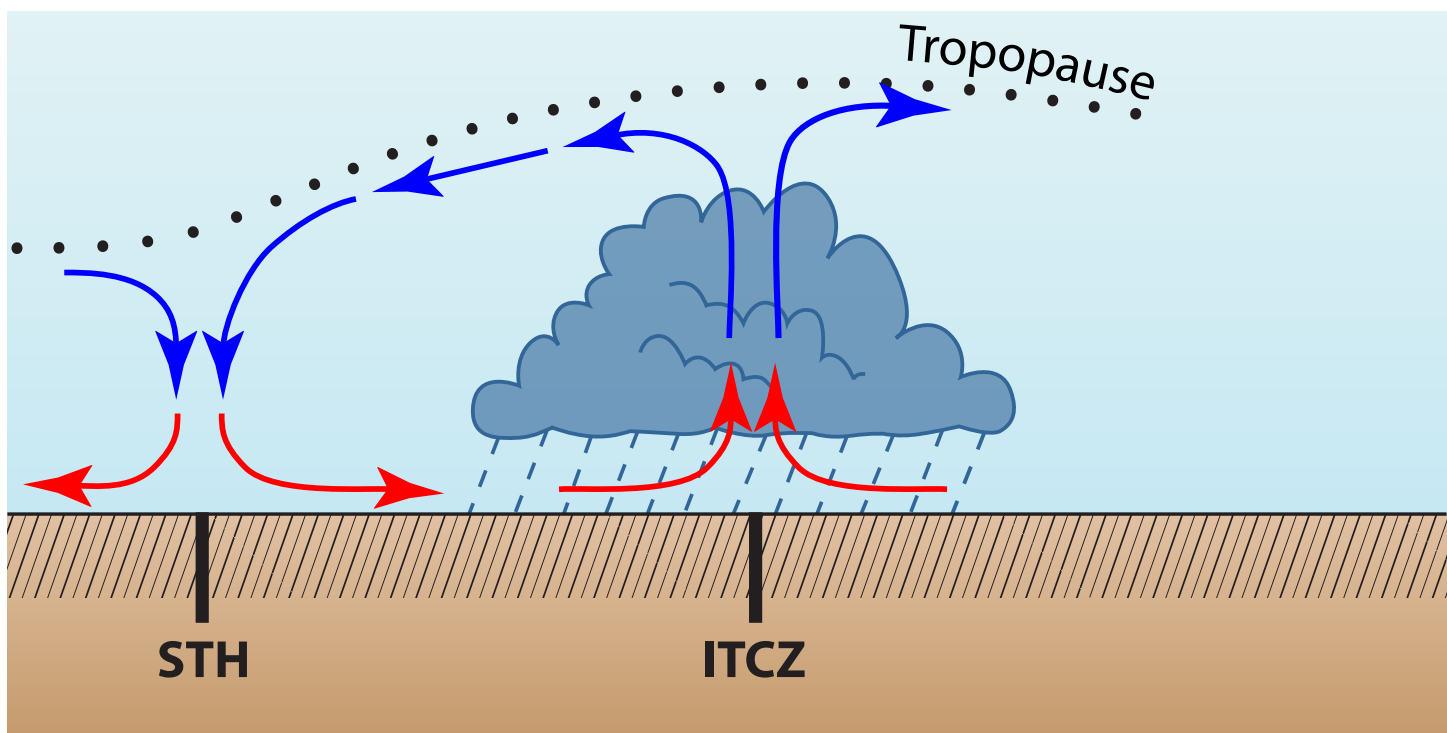


Figure 4.78a. The core of the Intertropical Convergence Zone migrates several degrees toward the north during the Northern Hemisphere summer, bringing summer rain into areas as far north as 15-25 degrees. Note that the entire Hadley cell has migrated poleward. The Equatorial zone continues to receive some precipitation (Source/Credit: Dennis I. Netoff).

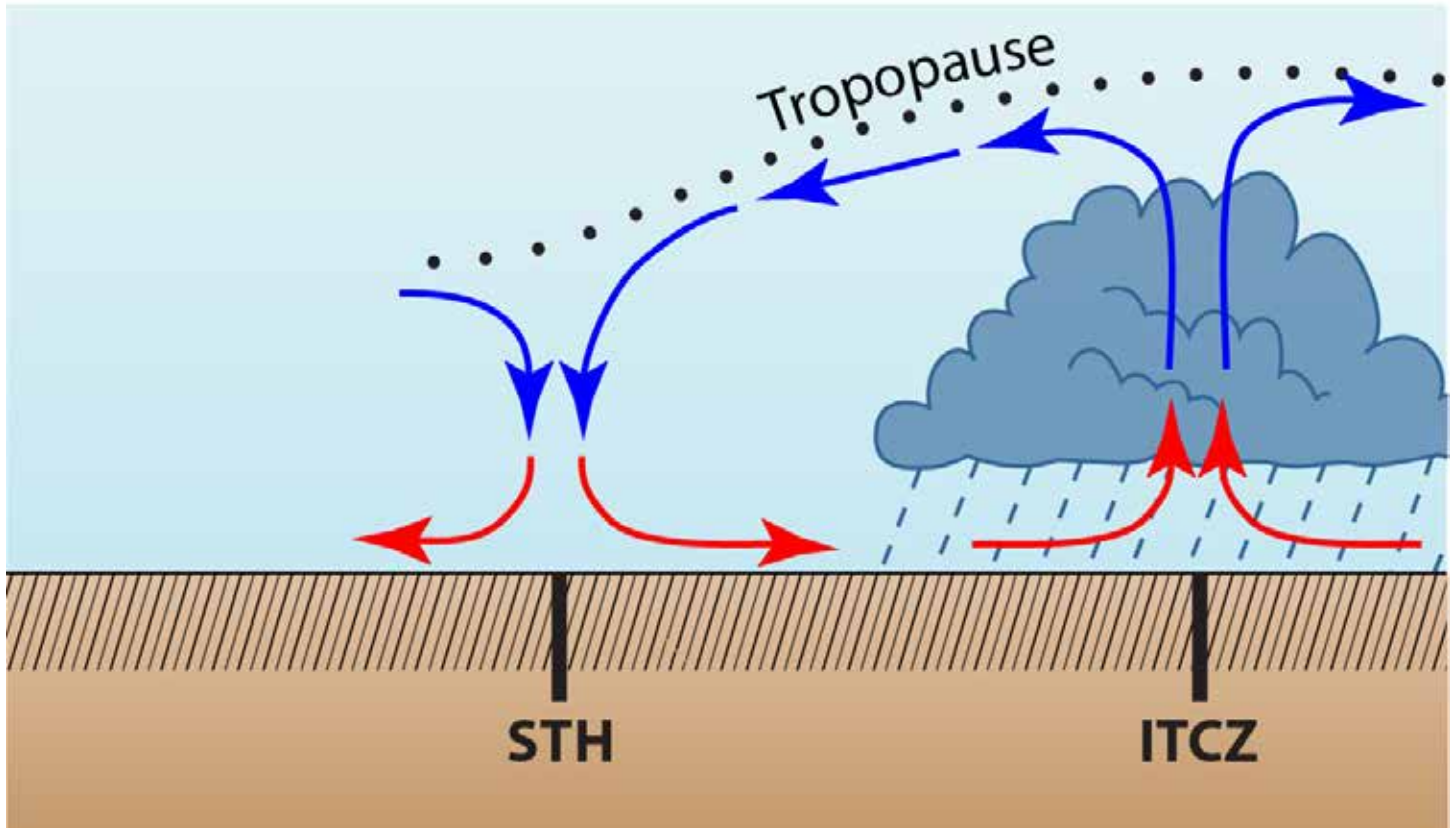


Figure 4.78b. The core of the Intertropical Convergence Zone migrates several degrees toward the south during the Northern Hemisphere winter, bringing summer rain into areas as far south as 15-25 degrees. Note that the entire Hadley cell has migrated toward the South Pole. At the same time, areas at 15-25 degrees north are under the domination of subsidence, and so are dry during several winter months. The Equatorial zone continues to receive some precipitation (Source/Credit: Dennis I. Netoff).

The distinctive zones of sparse precipitation at about 15-35 degrees latitude on the eastern side of all major ocean basins is due to the asymmetric nature of the Subtropical High (Figure 4.79). The dry climate extends to the west coasts of all continents at those latitudes, making some of them the driest deserts on Earth (e.g., the Atacama, the Sonora, the Namib). The oceanic Subtropical Highs are of the more permanent features of global pressure and they dominate the ocean basins at about 15-35 degrees latitude in the north and south Atlantic, the north and south Pacific, and the Indian Ocean Basins. The Westerly winds blow from their poleward side and the Trades from their equatorial side in both hemispheres. Stronger subsidence on the eastern side of the Subtropical High (west side of continents) plus the stabilizing influence of the cold ocean currents explains the large areas of sparse precipitation at those latitudes. On the other hand, the air along the western side of the Subtropical High (eastern side of continents, such as the southeastern part of the United States) experiences uplift and is de-stabilized by passage over a warm ocean current, so is wet.

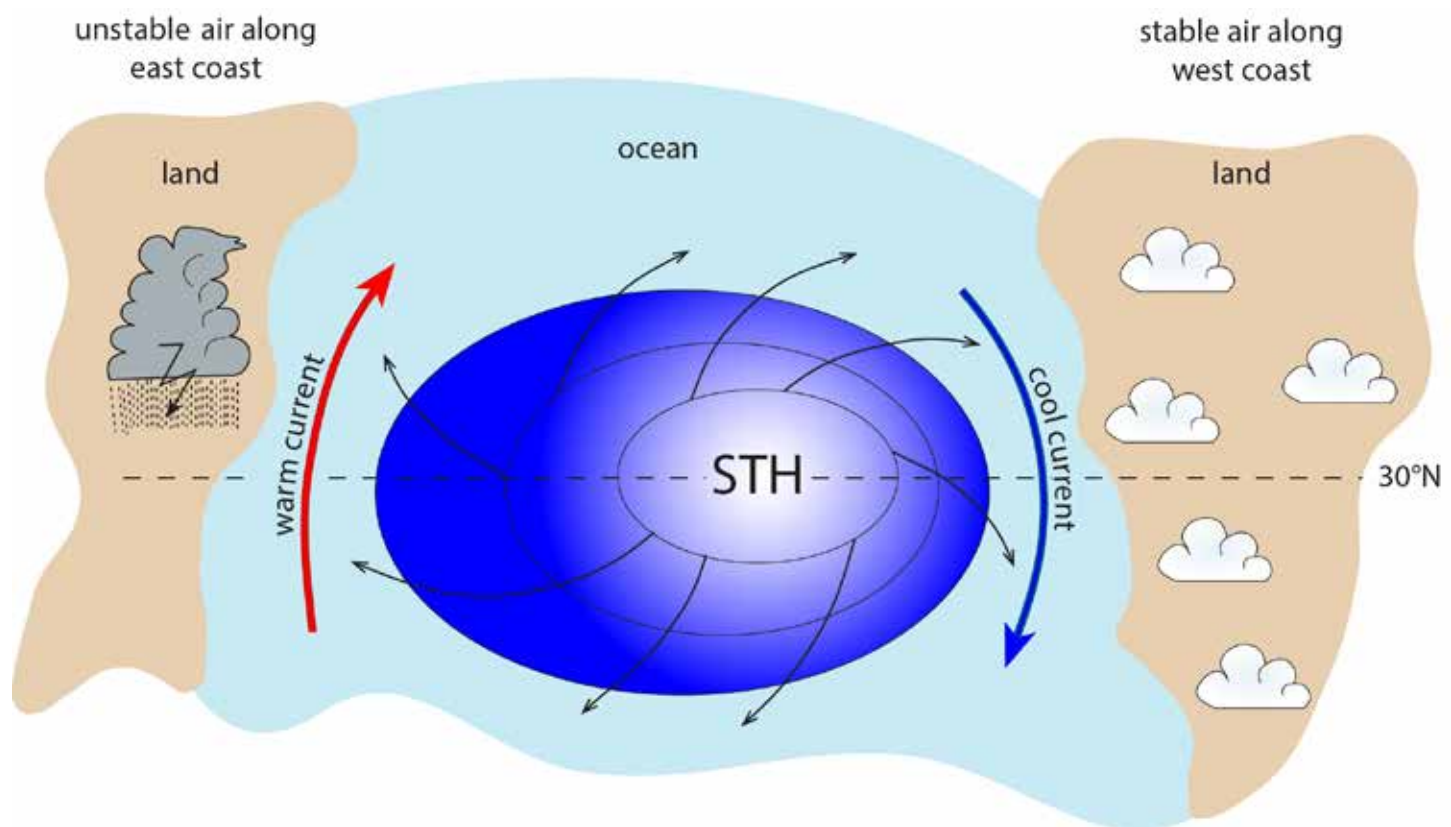


Figure 4.79. One of the more permanent features of global pressure in the existence of quasi-permanent oceanic Subtropical Highs over the major ocean basins. They dominate the ocean basins at about 15-35 degrees latitude in the north and south Atlantic, the north and south Pacific, and the Indian Ocean Basins. The Westerly winds blow from their poleward side and the Trades from their equatorial side in both hemispheres. Stronger subsidence on the eastern side of the Subtropical High (west side of continents) plus the stabilizing influence of the cold ocean currents explains the large areas of sparse precipitation at those latitudes. On the other hand, the air along the western side of the Subtropical High experiences uplift and is de-stabilized by passage over a warm ocean current, so is wet (Source/Credit: modified from Dennis I. Netoff and Ava Fujimoto-Strait, *Weather & Climate Lab Manual*).

Many of the wetter climates in the middle latitudes owe their precipitation to a combination of frequent frontal cyclones, mainly during the winter, monsoonal influences during the summer, and convective activity associated with thunderstorms and tropical cyclones (Figure 4.80). Precipitation may be enhanced by mountain barriers at these latitudes, such as the Appalachians and the Himalaya. Narrow coastal strips of heavy precipitation in places such as Norway, southern Chile, the Pacific Northwest, Columbia, and New Zealand are explained by a combination of frequent frontal cyclones, with orographic (mountain barrier) enhancement (Figure 4.81).

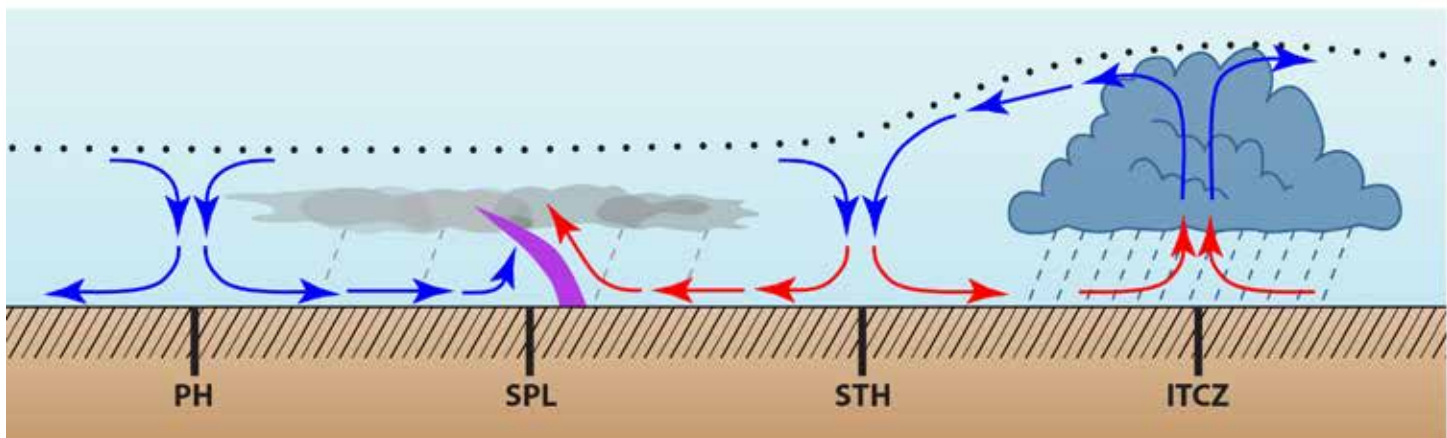


Figure 4.80. A mid-latitude belt of precipitation tends to be associated with frontal-cyclonic storms (here labeled SPL, Subpolar Low). The belt of storminess and precipitation migrates equatorward during the winter and poleward during the summer in respective hemispheres.

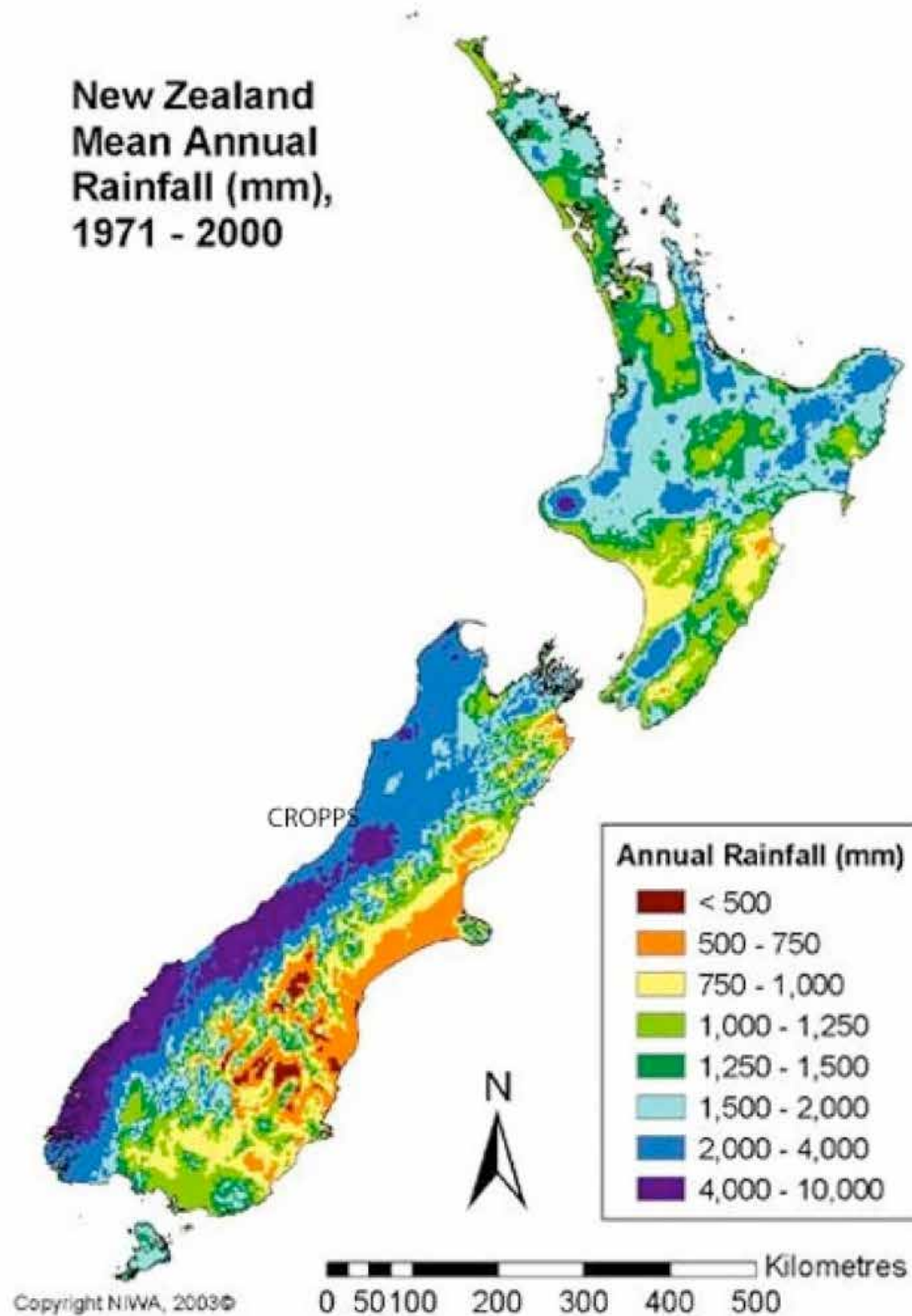


Figure 4.81. The huge amount of rainfall on western side of South Island, New Zealand is due to the combination of frontal-cyclonic activity and mountain barriers. This includes some of the wettest areas on Earth, with over 400 inches of liquid-equivalent rainfall per year (Source/Credit: New Zealand National Institute of Water and Atmospheric Research, NIWA).

Sparse precipitation in continental interiors (Eurasia, North America, and Australia) and the ice caps of Greenland and Antarctica are due to a combination of seasonal or permanent high pressure, being on the leeward side of mountain barriers, and frigid temperatures. The arid and semi-arid regions of the Tibetan Plateau, for example, are due to the Himalaya blocking moisture sources from the south, and to the massive Siberian Anticyclone that dominates Asia for six months.



## Chapter 5

# Air Masses, Fronts and Frontal Cyclones

In the middle latitudes, day-to-day weather is quite variable, especially during the cool season. Warm spells alternate with cooler weather, then relative warmth returns. Temperatures can change tens of degrees within a few hours. Along with these temperature changes come changes in wind direction, variations in air pressure and alternating foul weather (rain, snow, drizzle, extensive cloudiness) and clear skies. Many of the foul weather events are caused by the passage of frontal cyclones, which are large, migratory pressure cells containing two or more air masses and at least one front. One of the keys to understanding mid-latitude weather changes, therefore, lies in an understanding of the characteristics, movement and life cycle of these migratory systems and the air masses they contain.

### Air Masses

#### Air Mass Characteristics

An **air mass** is a large body of air that is characterized by relatively uniform temperature and moisture characteristics over a broad geographic region near the surface of the Earth. Air masses cover tens of thousands to over a million square miles. They can cover a substantial portion of a continent. Although they cover a large area, they are fairly shallow layers of air that average only a few thousand to a few tens of thousands of feet in depth. Their uniform characteristics are derived from the area in which they form; an area known as an air mass **source region**. Source regions are ideally large areas of relatively uniform terrain that are under the domination of high pressure systems. For example, the interior plains of Canada and Siberia are good air mass source regions during the winter when high pressure dominates. The Gulf of Mexico and tropical regions of the Atlantic and Pacific are good air mass source regions for warm, moist air masses. A fundamental difference in the moisture characteristics of air masses is the result of whether they are *continental* (land) or *maritime* (oceans) in origin. Maritime air masses are typically more moist (have higher dew points) than continental air masses for a given latitude.

In order for an air mass to acquire the characteristics of its source region, it must remain quasi-stationary for a period of time (a few days). High and low latitude areas tend to be good source regions; mid-latitudes are not because they typically are the battle-ground between air masses, and hence have very changeable weather.

Temporary stagnation of surface air requires that upper level winds must be gentle for a period of days. Strong upper level winds would remove the air from a region before it had time to develop into a well-defined air mass.

High pressure systems promote the development of air masses because of their characteristic vertical and horizontal motion. Strong subsidence and surface divergence tends to promote homogeneity because the air that is sinking is relatively uniform in terms of temperature and moisture, and because its temperature changes uniformly with elevation as it subsides. Low pressure systems, on the other hand, draw in air of differing character from all directions, favoring heterogeneity (Figure 5.1).

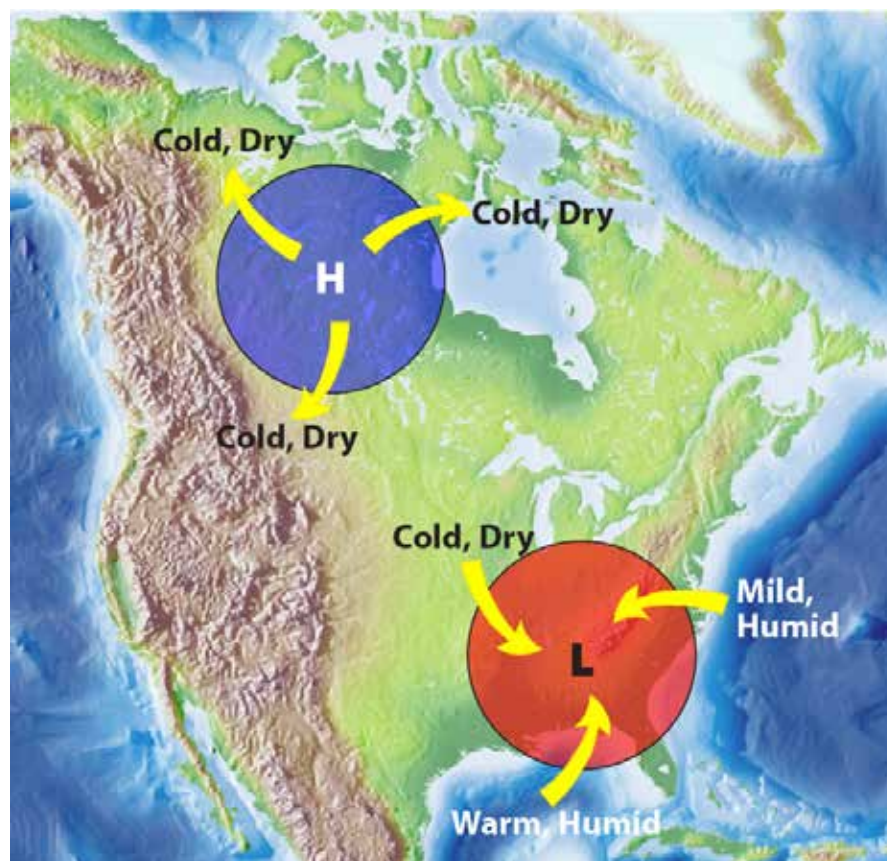


Figure 5.1. Areas of upper-level convergence and air subsidence, such as the high pressure area shown over Canada, favor the development of air masses because they promote the development of homogenous conditions. Surface divergence helps maintain homogeneity by spreading air of uniform character in all directions. Because of these factors, the humidity and temperature are uniform within the air mass at a given elevation. Areas of surface air convergence, such as that shown over the southeastern United States, are less likely to lead to air mass formation because the air that converges into a low pressure region comes from many areas that are dissimilar in terms of temperature and moisture characteristics.

Air masses can develop in low pressure areas, but the area of the low pressure must be very large and uniform in order to prevent the mixing of unlike air that is drawn toward the center of the low pressure region. The vast expanses of open ocean in the North Pacific and North Atlantic are examples of such low pressure areas capable of generating air masses.

In summary, air mass source regions are ideally:

- large
- uniform in terms of temperature and moisture
- fairly flat
- at either high or low latitudes
- characterized by light upper level winds
- high pressure areas

Once air masses acquire the characteristics of their source region, they eventually migrate to other areas, driven by local and planetary winds (Figure 5.2). Actual tracks of air masses and storms are quite variable, steered in large part by upper-level winds and pressure patterns. **Long after they move out of their source regions, however, air masses continue to retain the temperature, moisture and stability characteristics they inherited from their source region.** The source region exports air mass characteristics to other regions, sometimes thousands of miles away.

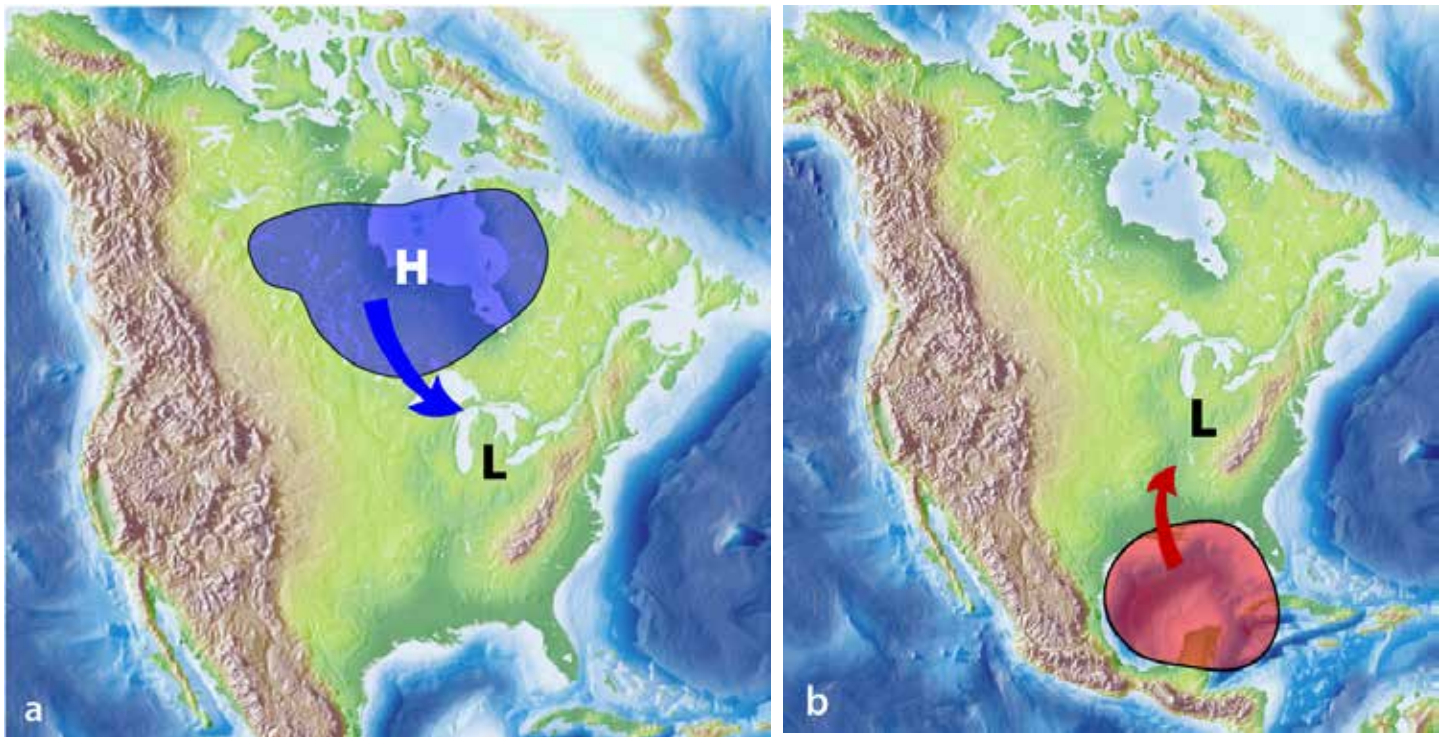


Figure 5.2a. Air flows from regions of high pressure to regions of low pressure. The cold air mass that developed over Canada moves out of a high pressure area toward the low pressure system near the Great Lakes. As it moves southward, it will bring cooler and drier air into the United States.

Figure 5.2b. A strong low pressure system associated with a major storm system acts to pull a moist air mass from the Gulf of Mexico toward it. This air mass will bring warmer and more humid conditions into the southeastern United States.

## Air Mass Classification

Air masses are classified according to their source region (Figure 5.3) as well as the modifications they undergo as they traverse foreign terrain. Important source region characteristics include temperature, moisture and stability of the air mass. The temperature and moisture characteristics are generally controlled by latitude and continental vs. maritime source. Continental air masses have lower water vapor content than marine air masses, and polar air masses are cooler than tropical air masses. In the abbreviated code for air masses, continental air masses are designated with a lower case **c**, and maritime air masses with an **m**. Polar air masses are designated with an upper case **P** and tropical ones with a **T**. Some air mass classifications use an **A** for Arctic, and an **E** for Equatorial. A third letter is abbreviated by a lower case letter that specifies its geographic origin: **g** for Gulf of Mexico, **a** for Atlantic, **p** for Pacific, **c** for Canadian and **s** for Sonoran. Air masses are sometimes given a fourth and fifth letter if sufficient information is available — **w** means that the air mass is warmer than the surface that it overlies, and **k** means that it is colder. If environmental lapse rates and zones of upper-level convergence and divergence are also known, the air mass may be designated **s** if conditions are stable, and **u** if they are unstable. These last two lower case letters help in determining whether extensive cloudiness is likely to develop, and what types of clouds may develop, as well as whether there is potential for abundant precipitation.

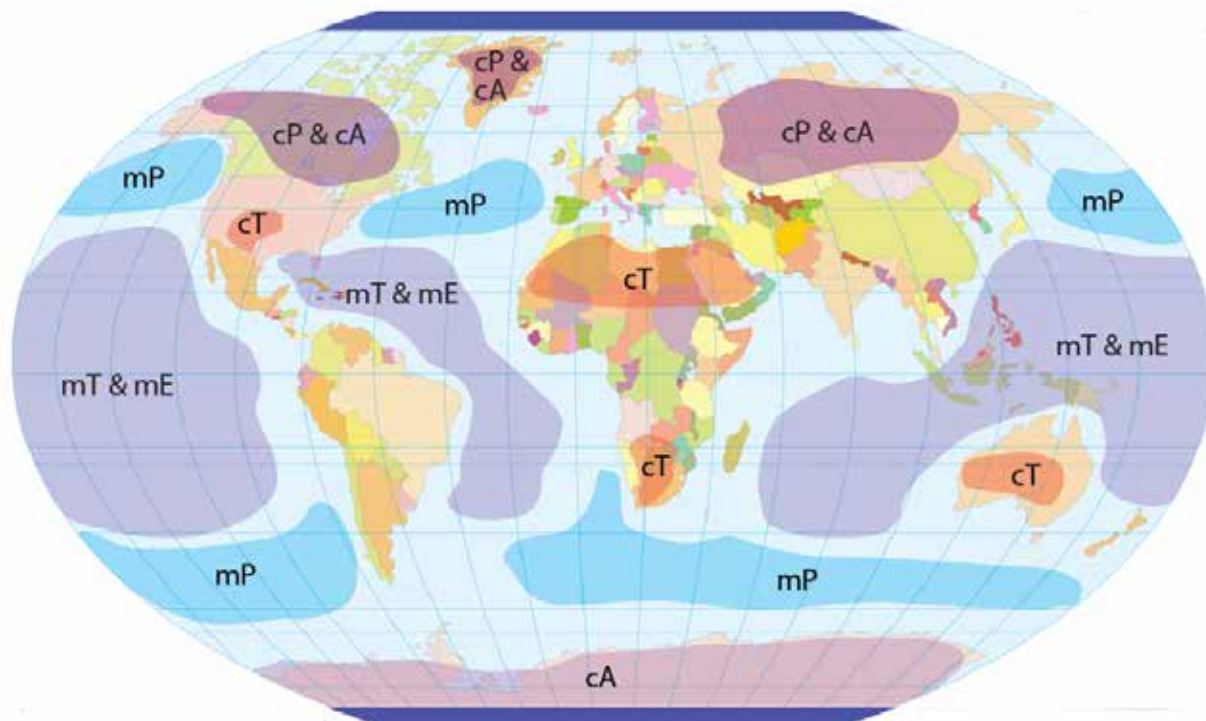


Figure 5.3. Generalized global map of air mass source regions. The first letter is lower case, and defines relatively moist air masses (*m* = maritime) versus drier air masses (*c* = continental). A second upper case letter defines warmer air masses (*T* = tropical) versus cooler air masses (*P* = polar). For example, an air mass forming over the Gulf of Mexico would be designated as a *mT* air mass (*m* = maritime, *T* = tropical). Some air mass classifications recognize Arctic source regions (*cA*), and Equatorial source regions (*mE*) (Source/Credit: [https://commons.wikimedia.org/wiki/Maps\\_of\\_the\\_world#/media/File:Eckert4.jpg](https://commons.wikimedia.org/wiki/Maps_of_the_world#/media/File:Eckert4.jpg)).

## ***Air Mass Modifications***

As air masses are carried away from their source regions by regional airflow patterns, they move into areas that differ from their source regions in terms of temperature and moisture conditions. As a result, the air mass begins to change its nature and eventually loses its original identity. For example, as a polar air mass from Canada (cPc air mass) travels into the southern United States, it is warmed and its humidity increases as moisture evaporates from the ground and into the air mass.

**Lake effect snow** provides an example of a much more rapid air mass modification. Lake effect snows are fairly common during the late fall and early winter, when polar air becomes frigid, but large water bodies such as the Great Lakes remain relatively warm (considerably above freezing). As the cold, dry, stable air from its cPc source region travels southward over Lakes Superior, Michigan and others, clouds form immediately as the air mass is warmed rapidly from the lake water (Figure 5.4a). As the moisture content (illustrated by the dew point) begins to rise, clouds thicken, and eventually snow may begin to fall (Figure 5.4b). A five letter air classification of the continental Polar Canadian air mass would be cPcku, the k indicates that the air mass is colder than the lake temperature and the u indicates that the air is becoming unstable from being heated from below as well as having moisture added to it.

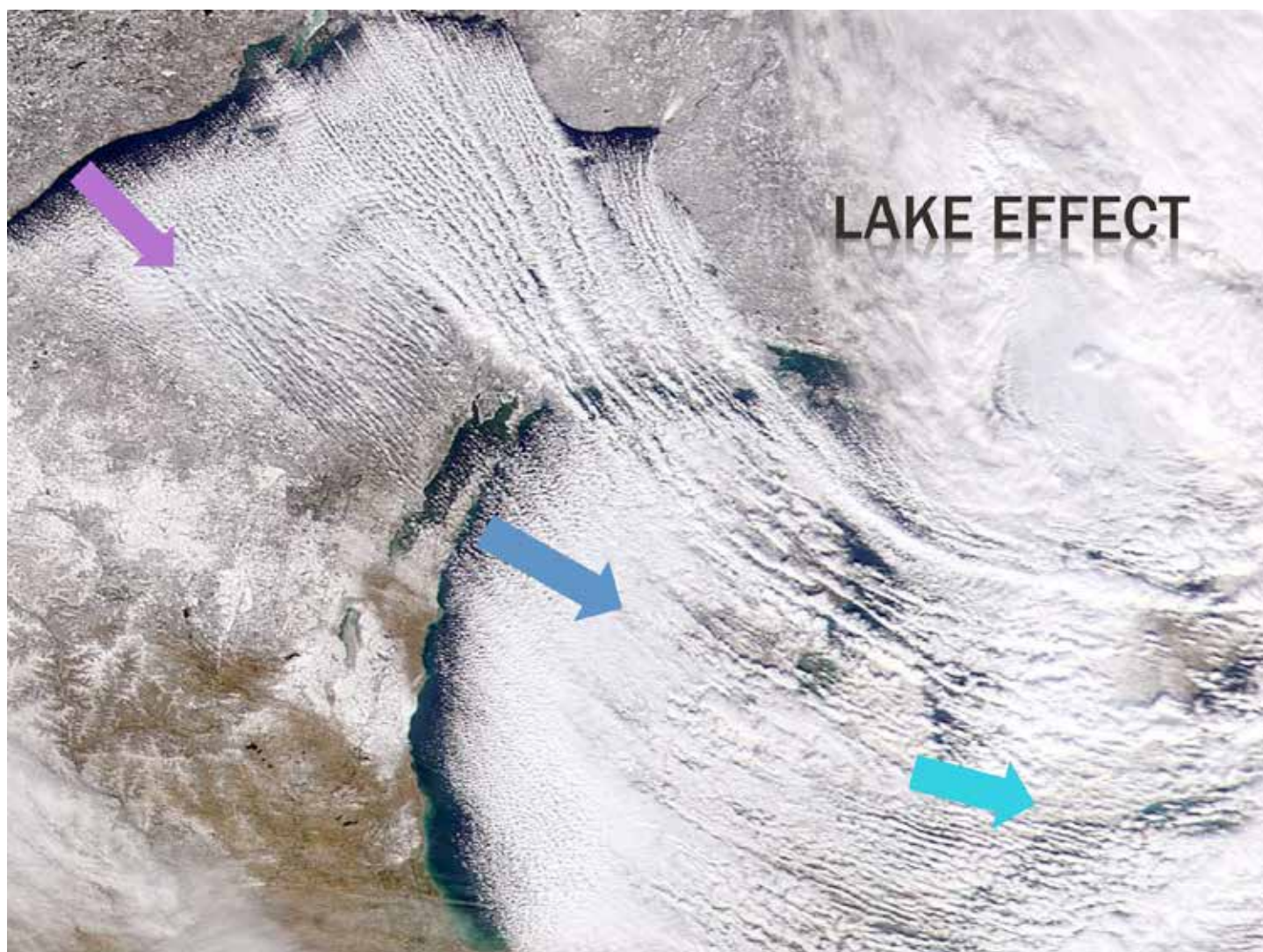


Figure 5.4a. Lake effect clouds and snow forming over the Great Lakes as a cPc air mass moves southeastward on December 5, 2000 (Source/Credit: NASA's SeaWiFS satellite).

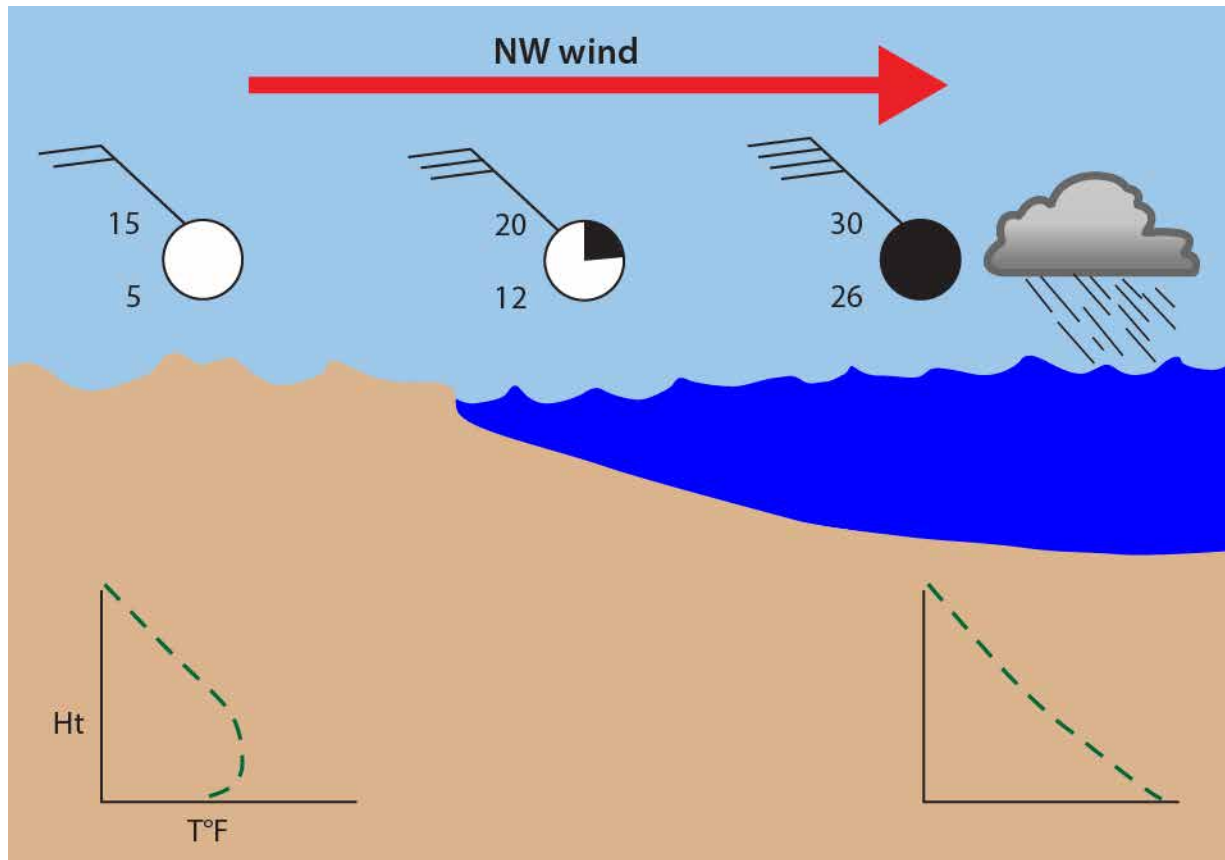


Figure 5.4b. Schematic cross-section of Lake Effect clouds and snow forming over Lake Superior. Some of the pertinent air mass modifications include: (1) an increase in temperature from 15-to-20-to 30°F within 100 or so miles, (2) increases in dew point (moisture content) from 5-to-12-to 26°F, (3) an increase in cloudiness from 0% to 100%, (4) Lake Effect snow, (5) an increase in wind velocity due to a reduction in frictional resistance, and a change from an inverted lapse rate (green dashed line, left) to a more normal lapse rate (green dashed line, right).

The rate and amount of such air modifications depends upon:

- **Speed of Motion.** The faster it moves into areas different from its source region, the more rapidly it changes.
- **Distance of Travel.** The further it travels from its source region, the more different it will become because the nature of the region into which it travels will become more different.
- **Dissimilarity of Areas Traveled Over.** The greater the difference between the source region and area traveled over, the more rapidly the air mass will lose its identity.



A more subtle example of air mass modification is illustrated by a cPc air mass invading the southern Great Plains in December 1990 (Figure 5.5). A five letter classification of the air mass at Lubbock or Midland would be cPcs, the s for stable air, indicated by stratiform clouds and fog.

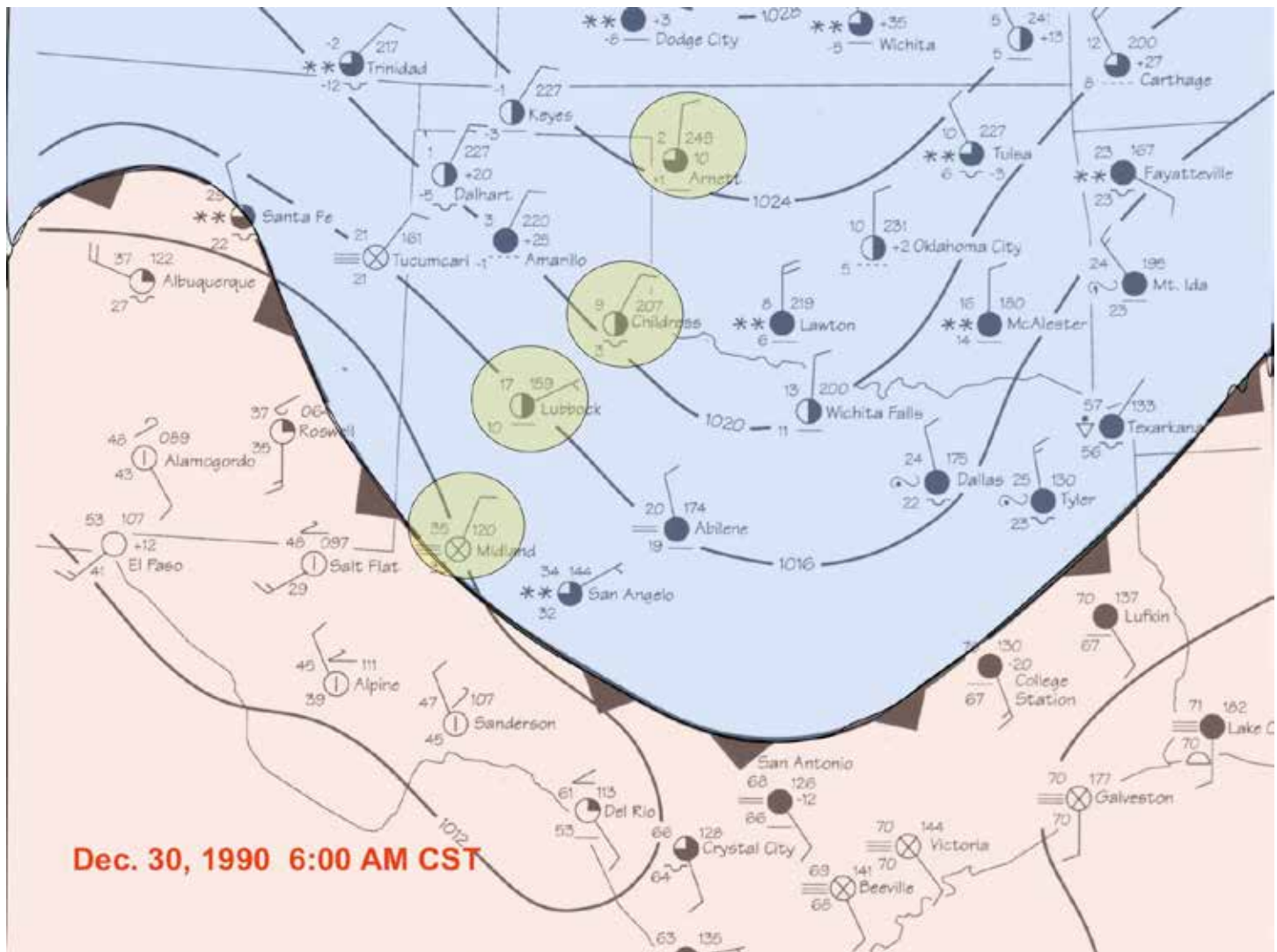


Figure 5.5. Modifications of a cPc air mass that is surging southward over Texas and Oklahoma on December 30, 1990. Areas in blue are under the domination of cPc air, whereas areas in pink are under mTg (maritime Tropical Gulf of Mexico) air. The zone of contact separating the two air masses is delineated by a cold front symbol (triangle linked with a solid line). Note the changes in air temperature from Arnett, Oklahoma to Midland, Texas (2°, 9°, 17°, 35°), and the changes in dew point (minus 1°, 3°, 10°, 33°). One of the results of these air mass modifications is the formation of fog in Midland, Texas (Source/Credit: modified from Dennis I Netoff and Ava Fujimoto-Strait, *Weather & Climate Lab Manual*, 2015).

## North American Air Masses

### Continental Tropical Sonoran Air Masses (cTs)

These are dry and warm-to hot air masses that form over subtropical desert and plateau regions of Mexico and the southwestern United States (Figures 5.6 and 5.7). These air masses often influence west Texas, and occasionally bring warm, dry weather well into the Great Plains states. Collision with Gulf of Mexico air masses (mTg) can develop the Texas **dry line**, which can cause severe weather (Figure 5.8).

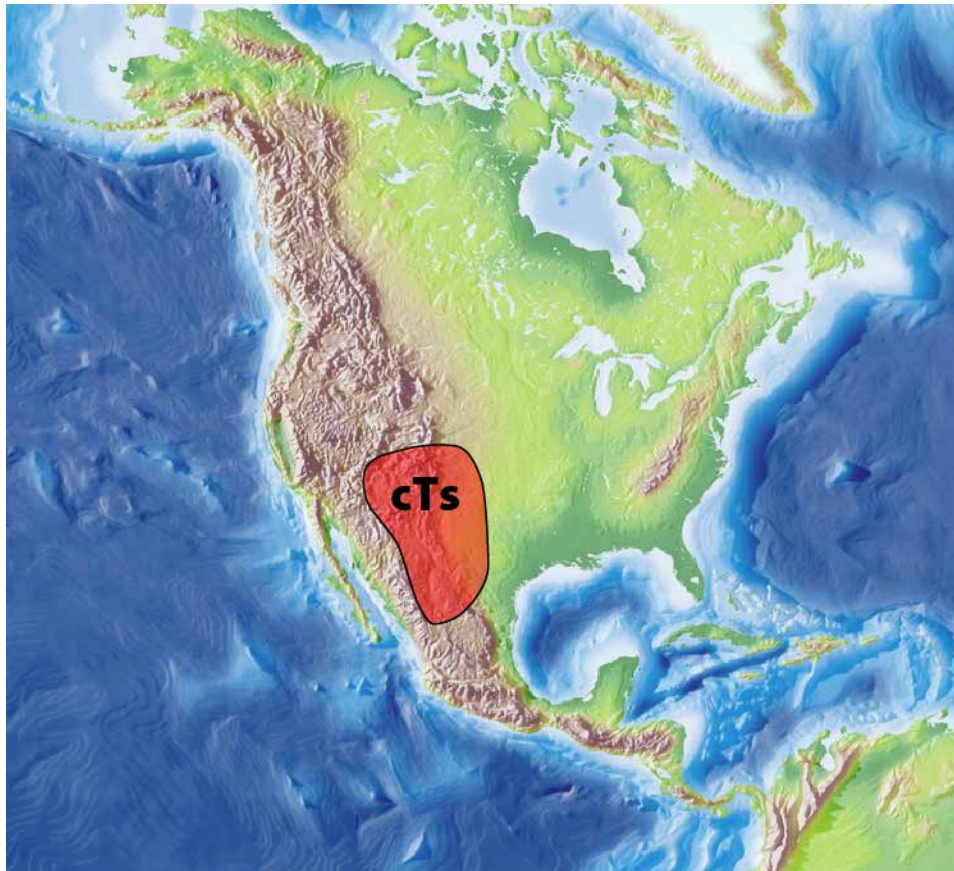


Figure 5.6. The deserts of northern Mexico and the southwestern United States are the source regions of cTs air masses.



Figure 5.7. The boojum “forest” of the Sonoran Desert in Mexico. Cloudless skies, subsiding air and extensive bare soil/rock with low moisture content make the desert area an ideal source region for warm and dry air masses (Credit/Source: Dennis I. Netoff).

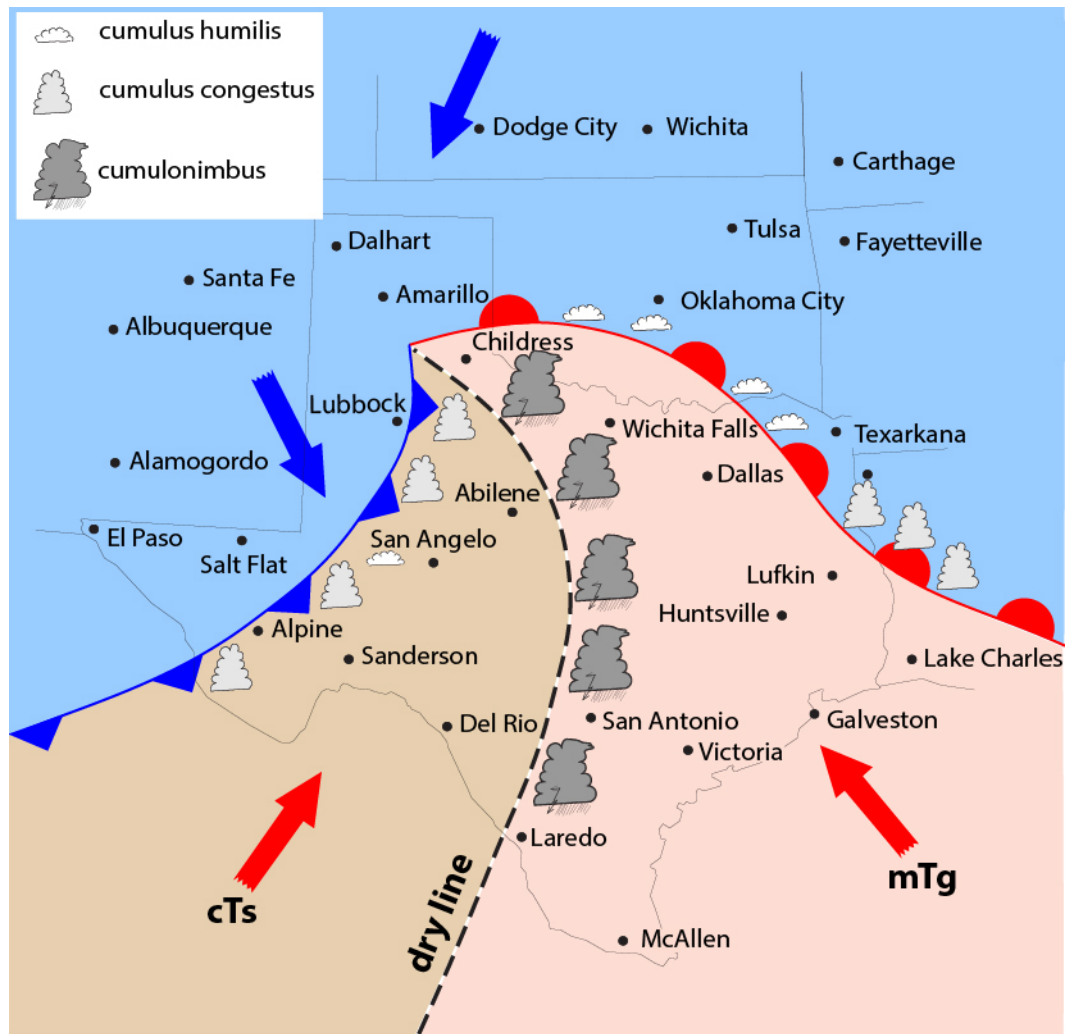


Figure 5.8. The conditions that give rise to a Texas dry line are illustrated in this diagram. Dry lines develop as warm, DRY air from northern Mexico (cTs) collides with warm MOIST air from the Gulf of Mexico (mTg). Because moist air weighs less than dry air, the moist air will rise upward and produce thunderstorms, some of which can be severe (Source/Credit: modified from Dennis I. Netoff and Ava Fujimoto-Strait, *Weather & Climate Lab Manual*, 2015).

Air masses from cTs source regions can bring incursions of warm, dry air into southeast Texas for brief periods of time, typically during the warmer months. Dewpoints and relative humidities within cTs air masses can drop down into the single digits. For example, on April 26, 2011, afternoon temperatures in Sanderson (west Texas) were in the upper 90s, whereas the dewpoint was 18°F and the relative humidity 5%. Not far to the east, near Rock Springs, the temperature, dewpoint and relative humidities were 98°, 67° and 37%, respectively (Figure 5.9).

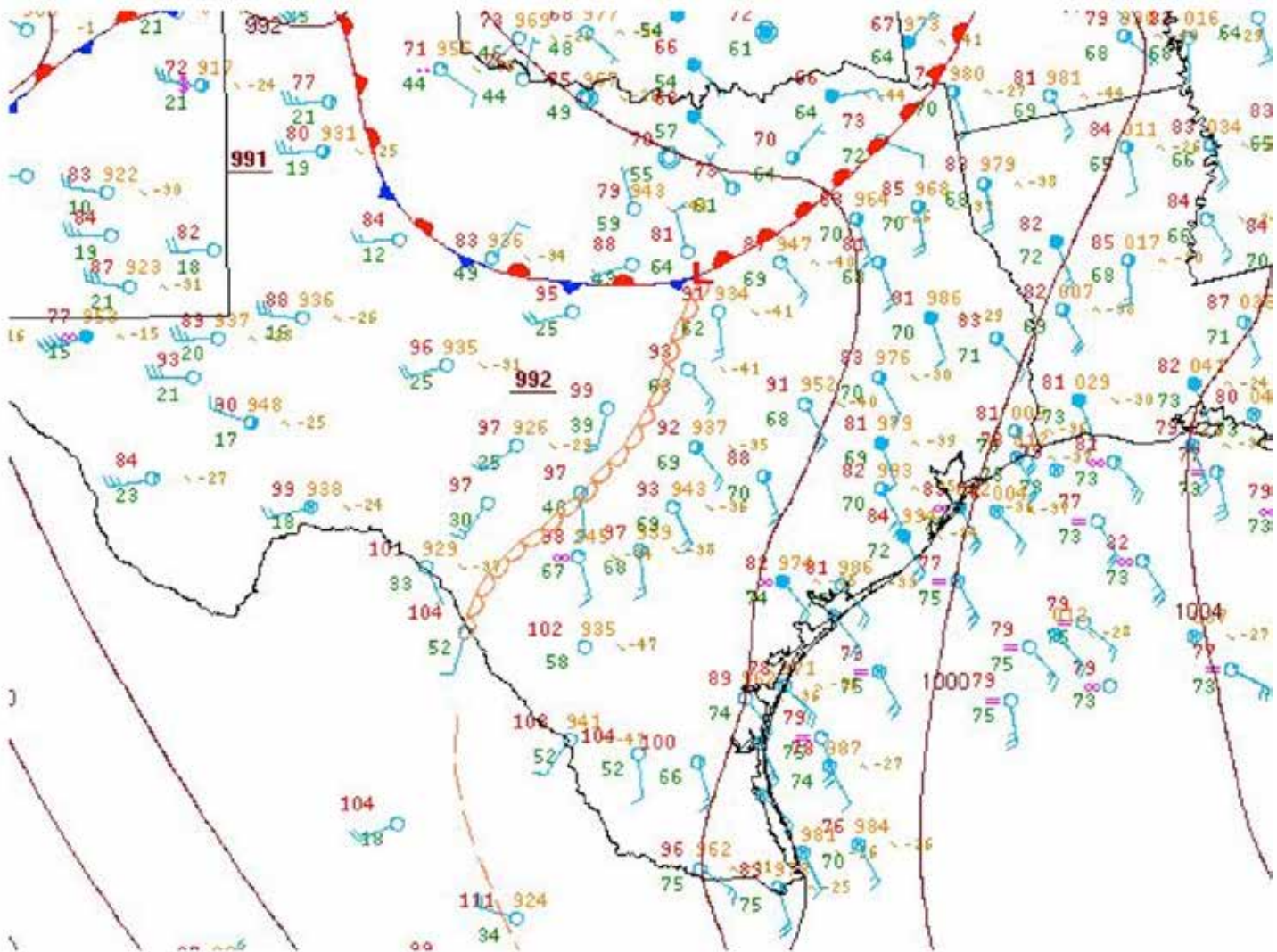


Figure 5.9. A dry line (small half-circles in light brown) in central-west Texas separates a cTs air mass to the west of the dry line from an mTg air mass in southeast Texas on April 26, 2011. Note the similarities in air temperature on either side of the dry line, but the very low dewpoints to the west of the dry line (source/credit: National Weather Service).

## Maritime Polar Pacific Air Masses (mPp)

Maritime Polar Pacific (mPp) air masses tend to be moist and cool to cold, depending on the season. They commonly form in areas of low pressure near the Aleutian Islands, and therefore typically bring overcast, drizzly, rainy or snowy conditions. Air mass temperatures are relatively mild for high latitudes because the ocean surface seldom freezes in the Gulf of Alaska. Notable exceptions occur when Siberian air over Russia travels over the Gulf of Alaska during the winter and early spring, bringing sub-freezing temperatures to vast ocean areas and creating misery for ocean-going vessels. Eventually they change their identity from Siberian air to cold maritime air.

Some of the most impressive extratropical storms on Earth occur in the North Pacific Ocean. The centers of some of these storms have central pressures that rival strong hurricanes and display a series of nearly-perfect concentric circles that also mimic the pattern of strong hurricanes (Figure 5.10). Examples include the “monster storms” of 2014, twice in 2015, and perhaps the most intense of all, 1977.



Figure 5.10. Remnants of super typhoon Nuri still had many of the characteristics of a tropical cyclone (intense, circular cyclonic winds) on November 8, 2014, even though it had lost its warm core and was at a high latitude of 54.87°N (Source/Credit: NWS GFS/NCEP).

Some of the most powerful North Pacific storms on record are remnants of exceptionally strong tropical cyclones (super typhoons in the Pacific Basin). Remnants of former typhoon Champi still had sustained winds of 81 mph (130 kph) well into the Gulf of Alaska in late October of 2015 (Figure 5.11). Super typhoon Nuri reached near-peak intensity on November 3, 2014 (Figure 5.12). Nuri was the most intense tropical cyclone worldwide in 2014, developing a central pressure of 910 millibars with sustained 1-minute winds of 180 mph (285 kph).

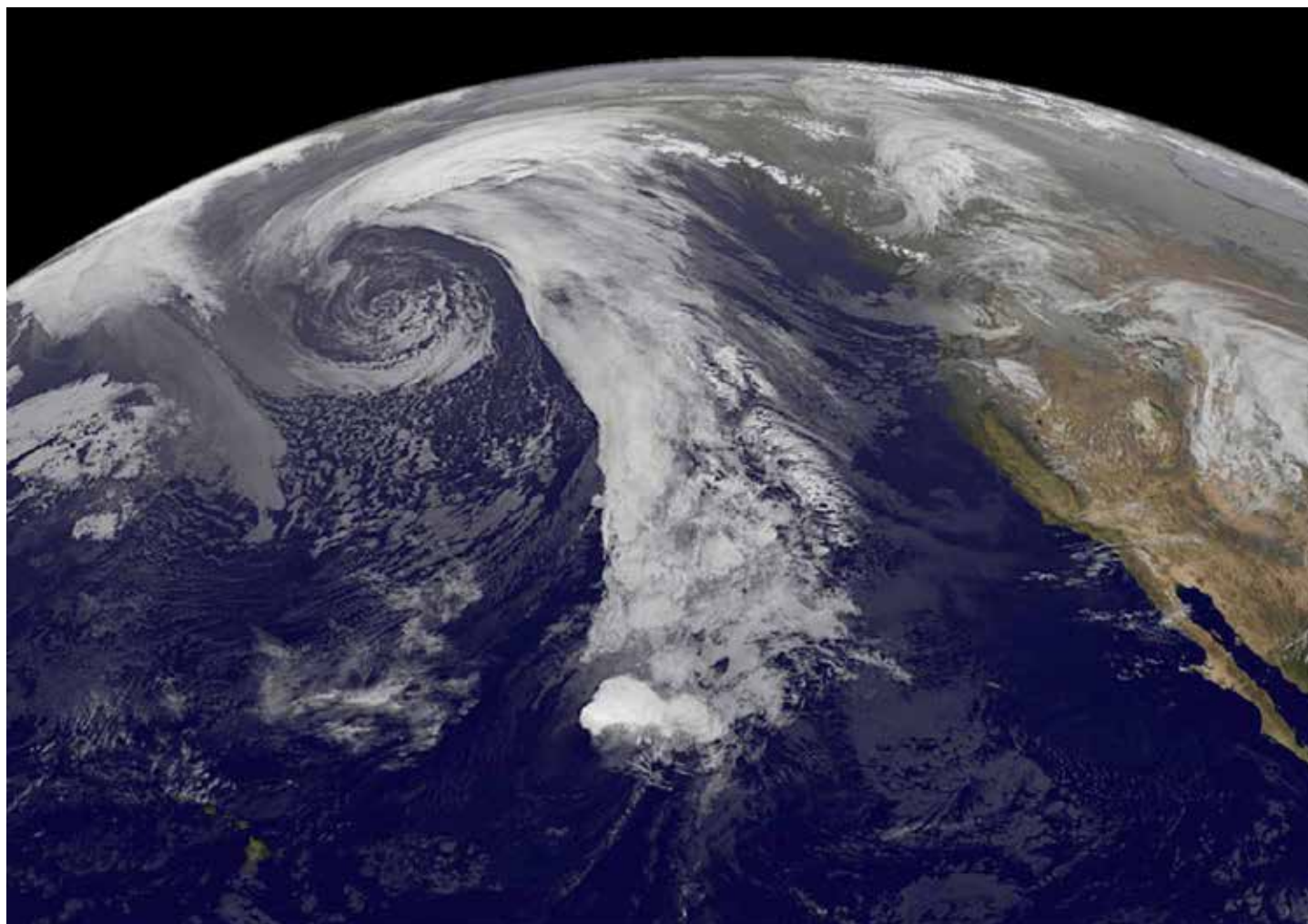


Figure 5.11. Remnants of former typhoon Champi on October 26, 2015, taken from the International Space Station. Although the storm by this time had lost most of its tropical characteristics, it still packed a lot of energy, with sustained winds of 81 mph (130 kph), and widespread precipitation (Source/Credit: Rapidscat, ISS).

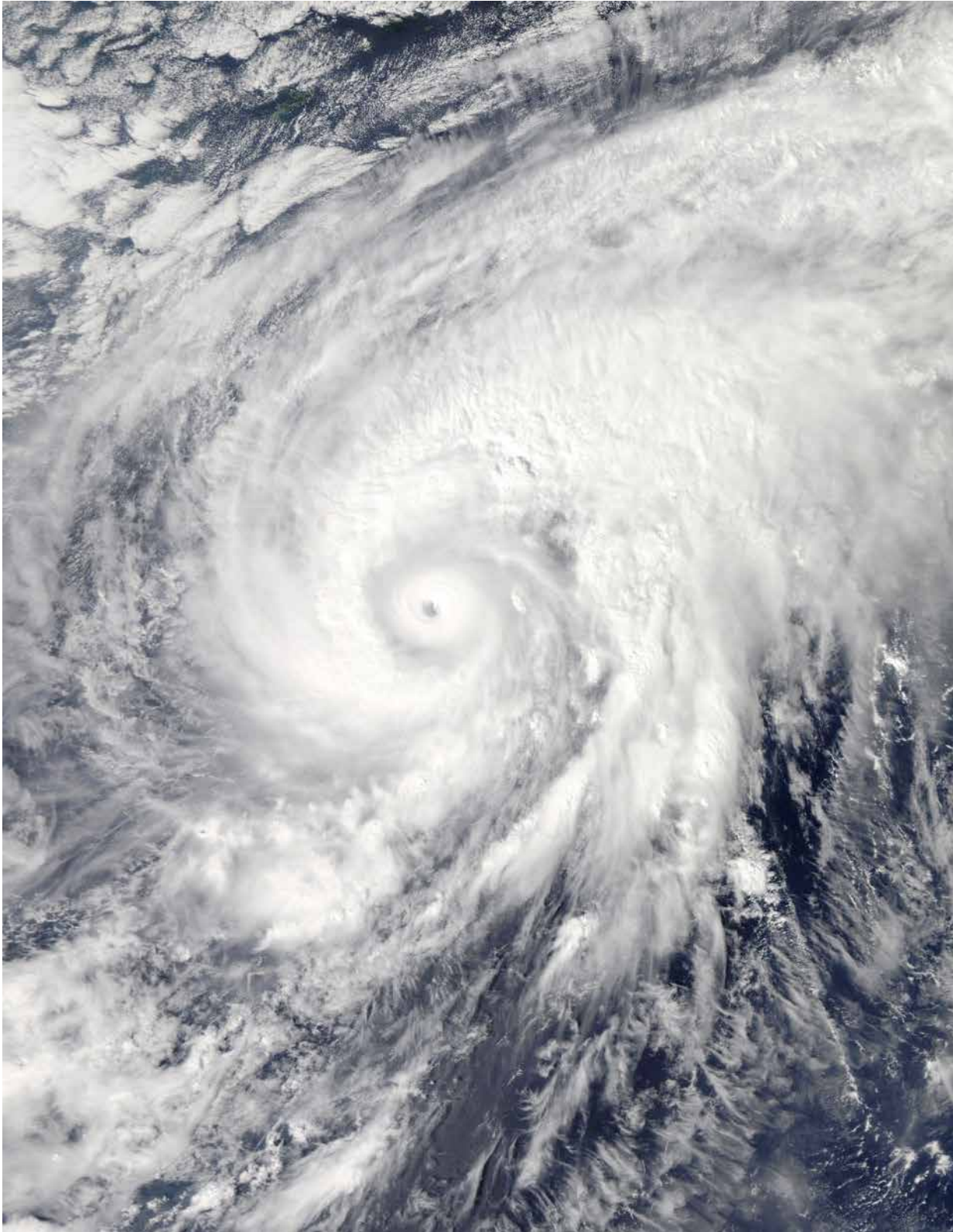


Figure 5.12. Typhoon Nuri at near-peak intensity on November 3, 2014. Nuri was the most intense tropical cyclone worldwide in 2014 developing a central pressure of 910 mb with sustained 1-minute winds of 180 mph (285 kph). As remnants of Nuri drifted northward into the North Pacific Ocean, it became one of the most intense extratropical cyclones ever recorded just 5 days after this image was taken (Source/Credit: NASA/GSFC/Earth Science Data and Information System).



The remnants of super-typhoon Nuri quickly traveled northward into the Bering Sea by November 7, 2014 (Figures 5.13a, 5.13b and 5.13c). The huge storm rocked the Bering Sea and shoreline. The lowest measured pressure was just under 930 millibars by a buoy at sea not far from the core of the storm on November 8th. Estimates of core pressure are 924 millibars (Hurricane Katrina made landfall with a pressure of 920 mb). On November 7th, the same buoy measured a pressure drop of 37.3 millibars in 6 hours. There was a widespread area of storm-strength winds (>57.5 mph, 93 kph) on November 8, 2014. On that date the pattern of closed, cyclonic isobars was approximately 1000 miles (1600 km) in diameter.

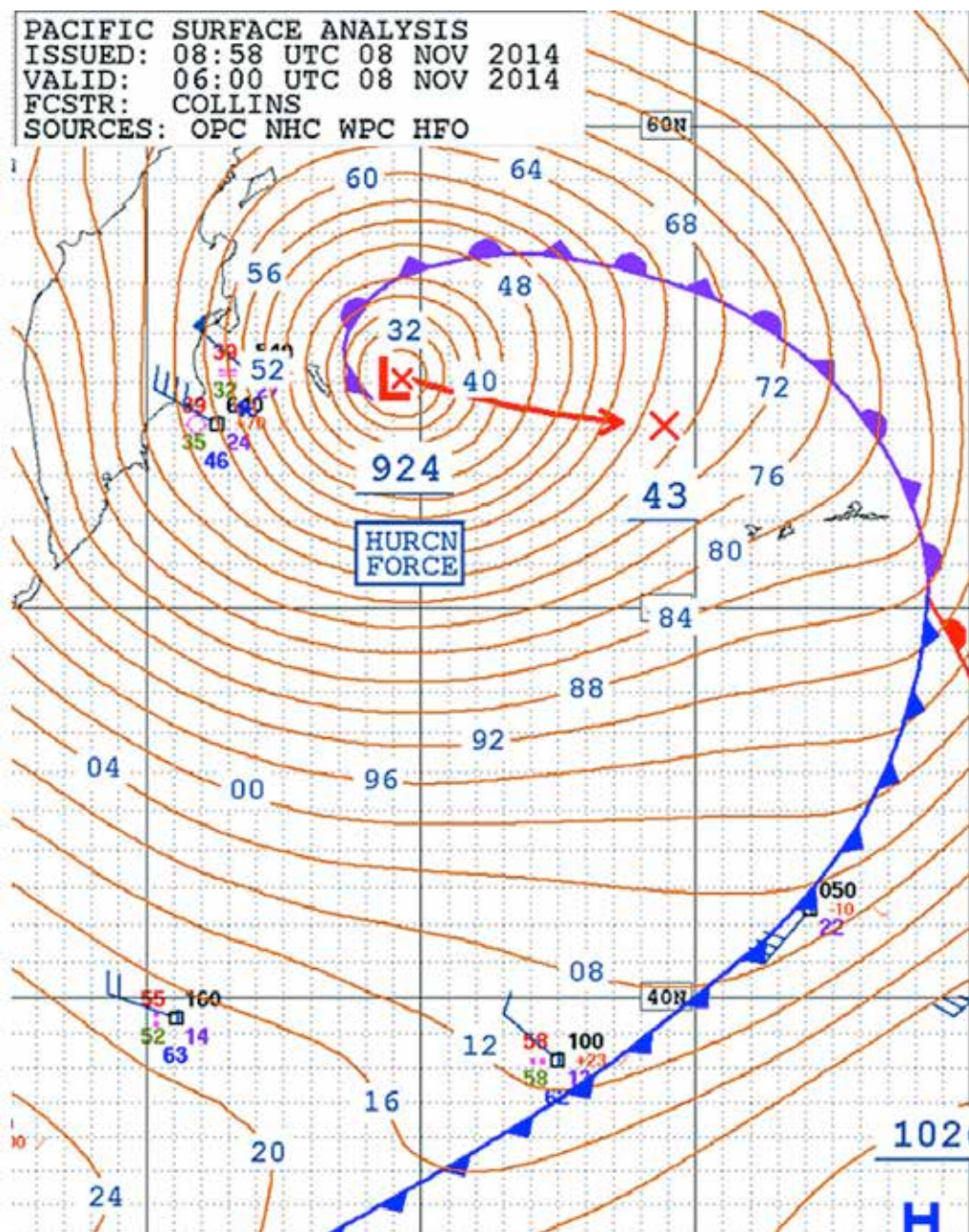


Figure 5.13a. Detailed surface map of the Bering Sea storm on November 8, 2014, when former Nuri was probably near peak intensity as an extratropical storm. Note the core pressure is estimated at 924 millibars. Parallels and meridians are spaced 10 degrees apart, so the parallels are roughly 690 miles apart (Source/Credit: OPC, NWS).

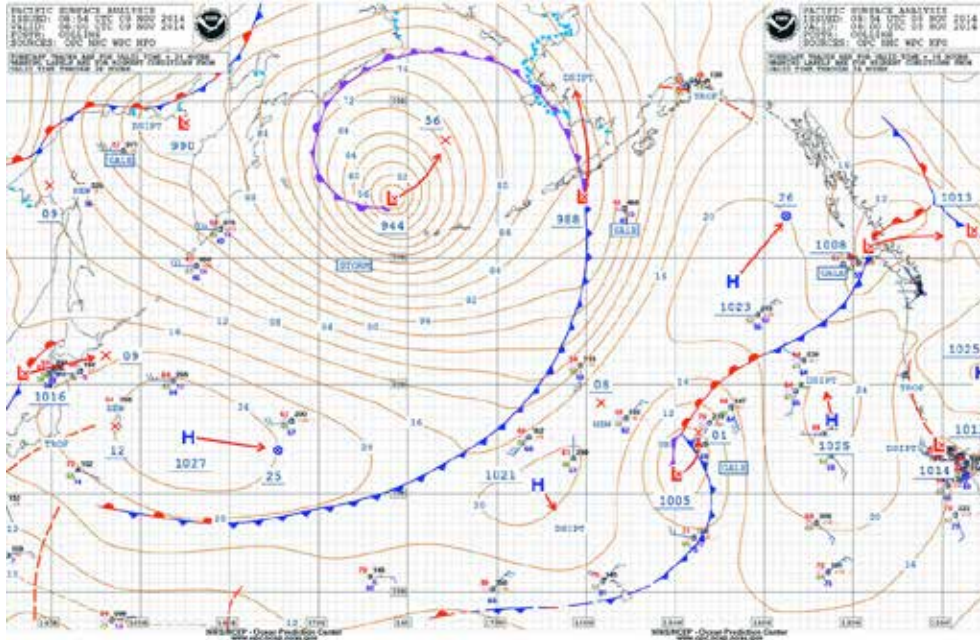


Figure 5.13b. Surface map showing the giant storm the following day (note change in scale). The storm had begun to lose intensity (fewer closed isobars), and the core pressure was now estimated to be 944 millibars. The length of the occluded front, cold front, and stationary front extending from the core to the periphery of the system measures roughly 5000 miles (8046 km), or the straight-line distance from Houston, Texas to Paris, France (Source/Credit: OPC, NWS).

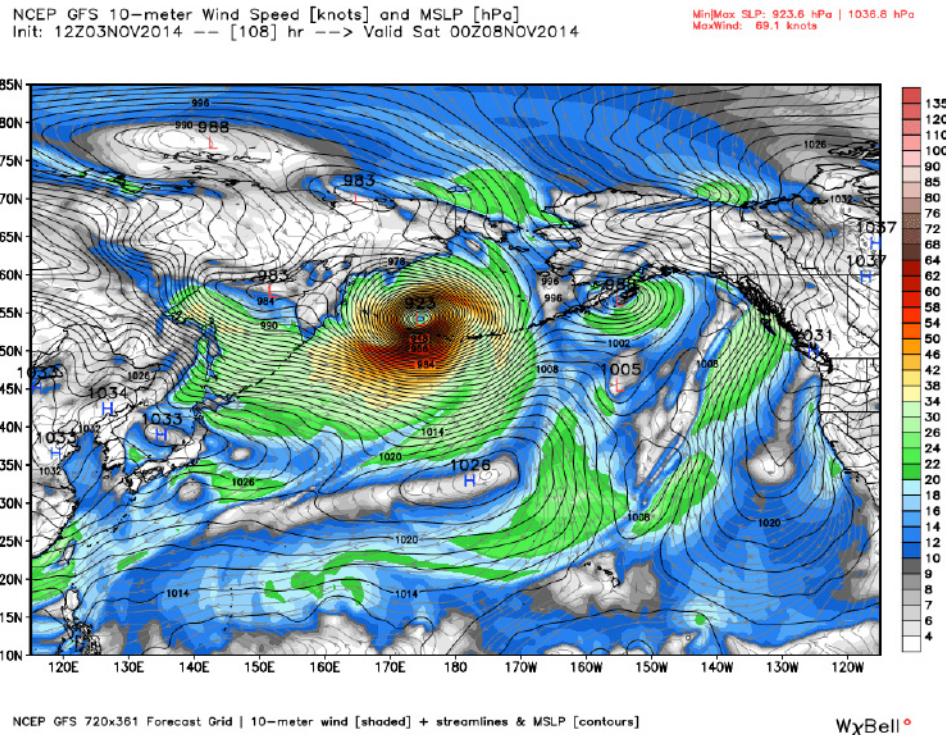


Figure 5.13c. GFS model forecast of surface pressures and winds when extratropical cyclone Nuri was expected to reach peak intensity on Friday evening November 7, 2014. Note the hurricane-like pressure field and the large area of high-velocity winds, represented by reds and browns. Browns indicate wind velocities of 64-80 knots (74-93 kph). Each increment of 5 degrees in latitude is roughly 345 miles, or 555 km (Source/Credit: NCEP).

Another powerful winter cyclone tore into the Aleutian Islands in mid-December 2015 (Figures 5.14a and 5.14b). The massive storm also had a surface isobaric pattern similar to tropical hurricanes. On December 13 the central pressure was estimated at 924 millibars. The lowest pressure directly observed at a fixed airport-based observation site was 938.9 millibars from the Adak Airport on Adak Island in the western Aleutians on Saturday, December 12. On December 16, there were sustained winds of 94 mph (151 kph) and gusts to 122 mph (196 kph). Hurricane-force winds caused 40-foot waves in the Bering Sea, although the Ocean Prediction Center estimated some waves at 63 feet. Central pressure dropped nearly 50 millibars in just 24 hours. Meteorologists refer to storms with a pressure drop over 24 millibars in 24 hours as *bomb cyclones*.

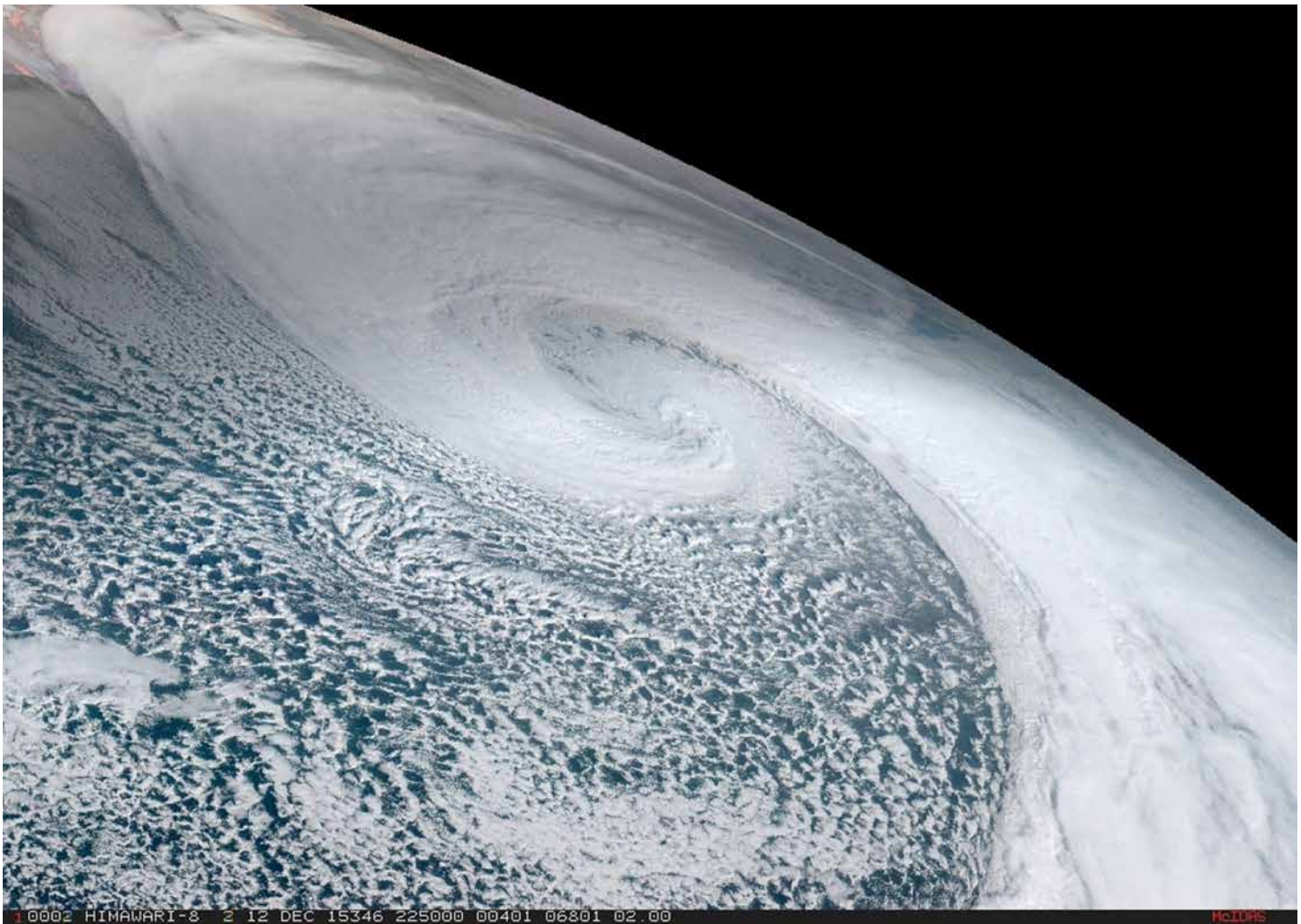


Figure 5.14a. Visible satellite image of the Bering Sea storm of mid-December 2015, three days after maximum intensity had been reached. The center of cyclonic circulation appears like a scorpion tail. Low, scattered water-vapor clouds dominate the southwestern sector of the storm. Higher, ice-crystal clouds are a more uniform white (Source/Credit: Japanese Meteorological Agency Himawari-8).

Some North Pacific storms, guided by upper-level flow patterns, travel far from their source, and many influence the conterminous United States. Prolonged periods of rainy weather over the Pacific Northwest during the winter are commonly caused by mPp air masses. About every five to seven days during the winter season, a new mPp air mass makes its way into the Pacific Northwest (Figures 5.15 and 5.16).

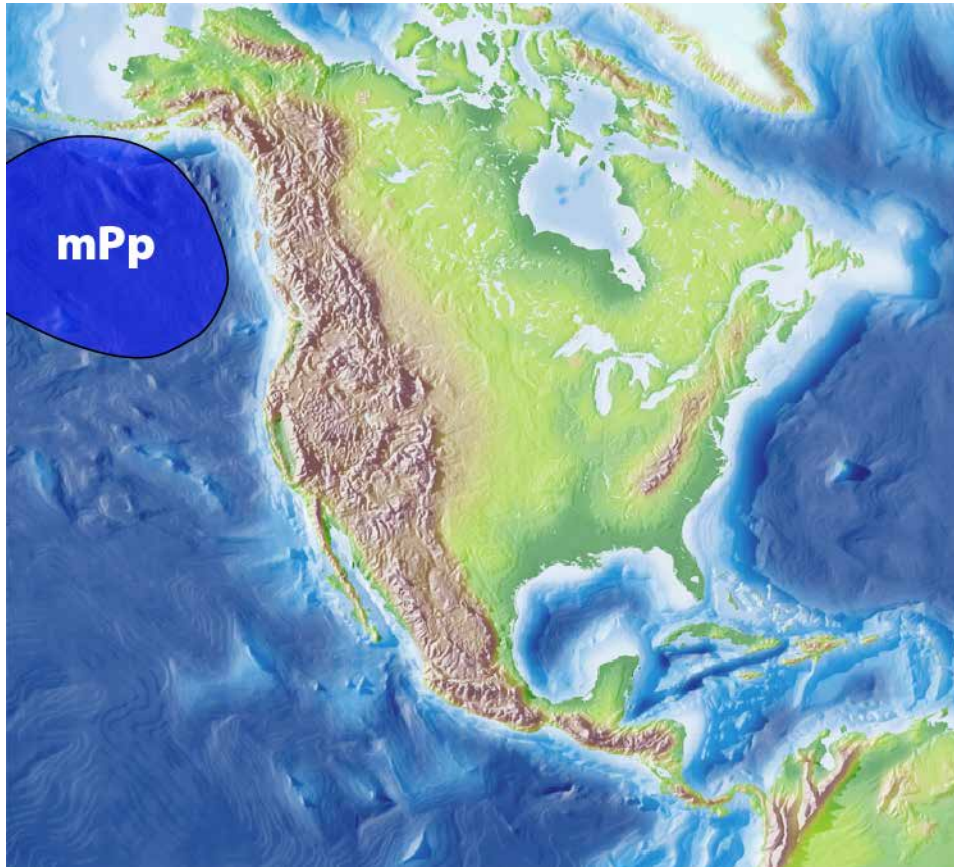
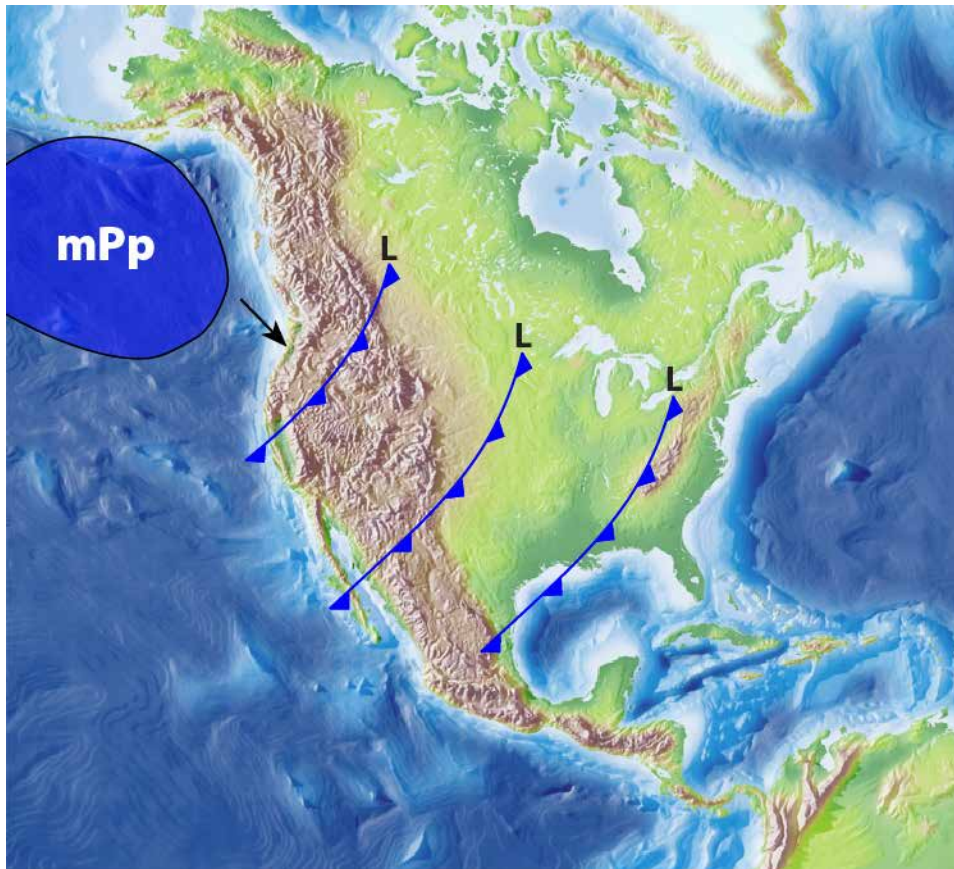


Figure 5.15. Many cool, moist, energetic North Pacific air masses and their associated storms are driven by upper-level winds to the coast ranges of Canada and the northwest United States. They typically bring low, overcast skies and periods of rain (lower elevations) and snow (higher elevations) to coastal areas and inland.



Figure 5.16. Moist air masses from the Pacific Ocean (mPp), driven by the upper-level winds, release much of their moisture along the coastal mountains as rain and snow. The wet climate of the Pacific Northwest is home to some of the most magnificent forests of the world, such as the redwood-fir forest here in the Klamath Mountains of northern California (Source/Credit: Nancy Netoff).

Fronts (cold fronts, warm fronts, occluded fronts) that form by the collision of warmer and colder air masses in the North Pacific may also be carried by upper-level winds toward the west coast of the continent (Figure 5.17). The weather along the Northwest coast of the United States may have temperatures in the 30s and 40s with plenty of overcast skies, rain, drizzle and fog. In the mountains to the east, snow is likely to be heavy as the moist air rises and cools. Some mPp air masses penetrate far inland and southward. By the time they reach the Plains states, their temperature may be even cooler than they were in the Pacific Northwest, due to the combined effects of continentality and the tendency for cold Canadian air to be drawn into these air masses.



5.17. As mPp air and its associated fronts move into the United States, they typically travel toward the east and south, occasionally all the way across the United States. The mPp air mass may slowly lose its identity as it mixes with colder air from the Canadian Plains and Southern Rockies.

## Continental Polar Canadian Air Masses (cPc)

These air masses develop over the Canadian Plains (Figure 5.18). They tend to be cold to severely cold and dry during the winter and spring months, and cool and dry during the summer and fall. During the winter, the days are short and the Sun angle is very low. This combination of factors allows very little energy from the Sun to be received over the course of the day. And, if the ground is covered in snow (Figure 5.19), much of the incoming solar energy is reflected rather than absorbed. The long, cold, clear nights allow plenty of time for what little radiation that was absorbed during the day to escape. In the middle of winter, cPc air masses can drop well below minus 30°F (minus 34°C), with wind chill equivalent temperatures that can approach minus 100°F (minus 73.3°C).

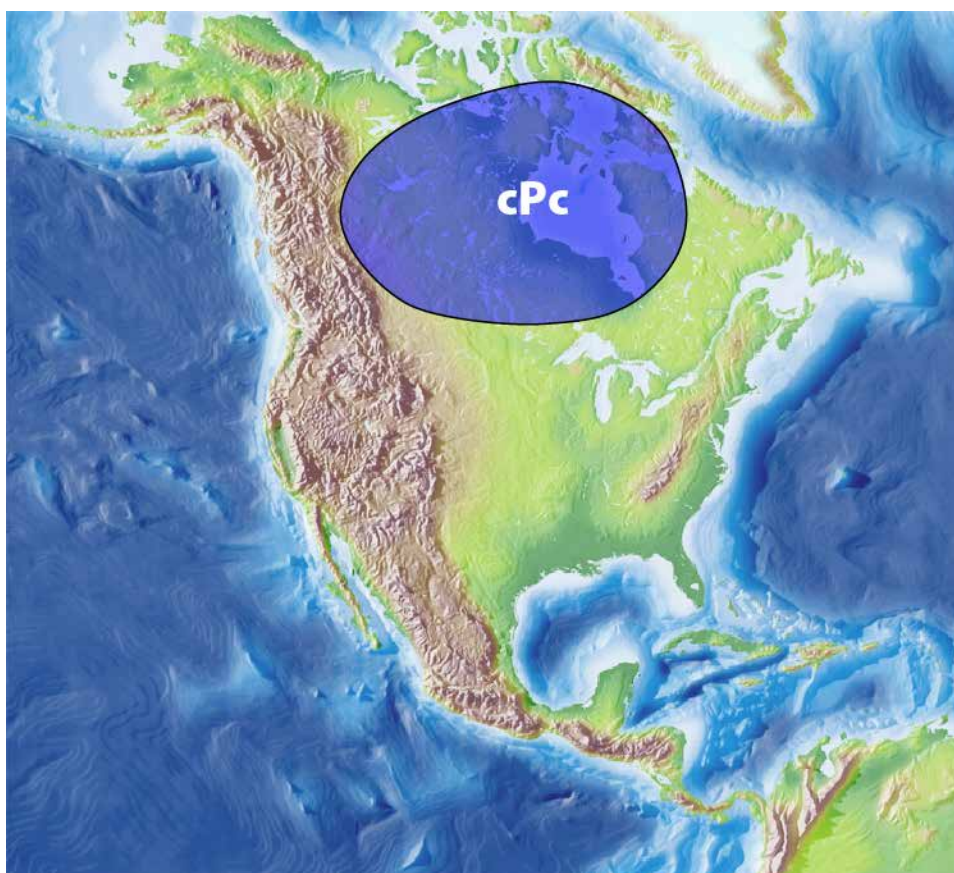


Figure 5.18. Continental Polar Canadian air masses (cPc) form at high latitudes over the deep interior of Canada. During winter at this latitude, the combination of snow-covered ground (high albedo) and long nights creates an energy deficit that produces these cold, dry air masses.



Figure 5.19. February 13, 2014 snow cover over North America. The cPc source region is an ideal birth place for cold, dry air, especially during the coldest part of winter. Ideal source region characteristics there include a large, high-latitude location, a relatively flat Canadian Plains, high pressure, and a snow-covered surface. Even areas marginal to the Arctic Ocean and Hudson Bay are little-affected by the nearby water because these water bodies remain frozen much of the winter, and well into spring. The coldest temperature ever recorded in Canada was minus 63°C (minus 81.4°F) in Snag, Yukon (Source/Credit: NASA).



Some cPc air masses travel straight from the Canadian Plains south into Texas and out into the Gulf, and occasionally deep into Mexico (Figure 5.20). The relatively flat nature of the Great Plains offers little resistance to their movement, and the Rocky Mountains and Appalachian Mountains help to funnel these air masses toward the south.

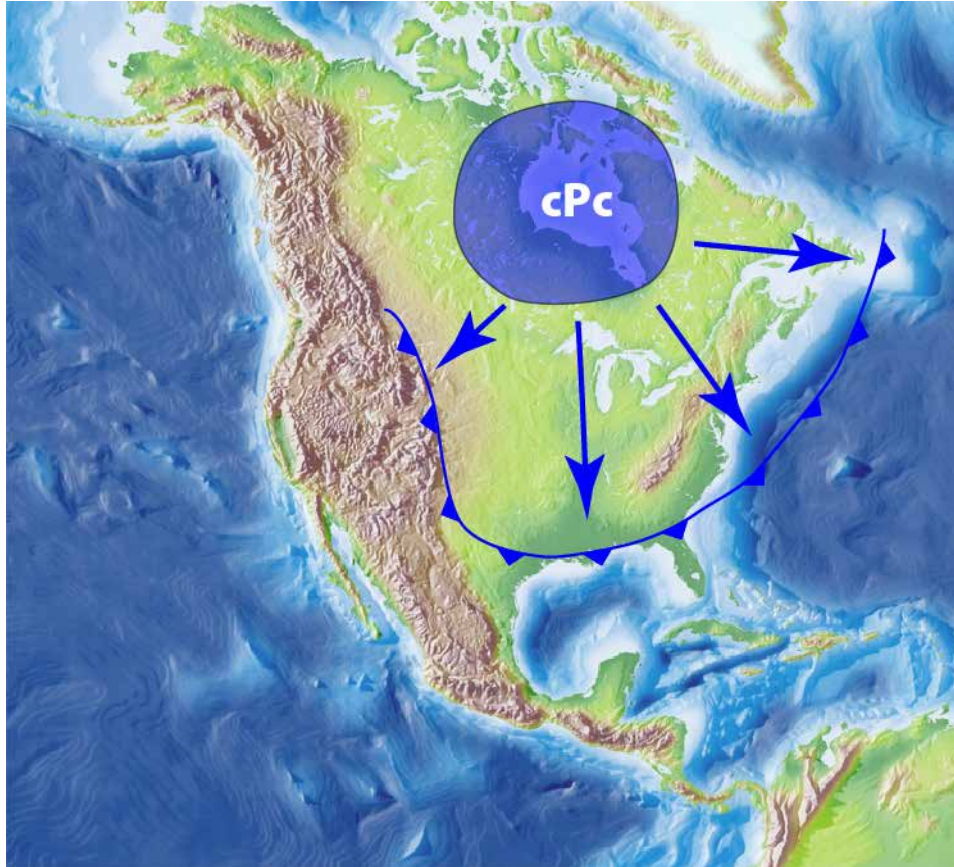


Figure 5.20. Continental Polar Canadian (cPc) air masses originate in Canada and move southward into the Central Plains. Typically, they stay to the east of the Rockies, which means that the western United States is not normally affected by them. However, cPc air masses from Alaska and mPp air masses do travel to the west of the Rockies.

Continental polar air masses often bring huge snowfalls to the southern and eastern United States (Figure 5.21). The moisture is not in the cPc air, but rather in the warmer, more humid air found in advance of these air masses. As these cPc air masses push into the warmer mT air masses, the rising and cooling air will often result in unusually heavy snowfalls that can bring most activity to a halt.



Figure 5.21. Two cars buried in deep snow on February 9, 2013 in Billerica, Massachusetts, courtesy of the collision of cPc air with warmer, more moist air to the south (Source/Credit: [http://commons.wikimedia.org/wiki/File:Winter\\_Blizzard\\_2013\\_](http://commons.wikimedia.org/wiki/File:Winter_Blizzard_2013_)).

Charles Russell's classic painting, *Waiting for a Chinook*, depicts the frozen desolation of the prairie that occurs with the invasion of a cPc air mass (Figure 5.22). The warm winds of the Chinook will clear the snow and enable the cow to find the tender grass below. If the Chinook doesn't come, the cow will weaken from cold and hunger and will become a meal for the wolves.

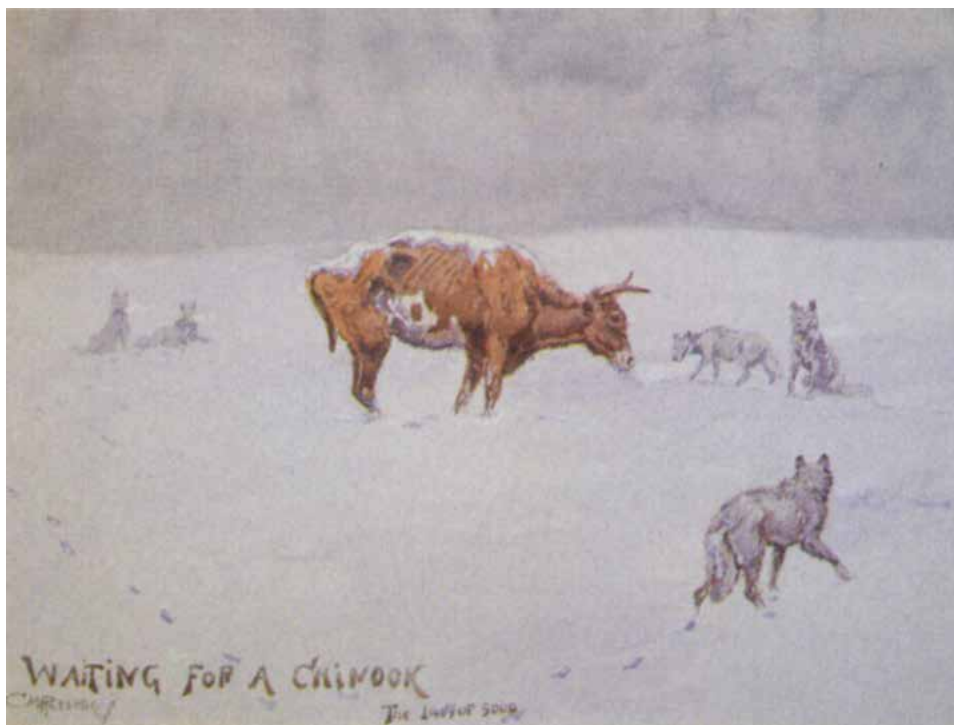


Figure 5.22. If a Chinook wind were to develop, the warm wind would melt the snow and uncover grass that the starving and weakened cow desperately needs to survive (Source/Credit: Charles Russell).

The most frigid air masses to impact the conterminous United States, and sometimes even northern Mexico are often designated as either cPc or cA air masses, but actually have a source region in Asia. Perhaps they should be classified as cPs (continental Polar Siberian) air masses. They are now referred to as the *Siberian Express*, and can bring subfreezing temperatures to places such as the lower Rio Grande Valley, where they can result in substantial crop losses. They often will cross the Arctic Ocean, blocked from entering Alaska and the North Pacific Ocean by an upper-level ridge. They are little affected by crossing a large ocean, because most of the Arctic Ocean is covered with insulating sea ice (Figure 5.23). Many of the low temperature records for January and February east of the Rockies are due to the invasion of Siberian air masses. Occasionally, they reach as far south as central Mexico and as far west as the coast of California, Oregon, and Washington (Figure 5.24).

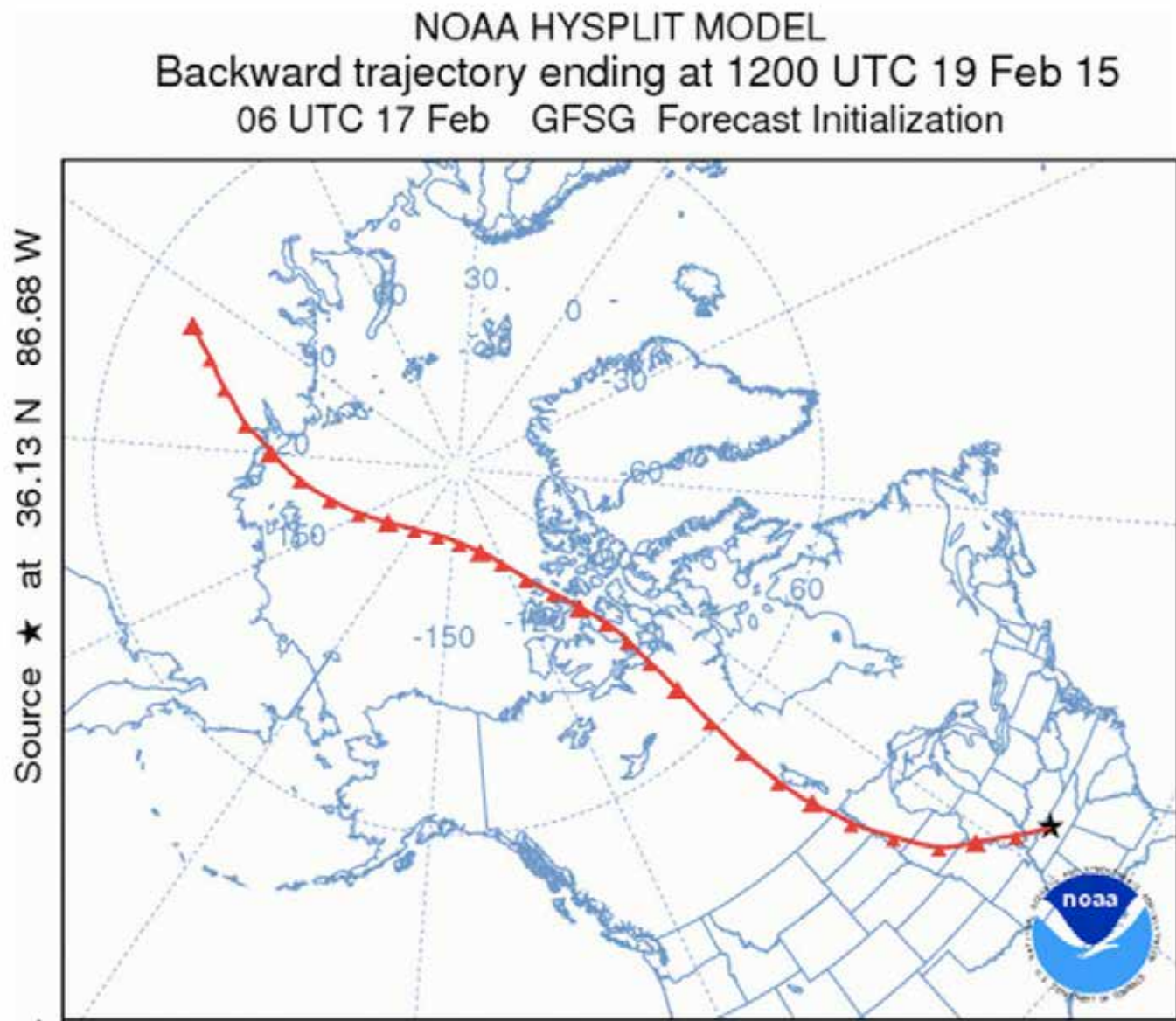


Figure 5.23. Track of the Siberian Express in mid-February of 2015. Cold temperatures associated with multiple outbreaks of the Siberian Express led to the partial freezing of Niagara Falls (Source/Credit: NOAA).

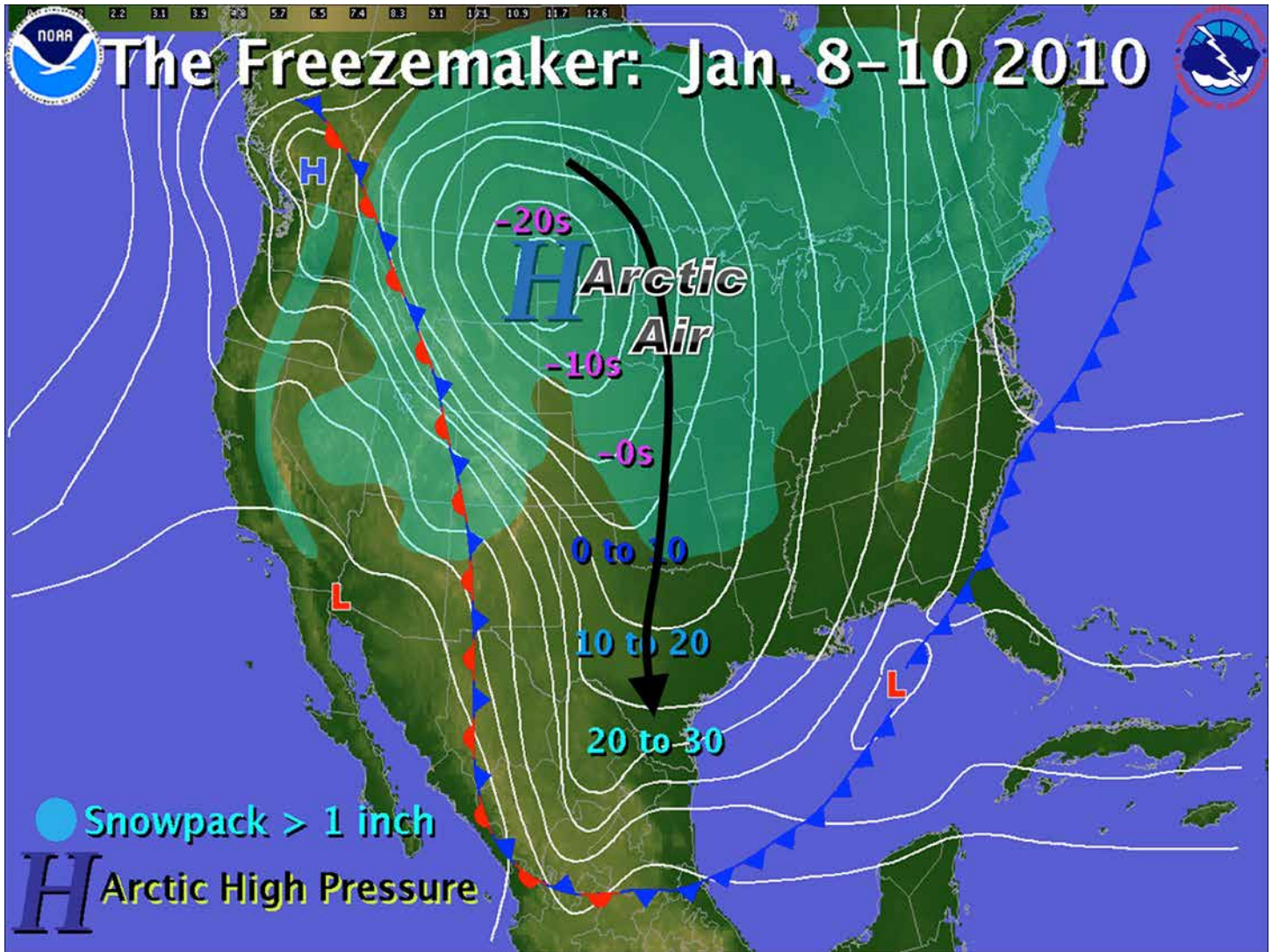


Figure 5.24. The Siberian Express of January 2010 brought sub-freezing temperatures well into Mexico. Negative temperatures occurred as far south as Kansas. The total distance that the Siberian Express traveled was about 8000 miles (~13,000 km), or about a third of the circumference of the Earth (Source/Credit: NOAA).

### Maritime Polar Atlantic Air Masses (mPa)

Off the northeast coast of Canada between Newfoundland and Greenland is the source region for maritime polar (mPa) air masses (Figure 5.25). These air masses, which are present all year, typically have little impact on North American weather because the Prevailing Westerlies normally carry these air masses to the east *away from* the United States. Because these air masses do travel to the east, they generate most of the winter storms that move into Europe from the North Atlantic. They are responsible for the frequent gray skies in Europe, especially in winter. In a sense, this air mass source region affects Europe in the same way that the mPp source region in the Gulf of Alaska affects the United States; i.e., it sends storms onto the land about every five to seven days during the cooler months.

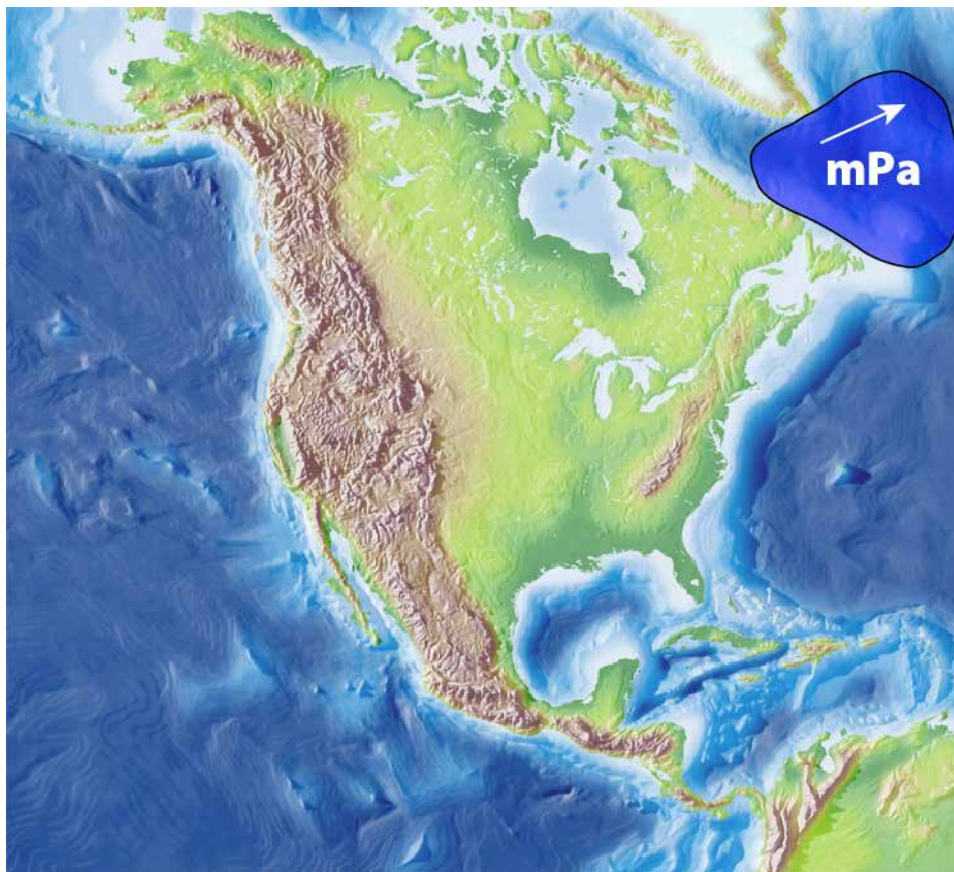


Figure 5.25. Maritime Polar Atlantic air masses (mPa) form in the area of the Icelandic Low and are normally carried eastward by the Prevailing Westerlies.

Deep low pressure systems that invade New England can, however, draw heavily on mPa air masses and their moisture. When this occurs, local residents experience a very different kind of winter storm. Instead of the typically cold and relatively dry storms caused by invasions of cPc air masses from central Canada, these storms tend to be associated with wet (and cold) conditions that make for some truly miserable weather. These are the famous New England **Nor'easters** (Figure 5.26 and 5.27).

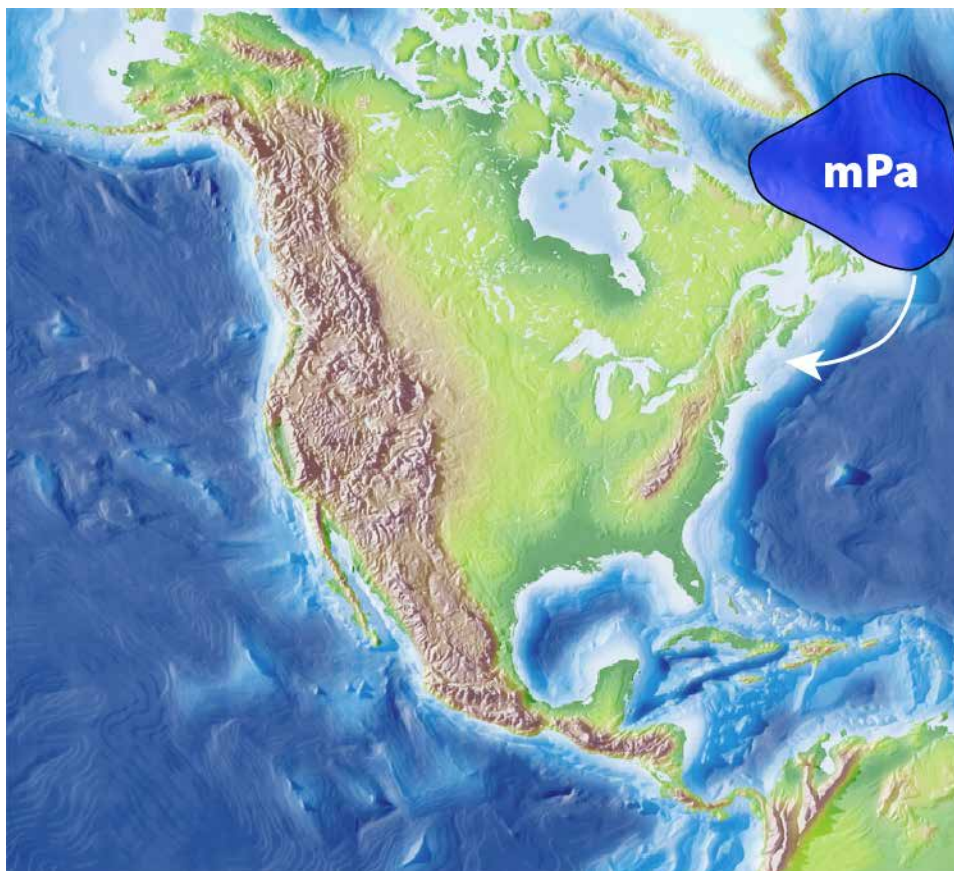


Figure 5.26. Occasionally, mPa air masses from the North Atlantic are carried westward into the United States contrary to their normal direction of travel.

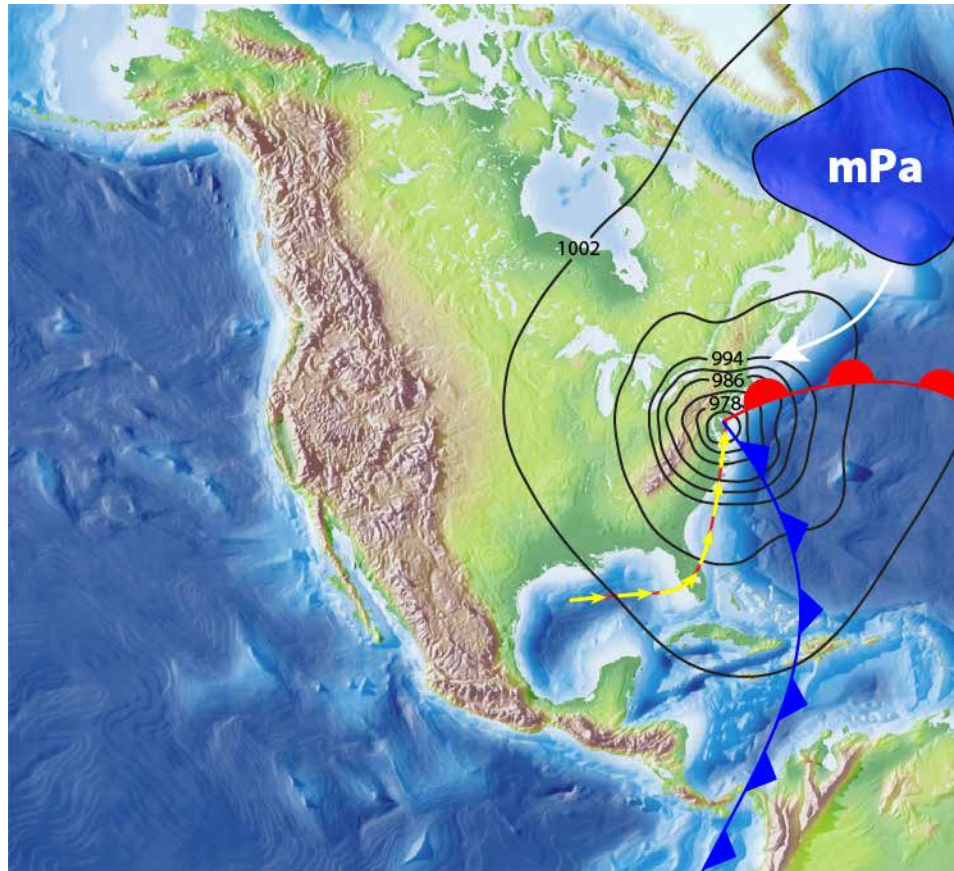


Figure 5.27 An mPa air mass can be drawn into the United States by strong low pressure systems over the continent. This condition produces Nor'easters, which can sometimes generate violent storms capable of causing extensive damage along the coast.



Nor'easters contain several key ingredients that make them exceptionally powerful and long-lived. A large trough in the upper-level flow, including the polar jet stream, sets up along the eastern half of the United States. A low pressure system typically develops over the Gulf region or over the southeastern states. The low is guided by upper level winds, initially to the east, then northeast along the coast along the eastern side of the upper-level trough. Here the clash of cold, polar air and maritime tropical air from the Atlantic energize the storm, and it intensifies. Precipitation also tends to become more intense, with snow or cold rain developing in the cold air mass, and warm rain on the marine side. Warm water from the Gulf Stream adds moisture and energy to the system.

As the storm continues up the eastern seaboard, the low pressure system deepens, and now a third air mass enters the scene, the mPa. As long as these factors persist, the storm can release copious amounts of warm rain, cold rain, freezing rain and snow over long periods of time. Some of the most memorable Nor'easters include the blizzard of 1888, the Ash Wednesday storm of March 1962, the New England blizzard of February 1978, the Halloween Nor'easter of 1991, the infamous storm of the century in March 1993 (Figures 5.28, 5.29a, 5.29b and 5.30), the Boston snowstorms of February 2015, and the January blizzard of 2016 (Figure 5.31).

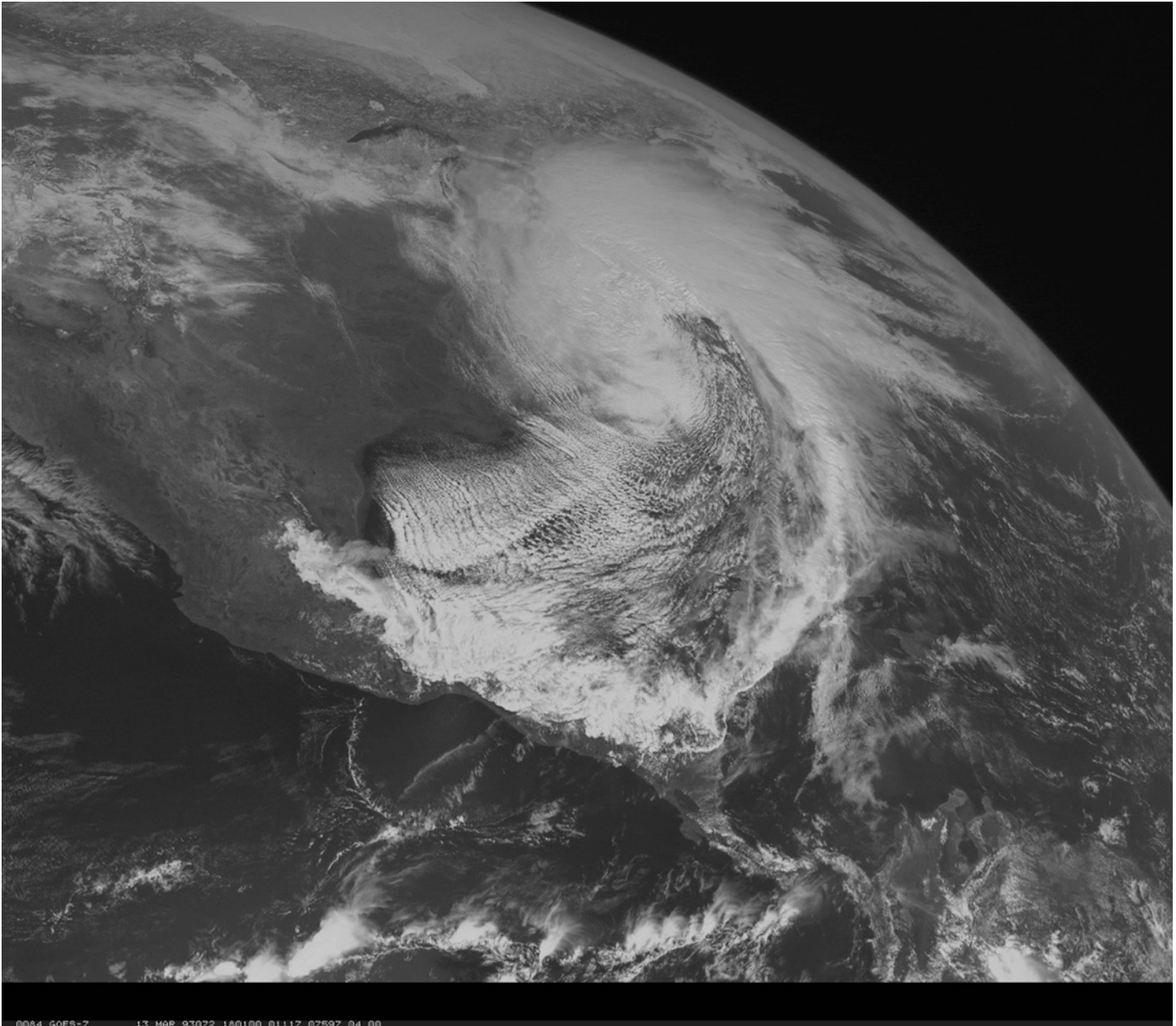


Figure 5.28. A GOES-7 satellite image of the March 1993 “storm of the century” taken on March 13 at 1:01 PM Eastern time. The storm at this time was only about half-way through its cycle in the United States. Note the widespread stratocumulus cloud streets over the Gulf of Mexico and the Atlantic Ocean. These are generated as cold air travels over warmer water. The long, thin clouds in the east-center of view mark the leading edge of the cold air mass, or cold front. Cold air had already plunged well into Central America (Source/Credit: NOAA).

<b>Heaviest snowfall totals from the March Storm of Century in 1933:</b>	
<b>Mount Le Conte, NT</b>	<b>56"</b>
<b>Snowshoe, WV</b>	<b>44"</b>
<b>Syracuse, NY</b>	<b>43"</b>
<b>Lincoln, NH</b>	<b>35"</b>
<b>Albany, NY</b>	<b>27"</b>
<b>Pittsburgh, PA</b>	<b>25"</b>

Figure 5.29a. Heaviest snowfall totals from the March 1933 storm (Source/Credit: data from NWS).

<b>Strongest wind gusts from the Storm of Century in March 1933:</b>	
<b>Mt. Washington, NH</b>	<b>144 mph</b>
<b>Key West, FL</b>	<b>109 mph</b>
<b>South Marsh Island, LA</b>	<b>92 mph</b>
<b>Myrtle Beach, SC</b>	<b>90 mph</b>
<b>Boston, MA</b>	<b>81 mph</b>
<b>La Guardia Airport, NY</b>	<b>71 mph</b>

Figure 5.29b. Strongest winds from the March 1933 storm. Mount Washington is notorious for strong winds (Source/Credit: data from NWS).

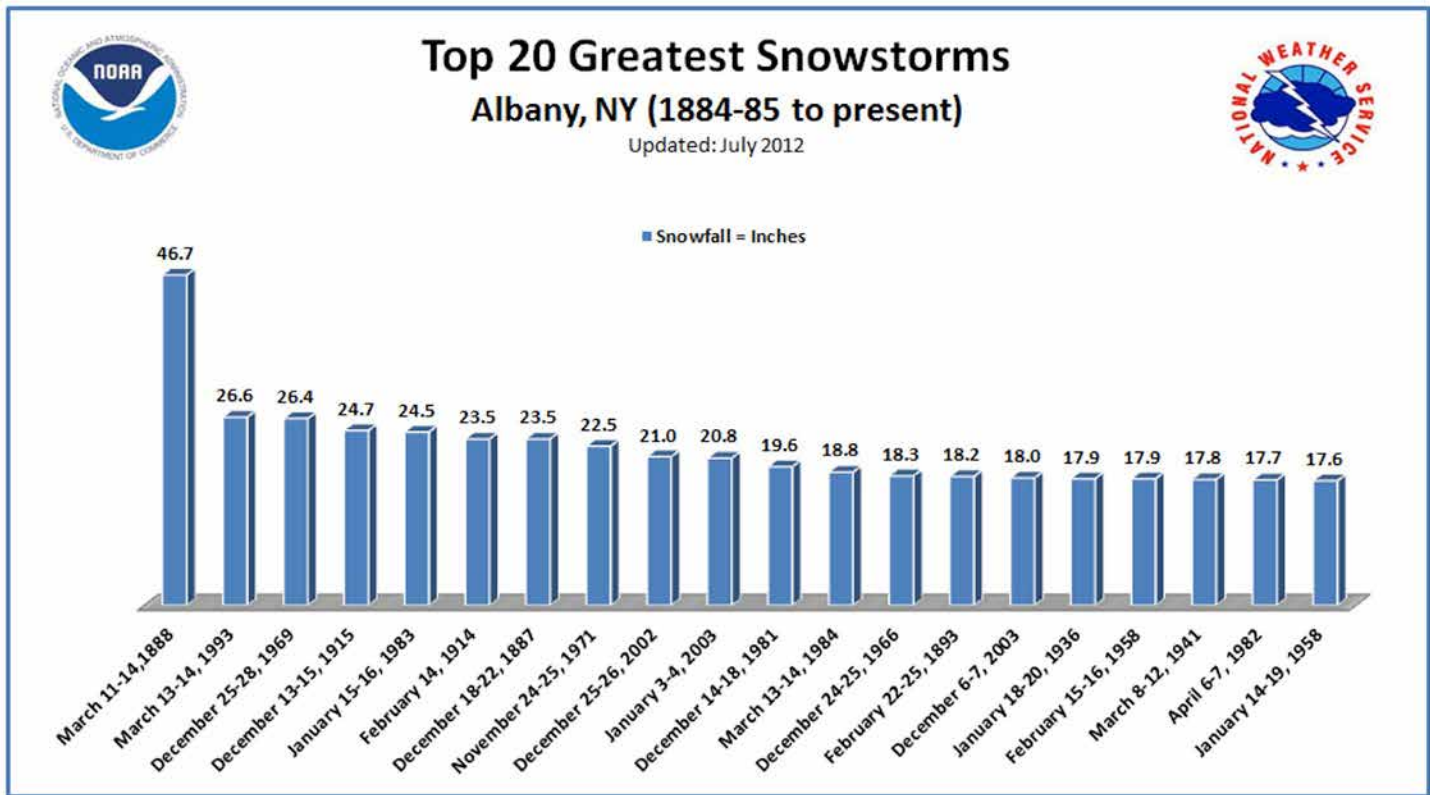


Figure 5.30. The top 20 greatest snowstorms for Albany, New York. 1993 storm vs. others. Although some places recorded record snowfall from this event, the Albany snowstorm of 1888 far eclipsed this value (Source/Credit: NOAA).

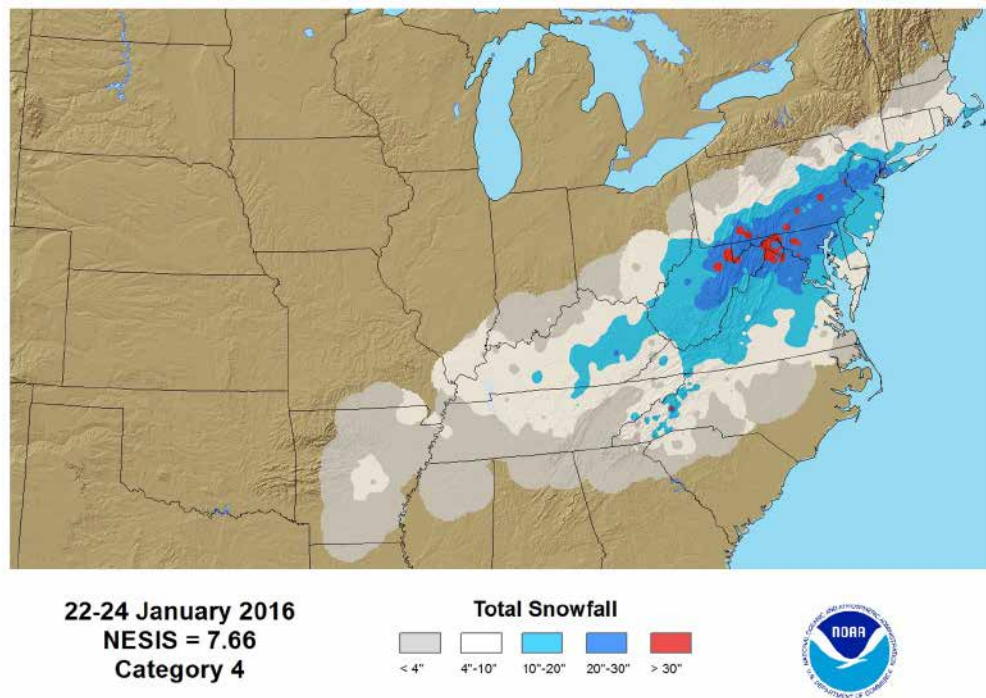


Figure 5.31. Total snowfall during 2016 blizzard from January 22-24, 2016 (Source/Credit: NOAA.)

In addition to heavy snows, Nor'easters can wreak havoc on the coast. Like a hurricane, they generate strong winds, big waves, and a storm surge that can destroy homes and buildings. Nor'easters can be powerful, destructive, and often deadly (Figure 5.32).



Figure 5.32. Damage from a strong Nor'easter that hit the Outer Banks of North Carolina in November, 2009 (Source/Credit: Charles Rocknak).

### **Maritime Tropical Pacific Air Masses (mTp)**

Off the southwestern coast of the United States and Mexico is a large maritime tropical (mTp) air mass source region in the Pacific (Figure 5.33). These air masses typically originate in the oceanic subtropical high pressure cells (STHs). The eastern side of these STHs (that affect the western side of the continents) are normally quite stable and dry, especially during the warm season. The dry season gets longer and drier progressing southward along the California coast from Eureka to San Diego. Average annual rainfall for Eureka is 40 inches (102 cm), San Francisco is 24 inches (61 cm), San Luis Obispo is 19 Inches (48 cm), and San Diego is a mere 10 inches (25 cm).

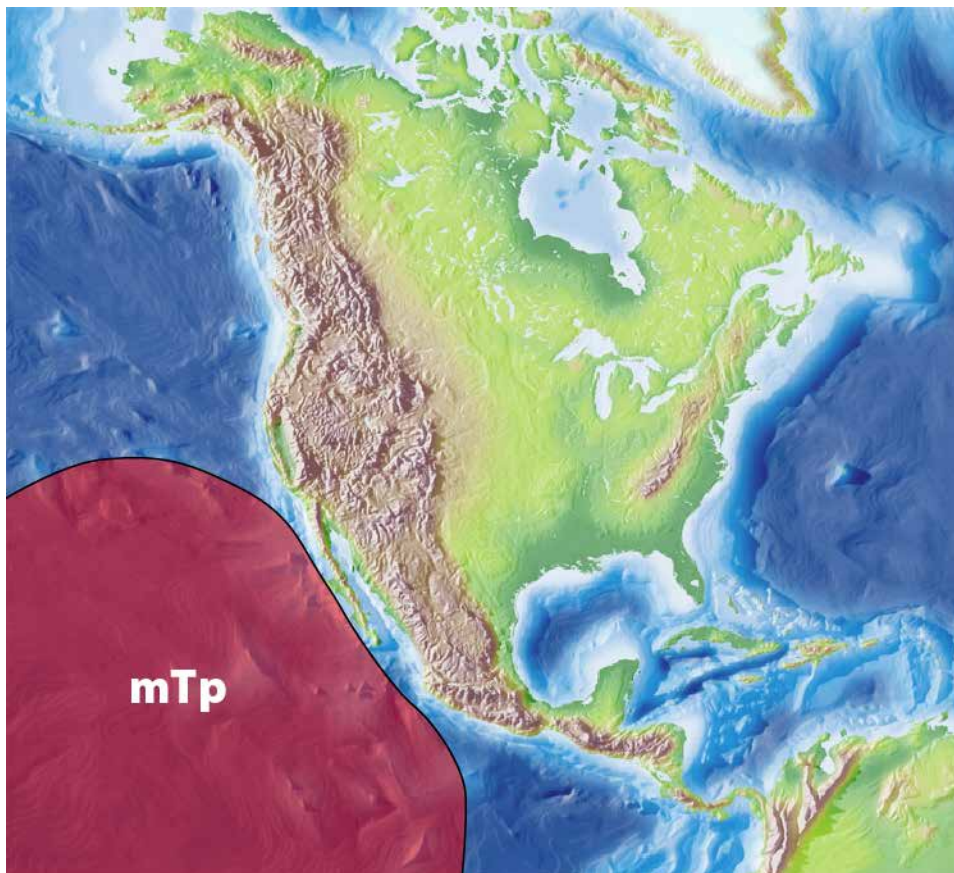


Figure 5.33. Maritime Tropical Pacific air masses (mTp) form over the warm waters of the tropical Pacific Ocean.

Coastal regions of California, Oregon and Washington are influenced by a set of geographic factors that create cool moist summers because of the **marine layer**. The *marine layer* is an extensive belt of cool coastal air that is typically anywhere from a few hundred to a few thousand feet thick. It can extend all the way from Washington to Baja, California, but tends to be best developed in California and Oregon.

The factors that contribute to the formation of the *marine layer* along mid-latitude west coasts include the summer season, the subtropical high, the Cold California Current and coastal mountains. Mid-latitude west coasts tend to be under the strong influence of the stable side of the quasi-permanent oceanic subtropical high during the warm months. The high sets up a clockwise circulation in the ocean basin, which in turn is responsible for the westerly winds and the Cold California Current. Strong subsidence on the eastern side of the subtropical high and advective cooling of air crossing the cold current establish a very persistent temperature inversion. The strong subsidence and persistent inversion discourage air mass uplift, and keep these coastlines summer-dry.

The thickness of the inversion layer depends largely on the strength of subsidence (Figure 5.34). Strong subsidence generates a very shallow marine layer, sometimes only 200-300 feet. Weak subsidence allows the inversion and therefore the marine layer to thicken considerably, occasionally to over 4000 feet. Below the inversion is the marine layer. Within the inversion, clouds and/or fog can form under stable atmospheric conditions. Stratus and stratocumulus clouds and/or fog may persist for days and give rise to local names such as the *May gray* or the *June gloom*. The coast ranges of California and Oregon are normally high enough to restrict the marine layer to a narrow belt along the coast, but unusually thick inversion layers may allow the layer to overtop the mountains and spill into the inland valleys, where they can have a temporary cooling effect on inland valley cities (Figure 5.35). Additionally, there are some gaps in the Coast Ranges (e.g., at San Francisco and Portland) that also allow the marine layer as well as fog to penetrate deep inland (Figure 5.36).

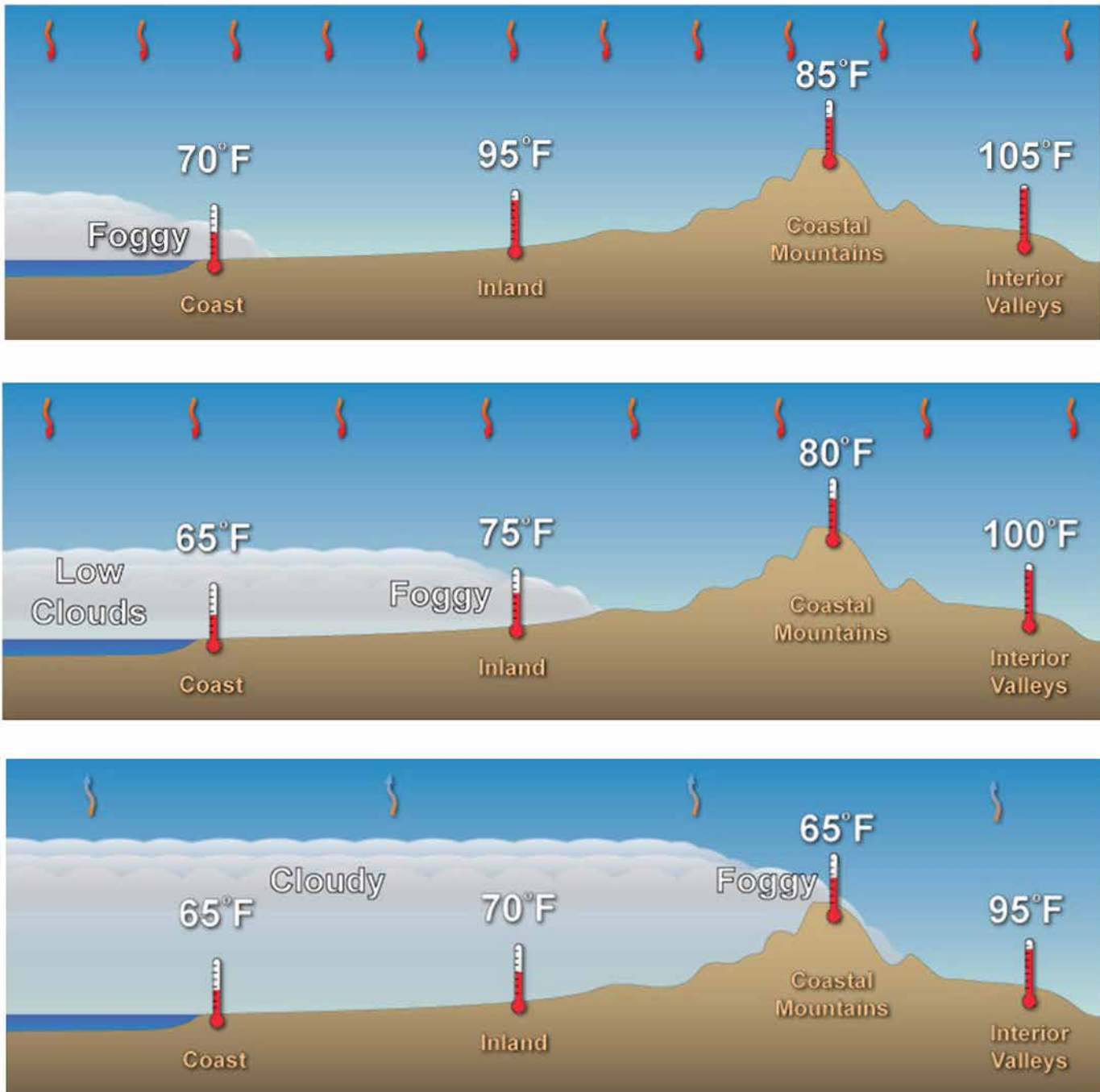


Figure 5.34. Strong subsidence (sinking) due to the upper level high pressure creates a thin marine layer that is confined to the coast. High inland temperatures tend to create a thermal low, increasing the airflow shoreward (upper diagram). A lessening of the subsidence allows for the development of a thicker marine layer and deeper penetration inland (middle diagram). Deep marine layers can cause the fog to thicken to the point that cool, foggy air spills over the mountains and may have a substantial, though temporary cooling effect on the Central Valley (Source/Credit: NWS).



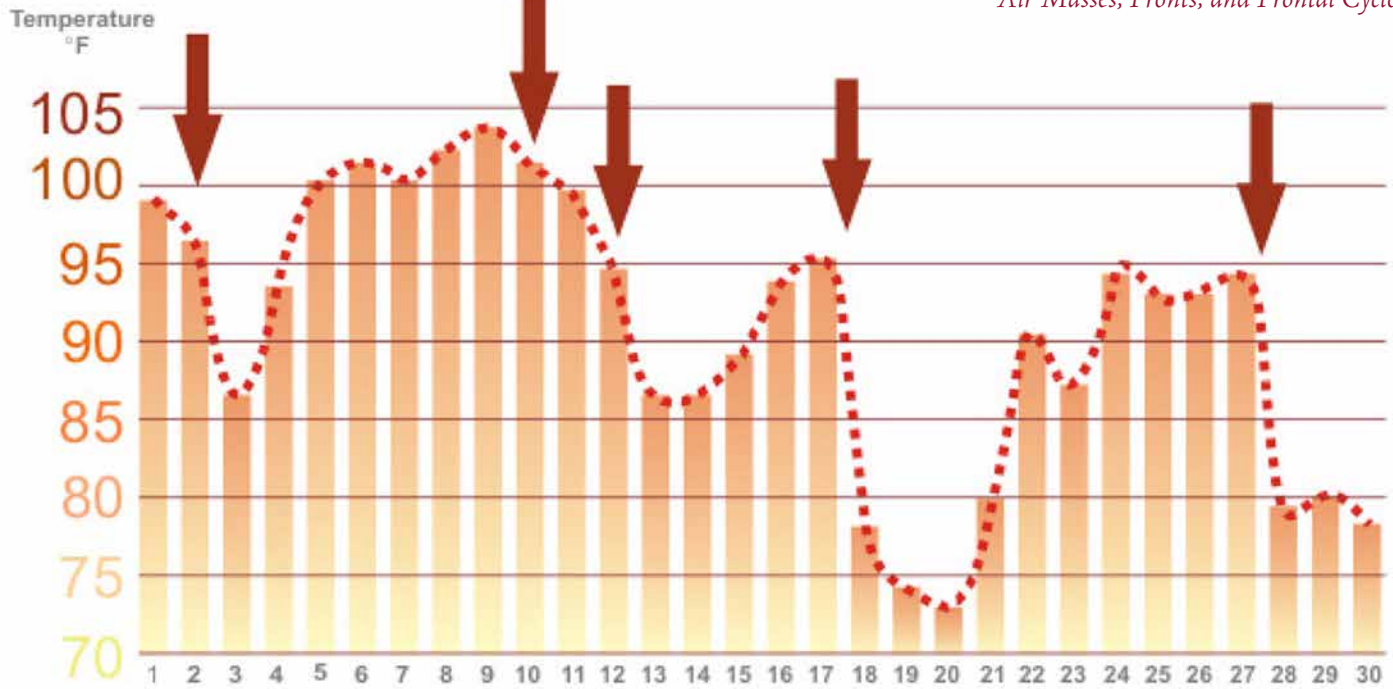


Figure 5.35. Bakersfield in the southern part of the Great Valley of California. Summertime highs are typically in the high 90s or low 100s, except for brief episodes when the marine layer penetrates inland. Arrows show the initial penetration of the marine layer and the pronounced cooling for a day or so (Source/Credit: NWS).



Figure 5.36. Advection fog that has developed in the marine layer. The fog in the distance almost hides one of the towers, which are 750 feet (230 m) above the ocean level. The top of the inversion is likely at about 750 feet. The image was taken on May 3, 2009. The Golden Gate marks one of the few gaps in the entire coast range system allowing the marine layer to occasionally penetrate inland to the Central Valley (Source/Credit: [https://en.wikipedia.org/wiki/San\\_Francisco\\_fog#/media/File:Golden\\_Fog,\\_San\\_Francisco.jpg](https://en.wikipedia.org/wiki/San_Francisco_fog#/media/File:Golden_Fog,_San_Francisco.jpg)).

There are several weather situations that cause a complete reversal from the dry summers of the southwestern United States. California and Baja, California are well known for their long summer droughts, hot and dry inland weather, but cooler coastal air thanks to the *marine layer*. The west coast of North America is typically free of hurricanes, the opposite of the mid-latitude east coast locations. Nearly every year, however, a rogue hurricane heads for the southwestern United States. Most are down-graded to tropical storms or depressions by the time they enter the United States. Even then they may pack strong wind gusts, cause dew points to skyrocket, and trigger showers, thunderstorms and flash floods. In mid-September 2016, the remnants of Hurricane Paine brought dew points in the Mojave Desert to the low 70s, reminiscent of southeast Texas dew points during September. The same storm helped fuel an outbreak of severe thunderstorms in Texas nearly a week later. In September of 1997, Southern California narrowly escaped the wrath of Hurricane Linda (Figure 5.37).

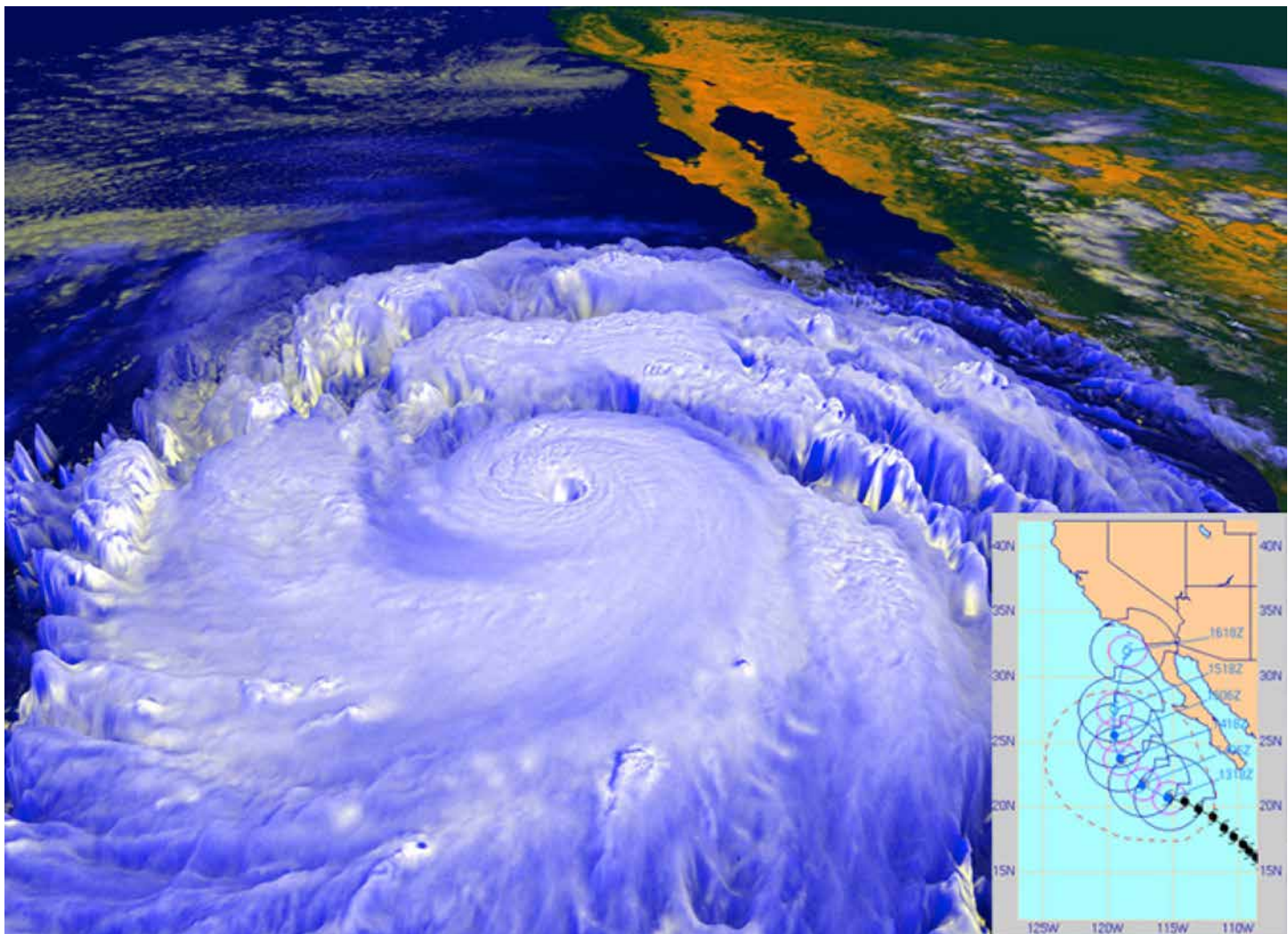


Figure 5.37. In September of 1997, Southern California was forecast to be in the path of the remnants of Hurricane Linda. Linda at one point was forecast to strike Southern California by the Naval Research Laboratory's Marine Meteorology Division. The storm eventually turned westward away from land, but still brought rainfall and high surf to parts of Southern California (Source/Credit: NASA/NOAA Inset image credit: NRL/NCEP).

A second reversal from the warm and dry summers of the southwestern United States arrives with some regularity, typically during early-to-middle July and occurs somewhat sporadically for one-to-three months or more. It is North America's analog to the Asian Monsoons, which bring warm, wet weather to much of Southeast Asia for the warm six months of the year. The *North American Monsoon* is shorter and less intense, but still very important to the economy of the southwest because as much as 30-40% of the annual precipitation can fall during this brief period. The setup for the onset of North American Monsoons is the development of a high pressure ridge over the Four Corners region to the western Great Plains and a thermal low around southern Arizona and southeastern California (Figure 5.38).

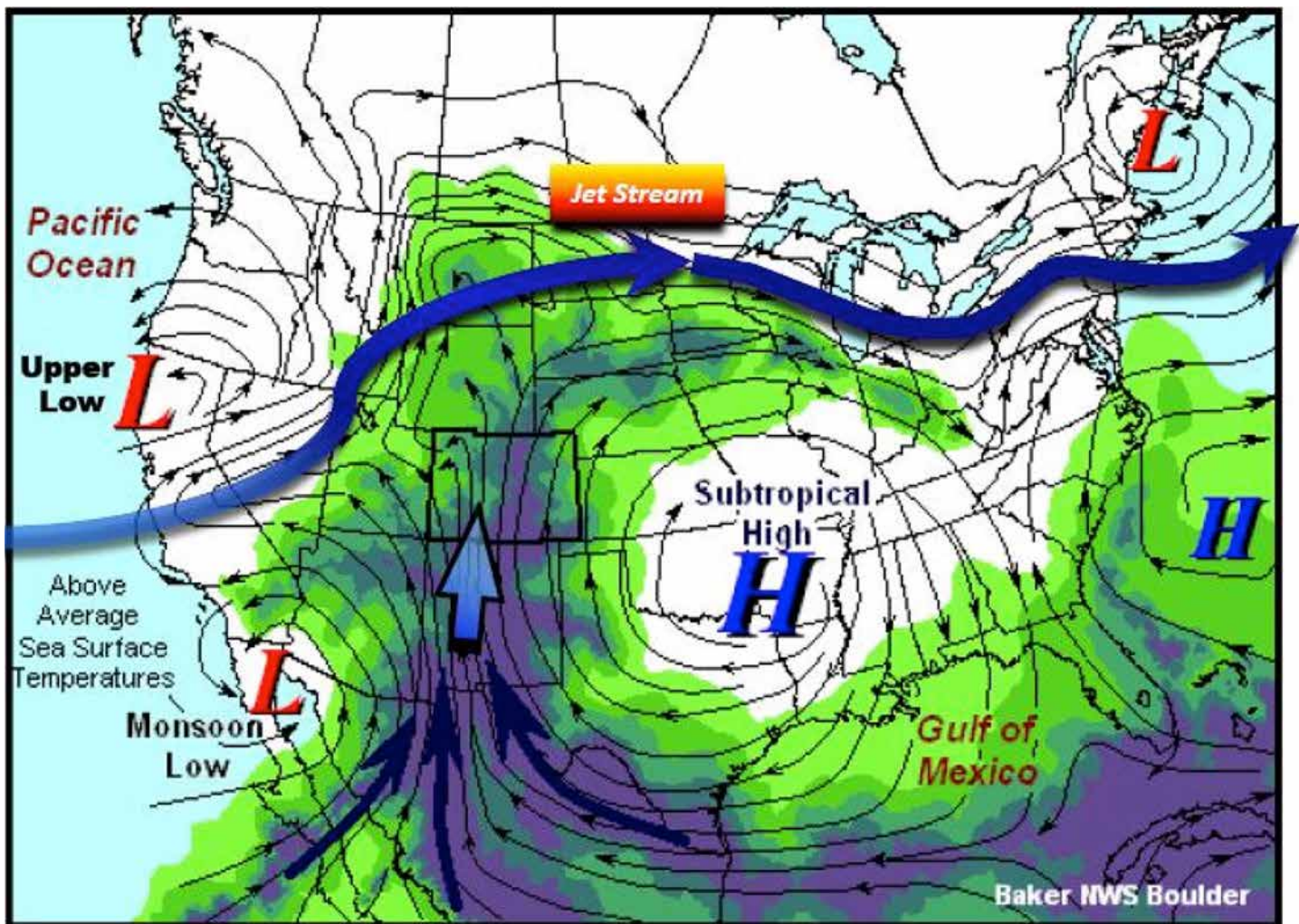


Figure 5.38. The ideal setup for the North American Monsoon is the development of a high pressure system in the vicinity of the Four Corners region to the western Great Plains. Intense heat in southern California, Arizona, and Baja California funnel warm, moist air from both the Sea of Cortez and the Gulf of Mexico into the Four Corners states, triggering abundant summer rains (Source/Credit: Mike Baker of NWS Denver WFO).

**Atmospheric rivers** can also bring huge amounts of moisture to the mid-latitude west coast. Atmospheric rivers are long, narrow belts of moisture-laden air that originate in tropical or subtropical latitudes, and are typically carried northeastward by a combination of upper-level flow and surface fronts (Figure 5.39). They often create large precipitation events, particularly in places like the west coast of North America during the winter, where they interact and are magnified by fronts and mountain barriers. They average just a few hundred miles wide, but can be thousands of miles long.

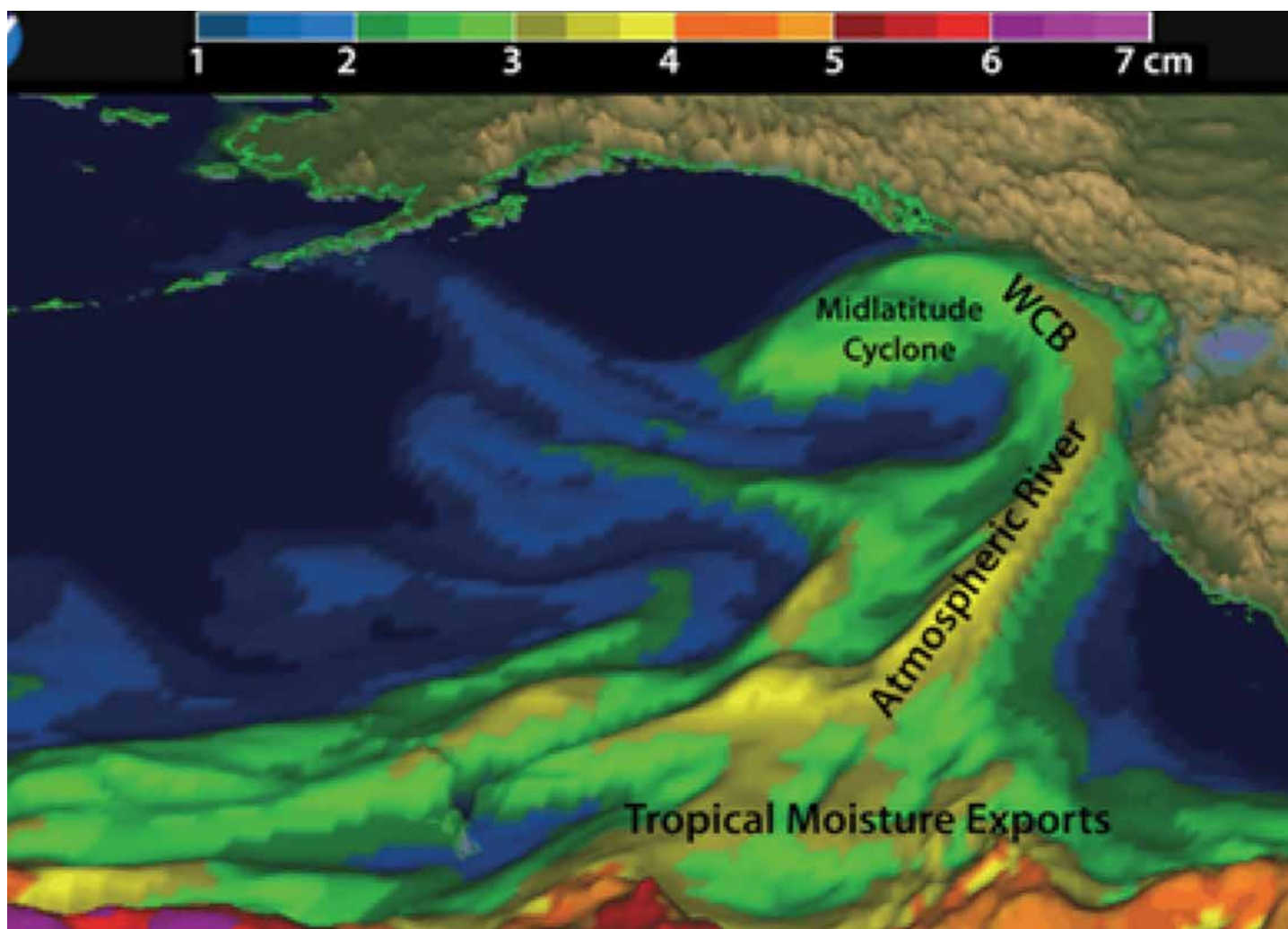


Figure 5.39. The Pineapple Express is an atmospheric river that transports massive amounts of water vapor from low-latitude oceans to higher latitudes. Atmospheric rivers are responsible for many mid-latitude flood events, some of which can be catastrophic. This depiction of an atmospheric river, adapted from NOAA/ESRL Physical Sciences Division, shows the river interacting with West Coast mountains and a mid-latitude cyclone over the northeast Pacific on February 5, 2015 (Source/Credit: NOAA).

## Maritime Tropical Air Masses from the Gulf of Mexico (mTg) and Atlantic (mTa)

These air masses dominate the warm-season weather in the entire southeastern United States. The warm waters of the Gulf and tropical Atlantic may exceed 85°F (29°C), and pump tremendous amounts of moisture into the air. The Bermuda High located off the east coast of the United States, provides a source of warm, moist, and often unstable air to the southeastern United States much of the year, and accounts for the high humidities experienced there, particularly during the summer and early fall (Figure 5.40). The high humidity keeps night-time temperatures warmer than they would otherwise be because it traps heat energy. The collision between cPc and mTg air masses frequently triggers severe storms, even during the winter.

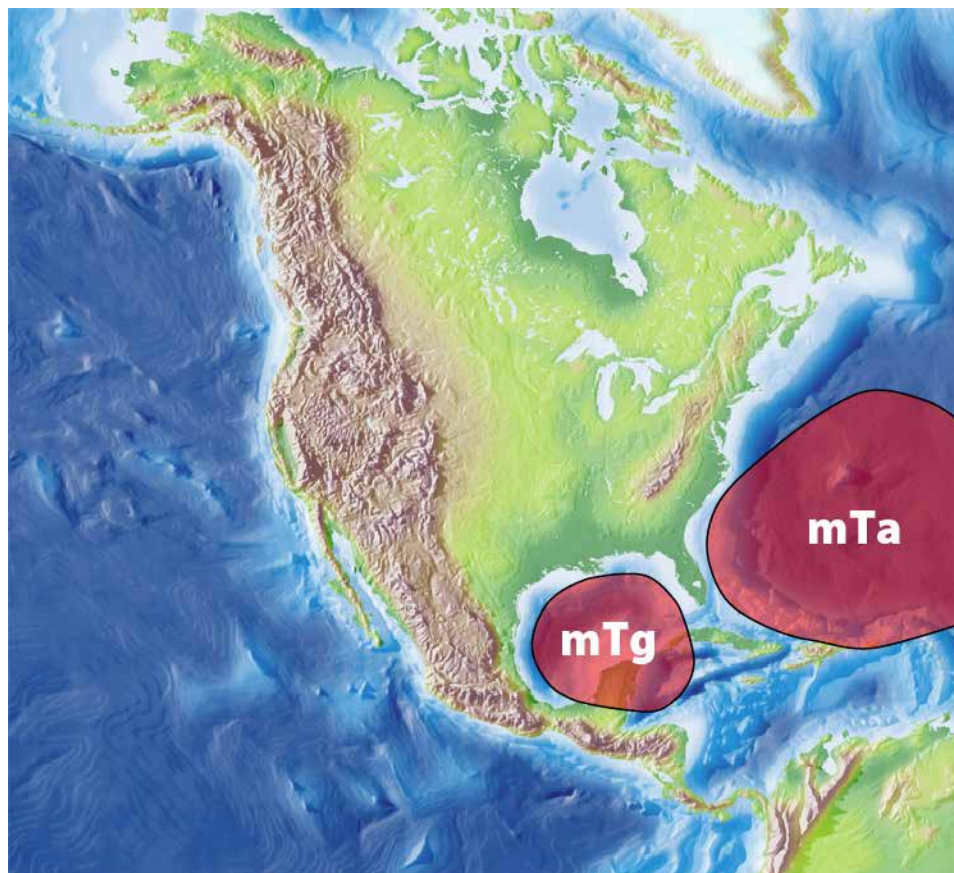


Figure 5.40. Maritime Tropical Gulf of Mexico air masses (mTg) and Maritime Tropical Atlantic air masses (mTa) form over warm, subtropical waters. Consequently, they are usually laden with moisture and are responsible for much of the rainfall that occurs from the Rockies eastward to the Atlantic. During the winter, these air masses are drawn into the interior of the continent by low pressure storm systems. During the summer, they are drawn into the interior by a combination of low pressure and airflow out of the Bermuda High. Although the air that sinks in the Bermuda High is originally dry, the air acquires moisture as it flows across the warm tropical waters of the South Atlantic and Gulf of Mexico.

During the warm season along the Gulf Coast, air masses originating in the Gulf of Mexico are often drawn onshore. During the daytime, these air masses are quickly modified by the warm ground. The warm ground heats the mTg air above it, and modifies its lapse rate (dashed green lines in the two temperature-height diagrams). As the lapse rate increases, the air becomes more buoyant, rises, and typically produces cumuliform clouds (Figure 5.41). Some of these clouds may transform into cumulonimbus clouds, bringing scattered thunderstorms to the Gulf States. In Texas, air masses may become further destabilized by uplift in the Texas Hill Country, as well as encountering fronts. The Texas Hill Country is arguably the most flash-flood prone area in the conterminous United States (Figure 5.42).

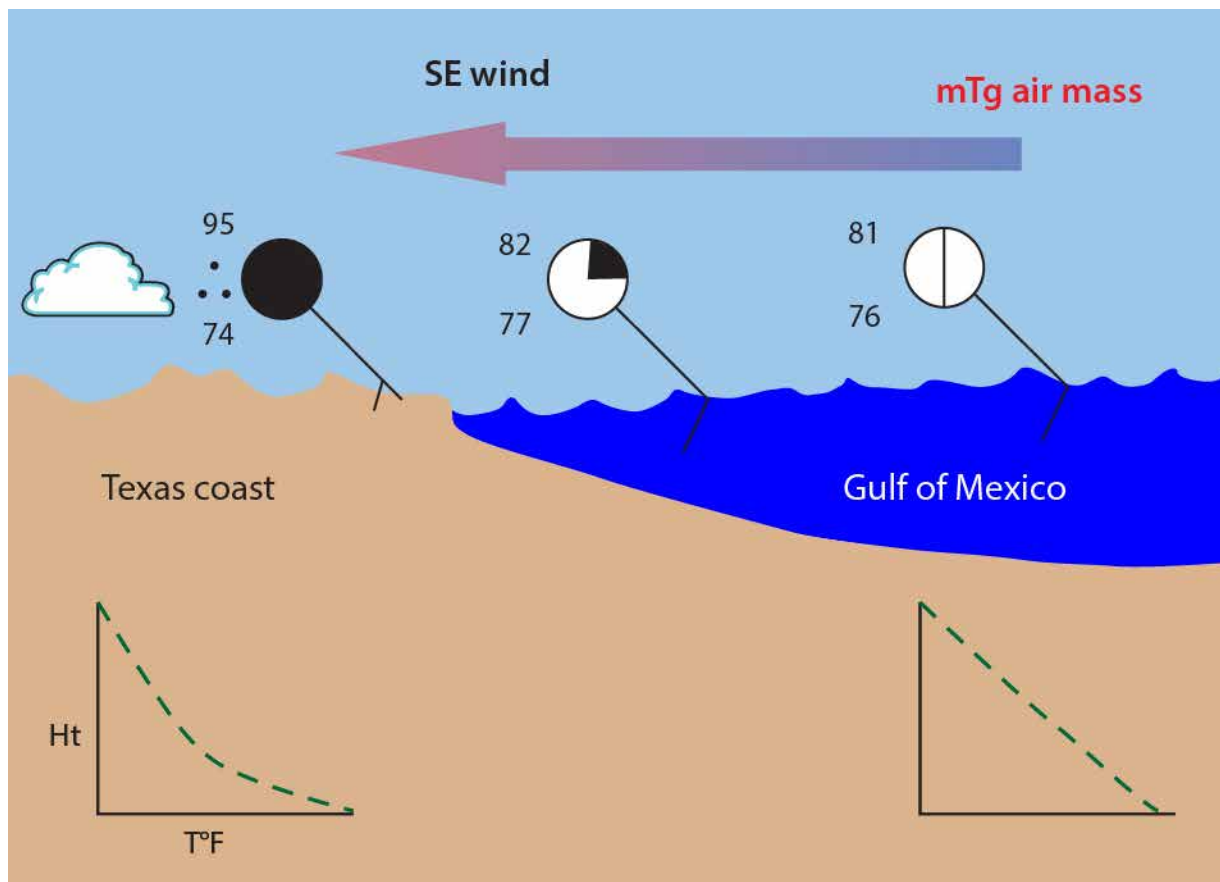


Figure 5.41. During the warm season along the Gulf Coast, air masses originating in the Gulf of Mexico are often drawn onshore. During the daytime, these air masses are quickly modified by the warm ground. The warm ground heats the mTg air above it, and modifies its lapse rate (dashed green lines in the two temperature-height diagrams). As the lapse rate increases, the air becomes more buoyant, rises, and typically produces cumuliform clouds. Some of these clouds may transform into cumulonimbus clouds, bringing scattered thunderstorms to the Gulf States. In Texas, air masses may become further destabilized by uplift in the Texas Hill Country, one of the most flash-flood prone areas in the conterminous United States.

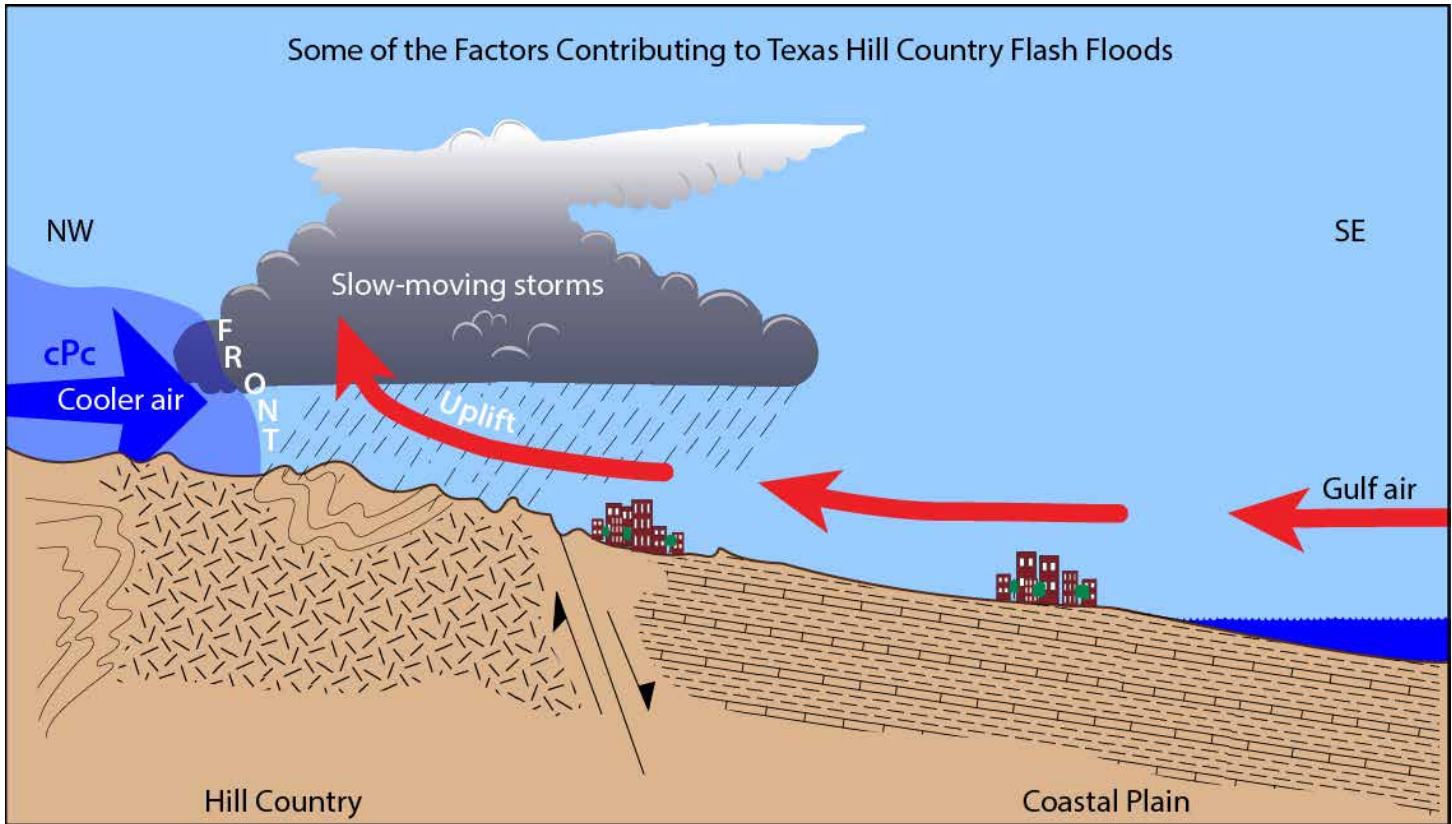


Figure 5.42. The Texas Hill Country is prone to long-lasting thunderstorms and flash-floods. Fronts that form the boundary between cooler polar air (cPc) and warmer tropical air (mTg) sometimes lose southward momentum and stall-out in the Hill Country, promoting prolonged precipitation events (Source/Credit: Baldwin, Cooper, Netoff, Solum and Degenhardt, *Geologic Hazards and Resources Laboratory Manual*, 2007).

During the cool season along the Gulf Coast, air masses originating in the Gulf of Mexico are often drawn onshore by large low pressure systems. In this scenario, the Gulf air mass is cooled at its base by colder land temperatures. Cooling tends to produce a stable temperature inversion (temperatures increase with height rather than decrease). Cooling may produce condensation, but the temperature inversion inhibits vertical motion, so stratiform clouds are produced (Figure 5.43). The result can be widespread cloudy skies and a prolonged spell of dreary weather.



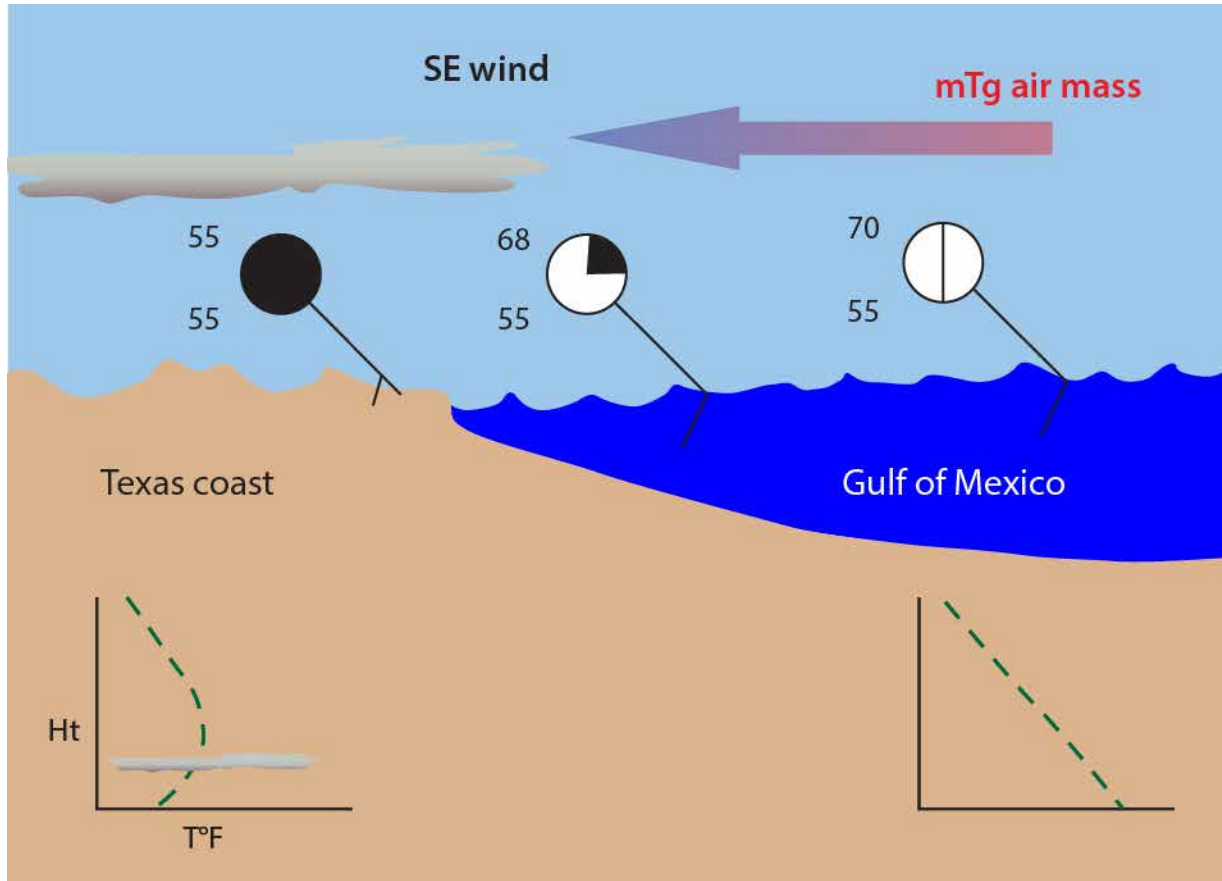


Figure 5.43. The cooling of Gulf air by the land during the wintertime can produce extensive stratiform clouds that make for a period of dreary weather. Cooling tends to produce a stable temperature inversion (green dashed line, left temperature-height diagram). If condensation occurs within the inversion layer, an extensive, but relatively thin cloud deck may occur.

Atmospheric rivers can amplify and concentrate moisture flow from mTg and mTa source regions. They can also destabilize the atmosphere, resulting in widespread thunderstorms and massive amounts of precipitation. The record-breaking precipitation over parts of Texas, Louisiana, Oklahoma, and Arkansas during the winter of 2016 was caused by an atmospheric river known as the *Mayan Express* (Figures 5.44, 5.45 and 5.46). The *Mayan Express* of 2016 was particularly noteworthy because some rainfall events lasted several days. Apparently, the upper-level trough that guided the *Mayan Express* stalled several times, causing staggering accumulations of precipitation.

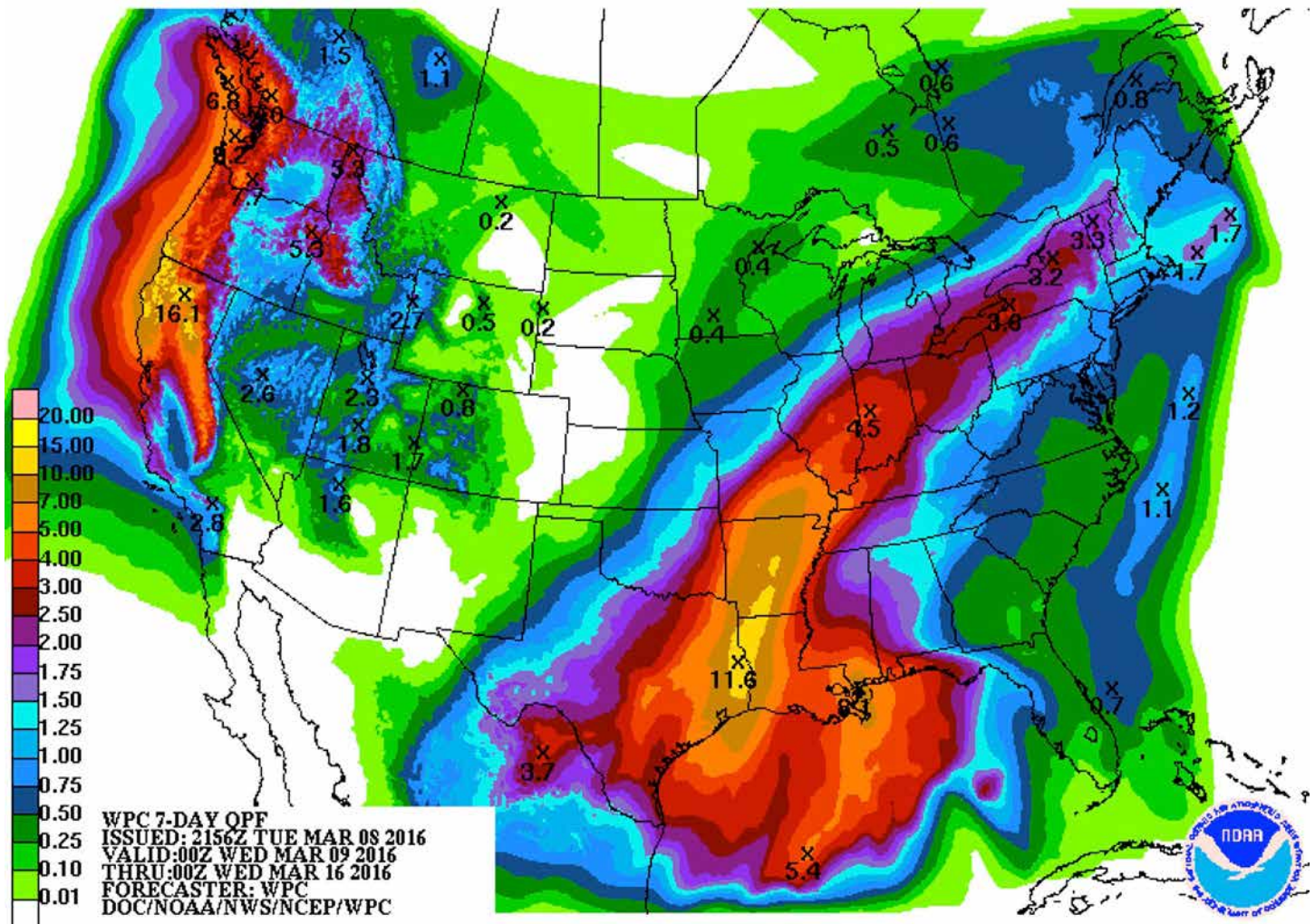
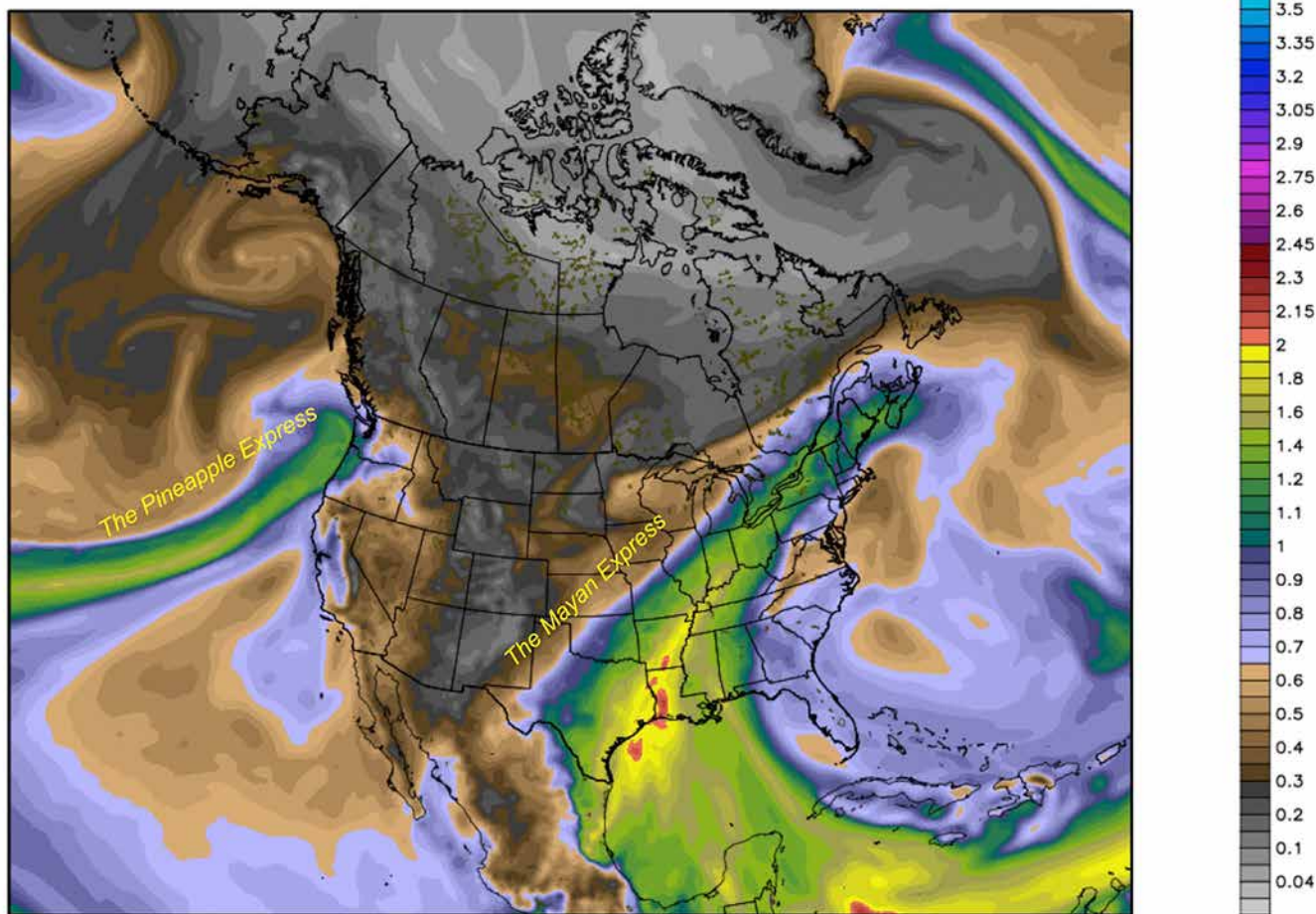


Figure 5.44. The projected 7 day rainfall totals (March 9-16) due to the *Mayan Express*. Note that some areas were forecast to receive as much as 20 inches (51 cm) of rain. Ironically, two atmospheric rivers were forecast to pelt the United States simultaneously (Source/Credit: NOAA/WPC).

NCEP GFS Precipitable Water [inch]  
Init: 12Z09MAR2016 -- [12] hr --> Valid Thu 00Z10MAR2016



GFS [T1534] 3072x1536 sflux Forecast Grid

WxBell<sup>®</sup>

Figure 5.45. Pineapple Express and the Mayan Express fuel moisture plumes to feed both eastern and western United States storms. The image shows precipitable water, or water vapor available for precipitation (Source/Credit: NCEP/NOAA).

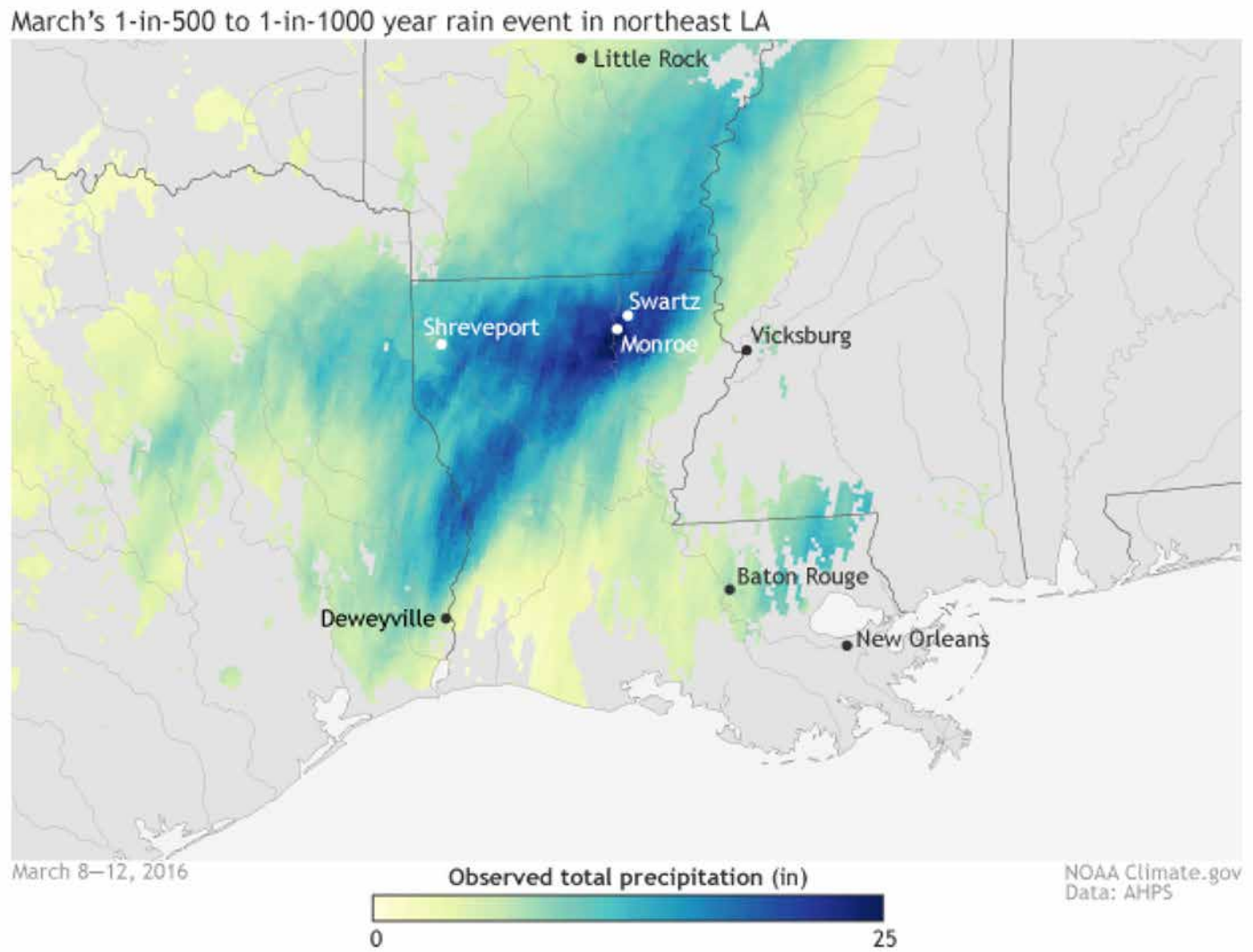


Figure 5.46. Actual precipitation from March 8-12, 2016. In a week, the *Mayan Express* brought over two feet of rain in parts of Louisiana. Some experts estimate that events such as these have a 1/500 to 1/1000 probability of occurring in any given year (Source/Credit: NOAA/AHPS).

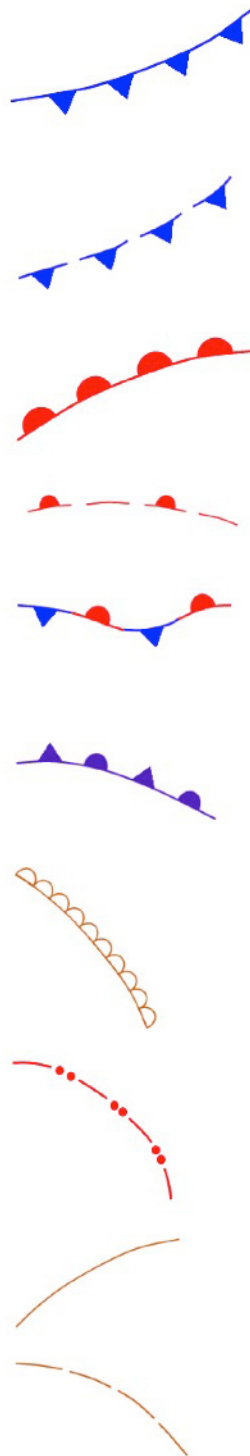
## Fronts

**Fronts** represent the surface boundary between unlike air masses. **When forecasters say that a front is moving into an area, they are really saying that one air mass is replacing another, and the weather is about to change.** The temperature and moisture characteristics of that area are due to be replaced by another air mass with different temperature and moisture characteristics. As the air masses collide, weather disturbances, in the form of strong wind, rain, sleet or snow, are often generated. **The greater the difference in air masses, the more severe the weather is likely to be.** Because the air masses differ, the following changes in weather conditions typically can be expected as a front passes and one air mass is replaced by another:

- temperature
- humidity
- cloud cover
- air pressure (which depends on temperature and moisture)
- wind speed and direction

## Types of Fronts

The four most common types of fronts depicted by the media, such as the Weather Channel or Accuweather are cold fronts, warm fronts, stationary fronts and occluded fronts. The National Weather Service, however recognizes several other types of fronts or discontinuities that can occur between two or more air masses (Figure 5.47). Each type of front tends to be associated with specific weather changes, and each is represented on a surface weather map by a specific symbol. For instance, weather maps display cold fronts with blue triangles; the triangles point in the general direction of frontal movement. Warm fronts are depicted on weather maps by a red line with red half-circles arranged along the side of frontal movement. Occluded fronts are depicted by purple triangles and half-circles on the same side of the frontal line. Dry lines, although not regarded as true fronts, act like fronts in that they are capable of producing uplift. They are depicted on weather maps by small, brown, open half-circles (dashed lines on some maps). The symbol for a stationary front is a line along which half-circles (red) and triangles (blue) alternate in sequence along opposite sides of the line. Fronts are often associated with cyclones. The National Weather Service has a standard set of symbols for fronts and other discontinuities (Figures 5.48a, 5.48b, and 5.48c). National Weather Service maps are published several times a day and can be accessed through their website.



**Cold front:** a linear zone separating a cold and warm air mass where the cold air is the aggressor and is replacing warm air with time. Shown is a cold front advancing toward the SSE.

**Cold frontogenesis:** a forming cold front. Other types of frontogenesis (e.g., warm frontogenesis) are similarly shown as symbols separated by a dashed line.

**Warm front:** a linear zone separating a cold and warm air mass where the warm air is the aggressor and is replacing cold air with time. Shown is a warm front advancing toward the NNW.

**Warm frontolysis:** a weakening, or dissipating warm front. Other types of frontolysis (e.g., cold frontolysis) are similarly shown by a dashed line with symbols on alternate dashes.

**Stationary front:** a linear zone separating cold and warm air masses that shows little or no movement in time

**Occluded front:** a linear zone where a cold front has overtaken a warm front. Surface air on either side of the front is typically cool to cold. Warm air has been displaced aloft.

**Dry line:** a linear zone separating warm, dry air from warm, moist air. Some weather maps depict dry lines by a series of black dashed lines. Dry lines are quite common in the south-central plains of the United States.

**Squall line:** a linear zone of convergence and associated uplift, typically associated with thunderstorms, that is non-frontal, but often occurs in advance of a cold front.

**Tropical wave:** a linear zone of non-frontal convergence in tropical or subtropical areas embedded within the trade winds.

**Trough (trof):** a linear zone of low pressure (vs. a circular cell). Some maps use the same symbol to depict an outflow boundary.

Figure 5.47. Symbols used by the National Weather Service to depict different kinds of fronts and discontinuities on surface weather maps (Source/Credit: modified from NWS).

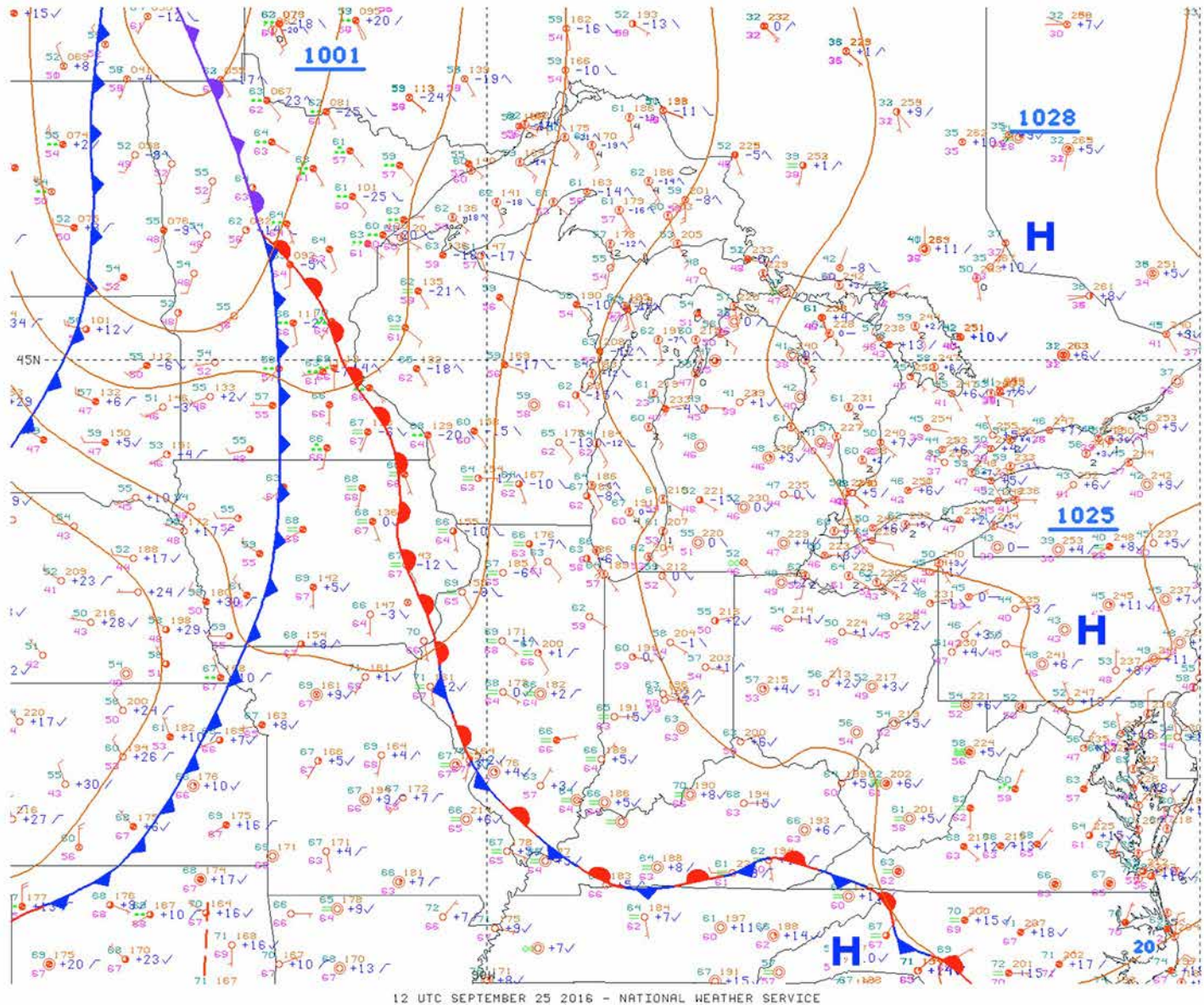


Figure 5.48a. Surface weather map for September 25, 2016 at 7:00 AM CDT. Frontal types depicted include two cold fronts (solid blue triangles), a warm front (solid red half-circles), an occluded front (solid purple half circles and triangles) and a stationary front (solid blue triangles and solid red half circles alternating). The light brown lines are isobars. Scores of weather station models with their appropriate symbols for weather observations are scattered across the map (Source/Credit: NWS).



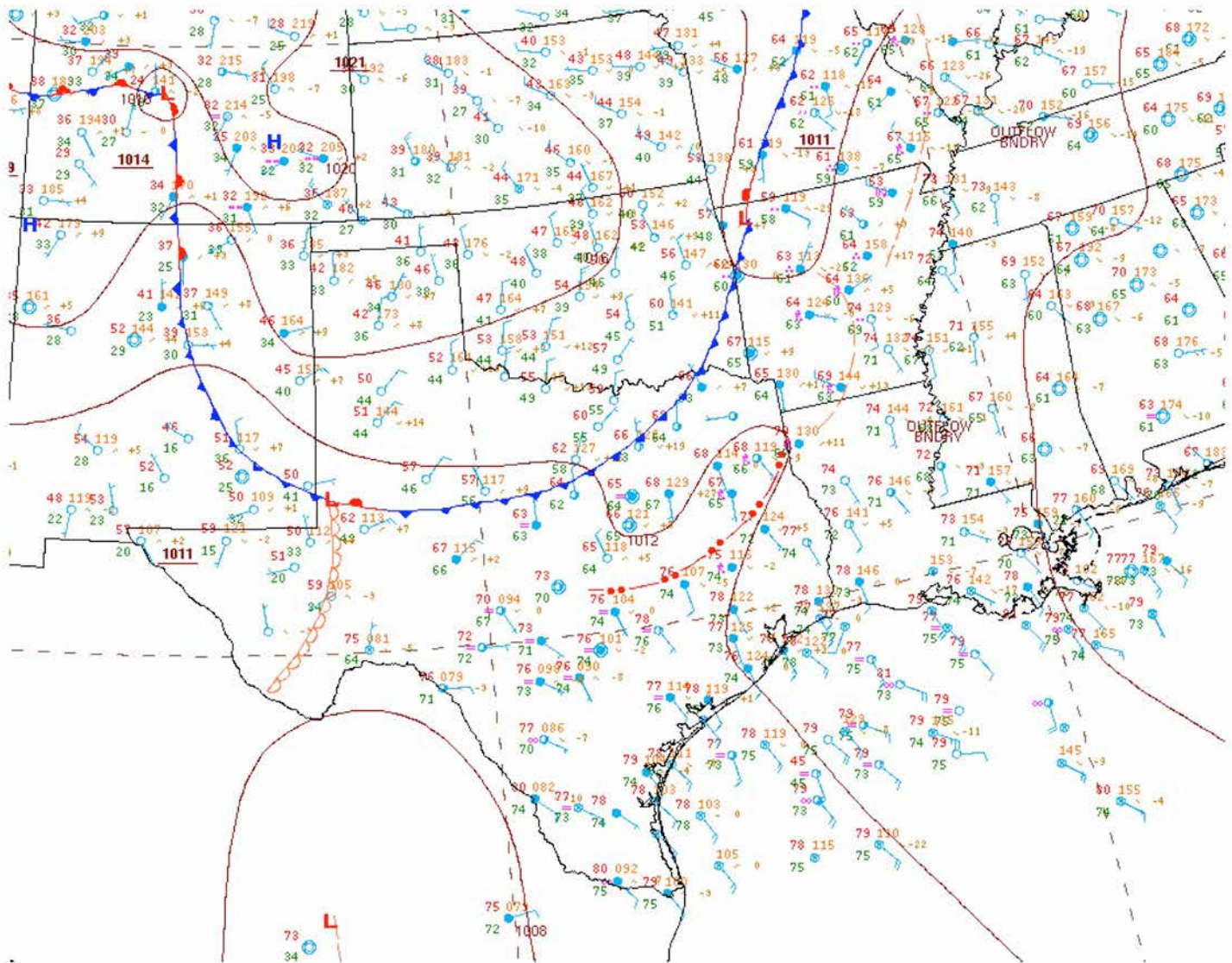


Figure 5.48b. Surface weather map for May 11, 2015 at 8:00 AM CDT. Frontal types depicted include a cold front (solid blue triangles), a warm front (solid red half-circles), a stationary front (solid blue triangles and solid red half circles alternating), a dry line (small, brown, open half-circles), and a squall line (red dots and dashes). The light brown lines are isobars. Scores of weather station models with their appropriate symbols for weather observations are scattered across the map (Source/Credit: NWS).

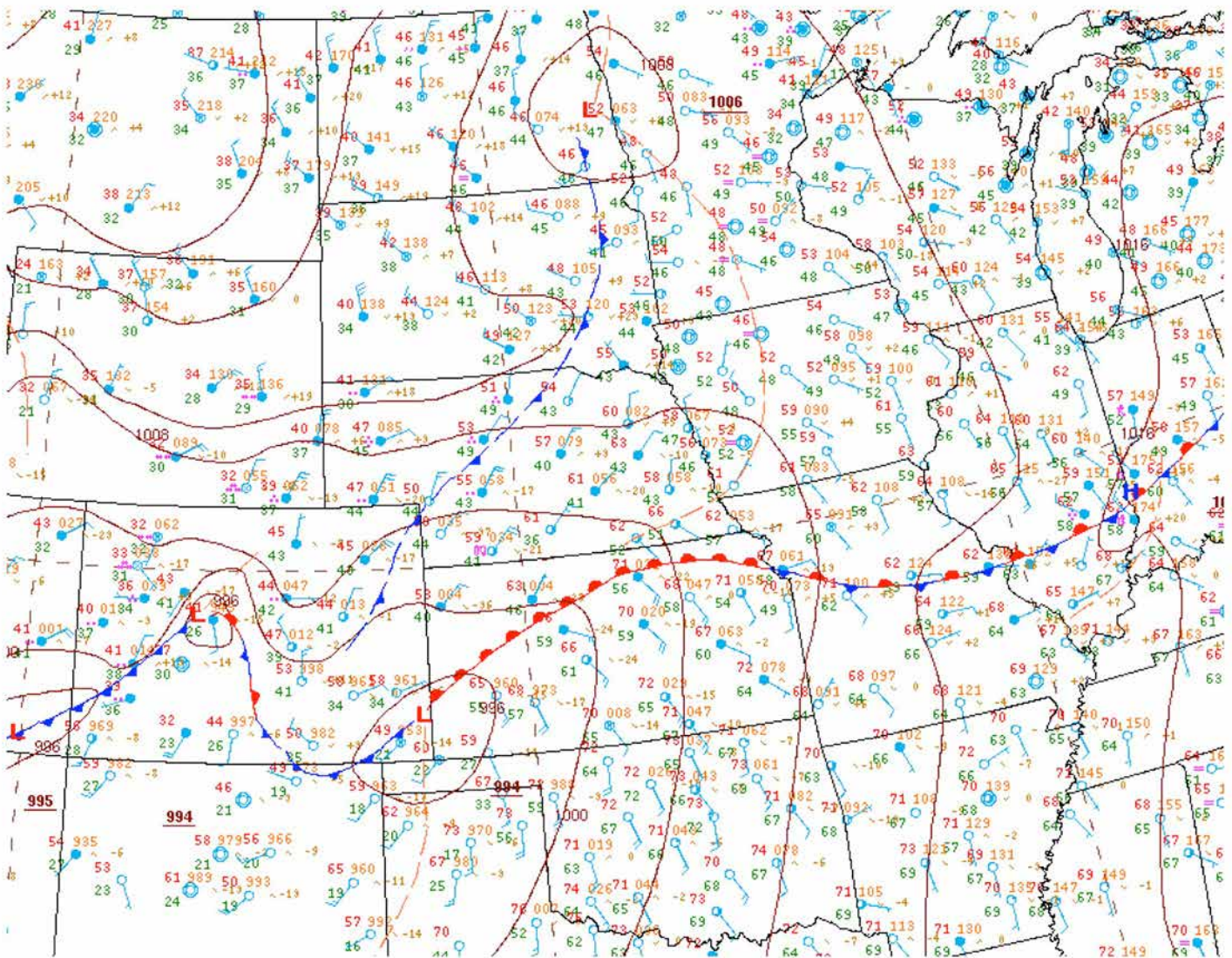


Figure 5.48c. Surface weather map for May 11, 2014. Frontal types depicted include a cold front (solid blue triangles), a warm front (solid red half-circles), a stationary front (solid blue triangles and solid red half circles alternating), and the dashed blue line with solid blue triangles on alternating dashes indicates cold frontolysis, or a dissipating cold front (Source/Credit: NWS).

## **Cyclones and Anticyclones**

When pressure systems on a surface map display a series of closed isobars in a circular or oval pattern, they are referred to as anticyclones or cyclones. Cyclones are low pressure centers frequently associated with foul weather. Anticyclones are high pressure centers and typically bring fair weather and clear skies. Large cyclonic and anticyclonic systems in the middle and high latitudes are often associated with two or more air masses, and fronts form at the line of contact. These **frontal-cyclones** are one of the most prominent weather producers in these latitudes.

## Anticyclones

On a weather map, an anticyclone appears as a series of concentric isobars, with higher pressure toward the center (Figure 5.49). This pattern may develop when cold, dry air sinks (subsides) toward the surface, or when air is forced to subside because of upper-level flow patterns (Figure 5.50). When the air approaches the surface, it is forced to flow outward (divergent flow). Because of the Coriolis Force, the outward-flowing air is deflected to the right of its direction of motion in the Northern Hemisphere, and so the air spirals outward from the center of the anticyclone in a clockwise fashion. In the Southern Hemisphere, the air spirals counterclockwise. **So, in the Northern Hemisphere, an anticyclone is characterized by air that flows downward, outward, and clockwise.** In the Southern Hemisphere, an anticyclone is characterized by air that flows downward, outward and counterclockwise.

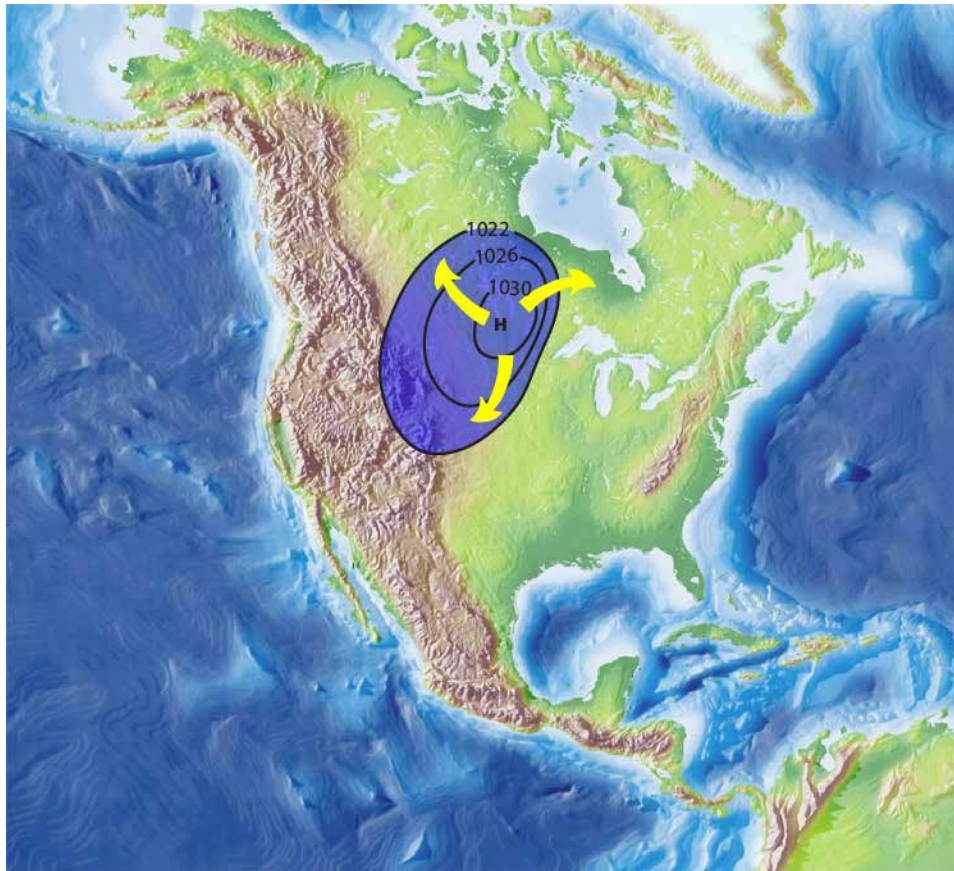


Figure 5.49. Anticyclones are represented by closed isobars in which the pressure increases toward the center of the pressure system. The cold, dry air in an anticyclone sinks towards the surface and then flows outward from the center of the system. In the Northern Hemisphere, the air flows outward in a clockwise fashion as a result of the Coriolis Force. In the Southern Hemisphere, it flows counterclockwise.

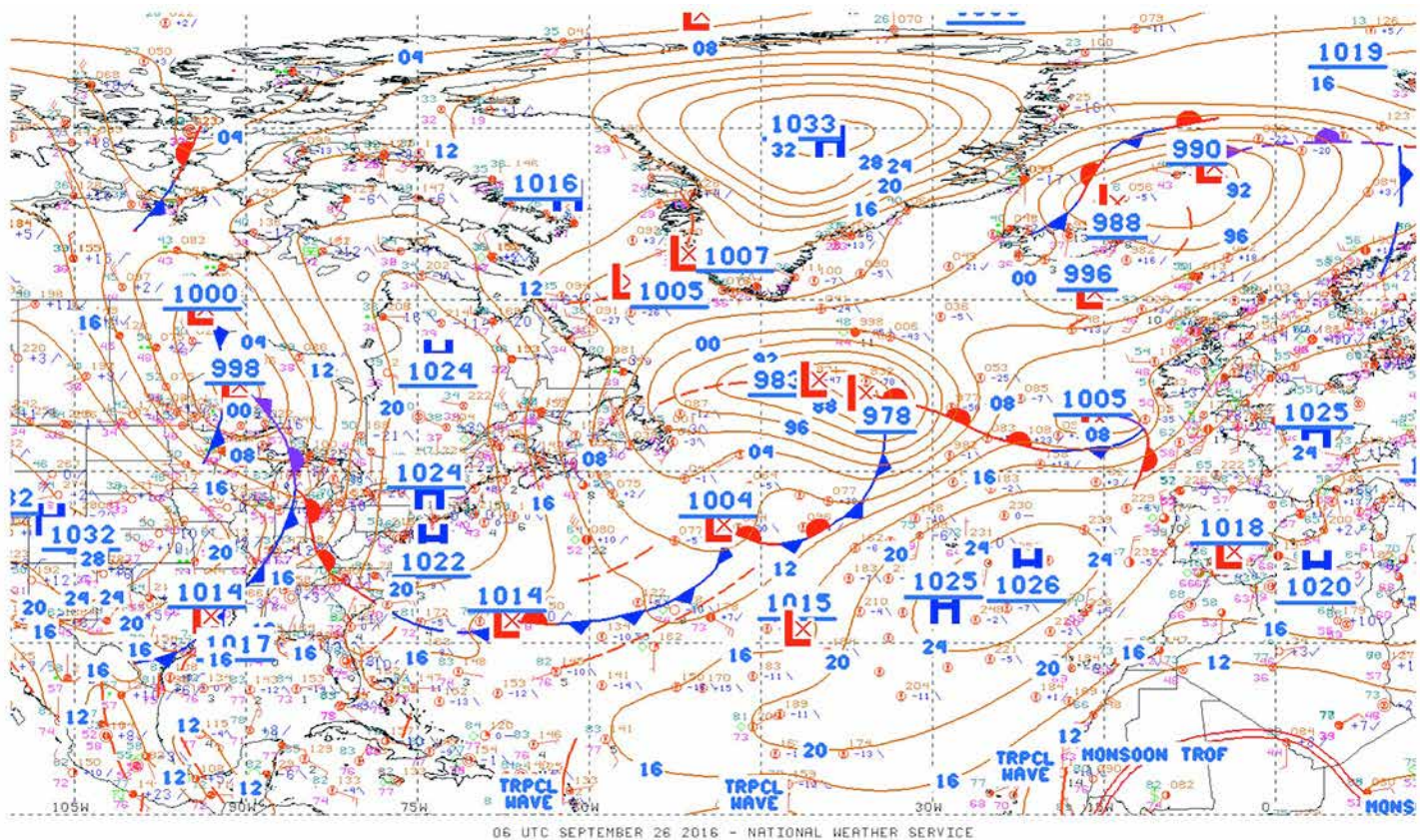


Figure 5.50. Surface weather map for September 26, 2016, 1:00 A.M. CDT. A series of frontal-cyclones are indicated over the eastern United States and Canada, mid-latitude North Atlantic Ocean and high-latitude Atlantic Ocean between Greenland and Europe. Each cyclone is associated with a variety of fronts and foul weather. There is a well-developed anticyclone (high pressure system) over Greenland due to the frigid temperatures. A second anticyclone to the west of the Iberian Peninsula (Spain and Portugal) is part of the quasi-permanent oceanic subtropical high, caused by upper level convergence. The anticyclones are associated with clearer skies (Source/Credit: NWS).

Anticyclones in the middle and high latitudes are associated with the source regions of cold, polar air masses. The average diameter of an anticyclone is the same as that of a typical air mass, i.e., about 1000 miles (1600 km). Because anticyclones are relatively cloudless, they cannot be directly detected from satellite imagery based on cloud patterns; rather, their existence is determined based on pressure and wind patterns.

## Cyclones

Cyclones are characterized by closed isobar patterns, approximately 500-1000 miles (800-1600 km) in diameter, in which the pressure *decreases* toward the center (Figures 5.51 and 5.50). Thus, they are low pressure systems and, as with all low pressure systems, they are characterized by rising air. As air flows toward the center of the cyclone, the Coriolis Force and pressure gradient force cause the air flow to be convergent. *In the Northern Hemisphere, cyclones are characterized by convergent, counterclockwise surface flow, and vertical uplift.* In the Southern Hemisphere, cyclones are characterized by convergent, clockwise surface flow and vertical uplift.

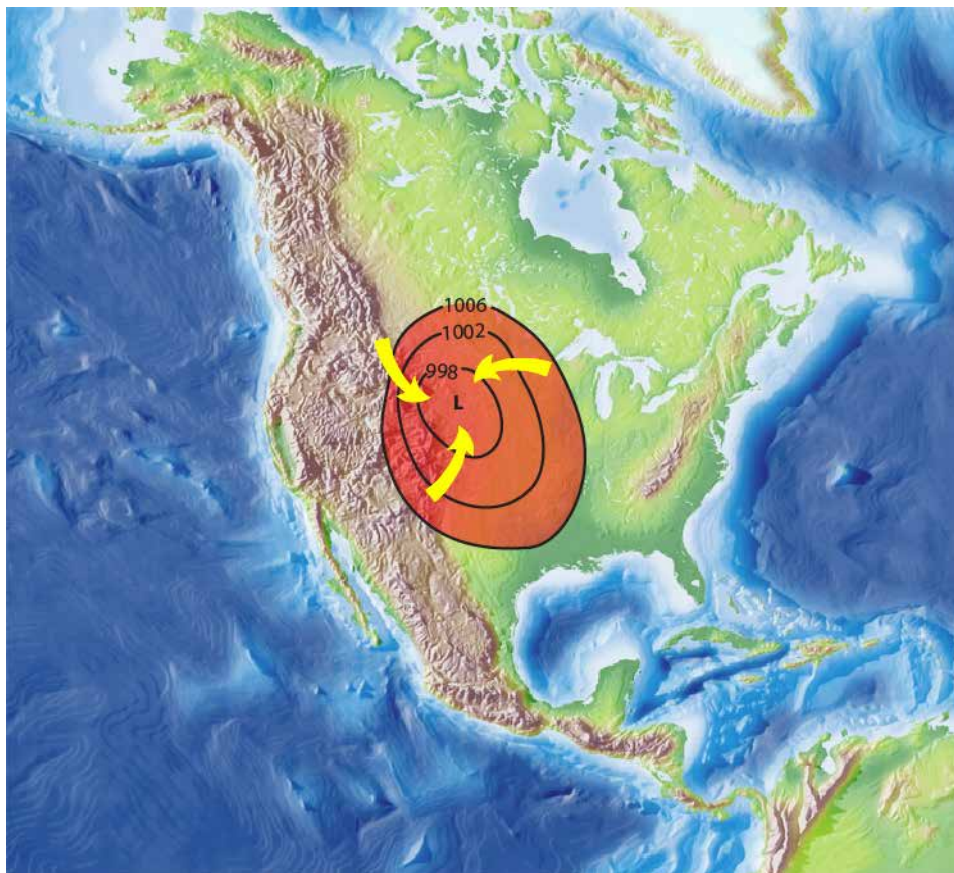


Figure 5.51. Cyclones are represented by closed isobars in which the pressure decreases toward the center of the pressure system. Air in a cyclone flows toward the center of the system and rises upward. In the Northern Hemisphere, the air flows inward in a counterclockwise fashion as a result of the Coriolis Force. In the Southern Hemisphere, it flows clockwise.

The pressure at the center of the cyclone is low because the air tends to be warm and moist, both of which decrease the density of the air. Furthermore, as the moisture in the rising air condenses, it releases heat energy to the air and warms it, thereby decreasing the pressure even more. As a result, the pressure gradient intensifies, winds blow more strongly, and precipitation usually occurs (Figures 5.52a and 5.52b). Cyclones are typically associated with stormy weather. Mariners have used barometers for over four centuries to detect falling pressure in hope of predicting foul weather.

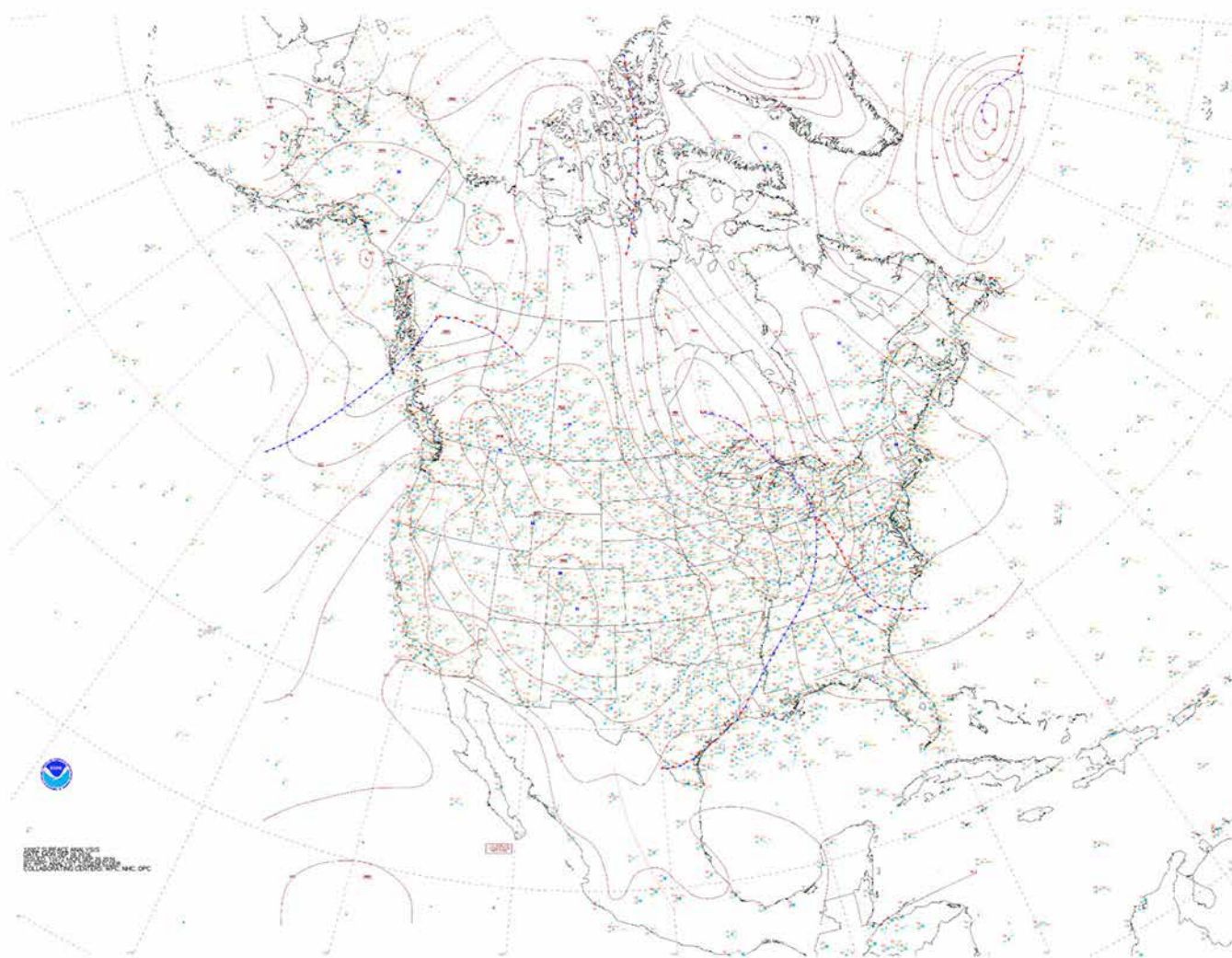


Figure 5.52a. Surface weather map for September 26, 2016 at 7:00 AM CDT. The eastern half of North America is dominated by a frontal-cyclone whereas much of the western side of the continent is dominated by an anticyclone. Another frontal-cyclone has entered British Columbia and will travel eastward, driven by upper-level westerly winds (Source/Credit: NWS).

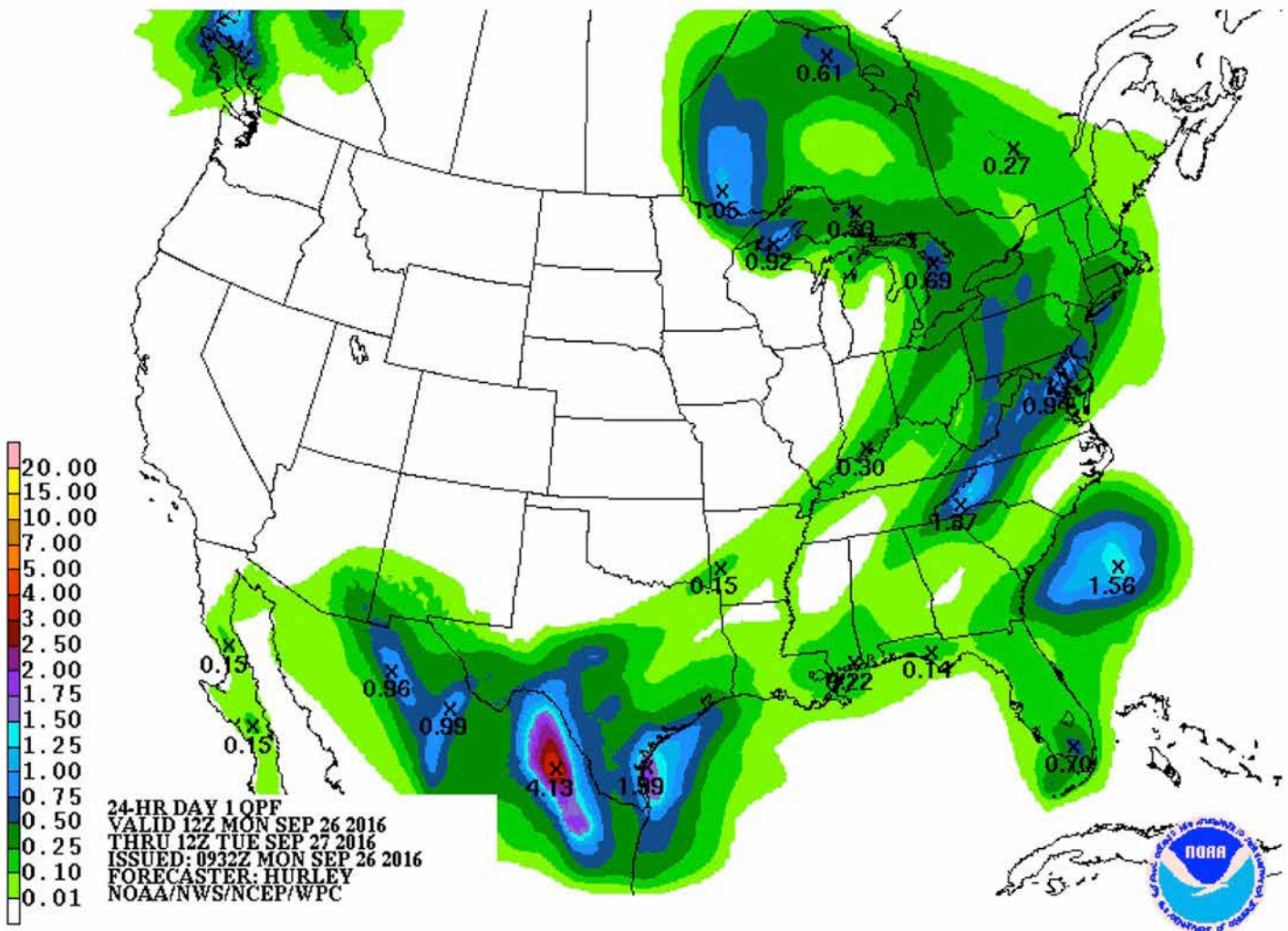


Figure 5.52b. Forecast precipitation for Monday, September 26, 2016. The linear belt of forecast precipitation coincides with a large frontal-cyclone. A second area of forecast precipitation in British Columbia is caused by an approaching frontal-cyclone (Credit/Source: NWS).

Because of their cloudiness, cyclones (including hurricanes) can be directly detected with satellite imagery. The clouds form a counterclockwise spiral pattern in the Northern Hemisphere and a clockwise spiral pattern in the Southern Hemisphere.



## Development of Frontal Cyclones

**Frontogenesis** refers to the development of fronts from non-frontal conditions. Frontogenesis is favored by convergent conditions that bring different types of air masses in contact. In the mid-latitudes of either hemisphere, traveling cyclones favor the development of fronts because they typically draw in air from different directions and therefore different source regions. **Frontolysis** represents the dissipation or decay of a frontal boundary. As frontal cyclones move, they encounter conditions where the air masses on either side of the front becomes progressively more similar (e.g., over open ocean waters away from their source regions). At some point the air masses become so similar in nature that they undergo frontolysis, and soon may disappear from the weather map.

Classic mid-latitude wave frontal-cyclones develop along the boundary between cold polar air to the north and warmer tropical or subtropical air to the south. This boundary is known as the **Polar Front**. The air around the North Pole flows from the northeast as part of the Polar Easterlies. South of the Polar Front, the air flow is from the west, i.e., it is part of the Westerlies. In short, air converges from opposite directions along the Polar Front (Figure 5.53).

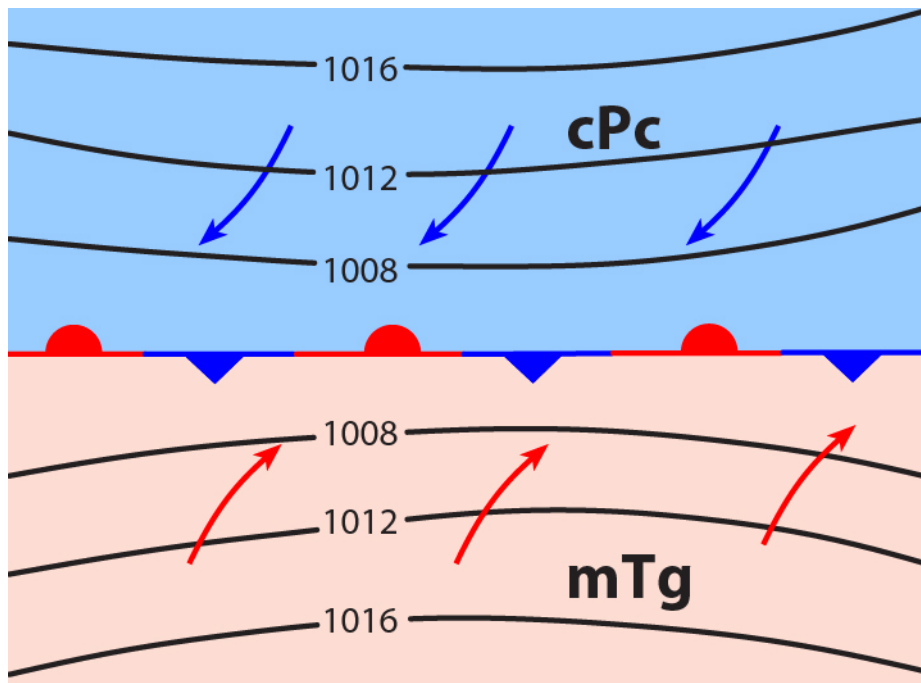


Figure 5.53. The Polar Easterlies and Westerlies converge along the Polar Front. If the boundary is stationary, a stationary front exists in the initial stage of development of a mid-latitude wave cyclone.

Because of the inherently unstable nature of the Polar Front boundary caused by the convergence of air flowing in opposite directions, and by temperature differences, a kink or bend (a deepening of pressure), eventually develops along the boundary (Figure 5.54).

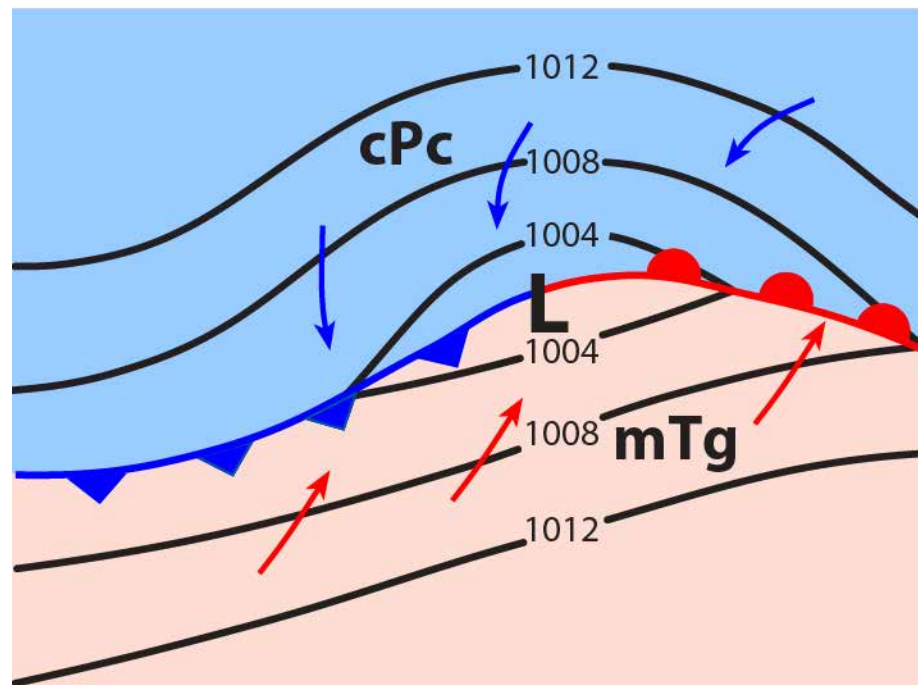


Figure 5.54. The convergence of opposing winds along the boundary between cold air to the north and warm air to the south produces an unstable situation. The instability eventually gives rise to an undulation, or wave, which evolves into a warm front and a cold front. As the undulation grows, a warm front develops on the eastern side of the wave as warm air moves northward and eastward. A cold front develops on the western side as cold air moves southward and eastward.

This bend, or deformation, of surface pressure is frequently linked to upper-level divergence. When viewed on a weather map, the pattern formed by the two air masses initially resembles a wave, hence the name mid-latitude wave cyclone. As soon as the bend develops, two fronts come into existence; a cold front to the west of the kink in the boundary, and a warm front to the east. This frontal pattern now resembles a wave, and the wave is carried eastward, and usually southward, by the Westerlies and other pressure conditions in the region. In addition to cold and warm fronts, stationary and occluded fronts occur in association with wave cyclones.

## Cold Fronts

A cold front occurs when a cold air mass overtakes and replaces a warm air mass (Figures 5.55a and 5.55b). In the United States, the most common air masses that interact to produce cold fronts are cPc air masses from Canada or Alaska, and mTa or mTg air masses from the Atlantic or Gulf of Mexico. Cool air masses traveling eastward from the Pacific (mPp) also affect weather in the United States.

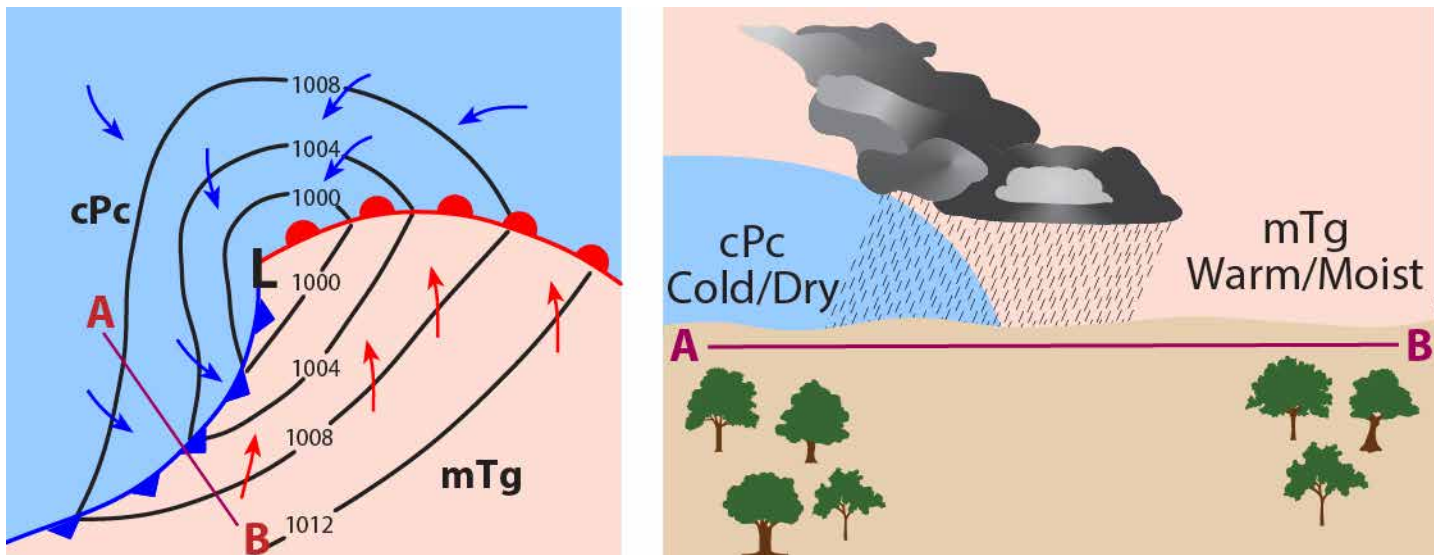


Figure 5.55a (left). Conditions that exist along the portion of the cold front are indicated by the transect from A to B.

Figure 5.55b (right). As the cold, dry, dense air from Canada collides with the warm, moist low density air from the Gulf of Mexico, the warm, moist air is forced upward along the frontal boundary. As the air rises and cools, precipitation is produced. Cold fronts have steep boundaries that produce rapid uplift and often severe storms.

**Cold fronts generally move faster than warm fronts** and have an average speed of about 25 to 30 mph (40 to 48 kph). Their rapid movement is associated with steep pressure gradients due to the greater difference in temperature and moisture between the cold and warm air masses, as well as to the fact that cold air is more efficient in displacing warm air than vice versa.

**The frontal boundary of a cold front is steep relative to that of a warm front.** Generally speaking, the boundary rises one foot for every 40 to 80 feet of horizontal distance (slope = 1/40 to 1/80). This rather steep slope, by frontal standards, is due to a combination of the rapid speed of motion of the cold air mass and friction with the ground. Because the lower part of the air mass is slowed by friction with the ground, while the upper part continues to move rapidly, the frontal boundary steepens.

Because warm, moist air is less dense than cold dry air, **warm air rises along the cold front boundary when the cold air collides with the warm air**. Because of both the rapid speed of motion of the cold air mass and the associated steep frontal boundary, the rapidly rising air cools quickly and releases its latent heat of condensation, adding further fuel for severe storms. **The steep frontal boundary of a cold front results in rapid uplift of moist air. This may result in the development of cumulonimbus clouds and potentially severe weather.**

As uplift produces condensation, there is also high potential for either intense rain or snow to occur, depending upon the temperature. In the spring, temperature and moisture differences between the polar and tropical air masses are at their greatest, and this is one reason why the most severe weather occurs at this time of the year.

Not all cold fronts are associated with severe weather. If the vertical lapse rate dictates stable air, cold fronts tend to produce stratiform clouds and less intense precipitation. Some cold fronts do not generate precipitation at all.

The approach and passage of a classic cold front in the Northern Hemisphere typically produces the following weather patterns, referred to as **cold front weather** (Figures 5.56a, 5.56b, 5.56c and 5.57a, 5.57b, 5.57c, 5.57d).

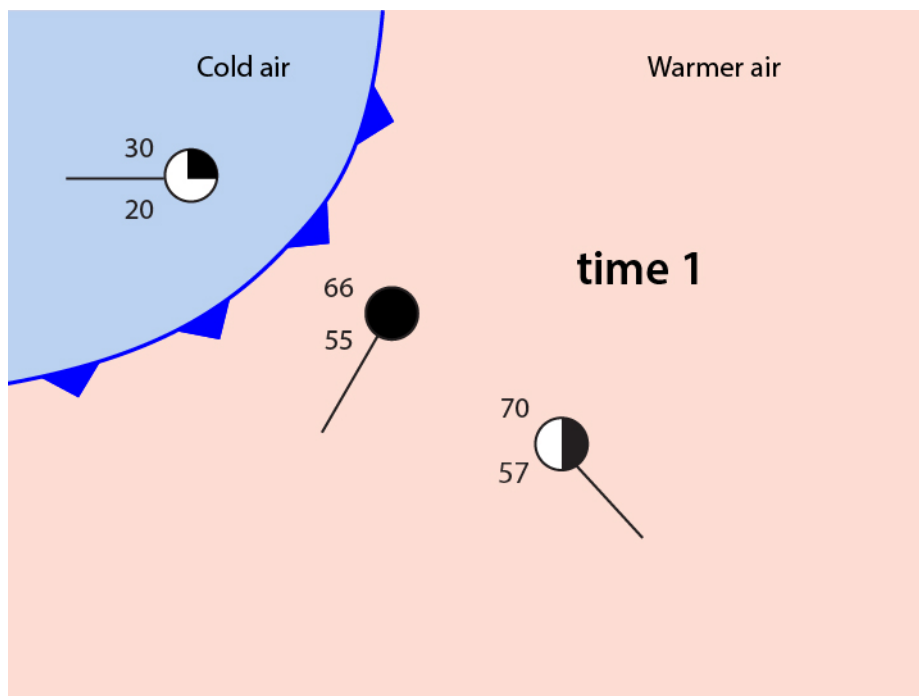


Figure 5.56a. Sketch of some of the weather characteristics that hypothetically occur within the cold and warm air masses separated by a cold front in the Northern Hemisphere. Note the temperatures (70, 66, and 30), dew points (57, 55, and 20), wind directions (SE, SW, W) and cloudiness (50, 100, and 25%) of the weather stations far in advance of the front, closer to the front, and behind the front. The following two figures illustrate changes that typically occur with time to each station as the front approaches and passes each station.

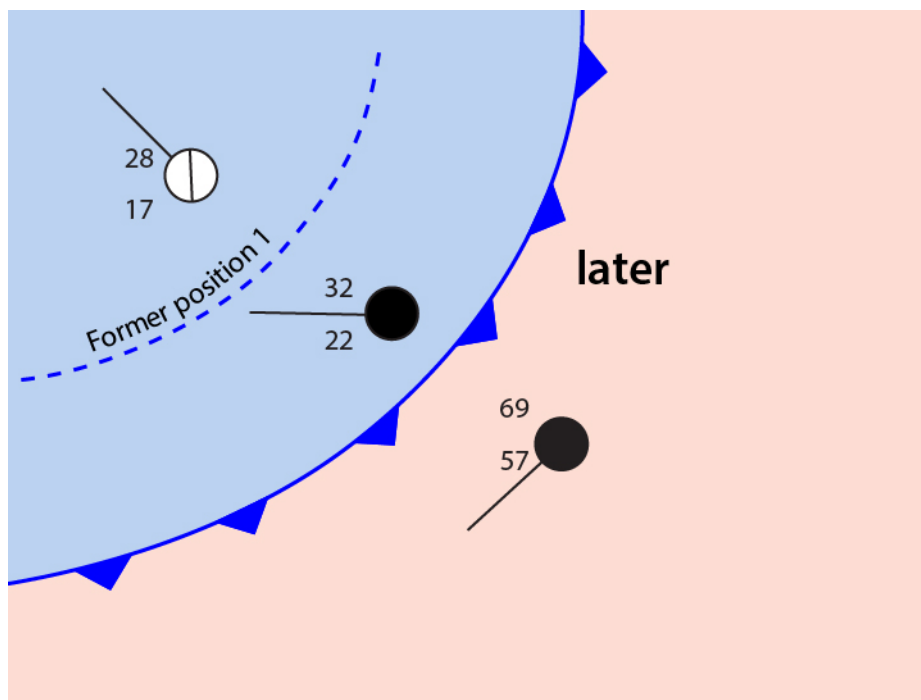


Figure 5.56b. Some time after time 1, the cold front advances and brings significant changes to the middle station. The dashed line marks the former position of the cold front.

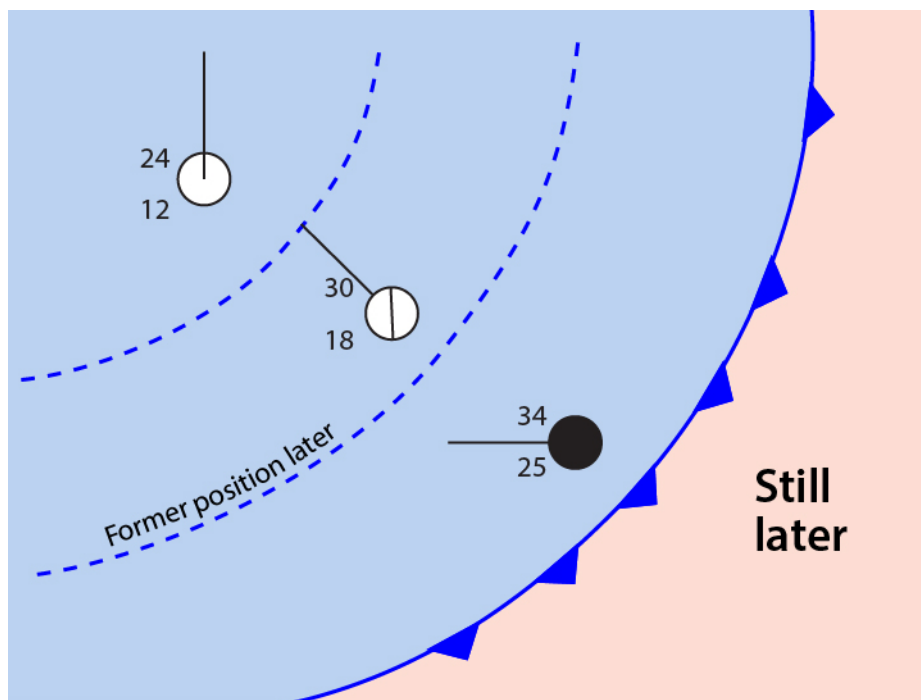


Figure 5.56c. At a still later time, the cold front advances farther, and all three weather stations are now under the domination of cold air. The dashed lines mark the former positions of the cold front.

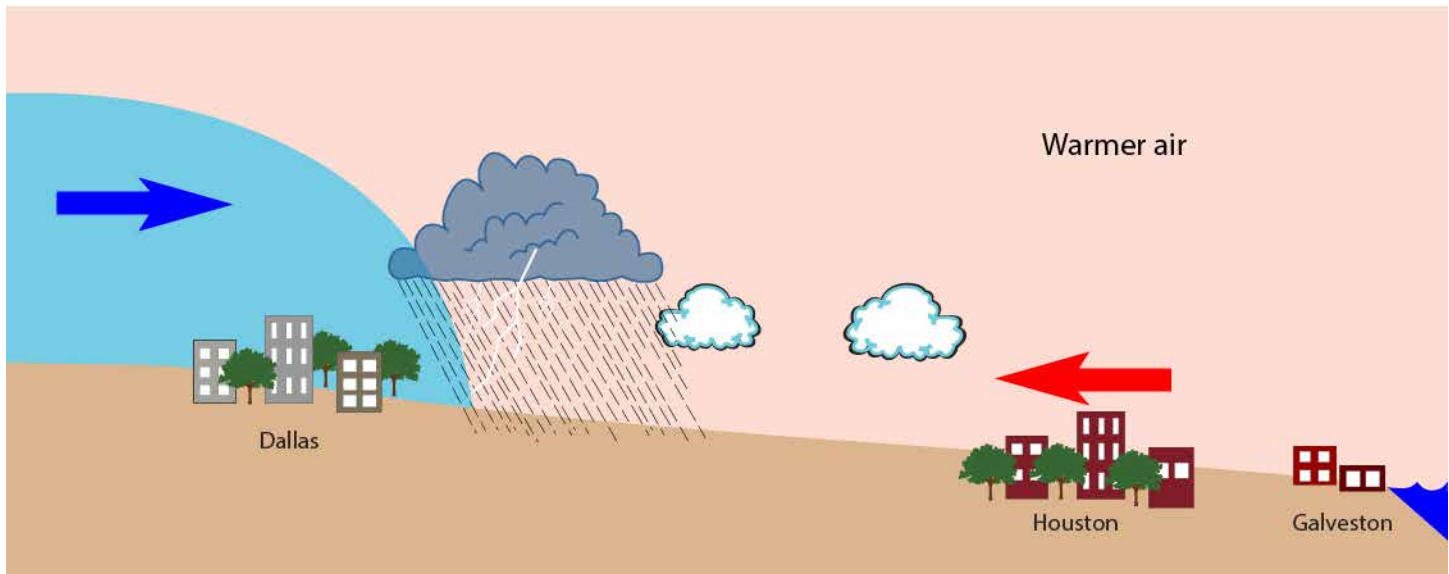


Figure 5.57a. Cross-sectional sketch of a cold front that has just moved through Dallas and is eventually headed for Galveston. The worst weather typically occurs in a narrow belt on either side of the cold front. Not all cold fronts follow this pattern. Sometimes, foul weather can take place considerably in advance of the cold front, or considerably behind the cold front. Some cold fronts do not produce any precipitation. The cold front might also lose momentum and stall, never reaching Galveston. After stalling it may become a stationary front, or even reverse direction and become a warm front.

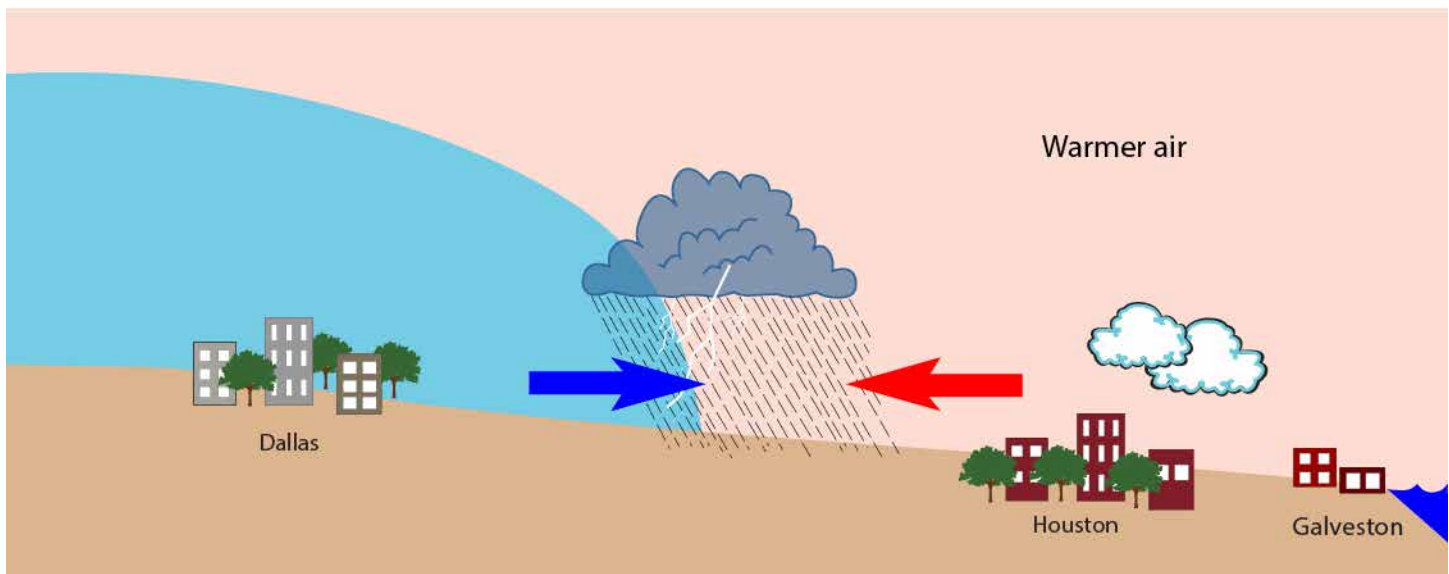


Figure 5.57b. Cross-sectional sketch of a cold front as it progresses toward Galveston. A pressure drop and a few scattered cumulus clouds might be clues that a front is approaching.

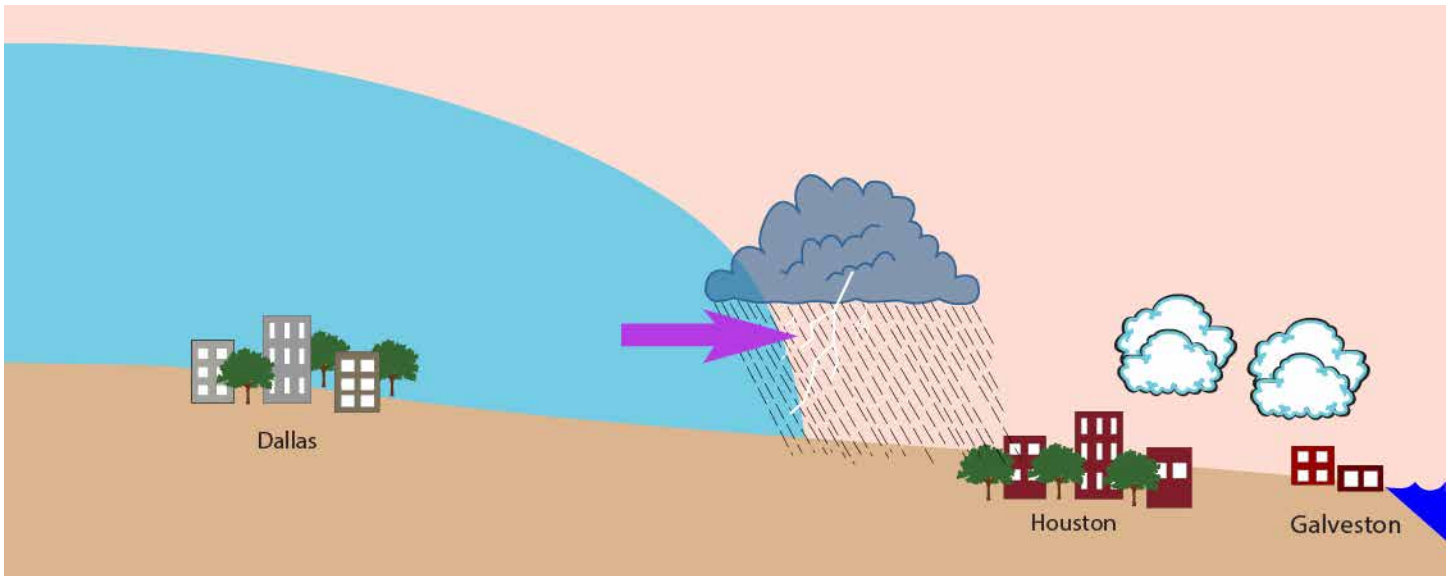


Figure 5.57c. Cross-sectional sketch of a cold front as it nears Galveston. A continued drop in pressure and an increasing cloud cover indicate the possible approach of a front.



Figure 5.57d. Cross-sectional sketch of a cold front as it rolls through Galveston. Shortly, the weather should improve and the pressure will begin to rise. The timetable for the front to travel from Dallas to Galveston could be hours to days, depending on the speed of the front.

- **Air pressure drops as the cold front approaches** due to the uplift of warm air and the condensation of the moisture in that air. Fronts of any type tend to generate low pressure belts, so their approach is signaled by a drop in pressure. This is the basis for decorative home barometers that indicate what the weather is going to do. If the pressure drops enough, it is a sure sign of an approaching low which may bring foul weather.
- **Cloudiness increases** as the front approaches. Initially, cirrus clouds may be present at high altitude, but as the front approaches the height of the clouds decreases and they commonly are replaced by cumuliform clouds (cumulus humilis, cumulus congestus or cumulonimbus).
- With the approach of the cold front, **winds shift** from southerly to southwesterly.
- After the front passes, the **winds shift** to the west, then northwest, and then north.
- After the front passes, both the **temperature and humidity drop** because colder, drier air has replaced the warmer, more moist air. As a result, the pressure begins to rise.
- After the front passes, the **skies begin to clear** because the humidity level in a cold air mass is low, the slope of the front lessens, and the atmosphere becomes more stable as high pressure moves in. The bluest, clearest skies occur in winter because the air is so dry at that time of the year. Under such dry conditions, very little light is scattered by moisture in the air, and so the sky appears deep blue.

In summary, warm, moist low-pressure conditions exist before a cold front arrives, and cold, dry, high-pressure conditions exist after it passes. Winds are initially from the south-south west, but they shift to the west-northwest and finally north after the front has passed.

The cold fronts that form on the leading edge of cPc air masses and move quickly southward are often termed **Blue Northers**. The term may be derived from the fact that once these very cold air masses pass, they leave in their wake exceeding deep blue skies.



The cold air mass typically takes the form of an anticyclone as it moves equatorward (Figure 5.58). The eastward movement of the eastern side of the anticyclone typically produces a cold front, whereas a warm front (or stationary front along the Rockies) may occur on the western side of the pressure system.

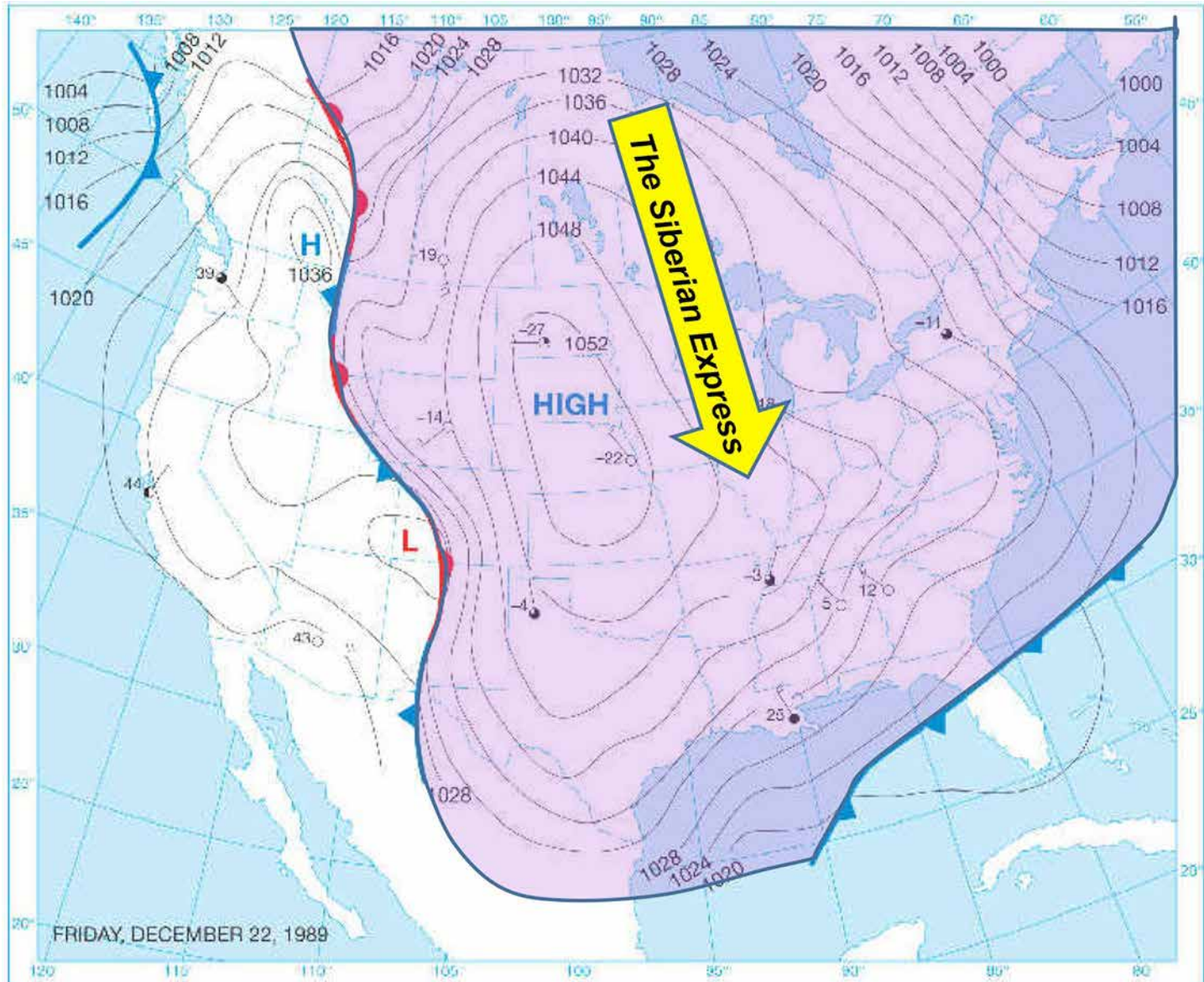


Figure 5.58. Anticyclones (highs) typically form the core of polar air masses. The colder the air in the core, the higher the atmospheric pressure. The central pressure shown here is just over 1052 millibars and the core temperature is between minus 22° and minus 27°F (minus 30° and minus 33°C). This cold-air outbreak on December 22, 1989 began as a Siberian air mass, crossed the North Pole, and maintained sub-zero temperatures all the way to north Texas. This event brought subfreezing temperatures as far south as the Gulf of Mexico (Source/Credit: NWS).

## Warm Fronts

A warm front occurs when a warm air mass replaces a cold air mass. In the United States, this generally means that an mTg air mass replaces a cPc air mass. The average speed of a warm front is 15 mph (24 kph), or about half that of a cold front (Figures 5.59a and 5.59b).

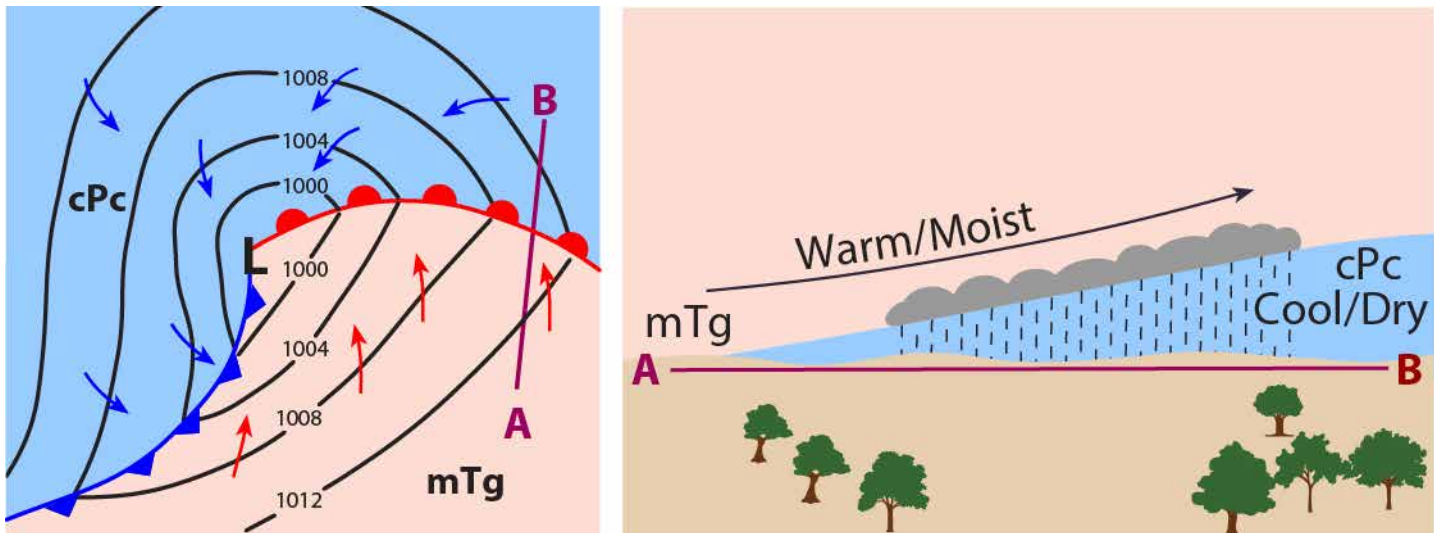


Figure 5.59a. (left) In a warm front, warm air rises up and over cold air as both air masses move to the east. Because the frontal boundary is gentle, the rate of uplift is slow and there is little cumulus cloud development and showers are generally gentle in nature. A cross-section of the transect from A to B is shown in Figure 5.59b.

Figure 5.59b. (right) The more gentle boundary of a warm front produces a slower rate of uplift and generally less severe weather than that of a cold front. Precipitation is often spread over a wider band along the frontal boundary. Cirrus clouds generally precede the arrival of the warm air mass by 12 to 24 hours. Note the lowering of the cloud base and the change in cloud type as the front draws nearer.

Warm fronts have a frontal slope of 1/100 to 1/200, which is considerably less steep than that of a cold front. The slope is more gentle because the warm air produces a streamlining effect as it overrides the cold air. Because of the slower rate of uplift and condensation along the more gently sloping frontal boundary, the storms associated with a warm front are typically less intense than those of a cold front. With sufficient vertical instability, however, warm fronts can generate severe thunderstorms, which can be tornadic.

Prior to the approach of the warm front, cooler, relatively dry, high pressure conditions exist in the area dominated by cPc air. However, as with a cold front, the pressure begins to drop as the front approaches and the warm, moist air is uplifted along the frontal boundary. After the front passes, warmer, more humid conditions occur and the pressure may be somewhat variable to steady for several hours.

The approach of a warm front is typically first indicated by cirrus and cirrostratus or cirrocumulus clouds about 12 to 24 hours in advance of the front (Figures 5.60a and 5.60b). As the front draws closer, the cloud deck continuously lowers, and the high-level cirroform clouds give way to altostratus or altocumulus, and finally low-level stratus, stratocumulus or nimbostratus (if precipitation occurs). Prior to the passage of the front, winds are from the east or northeast. Afterwards, the winds are from a southerly direction. Since warm fronts are broad bands of cloudiness and precipitation, often several hundred miles in width, and since they travel more slowly than cold fronts, warm front weather typically lasts much longer than cold front weather. The duration and intensity of weather associated with warm front weather, however, is variable, and depends on the size of the system, its rate of movement, and the stability characteristics of the atmosphere.

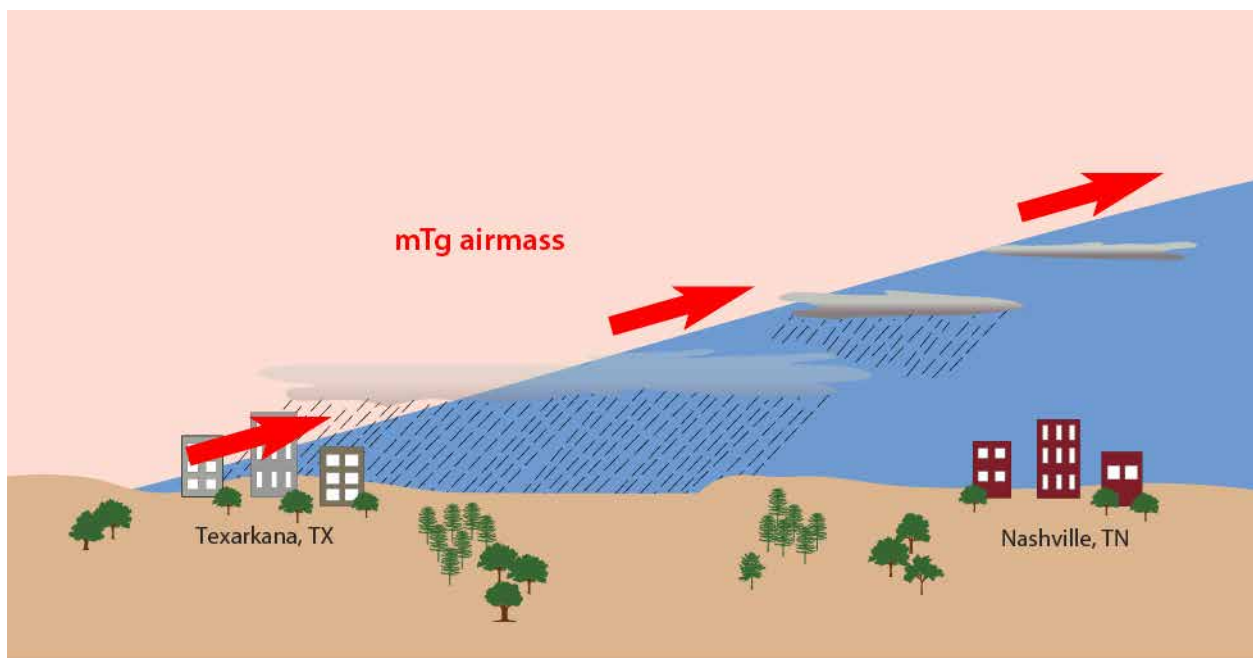


Figure 5.60a. Cross-sectional sketch of a warm front that is just about to pass over Texarkana, headed eventually for Nashville, Tennessee (500 miles/800 km) and beyond. The cloud cover and precipitation associated with warm frontal passage tends to be more widespread geographically, less intense and last longer than changes that accompany the passage of a cold front. The first signs of the approach of the warm front at Nashville are the appearance of high-level cirroform clouds and perhaps a slight drop in pressure. The occurrence of cirroform clouds, however, does not necessarily indicate the approach of any kind of front or bad weather.

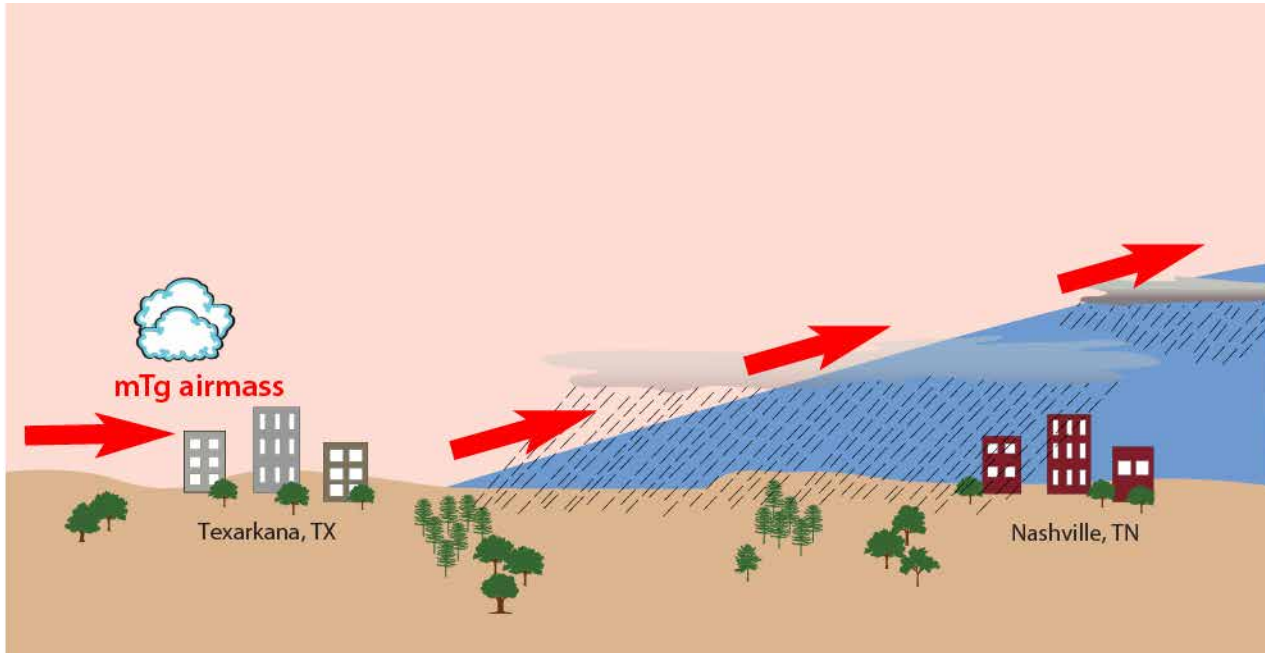


Figure 5.60b. Cross-sectional sketch of a warm front after passage over Texarkana. Texarkana should have experienced a slight change in wind direction from SE to S. More dramatically, Texarkana should observe a substantial warming trend after warm front passage as well as a large jump in dew points. Skies should partially clear, typically leaving scattered cumulus clouds. Nashville, still hundreds of miles ahead of the front, may notice a change from high, cirroform clouds (e.g., cirrus, cirrostratus, cirrocumulus), to slightly darker, middle-level clouds (e.g., altostratus or altocumulus) over time.

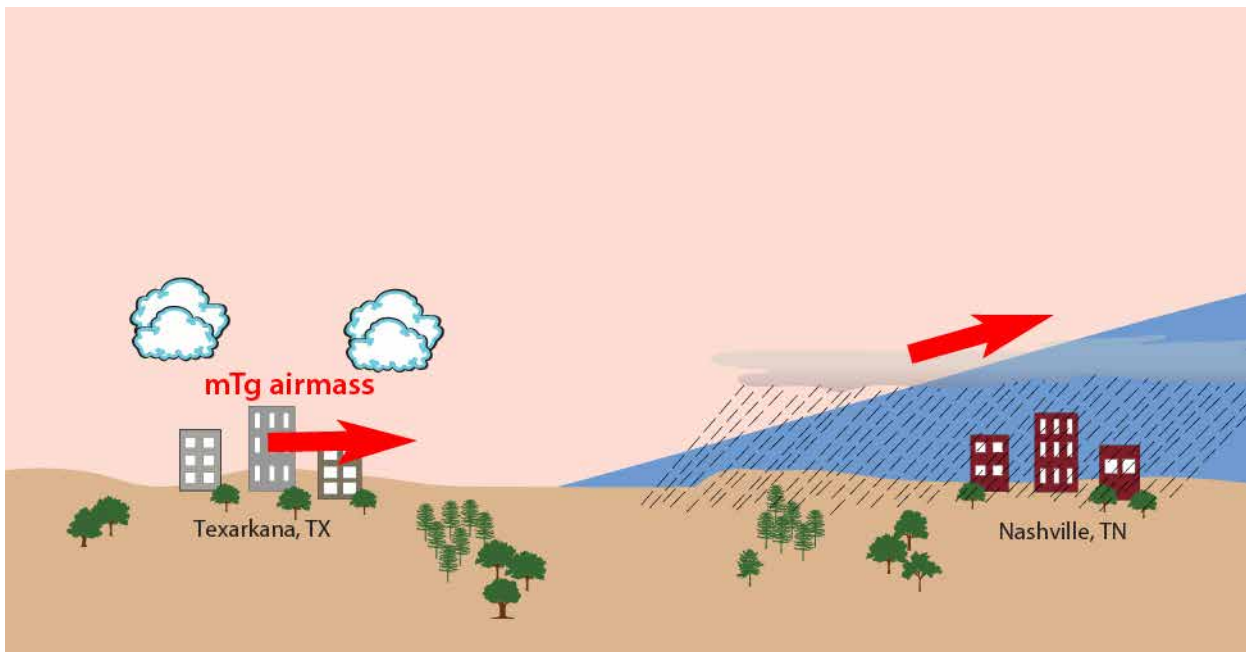


Figure 5.60c. Cross-sectional sketch of the warm front as it gets still closer to Nashville. Cloud cover over time should be increasing and getting lower in the sky. Light precipitation might begin to fall out of altocumulus or altostratus clouds. Depending on the temperature of the cold air, the precipitation type could be rain, freezing rain, sleet or snow. The sequence of high-to-middle-to-low-level clouds is a more reliable indicator of an approaching front than any single cloud type by itself.



Figure 5.60d. Cross-sectional sketch of the warm front as it passes over Nashville. Precipitation at Nashville should be steady and moderate in intensity, and last several hours. Low-level clouds (stratus, stratocumulus, nimbostratus) may cover the entire sky. Depending on the temperature of the cold air, the precipitation type could be cold rain (most commonly), freezing rain, sleet or snow. After the passage of the warm front, Nashville should experience weather changes similar to those of Texarkana as the front passed there.

In summary, cooler, drier, high-pressure conditions are slowly replaced by warmer, moister, low-pressure conditions after a warm front passes. Winds are initially from an easterly direction, but then shift to a southerly direction. Precipitation tends to be of lower intensity than that associated with cold fronts.

## Occluded Fronts

Cold fronts typically move faster than warm fronts. Eventually, they may overtake the warm front to form an occluded front (Figures 5.61a, 5.61b and 5.61c).

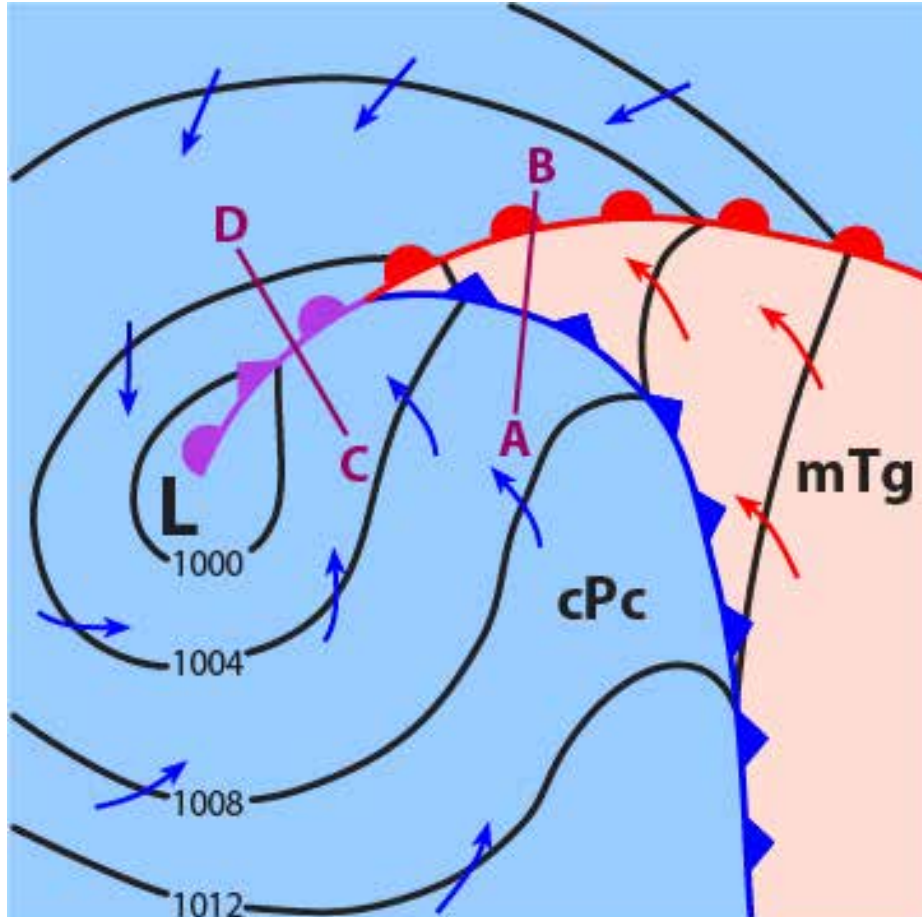


Figure 5.61a. Weather map of the initial stage of occlusion of a frontal cyclone. Part of the cold front has overtaken the warm front (purple symbol). As the occlusion progresses, the warm air wedge (mTg) will narrow and ultimately be lifted above the cooler air as the occluded front lengthens.

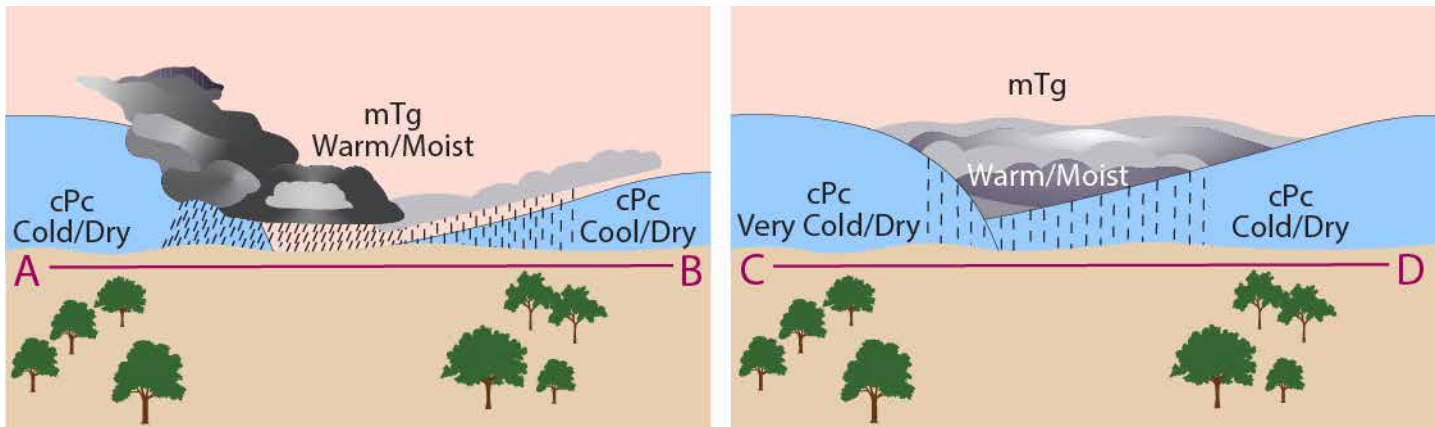


Figure 5.61b. (left). The line of transect A-B is depicted in cross-section just prior to occlusion.

Figure 5.61c. (right). The line of transect C-D is depicted in cross-section just after occlusion.

If the air behind a moving occluded front is colder than the air ahead of it, a **cold occlusion** occurs (Figure 5.62a, 5.62b, 5.62c and 5.61d). If the air ahead of the moving occluded front is the colder of the two, a **warm occlusion** occurs. When either occlusion occurs, the warm air is squeezed between the two colder air masses and forced upward.

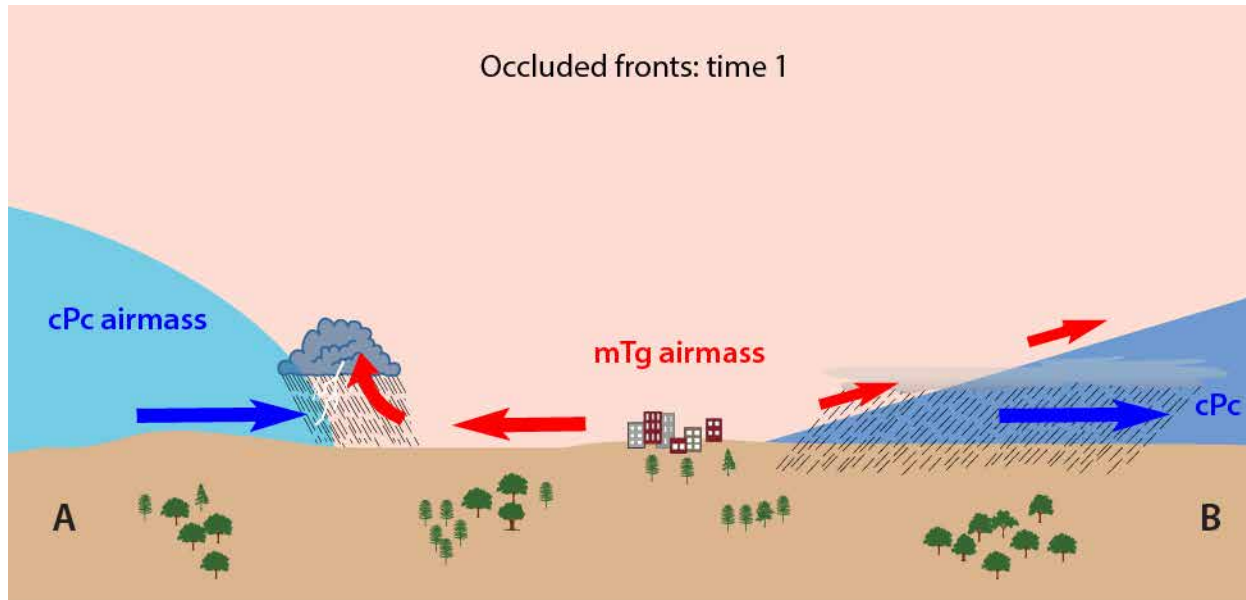


Figure 5.62a. Prior to occlusion, the area occupied by mTg air has gotten progressively smaller, whereas that occupied by cPc air has expanded.

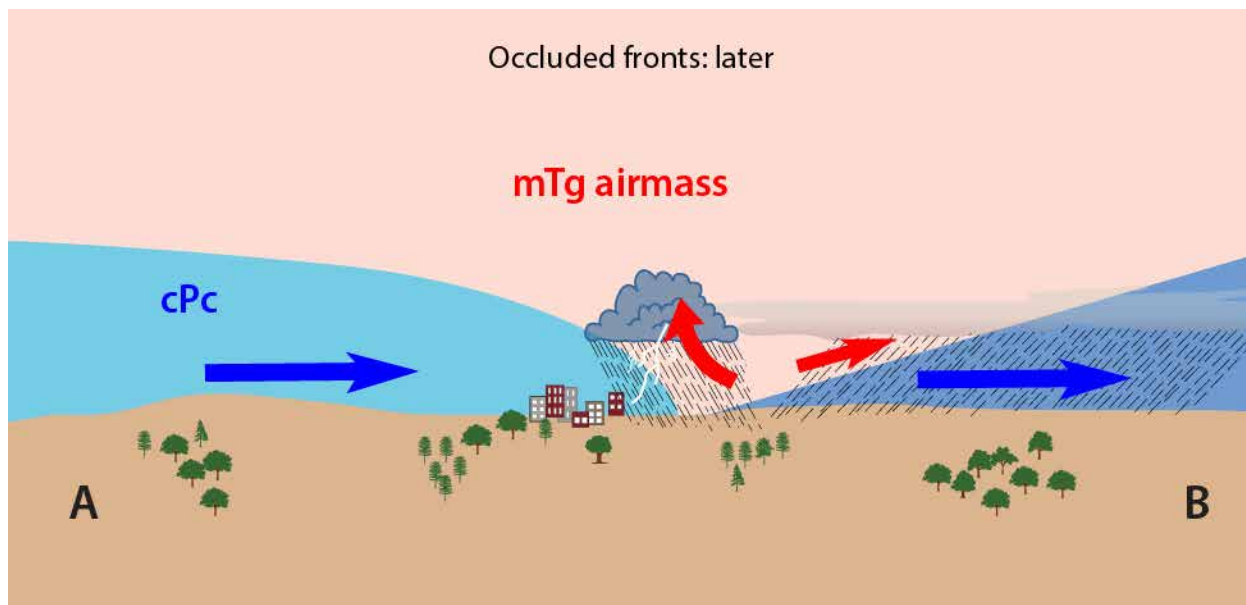


Figure 5.62b. During the incipient stage of occlusion, the cold front has just caught up with the warm front, pinching the mTg air off the ground. It was once thought that occlusion was the start of the end of the frontal cyclone, but satellite observations sometimes track foul weather for days following occlusion.

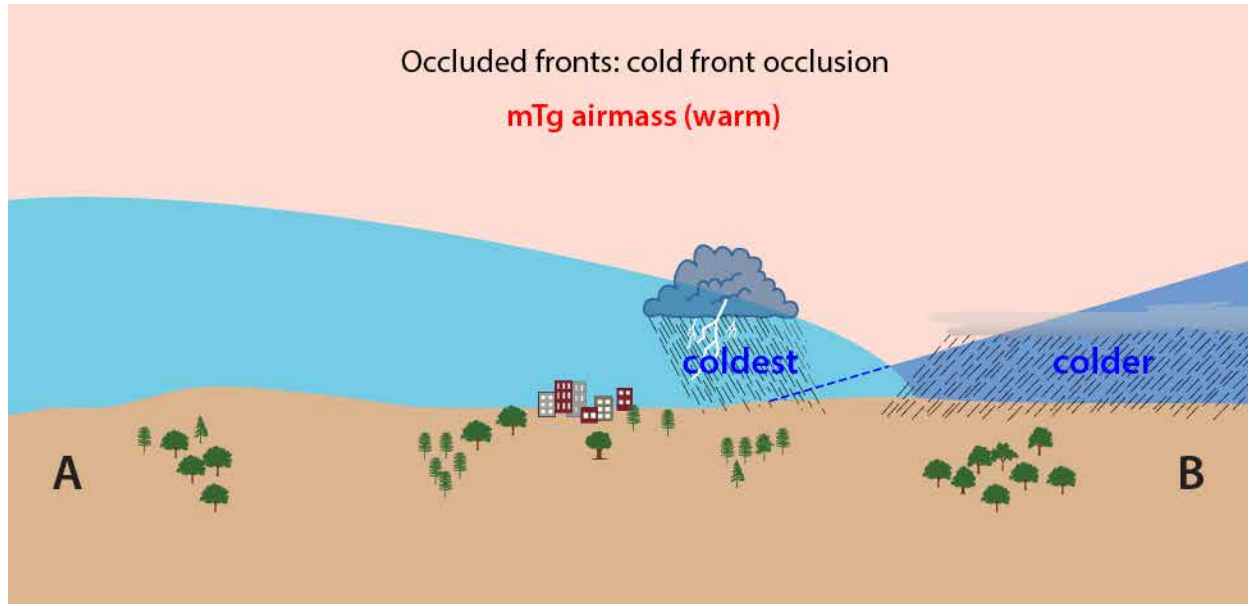


Figure 5.62c. Two basic types of occlusion are recognized. A cold front occlusion occurs when the air behind the cold front is colder than the air ahead of the warm front, destroying a portion of the warm frontal surface (dashed line).

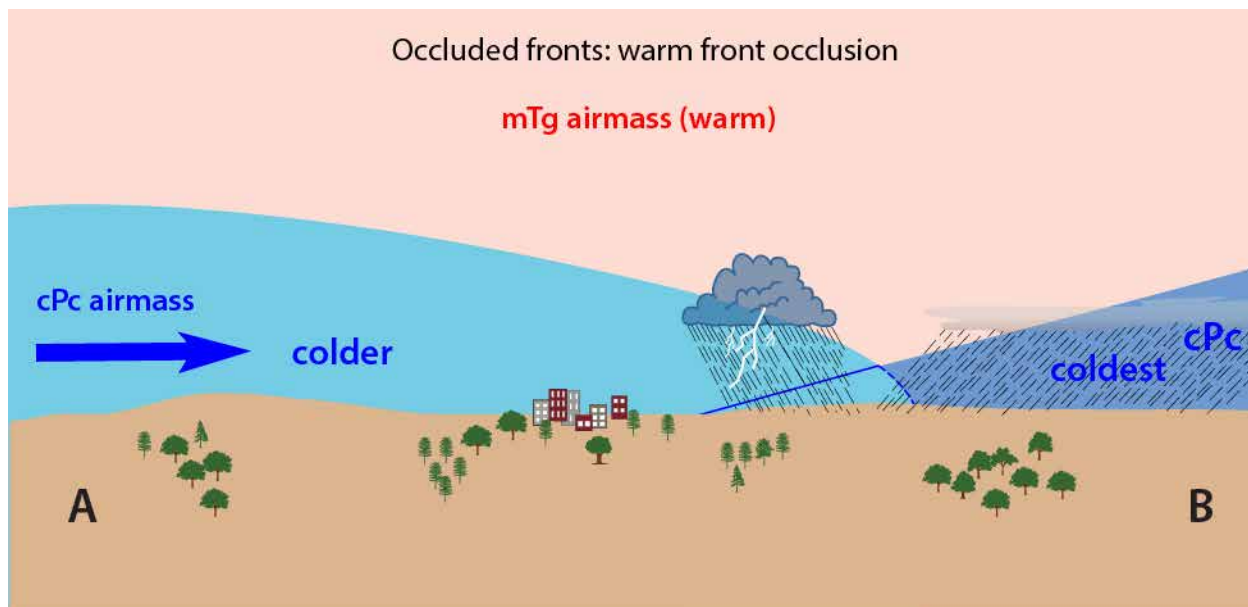


Figure 5.62d. A warm front occlusion occurs when the air ahead of the warm front is colder than the air behind of the cold front, destroying a portion of the cold frontal surface (dashed line). Note that both stable conditions (warm front) and unstable conditions (cold front) can coexist in the same storm system.

Occlusions commonly occur during the latter stages of development of frontal cyclones, when the fast-moving cold front has been given sufficient time to catch the more slowly-moving warm front. During all stages in the development of frontal cyclones, through occlusion, the entire system moves eastward because of the system's location within the sinuous upper-level westerly winds.



As the air masses along the occluded front mix and become more similar, a stationary front develops and in time, may dissipate.

The weather changes associated with the passage of an occluded front are not as variable as with warm and cold front passage, because the air masses on either side of the front are both cold. They are typically characterized by overcast skies, and periods of rain or snow. In some cases, however, when the overlying tropical air is quite unstable, thunderstorms may occur.

## Stationary Fronts

Stationary fronts develop when a front shows no appreciable movement over a period of hours. Stationary fronts may be linked to cold or warm fronts depending upon the relative movement of the frontal boundary (Figure 5.63a and 5.63b).

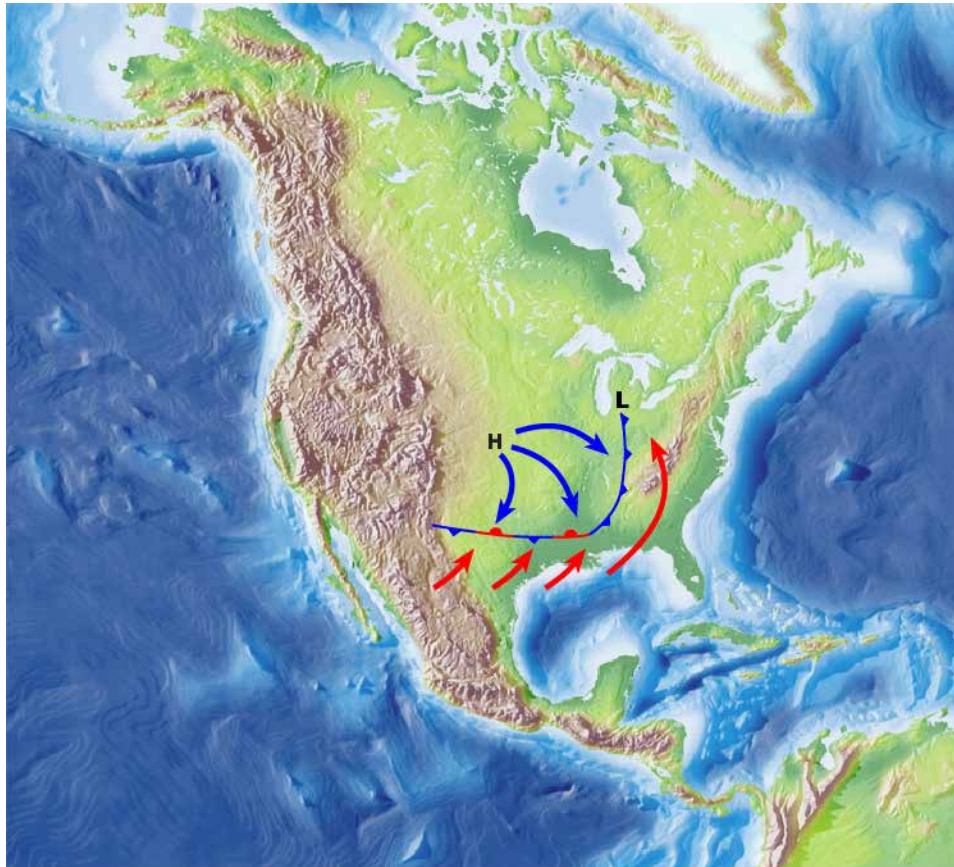


Figure 5.63a. Portions of cold fronts may lose momentum as they travel southward and southeastward and become transformed into a stationary front.

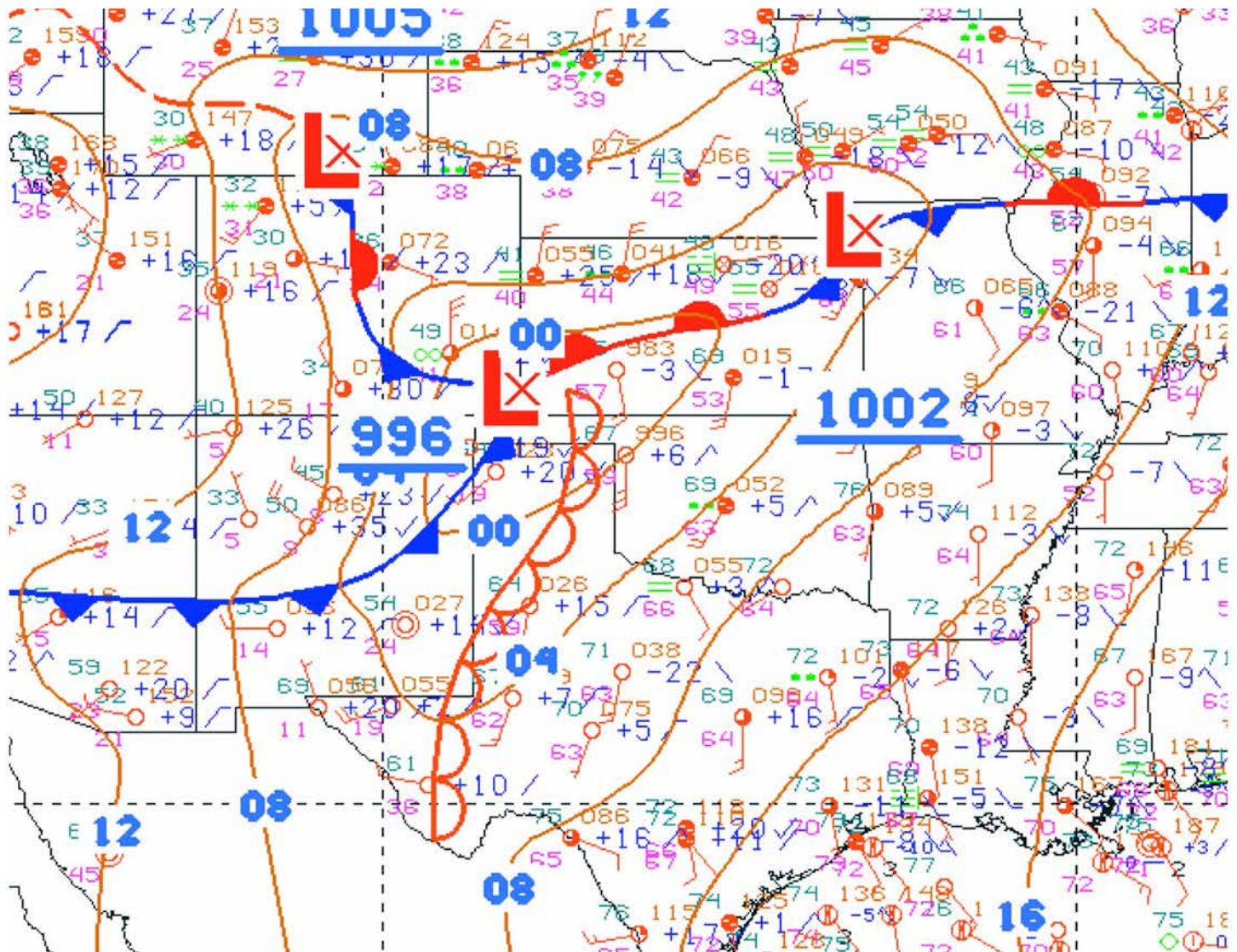


Figure 5.63b. Two stationary fronts have formed, one in Colorado, the other central Illinois and northern Missouri on April 9, 2015 at 1:00 AM CDT (Source/Credit: NWS).

### Stationary fronts develop when one of two conditions occur:

- The momentum associated with the cold air equals that of the opposing warm air and so the frontal boundary ceases to move. This can occur when a cPc air mass moves southward until it eventually slows and stalls. Alternatively, when a mTg air mass moving northward slows and stalls, it too can become stationary.
- The air masses are prevented from advancing by a mountain range that lies between them. This frequently occurs when, for example, a cPc air masses moves south out of Canada and to the west of the Rockies and a mTg air moves northward from the Gulf of Mexico to the east of the Rockies. Because air masses tend to be shallow, and the Rockies rise to more than 12,000 feet in many places, they can act as a wall that separates the cPc and mTg air masses.

Because neither air mass can displace the other in this situation, it is considered to be a stationary front. Because the front is not moving, cloudiness and precipitation can continue for days.

Much of the foul weather in the mid-latitudes is due to the passage of frontal cyclones, particularly during the cool season when polar air can penetrate well into the middle latitudes, and occasionally into tropical latitudes. The foul weather associated with warm, cold, occluded and stationary fronts is interrupted by clearer skies associated with the passage of large anticyclones. Mid-latitude cold-season weather forecasting is therefore largely a process of characterizing the weather of these huge, migratory frontal cyclones and anticyclones, and predicting their path and velocity of travel.

## The Dry Line

**Dry lines** form at the contact zone between warm, dry air and warm, humid air. In North America, they most frequently form in west Texas and New Mexico, and are sometimes referred to there as the *Marfa Front*. Although the National Weather Service does not give them legitimate frontal status, dry lines are discontinuities that separate air masses of different densities, and hence can induce uplift very much like a frontal boundary. They commonly trend north-south and link to large frontal cyclonic systems to the north (Figure 5.64).

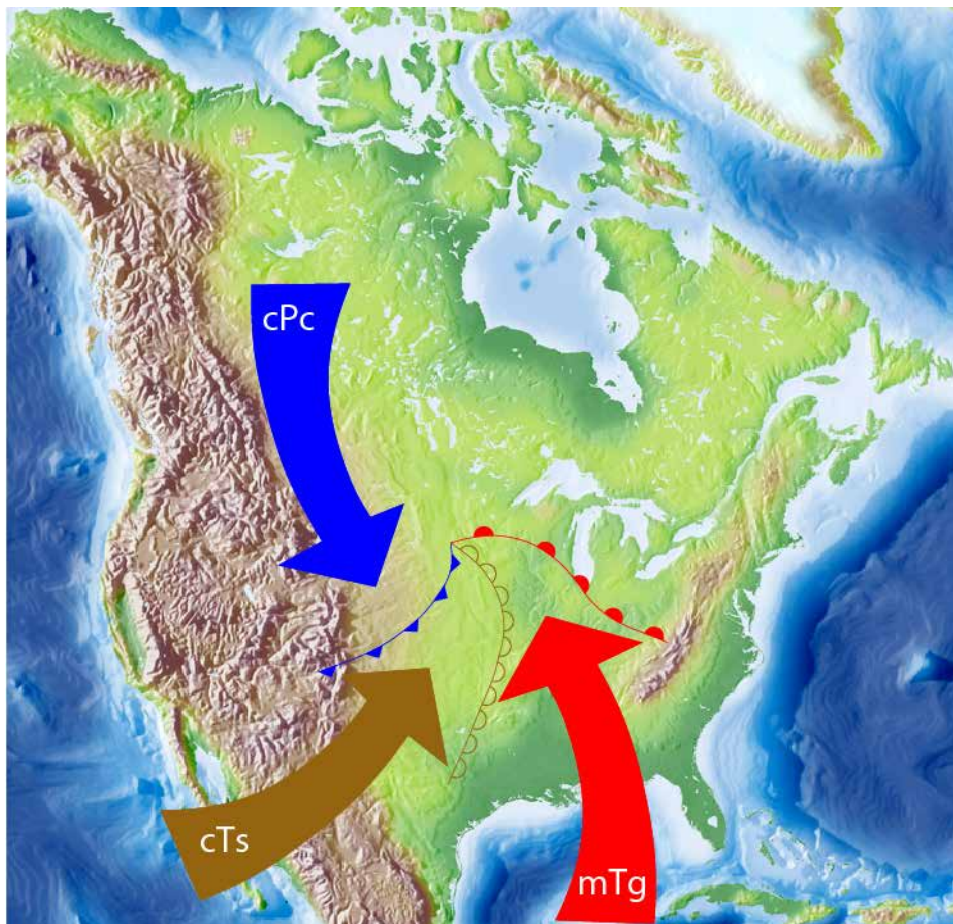


Figure 5.64. Sketch of a hypothetical cold front, warm front and dry line forming between cTs, mTg and cPc air masses. Dry lines typically form in west Texas, but then tend to march east and northeast. Warm, dry Sonoran air sometimes penetrates all the way into the Midwest and through the Texas Coastal Plain.

Dry lines are quite different from cold, warm and stationary fronts because the air temperature may be very similar on either side of the line, where cTs air meets mTg air. Variations in air density between the air masses are a function of differences in molecular composition rather than temperature. Although intuitively it may seem like moist air at a given temperature and pressure should be more dense than dry air, the opposite is true.

Avogadro's Law states that under the same temperature/pressure conditions, an equal volume of different gases contains the same number of molecules. Dry air is mostly  $N_2$  (~78%), with lesser amounts of  $O_2$  (~21%). Diatomic nitrogen has a molecular mass of 28, and diatomic oxygen 32. In moist air, some of the nitrogen and oxygen molecules are replaced by water vapor and  $H_2O$  has a molecular mass of only 18. **Moist air is less dense than dry air.**

Once formed, dry lines tend to move east and northeast. Severe thunderstorms are frequent along dry lines, and linear belts of thunderstorms may travel all the way to Kansas, Oklahoma and beyond during the evening hours (Figure 5.65). In the event that a given location experiences the passage of a warm front, dry line and cold front, a wide spectrum of precipitation types may follow (Figure 5.66).

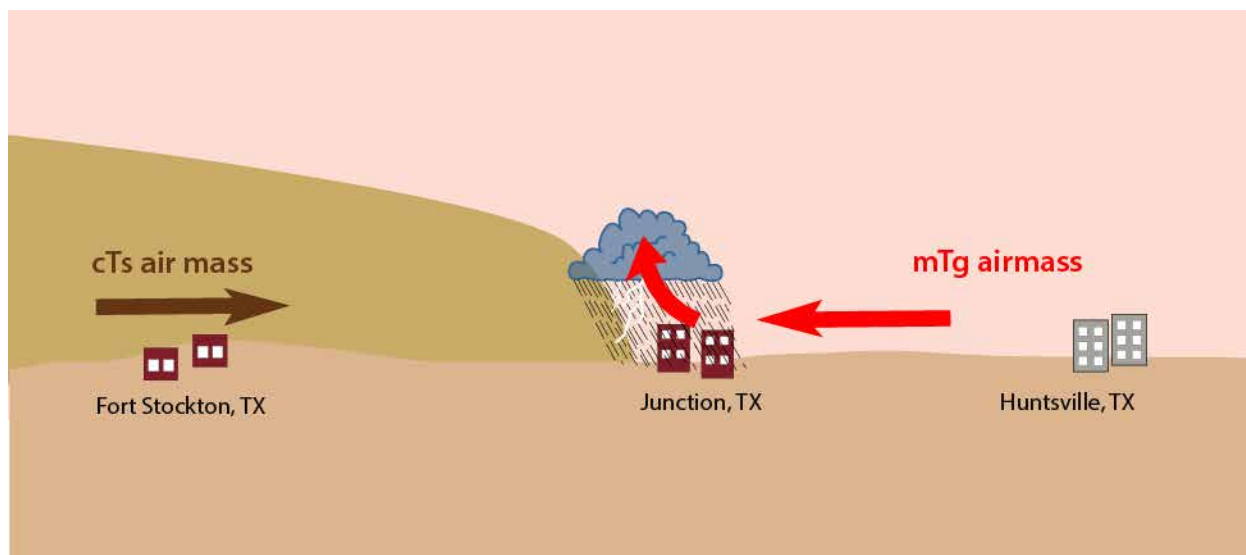


Figure 5.65. A hypothetical dry line, marking the transition zone between a cTs air mass and an mTg air mass is generating uplift and thunderstorms near Junction, Texas.

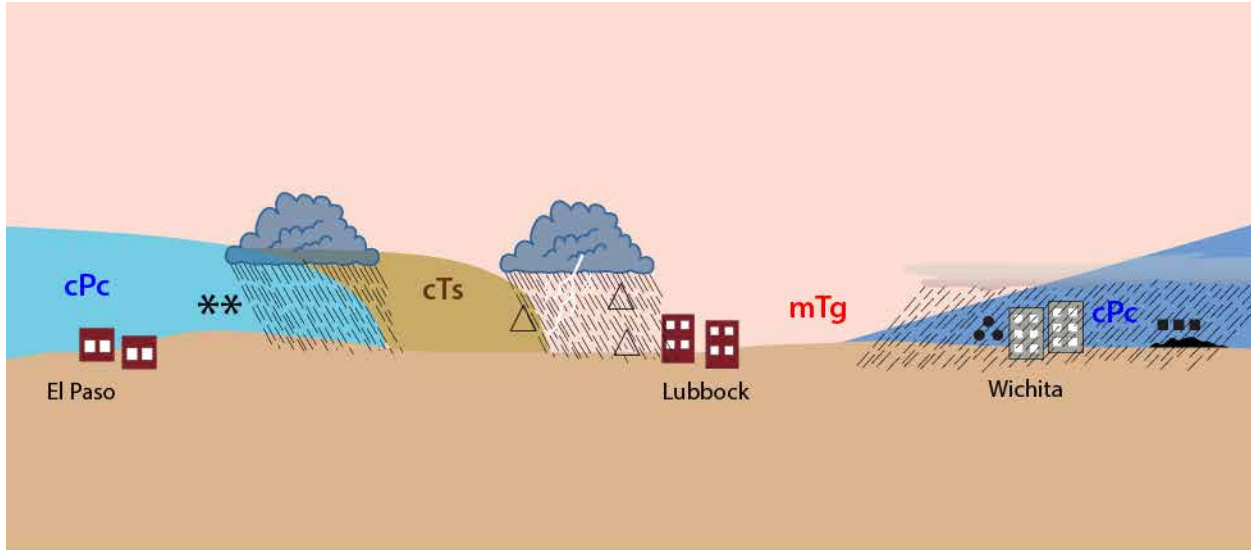


Figure 5.66. Schematic cross section of a cold front (just east of El Paso), dry line (Lubbock) and warm front (near Wichita, Kansas), marking the transition zone between a cTs air mass and an mTg air mass is generating uplift and thunderstorms near Lubbock, Texas. Large, diverse frontal cyclones such as this one can produce a variety of precipitation types, indicated here as snow, rain and hail (dry line), cold rain and freezing rain (Wichita, Kansas).

## **Tracks of Extratropical Storms in the United States**

When several years of data on frontal cyclone movement are analyzed, it appears that some of them tend to have preferred tracks. Preferred tracks implies that whatever kinds of foul weather occur within these systems, they have the opportunity to repeat themselves, enhancing precipitation in the process.

The tracks of extratropical storms determine the beltway of foul weather associated with those storms. Although the meandering nature of upper-level flow patterns changes daily, weekly, seasonally and decadally, there appear to be some preferred tracks (Figure 5.67), perhaps driven by topographic barriers or by anomalously warm and cold spots in the ocean basins. The following are brief descriptions of some of the storm tracks recognized in the conterminous United States.



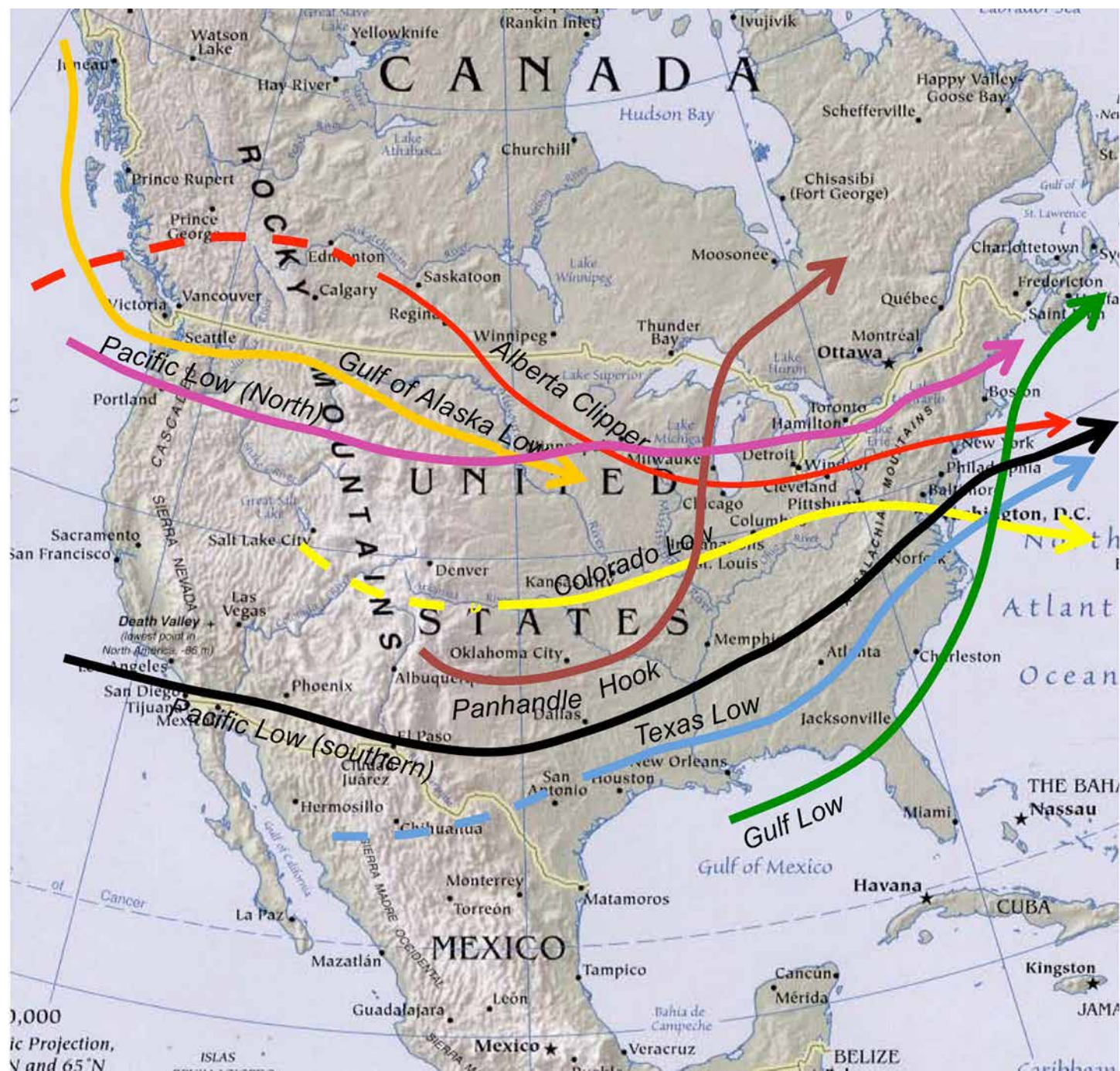


Figure 5.67. Map of some of the more common storm tracks in the conterminous United States (Source/Credit: CIA, modified).

## The Alberta Clipper

Many winter disturbances that travel across the Rockies can be rejuvenated and intensify as they arrive at the lee (downwind side) of the mountains. Two prime examples are the *Alberta Clipper* and the *Colorado Low*. They move swiftly, often covering hundreds of miles per day, hence the term clipper from the early sailing ships of the same name.

*The Alberta Clipper*, also sometimes known as the *Saskatchewan Screamer*, originates in or near the Canadian province of Alberta, southwestern Canada (Figure 5.67). A typical cold-season track takes the Clipper into the northern Great Plains, Great Lakes states and to the east coast. Most winter clippers leave a swath of moderate snowfall in their path. Although snowfalls are moderate, clippers often bring rapid drops in temperature and winds of 35-45 mph (56-72 kph).

## The Colorado Low

The Colorado Low forms over southern Colorado or extreme northern New Mexico. Similar to the Alberta Clipper, it tends to form from a pre-existing disturbance that weakens crossing the Rockies, but strengthens again once in the lee of the mountains. Upper-level winds commonly guide these storms to the east-northeast, where they are responsible for a considerable percentage of the winter snowfall in the Midwest. Some, however, head southeastward into Texas, and may be responsible for many of Texas' *Blue Northers*.

## The Gulf of Alaska Low

In the North Pacific, a common breeding ground for frontal cyclones is in the Gulf of Alaska. Multiple storms may develop simultaneously (Figure 5.68). If upper-level winds are favorable, the storms skirt the coast of Alaska and Canada, and then typically enter the United States somewhere between Washington and Northern California. These *Gulf of Alaska Lows*, already potent storms with strong winds and widespread precipitation, are further enhanced by multiple mountain barriers. The storms are most frequent during the cold season, but bring frequent rainfall to the Coast Ranges even during the summer. The Marquee at a community college in Northern Washington on the Strait of Juan de Fuca once read “people in Washington don’t tan — they rust.” These storms are also responsible for coastal gales of 40-70 mph (64-113 kph). Gulf of Alaska Lows can impact travel in the Pacific Northwest as well as the Rocky Mountains (Figure 5.69).

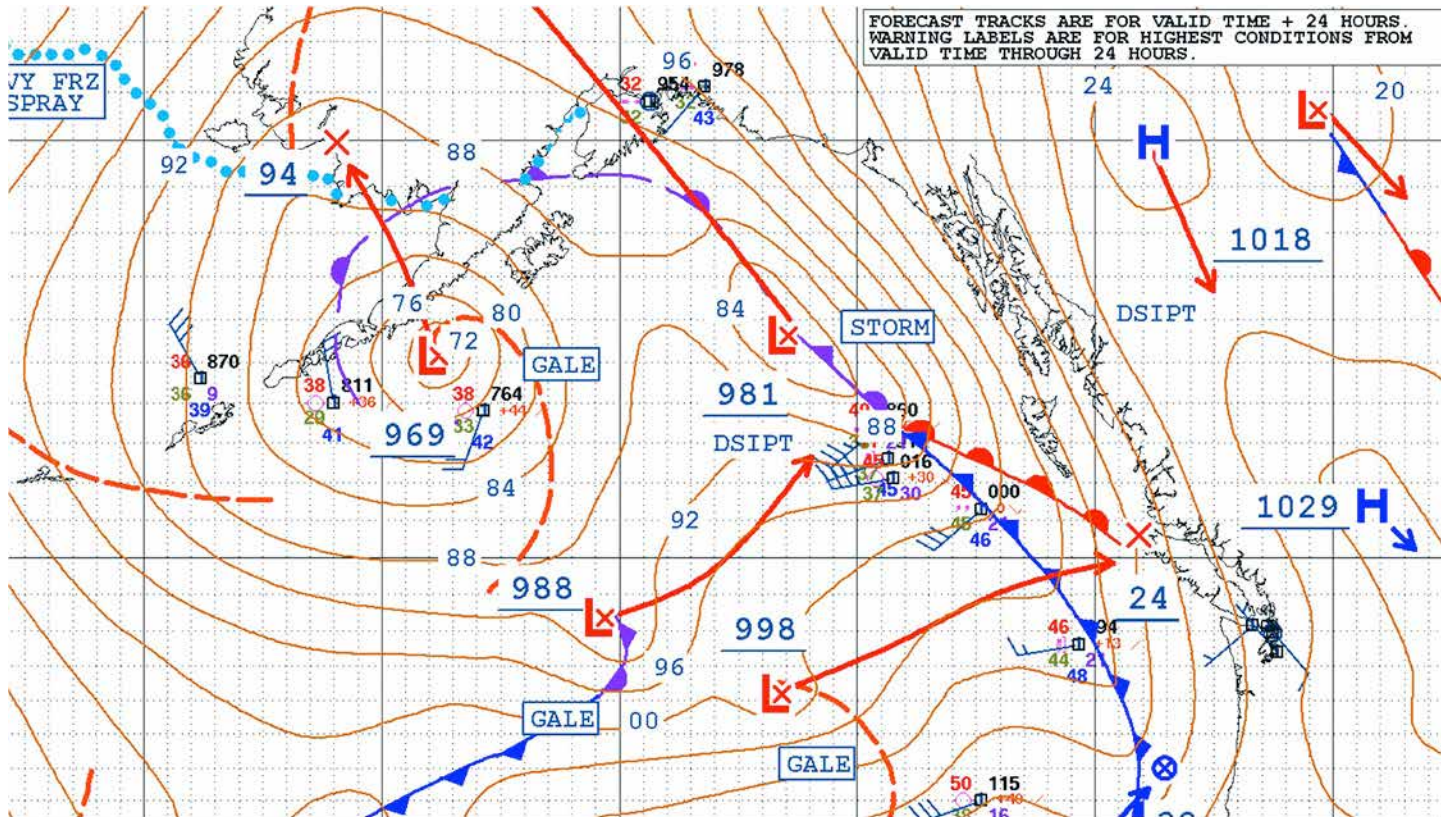


Figure 5.68. In the North Pacific, a common breeding ground for frontal cyclones is in the Gulf of Alaska. Multiple storms may develop simultaneously, as was the case here on February 21, 2016 (Source/Credit: NWS).

# Winter Storm To Impact Thanksgiving Travel

November 19<sup>th</sup> Forecast

Impact Level	Impacts	Timing	Strength
<ul style="list-style-type: none"> <li>Medium – This storm will impact Thanksgiving travel with rain and heavy mountain snow</li> </ul>	<ul style="list-style-type: none"> <li>Slick roads due to rain &amp; snow</li> <li>Chain controls and travel delays across the Sierra</li> <li>Potential for debris flows across NorCal burn scars</li> </ul>	<ul style="list-style-type: none"> <li>Starting Monday night, heaviest Tuesday</li> <li>Showers linger into early Thanksgiving Day</li> <li>Thunderstorms possible Wednesday</li> </ul>	<p>Rain</p> <ul style="list-style-type: none"> <li>Valley: 0.10"–0.40"</li> <li>Mountains: 0.5–2.0"</li> </ul> <p>Snow</p> <ul style="list-style-type: none"> <li>Heavy accumulations at pass levels</li> <li>Light snow down to 2500'</li> </ul>



Figure 5.69. Some of the impacts on Thanksgiving travel from a storm that originated in the Gulf of Alaska are illustrated by the sketch of the Sierra Nevada (Source/Credit: NOAA).

## The Gulf Low

The Gulf Low originates in the Gulf of Mexico where air masses are fueled by vast quantities of moisture from the warm Gulf water. Gulf Lows often make their way northeastward, moving along the east coast toward New England. During much of their course, they have the opportunity to maintain intensity because they continually draw moisture from the Gulf Stream. If they maintain intensity into the New England states, they become Nor'easters.

Nor'easters are responsible for a host of multi-billion dollar weather events, including the infamous storm of the century in 1993 (discussed earlier under mPa air masses). The Nor'easter of January 2015 illustrates typical characteristics of a Nor'easter (Figure 5.70). By January 27, several areas of Maine, New York, New Hampshire, Connecticut, Massachusetts and Rhode Island were covered with 15-25 inches (40-60 cm) of snow. Hurricane-force winds were felt along the coast. The pattern of upper-level winds determines exactly what path these Gulf Low storms take (Figure 5.71).

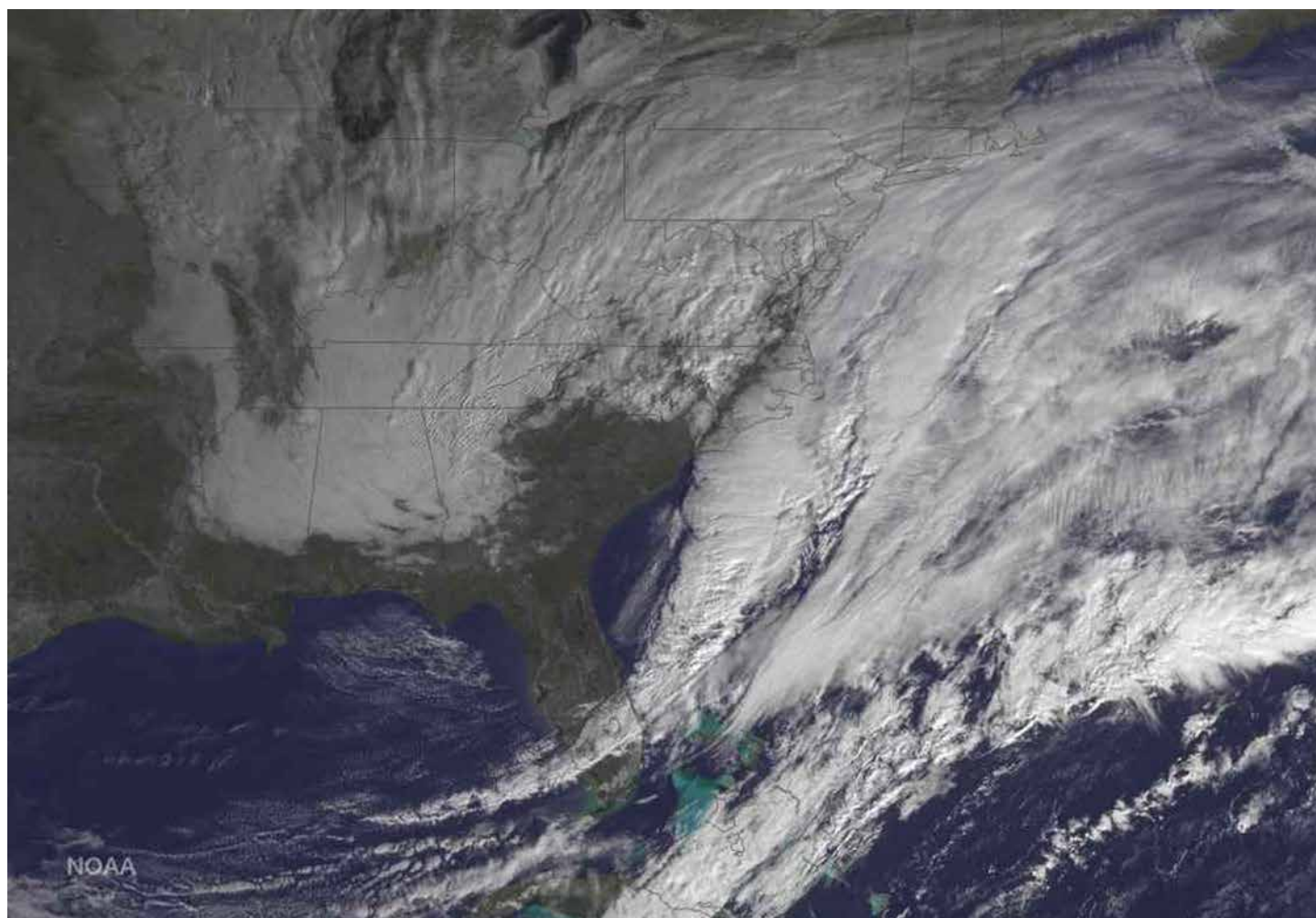


Figure 5.70. A satellite image of the Nor'easter blizzard on Monday morning January 26, 2015 (Source/Credit: NOAA/GOES 13 satellite).

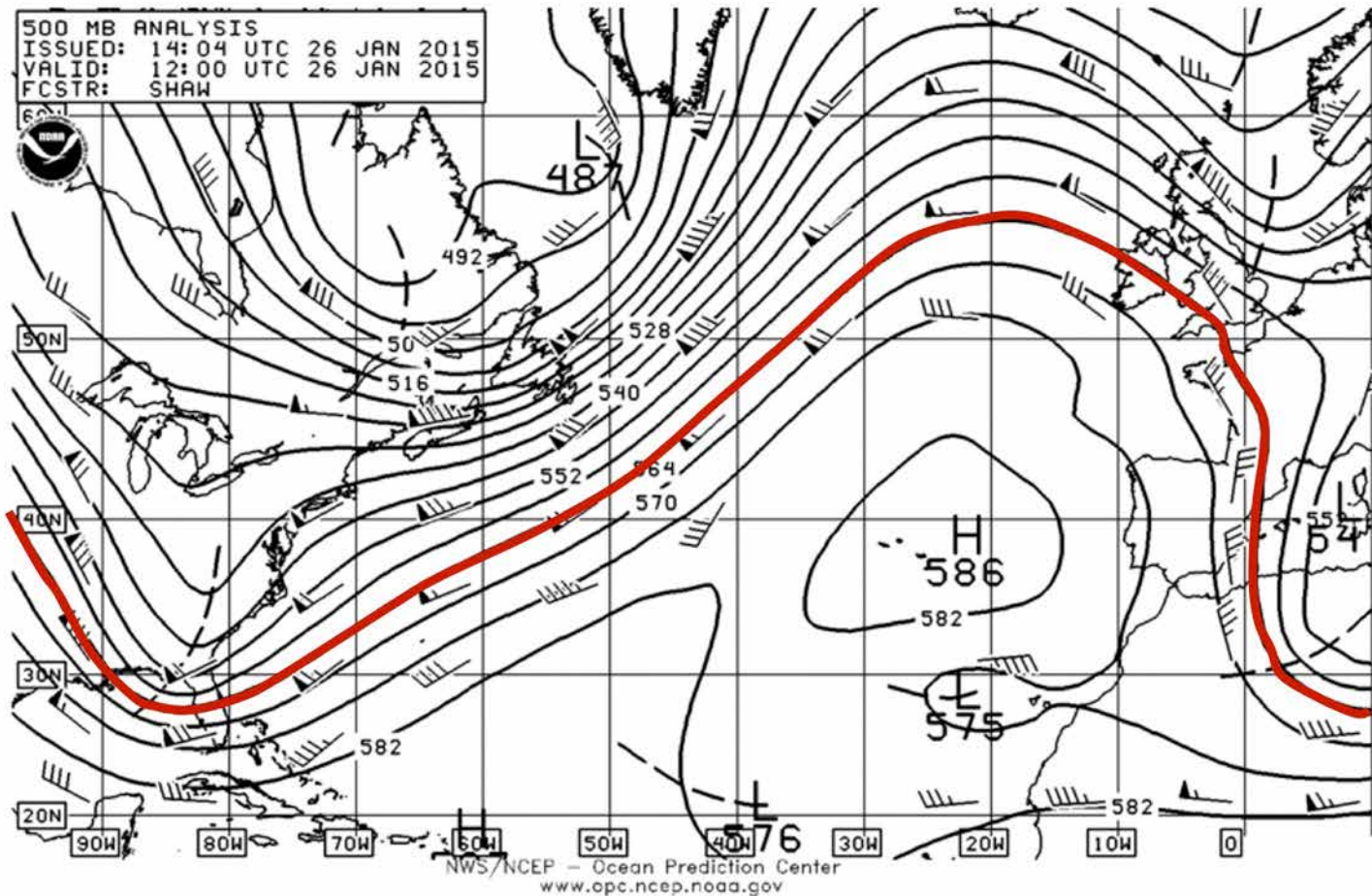


Figure 5.71. Upper-level steering winds on the 500 millibar chart on January 26, 2015 were responsible for directing the blizzard along the Atlantic coastline. High-velocity winds are indicated by the maroon line. Jet stream maximum winds at the 300 millibar level were sustained at 173 mph (278 kph) over Minnesota (Source/Credit: NOAA).

When a deep upper-level trough forms over Texas and the western Gulf, Gulf Lows may invade the mid-continent instead of skirting the east coast. This situation can lead to the famous *Mayan Express*, the atmospheric river that brought record-breaking precipitation over parts of Texas, Louisiana, Oklahoma, and Arkansas during the winter of 2016 (discussed earlier under mTg air masses).

## The Panhandle Hook

The *Panhandle Hook* has similarities to the *Colorado Low* and *Alberta Clipper*. It is a rejuvenated low that intensifies along the lee base of the New Mexico Rockies, and further intensifies over the Panhandle of Texas when it becomes energized by moisture from the Gulf of Mexico. The storm system then heads northeastward toward the Great Lakes, often dropping a wide belt of heavy snow en route. The Panhandle Hook is blamed on some of the wildest winter storms in the Midwest as well as the tragedy of the *Edmund Fitzgerald*.

The sinking of the *Edmund Fitzgerald* in 1975 is linked to another severe Panhandle Hook, but the exact cause of the sinking remains a mystery. The *Edmund Fitzgerald* was a Great Lakes iron ore freighter that was 729 feet (222m) long with a 75 foot beam (23m) and carried about 25,000 tons (22,680 tonnes) of cargo (Figure 5.72). She was crossing Lake Superior en route to a steel mill near Detroit when on November 10, 1975 encountered strong winds and massive waves from a Panhandle Hook. She sank in 530 feet (160m) of water, killing all 29 people on board. The catastrophic event was immortalized by Gordon Lightfoot's song *The Wreck of the Edmund Fitzgerald* in 1976.

*The Armistice Day Blizzard* of November 11-12, 1940 was an intense Panhandle Hook that intensified rapidly as it turned to the northeast. On the afternoon of November 11, most of the areas that were in the path of the storm were basking in 60°F (16°C) weather. During the evening as the storm approached, temperatures dropped, winds increased, and rain, sleet and snow fell progressively. The blizzard cut a path from Texas to Wisconsin, dropping as much as 27 inches (69 cm) of snow in places, and kicking up winds of 50-80 mph (80-130 kph). Several places in Nebraska to Michigan experienced temperature drops of 50°F (28°C).



Figure 5.72. The *Edmund Fitzgerald*, one of the largest freighters on the Great Lakes in the 1970s, sank on November 10, 1975, presumably from huge waves generated by strong winds from a powerful Panhandle Low (Source/Credit: David Arthur, Wikimedia).

One of the most favored theories on the cause of the sinking was from a series of wind-generated waves. Another freighter, the *Arthur Anderson*, was in the same vicinity as the *Fitzgerald* and reported two waves 35 feet (11 m) high. The *Anderson* reported wind gusts of 86 mph (139 kph) at about the time the *Fitzgerald* went down. The last communication between the *Anderson* and the *Fitzgerald* was at 7:10 PM, at which time there was no distress signal.



In 2005, NOAA conducted a computer simulation of conditions on Lake Superior from November 9-11. The analysis indicated peak sustained winds in the area of the sinking were about 50 mph (80 kph) and significant wave heights of 25 feet/7.5 m (Figures 5.73a and 5.73b). The convergence of two wave groups can produce rogue waves with heights significantly greater.

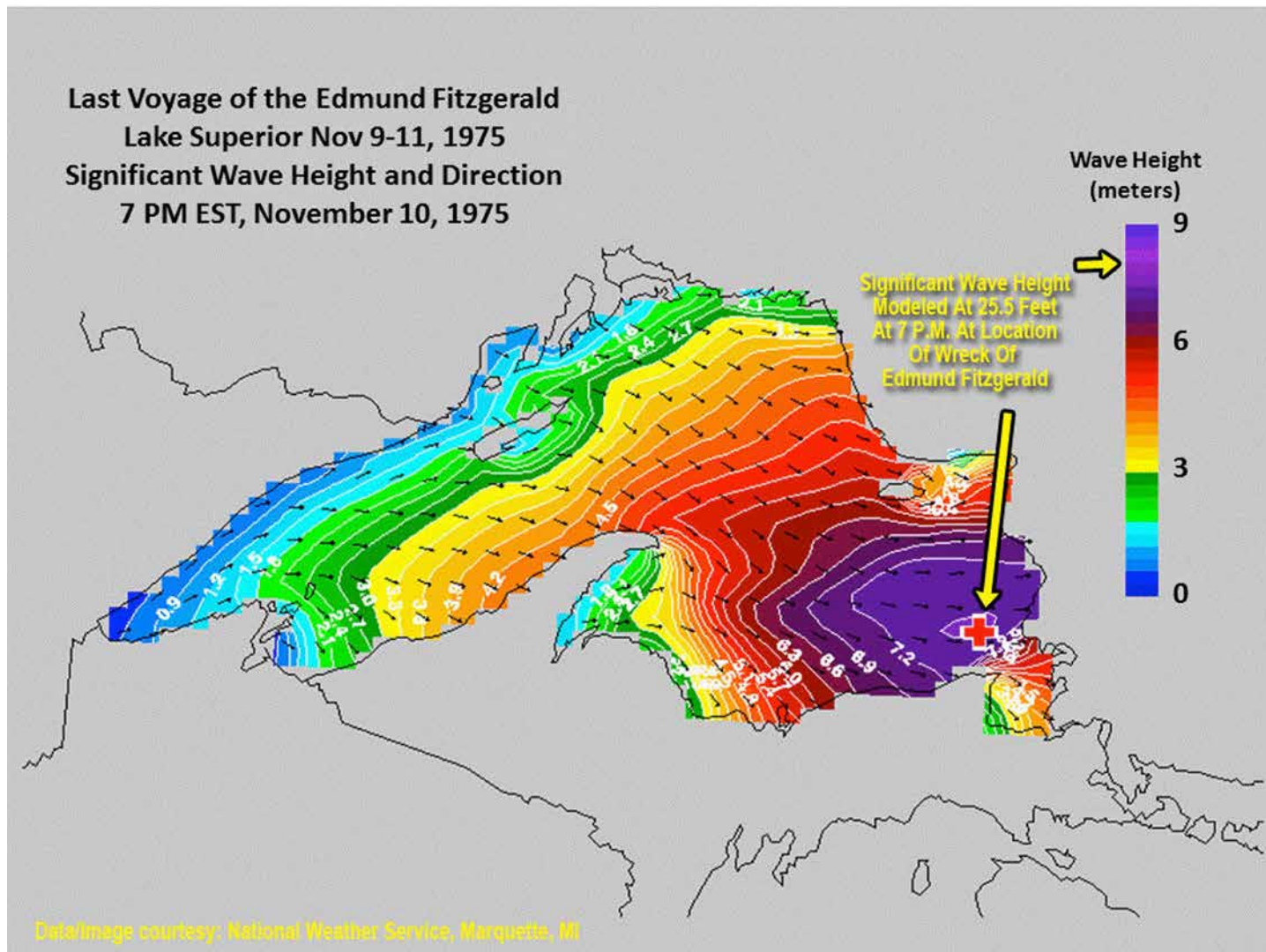
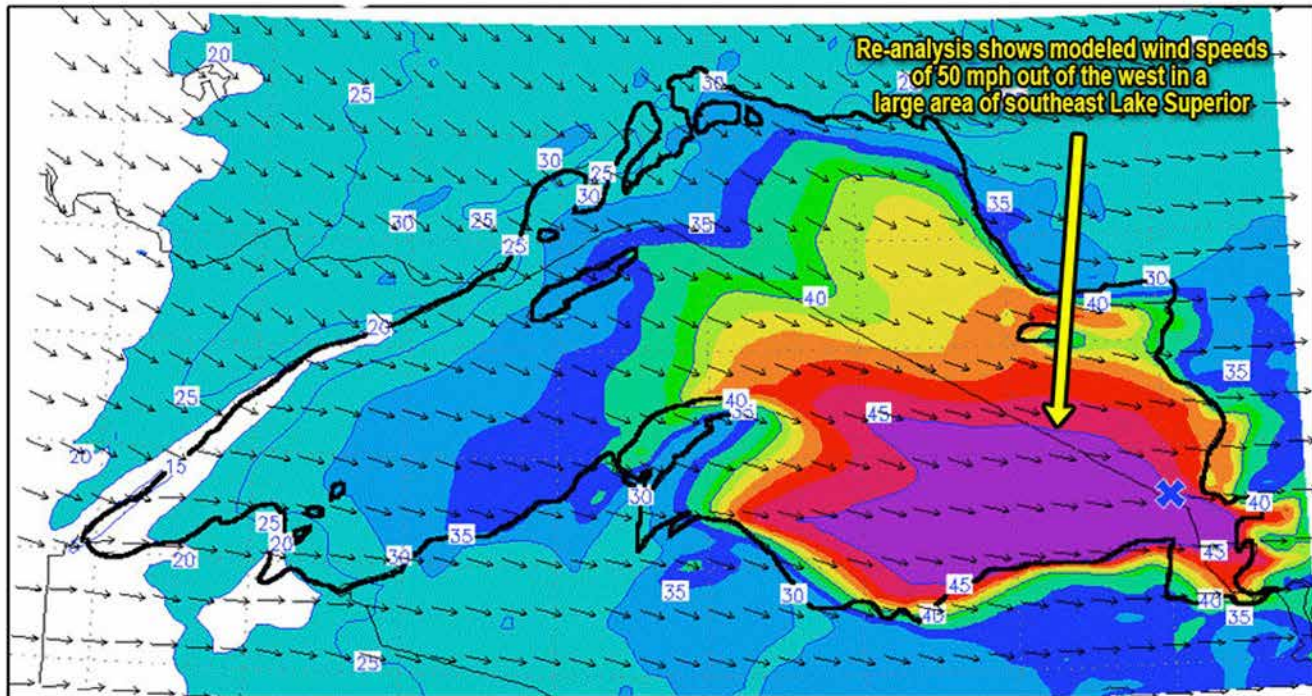
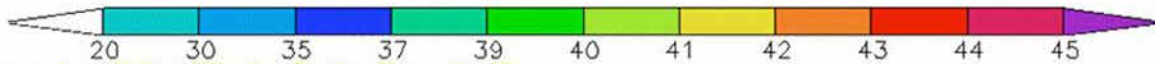


Figure 5.73a. A NOAA computer simulation of significant wave heights on Lake Superior at about the time of the sinking of the Edmund Fitzgerald (Source/Credit: NWS/NOAA).

## Modeled Wind Speed/Direction At 7 P.M. November 10, 1975



### 50 Meter Wind Speed (Knots) & Wind Direction



Data/Image courtesy: National Weather Service, Marquette, MI

Figure 5.73b. A NOAA computer simulation of wind speeds over Lake Superior at about the time of the sinking of the Edmund Fitzgerald (Source/Credit: NWS/NOAA).

## Pacific Lows

The Pacific Basin is the largest of the world's oceans, and the birthplace of a large number of both tropical and extratropical cyclones. Many of the extratropical cyclones that are generated in the north Pacific impact the conterminous United States. On any given year and season, their preferred tracks are variable, and not as easy to generalize as other storm tracks. Storm tracks here, as elsewhere, are dictated by the sinuous pattern of upper level winds, which are constantly changing. There are, however, some noteworthy examples of north Pacific storm tracks.

One of the most common north Pacific storm tracks begins near the islands of Japan and propagates eastward, typically reaching the west coast anywhere between southern California and Washington state (Figures 5.74a and 5.74b). Changes in the direction of upper-level winds may alter their landfall location along the coast. Many of the storm systems that impact the west coast during the cold season are either from this storm track or from the Gulf of Alaska (discussed earlier).

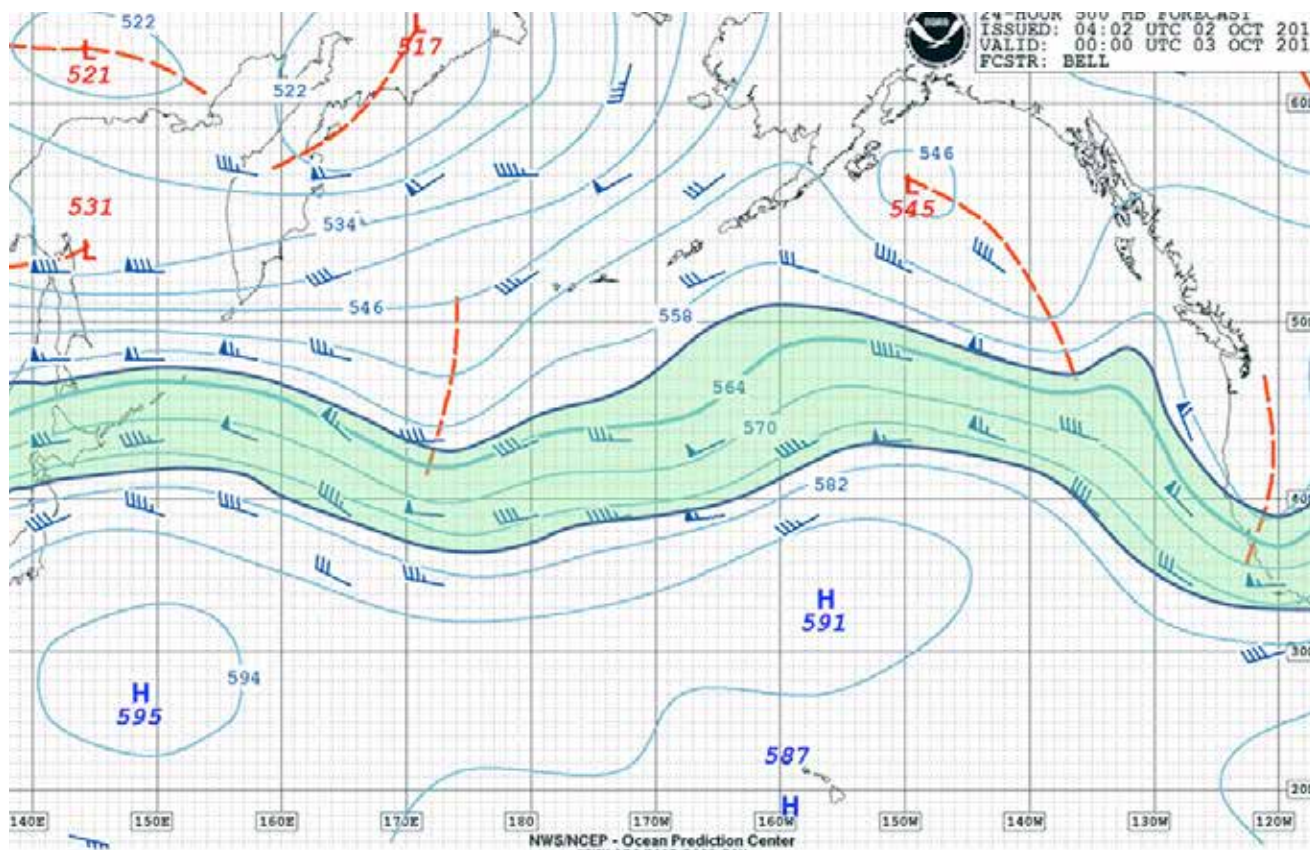


Figure 5.74a. A zonal flow pattern (upper-level flow with little variation in latitude) in the mid-latitudes of the Northern Hemisphere (green band) will steer surface storms from west to east across the Pacific Ocean from Japan to California. The map is a 24-hour forecast map of the 500 millibar chart for October 3, 2016. Compare this with the surface map to see where the actual storms are forecast. This is one of the most common storm tracks for the North Pacific Ocean (Source/Credit: NOAA).

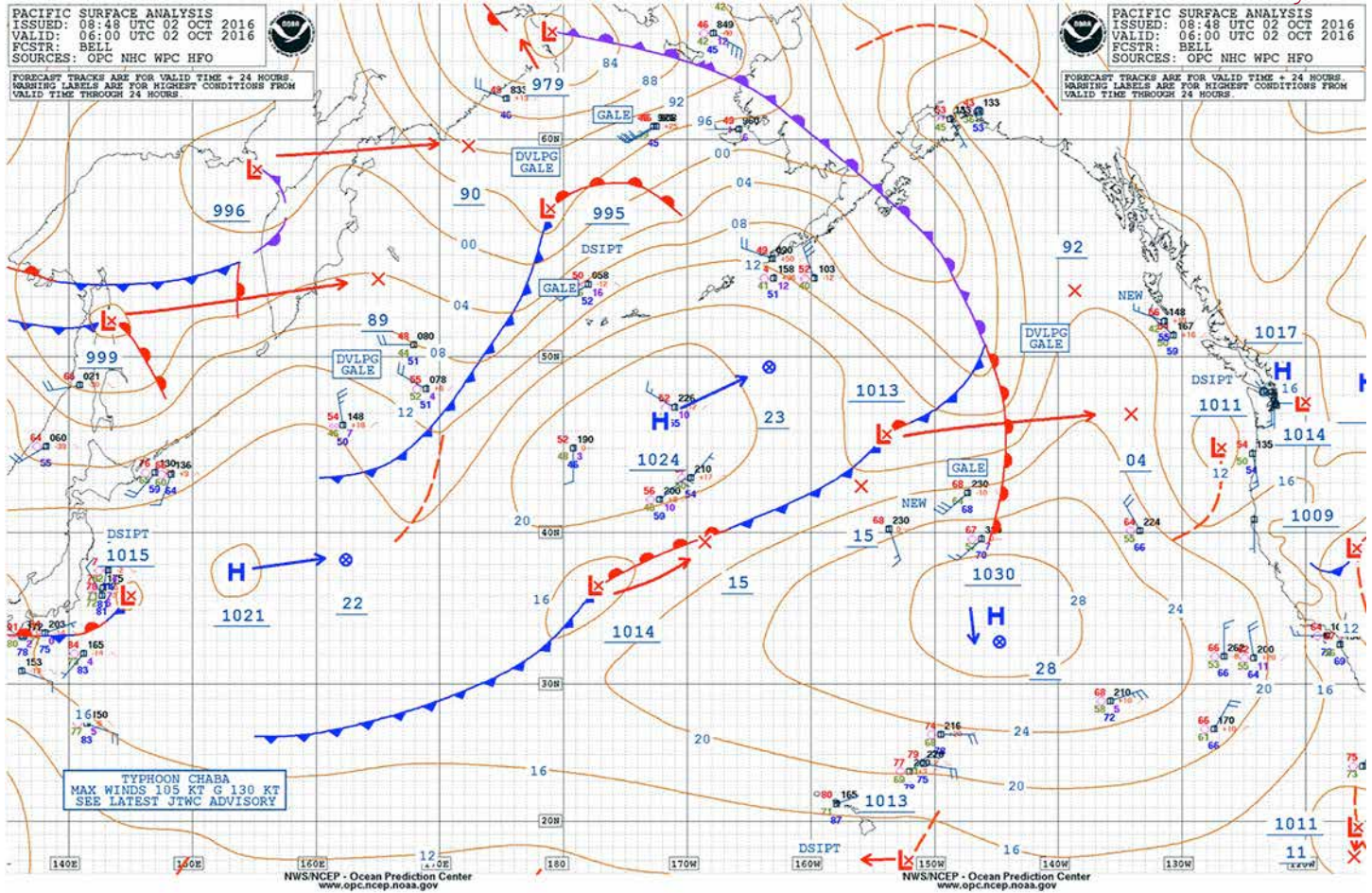


Figure 5.74b. Surface analysis of North Pacific cyclones (L) and anticyclones (H) for October 2, 2016. Red and blue arrows are forecast tracks, and follow the pattern of upper-level flow indicated on the 500 millibar contour chart (Source/Credit: NOAA).

The *Columbus Day Storm* (also *The Big Blow*) began in the tropical Pacific as Typhoon Freda. As it tracked 5000 miles (8000 km) across the Pacific, it became extratropical. Just before striking the west coast, upper-level winds caused a sudden deviation in its path toward the north-northeast (Figures 5.75) and tremendous intensification of the storm. It skirted the coast of Oregon and Washington and finally came ashore in Canada on October 12, 1962 (Figure 5.76) and degraded rapidly. Land-based wind velocities from the storm outrank even *The Perfect Storm* that hit the northeastern states in 1993. The storm took 46 lives and damage estimates were at \$230 million (\$1.8 billion in 2016 dollars).

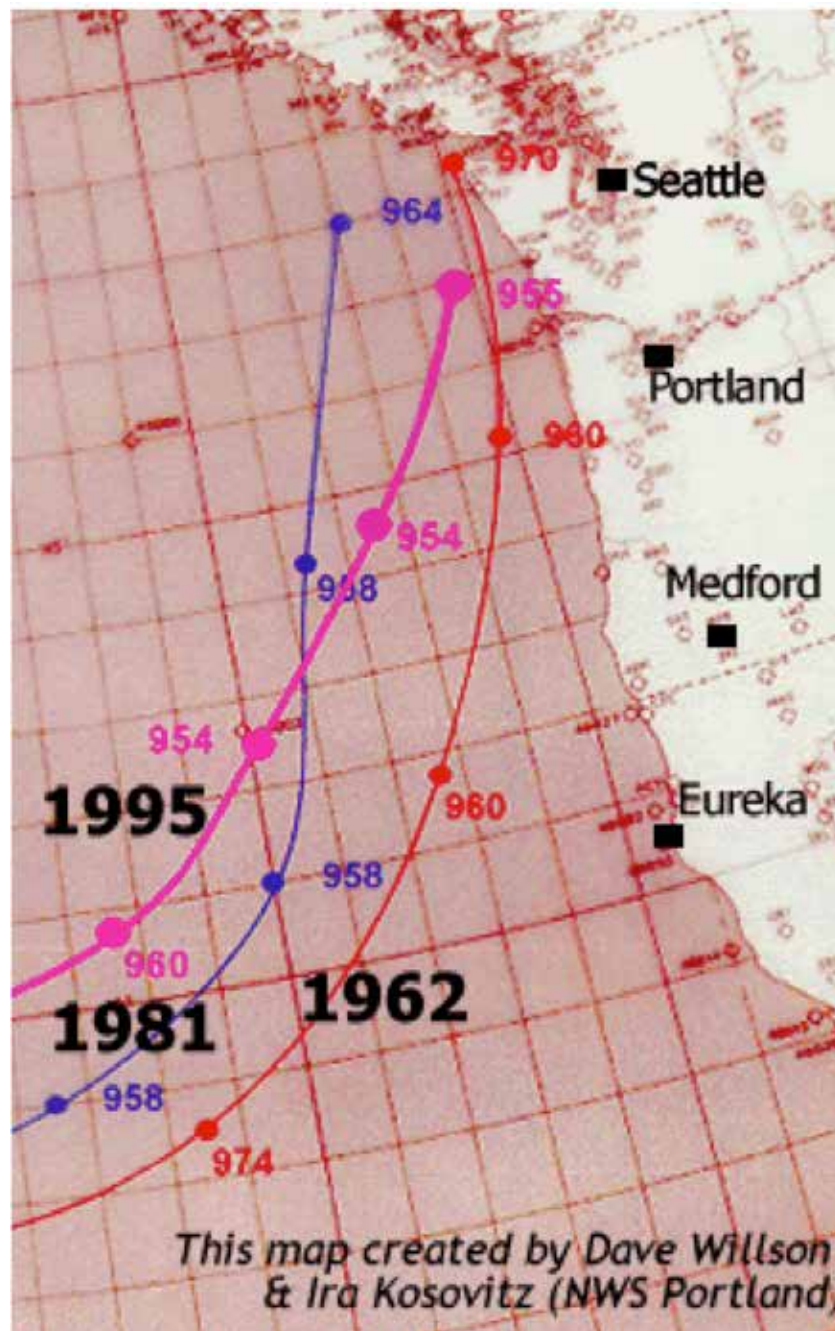


Figure 5.75. Similar pathways of some of the strongest storms to hit the west coast (Source/Credit: NWS, Dave Willson).

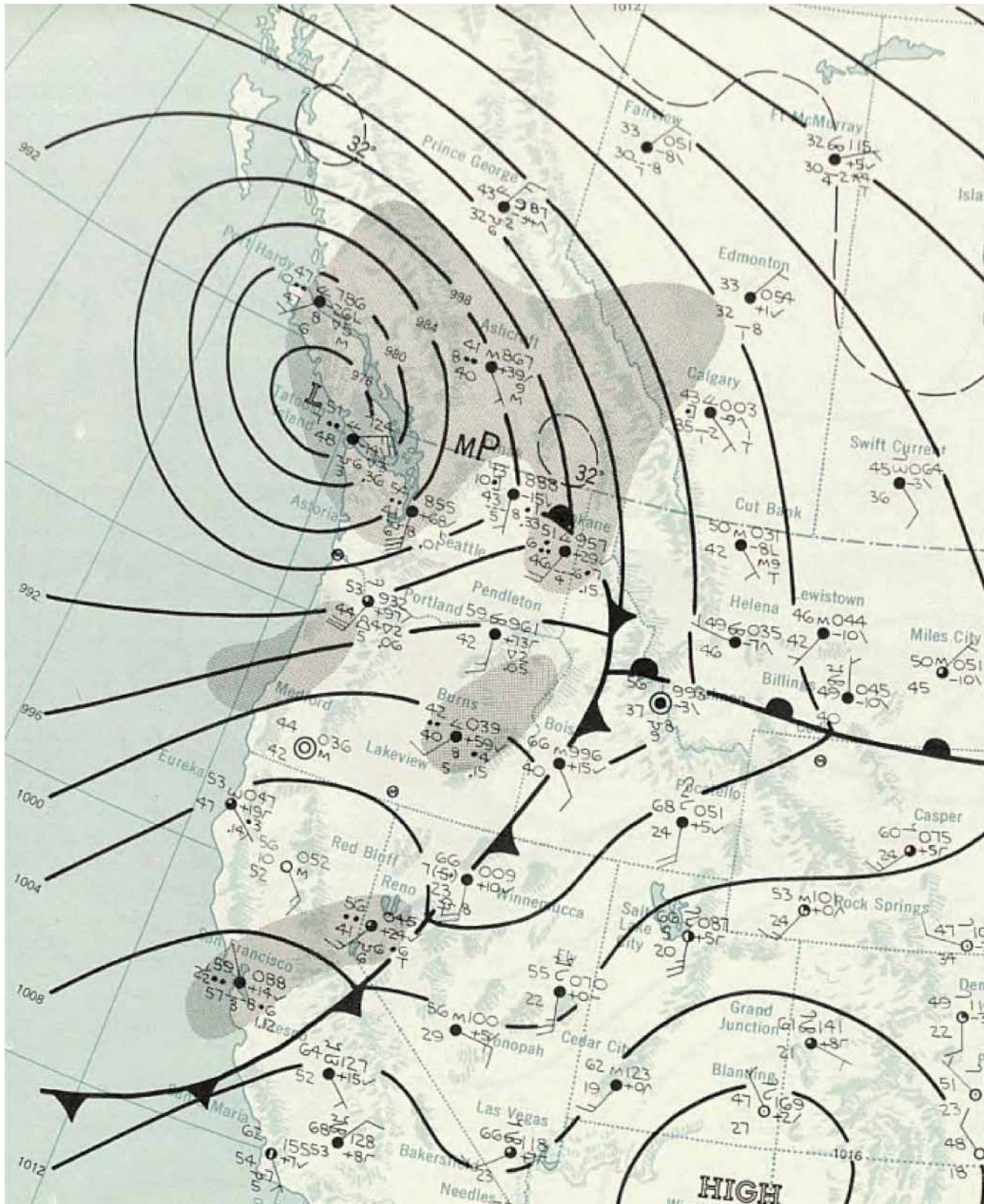


Figure 5.76. The Columbus Day Storm as it came onshore on October 12, 1962 (Source/Credit: NWS).

The lowest pressure recorded during *The Big Blow* was 960 millibars. Record rainfall was experienced in several places in central California. Although a couple of storms have produced slightly lower pressures, none can match the wind from the storm (Figure 5.77). Wind velocities of 127 mph (204 kph) were recorded at a weather station in Corvallis, Oregon, forcing its temporary abandonment.

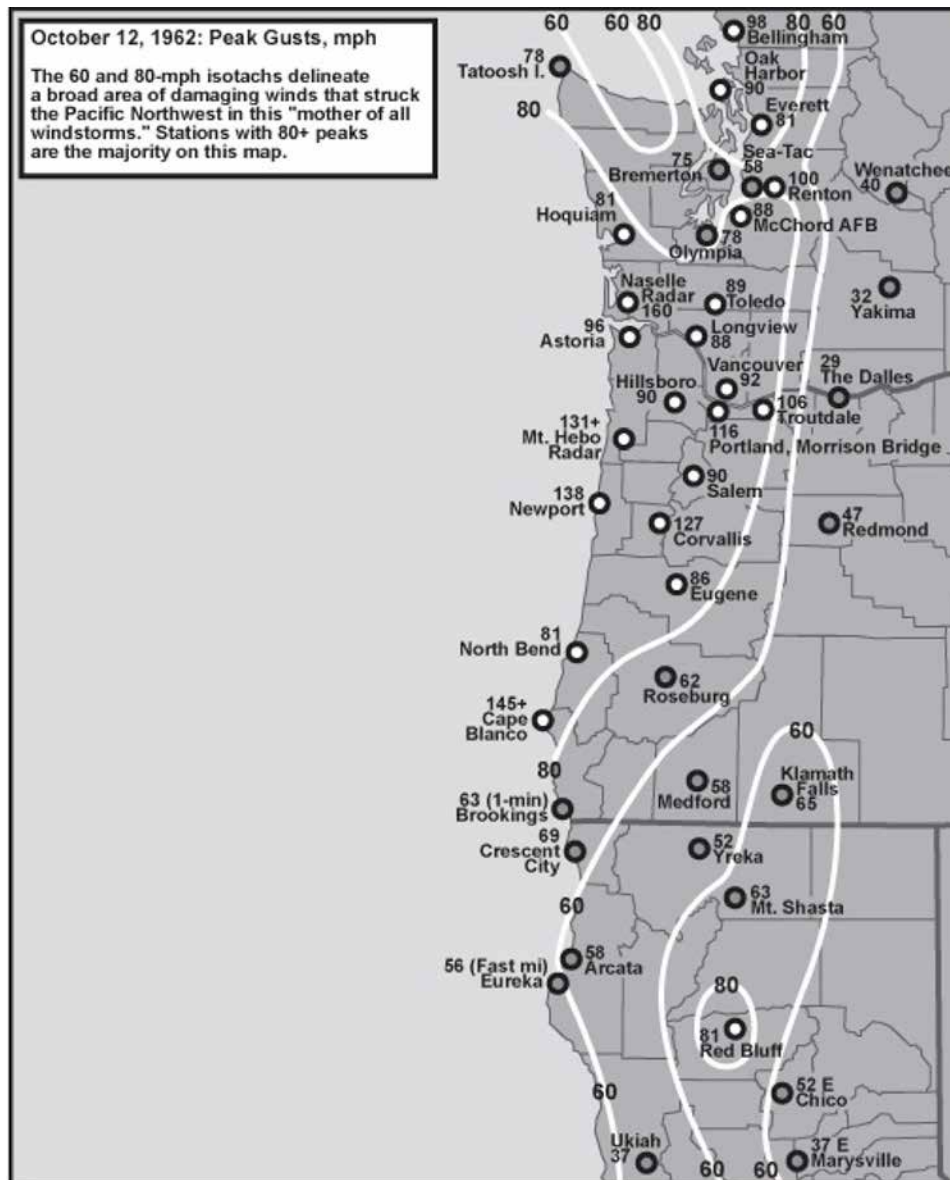


Figure 5.77. Map of peak wind gusts from northern California to British Columbia during the passage of the Columbus Day Storm of 1962. Cape Blanco, Oregon had gusts as high as 145 mph/233 kph (Source/Credit: NWS).

Significant deviations from the west-to-east migration of Pacific storms include storms out of the Gulf of Alaska (discussed previously in a separate section) and out of the subtropical and tropical ocean basins. The setup for the Gulf of Alaska storms that impact the United States is the development of strong upper-level **meridional flow**. *Meridional flow* occurs when the upper-level flow takes on more of a north-south pattern of high amplitude waves called

ridges and troughs. If the eastern side of a ridge sets up paralleling the west coast of the United States, surface storms are guided into the Pacific Northwest or California.

The most notorious of these storms that tap tropical and subtropical moisture sources in the east Pacific basin is a type of *atmospheric river* known as the *Pineapple Express*, discussed briefly earlier in this chapter. The *Pineapple Express* typically forms when polar air masses in the North Pacific expand well into the mid-latitudes in the form of a surface cold front. If there is a strong contrast in temperature between the polar and tropical air, a strong polar jet stream forms aloft. The *Pineapple Express* is a narrow band of moisture-laden air that forms along or just in advance of the front (Figure 5.78). If the front forms a southwest-to-northeast line between the Hawaiian Islands and the western states, the *Express* begins feeding moisture and energy to the coast, resulting in abundant amounts of precipitation. If the front stalls, then the *Express* can produce precipitation for longer periods.

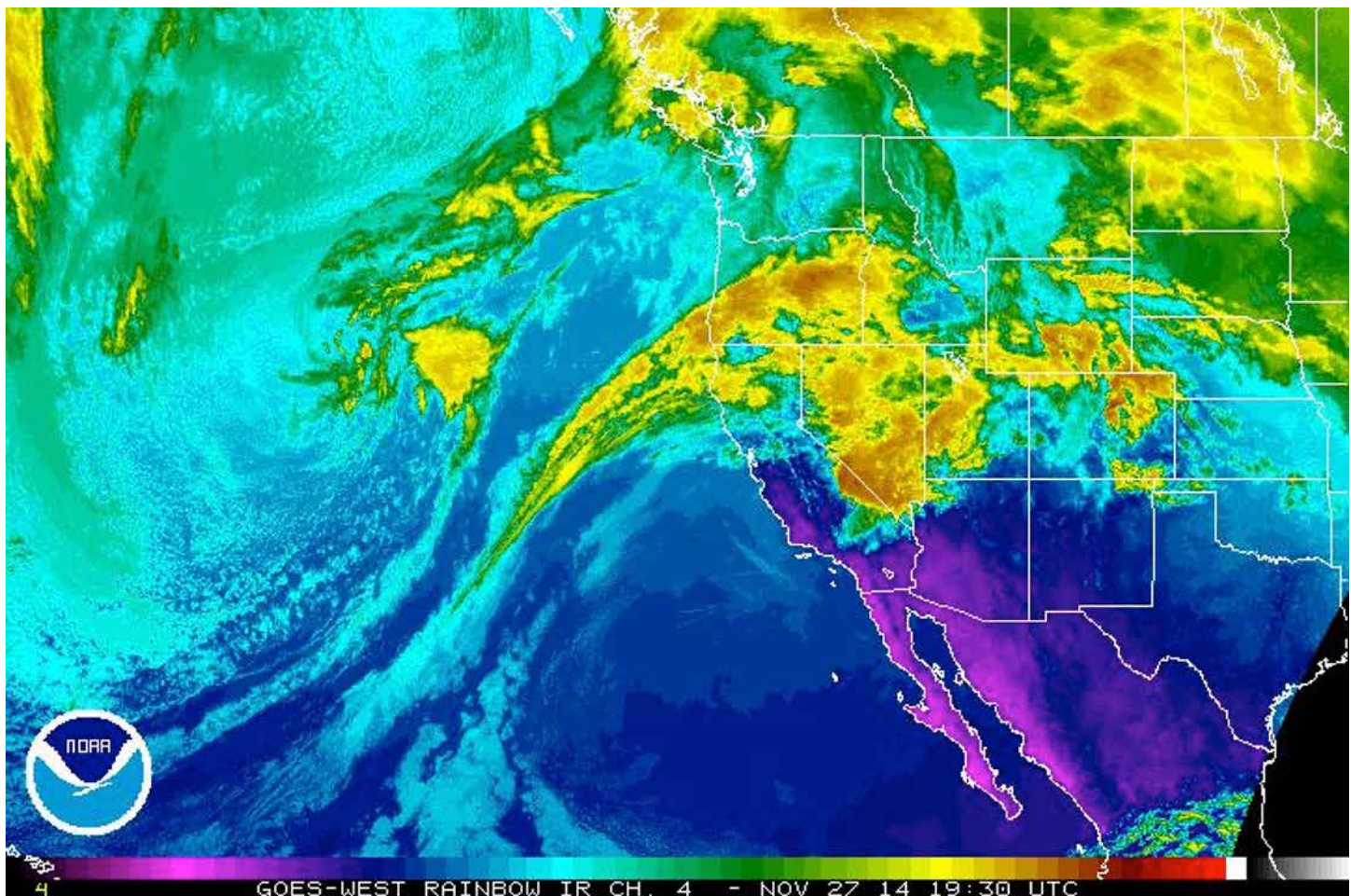


Figure 5.78. Satellite image of the Pineapple Express on November 27, 2014. The narrow plume of moisture near Hawaii broadens as it approaches the west coast (Source/Credit: NOAA/GOES).



## Impact of El Niño on Storm Tracks

Tropical ocean waters, especially those of the equatorial Pacific, undergo warming phases (El Niño) and cooling phases (La Niña), each phase lasting from several months to a couple of years. It has been long known that these cycles, now known as ENSO (El Niño/ La Niña Southern Oscillation) affect precipitation and temperature patterns along the Equatorial coast of Peru.

During the latter half of the 20th century, as satellite and buoy measurements of the Earth's surface and atmosphere began to accumulate, it became apparent that there was a much broader link between ENSO and global weather. The very strong impending El Niño predicted for 1997-1998 led to long-term weather forecasts and impacts, setting the stage for a test to check the accuracy of those predictions with actual observed patterns. Although some of their predictions failed to materialize, many proved to be accurate, especially in the conterminous United States.

Another massive El Niño occurred during 2015-2016, rivaling the record-breaking El Niño of the mid-1990s (Figure 5.79). Although there are several ways to attempt to compare the magnitude and duration of El Niño events, the most frequently used is the Oceanic Niño Index (ONI), which utilizes several parameters, among them sea surface temperature anomalies in the Equatorial oceans (Figure 5.80). Again, there was a golden opportunity to check theory against reality, comparing normal ENSO conditions (Figures 5.81a, 5.81b and 5.81C) with those observed.

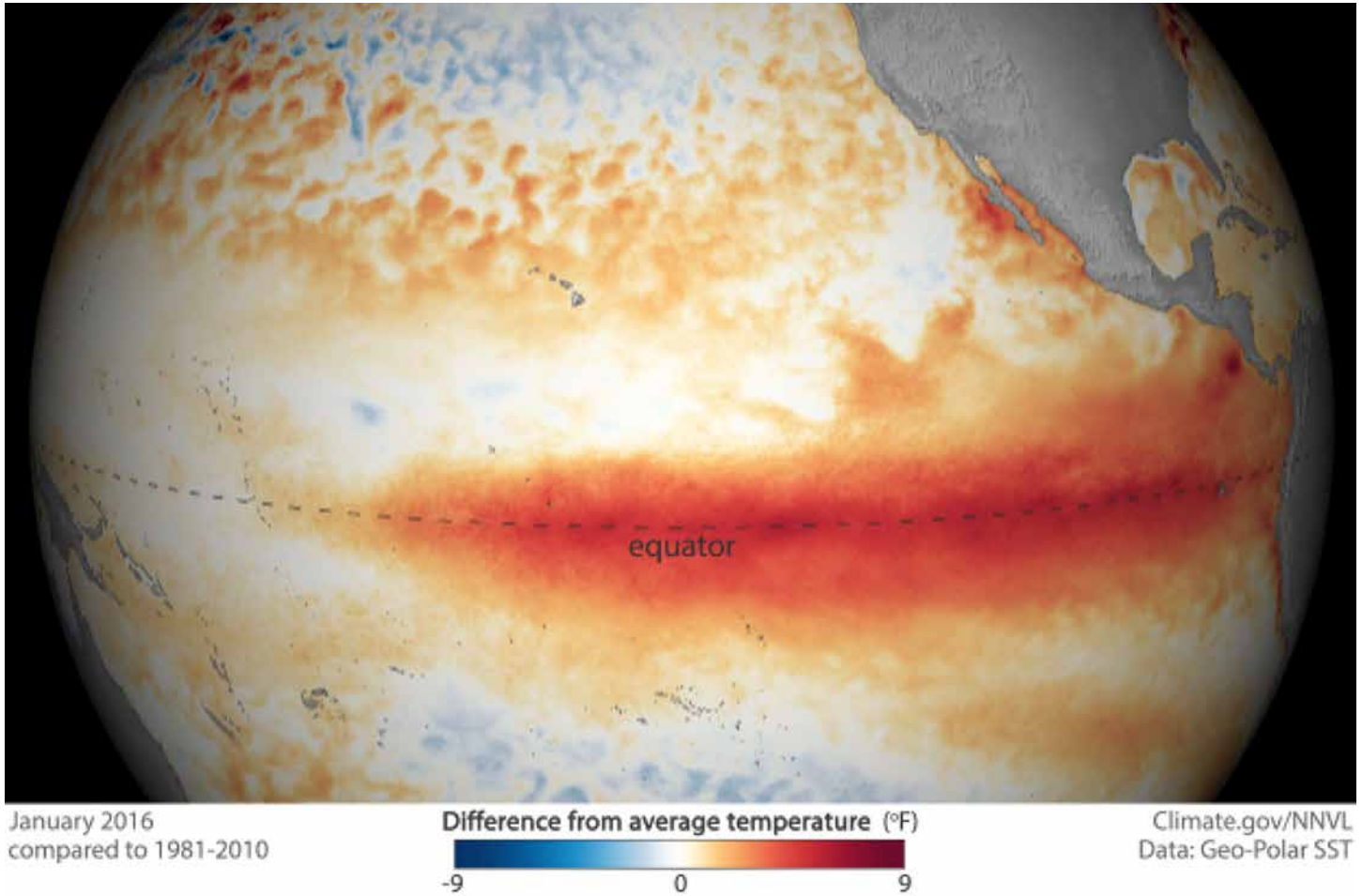


Figure 5.79. This satellite image shows sea surface temperature anomalies (departures from normal or average) for the month of January 2016. Orange and red colors are positive anomalies, and blue colors are negative anomalies. Averages are based on data from 1981-2010. The warmth in the equatorial east Pacific had already achieved the value of the record-breaking 1997-1998 El Niño (Source/Credit: Climate.gov/NNVL).

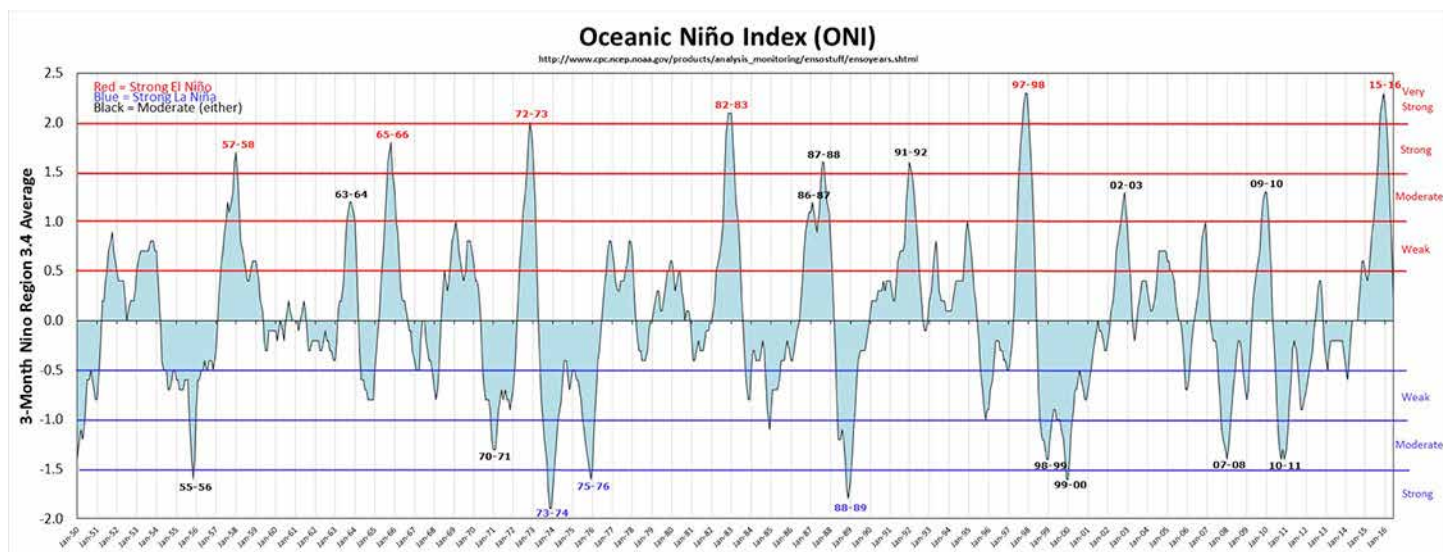


Figure 5.80. The Oceanic Niño Index from 1950 through most of 2016. Anything above or below 0.5 on the index for several months constitutes an El Niño (above 0.5) or a La Niña (below 0.5). Strong El Niño events are labeled in red. Using this index, it appears that the El Niños of 1997-1998 and 2015-2016 were the strongest on record (Source/Credit: NOAA/NCEP/CPC).

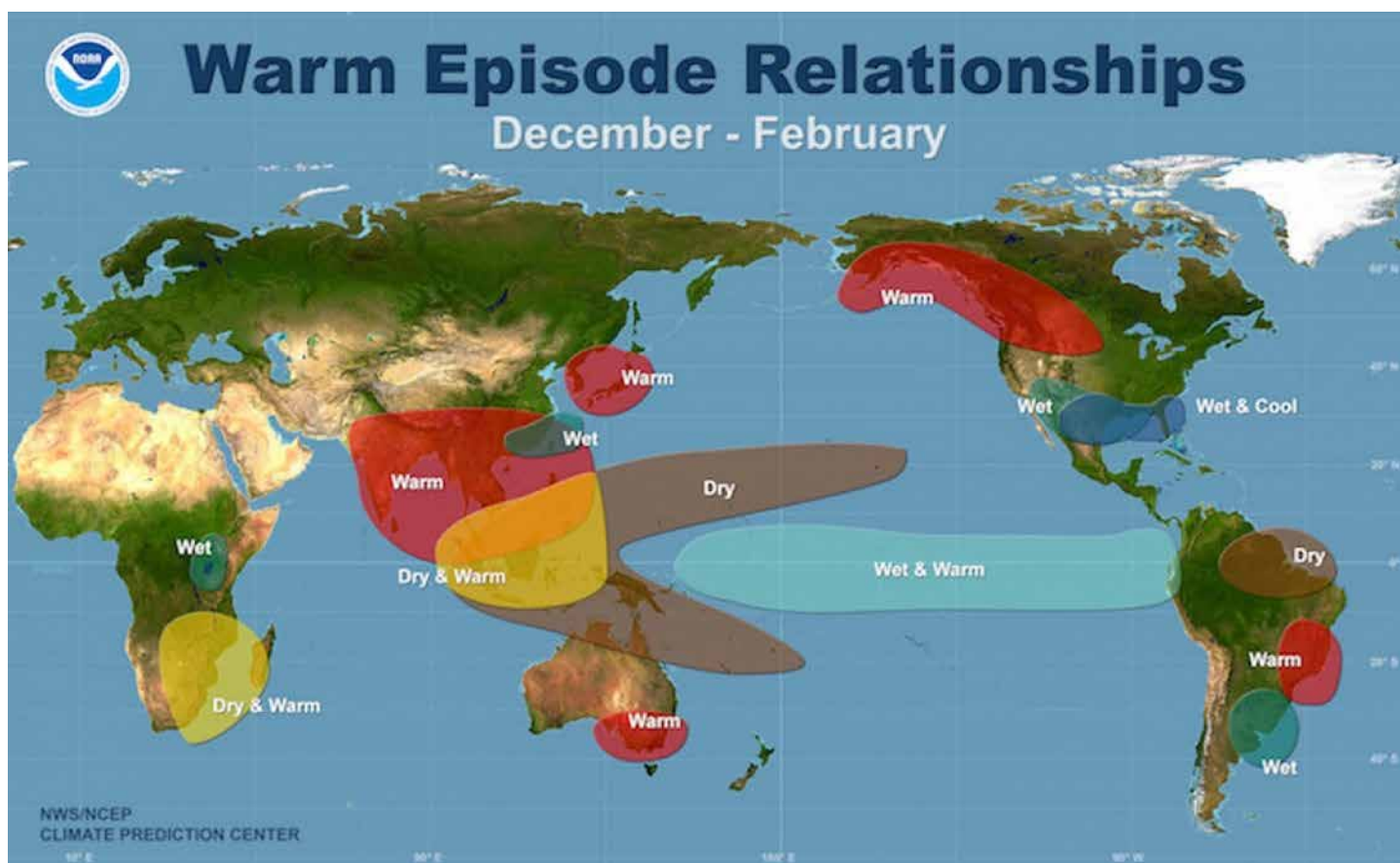


Figure 5.81a. Normal El Niño weather patterns around the globe (Source/Credit: NOAA).

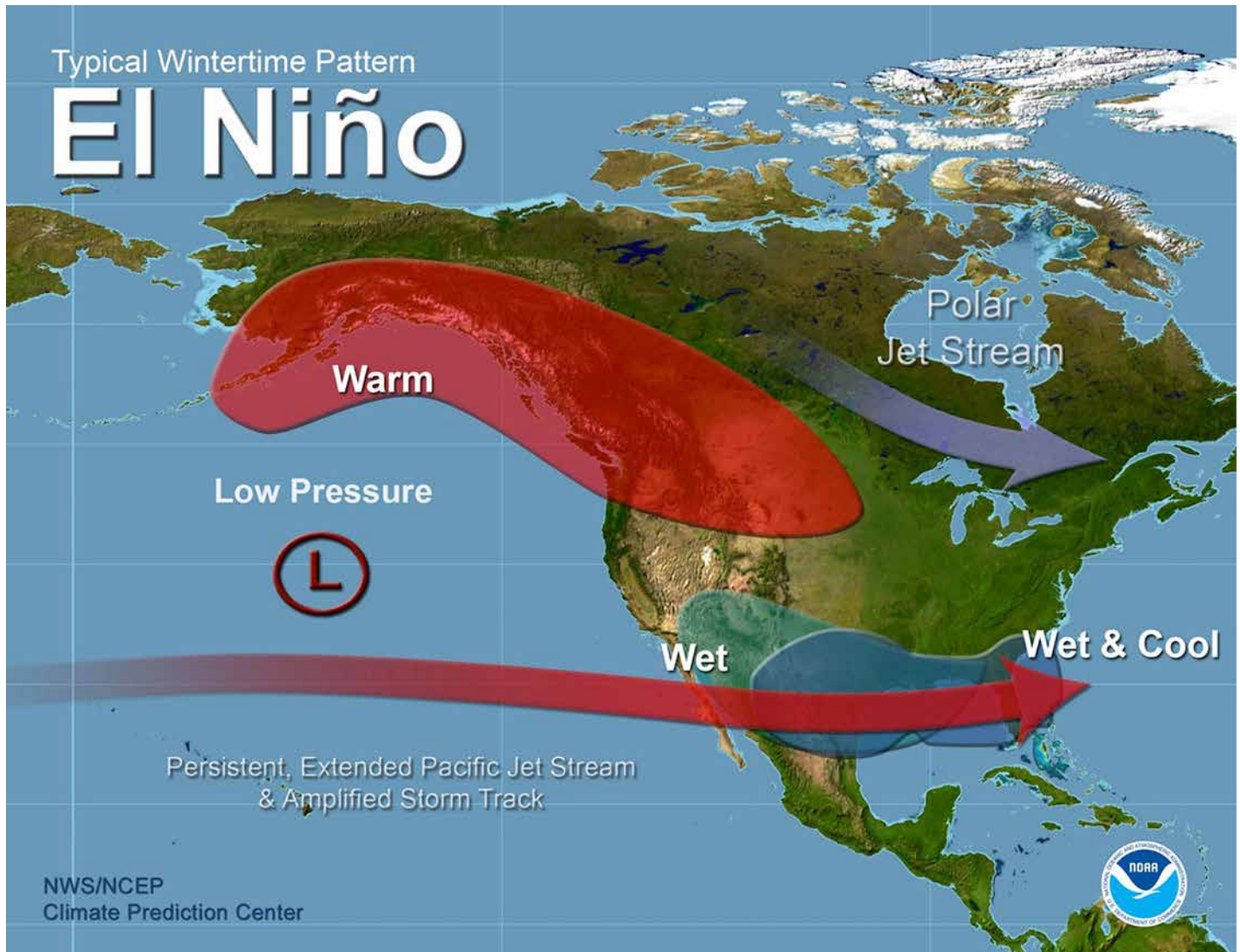


Figure 5.81b. Normal El Niño weather patterns for the eastern Pacific Basin and North America (Source/Credit: NOAA).

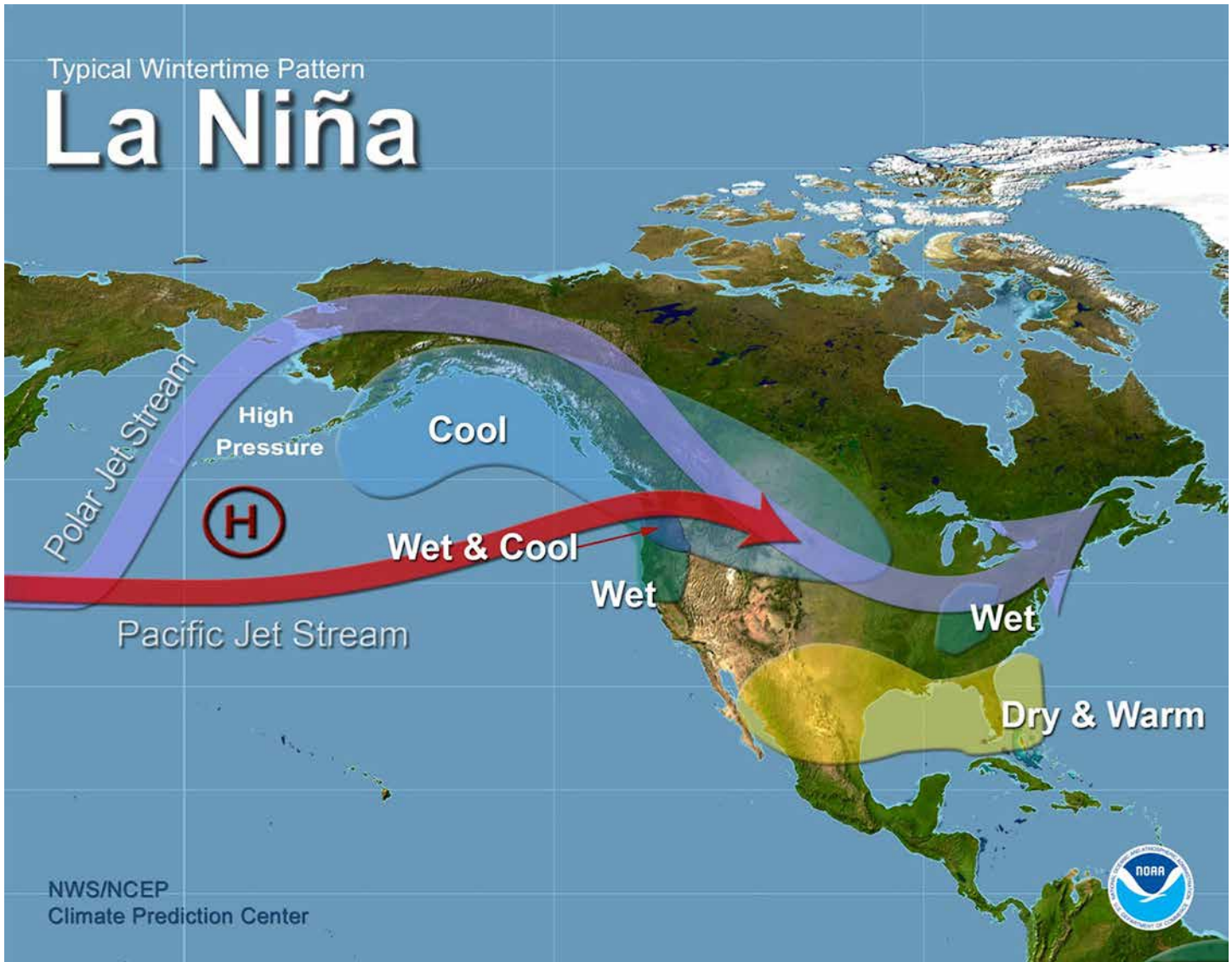


Figure 5.81c. Normal La Niña weather patterns for the Pacific Basin and North America (Source/Credit: NOAA).

By September, 2016 the El Niño event was over, and conditions were considered neutral. As expected, much of the southern tier of states were wetter than average, with many areas in Texas, Arkansas, Oklahoma and Louisiana getting record rainfall. During El Niños, the subtropical jet stream is energized by passage over warm waters and it is typically displaced south of its normal position. Although northern California was also predictably wet, southern California rainfall was actually below normal. The Pacific Northwest was warm and wet, instead of warm and dry as the normal pattern would have dictated. Apparently, the upper-level airflow pattern often took a northward swing just before the storms were set to drop rainfall on southern California (Figure 5.82), diverting the storms into the Northwest.

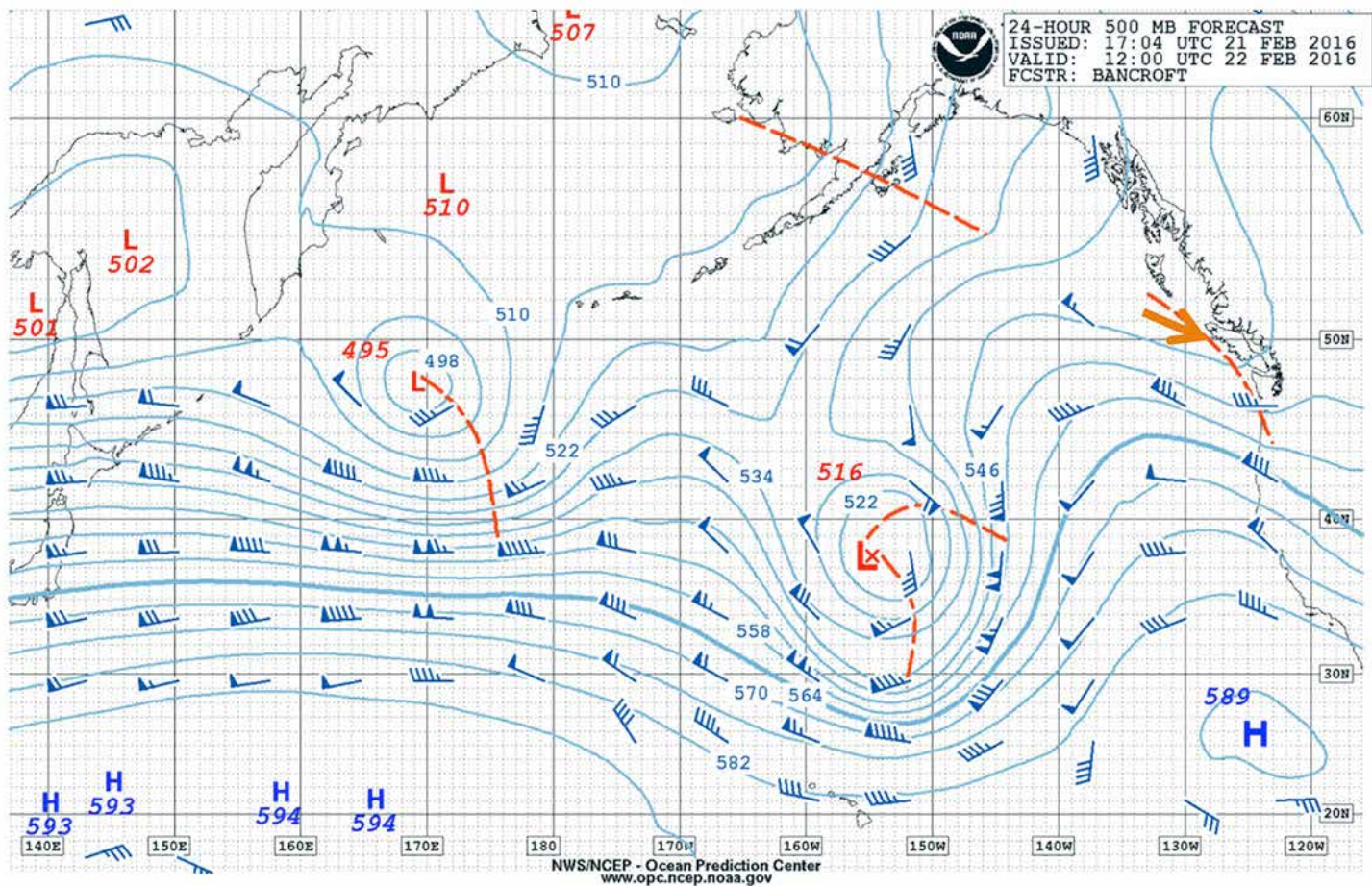


Figure 5.82. A trough and a ridge in the eastern Pacific Basin indicated on the upper-level 500 millibar chart (issued on November 21, 2016) will steer the surface storms into the Pacific Northwest, leaving southern California dry (Source/Credit: NWS).

With each ENSO cycle, meteorologists learn more about global connections, their causes, and why some warm or cold episodes do not fit the ideal pattern. Presently, agencies such as NOAA make probabilistic forecasts, but the cause-and-effect relationships in many regions are still unclear.

## Chapter 6

# Severe Weather

Thunderstorms, tornadoes, and tropical cyclones have in common that they produce severe weather, including some combination of heavy rainfall, hail, strong winds, local and regional flooding, frequent lightning, and storm surges. Global trends indicate a general decrease in death rates (per 100,000 population) from these events, the number of disasters reported and the number of people affected have increased dramatically over the past few decades (Figure 6.1). Much of the increase in reported global natural catastrophes has been due to meteorological and climatological events, with geophysical events remaining relatively constant (Figure 6.2). Although the trend in fatalities in the United States is similar to the global trend over the same period, monetary losses have seen staggering increases (Figure 6.3). These huge increases in monetary losses reflect not only population increase, but a multi-decadal migration of people to coastal zones and along river courses (Figure 6.4).

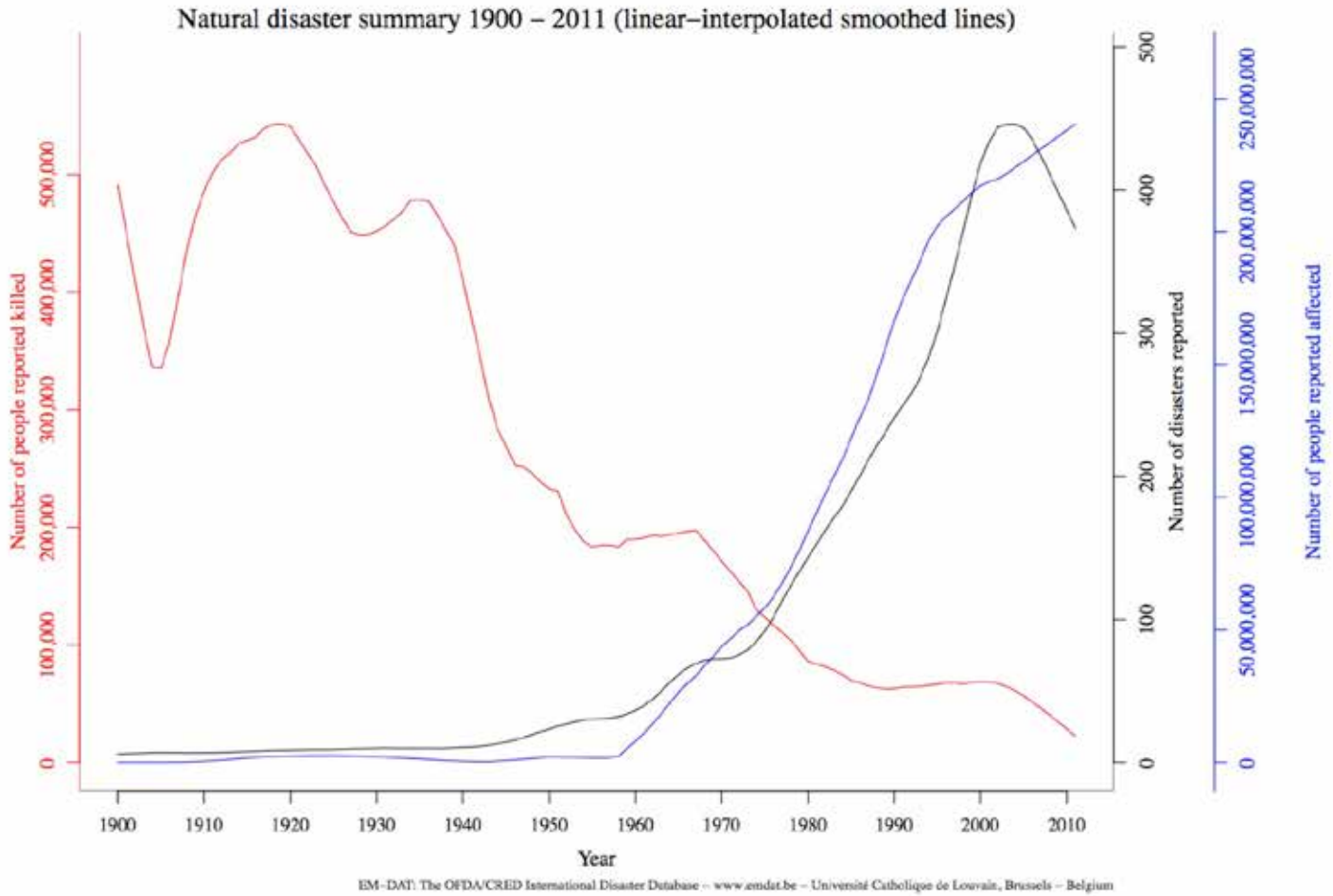


Figure 6.01. Since 1900, the trend in natural disasters has been toward lower death rates (per 100,000 population; red line), and increased numbers of people affected (blue line) as well as an increase in the number of disasters reported (black line) (Source/Credit: OFDA/CRED International Disaster DataBase – www.emdat.be-Université Catholique de Louvain, Brussels – Belgium).



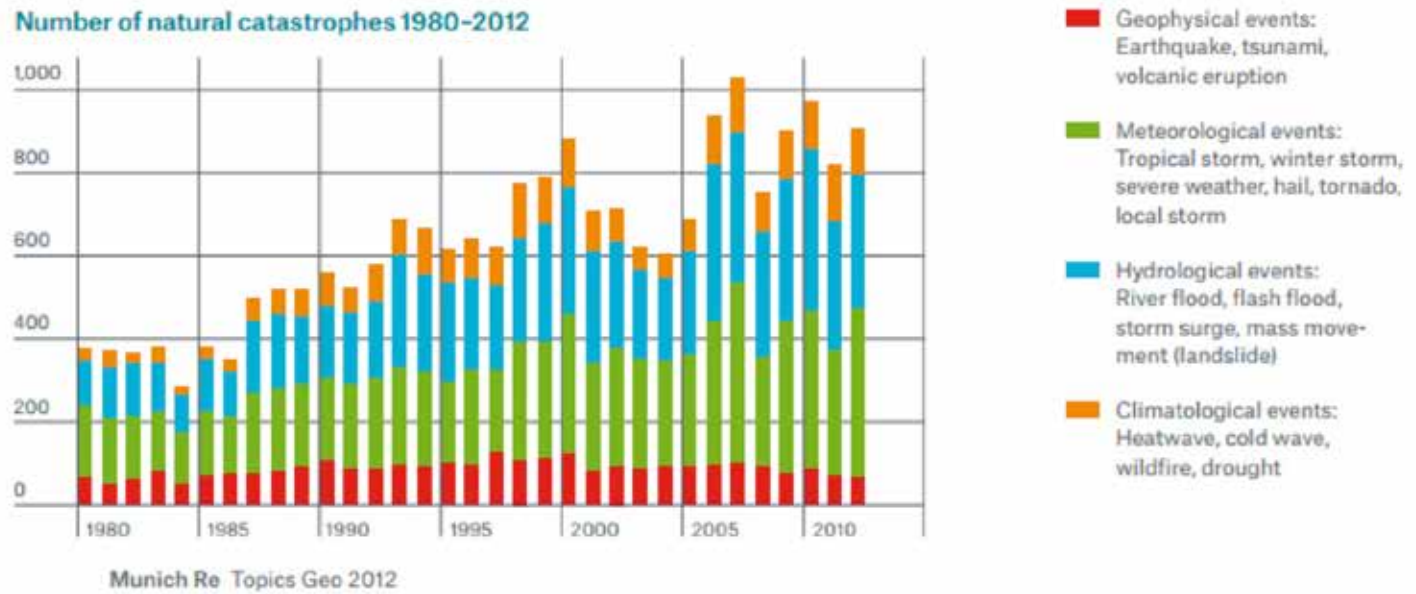


Figure 6.02. The number of reported global natural catastrophes has risen since 1980. The green, blue, and golden bars represent the cumulative number of reported weather/climate disasters, whereas the red bars represent geophysical events. Some atmospheric scientists attribute part of the rise in reported events to human-induced global warming (Source/Credit: Reinsurance Company Munich Re:Münchener Rückversicherungs-Gesellschaft Aktiengesellschaft in München Media Relations, Königinstraße 107, 80802 München, Germany).

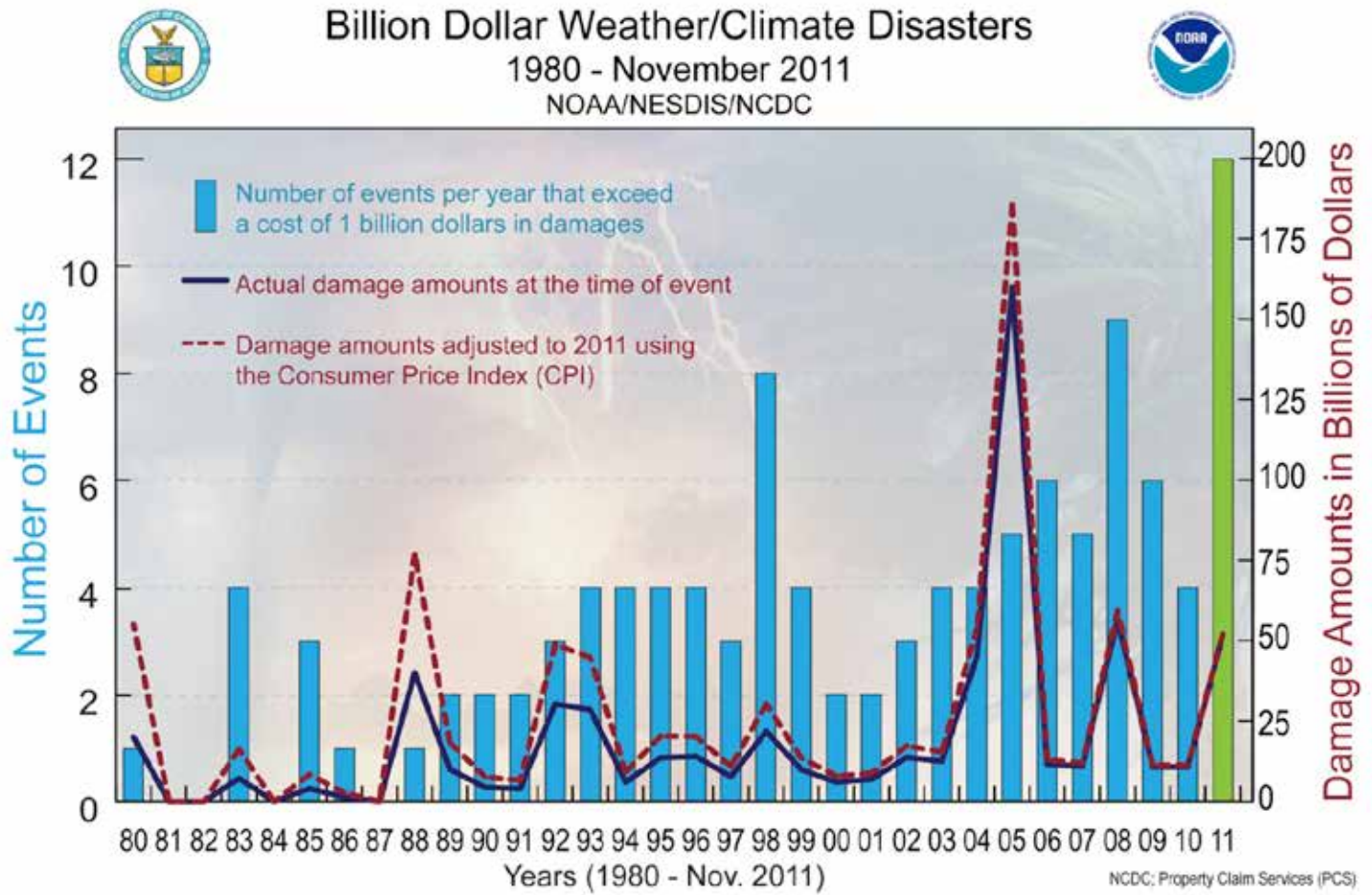


Figure 6.03. The number of billion dollar weather/climate disasters has generally increased in the United States since 1980, due in part to population increase as well as a shift in population toward the storm-prone coastal states (Source/Credit: NCDC/NOAA).

## Billion Dollar Weather Disasters 1980 - 2010

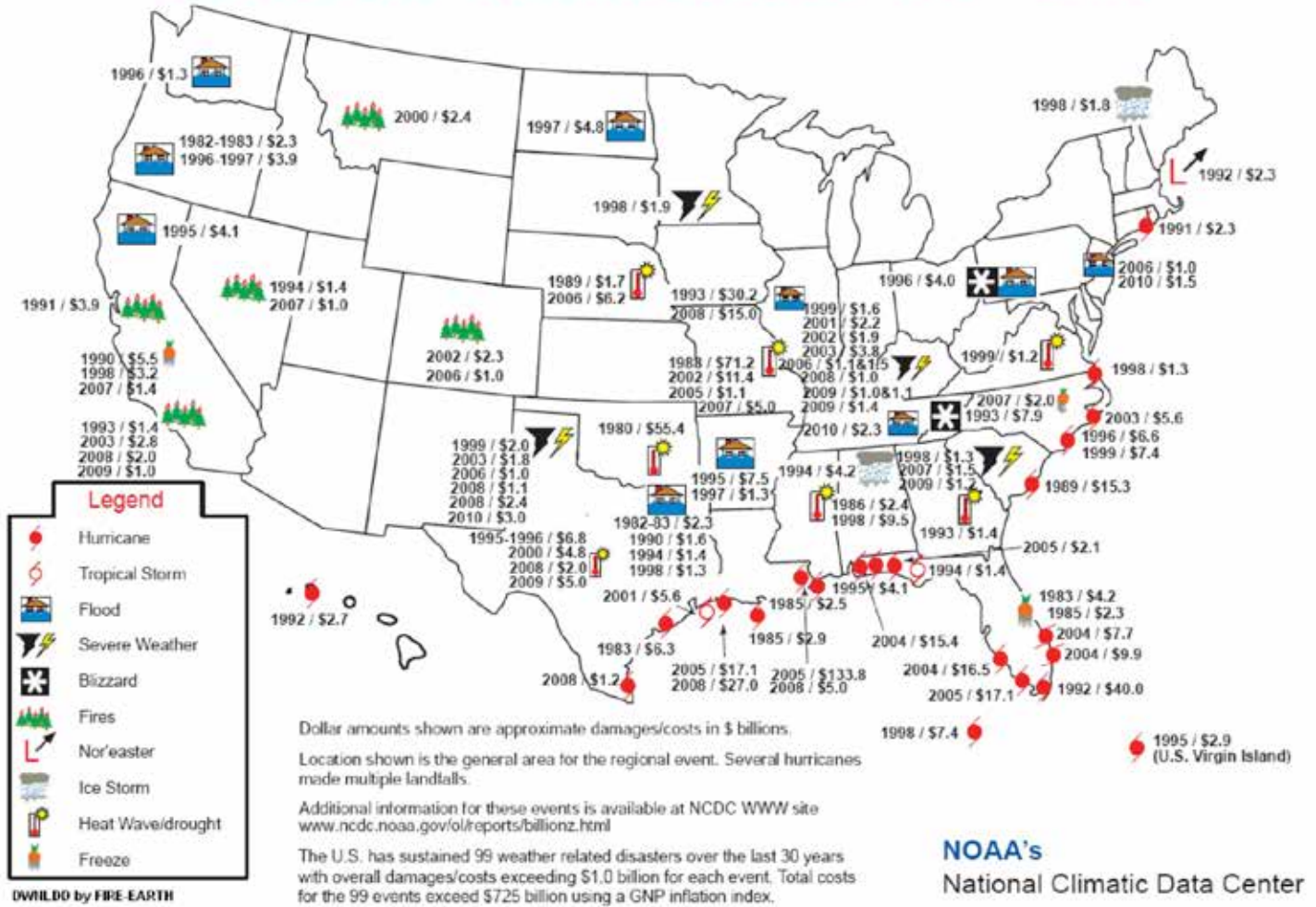


Figure 6.04. The United States has suffered a large number of billion-dollar weather disasters over the past few decades. The Rocky Mountain states and the upper Great Lakes states experienced relatively few disasters during this time. Texas, with its large size, high population, and great variety of weather events (severe thunderstorms, winter storms, tornadoes, tropical cyclones, drought, and wildfires) typically has the greatest annual number of billion-dollar disasters. Severe weather events in the Great Lakes states in 2014 and in New England in 2012 (e.g., Sandy) would change the geographic distribution somewhat in an updated map (Source/Credit: NOAA).

Individual weather events in the United States can account for massive monetary losses and substantial loss of lives (Figure 6.5). Storms such as hurricanes Katrina (2005), Sandy (2012), and Andrew (1992) are among the costliest natural disasters in U.S. history, with each of them costing tens of billions of dollars. Knowledge of their nature, time of occurrence, and direction of movement is critical in mitigating severe storm hazards as well as other weather/climate-related events.

### Most Expensive U.S. Weather Disasters Since 1980

Rank	Disaster	Year	Deaths	Damage (2013 dollars)
1.	<b>Hurricane Katrina</b> , LA/MS/AL	2005	1200	\$149,000,000,000
2.	<b>Drought</b> , Midwest/East	1988	7,500	\$79,000,000,000
3.	<b>Hurricane Sandy</b> , Northeast	2012	131	\$65,000,000,000
4.	<b>Drought</b> , Midwest/East	1980	10,000	\$56,000,000,000
5.	<b>Hurricane Andrew</b> , FL/LA	1992	26	\$45,000,000,000
6.	<b>Flood</b> , Mississippi River	1993	48	\$34,000,000,000
7.	<b>Drought</b> , Midwest/West	2012	123	\$30,000,000,000
8.	<b>Hurricane Ike</b> , TX/LA/MS	2008	112	\$29,000,000,000
9.	<b>Hurricane Wilma</b> , FL	2005	35	\$19,000,000,000
10.	<b>Hurricane Rita</b> , LA/TX	2005	119	\$19,000,000,000

**Source:** <http://www.ncdc.noaa.gov/billions>

Figure 6.05. Many of the most deadly and expensive natural disasters in the United States since 1980 have been weather/climate related. Surprisingly, drought has not only been among the most expensive weather/climate events, but also among the most deadly. Numerical data from recent storms (e.g., 2012 Hurricane Sandy, 2012 drought) will be adjusted upward with time due to inflation and added insurance claims (Source/Credit: NCDC/NOAA).

## Thunderstorms

Thunderstorms are local to regional-scale storms that are accompanied by lightning and thunder. They form almost exclusively from cumulonimbus clouds in a convectively-unstable atmosphere. They last from a few tens of minutes to a few tens of hours, and travel from a few miles from their point of origin to more than 1000 miles (~1600 km).

Although thunderstorms are extraordinary in terms of the amount of energy they liberate, they are quite common. Globally, about 1800 occur at any given time, 40,000 to 50,000 per day, and more than 16 million occur each year. In some areas, such as tropical rainforests, they are almost daily events. Conversely, there are many high-latitude areas where thunderstorms have never been observed.

### Origin of Thunderstorms

The formation of cumulonimbus clouds requires extensive vertical development of clouds, typically in the tens of thousands of feet. Cloud base may be just a few thousand feet above ground, whereas cloud tops may be in excess of 60,000 feet (~18,000 meters) in severe thunderstorms. Prerequisites for thunderstorm formation are therefore established when the air is buoyant for great thicknesses of the troposphere, a condition called a *deeply-convective atmosphere*.

Deep convection is favored by a condition where a body of air (an *air parcel*) is forced aloft, cools adiabatically, and achieves buoyancy because it becomes warmer than the surrounding *environmental air*. When the rising, cooling parcel of air becomes saturated with water vapor (i.e., the dewpoint has been reached), the water vapor condenses and a cloud is formed. The air parcel will continue to rise as long as it is buoyant (Figure 6.6). When the rising air parcel becomes cooler than the environmental air, often caused by the presence of an upper-level temperature inversion, uplift typically is halted, and the upper part of the cloud spreads out in response.

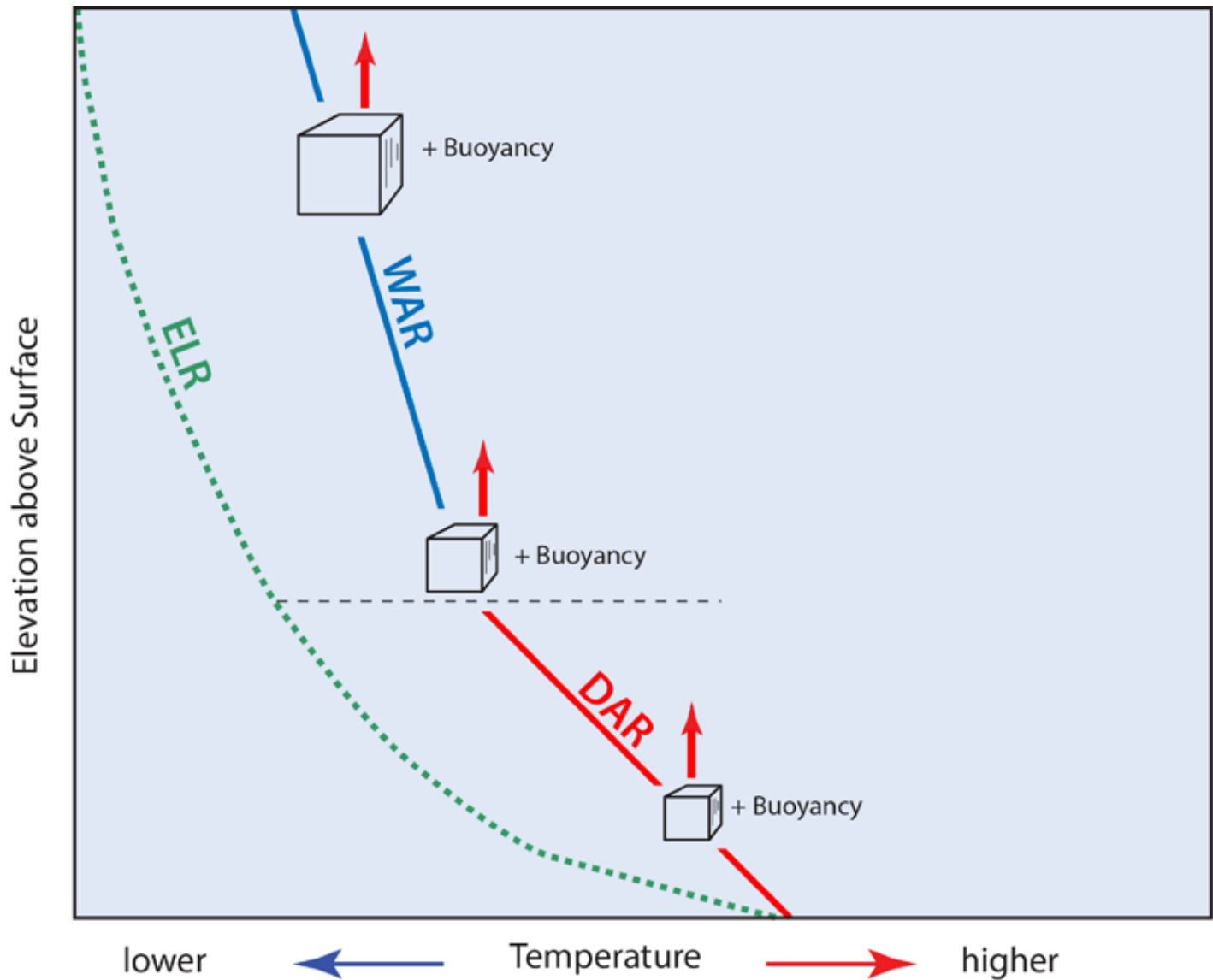


Figure 6.06. The dotted green line represents the environmental lapse rate (ELR), which would be the temperature profile of the atmosphere at a given time as measured by instruments at specified elevations above the ground surface. The ELR is constantly changing due to changing environmental conditions (e.g., solar heating from below, mid-level heating due to high pressure, advection of dissimilar air masses at different levels, etc.). If a volume of isolated air (an air parcel) is forced aloft, such as along a front or over a mountain, it will cool at pre-determined rates. As long as the air parcel remains unsaturated, it expands and cools at the dry adiabatic rate (DAR, solid red line). A rising air parcel that is saturated with respect to water vapor cools at a lesser rate, the wet adiabatic rate (WAR, solid blue line). In the above example, the air parcel (boxes) is warmer than the environmental air at any given elevation, so has positive buoyancy (red arrow) and a natural tendency to rise, whether being forced aloft or not (Source/Credit: Dennis I. Netoff).

The extent and intensity (velocity) of uplift depends on the relative buoyancy of the air parcel at any given elevation and the total amount of energy available for lift, often expressed as the **Convective Available Potential Energy (CAPE)**. CAPE values are expressed graphically by the amount of shaded area wherein a rising air parcel is warmer than the environmental air (Figure 6.7). A high CAPE value is commonly expressed as high instability, particularly when CAPE values are 2500J/kg (Figure 6.8). Violent storms may develop when CAPE values are between 2500 and 5000J/kg. CAPE values represent potential energy, and do not guarantee that violent convection will actually occur.

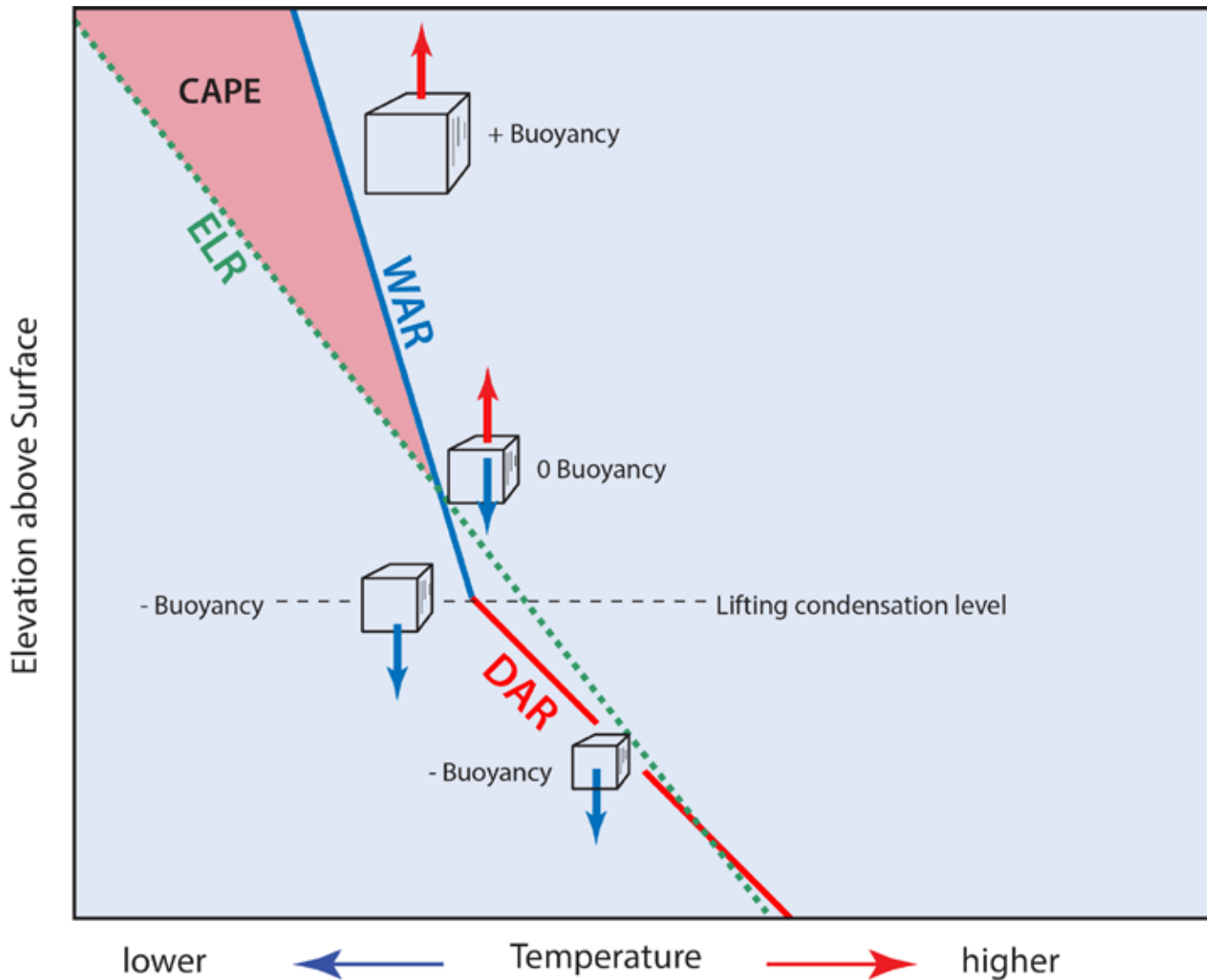


Figure 6.07. The dotted green line again represents the environmental lapse rate (ELR), whereas the solid red line is the dry adiabatic rate (DAR) and the solid blue line is the wet adiabatic rate (WAR). In the above example, the air parcel (boxes) is cooler than the environmental air below the “0 buoyancy” level, so it has negative buoyancy (blue arrow) and a natural tendency to resist upward displacement. Above the “0 buoyancy” level, the air parcel has positive buoyancy and should accelerate upward, producing a vertically-developed cloud. The greater the temperature difference between the buoyant air parcel and the environmental air, the stronger the vertical lift. The shaded pink zone (Convective Available Potential Energy; CAPE) represents the total amount of energy that the parcel has for upward acceleration. The greater the pink area (CAPE), the greater the potential for severe weather (Source/Credit: Dennis I. Netoff).

CAPE Value	Convection Potential
1	Stable
0-1000	Weak instability
1000-2500	Moderate instability
2500-4000	Strong instability
>4000	Extreme instability

Figure 6.08. CAPE values can be calculated if sufficient upper-level temperature/humidity measurements are taken. CAPE values can then be used to roughly estimate the convective potential of a rising parcel of air. CAPE values, however, represent potential energy when a parcel is lifted beyond the buoyancy level (also called the level of free convection). CAPE values range from stable (CAPE = 0) to extreme instability (CAPE >4000J/kg). Stable air is unlikely to produce deep convection, whereas extreme instability is potentially a breeding ground for severe thunderstorms (Source/Credit: modified from Rich Thompson, Storm Prediction Center, and others).



The environmental lapse rate within a thick portion of the troposphere will often display a zig-zag pattern with one, two or more temperature inversions. Although temperature inversions act as caps (i.e., suppress vertical uplift), they may actually promote a few violent storms by suppressing the formation of many non-violent ones and therefore conserve energy (Figures 6.9a and 6.9b). CAPE values for the United States are available from several internet sources (Figure 6.10) and, along with other assessments of convective potential in the atmosphere, are valuable in short-term severe storm forecasting.

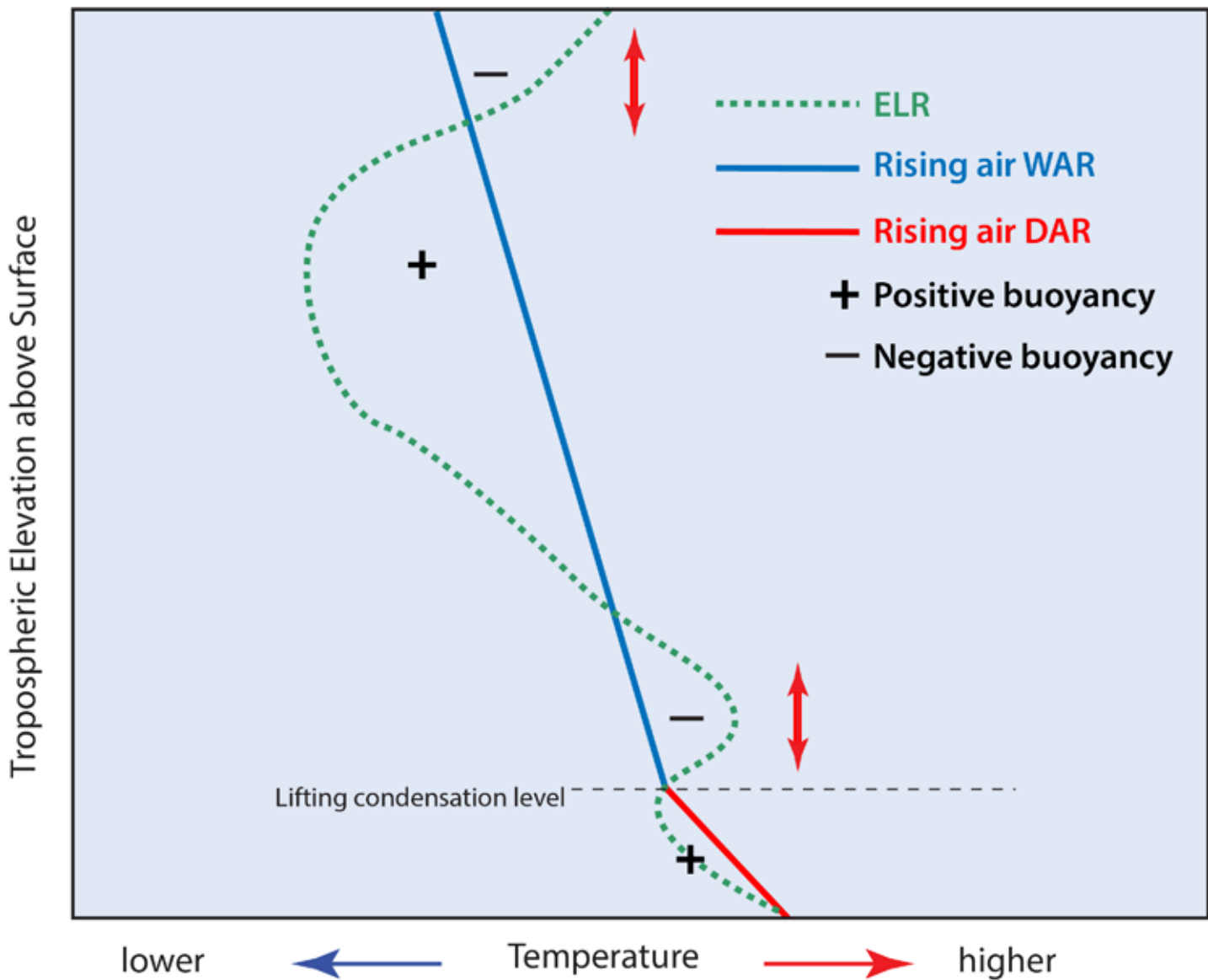


Figure 6.09a. The environmental lapse rate within the troposphere may display several temperature inversions (red arrows). This results in alternating zones of positive and negative buoyancy for a rising air parcel. Thick zones of positive buoyancy above the lifting condensation level may generate thick convective clouds, and ultimately thunderstorms (Source/Credit: Dennis I. Netoff).

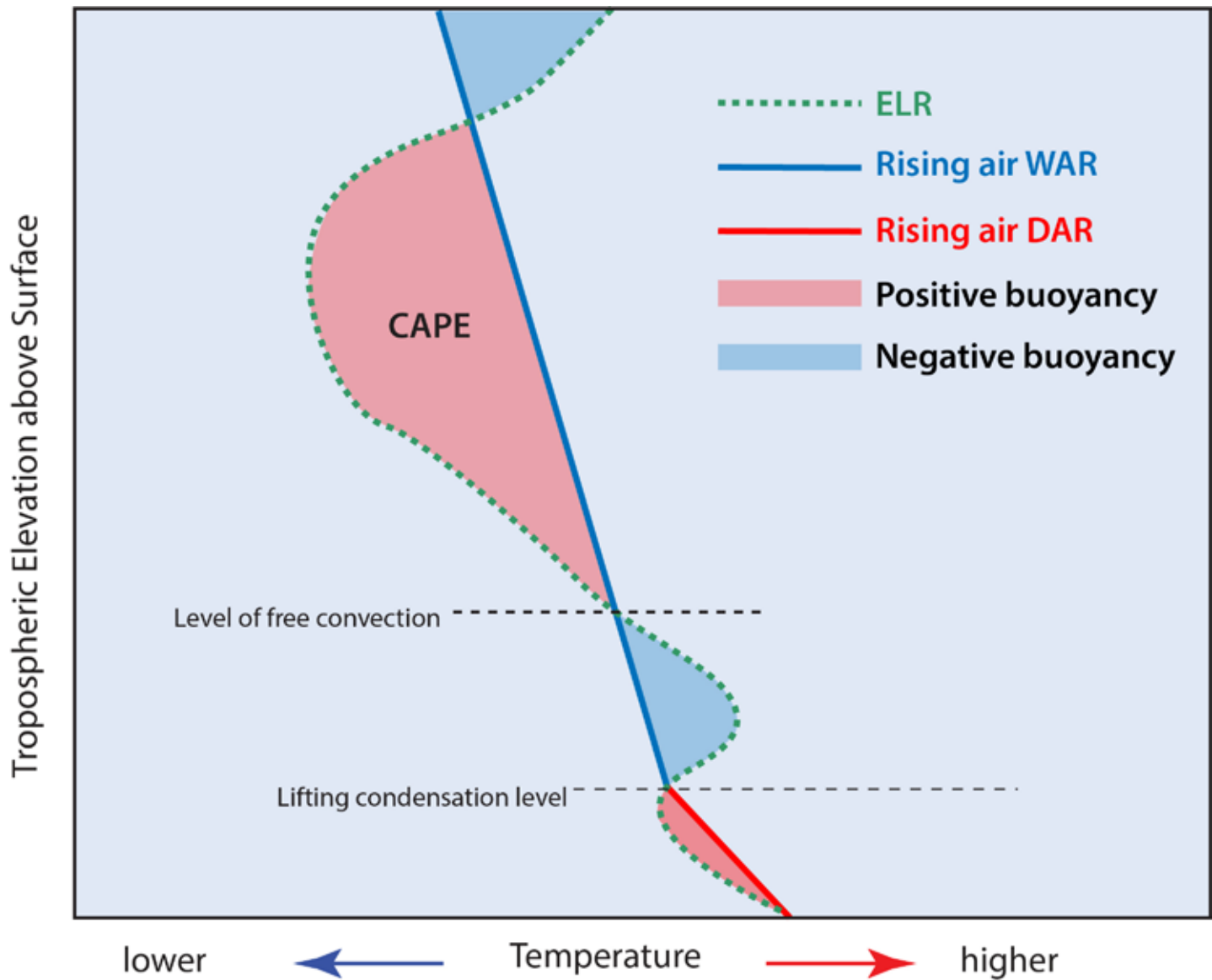


Figure 6.09b. The graph indicates the same atmospheric environment as Figure 6.09a, but with areas of positive and negative buoyancy shaded in pink and blue. The greater the surface area of shading, the more pronounced the positive or negative buoyancy. The high CAPE value in the middle troposphere indicates the potential for deep convection. If CAPE values are calculated  $>2500$  J/kg, thunderstorms are likely to develop. Values of  $>3500$  J/kg indicate the potential for severe storms. This is sometimes referred to as an atmosphere of high instability (Source/Credit: Dennis I. Netoff).

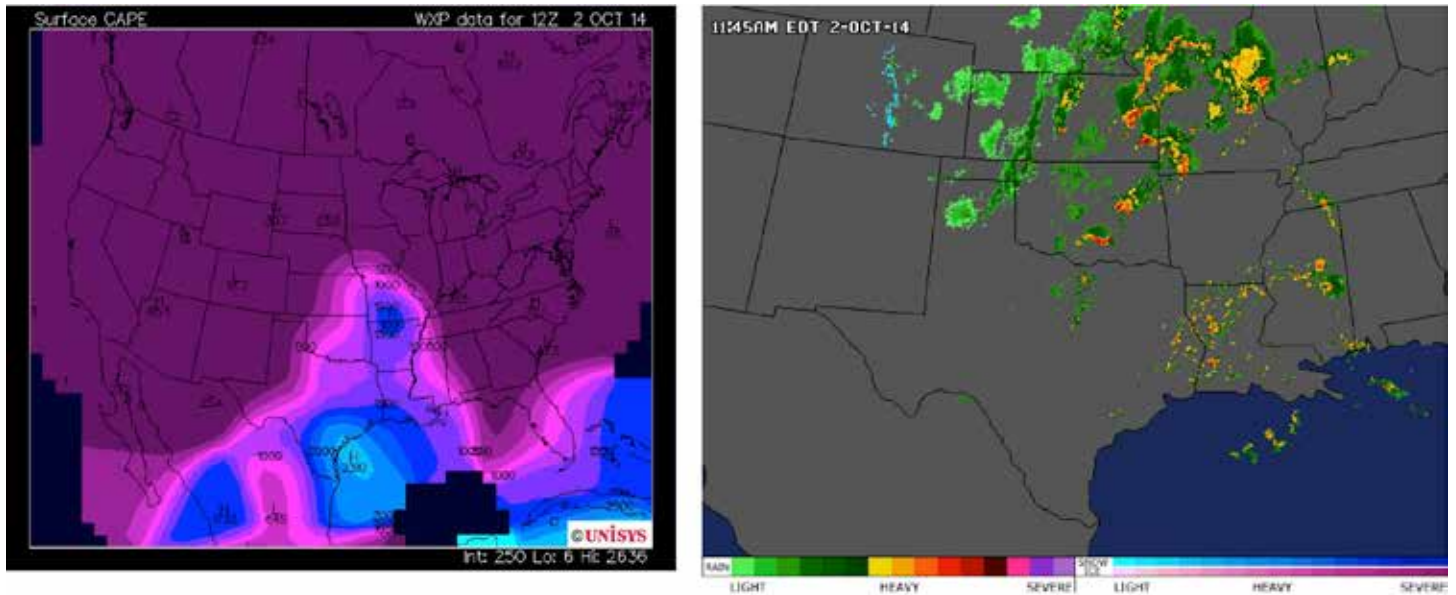


Figure 6.10. CAPE values for the United States on the morning of October 2, 2014 indicate the potential for deep convection in the south-central states, and northward into Arkansas and Missouri (left image, Source/Credit: UNYSYS). The image on the right shows several lines and pockets of severe thunderstorms at about the same time (right image, Source/Credit: Accuweather).

## Types of Thunderstorms Based on Uplift Triggers

In the middle latitudes during the warm season, much of the southeastern side of large continents is under the influence of warm, moist and unstable air. Cumulus and cumulus congestus clouds frequently form, but very few of them develop into cumulonimbus clouds and associated thunderstorms. What is often needed to generate thunderstorms is a thick layer of unstable air and some mechanism to initiate large-scale uplift — a boost or a triggering mechanism. Common triggering mechanisms include orographic barriers, fronts and upper-level divergence: these triggers are the basis for classification of thunderstorms (Figure 6.11).

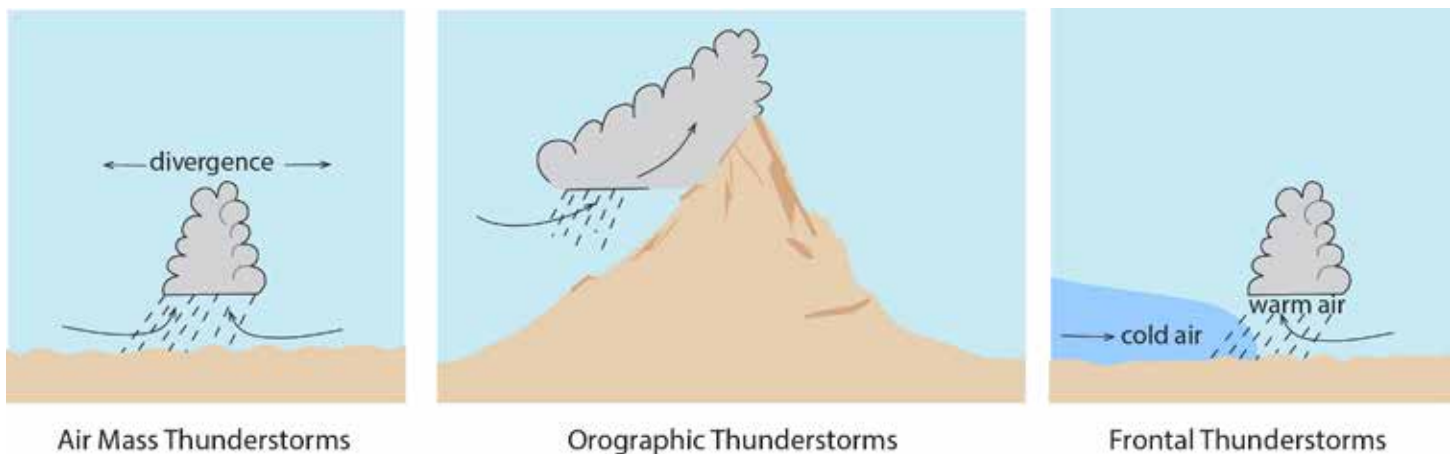


Figure 6.11. Types of mechanisms that initiate uplift. Air mass thunderstorms are the most difficult to predict because the upper level divergence that provides their development is not detectable by ground-based observations and their development may be quite sudden (Source/Credit: modified from Dennis I. Netoff and Ava Fujimoto-Strait, *Weather & Climate Lab Manual*).

## Air Mass Thunderstorms

During the summertime in the United States, a type of thunderstorm known as an **air mass thunderstorm** develops when the bottom layer of an mTg or mTa air mass is heated by the warm ground. Less often, this type of thunderstorm may develop when cool cPc air masses move southward and its bottom layer warms by conduction and radiation as it moves over warm ground. In both circumstances, heating may create instability which causes the air to become buoyant and rise.

Recent observations indicate that many, if not most, air mass thunderstorms require *upper-level divergence* to form. Upper level divergence can be caused by air molecules moving away from each other directionally, or it may be the result of accelerated upper-level flow velocity. Air mass thunderstorms most commonly occur during the mid-afternoon hours, when the environmental lapse rate is the steepest. Their geographic distribution is usually fairly random, and they are the most difficult type of thunderstorm to predict in terms of location. Many air mass thunderstorms form as single updraft and downdraft cells and grow randomly from scattered *cumulus congestus* clouds which appear on satellite imagery as popcorn balls (Figure 6.12). Larger and longer-lasting variants of air mass (and other) thunderstorms are supercell thunderstorms and mesoscale convective complexes.

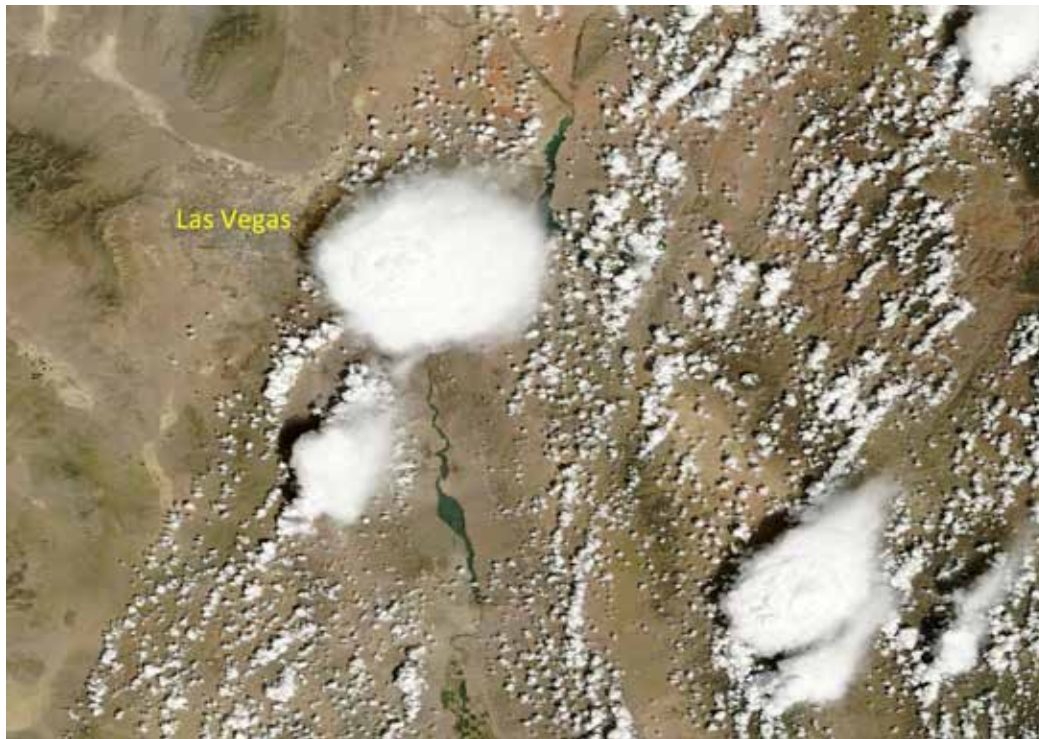


Figure 6.12. Air mass thunderstorms developing from a popcorn sky. The small, white puffs are cumulus humilis clouds, some of which are developing vertically into cumulus congestus clouds (larger puffs). The half-dozen large, white areas, such as the one just east of Las Vegas, are erupting cumulonimbus clouds. Lake Mojave is in the lower center of the image, and Lake Mead in the upper center. Local flash flooding followed the outbreak of severe thunderstorms that occurred here on August 14, 2014 (Source/Credit: NASA's Terra Satellite).

## Orographic Thunderstorms

Orographic thunderstorms get their initial lift from highlands or mountain barriers. They are common in practically all mountainous areas where relatively warm, moist, unstable air is forced to cross topographic barriers. The southern Rocky Mountains, for example, frequently develop mid-afternoon thunderstorms which then migrate toward the east as the day progresses. By evening, these can migrate all the way into Kansas, Nebraska and Oklahoma. Areas such as the Sangre de Cristo Mountains in New Mexico may generate over 60 thunderstorm days per year, which is greater, on average, than East Texas (Figure 6.13).

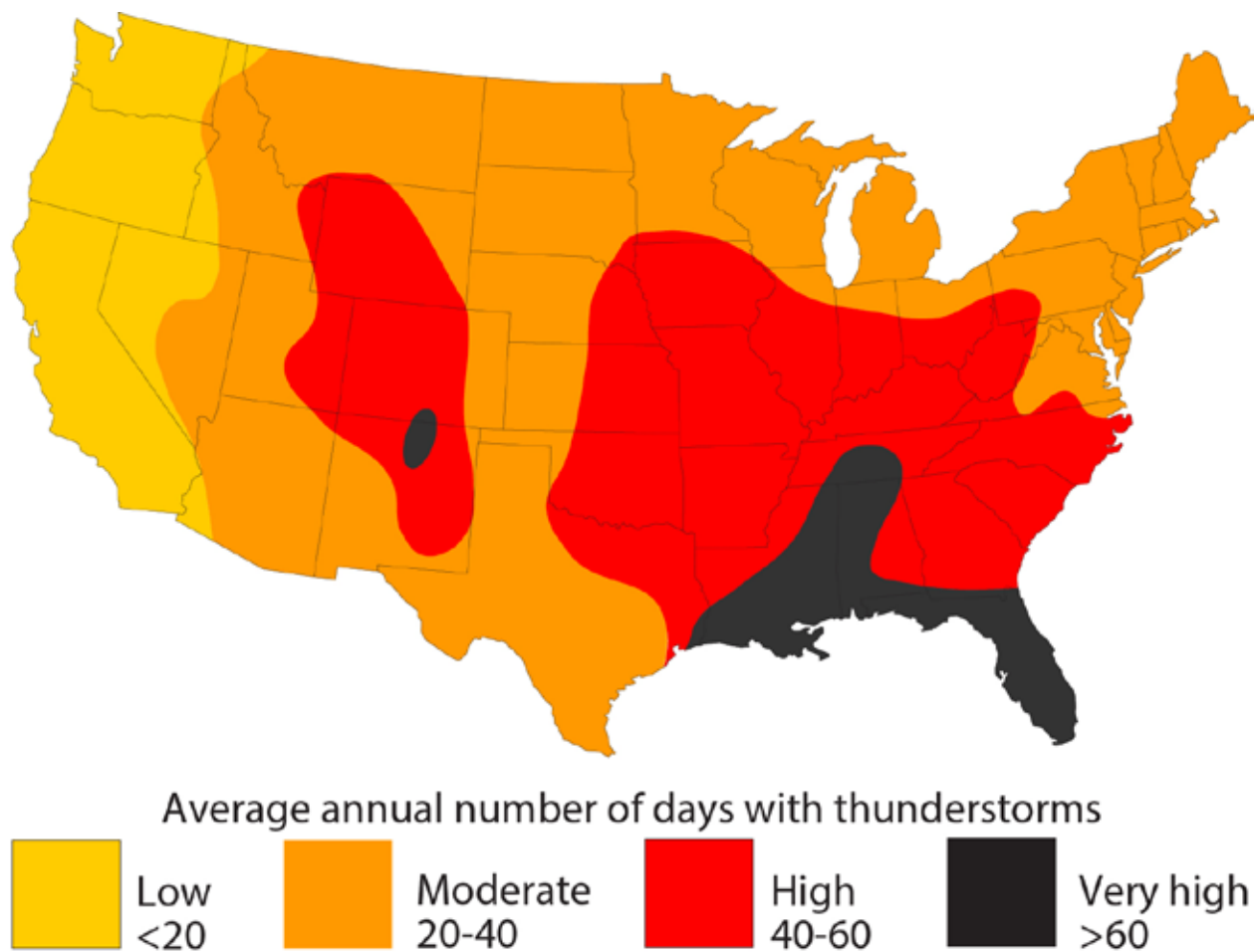


Figure 6.13. The orographic effect is evident in the high frequency of thunderstorms along the Rocky Mountain front from New Mexico to Wyoming. The broadest expanse of frequent thunderstorms is along the Gulf Coast where warm, moist unstable air dominates during much of the year (Source/Credit: modified from Dennis I. Netoff and Ava Fujimoto-Strait, *Weather & Climate Lab Manual*).

## Frontal Thunderstorms

**Frontal thunderstorms** form along the boundary between different types of air masses. Fronts supply the initial lift required to generate instability and often form lines of thunderstorms. Cold fronts, because of the steepness of the frontal boundary and the rapid rate of frontal advance, are efficient thunderstorm producers, especially when they clash with warm, moist unstable air from the Gulf of Mexico or the tropical Atlantic during the warm season (Figure 6.14). Cold front thunderstorms can occur at any time of the day or night. Other types of fronts, including stationary, occluded and warm, can produce thunderstorms if the upper-level 'support' is in place. Some of the most persistent and violent thunderstorms in Texas occur when cold fronts lose their momentum over the Texas Hill Country. **This area has recently been called the most flash-flood prone region in all of North America.**

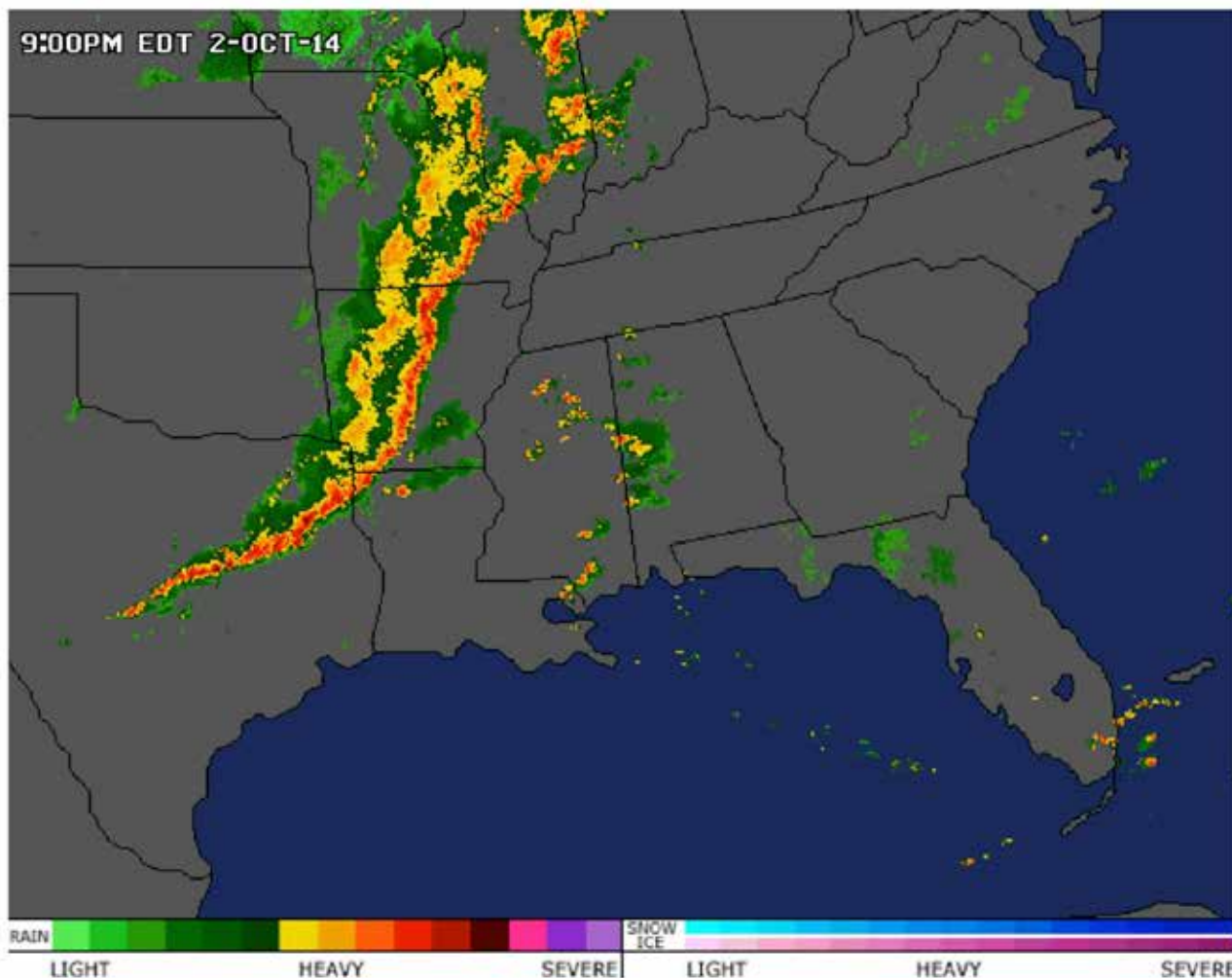


Figure 6.14. Frontal thunderstorms can occur along any type of front, but are most common along cold fronts, where there is rapid uplift of air, fast frontal movement and a large contrast in air masses on either side of the front. They are often referred to as squall lines, and can form along the front, behind the front, or a considerable distance ahead of the front. This long, linear belt of thunderstorms formed along a cold front boundary during the late afternoon hours of October 2, 2014 (Source/Credit: Accuweather/NWS).

The Texas Hill Country is the breeding ground for long-lasting and often dangerous thunderstorms and flash floods because of its geography (Figure 6.15). Environmental factors that favor their development include:

- (1) a nearby source of warm, moist, unstable air in the Gulf of Mexico;
- (2) uplift provided by the elevated Hill Country topography (Austin ~500 ft. elevation, Johnson City 1200 ft., Fredericksburg 1700 ft., Harper 2000 ft.);
- (3) slow-moving or stationary fronts that provide additional uplift;
- (4) periodic influx of moisture-laden air from tropical storms and hurricanes originating in both Gulf and Pacific source regions;
- (5) extensive areas of exposed bedrock or very shallow soils that promote rapid runoff of rainwater.

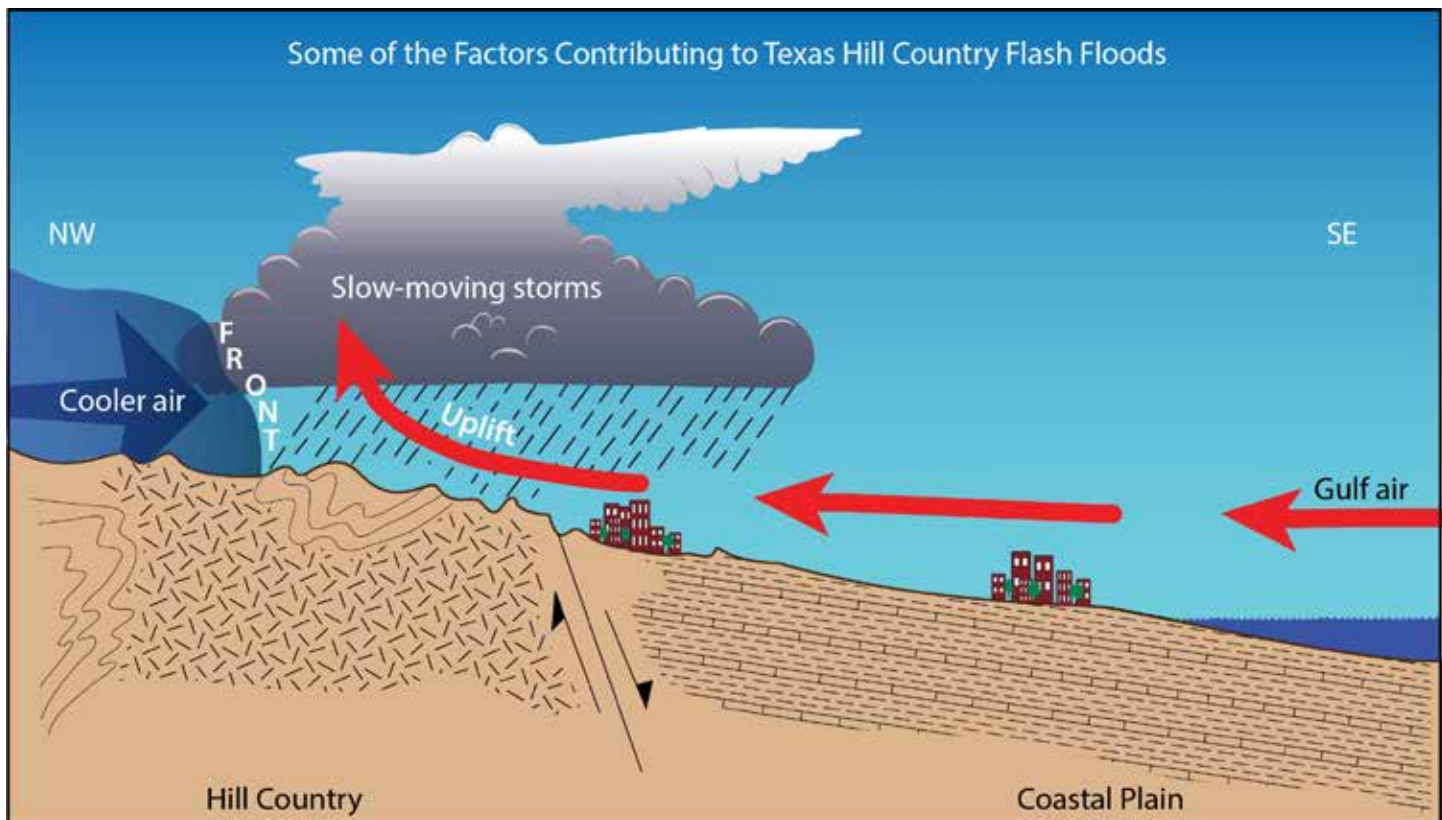


Figure 6.15. The Texas Hill Country has been tabbed as the most flash-flood prone area in the United States. Environmental factors that favor heavy, long-lasting thunderstorms include proximity to the Gulf of Mexico, orographic uplift, slow-moving or stalled fronts, periodic tropical storm moisture influx, and a high percentage of shallow soils and exposed bedrock (Source/Credit: Baldwin, Cooper, Netoff, Solum and Degenhardt, *Geologic Hazards and Resources Laboratory Manual*, 2007).



## Types of Thunderstorms Based on Size, Duration, and Severity

Thunderstorms can also be classified according to size, duration, and severity. **Single-cell thunderstorms** have a single dominant updraft and single downdraft and are typically small (a few square miles) and relatively non-violent (Figure 6.16). Many thunderstorms that develop within air masses are single-cell thunderstorms. They tend to be short-lived (20-30 minutes), although sometimes they can generate secondary thunderstorm cells that are of similar duration.



Figure 6.16. Single-cell thunderstorms typically have a single updraft and downdraft, are small in surface area, short-lived, and relatively non-violent. Gust fronts from these storms may give rise to other thunderstorms, such as the one building immediately to the left of the cumulonimbus cloud in the image center (Source/Credit: Bill Westphal, with permission).

**Multicell thunderstorms** contain clusters of updrafts and downdrafts (Figure 6.17). They are larger and of greater duration than single-cell thunderstorms, typically cover tens to hundreds of square miles, and may last for hours to over 12 hours. Multi-cell thunderstorms are frequently violent, and may become tornadic. In map view, they can either take the form of irregularly-shaped clusters, of linear belts, often called squall lines (Figure 6.14). Large supercell thunderstorms may be embedded in multi-cell thunderstorm clusters and linear belts (see section on severe storms).

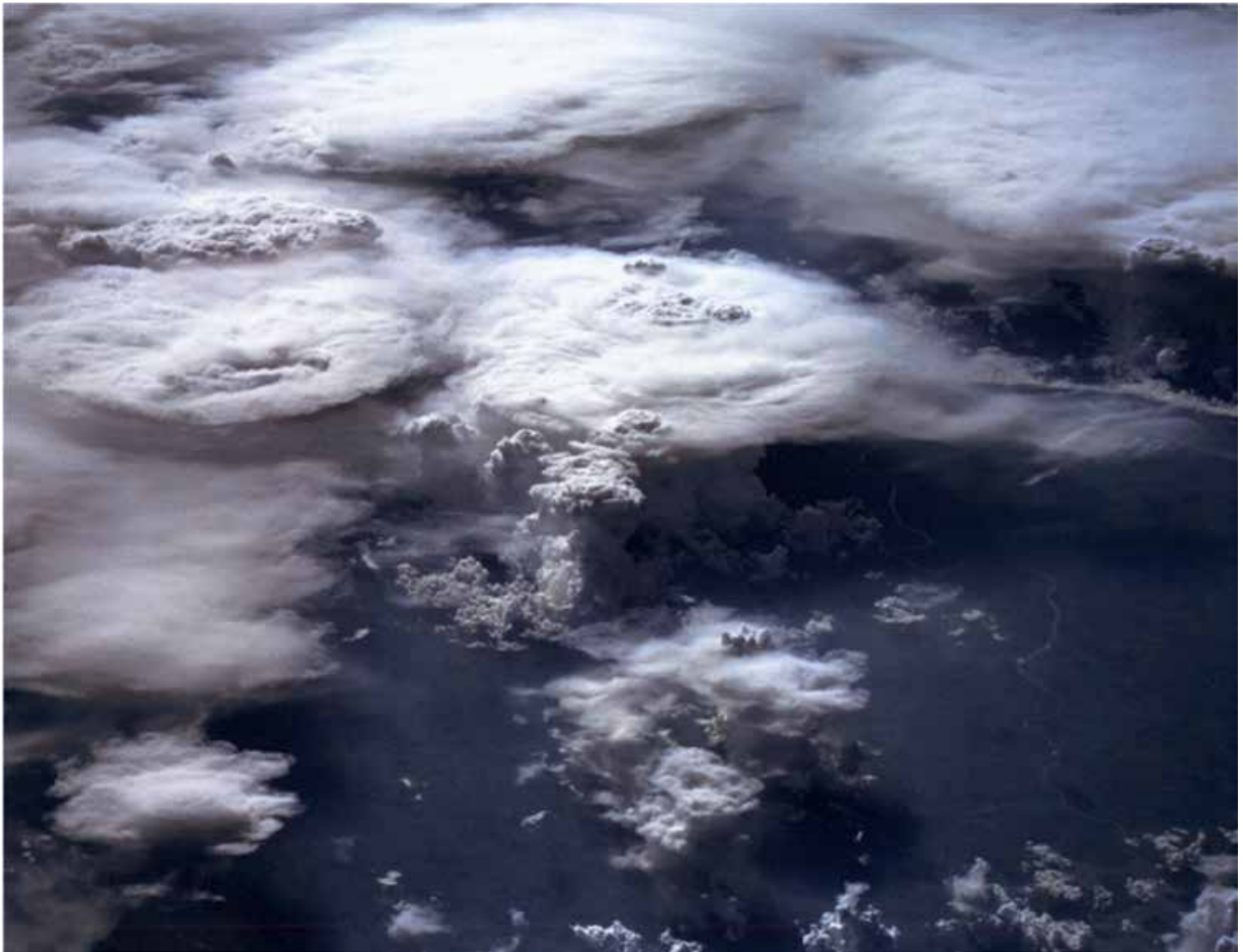


Figure 6.17. Multicell thunderstorms consist of several updrafts and downdrafts. They can cover tens to hundreds of square miles, and last for many hours. They are typically more violent than single-cell thunderstorms. They may form randomly-oriented clusters such as these in Amazonia or may form linear belts (Figure 6.14), often called squall lines (Source/Credit: NASA).

**Mesoscale convective complexes** (MCCs) are very large (area typically >40,000 square miles; ~100,000 square kilometers) clusters of thunderstorms, many of which may be violent (see section on severe storms). They may last >24 hours and cover distances of several hundred to over a 1000 miles; (1600 km). These complexes are common in the American Great Plains and in subtropical areas of South America, southeast Asia, Africa, and Australia (Figure 6.18). The reason for their low frequency in tropical latitudes is unclear, but may be related to the presence of a subtropical mid-level jetstream, which is uncommon in the equatorial latitudes.



Figure 6.18. Generalized distribution of some of the more frequent mesoscale convective complexes on Earth. With the exception of Africa, MCCs are relatively infrequent in the equatorial latitudes (Source/Credit: modified from maps of Laing and Fritsch, 1997, and other sources).

## Stages of Thunderstorm Development

### Cumulus Stage

All thunderstorms go through stages of development. In the case of air mass thunderstorms, these stages typically occur over the period of a few hours. In more severe thunderstorms, the stages last longer. In some orographic thunderstorms, the stages may progress in barely over an hour. Initially, small convective clouds appear in the atmosphere, indicating that the atmosphere is in a mild convective phase (Figures 6.19, 6.20 and 6.21). During the **cumulus** stage, the storm consists of vertically-growing cumulus clouds (Figure 6.21). Typically the cloud will grow to 20,000 or 30,000 feet in response to convectonal uplift of moist, unstable air. The rising column of air that generates the cloud is known as an **updraft** and vertical wind speeds in the updraft may reach 50 to 60 miles per hour. As condensation occurs, the air is warmed by the release of latent heat and this enables the cloud to continue growing in height and size. During this stage, the cloud contains much moisture but little, if any, precipitation, lightning or thunder. The edges and top of the cloud are fairly sharply defined.

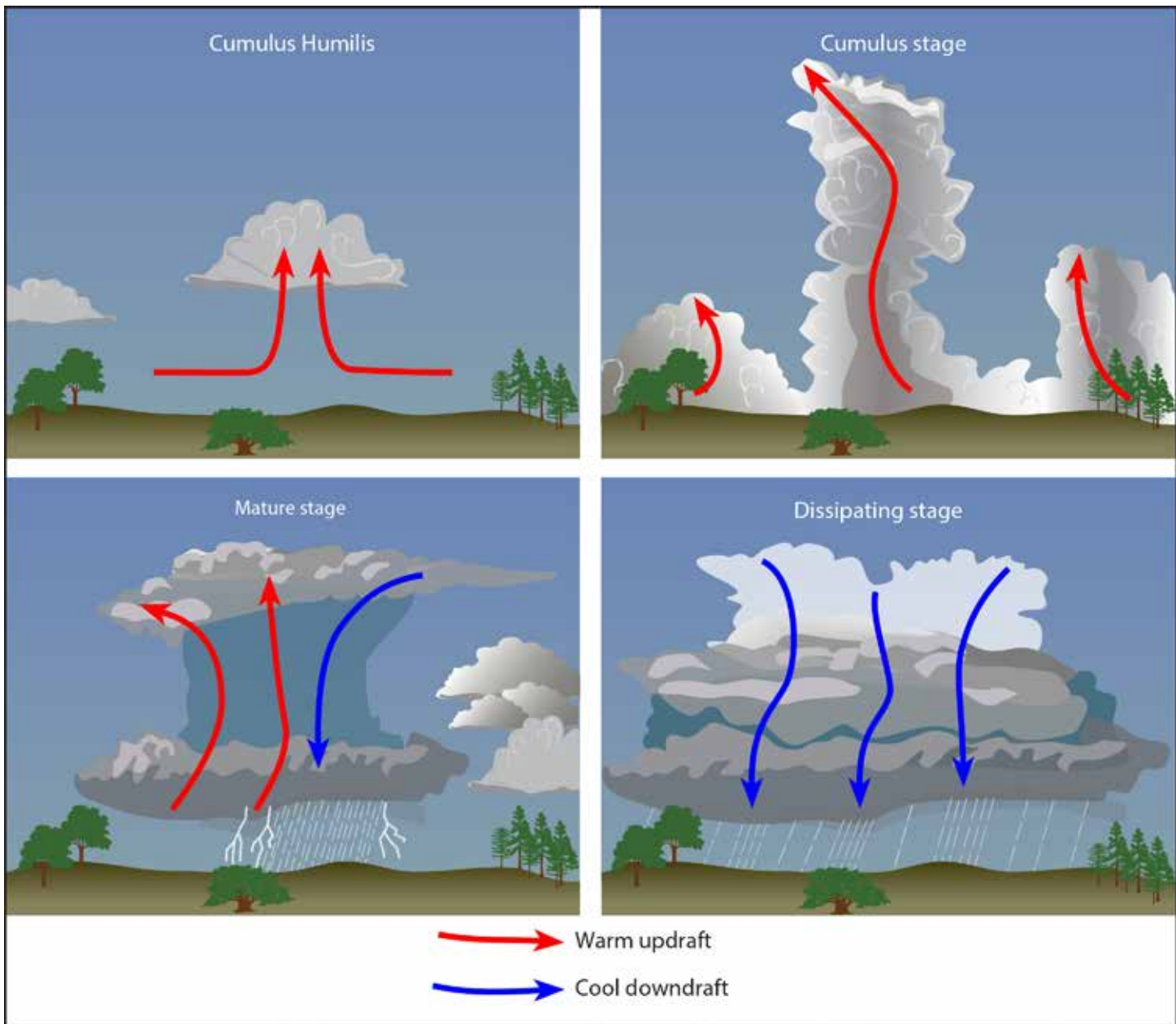


Figure 6.19. Thunderstorms develop from cumulonimbus clouds when violent updrafts and downdrafts coexist in the same cloud during the mature stage. All cumulonimbus clouds develop from clouds with less vertical development, beginning with cumulus humilis clouds. Cumulus humilis clouds signal limited vertical instability and are wider than they are tall. With increased instability, some cumulus humilis clouds develop into cumulus congestus (towering cumulus) clouds, arbitrarily when they are taller than wide. Cumulus congestus clouds signal deeper convection, but the vertical motion remains dominated by updrafts, and little if any precipitation falls. The most violent stage of development is the mature stage, and the vertical motion is characterized by strong updrafts and downdrafts side-by-side. During the dissipating stage, vertical motion largely consists of downdrafts which cuts off the supply of energy (latent heat of condensation) and the cloud begins to die. During the dissipating stage, light rain may be fairly widespread, but little if any lightning occurs. The upper portions of the cloud lose their sharp, bulbous or flat form, and become diffuse (Source/Credit: Dennis I. Netoff).

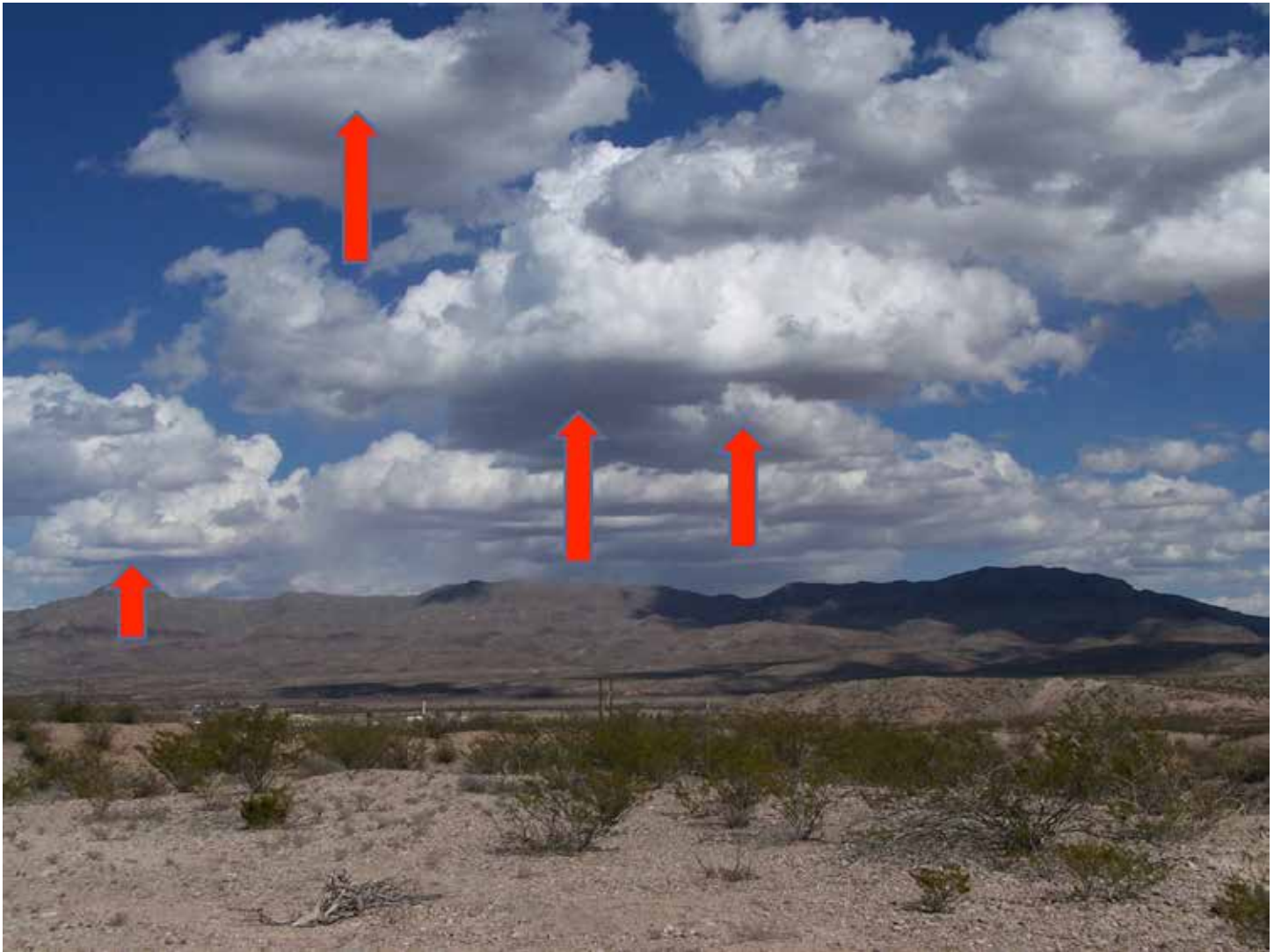


Figure 6.20. Mild, shallow convection forms cumulus humilis clouds. These flat-based clouds typically have greater width than height. With stronger and deeper convection, these may be transformed into cumulus congestus clouds, signaling the first, or cumulus stage of development (Source/Credit: Dennis I. Netoff).

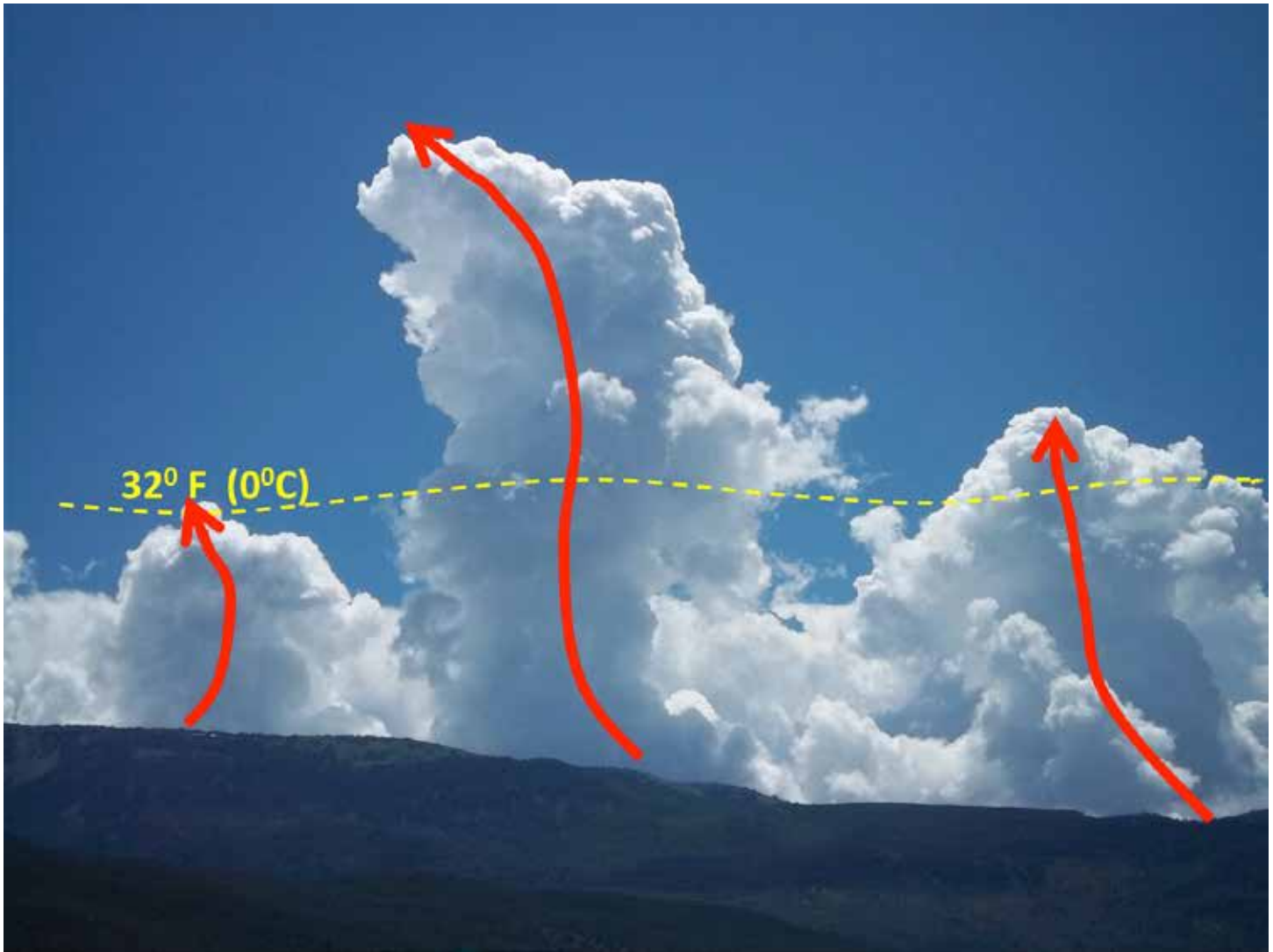


Figure 6.21. In the cumulus stage of development, rising columns of air known as updrafts carry moist air upward. As the air cools adiabatically by expansion, the dew point and/or the frost point is eventually reached and condensation and/or deposition occurs. These processes release heat energy to the air, and thus causing it to continue to rise. There is typically little or no precipitation, lightning or thunder during this stage (Source/Credit: Dennis I. Netoff).

## The Mature Stage

In the **mature stage**, strong updrafts and downdrafts take place side-by-side in the cloud, and precipitation occurs, as well as lightning and thunder (Figure 6.22). This is the most powerful phase of the storm. In addition, the entrainment of dry air that occurs as upper-level winds blow through the cloud causes evaporation to occur in some parts of the cloud. Because evaporation cools the air, some of the air in the cloud begins to sink forming a **downdraft**. Also, the rising column of air in the updraft eventually cools and begins to sink. When the cold downdraft hits the ground, the cold air flows outward away from the area below the cloud and creates a boundary between cold and warm air called a **gust front** that resembles a miniature cold front. The outward flow of air is called a **microburst** if it extends less than 2.5 miles (4 km), and a **macroburst** if it extends further. Gust fronts, microbursts and macrobursts can cause violent surface winds and turbulence, sometimes causing crippling dust storms called **haboobs** (Figure 6.23). Bursts of very cool surface air that are felt by observers well in advance of the actual thunderstorm are a reliable sign that a strong, mature thunderstorm is approaching. Just as a true cold front forces the uplift of warm, moist air, so too does the gust front. This forces even more air upward into the cloud. The combination of updraft and downdraft constitutes a **convection cell**. This stage may last from tens of minutes in a typical air mass thunderstorm to many hours in other types of thunderstorms.



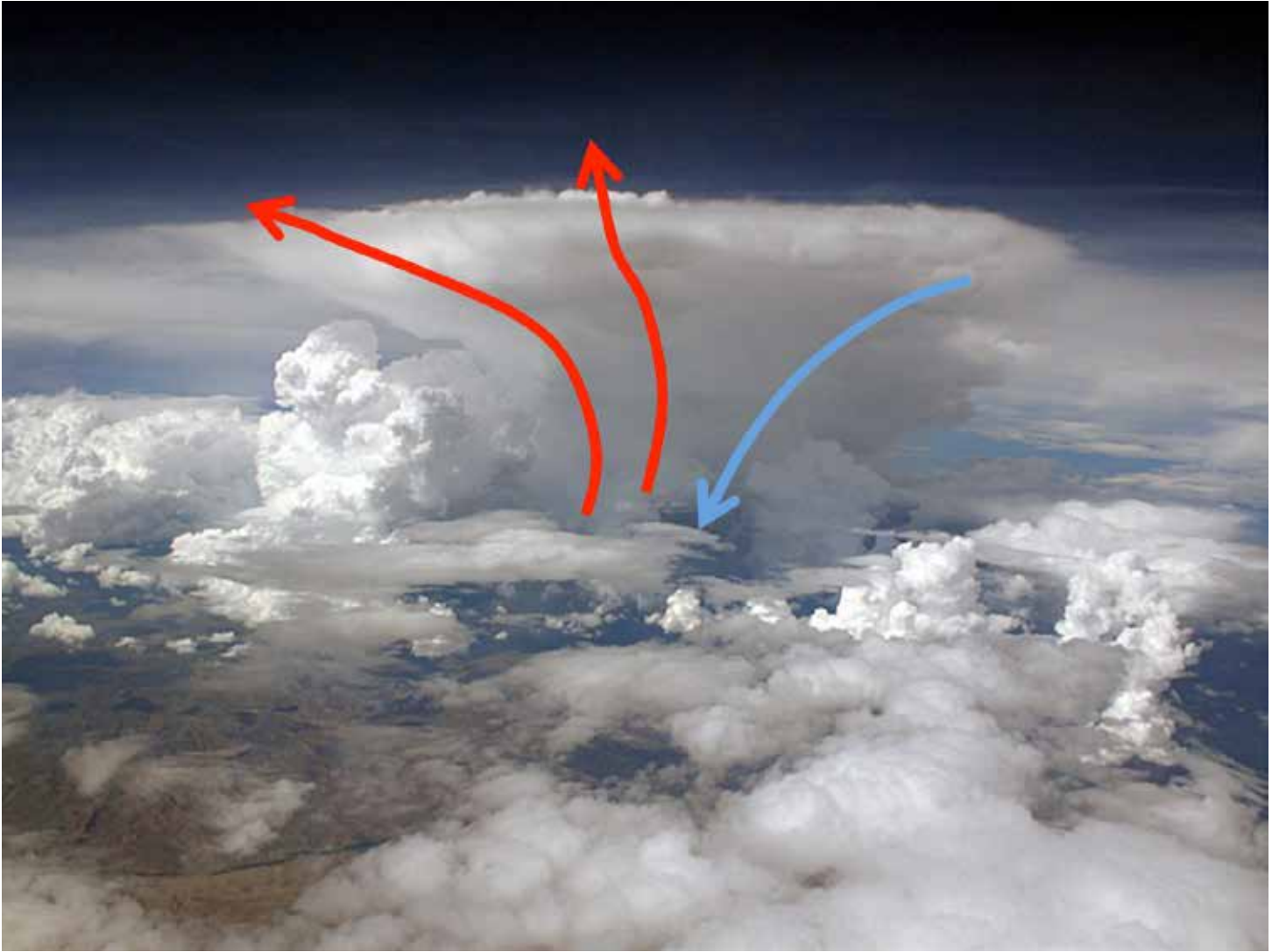


Figure 6.22. During the **mature stage**, updrafts and downdrafts occur side-by-side in the cloud. The most intense precipitation, lightning, vertical motion, and surface winds all occur during the mature stage. There may be a single updraft and downdraft, or multiple ones. Cumulonimbus clouds may extend from near-ground level to the tropopause or slightly into the lower stratosphere. The flat, anvil head of cumulonimbus clouds is the result of a cap or lid, an upper-level inversion. In severe thunderstorms, anvils may extend tens of miles from the base of the cloud due to upper-level winds. The ultimate lid is the tropopause, which limits all thunderstorm development, including hurricanes (Source/Credit: Bill Westphal, with permission).



*Figure 6.23. The haboob is a dust storm, often associated with a powerful gust front (winds 65 mph) such as the one illustrated here that struck Lubbock, Texas on June 18, 2009 (Source/Credit: NOAA).*

## The Dissipating Stage

If the supply of moist air that has been feeding the cloud is exhausted, or if the air becomes stabilized vertically by temperature changes, the cloud no longer has access to a source of energy and lift and it begins to dissipate (Figures 6.24 and 6.25). During the **dissipating stage**, uplift stops and downdrafts form throughout the cloud. With no source of latent heat, the storm quickly weakens. One of the mechanisms by which the updraft may shut down is by precipitation into the updraft. As raindrops fall through the air, they create drag on the air which tends to pull it downward. If the downward drag is great enough, it can stop the upward motion of the air.



Figure 6.24. During the dissipating stage, uplift stops and downdrafts form throughout the cloud. With no source of latent heat, the storm quickly weakens. The early dissipating stage at White Canyon, Utah, is indicated in this June 24, 2008 image. Light, widespread rain signals predominantly downdrafts. The upper boundary of the cloud is fibrous and diffuse (Source/Credit: public domain, Rafikimambo at en.wikipedia/from Wikimedia Commons, PD. File:CloudOverUtah.jpg).

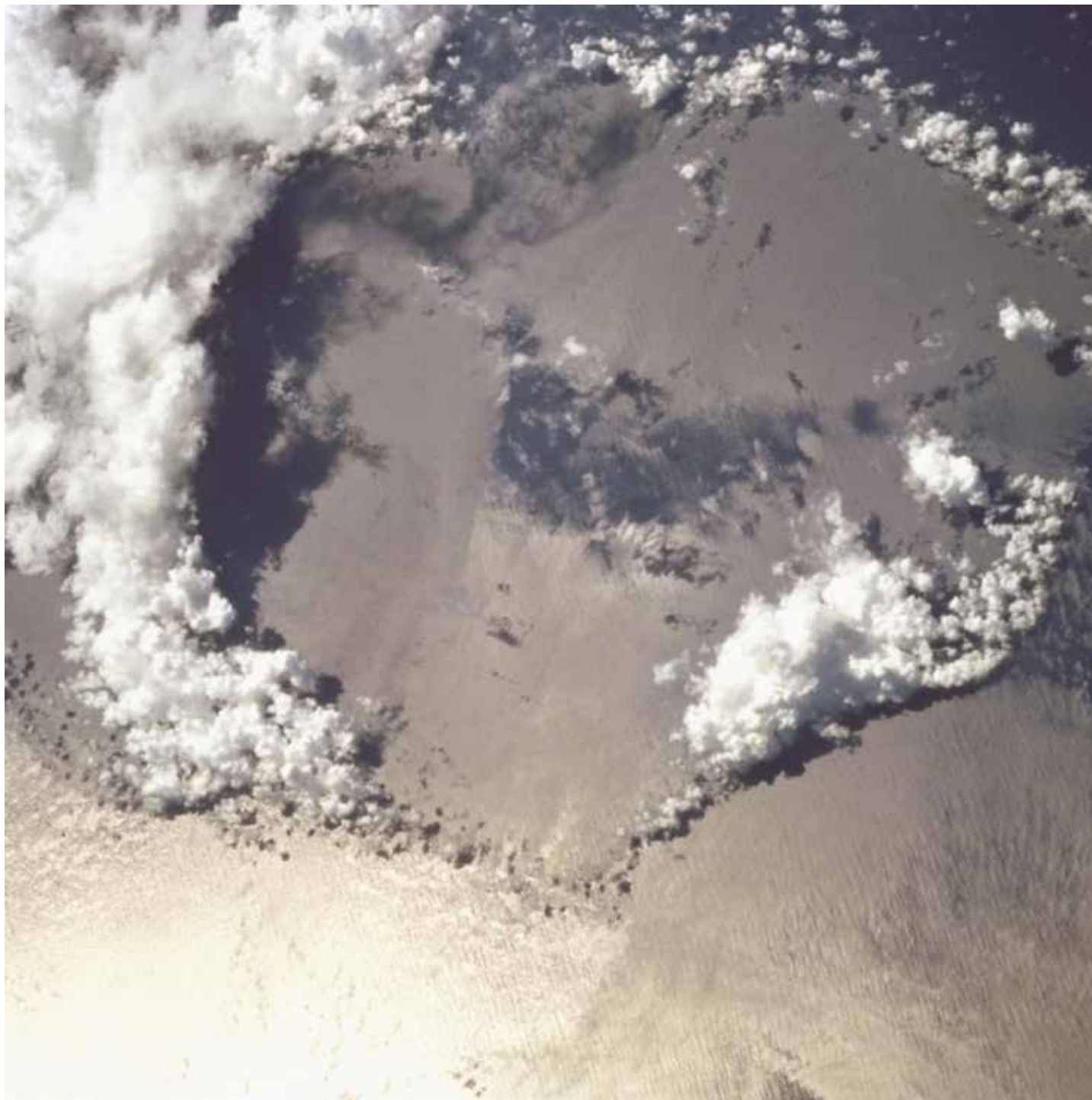


*Figure 6.25. Some thunderstorms collapse violently during the dissipating stage, and the original cloud disappears except for a ring of cumulus clouds marking the former outer margin of the cumulonimbus cloud (Source/Credit: NASA).*

During the dissipating stage, light, widespread rain may occur throughout the cloud. The upper boundary of the cloud often becomes fibrous and diffuse, as cloud dissipating processes dominate over cloud-forming processes. Lightning is infrequent during the dissipating state, although electrical charges may still be maintained from when the storm was mature. As some thunderstorms dissipate, new ones may form, and several stages of development can be seen at the same time (Figure 6.26).



Figure 6.26 The cluster of clouds over Swifts Creek, Australia illustrates several stages of thunderstorm development in a single image. In the middle background, a cumulonimbus capillatus incus cloud is in the early dissipating stage, and its anvil is beginning to become fibrous and diffuse. As the first-formed cloud begins to dissipate, newer cumulus congestus clouds have developed in the middle foreground, and still newer cumulus humilis clouds are forming in the right foreground (Source/Credit: Fir0002/Flagstaffotos.com.au, with permission).

## Severe Thunderstorms and Tornadoes

Thunderstorms differ in severity and duration. Accordingly, meteorologists distinguish typical thunderstorms such as those just described as severe or supercell thunderstorms. **Severe thunderstorms** are characterized by surface wind speeds of at least 58 mph (93 km/h), hail at least 1 inch (2.5 cm) in diameter, and cloud heights that may exceed 60,000 feet (Figure 6.27). Severe thunderstorms last longer than typical thunderstorms and may be tornadic. In satellite view, they typically have broad, flat-topped anvils that are extended down-wind, often with conspicuous overshooting tops (Figures 6.28 and 6.29). In severe thunderstorms, the convection cell is tilted in such a way that precipitation falls into the downdraft and this strengthens the intensity of the downdraft. Portions of the cloud may display numerous, pendant pouches called **mammatus** (Figure 6.30), indicating an unstable interface between air above and below them. Strong downdrafts may generate turbulent gust fronts and dust storms (haboobs) that extend far from the main cloud. Strong gust fronts may also initiate new cumuliform cloud development which may give birth to new thunderstorms. A stable form of turbulent flow near the terminal portion of the gust front may result in a **shelf** cloud and/or **roll cloud** (Figures 6.31a, 6.31b, 6.31c and 6.32a, 6.32b).

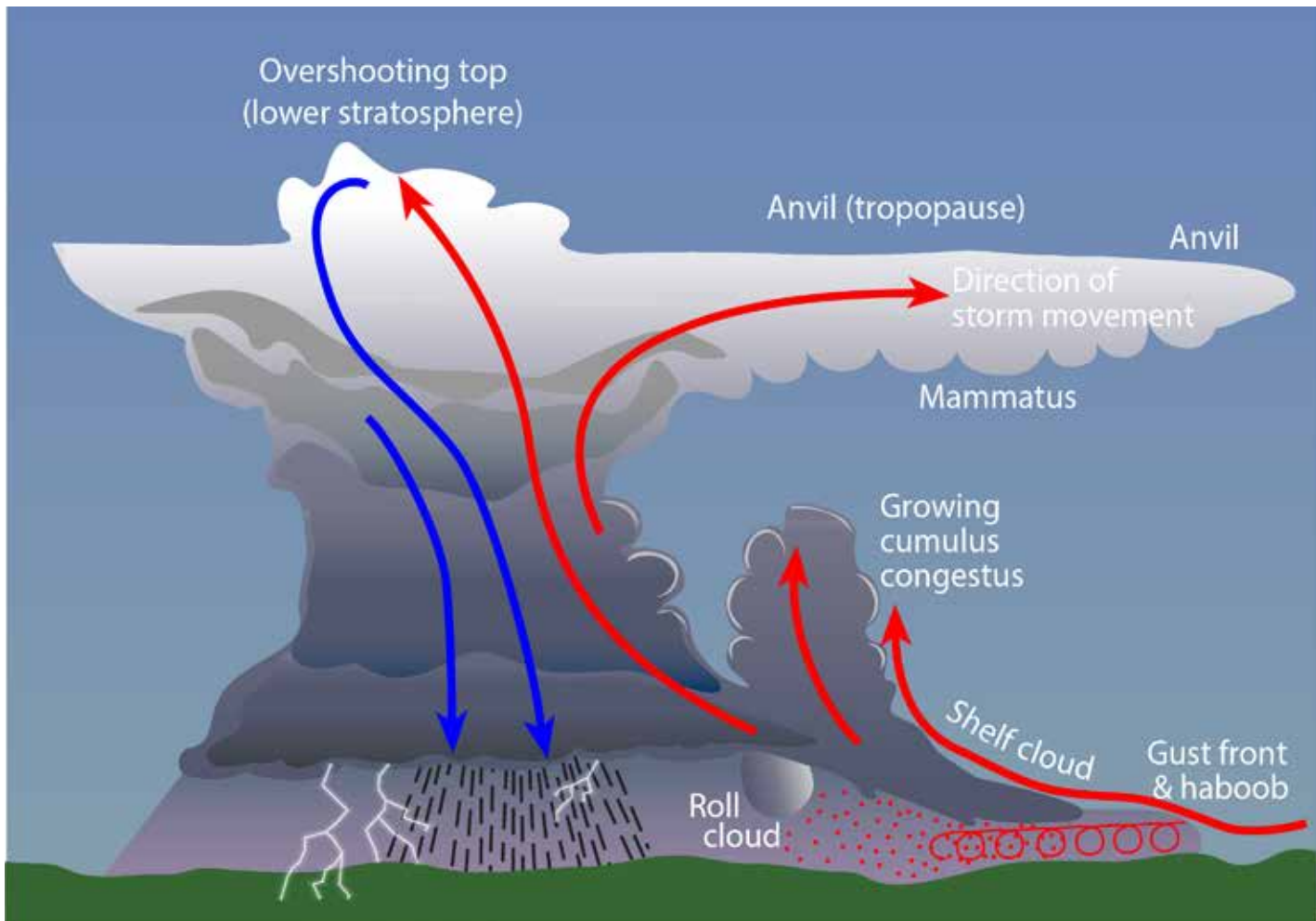


Figure 6.27. Characteristics of a severe thunderstorm. Severe thunderstorms may have one or more very strong updrafts and downdrafts, each pair causing strong differences in electrical charge within the cloud. A flat-headed anvil typically forms at the tropopause, where there is an exceptionally strong temperature inversion. Upper-level winds extend some anvils for dozens of miles in advance of the surface storm. Strong updrafts may have sufficient momentum to cause the cloud top to temporarily invade the lower stratosphere, the overshooting top. Vertical instability may result in mammatus on the underside of the anvil. On the surface, gust fronts may extend several miles from the main downdrafts, often forming haboobs (dust storms) if there is loose soil. A streamlined, wedge-shaped shelf cloud may form over the dense gust front, as well as a new cumulus or cumulus congestus cloud. On rare occasions, turbulence in the cold, stable air within the gust front will cause a roll cloud to form, rotating on a horizontal axis (Source/Credit: Dennis I. Netoff, modified from several sources).



Figure 6.28. Strong thunderstorms erupted in the late afternoon on August 5, 2014 over Borneo, Indonesia. The cirroform anvils are all being swept to the south (toward lower left) by strong upper-level winds. Overshooting tops jut above the anvil of several clouds. Lower-level winds, indicated by smoke plumes (right-center) and lines of cumulus humilis clouds (cloud streets, lower left) are easterly (blowing from lower right toward upper left). The image was taken from the International Space Station, some 205 miles (330 km) above the clouds (Source/Credit: NASA).





Figure 6.29. Severe thunderstorm with a flat anvil at the tropopause and an overshooting top. Clusters of cumulus humilis and cumulus congestus clouds are scattered in the foreground, some of which may become thunderstorms (Source/Credit: NASA).



Figure 6.30. Mammatus clouds, such as these near Wichita Falls, Texas, are characterized by bases that have pouch-like protuberances that extend downward from their bases. These features develop in response to downdrafts of cold air within the cloud. Two tornadoes touched down within 30 minutes of the time that this photograph was taken, indicating the severity of the storm (Source/Credit: Dennis I. Netoff).



Figure 6.31a. Shelf clouds are one of the most photographed parts of thunderstorms. They are typically low, wedge-shaped clouds associated with the convergence of cold gust fronts and warm peripheral air. The leading part of the shelf cloud is often streamlined, whereas the underside may appear ragged and turbulent (Source/Credit: NOAA).



Figure 6.31b. A shelf cloud in Saskatchewan, Canada is illuminated by the rising Sun in August 2001. The wedge-shaped leading edge is attached to the main thunderstorm mass above (Source/Credit: NOAA, Jeff Kerr; <http://apod.nasa.gov/apod/ap080122.html>).



Figure 6.31c. A shelf cloud has formed along the leading edge of a thunderstorm near Enschede in the Netherlands on July 17, 2004. Shelf clouds typically form as warm, moist air ahead of an approaching thunderstorm is lifted along an outflow of cooler, denser air from the heart of the thunderstorm (Source/Credit: Photo by John Kerstholt.<br>From english wikipedia (and meta).  
{{GFDL}}).



*Figure 6.32a. Roll clouds are rarely observed in association with thunderstorms, with the exception of this one from Racine, Wisconsin, taken on June 1 2007. Roll clouds spin on a horizontal axis, typically with the leading edge showing an upward movement. They are somewhat more common over the Gulf of Carpentaria in Australia, for reasons that are unclear (Source/Credit: Eazydp, courtesy Wikipedia).*



*Figure 6.32b. The leading edge of a roll cloud in Lubbock Texas on September 25, 2007. The roll cloud rotates on a horizontal axis, and although the movement within the cloud is clearly visible to a ground observer, the cloud position changes very little. Most roll clouds in the United States are associated with the passage of cold fronts and associated thunderstorms. They are fairly rare throughout most of the world, with the exception of the Gulf of Carpentaria, Australia, which is reputedly the only place on Earth where they can be predicted with any accuracy. The roll clouds in Australia are reputed to be the largest clouds on Earth, some stretching for over 600 miles (1000 km) (Source/Credit: NOAA/NWS).*

**Supercell thunderstorms** are unusually large types of severe thunderstorms (thousands of square miles), of long duration (1-4 hours or more; hence the name supercell), have stronger updrafts and surface winds than ordinary thunderstorms, and are responsible for nearly all of the intense tornadoes in the United States ((Figures 6.33 and 6.34). They can produce hailstones from the size of marbles to softballs (Figure 6.35). Updrafts, downdrafts, and outflow winds may exceed 100 mph (160 km/hr).

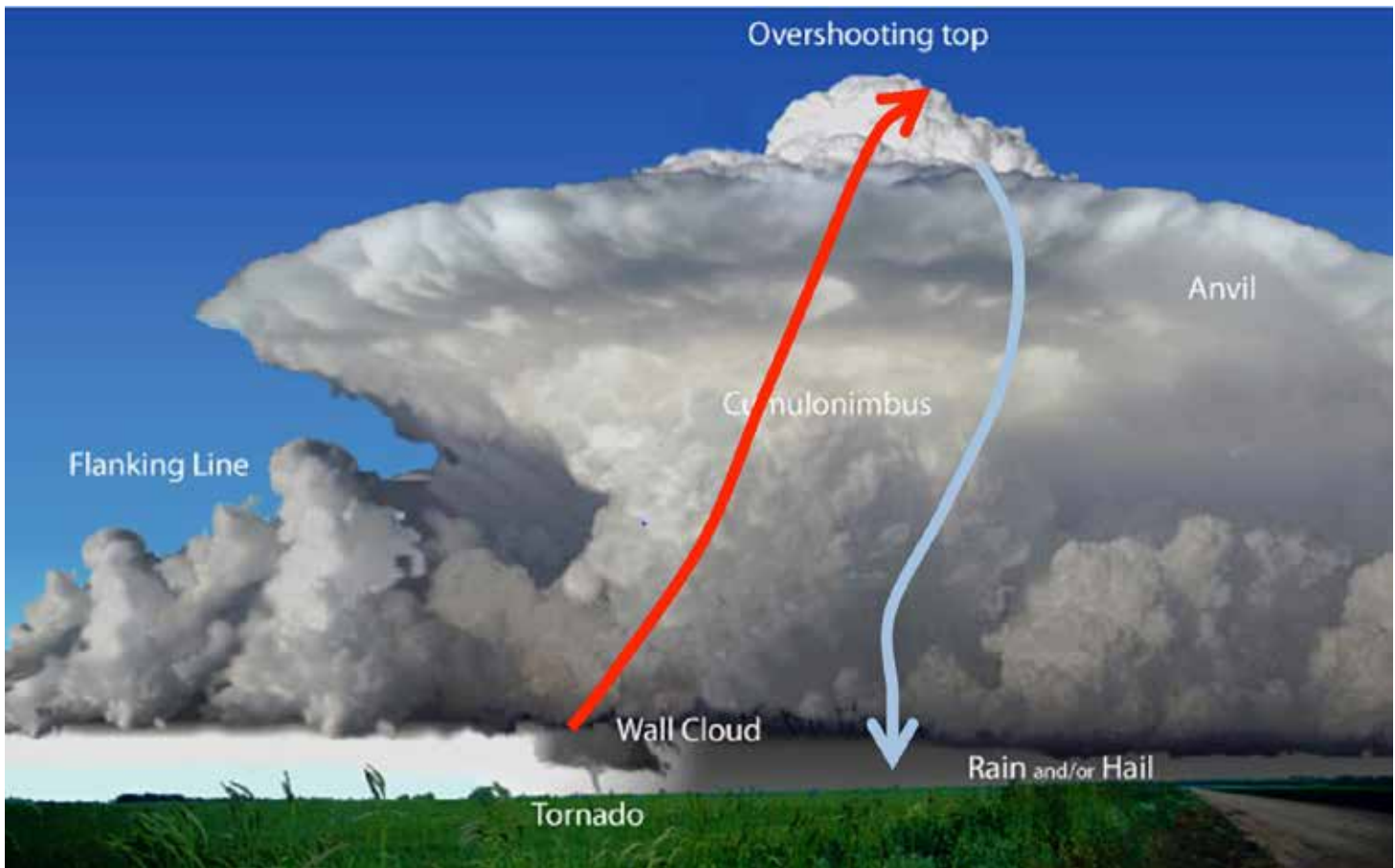


Figure 6.33. Supercell thunderstorms have several features that distinguish them from lesser thunderstorms. Updrafts are tilted by strong upper-level winds, so that they do not conflict with adjacent downdrafts. Updrafts and downdrafts are exceptionally strong, and can keep golf-ball to softball hail stones suspended in the cloud, making hail and damaging winds major hazards with these types of storms. Even more significant is the existence of a mesocyclone, a large, rotating cyclonic shaft that may extend throughout most of the vertical extent of the cloud. The base of the mesocyclone is often characterized by a streamlined, rotating protuberance called a wall cloud. The wall cloud can tighten, spin progressively faster, extend downward as a funnel cloud, and when it reaches the surface can become a tornado (Source/Credit: modified from NOAA/NWS).





Figure 6.34. The anvil of this supercell thunderstorm is quickly forming and mammatus are beginning to develop on the underside of the anvil. The storm produced golf-ball sized hail over Chaparral, New Mexico on April 3, 2004, causing considerable local damage. Compare this photo with the upper part of the sketch of a supercell in Figure 6.33 (Source/Credit: <http://www.srh.noaa.gov/elp/swww/v8n1/Chaparral%20Supercell%20.JPG>).



Figure 6.35. Golfball-to-baseball sized hailstones that fell from a supercell thunderstorm northwest of Charleston, South Carolina on July 1, 2012. Hailstones of this size fall at velocities of 60-80 mph (29-36 m/s) and can cause extensive damage to roofs, crops and cars, and can threaten human lives (Source/Credit: NOAA).

At some time in their life cycle, supercell thunderstorms contain a **mesocyclone** (Figure 6.36), a large-scale (typically a mile or more) cyclonic circulation pattern that may extend throughout much of the thickness of the cumulonimbus cloud. The lower portion of the mesocyclone may be visible as a streamlined, striated, rotating mass. It may manifest itself as a sag on the underside of the cumulonimbus cloud, called a **wall cloud** (Figure 6.37). The cyclonic circulation of the wall cloud may diminish in diameter, causing the spin velocity to increase. A funnel cloud may develop from the wall cloud, which can then touch ground to become an actual tornado (Figures 6.38a and 6.38b). A satellite view of a supercell thunderstorm typically displays an immense, flat-topped anvil which may cover thousands of square miles and extend for over a hundred miles beyond the cloud. Numerous overshooting tops may rise above the anvil (Figures 6.39a and 6.39b).



Figure 6.36. The lower portion of a mesocyclone is visible as a streamlined, rotating mass at the base of a cumulonimbus cloud in Nebraska on June 6, 2010 (Source/Credit: NOAA).



Figure 6.37. A wall cloud near Miami, Texas in 1980. Wall clouds are protuberances below the main cloud base of a cumulonimbus cloud. They often represent the visible base of a mesocyclone within the cloud. The wall cloud usually has a strong cyclonic (counter-clockwise in the Northern Hemisphere) spin that may become tornadic (Source/Credit: Brad Smull, NOAA Photo Library, NOAA Central Library; OAR/ERL/National Severe Storms Laboratory (NSSL) - nssl0092, National Severe Storms Laboratory Collection <http://www.photolib.noaa.gov/nssl/nssl0092.htm>).



*Figure 6.38a. Funnel cloud emanating from a rotating wall cloud and mesocyclone. (Source/Credit: Justin 1569 at en.wikipedia).*

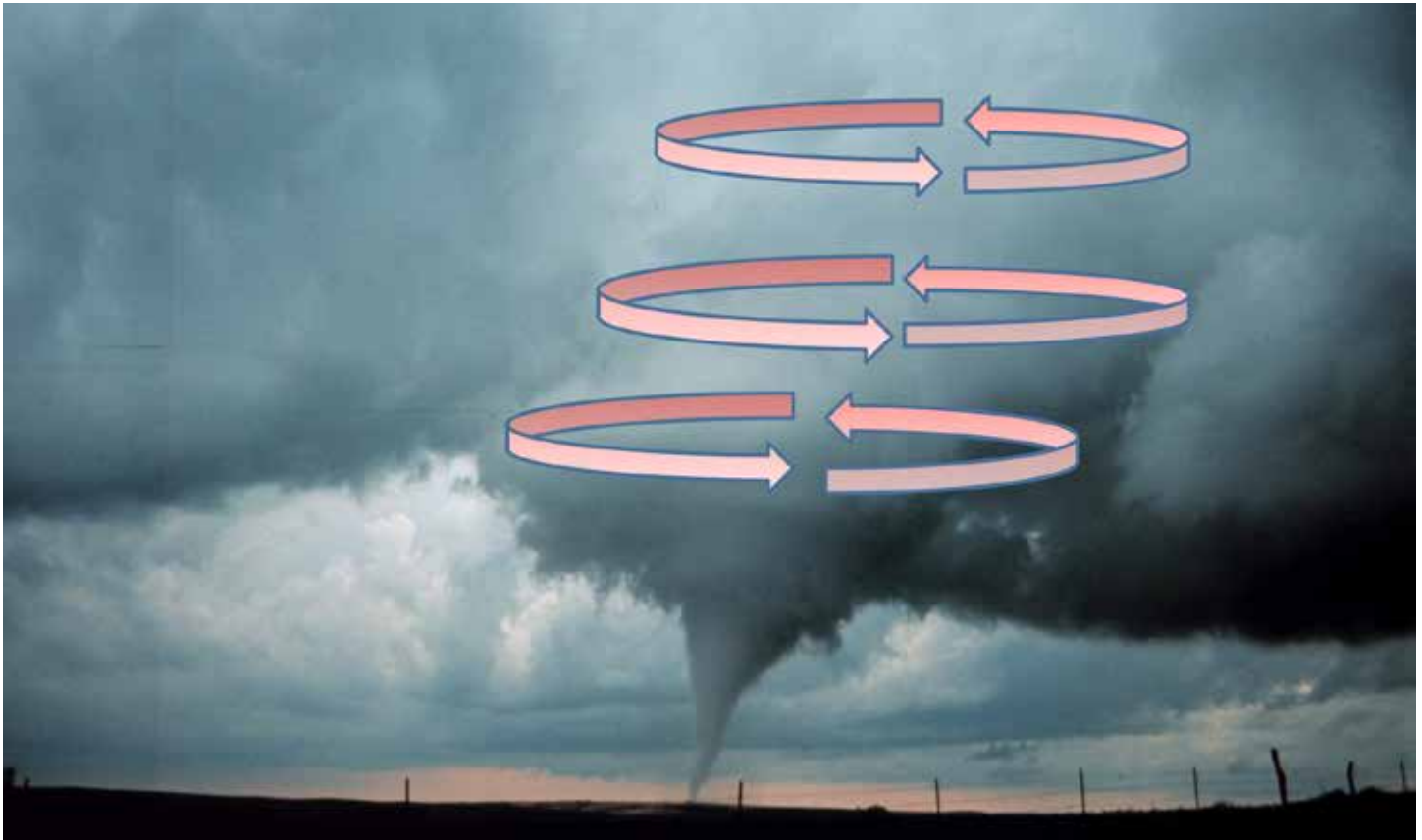


Figure 6.38b. A mesocyclone is a large, wide column of rotating air within a cumulonimbus cloud. Some mesocyclones can be detected as a large protuberance extending from the underside of the cloud known as a wall cloud. Smaller, more rapidly-rotating vortices that extend to the ground become tornadoes (Source/Credit: NOAA).

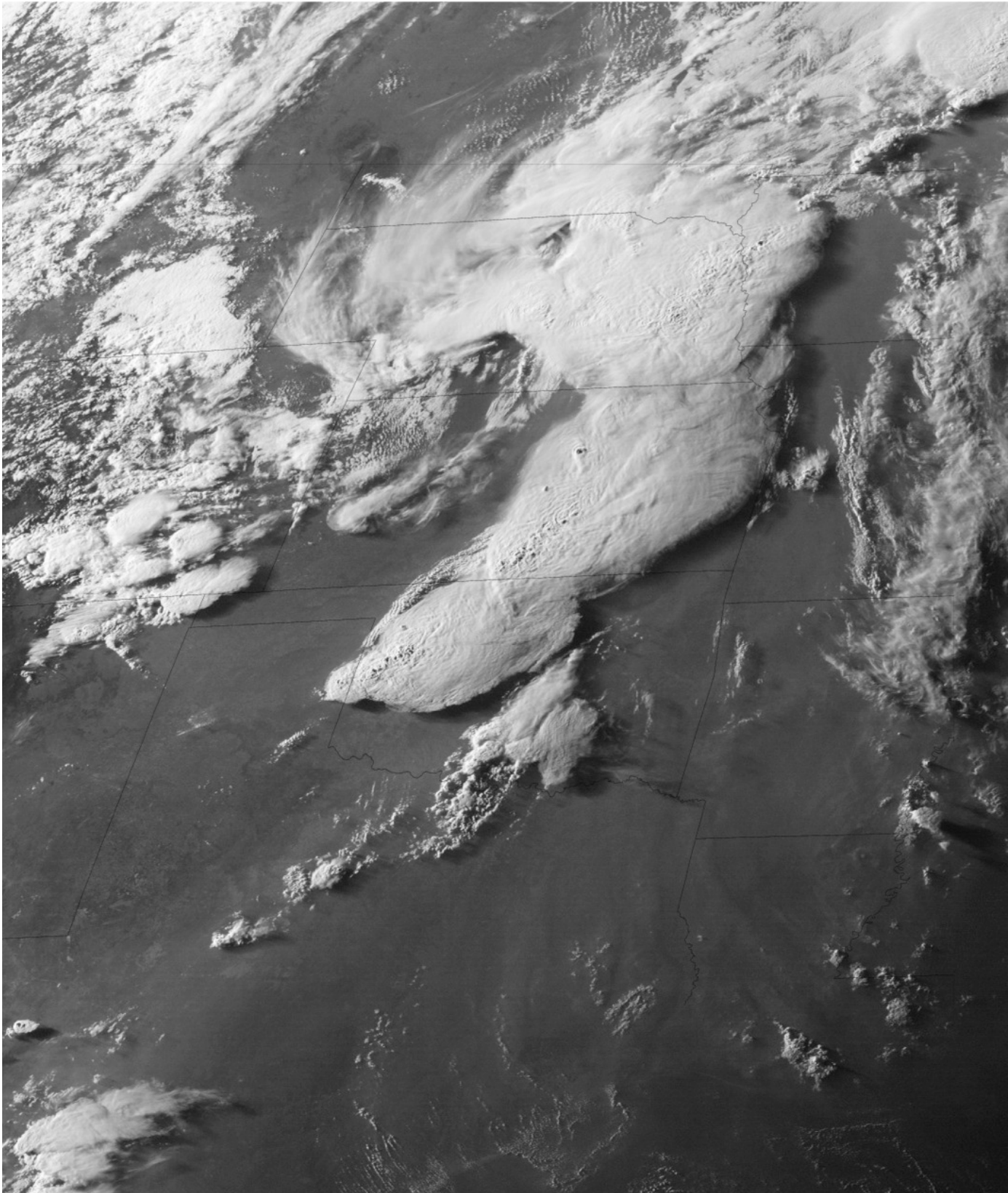


Figure 6.39a. Two large clusters of supercell thunderstorms merge in the region from northern Texas, through Oklahoma, Kansas and well into eastern Nebraska on May 19, 2012. The merging, flat-topped anvils extend toward the northeast in the direction of upper-level winds, in approximately the same direction as the storm tracks. The dark, bulbous spots on top of the anvils are overshooting tops (Source/Credit: NASA, geostationary GEOS-East satellite).

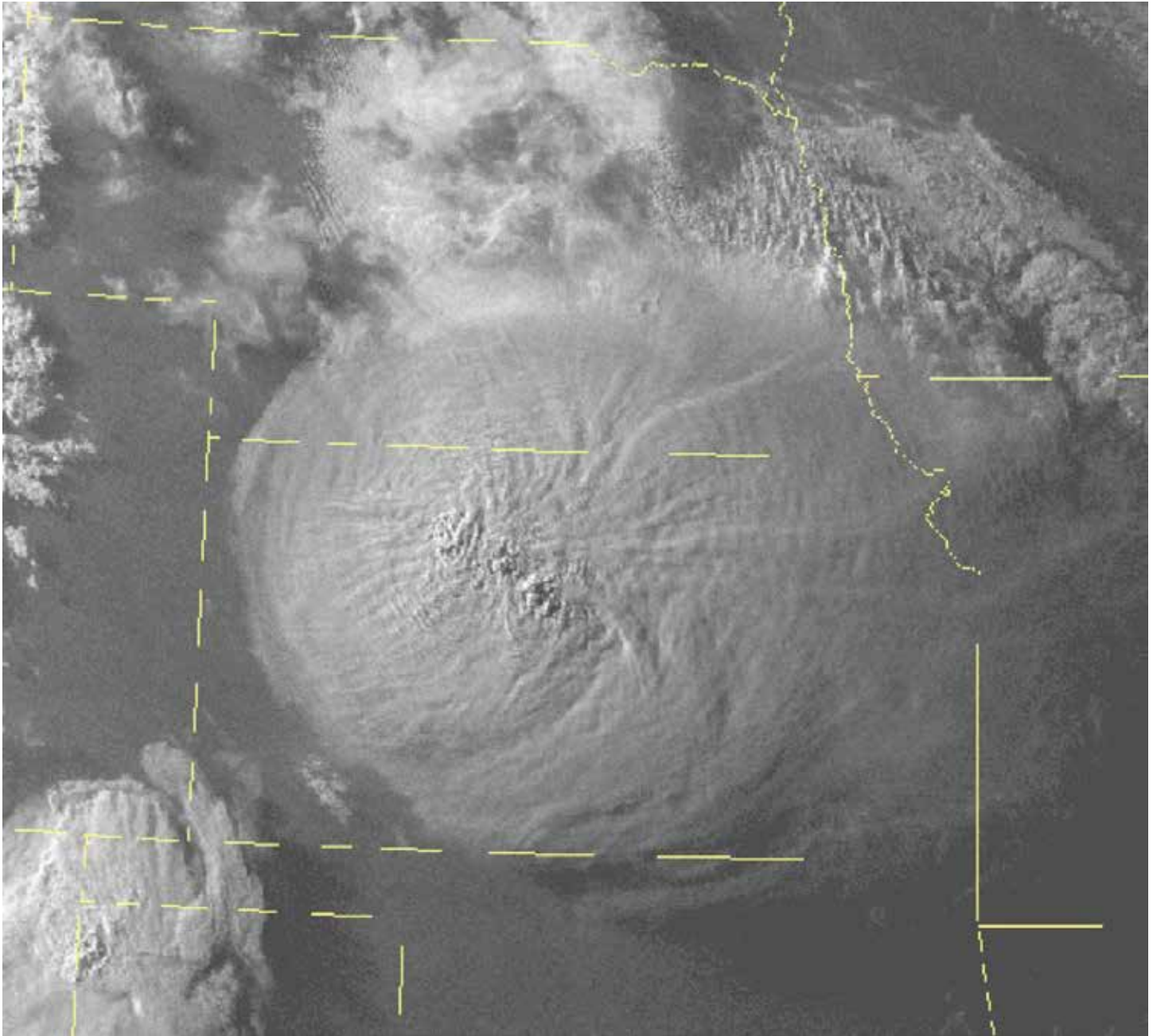


Figure 6.39b. The anvil of this supercell thunderstorm in Kansas on July 7, 2004 is unusually large (>50,000 sq mi; 130,000 sq. km). Although the anvil has its greatest extent eastward of the main storm, it is surprisingly symmetrical, presumably due to fairly gentle upper-level winds. Several overshooting tops extend above the flattish anvil (Source/Credit: NWS).



Environmental conditions that promote supercell development include the same as those for all thunderstorms (moist, unstable air, high CAPE values and a triggering mechanism), and additionally include strong shearing winds aloft. In the Great Plains, surface winds are typically out of the south or southeast, with mid-level winds out of the southwest, and high-level winds out of the west or northwest. Winds thus turn clockwise with increasing height above the surface (Figure 6.40). High wind shear not only can initiate mesocyclone circulation, but can intensify the storm by tilting it in the direction of the powerful upper-level winds. The tilting tends to increase separation between the updrafts and downdrafts of the storm, so that they do not interfere dynamically with each other.

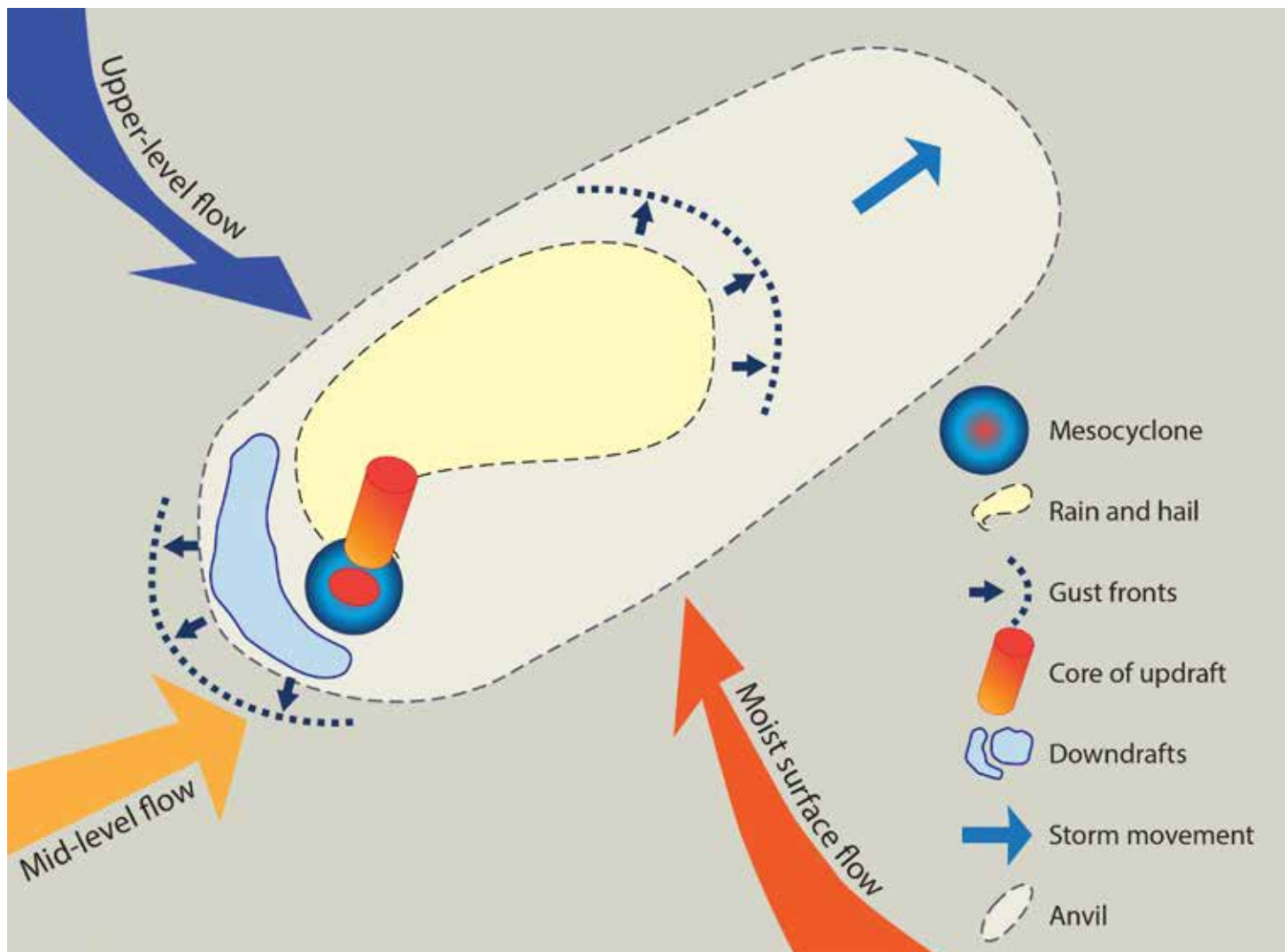


Figure 6.40. Some of the environmental conditions that favor the development of supercell thunderstorms include strong buoyancy (high CAPE values), an updraft core that is tilted in the direction of the strong downdrafts, strong wind-directional shear with height (i.e., change in wind direction with height), and the development of a mesocyclone (Source/Credit: Dennis Netoff, modified from NOAA and other sources).

Both severe and supercell thunderstorms often develop in a **squall line** that occurs either along the cold front boundary or ahead of it (Figures 6.41a, 6.41b and 6.41c). Those squall lines that form ahead of the front develop as a result of vertically-oriented undulations, (waves) in the airflow ahead of the frontal boundary. During the upward-directed component of the undulation, uplift of moist air occurs that can lead to rapid condensation and the production of a squall line.



Figure 6.41a. Squall line moving rapidly across the Indiana plains on April 11, 2007 (Source/Credit: NOAA/Bob Hammitt).

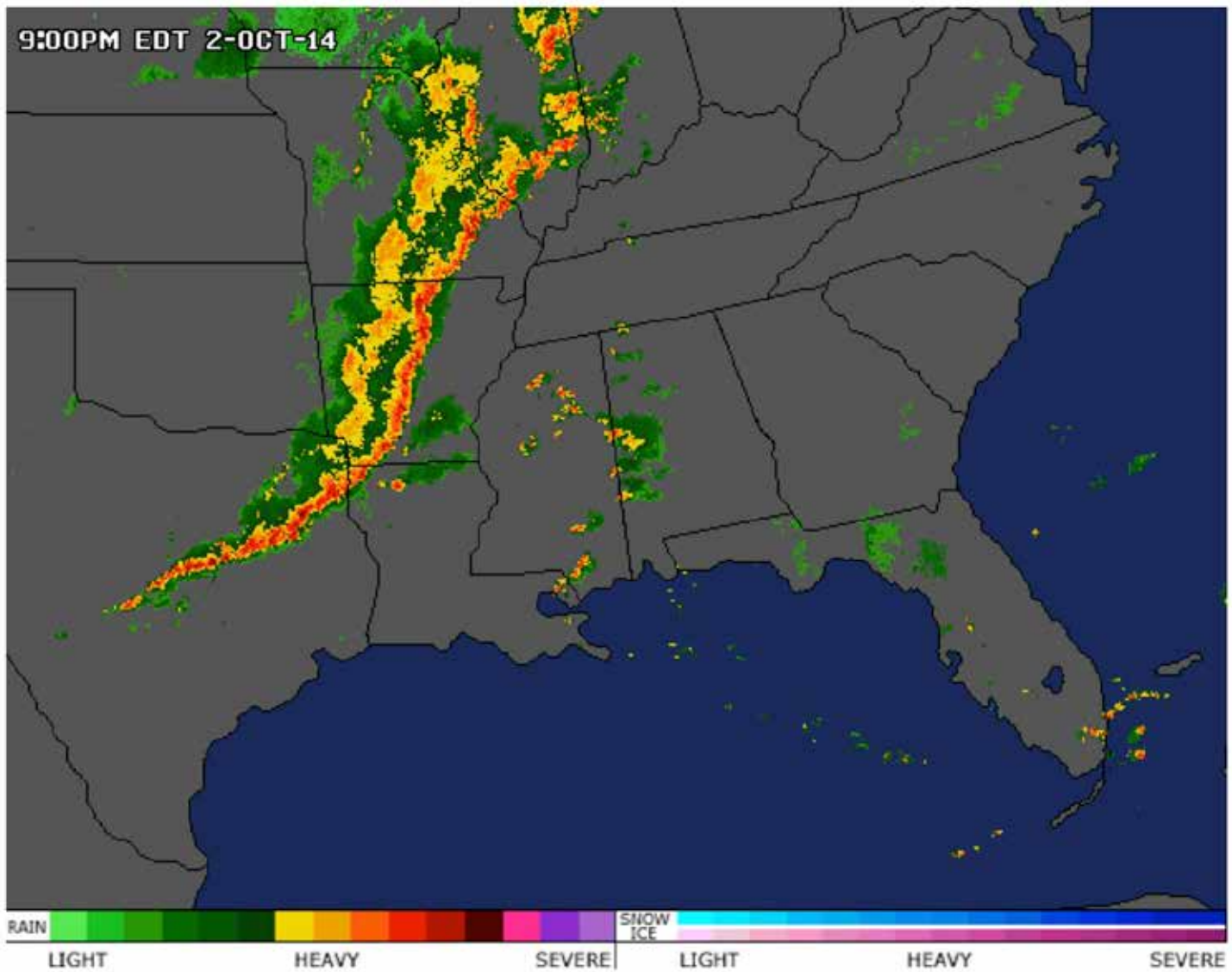


Figure 6.41b. Satellite image of an intense squall line associated with a fast-moving cold front in north-central Texas on October 2, 2014. Although squall lines can occur with or without fronts, they most commonly are associated with fast-moving cold fronts, where there is rapid uplift of air, fast frontal movement and a large contrast in air masses on either side of the front. Cold-front squall lines can form along the front, behind the front, or a considerable distance ahead of the front (Source/Credit: NWS).



*Figure 6.41c. Squall line from space. The line of severe thunderstorms formed along a cold front that had moved into the North Atlantic Ocean near Bermuda (Source/Credit: NASA, taken in June 1985).*

Occasionally hundreds or even thousands of thunderstorms will cluster together into a large circular or oval-shaped storm system to form what is known as a **Mesoscale Convective Complex** (MCC) (Figures 6.42 and 6.43). These large, slow moving storms, which generally form in the late afternoon or early evening and may have a life of 8 to 24 hours, can cause great damage from strong winds, lightning strikes, and flash flooding as they traverse an area. They also bring beneficial spring and summer rain to much of the Midwest and Great Plains. Many tornadoes that occur at night are spawned by MCCs. These systems often reach their peak intensity in the hours just beyond midnight, which makes them particularly dangerous because most people are asleep at this time and may be unaware of warnings issued.

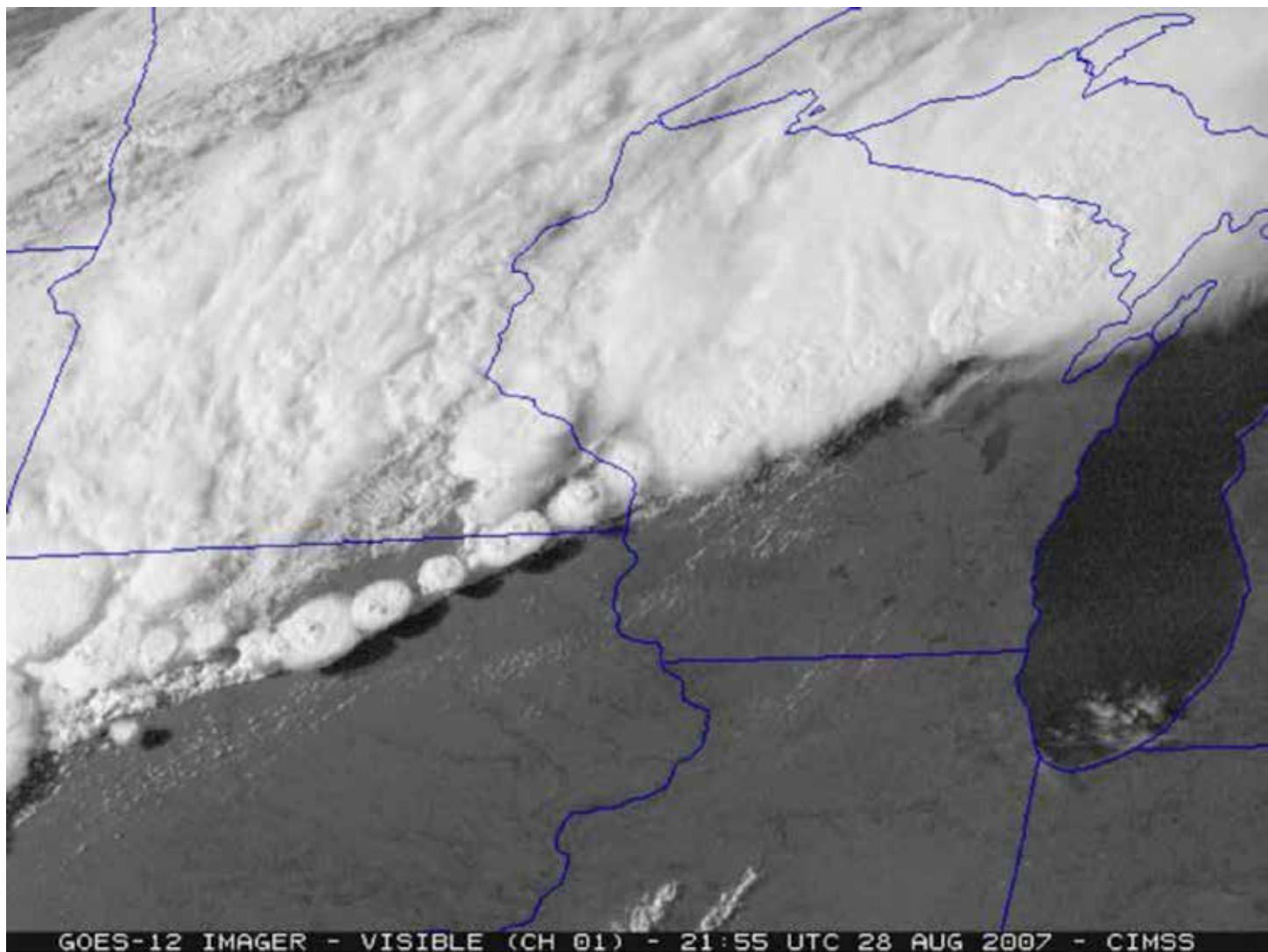


Figure 6.42. Mesoscale convective complexes are massive clusters of thunderstorms that can cover well over 100,000 square kilometers (~40,000 sq mi). This one on August 28, 2007 covered parts of Iowa, Minnesota, and Wisconsin. Some of the thunderstorms generated surface gusts of 60-80 mph and large hail. Individual cells with anvil tops are lined up along the leading edge of the system. Cell movement was mainly toward the northeast (Source/Credit: NOAA).

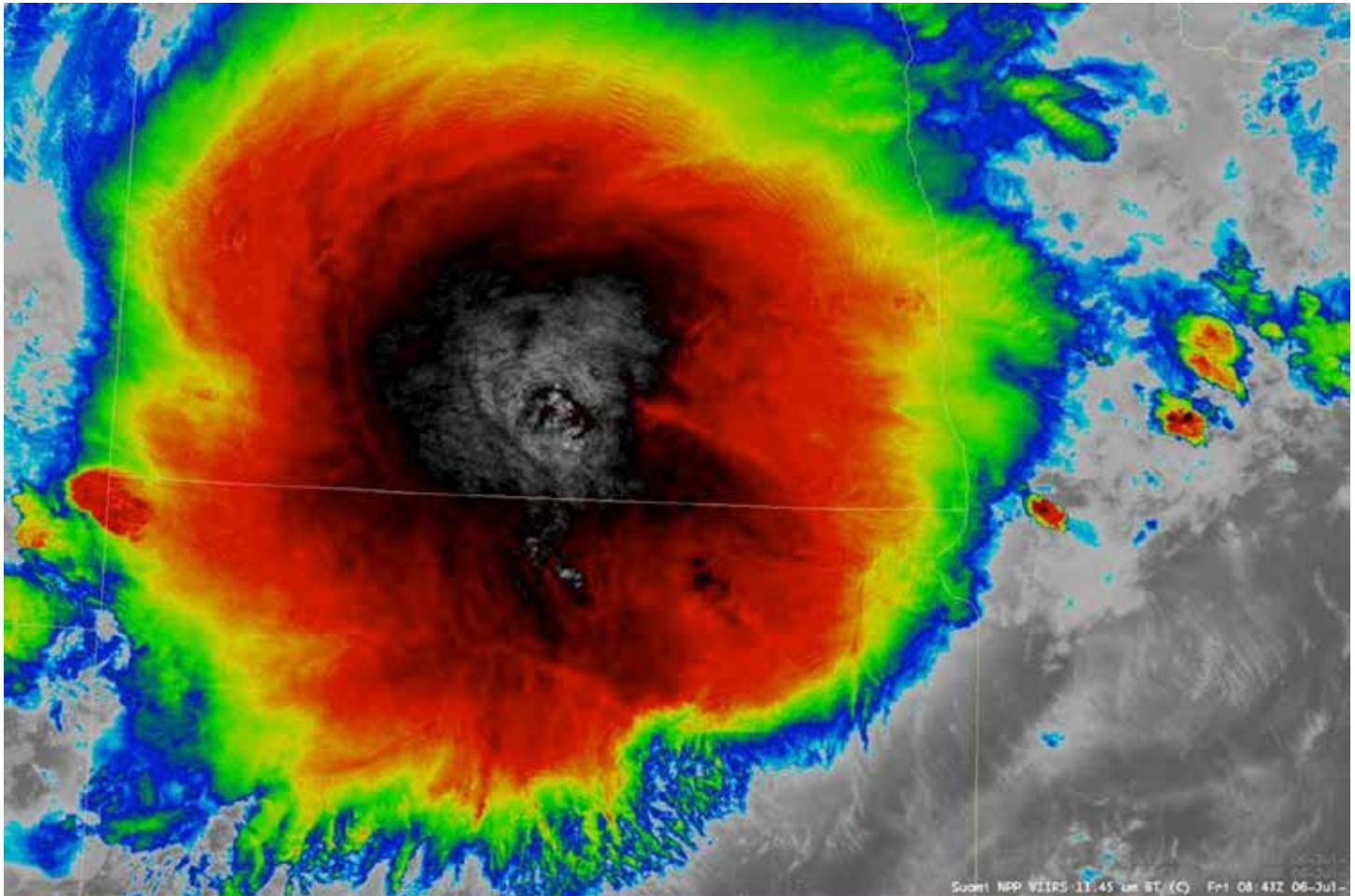


Figure 6.43. A large mesoscale convective complex developed over eastern North and South Dakota and extreme western Minnesota on July 6, 2012. The image shows the thunderstorm complex at maximum development at about 3:43 AM local time. Surface wind gusts of 59 mph and cloud-top temperatures of minus 119°F (-84°C) were recorded (Source/Credit NOAA/GOES-13 satellite).

A mesoscale convective complex is classified by the National Weather Service as a subtype of **mesoscale convective system**, along with a **mesoscale convective vortex** (MCV). Because of its immense size, it is usually identified by satellite observation. MCCs often begin as lesser storm systems, but are transformed into these massive system complexes during the late afternoon of early evening. Some MCCs have their origin in the Rocky Mountains, then are carried eastward by upper-level winds during the evening and overnight hours. These *orogenic complexes* bring frequent nighttime thunderstorms to the Great Plains (Figure 6.44).



Figure 6.44. A severe thunderstorm forming over the Colorado Rockies on June 7, 2012. During the North American monsoon season, moist air from the Gulf of Mexico frequently generates mid-day thunderstorms over the Southern Rockies. As upper-level winds carry them eastward into Kansas, Oklahoma and Nebraska, they can build into orogenic complexes, a form of mesoscale convective complex (Source/Credit: Royal Meteorological Society).

The high frequency of MCCs in the Great Plains during the spring and summer is due largely to three factors:

- (1) this is an area of frequent, migratory upper-level troughs in the atmosphere, and strong upper-level divergence often occurs just east of the axis of these troughs;
- (2) at night, a low-level jet coming off the Gulf of Mexico provides an abundant source of moisture (and energy) for severe thunderstorms, and;
- (3) strong surface convergence and uplift is provided by a mid-tropospheric mesoscale vortex. MCCs occur with some frequency in a few other areas of the world, mostly in lower-mid latitude locations (Figure 6.45).

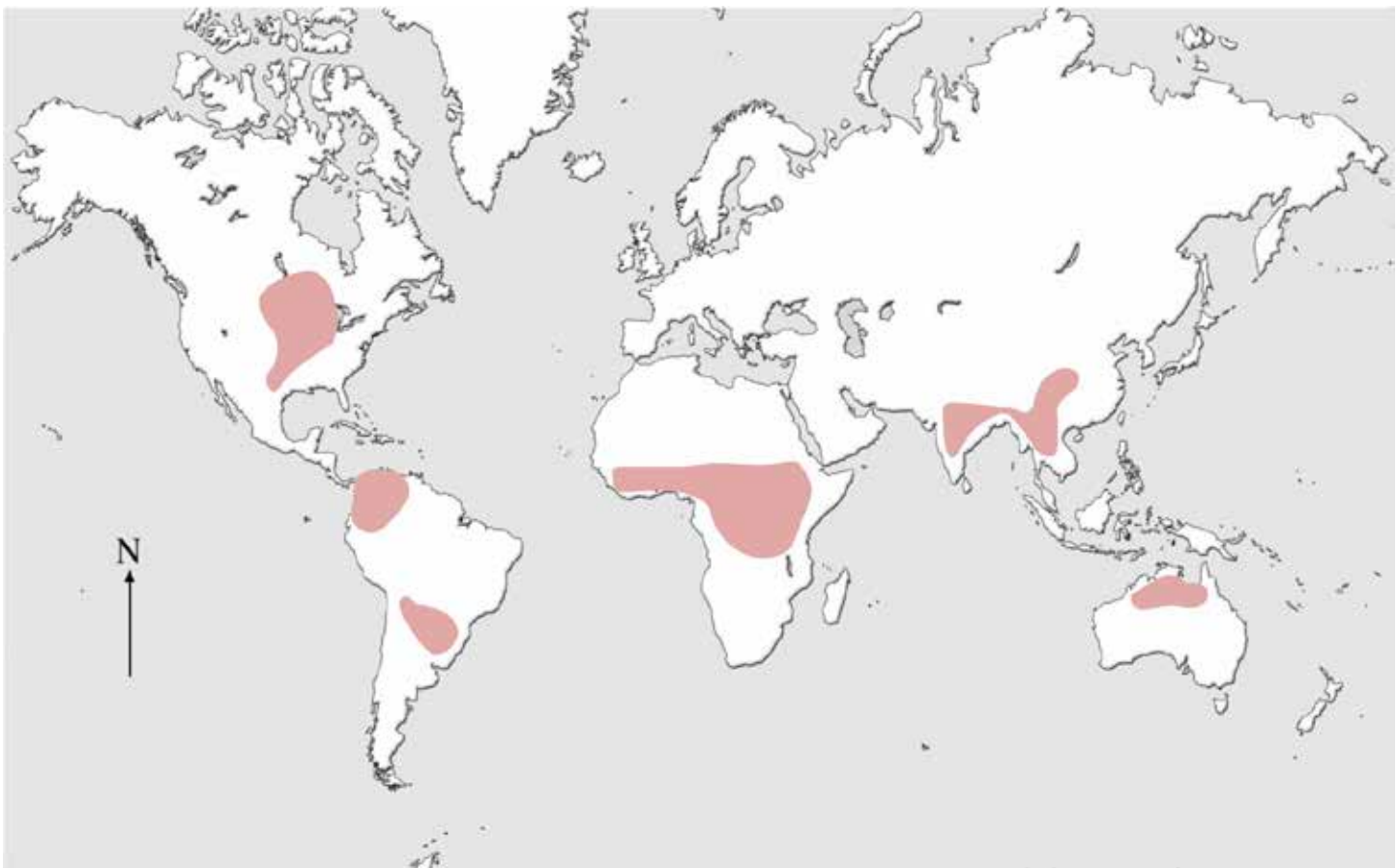


Figure 6.45. Generalized distribution of some of the more frequent mesoscale convective systems on Earth. With the exception of Africa, MCCs are relatively infrequent in the equatorial latitudes (Source/Credit: modified from maps of Laing and Fritsch, 1997, and other sources).



## Thunderstorm Hazards

### Strong Updrafts, Downdrafts and Surface Winds

The updrafts and downdrafts in a severe thunderstorm, both of which can reach speeds of 100 miles per hour, produce violent wind shear that can threaten aircraft as well as structures on the ground. Planes that have the misfortune of flying into these clouds can literally be torn apart by the violent wind shear inside the clouds. For example, in World War II a bomber squadron of eight planes flew into a line of cumulonimbus clouds — but only two came out. The other six were either torn apart or sent plunging to the ground by downdrafts.

Another tragic example of the power of these storms is provided by the account of a gliding contest held in 1939. Gliders stay aloft by riding on thermals, which are updrafts of warm air. Fair weather cumulus clouds provide good updrafts for gliding; however, the updrafts under a cumulonimbus cloud are too strong to be used safely as the pilots found out. During the contest, five gliders entered a cumulonimbus cloud whereupon their planes were broken apart by violent winds. The pilots attempted to parachute to safety but updrafts caught their chutes and carried them upwards tens of thousands of feet, well above the altitude at which there is enough oxygen to breathe and well into the realm of sub-freezing temperatures. Four of the pilots died when they were carried to an altitude of 6 miles, an altitude at which they froze to death, asphyxiated or were killed by lightning or hailstones.

Planes try to stay at least 20 miles away from well-developed cumulonimbus clouds, not only to avoid being endangered by updrafts or slammed downward by downdrafts, but because the updrafts are capable of throwing hail out of the sides and top of the cloud to distances of several miles. If sucked into a jet engine, these stones could damage or destroy engines.

The cool downdrafts that occur in association with thunderstorms can be refreshing and pleasant to feel on a hot summer day; but, if well developed, they can pose a threat to planes, ships and structures such as homes. The threat of downdrafts to planes is greatest when a plane is landing. While on approach to a runway, the pilot reduces air speed in order to lose elevation. If a downdraft is occurring near the runway, the pilot will first experience an unwanted lifting action as air that hit the ground flows sideways towards the plane and adds lift to it (Figure 6.46). To compensate, the pilot may make the mistake of further reducing speed to continue descending. However, the plane may then fly into the heart of the downdraft, where the air is moving straight downward. By then, it is usually too late to recover. Because of the reduced speed of the craft and the low altitude, the pilot cannot compensate by accelerating and adding lift, so the plane is slammed into the ground.

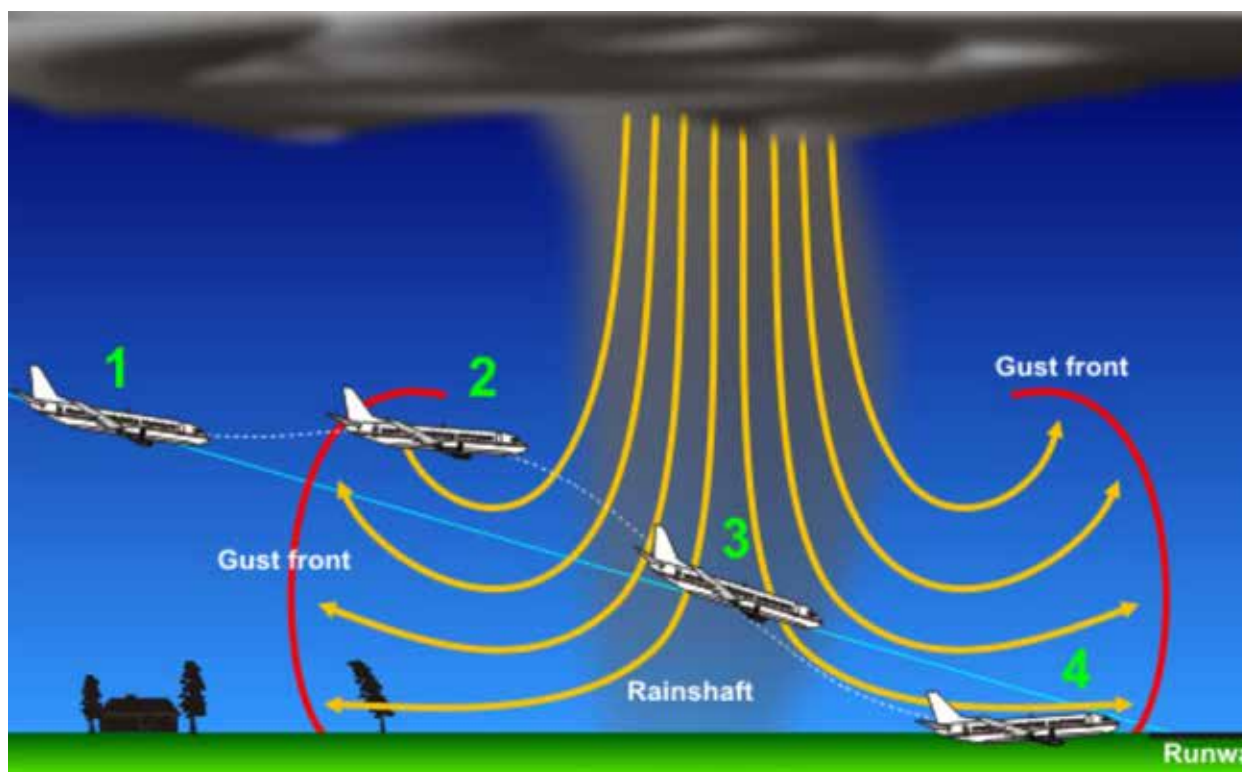
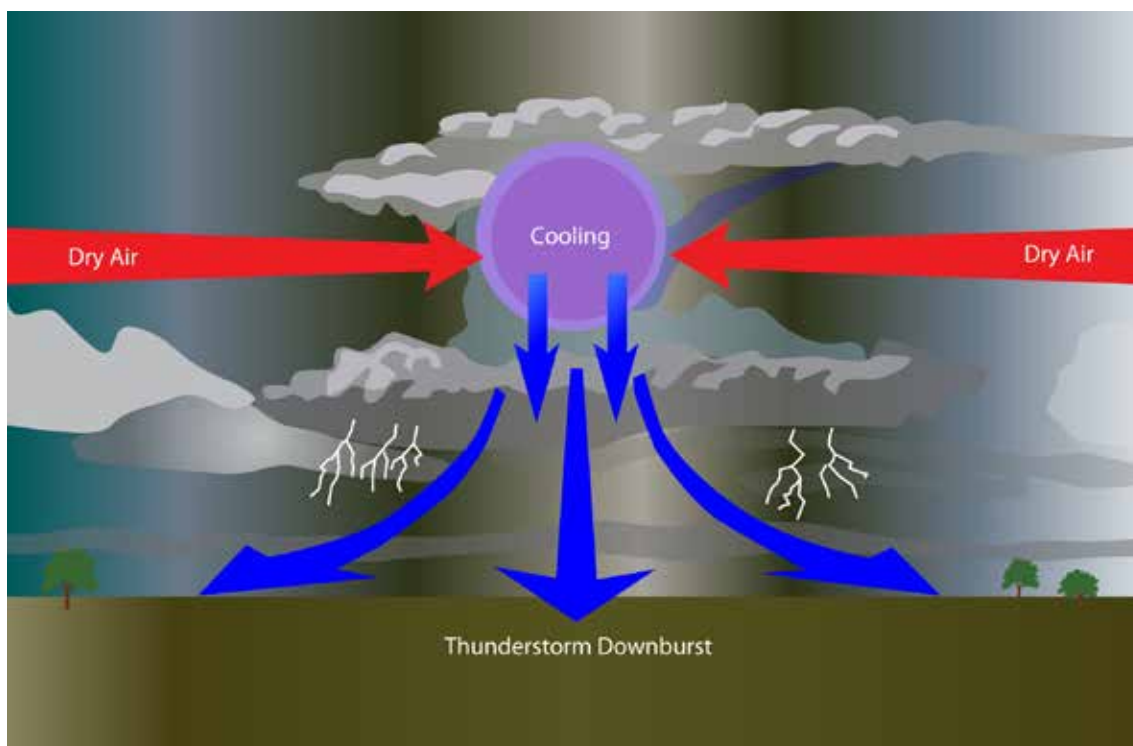


Figure 6.46. A descending airplane is lifted upward by the airflow associated with the gust front produced by a cloud. In response, the pilot reduces speed; but when the plane enters the downdraft, the airplane may be too low and moving too slow to regain altitude before being slammed into the ground by the downdraft directly below the cloud. New instrumentation at major airports is helping to reduce this threat by detecting these downdrafts. However, as rule of thumb, planes should not land if a cumulonimbus cloud is above the runway (Source/Credit: NOAA).

Many of the worst airline disasters have occurred as a result of downdrafts. Fortunately, pilots know about downdrafts nowadays and they often abort landings if a cloud is above the runway.

**Straight-line winds** associated with thunderstorm downdrafts and cold outflow can produce extensive damage. Gusts of over 100 mph (160 km/hr) are capable of downing trees (Figure 6.47), destroying mobile homes, overturning vehicles, and causing structural and cosmetic damage to homes and other structures (Figure 6.48). Damaging straight-line winds can be associated with all varieties of severe thunderstorms, ranging in size from tens to tens-of-thousands of square miles. The National Weather Service has considerable literature concerning hazards and precautions associated with straight-line winds (Figures 6.49a, 6.49b and 6.49c).



Figure 6.47. Hundreds of trees were felled by straight-line winds in Burnett County, Minnesota in 2011 (Source/Credit: NOAA/NWS Duluth, MN and the Burnett County Sheriff's Department).



Figure 6.48. Manufactured homes (image) and mobile homes are particularly susceptible to wind damage from thunderstorms. This home was completely destroyed by an eastern Iowa derecho in July of 2011 (Source/Credit: NOAA/NWS, courtesy of Kip Ladage).

<b>Product</b>	<b>What It Means</b>	<b>You Should...</b>
<b>Hazardous Weather Outlook</b>	<i>Will there be severe thunderstorms or tornadoes in the next several days?</i>	<i>If severe weather is expected, check back for later forecasts, information, and possible watches.</i>
<b>Severe Thunderstorm Watch</b>	<i>Conditions are favorable for thunderstorms to produce large hail, damaging winds, and possibly a tornado in and around the watch area during the next few hours.</i>	<i>If the watch includes your county, or one close to you, you should remain weather-aware and pay attention to what is going on. If there are storms nearby, check your <a href="#">weather source</a> to see if there are warnings.</i>
<b>Tornado Watch</b>	<i>Conditions are particularly favorable for the development of tornadoes, along with hail and damaging winds, in and around the watch area during the next few hours.</i>	<i>If the watch includes your county, or one close to you, you should remain weather-aware and pay attention to what is going on. If there are storms nearby, check your <a href="#">weather source</a> to see if there are warnings.</i>
<b>Severe Thunderstorm Warning</b>	<i>A storm with large hail and/or damaging winds has been indicated on radar or observed by storm spotters.</i>	<i>Listen closely to the warning - it will tell you exactly what to expect (hail size and wind speed). If you are outside, go indoors immediately.</i>
<b>Tornado Warning</b>	<i>A tornado has either been seen, or there are signs on radar that a tornado could be forming.</i>	<i>If you are in the warned area, <b>now</b> is the time to put your safety plan into action. Seek shelter immediately.</i>

Figure 6.49a. The National Weather Service puts out a series of outlooks, watches and warnings to alert people of potential thunderstorm hazards (Source/Credit: NOAA/NWS).

## Straight-Line Winds

Straight-line wind safety is similar to tornado safety.

If you are. . .

- **Inside of a well-built home or building -**
  - Move to the lowest floor and stay away from windows.
  - Taking shelter in a basement is strongly encouraged, especially if you are surrounded by trees that could fall onto the building or house.
- **In a mobile home or manufactured home -**
  - Move to a stronger building or storm cellar if one is nearby
  - Mobile and manufactured homes can usually withstand low-end straight-line wind storms, but as winds reach or exceed 70 mph, the risk of these homes being blown apart or struck by falling trees increases greatly.
- **Driving -**
  - Keep both hands on the wheel and slow down.
  - Pull over to the shoulder and stop, making sure you are away from trees or other tall objects that could fall onto your vehicle. **DO NOT** stop in the middle of a lane under an overpass. This could lead to an accident.
  - Take extra care in a high-profile vehicle such as a truck, van, SUV, or when towing a trailer
    - These are more prone to being pushed or even flipped by straight-line winds
    - If possible, orient your vehicle so that it points into the wind
  - Stay in the car and turn on the hazard lights until the wind subsides.
- **Caught outside -**
  - Take cover in a well-built building, or use this building to block the wind if you cannot get inside.
  - If no building is nearby, find the lowest spot and crouch low to the ground.
  - Stay away from trees or power lines, since these are easily felled by straight-line winds.
    - If you are in the middle of a forest, move to the lowest/smallest stand of trees
  - Stay clear of roadways or train tracks, as the winds may blow you into the path of an oncoming vehicle
  - Watch for flying debris. Tree limbs, street signs, and other objects may break and become flying projectiles in the wind.



If you venture outside after the storm has passed, be alert for downed power lines. Do not touch any downed wires or anything in contact with the wires.

Figure 6.49b. The National Weather Service issues statements of advice about coping with straight-line winds in various situations (Source/Credit: NOAA/NWS).

Long-lived squall lines that form a linear front in plan view and move in more-or-less straight lines are called *derechos* (Spanish “straight”). They can last over 12 hours and produce damaging straight-line winds for hundreds of miles. *Derechos* are more common in the eastern United States than in most other parts of the world (see chapter 4 for expanded discussion of *derechos*).

## Lightning

**Lightning** is the rapid discharge of electricity (a huge spark) within a cloud, from cloud to cloud, or cloud to ground (Figure 6.50). Positive and negative charges in a cumulonimbus cloud tend to separate, and when the electrical potential exceeds the insulating capacity of the air, an immense discharge occurs. Although the most frequent cause of lightning in the atmosphere is from thunderstorms, lightning can also originate from intense forest fires, volcanic eruptions, nuclear detonations and heavy snowstorms.

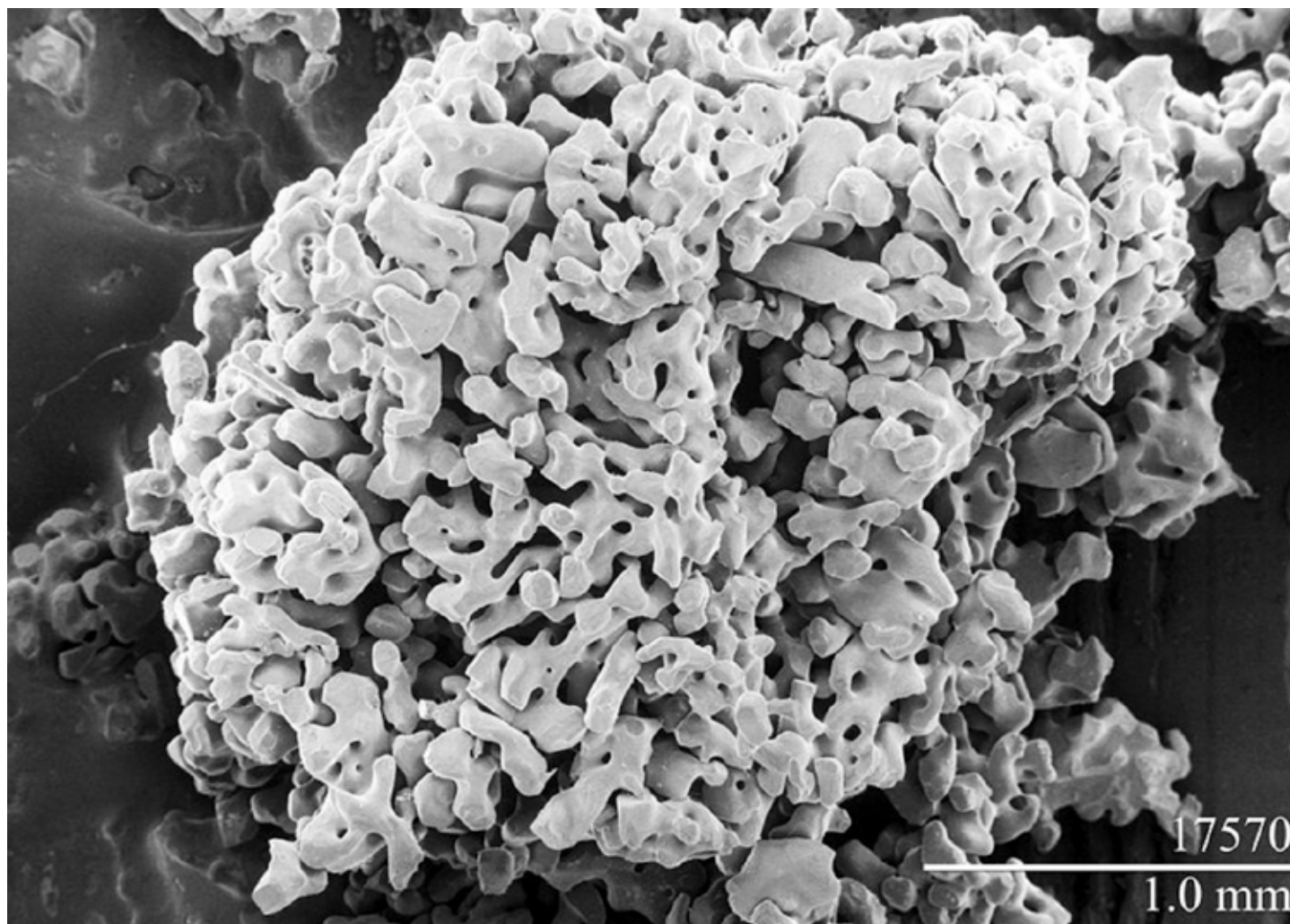


Figure 6.50. Lightning can occur within a cloud, from cloud to cloud, or from cloud to ground (Source/Credit: NOAA).

**Thunder** is a compressional sound wave caused by lightning. Lightning heats the air to somewhere between 18,000°F and 54,000°F (~10,000-30,000°C), causing instantaneous expansion of air and a compressional wave that radiates in all directions. The faster the air is heated, the more explosive the acoustic wave. Whereas lightning travels at the speed of light (about about 670 million mph in the atmosphere), the clap from thunder travels at the snails-pace of sound (~770 mph or 1235 km/h at sea level). The speed of sound varies with altitude as a function of temperature and pressure. The time lag between seeing a lightning flash and hearing the thunder depends on distance from the observer. As a rule of thumb, every second in lag time means about 1100 feet (~335 m) distance. If the lag time is 5 seconds, the origin of the electric spark is about a mile away (5 X 1100 = 5500 ft). A lightning flash can be seen for many tens of miles under ideal atmospheric conditions, whereas thunder is seldom heard from more than about 20 miles from the source.

Although the exact mechanisms by which clouds acquire charges are not fully understood, in most cases the base of a cloud develops a negative charge. One theory maintains that this charge separation results from the interaction of graupel, snow crystals, and supercooled water droplets. **Graupel** is a low-density form of ice that results from supercooled water droplets freezing on snow crystals (Figure 6.51). When graupel collides with snow crystals and supercooled water droplets, electrons are torn off the rising ice crystals, leaving them with a positive charge. The newly-acquired electrons leave the graupel with a negative charge. When cloud temperatures are below about 5°F (-15°C), the snow crystal winds up positively charged and the graupel winds up with a negative charge. The heavier, negatively-charged graupel tends to accumulate in the middle part of the cloud, whereas the lighter snow crystals are carried higher, giving the upper part of the cloud a positive charge. If cloud temperatures are above ~5°F (-15°C), the positive and negative charges are reversed (Figure 6.52).





*Figure 6.51. Photomicrograph of graupel. Graupel is a fragile, low-density form of ice that forms when supercooled water droplets freeze on snow crystals. Bar scale is 1.0 mm, or about 0.039 inches (Source/Credit: Agricultural Research Service. USDA).*

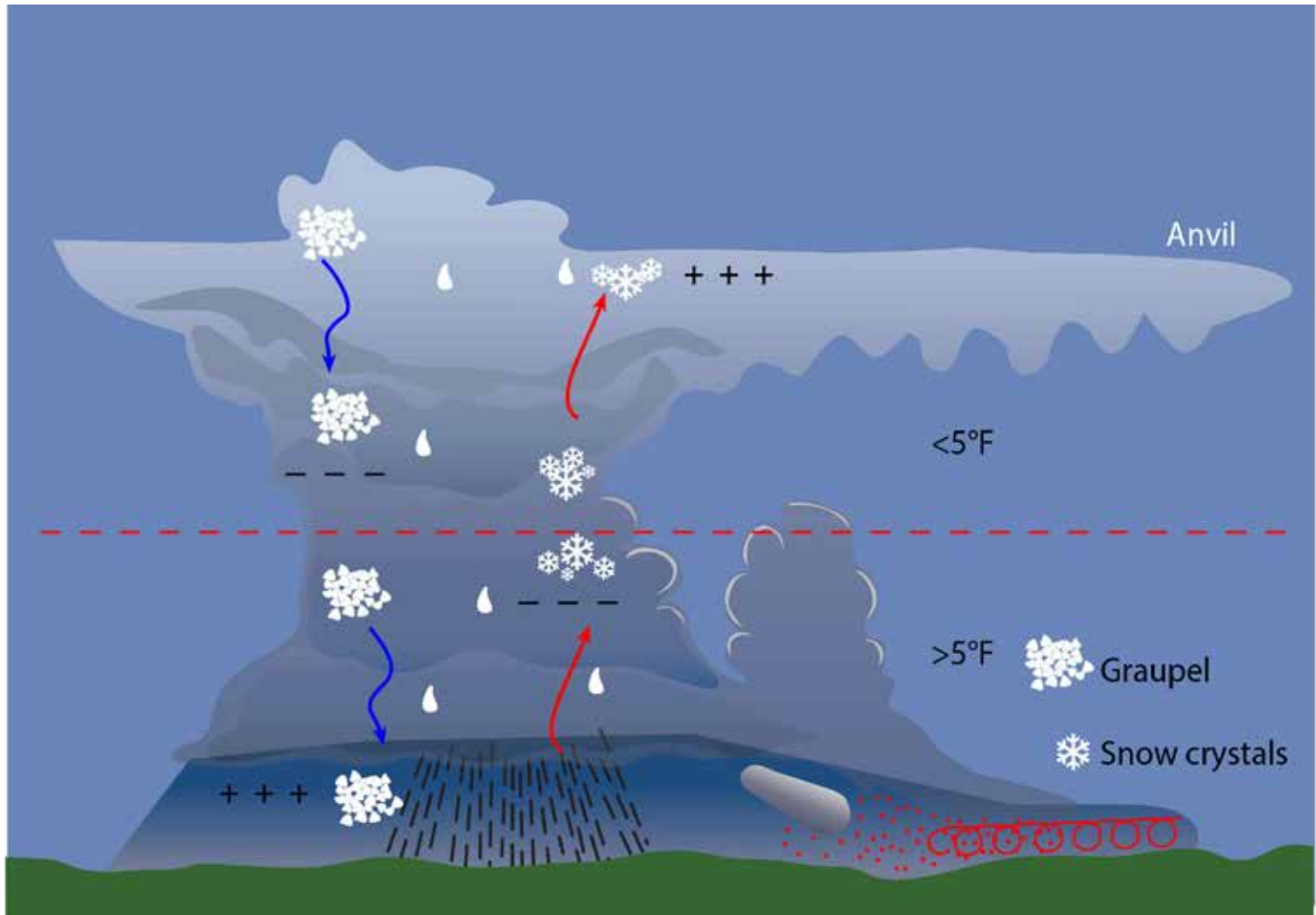


Figure 6.52. One theory on the origin of charge separation maintains that it results from the interaction of graupel, snow crystals, and supercooled water droplets. At temperatures below about 5°F (-15°C), the snow crystal winds up positively charged and the graupel winds up with a negative charge. The negatively-charged graupel tends to accumulate in the middle part of the cloud, whereas the lighter snow crystal is carried higher, giving the upper part of the cloud a positive charge. If cloud temperatures are above ~5°F (-15°C), the positive and negative charges are reversed (Source/Credit: Dennis Netoff, modified from several sources).

In clouds that have negative charges concentrated near their base, the negative charge in the bottom of a cloud repels the negative charges in the ground below because like charges repel one another. As a result, the ground becomes positively charged (Figure 6.53). When the voltage potential becomes great enough, an electrical charge begins to work its way toward the ground in the form of a thin filament of electricity known as a **stepped leader**. The stepped leader travels in a series of 160 ft. (50m) steps toward the ground producing the characteristic zigzag pattern of most lightning strokes. As the leader approaches the ground, positive charges in the ground begin to move upward toward the leader. This usually occurs by way of the tallest objects in an area which is why it is not safe to stand near a tree during a thunderstorm (Figure 6.54). When they meet, a rapid discharge of electricity occurs from the ground upward to the cloud. This discharge is called a **return stroke**. The return stroke generally follows the zigzag path that was taken by the stepped leader on its way toward the surface. We do not normally see the stepped leader because it is less powerful and more faint than the return stroke.

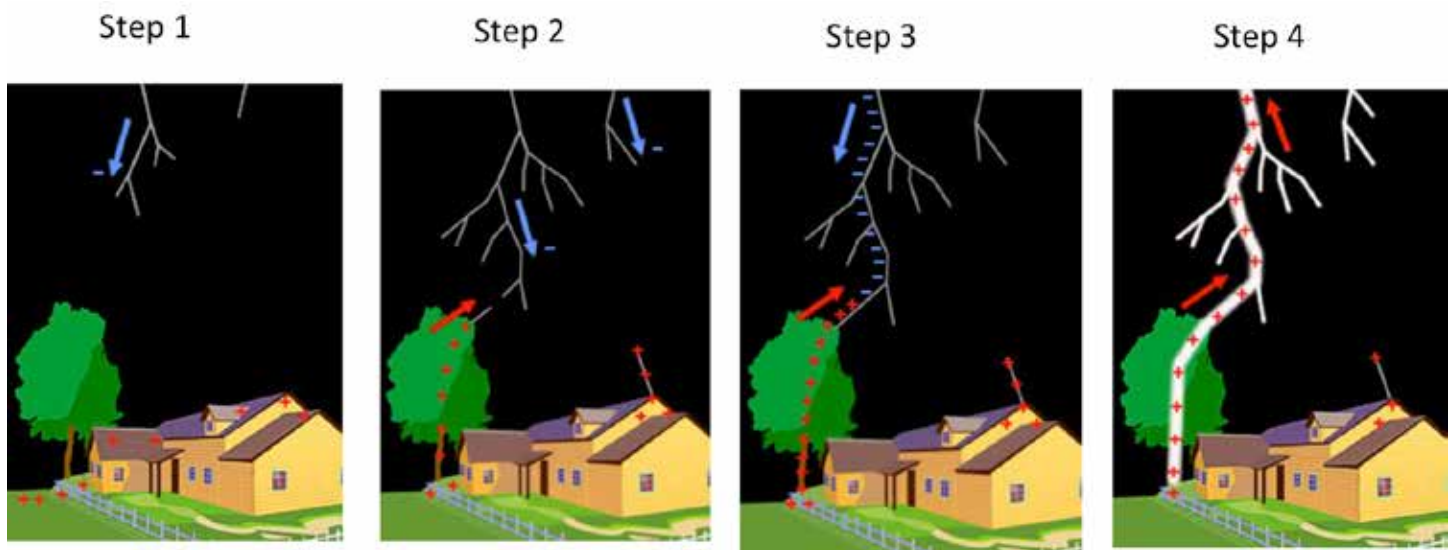


Figure 6.53. The initial stage of electrical discharge between the cloud and the ground is a faint, negative stream of electrons referred to as a stepped leader. Subsequent steps of about 160 feet (50 m) and a millionth of a second in duration carry the stepped leader closer to the ground. After thousands of steps, the leader is close enough to the ground to cause an influx of positive charges that meet the stepped leader and close the electrical circuit. Once the electrical connection is made, a stream of electrons flows toward the ground along the established channel. Immediately following this, a return stroke of positive charges carrying perhaps 30,000 amperes creates a brilliant visible flash (Source/Credit: NOAA).



Figure 6.54. Lightning prefers to strike tall objects because they represent the shortest path of the lightning bolt through the atmosphere (Source/Credit: NOAA/NSSL).

Lightning is a major weather-related hazard (Figure 6.55a and 6.55b). More than 21 million cloud-to-ground lightning strikes occur in an average year. In the United States, approximately 85 to 100 people are killed each year by lightning, and more than 500 are injured. The odds of any individual being hit in a year are about 350,000 to one. By way of comparison, the odds of you being hit by a car is about one in 7000. Nonetheless, precautions should be taken when thunderstorms are in your area.

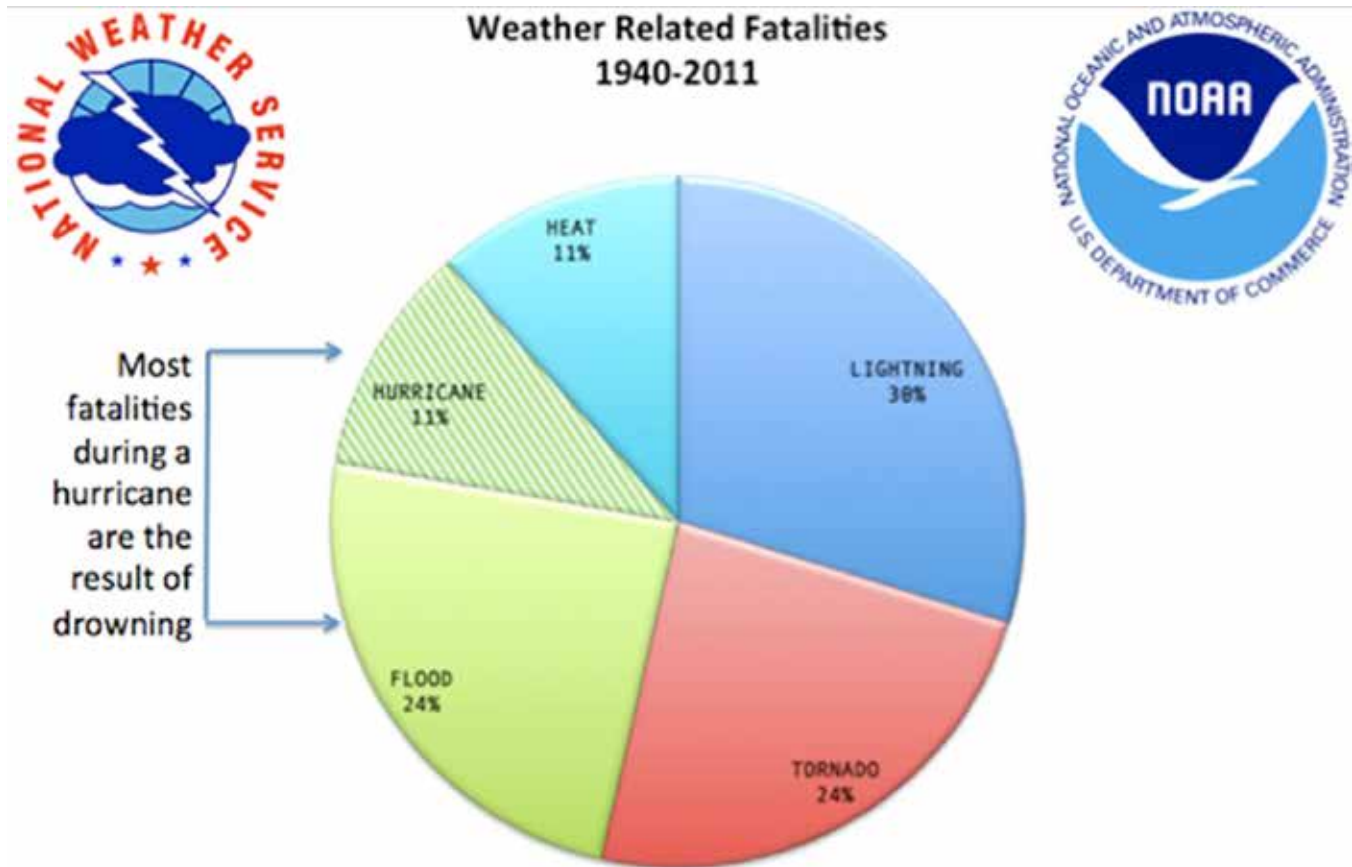


Figure 6.55a. Over a 70+-year time span, lightning is #1 in weather-related fatalities, followed by tornadoes and floods, with heat tied for 4th place. Heat and hurricane deaths have steadily risen proportionately in recent decades, in part because of population movement toward the South and toward the coasts (Source/Credit: NWS/NOAA).

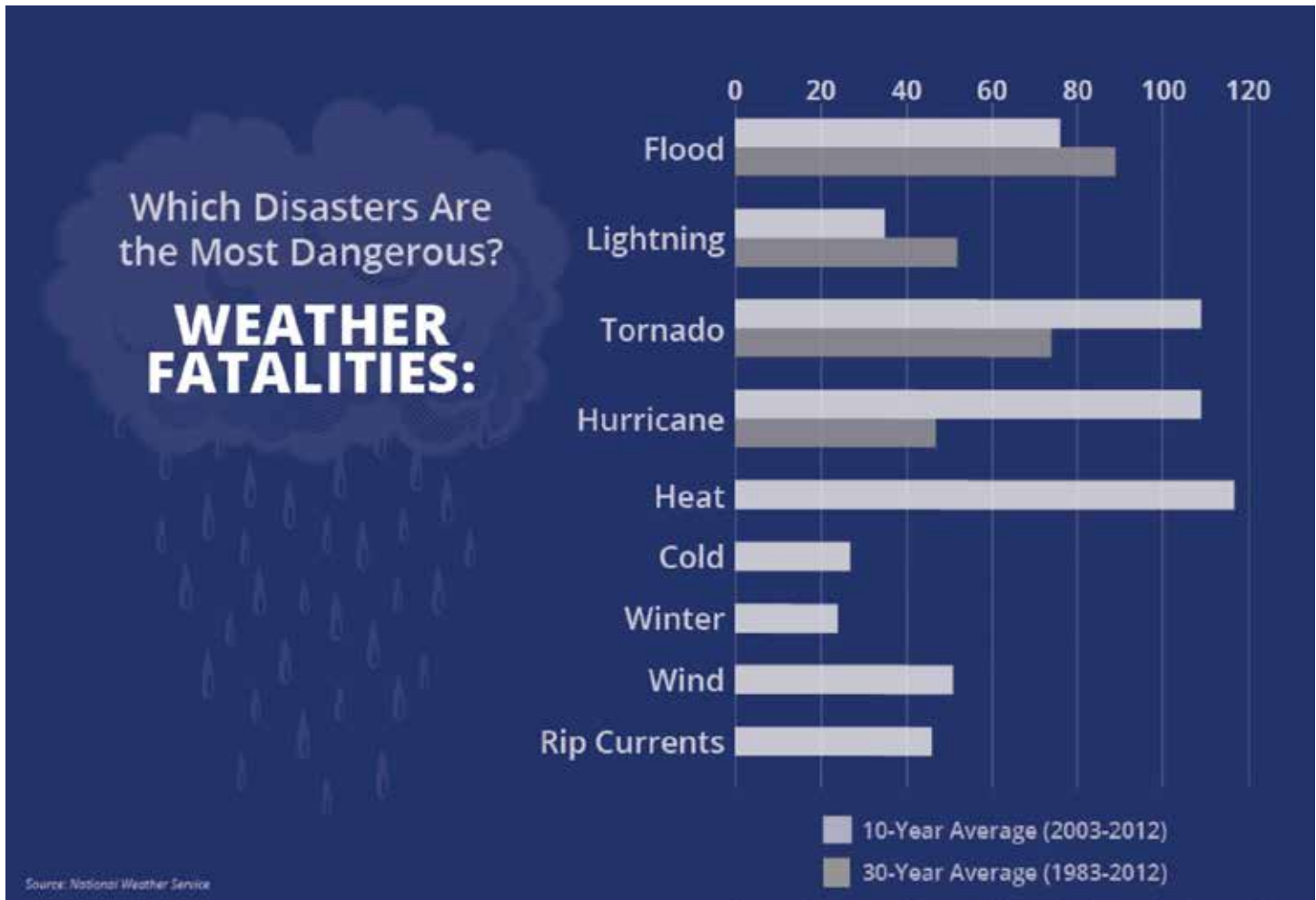


Figure 6.55b. Data on weather-related hazards in the United States varies with the time interval used. Single events with large fatalities, such as hurricane Katrina in 2005, make the 10-year average from 2003-2012 among the leader in fatalities, whereas the 30-year average has hurricanes in 4th place among floods, lightning, tornadoes and hurricanes. Over the past few decades, heat is consistently #1 in average weather fatalities (Source/Credit: NWS/NOAA).

In addition to the precautions above, NOAA offers some interesting myths and facts about lightning safety (some items abbreviated/modified):

**Myth:** Lightning never strikes the same place twice.

**Fact:** Lightning often strikes the same place repeatedly, especially if it's a tall, pointy, isolated object. The Empire State Building is hit nearly 100 times a year.

**Myth:** If it's not raining or there aren't clouds overhead, you're safe from lightning.

**Fact:** Lightning often strikes more than three miles from the center of a thunderstorm, far outside the rain or thunderstorm cloud. Lightning can strike 10-15 miles from the thunderstorm.

**Myth:** A car's rubber tires protect you from lightning by insulating you from the ground.

**Fact:** Most cars are safe from lightning, but it is the metal body of the car that

protects, not the rubber tires. Open-air vehicles (convertibles, backs of pickups, motorcycles, bikes, recreational vehicles) offer no protection from lightning.

**Myth:** If outside in a thunderstorm, you should seek shelter under a tree to stay dry.

**Fact:** Being underneath a tree is the second-leading cause of lightning casualties.

**Myth:** Sheet lightning forms without an actual lightning bolt.

**Fact:** Sheet lightning is from a lightning bolt that cannot be seen, typically because it is obscured by clouds.

**Myth:** If you are in a house, you are 100% safe from lightning.

**Fact:** Houses are relatively safe as long as you avoid anything that conducts electricity. Stay off corded phones and away from electrical appliances, wires, TV cables, computers, plumbing, metal doors and windows.

**Myth:** If thunderstorms threaten while you are outside playing a game, it is OK to finish it before seeking shelter.

**Fact:** Many lightning casualties occur because people do not seek shelter soon enough. Seek proper shelter immediately if you hear thunder.

**Myth:** If a lightning victim is electrified, you can be electrocuted if you touch them.

**Fact:** The human body does not store electricity. It is safe to give a lightning victim first aid.

**Myth:** Texas, because of its size, is the lightning capital of the U.S., whereas Amazonia (Brazil) is the world's lightning capital.

**Fact:** Florida is the lightning capital of the U.S.; equatorial Africa is the world capital.

**Myth:** Heat lightning is lightning that occurs in clear air, and is no threat to humans.

**Fact:** Heat lightning is caused by regular thunderstorms that are too distant to see the actual lightning bolt or hear thunder; dim, flickering light on the horizon is typically reflected light from distant cumulonimbus clouds that may be >100 miles (160 km) away.

**Myth:** Dry lightning occurs without a cumulonimbus cloud.

**Fact:** Dry lightning is generated from a cumulonimbus cloud that does not produce rain at the Earth's surface; virga may form, but evaporates prior to reaching the surface. Dry lightning produces lots of forest and brush fires.

When Benjamin Franklin discovered that lightning was a form of electricity, the door was opened to help minimize the threat that lightning poses to structures. Franklin realized that if a metal rod (a lightning rod) were attached to a house and grounded, lightning would travel through the rod and into the ground. In effect, the discharge takes the path of least resistance, and that path is through the rod, not through the house. In fact, Franklin installed a lightning rod on his own home, and a few years later lightning hit it. The rod spared his home from the strike. Modern lightning rod systems are used extensively in high-rise structures, especially those that house critical facilities (Figures 6.56a and 6.56b).

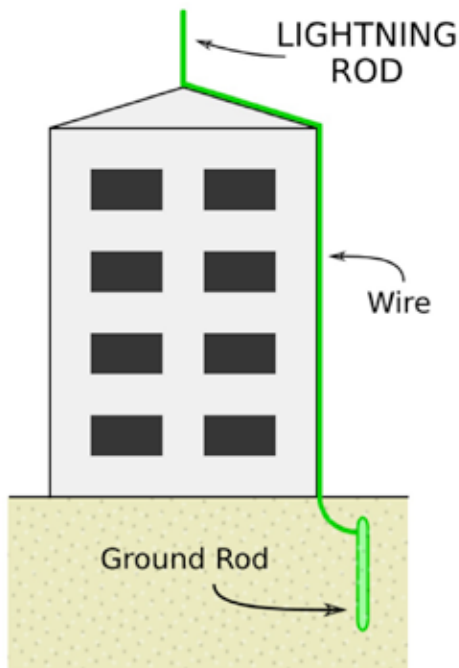


Figure 6.56a. (left) Simple lightning protection systems have one or more lightning rods at high points on the structure that are grounded by a wire(s) leading from the rod to the ground (Source/Credit: <https://commons.wikimedia.org/wiki/User:Wdchk>).

Figure 6.56b. (right) Critical facilities, such as the air traffic control tower at Chicago's Midway International Airport, have advanced lightning protection systems. There are hundreds of air traffic control towers in the United States, and only one reported accident involving lightning strikes (Source/Credit: AP, March 12, 2013).



The geography of thunderstorm-generated lightning follows a fairly predictable pattern. Thunderstorms require warm, moist, unstable air, and are often triggered by afternoon ground heating. Land areas heat up and become unstable in the early afternoon more readily than water, so land masses have a much higher frequency of lightning strikes than over oceans, even in the tropics (Figure 6.57). Tropical latitudes generate more land-based thunderstorms than any other region, because requisite conditions are met most of the year. Higher latitudes show progressive decreases in thunderstorm activity, and become more concentrated during the warm season. In the mid-latitudes, the eastern sides of continents show a much higher frequency of lightning strikes than the western sides because of proximity to warm ocean currents and monsoonal flow patterns.

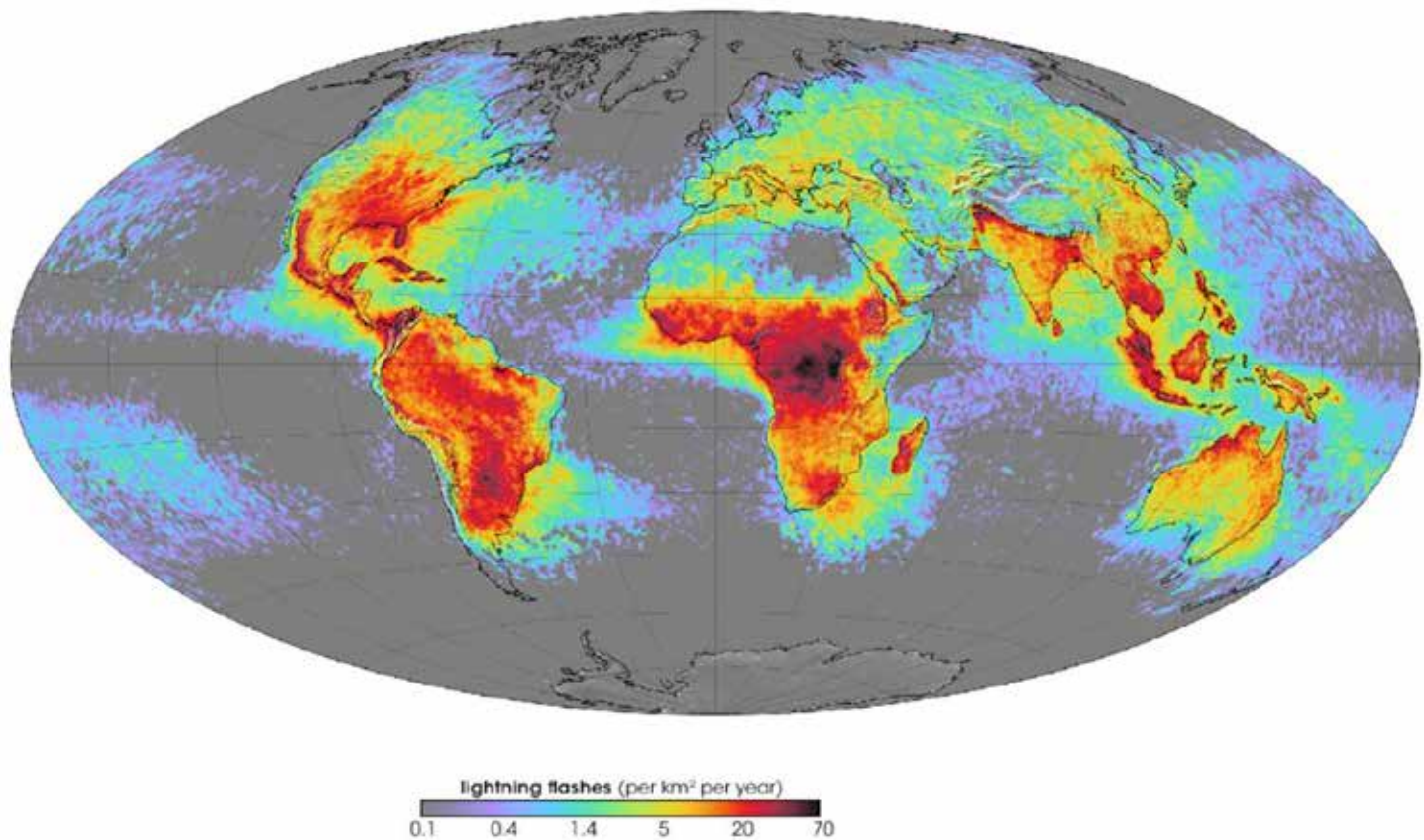


Figure 6.57. The world map shows the distribution of lightning strikes per year. Several general patterns include (1) lightning strikes are far more abundant over land than water, (2) the frequency of strikes over land decreases with increasing latitude, (3) in the mid-latitudes, the eastern side of continents (e.g., the southeastern United States and China) has a higher frequency than the western side (Source/Credit: NASA).

## Hail

Hail is a solid form of precipitation that forms exclusively from cumulonimbus clouds. The strong updrafts of cumulonimbus clouds are required to keep large hailstones aloft; the larger the stone, the stronger the updraft needed to keep it suspended. As hailstones are carried by downdrafts and updrafts, they grow by contact with supercooled water drops and other solid objects. Supercooled water droplets are abundant in the middle and middle-upper parts of cumulonimbus clouds where temperatures are between 32°F (0°C) and -40°F (-40°C). In *dry growth*, supercooled water droplets freeze instantly when they collide with snow crystals or hail stones, forming cloudy layer of ice. In other areas of the cloud, supercooled water droplets may be sparse, and water vapor may sublime onto the hailstone, forming an opaque layer of ice. A layer of clear ice may form during *wet growth*, where supercooled water droplets accrete onto ice nuclei and slowly spread across the ice surface. Because of slow growth, a layer of clear ice forms. In *dry growth*, supercooled water droplets freeze on contact, which traps lots of air bubbles, creating a cloudy appearance.

Alternating clear and opaque ice tends to form concentric bands (onion-skin layering) that are visible when hailstones are cut (Figure 6.58). Some hailstones combine with other hailstones during their descent through the cloud, giving the hailstone an irregular shape, often lacking the onion-skin layering. When the size of the hailstone is greater than the strength of the updrafts, it falls toward the ground. Many hailstones experience partial or total melting as they fall through warmer, near-surface air.



Figure 6.58. Concentric banding in hailstone that fell on October 20, 2008. The transparent/translucent layers are produced by wet growth of supercooled water droplets, whereas the cloudy, opaque layers form from dry growth (Source/Credit: [http://commons.wikimedia.org/wiki/File:Hagelkorn\\_mit\\_Anlagerungsschichten.jpg](http://commons.wikimedia.org/wiki/File:Hagelkorn_mit_Anlagerungsschichten.jpg))

The size of a hailstone is therefore limited by the strength of the strongest updraft within the cloud. Estimates of the fall velocity of objects of various sizes and densities gives estimates of the strength of updrafts in the cloud from which it fell (Figure 6.59). Pea-sized hail falls at about 24 mph (11 m/s), whereas baseball-sized hail falls at about 81 mph (36 m/s). The largest recorded hail stones in the world are about softball-sized (Figures 6.60 and 6.61) with a fall velocity of about 103 mph (46 m/s).

### Estimating Hail Size

Hail size is estimated by comparing it to a known object. Most hail storms are made up of a mix of sizes, and only the very largest hail stones pose serious risk to people caught in the open.

Hailstone size	Measurement		Updraft Speed	
	in.	cm.	mph	m/s
bb	< 1/4	< 0.64	< 24	< 11
pea	1/4	0.64	24	11
marble	1/2	1.3	35	16
dime	7/10	1.8	38	17
penny	3/4	1.9	40	18
nickel	7/8	2.2	46	21
quarter	1	2.5	49	22
half dollar	1 1/4	3.2	54	24
walnut	1 1/2	3.8	60	27
golfball	1 3/4	4.4	64	29
hen egg	2	5.1	69	31
tennis ball	2 1/2	6.4	77	34
baseball	2 3/4	7.0	81	36
tea cup	3	7.6	84	38
grapefruit	4	10.1	98	44
softball	4 1/2	11.4	103	46

Figure 6.59 Estimates of hailstone velocity based on size is only approximate, since the density is somewhat variable and few hailstones are perfect spheres. Larger stones have greater mass and higher fall velocities, and pose the greater hazard to humans and crops (Source/Credit: NOAA /NWS /NSSL).



Figure 6.60. The former record-holder hailstone fell on June 22, 2003 in south-central Nebraska. It had a diameter of 7 inches (~18 cm) and a circumference of 18.75 inches (~48 cm). Larger hailstones have been reported elsewhere on Earth, but never verified (Source/Credit: NOAA).



Figure 6.61. A new North American record for hailstone size was set in Vivian, South Dakota on July 23, 2010. Its 8-inch (20.3 cm) diameter exceeds the 7-inch (17.8 cm) diameter of the hailstone that fell in Aurora, Nebraska in 2003. It also eclipses the 1.67 pound weight record of the Coffeerville Kansas hailstone of 1970 at an amazing 1.94 pounds. Its 18.625-inch circumference will remain second to the Aurora Nebraska hailstone, which measured 18.75 inches (Source/Credit: NWS Aberdeen, SD).

Large, massive hailstones cause millions of dollars of crop losses annually and can do serious damage to automobiles, houses, and other objects (Figure 6.62). Over 7000 major hailstorms were reported in the United States in 2012. A single hailstorm in St. Louis, Missouri in 2001 caused over \$2 billion with baseball-sized hail, and one in Colorado in 1990 caused \$1.1 billion in damages. A list of notable hailstorm events illustrates the kind of damage done by hail, as well as the diverse geographic locations involved (Figure 6.63).



Figure 6.62a. Hail damage to a vehicle in Lubbock County, Texas on April 29, 2012 (Source/Credit: NOAA).



*Figure 6.62b. The hail superstorm. On May 12, 2000, a supercell thunderstorm developed in west-central Wisconsin. Hail up to the size of baseballs and winds exceeding 60 mph produced incredible damage in several counties. Property damage in Wisconsin was estimate at \$122 million (Source/Credit: NOAA).*





*Figure 6.62c. Hail damage to the windows and siding of a home in Lubbock County, Texas on April 29, 2012 (Source/Credit: NOAA).*

Date	Location	Description
July 6, 1928	Potter, Nebraska	Early record-holding hailstone at 7 inches diameter and 1.5 lbs.
September 2, 1960	Southern California	Baseball-sized hail in an area where thunderstorms are rare.
September 3, 1970	Coffeyville, Kansas	Record-breaking hailstone at 1.67 lb. and 17.5-inch circumference.
July 30, 1979	Ft. Collins, Colorado	Grapefruit-sized hail, 2500 autos severely damaged, one fatality.
July 11, 1990	Denver, Colorado	Softball-sized hail causes \$1.1 billion damage to roofs, cars.
July 23, 2010	Vivian, South Dakota	Record-breaking hailstone at 1.94 lbs; many baseball-to-softball-sized hailstones.
April 28, 2012	St. Louis, Missouri	Several hailstorms batter St. Louis; second costliest hailstorm in U.S. at \$1.6 billion.

Figure 6.63. Notable hailstorms in U.S. history (Source/Credit: [http://en.wikipedia.org/wiki/List\\_of\\_costly\\_or\\_deadly\\_hailstorms](http://en.wikipedia.org/wiki/List_of_costly_or_deadly_hailstorms)).

Hailstorm frequency in the United States coincides roughly with thunderstorm frequency, but with some notable exceptions (Figures 6.64a, 6.64b and 6.64c). The most obvious of these is the high frequency of severe hail events in the Great Plains, whereas the highest frequency of thunderstorms is along the Gulf Coast. Texas, with several large population centers in the northern part of the state, typically ranks number one in terms of damaging hail events. The metropolitan areas with populations exceeding 50,000 people that are typically in the top 10 in the country with respect to hail damage include, in general decreasing order, Amarillo TX, Wichita KS, Tulsa OK, Oklahoma City OK, Midwest City OK, Aurora CO, Colorado Springs CO, Kansas City KS, Fort Worth TX, and Denver CO.

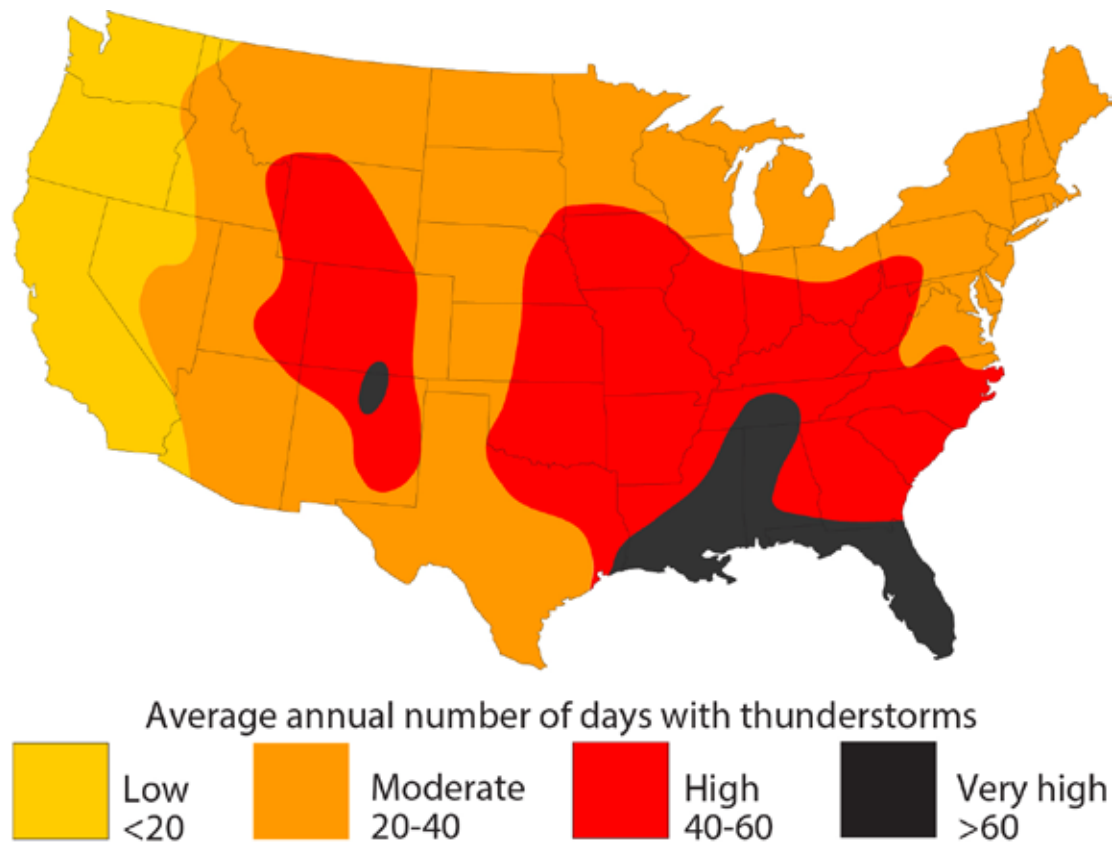


Figure 6.64a. The highest frequency of thunderstorms in the United States is along the Gulf Coast where warm, moist unstable air dominates during much of the year. A secondary area of frequent thunderstorms occurs in a belt from New Mexico to northern Wyoming, and is orographically-enhanced (Source/Credit: modified from Dennis I. Netoff and Ava Fujimoto-Strait, *Weather & Climate Lab Manual*).

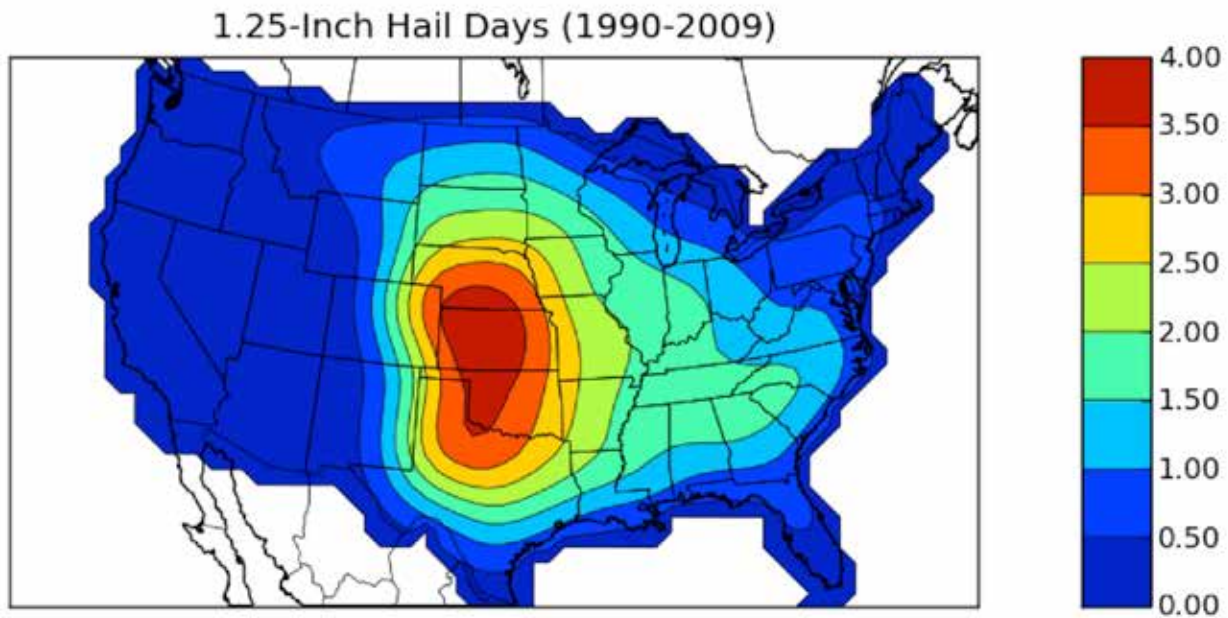


Figure 6.64b. Frequency of 1.25-inch (~3.2 cm) hail days per year in the United States (Source/Credit: contour map created by Harold Brooks, NSSL and Tom Grazulis, Tornado Project and NWS records).

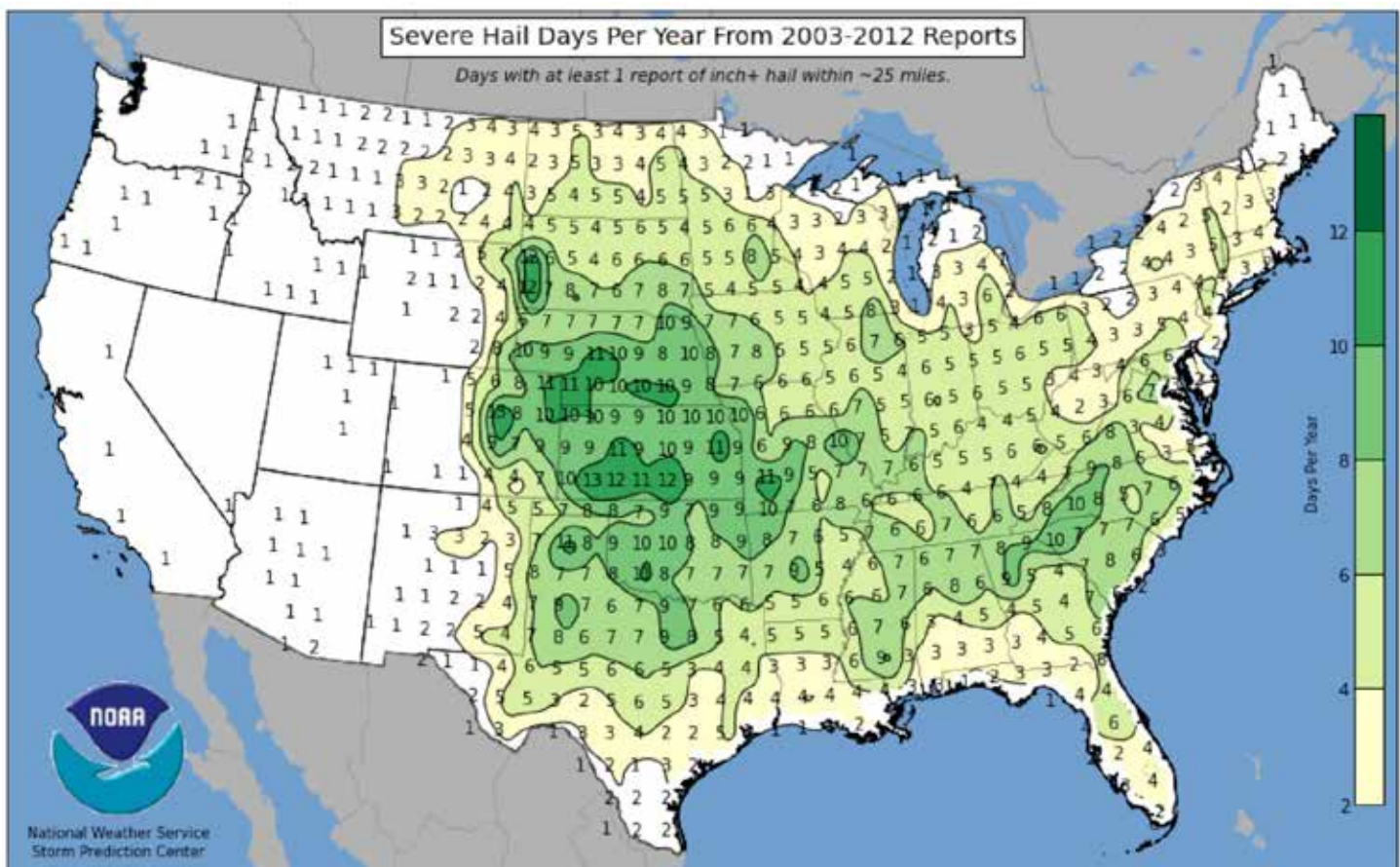


Figure 6.64c. A detailed map of the frequency of severe hail days in the United States shows a concentration in the central Great Plains, but with two additional areas of high frequency in eastern Colorado and Wyoming. The tri-state area that includes northeast Colorado, northwest Nebraska, and eastern Wyoming is called hail alley (Source/Credit: NOAA).

## Floods

Many **floods**, especially flash floods, result from thunderstorms. Flash floods, unlike regional floods, typically occur within a few hours of a rainfall event, and are therefore difficult to give adequate advance warning. Floods are typically one of the most expensive weather-related hazards in the United States in any given year. Over the past century, floods, including flash floods, were ranked the number one natural disaster with respect to lives lost and property damage, according to the United States Geological Survey. Many of the catastrophic flash floods in the United States have been associated with thunderstorms produced by land-falling tropical storms and hurricanes (Figure 6.65). In September 2014, widespread thunderstorm-induced flash floods devastated Arizona, New Mexico, and west Texas from the remnants of hurricanes Norbert and Odile, long after they had made landfall in Mexico (Figure 6.66).

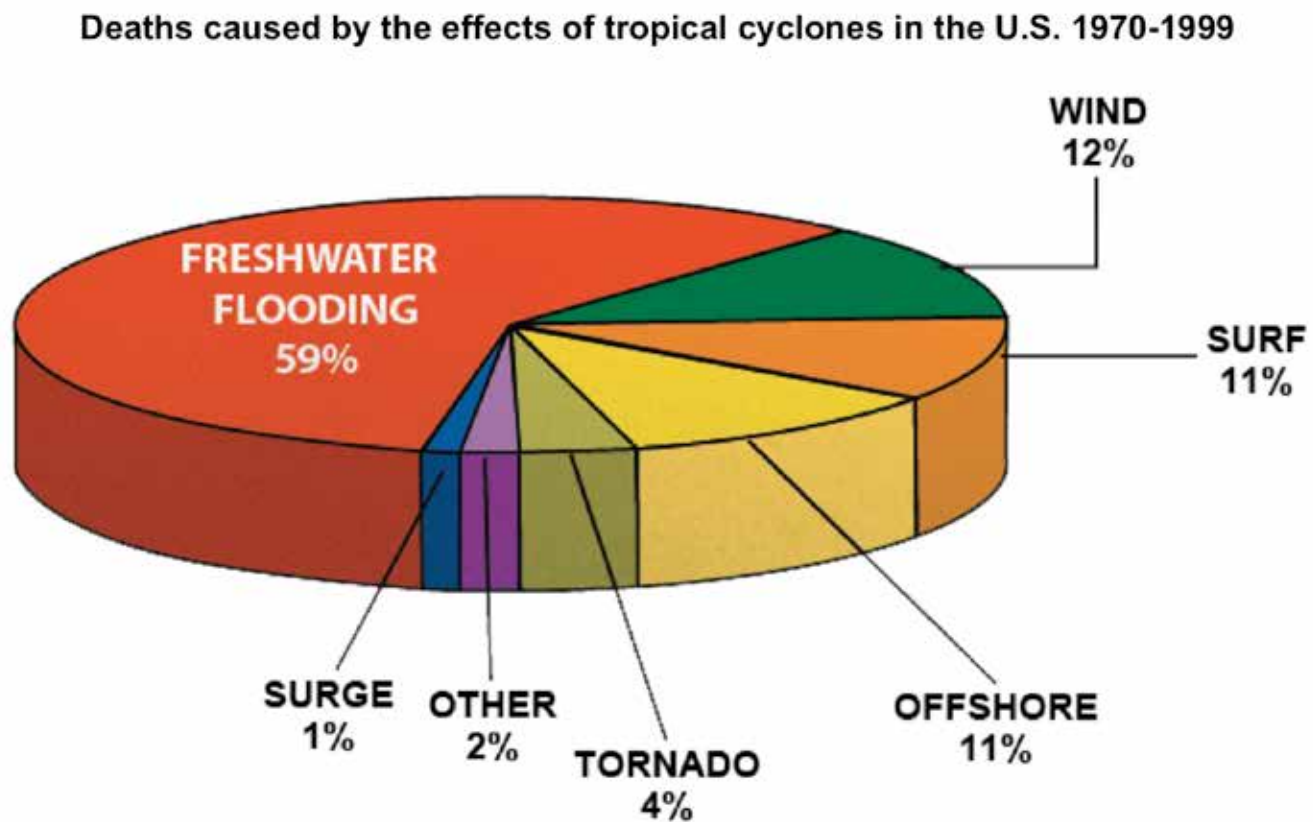


Figure 6.65. Many of the catastrophic flash floods in the United States have been associated with thunderstorms produced by landfalling tropical storms and hurricanes. The flood deaths do not include casualties caused by salt-water inundations due to tropical cyclone storm surges (Source/Credit: NOAA).



Figure 6.66. Hurricane Odile made landfall near Cabo San Lucas on September 14, 2014 as a Category 3 hurricane with sustained winds of 127 mph (204 km/h). Torrential rains and flash floods occurred sporadically on the Baja Peninsula as the storm moved northwestward. Several days later, remnants of the storm turned to the northeast, hitting the southwestern deserts of the United State. Just a week earlier, the remnants of Hurricane Norbert made a similar track and delivered over 3 inches of rain to Phoenix, AZ and Las Vegas, NV (Source/Credit: NASA).

Flash floods are very common in arid or semi-arid regions such as the western United States. Steep slopes, rocky terrain, lack of vegetation cover, and low-permeability soils combine to make these regions flash-flood prone (Figures 6.67a, 6.67b, 6.67c and 6.67d). Normally-dry water courses are suddenly engulfed in a wall of swift-moving water, which can cause extensive damage within just a few hours. The Texas Hill Country has been labeled the most flash-flood prone region in North America.



*Figure 6.67a. Normally dry desert stream beds, known as arroyos, are prone to flash floods. When flash floods occur in these channels, they usually develop in response to rain that fell on nearby mountain ranges – not onto the area immediately adjacent to the arroyos. As the water runs down the mountains, it is channeled into the arroyos, causing them to fill rapidly with water. A wall of water can literally form as the flood wave moves down the channel (Source/Credit: Dennis I. Netoff).*



Figure 6.67b. El Rosario arroyo in Baja, Mexico during a flood. Highway 1, the only paved north-south highway in the Baja Peninsula, goes across the bottom of the arroyo (Source/Credit: Dennis I. Netoff).





Figure 6.67c. Slot canyons (narrow, deep, bedrock-walled canyons) are highly susceptible to flash floods. The image is Antelope Canyon, a popular area near Lake Powell for hikers and photographers on the Arizona-Utah border. When water fills these narrow canyons or stream channels, there is no place for the water to go but up. Floods in such areas are deadly, as there is no easy escape from the fast-flowing water. In 1997, 11 hikers drowned in the canyon due to torrential rains from a thunderstorm that was 7 miles (11 km) away (Source/Credit: Public Domain <http://commons.wikimedia.org/wiki/User:Selby02>, Lucas Löffler).



*Figure 6.67d. Frontal lobe of a flash flood on the Paria River, northwest of Lake Powell, Utah. Severe High Plateau thunderstorms some distance away were responsible for the resultant floods (Source/Credit: Dennis I. Netoff).*

In addition to lightning, hail and floods, cumulonimbus clouds are also responsible for some of the most feared atmospheric phenomena — tornadoes.

## Tornadoes

Tornadoes are intense cyclonic vortices that emanate from cumulonimbus clouds and are in contact with the ground. They are an extreme type of cyclonic storm. Most tornadoes occur in association with cold fronts characterized by intense thunderstorm activity. The most aggressive fronts that provide maximum lift and instability occur when the contrast in converging air masses is the most pronounced, typically during the spring. Consequently, most tornadoes occur in spring when mTg or mTa and cPc air masses collide in the mid-latitudes. Approximately 75% of tornadoes **travel from southwest to northeast along the frontal boundary** (Figure 6.68).

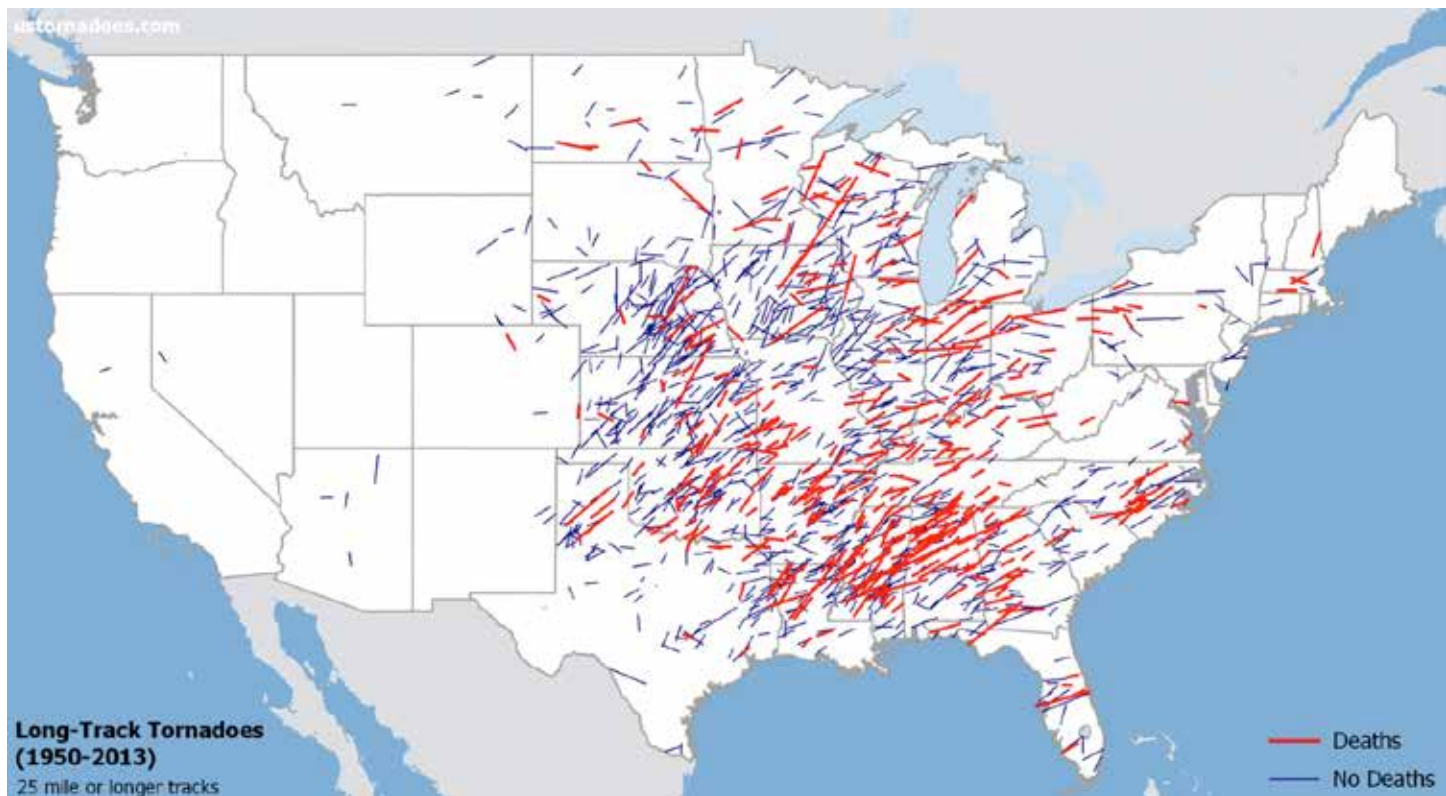


Figure 6.68. Most tornadoes in the United States travel from southwest to northeast, rolling along a cold front boundary. The map only indicates tornadoes with a track length of 25 miles or greater. Tornadoes with shorter tracks have similar paths, but are difficult to resolve on a U.S. map. Note that some tracks are oriented in virtually every direction, and that tornadoes are rare west of the Rocky Mountains (Source/Credit: Ian Livingston/SPC Data).

The United States has an average of about 700 tornadoes per year, which gives it the dubious distinction of having the greatest number of tornadoes of any country on Earth. More than 1100 have occurred in some years. The reason for the high frequency of tornadoes in the United States is due to its mid-latitude location, proximity to warm, moist air masses,

orientation of the western mountains, proximity to southwest deserts and frequent, strong polar and subtropical jet stream divergence aloft. Most of the mountain ranges in America, such as the Appalachians and the Rockies, are aligned approximately north-south, rather than east-west. This alignment allows very cold polar air to penetrate far southward and collide with warm, moist tropical air masses that are moving northward.

The unimpeded track of polar air southward is provided by the north-south trend of the Rocky Mountains and the Appalachians (Figure 6.69). In most other areas of the world, there are major mountain ranges that run east-west, such as the Himalayas and Alps, that deter cold polar air from meeting tropical air. The mountains are high enough that they serve as a barrier to air mass movement and thereby prevent the collision of radically different air masses.

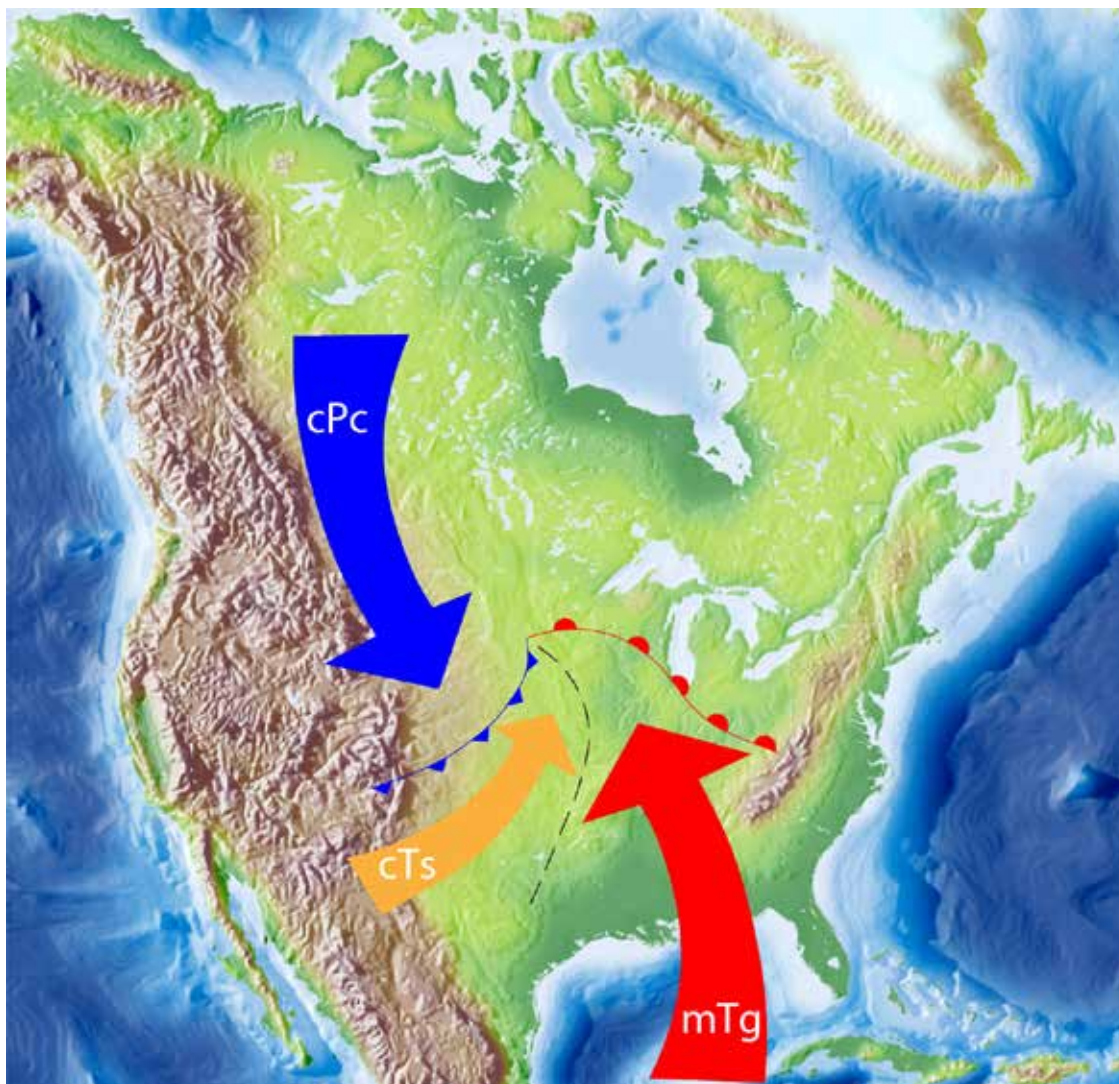


Figure 6.69. The north-south orientation of the Appalachian Mountains in the eastern United States and the Rockies in the west allow mTg air masses from the Gulf of Mexico and cPc air masses from Canada to meet in the heartland of the country. As the warm, moist air is uplifted along cold front boundaries, severe and supercell thunderstorms may develop which can give rise to tornadoes. Severe thunderstorm development is also promoted by the collision of cTs and mTg air masses (Source/Credit: Dennis I. Netoff, modified from several sources).

The rapid uplift of warm, moist maritime tropical air is necessary for tornadoes to develop because condensation releases heat energy that warms the air and decreases the air pressure in the cloud. This uplift is further promoted and accelerated by the presence of strong divergence aloft (often jet stream) as well as the superposition of dry, desert air in the middle troposphere coming from the southwestern deserts (Figure 6.70).

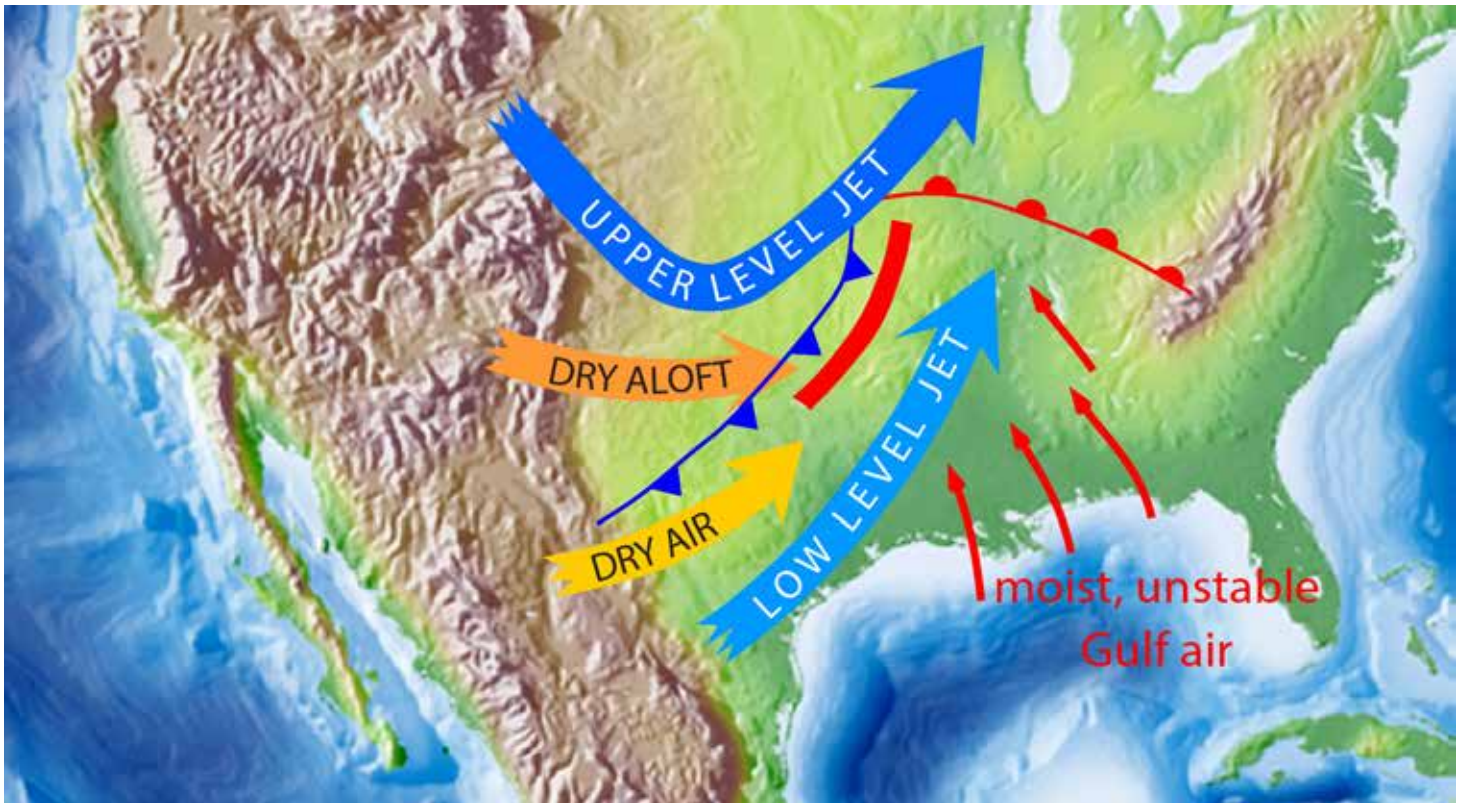


Figure 6.70. Conditions favoring severe thunderstorms and tornadoes in the Great Plains. The curved red bar represents the area of greatest tornado probability, based on the history of tornadoes relative to these geographic factors (Source/Credit: modified from Dennis I. Netoff and Ava Fujimoto-Strait, *Weather & Climate Lab Manual*).

Most thunderstorms in the world never generate tornadoes. A critical factor that promotes tornadic thunderstorms is the development of a **mesocyclone** within severe thunderstorms. Mesocyclones are large, rotating cylinders with a nearly-vertical axis that typically extend much of the height of the cloud that houses them. Mesocyclones are thought to develop as rotating cylinders with a horizontal spin axis. This generally requires that there be a large amount of wind shear in the atmosphere.

**Wind shear** can develop in two ways. A typical setup for severe thunderstorms in the western Great Plains (Figure 6.70) indicates surface air out of the southeast, a low-level jet out of the southwest, a mid-level flow of dry air from the west, and a high-level polar jetstream out of the northwest. The clockwise veering of winds with height is called **directional wind shear**, and can initiate a large-scale cylindrical spin in the lower troposphere (Figure 6.71). A cylindrical spin can also be initiated by a dramatic increase in wind velocity with height (Figure 6.72),

called **speed shear**. The combination of directional and speed shear favors the development of mesocyclones that may become tornadic. The final stage in the development of a mesocyclone is provided by the vertical uplift of a portion of the rotating cylinder by a strong thunderstorm updraft (Figure 6.73).



Figure 6.71. The clockwise veering of winds with height is called *directional wind shear*, and can initiate a large-scale cylindrical spin in the lower troposphere. In the western Great Plains directional wind shear is typically provided by a flow of surface air out of the southeast, a low-level jet out of the southwest, a mid-level flow of dry air from the west, and a high-level polar jetstream out of the northwest (Source/Credit: NOAA).

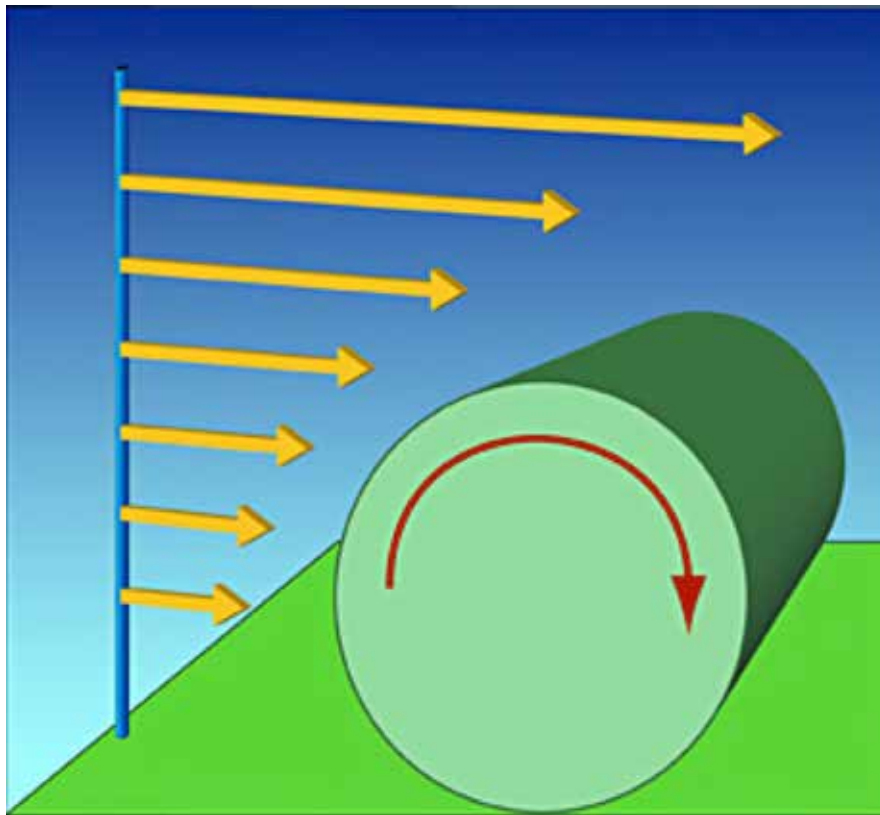


Figure 6.72. A cylindrical spin can be initiated by a dramatic increase in wind velocity with height, called speed shear. Some speed shear is nearly always present in the lower troposphere because of the loss of frictional resistance of airflow with height. The combination of directional and speed shear favors the development of mesocyclones that may become tornadic (Source/Credit: NOAA).

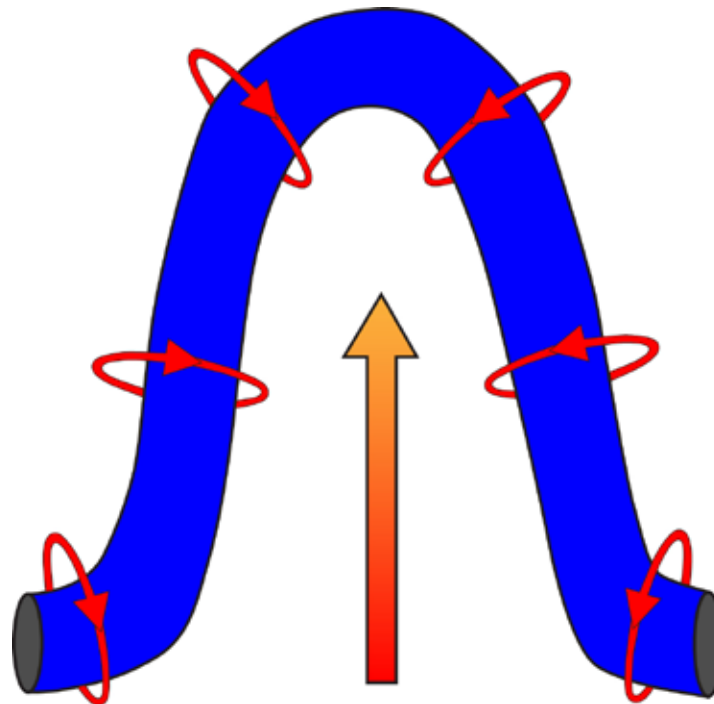


Figure 6.73. As a horizontally-rotating cylinder gets picked up by a strong updraft in a severe thunderstorm, both cyclonic and anticyclonic vortices are created side-by-side (Source/Credit: NOAA).

The transformation from a mesocyclone to a tornado involves a reduction in the diameter of the rotating, vertical cylinder, perhaps by a rapid pressure drop. This transformation can sometimes be visible at the base of a cumulonimbus cloud as the rotating wall cloud develops into a funnel cloud and then into a mature tornado (Figure 6.74). Initially, a condensation funnel develops which is relatively free of surface debris and therefore is light gray in color. As the funnel lowers to the ground, more and more debris is picked up and the funnel takes on a darker appearance, typically dark brown or reddish-brown (depending on the soil for the area) (Figures 6.75a and 6.75b).



Figure 6.74. The lower part of a mesocyclone is indicated by the rotating wall cloud (yellow arrows) at the base of this cumulonimbus cloud. The cloud later produced a category F5 tornado that struck Elie, Manitoba on June 22, 2007. A distinct, light-gray condensation funnel has developed, and two or three others appear to be developing to the right of the funnel (Source/ Credit: Justin 1569 at en.wikipedia).





*Figure 6.75a. When a funnel cloud extends to the ground, it becomes a tornado. The blue-gray color of the upper portion of the vortex contains mostly condensed water (the condensation vortex), and very little debris. Close to the ground, the vortex becomes light brown, and consists of both condensed water and high proportions of rotating debris. This EF5 tornado struck Elie, Manitoba on Friday, June 22, 2007. This funnel is easy to see because of the general lack of rain; many others are obscured by heavy rainfall (Source/Credit: Justin 1569 at en.wikipedia).*



Figure 6.75b. The tornado near Anadarko, Oklahoma has a tube-like condensation funnel that is generating a translucent dust cloud where it impacts the surface. Note that the tornadic winds are much wider than the funnel (Source/Credit: Public domain. <http://www.nssl.noaa.gov/headlines/dszpics.html>).

The rotation of the mesocyclone can be detected with a special type of radar system known as a **Doppler radar** (Figures 6.76a, 6.76b and 6.76c). In a Doppler radar image, the mesocyclone appears as a color coded, comma-shaped form called a **hook echo**. The ability to identify hook echoes allows for the early detection of tornadoes (or possible tornadoes) before they become visible to observers on the ground.



Figure 6.76.a. The radar tower of a modern WSR-88D Doppler radar system. Doppler radars emit radio waves that reflect off of raindrops in a cloud. If the raindrop is moving toward the radar, the wavelength of the radio wave is shifted toward the blue end of the spectrum. In contrast, if the raindrops are moving away from the radar, the radio wavelengths are shifted toward the red end of the spectrum. When a mesocyclone and tornado develop, the spiral flow of air into the system causes some of the raindrops to move toward the radar, while others move away. It is through the detection of the shift in wavelength associated with these motions that a Doppler radar can locate mesocyclones and tornadoes even if they are invisible to observers on the ground. This makes Doppler radar one of the most important technologies used by meteorologists to save lives by providing advance warning of tornadoes (Source/Credit: NOAA).

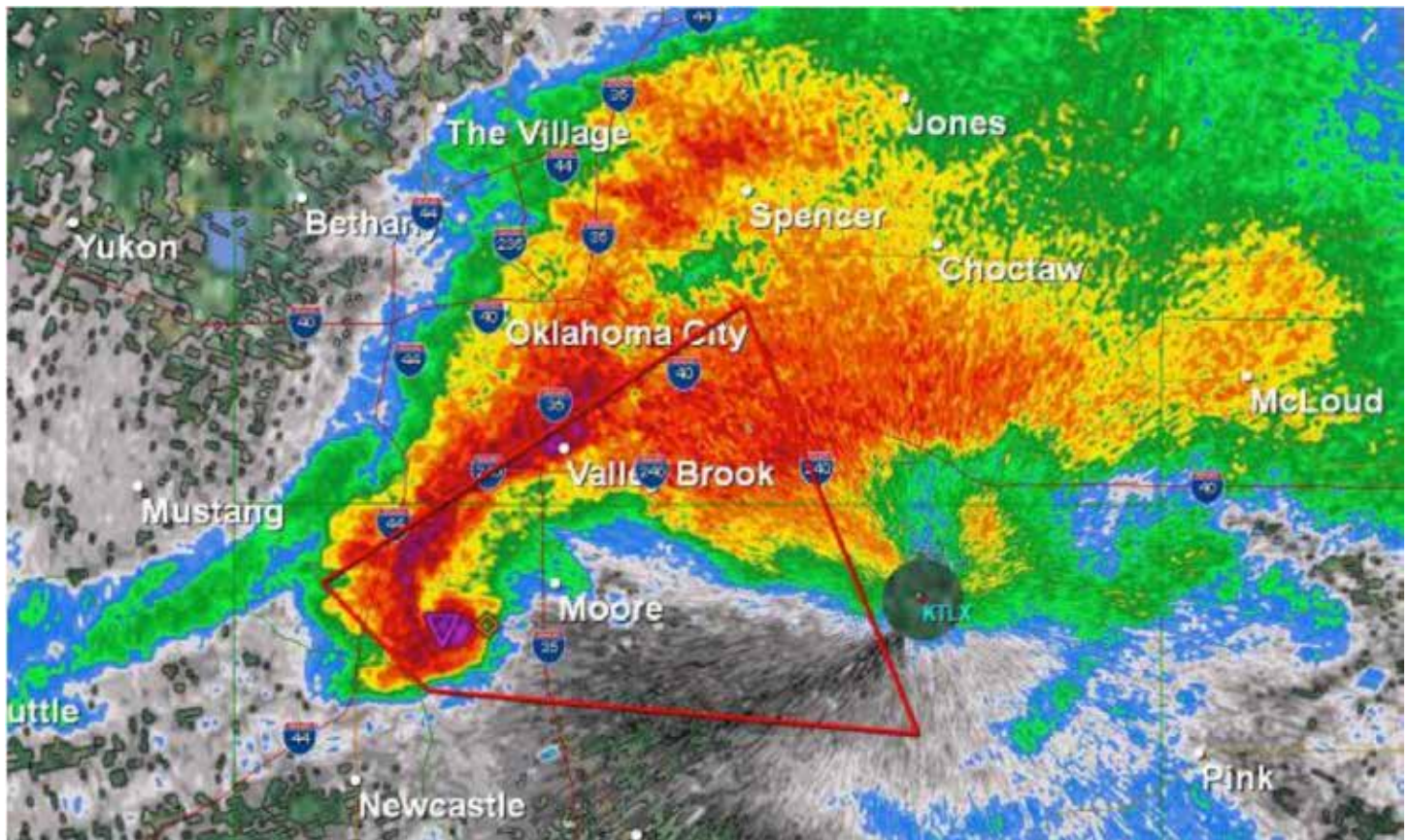


Figure 6.76b. The Doppler radar image of the EF5 tornado that hit Moore, Oklahoma on May 20, 2013 displays the tell-tale hook echo that indicates a probable tornadic vortex. The hook echo is the comma-shaped pattern and indicates that there is a counterclockwise rotation in the storm. The unusual Moore tornado was exceptionally large, with a diameter of over 1.3 miles (2 km) that is clearly visible just to the west-southwest of the city of Moore (Source/Credit: NOAA).

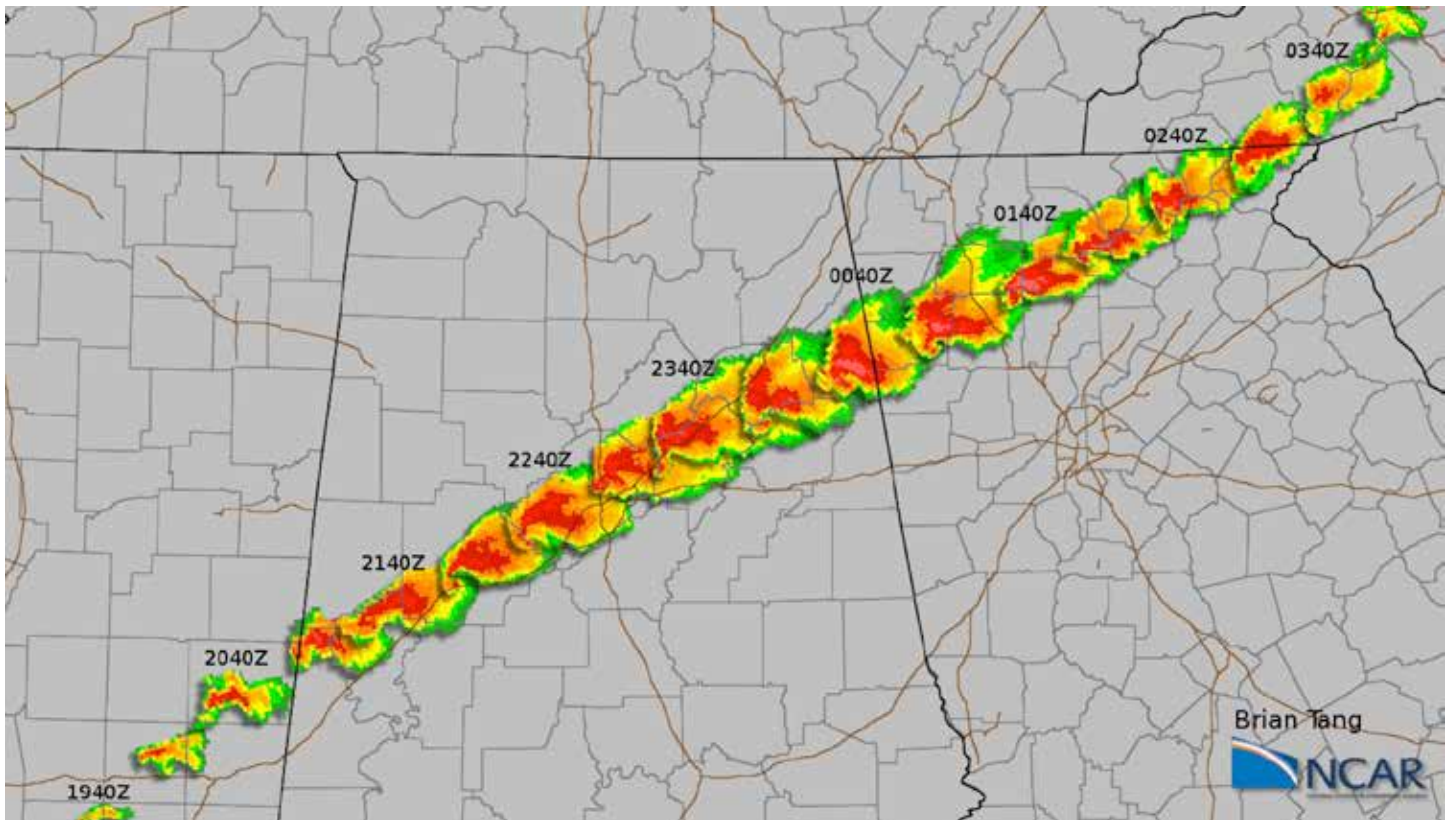


Figure 6.76c. Composite radar imagery of a long-track tornadic supercell on April 27, 2011. What appears to be a single supercell is actually two, with the second developing at the expense of the first. Five tornadoes were produced by the two supercells. A close examination of the radar images shows several well-developed hook echoes (Source/Credit: Brian Tang/NCAR).

Tornadoes are the most intense storms on Earth. Although direct measurements of tornadic winds are extremely difficult to make, Doppler radar estimated near-surface winds near Oklahoma City on May 3, 1999 at about 318 mph (512 km/h), the current world record. The former record was a tornado near Red Rock, Oklahoma on April 26, 1991 at 286 mph (460 km/h), also estimated by Doppler radar. There are only a couple reliable direct measurements of the pressure drop inside a tornado. On April 27, 2007, *in situ* measurements of pressure and wind velocity were made in an EF2 tornado in the Texas panhandle town of Trulia. Winds were clocked at 113 mph (182 km/h) and the pressure drop was 194 mb, the largest measured pressure fall ever recorded within a tornado. More powerful tornadoes (EF4 or EF5) would most likely have much greater pressure drops and higher wind velocities.

Tornadoes are difficult to obtain direct ground-based measurements, not only because because of the strong winds and immense pressure drops, but because of their small size and brief duration on the ground. Tornadoes average only a few hundred yards in diameter, stay on the ground continuously for just a few miles, and only remain in contact with the ground for a few minutes (Figures 6.77a and 6.77b). Many exceptions have occurred. A list of some of the widest tornados in the United States includes the El Reno, Oklahoma tornado of May 31, 2013 (2.6 mi./4.2 km), the F4 Mulhall Oklahoma tornado in 1999, with a damage swath of nearly 4 mi. (6.4 km), the F4 Hallam, Nebraska tornado of May 22, 2004 ( 2.5 mi./4.0 km) and in Edmonson, Texas on May 31, 1968, with a damage-path width of 2 to 3 miles (3.2 to 4.8 km).

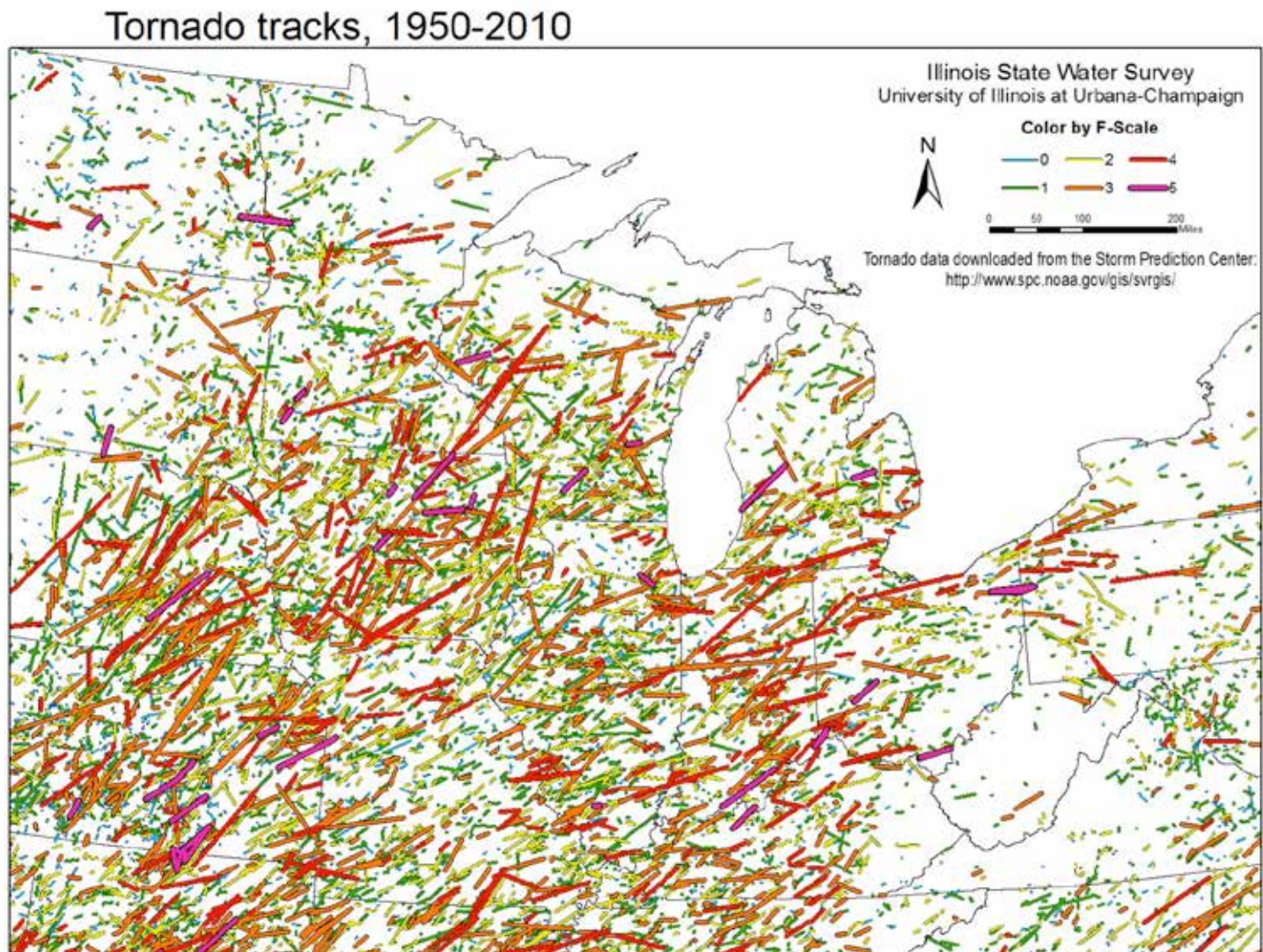


Figure 6.77a. Tracks of tornadoes from 1950-2010 for much of the central-northern part of the United States. Different colors are used for F-scales 0-5. The preferred direction is clearly southwest to northeast, although there are many exceptions. Most of the tracks are short (Source/Credit: Illinois State Water Survey).

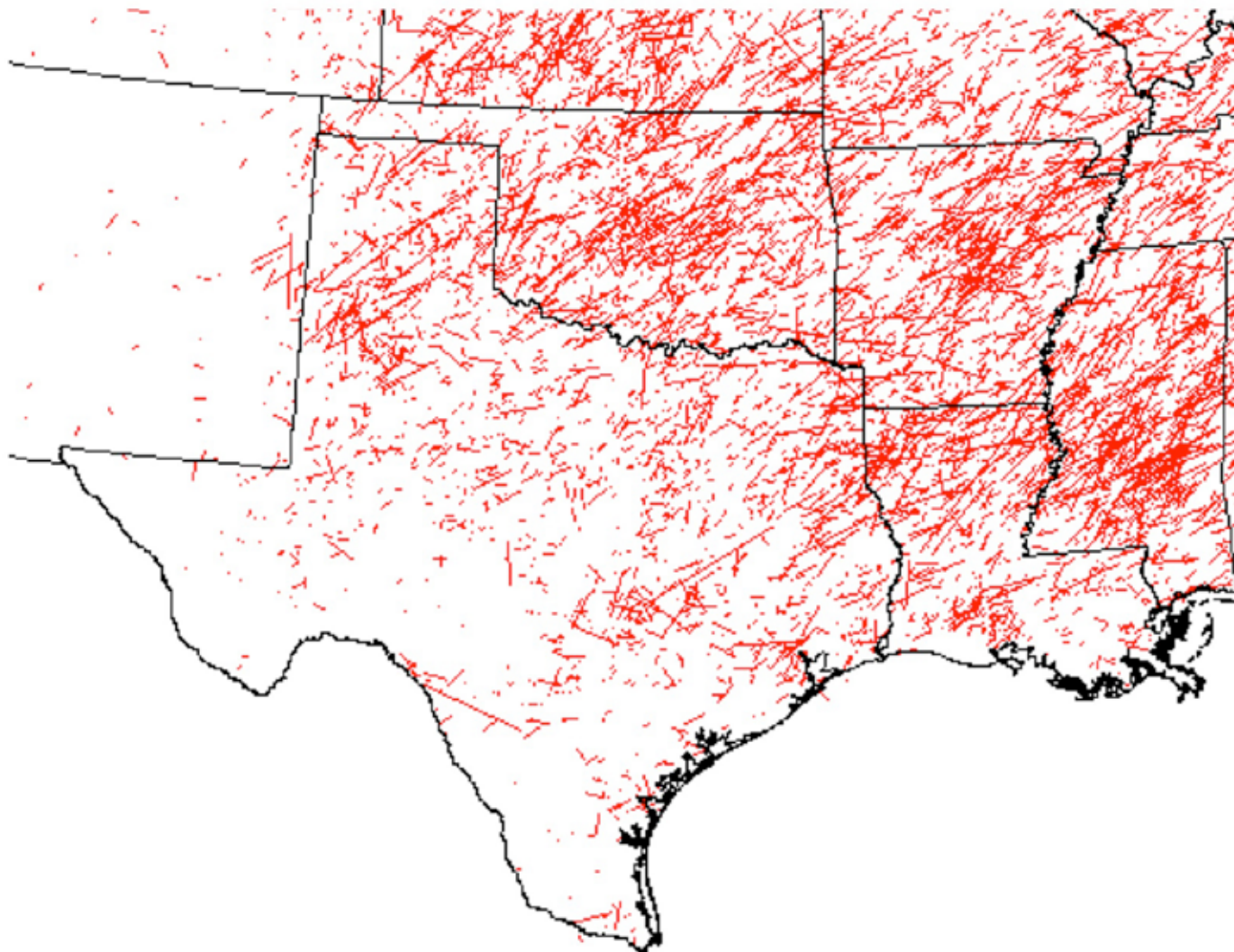


Figure 6.77b. The tornado tracks in the south-central section of the United States from 1950-2011 also show a preferred direction from southwest to northeast, and most of the tracks are short. In south and west Texas, the pattern is more erratic, and only a few long tracks have been reported (Source/Credit: NOAA).

Records for the longest continuous tornado tracks are difficult to verify, in part due to technology that existed during earlier times, and the fact that some supercells can spawn multiple tornadoes, the tracks of which are sometimes hard to distinguish. A tornado or tornado family with a track of some 293 miles (472 km) on May 26, 1917 cut a swath from Missouri, across Illinois and into Indiana. A tornado in the tri-state area of Missouri, Illinois and Indiana on May 18, 1925 had a continuous ground track of 219 miles (352 km) and is thought to have been in direct contact with the ground for 3.5 hours, with a record forward motion of 73 mph/117 km/h (Figures 6.78 and 6.79).

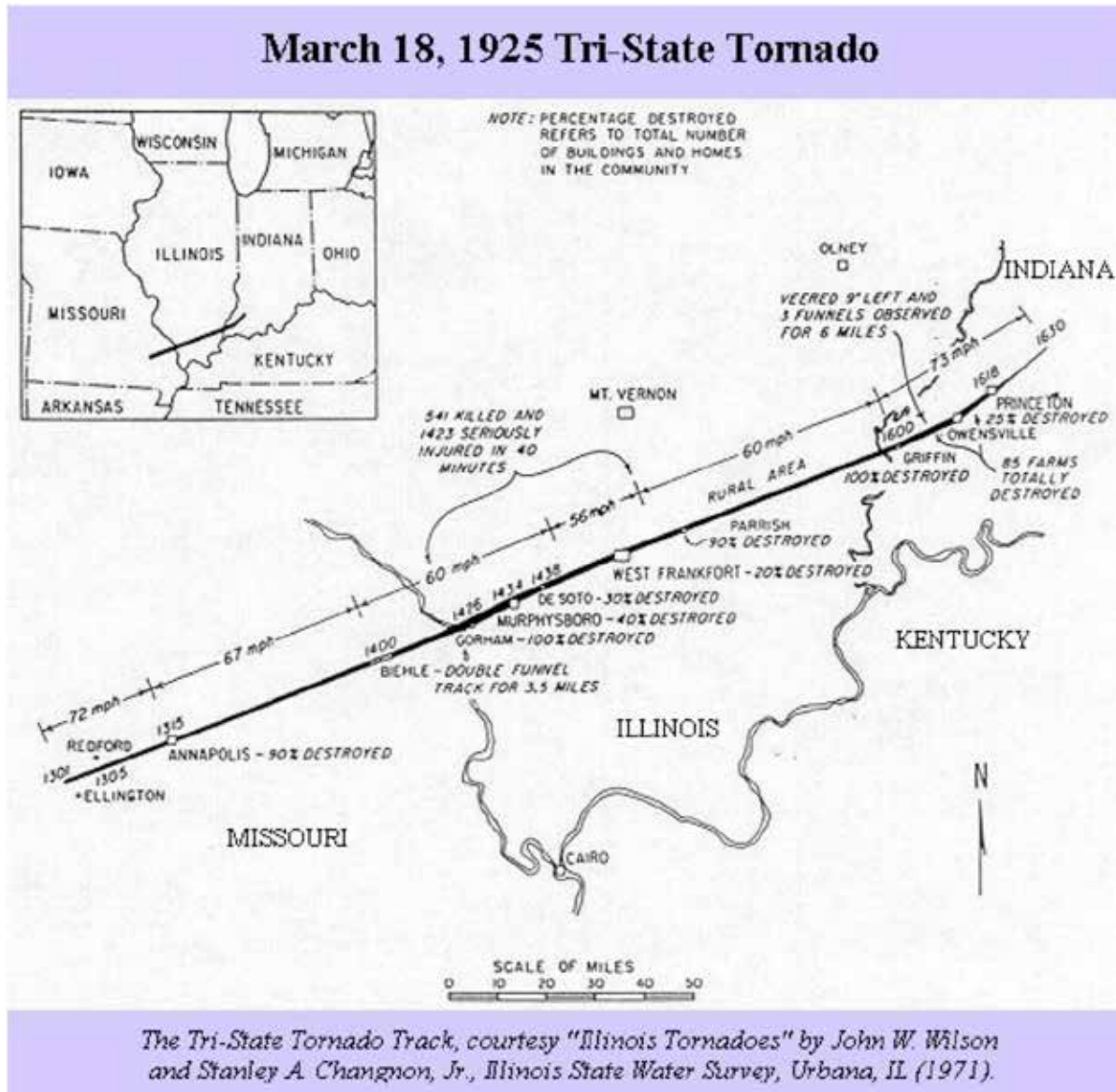


Figure 6.78. The tri-state tornado of March 18, 1925 still ranks as the deadliest single tornado in U.S. history. It began in Missouri and ended in southern Indiana 3.5 hours later, leaving a path over 200 miles long and killing 695 people. There is speculation today, as a result of an exhaustive study and report issued in 2013, that the reported single tornado could have actually been a family of closely-spaced tornadoes. Hail 4.5 inches (11 cm) in diameter fell in some places. The estimated damage (in 2014 dollars) was nearly \$2 billion. The tracks of several lesser tornadoes are given (Source/Credit: Public domain; [http://en.wikipedia.org/wiki/Tri-State\\_Tornado#mediaviewer/File:Tri-State\\_Tornado\\_cyclone\\_track\\_map\\_key.jpg](http://en.wikipedia.org/wiki/Tri-State_Tornado#mediaviewer/File:Tri-State_Tornado_cyclone_track_map_key.jpg)).





Figure 6.79. As the tri-state tornado entered Indiana from southern Illinois, it leveled essentially 100% of the small town of Griffin, killing 26 people. At that point, the entire storm was traveling northeastward at an amazing 73 mph (118 km/h). Three separate funnels were seen on the ground. Just outside Griffin, 85 farms were destroyed (Source/Credit: <http://commons.wikimedia.org/wiki/File:1925tornado-p2o-b.jpg>).

Another devastating super outbreak of tornadoes occurred on April 3-4, 1974, producing a then-record 148 tornadoes in just 24 hours (that record has now been superseded by the April 25-28, 2011 outbreak, which produced 355 tornadoes; 211 of them occurred within 24 hours). The paths of the tornadoes were mapped by Ted Fujita of the University of Chicago, who developed the Fujita tornado intensity scale. Although the paths vary considerably in length, there is a remarkable similarity in their southwest to northeast direction of travel (Figure 6.80). Xenia, Ohio, where half the city was leveled, was perhaps the hardest hit city during the course of the tornado outbreak (Figures 6.81a and 6.81b).

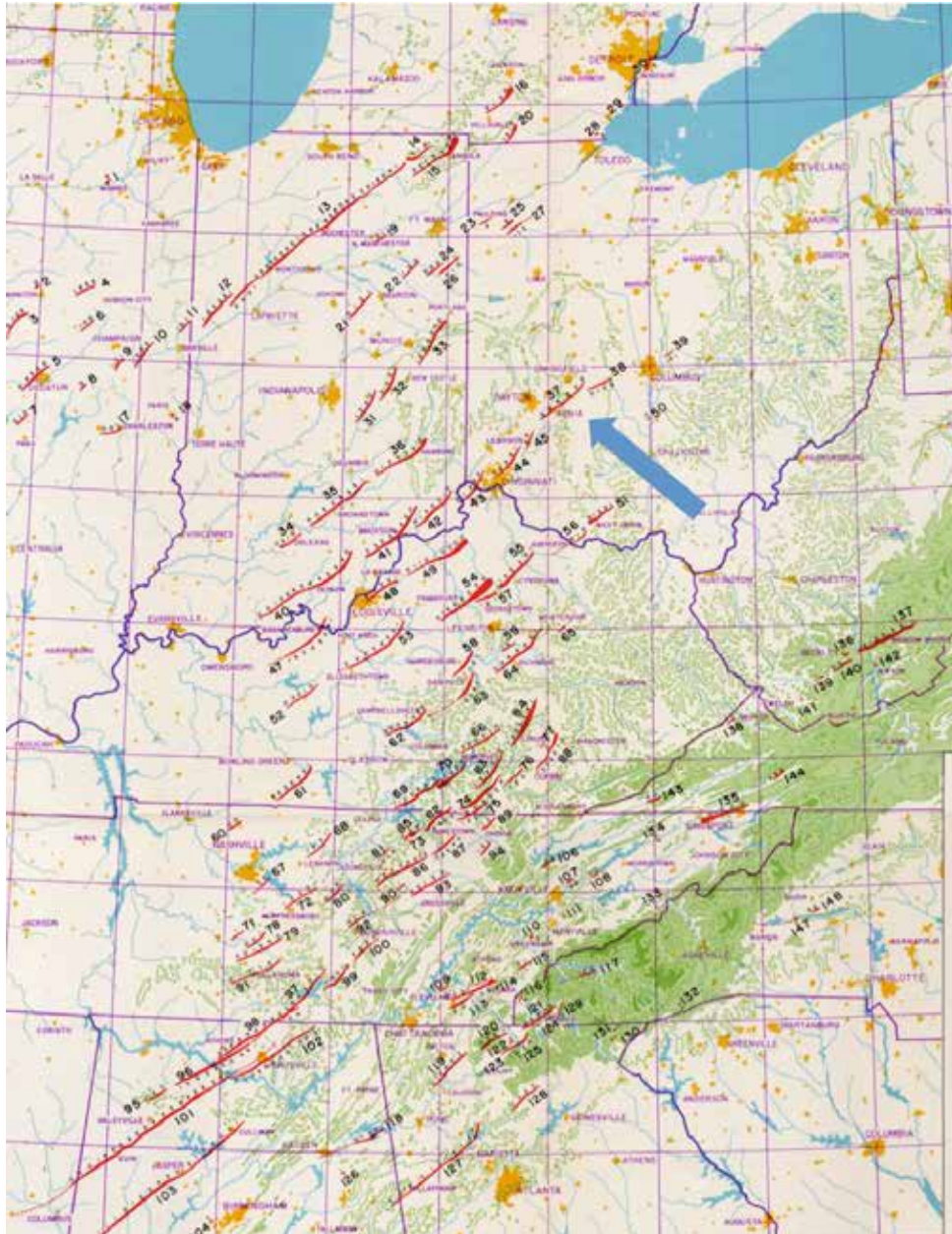


Figure 6.80. Detailed map of the Super Outbreak of tornadoes on April 3-4, 1974 that produced a record 148 tornadoes in just 24 hours. The tornado paths and intensity analysis (very small numbers given along red tracks) then-record were hand drawn by Dr. T. Theodore Fujita of the University of Chicago. Although the paths vary considerably in length, there is a remarkable similarity in their southwest to northeast direction (Source/Credit: the National Weather Service, Courtesy of Ted Fujita).



*Figure 6.81a. Xenia, Ohio was one of several hard-hit towns that experienced F5 tornadoes during the 1974 Super Outbreak. Railroad cars were lifted and turned over as the tornado passed over a freight train near the town's center. The debris vortex was wide, intense, and particularly destructive (Source/Credit: NOAA).*



Figure 6.81b. The Xenia High School, a well-built brick structure with steel reinforcement, was demolished by the direct hit of the tornadic vortex. A school bus was lifted, moved, and dropped onto the stage that students had been practicing on just a few minutes previously (Source/Credit: <http://www.erh.noaa.gov/iln/Xenia1974/08pics.php>).

Some tornadoes consist of a single, main vortex surrounded by multiple, smaller suction vortices that move counterclockwise around the main funnel (Figures 6.82a and 6.82b). These vortices are created when air within the center of the tornado sinks and flows outward along the ground away from the funnel. As this air encounters air rushing into the funnel, the wind shear causes rotating vortices to develop. These add to the destructive potential of the tornado and can account for the patterns of random destruction that are often caused by tornadoes.

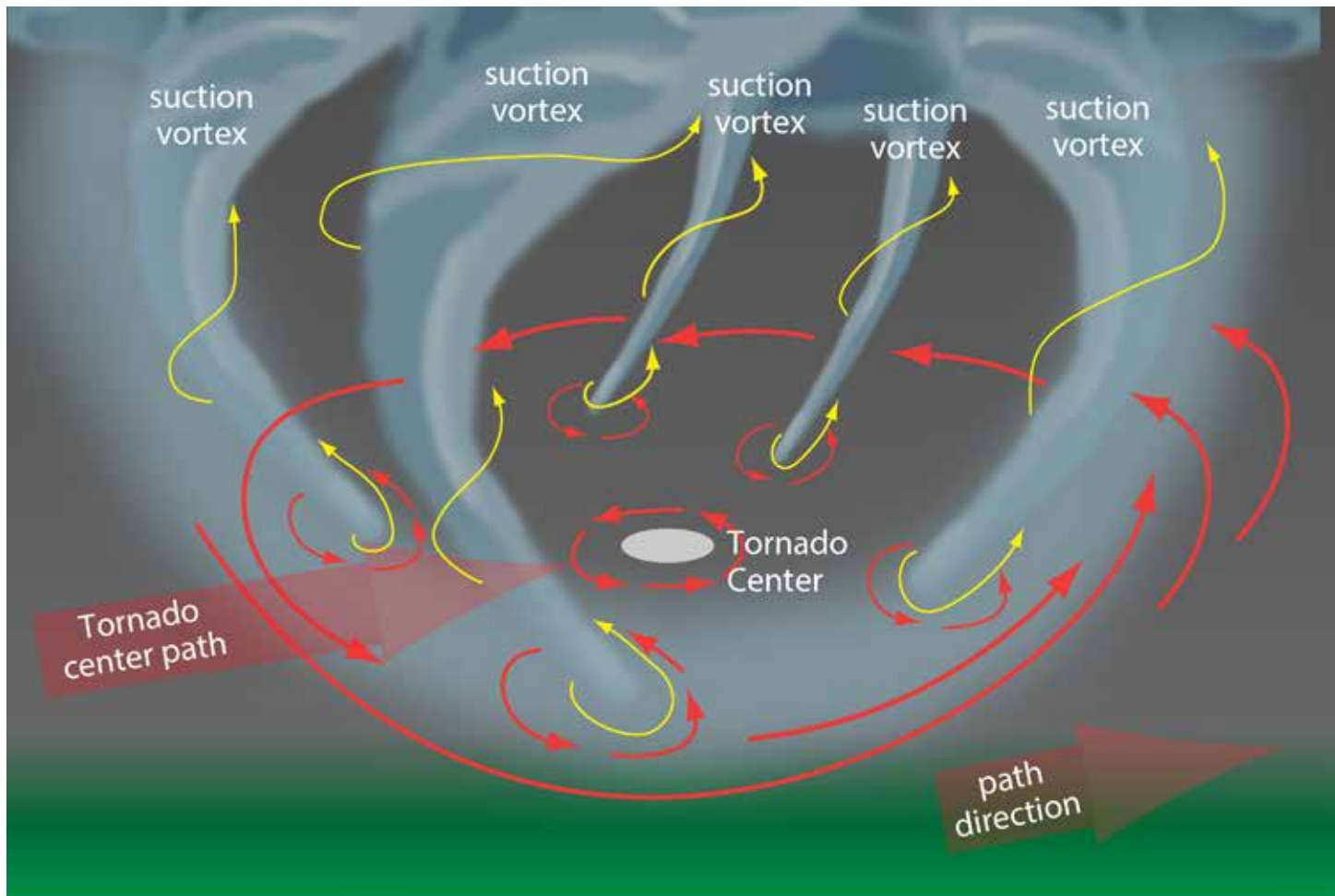


Figure 6.82a. Some strong tornadoes are made of multiple suction vortices. Each vortex is typically 30-100 ft (10-30 m) in diameter. Certain quadrants of each suction vortex can add to the maximum wind speed of the main tornado (Source/Credit: Dennis I. Netoff).



Figure 6.82b. The rotation of a tornado's funnel often produces a spiral-like pattern of disturbed ground along its path. If the tornado had multiple suction vortices, additional patterns of disturbed ground may be discernible along the path of the main funnel (Source/Credit: NOAA).

The damage caused by tornadoes is due to their high winds, and to a much lesser degree to the drop in pressure that occurs as the funnel passes over. The idea that pressure changes cause houses to explode gave rise to the myth that opening windows in a house could prevent the house from 'exploding' by allowing the air pressure inside the house to equalize with that outside. If a tornado vortex passes close to a house or other structure, winds in excess of 300 mph are possible. At 300 miles per hour, every square inch of a surface exposed to the wind experiences a force of 800 pounds per square inch. So, **it is primarily the wind, not the change in pressure, which causes damage.**

Dr. Theodore Fujita of the University of Chicago developed the **Fujita Intensity Scale** in an attempt to measure the local damage done after passage of a tornado. The scale is based on a post-tornado survey of damage sustained by a range of structures, each with a different vulnerability to wind damage. The original scale was from F0 (minimal damage) to F6 (inconceivable damage). Each category was assigned a range of wind velocities that were thought to be responsible for the damage. The scale has been thoroughly revised

and replaced by the **Enhanced Fujita Scale** (Figure 6.83), which is based on more objective criteria and more categories than the original scale. An excellent illustration and description of damage done in each ranking on the EF scale was published following the April 27, 2011 tornadoes near Huntsville, Alabama (Figure 6.84). The National Weather Service has published several abbreviated as well as very detailed descriptions with photographs to help surveyors determine what EF-scale numbers to assign along tornado tracks (Figures 6.85a to 6.85s).

Fujita Scale (Developed in 1971, used through January 2007)			Enhanced Fujita Scale (Implemented February 2007)		
Rating	Winds	Expected Damage	Rating	Winds	Expected Damage
<b>F0</b>	< 73 mph	Light damage. Damage to chimneys and billboards; branches broken off trees; shallow-rooted trees pushed over.	<b>EF0</b>	65-85 mph	Minor damage. Shingles or parts of roof peeled off; damage to gutters/siding; branches broken off; shallow-rooted trees toppled.
<b>F1</b>	73-112 mph	Moderate damage. Surface peeled off roofs; mobile homes pushed off foundations or overturned; moving autos blown off roads.	<b>EF1</b>	86-110 mph	Moderate damage. More significant roof damage; windows broken; exterior doors damaged or lost; mobile homes badly damaged or overturned.
<b>F2</b>	113-157 mph	Considerable damage. Roofs torn off frame houses; mobile homes demolished; boxcars overturned; large trees snapped or uprooted; light-object missiles generated; cars lifted off ground.	<b>EF2</b>	111-135 mph	Considerable damage. Roofs torn off well-constructed homes; homes shifted off their foundation; mobile homes completely destroyed; large trees snapped or uprooted; cars may be tossed.
<b>F3</b>	158-206 mph	Severe damage. Roofs and some walls torn off well-constructed houses; trains overturned; most trees in forest uprooted; heavy cars lifted off ground and thrown.	<b>EF3</b>	136-165 mph	Severe damage. Entire stories of well-constructed homes destroyed; significant damage to large buildings; homes with weak foundations may be blown away; trees begin to lose bark.
<b>F4</b>	207-260 mph	Devastating damage. Well-constructed houses leveled; structures with weak foundations blown some distance; cars thrown and large missiles generated.	<b>EF4</b>	166-200 mph	Extreme damage. Well-constructed homes leveled; cars thrown significant distances; top story exterior walls of masonry buildings likely collapse.
<b>F5</b>	261-318 mph	Incredible damage. Strong frame houses leveled and foundations swept clean of debris; automobile-sized missiles fly through the air in excess of 100 meters; trees debarked; incredible phenomena occur.	<b>EF5</b>	> 200 mph	Incredible damage. Well-constructed homes swept away; steel-reinforced concrete structures critically damaged; high-rise buildings sustain severe structural damage; trees usually completely debarked, stripped of branches, and snapped.

Figure 6.83. A comparison of estimated wind speeds associated with F0 (EF0) to F5 (EF5) on the original versus enhanced Fujita scales. The original Fujita scale was adopted in the United States in 1971 and the Enhanced Fujita Scale in 2007 (Source/Credit: NOAA).







EF Rating	Wind Speeds	Expected Damage		
<b>EF-0</b>	65-85 mph	'Minor' damage: shingles blown off or parts of a roof peeled off, damage to gutters/siding, branches broken off trees, shallow rooted trees toppled.		
<b>EF-1</b>	86-110 mph	'Moderate' damage: more significant roof damage, windows broken, exterior doors damaged or lost, mobile homes overturned or badly damaged.		
<b>EF-2</b>	111-135 mph	'Considerable' damage: roofs torn off well constructed homes, homes shifted off their foundation, mobile homes completely destroyed, large trees snapped or uprooted, cars can be tossed.		
<b>EF-3</b>	136-165 mph	'Severe' damage: entire stories of well constructed homes destroyed, significant damage done to large buildings, homes with weak foundations can be blown away, trees begin to lose their bark.		
<b>EF-4</b>	166-200 mph	'Extreme' damage: Well constructed homes are leveled, cars are thrown significant distances, top story exterior walls of masonry buildings would likely collapse.		
<b>EF-5</b>	> 200 mph	'Massive/incredible' damage: Well constructed homes are swept away, steel-reinforced concrete structures are critically damaged, high-rise buildings sustain severe structural damage, trees are usually completely debarked, stripped of branches and snapped.		

Figure 6.84. . Examples of damage from the complete range of EF-scale rankings from the April 27, 2011 tornadoes that hit the Huntsville, Alabama area (Source/Credit: <http://www.srh.noaa.gov/images/hun/stormsurveys/2011-04-27/EF-Ratings.png>).





Figure 6.85a. Trees were sheared by an EF0 tornado in Toledo, Ohio on June 5, 2010 (Source/Credit: NWS/NOAA).



*Figure 6.85b. Felled tree limbs and debris from an EF0 tornado near Melbourne, Florida on January 21, 2010 (Source/Credit: NOAA).*



Figure 6.85c. A sheared tree trunk did minor damage to a structure from an EF0 two miles west of Columbia in Adair County, Kentucky on June 9, 2010 (Source/Credit: NWS).



Figure 6.85d. Damage from an EF1 tornado in Indiana on October 18, 2007 included overturned single-wide and double-wide trailers and partially sheared trees (Source/Credit: NOAA).



Figure 6.85e. Damaged house siding and uprooted tree from an EF1 tornado in central Kansas on April 14, 2012 (Source/ Credit: NOAA).



Figure 6.85f. Roof damage from an EF2 tornado on May 7, 2012 near Tulsa, Oklahoma (Source/Credit: [http://www.srh.noaa.gov/tsa/?n=weather-event\\_2012aprfflood](http://www.srh.noaa.gov/tsa/?n=weather-event_2012aprfflood)).



Figure 6.85g. Damage of a house, barns and machinery from an EF2 tornado in Indiana on Oct 18 2007. The wood framed pole barn was completely destroyed. The red combine sits where the barn was, and the metal grain bins were demolished (Source/Credit: NOAA).



Figure 6.85h. An example of the kind of damage done by an EF3 tornado that hit St. Louis on May 31, 2013 (Source/Credit: NWS, St. Louis Missouri).





Figure 6.85i. Completely destroyed buildings due to an EF3 tornado that ravaged Wilkin, North Dakota in 2010 (Source/Credit: NOAA).



Figure 6.85j. Uprooted, sheared trees and a leveled building from the EF3-EF4 tornado that struck North Dakota and Minnesota in 2010 (Source/Credit: NOAA).



Figure 6.85k. A building completely sheared from its concrete slab from the EF3-EF4 tornado that struck North Dakota and Minnesota in 2010 (Source/Credit: NOAA).



Figure 6.85l. A low, oblique aerial view of complete destruction of the Plantation subdivision near Mayflower, Arkansas from an EF4 tornado that struck on April 27, 2014. Most of the homes were leveled and swept clean off their foundations. Later inspection revealed a lack of properly constructed walls and foundation anchor bolts (Source/Credit: NOAA).



Figure 6.85m. Tree foliage stripping and de-barking from an EF4 tornado near Louisville, Mississippi on April 27, 2014 (Source/Credit: NOAA).



Figure 6.85n. Severe damage from the EF4 Wadena Tornado that struck Wadena County, Minnesota on June 17, 2010. The tornado had a maximum width of 1.1 miles/1.8 km and a track of about 10 miles/16 km (Source/Credit: NOAA).



Figure 6.85o. More damage from the EF4 Wadena Tornado that struck Wadena County, Minnesota on June 17, 2010. There were 74 tornadoes that occurred during the tornado outbreak (Source/Credit: NOAA).



Figure 6.85p. A house that was completely destroyed by the EF4 tornado in Hattiesburg, Mississippi on February 10, 2013 (Source/Credit: NOAA).





Figure 6.85q. Complete devastation of two blocks of a suburban area in Moore, Oklahoma from an EF5 tornado on May 20, 2013 (Source/Credit: Oklahoma National Guard).



Figure 6.85r. A large, well-built home just south of Oklahoma City that sustained EF5 tornado damage during the Washington-Goldsby Tornado of May 24, 2011 (Source/Credit: NOAA).



Figure 6.85s. A chaotic pile of debris is all that remains of the Briarwood Elementary School in Moore, Oklahoma after an EF5 tornado on May 20, 2013 (Source/Credit: NOAA).

In addition to the obvious threat posed by the collapse of buildings, tornadoes also lift massive quantities of debris into the air and hurl them at tremendous speeds. Everything becomes a lethal weapon at such speeds. Even pieces of straw can impale a person. Pieces of straw have been found driven into telephone poles and glass windows (Figure 6.86).



Figure 6.86. A wooden 2 x 4 was driven into a metal trailer by tornadic winds on March 3, 2012 (Source/Credit: NOAA).

It is mainly because of the hazard posed by flying debris that people are advised to go into their basements during a tornado. Being below ground minimizes one's exposure to the debris. If no basement is available, then one should seek shelter under a stairwell or in a bathroom or closet near the center of the house and on the first floor. These areas are small and relatively strong.

People who live in the Midwest, which is an area particularly susceptible to tornadoes, sometimes construct a tornado shelter in their home (Figures 6.87a and 6.87b). Plans can be purchased for about \$5 from Texas Tech University. Research at Texas Tech has shown that relatively safe areas can be created by reinforcing a small room such as a closet with concrete and adding a metal door. Plywood can even be used if the shelter is assembled properly. The cost of retrofitting a home varies from a few thousand dollars to tens of thousands of dollars. Some companies sell prefabricated shelters that are placed below ground. The benefit of these is that you do not have to alter your existing home. The downside is that you would have to leave your house to get to the shelter, and this requires precious time that you may not have.

### Protecting life and property

Structural engineers say people stand the best chance of surviving a tornado inside a safe room with reinforced walls and no windows. Such a unit can cost \$3,000 to \$7,500. Example of a safe room:

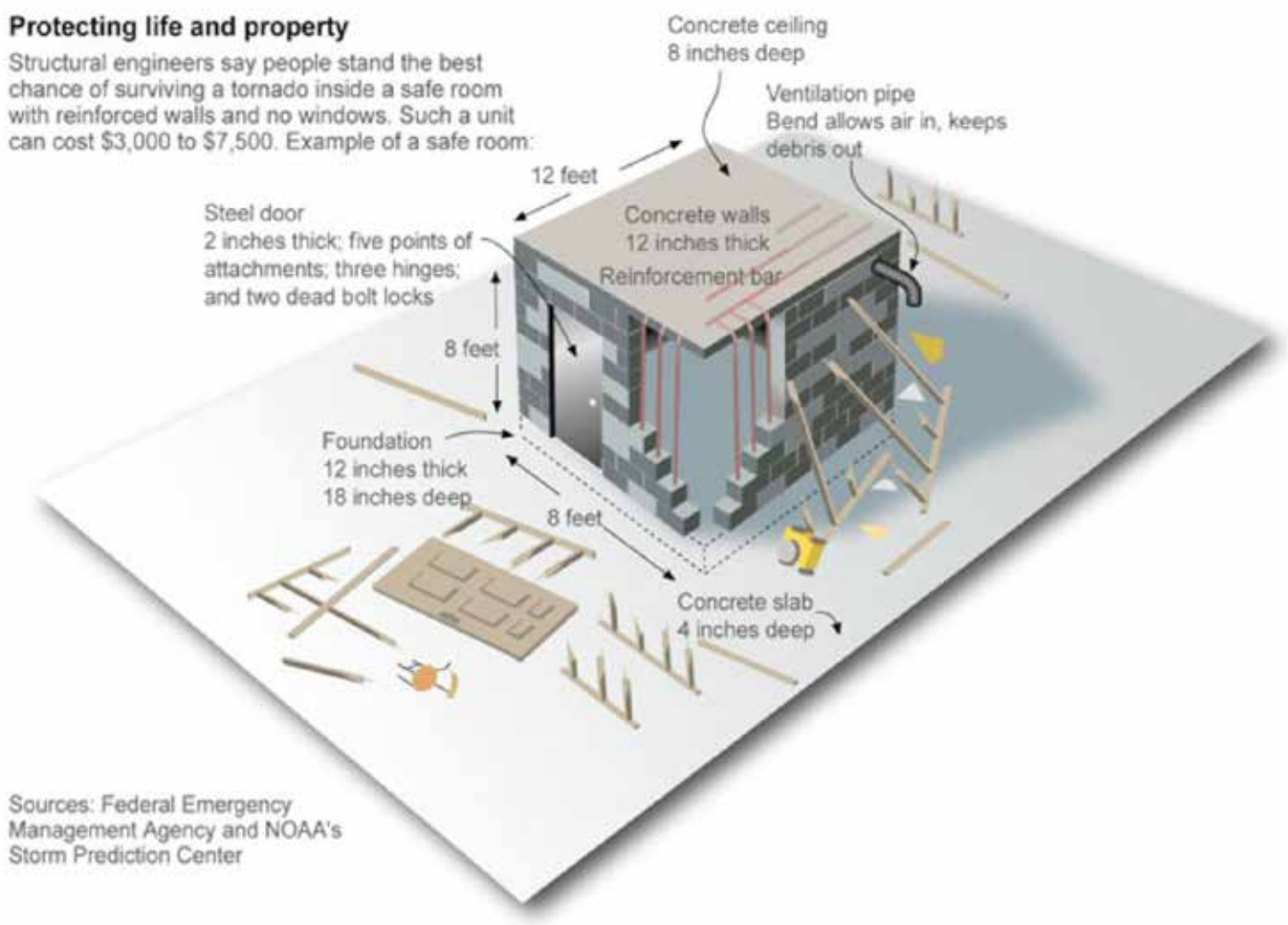


Figure 6.87a. There are several designs for storm shelters that are designed to withstand tornadic winds. Some of these can be built when the home is constructed, whereas others can be retrofitted (Source/Credit: FEMA and NOAA).



Figure 6.87b. Concrete storm shelters that are tied to the foundation slab (Source/Credit: NOAA, Department of Homeland Security, NWS, Red Cross).

The National Weather Service issues watches and warnings before a tornado strikes. A tornado **watch** means that conditions are right for a tornado to develop, although none have yet been detected. A **warning** means that a tornado either has been sighted, or rotation has been detected on Doppler radar, and people need to take cover immediately.

Unfortunately, many tornadoes strike at night when people are asleep and they do not hear the broadcast of the watch and warning. However, for a relatively small amount of money (about \$50), you can purchase a *weather alert radio*. These radios continuously monitor signals from the National Weather Service, and if a watch or warning is issued, a loud alarm goes off. You can then turn on the radio and find out what is happening in your area. Watches and warnings can be issued for any type of severe weather, including floods.

Cloud size, form and activity can also help determine whether a tornado is likely to occur. When a cumulonimbus cloud develops severe turbulence, the sort required to generate tornadoes, the bottom of the clouds typically develop protrusions. When fully developed, these protrusions give the bottom of cloud the appearance of an egg carton. This type of cloud is referred to as a **mammatus cloud**, and while they do not always indicate that a tornado will develop, they serve as a sign that they might develop. In addition, the extreme turbulence in a tornadic cloud often results in large hail. Most tornadoes are associated with hail. Other signs of tornadic potential include the development of a rotating wall cloud, an

overshooting top, more than 30 lightning strikes per minute and very strong downdrafts and surface winds (Figure 6.88).

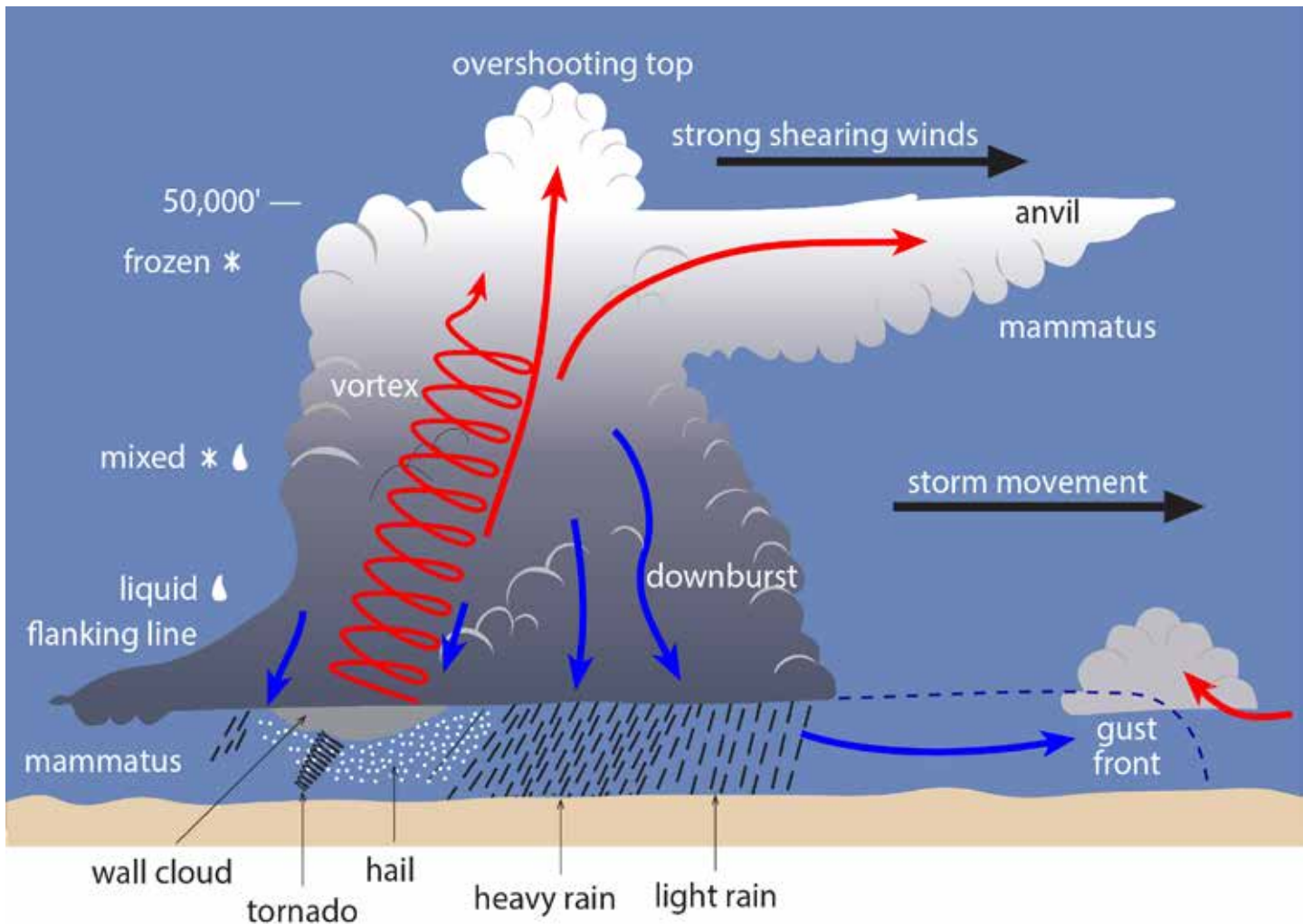


Figure 6.88. The structure and characteristics of a tornadic supercell thunderstorm. In this example, the updraft is so powerful that it has punched through the tropopause at 50,000 feet to form an overshooting, cauliflower-like top. The anvil that extends a substantial distance downwind from the main trunk of the cloud is a sign of strong upper-level winds blowing from left to right in the diagram. Strong upper-level winds aid in the development of severe thunderstorms by providing a mechanism of uplift, as well as wind shear that can tilt the cloud and keep the rain falling in the downdraft, rather than the updraft. Of particular interest is the fact that the mesocyclone is a huge column of rotating air that produces both the wall cloud and the tornado, which is only a small part of the mesocyclone. Heavy rain and hail normally precede the occurrence of a tornado, which occurs on the back side of the cloud. Ironically, once the tornado passes, the skies clear quickly, assuming the cloud that gave rise to the tornado was an isolated thunderstorm. The gust front on the leading side of the cloud causes forced uplift of air that can either continue to feed the storm, or create a new cloud ahead of it (Source/Credit: modified from Dennis I. Netoff and Ava Fujimoto-Strait, *Weather & Climate Lab Manual*).

In addition to forming along cold fronts, non-frontal tornadoes can develop during the summer, especially during late afternoon or evening, when the ground is hot and thermals generate cumulonimbus clouds. They are also produced in association with hurricanes. In fact, one of the largest outbreaks of tornadoes, more than 140 in one day, occurred in association with a hurricane. Although tornadoes can occur anytime, they are most likely to develop in the spring, when vigorous cold fronts encounter warm, moist, unstable air from the Gulf, and the Polar jet stream creates strong upper-level divergence. Even though **tornado alley** is the king of the world's tornadic activity (Figure 6.89) they can also occur in other places (Figure 6.90).

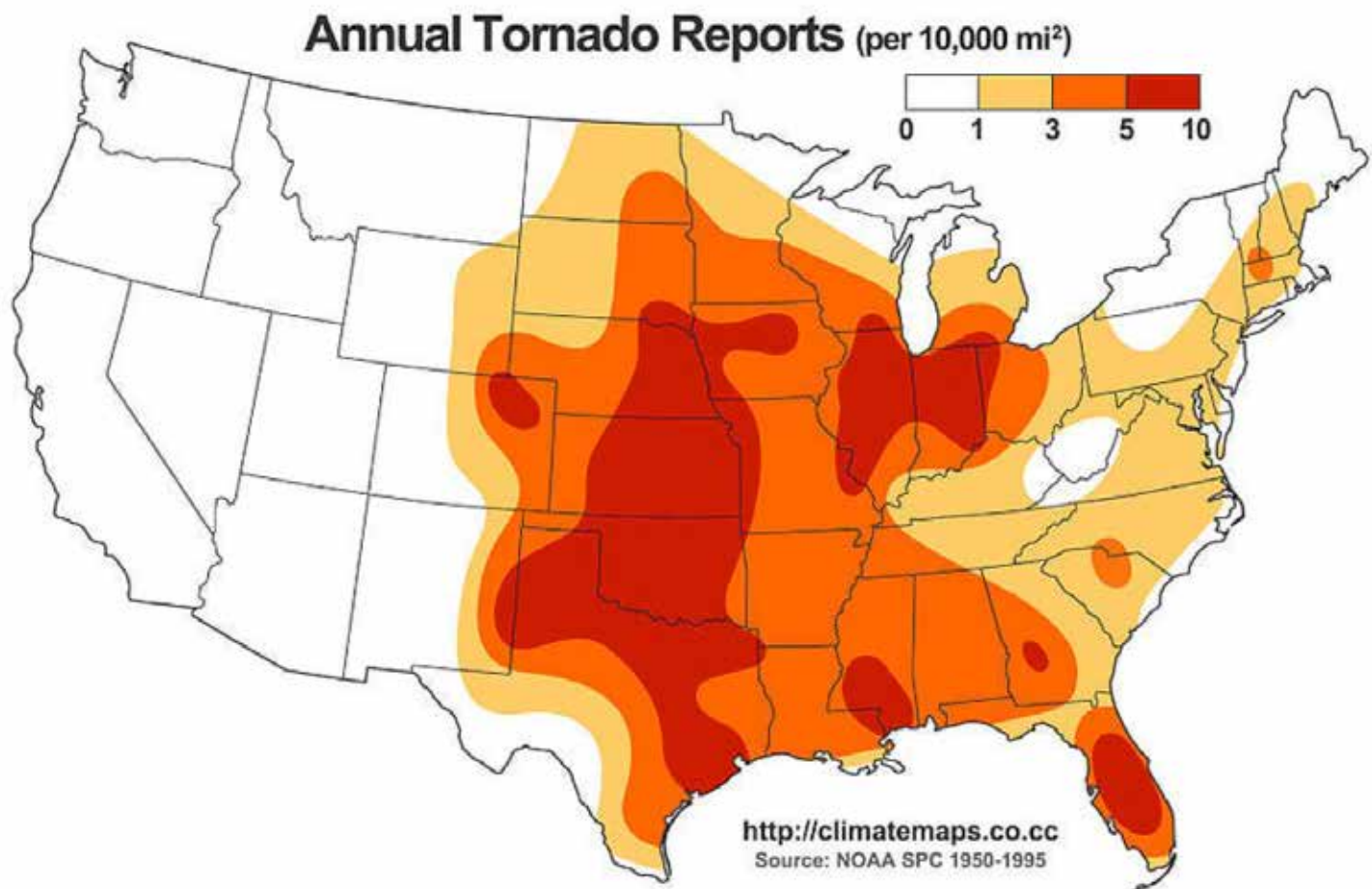


Figure 6.89. Many attempts have been made to portray tornado-prone areas on maps. This one is based on annual tornado reports per unit area of land from 1950-1995. Based on this map, tornado alley could be defined in the traditional way, from Texas to the Dakotas, or more broadly to include portions of the Midwest and the Southeast, including peninsular Florida. Even areas included in the white band on this map (0-1 reports per 10,000 mi<sup>2</sup> [square miles]) have reported some tornadoes during this and subsequent time periods (Source/Credit: NOAA/SPC).



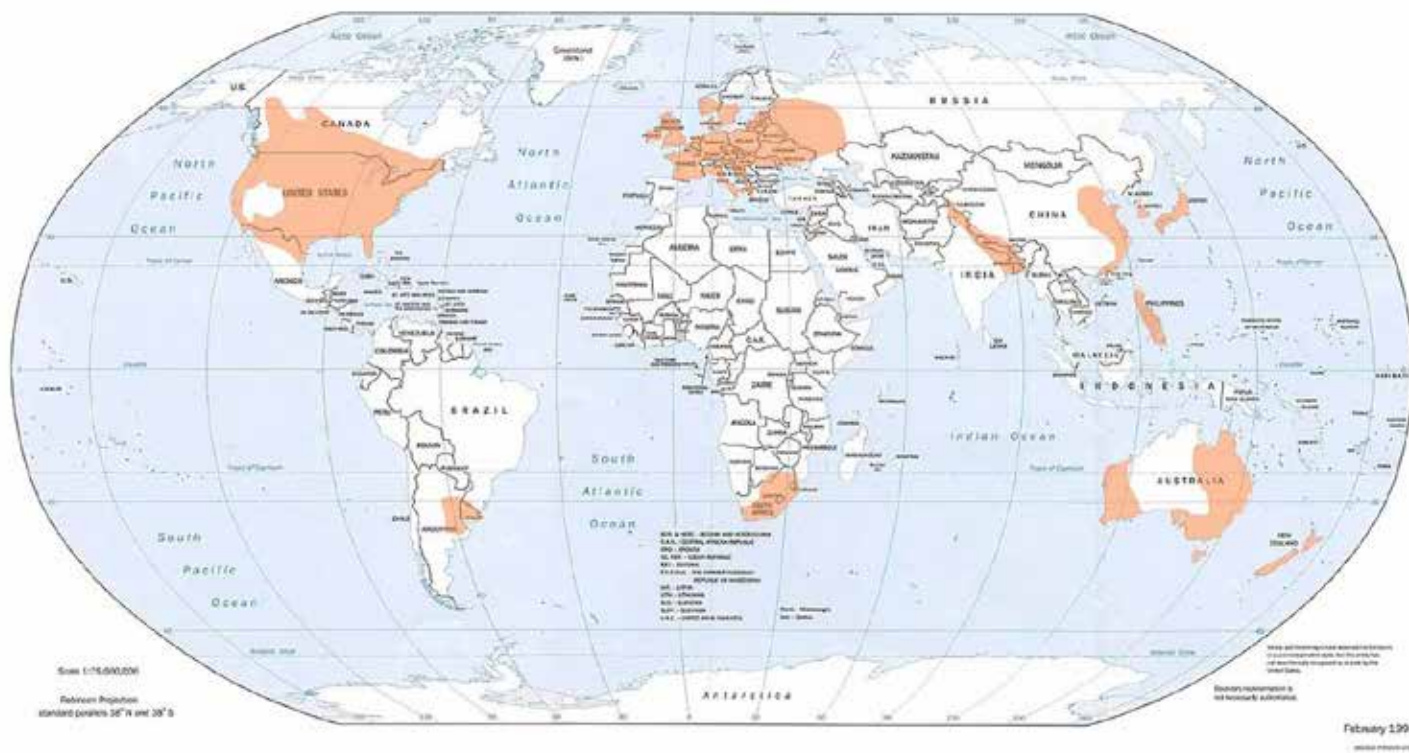


Figure 6.90. Geographic distribution of tornadoes globally through 1995. Mid-latitude North America is clearly the tornado king of the world. Note the relative absence of tornadoes in the tropical latitudes and high latitudes (Source/Credit: NOAA).

In a discussion of tornado frequency and damage, a distinction should be made between actual tornadoes produced by thunderstorms and other far-less dangerous features that are in some respects similar to tornadoes. **Dust devils** are small, local, short-lived, mostly cyclonic vortexes that pose little threat to property and lives (Figure 6.91). They typically form through local convection and wind shear on warm afternoons. Waterspouts, on the other hand, can be tornadic or fair weather (Figure 6.92a and 6.92b). **Tornadic waterspouts** occur over water in association with thunderstorms, and are therefore potentially dangerous. **Fair weather waterspouts** are typically smaller, less intense, and associated with cumulus clouds.



Figure 6.91. Dust devils are fairly common in arid regions on warm days when surface air becomes buoyant. This one moved over a cotton field near Smyer, Texas on May 31 2009. A similar one took a path right through Texas Tech's Mesonet Station on June 11, 2009 and registered a 53 mph wind gust. Although most dust devils are not considered dangerous, a few have the capacity to move large debris, and can do local damage (Source/Credit: West Texas Mesonet WTM/NWS).



*Figure 6.92a. Twin tornadic waterspouts were caught over Lake Michigan on September 12, 2013 (Source/Credit: Mike Madsen, Kenosha Police Department).*



Figure 6.92b. A fairly extensive fair weather waterspout formed over Ross Barnett Reservoir near Jackson, Mississippi on July 23, 2014 (Source/Credit: NWS, photo by Glenn Page, taken from Goshen Springs).

## Hurricanes

Hurricanes are rotating low-pressure systems, so they are also cyclonic storms, but on a much larger scale than tornadoes. In the western Pacific, they are called **typhoons**; in the Indian Ocean, **cyclones**; and in Australia, they are called **willy-willies** (Figure 6.93).

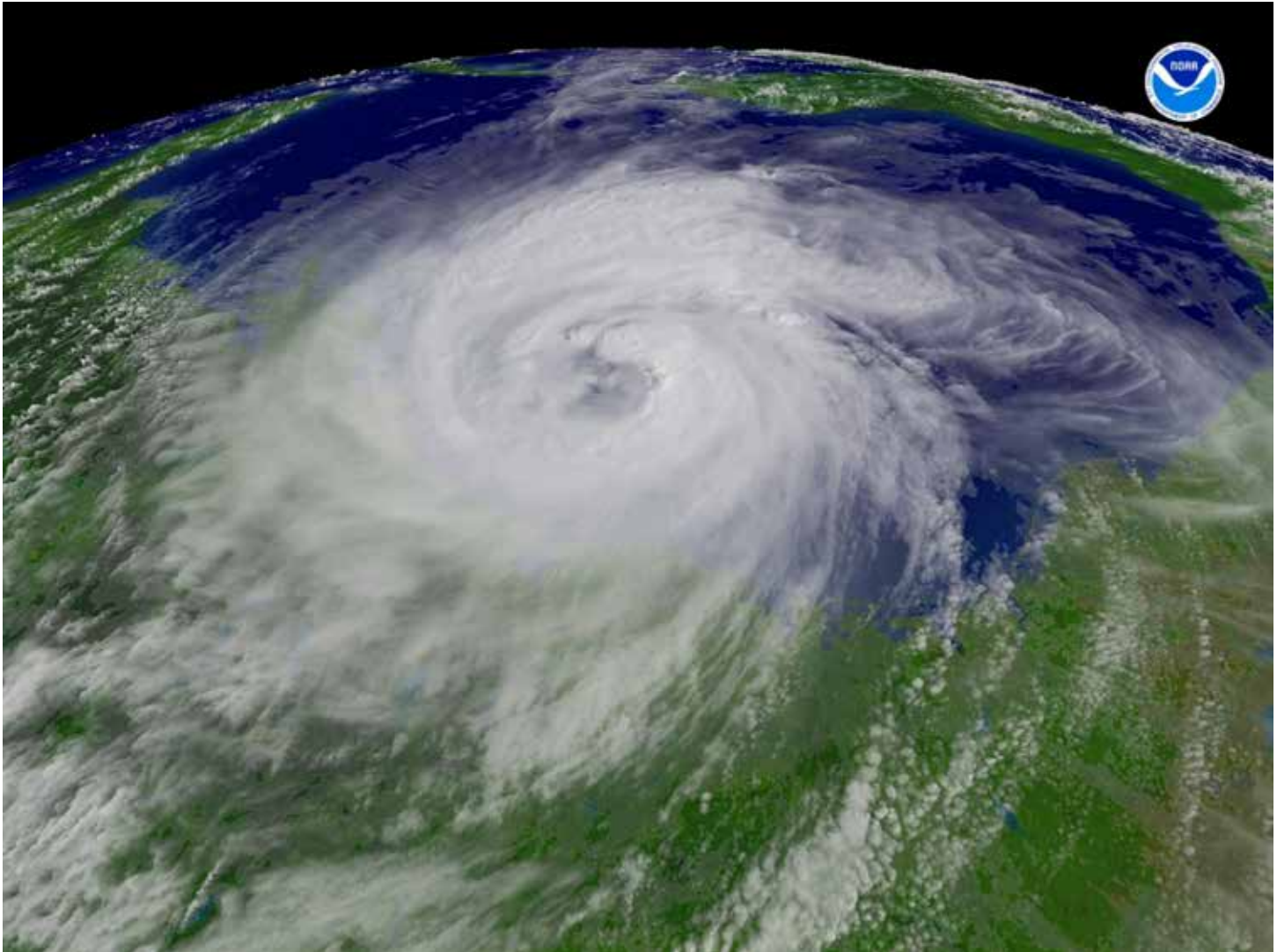


Figure 6.93. Satellite image of Hurricane Ike making landfall on the Texas coast on September 12, 2008. View is toward the southeast. Mexico's Yucatan Peninsula is near the horizon on the right. A portion of Hurricane Ike's dissipated eye went over Sam Houston State University (Source/Credit: NOAA).

## Hurricane Formation

By definition, a **hurricane is a tropical cyclone with sustained wind speeds of 74 miles per hour or greater**. They form over the warm waters of the ocean between 5° and 20° north and south of the Equator. They seldom form at lower latitudes because of the low Coriolis Force there. Like all severe storms, hurricanes derive much of their energy from the release of latent heat during the condensation of water that was initially evaporated from the surface. The huge amount of energy required to feed a hurricane can only be derived from the evaporation of warm water over vast areas of the ocean. In general, **the water temperature must be at least 80°F to generate sufficient water vapor to form hurricanes**. Hurricanes typically form in the lower mid-latitudes over warm bodies of water. They can be sustained farther poleward only if they remain over warm ocean currents.

Hurricane formation also requires the existence of a pre-existing weather disturbance, such as an **easterly wave**. An easterly wave is a weak, low-pressure cell in the tropics that appears as bent isobars on a weather map. The bend in the isobars is aligned along a north-south axis (Figure 6.94). These pressure disturbances travel from east to west in the Trade Wind Belt. Behind (east of) the wave, convergence of air and uplift occurs that helps pump moisture into the atmosphere and intensify the storm. West of the wave, air subsidence occurs, promoting clear conditions.

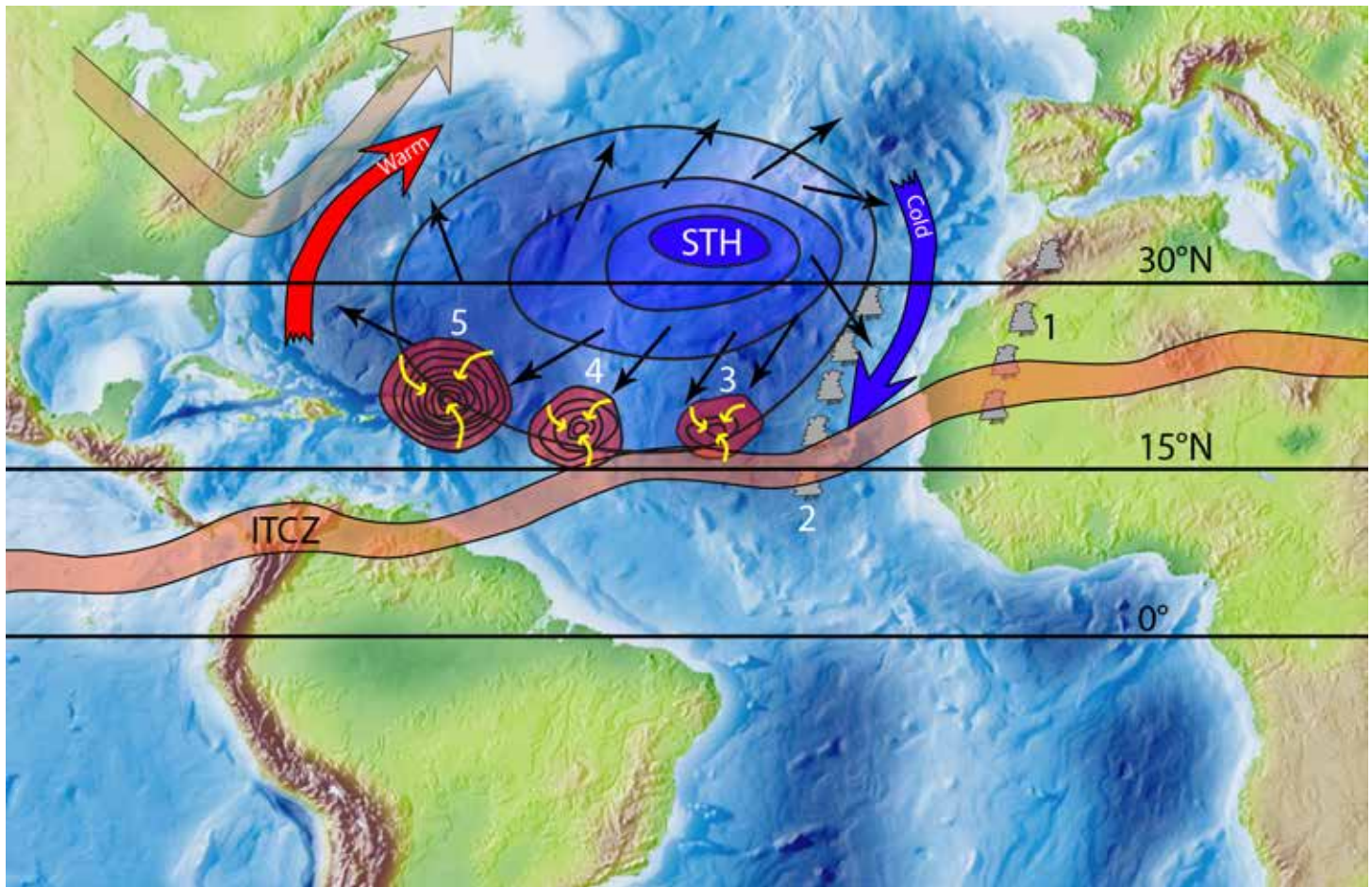


Figure 6.94. Waves that develop in the Intertropical Convergence Zone (ITCZ) travel from east to west in the Trade Wind belts. On the eastern side of the wave, conditions favor uplift and the formation of clouds (Stage 1). Intensification of storm activity associated with these clouds can lead to the development of a tropical disturbance (Stage 2). As the 'Easterly Wave' continues to meet air flow coming out of the Bermuda High Pressure system, the clouds can develop in size and number, and ultimately form a cyclonic, tropical depression which is revealed by closed, widely-spaced isobars (Stage 3). Further intensification of the storm can lead to the formation of a tropical storm (Stage 4), and eventually a hurricane (Stage 5). Notice how the isobars become more closely spaced and greater in number as the sequence progresses. Once the sustained winds in a tropical storm exceed 74 mph, the system is considered to be a hurricane.

In addition to warm waters, rotation and an easterly wave, hurricanes require at least two more conditions in order to develop. One of these is a condition in which **upper level divergence of air at the top of the storm exceeds lower level convergence of air into the storm**. The rate of airflow into the hurricane at its base must be less than the rate of airflow out of its top. Favorable conditions for hurricane development and intensification include a strong upper-level anticyclonic outflow pattern to compliment the strong cyclonic surface inflow (Figure 6.95).

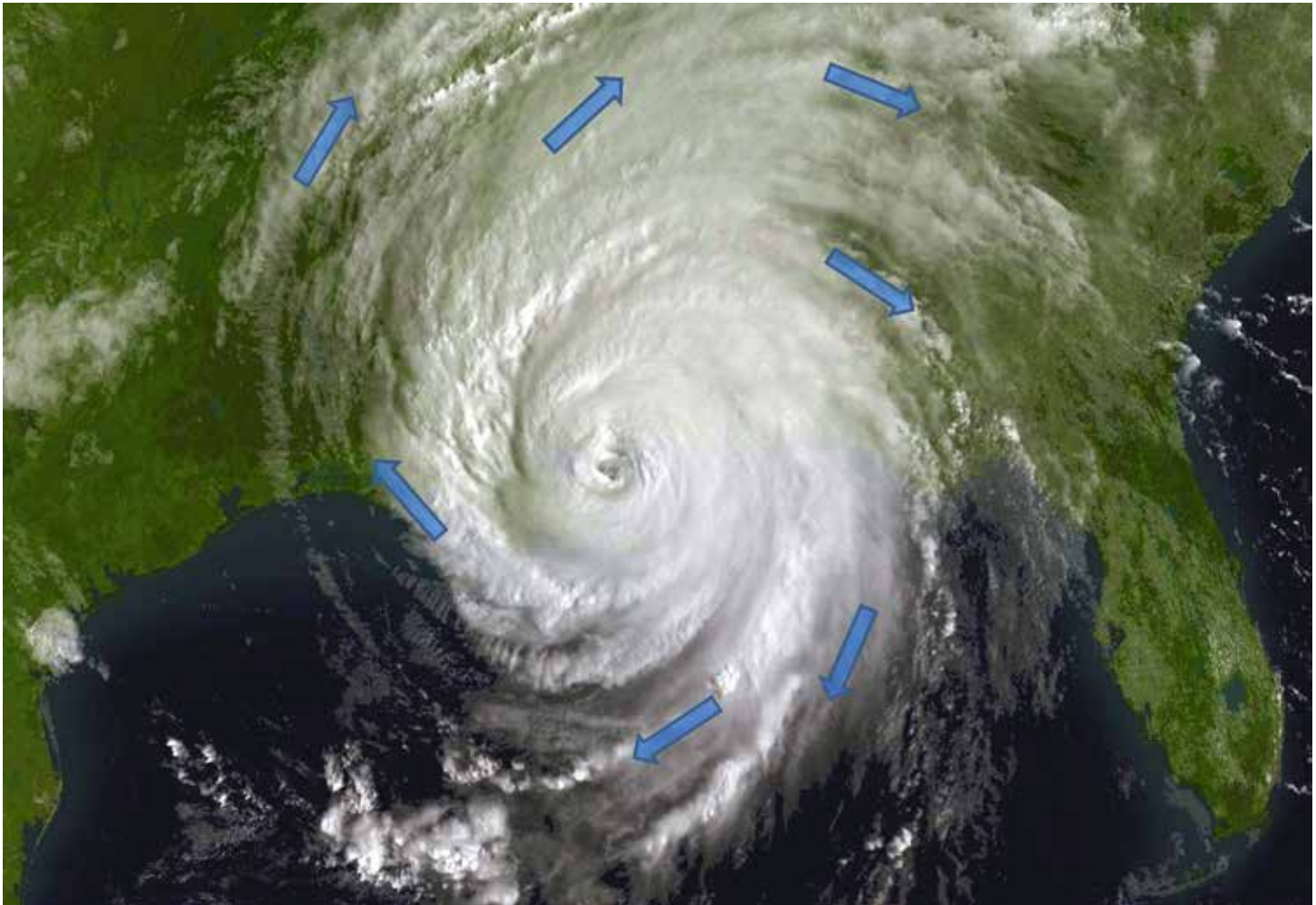


Figure 6.95. Upper-level anticyclonic flow pattern (blue arrows) of Hurricane Katrina as it was making landfall on August 28, 2005 (Source/Credit: NOAA/NASA).

Strong, **unidirectional winds** (from one direction) near the tropopause create shear, which is not conducive to hurricane development. Wind shear impedes intensification of tropical storms that might become hurricanes.



Hurricanes begin as **tropical depressions** that have several closed isobars and sustained winds of 23 to 39 miles per hour (53 to 63 kph) (Figure 6.94). As the pressure continues to drop, the storm intensifies to form a **tropical storm** with sustained winds of 40 to 74 miles per hour (64 to 119 kph). Now, the isobars become more closely-spaced, and more circular. Tropical storms are given names, and each hurricane basin has a separate set of names for a given year (Figure 6.96).

Names for North Atlantic Storms					
2020	2021	2022	2023	2024	2025
Arthur	Ana	Alex	Arlene	Alberto	Andrea
Bertha	Bill	Bonnie	Bret	Beryl	Barry
Cristobal	Claudette	Colin	Cindy	Chris	Chantal
Dolly	Danny	Danielle	Don	Debby	Dorian
Edouard	Elsa	Earl	Emily	Ernesto	Erin
Fay	Fred	Fiona	Franklin	Francine	Fernand
Gonzalo	Grace	Gaston	Gert	Gordon	Gabrielle
Hanna	Henri	Hermine	Harold	Helene	Humberto
Isaias	Ida	Ian	Idalia	Isaac	Imelda
Josephine	Julian	Julia	Jose	Joyce	Jerry
Kyle	Kate	Karl	Katia	Kirk	Karen
Laura	Larry	Lisa	Lee	Leslie	Lorenzo
Marco	Mindy	Martin	Margot	Milton	Melissa
Nana	Nicholas	Nicole	Nigel	Nadine	Nestor
Omar	Odette	Owen	Ophelia	Oscar	Olga
Paulette	Peter	Paula	Philippe	Patty	Pablo
Rene	Rose	Richard	Rina	Rafael	Rebekah
Sally	Sam	Shary	Sean	Sara	Sebastien
Teddy	Teresa	Tobias	Tammy	Tony	Tanya
Vicky	Victor	Virginie	Vince	Valerie	Van
Wilfred	Wanda	Walter	Whitney	William	Wendy

Figure 6.96. These names, approved for North Atlantic hurricanes for the period 2020 through 2025, are reused every sixth year; however, the names of infamous hurricanes may be retired. For example, the names Katrina, Rita, Stan and Wilma were retired after the record 2005 hurricane season. North Atlantic hurricane names for 2026 will be the same as 2020, except for retired names (Source/Credit: NOAA).

Hurricanes average approximately 340 miles in diameter and have a central pressure of 931 to 965 millibars (standard sea level pressure is 1013.2 mb.). They travel at an average speed of about 10 to 31 mph, but often accelerate in higher latitudes. They typically travel from east to west for several days with the Trade Winds, but as they migrate into higher (more than 30°) latitudes, they change course and flow toward the northeast in the Westerly Wind Belt (Figures 6.97a and 6.97b).



Figure 6.97a. Paths of tropical storms and hurricanes from 1949-2008 in the east Pacific basin and 1851-2008 in the north Atlantic basin. Major hurricanes (category 3 or greater) are shown in yellow; lesser hurricanes and tropical storms are shown in solid red; lesser disturbances are shown in dashed red. North Atlantic tropical storms indicate the importance of the trade winds and westerlies in determining direction of movement, although there are many exceptions (Source/Credit: NOAA).

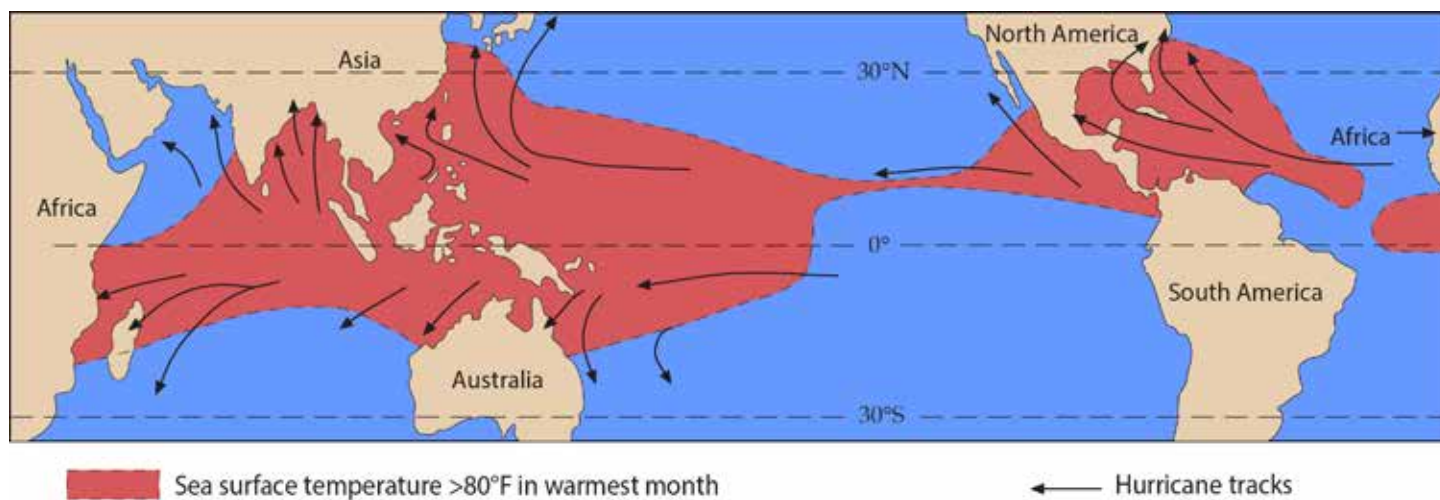


Figure 6.97b. Global breeding grounds for tropical storms and hurricanes (Source/Credit: modified from Dennis I. Netoff and Ava Fujimoto-Strait, *Weather & Climate Lab Manual*).

Hurricanes dissipate when the source of their energy is cut off or when upper-level winds become unfavorable. Energy, in the form of the latent heat of condensation, is progressively cut off when hurricanes make landfall, where they may be downgraded to tropical storm intensity within hours (Figures 6.98a and 6.98b). They lose intensity much more slowly as they move into higher latitudes over cold waters. Hurricanes may die a more subtle death when they encounter upper-level winds that are strong and unidirectional, which disrupts their upper-level outflow pattern.

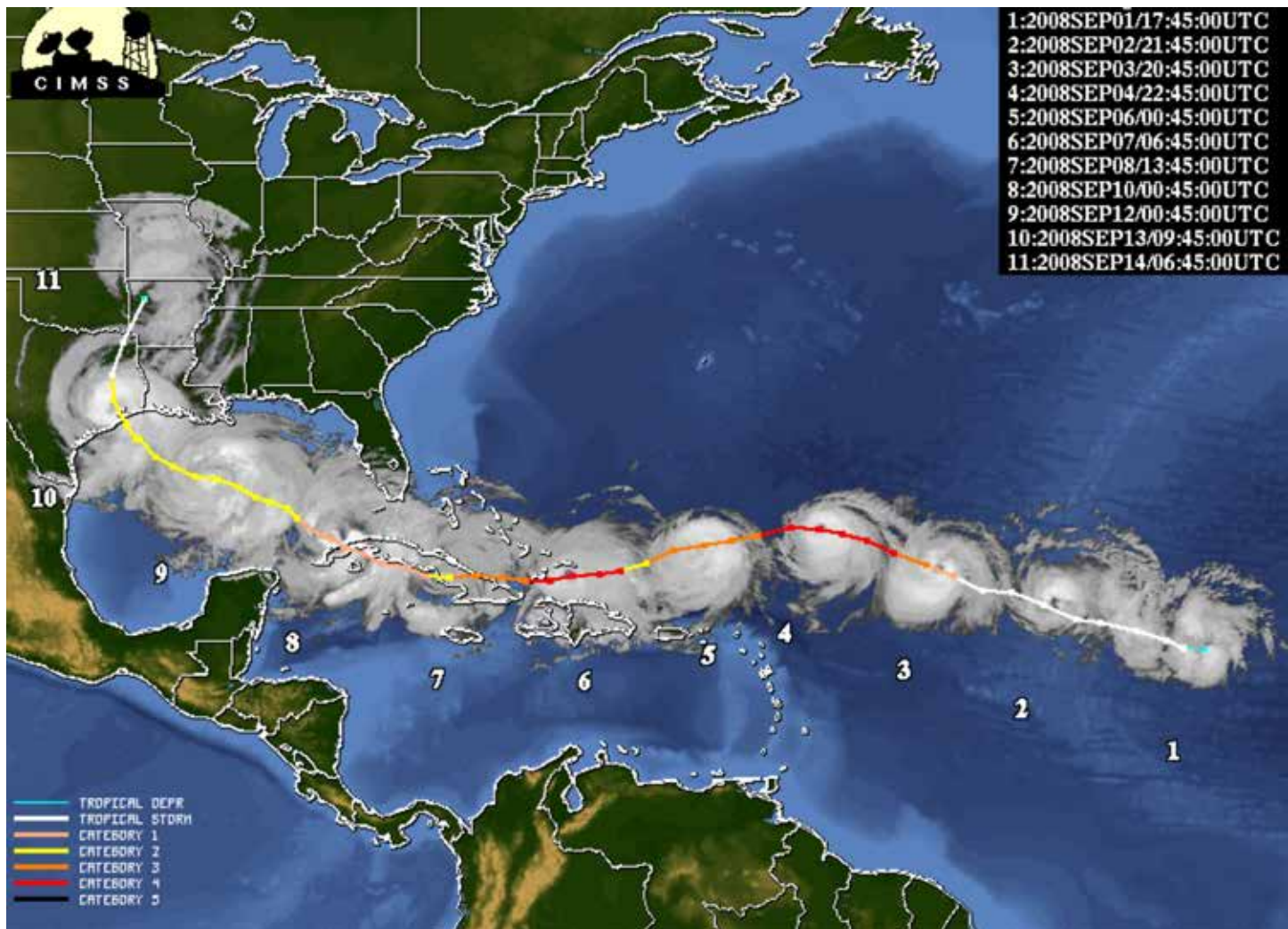


Figure 6.98a. Montage of Hurricane Ike's long-lived path in September of 2008. The hurricane was a strong category 4 storm on September 4, with sustained winds of 145 mph. It made landfall on Galveston Island as a strong Category 2, with a Category 5 equivalent storm surge. The storm recurved just after passing over Huntsville, steered in part by a cold front, and lost many of its tropical storm characteristics within two days. Damage is estimated at \$38 billion (2012) dollars. It caused the largest evacuation in Texas history (Source/Credit: NOAA).

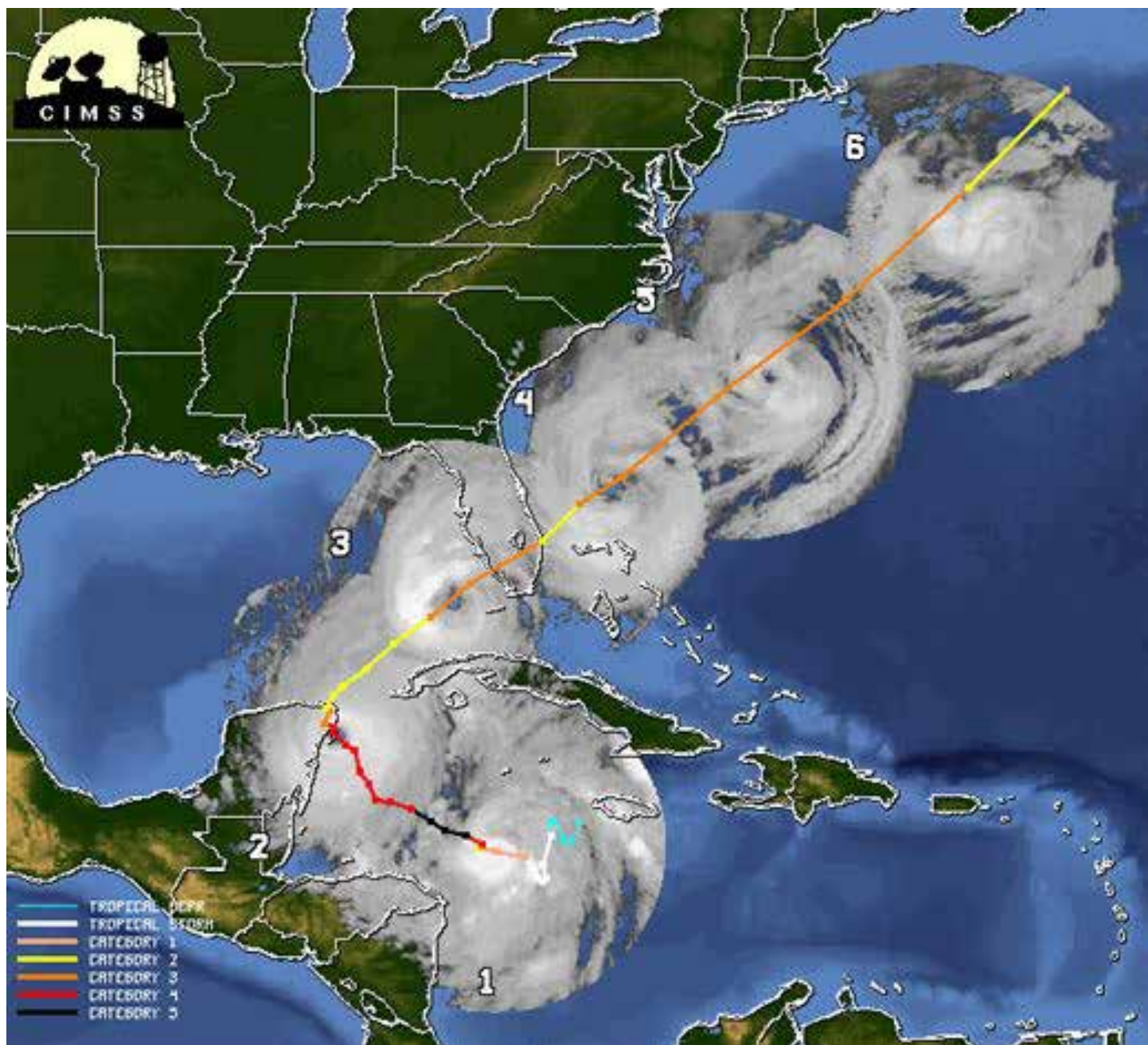


Figure 6.98b. Path of Hurricane Wilma during the fall of 2005. Wilma, even after recurving to the north and then northeast, remained largely over water, and had sustained hurricane winds well into higher latitudes (Source/Credit: NOAA).

## Hurricane Structure

Hurricane anatomy is the most distinctive of all of the Earth's storms. At the center of the hurricane is a 5 to 22 mile diameter region of calm, clear conditions known as the **eye** (Figure 6.99). The eye is surrounded by a towering wall of cumulonimbus clouds, approximately 18 miles in width, known as the **eyewall (collar)**. It is in the eyewall that wind speeds are the greatest in a hurricane. Spiraling inward toward the eyewall are bands of cumulonimbus clouds that are arranged in the classic pinwheel form that characterizes hurricanes. These clouds constitute the convergent, counterclockwise **spiral bands**. In the Northern Hemisphere, hurricanes rotate counterclockwise, whereas in the Southern Hemisphere, they rotate clockwise.

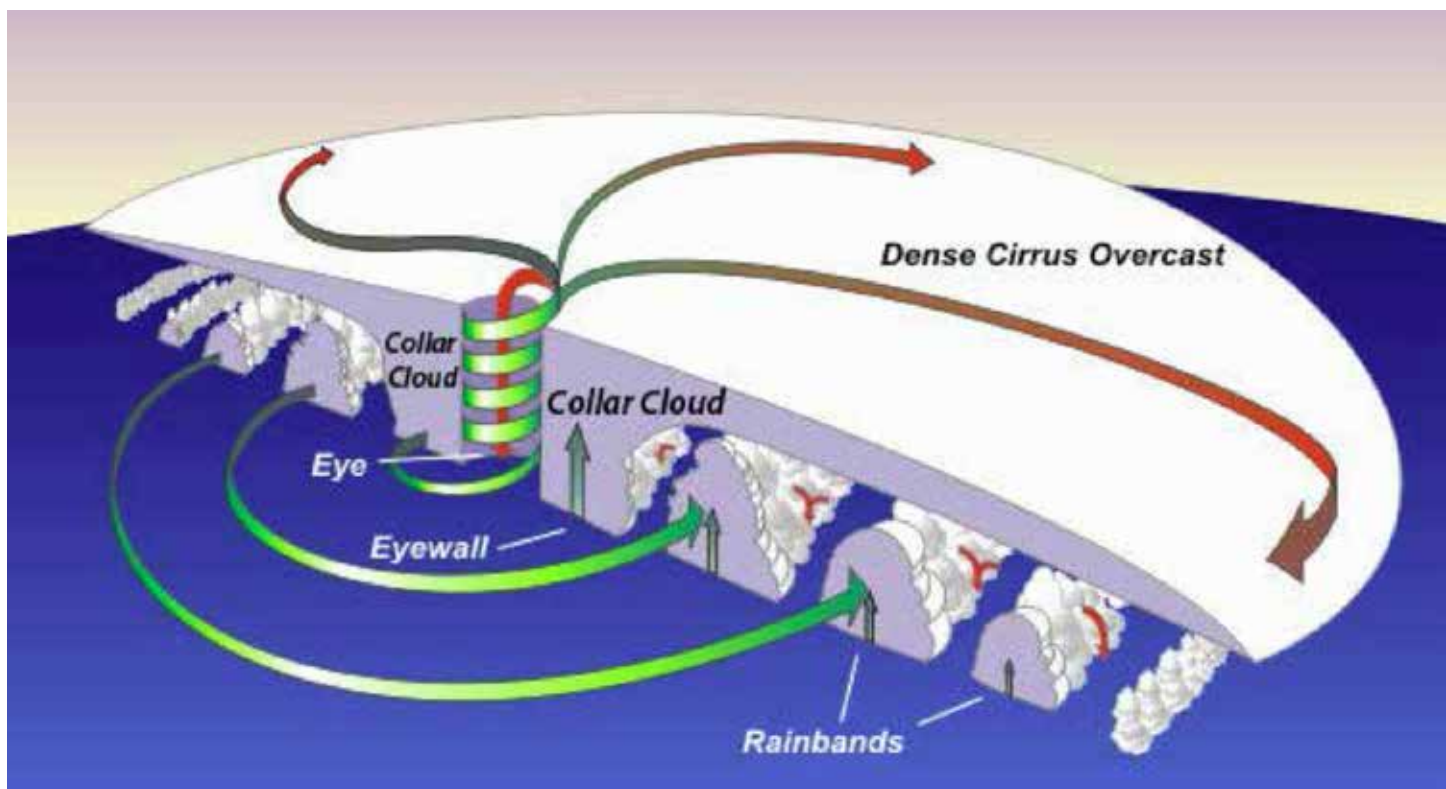


Figure 6.99. The internal structure of the hurricane. The warm, moist air that moves toward the center of the low pressure rises upward to produce bands of cumulonimbus clouds that spiral inward to the eye of the hurricane. The most intense storm activity is in the collar clouds that envelope the eye. Some of the air flows outward away from the center and then sinks on the outer edges of the storm. The subsiding air in this area accounts for the rather sharp boundary of hurricanes — and the clear skies that immediately precede their arrival. The remaining air that rose in the collar clouds sinks in the eye. Because it is dry, and because it is heated adiabatically by compression, its relative humidity is lowered as it subsides. This accounts for the clear, dry conditions in the eye. The contrast between the raging fury surrounding the eye, the calm that prevails in the eye is truly striking (Source/ Credit: NOAA).

Many of the anatomical characteristics of hurricanes are evident from satellite images of the infamous 2005 hurricanes Rita and Katrina (Figure 6.100a, 6.100b and 6.100c). The 2005 North Atlantic hurricane season was the most memorable in recorded history, with 27 tropical storms (old record 21), most hurricanes (15; old record 12), most category 5 hurricanes (4; Emily, Katrina, Rita and Wilma), most hurricane names to be retired (6; previous record 4), most monetary damage (more than \$150 billion; old record ~ \$50 billion), and strongest hurricane intensity (Wilma, with a central pressure of 882 mb).



Figure 6.100a. Spiral inflow bands and large, distinct eye of Katrina on August 28, 2005, when surface pressure was estimated at 902 mb. This is the lowest pressure ever recorded in this part of the Gulf of Mexico (Source/Credit: NASA).



*Figure 6.100b. The eye of Hurricane Rita is clearly visible in this satellite image of September 23, 2005 (Source/Credit: NOAA).*



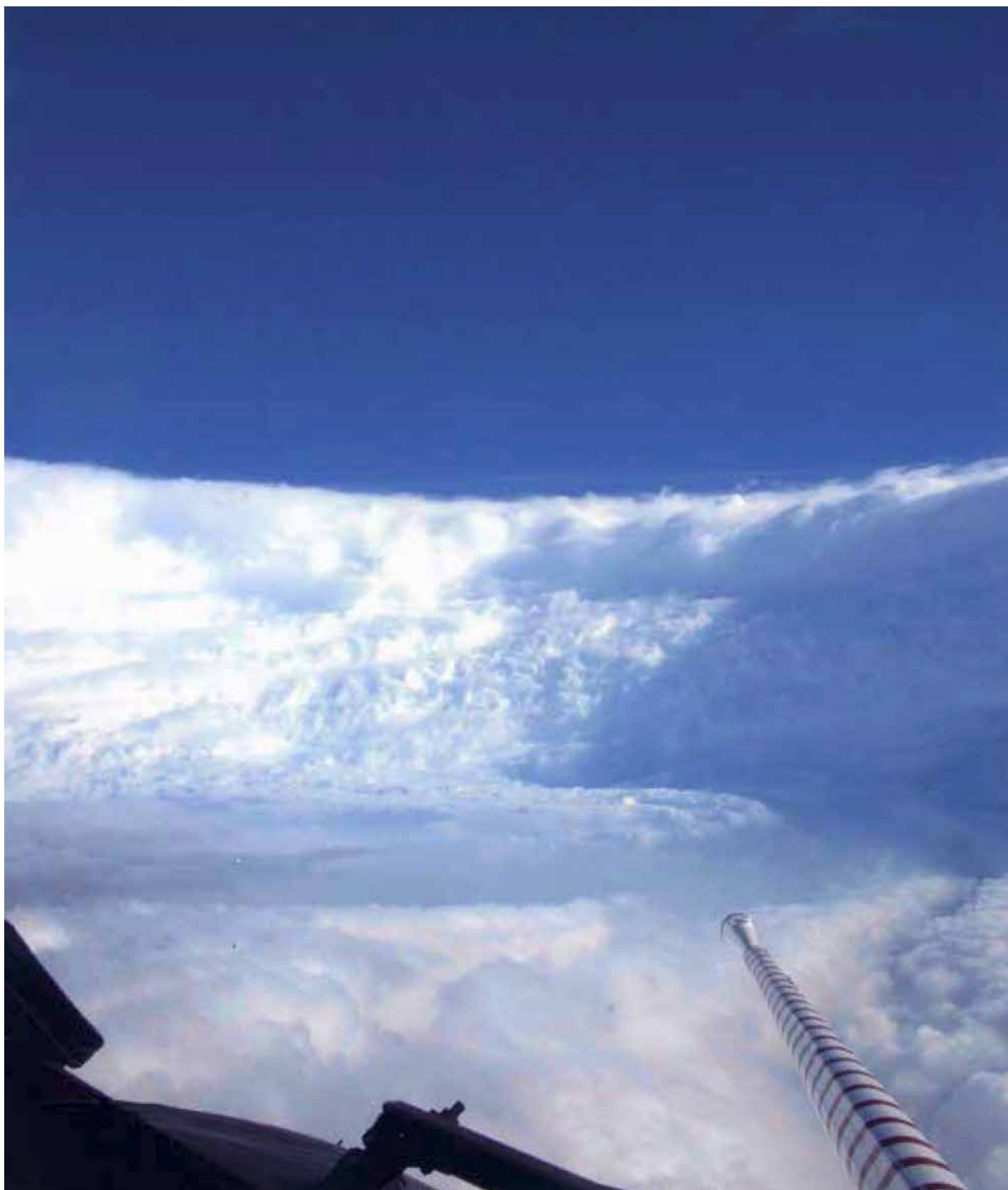


Figure 6.100c. This is the eye wall of Hurricane Rita as photographed from a hurricane chase plane as it circled within the eye of the storm (Source/Credit: NOAA).

The eye of the hurricane is a small region of calm, clear skies, surrounded by some of the most violent winds and storm activity that occur any place on the planet. Air within the eye subsides, and is heated adiabatically, accounting for the relatively clear skies there.

A typical scenario of a hurricane in the Gulf of Mexico that is heading toward the northwest toward Galveston Island begins with scattered, high-level cirrus clouds and high humidity. If the eye of the storm makes landfall to the southwest of Galveston, surface winds will initially come from the northeast, then east and finally from the southeast (Figure 6.101a, 6.101b, 6.101c and 6.101d). Slightly to the southwest of Galveston, where the eye passes overhead, the skies will clear briefly and the Sun will shine, giving the illusion that the storm is over. But the skies there will begin to darken again and suddenly the full force of the other side of the eyewall will hit.

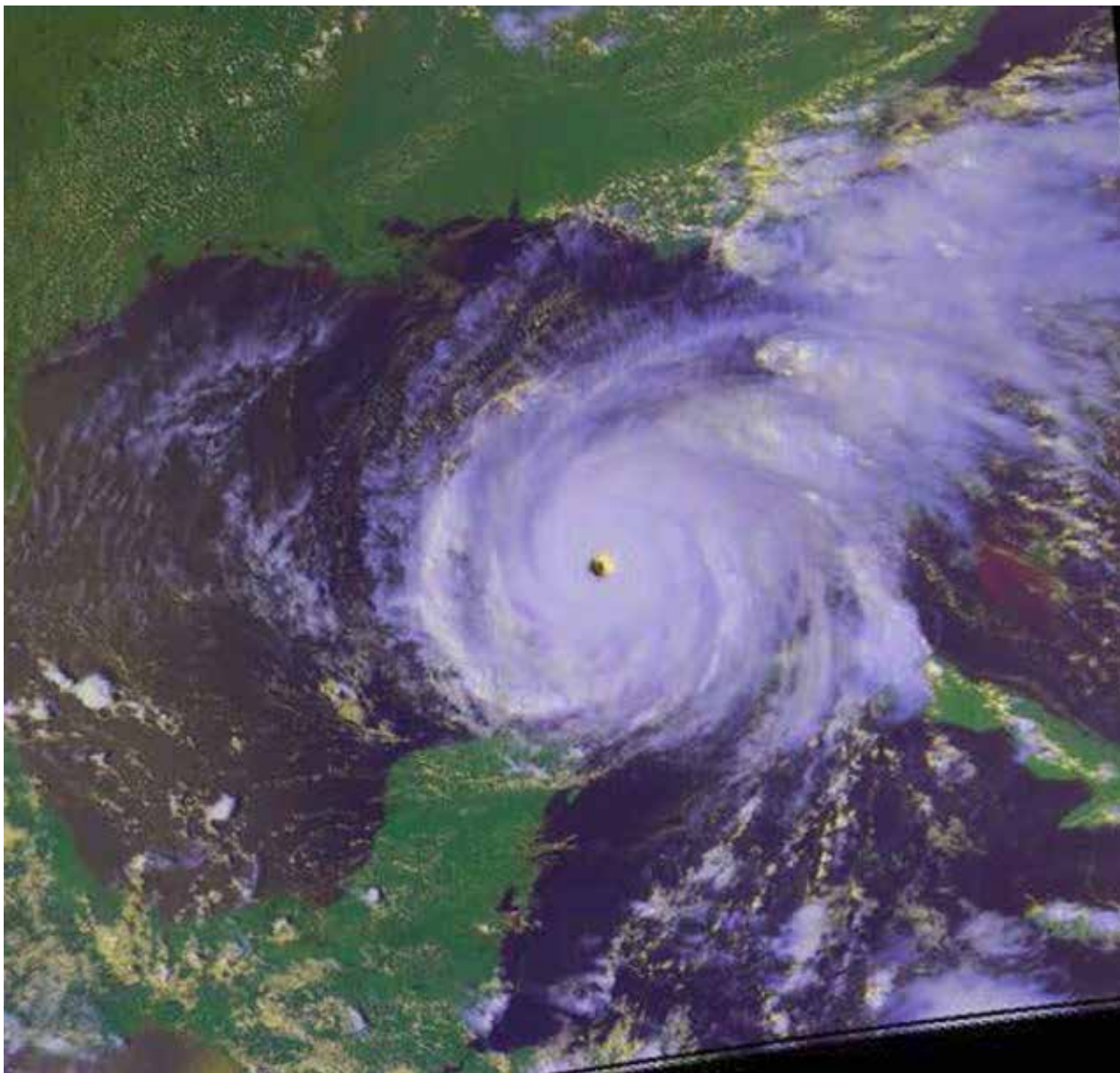


Figure 6.101a. Time series of satellite images of Hurricane Rita in the Gulf of Mexico. Rita's path was very typical for Gulf hurricanes in September and October, beginning with a westward trajectory on Wednesday September 21, 2005, with sustained winds of 165 mph (Source/Credit: NOAA).

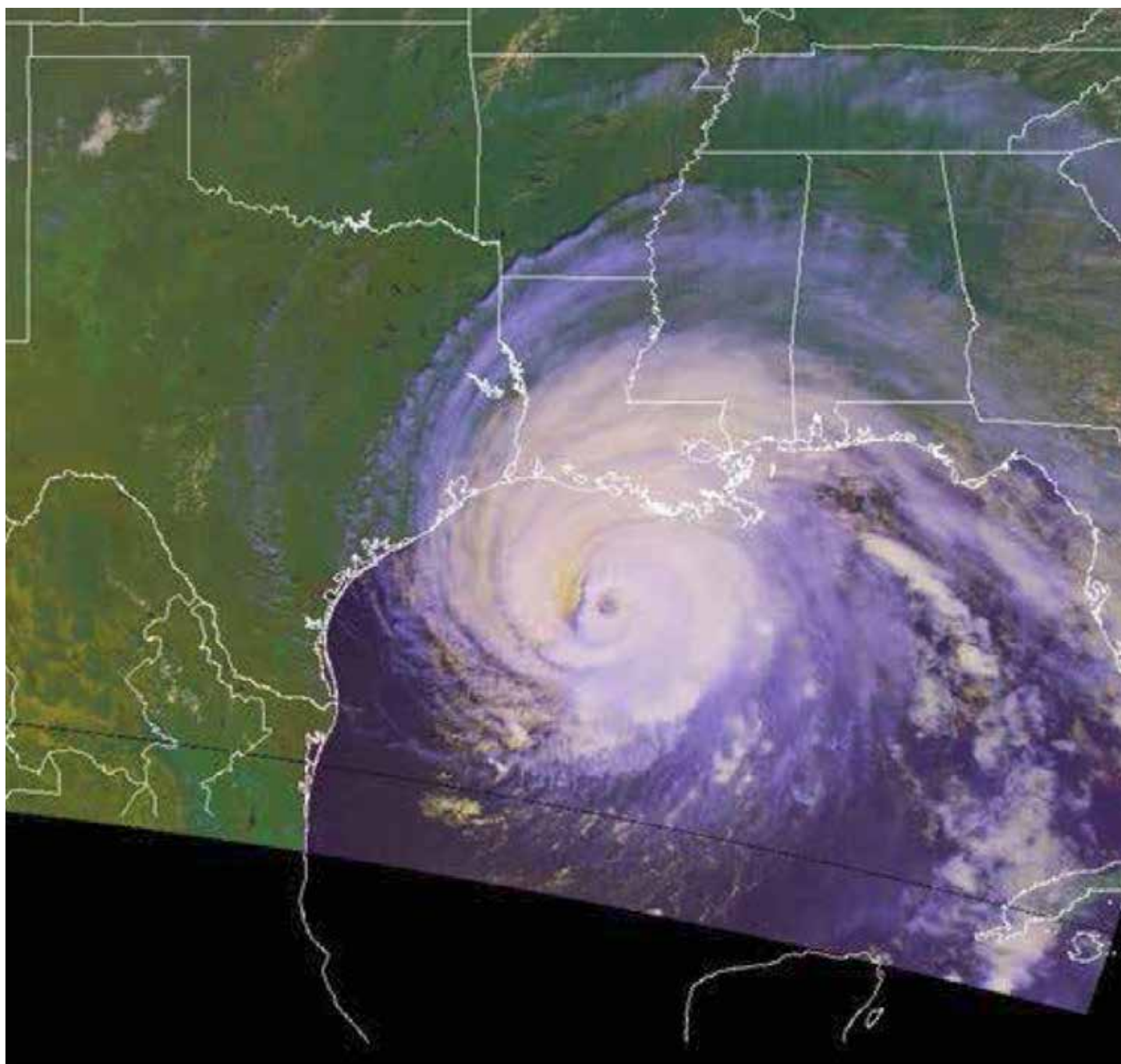


Figure 6.101b. Rita turns to west-northwest on Friday, September 23 and finally recurves to the north with landfall on September 24 (Source/Credit: NOAA).

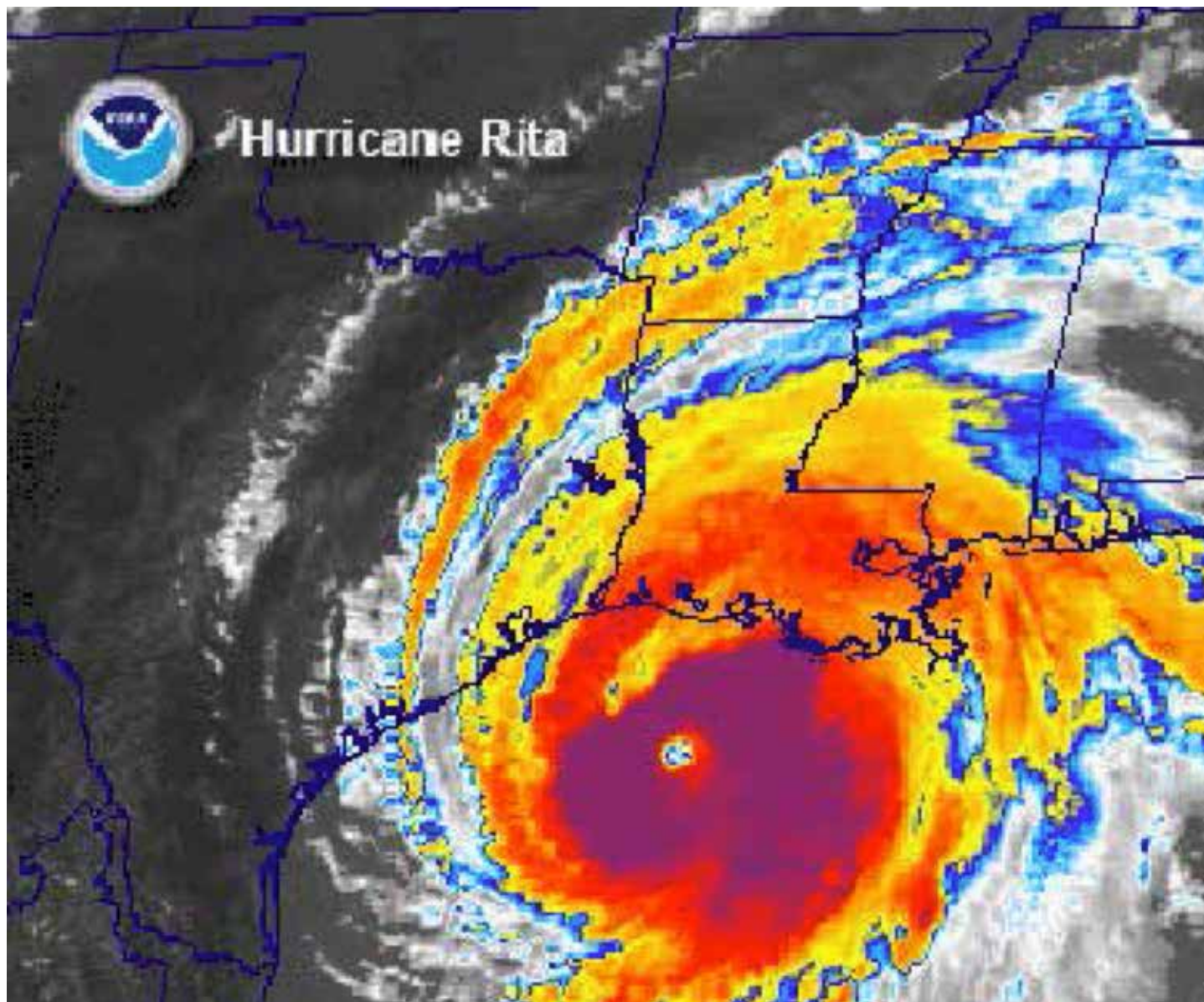


Figure 6.101c. Infrared image of Rita showing concentration of precipitation around the well-defined eye on Friday, September 23 (Source/Credit: NOAA).

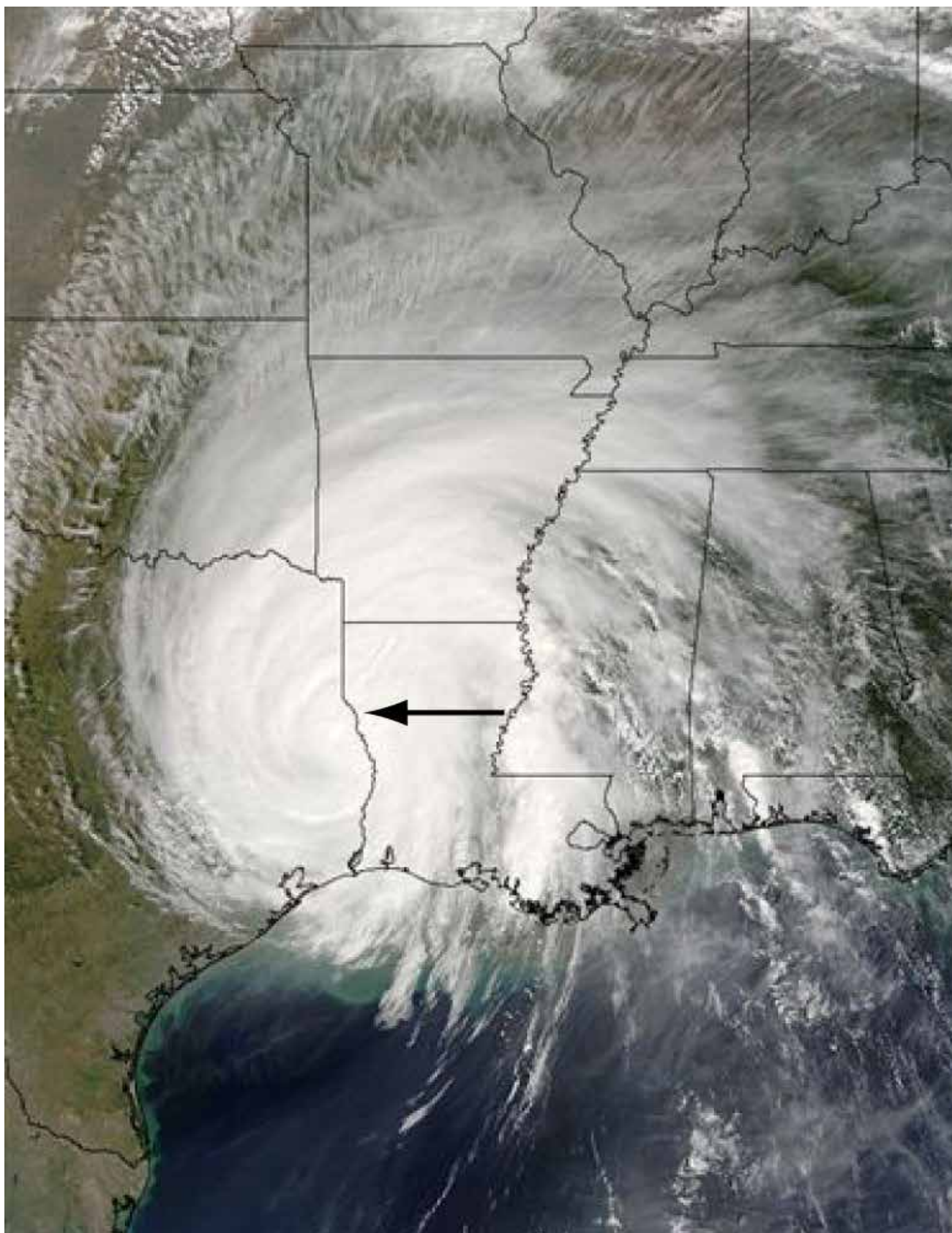


Figure 6.101d. Rita recurves to the north on Saturday, September 24, 5:00 AM a few hours after landfall. Within a few hours, the eye of the storm had completely disappeared, and sustained winds were down to about 50 mph. The approximate location of the “eye”/center of the storm is indicated by the arrow (Source/Credit: NOAA).

Birds have been found in the eye of a hurricane. Having survived the trip into the eye, they dare not venture back into the eyewall clouds, and so they must travel with the hurricane until it dissipates. The hurricane, in effect, imposes a forced migration on these birds.

Wind is certainly a destructive force in hurricanes, but the greatest damage that they cause is from storm surges and flooding. A **storm surge** is an elevated dome of water that develops under a hurricane as a result of three elements; the low pressure (which elevates the sea surface), the flow of water toward the eye as wind pushes it along, and astronomical high tides (Figure 6.102a and 6.102b).



Figure 6.102a. When a hurricane approaches, the combination of low pressure and airflow toward the center of the storm causes the surface of the ocean to bulge upward, creating a powerful and dangerous storm surge. Because of high winds, the waves on top of the storm surge are bigger than normal and this combination sets the stage for massive destruction in low-lying coastal areas. The threat of a storm surge, and strong winds, is why residents should always evacuate coastal areas when a hurricane approaches (Source/Credit: NOAA).

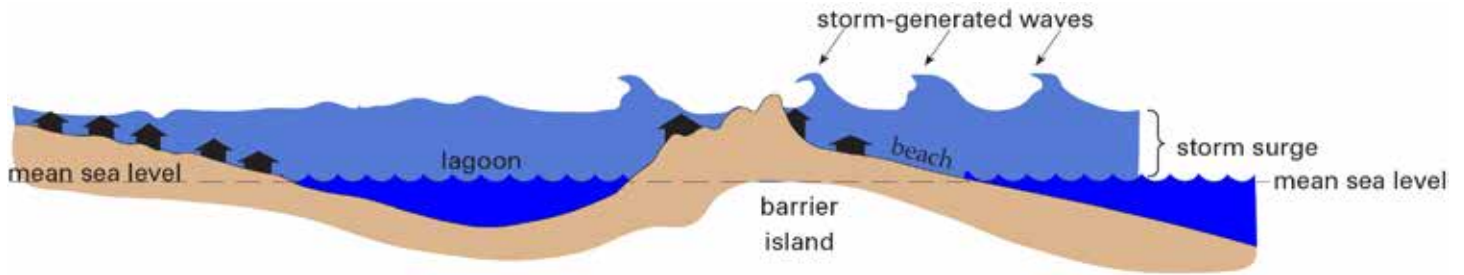


Figure 6.102b. Galveston Island, like all barrier islands, is particularly susceptible to the damaging effects of storm surges. This is because barrier islands are actually low-lying, narrow strips of sand that storm surges can wash over and then reach the mainland. During the infamous Galveston Hurricane of 1900, the highest spot on Galveston was a mere 8 feet above sea level. The storm surge was approximately 15 feet high, which means that the entire island was inundated under several feet of water. Following this devastating storm, which killed 6000-10,000 people, a 17-foot high seawall was built to protect part of the island. However, a major storm surge could still cross this protected part of the island, causing massive destruction. Because the island is made of sand, the storm surge picks up sand on the ocean side of the island and carries it to the back side of the island, where it may be deposited in the lagoon. This effect literally causes the island to move toward the mainland over time. Barrier islands are unstable piles of sand, which makes them very vulnerable to the effects of storm surges (Source/Credit: modified from Dennis I. Netoff and Ava Fujimoto-Strait, *Weather & Climate Lab Manual*).

The maximum storm surge is typically experienced in the right-front quadrant of a hurricane making landfall, and is about 40 to 50 miles in breadth (Figures 6.103a, 6.103b and 6.103c). In extreme cases, the surge can be 30 to 40 feet high, although most are on the order of ten feet. Large wind waves are superimposed on the storm surge, adding to their destructive potential. The right front quadrant is also the preferred location for the development of tornadic thunderstorms, particularly in Texas (Figure 6.104).

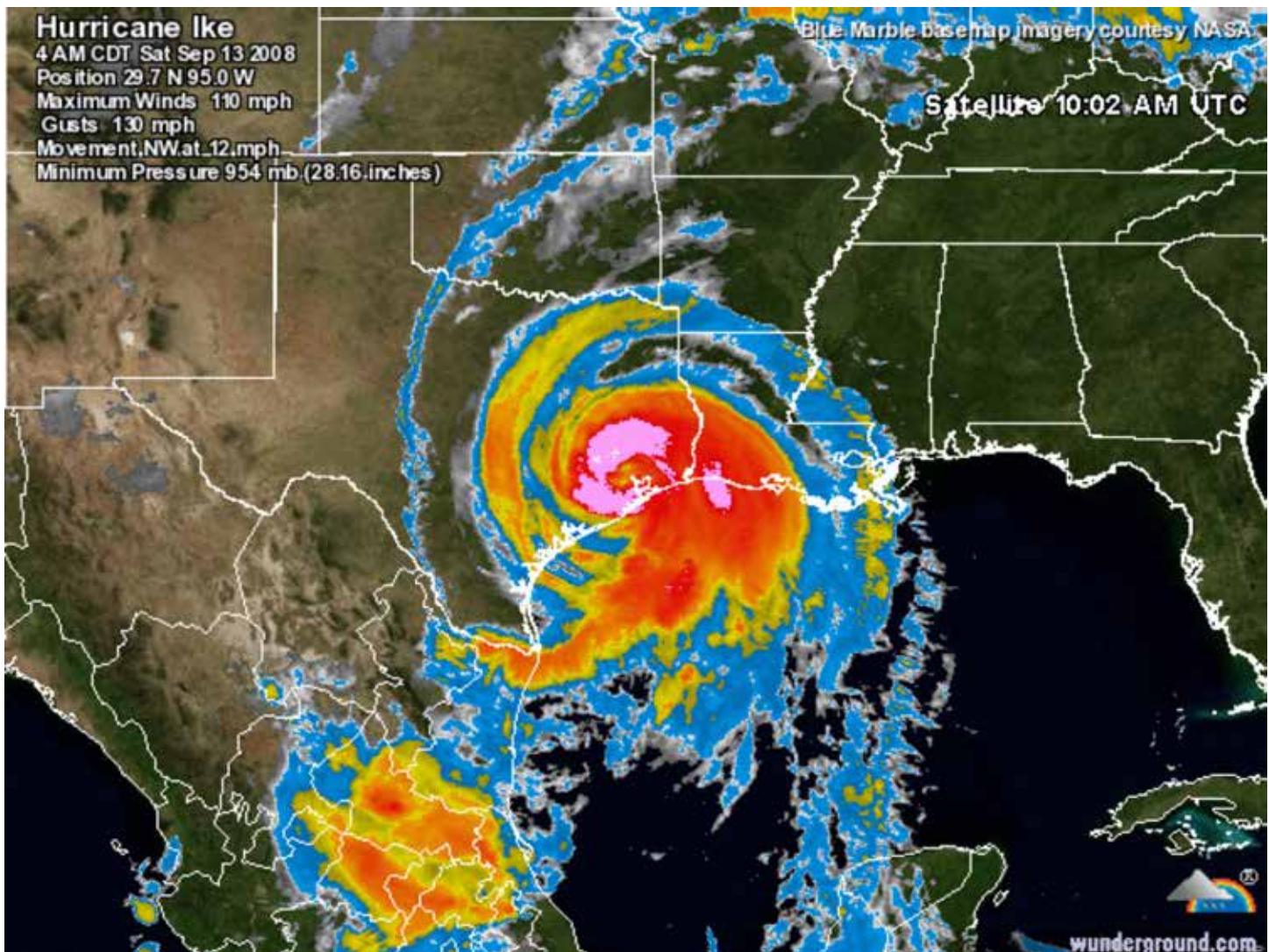


Figure 6.103a. Satellite image of Ike about two hours after making landfall. The area around the eyewall and the right quadrants of the system are still very strong (pink and red colors) because they are being energized by a strong shoreward flow of moisture, whereas the left quadrants are dissipating due to the admix of dry, land-based air (Source/Credit: NOAA).



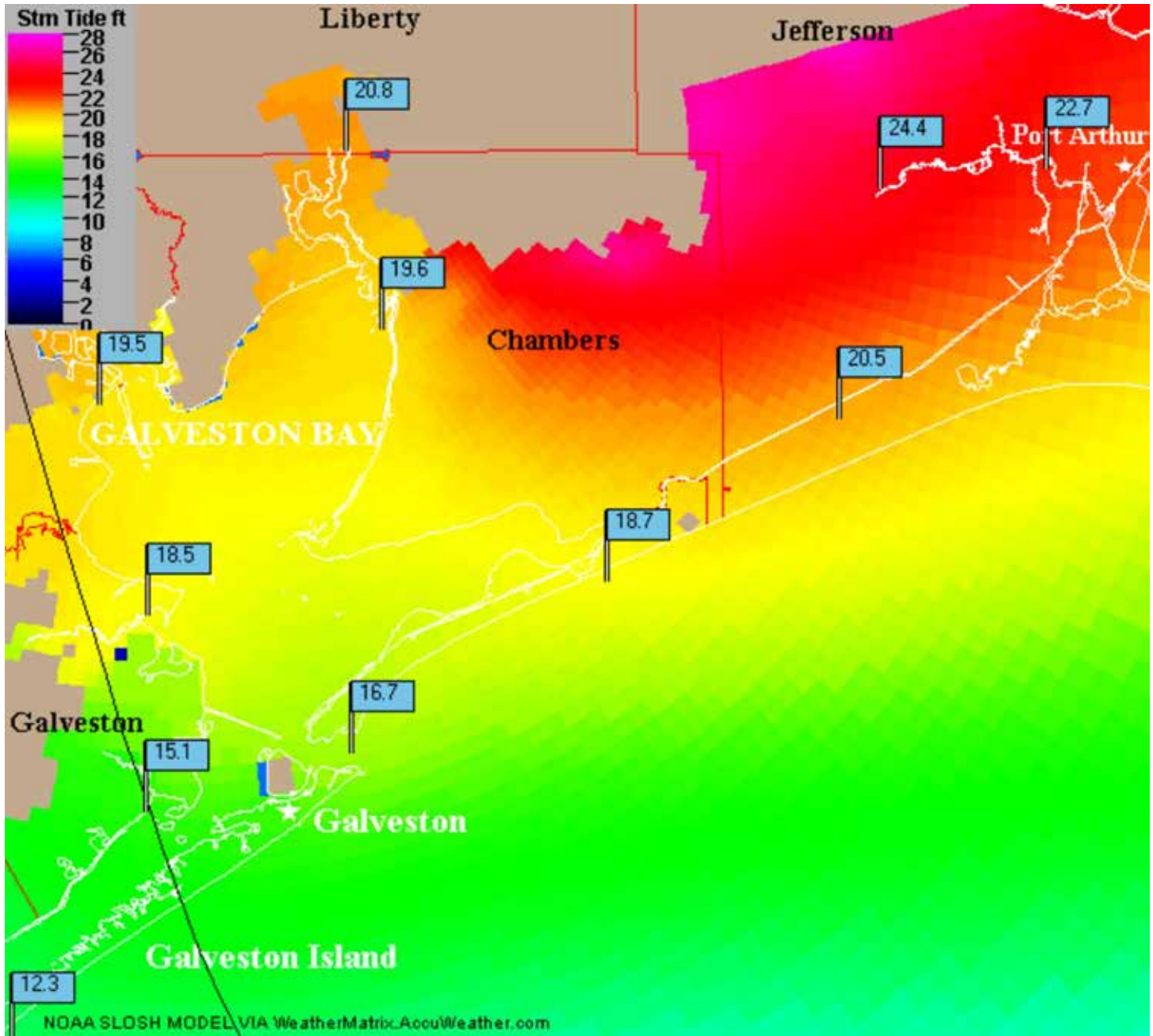


Figure 6.103b. The NOAA SLOSH MODEL prediction of the magnitude of Ike's storm surge in the right-front quadrant of the hurricane. The prediction was made about a day prior to landfall on September 12; the actual path of the storm was just east of this model prediction (Source/Credit: NOAA).

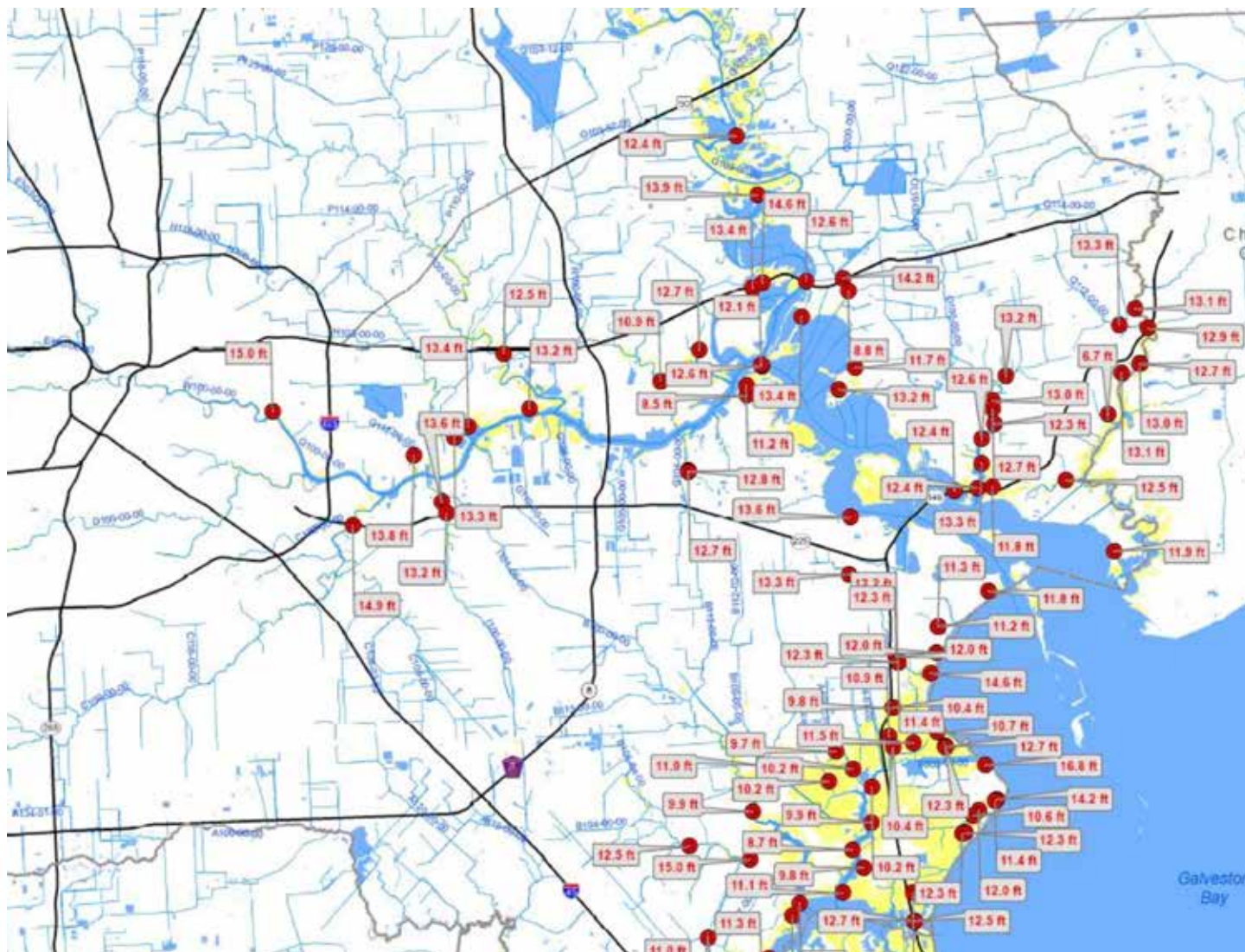


Figure 6.103c. Actual measured storm surge (in ft) in Galveston Bay and the San Jacinto Estuary along the path of Hurricane Ike (Source/Credit: Harris County Flood Control District).

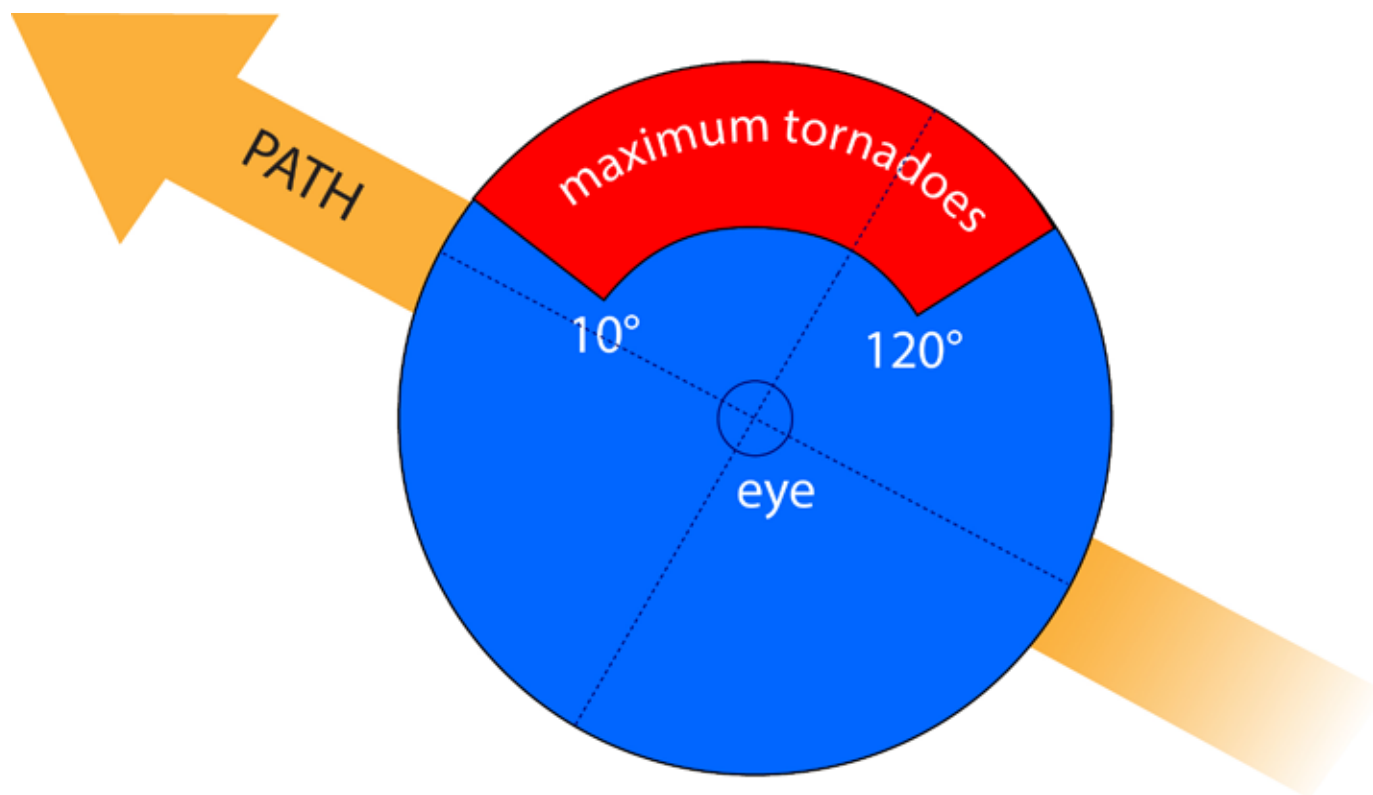


Figure 6.104. The right-front quadrant is also the preferred location for the development of tornadic thunderstorms, particularly in Texas (Source/Credit: modified from Dennis I. Netoff and Ava Fujimoto-Strait, *Weather & Climate Lab Manual*).

Along low-lying coasts, a rise in sea level of only a few feet can wreak havoc because the water can extend so far inland. Consequently, developed coastal areas, such as those along the Gulf Coast and the East Coast, are particularly susceptible to damage by storm surges (Figure 6.105a, 6.105b, 6.105c, 6.105d and 6.105e). Homes, hotels, stores, bridges and roads can easily be washed away by storm surges. Unfortunately, some people fail to realize this and refuse to evacuate coastal areas.



Figure 6.105a. The storm surge created by Hurricane Katrina when it made landfall in south Plaquemines Parish, Louisiana on August 29, 2005 drove shrimp boats and pleasure boats onto this highway and severely damaged the road. Many boats, roads and bridges were destroyed by the hurricane (Source/Credit: NOAA).



Figure 6.105b. Figures 6.105b- 105e illustrate the susceptibility of a low-lying coastline such as the Gulf Coastal Plain to coastal flooding, erosion, and deposition by hurricanes. Each photo pair is a before and after Ike landfall. Note that even areas in the left-front quadrant sustained considerable damage. Damage in the right front quadrant was more extensive and intensive because of the stronger winds, greater storm surge and higher amounts of rainfall (Source/Credit: USGS).

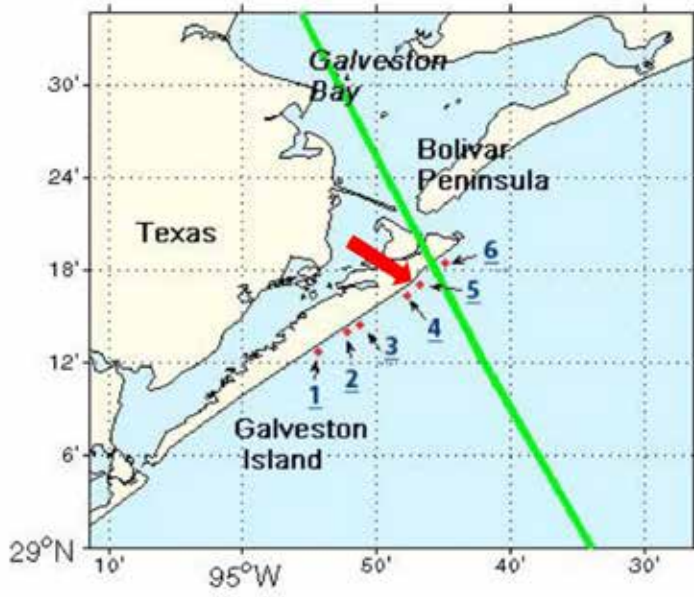


Figure 6.105c.

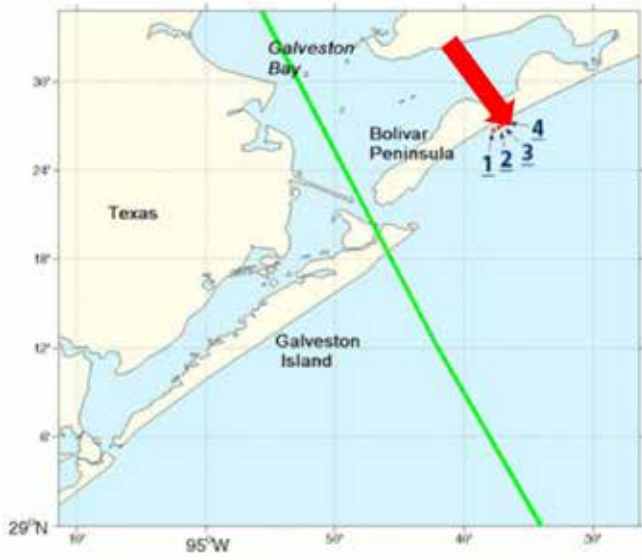


Figure 6.105d.



Figure 6.105e.

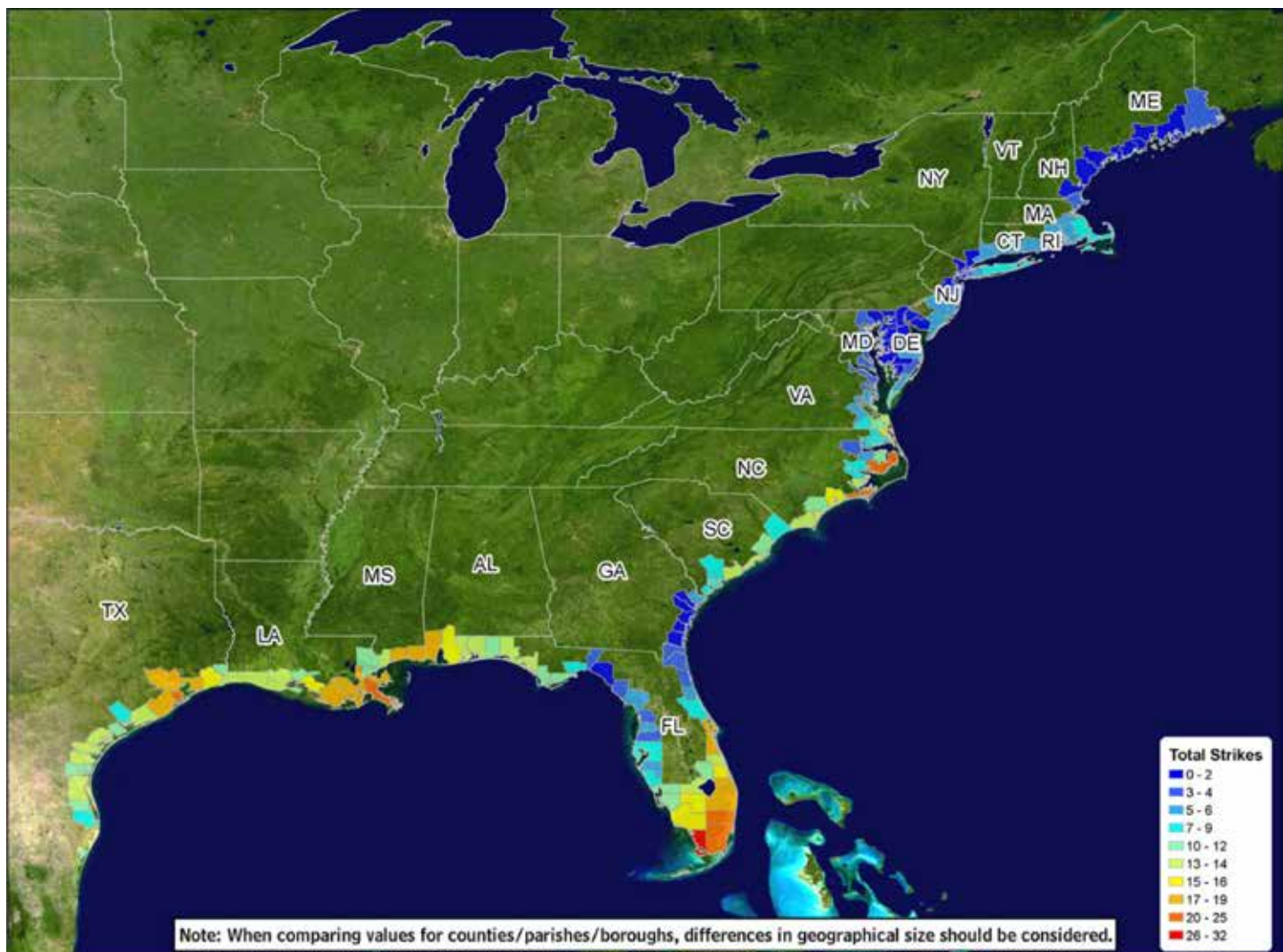


In some parts of the world, people understand the dangers of storm surges but have no option but to live with the threat. Bangladesh is one such place. This country is located between India and Myanmar along the coast of the Bay of Bengal. Much of Bangladesh is a delta that has been formed by the deposition of sediment into the bay. Because it is a delta, it is very low-lying, and because of overpopulation and the ever-growing need for more land and food, many people have moved out onto these low-lying areas in order to farm them. This, combined with the shape of the Bay of Bengal, creates a tremendous threat from storm surges. When hurricanes travel into the bay, the narrowing width of the bay acts to funnel the water and raise the water level to as much as 40 feet above normal sea level. In 1974, a 40-foot surge caused the death of 250,000 people.

At times, more than half of the country of Bangladesh is flooded. Because of its location and its susceptibility to storm surges, this country faces a virtually impossible task of developing economically. It appears that periodic natural disasters on the scale of the entire country, combined with overpopulation, will forever doom the majority of people in that country to a life of poverty.

By way of comparison, the worst natural disaster (in terms of lives lost) to strike the United States occurred in 1900. That year, a hurricane swept through the Gulf of Mexico and struck Galveston Island. The storm surge was so high that it swept completely over parts of the low-lying barrier island. Over six thousand people were killed in this storm. The construction of the Galveston seawall was in response to the 1900 hurricane devastation.

The East coast of the United States has many barrier islands, and, like Galveston, most are developed to varying degrees. All of these islands are potentially subject to the same fate as Galveston (Figure 6.106). This is one reason why many people argue that barrier island development should cease, and that the islands should be left in a natural state. In a natural state, they provide habitat for various species, and they also reduce the brunt of storm surges along the continental coast, thereby helping to mitigate damage in those areas. Once developed, habitat is lost and beaches usually erode, thereby diminishing the width of the islands. But, no matter what ecological arguments that may be put forward to preserve the islands, it is clear that those who choose to live on these islands risk both their property and their lives.



### Total number of hurricane strikes by counties/parishes/boroughs, 1900-2009

Data from NWS NHC 46: Hurricane Experience Levels of Coastal County Populations from Texas to Maine. Jerry D. Jarrell, Paul J. Hebert, and Max Mayfield. August, 1992, with updates.

Figure 6.106. The entire Gulf and Atlantic coast is susceptible to hurricane damage, particularly the barrier islands. Historically, there are some obvious hotspots, including the Carolina Outer Banks, Peninsular Florida, the Mississippi Delta, and the Galveston-Houston area (Source/Credit: National Weather Service and National Hurricane Center).

Another illustration of the extreme susceptibility of low-lying, heavily populated coastlines to tropical cyclone hazards is Hurricane Sandy (Figure 6.107), which has become the second-most expensive natural disaster in U.S. history, with a price-tag of about \$71 billion (2012 USD). Hurricane Sandy was unusual in that it was drawn landward in late October and merged with an extra-tropical cyclone to produce foul weather from the coast of the New England states to the Great Lakes. Normally, hurricanes that make their way along the eastern coastline are deflected toward the northeast as they interact with extra-tropical cyclones. A blocking high pressure system off the Canadian coast caused Sandy to go the opposite direction (Figure 6.108). Significant snow fell at higher elevations in the Appalachians (Figure 6.109).



Figure 6.107. Oblique satellite image viewed toward the south (see peninsular Florida in upper-right) of Hurricane Sandy after merging with an extra-tropical frontal cyclone on October 29, 2012. At one point, even though it only reached a category 3 status, Superstorm Sandy became the largest North Atlantic hurricane in history, with a diameter of 1100 miles (1800 km). After landfall, Sandy caused gale-force winds from the Atlantic coast to the Great Lakes (Source/Credit: NOAA).

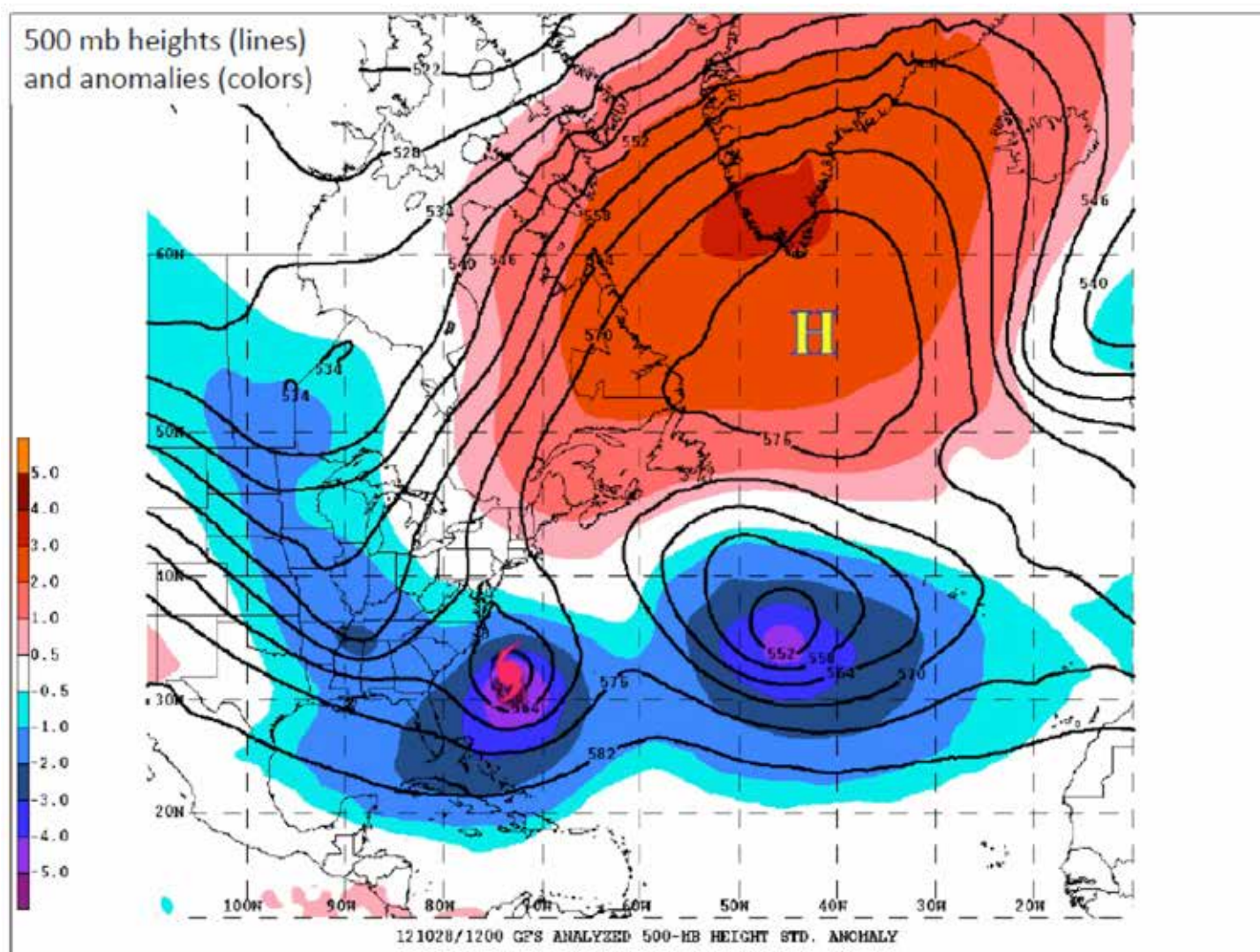


Figure 6.108. A very dominating upper-level blocking high pressure system (red, with H) that is clearly visible on this 500 mb chart on October 28, 2012 diverted Sandy landward, where it merged with an extra-tropical system (Source/Credit: NOAA).

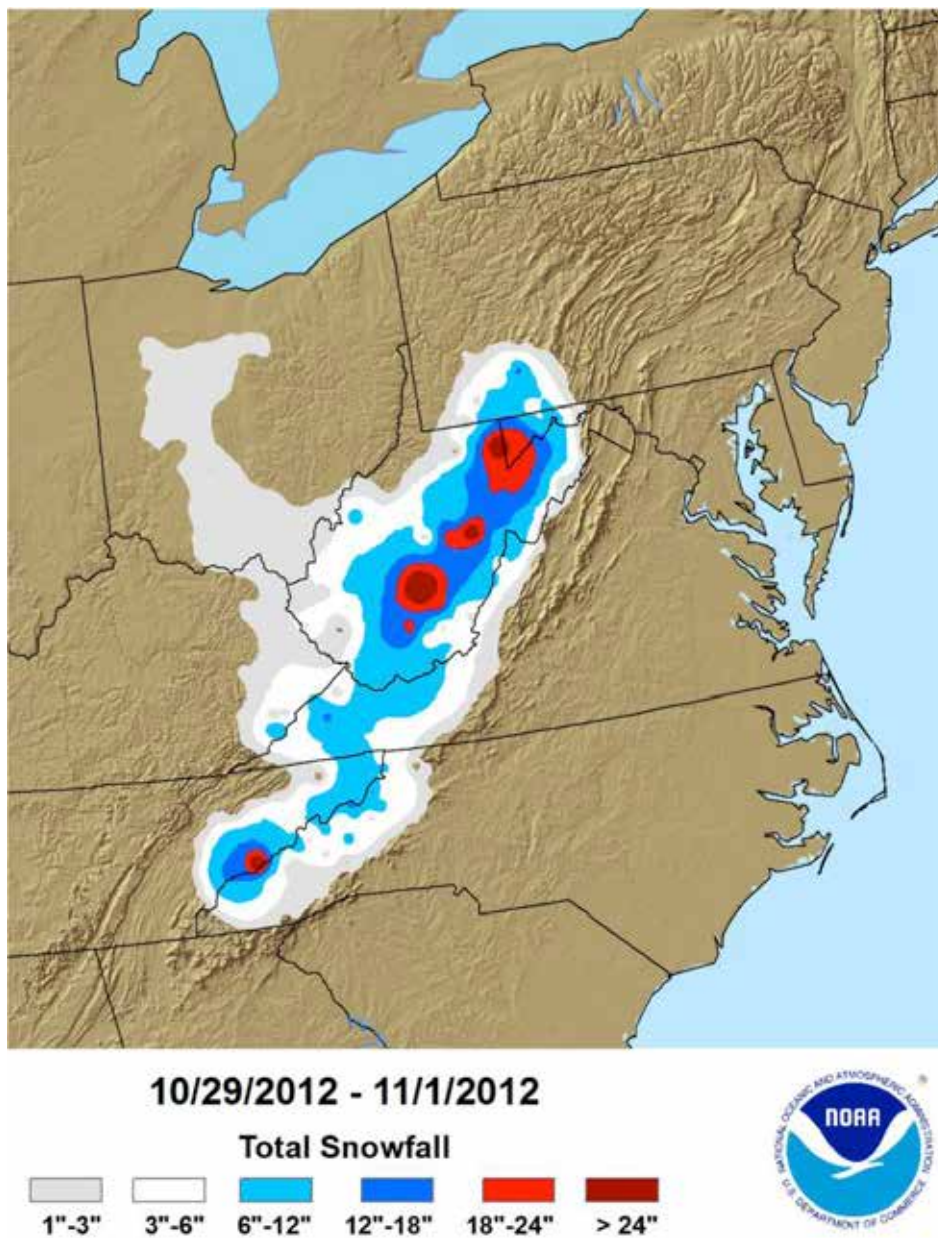


Figure 6.109. The merging storm systems brought heavy snowfall to the higher elevations in the Appalachians over a four-day period of October 28-31 (Source/Credit: NOAA/National Climatic Data Center).

Hurricanes can have far-reaching impacts long after they make landfall. Dramatic examples are those Hurricanes Norbert and Odile in September of 2014 (Figure 6.110). Both were East Pacific hurricanes that made landfall in Mexico, but drifted northeastward as they entered the United States. Extensive flash-flooding occurred from Arizona to west Texas, then northward to the Great Plains. Phoenix and Las Vegas both received over 3 inches of rain from the combined storms.



Figure 6.110. Hurricane Odile made landfall near Cabo San Lucas on September 14, 2014 as a Category 3 hurricane with sustained winds of 127 mph (204 km/h). Torrential rains and flash floods occurred sporadically on the Baja Peninsula as the storm moved northwestward. Several days later, remnants of the storm turned to the northeast, hitting the southwestern deserts of the United States. Just a week earlier, the remnants of Hurricane Norbert made a similar track and delivered over 3 inches of rain to Phoenix, AZ and Las Vegas, NV (Source/Credit: NASA GOES Satellite Sept 14, 2014).

The intensity and potential for destruction of hurricanes is rated on a scale known as the **Saffir-Simpson Scale**. This scale, with categories from 1 (minimal hurricane) to 5 (catastrophic with sustained winds over 155 miles per hour), is based on estimates of the amount of damage the storm would cause should it make landfall (Figure 6.111).

The Saffir-Simpson Hurricane Intensity Scale				
Category	Wind (mph)	Pressure (approx.)	Storm Surge (approx.)	Damage
1	74-95	>980	4-5	minimal
2	96-110	965-979	6-8	moderate
3	111-130	945-964	9-12	extensive
4	131-155	920-944	13-18	extreme
5	over 155	<920	over 18	catastrophic

Figure 6.111. Note: Classification by central pressure was ended in the 1990s and wind speed alone is now used. These estimates of the central pressure that accompany each category are for reference only. (Note: Because of the mismatch in actual and predicted storm surge from Hurricane Ike in 2008, storm surge estimates have officially been dropped from the Saffir-Simpson Scale by the National Hurricane Center. They are given here only as a crude approximation) (Source/Credit: modified from Netoff and others. Geologic Hazards & Resources Lab Manual).

Fortunately, category 4 and 5 storms are rare. The 2005 North Atlantic Hurricane season (Dennis, Katrina, Rita, and the record-breaking Wilma) was an exception (Figure 6.112). The greatest potential damage from wind and storm surges is in the right front quadrant of a hurricane. This is because this area experiences high winds associated with both the low pressure system of the storm and the motion of the storm. As hurricanes make landfall along the Gulf coast, the right front quadrant typically not only has the greatest storm surge and strongest winds, but also the heaviest rainfall, greatest number of lightning strikes, and the highest frequency and intensity of tornadic thunderstorms.



Figure 6.112. Paths of hurricanes in the Atlantic and Gulf region during the 2005 hurricane season (Source/Credit: NOAA).

In summary, all severe storms are low-pressure systems in which air flows inward and upward, and moisture condenses as the air rises. As the moisture condenses, heat energy is released which warms the air and further decreases the pressure. This intensifies the pressure gradient and causes the wind to blow even harder. If the low pressure pattern appears as closed, concentric isobars on a map, the storm is cyclonic in nature. In such cases, the air will flow not only inward and upward, but will begin to spiral in a counterclockwise manner in the Northern Hemisphere, and clockwise in the Southern.



# Chapter 7

## Climate and Ecosystems

### *Climate Classification*

Climate is long-term weather. The climate of a given region is the sum total of all of the elements of weather (temperature, pressure, winds, moisture, air masses and storms) taken over a long time period. The climate of a region is the long-term summation of just about everything that has been discussed so far in this book, averaged over the long haul. Some of the main factors that control climate include such things as **latitude, elevation, mountains and highlands, land and water distribution, the influence of ocean currents, the dominant pressure and wind systems, and air masses and storms.**

For example, some of the phrases that describe the climate of Houston, Texas might include: warm to hot summers, with typical daytime highs in the 90s and night-time lows in the 70s; mild winters, with daytime highs typically in the 50s and 60s and lows in the 30s and 40s; abundant rain in virtually all months of the year (i.e., no drought, on average); prevailing winds out of the southeast during the warmer months, with brief cool, northerly winds in the colder months; high humidity during the warm season, and variable humidity in the cold; periods of overcast skies and rain or drizzle during the colder months, whereas during the warm months, frequent cumuliform clouds and periods of intense precipitation and thunderstorms, and severe, sporadic fall coastal weather associated with the invasion of tropical storms.

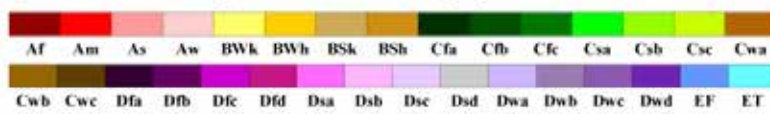
The **climatic controls** that produce these characteristics for Houston include: low (~30°) latitude and low elevation, so the Sun's rays are always high in the sky, and the daylight hours are fairly long any time during the year; abundant rain is due to nearness to the source of warm, moist, Gulf air masses and to convectional precipitation (thunderstorms) in the summer, and frontal-cyclonic precipitation (long periods of overcast skies and rain/drizzle) during the winter; late summer and fall tropical storms and hurricanes are common in subtropical latitudes, especially where there are vast areas of warm ocean water, and warm coastal ocean currents.

Weather and climate elements, therefore, characterize the climate of an area, whereas a group of climatic controls helps to explain why those characteristics occur. Since certain climatic controls are associated with latitude and relative location on the continent, the controls tend to repeat themselves in regular geographic patterns. This results in certain regions, determined by latitude and relative position on the continents, having fairly similar climatic characteristics over large areas, and this is the basis for identifying and differentiating global climates. These climatic regions, in turn, tend to have a distinctive vegetation assemblage, which is in large part a result of the prevailing climatic characteristics. Climate and vegetation are important factors that contribute to soil character, so there is a general relationship, at least on a global and regional scale, between climate, vegetation and soils. Ecosystems include the biological, physical and chemical aspects of distinctive assemblages of plants and animals and how they interact. Ecosystems occur at all scales, from microscopic to global. Ecosystem characteristics and function greatly influence the way that humans live with and use the land.

Several attempts have been made to classify climate on a global and regional scale, each one with strengths and weaknesses. One of the most widely used classifications was devised by the German climatologist **Wladimir Koeppen (1846-1940)** (Figure 7.1). The classification attempted to define the climatic characteristics that delineated broad zones of vegetation communities. Koeppen assumed that two climatic parameters, temperature and precipitation, were of paramount importance in determining the location and extent of these communities. Within certain limits of temperature and precipitation, the climate was sufficiently homogenous to produce a single, dominant climax ecosystem. Similarly, adjacent regions that were defined by different limits of temperature and precipitation produced a distinctly different ecosystem. Between ecosystems there may be a broad or sharp transition, or ecotone, between systems. These global-scale terrestrial ecosystems are often referred to as **biomes**. They are characterized by specific plant communities, and usually named after the predominant vegetation in the region. Examples of terrestrial biomes that have come under recent scrutiny because of their rapid degradation include the **tropical rainforest, grasslands, the Arctic tundra and the tropical savanna** (Figure 7.2).

### World Map of Köppen–Geiger Climate Classification

updated with CRU TS 2.1 temperature and VASCLimO v1.1 precipitation data 1951 to 2000



**Main climates**

- A: equatorial
- B: arid
- C: warm temperate
- D: snow
- E: polar

**Precipitation**

- W: desert
- S: steppe
- f: fully humid
- si: summer dry
- w: winter dry
- m: monsoonal

**Temperature**

- h: hot arid
- k: cold arid
- a: hot summer
- b: warm summer
- c: cool summer
- d: extremely continental
- F: polar frost
- T: polar tundra

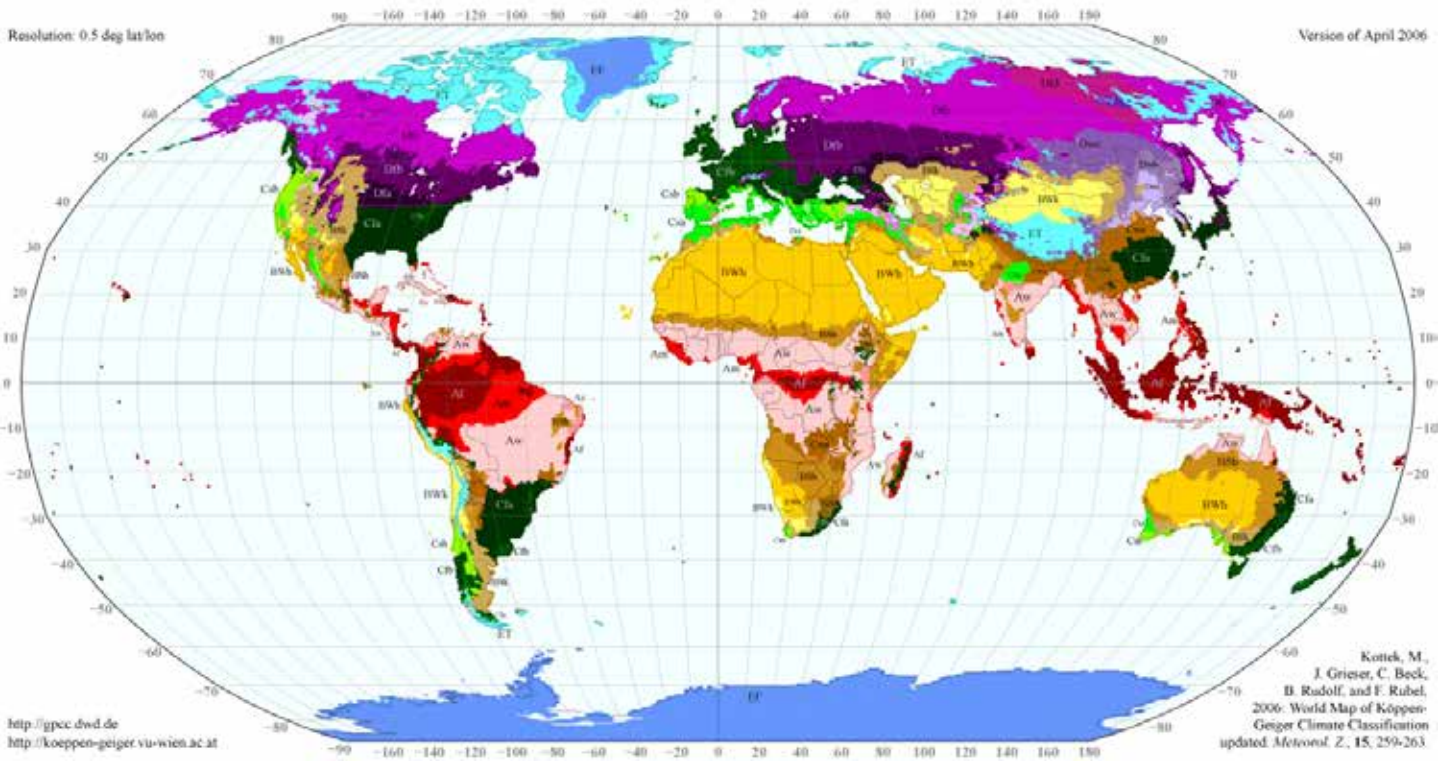


Figure 7.1. Climatic regions of the globe, modified from W. Koeppen and others. In general, the climatic types progress from A through E with increasing latitude. Types A, C, D, and E are defined primarily by temperature, whereas B climates are defined by inadequate precipitation (Source/Credit: M. Kottek, J. Grieser, C. Beck, B. Rudolf, and F. Rubel, 2006: World Map of Köppen-Geiger Climate Classification, updated. Meteorol.Z., 15, 259-263). See Appendix 1 for a slightly larger version of this map.

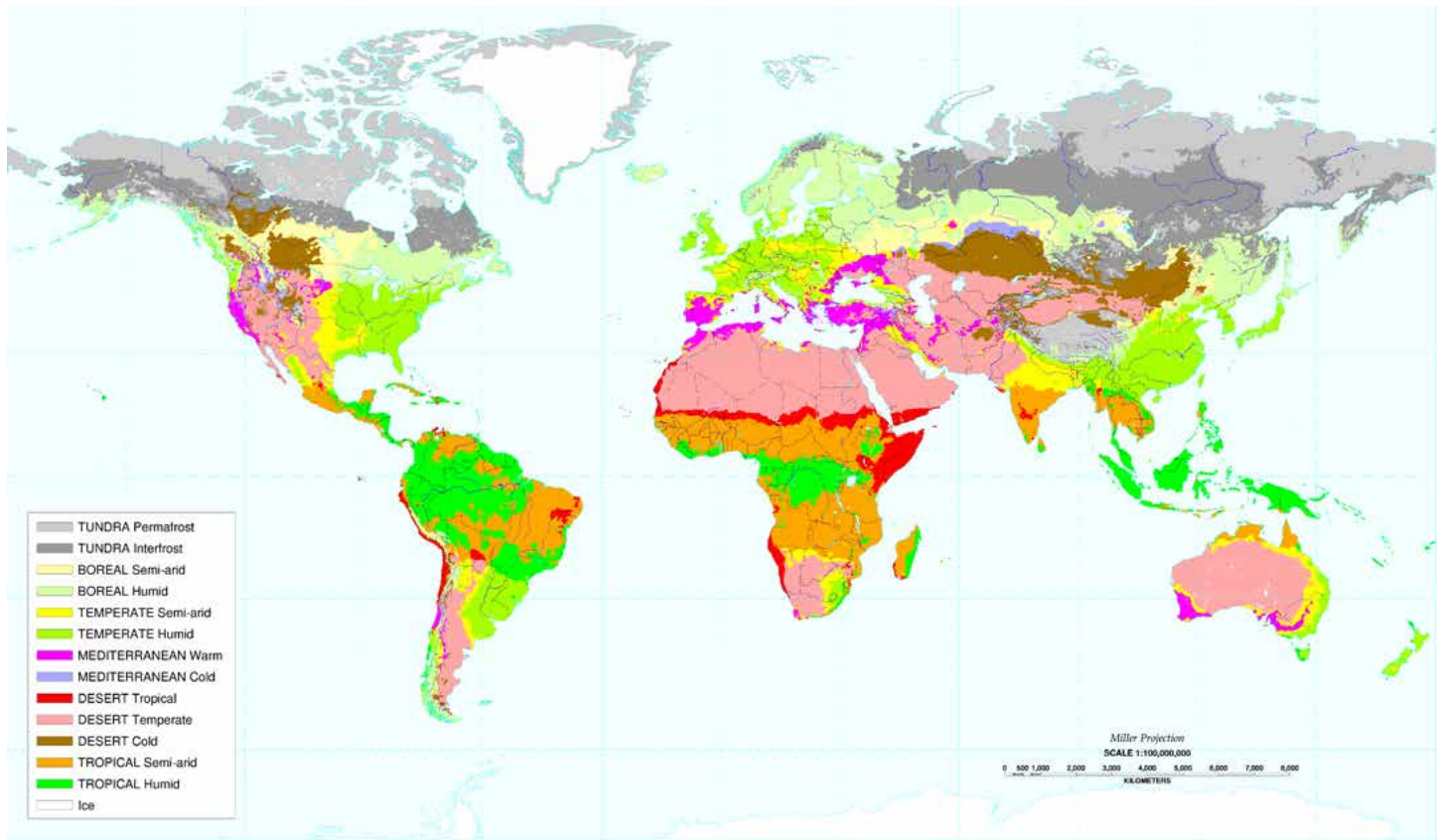


Figure 7.2. Major terrestrial ecosystems or biomes. The terrestrial ecosystems, on a global scale, correspond to the Koeppen climates. Factors other than climate also influence the distribution of ecosystems, so the correlation between climate and ecosystems is imperfect (Source/Credit: FAO).

Koeppen and his followers searched for the temperature and precipitation limits that define the boundaries of a biome, or ecosystem at any scale. For example, certain species of plants within the tropical rainforest require an average annual temperature of **64.4°F** or higher in order to persist, and the monthly precipitation must be more than what is lost through evaporation and plant transpiration (**evapotranspiration**), generally greater than **2.4 inches** per month.

Any climatic factors that generate climatic stress on plants can affect the distribution of vegetation communities. Examples include such things as seasonal or long-term drought, extreme temperatures (both high and low), available sunshine, soil moisture storage, strong, desiccating winds and catastrophic meteorological events (e.g., tornadoes and hurricanes).

Climate is perhaps the most important single factor in determining the type, density and distribution of vegetation. Vegetation, in turn, greatly influences the type, abundance and diversity of animals that can be supported in that environment. Climate and vegetation are the major factors that determine the soil type that evolves in that biome (Figure 7.3). The type of soil strongly influences the capacity of that soil to grow certain types of crops, and so directly affects human utilization of the land.

## Global Soil Regions

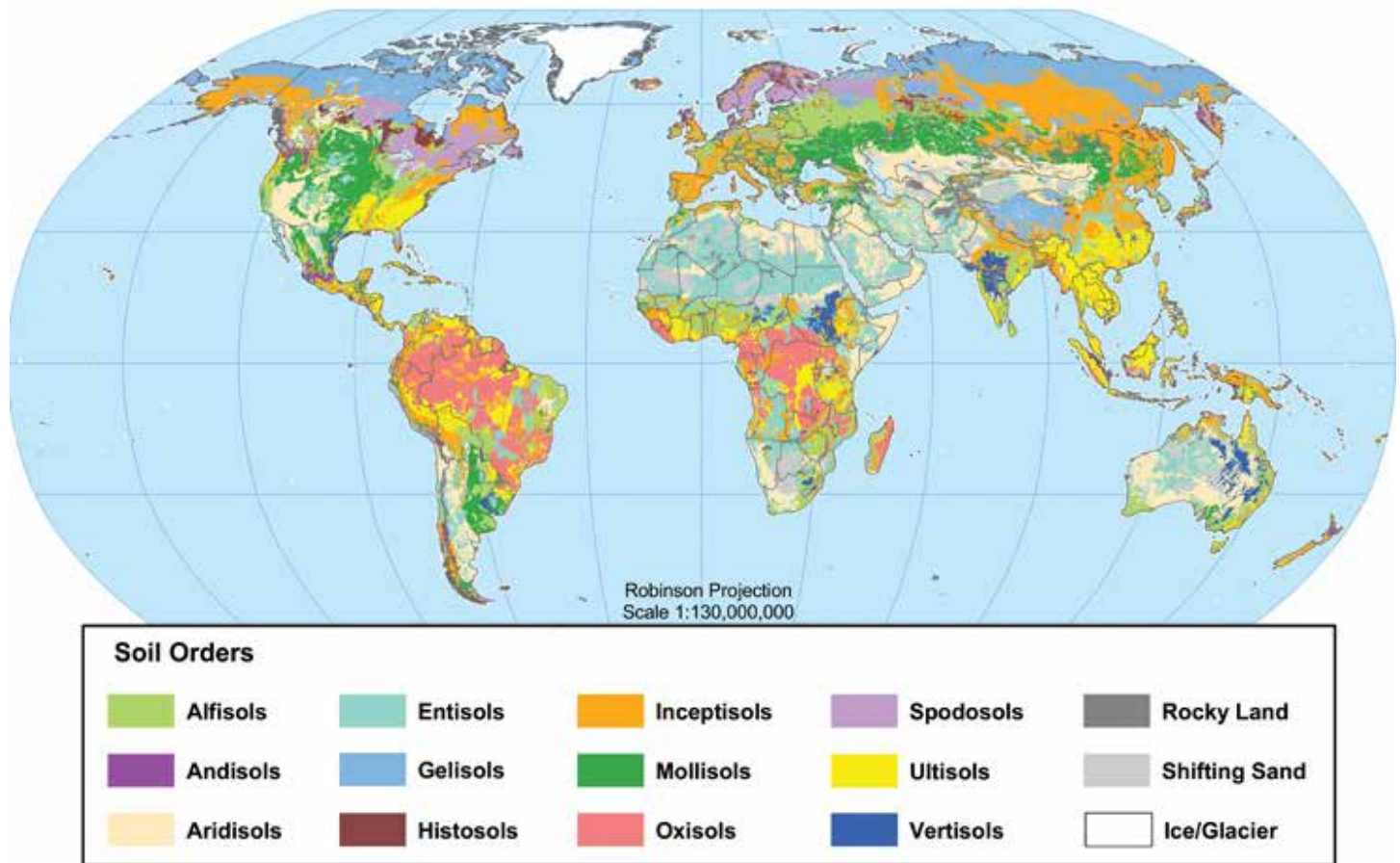


Figure 7.3. Global soil types. Climate and vegetation strongly influence the development of soil characteristics, so there is a general relationship between climate, vegetation and soils. Note, for example, the correlation between BS climate, grassland ecosystems and mollisols on the maps depicted in Figures 7.1 through 7.3 (Source/Credit: USDA).

Climate influences all aspects of our lives, including where we choose to live, the types of buildings and homes we live in, the types of clothes we wear, and the types of hazards we must deal with, such as snow and ice on roads. It is intimately associated with the type and rate of spread of certain diseases. It affects land and sea transport, and thereby the distribution of people, goods, medicine, food and clothing. Few things are not influenced directly or indirectly by weather and climate. It also influences our seasonal recreational activities, including the sports we watch or participate in (e.g., snow skiing and ice skating vs water skiing).

Climate affects our very existence and ability to sustain ourselves. For example, the mid-west of the United States is farm country and it feeds much of the nation. This is possible because the combination of climate and soils provides better conditions for agriculture than most other areas of the world. Favorable climate and soil provide a surplus of agricultural products that are shipped all over the world, helping maintain a healthy economy.

Climate also influences the geographic distribution of diseases. Malaria, for example, is confined to the tropics because the mosquitoes that carry the virus are limited to that area by climatic conditions; specifically, they cannot survive cold winters. We all know that colds are more common during winter. This results from three climate-related factors. The first is that many cold viruses are killed in summer by the more intense ultraviolet light at that time of the year. The lower levels of sunlight in winter result in a greater number of cold viruses. The second is that cold conditions are also dry conditions, and this causes the mucous membranes in our nose to dry and crack, providing a *port of entry* for viruses. Finally, because of the cold conditions during winter, we stay inside more and, as a result, are subjected to an onslaught of viruses transmitted by the people around us.

## Basic Climate Patterns

Temperature and precipitation, and the seasonal distribution of each, are the two main criteria for defining climatic regions. Some of the basic patterns of these variables include:

- Temperature Patterns
  - Mean annual temperature decreases with increasing latitude.
  - The annual range of temperatures increases with increasing latitude.
  - The annual temperature range is greater for continental interiors than for coastal areas at similar latitudes.
  - Temperatures are warmer for areas affected by warm ocean currents and colder for those affected by cold currents.
- Amount of precipitation
  - Abundant year-round precipitation occurs along the Equator.
  - Higher levels of precipitation occur along windward coasts.
  - Precipitation is sparse in areas of seasonal or persistent high pressure.
  - The leeward side of mountains is drier than the windward side.
  - Lower levels of precipitation occur on leeward coasts.
  - Lower levels of precipitation occur in areas affected by continental air masses.
- Seasonal Patterns of Precipitation
  - Abundant precipitation throughout the year (e.g., persistent Intertropical Convergence Zone [ITCZ] or frontal cyclones).
  - Summer drought (e.g., summer domination by the Subtropical High [STH]).
  - Winter drought (e.g., winter monsoons).

## Climograms

**Climograms** are graphical devices that are used to portray monthly information about temperature and rainfall in order to provide a visual summary of the climate (Figure 7.4). The line at the top of the climogram is a plot of the average monthly temperature over the course of the year. The temperature scale used here is represented by a red line that plots mean monthly temperatures, with the scale (degrees F) given on the vertical axis on the right side of the climogram. The bars at the bottom of the climogram show the average monthly rainfall values and the scale is given on the vertical axis on the left margin of the climogram.

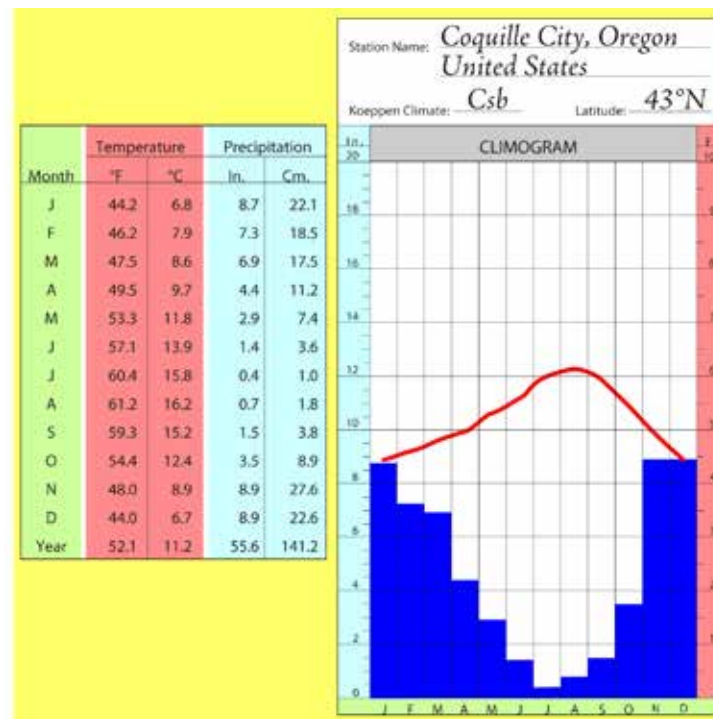


Figure 7.4. A climogram of Coquille City, Oregon. Temperatures are mild year-round, and there is a distinct winter-wet and summer dry precipitation pattern. Temperatures are mild because of the combined influence of the westerly winds, maritime influence, and cold California ocean current. Wet winters are the result of frequent passages of frontal cyclones; drier summers result from the poleward migration of the dry (stable) side of the oceanic subtropical high (STH).

The temperature and moisture characteristics of a place that are portrayed graphically on a climogram are determined by a set of climatic controls. The climatic controls are determined by relative geographic location. Temperature and annual temperature range are clues to latitude and continentality (location in the continental interior) vs maritimity (coastal location, particularly a windward coast). Precipitation type and amount are clues to latitude, relative position on the continent, proximity to mountain barriers and domination by high vs low pressure systems. For example, if there is virtually no change in monthly average temperatures over the course of a year, and if the temperature values were also high, this would indicate an equatorial latitude. Further evidence of low latitude would be abundant



precipitation in all months. If two places were located at 40°N, and one had a large annual temperature range, whereas the other had a small range, this would suggest that the former was located in the continental interior and the latter along a coast. Dry summers for a lower mid-latitude location such as Los Angeles, California or Santiago, Chile (34°N and 34°S) indicate position on the western side of the continent, dominated by the drought producing effects of the subtropical high and cold ocean current. Large annual temperature ranges, with summer months in the 60s or 70s and winter months near zero, indicate higher latitudes, perhaps in Canada or northern Russia.

For example, the temperature pattern in the climogram and data table in [Figure 7.4](#) suggests a mid-latitude, Northern Hemisphere location. High latitudes would have colder temperatures (one or more months below freezing), and low latitudes would be much warmer. The small annual temperature range (difference between the warmest and coldest monthly mean; in this case  $61.2 - 44.0 = 17.2^{\circ}\text{F}$ ) implies a coastal location, moderated by winds coming from the ocean most of the year. The coolness of the summer months is likely due to the influence of a cold current, such as off the west coasts of continents in the mid-latitudes. Very wet winters and dry summers are consistent with a mid-latitude, west coast location, where frontal-cyclones bring abundant winter rainfall, but are blocked during the summer by the dry side of the oceanic STH. The climogram represents Coquille City, Oregon, at 43°N on the coast. Other mid-latitude west coast locations should be affected by similar climatic controls, and so should have the same temperature and moisture characteristics.

## Koepfen Climate Classification

Since Koepfen devised the climate classification system to define the limits of vegetation communities, there is a close correlation of climatic types with vegetation and soil. The major Koepfen climate types are **A, B, C, D, E,** and **H**. Climate types A, C, D, and E are based on temperature. B climates are defined according to inadequate precipitation. The H climates are those that occur in highlands and mountains, where climate, vegetation and soil types change rapidly with increase in elevation. The Koepfen climates A through E are generally arranged according to latitude. For example, the **A (tropical) climates** occur in the tropics, the **B (arid/semiarid) climates** occur in the subtropics (i.e., the Subtropical High Pressure belt) and in orographic rain shadows, the **C (moist mid-latitude with mild winters) climates** occur in the mid-latitudes, the **D (moist mid-latitude with severe winters) climates** in the high mid-latitudes, and the **E (polar) climates** occur in the polar regions. The correspondence between climate type and latitude is not perfect because latitude is certainly not the only factor affecting climates. Similarly, there will be discrepancies in the relationship between climate, vegetation and soils, because climate is not the only factor that affects their distribution.

Within each of the major categories, there are subcategories indicated with lower-case letters. Each letter signifies a unique characteristic of that climate. In many cases, the second letter indicates the precipitation regime, and the third indicates the nature of the summer or winter temperature extremes. For example, in the **Cfa climate** (which includes all of East Texas) the letter **C** signifies that the climate is a humid, mild mid-latitude climate (i.e., no monthly average temperature is below freezing). The second letter, **f**, signifies adequate precipitation throughout the year. The third letter, **a**, signifies a long, hot summer season.

Climate classification is not just a simple task of memorizing letters, names and numbers. It is an attempt to understand relationships between physical and biological systems, and to attempt to establish cause and effect on regional to global scales. An understanding of ecosystem location and dynamics aids us in making sound judgments about managing the land. Understanding the complex relationships between climate and ecosystems will also aid in predicting and coping with present and future climatic change.

## **Tropical Climates (A Climates)**

**Tropical climates are winterless climates.** All monthly mean temperatures are above 64.4°F. Many tropical plants will not survive colder temperatures. The three major subtypes for tropical climates are **Af**, **Am**, and **Aw**. The letters f, m, and w represent rainfall regimes. The **tropical humid** (or **tropical wet**) (Af) climate has uniform, plentiful rainfall throughout the year. The **tropical monsoon** climate (Am) experiences massive amounts of rainfall during the summer, but has dry winters. The **tropical wet-dry climate** (Aw) has a pronounced winter drought and moderate, high-Sun precipitation.

## Tropical Humid (Tropical Wet) Climates (Af)

The tropical wet climate is a lowland climate (typically less than 3000 feet, or less than 1000 meters) associated with the Equatorial Low pressure system and the convergence of the Northeast and Southeast Trade Winds. Although this pressure trough migrates north and south with the vertical rays of the Sun, the pressure trough is broad enough to dominate equatorial latitudes throughout the year (Figure 7.5). Surface convergence, the availability of warm, moist air from widespread tropical oceans, and daily heating of the ground to destabilize air combine to generate substantial rainfall in all months of the year. Rain falls almost daily in this climate, and it follows a somewhat predictable cycle. In the early morning, the air is damp and the skies are relatively clear. As the Sun warms the Earth, added moisture and an increase in the environmental lapse rate typically result in cumulonimbus cloud development. By the afternoon, cumulonimbus clouds form, and thunderstorms bring abundant rainfall. Once the air begins to cool as nightfall approaches, the clouds dissipate — until the next day when the cycle repeats itself. Rainfall amounts average between 68 and 98 inches (173 and 249 cm) per year (Figures 7.6a and 7.6b), though the maximum may exceed 200 inches (508 cm).

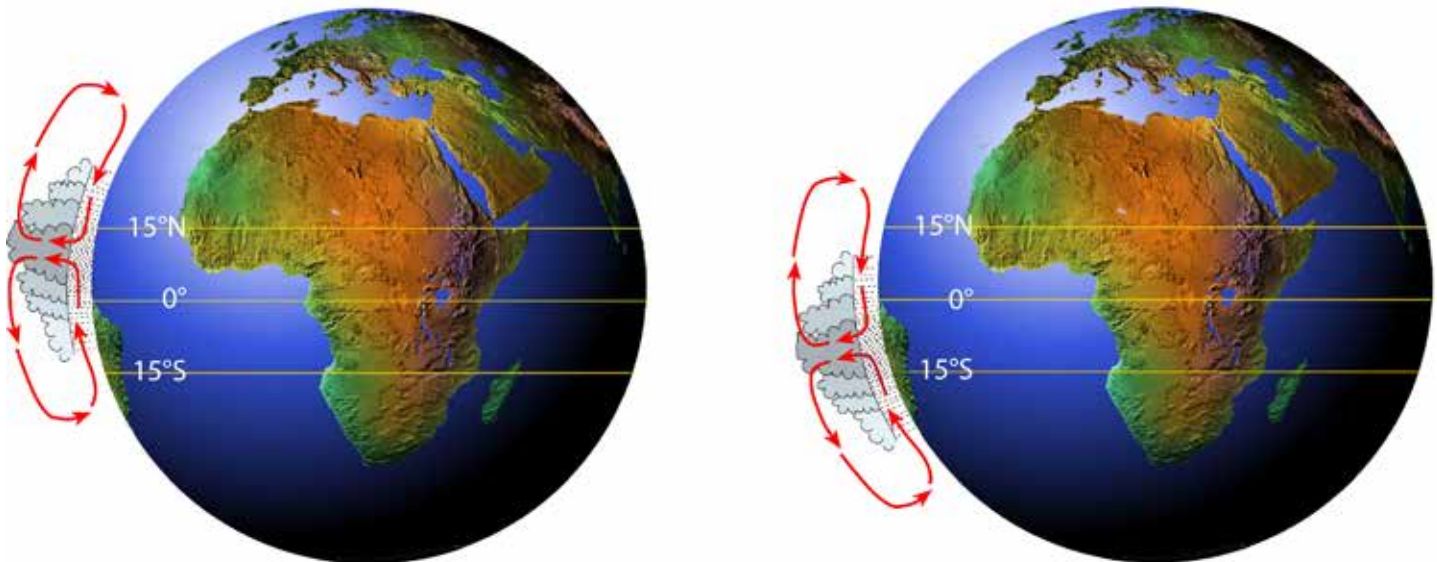


Figure 7.5. Cross-section of the Hadley cell and the seasonal movement of the Intertropical Convergence Zone (ITCZ). Latitudes of a few degrees on either side of the Equator are under the influence of the rain-producing ITCZ in all seasons. Zones at around 15°N/S are alternately under the influence of the rainy ITCZ (summer) and drought-producing subtropical high (STH) during the winter.

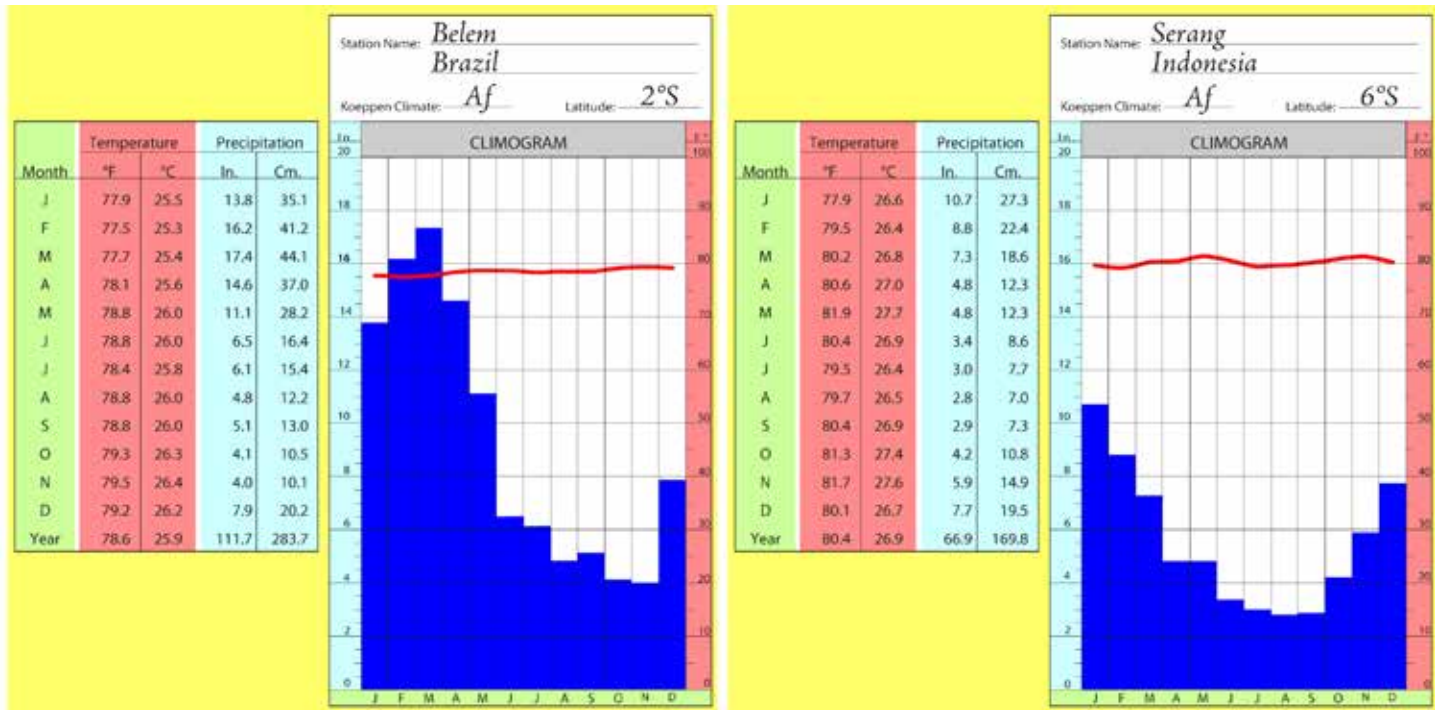


Figure 7.6a. (left) Climogram of Belem, Brazil, a tropical humid (Af) climate.

Figure 7.6b. (right) Climogram of Serang, Indonesia, also a tropical humid (Af) climate. These climates are characterized by uniformly warm temperatures in all months (more than 64.4°F), and adequate moisture in all months (more than 2.4 inches/month).

The equatorial location results in a very small annual temperature range of only a few degrees Fahrenheit. The high moisture content of the air, in conjunction with its low elevation, limits daily temperature fluctuations to only 14° to 18°F (7.8° to 10°C). The equatorial location also means that there is always very close to 12 hours of daylight and darkness every day of the year. This climate is one of overarching *sameness* from one day to the next. It is always warm and humid.

The copious rainfall, high temperatures and abundant solar radiation **give rise to the most prolific and biologically diverse biomes of the world**, the **tropical rainforests**. There is little climatic stress on vegetation, so there are endless habitats for both plants and animals. In addition, these areas were never glaciated during the Pleistocene (~2.588 million to ~12000 years ago), so the ecosystem composition has changed very little over millions of years.

Although tropical rainforests cover less than 10% of the Earth’s land surface, and constitute only one-third of the forests of the world, they contain more than 50% of the vegetation biomass and 40 to 50% of all of Earth’s plant and animal species. For example, more than 1000 species of beetles have been found in a single tree, and more than 43 species of ants, which is more than found in all of Britain. Several hundred species of trees may be found in an area the size of a football field. Unfortunately, many of the species in the rainforests are threatened

with extinction because of the cutting and burning of rainforests for lumber and to create agricultural land.

The tropical rainforest is dominated by **broadleaf evergreen trees**, which are in competition for available sunlight and space (Figures 7.7a and 7.7b). This results in a very dense canopy of trees, and very little direct sunlight actually reaches the forest floor in the true rainforest. Competition for sunlight is also reflected in the structure of the forest, which is sometimes described as *three-tiered*. The tallest trees make up the emergent layer, some 100 to 150 feet in height (Figure 7.8). The main canopy is somewhat lower, and tends to form a continuous canopy of coalescing tree crowns. The bottom tier of trees, typically only a few tens of feet in height, is discontinuous, much like the emergent tier. Each lower layer is better adapted to shade. The forest floor, contrary to popular misconception, is relatively devoid of ground cover because of the lack of direct sunlight. The tropical rainforest is considered the **climatic climax** community of the Af and some Am climates. Climatic climax vegetation is in relative equilibrium with the prevailing climate, provided that the vegetation is not disturbed by fire, disease or humans.



Figure 7.7a. The “pre-montane” forest in Mindo, Ecuador is very similar to the tropical rainforest that occurs at slightly lower elevations. The montane forest is moist, green and lush, like the tropical rainforest, but somewhat cooler because of higher elevations. Even though there is a season of sparse rainfall, the constant cloudiness and high humidities of the cloud forest keep it evergreen year-round. The abundance of epiphytes, mosses, ferns, orchids and algae reflect the moist nature of the montane forest (Source/Credit: Richard Payne).



Figure 7.7b. Broadleaf evergreen forests that are similar to the tropical rainforest extend as far north as Puerto Rico, at  $\sim 18^\circ\text{N}$  latitude. (Source/Credit: Guy Smith Memorial Slide Collection, USDA).

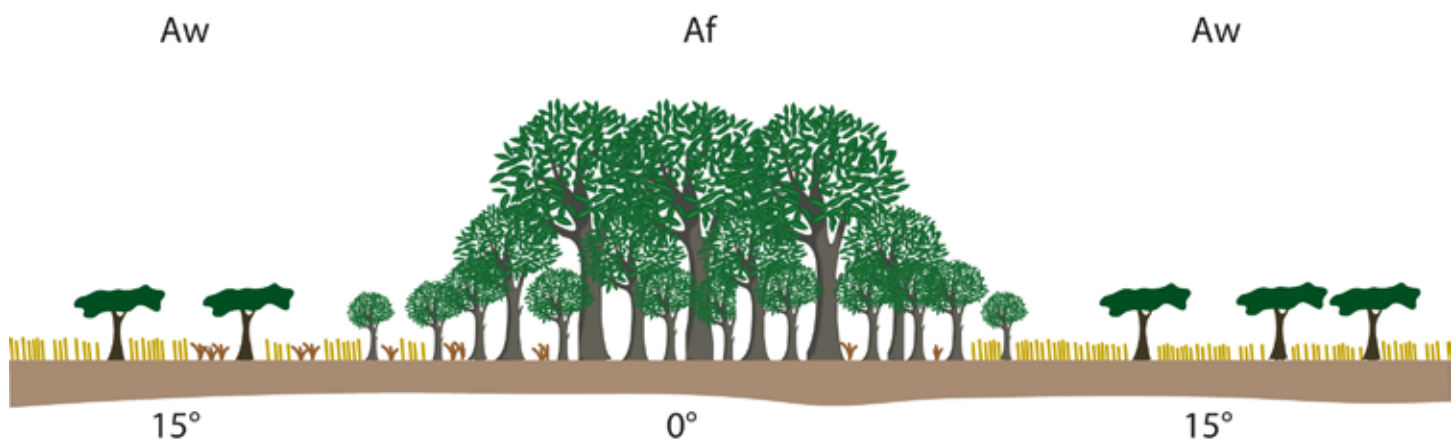


Figure 7.8. Latitudinal cross-section of climate and ecosystems from the tropical rainforest at equatorial latitudes to the tropical savanna at approximately  $8^\circ$  to  $23^\circ\text{N/S}$ . In the transition zone between these ecosystems is the semi-deciduous tropical forest, where the forest canopy is continuous, but the three-tiered nature of the tropical rainforest gives way to a single, continuous canopy.

In every ecosystem, disturbances occur that temporarily remove the climatic climax vegetation. These **successional vegetation communities** in the tropics are represented by the **tropical jungle**, a low, nearly impenetrable ground cover of vegetation whose species composition changes continually until the climax community is re-established. The dense ground cover requires abundant direct sunlight, so many river banks, or **riverine** communities, have jungle structure.

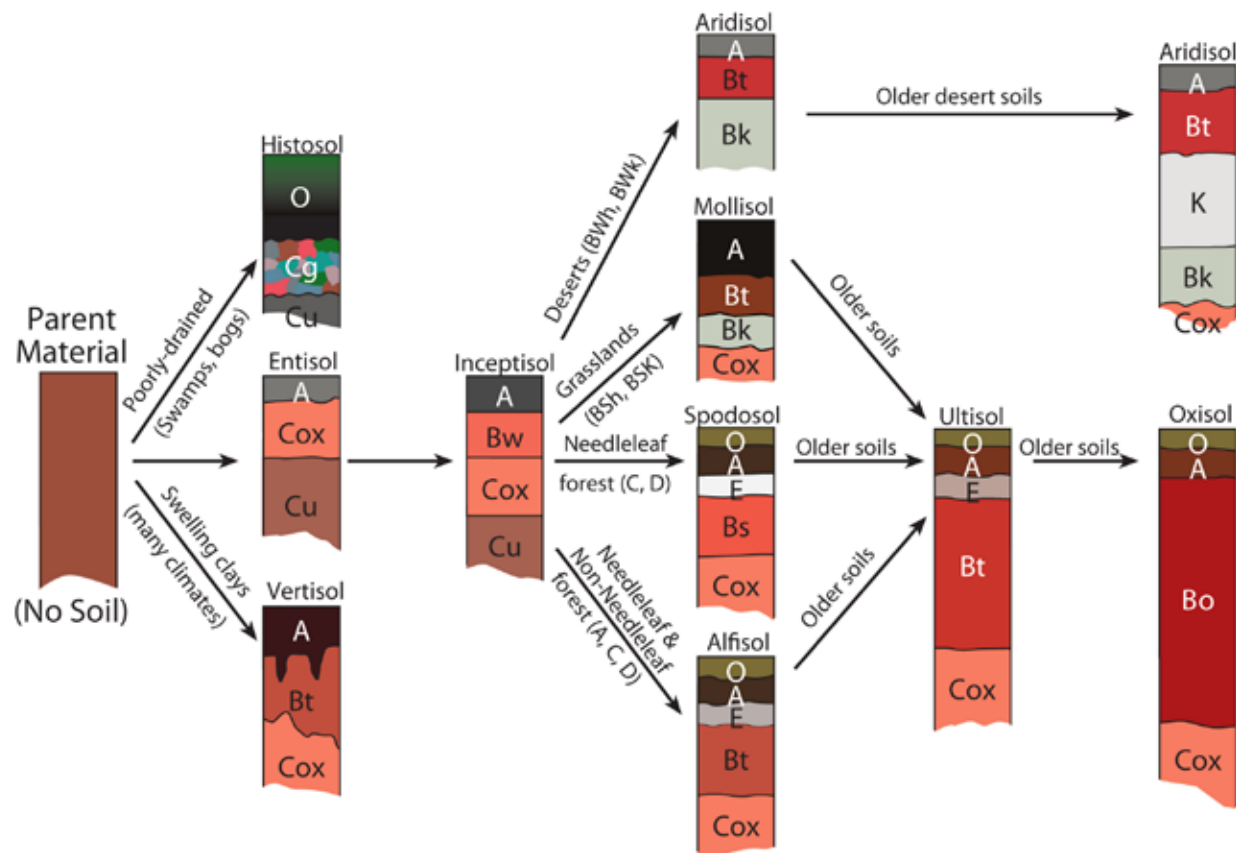
Other adaptations to competition for sunlight are seen in **lianas**, which are climbing woody vines and **epiphytes**, which are plants that live on other plants in order to maintain a position that is high enough in the canopy to guarantee sufficient sunlight for photosynthesis. Many of the potted household plants in the United States, such as the bromeliads, (e.g., Fosters favorite) are epiphytes. Some trees have **buttressed roots** (Figure 7.9), which may be an attempt to gain structural support in soils that are frequently water-saturated.



Figure 7.9. Buttressed roots and lianas in the tropical rainforest, Australia. The flared base of the trunk offers structural support in soils that become water-saturated. The climbing, woody lianas have completely encased the tree trunk (Source/Credit: Marcus Gillespie).



Soils in the tropics tend to be very old and heavily altered by chemical, physical and biological weathering. As soils develop, they tend to exhibit layers, called **horizons**. Soil horizons are distinguished from each other by such things as color, and the relative proportion of sand, silt, and clay, primary and secondary minerals and organic content. As soils develop progressively through time, they tend to lose their original geological characteristics, and take on properties that are determined by factors such as climate, organisms (including vegetation), slope and degree of weathering (Figure 7.10).



- O Horizon:** Surface horizon dominated by organic matter (e.g., leaves) in various stages of decay
- A Horizon:** Surface horizon or beneath O horizon dominated by mineral matter, but with sufficient humus to darken color
- E Horizon:** A light-gray subsurface horizon that has been leached of pigments by organic acids produced by the decay of needleleaf litter
- Bw Horizon:** A young B horizon that has been slightly reddened by oxidation, but is not yet clay-enriched
- Bs Horizon:** Illuvial accumulation of amorphous organic matter – sesquioxide ( $\text{Al}_2\text{O}_3$ ;  $\text{Fe}_2\text{O}_3$ ) complexes
- Bk Horizon:** A light-colored B horizon due to the coating of mineral grains by carbonates
- Bt Horizon:** A 'mature' B horizon that is reddened by oxidation as well as clay-enriched
- Bo Horizon:** A deep red, highly weathered and leached B horizon rich in residual sesquioxides; usually restricted to very old soils in tropical climates
- Cox Horizon:** An oxidized horizon beneath a B or A horizon
- K Horizon:** Similar to a Bk horizon, but so greatly enriched in carbonates that the horizon is white
- Cg Horizon:** A 'gleyed' subsurface horizon that shows patchy zones of blue, gray and green colors from reduced conditions; may be local areas of oxidized material
- Cu Horizon:** Unweathered parent material

Figure 7.10. Soil development chart. Soils develop in stages through time, influenced by such things as the geologic material from which they form (the parent material), climate, vegetation, slope angle and aspect and time. Soils on the right-hand side of the chart are generally older (more mature) than those on the left (Source/Credit: modified from Dennis I. Netoff and Ava Fujimoto-Strait, *Weather & Climate Lab Manual*).

The soil types in the tropical rainforests are **oxisols** and **ultisols**, with lesser areas of **inceptisols** (Figures 7.11a, 7.11b and 7.11c). **Oxisols** are deeply and intensely weathered. The original mineral content of the soil has been so intensely altered that only the most chemically resistant minerals and compounds remain. They are dominated by iron and aluminum oxides and hydroxides and clay minerals. The iron oxides impart a rich red color to the **B horizon** of the soil. These very old soils have thick weathering profiles, and the oxidized **C horizon** may extend tens of feet into the subsurface. Many of the important nutrients have been removed from the soil profile by countless years of downward percolating water, a process called **leaching**. **Excessive leaching has left these soils relatively infertile, in terms of producing high-protein crops such as grains and corn.** The limited amount of nutrients that are made available in the soil by chemical processes are either held in the vegetation canopy or the uppermost few inches of the *topsoil*, the **A horizon** of the soil. When these areas are cleared for high-protein agricultural use, their fertility is limited to just a few years, after which they must either be abandoned, or heavily fertilized.

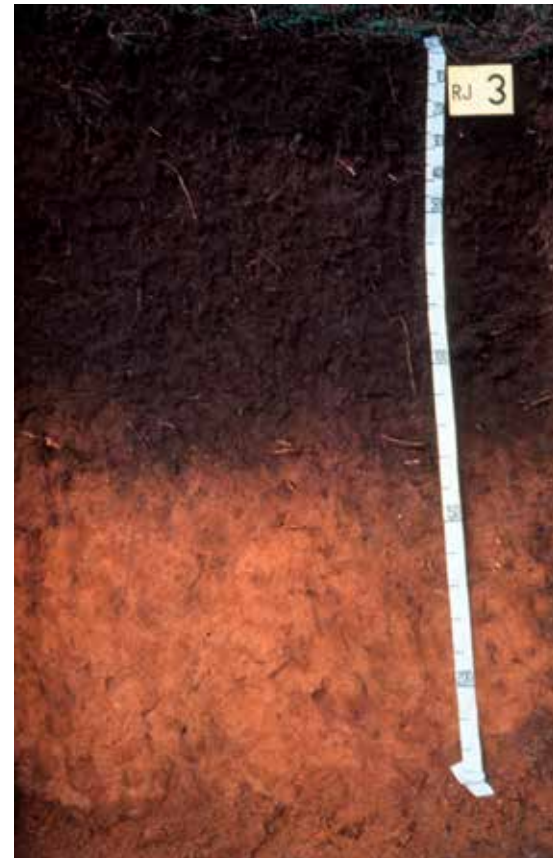
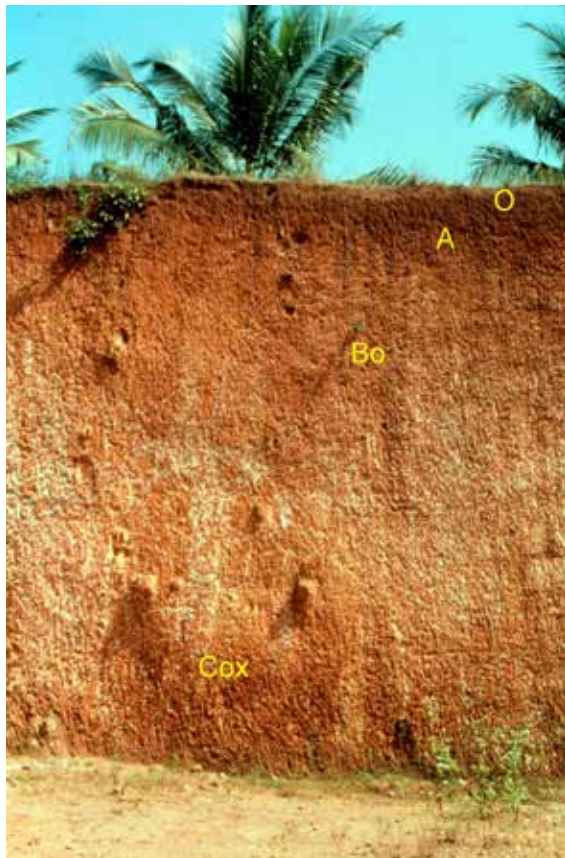


Figure 7.11a (left). A relict oxisol (formed in a previous time when conditions were more tropical humid) in India. Note the (1) deep weathering profile, (2) deep reddish colors, indicating large amounts of oxidized iron, and (3) the vague boundaries between soil horizons. Oxisols and their slightly less-weathered counterparts, ultisols, are the old, mature soils of the tropics (Source/Credit: USDA Guy Smith Memorial Slide Collection).

Figure 7.11b (right). Although many oxisols and ultisols have thin A horizons because of the rapid rate of humus decomposition, some form under conditions that are favorable for thick A horizon development, and they can be moderately fertile (Source/Credit: USDA Guy Smith Memorial Slide Collection).



Figure 7.11c. Oxisol and superimposed ultisol formed on volcanic ash on Hawaii. The abundant rainfall and continuous growing season make these soils well-suited for growing carbohydrate-rich crops such as sugar cane. Their ability to produce high-protein crops is somewhat limited by their low nutrient content, which is in part due to the long, intense weathering and leaching (Source/Credit: USDA Guy Smith Memorial Slide Collection).

When clay-rich oxisols and ultisols are exposed to the Sun due to deforestation, the soil bakes into a hard, brick-like condition. When the soil reaches this state, it is referred to as a **laterite**. Lateritic soils are so hard that they have been used for centuries as construction material.

Floodplain soils in the tropical rainforest are not as well developed in terms of age or horizons, but their fertility is replenished by each year's receding floodwaters (Figure 7.12). Floodwaters deposit sand, silt, and clay, as well as organic nutrients. These inceptisols are some of the most productive of all tropical soils.



Figure 7.12. Satellite image of the Amazon River during flood stage and the surrounding tropical jungle (along water courses) and tropical rainforest (interior, away from water courses). The frequent flooding renews soil nutrients, and keeps the agricultural potential of these inceptisols (young soils) high. A curious pattern of cumulus humilis clouds have formed over the forested area, but the water courses are almost devoid of clouds. This is likely due to the more buoyant air over the forests as a result of higher temperatures and greater moisture content than the air over water (Source/Credit: NASA's Earth Observatory, August 29, 2009).

It has been estimated that approximately half of the rain that falls in a tropical rainforest each day comes from the transpiration of water from the plants themselves. This means that, if a large area of the rainforest is cleared, it can literally alter the climate by reducing rainfall. And, if the cloud cover is diminished by the reduction in water vapor, temperatures at the

surface will increase, as will wind speeds when the trees are removed. The combination of higher wind speeds and higher temperatures enhance the drying of the soil (and the forest environment in general), further altering the nature of the forest and threatening species.

Several valuable species of trees are lumbered in the tropical rainforest, including hardwoods such as teak, mahogany, rosewood and ebony. Harvesting them is expensive, however, because of the species diversity, resulting in astronomical costs of some of the lumber produced.

## Tropical Monsoon Climates (Am)

Tropical monsoon climates occur along coastal zones of Southeast Asia, India, the Caribbean, Indonesia and the northeastern coast of South America (Figure 7.01). These climates are dominated by monsoon winds which bring moisture during the season of high Sun. **The moist air is de-stabilized as it is heated over land, and the precipitation greatly enhanced by orographic barriers.** Monsoon climates typically have well over 100 inches (254 cm) of annual rain, despite having a dry season. This climate experiences a short dry season during which precipitation drops to below 2.4 inches (6 cm) for one or more months of the year. Because the dry spell is typically short, the soil moisture remains high year-round, and the ecosystem is very similar to the tropical rainforest, though not as species-diverse, and some of the trees may be deciduous. The three-tiered effect may not be as conspicuous as in the tropical rainforest. Ground-cover vegetation is abundant where sunlight can penetrate the forest canopy, such as on steep slopes. The maximum temperature often occurs during the season of low Sun because of reduced cloud cover at this time of the year (Figure 7.13). One of the main crops in this region is rice production, concentrated on the fertile inceptisols of floodplains and deltas.

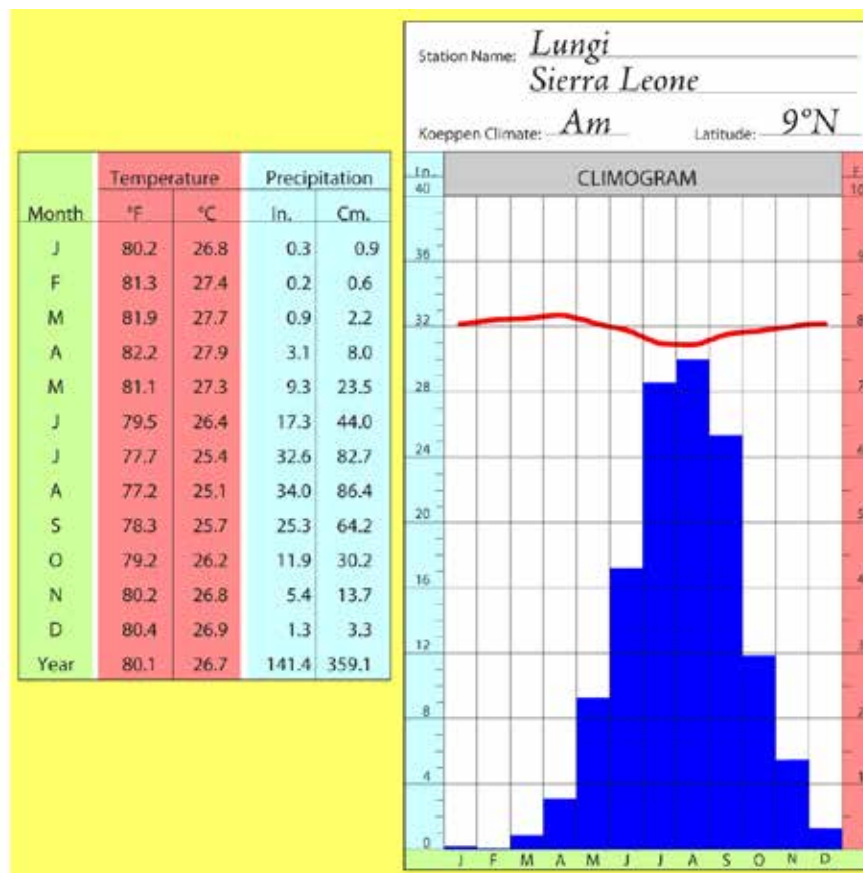


Figure 7.13. Climogram for Lungi, Sierra Leone, an Am (tropical monsoon) climate. Although there is very little annual temperature range, there is a very distinct wet-and-dry cycle caused by the monsoonal circulation. Monsoon climates, as defined here, have annual rainfall that averages more than 100 inches (more than 161 cm). Elevation of Lungi is 82 feet (25 m).

## Tropical Wet and Dry Climates (Aw)

Between the tropical humid region and the dry subtropical high pressure belt, occurs a transitional climate known as the **tropical wet and dry climate**. This climate has a distinct wet season that occurs when the Intertropical Convergence Zone moves overhead during the season of high Sun (Figure 7.14), and a distinct dry season that occurs when the subtropical belt of high pressure moves over the region during the season of low Sun. Precipitation may fall below 2.4 inches per month for as many as six months, producing considerable climatic stress on vegetation. During the wet season, precipitation is sufficient, but typically far below the values measured in the tropical monsoon climates (Figure 7.15). Because the dry season is longer than that of the monsoon climate, some of the trees may lose their leaves in order to conserve moisture. This creates a **semi-deciduous tropical forest** (Figure 7.16) which bears some resemblance to the tropical rainforest along its wetter margins (see Figure 7.8). In the drier margins of the Aw climates, the trees become so widely spaced that their crowns no longer overlap, creating an open forest similar to what are called woodlands in the mid-latitudes (Figure 7.17). As the trees become even more widely spaced, the dominant form of vegetation is a vast ground cover of grasses and shrubs. This is the famous **tropical savanna**, the setting for scores of Hollywood movies (Figure 7.18). In South America the savanna grassland areas are called **llanos** or **campos**. Many ecologists conclude that the structure of the savanna may be in large part due to forest and grassland fires, both natural and human-induced (Figure 7.19). Many trees have adapted to this by becoming *fire resistant*. They have fire-tolerant bark and leaves (Figures 7.20a, 7.20b and 7.20c) as well as deeper roots in order to gain access to deeper sources of ground water which are more reliable than shallow sources.





Figure 7.14. Convective afternoon showers in the Cerrado of Brazil. Much of the precipitation in the A climates is convective in origin. The humid air becomes convectively unstable in the afternoon hours when lapse rates are high, and afternoon thunderstorms frequently occur (Source/Credit: Richard Payne).

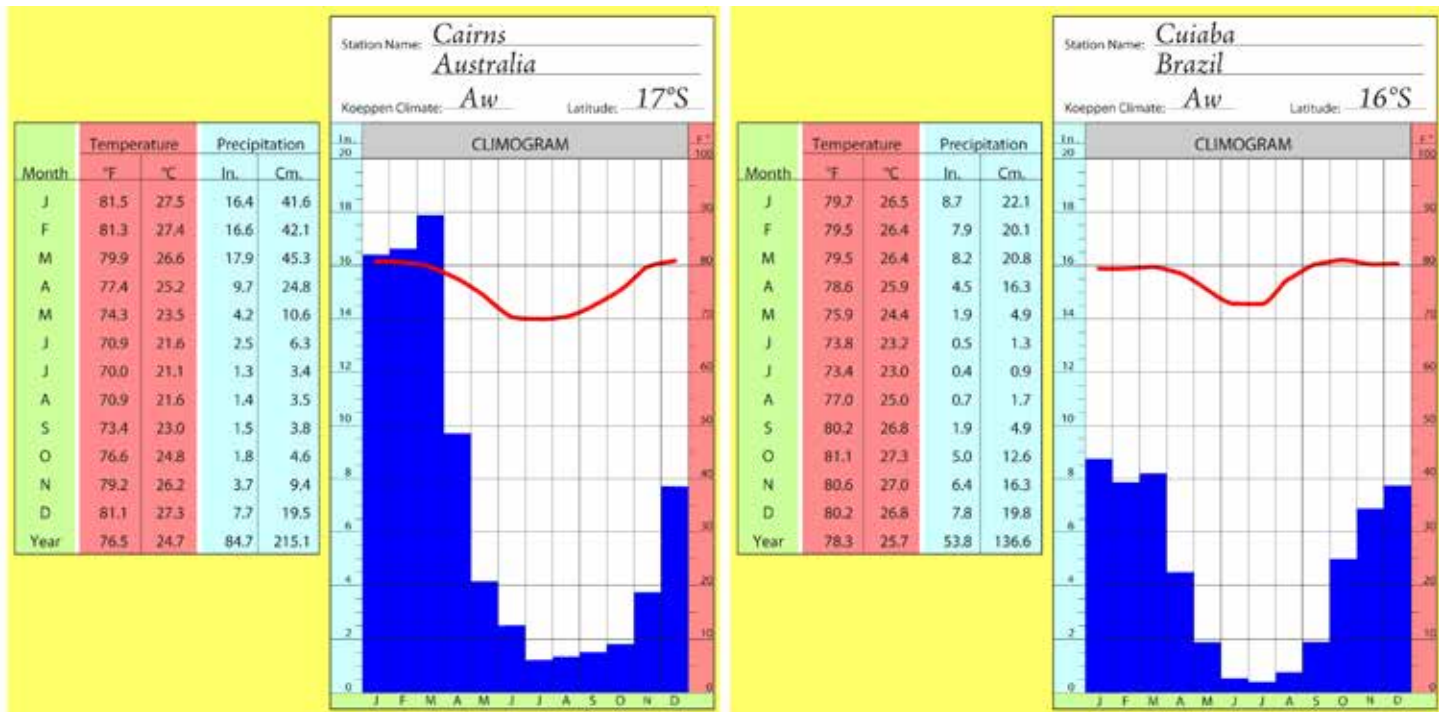


Figure 7.15. Climograms of Cairns, Australia, at 17°S and Cuiaba, Brazil, at 16°S. The Aw (tropical wet-and-dry) climates have 3-6 months of drought during the low-Sun season, and 6 or more months of adequate (more than 2.4 inches/month) precipitation during the high-Sun season. The alternating influence of the ITCZ and the STH is largely responsible for the seasonal precipitation pattern (see Figure 7.5, at 15° to 18° latitude).



Figure 7.16. The semi-deciduous tropical forest of the Cerrado, Brazil (Source/Credit: Richard Payne).



Figure 7.17. Low, oblique aerial photograph of savanna vegetation in northern Australia, in the Bungle-Bungle massif. The vegetation community consists of scattered trees, or tree clusters, separated by a vast understory of grasses and shrubs (Source/Credit: Dennis I. Netoff).



Figure 7.18. Flooded grassland savanna of the Pantanal region, Brazil (Source/Credit: Richard Payne).



Figure 7.19. Fire in the eucalyptus savanna of northern Australia, west of Katherine. Fire is a natural component of the savanna ecosystem and has undoubtedly helped shape the structure of the savanna landscape over millennia. Today, human-induced fire is a common practice to destroy the ground-cover shrubs to promote grassland succession (Source/Credit: Dennis I. Netoff).



Figure 7.20a. Fire-resistant trees, such as dozens of species of the Australian eucalyptus, are unscathed after a grass-brush fire only weeks prior to this photo (Source/Credit: Dennis I. Netoff).



Figure 7.20b. (left) The baobab tree (Australian boab). The odd-looking tree, sometimes described as an upside down tree with its roots exposed, is another fire-tolerant species of the Australian savanna (Source/Credit: Dennis I. Netoff).

Figure 7.20c. (right) Baobabs can live for well over 1000 years. Ghost gum and baobab, northern Australia savanna (Source/Credit: Dennis I. Netoff).

Aw climates are located poleward of Af climates and equatorward of the subtropical high pressure belts (see Figure 7.1). This climate occurs both north and south of the Amazon rainforest, in western Central America, in south central and eastern Africa, in western Central America, and parts of India and Southeast Asia. Because this climate occurs poleward of the moist tropics, the annual temperature range increases, ranging from 5°F to 20°F (2.8°C to 11.1°C). The daily temperature range also increases, reaching a maximum during the dry, low-Sun season

when there is less moisture in the air to trap heat at night. Rainfall values average 40 to 60 inches (102 to 152 cm).

Soils in the Aw climates are typically not as heavily weathered and leached as they are in the Af climates. There are still, however, considerable areas of ultisols, but **alfisols** are also common (Figure 7.21). Soils tend to be more nutrient-rich than the oxisols of the Af climates. Inceptisols dominate on the fertile and heavily farmed floodplains.

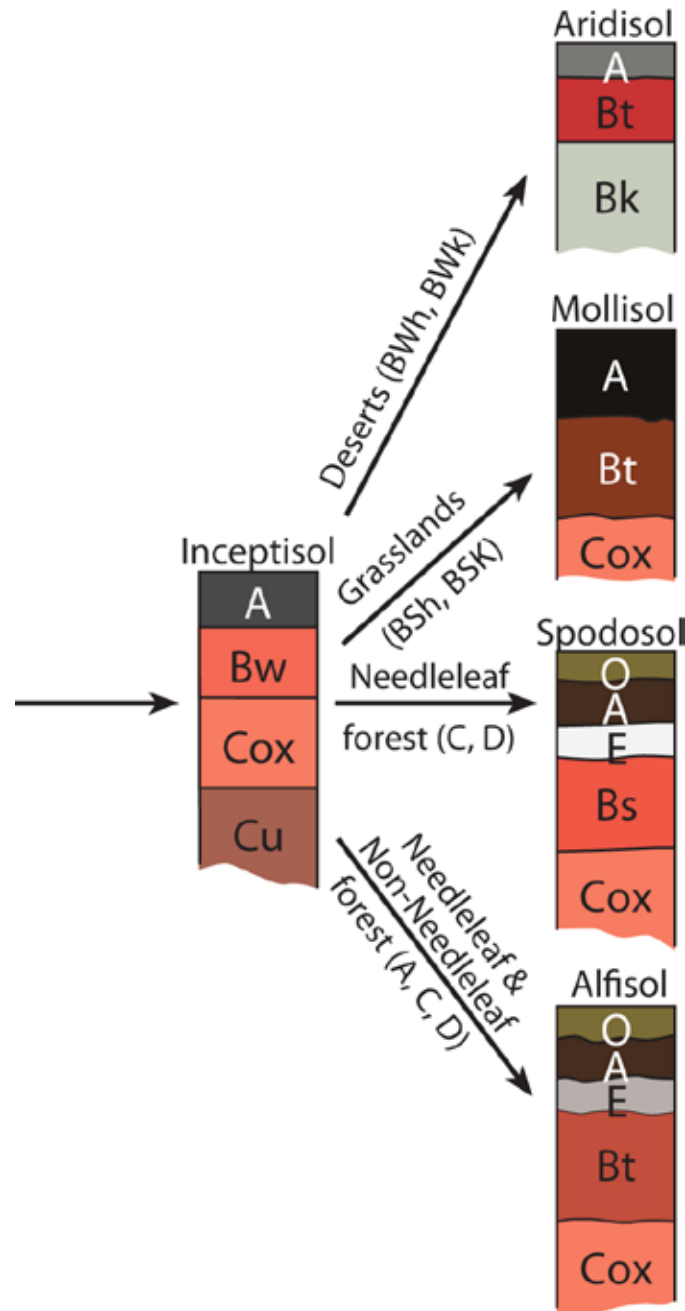


Figure 7.21. Mature soils, such as aridisols, mollisols, spodosols and alfisols, tend to reflect in their characteristics the strong influence of climate and vegetation. Humid climates promote the development of moderate to heavy leaching, and forest growth (Source/Credit: modified from Dennis I. Netoff and Ava Fujimoto-Strait, *Weather & Climate Lab Manual*).

## ***Arid (BW) and Semi-arid (BS) Climates***

Arid and semi-arid climates are those in which **potential evapotranspiration exceeds precipitation**. This is an environmental condition that has to do with both temperature and precipitation. The amount of moisture that is held in the soil layer is determined by not only how much precipitation actually falls to the surface, but also how much is immediately lost back to the atmosphere, which depends mainly on temperature. For example, areas in the subtropics that receive 14 inches (36 cm) of precipitation would also have very high evapotranspiration rates. Consequently, they may be considered deserts because only a small fraction of those 14 inches actually makes its way into the soil, and it is soil moisture that plants depend on for growth and survival. High-latitude areas with similar precipitation will support forests because the average annual temperatures are so low that relatively little evapotranspiration occurs.

Arid and semi-arid climates also have highly variable precipitation from month to month and year to year. Much of the rainfall that occurs is produced by isolated thunderstorms. This means that some areas may be drenched, while areas in close proximity receive little or no rainfall. Heavy downpours from isolated thunderstorms, combined with the rocky terrain of many deserts, which limits infiltration and increases runoff, often combine to produce flashfloods.

There are two major B climate areas in the world. The first occurs on the stable, eastern side of the oceanic subtropical highs (affecting the western sides of the continents), at approximately 20° to 30° latitude (see Figure 7.1). This area is characterized by dry, sinking air that is heated adiabatically by compression as it subsides. The heating of the air by compression causes the relative humidity to decrease, making the air effectively very dry. The air is further stabilized by passage over the cold coastal ocean currents (Figures 7.22a and 7.22b). The second major region of B climates occurs in the mid-latitudes of continental interiors, particularly on the lee side of mountains. Remoteness from moisture sources and the *rainshadow effect* on the lee side of mountains causes these areas to be dry (Figures 7.23a, 7.23b 7.23c and 7.23d).

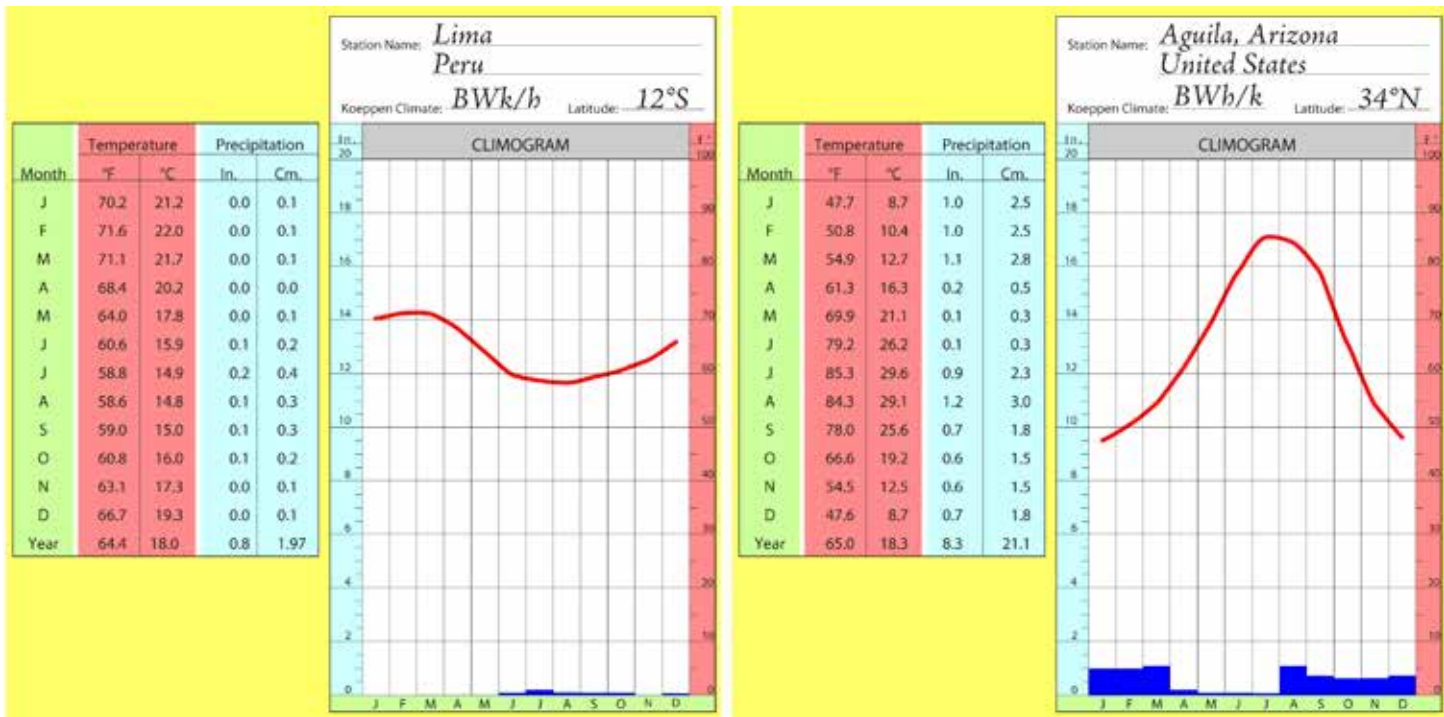


Figure 7.22a. (left) Climogram of Lima, Peru. Lima is a west coast desert, and is amazingly cool and dry for its latitude, thanks to the cold Peru Current and the strong subsidence on the stable side of the STH.

Figure 7.22b. (right) Climogram of Aguila, Arizona. Aguila, not far from Phoenix, owes its aridity to its proximity to the stable side of the STH as well as to mountain barriers. Both are BW climates, on the boundary between hot (h) and cold (k) deserts.

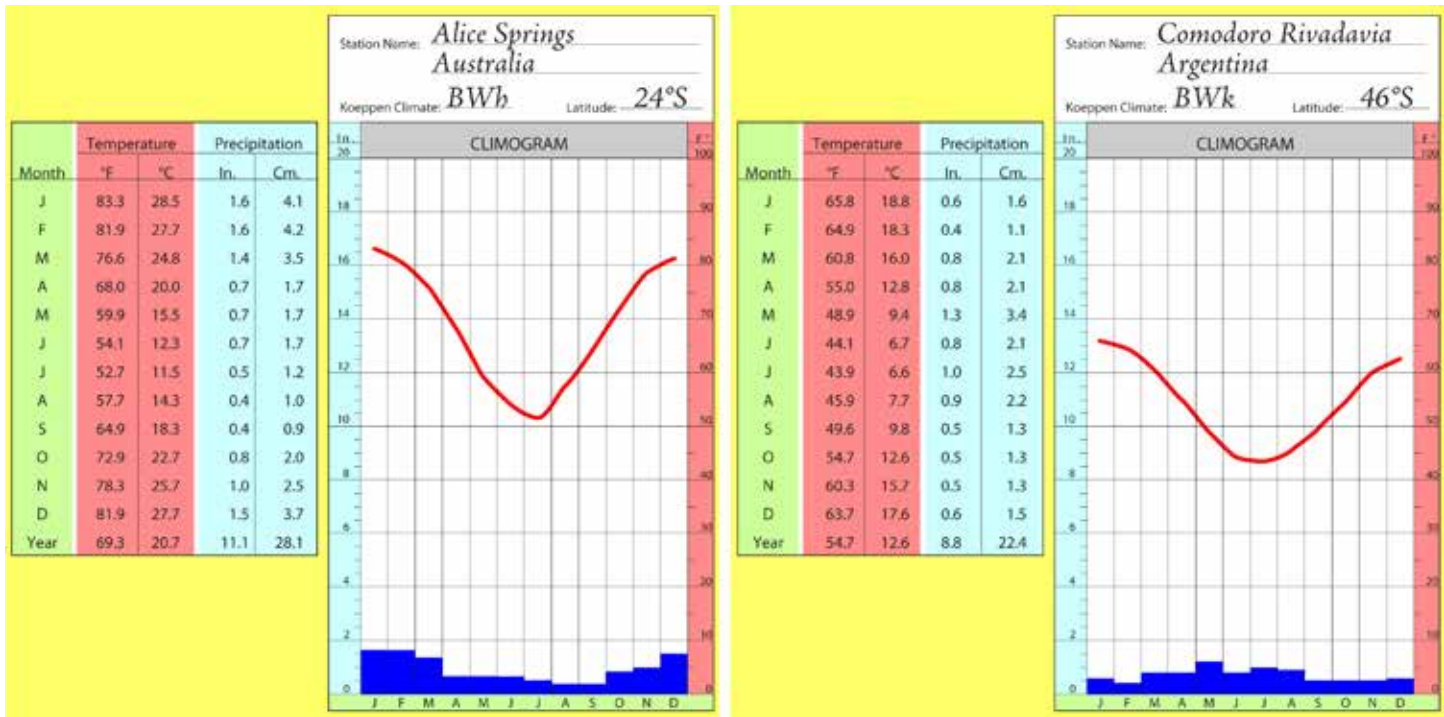


Figure 7.23a. (left) Climogram of Alice Springs, Australia. Alice Springs is a BWh climate in the Australian Outback. Its location in subtropical latitudes and its interior location cause aridity.

Figure 7.23b. (right) Climogram of Comodoro Rivadavia, Argentina. Comodoro Rivadavia is a mid-latitude, cold desert (BWk). It is located on the east coast, but the Andes Mountains block moisture from the prevailing westerly winds to produce aridity.



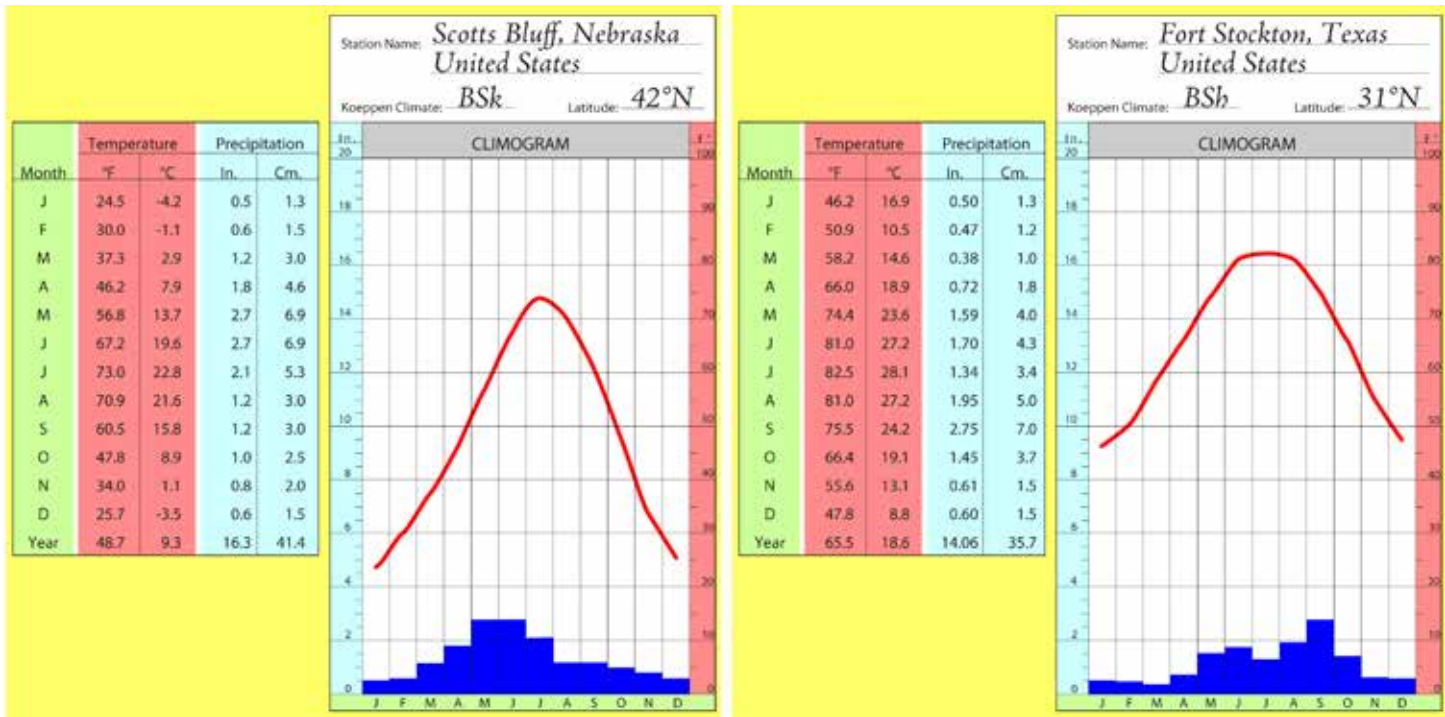


Figure 7.23c. (left) Climogram of Scotts Bluff, Nebraska. Scotts Bluff is a mid-latitude steppe climate (BSk) located in the continental interior, and to some degree, in the rainshadow of the Rocky Mountains.

Figure 7.23d. (right) Climogram of Fort Stockton, Texas. Fort Stockton is a borderline hot steppe (BSh) or hot desert (BWh).

Arid and semi-arid climates occupy more land area than any other climate type. They cover approximately 26% of the Earth’s surface and appear as large brown areas when viewed from space. This fact places a fundamental limit on the amount of land available to supply food for the world’s rapidly growing population, which is expected to reach about 8.9 billion by the year 2050.

## Deserts (BWh and BWk)

The geographic distribution of deserts is largely controlled by the stable side of the subtropical high in conjunction with cold ocean currents, and large continental interiors bordered by mountain barriers. West coast deserts include the Sonoran Desert of the United States and Mexico, the Atacama of Chile, the famous Sahara, the Namib Desert of South Africa, and the Great Sandy Desert of northwest Australia (Figure 7.24). Deserts that are caused by inland location and mountain barriers include the Gobi, the Great Australian, and to some extent, the Great Basin (Figure 7.25).

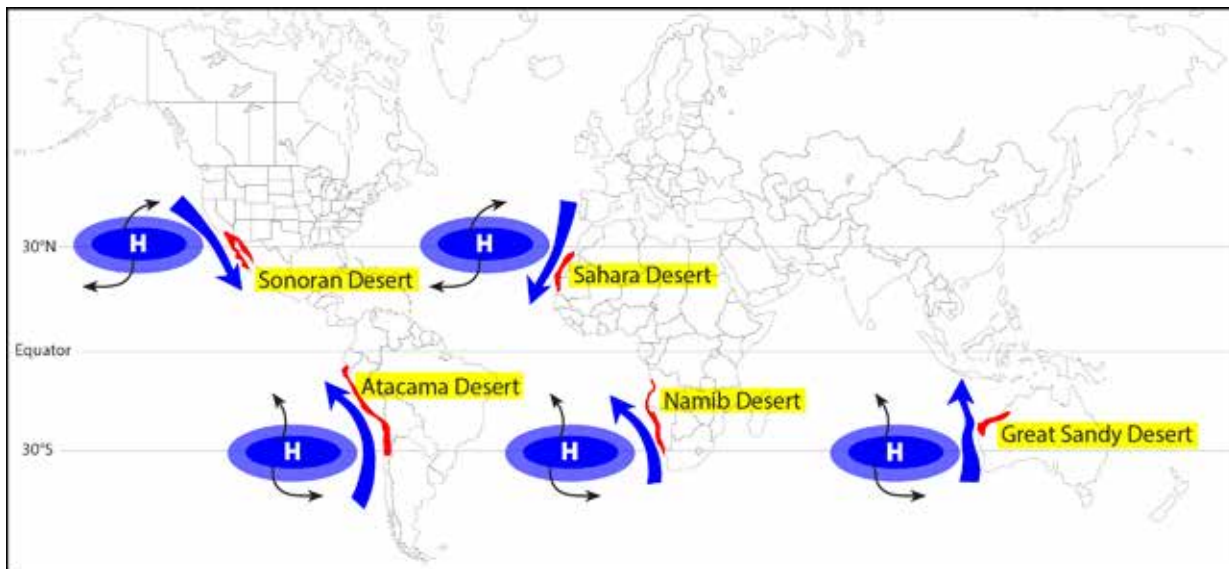


Figure 7.24. The world's west coast deserts are typically located in the lower-mid-latitudes, dominated by the stable, dry side of the Subtropical High as well as cold ocean currents (Source/Credit: modified from Koeppen and others).

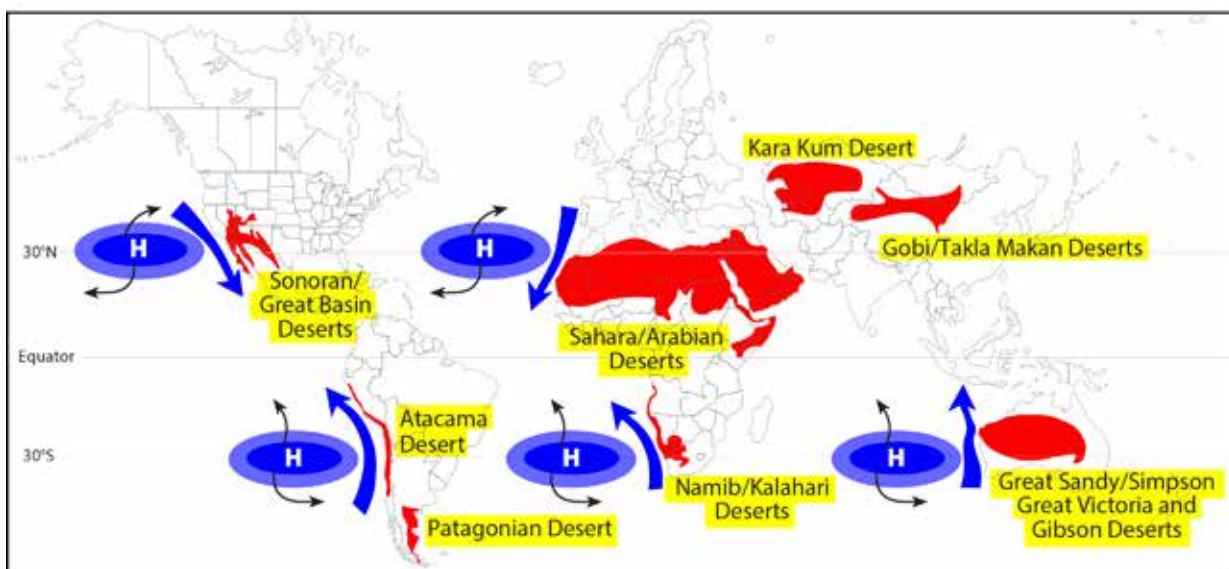


Figure 7.25. Map of some of the world's better-known inland deserts. These deserts are controlled mainly by continentality, but many are in part due to the added effects of mountain barriers (Source/Credit: modified from Koeppen and others).

Plants that grow in this region tend to be widely-spaced, with lots of bare rock or ground between individual plants (Figures 7.26a and 7.26b). Drought-tolerant plants are known as **xerophytes**, and have developed a variety of mechanisms that enable them to survive the extreme dryness of this climate. One such mechanism is a reduction in leaf size, or microphyllous leaves (Figure 7.27). The reduction in leaf size significantly reduces water loss by plant transpiration. In the case of many succulents, such as cacti, the leaves have evolved into thorns, which also help to protect the plants from predation (Figures 7.28a, 7.28b and 7.28c). Accompanying this evolutionary adaptation was the movement of the chlorophyll into the trunks of the cacti, giving them their green color. The skin of the trunk photosynthesizes. **Succulents have special moisture-storage cells**, which allow them to store large amounts of water after rains, then gradually shrink and desiccate when little soil moisture is available during drought (Figure 7.29).



Figure 7.26a. (left) Desert vegetation of Panamint Valley, California, in the Mojave Desert (Source/Credit: Dennis I. Netoff).  
Figure 7.26b. (right) Desert vegetation in the Chihuahuan Desert of Big Bend, Texas. Although the plant associations are quite different floristically, they have in common that there is an obvious absence of trees, lots of bare rock/ground and the plants are predominantly xerophytic (Source/Credit: Dennis I. Netoff).



Figure 7.27. The Palo Verde of the Sonoran Desert in Arizona. The microphyllous nature of the leaves reduces moisture loss by transpiration. The twigs and branches, like the leaves, are green. Palo Verde means green stick (Source/Credit: Dennis I. Netoff).



Figure 7.28a. Cacti of the Sonoran and Chihuahuan Deserts. The Giant Saguaro is the world's tallest cactus, sometimes growing to more than 60 feet (near Lake Roosevelt, Arizona) (Source/Credit: Dennis I. Netoff).



Figure 7.28b. (left) The small barrel cactus is rooted in the minute cracks of granite bedrock (Baja Peninsula, Mexico) (Source/Credit: Dennis I. Netoff).

Figure 7.28c. (right) A large barrel cactus (foreground) and abundant Prickly Pear cacti (middle background) form part of a complex desert ecosystem at Rockhound State Park, near Deming, New Mexico (Source/Credit: Dennis I. Netoff).



Figure 7.29. Eating the fleshy fruit of cactus in the Great Basin Desert of Nevada (Source/Credit: Dennis I. Netoff).

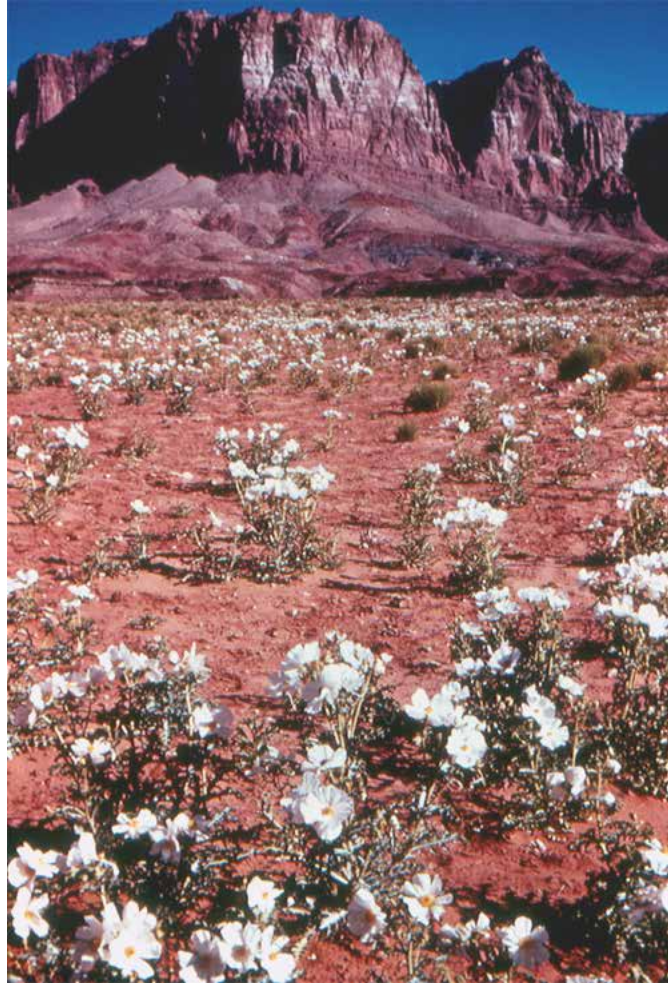
The leaves of many plant species in desert environments, including the trunks of cacti, are covered by a waxy substance that also limits evapotranspiration. Thick, leathery, **sclerophyllous** leaves also reduce moisture loss (Figures 7.30a and 7.30b). Some xerophytes secrete chemotoxins (poisons) into the soil that inhibit the growth of roots from neighboring plants. This is a form of chemical warfare between plants that is intended to maximize the amount of water available to the poison-secreting plants. Some desert plants avoid drought by existing as seeds in the soil, until sufficient soil moisture is stored to cause germination (Figure .731). Other desert plants, called **halophytes**, have adapted to high amounts of salt in the soil, which are toxic to most plants.



Figure 7.30a. The creosote bush, a common xerophyte of the Chihuahuan Desert. The creosote leaves are thick-skinned and have waxy coatings on the leaves (Source/Credit: Dennis I. Netoff).



Figure 7.30b. The Ocotillo plant is also a common xerophyte of the Chihuahuan Desert. The Ocotillo will shed all of its leaves when stressed because of drought. Within three days after a healthy rain, new leaves emerge (Source/Credit: Dennis I. Netoff).



*Figure 7.31. Desert annuals in full bloom at the base of the Vermillion Cliffs in Utah. Annuals can avoid long periods of drought-induced stress by residing in the desert soil for long periods as seeds. When the rains come, and the soil becomes moist, the seeds germinate and quickly go through their life cycle (Source/Credit: W.C. Bradley).*

**Aridisols** are common mature soils of the BW climates. Aridisols tend to have a very thin, pale A horizon, because of the sparse cover of vegetation, and an accumulation of whitish salts at depth, the **Bk** or **K** horizon (Figures 7.32a and 7.32b). Because of the lack of removal of nutrients by leaching, they have a high inherent fertility. Lack of water and humus, and the presence of salts typically limit their agricultural use. In some deserts, exotic streams pass through the area, and the resulting floodplain inceptisols can be very fertile. The forested riverine vegetation along these streams stand in sharp contrast to the surrounding sparse desert vegetation. Riverine vegetation can consist of tree growth, even in the driest climates, because of the occurrence of water at shallow depth on floodplains. Tree clusters can also occur as desert oases where geological conditions create seeps and springs (Figures 7.33a and 7.33b).



Figure 7.32a. Aridisol, Williams Fork Valley, Colorado. The sparse, slow-growing vegetation produces very little vegetative input to the soil, so the A horizon tends to be thin and pale in color. The white Bk horizon is rich in calcium carbonate (Source/Credit: Dennis I. Netoff).



Figure 7.32b. Cotton growing on an aridisol near Tucson, Arizona (Source/Credit: Dennis I. Netoff).



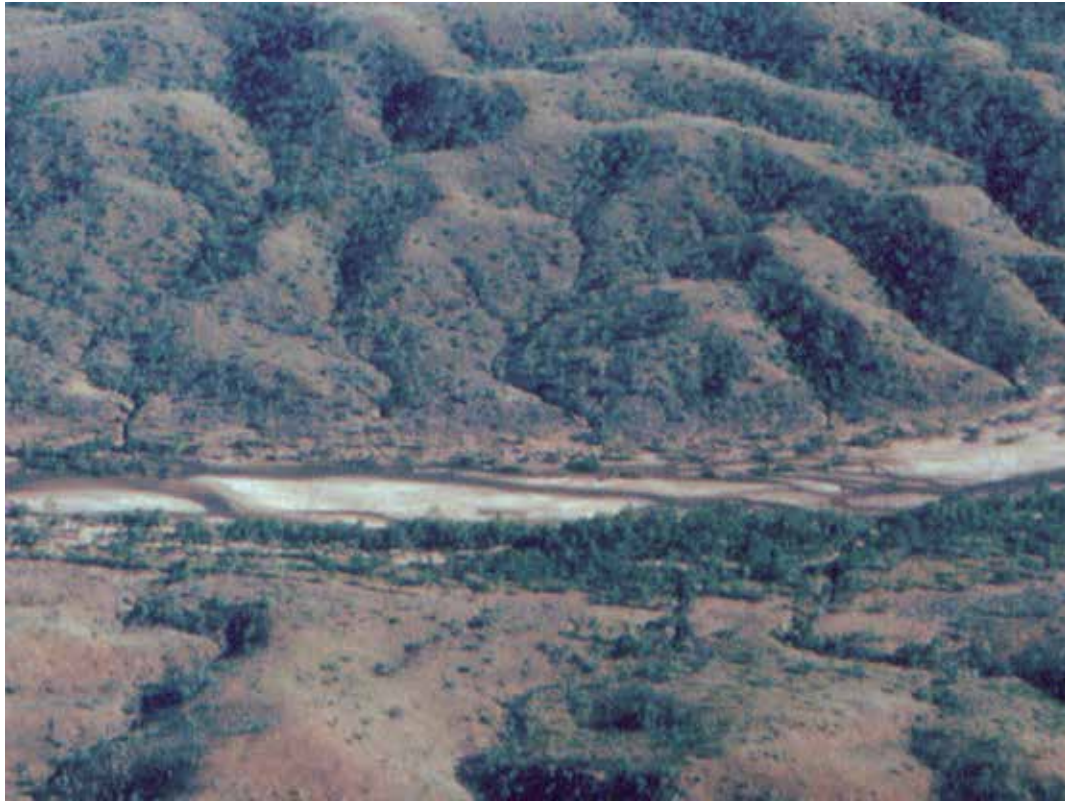


Figure 7.33a. (left) The dense riverine forest of the Ord River, Australia, contrasts with the sparsely-vegetated Savanna on higher ground (Source/Credit: Dennis I. Netoff).



Figure 7.33b. (right) Desert oasis of palm and cottonwood, Big Bend National Park, Texas. A spring at the base of the trees provides water (Source/Credit: Dennis I. Netoff).

Desert winds are notoriously strong and sporadic in time and place. Winds in the Great Basin and Colorado Plateau of the United States have been clocked at nearly 100 mph, and desert sand storms in the Sahara sometimes last for weeks. These strong, desiccating winds also impose climatic stress on plants. Dust storms originating in the Gobi Desert of Asia can blanket much of mainland China, and then carry clay-sized particles all the way across the Pacific to the United States (Figure 7.34).

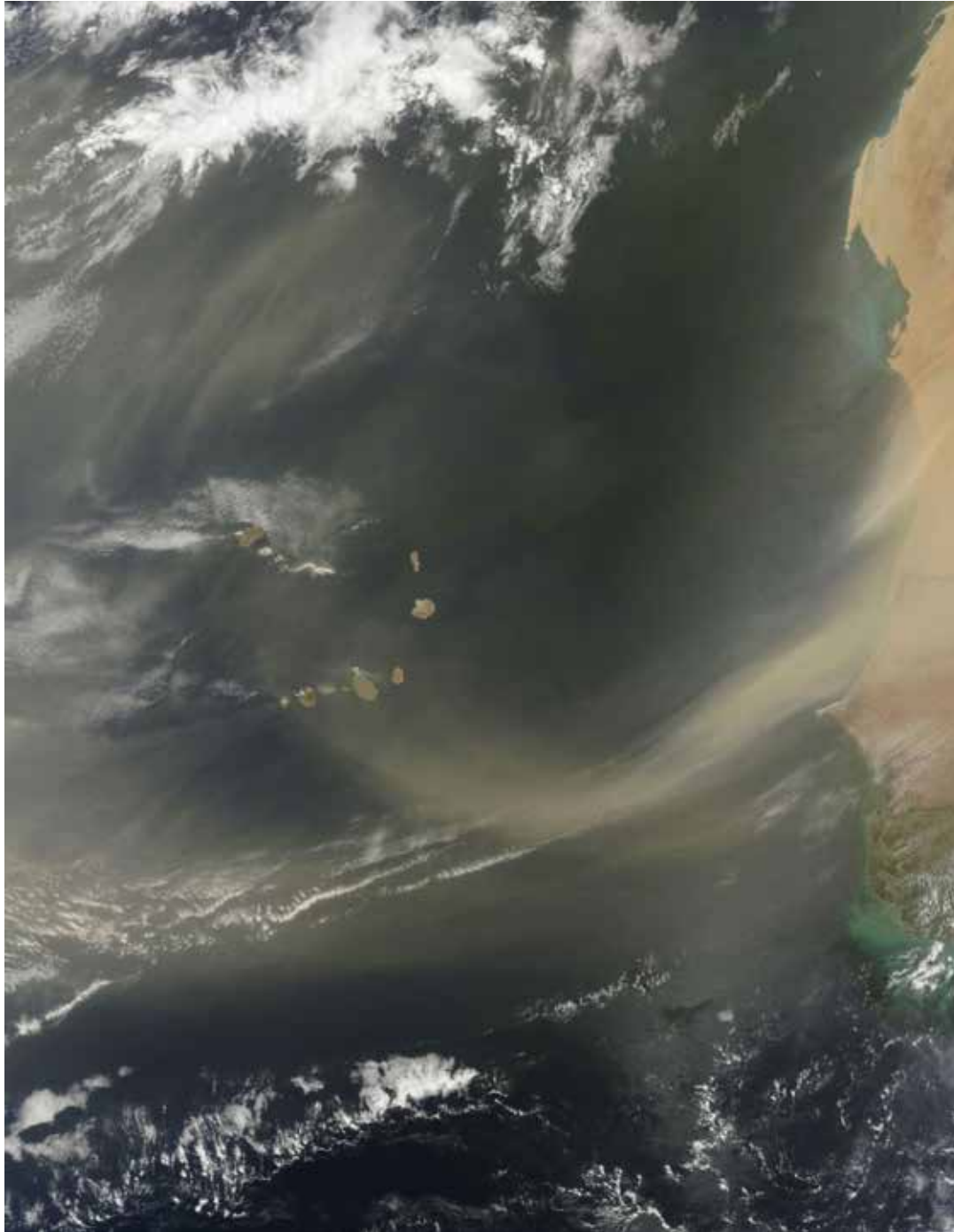


Figure 7.34. Two distinct Saharan dust plumes are blowing westward off the coasts of Mauritania and Senegal. The curved plume extends over 400 miles (640 km) from Africa to the Cape Verde Islands (Source/Credit: NASA Earth Observatory, June 22, 2009).

A common misconception about deserts is the belief that all deserts are hot and covered with sand dunes (Figures 7.35a and 7.35b). In fact, many are cold, and even hot deserts can be cold at night. In the Koeppen system, hot deserts are designated with the letters **BWh**. The *h* is for the German word *heiss* which means hot. These occur primarily in the subtropical high pressure belts, and include such deserts as the Sahara in North Africa, the Namib in South Africa, and the Great Sandy and Great Victoria Deserts in Australia. Because of the lack of moisture in the air in these regions, daytime temperatures frequently exceed 104°F (40°C) and can drop below 77°F (25°C) at night as infrared radiation escapes to space. As a result, the daily temperature range can be large. These climates have a mean annual temperature above 64°F (18°C), but daily temperatures can exceed 120°F (49°C) during the hot summer. The soil temperatures can be much higher. For example, surface soil temperatures in the Mojave Desert have been known to reach 200°F (93°C)! This is why so many desert animals burrow underground and tend to be nocturnal. During midday, the relative humidity may drop to 5%, or less.



Figure 7.35a. (left) Sand dunes, such as those found in this dune field on the floor of Death Valley, California, are common in deserts because of the lack of vegetation, lack of soil moisture, abundant supply of loose material and fierce desert winds (Source/Credit: Dennis I. Netoff).

Figure 7.35b. (right) Partly stabilized dunes of the Great Sandy Desert in Australia, near Coral Bay. The low ridge in the background is a dune (Source/Credit: Dennis I. Netoff).

Cold deserts are designated as **BWk** in the Koeppen system. The **k** is derived from the German word *kalt*, which means cold. These deserts occur in the mid-latitudes in the interiors of continents, and usually in rain shadow positions (Figure 7.36). They have a mean annual temperature below 65°F (18°C) and include such deserts as the Gobi Desert in Asia and the Great Basin Desert of the United States. Because of the effects of latitude and continentality, these climates have large annual temperature ranges. Summertime temperatures during the afternoon can exceed 104°F (40°C), but minimum winter temperatures may drop below minus 31°F (minus 35°C). The high latitude deserts can also have very high diurnal (day-night) temperature variations and spring and summer afternoons can exceed 100°F. Shortly after the Sun sets, the night temperature can drop well below freezing.



*Figure 7.36. The Big Sage dominates the desert vegetation in this part of the Great Basin Desert in Nevada (Source/Credit: Dennis I. Netoff).*

## Steppe Climates (BSh and BSk)

Semi-arid climates support grassland ecosystems, and are transitional between deserts and forests. The **S** designation in the Koeppen classification represents *steppe*, which is Russian for grasslands. Grasslands are well adapted to drought, because they go into dormancy (*turn brown*) during the dry season, or when the amount of sunlight is insufficient (Figure 7.37). The famous Australian Bundle-Bundle grass has blades that are akin to the spines on North American cacti, presumably for protection against grazing (Figures 7.38a and 7.38b).



Figure 7.37. The short grass prairie in central-western Kansas. Estimated annual precipitation is 15 inches. Mollisol soils develop under continuous grassland vegetation. Because grasses contribute large amounts of vegetative matter to the soil each year, the A horizons are thick and dark in color (Source/Credit: Dennis I. Netoff).



Figure 7.38a. (left) Australia's Bundle-Bundle grass, which is composed of mounds of very rigid, sharp-tipped blades that are effective in warding off many animals (Source/Credit: Dennis I. Netoff).



Figure 7.38b. (right) Close-up of the rigid bladed Bundle-Bundle grass (Source/Credit: Dennis I. Netoff).

In the conterminous United States, there is considerable variation within the grassland ecosystem. A transect from Indiana to eastern Colorado illustrates the principal changes that take place in climate, vegetation, and soils. The wetter eastern portion consists of the **tall grass prairie** which is a luxuriant growth of grasses that attained heights that could hide a person on horseback during the era of settlement of the plains. Extensive tall grass prairie once stretched from Indiana through Iowa, where annual precipitation is well over 20 inches. Little of the tall grass prairie remains today, largely because of farming and grazing. Due to increasing aridity, the tall grass prairie becomes shorter toward the west, and gives way to **short grass prairie** in Kansas. Here grasses grow a few feet in height but still provide the soil with a large supply of organic matter at the end of the growing season. Soils in the tall and short grasslands are typically **mollisols** which have a distinctive dark, spongy, humus-rich *mollic* A horizon, the result of large inputs of organic matter from the decay of grasses over thousands of years (Figure 7.39).

## Mollisol

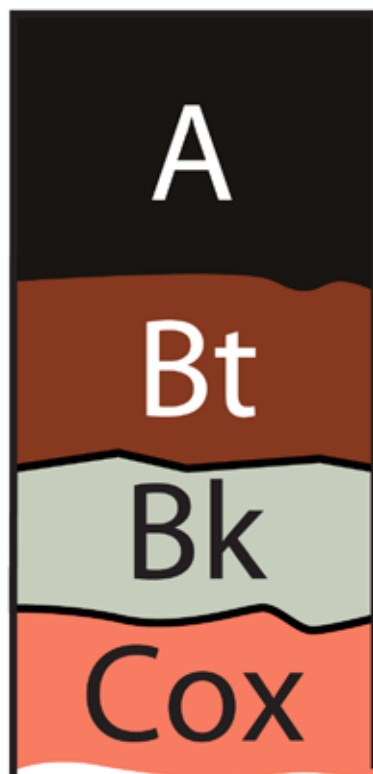


Figure 7.39. Closeup of mollisol. The thick, dark-colored, soft A horizon is rich in humus as well as important nutrients for high-protein plant growth. Mollisols are some of the most fertile soils on the planet. The small amount of accumulation of calcium carbonate (white material) is an indicator of incomplete leaching of the soil horizons, and therefore an arid or semi-arid climate (Source/Credit: Dennis I. Netoff).

In the driest western margins of the grassland transect in the Colorado Piedmont, where the precipitation drops to 10 to 15 inches, grasses are even more stunted and grow in bunches — the bunchgrass community. Soils there take on the characteristics of **aridisols** (Figure 7.40).



Figure 7.40. Aridisol in the Colorado Piedmont just east of Fort Collins in the Cache La Poudre drainage. The parent material is stream gravel (stones are visible). The white K horizon is heavily enriched with calcium carbonate and hence is an old soil (more than 100,000 years). The horizons from top to bottom are A, Bt, K, Bk, and Cox (Source/Credit: Dennis I. Netoff).

Soil parent material, the geologic material from which soils are derived, can have a strong influence on vegetation and soil development. In northwest Nebraska, there are 20,000 square miles of sandy parent material called the Nebraska Sand Hills which were active sand dunes just a few thousand years ago. Sand does not hold moisture well, and so the vegetation is more **xeric** (drought-tolerant) and stunted than in the surrounding plains. Grasses are shorter, more sparse and there are many desert-dwelling plants such as the cactus that occupy the Sand Hills. The relative youth of these soils, and their sandy character makes these **entisols** immature with only the incipient development of soil horizons (Figure 7.41a and 7.41b).

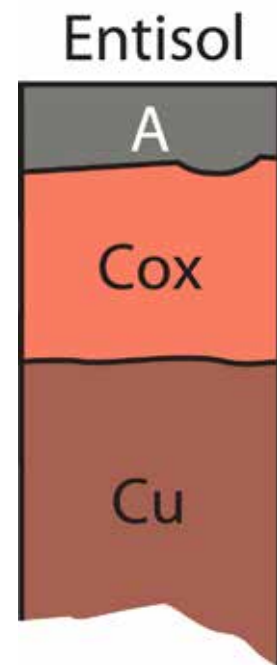


Figure 7.41a. (left) The sparse grass cover in the BSk climate of the Sand Hills of Nebraska. Most of the soils in the Sand Hills are poorly-developed entisols, since the sand dunes have been stabilized for only a few thousand years (Source/Credit: Dick Payne).

Figure 7.41b. (right) Entisol horizons (Source/Credit: (Source/Credit: modified from Dennis I. Netoff and Ava Fujimoto-Strait, Weather & Climate Lab Manual).

As with the true desert climates, the semi-arid climates can be divided into two main subtypes based on temperature. These subtypes are the hot semi-arid climates (BSh) which have average annual temperatures of 65°F or more (18°C), and cold (BSk) subtypes, with a mean annual temperature below 65°F.



## C Climates

The C climates occur in the mid-latitudes and typically have sufficient precipitation to support forest or woodland growth. They have distinct summer and winter seasons, but the winters are mild. According to Koeppen, the coldest monthly temperature in winter is between 32°F (0°C) and 64°F (18°C). *Average* monthly temperatures do not drop below freezing even though there may be short spells of below freezing temperatures. From the standpoint of plant biology, the 32-degree temperature is of significance because many plant species cannot tolerate hard, long freezes.

The C climates may be divided into several subtypes based on the precipitation regime and the nature of the summer. The precipitation regime is indicated with the second, lower-case letter in the three-letter climate designation. The **f** subtype means adequate moisture in all months, typically more than 1.2 inches. This is biologically significant in that there is little climatic stress from drought. Drier-than-normal years do, however occur in virtually all climatic types. The **s** subtype experiences a summer dry season, and the **w** subtype is distinguished by a winter dry season.

The nature of the summer is indicated by the third letter (a, b, or c,) in the C climate designation. The **a** subtype has long hot summers, the **b** has mild summers, and the **c** subtype has the short, cool, summers.

### *Humid Subtropical Climates (Cfa)*

These climates are found primarily along the east side of continents between 25° and 40° latitude (see [Figure 7.1](#)). In the United States, this includes most of the southeastern sector of the country. Humid subtropical climates are bordered by drier climates to the west (BS) and colder climates to the north (Dfa climates).

Much of this area on the eastern sides of continents tends to coincide with the subtropical high pressure belts, which are normally characterized by dry conditions. The **western** side of the oceanic subtropical highs (that affect the **eastern** sides of the continents), however, provide adequate-to-abundant precipitation. Instead of strong subsidence, there is a tendency toward uplift and cloudiness. The air is further destabilized by passage over warm ocean currents (Figure 7.42). Areas such as the southeastern part of the United States tend to receive heavy convective precipitation during the summer, mainly from thunderstorms, whereas in the winter, abundant precipitation is associated with the frequent passage of frontal cyclones (Figures 7.43a and 7.43b).

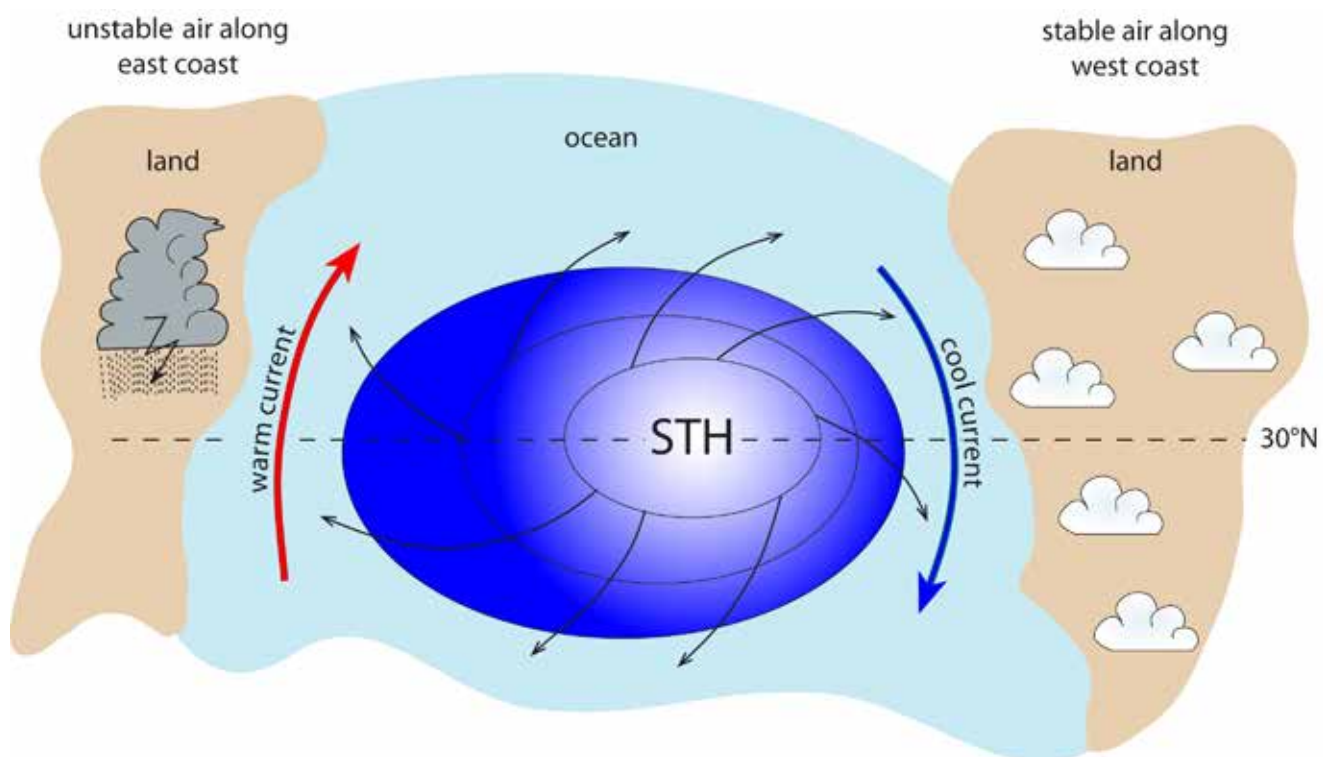


Figure 7.42. The western side of the oceanic subtropical high brings warm and moist tropical and subtropical air toward the continent. The air becomes further destabilized by passage over a warm ocean current, which adds moisture and heat energy to the air. The eastern side of the subtropical high is characterized by very strong subsidence, and a cold current which promotes atmospheric stability and relative drought (Source/Credit: modified from Dennis I. Netoff and Ava Fujimoto-Strait, *Weather & Climate Lab Manual*).

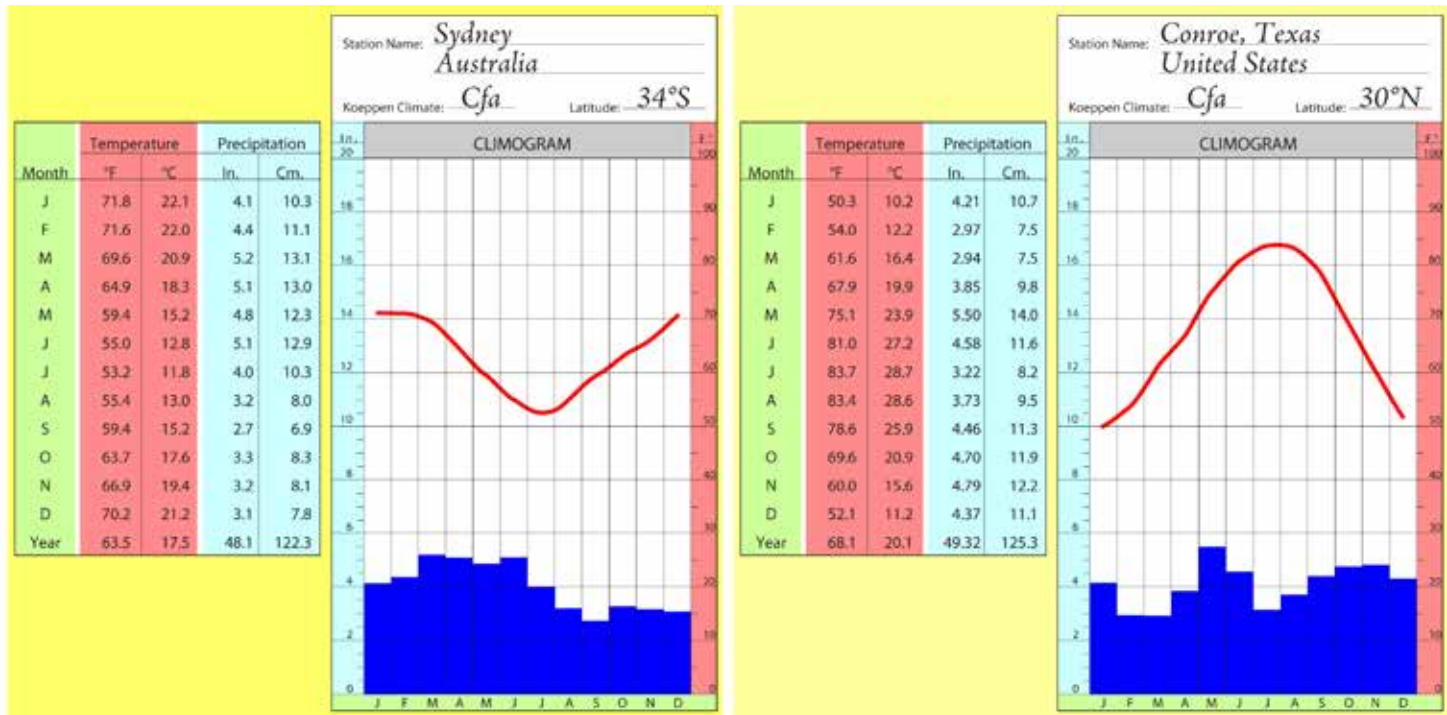


Figure 7.43a. (left) Climogram of Sydney, Australia.

Figure 7.43b. (right) Climogram of Conroe, Texas. Humid subtropical climates have mild winters, warm, humid summers and fairly-evenly distributed, but adequate precipitation year-round.

Because of the abundant rainfall and warm summers, this climate is noted for lush vegetation, such as the Piney Woods and Big Thicket of East Texas. Although the climatic climax ecosystem is the **mid-latitude deciduous forest** (Figure 7.44), extensive areas of the Cfa climate in the United States are needle leaf evergreen, the **southeastern pine forest** (Figures 7.45a, 7.45b and 7.45c). Further north, the pine trees give way to forests dominated by oak trees. In swampy areas, water-tolerant species dominate, such as cypress, sedges, and grasses. **Histosols** are the primary soil type (Figures 7.46a, 7.46b and 7.46c).



Figure 7.44. A broadleaf deciduous oak-hickory forest of the southern Appalachians in the United States (Source/Credit: Dennis I. Netoff).

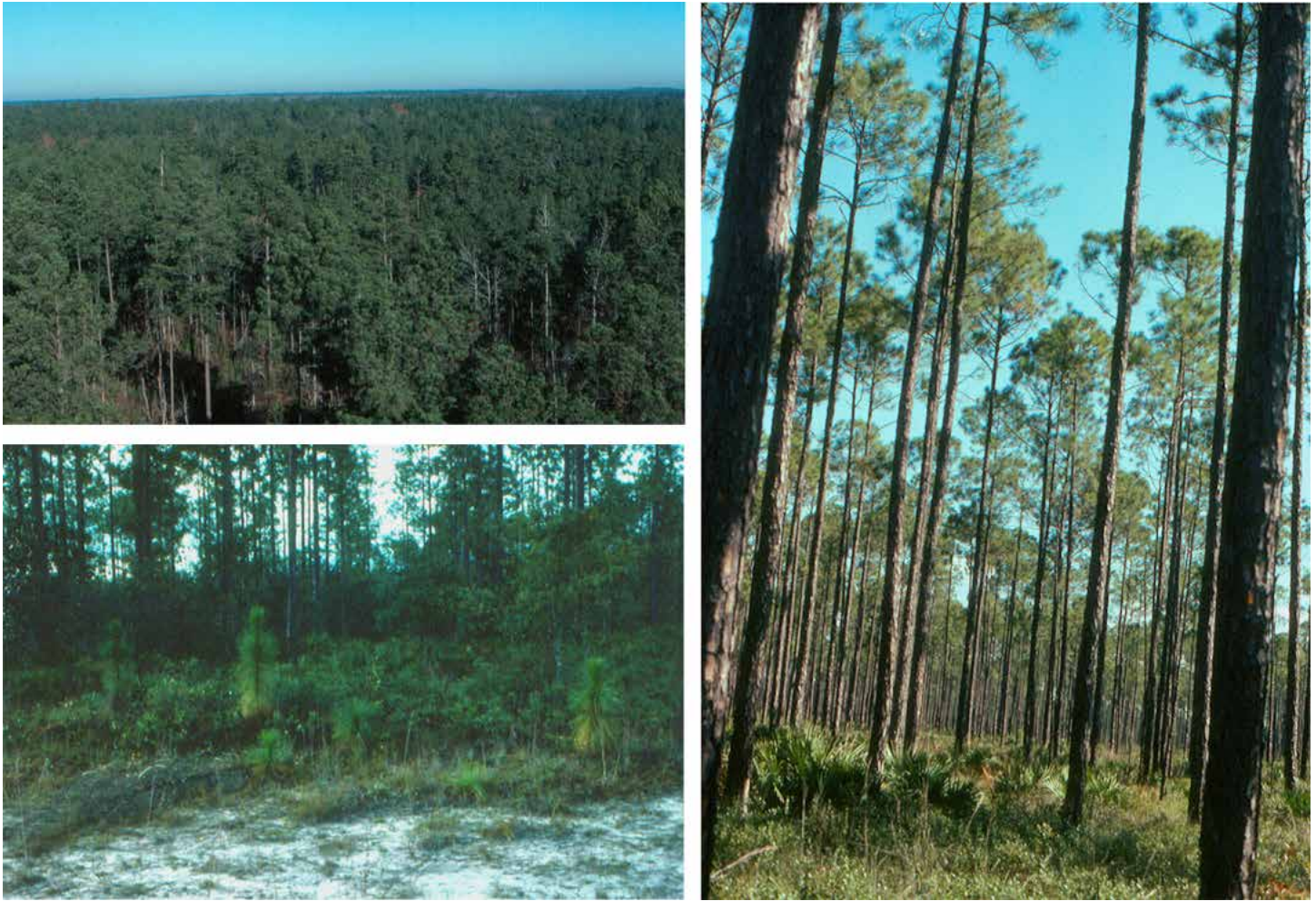


Figure 7.45a. (top) The southeastern pine forest stretches from East Texas to Florida. Although the climatic climax vegetation in the Cfa climate is a mid-latitude broadleaf deciduous forest, frequent fires, sandy soils and periodic drought have favored the dominance of pines in many areas. Large tracts of land are occupied by relatively few species, such as the Longleaf Pine, the Slash Pine and the Loblolly Pine. The forest appears very uniform from a fire tower in Louisiana (Source/Credit: Dennis I. Netoff).

Figure 7.45b. (bottom) Pine seedlings coming up after a burn (Source/Credit: Dennis I. Netoff).

Figure 7.45c. (right) Successional pine stand in Florida. Many pines are fire-tolerant and seedlings grow quickly after a burn (Source/Credit: Dennis I. Netoff).



Figure 7.46a. (left) Soils in waterlogged environments are typically histosols, characterized by a thick accumulation of peaty humus in the O horizon, and reducing (vs oxidizing) colors in the Cg, or gleyed horizon (Source/Credit: modified from Dennis I. Netoff and Ava Fujimoto-Strait, *Weather & Climate Lab Manual*).

Figure 7.46b. (top right) The buttressed roots of a stand of cypress in the water-logged shoreline of Reelfoot Lake in Tennessee (Source/Credit: Dennis I. Netoff).

Figure 7.46c. (top right) Hydrophytic species of trees, grass and sedges of the Florida Everglades (Source/Credit: Dennis I. Netoff).

The warm and wet nature of the Cfa climate is conducive to the development of deep, reddish-orange, heavily-leached ultisols (Figure 7.47). Ultisols, like their tropical counterpart oxisols, have limited fertility and generally require fertilization for high-protein plant production. More recently-developed soils, such as alfisols and inceptisols, occur where there has been recent erosion or deposition.

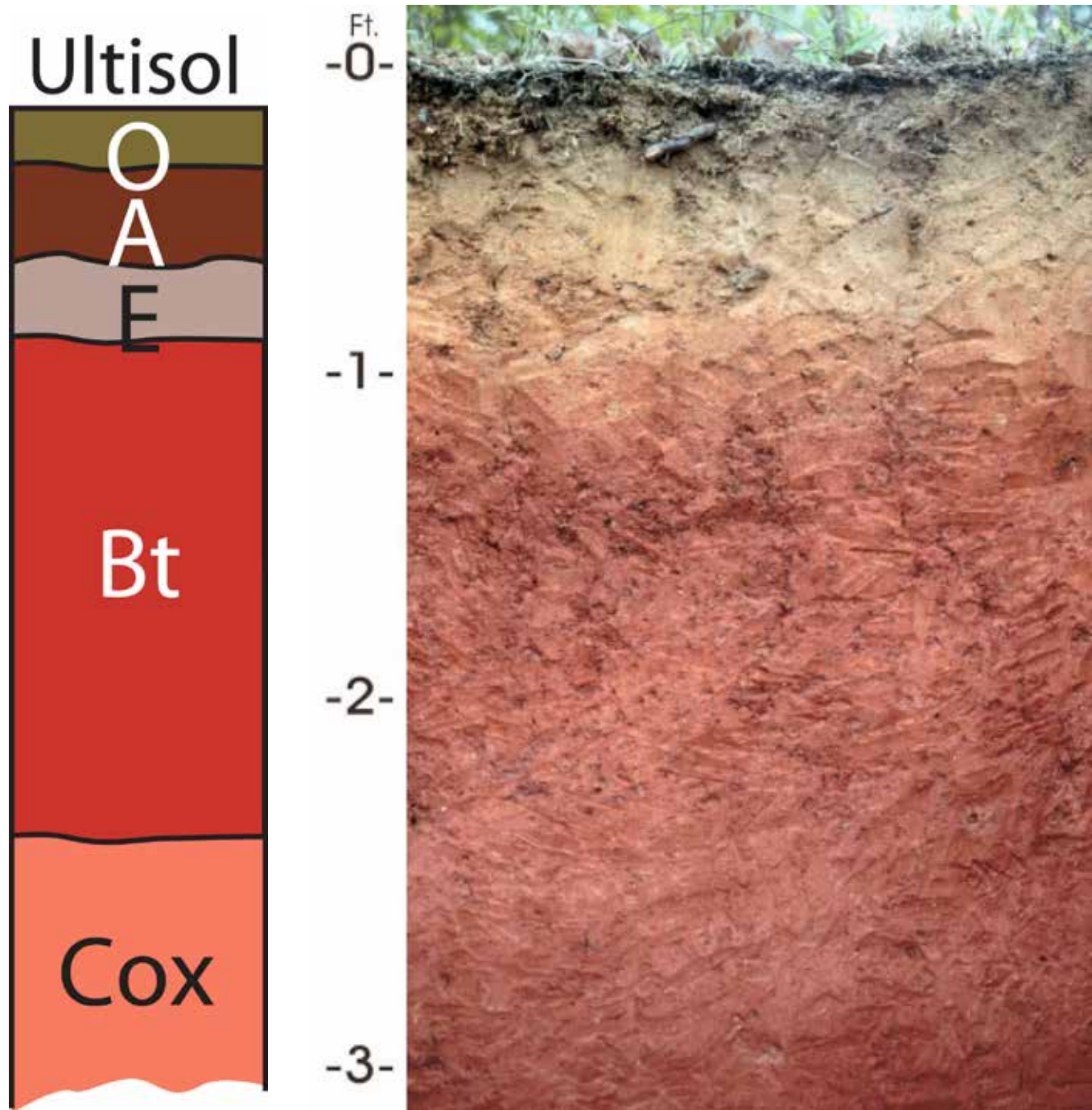


Figure 7.47. Ultisols have strong affinities to the deeply weathered, heavily leached red soils of the A climates. They occur in Cfa climates where the soils are very old on stable land surfaces. The image on the left is the Bama soil, which is the state soil of Alabama (Source/Credit: (left) modified from Dennis I. Netoff and Ava Fujimoto-Strait, *Weather & Climate Lab Manual*).

In the Cfa climate of the Texas Coastal Plain, there are clay-rich soils dominated by the clay mineral montmorillonite which are locally notorious for their shrink-swell capacity. These **vertisols** are characterized by the presence of deep cracks during periods of drought (Figure 7.48). As they shrink and swell, they cause extensive damage to roads, pipelines, house foundations, driveways and other structures.

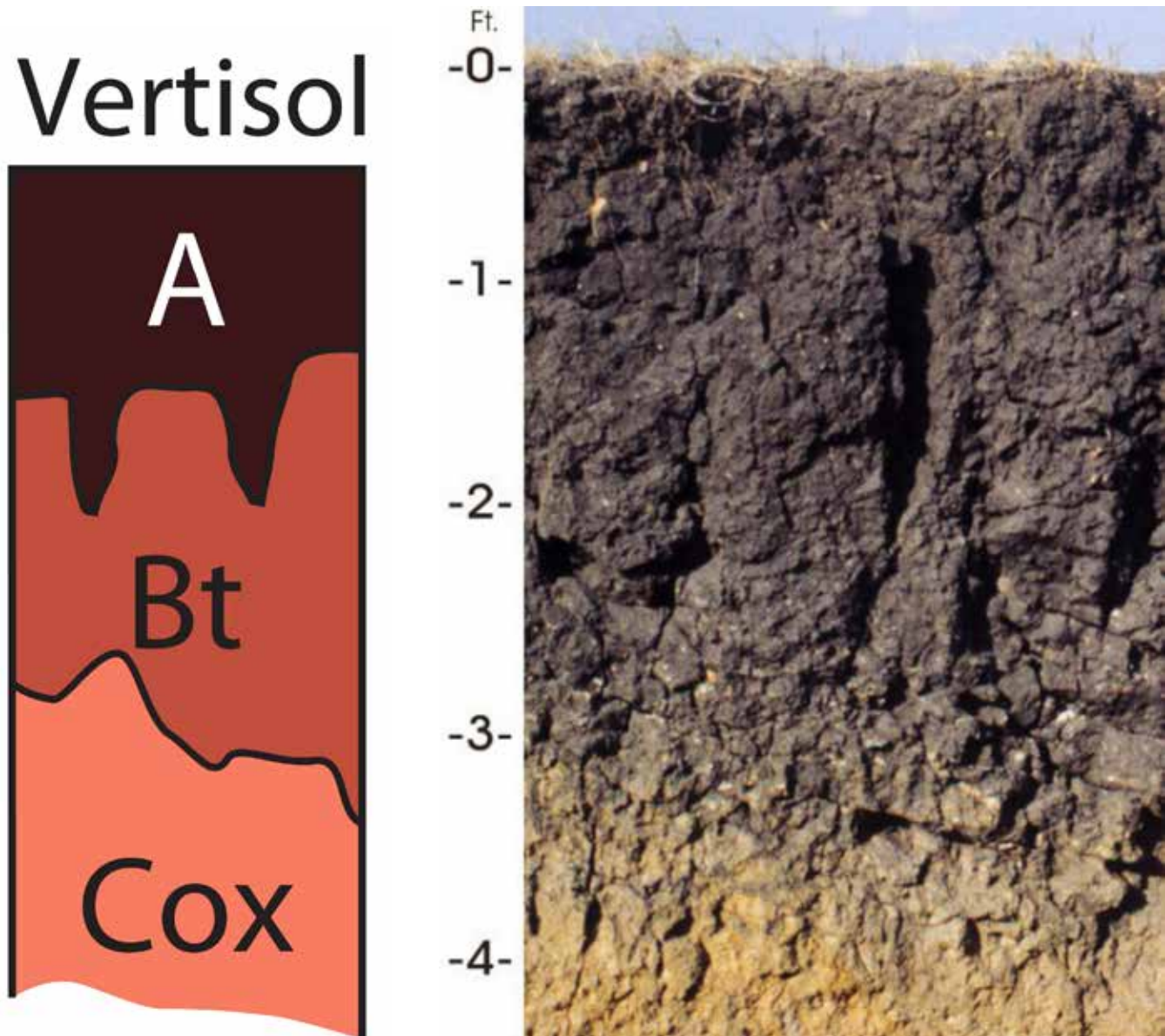


Figure 7.48. Vertisols, sometimes called expandable soils, develop on parent material that is dominated by the clay mineral montmorillonite. Vertisols are therefore more controlled by bedrock geology than by climate. The soil has a huge capacity to expand when wet and shrink when dry. Shrinkage during dry spells tends to develop deep cracks, and the A horizon material mixes with that of the B horizon. Expansion and contraction can cause structural damage to roads, building foundations, driveways and pipelines. The image on the right is the Houston Black soil, which is the state soil of Texas (Source/Credit: (left) soil horizons modified from Dennis I. Netoff and Ava Fujimoto-Strait, *Weather & Climate Lab Manual*).

## Mediterranean Climates (Csa or Csb)

Mediterranean climates, named after the areas marginal to the Mediterranean Sea in Europe, are typically found at approximately the same latitude as the Cfa climates, but on the **western** side of the continents, affected by the stable, dry side of the subtropical high during the warm months. Cold ocean currents further stabilize the air and also provide cool summer temperatures, particularly in coastal locations such as San Francisco and Santa Barbara, California (Figures 7.49a, 7.49b and 7.49c). A few tens of miles inland, summer temperatures can exceed 100°F. During the winter, the subtropical high migrates equatorward, allowing the frequent invasion of rain-generating frontal cyclones. Coastal mountains intensify the winter rain season. These climates tend to be positioned poleward of the world’s west coast deserts and steppes, but equatorward of the marine west coast climates. As the second letter s in the designation indicates, a pronounced dry season during the summer is typical. For example, both San Francisco and Sacramento, California average no rainfall during the months of July and August. Annual rainfall levels are also somewhat low, averaging only 15 to 35 inches (38 to 89 cm) per year. Hot summers (a) versus mild summers (b) are typically the difference between coastal and inland locations.

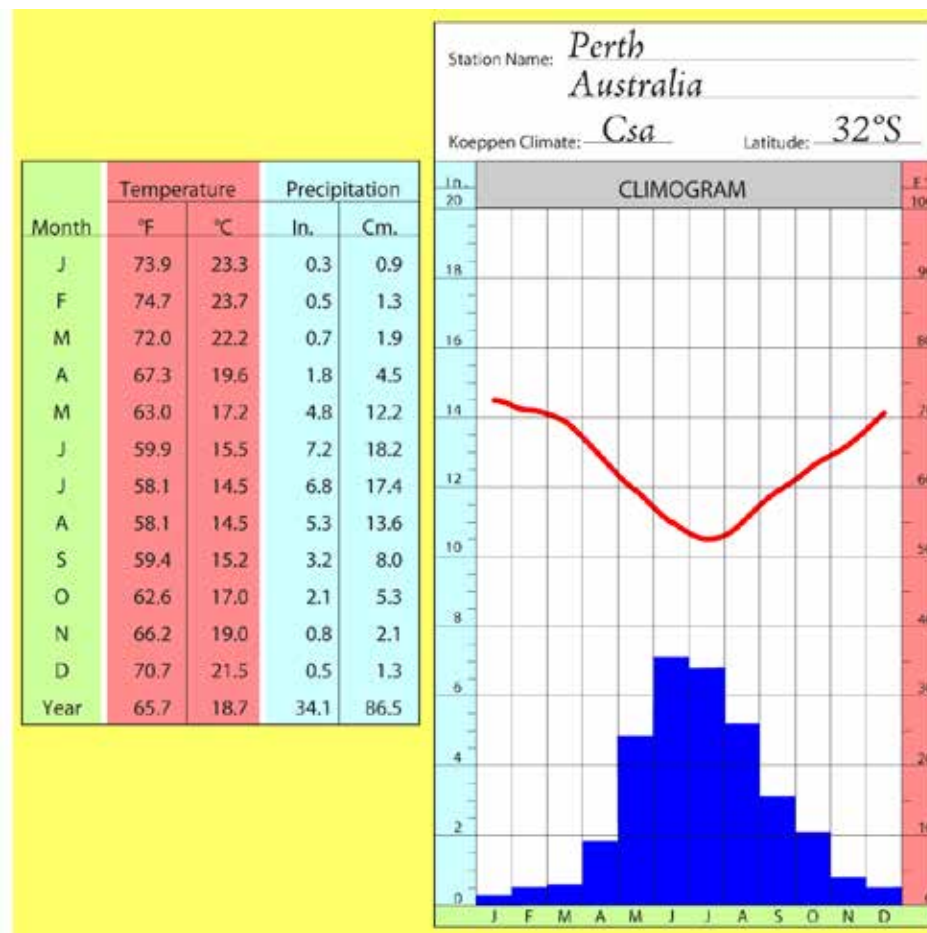


Figure 7.49a. Climogram of Perth, Australia.



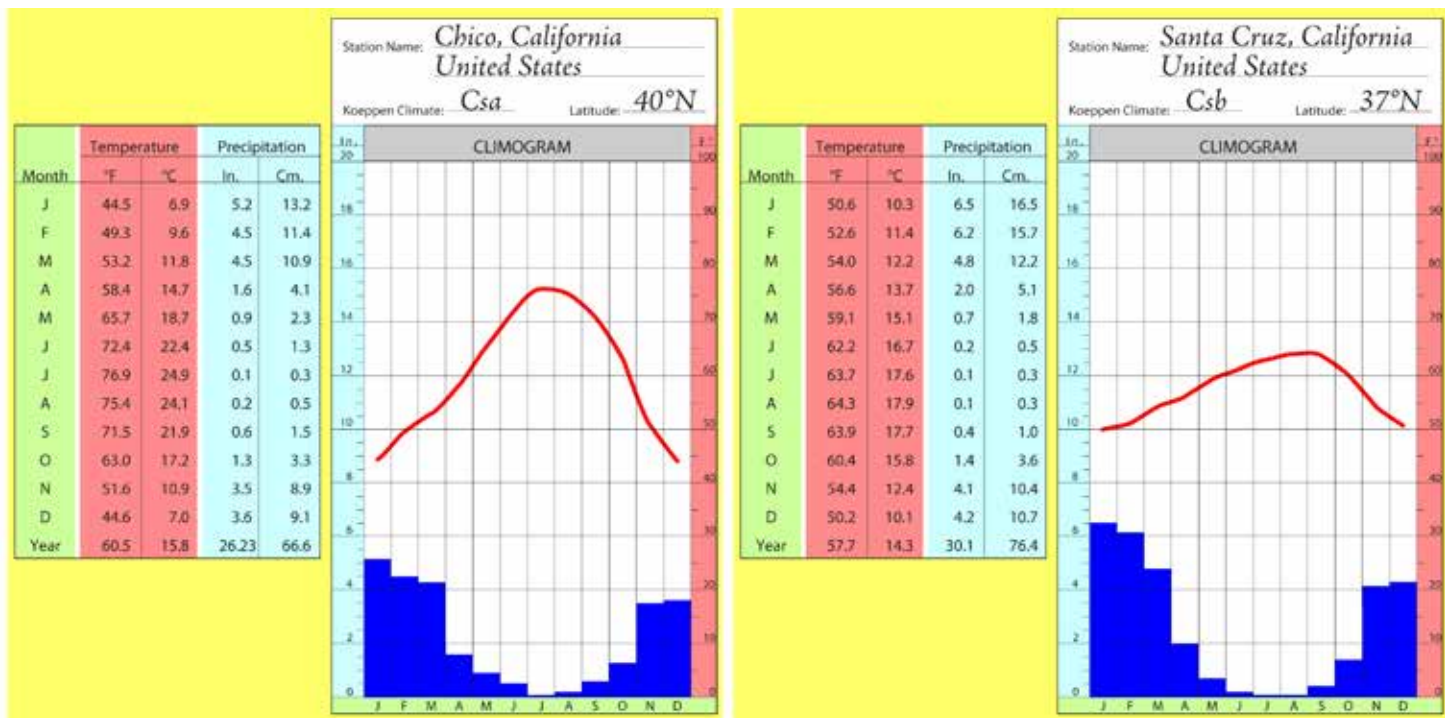


Figure 7.49b. (left) Climogram of Chico, California.

Figure 7.49c. (right) Climogram of Santa Cruz, California. All Cs climates have distinctive drought during the summer. Winters are mild with frequent rainy spells brought by the passage of frontal cyclones. The constancy of the temperature of Santa Cruz is due to its coastal location and nearness to the cold California Current.

The dry conditions, and moderate temperatures caused by the coastal position, make this an ideal climate for many people. The dry summer season is especially attractive to vacationers who can choose almost any form of outdoor recreation and not have to be concerned with foul weather. Dry summers, however, mean heavy reliance on either imported water or groundwater to drive the thriving agricultural economy that characterizes most Mediterranean regions. The California Water Plan, which delivers water from rainy northern California to dry southern California, is one of the largest engineering projects ever undertaken by humans.

In spite of the overall aridity of this climate, advection fogs are common along the coast. These occur when warm, moist air from the ocean passes over cold coastal ocean currents, such as the California Current (Figure 7.50). As the warm, moist air cools, the relative humidity climbs and fog results. At night, these fogs can penetrate inland, but are driven back to their coastal location the following day by local heating of the land.



*Figure 7.50. Advection fogs are common in coastal Cs climates such as here in Santa Cruz, California. Relatively warm air from the subtropical high cools with passage over the cold coastal currents producing fog (Source/Credit: Dennis I. Netoff).*

The summer drought, when evaporation and transpiration rates are at their highest, produces a great amount of climatic stress on vegetation. Trees tend to be stunted and scattered, somewhat like that of the tropical savanna. Thick, leathery sclerophyllous leaves are common on trees as well as shrub forms (Figures 7.51a and 7.51b). Two common ecosystems in the Mediterranean climates are the **chaparral** and the **Mediterranean oak-woodland**, both of which display xerophytic characteristics (Figures 7.52a, 7.52b, 7.52c, 7.52d and 7.52e). Soils in the Mediterranean climates are quite variable, because of vegetation, slope and recent erosion or sedimentation, but they are agriculturally rich in lowlands such as the Central Valley of California and the Willamette Valley of Oregon. Common mature soils in coastal California and Oregon include mollisols (grassy ground cover) and alfisols (closed forests), although immature soils such as entisols and inceptisols are common on slopes that have experienced recent erosion or sedimentation.



Figure 7.51a. (left) Sclerophyllous leaves of the California coastal oak (Source/Credit: Dennis I. Netoff).

Figure 7.51b. (right) Sclerophyllous leaves of the Manzanita in the Mediterranean climate of California. Both the California coastal oak and the Manzanita are evergreen but can withstand the stress of summer drought and occasional winter cold because of the woody structure of the leaves and the waxy surface coating (Source/Credit: Dennis I. Netoff).



Figure 7.52a. The chaparral is a low, woody, dense shrub community that may be in part the result of frequent fire (Source/Credit: Dennis I. Netoff).



Figure 7.52b. The oak-woodland community has a structure similar to that of the tropical savanna. A distinctive aspect of the oak-woodland is that the vast under-story of grasses is winter green, when the rains occur (Source/Credit: Dennis I. Netoff).



Figure 7.52c. A Mediterranean oak-woodland community (Source/Credit: Dennis I. Netoff).



Figure 7.52d. A chaparral community (Source/Credit: Dennis I. Netoff).



Figure 7.52e. A Mediterranean oak-woodland community (Source/Credit: Dennis I. Netoff).

In California, the Santa Ana winds that follow the dry season fan the flames of fires that occur every year throughout Southern California. As a result, hillsides are set ablaze by raging fires that are difficult to control and which cause millions of dollars of property damage almost every year in the State. When the winter rains return, the denuded hillslopes frequently experience massive landslides (Figure 7.53).



Figure 7.53. Campground in Cable Canyon, southern California. A debris flow occurred on December 25, 2003 that killed several people. The debris flow was triggered by heavy rains, but was facilitated by removal of the protective vegetation cover by a wildfire during the previous October (Source/Credit: USGS, image by Sue Cannon).

## Marine West Coast Climates (Cfb or Cfc)

Marine west coast climates are typically located along west coasts poleward of the Mediterranean climates at latitudes of 40° - 60° or so. They are cooler and wetter than the Mediterranean climates. The blocking effect of the dry side of the subtropical high is less effective than in the Mediterranean climates, so even the summer months receive adequate precipitation (Figures 7.54a and 7.54b). Westerly winds bring cool, moist air from the ocean onto the continent. The ocean moderates temperature extremes resulting in warmer conditions during the winter than would be expected for that latitude, and cooler summers as well. During winter, the average temperature remains above freezing which is in marked contrast to locations in the continental interior at similar latitudes, such as Winnipeg, Canada, where the average monthly temperature in January is just below 0°F (minus 18°C).

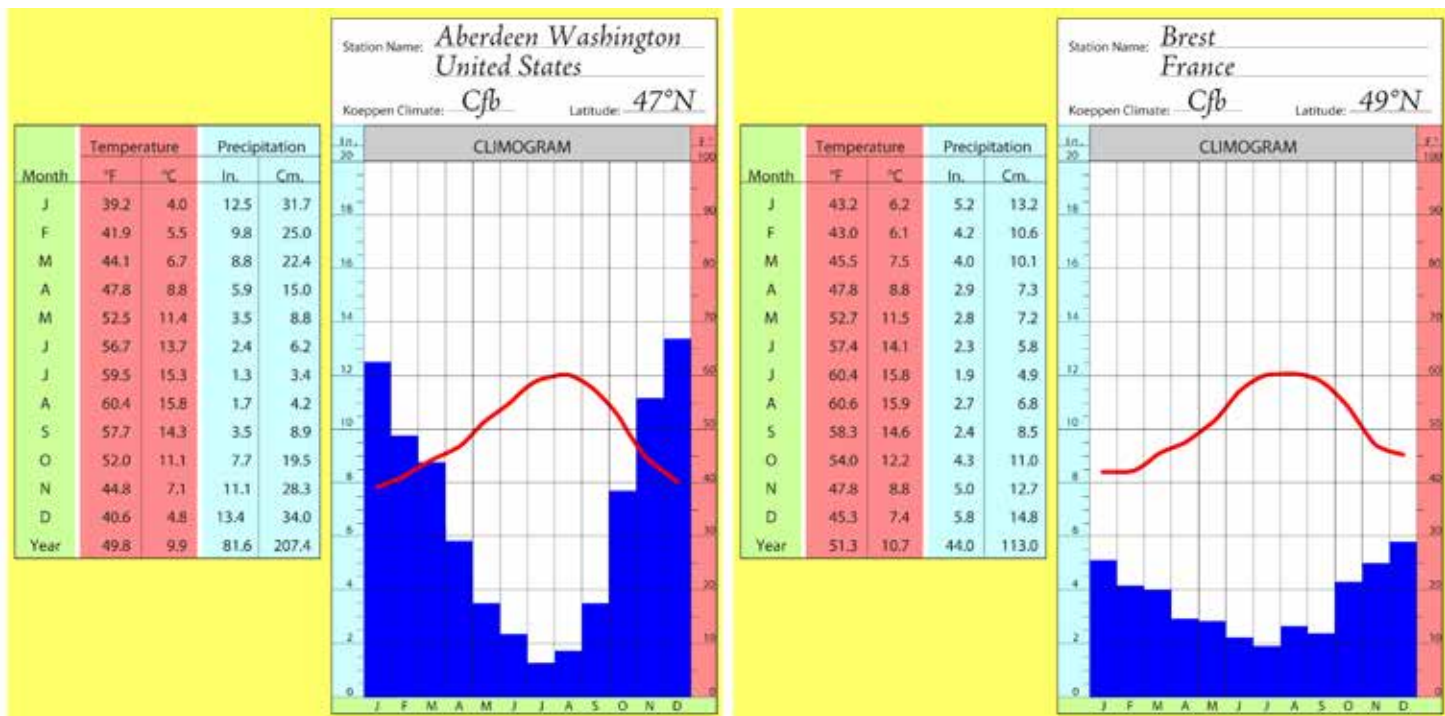


Figure 7.54a. (left) Climogram of Aberdeen, Washington. Marine West Coast climates experience year-round frontal cyclonic activity which brings abundant rain in all months. Although Aberdeen is on the coast, the nearby coastal mountains magnify the precipitation.

Figure 7.54b. (right) Climogram of Brest, France.

There are five general locations of marine west coast climates on Earth, each generally located poleward of the Mediterranean climates (see Figure 7.1). In North America, South America, southern Africa and Tasmania-New Zealand they are typically restricted to coastal areas by the presence of mountains, or occur on isolated islands. Only in Northern Europe, where the Alps trend east-west, allowing deeper penetration of maritime air masses onto the continent, do marine west coast climates have considerable east-west extent.



Because of the marine influence, the frequent passage of frontal-cyclones and orographic effects along mountainous coasts, precipitation levels average more than 50 inches per year, and several locations exceed 100 inches. This is one of the cloudiest, rainiest, foggiest climates in the world. For example, in Bahia Felix, Chile near the Straits of Magellan, rain falls 325 days a year. In 1916, rain fell on 348 days. Even when it is not raining, skies are often overcast. A statement on the Marquee at Peninsula College, located on the Strait of Juan de Fuca on the north flank of Washington's Olympic Mountains once stated: *people in Washington don't tan, they rust.*

At higher elevations, the heavy precipitation produces beautiful snow-capped peaks and many modern-day glaciers. The Pacific Northwest region of the United States is noted for its spectacular glacially-carved landscape. The lofty volcanic highlands of Mt. Shasta in northern California, Mt. Hood in Oregon and Mt. Rainier in Washington are so deeply covered with snow that roads to higher elevations typically do not open until mid-summer because of heavy snow drifts and the difficulty in keeping the roads open.

Most marine west coast climates experience a tendency for **summers to be considerably drier than winters because of the poleward migration of the stable, dry side of the Subtropical High**. Some frontal cyclones, however, penetrate these areas in all summer months, so the soils tend to have adequate soil moisture year-round. The **f** designation means adequate moisture in all months. The higher latitude and the marine influence keep the summers mild to cool (C**f** and C**f**c).

The abundant precipitation in this area supports lush, mid-latitude forests. In North America, the dominant trees of the marine west coast climates are **needleleaf evergreen**, and form an ecosystem that is similar in appearance to the **northern coniferous forests** of the Canadian Plains (Figure 7.55). Some of the tallest tree species on Earth inhabit the marine west coast climates and the cooler margins of the Mediterranean climates. Vast, evergreen expanses of **fir** (e.g., the **White fir** and the **Douglas fir**), spruce (e.g., the **Sitka spruce**), **pine** (many species), **cedar** (e.g., the **incense cedar**), **redwood** and **hemlock** dominate the landscape. Arguably among the tallest species of either plant or animal that ever inhabited the face of the Earth is the Douglas fir or the Coastal redwood, both reputedly some 374 feet in height. The wettest areas are known as mid-latitude rainforests (e.g., the Olympic Peninsula in Washington). Here there is green everywhere, including abundant mosses, ferns, lichens and the dense foliage of the forest canopy (Figure 7.56). In Europe, broadleaf deciduous forests are more common than the needleleaf forest (Figure 7.57). The exact reason for the occurrence of the broadleaf forests in Europe is unclear, but it may have to do with species impoverishment during glacial times when much of the northern European Plains were overrun repeatedly by glacial ice.



Figure 7.55. Coniferous forests dominate the marine west coast climate of North America. These are needleleaf evergreen trees such as fir, pine, spruce, cedar and hemlock (Source/Credit: Dennis I. Netoff).



Figure 7.56 The Olympic Peninsula is home to one of the few temperate rainforests in the world. Individual trees can be well over 200 feet in height making the forest floor damp and dark (Source/Credit: Dennis I. Netoff).



*Figure 7.57. Unlike North America, much of the Northern European Cfb climate is dominated by broadleaf deciduous trees, such as this chestnut-oak stand in northwest France (Source/Credit: Christopher Baldwin).*

Soils tend to be acidic under the needleleaf forest. They include **spodosols**, alfisols and, in some places, highly weathered ultisols. Steep slopes are largely stripped of mature soils and tend to be thin, acidic and poorly developed. Their agricultural potential is limited. Floodplains and old lake floors, however can be quite productive.

## Humid Continental and Continental Subarctic (D) Climates

The **D** climates are restricted to the large, middle-to-high latitude (40° to 70°), Northern Hemisphere continents of North America and Eurasia. **There are no widespread Southern Hemisphere D climates** because of the occurrence of vast oceans at the appropriate latitudes. The D climates are characterized by very cold winters with at least one month averaging below 32°F (0°C). To distinguish D and E climates, the D climates must have at least one month more than 50°F (10°C). With one or more months below freezing, **cold season precipitation is largely in the form of snow** and the snow may persist for days to months, depending on the amount of snowfall and the duration of sub-freezing months. The subtypes within this climate group have many of the second and third letter designations as does the C climate group. An exception is in Siberia, where there may be one or more winter months below minus 36.4°F (minus 38°C), and the third lower case letter **d** is used.

The cold winter conditions result from a combination of low-Sun angle during the winter, short winter daylight hours and the high albedo of the snow-covered ground surfaces during winter. These are referred to as *continental climates*, even though many of them extend to the Arctic coast as well as to the eastern side of North America and Eurasia. Proximity to the Arctic Ocean does very little to warm coastal areas because of the extensive cover of ice over the Arctic Ocean during much of the winter. East coast locations, likewise, feel very little *maritime* influence because the winter *monsoon* winds generally blow from the continent to the ocean.

## Humid Continental Climates (Dfa and Dfb)

The humid continental climates occur from 40° to 50°N in North America, and from 40° to 60°N in Central and Eastern Europe (see Figure 7.1). It is also the climate of Northern China, Korea and most of Northern Japan. The precipitation is considered adequate in all months, although there is a definite monsoonal effect so that winters are drier than summers. The spring or early summer precipitation maximum is caused by the invasion of mT air masses at this time of the year. Frontal cyclones can occur in any month (Figures 7.58a, 7.58b and 7.58c). Winters tend to have sparse precipitation, in terms of liquid-equivalent snowfall, but low temperatures allow much of this moisture to infiltrate into the ground. The annual temperature range is large and increases with increasing latitude. For example, the annual temperature range is 47°F (26°C) for Saint Louis, Missouri, but increases to 68°F (38°C) for Winnipeg, Canada.

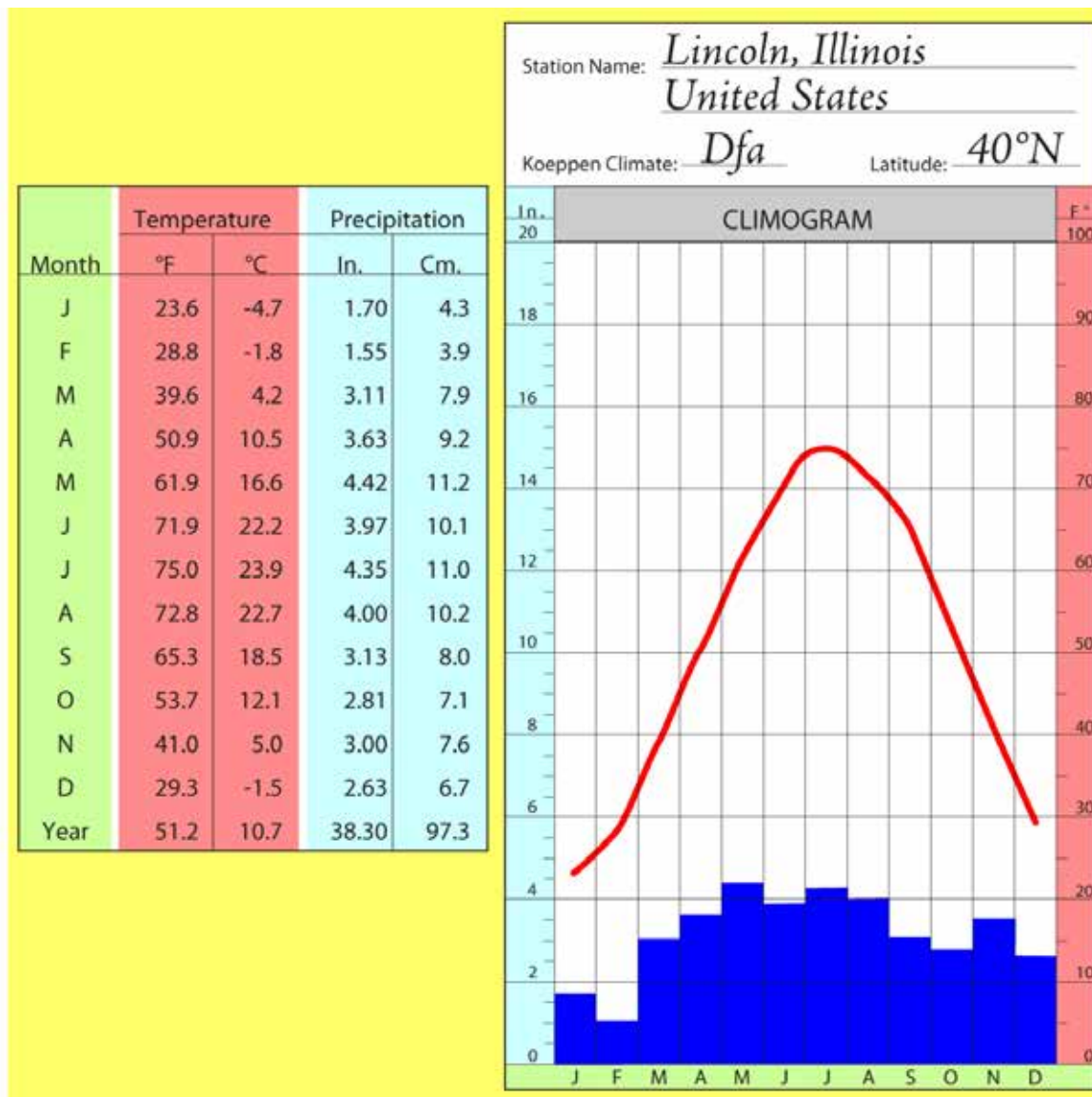


Figure 7.58a. Climogram of Lincoln, Illinois. This location has hot summers, and cool winters.

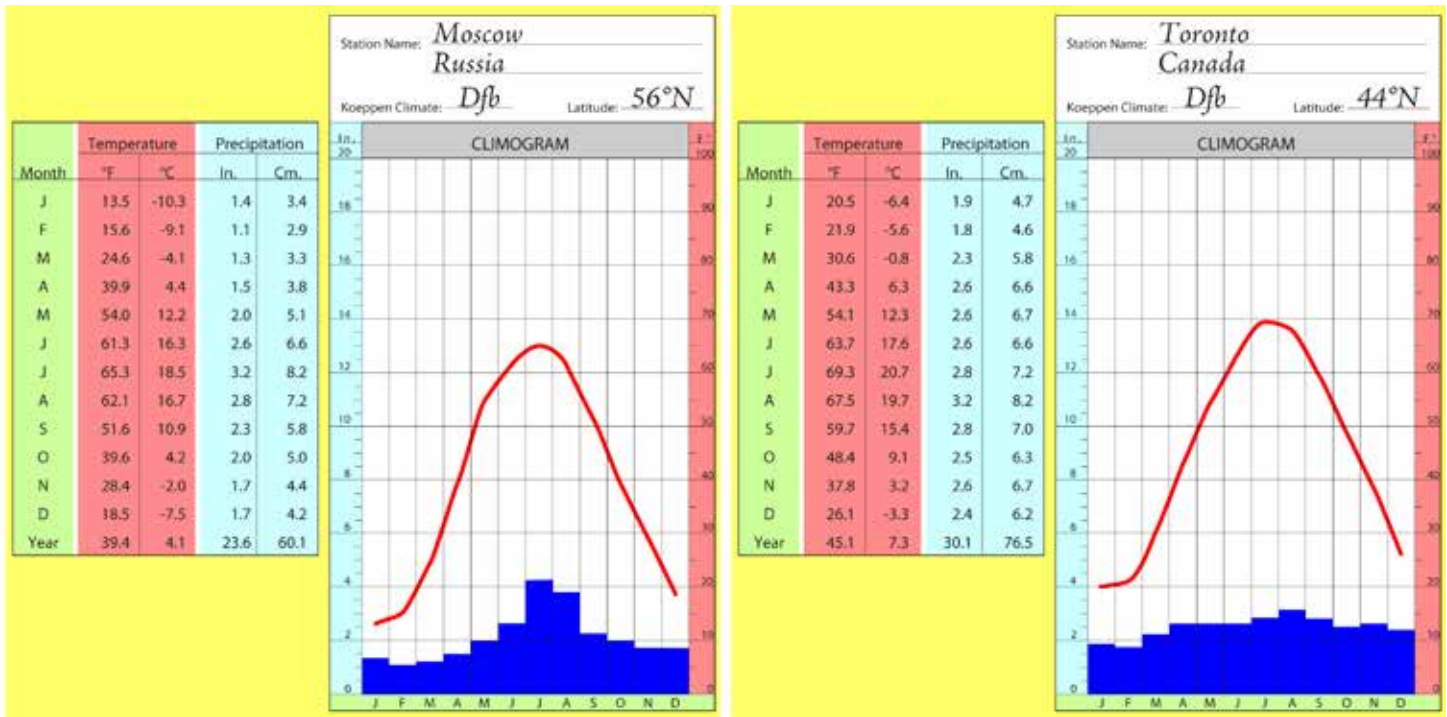


Figure 7.58b. (left) Climogram of Moscow, Russia. This location and Toronto have long and very cold winters, with mild summers.

Figure 7.58c. (right) Climogram of Toronto, Canada.

The wetter areas within this climate are dominated by either deciduous forests, coniferous forests or mixed forests, which represent a combination of coniferous and broadleaf deciduous (Figure 7.59). The spodosols of the coniferous forests tend to be acidic and of limited agricultural productivity, unless neutralized and fertilized. Mixed forests and broadleaf forests typically develop less acid soils called alfisols, which are more fertile than the spodosols. Along the drier margins of the humid continental climates, forests give way to grasslands. The grassland areas within this climate zone constitute one of the major agricultural regions of the world. The grassland soils are largely mollisols and are characterized by a soft, black layer that is rich in decomposed organic matter called **humus**. The upper horizons of many of the world's mollisols are derived from wind-blown geologic material called **loess**. The mineralogical character of loess, in conjunction with the high humus content and incomplete leaching of soluble minerals in the mollisols, makes them one of the richest agricultural soils on Earth.



Figure 7.59. A mixed forest of pine, spruce, and birch in the Dfa climate of New Hampshire (Source/Credit: Dennis I. Netoff).



## Continental Subarctic Climates (Dfc, Dwc, Dfd, Dwd)

Continental subarctic climates are generally located poleward of the humid continental climates. Summers are cool and short, and winters are long and cold to frigid. In the Dfc climates, there are only one to three summer months with average temperatures above 50°F (10°C). In North America, these climates extend from Alaska through Canada; and in Eurasia they extend from Norway through much of Siberia. They occupy the source regions for continental polar (cP) air masses. **This climate has the largest temperature range of any climate in the world.** For example, the town of Yakutsk in Siberia has an average annual temperature range of 113°F (63°C)! Winter temperatures in Siberia are among the harshest on Earth, rivaling those of interior Greenland and Antarctica (Figures 7.60a and 7.60b). The warmest month in summer averages 45°F (7°C), but in winter the coldest month averages minus 68°F (minus 56°C). Given the annual range, this means that the average change in monthly temperature is also the greatest of any place in the world.

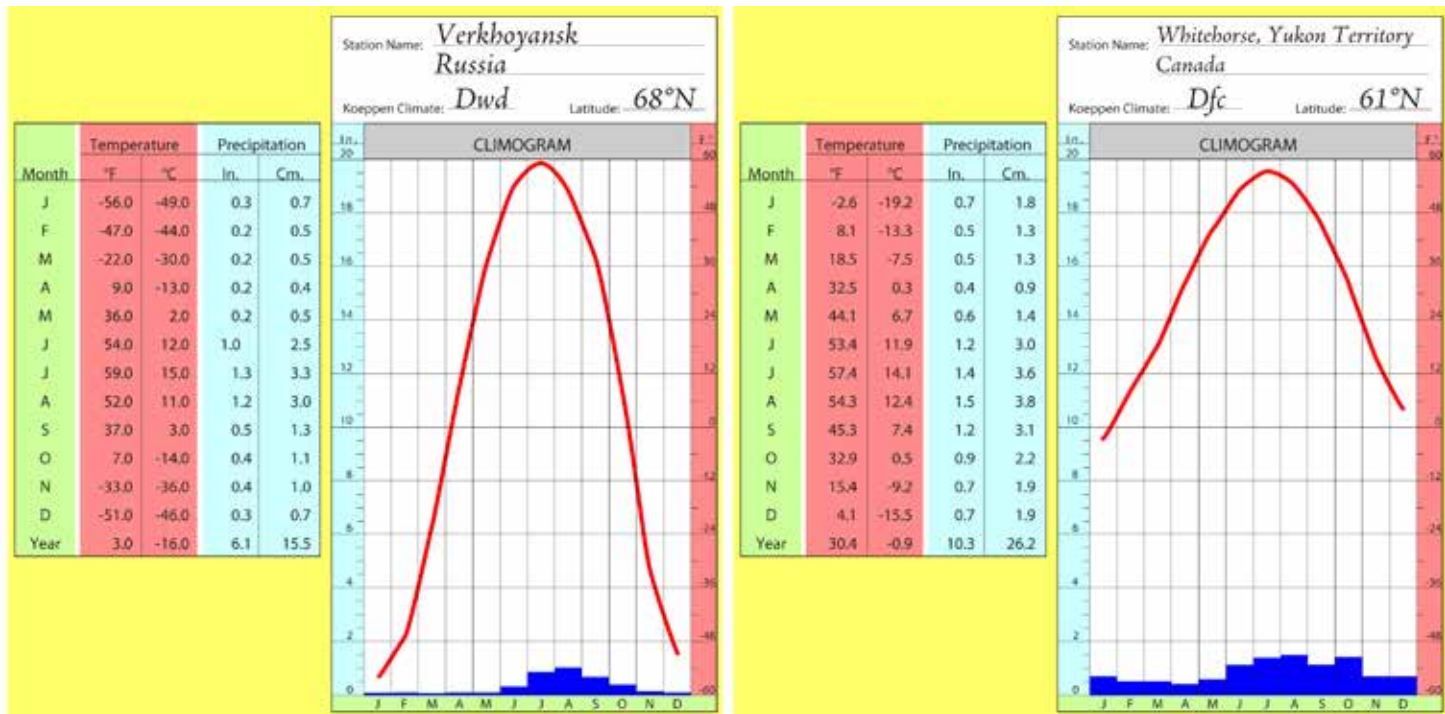


Figure 7.60a. (left) Climogram of Verkhoyansk, Russia. Both Verkhoyansk and Whitehorse have long, bitterly cold winters. Winters tend to have sparse precipitation because of the influence of the Siberian and Canadian anticyclones. In Siberia, there are vast areas dominated by a single species of tree, the Siberia Larch. The winters are so severely cold that the ground freezes to depths of tens of feet. As a result, the larch drops its needles during the winter.

Figure 7.60b. (right) Climogram of Whitehorse, Yukon Territory, Canada.

The severe winters and recent glaciation in the subarctic climate have resulted in a broad, uniform, coniferous forest called the **northern coniferous forest** in North America, and the **boreal forest** or **taiga** in Eurasia. This forest type covers the largest amount of forested area

in the world. Although precipitation levels are low in this climate, typically averaging less than 20 inches (51 cm) per year, these vast forests can be maintained by a relatively small supply of water. This is largely due to the growing season being so short and because cold temperatures reduce evaporation rates, thus much of the surface water infiltrates into the soil and can be utilized by the trees. The coniferous trees do well in cold climates. They have low moisture and nutrient requirements, are relatively drought tolerant, have flexible limbs to shed winter snow and have a waxy coating on their needles to inhibit moisture loss. Within the northern coniferous forest, there are stands of broadleaf deciduous trees that probably represent *successional* communities.

In the northern coniferous forest, thousands of square miles of land may be dominated by just a handful of species of needleleaf trees. This forest is sometimes referred to as species impoverished, in contrast to the biodiversity found in the tropical rainforest. These large, pure tracts of trees lend themselves to a lumbering activity called **clear-cutting**. **Lumbering is one of the major economic activities of this ecosystem**. Lumber is used for such things as construction, siding, pulp, paper products and plywood.

Severe climatic conditions and recent glaciation have restricted soil development in much of the subarctic climates. Mature soils may be alfisols or spodosols, but more frequently they are the immature entisols or inceptisols. Depressions left from glacial erosion are typically swampy, boggy areas dominated by **hydrophytic** (water-tolerant) plants and histosols (Figure 7.61). Constant freezing and thawing of the upper horizons causes heaving of the soil, further limiting their development.



Figure 7.61. Repeated glaciation during the recent geologic past has left thousands of depressions in the high-latitude landscape of the continental subarctic climates. These are initially the site of lakes, which gradually are filled with mineral as well as organic, swampy sediment. Soils that develop on these boggy sites are typically histosols. Peat is being mined in the dark-colored histosol in the middle foreground in the Front Range of Colorado (Source/Credit: Dennis I. Netoff).

This area is also characterized by the presence of **permafrost**, which is permanently frozen soil. The layer above the permafrost zone usually thaws during the summer; but, because the underlying ground remains frozen, the water cannot readily drain. As a result, the upper soil becomes saturated, and many bogs and shallow lakes develop as a result of this condition. During winter, the ground freezes solid again, and when the soil freezes, its volume expands. Most of the permafrost occurs in patches of various sizes, separated by non-permafrost zones.

The constant freezing and thawing makes construction and maintenance of roads, railroads and runways very difficult because the ever shifting ground breaks them apart. Homes and buildings must be built either on stilts or on a gravel layer in order to keep the heat associated with the building from melting the underlying permafrost. If this is not done, the uneven heating will melt part of the ground and cause the building to lean.

## Polar (E) Climates

In the Koeppen system, polar climates are those in which no month has an average temperature of above 50°F (10°C). Generally, this temperature represents the minimum temperature required for tree growth, and thus has great biological significance. The Koeppen system distinguishes two polar climates, the **tundra climate (ET)** and the **ice cap climate (EF)**.

### Tundra Climates (ET)

The tundra (ET) climate occurs along the coastal fringes of the Arctic Ocean and is dominated virtually year-round by polar air masses. Proximity to the ocean keeps the temperature warmer than it would otherwise be. The warmest month(s) are between 32°F (0°C) and 50°F (10°C), so there is a brief season for plant growth (Figure 7.62). Precipitation typically averages less than 14 inches (36cm) per year. The very short growing season and the severe winter cold and desiccating winds prevent tree growth. The tundra is a treeless expanse of low growing plants that include lichens, mosses, sedges and herbaceous plants (Figures 7.63a, 7.63b and 7.63c). These plants provide ample food for reindeer, musk ox and caribou.

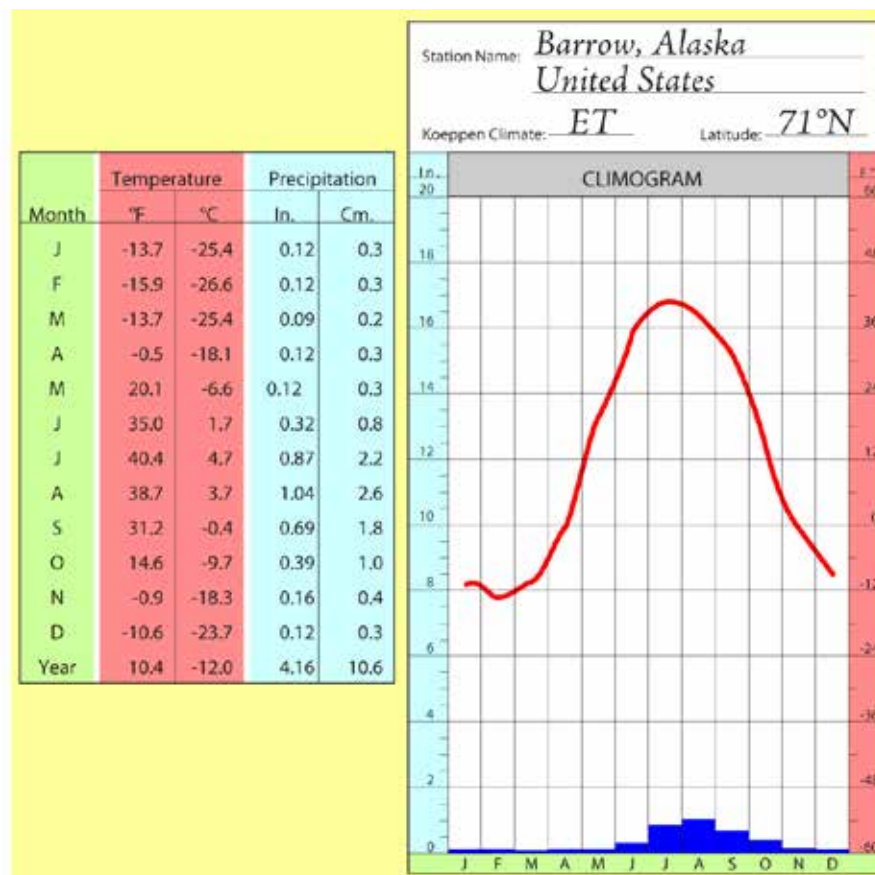


Figure 7.62. Climogram of the tundra (ET) climate of Barrow, Ala



Figure 7.63a. Tundra plants of the Arctic are well-adapted to long periods of bitter cold as well as strong, desiccating winds. Although summer days are long, the Sun's rays are at a very low angle and so temperatures remain cool. Purple saxifrage cushion is known as the 'Arctic compass' because the small (less than 0.5 inch; less than 1 cm) flowers only grow on the south-facing slope (Source/Credit: Christopher Baldwin).



Figure 7.63b. Lichens carpet the bedrock on a steep valley side in Svalbard (Source/Credit: Christopher Baldwin).



Figure 7.63c. The rocky 'patterned ground' in Spitzbergen is covered by a low growth of lichens, mosses, grasses and sedges (Source/Credit: Christopher Baldwin).

Permafrost is even more common in the ET climates than in the subarctic climates, and presents the same problems for construction. Soils are poorly developed entisols and inceptisols, except for the humus-rich histosols that form in water-logged bogs.

## Ice Cap Climates (EF)

This climate occurs at very high latitudes, typically poleward of 65° in both hemispheres. No monthly mean temperatures are above freezing (Figure 7.64). With the exception of the Antarctic Dry Valleys, these are realms of perpetual ice and snow. The EF climates include most of Greenland and Antarctica. Although daylight may last 24 hours during the summer, the **Sun angle is so low that little warming occurs. The high albedo of the snow and ice covered surface also helps maintain cold temperatures year-round.** As a result, this climate zone is nearly devoid of vegetation and soil.

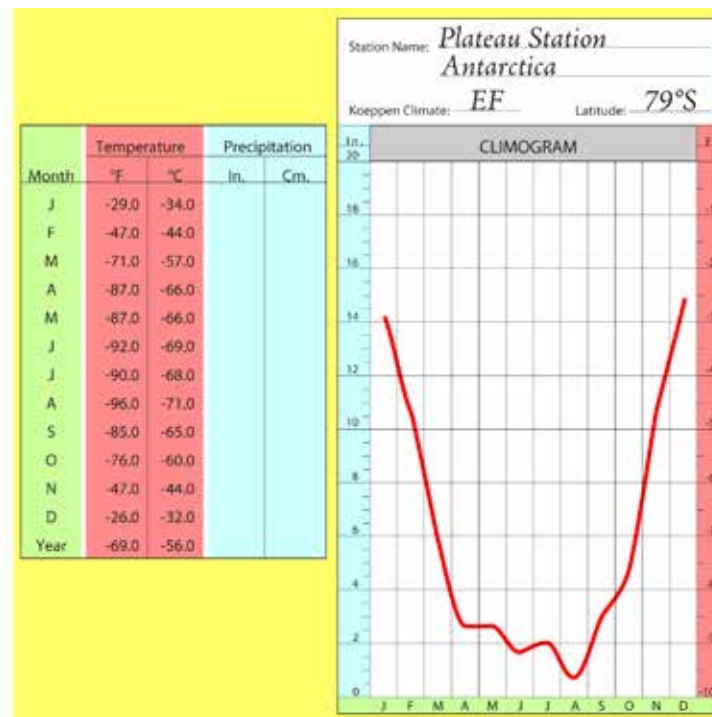


Figure 7.64. Climogram of an Icecap (EF) climate at Plateau Station, Antarctica. The average annual temperature of minus 69°F (minus 56°C) makes it one of the coldest places on Earth.

The extensive, thick (nearly 2 miles [3.2 km]) Greenland and Antarctic ice caps give the illusion of excessive snowfall, but this is hardly the case. Moderate to meager snowfall tends to linger and accumulate because of the bitter cold temperatures and low evaporation rates, and almost total absence of melting. Much of Greenland and Antarctica receive less than 10 inches (25 cm) of liquid-equivalent precipitation per year (again, the rule of thumb is that it takes about 10 inches of dry snow to equal one inch of liquid water).

Because of the high pressure generated over the cold, dry, ice covered surfaces of Greenland and Antarctica, both areas are characterized by **frequent strong winds that diverge toward the coast.** These winds that flow downhill in response to density and gravity are called **katabatic winds.** They are accelerated by gravity, and the smooth, ice-covered surface that



they blow across offers little frictional resistance to flow. At Mawson, on the Antarctic coast, winds exceeding 58 mph (50 knots) have been recorded every month of the year. Wind-chill equivalent temperatures can drop below minus 150°F (minus 101°C), making this a truly inhospitable place.

## Highland Climates (H)

The mountainous areas of the world are characterized by extreme variability of climate conditions over short areas. This altitudinal zonation of climate produces a corresponding altitudinal zonation of vegetation and soils. Rapid changes in climate, vegetation and soils are the result of:

- rapid changes in elevation over short horizontal distances which cause significant changes in temperature and precipitation (Figure 7.65).

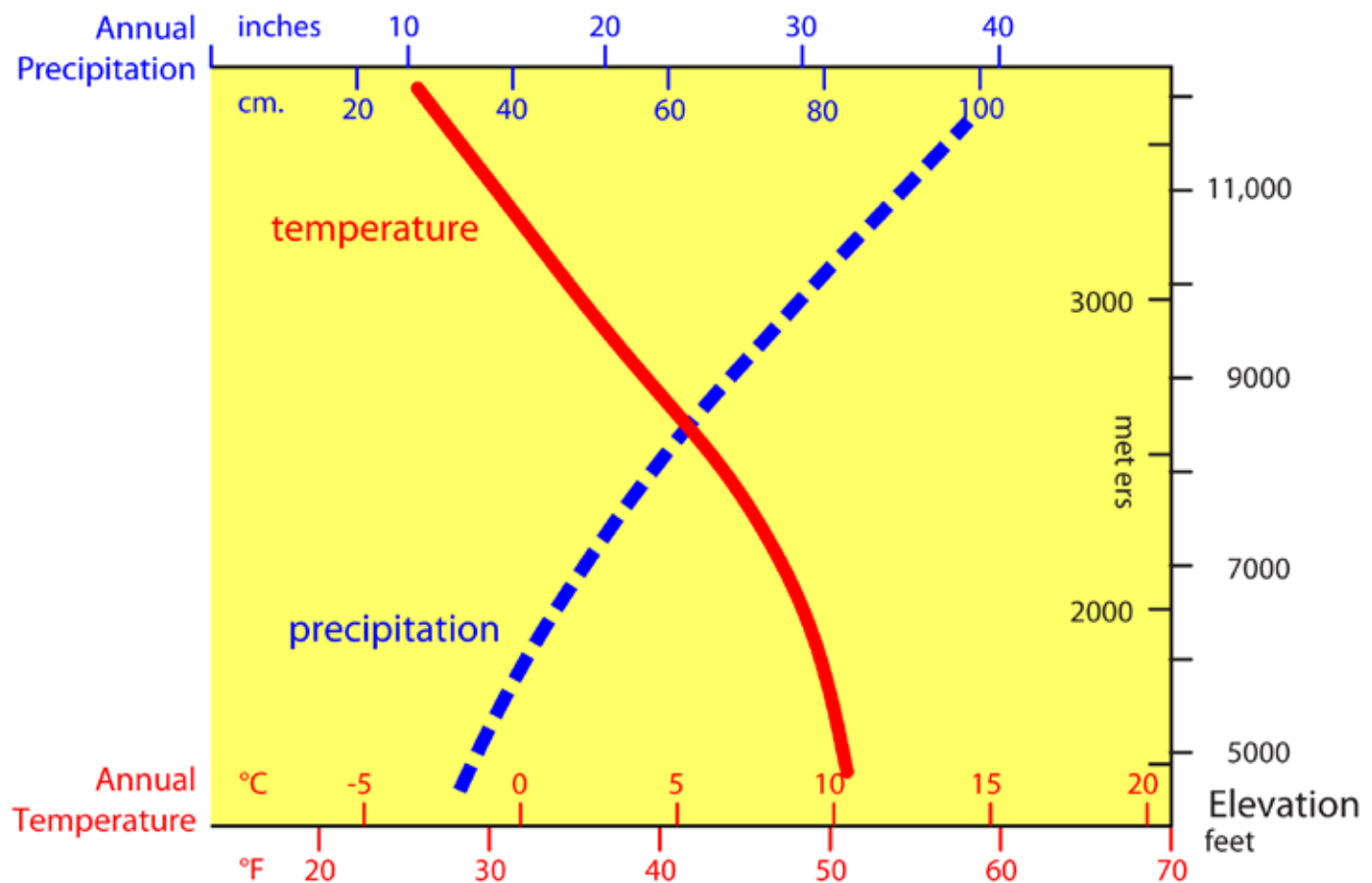


Figure 7.65. Highland climates are characterized by rapid changes in temperature and precipitation with elevation. The data shown depict changes from the base of the Front Range near Boulder, Colorado to the alpine tundra near the Continental Divide.

- windward-leeward effects, which have pronounced effects on rainfall (Figure 7.66).

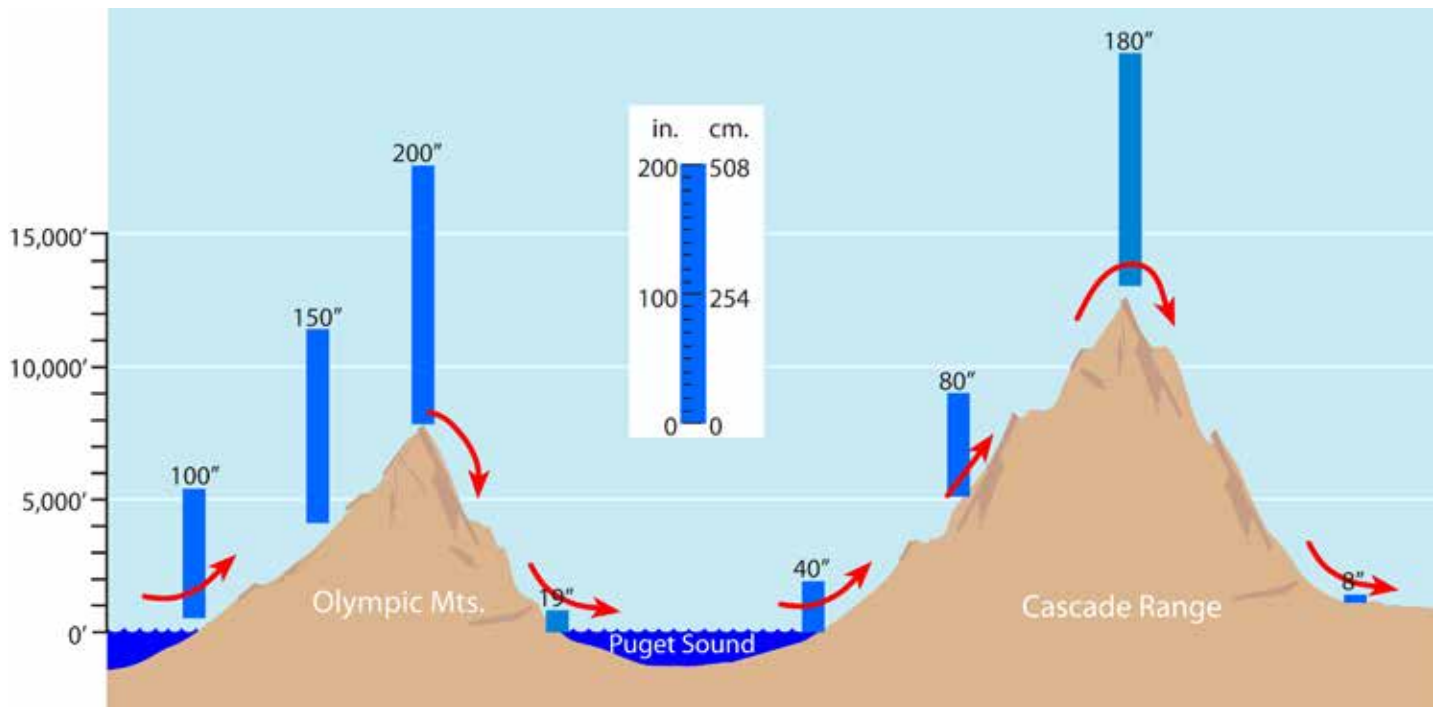


Figure 7.66. A west-to-east precipitation transect from the Pacific coast to central Washington. Windward slopes receive most of the rain and snow. Leeward slopes are dry, and are sometimes referred to as 'rainshadow deserts.' The crest of the Cascade Range has nearly 200 inches of precipitation, whereas Yakima, at the leeward base of the mountains only a few miles away, receives only 8 inches (Source/Credit: modified from Dennis I. Netoff and Ava Fujimoto-Strait, *Weather & Climate Lab Manual*).

- aspect effects (i.e., north vs south-facing slopes), which also have pronounced effects on temperature and soil moisture. South-facing slopes are significantly warmer and drier than north-facing slopes.

The result of this altitudinal zonation is a compression of ecosystem types in a fairly small area making it impossible to display them in detail on a continental or global-scale map. Consequently, Koeppen simply referred to these climates as *H* for highland climates.

Mountainous areas in practically every climatic zone have their own regional or local names to define ecosystem changes based on elevation. For example, in Guatemala, at about 15°N latitude, lower elevations are called the *Tierra caliente* (hot land), and with increasing elevation is found the *tierra templada* (temperate land), then the *tierra fria* (cold land), and finally the *tierra helada* (frozen land). In the western United States (30°N to 45°N), the base of a mountain may lie in a desert (BW) or steppe (BS) climate zone which may give way to a oak-woodland community, then a lower montane forest (Figures 7.67a and 7.67b), a *subalpine forest* (Figure 7.68) and finally the *alpine tundra* (Figure 7.69). The alpine tundra is similar to the high-latitude Arctic tundra in that it is generally treeless (Figures 7.70a and 7.70b). The plants of the alpine tundra are well adapted to severe cold, desiccating winter winds, and a short growing season.



Figure 7.67a. Spruce-fir forest in the montane zone of the Sierra Nevada at an elevation of about 7000 feet (Source/Credit: Dennis I. Netoff).



Figure 7.67b. Ponderosa Pine forest at the Val Verde site in the San Juan Mountains of Colorado at a similar elevation (Source/ Credit: Dennis I. Netoff).



Figure 7.68. The transition zone (ecotone) from the sub-alpine forest to the alpine tundra in the Colorado Front Range (Source/ Credit: Dennis I. Netoff).

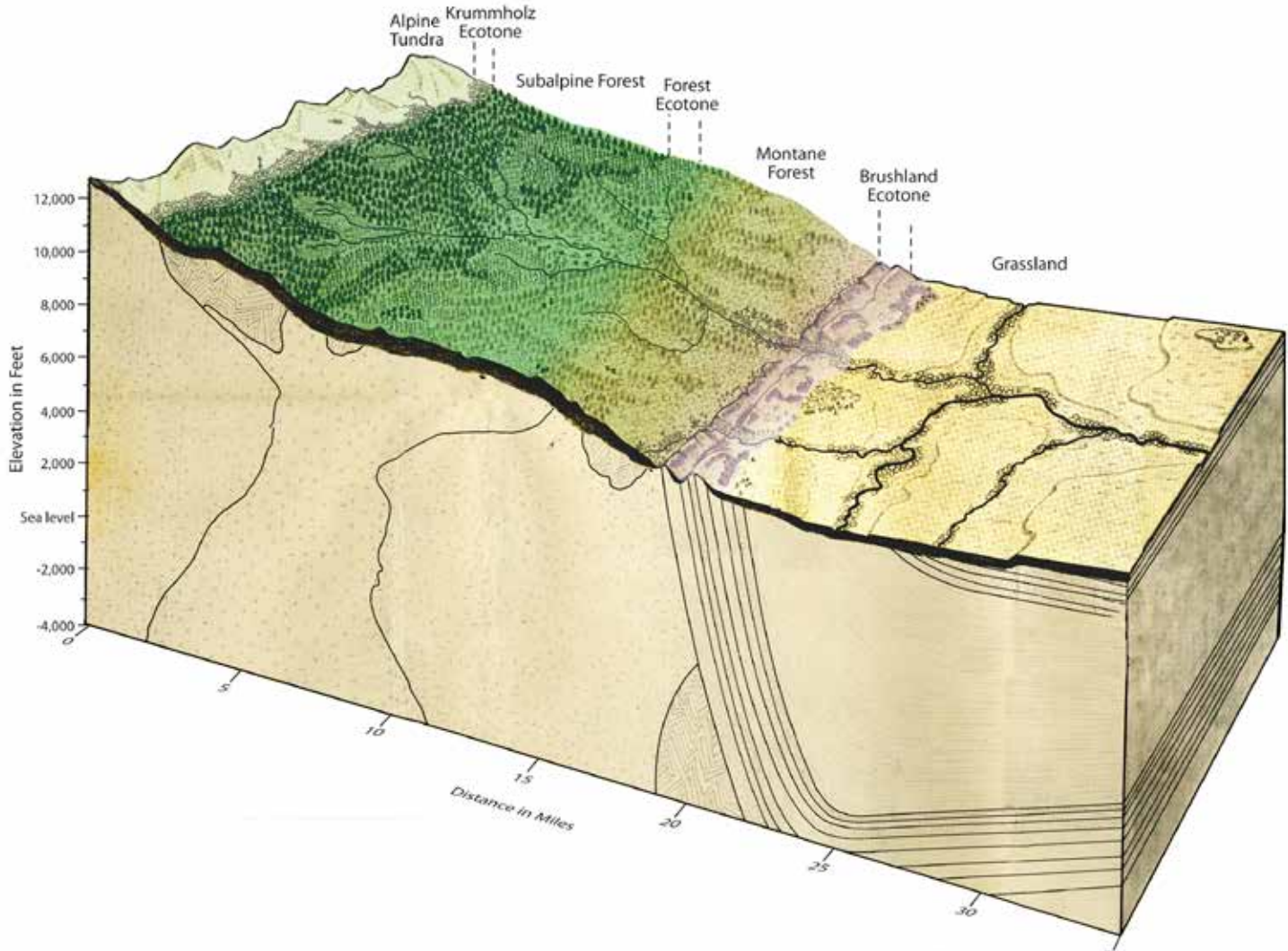


Figure 7.69. Vegetation transect from the grassland ecosystem at about 5000 feet elevation to about 13,000 feet at the Continental Divide in the Colorado Front Range. From lower to higher elevations are the grasslands, the brushland ecotone, the lower montane forest, the upper montane forest, the subalpine forest, the Krummholz ecotone and the alpine tundra (Source/Credit: Nancy Stonington).



Figure 7.70a. The alpine tundra of the Colorado Front Range at about 12,500 feet elevation. The alpine tundra is similar to the Arctic tundra in that there is a conspicuous absence of trees and the plant community consists of low-lying, cold-tolerant species. (Source/Credit: Dennis I. Netoff).

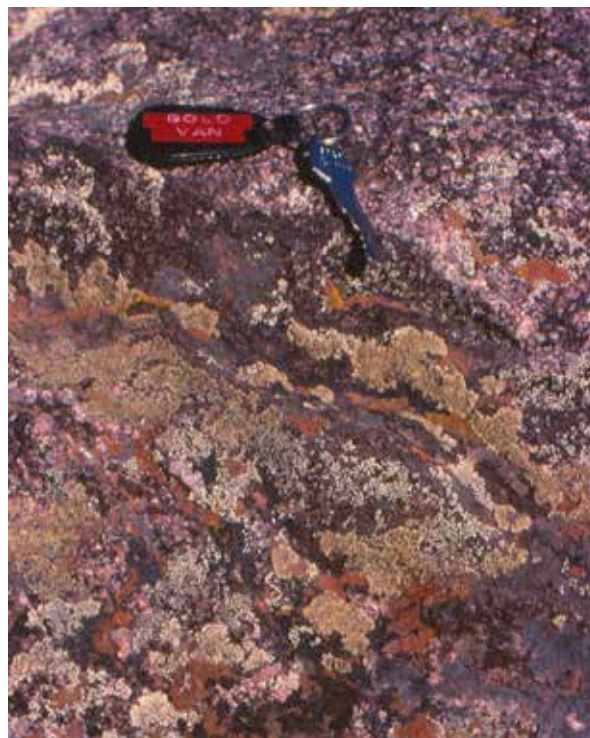


Figure 7.70b. Lichens occupying a bedrock surface in the alpine tundra of the Colorado Front Range. Several species of lichen are present. Lichens are considered one of the pioneer plants in the tundra. They slowly break down the bedrock and produce soils that are necessary for most of the other tundra plants (Source/Credit: Dennis I. Netoff).

Mature soils in mountainous areas include *alfisols* (broadleaf and mixed forests), *spodosols* (needleleaf forests), *mollisols* and *histosols* (grasslands and swamps), and occasionally ultisols where the landscape has been stable for long periods of time. More frequently, steep slopes and recent glaciation result in immature *entisols* and *inceptisols* (Figures 7.71a and 7.71b).



Figure 7.71a. (left) Soils of the higher elevations in mountainous climates are typically immature, because of recent erosion, deposition, and severe winter cold. The entisol in the subalpine forest has an A/Cox profile, and is developed on young glacial deposits (Source/Credit: Dennis I. Netoff).

Figure 7.71b. (right) The entisol in the alpine tundra is even less well-developed, with a total profile thickness of just over a foot (Source/Credit: Dennis I. Netoff).



Because of the altitudinal zonation of climate and vegetation, it is possible to have tundra and even ice cap at the Equator (Figures 7.72a and 7.72b).



Figure 7.72a. Alpine tundra on the Equator at more than 13,000 feet (4000 m) at Papallacta Pass, Ecuador (Source/Credit: Richard Payne).



*Figure 7.72b. Close-up of vegetation in Papallacta Pass, more than 13,000 feet, 4000 meters (Source/Credit: Richard Payne).*

## Chapter 8

# Climate Change

One of the most hotly-debated topics in all of the sciences in the 21<sup>st</sup> century is climate change. More specifically, the debate centers around the assertion that the period since the 1950s has seen **global warming**, and warming has accelerated in the past three decades. Moreover, statements such as those made by the Intergovernmental Panel on Climatic Change (IPCC) in 2013 that there is unequivocal evidence that human activities are mostly to blame for recent global warming have come under vicious attack by skeptics of global warming and its cause. Just a few decades ago, the topic of climate change was mostly discussed within the hidden realm of atmospheric scientists called paleoclimatologists. Today, it is virtually impossible to go to a book stand, pick up a newspaper, surf the world wide web, or listen to the news on TV, without hearing about the topic of climate change (Figure 8.1). Although the debate will continue for some time, there is **no debate that past, present, and future climate change has impacted human activities and will continue to do so, perhaps on an unprecedented scale.**

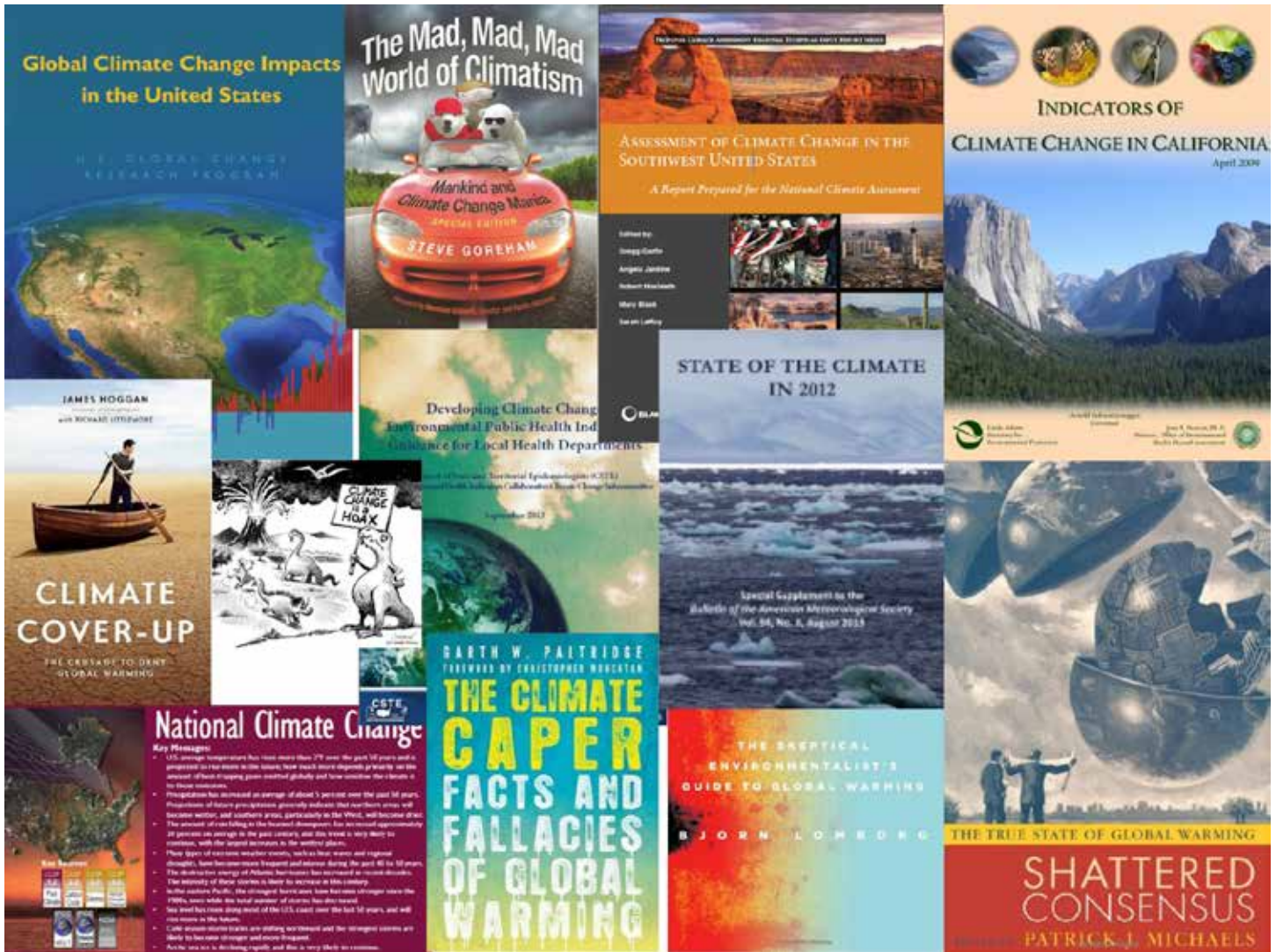


Figure 8.1. The debate over climate change has intensified over the past three decades. At one end of the spectrum is a host of government publications that methodically state the direction and exact magnitude of climate change and the degree to which humans are responsible for it. At the opposite end of the spectrum are those that flat-out deny that global warming is real, or at the least, deny that human activities are at all responsible. Lively, open debates about climate change are not only healthy but of critical importance to human sustainability.

## Evidence of Past Climatic Change

Climatic change, on any time scale, is the norm for planet Earth. Europe just emerged from the *Little Ice Age* in the 19<sup>th</sup> century. Records of wine grape harvests in Europe tell of years of good and bad short-term climate change. The *Medieval Warm Period*, from about AD 800-1300, saw the Norse colonization of the Americas and Viking settlements in Greenland. It may have also caused warmer and drier conditions in the Great Plains that re-activated thousands of square miles of sand dunes in places like the Sand Hills of Nebraska. The *dust bowl days* of the 1930s recorded several years of extreme drought, with dire consequences to farmers and ranchers in the western Great Plains. West Texas was partly covered with woodland a mere 18,000 years ago; now much of it is desert. Climatic change at the end of the Ordovician (440 million years ago) contributed to the extinction of some 85% of the Earth's land plants and animals.

Tropical flora occupied latitudes as high as 45 degrees at the start of the Eocene, about 56 million years ago. Dramatic variations in climate are undoubtedly linked to global extinctions (Figure 8.2). The present icehouse climate of the Earth began 34 million years ago, and then went into deep refrigeration about 2 million years ago. The present period of relative warmth began only 10,000 years ago. **One of the most compelling scientific questions of the 21<sup>st</sup> century is concerned with the magnitude, causes and impacts of global warming.**

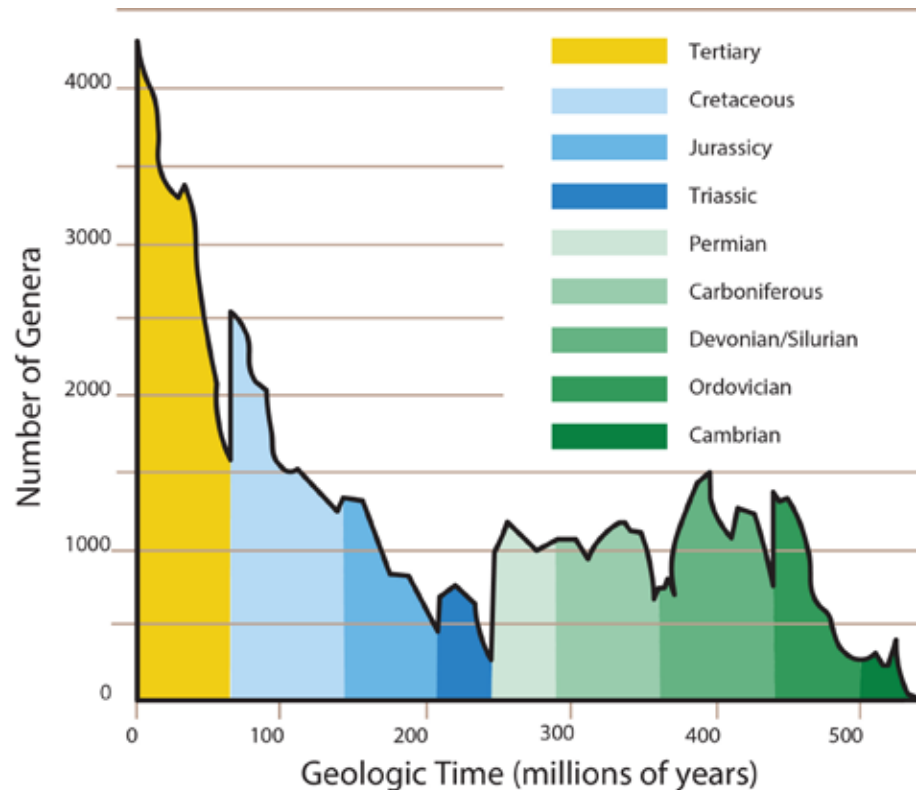


Figure 8.2. Several of the mass extinctions in Earth history have been linked to climatic change. The number of genera of plant and animal species is plotted against time for the past 550 million years. The Late Permian extinction was the most devastating in all of Earth history. The Late Cretaceous extinction brought a rapid end to the 150 million year reign of the dinosaurs.

Given all the variables that influence climate, it is amazing that the climate of the Earth has remained habitable for the past 3.8 billion years. There has never been a time in the history of this planet when the temperatures dropped so much that the entire planet froze (some *snowball Earth* advocates might debate this), nor has the temperature ever risen so high that life was extinguished. That such a relatively small temperature range could be maintained for billions of years is extraordinary. We owe our existence to a narrow range of climate changes.

The fact that climates do change is borne out by a variety of different types of evidence that includes such things as:

- Glacial landforms and deposits
- The geologic record of sea level changes. Assemblages of plant and animal fossils. Tree ring data
- Oxygen isotopes from glacial ice cores
- Buried soils
- Loess (wind-deposited silt) sheets
- Freshwater and playa lake deposits
- Remote sensing from satellites
- Written records

The picture that is emerging from climatological research is that the Earth's climate is highly changeable, as it has been throughout geologic time. In general, the bulk of the past 4.6 billion years has been characterized by a **greenhouse climate**, with temperatures warmer today and a conspicuous **absence of continental ice**. The greenhouse Earth occasionally shifts temporarily to **an icehouse climate** with continental and alpine glaciers covering a sizable portion of the continental land masses. Icehouse climates are usually brief, lasting from a hundred thousand years to a few million years (Figure 8.3).

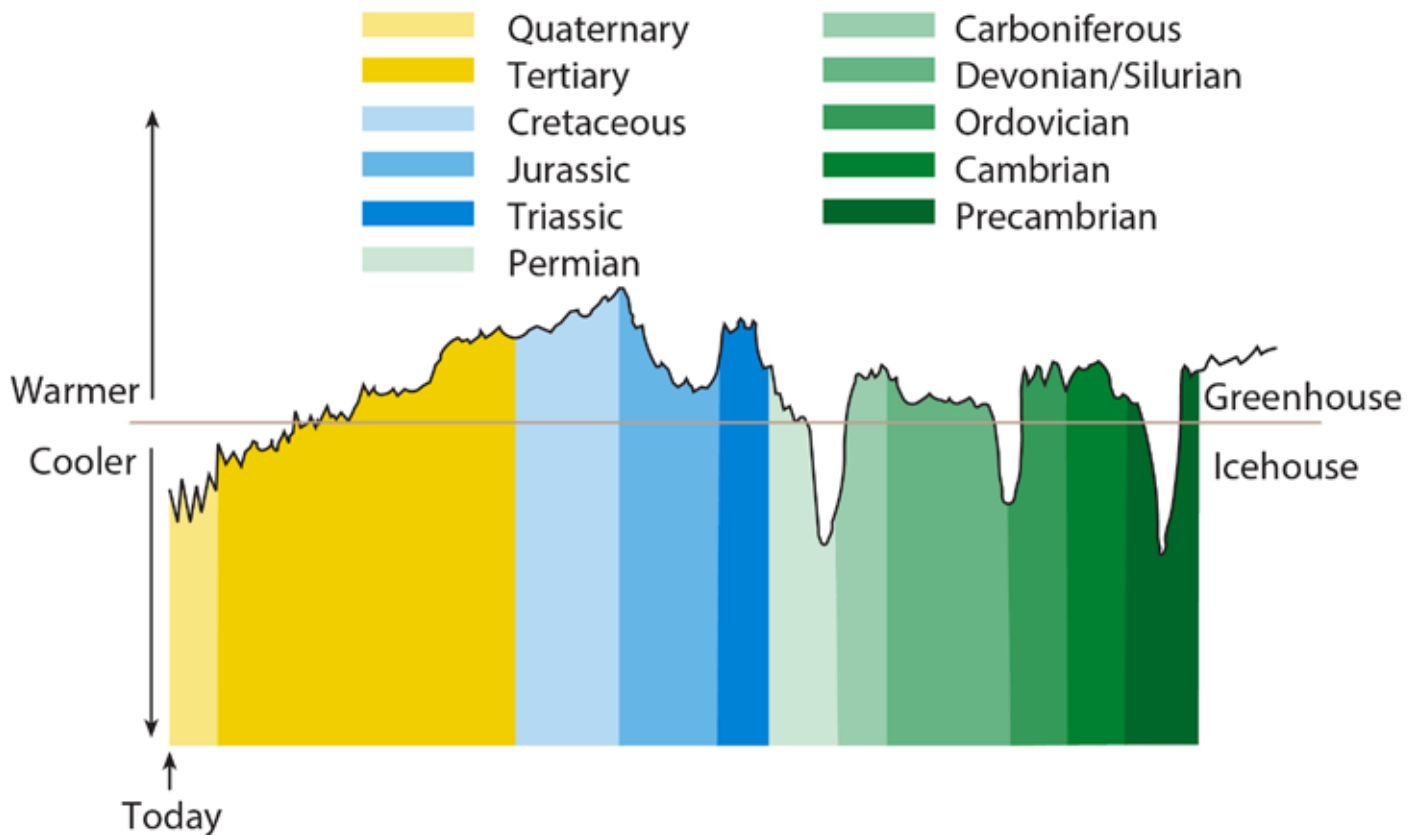


Figure 8.3. Most of the 4.6 billion year history of the Earth has been characterized by relatively warm, ice-free greenhouse climates, punctuated by brief periods of icehouse climate. The graph is a very crude estimate of temperature variations over the past 750 million years.

Icehouse climates constitute less than one percent of geological time. Humans have evolved in the present icehouse climate, which is atypical compared to the prevailing greenhouse climate of the Earth.

One of the goals of **paleoclimatology** is to decipher these changes using the types of data listed above, and to develop explanations to account for these changes. Since climate affects all aspects of life on Earth, an understanding of the causes of climate change can help us to better prepare for future climate change, and possibly take action to stop climate changes caused by human activities, or at least mitigate the consequences of those changes.

## Theories of Climate Change

Climatic change can be driven by external, or extraterrestrial causes, terrestrial causes, or a combination of both. **No single theory of climatic change can explain the frequency and magnitude of all of the changes that are known to have occurred in Earth history.** The following discussion of some of the theories of climatic change barely touch on the breadth and complexity of understanding climatic change. It has been estimated that there has been about one theory of climatic change proposed each year since the general acceptance of the glacial theory in the mid-1800s. Only in the past few decades, however, have we been able to get reliable age dating of climatic variability, and have been able to test theories with computer models that simulate the atmosphere.

### Variations in Solar Output

The average amount of energy received at the top of the atmosphere when the Sun is directly overhead is known as the **solar constant** and is equal to 2 calories/cm<sup>2</sup>/minute. However, recent satellite measurements of solar output indicate that the amount varies by about 1% through time, so the solar constant is not a true constant. Satellite data gathered since the early-1980s has revealed both cyclic and non-cyclic changes in solar output. The phrase solar constant is more frequently referred to today as the **total solar irradiance**. The value of the total solar irradiance is about 1361 watts/square meter, measured outside the Earth's atmosphere adjusted to an Earth-Sun distance of 93 million miles.



While this one percent variation in output may not seem significant, it may be capable of causing important changes in global average temperatures. For example, between 1615 and 1715 A.D., the amount of energy given off by the Sun diminished slightly. At this time, there were virtually no sunspots on the Sun (Figure 8.4).

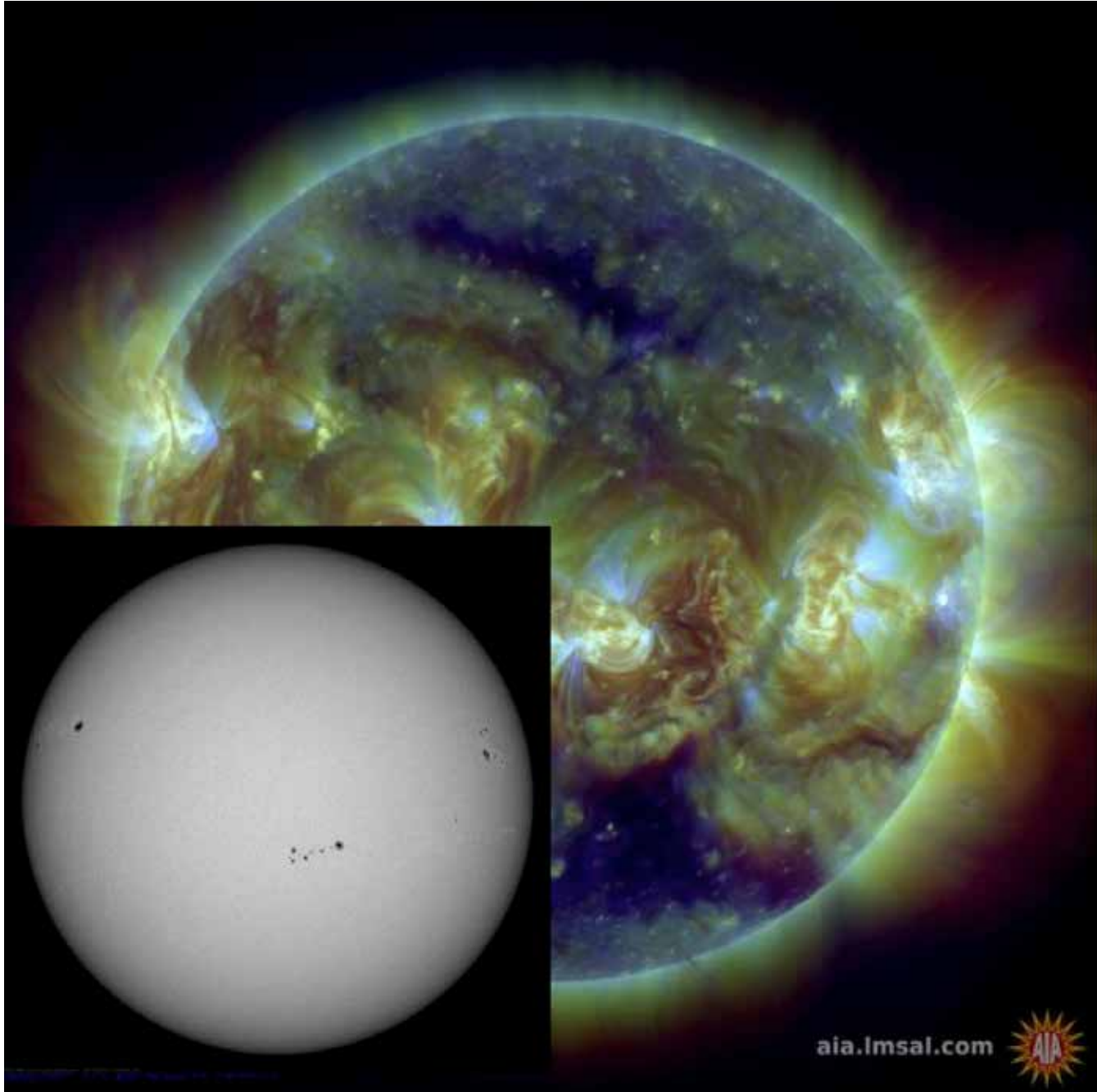


Figure 8.4. Sunspots are actually cool spots (~8,000°F; 4300°C) on the Sun. When they are abundant, however, the overall output of solar energy increases. Sunspots increase and decrease in a cycle of approximately 11 years. The image above is of sunspot activity on March 14, 2014. The inset shows several areas of sunspot activity. The larger image, taken in different wavelengths, shows the intense geomagnetic activity associated with the sunspots. A hiatus in sunspot activity may have contributed to a period of reduced global temperatures during the 17<sup>th</sup> and 18<sup>th</sup> centuries known as the Little Ice Age (Source/Credit: NASA/SDO Solar Dynamics Observatory).

This period of reduced sunspot activity is called the **Maunder Minimum** after the person who described it (Figure 8.5).

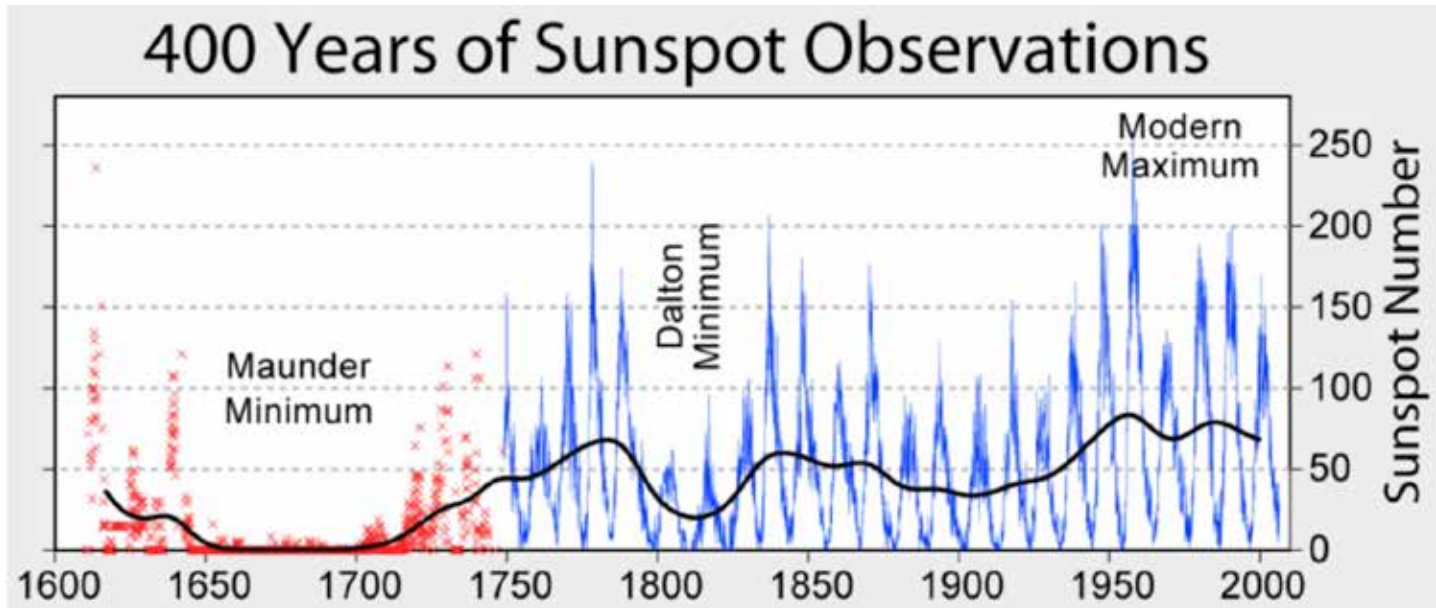


Figure 8.5. Sunspot activity was greatly reduced during the 17<sup>th</sup> century. This period, known as the Maunder Minimum, roughly coincided with cooler-than-normal temperatures on Earth, the Little Ice Age. The blue line represents sunspots reported by several observatories; the red dots are sporadic observations, and actual numbers may have been somewhat different than shown. Although the correlation between the Maunder Minimum and the Little Ice Age is real, it is unclear if the low sunspot activity was the actual cause of reduced global temperatures (Source/Credit: Robert Rohde, Global Warming Art project).

This period was one of exceptional cold in Europe and the Americas and is referred to as the **Little Ice Age**. During this time, the Viking colonies disappeared from Greenland and advancing glaciers overran Swiss villages. Canals in Holland froze repeatedly and for long periods of time. The estimated drop in average global temperature was only 1.8°F (1.0 °C). Either minor changes in solar output can have significant effects on climate, or, as other scientists argue, there were other factors involved in causing the Little Ice Age. Sunspot cycle 24 hit a trough and surprisingly, remained low until early 2010. The expected peak in 2013-2014 has instead resulted in an erratic series of ups and downs, with overall sunspot activity considerably below that of the previous peaks. If the size of the peak remains small throughout the cycle, this will likely become the weakest sunspot maximum since 1906 (Figure 8.6).

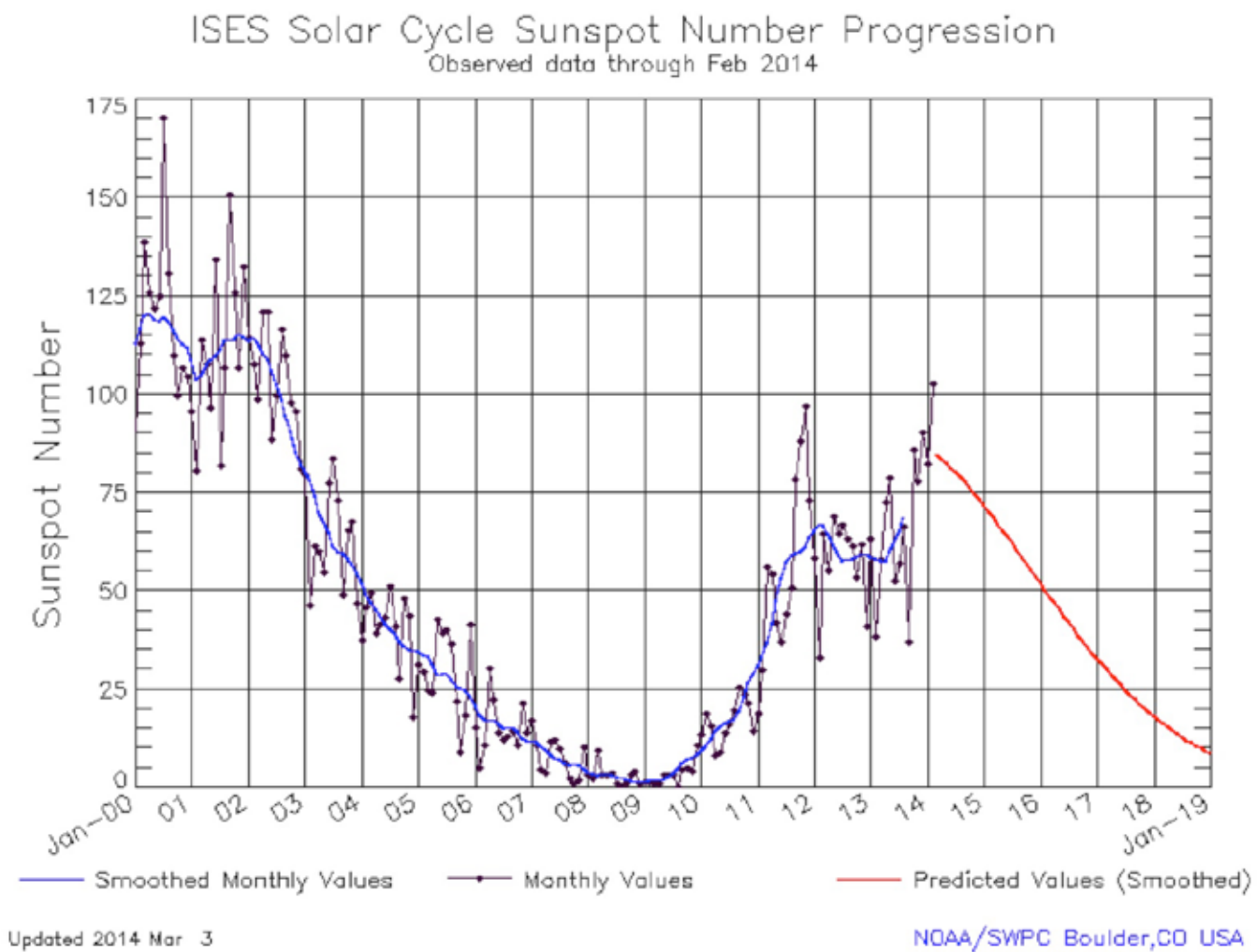


Figure 8.6. Sunspot cycle 23 began with a double peak between 2000 and 2002. The sunspot trough that began in 2006 lasted an unusually long time, and finally started to rebound in early 2010. Sunspot cycle 24 was expected to peak at around 2013-2014, but instead shows an erratic pattern that overall is much smaller than the previous peak in 2000-2002 (Source/Credit: NOAA/SWPC).

Variations in sunspot number and total solar irradiance (output) from 1979 to 2014 show an overall slight downward trend of solar irradiance, which argues against it being the sole cause of recent decadal warming (Figure 8.7).

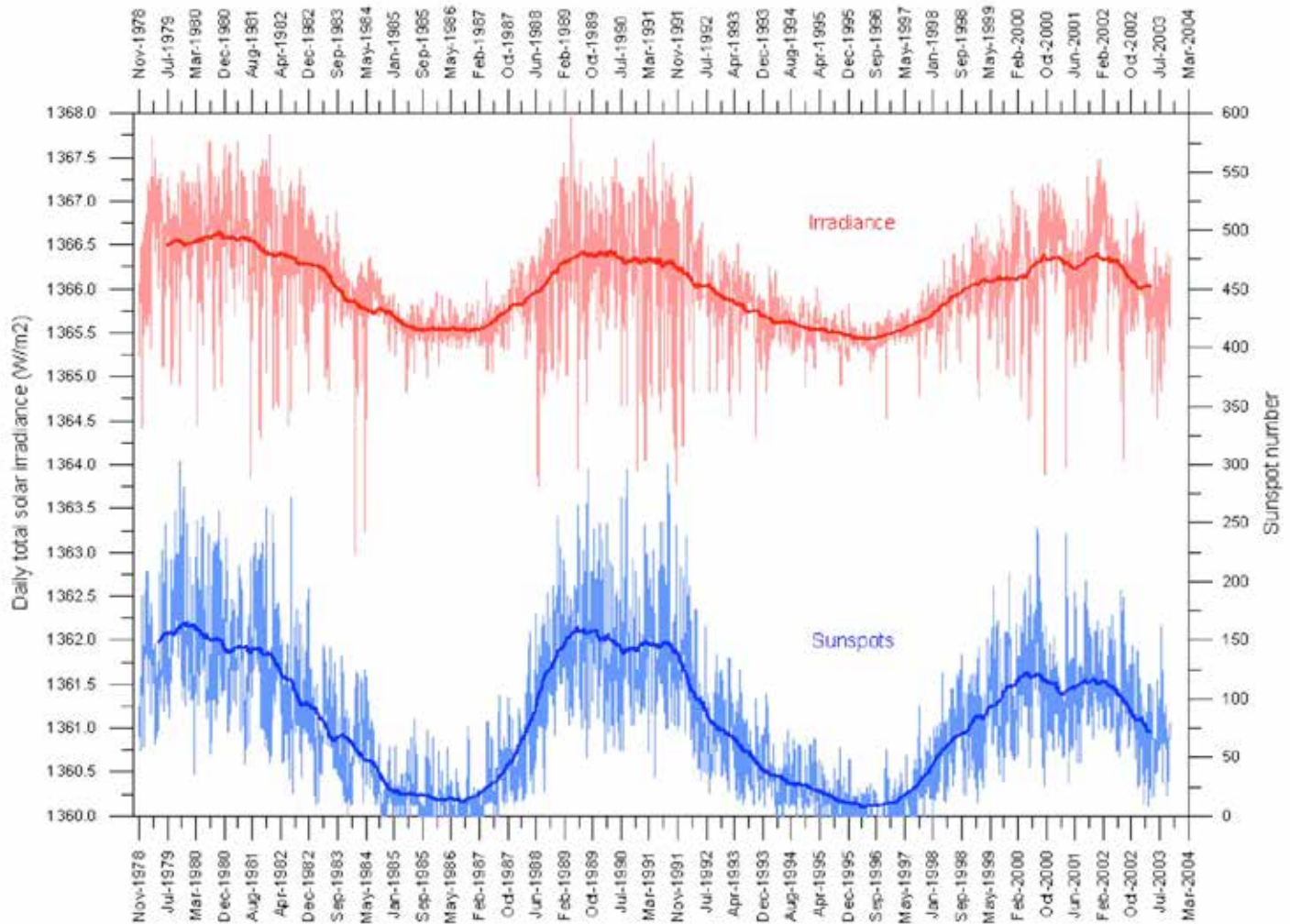


Figure 8.7. Variations in sunspot number and total solar irradiance (output) from 1979 to 2014. The light red and blue squiggles represent daily variations, whereas the solid darker lines are running averages. The overall downward trend of solar irradiance argues against it being the sole cause of recent decadal warming (Source/Credit: NOAA/National Geophysical Data Center).

## Orbital and Axial Variations

The geometric relationships between the Earth and the Sun, including such things as the angle of axial tilt, the shape of the Earth's orbit, and the time of the year when the Earth is closest or most distant from the Sun, help determine the radiation received at various latitudes during the course of the year. Changes in any of these orbital and axial parameters can change the distribution of solar energy intercepted by the Earth's surface, and therefore can cause temperature variations. **Orbital and axial variations are thought to be a major influence in the 100,000-year glacial-interglacial climatic cycles that have occurred during the Quaternary, the past 1.8 million years of geologic time (Figure 8.8).**

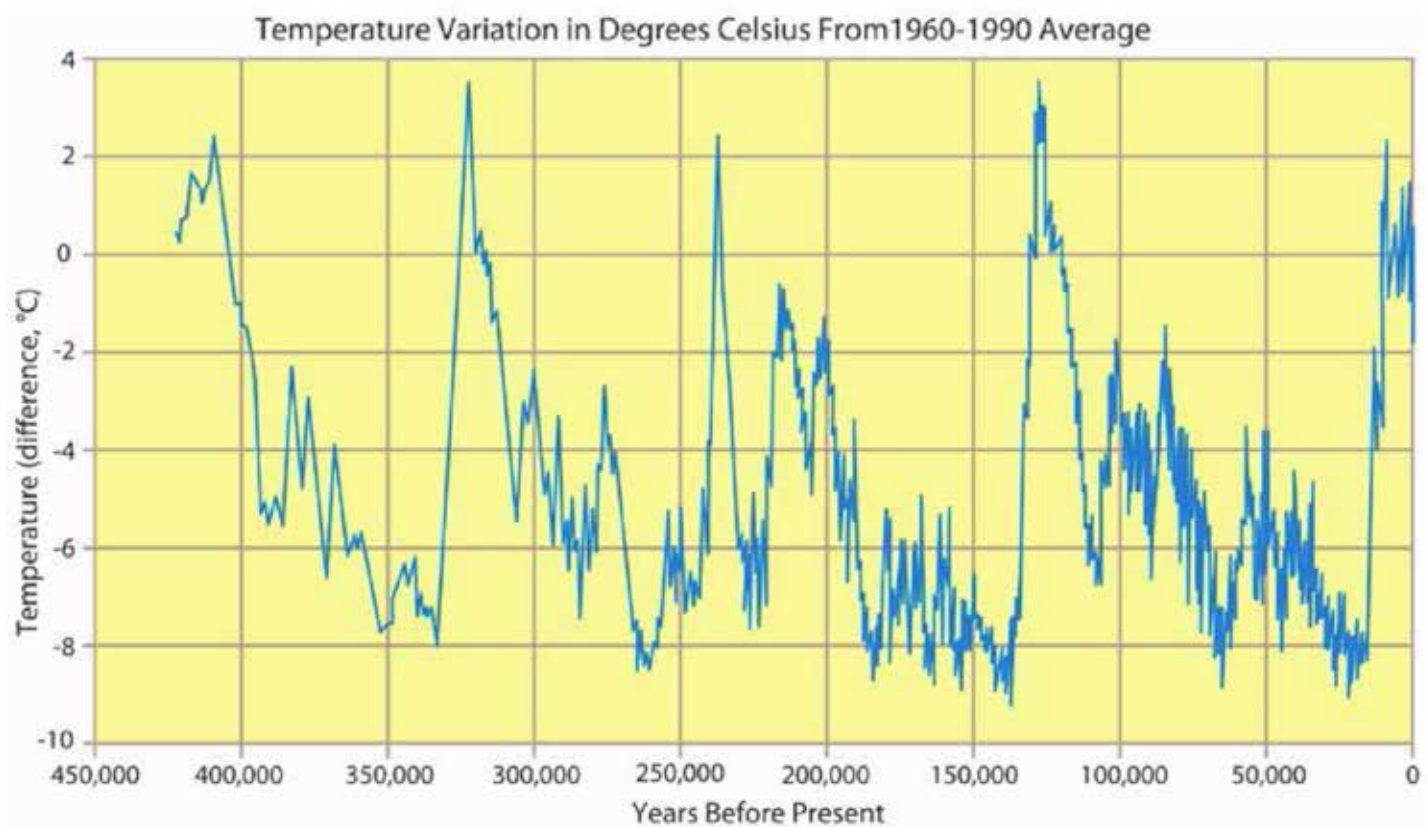


Figure 8.8. The 100,000-year temperature cycles show some correlation with changes in the shape of the Earth's orbit (orbital eccentricity), particularly for the past 900,000 years. Milutin Milankovich hypothesized these cycles long before data from sea floor sediments and ice cores verified them. Some of the other temperature fluctuations correlate with changes in the axial tilt (41,000-year cycle) and the wobble of the Earth's axis (23,000-year cycle). Warm interglacials, such as the present one (peak from 10,000 to 0 years), are relatively brief (Source/Credit: NOAA).

The astronomical theory dates back to the mid-1800s, but gained little acceptance until the early 20<sup>th</sup> century. Scientists such as Wladimir Koeppen and Alfred Wegener demonstrated the importance of **summer insolation values in the Northern Hemisphere as the primary control of ice sheet growth and disappearance**. The Serbian astronomer-mathematician Milutin Milankovich published a series of papers on climate change that involved orbital and axial variations, beginning in 1912. The popularity of his theory waxed and waned until the 1970s when evidence from deep sea sediment cores as well as the Greenland and Antarctic ice cores verified cyclic patterns of climatic change that generally coincided with the 100,000-year cycles predicted by Milankovich decades earlier. The **Milankovich Theory** maintains that predictable changes in the Earth's orbit, degree of axial tilt, and the timing of perihelion and aphelion create the basic rhythm of the mid-to late-Quaternary glacial and interglacial cycles.

The Earth's orbit is elliptical, but the shape of the ellipse changes over a 100,000-year cycle from being nearly circular to highly elliptical (Figure 8.9). As a result, the distance of the Earth's closest approach (perihelion) and farthest approach (aphelion) varies by as much as 11.5 million miles. Right now, the distance varies by only three million miles. When the orbit is most eccentric, the amount of energy received from the Sun decreases by several percent.

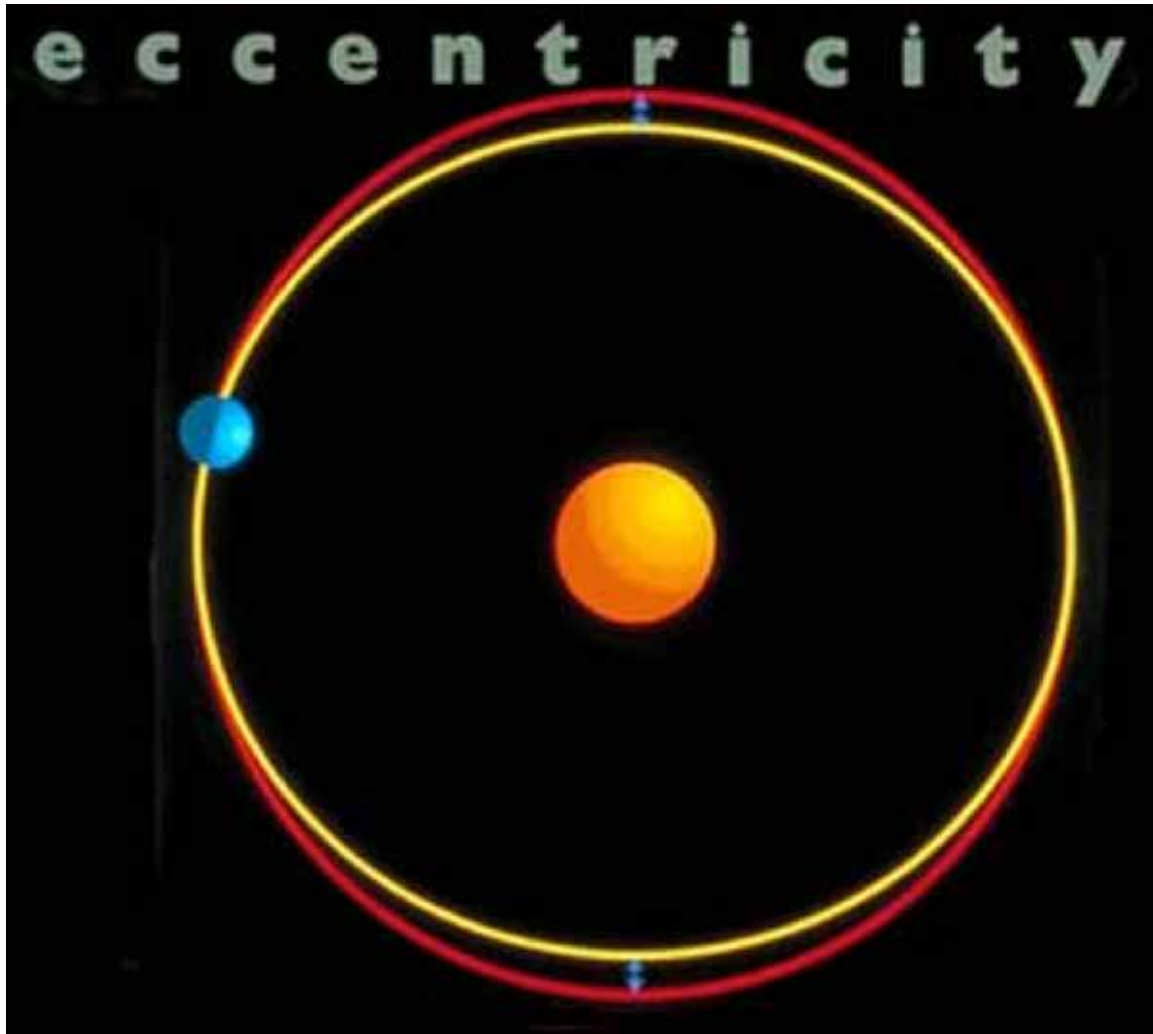


Figure 8.9. Changes in the shape of the Earth's orbit (eccentricity) affect the seasonal radiation budget of the Earth, and are thought to play a significant role in the 100,000-year temperature cycles during the past million years or so. When the Earth's orbit is nearly circular, eccentricity is close to 0.00. When the orbit is more elliptical, eccentricity is about 0.06. There are both 100,000 and 400,000-year frequencies to eccentricity (Source/Credit: NOAA).

During the current phase of the cycle, the orbit is only slightly elliptical, and the Northern Hemisphere summer occurs when the Earth is most distant from the Sun. If summer were to occur when the Earth were even further from the Sun than it now is, this would result in cooler summers and would favor ice development because less snow would melt during the summer and winters would last longer. In contrast, when the Northern Hemisphere summer occurs during perihelion, summers are warmer and would favor an ice-free North America and Eurasia.

Although the Earth's axial tilt is now  $23.5^\circ$ , it varies from about  $22^\circ$  to  $24.5^\circ$  over a 41,000-year cycle (Figure 8.10). Because it is the axial tilt that is responsible for the seasons, changes in the axial tilt (obliquity) affect the intensity of the seasons. During those periods when the axial tilt *decreases*, the seasonal temperature extremes from winter to summer decrease and this favors glacial development. This is because the summers are not as hot, and so more ice survives the summer season. Also, milder, warmer winters favor enhanced snowfall due to the ability of warmer air to contain more moisture. Therefore, ice ages are favored when the axial tilt is smallest.

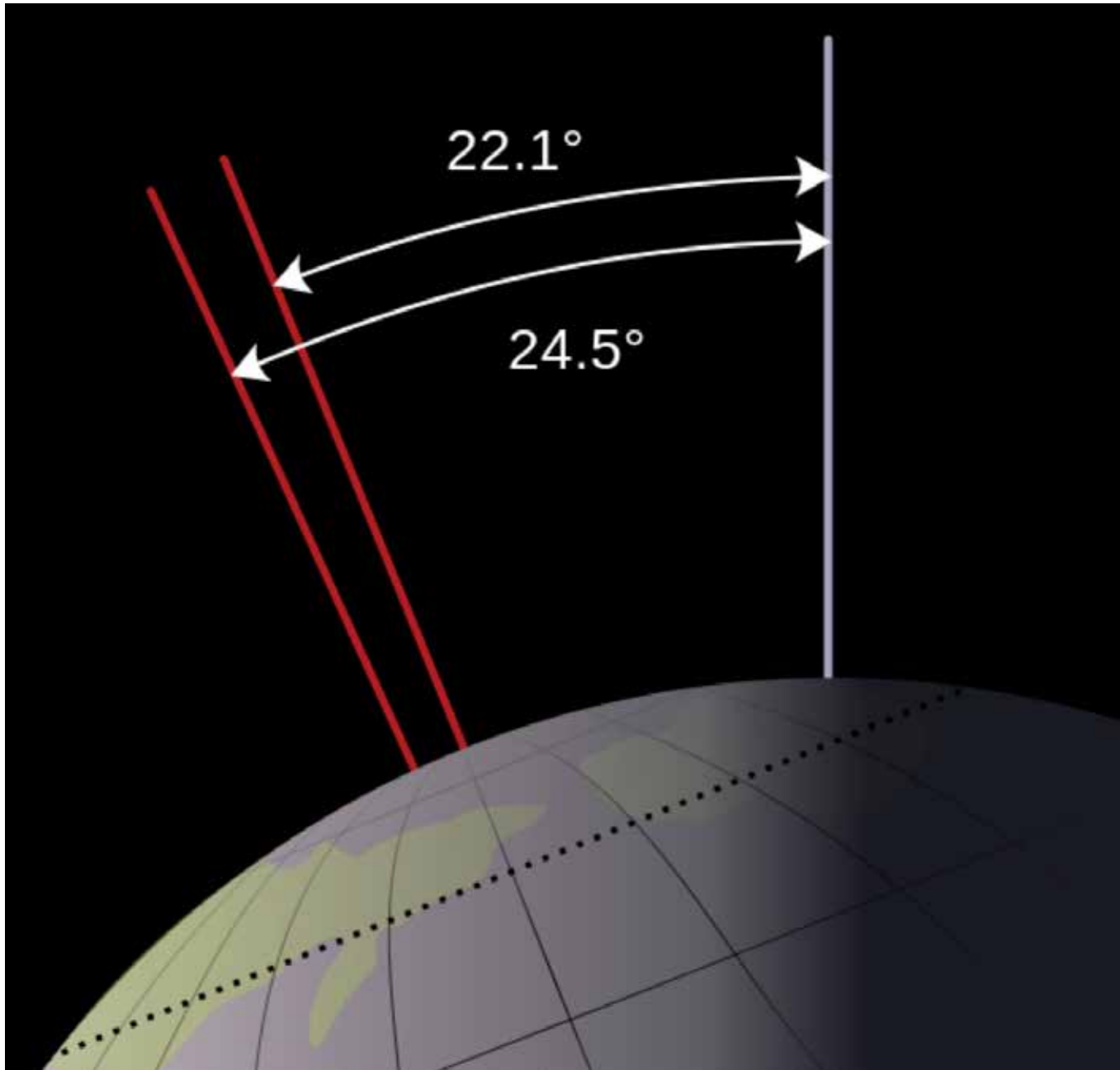


Figure 8.10. The 41,000-year tilt cycle varies about a degree from the current  $23.4^\circ$  (usually expressed as  $23.5^\circ$ ). Even through these subtle variations are too small to cause glacial-interglacial cycles, they can periodically amplify the effects of other orbital factors (Source/Credit: NASA).



Another variation in the orbit is referred to as the **precession of the Earth's axis** and results from the fact that the Earth wobbles on its axis like a spinning top. A complete wobble takes 23,000 years (Figure 8.11). Currently, the axis is pointed in such a way that the North Pole points toward the North Star. However, about 11,000 years from now, the axial wobble will cause the axis to point in a different direction in space toward the star Vega. In another 11,500 years, it will once again point towards Polaris, the North Star.

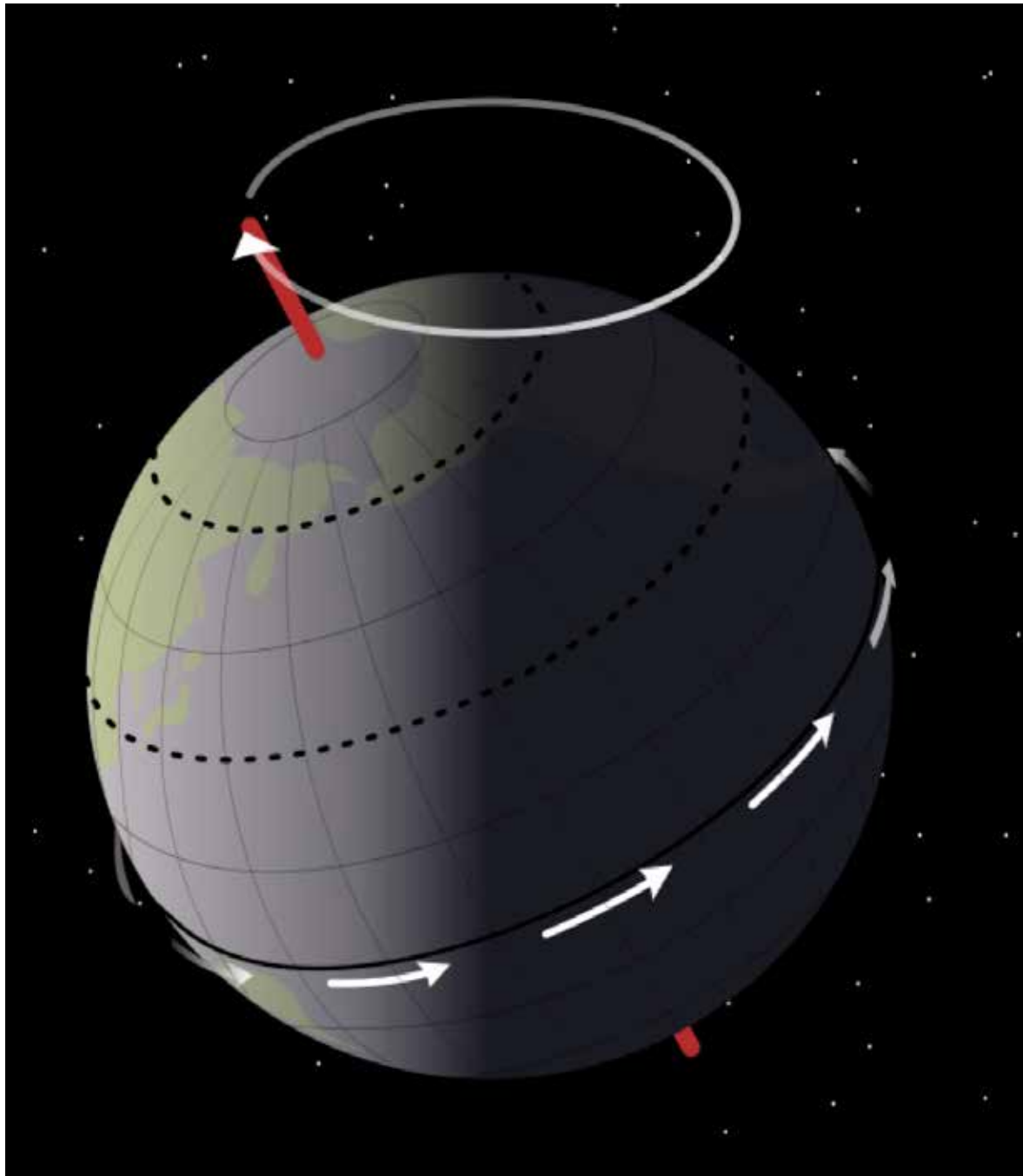


Figure 8.11. The 23,000-year wobble cycle of the Earth. The wobble cycle is similar in effect to the tilt cycle in that it cannot by itself force glacial-interglacial temperature fluctuations, but can amplify the effects of other factors such as that of orbital eccentricity (Source/Credit: NASA).

Because of the wobble, the seasons can reverse in relation to the time of closest approach. For example, our summer now occurs when the Earth is at its most distant point from the Sun (Figure 8.12). This favors glacier development because it makes our summer slightly cooler than it would otherwise be. However, because of the wobble, the Northern Hemisphere's summer will eventually occur when we are closest to the Sun, making our summers slightly warmer.

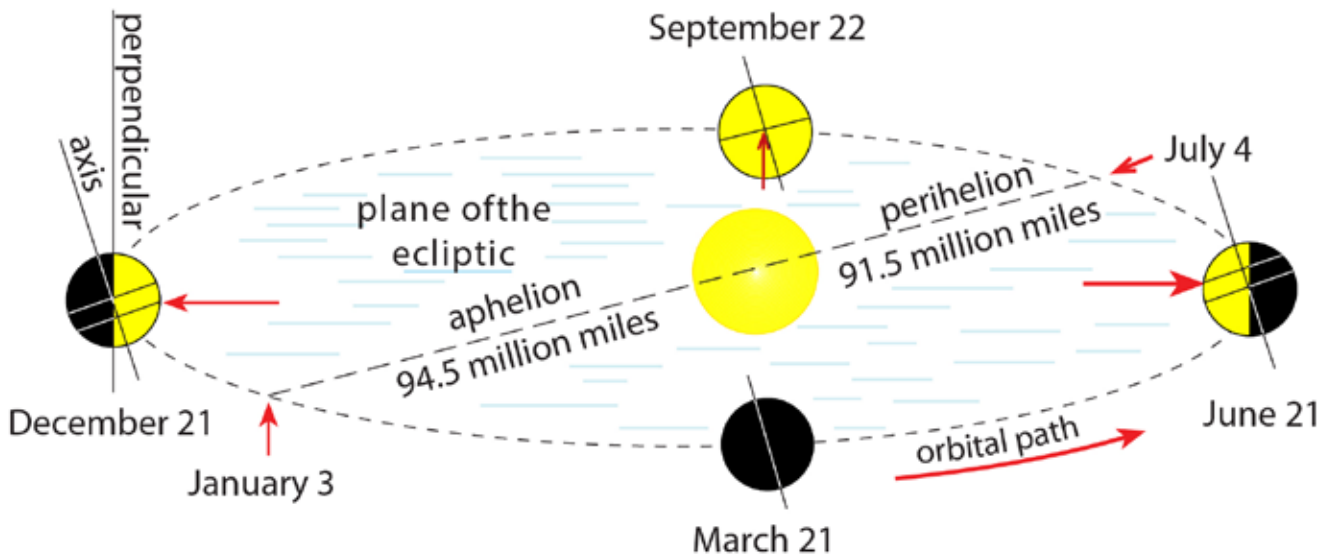
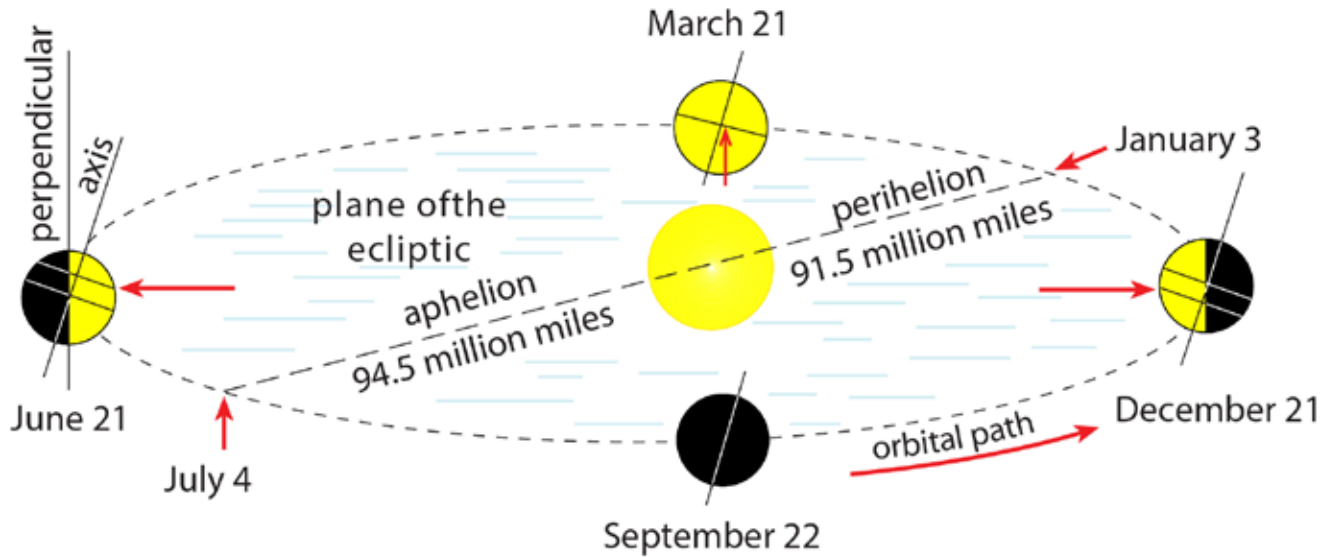


Figure 8.12. In 11,500 years, aphelion will occur in January, favoring colder Northern Hemisphere winters (Source/Credit: modified from Dennis I. Netoff and Ava Fujimoto-Strait, *Weather & Climate Lab Manual*).

Data from ice cores show that, during the last 900,000 years, major episodes of glaciation occur approximately every 100,000 years, which correlates very well with the 100,000-year cycle in the eccentricity of the Earth's orbit (Figures 8.13a and 8.13b). In addition, there are smaller episodes of glaciation that are superimposed onto this larger cycle. These occur every 41,000 years and 23,000 years. These smaller cycles correspond to the cycles associated with changes in the axial tilt and precession, respectively.

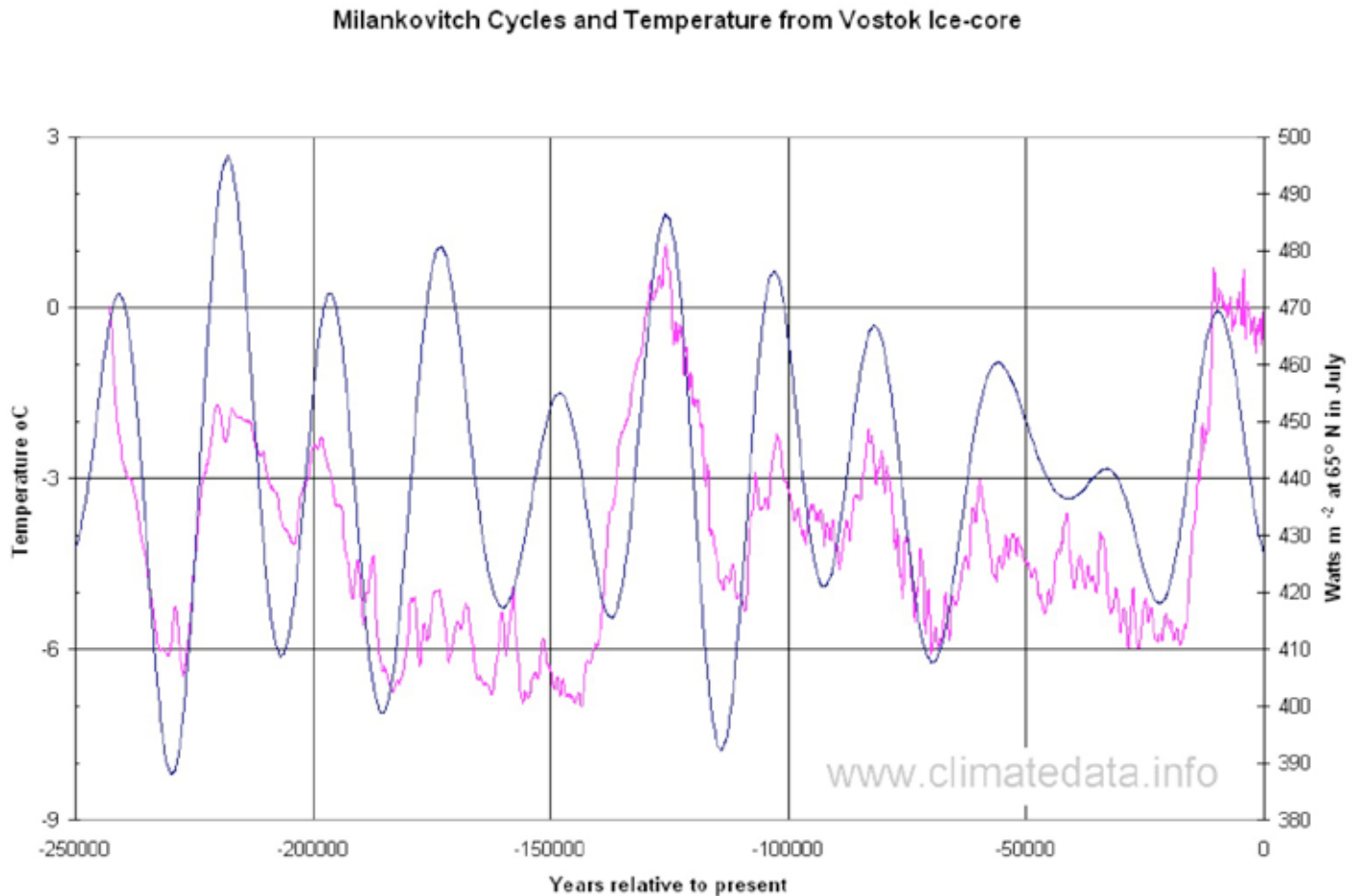


Figure 8.13a. The Milankovitch cycles show general agreement in magnitude and timing compared to temperature reconstructions (pink line) from the Vostok ice core. The Milankovitch curves (purple) show variations in insolation at 65°N latitude in July. Small adjustments in the timing of the Vostok curves have been made to show better agreement to insolation peaks and troughs. In spite of this, there are still discrepancies in some of the peaks and troughs (especially between about 150,000 and 170,000 years), indicating that the Milankovitch cycles cannot explain all of the variability in temperature for the past 250,000 years (Source/Credit: [www.climatedata.info](http://www.climatedata.info)).

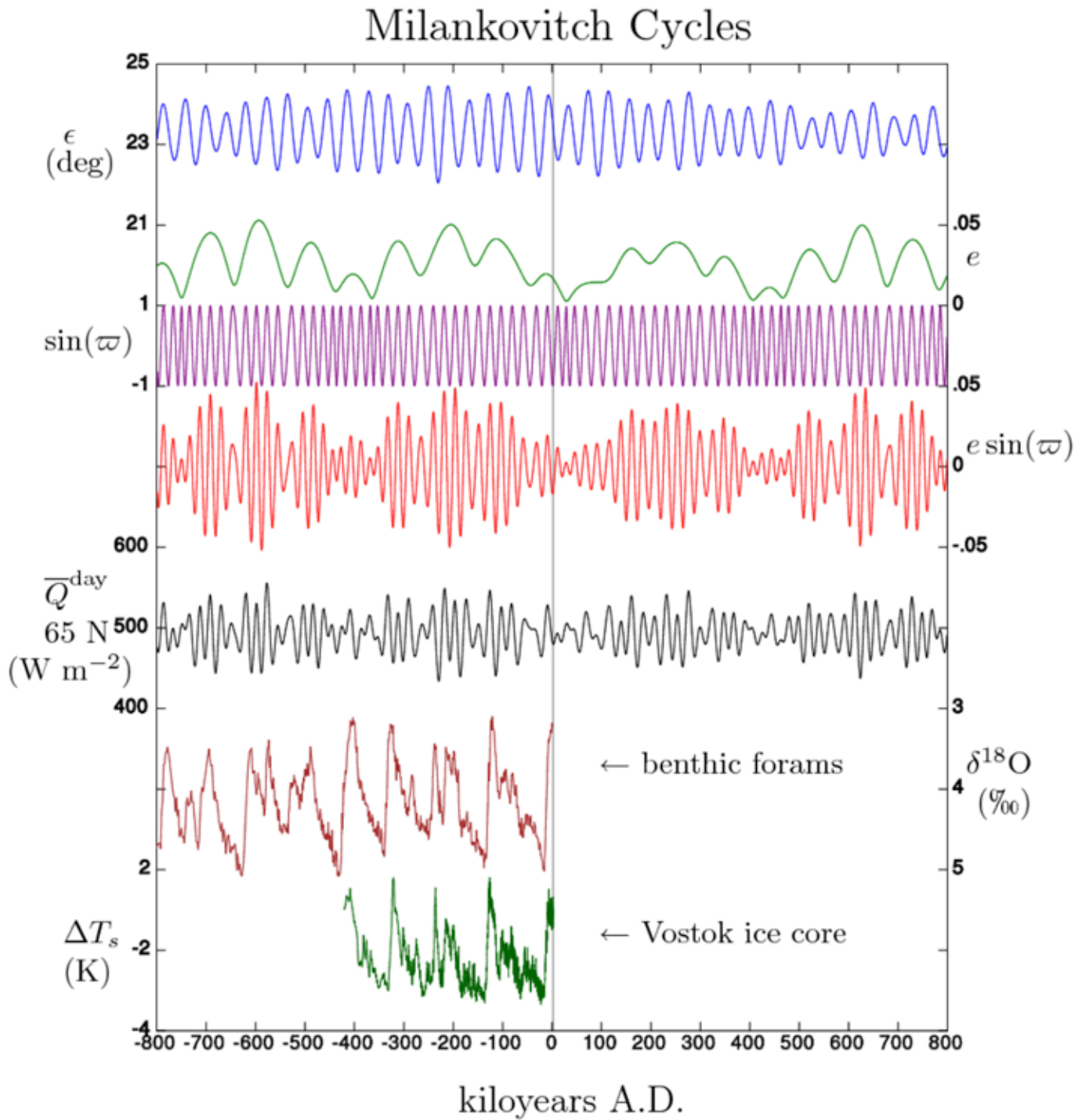


Figure 8.13b. The Milankovitch insolation cycles for the past 800,000 years are based on changes in the axial tilt (blue, top), orbital shape (green, 2<sup>nd</sup> line), longitude of perihelion (~precession, purple, 3<sup>rd</sup> line), and precession index (precession and obliquity, red, 4<sup>th</sup> line). Together, they generate the insolation curve for 65°N (black, 5<sup>th</sup> line). The final two curves show proxy data (temperature data inferred from indirect methods) from deep sea fossils and the isotope evidence from the Vostok ice cores (Source/Credit: NASA; <http://aom.giss.nasa.gov/srorbpar.html>).

The three orbital and axial changes are occasionally in or out of phase and create either warmer or colder than average conditions in the atmosphere. At present, the conditions are acting in sync to create conditions that should lead to the onset of another ice age within the next few tens of thousands of years. However, other factors also contribute to warming and cooling trends, and may periodically outweigh the influences of orbital and axial variations.

## Galactic Dust

As our solar system orbits the center of the Milky Way Galaxy once every 225 million years, it periodically passes through regions of relatively high concentrations of gas and dust (the material from which future solar systems will form) (Figures 8.14a and 8.14b). Such concentrations block some sunlight from reaching the Earth, just as a cloud blocks light from reaching the Earth's surface. In such cases, global average temperatures may decline, and if they interact with the orbital changes described above, could facilitate cooling.



Figure 8.14a. Galactic dust, such as the vast cosmic cloud shown in the Great Nebula of Orion, is periodically intercepted by the Earth as the solar system orbits the Milky Way Galaxy. Although encounters with interstellar dust are not thought to be the cause of recent icehouse climates, they may have contributed to earlier ones (Source/Credit: March 20 2013 NASA).

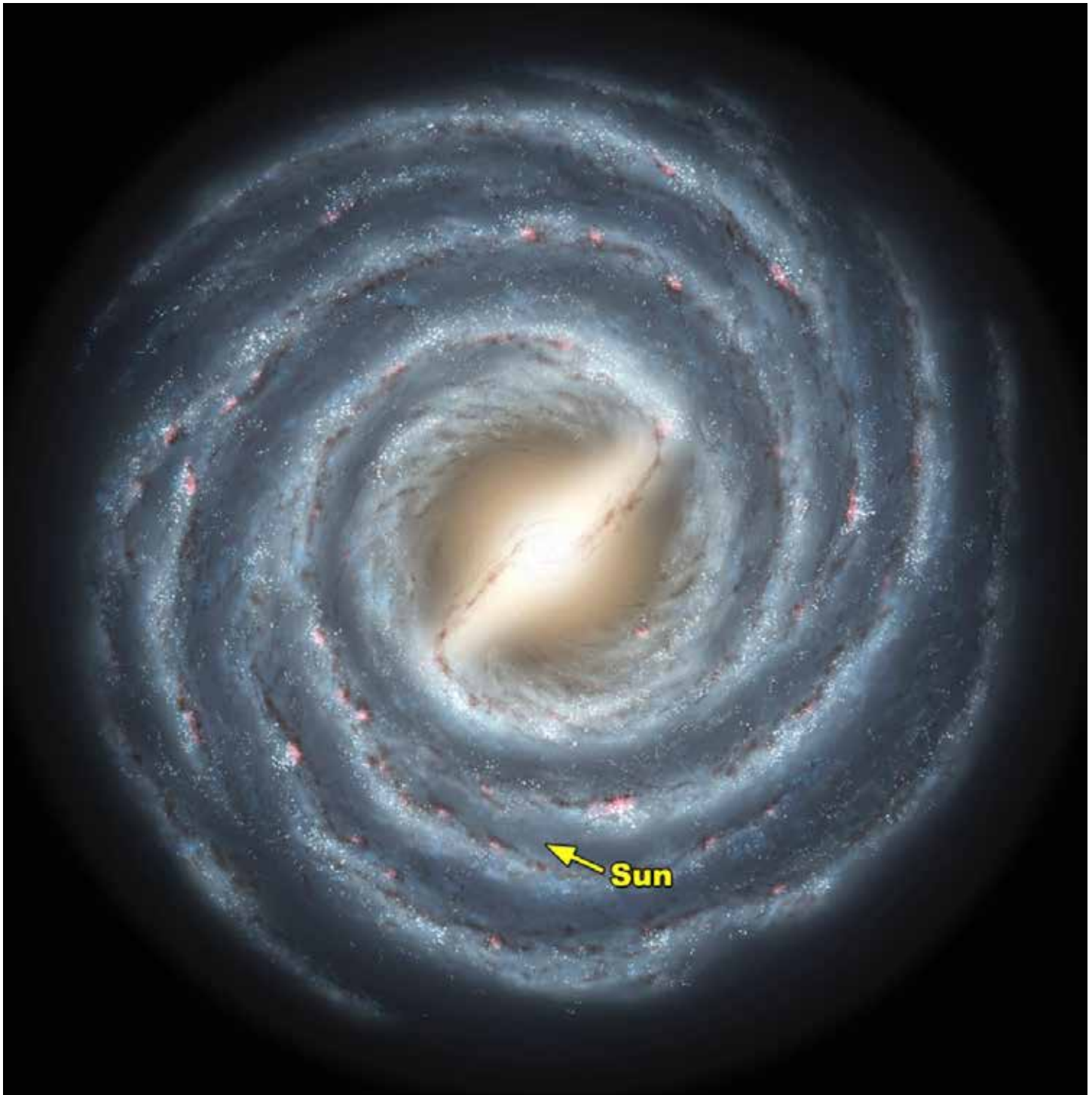


Figure 8.14b. The Milky Way Galaxy is a type of spiral galaxy, similar to the nearby Andromeda Galaxy. In this artistic plan view of the Milky Way Galaxy, several spiral arms are apparent. The solar system lies in one of the spiral arms. The entire galaxy revolves, and the solar system makes one complete revolution every 230 million years. Some scientists correlate four periods of global cooling during the past 520 million years with the crossing of the solar system through Galactic arms four times. The increase in density of the galactic clouds not only might influence the transparency of the Earth's atmosphere, but the increase in mass of the solar system may attract more comets from the Oort cloud, further affecting the amount of atmospheric particulates (Source/Credit: NASA Caltech).

Some scientists correlate four periods of global cooling during the past 520 million years with the crossing of the solar system through galactic arms four times. The increase in density of the galactic clouds not only might influence the transparency of the Earth's atmosphere, but the increase in mass of the solar system may attract more comets from the Oort cloud, further affecting the amount of atmospheric particulates. Although most scientists do not support the idea that galactic dust contributed to recent cooling, there is some evidence of cosmic dust recovered in the Camp Century ice core in Antarctica. High concentrations of iridium and nickel were found in a portion of the ice core dated at about 14,000-20,000 years, at the height of the most recent glacial stage.



## **Plate Tectonics and Continental Drift**

In the middle of the 20<sup>th</sup> century, scientists such as Ewing and Donn suggested that Quaternary glacial cycles can only occur if there are large continents (e.g., North America and Eurasia) at fairly high latitudes, and if there is sufficient moisture influx in the form of snow onto these continents to build ice sheets (Figures 8.15a, 8.15b and 8.15c). The theory of plate tectonics provides a mechanism by which not only can continents move in and out of high latitude areas over time, but also periodically sets up the proper ocean circulation to nourish high-latitude airmasses with sufficient water vapor to build massive glaciers. Different rates of seafloor spreading can cause a substantial rise or fall in sea level, affecting global albedo, ocean circulation, biological productivity and degree of continentality.

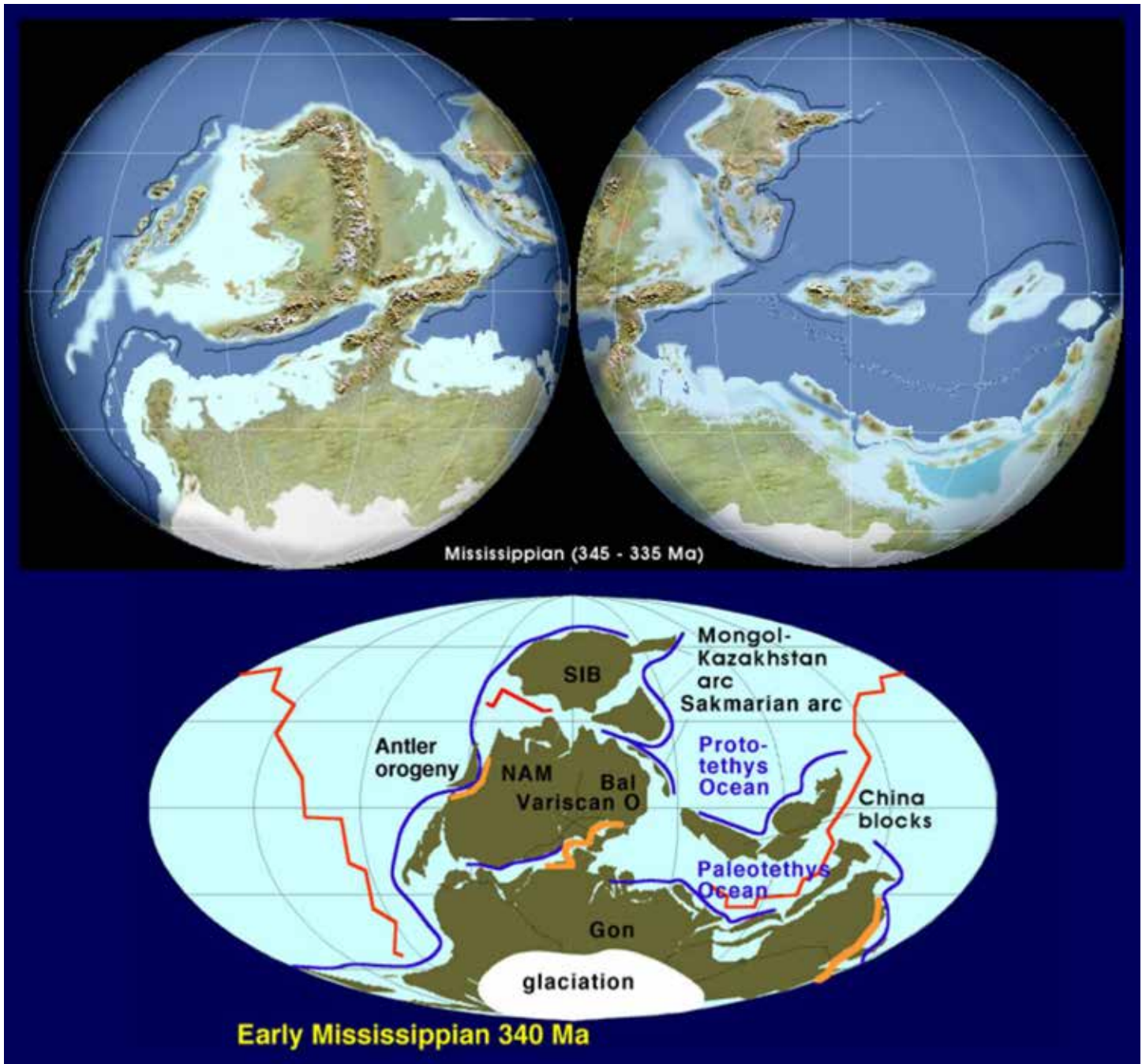


Figure 8.15a. Mississippian, 340 million years ago. Plate tectonics is responsible for the movement of the continents and the opening and closing of ocean basins. Plate movement can affect climate in many ways, including positioning of continents at high latitudes, the distribution of ocean currents and sea level rise and fall. At the close of the Paleozoic, the continents were clustered around the South Pole, contributing to a long series of glacial-interglacial cycles (Source/Credit: Ron Blakey, with permission).

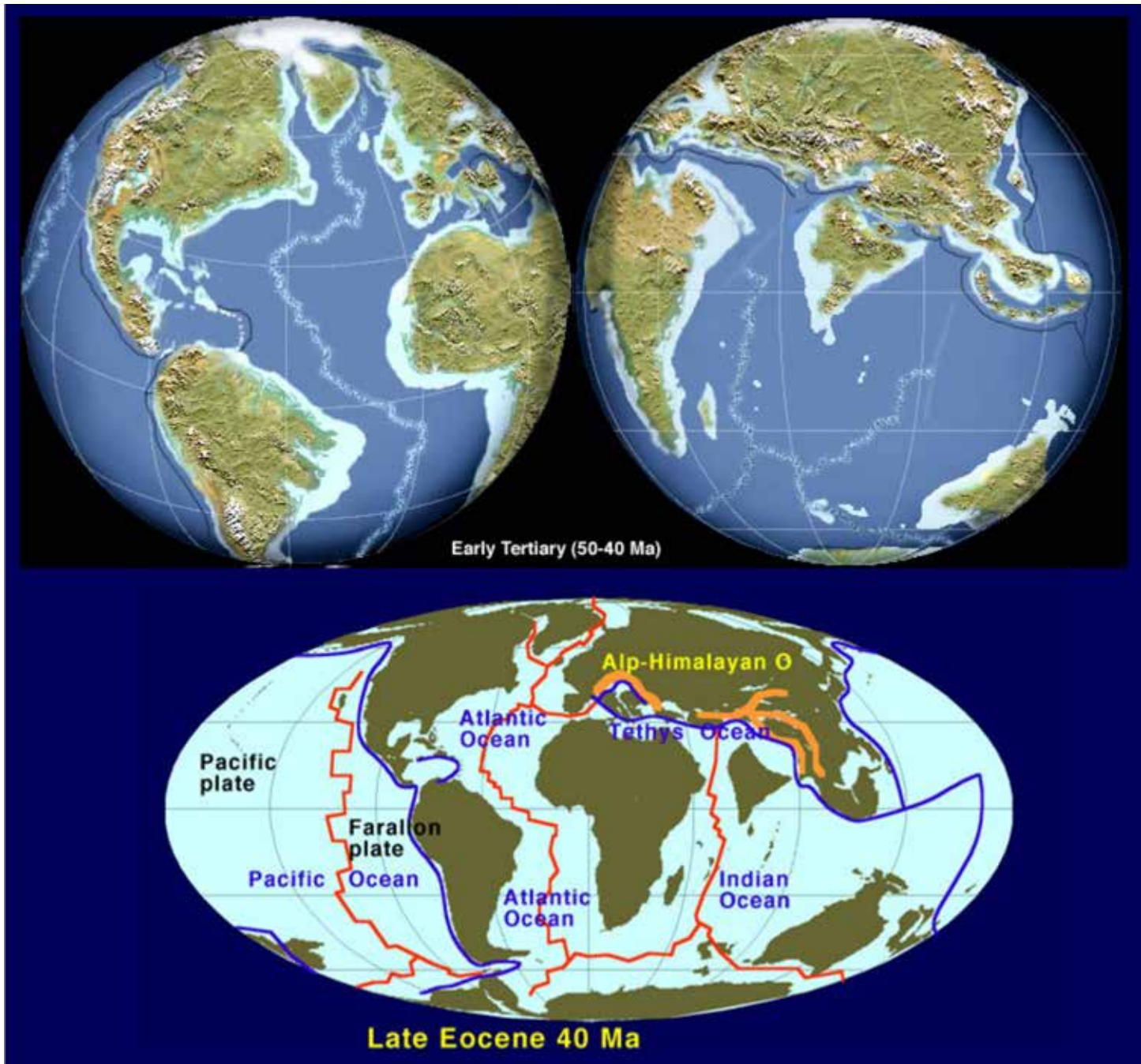
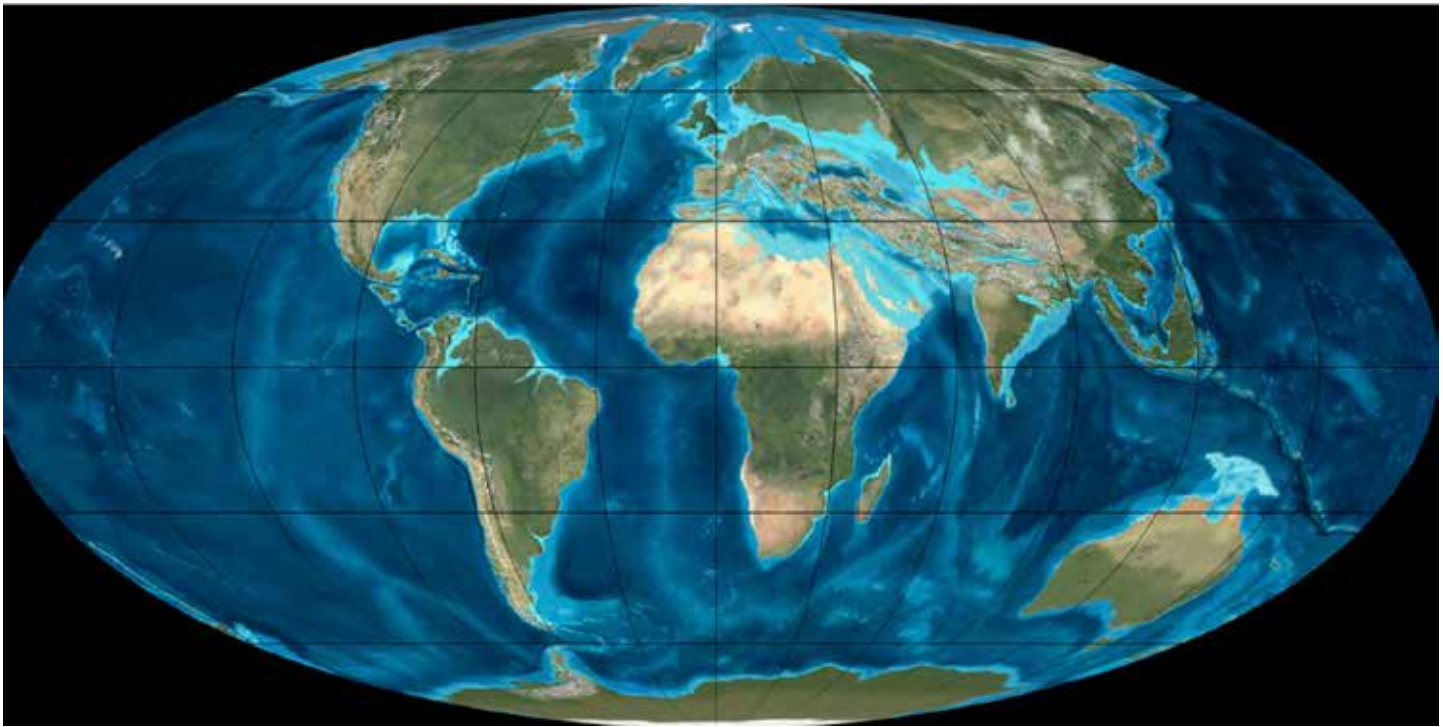


Figure 8.15b. Late Eocene, 40 million years ago. By the Late Eocene, North America, Eurasia, Greenland and Antarctica had drifted to high latitudes, setting the stage for glacial-interglacial cycles. Although Southern Hemisphere glaciation began soon thereafter, North America and Eurasia would not be occupied by large ice sheets until about 2 million years ago (Source/Credit: Ron Blakey, with permission).



*Figure 8.15c. During the Oligocene, about 35 million years ago, Australia had separated from Antarctica and the Drakes Passage opened between Antarctica and South America. This set up an ocean current system that encircles Antarctica, rather than the previous circulation that brought large amounts of warm tropical water to Antarctica. The result was the cooling of Antarctica and the onset of glaciation about 34 million years ago (Source/Credit: Ron Blakey, with permission).*

For example, when Antarctica drifted to the south polar region, the land cooled more during winter than the water that once occupied the region, and it also reflected more sunlight. This combination led to an accumulation of snow. As more and more snow accumulated and turned into glacial ice, the albedo increased even more and temperatures dropped accordingly. Eventually, the entire continent plunged into a multi-million year ice age. Ice now reaches depths of more than two miles in places. Because of its size and high albedo, the amount of energy reflected by Antarctica has a significant cooling effect on the average global temperature of the Earth.

## Atmospheric Composition

The greenhouse effect involves transmission of large amounts of incoming solar radiation, absorption by the Earth's surface, re-radiation at longer far-infrared wavelength, and absorption in the atmosphere by greenhouse gases such as water vapor, carbon dioxide and a host of trace gases. Changes that affect any one of the steps in this process can affect the radiation balance of the Earth. For example, changes in the transparency of the atmosphere affect the albedo of the atmosphere, and thereby affect the ability of insolation to penetrate to the surface. Transparency also affects the ability of terrestrial energy to return to space. Several processes contribute to changes in atmospheric transparency.

- **Volcanic Ash:** When volcanoes erupt, they inject dust-sized aerosols into the atmosphere that are capable of blocking sunlight. Some eruptions release large amounts of sulfur and are particularly effective at blocking sunlight because the sulfur combines with water to form sulfuric acid droplets that are highly reflective. The increase in albedo of the atmosphere decreases surface temperatures. The eruption of Mt. Pinatubo in the Philippines in 1991 sent millions of tons of ash and sulfur into the atmosphere (Figure 8.16).



Figure 8.16. The eruption of Mt. Pinatubo in 1991 injected millions of tons of volcanic ash as well as sulfur into the atmosphere, both contributing to nearly two years of cooler-than-expected temperatures. The sulfur reacted with atmospheric gases to become tiny droplets of sulfuric acid, and caused significant stratospheric cooling for over three years (Source/Credit: USGS).

These aerosols rose to elevations of 19 miles (30 km), well into the stratosphere. Since there are virtually no clouds in the stratosphere, there is no rain, and therefore the only way to cleanse the aerosols is by gravity settling. The net effect of the Pinatubo eruption was to cool temperatures through 1992, in spite of the overall trend of global warming. A single large eruption can cause an average drop in global temperature as much as 2°F (1°C) or more for a period of a few years. Local temperatures can drop by as much as 5°F (3°C). A slight increase in global volcanism from 2008-2012 is thought to have reduced the rate of global warming. Icelandic eruptions in 2010 spread volcanic ash and sulfur aerosols over much of Europe, causing major airports to close for extended periods (Figure 8.17).



Figure 8.17. The eruption of an Icelandic volcano in May and June 2010 injected millions of tons of volcanic ash as well as sulfur into the atmosphere. Increased global volcanism in the period 2005-2014 is thought to have reduced the rate of global warming during that period. Ash clouds from this and later eruptions spread over western Europe and caused thousands of flight delays and local surface traffic problems (Source/Credit: NASA).

One of the most famous instances of short-term climate change produced by a volcanic eruption occurred following the massive eruption of Mount Tambora in Indonesia in 1815 (Figure 8.18). In North America, the year 1816 was known as **the year without a summer** because snow remained on the ground in June in some parts of the continent. Crops in New England were damaged by frost in every summer month.

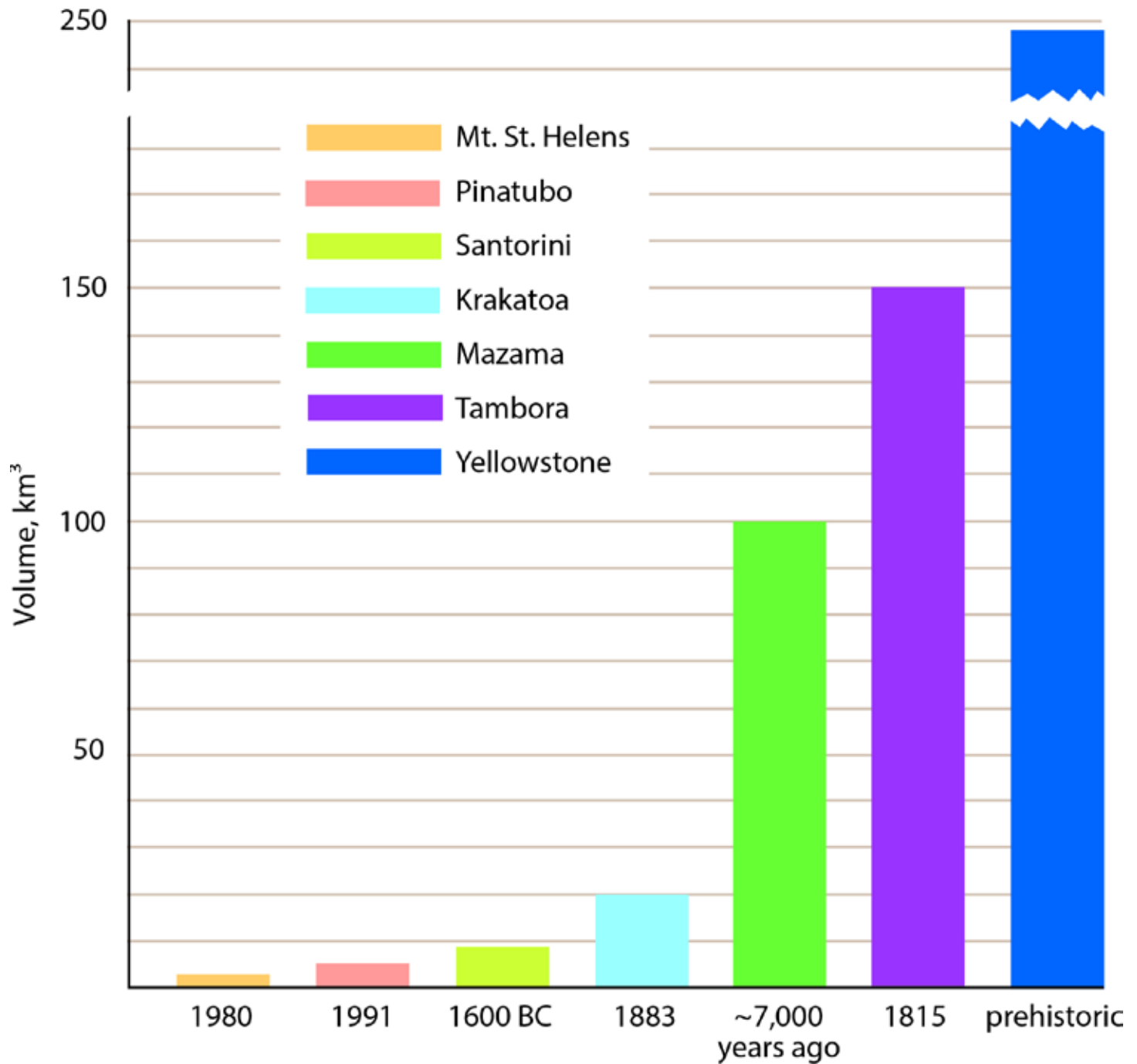


Figure 8.18. Estimated volume of volcanic ash injected into the atmosphere by notable eruptions. The Mount Tambora eruption of 1815 was followed by the year without a summer and was one of the coldest years on record for most of New England and western Europe (Source/Credit: data mainly from USGS).

Sustained volcanic activity can affect long-term climate. Two of the great mass extinctions in Earth history were accompanied by massive outpourings of volcanic rock. The Permian-Triassic extinction event led to the demise of an estimated 90% of life forms on Earth some 252 million years ago. It is the only mass extinction of insects in Earth history. It coincided with the largest outpouring of continental volcanic rock in the past 500 million years. The estimated areal extent of the basalt flows and tuffs (ash layers) combined was 2.7 million square miles (7 million km<sup>2</sup>), enough to cover 90% of the conterminous United States (Figure 8.19). Although other mechanisms have been proposed to explain the extinction event, the injection of volcanic gases and aerosols into the atmosphere from the million+-year period of volcanism might have altered global climate and changed the composition of the atmosphere sufficiently to cause the mass extinction.



Figure 8.19. The **Siberian Traps** are an extensive area of volcanic rocks that erupted across the Permian-Triassic boundary. They coincide with the greatest mass extinction in Earth history. The original areal coverage may have been as much as 2.7 million square miles (7 million km<sup>2</sup>), nearly 90% of the size of the conterminous United States. Changes in atmospheric gases and aerosols from the succession of volcanic eruptions could have altered Earth's climate sufficiently to cause the extinction event (Source/Credit: base map is Courtesy of the University of Texas Libraries, The University of Texas at Austin).



The end of Cretaceous extinction, which included the demise of all species of dinosaurs, was also accompanied by massive outpourings of volcanic rock. The modern Deccan Plateau in India is made of volcanic rocks that range from 68 to about 60 million years old. The original extent of the volcanic rocks may have been close to 580,000 square miles (1.5 million km<sup>2</sup>), approximately the size of present-day India. Although meteoric impact is the preferred theory to explain the Cretaceous extinction, no doubt volcanism played an important role.

- **Greenhouse Effect:** Certain gases in the atmosphere, such as carbon dioxide, methane, nitrous oxides, water vapor and man-made chlorofluorocarbons (CFCs) absorb outgoing terrestrial infrared radiation. The abundance of these greenhouse gases has a profound effect on atmospheric temperature. A decline in their quantity causes global cooling, whereas an increase in their concentration causes warming.

The actual concentration of greenhouse gases in the atmosphere depends on the balance of inputs (sources) and removal (sinks). The sources and sinks are complex, resulting from the interplay of geologic, cosmogenic and biological processes. Long periods of increased volcanic activity associated with continental rifting can cause changes in the concentration of greenhouse gases. For example, during the Mesozoic Era when dinosaurs roamed the Earth, the average global temperature was about 18°F (10°C) warmer than it is today. This temperature coincided with higher carbon dioxide levels that are believed to have been generated by volcanism during the break-up of the supercontinent during that period.

## Impacts (Comets, Meteors, Asteroids)

The Earth's atmosphere is dense enough to cause most extraterrestrial objects to burn up in the atmosphere. The nighttime display of shooting stars is testimony to the frequency of these events. It is estimated that 50-100 tons of meteoric debris are intercepted by the Earth each day.

Larger meteors may either break up and explode violently in the atmosphere, or impact the surface, often forming a distinctive crater surrounded by deformed and shocked rock masses. Meteor Crater, Arizona was an actual impact of a 55-yard wide iron-nickel meteor (Figure 8.20). The violent explosion that rocked Siberia, the Tunguska event in 1908, was first thought to have been caused by a meteor or cluster of meteors that were vaporized in the atmosphere. Recent evidence suggests that it was caused by the impact of a rocky-ice comet (Figure 8.21).

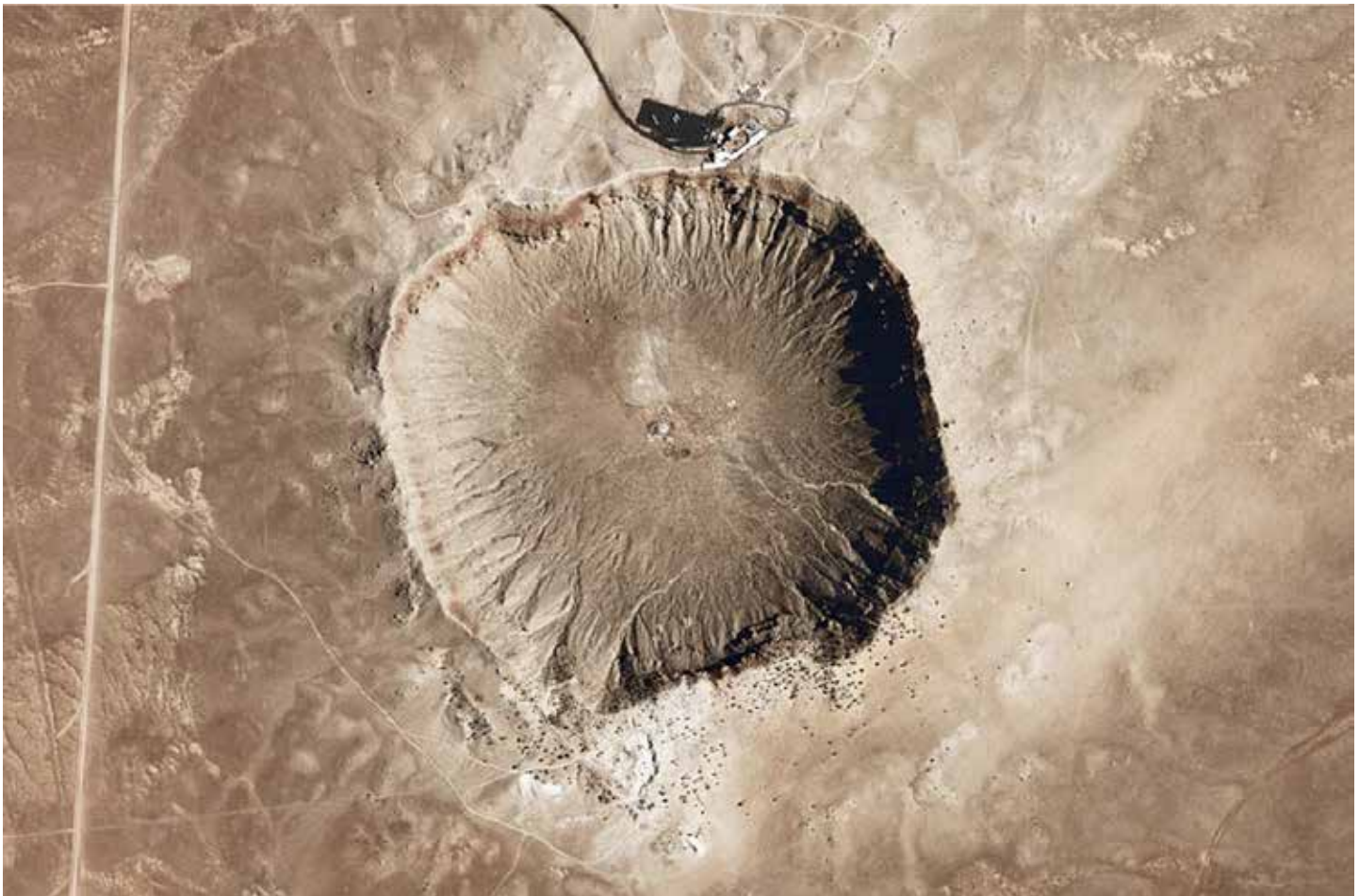


Figure 8.20. Meteor Crater in Arizona is the best-preserved impact site on Earth, owing to the desert climate and the youthfulness (~50,000 years ago) of the event. Even though the impact was caused by a modest-sized iron-nickel meteor, estimated to have been 55 yards (~50 m) in diameter, it created a sizeable crater. The modern crater is 3900 feet (1200 m) wide and 570 feet (170 m) deep. The impact velocity was probably about 8 miles per second (12.8 km/s), meaning that it traveled through the Earth's troposphere in just over a second. The impact was too small to have created any long-lived episodes of global climate change (Source/Credit: NASA Earth Observatory).



*Figure 8.21. Image of noctilucent clouds taken from the International Space Station on July 13, 2012. Noctilucent clouds are the highest clouds that form in the atmosphere, typically from 47-53 miles (76-85 km) above the surface in the mesosphere. They are ice crystal clouds that can only form at temperatures of about minus 184°F (minus 120°C). Recent studies indicate that they tend to form around dust nuclei that can be either of human origin (e.g., the Space Shuttle) or from meteoric dust. Noctilucent clouds were seen hundreds of miles from the Tunguska site in 1908, possibly the result of a comet beginning to vaporize in the mesosphere (Source/Credit: NASA).*

The best-documented example of an impact-induced global change in climate is 66 million years ago. It marks the close of the Cretaceous Period and the end of the era of dinosaurs. The main culprit was a meteor estimated to be 6 miles (10 km) in diameter (Figure 8.22). Although the exact site of impact is still under debate, the leading candidate is the Chicxulub site in the Yucatan Peninsula of Mexico. Widespread volcanism in the Deccan Traps of India also likely contributed to the climate change. There is evidence that Deccan Traps volcanism preceded the great impact. Perhaps there was a one-two punch, with thousands of years of volcanism wiping out or threatening many species, followed by a massive impact.



Figure 8.22. Artistic rendering of the end of Cretaceous meteoric impact at the proposed Chicxulub site (Source/Credit: Don Davis, NASA).

## Anthropogenic

Humans have entered a new, unprecedented phase in their history. For the first time in the history of our existence, we have acquired the capability to significantly alter the composition of our atmosphere and, in so doing, alter the climate of our planet. The changes that we are bringing about are unintentional, but seemingly profound. We may be embarking on a path that will inevitably change the world's climate. How much and how fast it will change is a matter of vigorous debate, but that we are forcing change is no longer questioned by the majority of the scientific community. Recently (2013) the IPCC (International Panel on Climate Change), one of the most prestigious groups of scientists ever assembled, issued bold statements about recent changes in global climate:

Warming of the climate system is unequivocal, and since the 1950s, many of the observed changes are unprecedented over decades to millennia. The atmosphere and ocean have warmed, the amounts of snow and ice have diminished, sea level has risen, and the concentrations of greenhouse gases have increased.

There are many possible consequences of altering the climate, some may even be beneficial. However, because of the rate at which the climate is changing and our inability to adapt rapidly to its effects, most scientists agree that the majority of the changes will have a negative impact. However, if we understand the causes of climate change, we may at least take actions to slow down the process, giving us more time to cope with and adapt to the manifold impacts of climatic change.

Since the Industrial Revolution a couple hundred years ago, we have been consuming fossil fuels at an ever-increasing rate. One of the by-products of fossil fuel consumption is the release of carbon dioxide, an important greenhouse gas (Figure 8.23a). A significant relationship between carbon dioxide and temperature levels through time suggests cause and effect (Figure 8.23b). However, correlations in no way prove cause and effect. In 2013, carbon dioxide levels rose to more than 400 ppm, the highest level in the past 600,000 years (Figure 8.24). Glacial ice cores spanning the last 800,000 years of time have also demonstrated a correlation between carbon dioxide levels and temperature. However, it can also be argued that the change in carbon dioxide is the result of, and not the cause of temperature fluctuations. Whatever the historical causes of past warming trends, it is certain that carbon dioxide traps energy; therefore, if carbon dioxide levels go up, temperature levels should do the same.

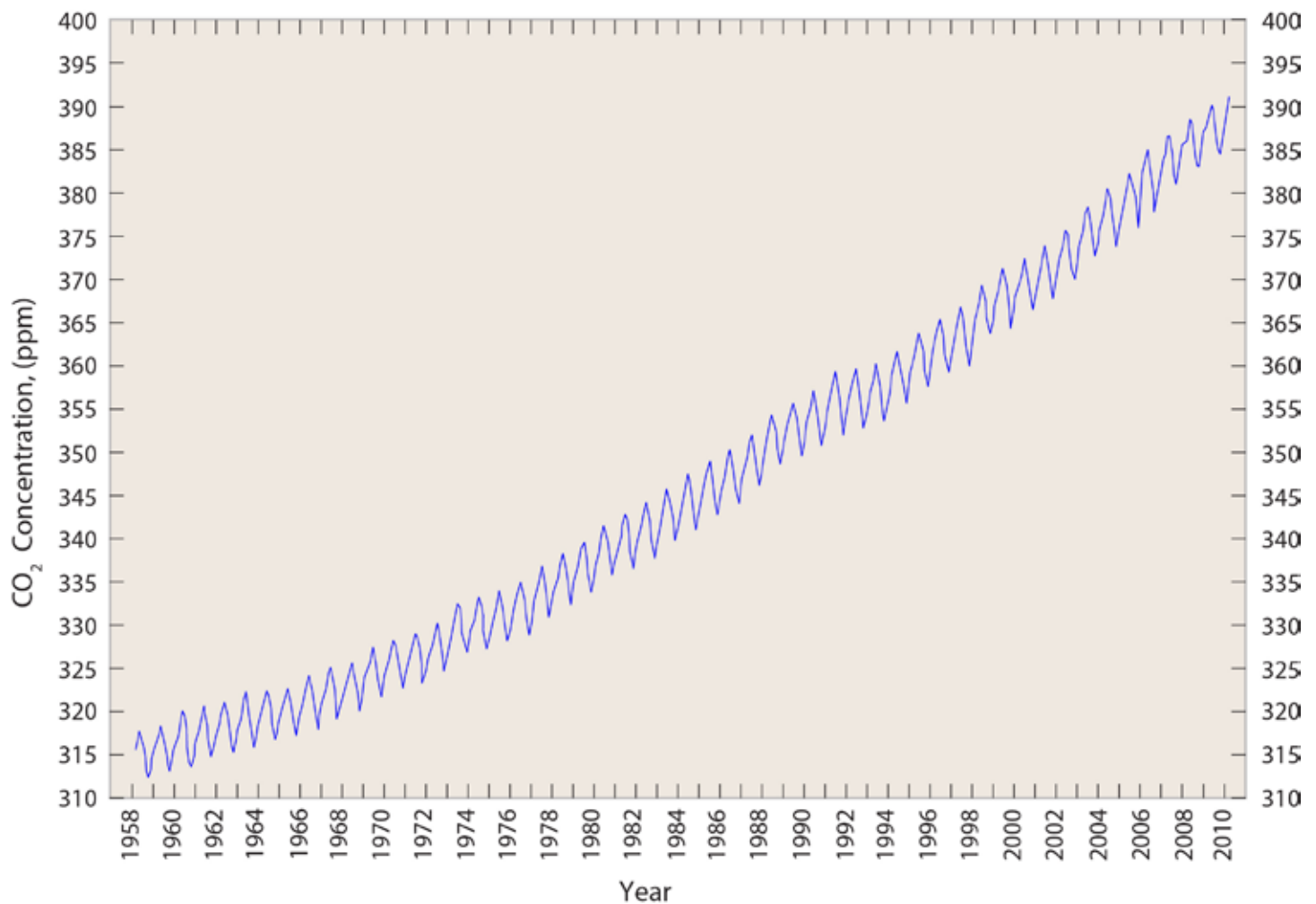


Figure 8.23a. The seasonal and decadal variation of carbon dioxide in the atmosphere. Early data was based mainly from readings at the Mauna Loa Observatory in Hawaii. Now there are dozens of monitoring sites all over the world that reflect the same trends over time. Maximum concentration occurs in the Northern Hemisphere winter (more land in the Northern Hemisphere), when most plants are dormant and are not taking in carbon dioxide. Carbon dioxide levels have risen primarily as a result of the burning of fossil fuels. In the summer of 2013, the CO<sub>2</sub> content momentarily reached 400 ppm, the highest it has been in several hundred thousand years (Source/Credit: NOAA).

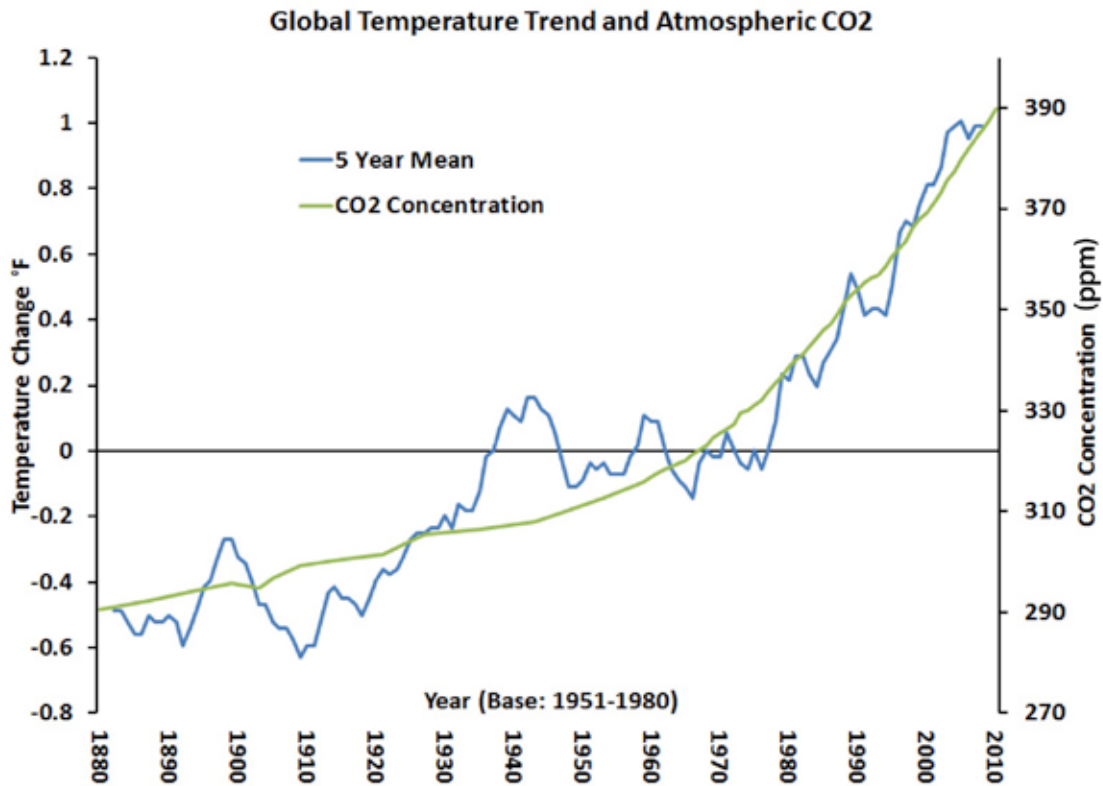


Figure 8.23b. Recent changes in global temperature correlate with changes in carbon dioxide, leading many atmospheric scientists to conclude that increases in CO<sub>2</sub> cause higher temperatures. Others argue that the correlation suggests that global temperature change is causing CO<sub>2</sub> increases (Source/Credit: NASA-GISS, CDIAC, NOAA ESRL).

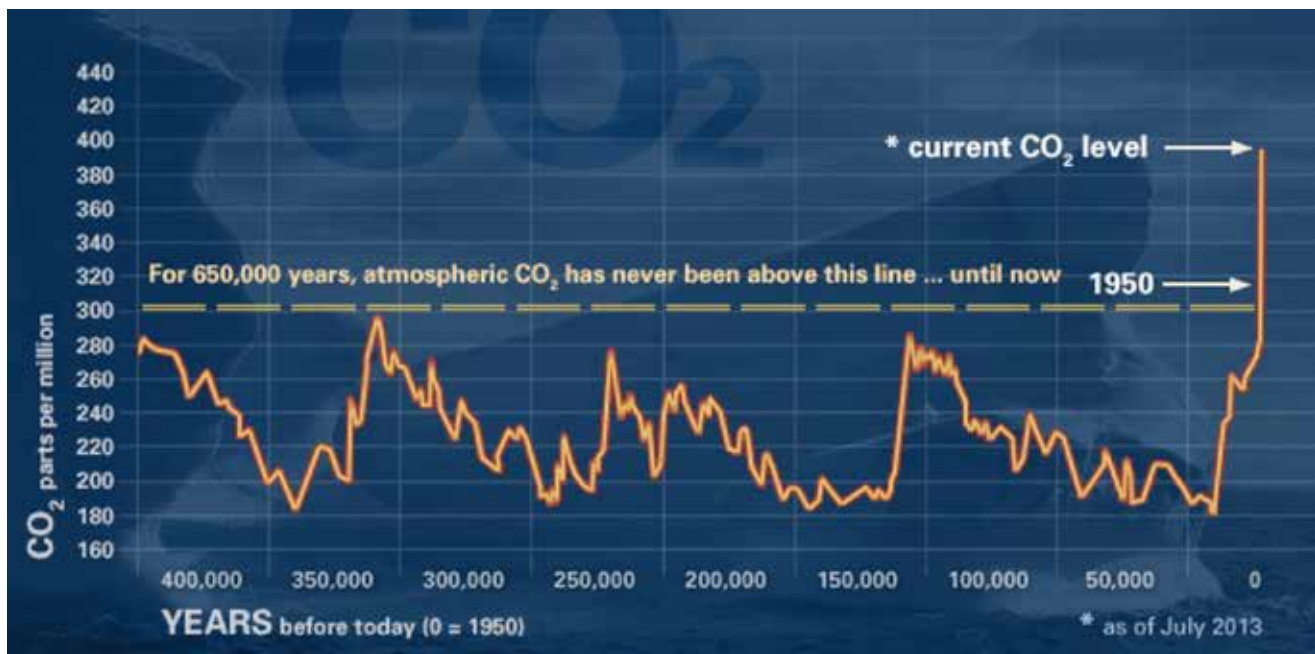


Figure 8.24. Although CO<sub>2</sub> concentrations in the atmosphere have only been measured with high accuracy since 1958, CO<sub>2</sub> trapped in the Antarctic ice cores and deep-sea carbonate fossils have extended the CO<sub>2</sub> curve for over 650,000 years. If the data is accurate, the CO<sub>2</sub> concentrations today are far greater than they have been for the entire length of the record (Source/Credit: Earth Observatory NASA).

The debate on global warming focuses on the cause of the warming, not that the Earth has warmed over the past few decades. Although the majority of atmospheric scientists cite increases in carbon dioxide as the principal cause, there is no doubt that other factors are involved. Several European paleoclimatologists assert that the warming of the last two centuries is primarily the result of changes in solar output.

Continued global population growth, coupled with the trend of increased global industrialization, should result in an even greater imbalance between carbon dioxide sources versus sinks. The 2013 IPCC report contained several scenarios for increases in carbon dioxide projected to the year 2100. Estimates ranged from a low of 550 ppm to a high of >900 ppm.

An average of these two extremes would put carbon dioxide levels at 788 ppm in 2100, almost a doubling of the 2014 level of 396 ppm. Levels are expected to continue to increase until we switch to alternative energy sources and fossil fuel consumption drops dramatically.



Evidence now suggests that the temperature has already increased between 0.9°F and 1.8°F (0.5° and 1°C) during the last century (Figure 8.25). Some models predict a temperature increase as much as 6.4° to 10.4°F (3.6° to 5.8°C) by 2100, perhaps the most rapid temperature change in the past two million years.

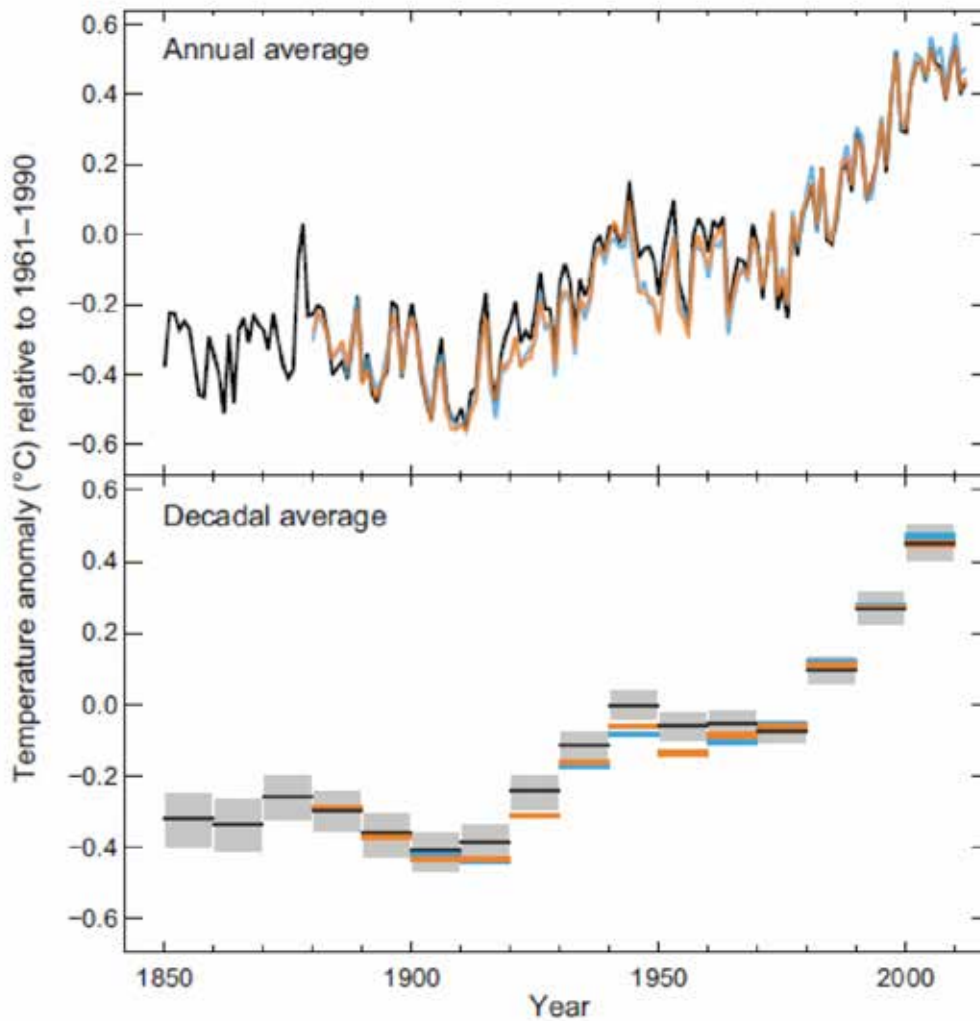


Figure 8.25. Instrumental records from 1850-2012 indicate that average global land and sea temperatures have risen nearly 1°C (Source/Credit: IPCC 2013).

Other greenhouse gases have shown significant increases since the start of the Industrial Revolution (Figure 8.26). Methane ( $\text{CH}_4$ ) is the most important with respect to its warming impact, followed by nitrous oxide ( $\text{N}_2\text{O}$ ). The 2013 IPCC report has included tropospheric ozone ( $\text{O}_3$ ) as an important greenhouse gas (Figure 8.27). The concentration of carbon dioxide, methane, and nitrous oxide had risen 40%, 150%, and 20% above pre-industrial levels as of 2011.

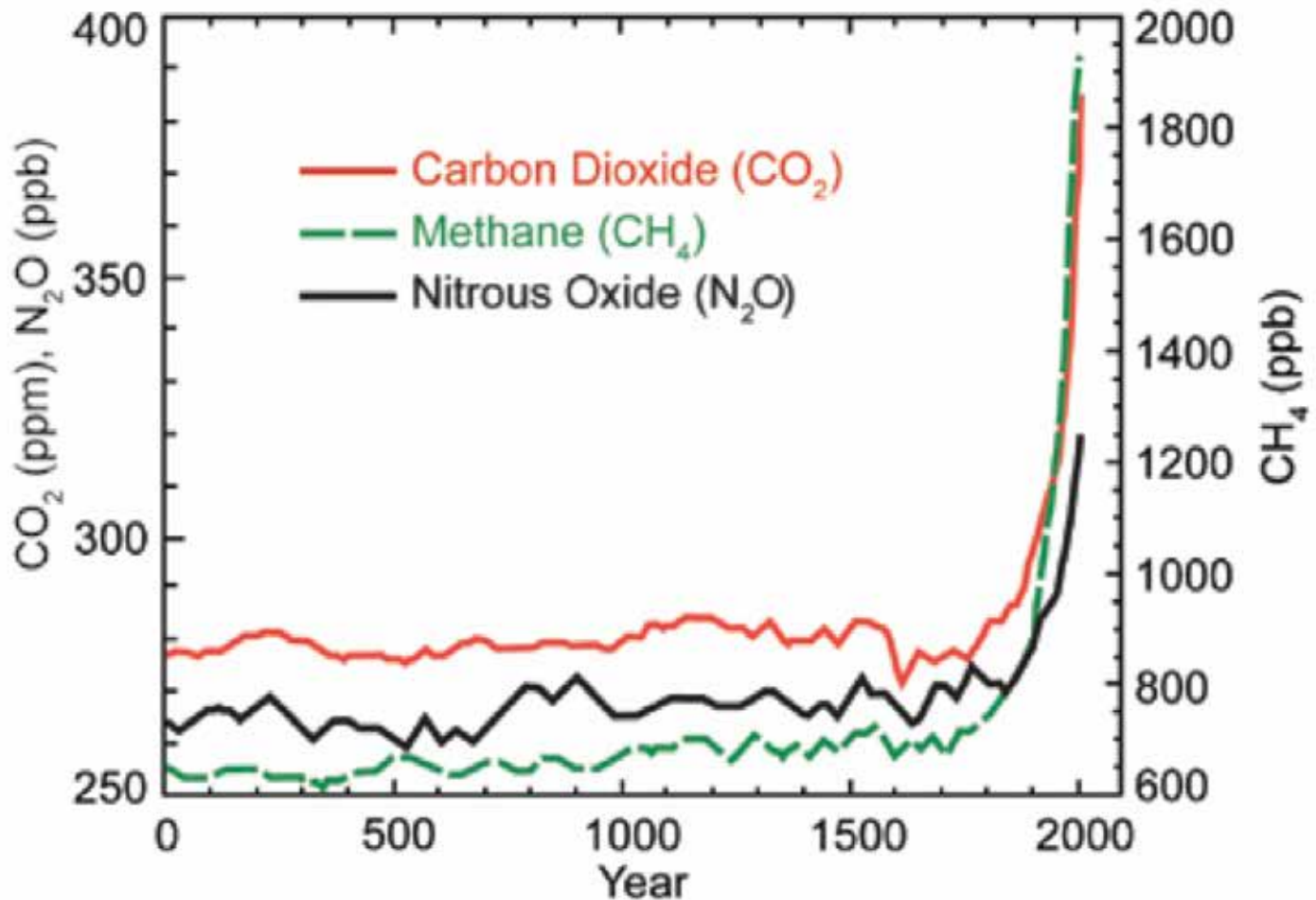


Figure 8.26. Changes in concentration of carbon dioxide, methane, and nitrous oxide over the past two millenia. Increases in concentrations since 1750 are primarily from human activities. Concentrations are expressed in parts per million (ppm) and billion (ppb) (Source/Credit: *Global climate change impacts in the United States 2009*).

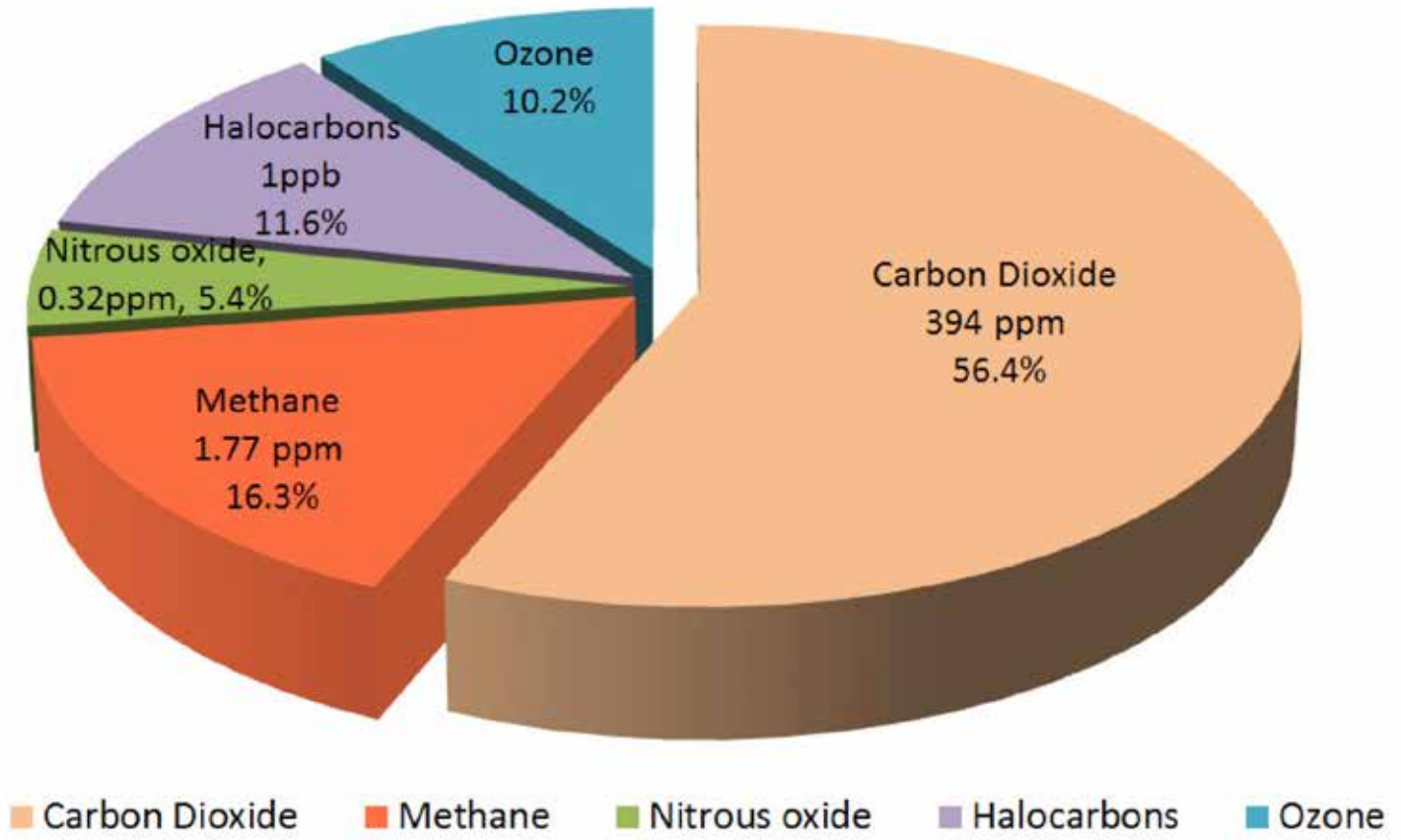


Figure 8.27. Relative importance of greenhouse gases to global warming other than water vapor in 2013. Carbon dioxide dominates as the second most abundant (after water vapor) tropospheric greenhouse gas, even though some of the others are gaining in relative importance (Source/Credit: NASA).

Greenhouse gases have natural as well as anthropogenic origins (Figure 8.28). The cause of much of the increase in carbon dioxide is thought to be fossil fuel combustion, although burning of any hydrocarbon fuel (wood, grass) releases some. Natural sources of methane include the by-product of animals as well as plants in low oxygen environments (e.g., swamps). Anthropogenic sources of methane include rice fields, cattle, coal mining, and using natural gas. Natural sources of nitrous oxide include microbial processes in water and soil. Nitrogen-based fertilizers, fossil-fuel power plants, and vehicle emissions are major sources of anthropogenic nitrous oxide. Tropospheric ozone is largely anthropogenic and is in much higher concentrations in urban and industrial regions. Chlorofluorocarbons are exclusively anthropogenic. Although they are a very small component of greenhouse gases, they are very potent absorbers and have a long residence time (average length of time) in the atmosphere. Although they occur in many different chemical combinations, collectively, they are now approximately of the same importance as tropospheric ozone as a greenhouse gas.

### World GHG Emissions Flow Chart

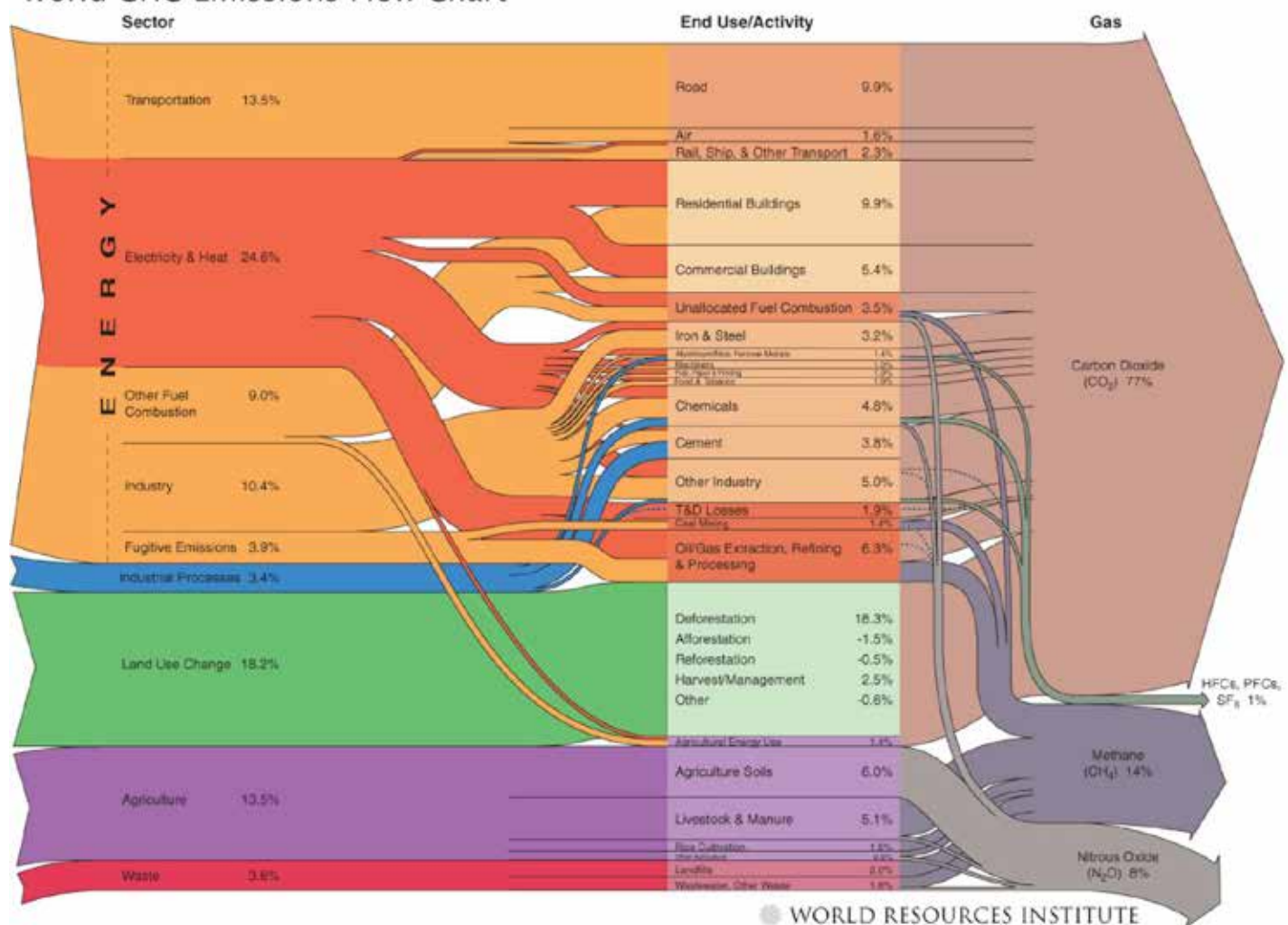


Figure 8.28. World greenhouse gas emissions flow chart. The energy sector is the number one contributor to greenhouse gases globally, and carbon dioxide is the most abundant gas emitted (Source/Credit: World Resources Institute).

Aerosols are tiny solid or liquid colloidal particles in the atmosphere. Aerosols have natural sources as well as anthropogenic sources. They are typically smaller than one micron in diameter, so may be kept aloft in the atmosphere indefinitely. Even though they are not true greenhouse gases, many play a role in atmospheric heating and cooling, although their exact role is poorly understood. The 2013 IPCC report indicates with reasonable confidence that the net role of all tropospheric aerosols is toward cooling (Figure 8.29).

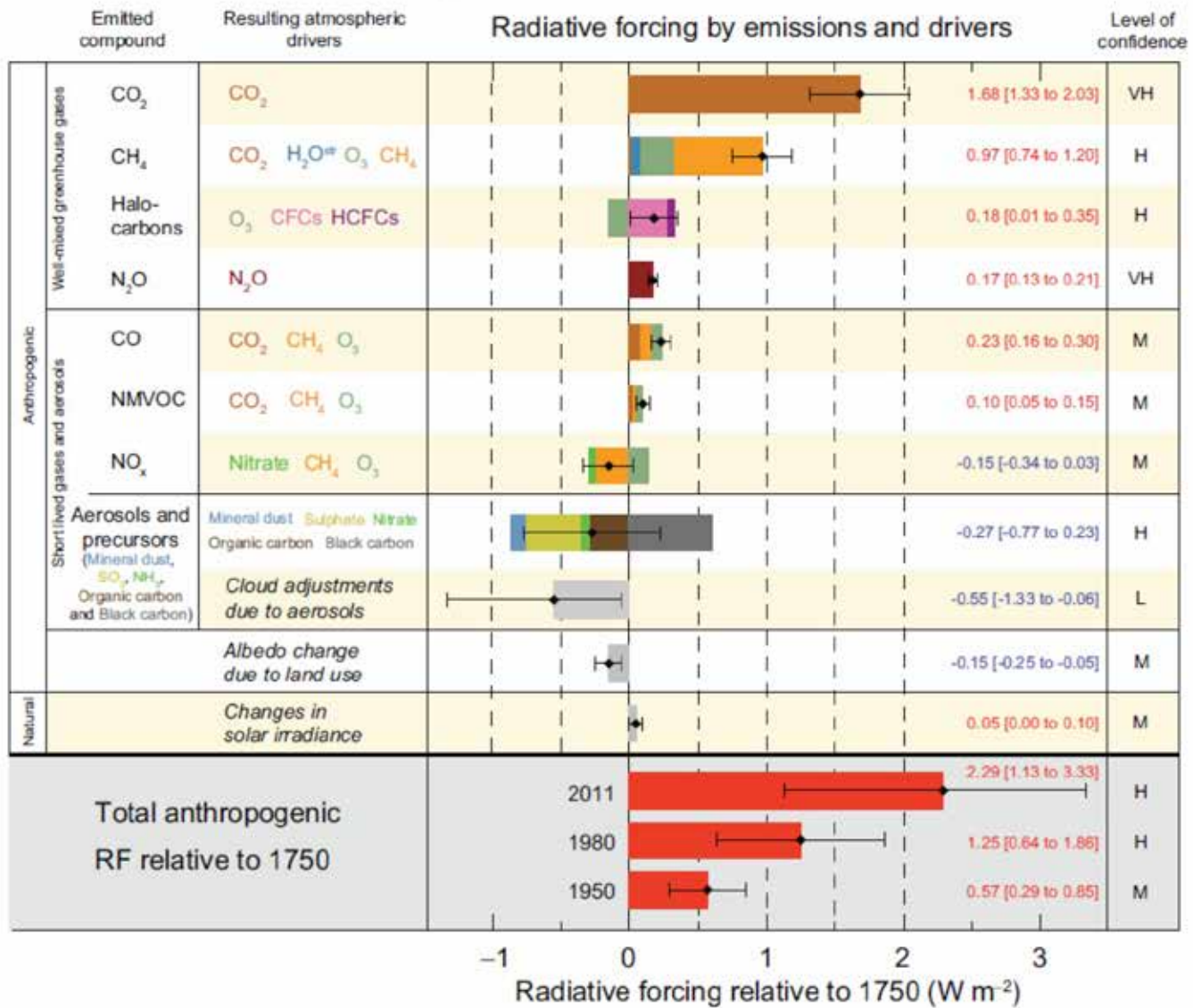


Figure 8.29. One of the most instructive graphics provided by the 2013 IPCC report is a list of the principal gases, aerosols, and other influences that tend to warm the troposphere, called **positive radiative forcing** (bar graphs extending to the right of the solid vertical line, middle of graph), and **negative radiative forcing** (cooling effect, bar graphs to the left of the line). Radiative forcing estimates represent year 2011 relative to 1750. Values are global average radiative forcing. The best estimates of the net radiative forcing are shown as black diamonds with corresponding uncertainty intervals; the numerical values are provided on the right of the figure, together with the confidence level in the net forcing (VH – very high, H – high, M – medium, L – low, VL – very low). Albedo forcing due to black carbon on snow and ice is included in the black carbon aerosol bar. Volcanic forcing is not included because of its episodic nature. Total anthropogenic radiative forcing is provided for three different years relative to 1750 (Source/Credit: IPCC 2013).

## Current and Future Trends and Impacts of Global Climate Change

### Climate Modeling

Climate modeling is the best single resource to test theories on current climate change as well as to speculate what future climates will occur, and how these will affect human activities. Climate modeling has improved vastly in just the past dozen or so years. All climate models have inherent flaws, because (1) climate models are never better than what they are programmed to do, and so are limited by human understanding of a very complex system, and (2) climate models cannot predict future technologies and how they might change human activities, nor can models predict natural variables (e.g., volcanism, impacts) that can greatly influence climatic outcomes. They are, however, an extremely important tool if we want to understand the present climate system and predict future climate change.

Tremendous effort has been put forth by climatologists to predict the consequences of such things as the increase in concentrations of carbon dioxide and other greenhouse gases into the atmosphere. These predictions are based on complex computer models that utilize temperature and moisture data gathered from all over the world, as well as equations used to describe physical and chemical processes. They also utilize assumptions about trends in fossil fuel use and deforestation. Because of the limitations of both the amount and quality of data, limitations in the accuracy of equations, and the impossibility of knowing exactly what people will do in the future, the models have limits. Nonetheless, methods have been devised to check the reliability of the models, and this has given the scientific community some confidence in climate predictability. Every model in use predicts that warming will occur if greenhouse gases continue to increase, though they may differ in the predicted amounts.

It should be emphasized that the scientific community is not predicting that global warming will lead to disastrous negative impacts in all regions of the globe. Although many of the predicted consequences will have negative impacts, such as the extinction of some species, the declining ability to produce food, increased droughts and heat waves, and the impacts of rising sea levels, other regions will experience beneficial effects of a warming globe. High latitude tundra will become forested. Some semi-arid regions will become wetter. Increased carbon availability by plants may produce healthier species. Permafrost areas may become more productive wetlands.

Since the first decade of the 21<sup>st</sup> century, a vast number of climatic scientists have asserted that humans have had an increasing impact on climatic warming, and there has been increased awareness of the potential consequences of warming. Government and private agencies in most industrialized countries have warned of the threat of global warming (e.g.,

the National Academy of Sciences, the American Association for the Advancement of Science, the National Research Council). Intelligence agencies in the United States have likewise stated the potential economic and environmental impacts of climatic change, including threats to our national security. Even the industrial sector, which for decades has been reluctant to accept the premise of anthropogenic climatic change, has been issuing statements of vital concern over climatic change and the urgency to do something about it.

The following sections of this chapter attempt to generate some scenarios of present and near-future trends in global and regional climate, and what impact they might have on human activity. These might be thought of as a work in progress, rather than predictions. They are based on careful analyses of past climates and computer models of past, present and future climates. With better understanding of the climate system, future scenarios will be revised and fine-tuned.

## Temperature

### Land

Warming of the global climate system is real. Since the 1950s, many of the observed changes, in particular the greenhouse gas concentrations, are unprecedented over decades to millennia. The past three decades have seen warmer surface temperatures than any preceding decade since 1850). In the Northern Hemisphere, the period from 1983–2012 was arguably the warmest 30-year period in the last 1400 years.

Global temperatures have increased between 0.9°F and 1.8°F (0.5° and 1°C) during the last century, with land areas experiencing a greater increase than oceans (Figure 8.30). Future increases are likely to continue throughout the 21<sup>st</sup> century, but the exact amount depends primarily on future emissions of greenhouse gases, and to a lesser extent on land-use patterns. Computer models therefore generate multiple scenarios of future climate and climatic impact, typically ranging from best-case scenarios (lowest future emissions) to worst-case scenarios (highest emissions).

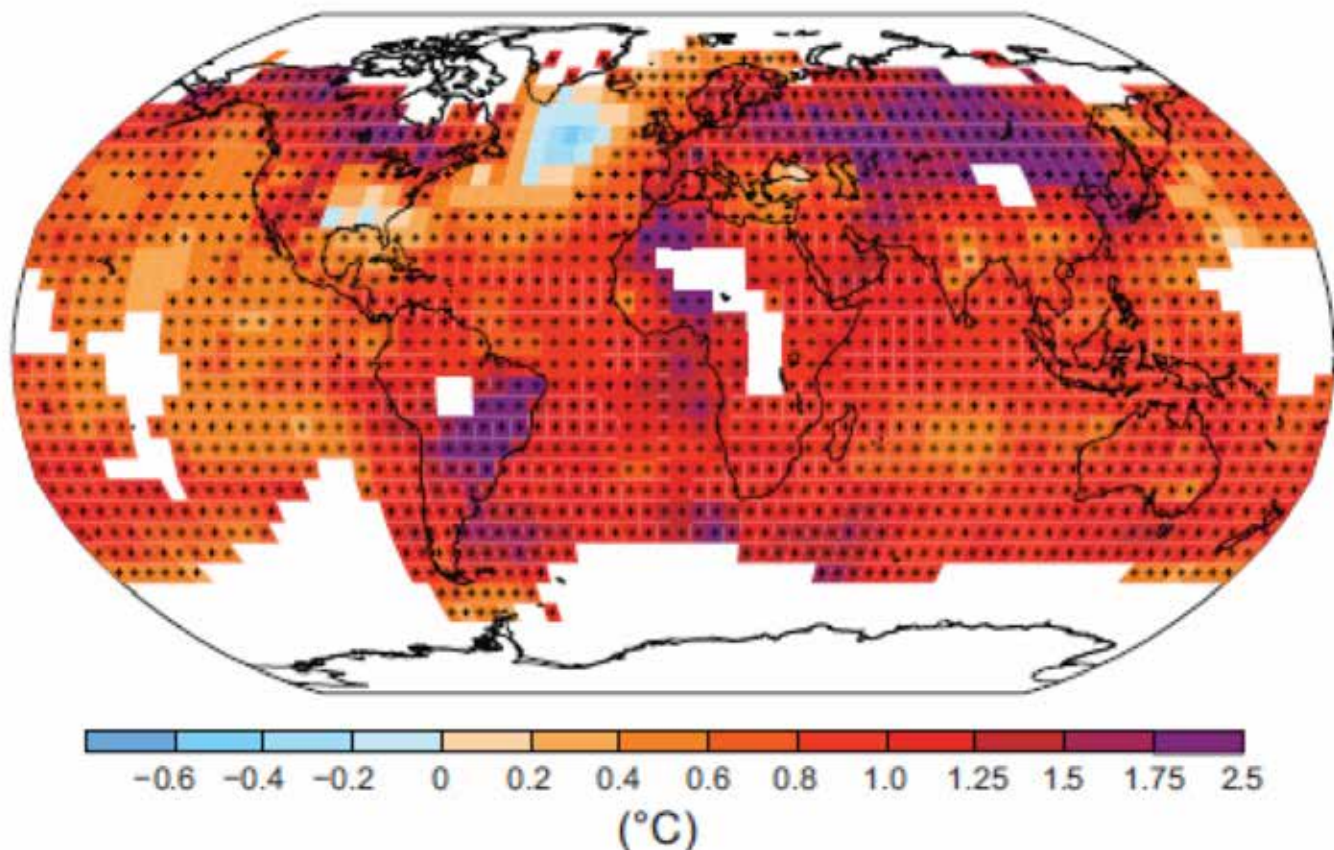


Figure 8.30. Observed change in surface temperatures from 1901 to 2012, expressed as positive and negative temperature anomalies. White areas represent insufficient data to establish trends for the entire time period. Positive trends in temperature dominate, with land slightly greater than oceans (Source/Credit: IPCC 2013).



Some models predict a temperature increase as much as 6.4° to 10.4°F (3.6° to 5.8°C) by 2100, perhaps the most rapid temperature change in the past two million years (Figures 8.31a and 8.31b). The 2013 IPCC report has revised its temperature projections to 2100 downward from the 2007 report, suggesting a more modest increase of 2.7° to 3.6°F (1.5° to 2.0°C), with a worst case scenario (high emissions) of 4° to 9°F (2.6° to 4.8°C). Even small changes in average temperature can have profound effects. For example, at the height of the last glacial period 18,000 years ago, the global average temperature was only 7°F cooler than today. Many areas will experience a much larger change in temperature.

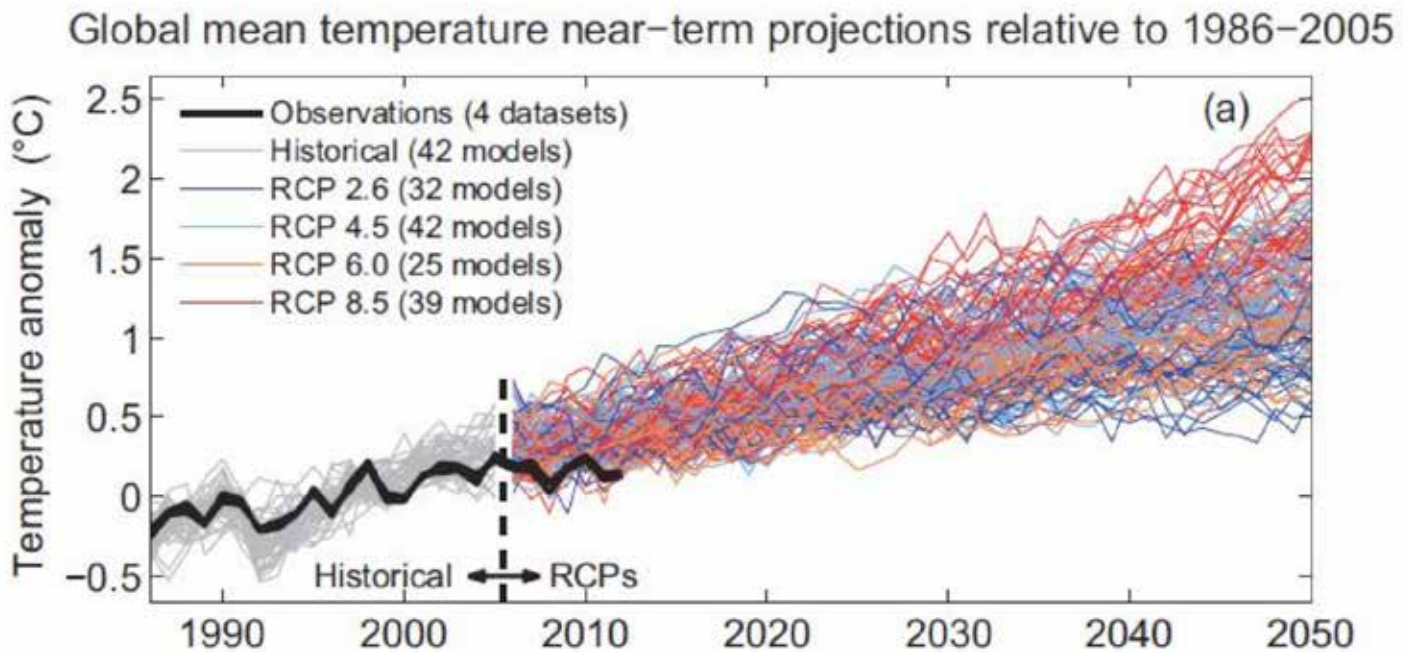


Figure 8.31a. Multiple computer models are used in forecasting future climate, and have the advantage over single models in that they give a range in results. All models indicate a rise in temperature from the 1986–2005 average to the year 2050 (Source/Credit: IPCC 2013).

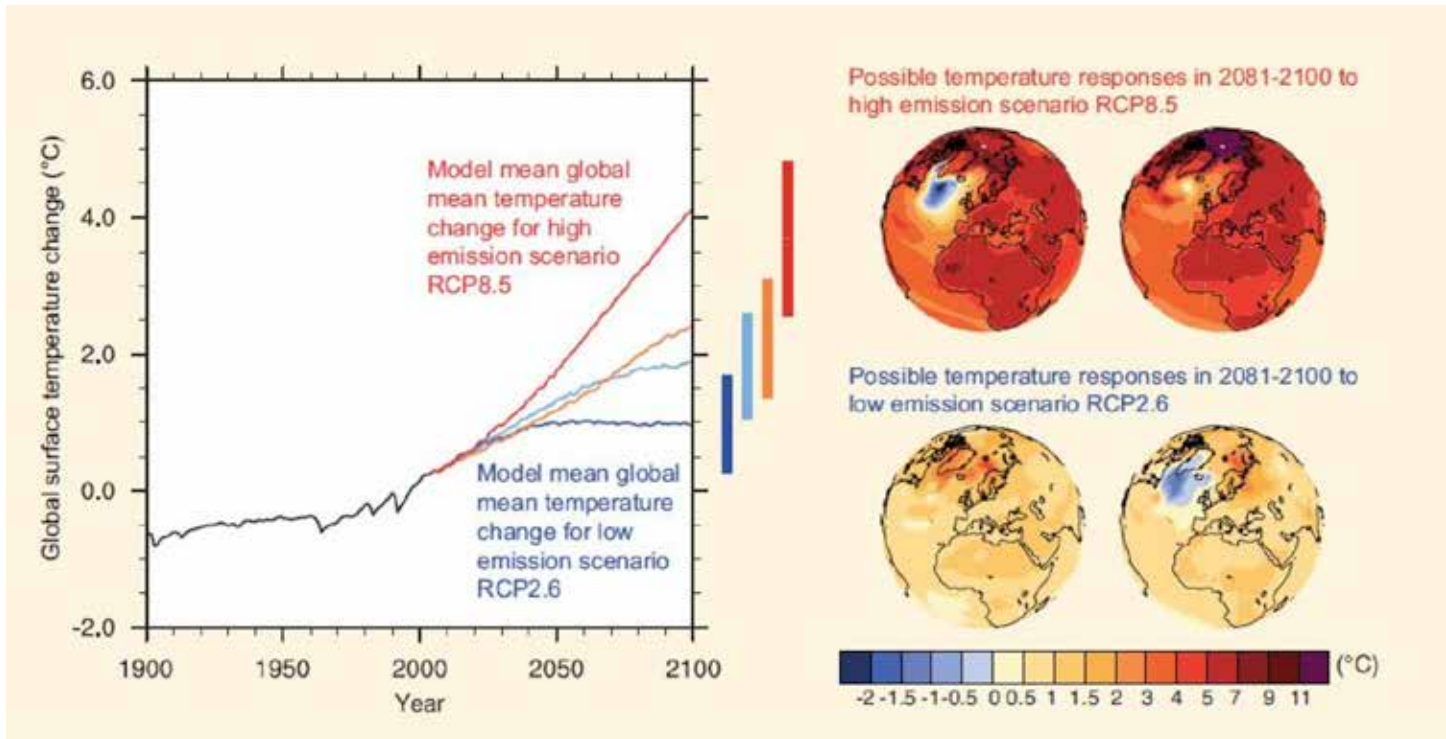


Figure 8.31b. Simplified forecasts of future climate for high and low emissions scenarios. The graphs on the left illustrate global averages, whereas the globes on the right illustrate geographic variations. Note the negative anomalies in the North Atlantic (Source/Credit: IPCC 2013).

The predicted temperature changes will not be uniform globally; some places will experience relatively little change, such as the tropics, whereas other places will experience far more change. Polar and subpolar latitudes will most likely be affected more than any other region. Average temperature increases in the Arctic over the past 100 years have been roughly twice that of the global average, and that trend is expected to continue. The extent of Arctic sea ice has decreased 3.5 to 4.1% per decade since 1979 when reliable satellite monitoring began. The average annual temperature in the Arctic is predicted to increase as much as 20°F (11°C) by the end of this century, with winter warming most pronounced, according to the 2013 report of the IPCC.

**High and low latitude temperature contrasts:** As polar regions warm more than the tropics, the temperature contrast between the high and low latitudes will decrease. Since latitudinal temperature contrasts are the prime cause of the Earth's pressure and wind systems, the intensity of the global wind belts may change, and this would affect such things as ocean currents and the distribution of rainfall. Latitudinal temperature contrasts control the position and strength of jetstreams (both polar and subtropical jetstreams) in the upper troposphere. Since upper-level flow patterns steer surface cyclones and anticyclones, it is likely that middle and high latitude precipitation patterns will be impacted by global warming.

**Upwelling:** The richest fisheries in the world are located along the west coasts of continents where ocean upwelling occurs. **Ocean upwelling** is the movement of deep water up to the surface in response to the effects of wind on the ocean surface. As the deep water is brought to the surface, it carries nutrients up to the shallow layer of the ocean water, and these nutrients serve as the basis for a rich marine food chain. Half of the world's fish supply comes from only 10 upwelling zones.

Already, almost every one of these upwelling zones is being harvested at rates faster than nature's ability to replenish them. Fish supplies are dwindling and fish populations are threatened by this over-fishing. If global warming continues and the Trade Winds diminish in intensity, then upwelling will also diminish. This would result in further reductions in global fish production.

**Spread of tropical diseases:** One of the widespread impacts of current and future warming of the climate is the spread of tropical diseases. Because climate controls the geographic distribution of insects, diseases, and crop pests, climate change will inevitably lead to a change in their distribution. **Of particular concern is the potential for movement of tropical diseases and pests into the mid-latitudes.** As temperatures warm and winters become milder, tropical insects and diseases will be able to expand their range. This has implications for both agriculture and human health.

Roughly 37% of the losses in agriculture and 25% of the losses in forestry are due to pests. Warmer temperatures could increase this rate significantly. To illustrate how significant this is, consider that a 20% reduction in rice losses alone could feed 180 million people per year. Food lost to pests is food lost to people.

Tropical diseases include such things as:

- **Hookworm:** this is an intestinal worm that causes progressive anemia (loss of red blood cells).
- **Dysentery:** Dysentery is a potentially deadly intestinal infection that causes pain, fever and severe diarrhea, often with the passage of blood and mucus. Millions die from it every year.
- **Malaria:** Malaria is caused by a parasite (transmitted by mosquito bite) that infects the liver and blood. It causes chills and fever, and leaves people susceptible to recurrent bouts with the disease. It can be fatal if left untreated. At present, between 300 and 500 million people are infected by malaria and two million die each year from this disease. As a result of warming, an additional 46% to 60% of the world's population will live within the transmission zone for malaria.

- **Bubonic plague:** This is a usually fatal infection, transmitted by fleas and small rodents, which is characterized by chills, fever, vomiting, and diarrhea.
- **Dengue fever:** This sickness is also transmitted by mosquitoes. It causes fever and chills and can be fatal. A temperature increase of 5°F to 7°F (2.8°C to 3.9°C) could double the transmission rate of this disease.

## Oceans

More than 90% of the increase in energy stored in the Earth's climate system over the past 40 years is in the oceans. The most pronounced increase in energy stored is in the upper 2300 feet (700 m). As a global average, the upper 250 feet (75 m) warmed by about 0.2°F (0.11°C) per decade over this period. Oceans are projected to warm between 0.5°F (0.3°C) and 3.6°F (2°C) in the top 300 feet (~100 m) by the end of the 21<sup>st</sup> century.

It also appears that regions of high ocean salinity (dissolved salts) have become more saline, while regions of low salinity have become fresher. The implication of these changes in salinity are that rates of evaporation and precipitation are changing over the oceans. It also appears that the oceans in general have become more acid over the past few decades (Figure 8.32). The 2013 IPCC report estimates acidity increases of nearly 26% since the start of the Industrial Revolution.

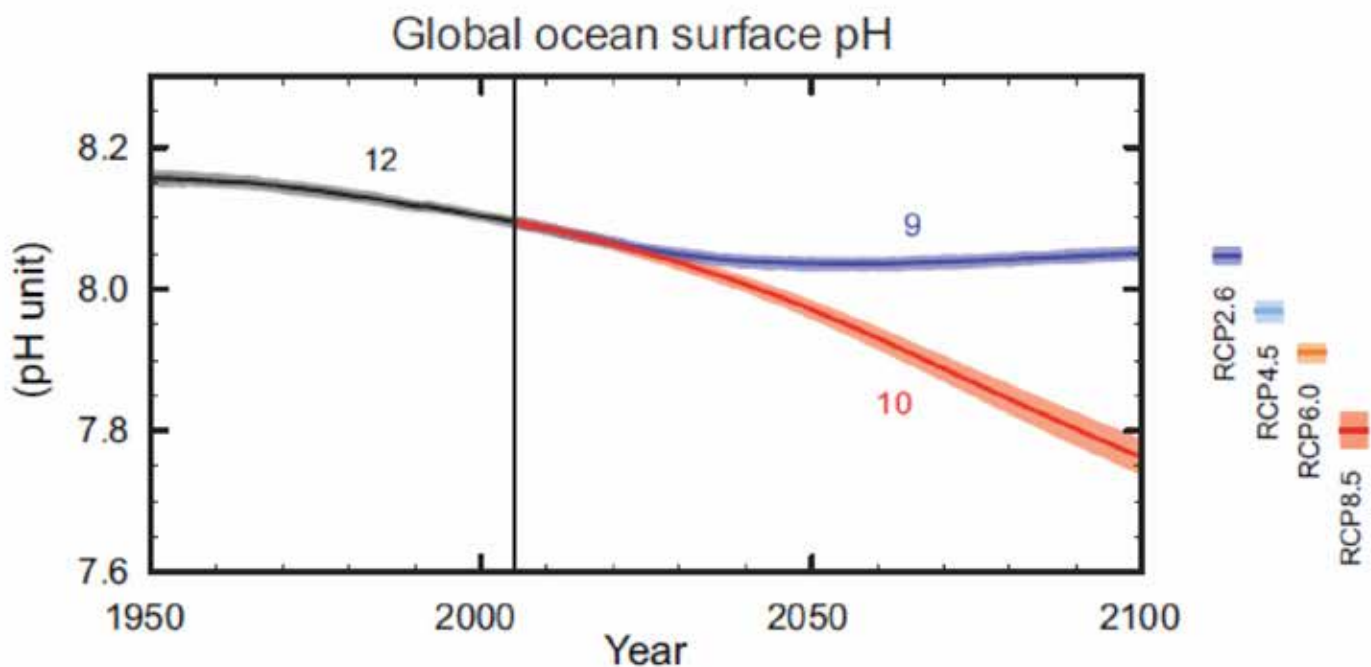


Figure 8.32. Global changes and projected scenarios in the pH of the ocean surface (Source/Credit: IPCC).

One of the possible impacts of global warming is a change in ocean circulation. In particular, scientists are concerned that the Gulf Stream may shut down in the North Atlantic as a result of the influx of fresh water from melting mountain glaciers and the Greenland Ice Cap (Figure 8.33). So, ironically, global warming could actually cause Western Europe to be plunged into very cold conditions. Because of the influence of the Gulf Stream, Western Europe is far warmer than it would otherwise be. If the **thermohaline circulation** in the North Atlantic shuts down, temperatures in this area would be comparable to those in Canada, which is located at similar latitude. The North Atlantic thermohaline circulation is tied to a global pattern so that changes in one part of the circulation system might trigger changes elsewhere (Figure 8.34).

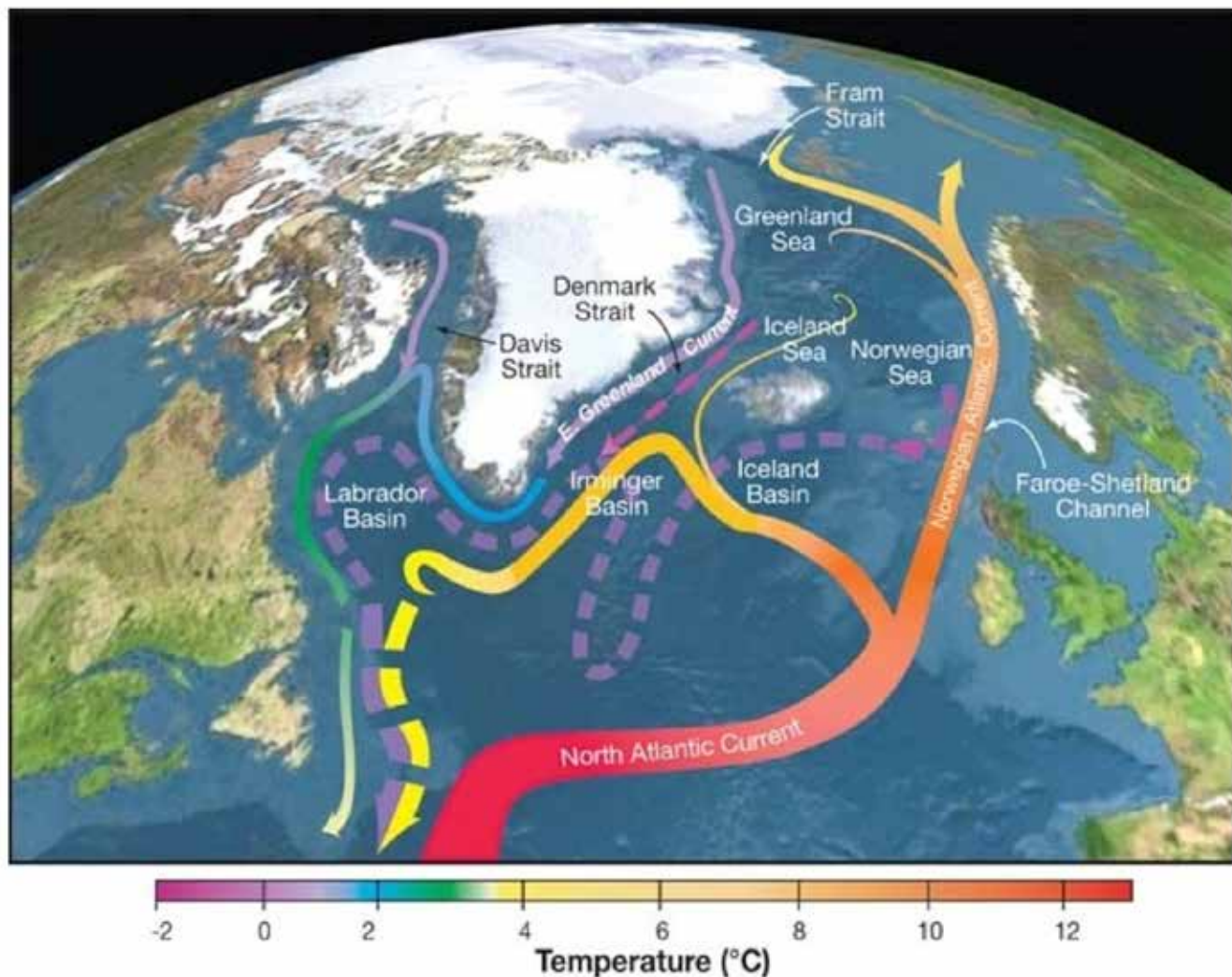


Figure 8.33. The North Atlantic thermohaline circulation is part of a world-wide conveyor belt of slow-moving ocean currents driven by density differences compared to the surrounding water. Surface currents are in solid lines; deep currents are in dashed lines. The surface component of the current system is partially controlled by prevailing surface winds and is much faster than the currents that move along the ocean floor. The warm, near-surface currents (red, orange, and yellow) transport huge amounts of heat energy poleward, keeping northern Europe much warmer than North America at similar latitudes. The failure of the warm surface currents might send temperatures in Europe plunging (Source/Credit: R. Curry, Woods Hole Oceanographic Institution/Science/USGCRP).

## Thermohaline Circulation

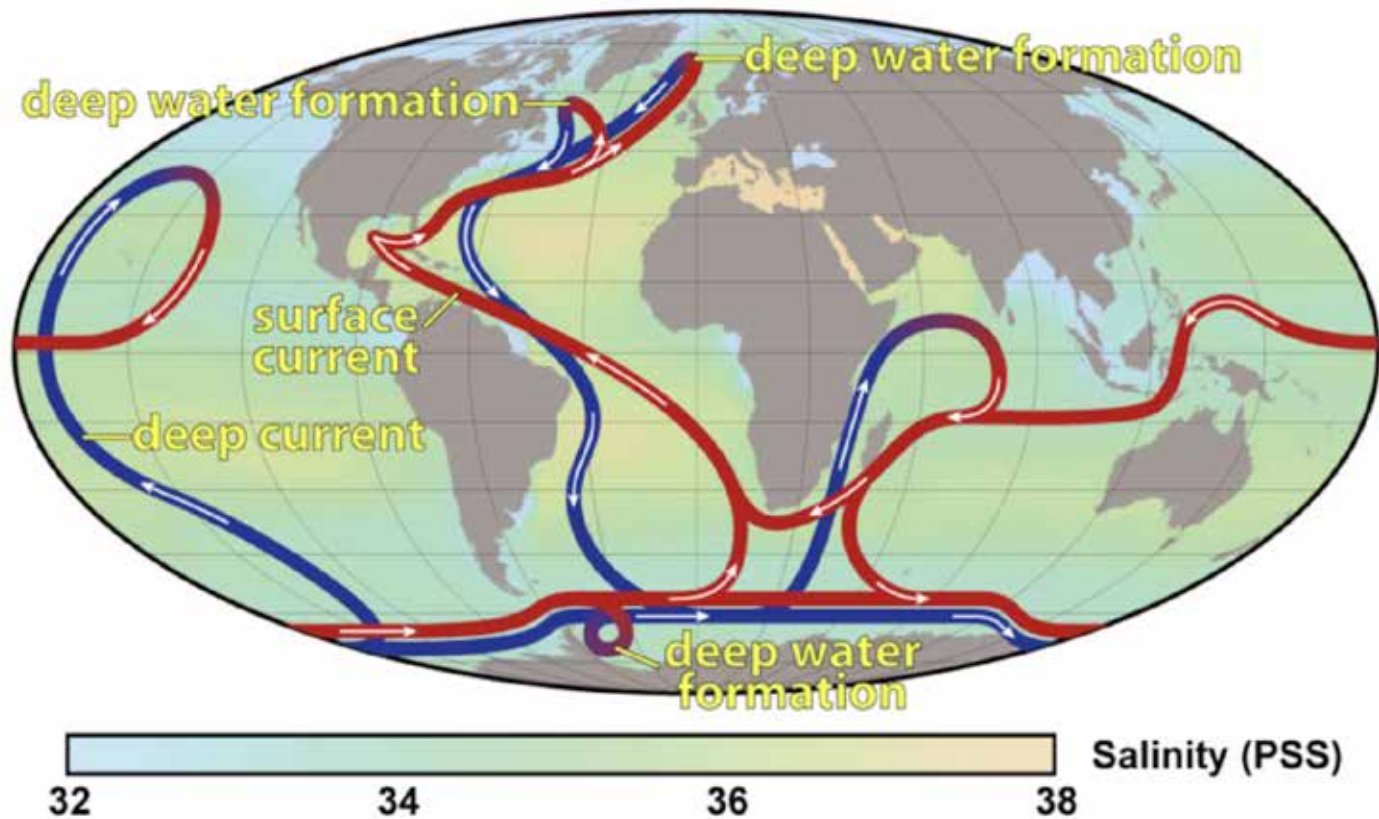


Figure 8.34. Surface, wind-driven circulation of ocean currents are linked to slow-moving subsurface circulation that is density-driven, the thermohaline circulation. Together, these currents move a vast amount of water both poleward and equatorward, helping maintain the present latitudinal temperature patterns. One complete cycle of circulation takes about 2000 years (Source/Credit: NASA Earth Observatory).

Previous paleoclimatic events have been linked to the failure of thermohaline circulation in the North Atlantic. One occurred at the end of the last ice age when melting glaciers pumped massive quantities of fresh water into the North Atlantic, just as is now happening. A large pool of freshwater in the Atlantic has already been discovered. What is particularly disturbing is the interpretation that the ice age shut down took only decades to occur. Climate change is not something that always occurs slowly or predictably. Major changes might occur within our lifetime. Indeed, they may have already begun.

## **Extreme Weather Events** (*Heat Waves, Drought, Tropical Storms, Tornadoes*)

Extreme weather events (droughts, heat waves, cold snaps, dust storms, violent storms) are influenced by changes in temperature, moisture content (humidity), and circulation patterns of the atmosphere. Some analyses indicate that there have been systematic changes in certain extreme weather events since 1950, and these may become even more frequent during the 21<sup>st</sup> century. Other observed changes that have occurred may be multi-decadal oscillations that are not necessarily tied to climate change.

Several studies in different sectors of the world indicate that the number of cold days and nights has decreased and the number of warm days and nights has increased. The frequency of heat waves has apparently increased in large parts of Europe, Asia and Australia, and some parts of North America. Heat waves impact large numbers of people and are associated with increases in respiratory ailments and heart problems.



The 2003 heat wave in Europe brought the highest summer temperatures since 1540 (Figure 8.35). France was particularly hard hit, with over 14,000 heat-related deaths. Northern France, which typically has mild temperatures during the summer, had seven days that exceeded 104°F (40°C). Record high temperatures were set in many cities in Spain, Italy, Germany, and Switzerland, with maximum temperatures ranging from 102°F (39°C) to 115°F (46°C).

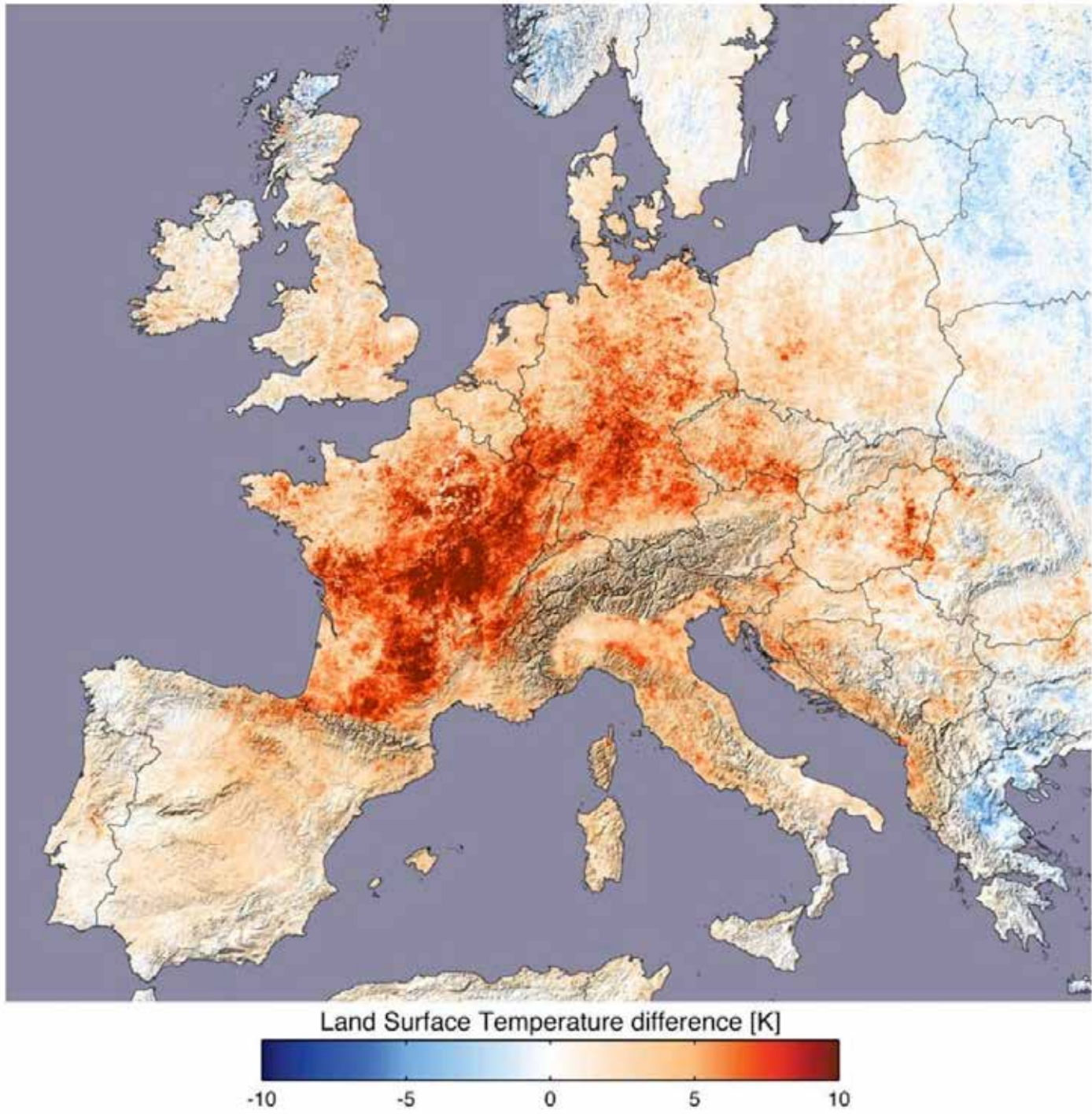


Figure 8.35. Temperature anomalies during from July 20-August 20, 2003 in Europe compared to temperatures over the same time period in the years 2000, 2001, 2002, and 2004. Much of France was 18°F (10°C) warmer than average (Source/Credit: Reto Stöckli, Robert Simmon and David Herring, NASA Earth Observatory, based on data from the MODIS land team).

In July 2006 more than 220 people died in a North American heat wave. Temperatures in South Dakota reached a reported high of 130°F (54°C), one of the highest temperatures ever recorded in North America. In June 2010 parts of Russia reported the highest temperatures in 1000 years. Wild fires, drought, and the heat wave accounted for thousands of deaths, including many who drowned while swimming drunk (Figure 8.36). Heat waves also occurred in North America and China during summer 2010 (Figure 8.37). The number of unusually hot summer temperatures in the contiguous United States has increased over the past hundred years (Figure 8.38). Whether the increase is solely due to climate change or is partly related to other factors (urban effects, better monitoring) is unclear. Heat waves are expected to increase throughout the 21<sup>st</sup> century, but the magnitude of change depends largely on the future emissions scenario.

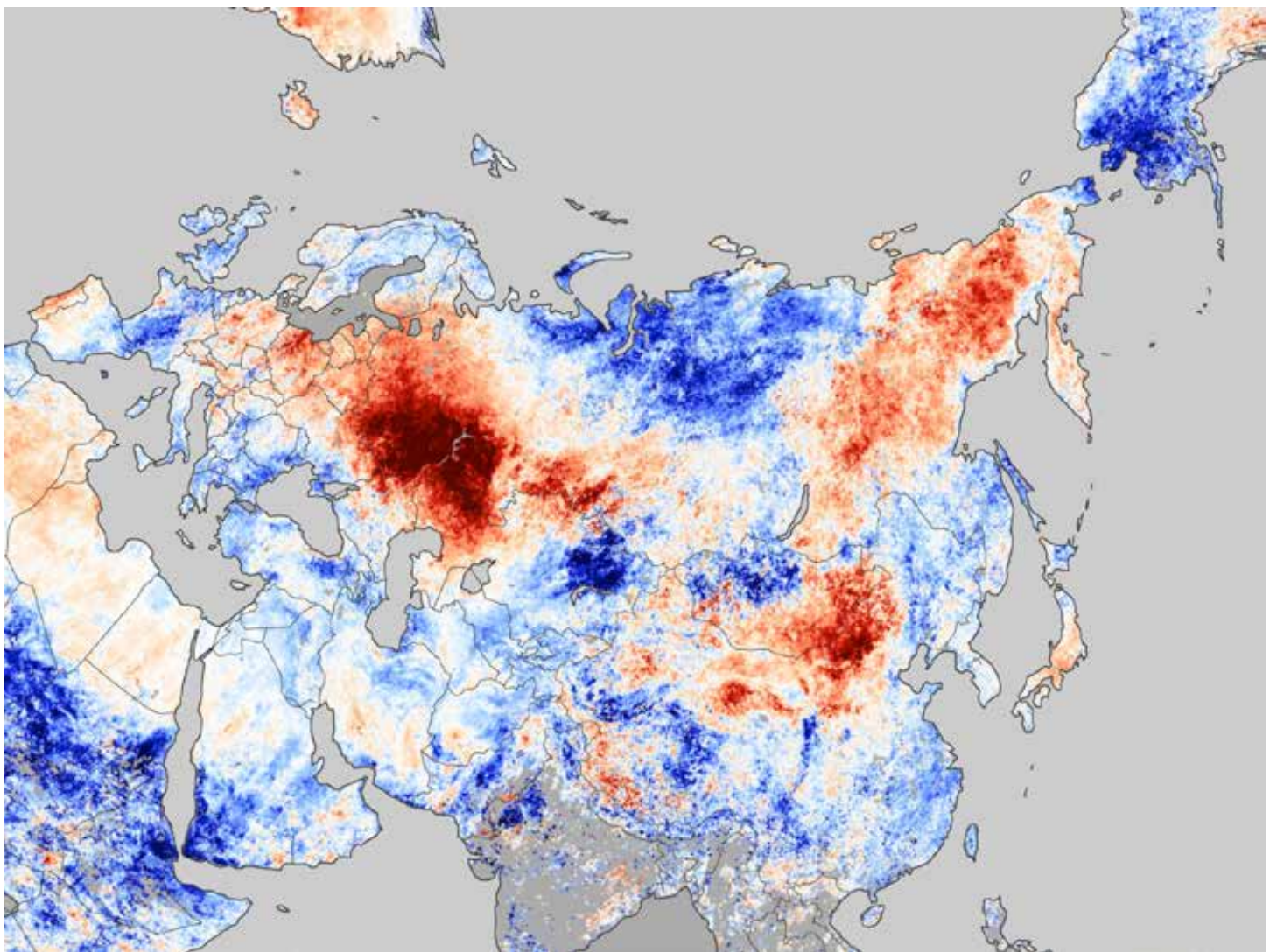


Figure 8.36. The Russian heat wave of July 20-27, 2010. The image shows temperature anomalies compared to averages from 2000-2008. Warmer than average temperatures are in orange and red, whereas cooler temperatures are in blue and oceans gray (Source/Credit: NASA Earth Observatory/MODIS).

# Temperature Anomalies June 2010

(with respect to a 1971-2000 base period)

National Climatic Data Center/NESDIS/NOAA

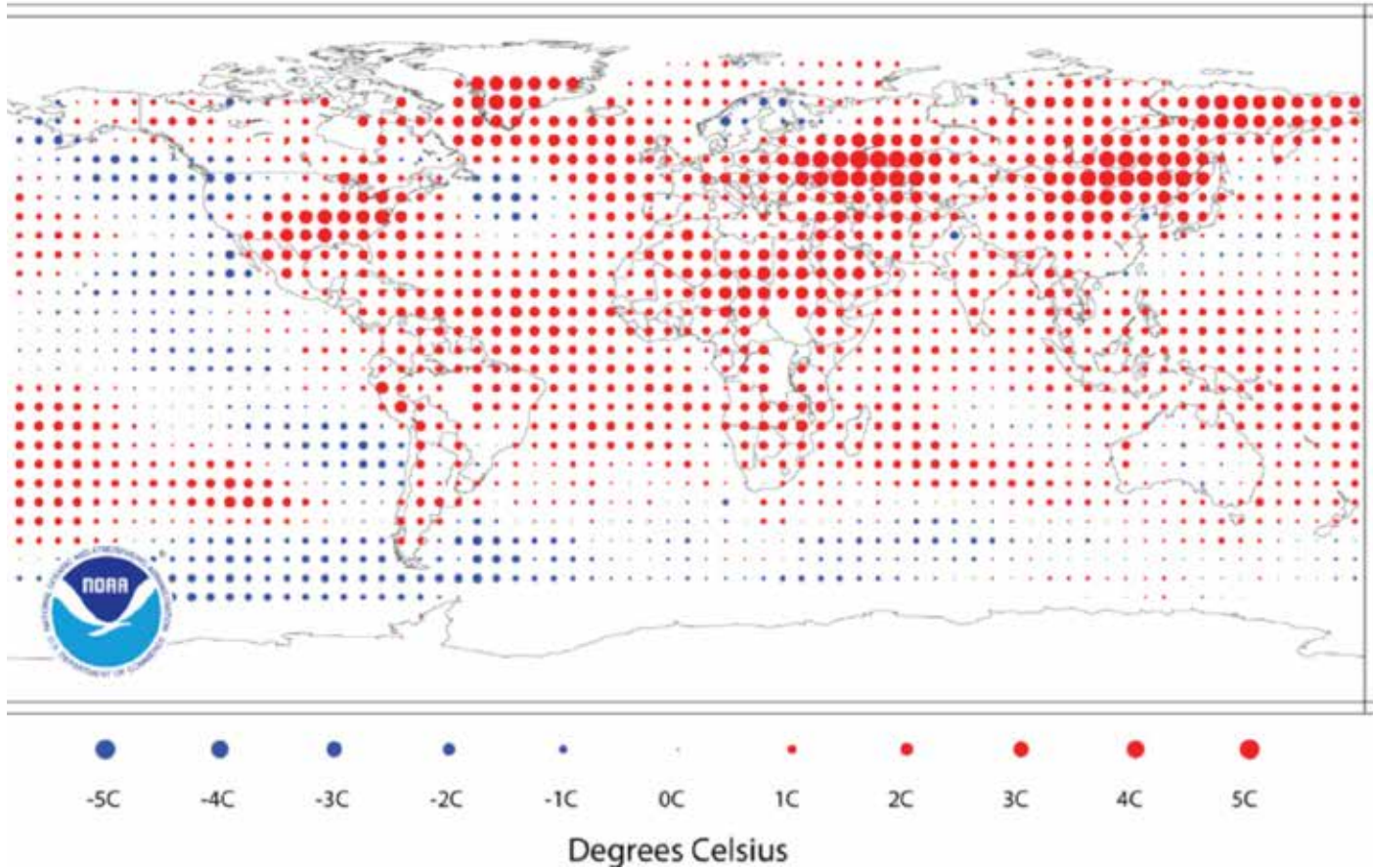
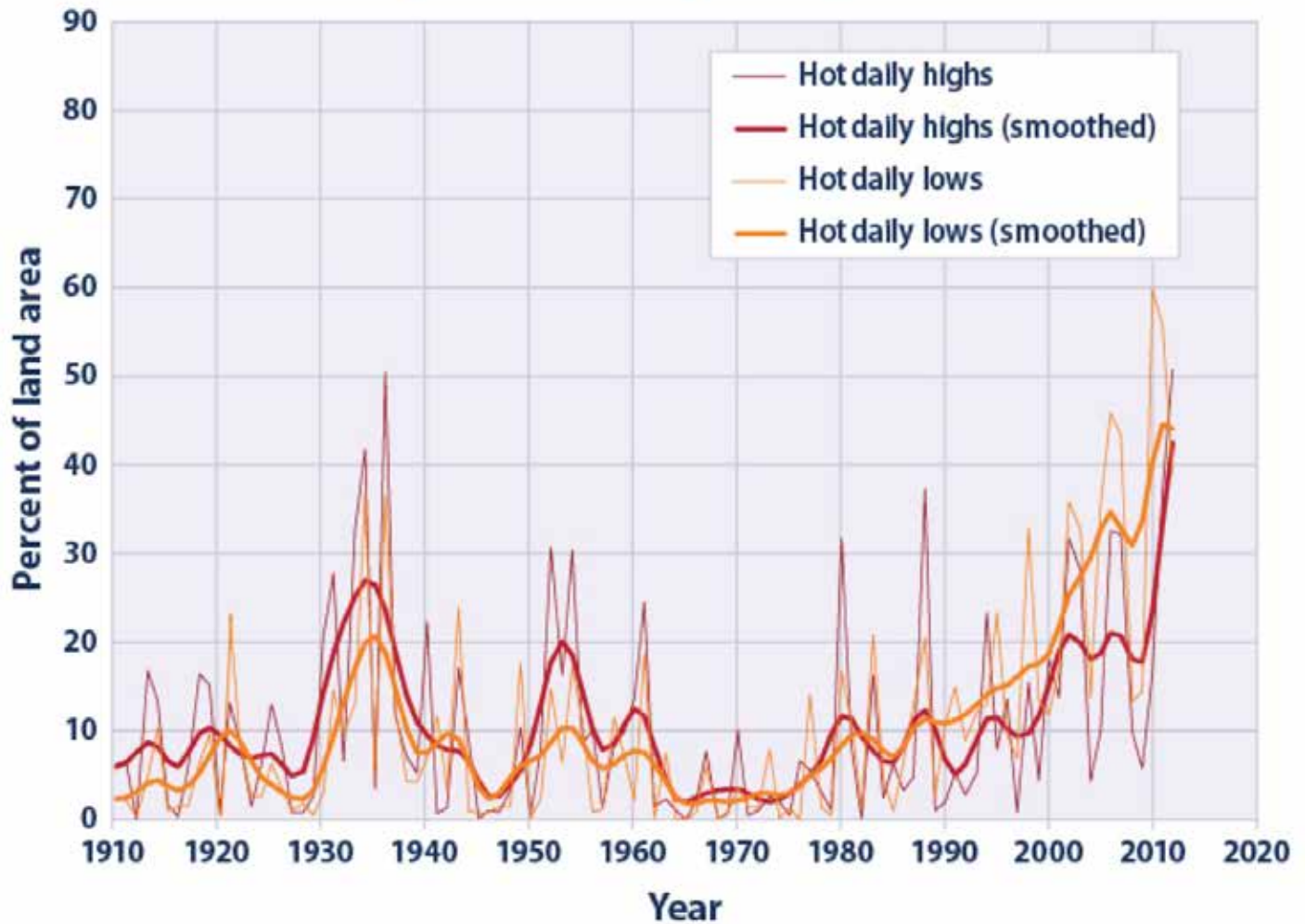


Figure 8.37. Global temperature anomalies in June 2010. Heat waves affected Russia, China, the United States, and to a lesser degree, north Africa (Source/Credit: NOAA/NCDC).

### Area of the Contiguous 48 States with Unusually Hot Summer Temperatures, 1910–2012

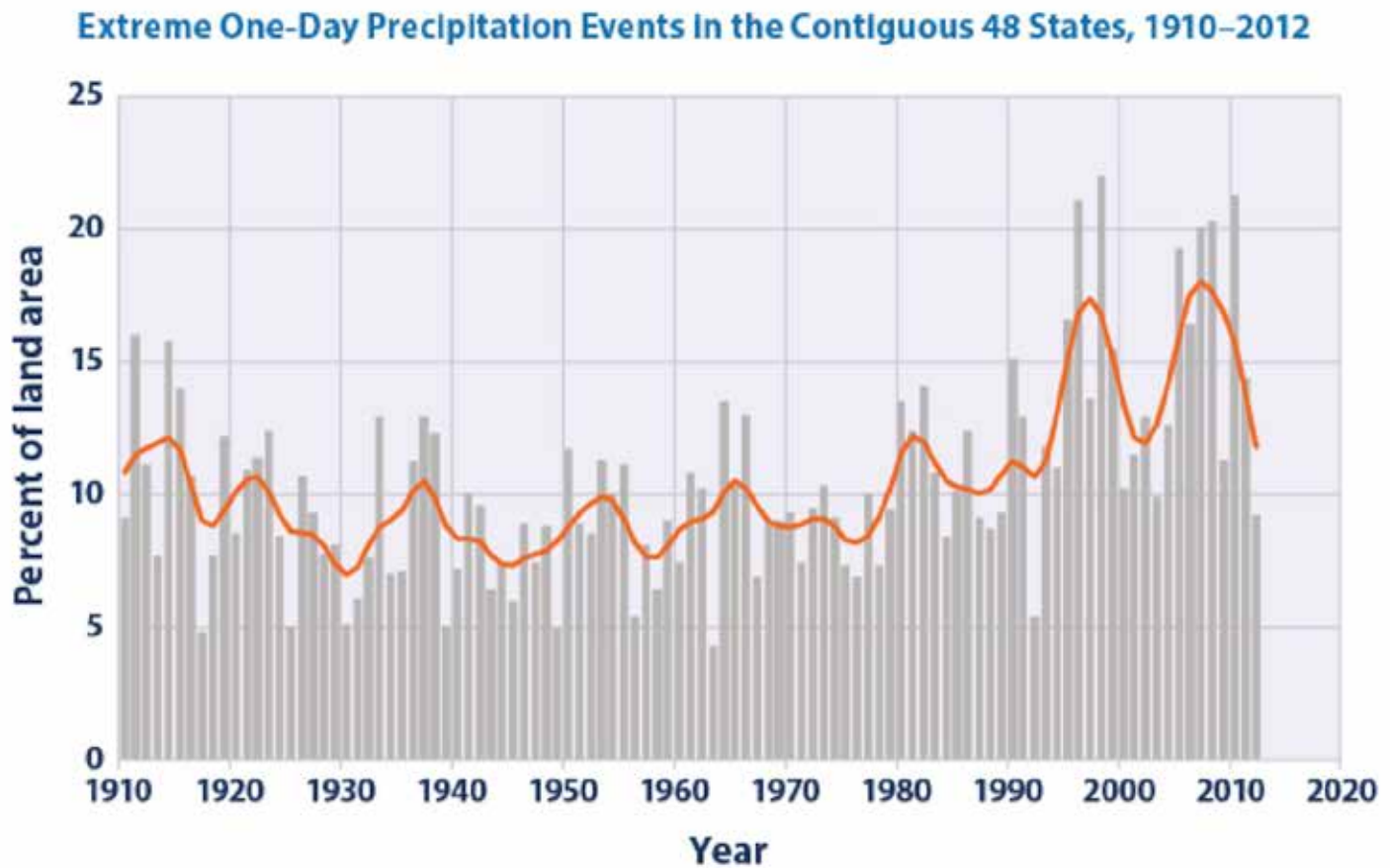


Data source: NOAA (National Oceanic and Atmospheric Administration). 2012. U.S. Climate Extremes Index. Accessed October 2012. [www.ncdc.noaa.gov/extremes/cel](http://www.ncdc.noaa.gov/extremes/cel).

For more information, visit U.S. EPA's "Climate Change Indicators in the United States" at [www.epa.gov/climate-change/indicators](http://www.epa.gov/climate-change/indicators).

Figure 8.38. The number of summer hot days in the contiguous United States shows considerable variability from year to year, but a general increase from 1910-2012. Whether the increase is solely due to climate change or is partly related to other factors (urban effects, better monitoring) is unclear (Source/Credit: NOAA 2012).

There also appears to be an increase in the number of heavy precipitation events in certain regions (Figure 8.39). Higher water-vapor content and warmer surface temperatures both tend to destabilize the lower atmosphere, inducing deeper convection and increased probability of precipitation. In other regions, there is no apparent trend over time in extreme weather events.



Data source: NOAA (National Oceanic and Atmospheric Administration). 2013. U.S. Climate Extremes Index. Accessed March 2013. [www.ncdc.noaa.gov/extremes/cel](http://www.ncdc.noaa.gov/extremes/cel).

For more information, visit U.S. EPA's "Climate Change Indicators in the United States" at [www.epa.gov/climatechange/indicators](http://www.epa.gov/climatechange/indicators).

Figure 8.39. Extreme one day precipitation events in the contiguous United States shows a slight increase from 1910-2012. The image indicates the percentage of the land area where a much greater than normal portion of total annual precipitation has come from extreme single-day precipitation events. The gray bars represent individual years, whereas the red line is a nine-year weighted average (Source/Credit: NOAA/EPA 2013).

Whereas the link between heat waves and a warming climate seems apparent and readily explainable, the connection with tropical storms and tornadoes is less clear. The most intensely studied hurricane breeding ground in the world is the North Atlantic Ocean basin. In the past decade or so, there has been an increase in the frequency of North Atlantic hurricanes (Figure 8.40). Although this trend may be attributable to natural decadal cycles, there are a growing number of researchers who link the trend to global warming. North Atlantic Hurricanes have not only increased in frequency, but also intensity (Figure 8.41). This may be the result of an increase in ocean temperatures as well as a larger body of warm ocean water. Warmer water means more water vapor injected into the atmosphere, which is the fuel for many severe storms. While it is not possible to say conclusively that recent hurricanes such as Katrina, Rita, Ike and Sandy were bigger than would have occurred in the absence of global warming, some meteorologists believe that at least some of their intensity, as much as 7%, may have been caused by warmer ocean temperatures. Anthropogenic warming already appears to be affecting storm intensity and frequency.

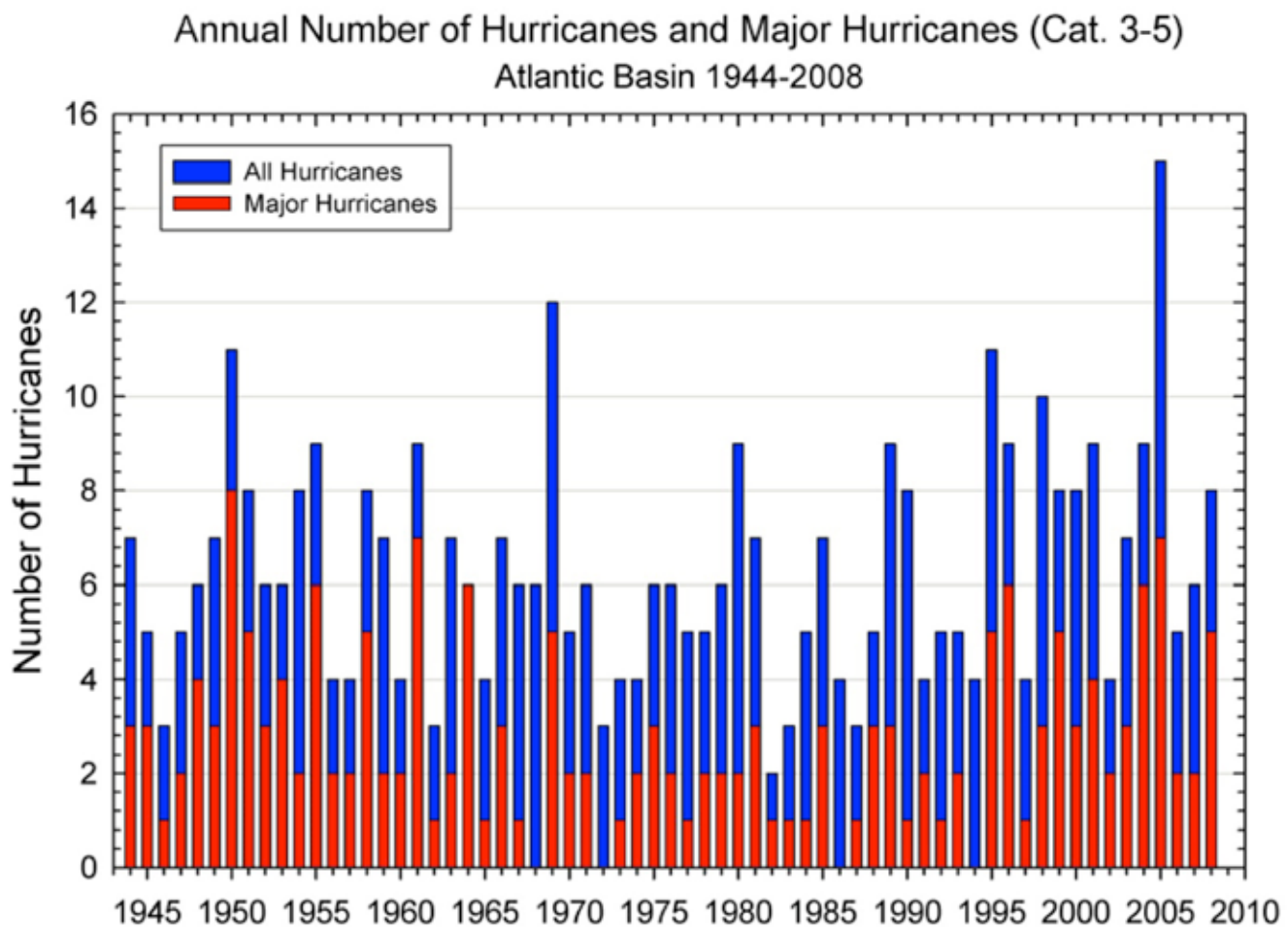
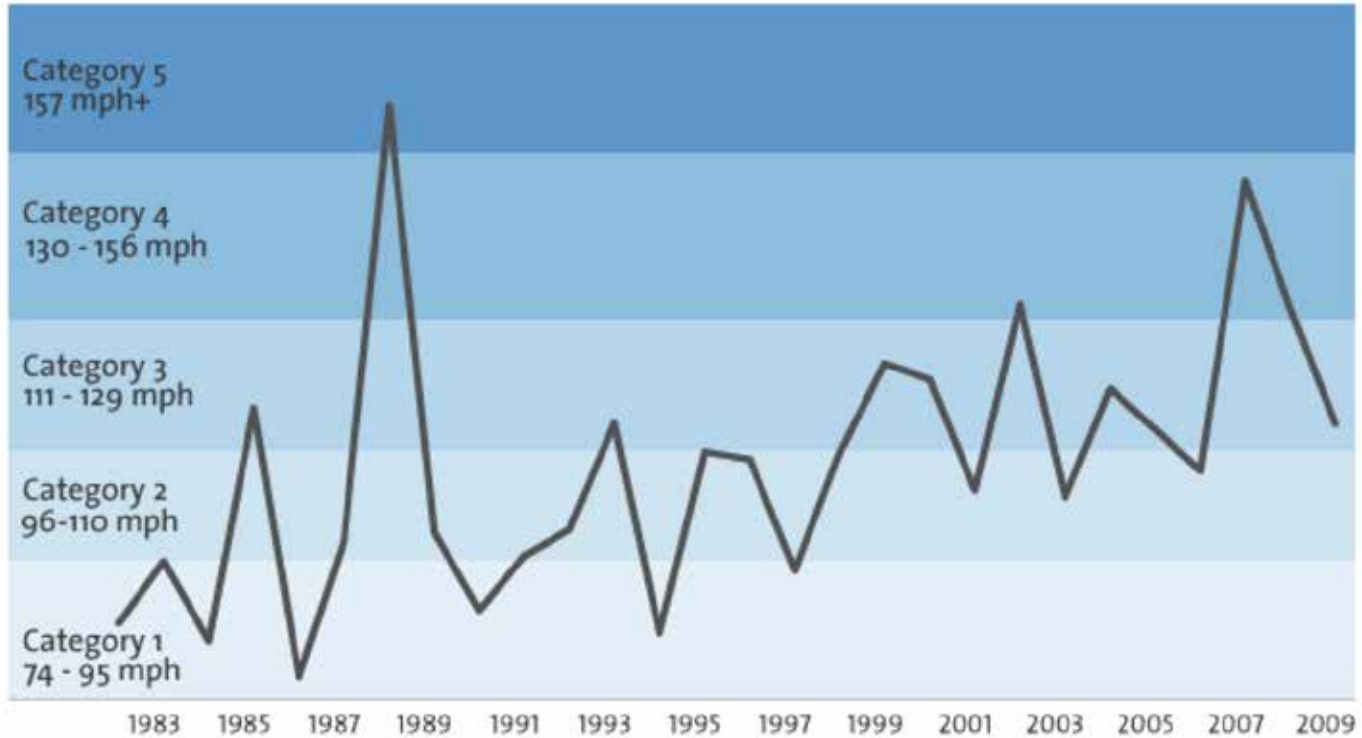


Figure 8.40. The graph compares the annual number of all hurricanes to the annual number of major hurricanes (category 3-5) for the North Atlantic Basin from 1944-2008. Whereas the major hurricanes show a crude multi-decadal trend, the numbers of all hurricanes are more sporadic. Although we appear to be in an era of higher-than-normal activity, there are significant variations from one year to the next, negating any accurate predictive capability (Source/Credit: NCDC).

# The Rising Strength of North Atlantic Hurricanes

On average, the maximum wind speed of hurricanes in the North Atlantic basin has jumped 25 mph in just under three decades. That's a much higher increase than any other basin around the world.



Source: Jim Kossin, National Climate Data Center  
Analysis included only storms that reached Category 1 hurricane strength or greater.



Figure 8.41. The average maximum wind speed of North Atlantic hurricanes appears to be increasing over the last three decades. The reason for the large increase in strength here compared to other ocean basins is not known (Source/Credit: Jim Kossin, NCDC).

There is some rationale to think that some areas in subtropical latitudes that are today almost free of hurricane activity could become more susceptible with global warming. Southern California, for example, has not had a hurricane make landfall since 1900, and there have only been two tropical storms that have penetrated the area. The reasons for the near-absence of hurricanes there is that (1) the area is swept by the cold California Current, keeping temperatures well below the 80°F (27°C) level that is required for hurricane formation and maintenance, and (2) upper-level winds off the coast are typically unidirectional and have strong shear; hurricanes require anticyclonic flow aloft. Although hurricanes do form in the fall of the year off the coast of Mexico, most of them travel northeast out into the open ocean. The few hurricanes that head northward toward California are typically weakened by passage over the cold California Current and the upper-level shearing winds (Figure 8.42). With global warming, one might speculate that higher ocean surface temperatures combined with reduced upwelling of cold water might allow some hurricanes to penetrate the Los Angeles lowlands, home to 22 million people.

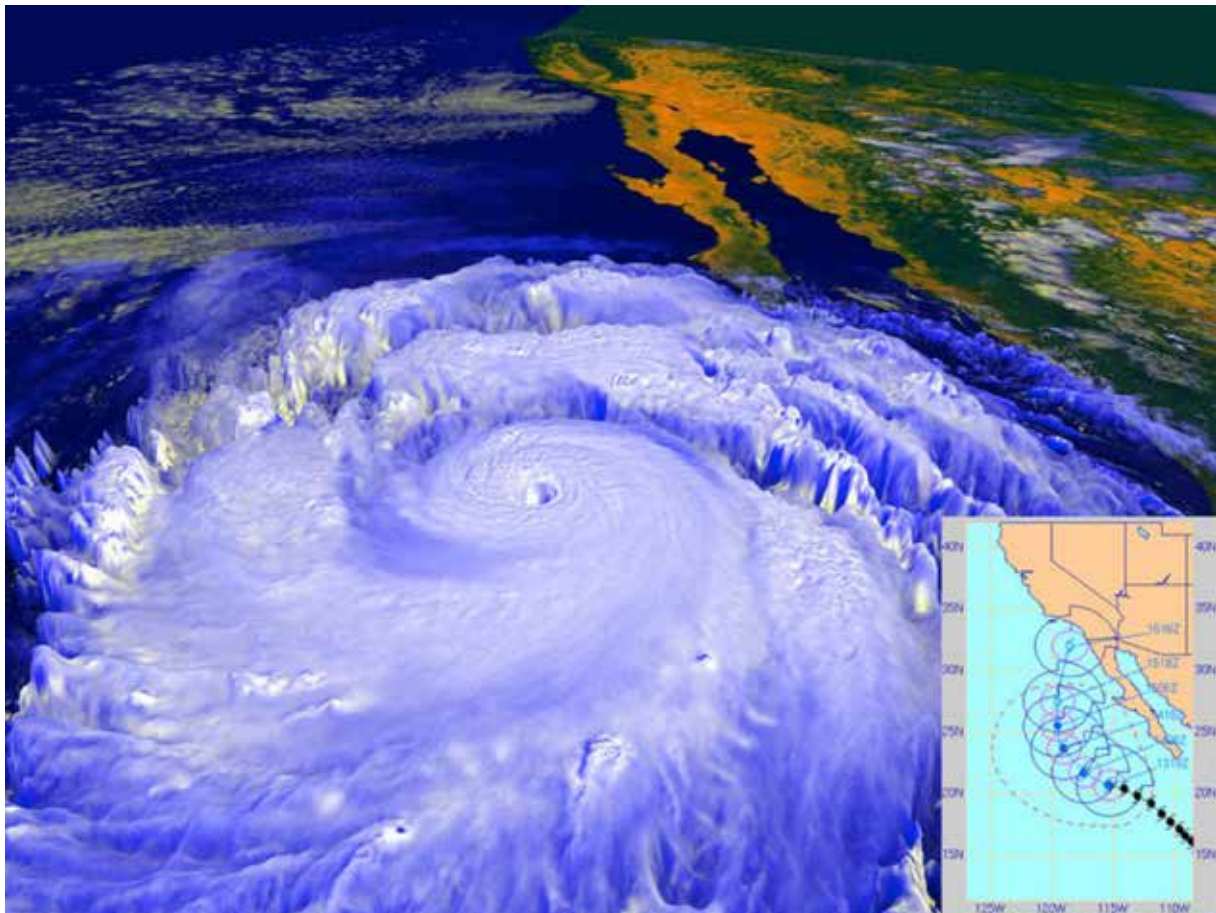


Figure 8.42. Although hurricanes commonly form in the east Pacific Basin during the fall of the year off the coast of Mexico, most of them travel northeast out into the open ocean. The few hurricanes that head northward toward California are typically weakened by passage over the cold California Current. The image shows hurricane Linda in 1997 (computer enhanced image), which was forecast to strike Southern California, but veered west at the last minute. With global warming, one might speculate that higher ocean surface temperatures combined with reduced upwelling of cold water might cause an occasional hurricane to penetrate the Los Angeles lowlands, home to 22 million people (Source/Credit: NASA/JPL; NRL/NCEP).



The connection between global warming and recent tornadic activity is also unclear. Intuitively, the increase in water vapor content of the atmosphere and higher surface temperatures would seemingly cause more severe thunderstorms, and hence more tornadoes. There is evidence of some decadal fluctuations in the frequency of tornadoes and strong tornadoes, but no clear long-term time trend has been established (Figures 8.43a and 8.43b). There is also an obvious bias in detection of tornadoes. Prior to the 1960s, tornadoes had to be verified by ground observers. Now, satellite imagery and Doppler Radar can spot the telltale signs of tornadoes remotely.

U.S. Annual Count of EF-1+ Tornadoes, 1954 through 2012

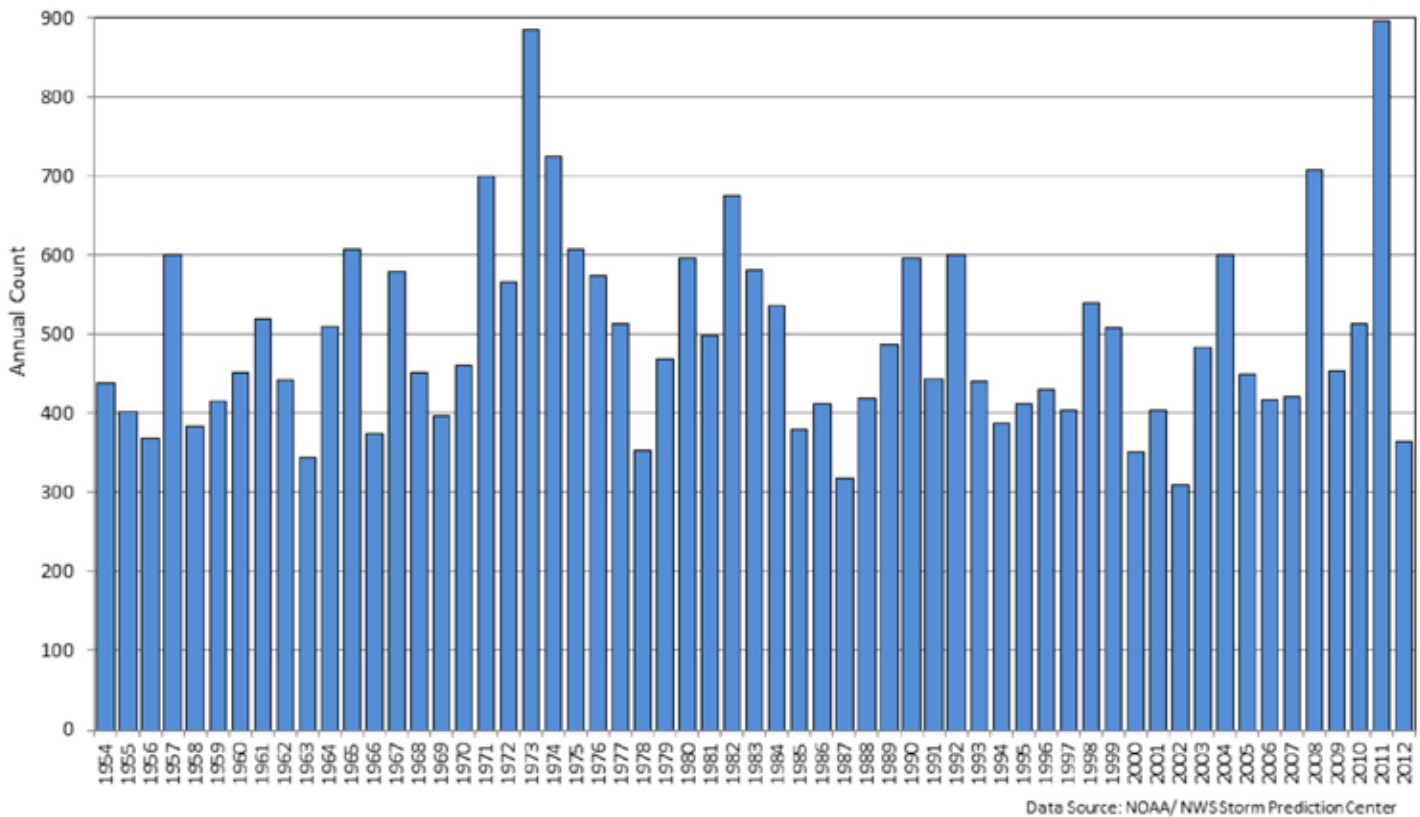


Figure 8.43a. Annual count of EF1+ tornadoes from 1954 through 2012. Although there appears to be a crude decadal cycle, there does not appear to be a positive link between global warming and tornado frequency over the past few decades. It should be pointed out that part or all of the apparent trend toward an increase in frequency since 2000 may be simply be due to better spotting techniques and not an actual increase in tornado activity (Source/Credit: NOAA/SPC/NWS).

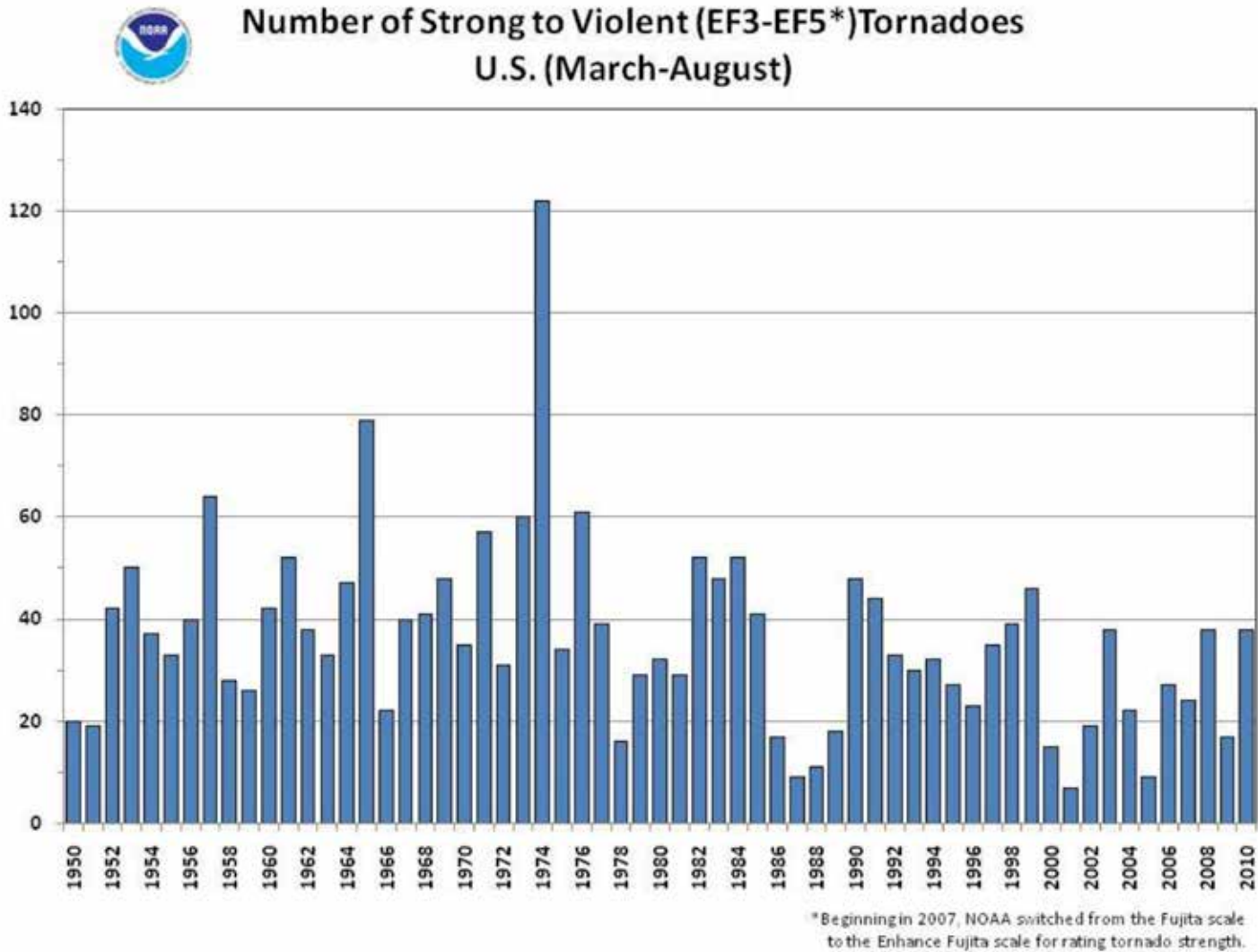


Figure 8.43b. Annual count of EF3-EF5 tornadoes from 1954 through 2010. Although there appears to be a crude decadal cycle, there does not appear to be a positive link between global warming and tornado frequency over the past few decades (Source/Credit: NOAA/SPC/NWS).

Storm damages associated with hurricanes and tornadoes were so costly to the insurance industry in the period 1990-2014 that it concluded that it might be bankrupted by future weather disasters. So, the insurance industry, which is not noted for radical environmental positions, has taken a policy stand and stated that it believes global warming is real and poses a genuine threat. The industry has called for actions to be taken to minimize global warming. The impacts of Katrina, Rita, Ike and Sandy caused more than \$200 billion dollars in damages. If this is a portent of things to come, it is clear that an intensification of the hydrologic cycle can have a very substantial impact on national economies.

## Precipitation

Precipitation trends for the 150-year instrumental period are in general much more complex than temperature patterns (Figure 8.44), and precipitation forecasts for the next few decades are made with far less confidence than temperature (Figure 8.45). Temperature patterns for the instrumental period are driven principally by increases in greenhouse gas concentrations, which are thoroughly mixed in the atmosphere. This allows computer models to make forecasts with a relatively high degree of confidence.

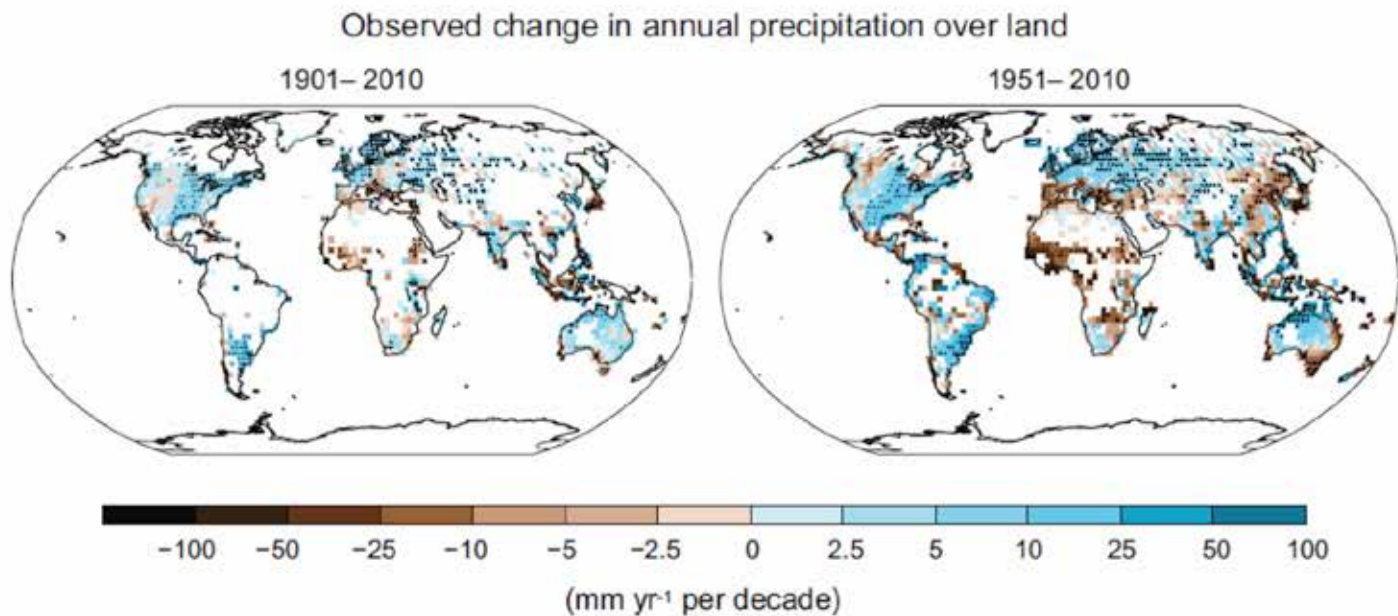


Figure 8.44. Precipitation changes over land over the past 110 years (left) and 60 years (right) indicate that some areas have become wetter (e.g., New England and northern Europe) whereas other have become drier (e.g., subtropical Africa). The patterns, however, are complex and the trends observed in one time interval are often not observed in another. The 60-year trend for China, for example, indicates drier conditions, whereas the 110-year trend indicates little change. Pre-satellite instrumental data for places like Greenland, Antarctica, and in the developing world are sparse, so trends are not detected (IPCC 2013).

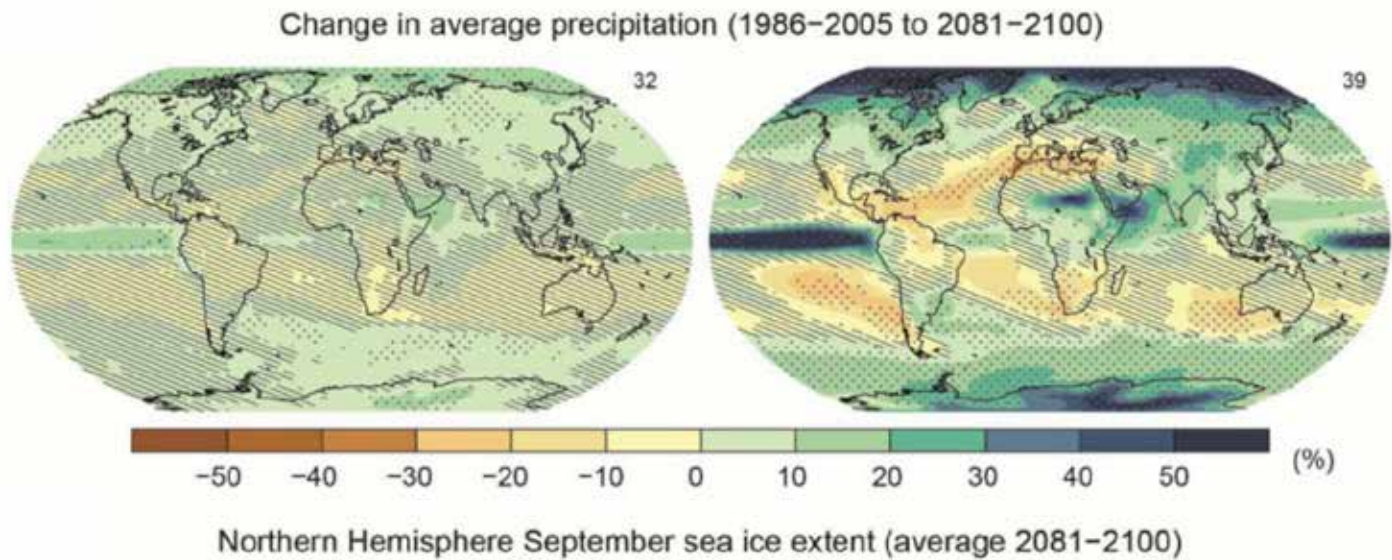


Figure 8.45. Actual changes in precipitation (left) and precipitation forecast to the end of the 21<sup>st</sup> century (right). Although the forecast map clearly shows areas of increased and decreased precipitation, the confidence level of the forecast is relatively low (Source/Credit: IPCC 2013).

Precipitation is controlled by a much broader set of factors, such as

- (1) The moisture content of the atmosphere,
- (2) Areas of convergent and divergent flow
- (3) Mechanisms that produce uplift,
- (4) The convective potential of the air, including lapse rates,
- (5) Storm tracks and intensities, governed largely by upper-level and surface pressure patterns,
- (6) Multi-year and multi-decadal oscillations in ocean temperatures and currents, such as El Niño/La Niña in the equatorial Pacific Basin,
- (7) The concentration and type of condensation nuclei in the air, partially controlled by human activities, and
- (8) The intensity and duration of monsoonal circulation. Illustrations of how some of these factors make decadal precipitation forecasts difficult are given in the following.

One obvious scenario follows that with an increase in temperature, there will be an increase in evaporation from the world's oceans, and an increase in the water vapor content of the air. This should lead to more cloudiness, and presumably an increase in precipitation. However, an increase in cloudiness decreases the transparency of the atmosphere, and increases the albedo. Both tend to reduce surface temperatures, thereby retarding the initial temperature increase.

There has been much speculation about how global warming will affect the El Niño and La Niña events in the tropical Pacific. The typical El Niño event has regional as well as global precipitation implications (Figure 8.46). An El Niño event refers to the superposition of a warm body of water over the eastern tropical Pacific basin, the opposite of the normal cold water that comes from upwelling and the cold Peru Current (Figures 8.47a and 8.47b). El Niño events are known to affect the precipitation patterns of much of the world, typically bringing drought to Australia, but enhanced rainfall to the west coast of the United States. The warm water ponds against equatorial South America, but then spreads poleward, affecting ocean temperatures as far away as California and Oregon. The warmer water injects more water vapor into the tropical and subtropical atmosphere which would seem to be more conducive to the formation of tropical storms and cyclones. However, an intense El Niño favors strong, unidirectional upper-level winds in the low latitudes which tend to suppress tropical storm development. Global warming is forecast to slightly enhance the normal circulation in the tropical Pacific (Figure 8.47c).



High Resolution Images can be found at:  
<http://www.cpc.ncep.noaa.gov/products/precip/CWlink/ENSO/ENSO-Global-Impacts/>

Figure 8.46. Typical precipitation impacts of summer and winter El Niño (warm episode) events (Source/Credit: NOAA/NWS/NCEP/Climate Prediction Center).

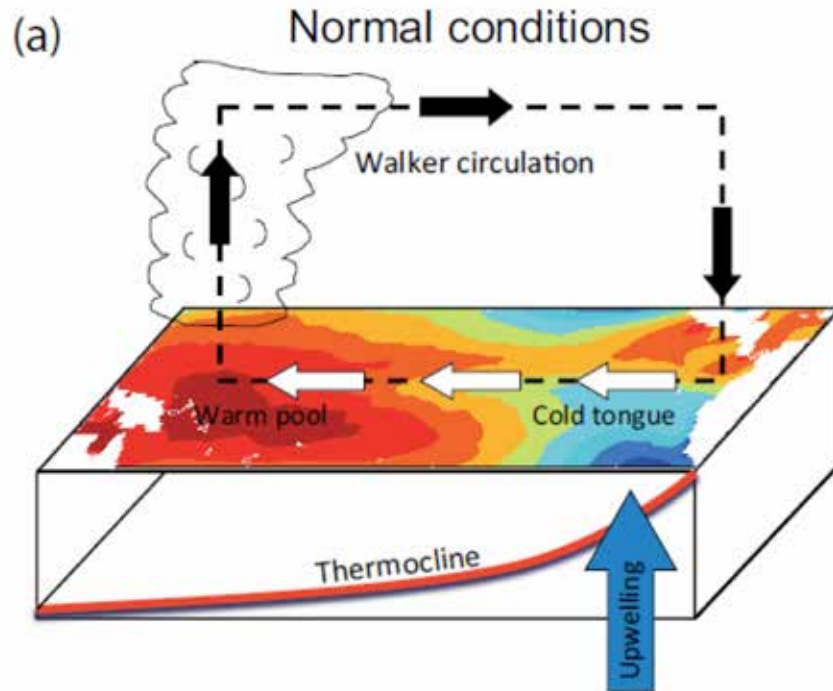


Figure 8.47a. Under normal conditions, warm water pools over the western Pacific basin (Australia, Indonesia), and cold water over the eastern basin (equatorial South America). This sets up a vertical circulation called the Walker Circulation, creating dry conditions along South America and wet conditions in Indonesia. Strong upwelling brings nutrients to the surface, resulting in one of the richest anchovy fisheries of the world (Source/Credit: IPCC, 2013).

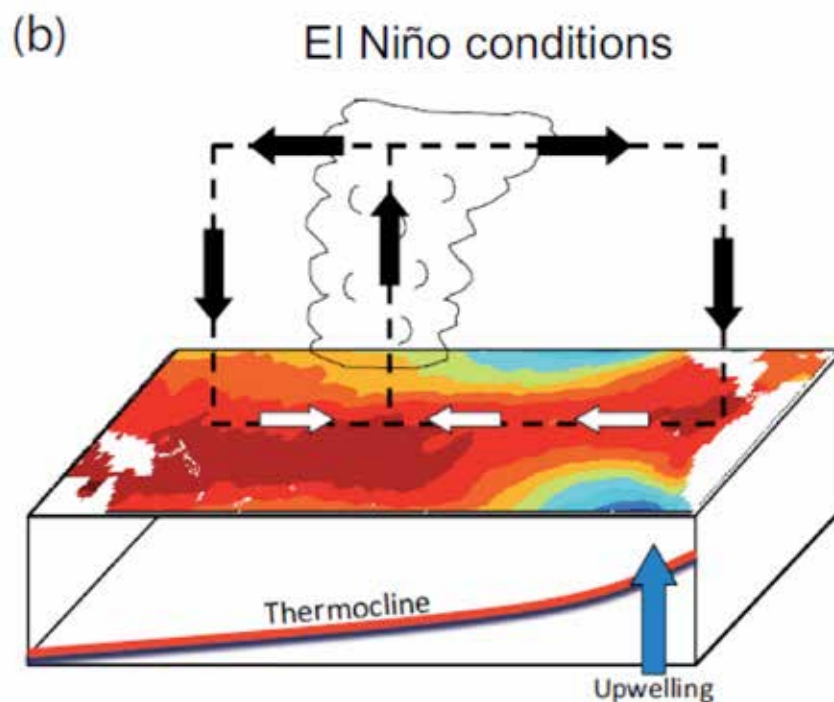


Figure 8.47b. Under El Niño conditions, warm water pools over the eastern Pacific basin, changing the Walker Circulation, creating dry conditions over Australia and wetter conditions over the warmest water. Upwelling is suppressed, and the anchovy industry suffers massive losses (Source/Credit: IPCC, 2013).

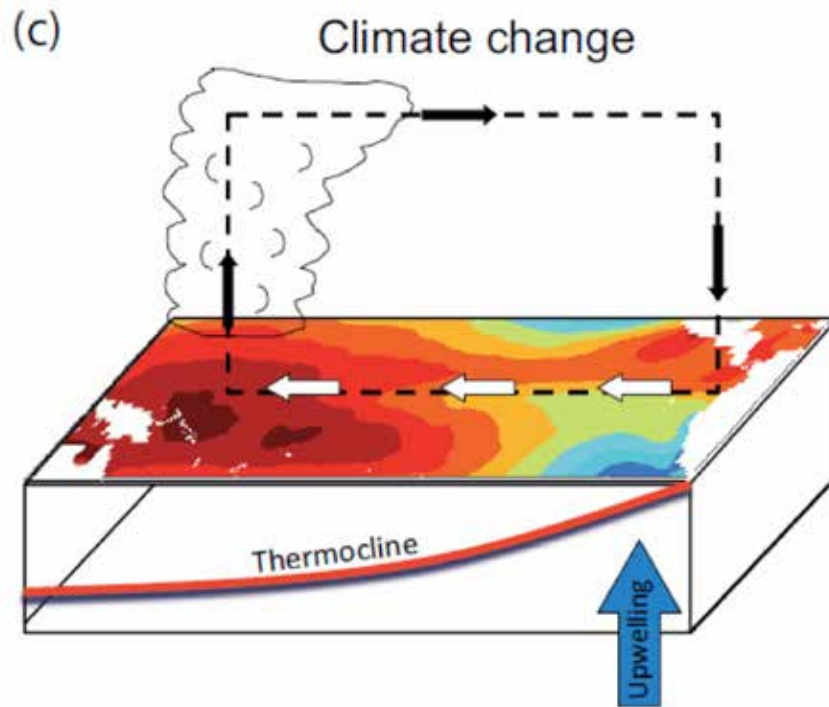


Figure 8.47c. One model of future climate shows an enhancement of the normal conditions, including a larger pool of warm water over the western Pacific basin (Australia, Indonesia), but a slightly reduced pool of cold water over the eastern basin (equatorial South America). The Walker Circulation is maintained. The impact of this change in Pacific circulation has on global weather is unclear (Source/Credit: IPCC, 2013).

The monsoons wind system is the most important regional wind system on Earth. Summer monsoons bring rain that is essential to the agricultural and grazing systems that support over two-thirds of the world's population. Failure of the summer monsoons (too much, too little, too soon, too late) threatens not only the well-being of these people, but the health of the global economy. The most pronounced monsoon wind system is in south, east, and southeast Asia. Less intense monsoons, some of shorter duration, occur in Africa, Australia, South America and North America (Figure 8.48).

Physical Map of the World, June 2003

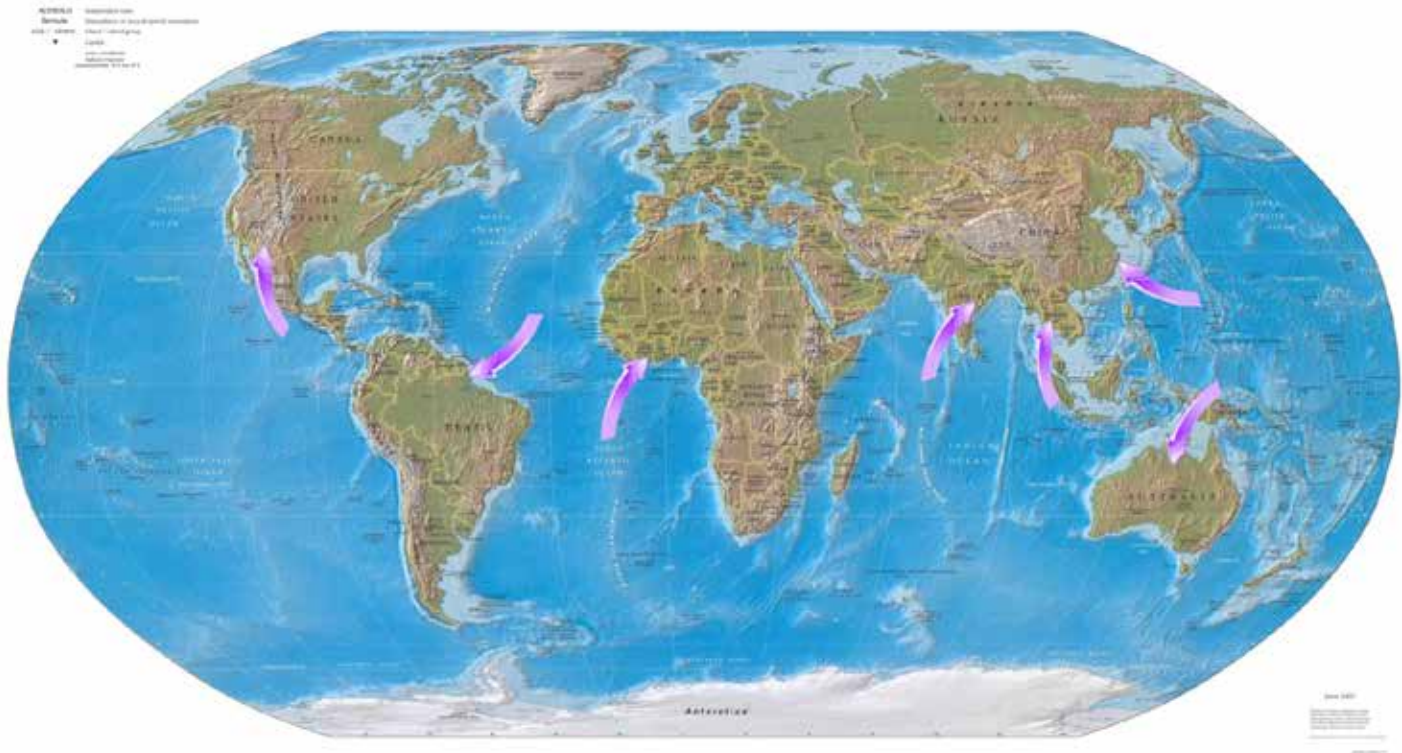


Figure 8.48. Some of the regions of the world that experience monsoon wind systems or monsoon tendencies. These are regions that rely on summer monsoons for much of their annual rainfall (Source/Credit: Courtesy of the University of Texas Libraries, The University of Texas at Austin).



The strength and duration of the monsoons is controlled by several factors, including temperature contrast between land and ocean, water vapor content of the air, convective potential of the air, the presence of orographic barriers, and aerosol content of the air. Aerosol content is a function of land use practices and vegetation type and density. Monsoon rainfall is projected to become more intense and cover a larger area with global warming, but local patterns may be exceptions. Human activity can influence monsoonal precipitation in several ways. Increased temperatures lead to higher evaporation rates, higher water vapor content of the air, and greater potential for rainfall. Higher aerosol content of the air as a result of poor land use practice tends to produce surface cooling, moderating the influence of higher moisture content (Figure 8.49). Higher aerosol content, particularly hygroscopic nuclei such as certain clay minerals, should induce more condensation and make more rain-bearing clouds, but too many of them theoretically can inhibit the growth of cloud droplet to raindrop size.

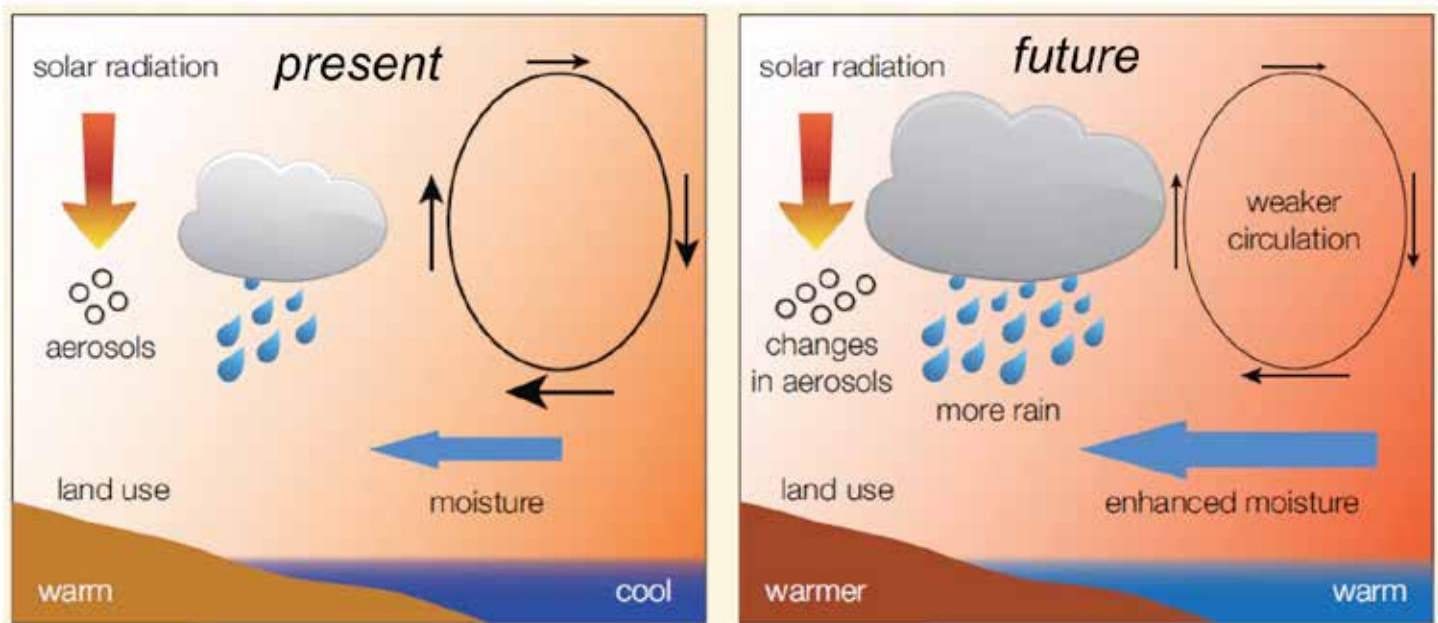


Figure 8.49. Human activity can influence monsoonal precipitation in several ways. Increased temperatures lead to higher evaporation rates, higher water vapor content of the air, and greater potential for rainfall. Higher aerosol content of the air as a result of poor land use practice tends to produce surface cooling, moderating the influence of higher moisture content. Higher aerosol content, particularly hygroscopic nuclei such as certain clay minerals, should induce more condensation and make more rain-bearing clouds, but too many of them theoretically can inhibit the growth of cloud droplet to raindrop size (Source/Credit: IPCC 2013).

There is much concern that global warming might destabilize the vegetation patterns of the semi-arid and arid portions of places such as the Great Plains of the central United States bringing back images of the Dust Bowl days of the 1930s. Deteriorating vegetation cover leaves the soil exposed to the fierce winds of the Great Plains. Scientists from the United States Geological Survey and the University of Nebraska have recently developed scenarios of dune reactivation caused by relatively minor changes in temperature and precipitation patterns.

The largest fossil sand dune field in North America is in the Sand Hills of Nebraska (Figure 8.50). The dune field covers over 20,000 square miles (~52,000 km<sup>2</sup>), nearly a third of Nebraska (Figure 8.51). It probably formed during the Ice Ages, when strong northwest winds picked up massive amounts of sediment shed from the Rocky Mountains. Today, the dunes are stabilized by grass cover from spring and summer moisture brought in by southeast winds from the Gulf of Mexico. Careful analysis of dune morphology, however, indicates that a large portion of the dune field was formed by winds from the southwest, coming from the desert areas of New Mexico, Texas, and Mexico. Recent thermoluminescence dating of the sand grains in those dunes suggest that they formed much more recently than the rest of the dunes, probably about 1000 years ago. This coincides with the Medieval Warm Period of the North Atlantic. Perhaps subtle changes in the temperature of the North Atlantic Ocean caused a change in the wind regime in North America, activating thousands of square miles of sand dunes.

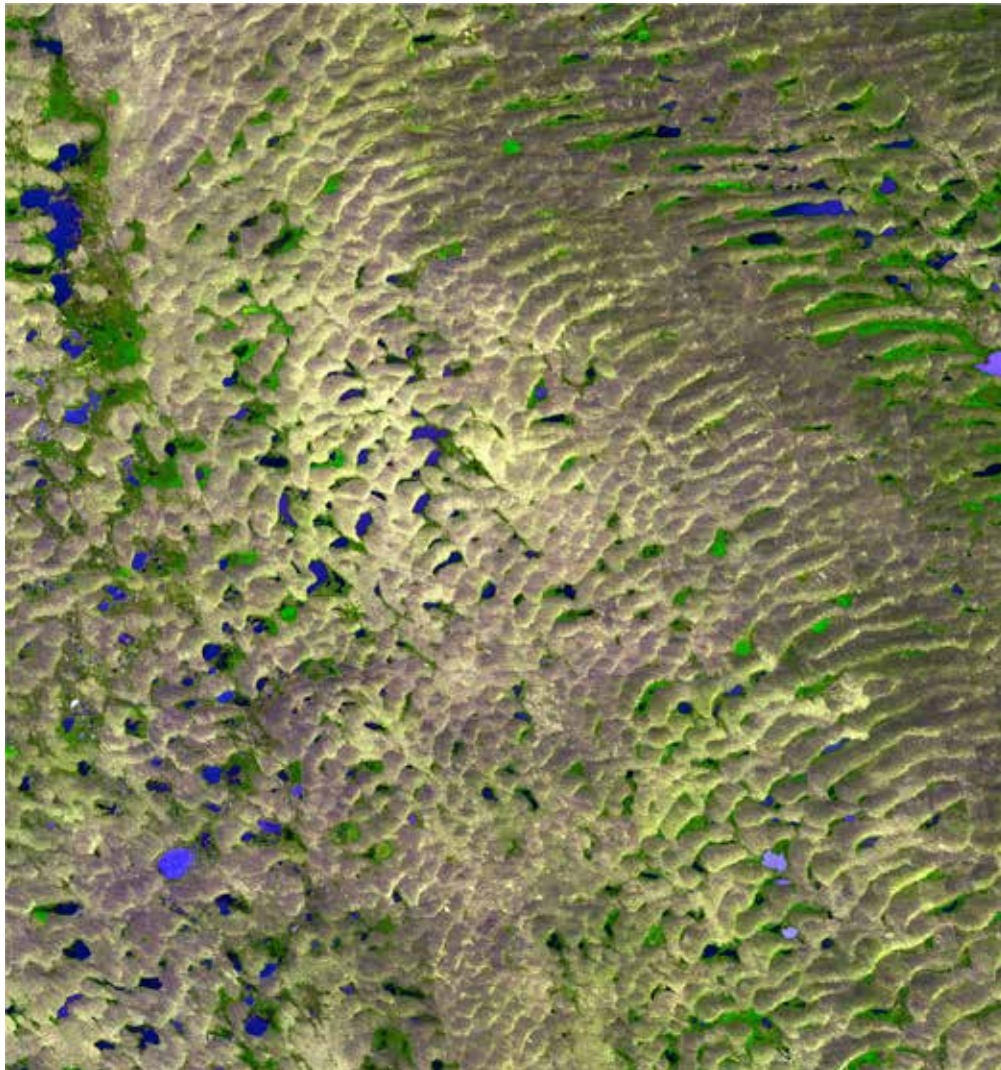


Figure 8.50. The satellite view of a portion of the Sand Hills of Nebraska shows the pattern of wind-deposited sand dunes that were laid down by northwest winds during the last ice age. The modern dunes are stabilized by a nearly-continuous grassland cover. Grasses exist because spring and summer winds out of the southeast bring moisture from the Gulf of Mexico (Source/Credit: NASA/GSFC/METI/Japan Space Systems, and United States/Japan ASTER Science Team).

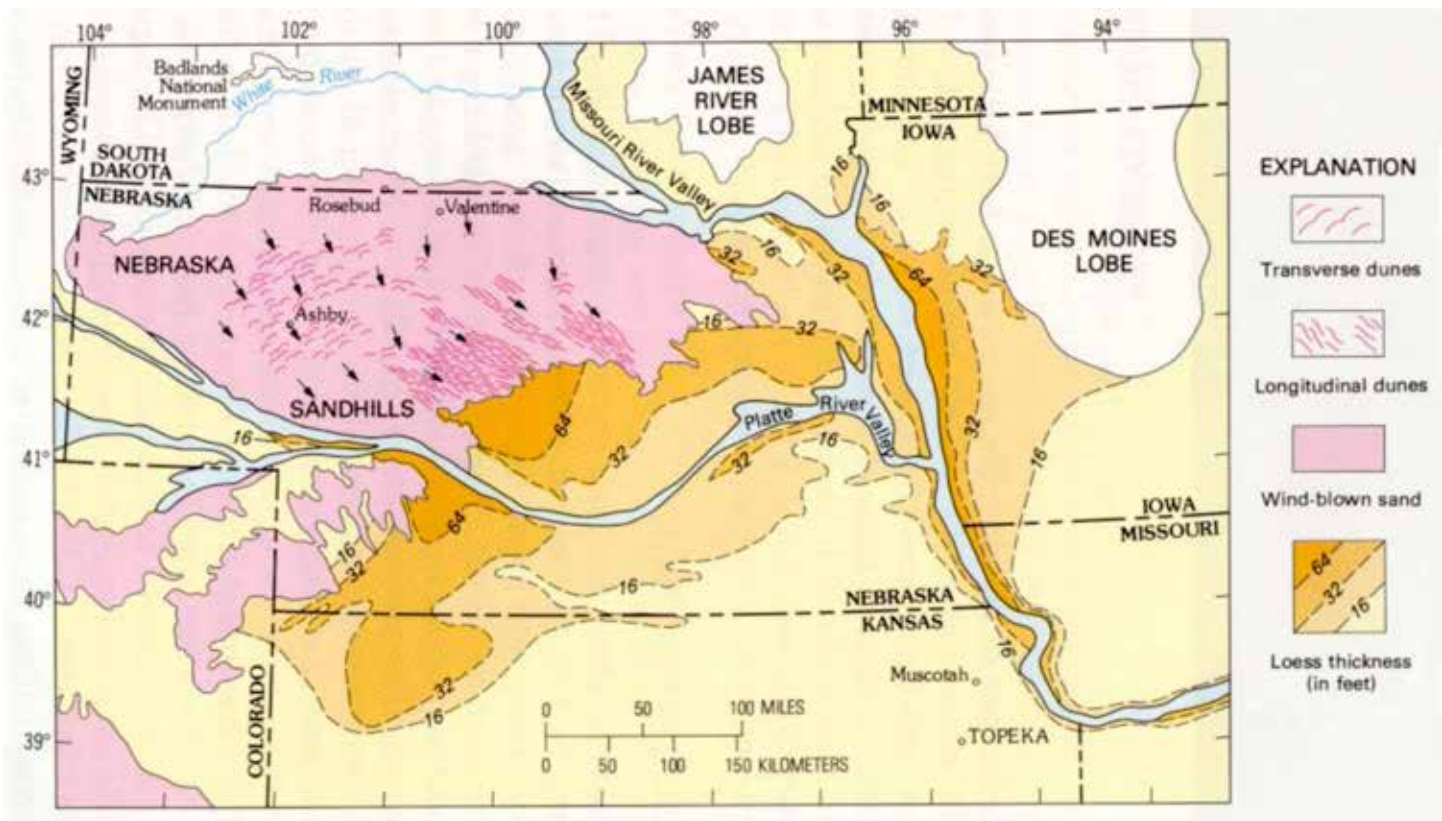


Figure 8.51. The pink area represents over 20,000 square miles of Nebraska covered by a fossil dune field, the **Sand Hills**. Patterns of orange and yellow represent wind-deposited material called loess, which is finer-grained than sand dunes. Together, they cover most of Nebraska. Although most of the state is covered with stabilizing grasses and shrubs, evidenced suggests that large portions of the dune field were re-activated a mere 1000 years ago during the Medieval Warm Period. The implication is that minor future changes in temperature and/or precipitation could drastically change the landscape of Nebraska (Source/ Credit: USGS).

**Hydrologic cycle:** With warmer temperatures come greater amounts of evaporation, greater amounts of rainfall, and perhaps more intense rainfall. In the past decade or so, there has been an increase in the frequency of tornadoes in the United States as well as North Atlantic hurricanes. Although this trend may be attributable to natural decadal cycles, there is a growing number of researchers who link the trend to global warming. North Atlantic hurricanes have not only increased in frequency, but intensity. This may be the result of an increase in ocean temperatures as well as a larger body of warm ocean water. Warmer water means more water vapor injected into the atmosphere which is the fuel for many severe storms. While it is not possible to say conclusively that recent hurricanes such as Katrina, Rita, Ike and Sandy were bigger than would have occurred in the absence of global warming, some meteorologists believe that at least some of their intensity, as much as 7%, may have been caused by warmer ocean temperatures.

The connection between global warming and **drought** is unclear. In earlier studies, there was widespread concern that warming was at least partially the cause of widespread desertification, the transformation of grassland ecosystems to desert ecosystems. During the 1970s, desertification in the Sahel region of Africa transformed hundreds of thousands of square miles of grasslands and savanna into barren desert (Figure 8.52).

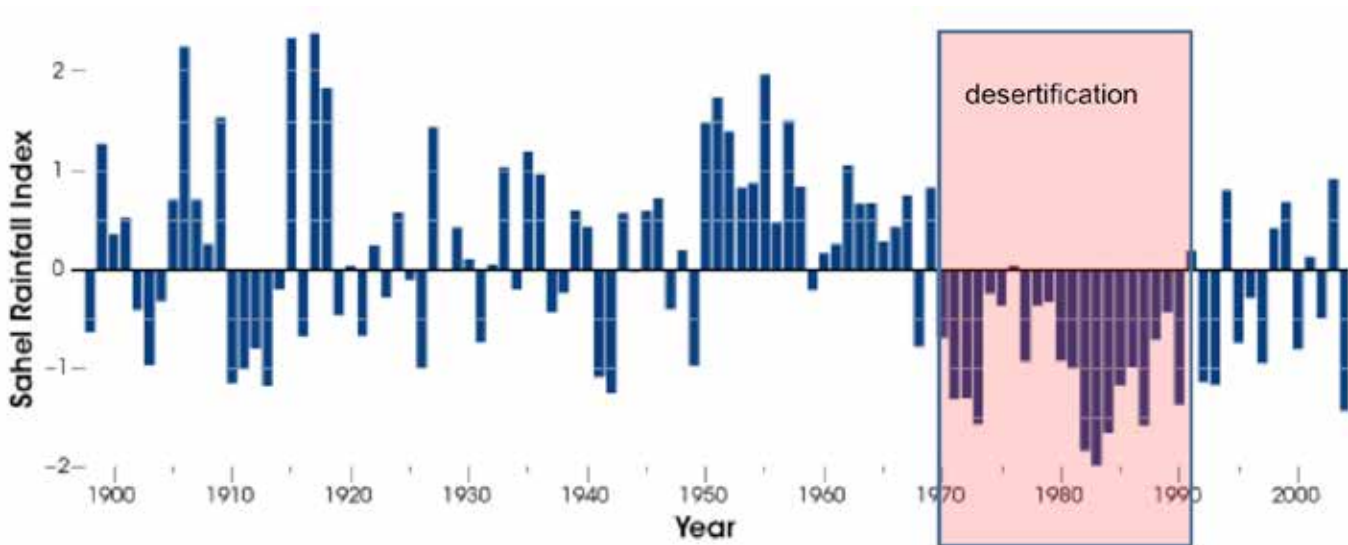


Figure 8.52. The graph indicates fluctuations in rainfall in the Sahel region of North Africa. Decadal cycles occur, including a very dry period from 1970 until 1990 (box insert). That period coincides with the great desertification of the Sahel, when over 100 million people died from famine. Since that period, rainfall totals have rebounded some, and the desertification has been reversed. Initially, the desertification and drought were blamed on global warming. It now appears that desertification was part of a natural drought cycle that was accentuated by poor land use practices (overgrazing and burning vegetation for fuel) (Source/Credit: NOAA graph, modified from Mitchell, 2005).

The 2013 IPCC report has shifted its position on anthropogenic causes of drought from earlier climatic assessments. In particular the droughts during the 1970s and beyond are now thought to be a sign of decadal cycles rather than strictly human-induced. The present cycle of drought in the western United States is likewise thought to be largely part of decadal cycles, although exacerbated by regional warming and land use practices.

**Ecosystems:** Climate is a fundamental control in the distribution of ecosystems. Changes in climate will change ecosystem distribution. The two main components of the climate system that control the general global pattern of ecosystems (biomes) are temperature and precipitation. Global warming and precipitation changes associated with it will undoubtedly change the geographic distribution of ecosystems. Some may expand, while others may shrink, and still others may disappear.

Ecosystem components are not highly mobile, so there is a time lag between climate change and ecosystem response. Time is needed for forests and grasslands to reestablish themselves

in new areas. The ability to *migrate* is hindered by the fact that people have put a lot of land under plow, and this interferes with the migration of plants and animals. As forests or grasslands shrink, expand or die out, then the animals that live in them will be threatened as well.

A study published in the journal *Nature Climate Change* (April 2013) suggests that the Koeppen-Geiger climate boundaries are changing at an accelerated pace due to changes in temperature and precipitation patterns (Figure 8.53). The implication of accelerated change is that species of plants and animals in each climatic zone will have less time to adapt to changes. Certain regions will undergo more change than others. In general, tropical latitudes will be least affected, whereas middle and high latitudes will be progressively impacted. High latitude continental subarctic, tundra, and ice cap climates in the Northern Hemisphere will undergo dramatic changes. Mid-latitude climates with cool and mild summer temperatures will become warm to hot.

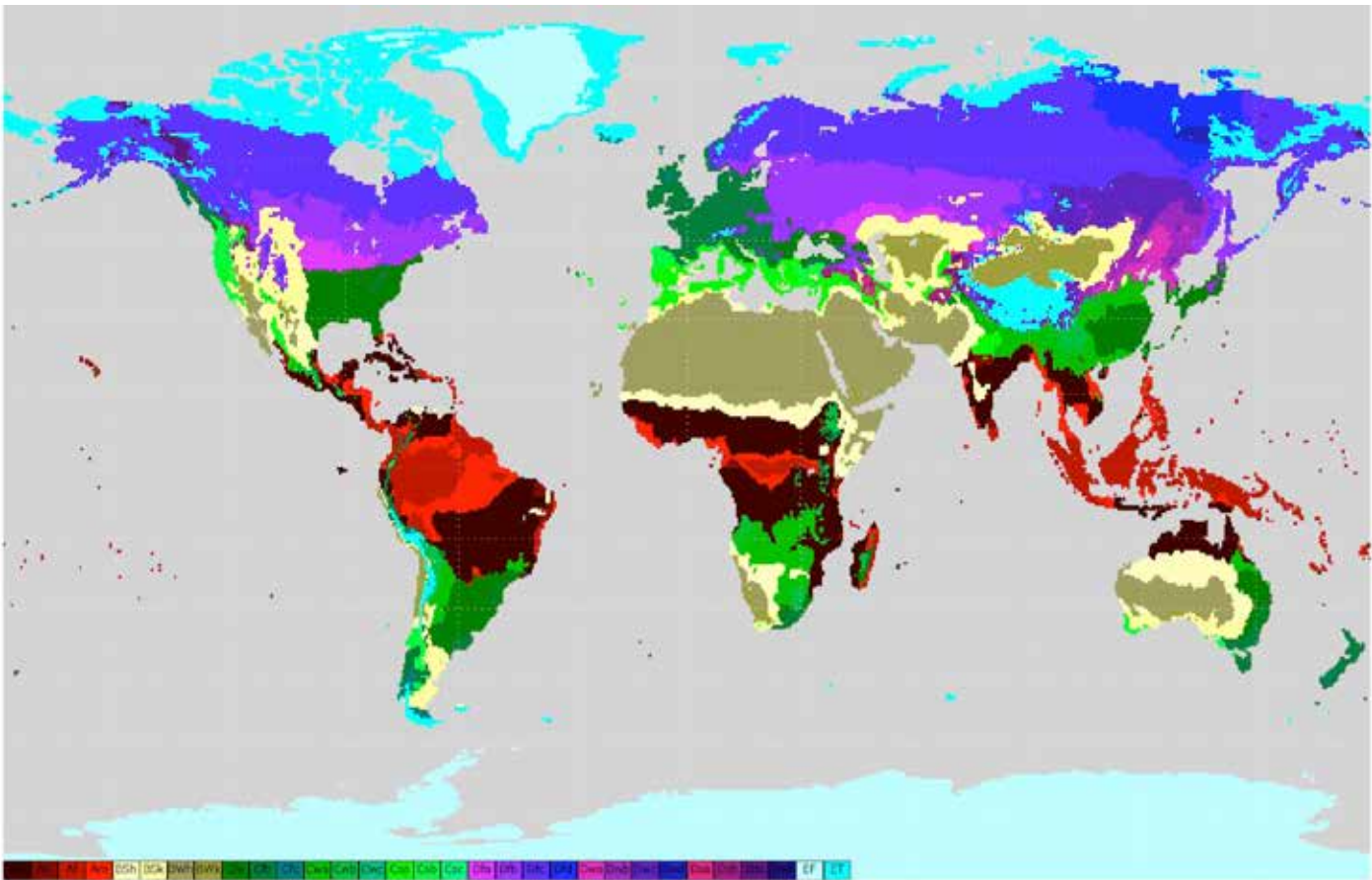


Figure 8.53. The Koeppen-Geiger climate boundaries are apparently changing at an accelerated pace due to changes in temperature and precipitation patterns, a recent scientific study claims. Certain regions will undergo more change than others. In general, tropical climates Af, Am and Aw (red and black) will be least affected. Arid and semi-arid climates (BW, sage and BS, yellow) will expand in some areas and shrink in others. Humid subtropical climates (Cfa, dark green) will expand poleward, as will most of the D climates (purple and dark blues). Tundra and ice cap climates (light blues) of the Northern Hemisphere will shrink. Mid-latitude climates with cool and mild summer temperatures will become warm and hot. The implication of accelerated change is that species of plants and animals in each climatic zone will have less time to adapt to changes (Source/Credit: Public domain Wikimedia).

Even subtle things, such as a change in the timing of insect maturation and the blooming of flowers, can threaten both insects and flowers with extinction by throwing the pollination process out of sync with the life cycles of the plants and insects. Without the insects, the flowers can't reproduce, and without the flowers, the insects lose a source of food. Some species of flowers rely on a single species of insect for pollination. Likewise, some insect species depend entirely upon one species of plant for their survival. Such species are particularly vulnerable to the effects of rapid climate change.

Marine ecosystems will also be subject to change. As ocean waters warm, some species of coral begin to die. This occurs when the water temperature causes the corals to expel algae that live in symbiotic relationship with them. The process results in a loss of color for the coral and is called **bleaching**. This bleaching process is occurring in many places right now, although it is not certain whether or not the phenomena is entirely the result of temperature increases.

The United States Geological Survey is studying the impact of windblown dust and increasing CO<sub>2</sub> levels in the atmosphere on reef systems such as in the Virgin Islands (Figure 8.54). The ocean absorbs 22 million tons of CO<sub>2</sub> per day, and that number has increased in the past few decades. More dissolved CO<sub>2</sub> means more carbonic acid (H<sub>2</sub>CO<sub>3</sub>), which can adversely affect calcium-building organisms such as coral reefs, lobsters, clams, snails, oysters, and phytoplankton.



Figure 8.54. The marine ecosystem is affected in many ways by human activities, including global warming, ocean pollution, pathogens in wind-blown dust, overfishing, and acidification. The United States Geological Survey is studying the impact of windblown dust and increasing CO<sub>2</sub> levels in the atmosphere here in the Virgin Islands. The ocean absorbs 22 million tons of CO<sub>2</sub> per day, and that number has increased in the past few decades. More dissolved CO<sub>2</sub> means more carbonic acid (H<sub>2</sub>CO<sub>3</sub>), which can adversely affect calcium-building organisms such as coral reefs, lobsters, clams, snails, oysters, and phytoplankton (Source/Credit: USGS).

Reefs are the *tropical rainforests of the sea*; more species of life are found there than in any other area of the ocean. So, when a reef dies many animals die as well. This also reduces fish harvests because many fish begin their lives in the reef area. In the Caribbean Sea, some estimates indicate that 80% of the coral has been destroyed in the past 40 years. Globally, there appears to be a decline in coral reefs of about one percent per year.

Another unexpected effect of global warming is that some plants will grow faster than others in response to increased carbon dioxide levels. Although there may be obvious benefits to this, it can be disruptive to the natural balance of competition among plant species and could result in less diverse forests. For example, beech trees grow faster than sugar maples in enriched carbon dioxide environments. As both compete for light, this can give the beech tree a slight advantage, thereby diminishing the number of sugar maple trees.

Another result of growth in an enriched carbon dioxide atmosphere is that plants produce more carbohydrate-rich tissues and less protein. As a result, insects have to eat more plant tissue to obtain the necessary protein. They also suffer from decreased growth and possible loss of vitality. For example, in one study the buckeye butterfly larvae ate about 15% more plant material than normal, but they took 10% longer to reach maturity and they were visibly weaker. In addition, sagebrush-eating grasshoppers needed 36% to 58% more food when fed plants raised at high carbon dioxide levels.



## Cryosphere

### Sea Ice and Snow Cover

Globally, floating sea ice and land ice have been diminishing over the past few decades (Figure 8.55). The most consistent decline in sea ice has been over the Arctic Ocean (Figure 8.56). Arctic sea ice tends to reach maximum extent in late March or April, and a minimum in September (Figure 8.57). Arctic sea ice is expected to continue to decline throughout the 21<sup>st</sup> century, virtually disappearing by 2100 (Figure 8.58).

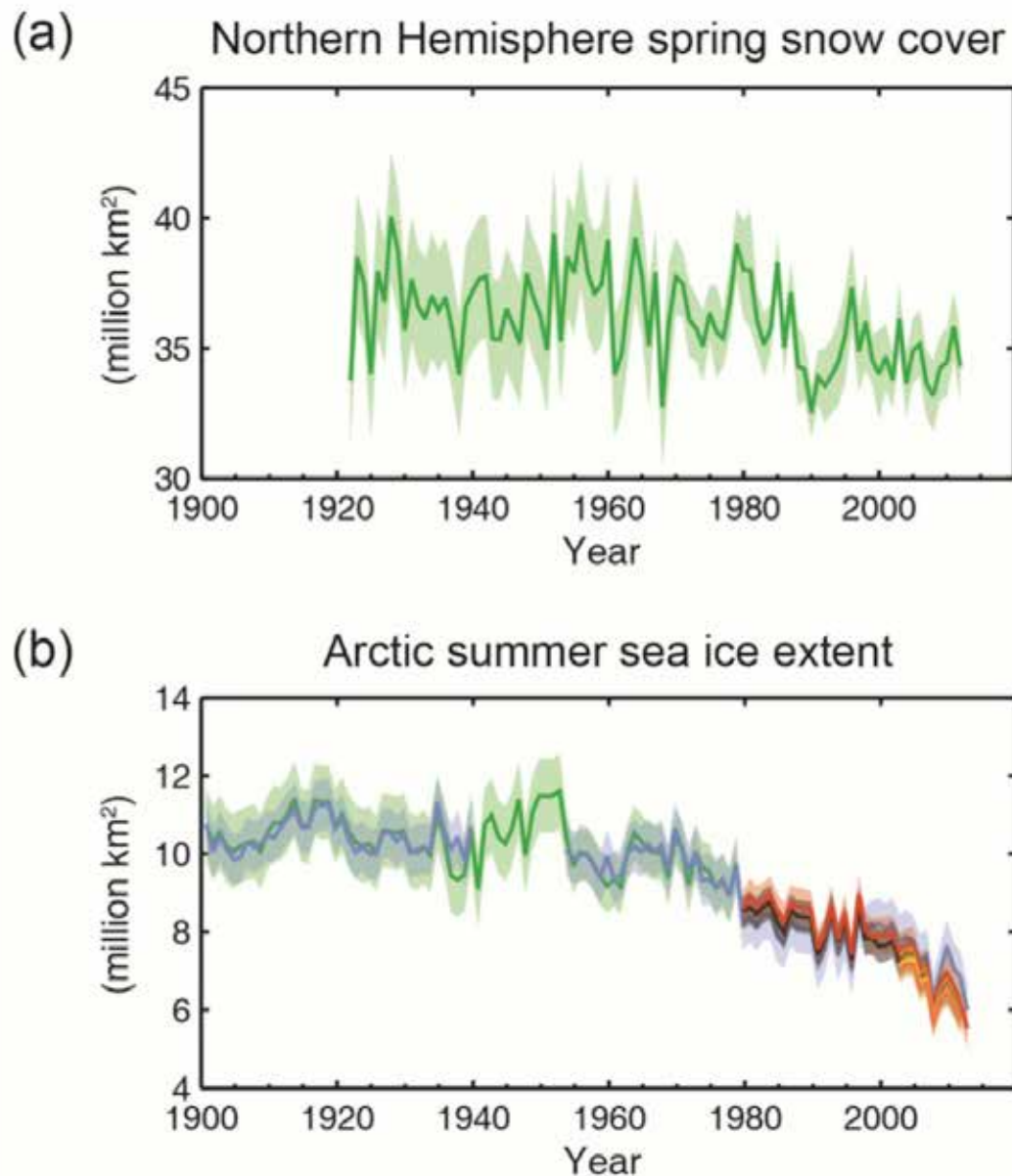


Figure 8.55. Northern Hemisphere spring snow cover from 1920-2012 shows considerable year-to-year variation, and a slight downward trend overall. The downward trend is much clearer for Arctic summer sea ice extent from 1900-2012. Arctic summer sea ice extent has only been carefully monitored since the satellite era (Source/Credit: IPCC 2013).

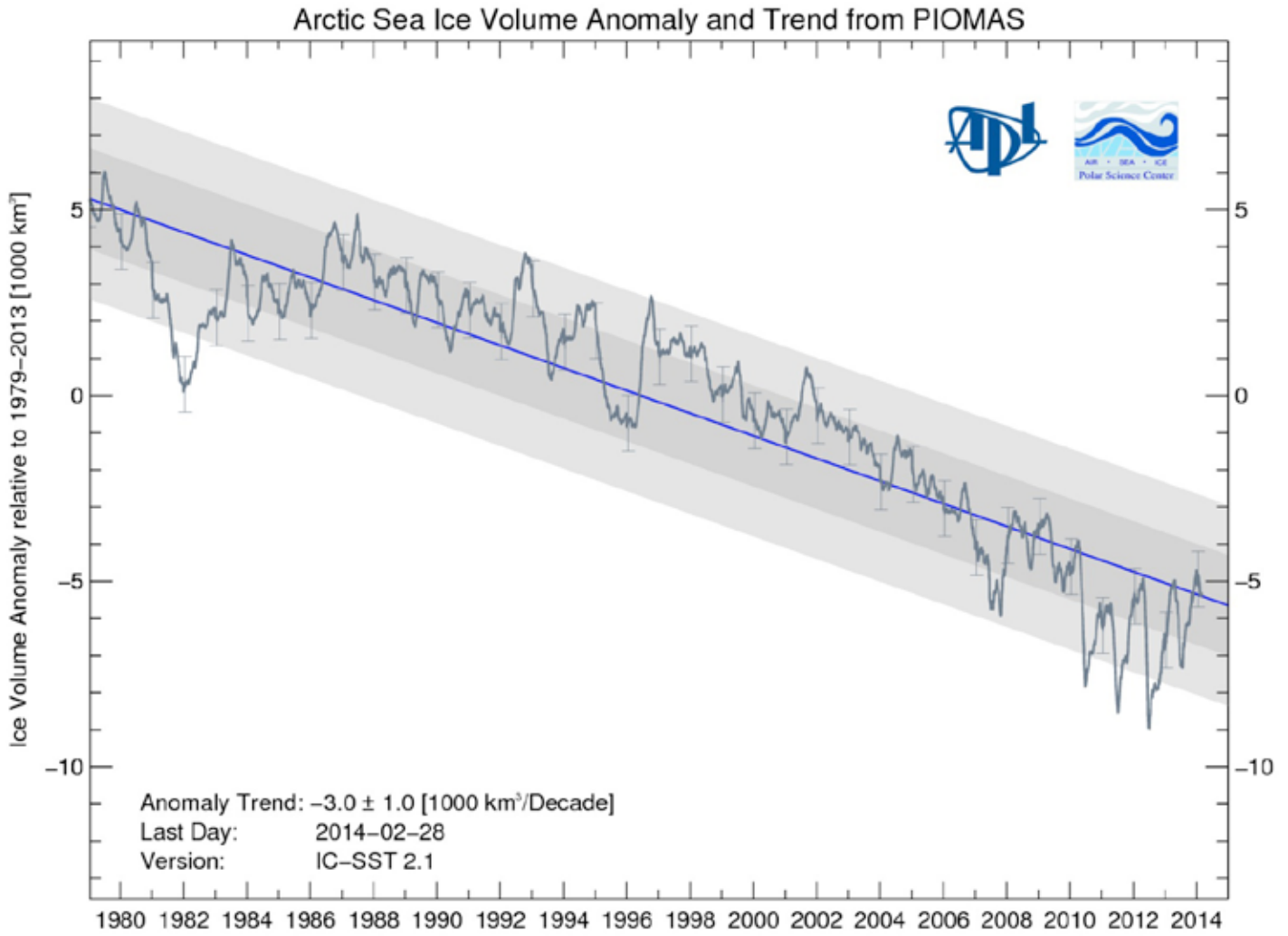


Figure 8.56. Arctic sea ice volume anomaly. Sea ice volume anomalies are computed daily relative to the 1979-2011 average. The trend line is shown in blue. Shaded areas indicate one and two standard deviations from the trend line. Although significant year-to-year variations occur, the overall trend is toward declining ice volume (Source/Credit: PIOMAS).

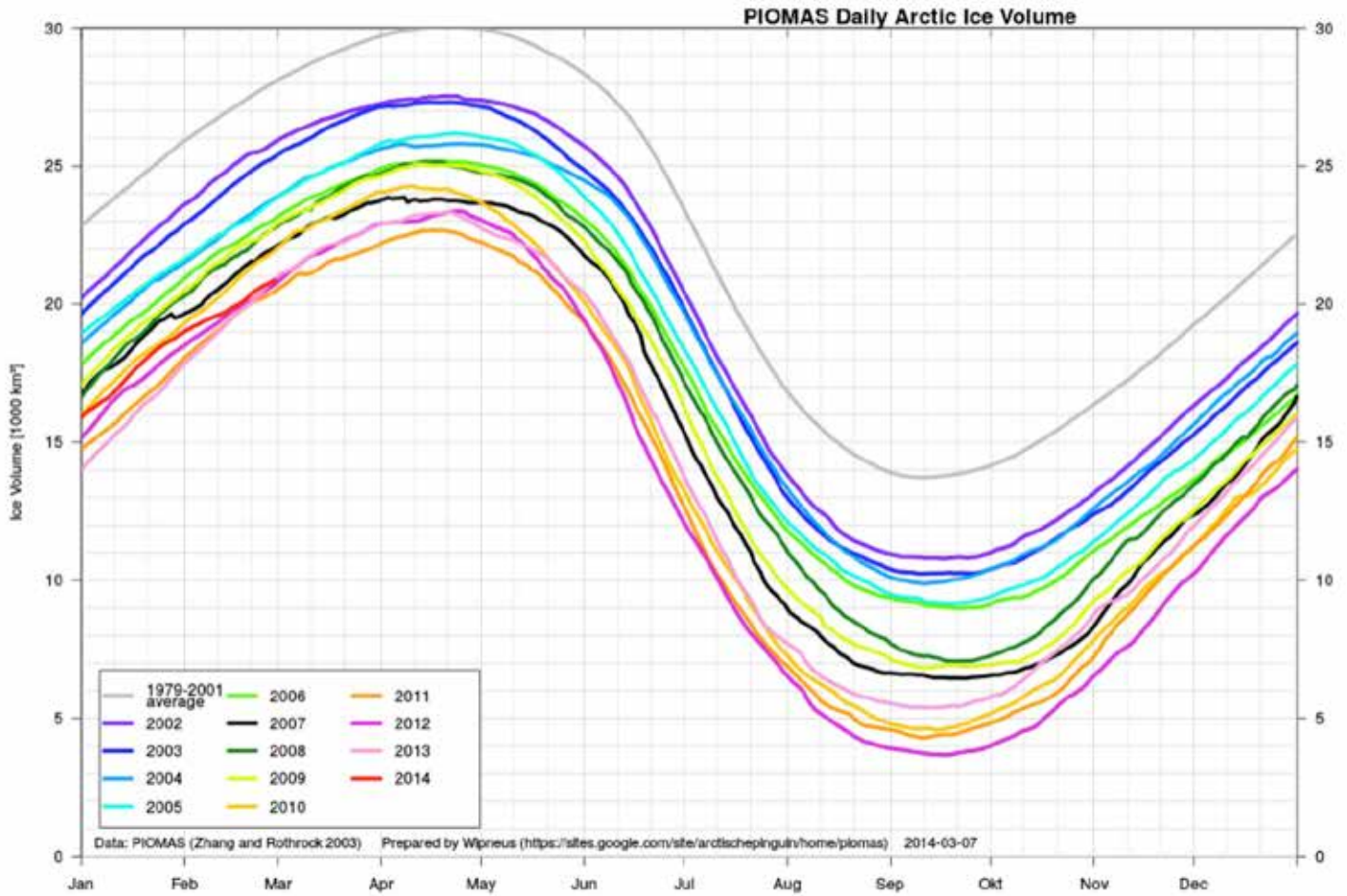


Figure 8.57. Accurate records of Arctic sea ice are available from 1979. The graph shows daily Arctic sea ice volume from 2002 through early March 2014. The light gray line (top) shows the average sea ice extent for 1979-2001. Arctic sea ice tends to reach a maximum in March or April, and a minimum in late September. The overall trend is downward, with 2012 having the least sea ice in the period of accurate satellite monitoring (Source/Credit: PIOMAS).

## Northern Hemisphere September sea ice extent (average 2081–2100)

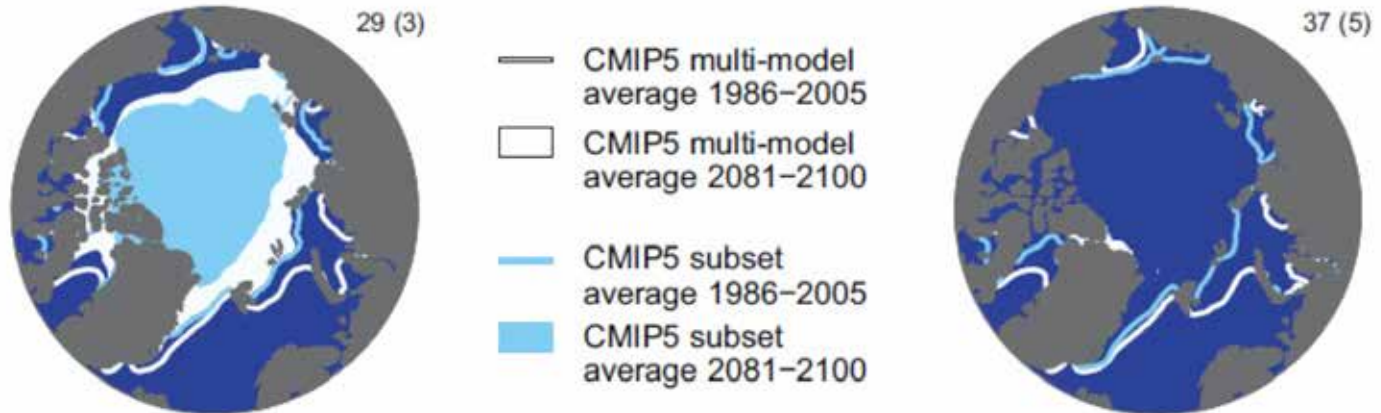


Figure 8.58. Arctic sea ice is expected to continue to decline throughout the 21<sup>st</sup> century, virtually disappearing by 2100 (Source/Credit: IPCC 2013).

The extent of floating sea ice in Antarctica differs from one ice shelf to the next. Some areas show expansion of sea ice, whereas others show decline. The January 2014 sea ice extent around Antarctica was 30% above the average for the period 1981–2010, the second largest on record. The most reliable data for Antarctica indicates that it is very likely that sea ice has increased at a rate of about 1–2% per decade between 1979 and 2012. The reason for this trend is unclear. This trend is expected to reverse later in the century.

The loss of sea ice is extremely important and is the primary reason why the temperatures in polar regions will rise more than in other areas. The loss of sea ice *decreases* the albedo of these areas and results in more absorption of heat energy. White ice, which is reflective, is replaced by blue water, which absorbs energy. This, in turn, raises the temperature even more. This type of response to a change in a system is referred to as **positive feedback**. With positive feedback, an initial change in the system that leads to a movement away from the normal condition, causes other changes which move the system even further away from the normal condition. By increasing carbon dioxide levels, the temperatures goes up, which causes sea ice to melt, which causes temperatures to go up even more. **There are multiple positive feedback processes in the climate system that can accelerate warming.**

The Northern Hemisphere snow cover on land has shown moderate overall decreases in the past few decades, presumably due to global warming. Spring and summer losses in snow cover dominate, with very little observable trend during the winter and fall (Figure 8.59).

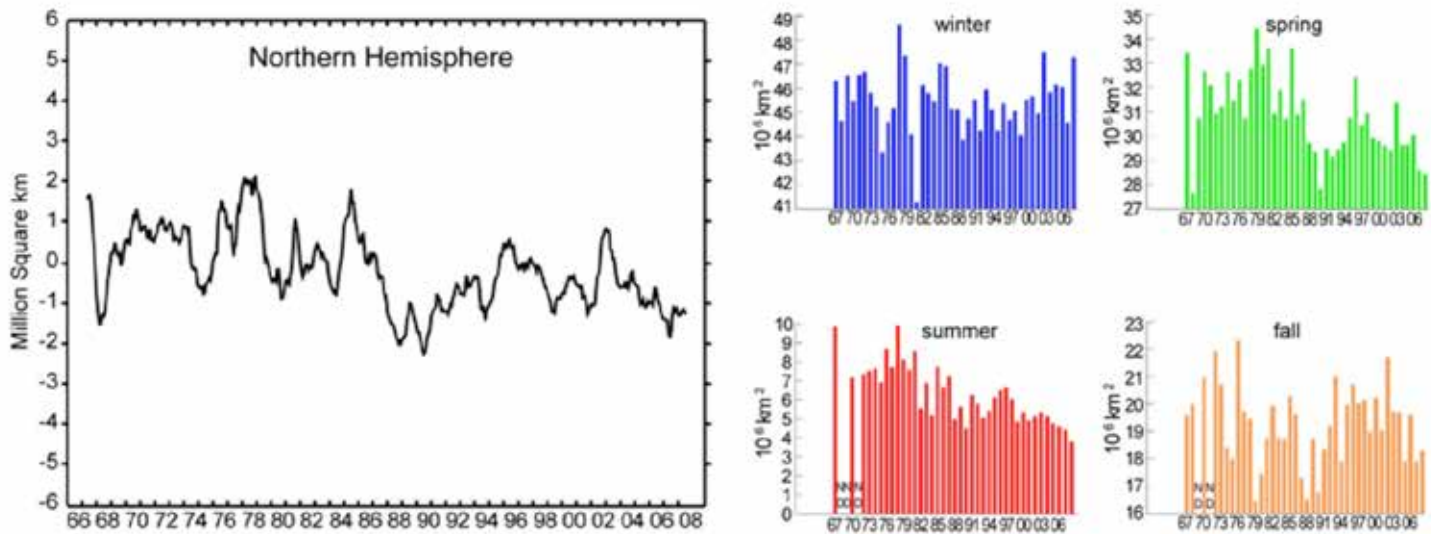


Figure 8.59. Changes in Northern Hemisphere snow cover from 1966-2008. Spring and summer losses are most obvious. The winter and fall snow cover are about the same throughout the period (Source/Credit: NOAA).

## Permafrost

**Permafrost** is permanently frozen ground in high latitudes and high elevations, mostly in the Northern Hemisphere (Figure 8.60). As the Arctic warms, permafrost thaws (Figure 8.61). Permafrost temperatures have increased in virtually all Northern Hemisphere high latitudes since the early 1980s. In northern Alaska, some regions have warmed as much as 5°F (3°C). In Russia, permafrost temperatures are thought to have warmed about 3.5°F (2°C). Permafrost temperatures are expected to continue to rise throughout the 21<sup>st</sup> century.

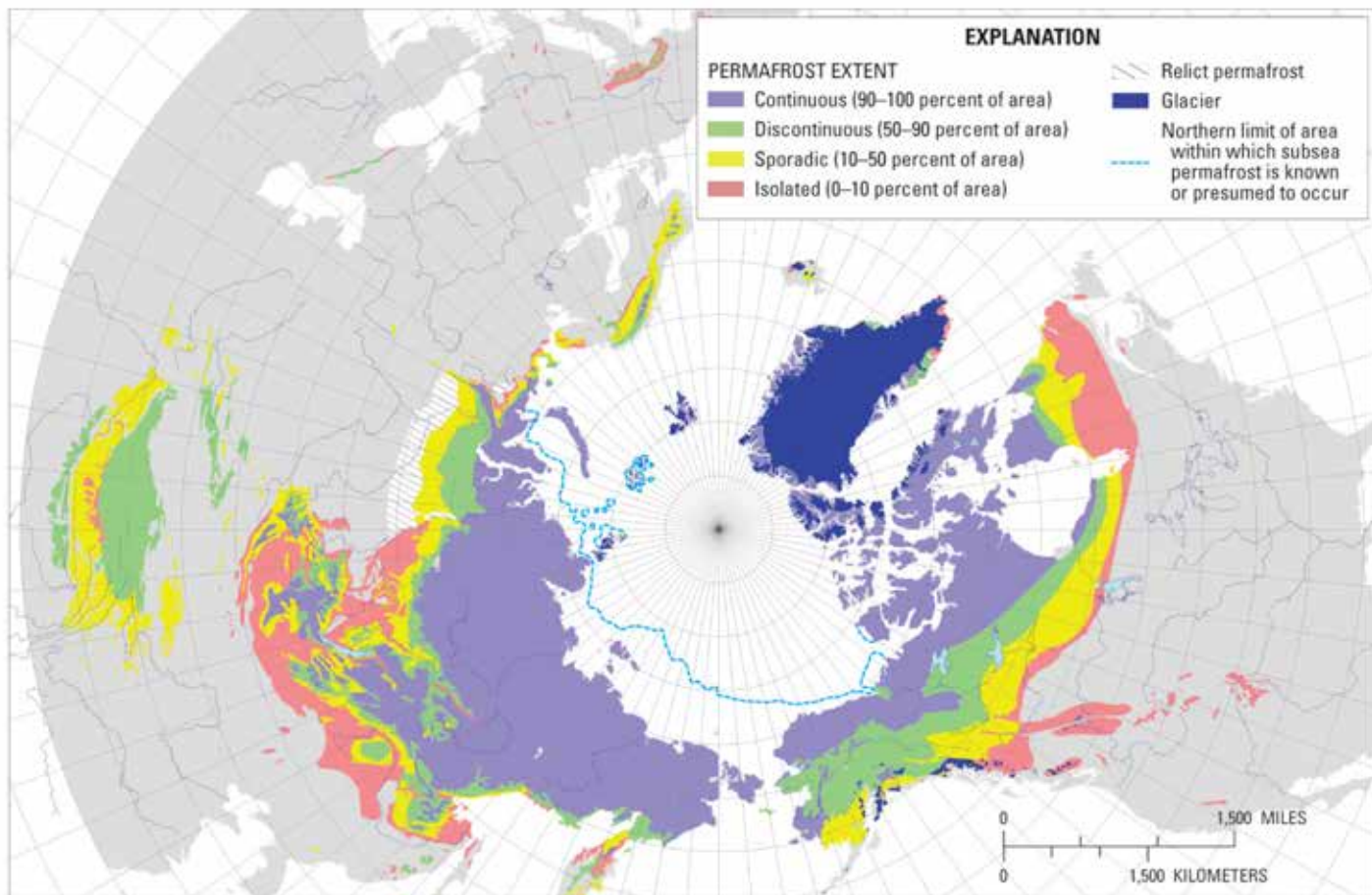


Figure 8.60. In high latitude land areas of the Northern Hemisphere, there are extensive areas of **permafrost**, a part of the soil that never thaws. The areas that have over 90% of the land area underlain by frozen ground are the continuous permafrost zone (light purple). The Greenland Ice Sheet is shown in dark purple. Other areas (colors) have less than 90% permafrost in the subsurface. Global warming will cause a thawing of portions of permafrost regions, and each zone will retreat poleward. Among the environmental consequences will be the release of carbon dioxide and methane gases, further enhancing the greenhouse effect (Source/Credit: USGS).



Figure 8.61. In some permafrost zones, there are lenses and wedges of nearly pure ice at the surface, some relicts of the ice age. The soil and ice thaw, causing collapse and chaotic ground surface of mounds and lows, some of which are occupied by standing water during the summer (Source/Credit: Miriam Jones, USGS).

Thawing of the permafrost results in the release of carbon dioxide and methane from the soil as dead organic matter within the soil begins to decompose (Figure 8.62). This release of additional carbon dioxide will add to the greenhouse effect and is another example of positive feedback. Every year, people add about **two billion tons** of carbon dioxide into the atmosphere. The permafrost contains about **300 billion tons**, or 14% of the world's carbon. If a large area of the permafrost thaws, there will be a huge influx of carbon dioxide and methane into the atmosphere that far exceeds direct human contribution.



Figure 8.62. One of the consequences of global warming is the thawing of permafrost in the soil that now supports boreal forests and arctic tundra ecosystems. As the soil thaws, land sinks, and some areas have ponded drainage. Thermokarst lakes replace forest and tundra. The carbon that was formerly locked in frozen soil becomes alive with microbial activity, releasing large amounts of methane gas, seen above as bubbles frozen in the ice (Source/Credit: Miriam Jones, USGS).



## Sea Floor Methane Hydrates

Another concern is the existence of frozen methane ice deposits on the continental shelf of Alaska and elsewhere (Figure 8.63). Because **methane absorbs ten times more energy per molecule than carbon dioxide**, it is a far stronger greenhouse gas than carbon dioxide. However, at present, it does not contribute as much to the greenhouse effect because there are fewer methane molecules in the atmosphere than carbon dioxide molecules. There is a very real possibility that as the polar seas warm the seafloor methane ice will thaw, releasing tremendous quantities of methane into the atmosphere and further contributing to global warming. There are 15 trillion tons of methane in these deposits. This is another positive feedback mechanism that could cause the climate to shift much more rapidly than expected.

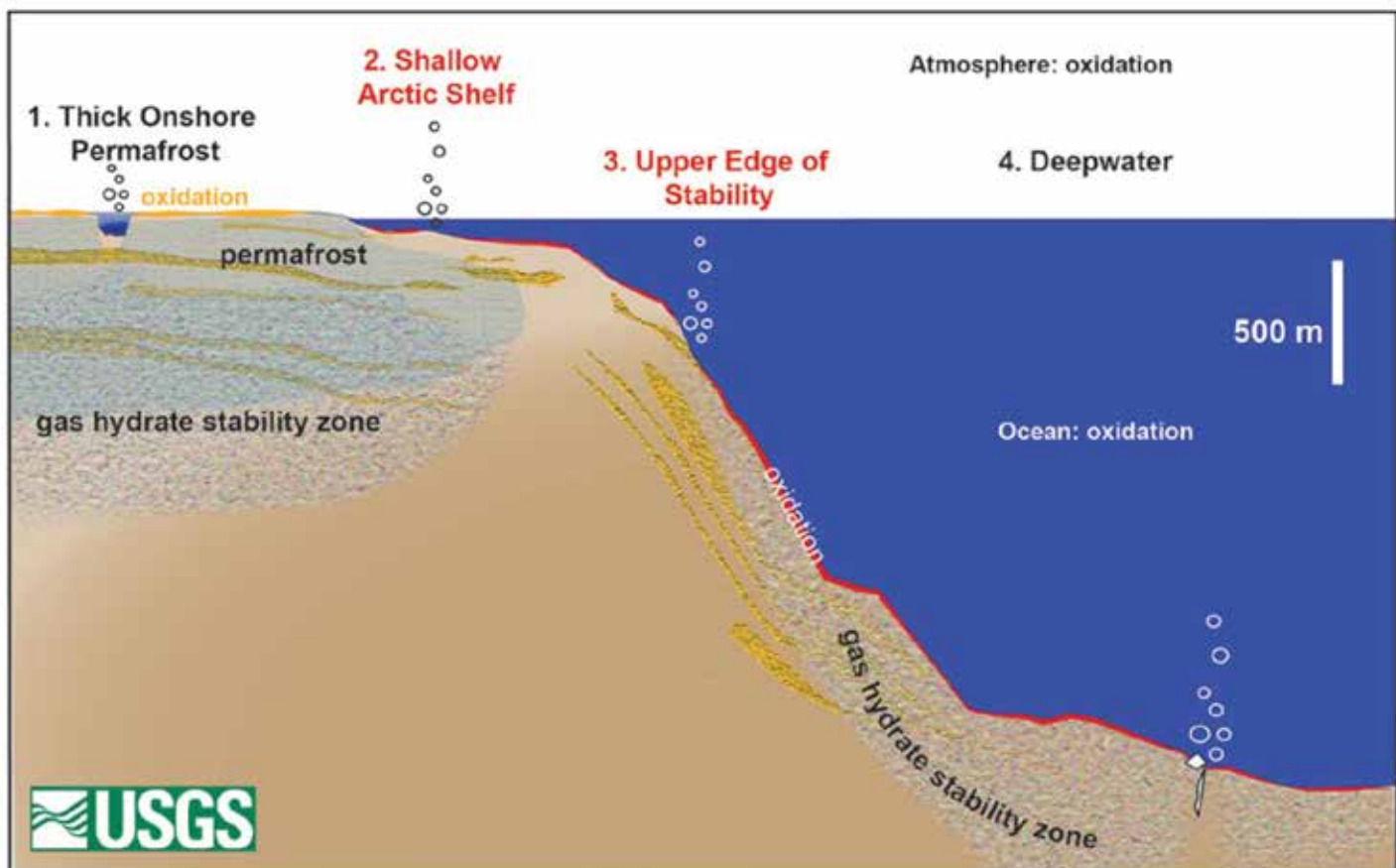


Figure 8.63. The temperature-pressure conditions in some sea-floor regions causes methane and other gases to combine with water and remain frozen for centuries on the sea floor. These **methane hydrates** contain vast amounts of methane, and become unstable with a slight warming of the bottom waters. This provides another positive feedback mechanism, where global warming releases methane, which in turn causes more warming, which releases more sea-floor methane, and so on (Source/Credit: USGS).

## Glaciers and Ice Caps

Over the last two decades, the Greenland and Antarctic ice sheets have been losing mass and volume. Glaciers have continued to shrink almost worldwide, with only minor exceptions (Figure 8.64). Some Alaskan and Argentinian glaciers began retreating nearly a hundred years ago (Figure 8.65).

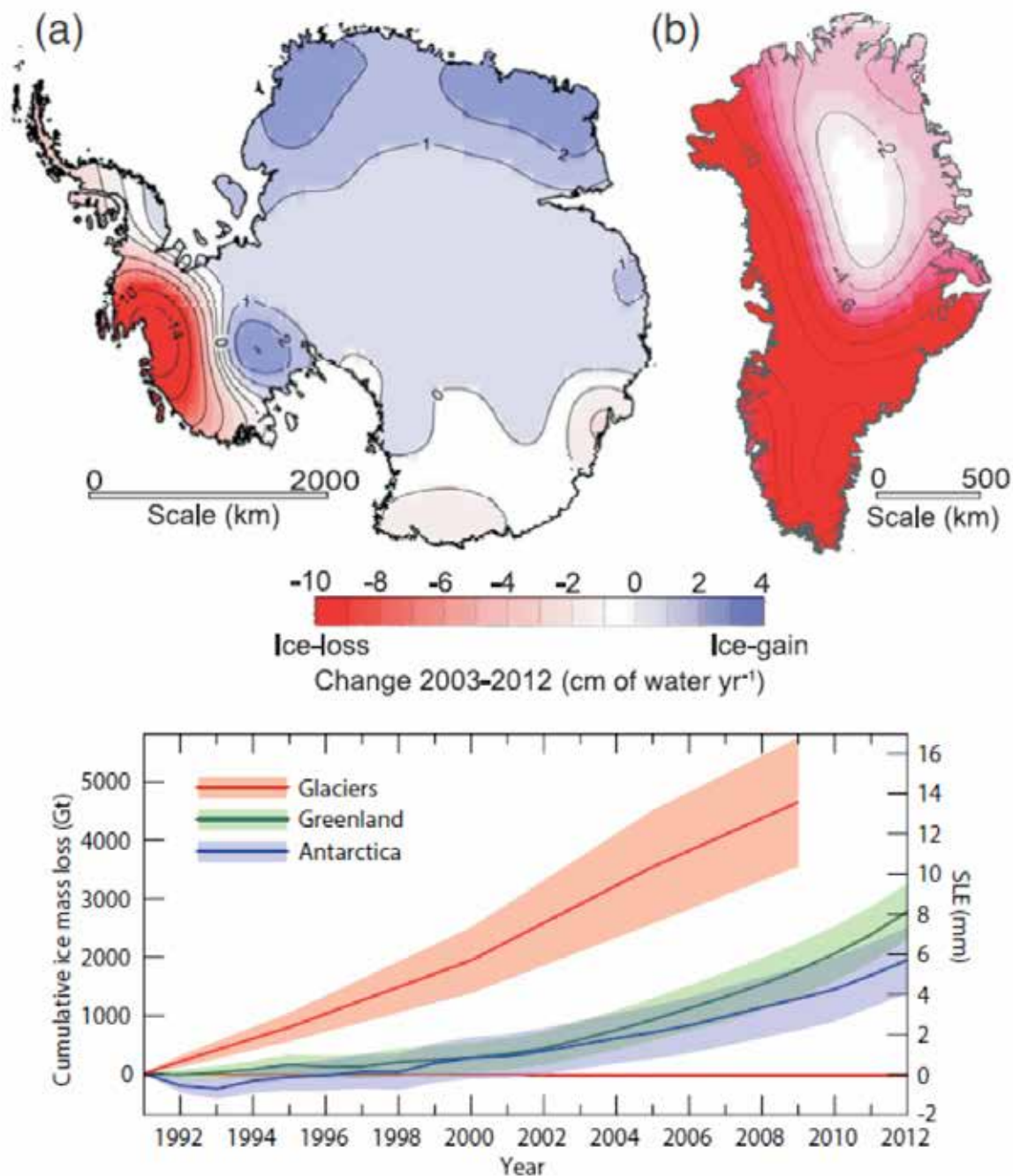


Figure 8.64. The lower graph indicates the cumulative mass loss of global glaciers from 1991-2012 (pink), as well as losses for Greenland (green) and Antarctica (blue). The upper images indicate spatial distribution of ice losses and gains for Antarctica and Greenland (Source/Credit: IPCC).

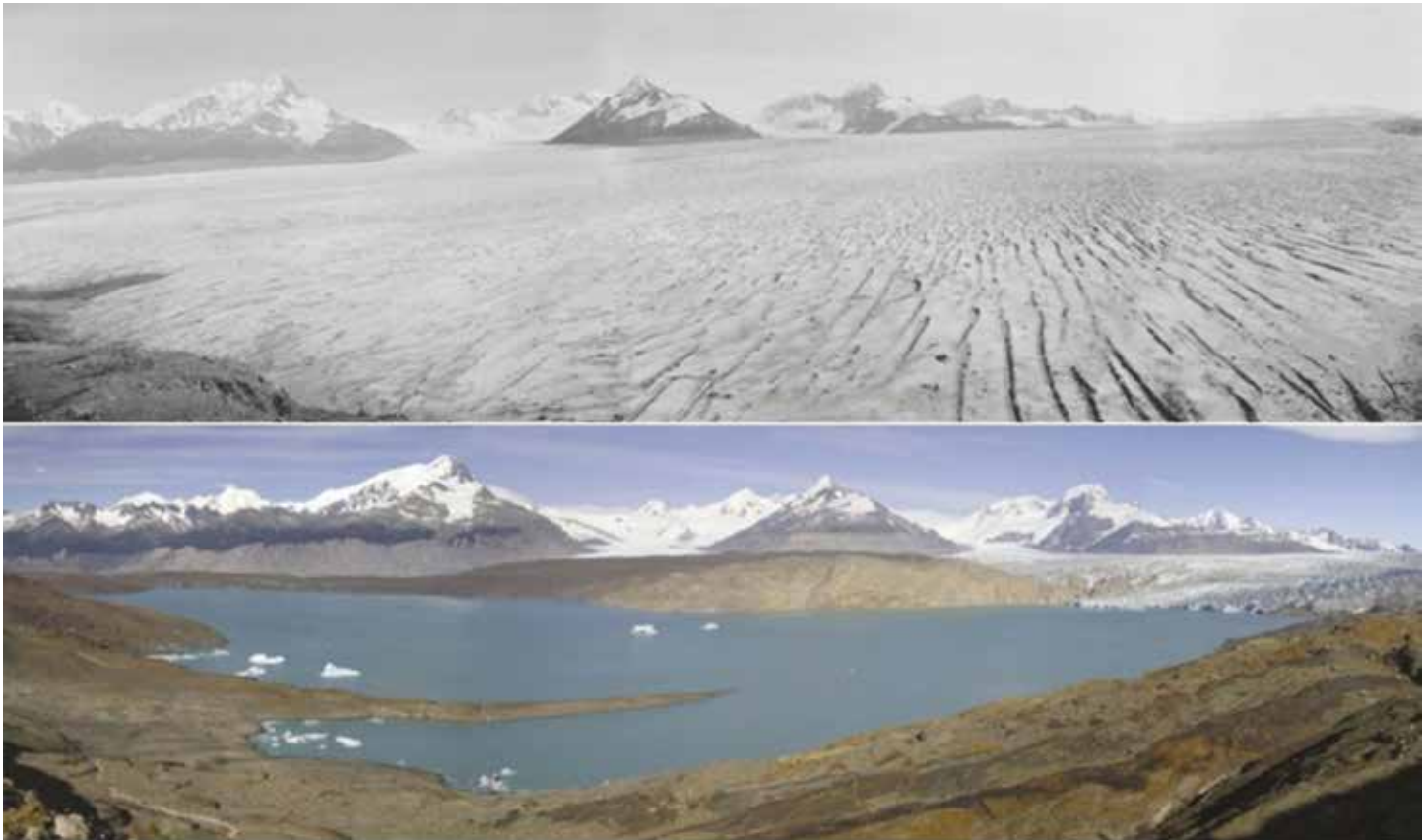


Figure 8.65. The majority of mountain glaciers throughout the world have retreated significantly during the past 100 years or so, presumably in response to global warming. Argentina's Upsala Glacier has retreated dramatically since 1928. Interestingly, a lesser proportion of mountain glaciers have been stable, or have advanced during the same time interval (Source/Credit: Greenpeace).

The Greenland ice sheet has experienced the most dramatic and consistent losses over the past few decades of accurate monitoring (Figure 8.66). The average rate of ice loss from the Greenland ice sheet has very likely increased from an estimated 34 gigatons per year over the period 1992–2001 to 215 gigatons per year over the period 2002–2011. Global glacier volume is expected to continue to decrease throughout the 21<sup>st</sup> century.

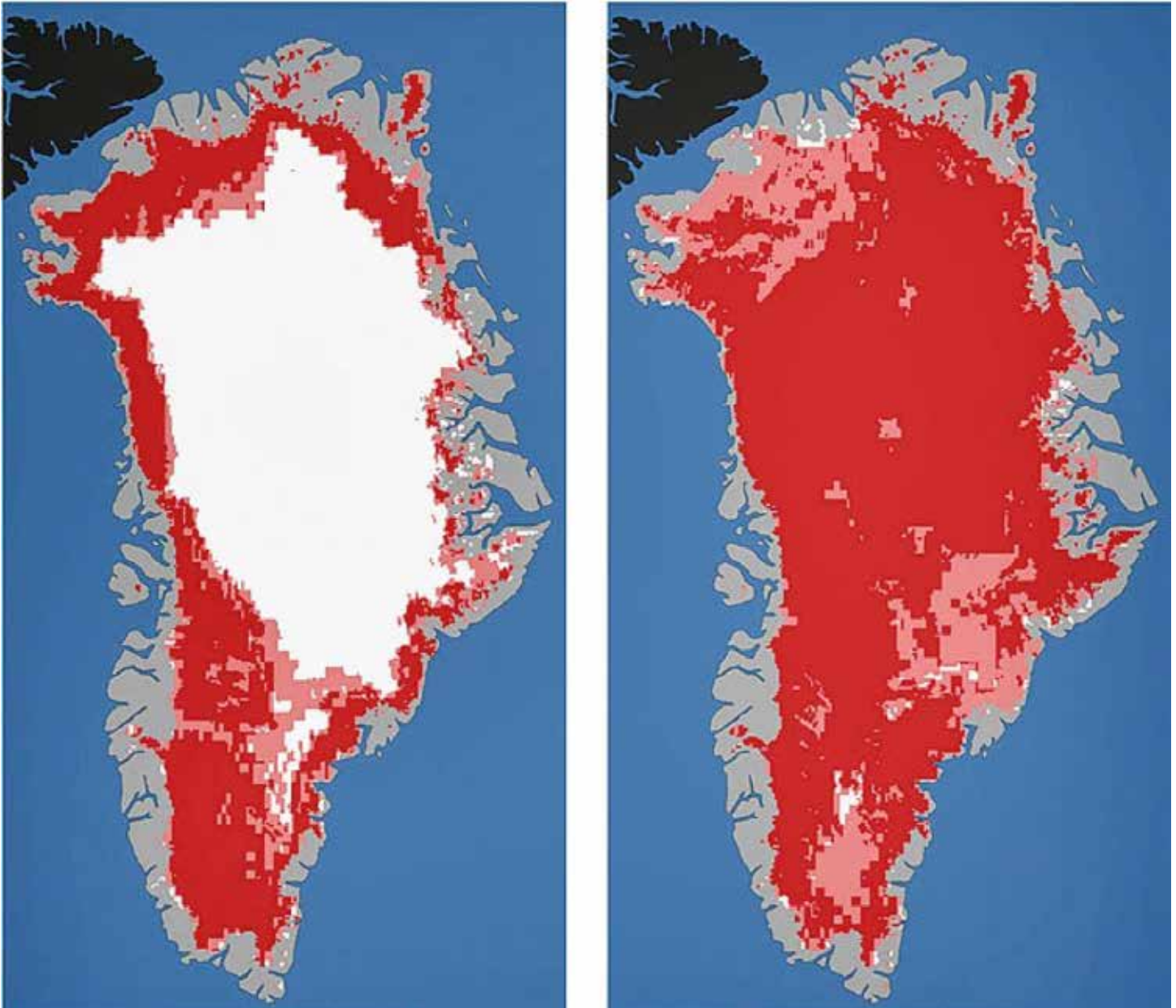


Figure 8.66. The lower graph indicates the cumulative mass loss of global glaciers from 1991-2012 (pink), as well as losses for Greenland (green) and Antarctica (blue). The upper images indicate spatial distribution of ice losses and gains for Antarctica and Greenland (Source/Credit: IPCC).

Temperature and ice mass trends for Antarctica are not as consistent as Greenland. Although Antarctica shows a slight decadal loss in ice volume, temperature trends of the surface of the ice sheet show both warming and cooling (Figure 8.67). It should be noted that much of the data for ice volume and temperature in Antarctica are from recent satellite measurements. There are very few ground-based observations to ground truth the satellite data.

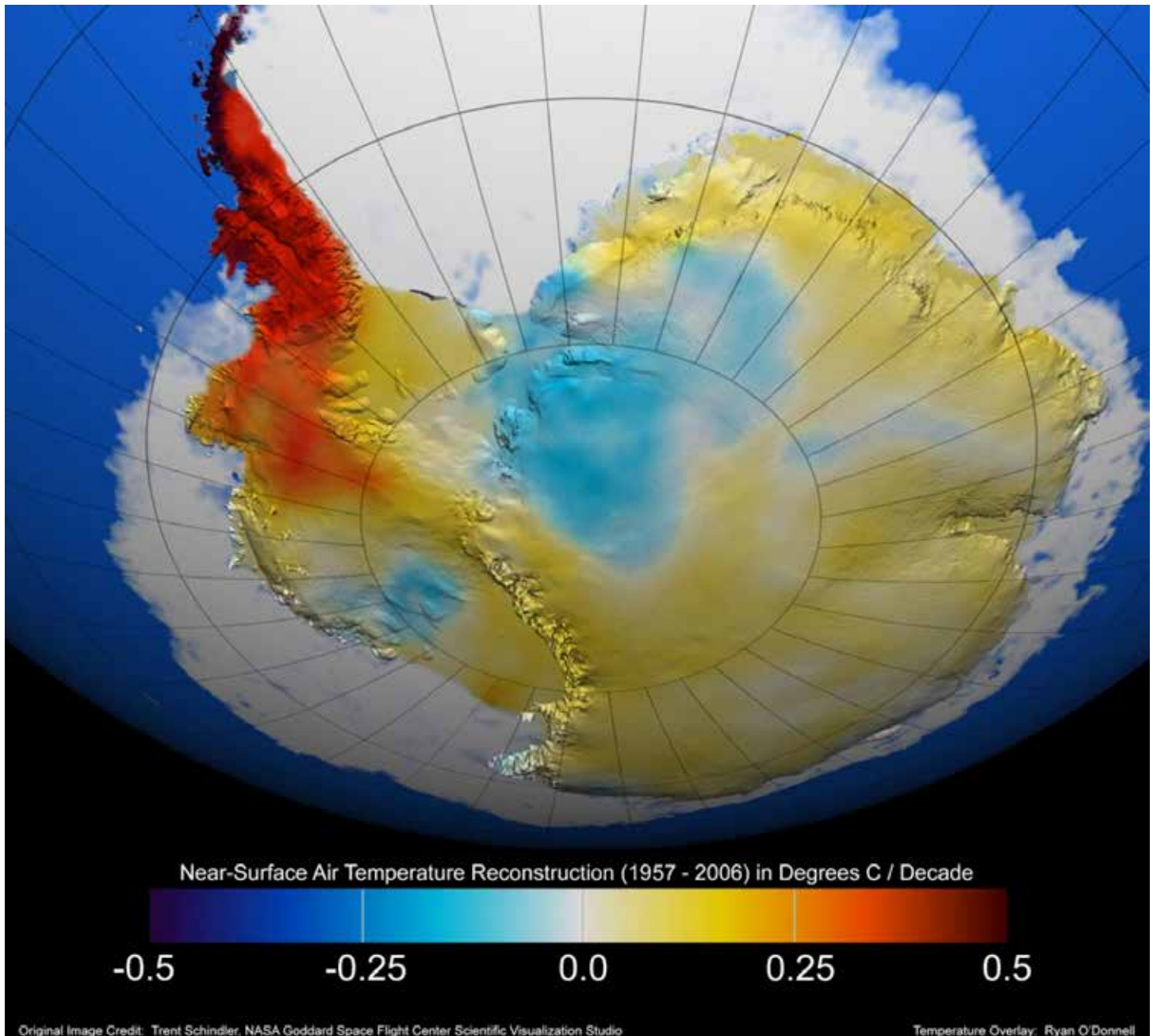


Figure 8.67. Near-surface air temperature reconstruction in degrees C/decade for the period 1957-2006. Interestingly, some areas seem to have been cooling, whereas others warming. This contrasts with the high-latitude temperature trends in the Northern Hemisphere, where temperatures have been increasing for the same time period (NASA, Trent Swindler).

## Sea Level

The rate of global sea level rise since the mid-19<sup>th</sup> century has been larger than the rate for the last 2000 years. From 1901–2010, global mean sea level rose by about 0.6 feet (0.19 m). The IPCC (2013) estimates the mean rate of global average sea level rise was 0.07 inches (1.7 mm) per year between 1901 and 2010. The rate had risen to 0.13 inches (3.2 mm) per year between 1993 and 2010. This compares with the average global rate of sea level rise of about 0.06 inches (1.4 mm) per year for the past 6000 years. Global tide-gauge data is consistent with more recent satellite altimeter data regarding rates of sea level rise (Figure 8.68). At least 75% of the rise in sea level for over the past century has been due to the combined effects of thermal expansion of the ocean and the melting of glaciers.

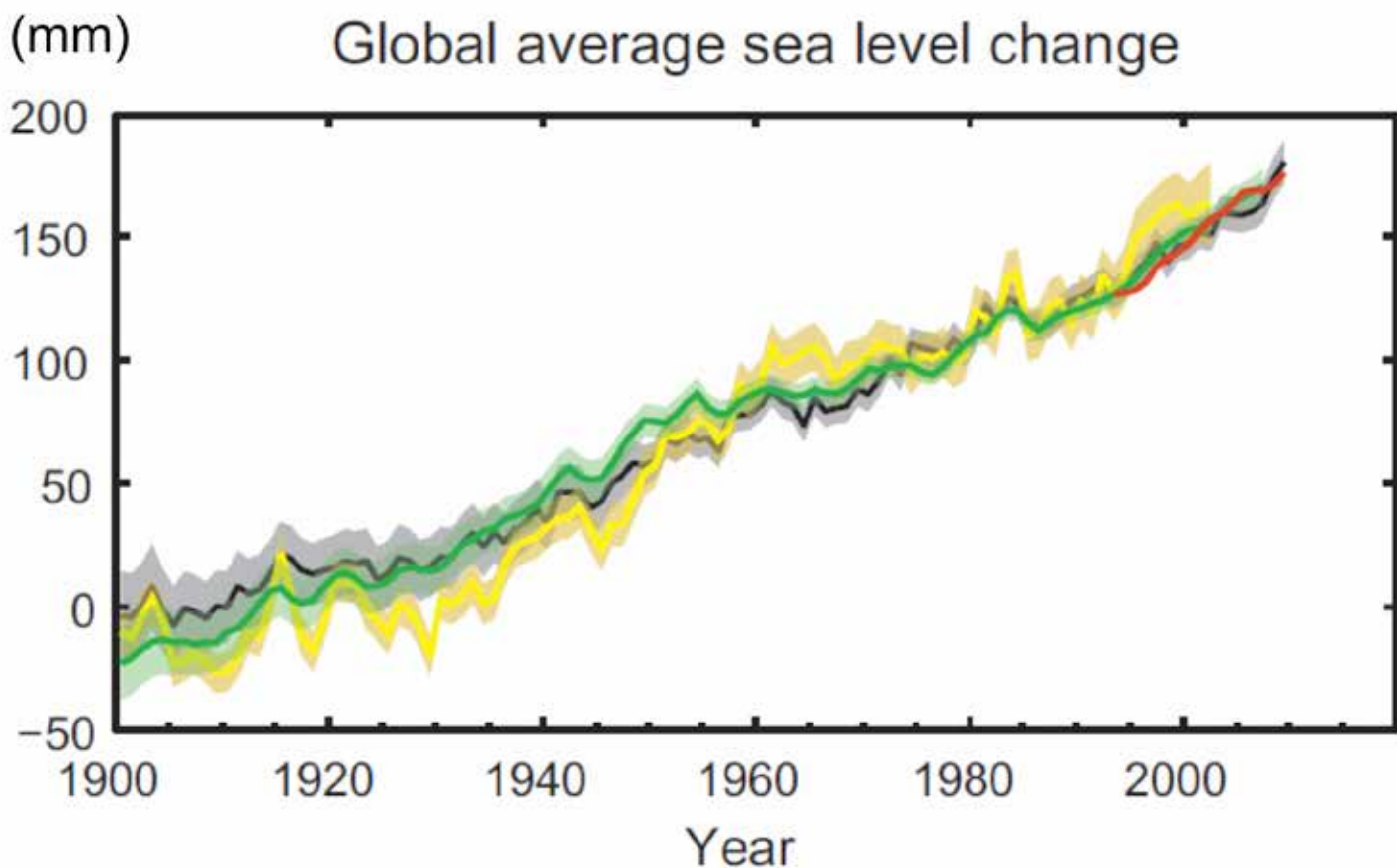


Figure 8.68. Global sea level has risen an average of about 200 mm (8 inches) over the past 115 years relative to the 1900–1905 mean. The red line represents the first year of satellite altimetry data in 1993 (Source/Credit: IPCC2013).

Global sea level is expected to rise at an increasing rate through the end of the 21<sup>st</sup> century (Figure 8.69). An interesting analog to the amount of sea level rise that might result from long-term global warming is the middle of the last interglacial period, from about 129,000 to 116,000 years ago. Global temperatures during that time are estimated to have been about 3.6°F (2°C) warmer than today. Geologic evidence suggests that average sea level was between 16 and 33 feet (5-10 m) higher than today's for a duration of several thousand years. A rise in sea level of several feet to tens of feet sounds inconsequential, but it would threaten all low-lying coastal regions, where 10% of the global population resides (Figure 8.70). Continued sea level rise in future centuries could result in a global sea level rise of over 200 feet (~60 m) if all glaciers melted (Figure 8.71).

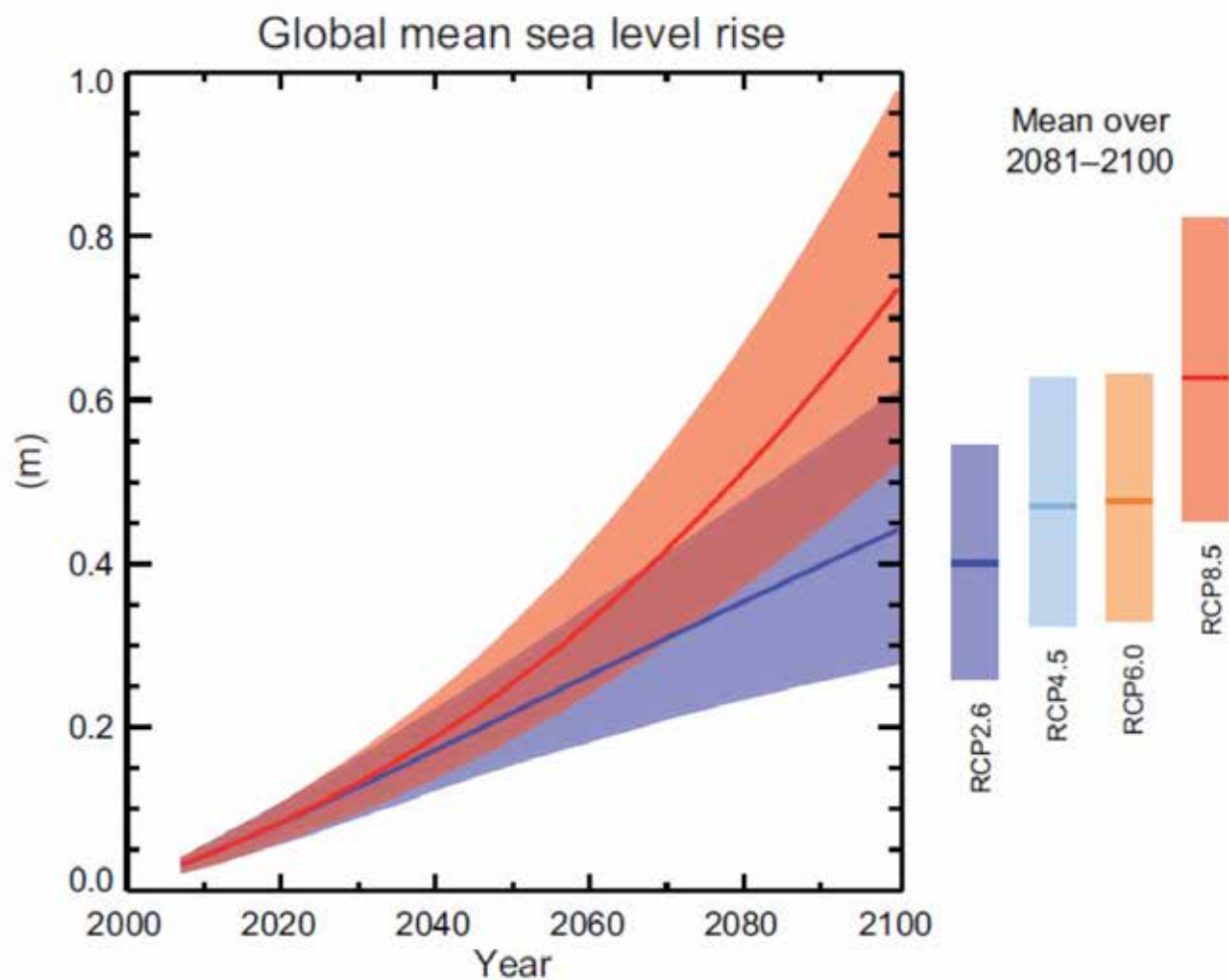


Figure 8.69. Different computer scenarios of projected sea level rise to the end of the 21<sup>st</sup> century, in meters (Source/Credit: IPCC 2013).



Figure 8.70. The map indicates the degree of vulnerability of the coastal areas of the United States to sea level rise. Included in the vulnerable areas are large numbers of nuclear power plants (Source/Credit: USGS).

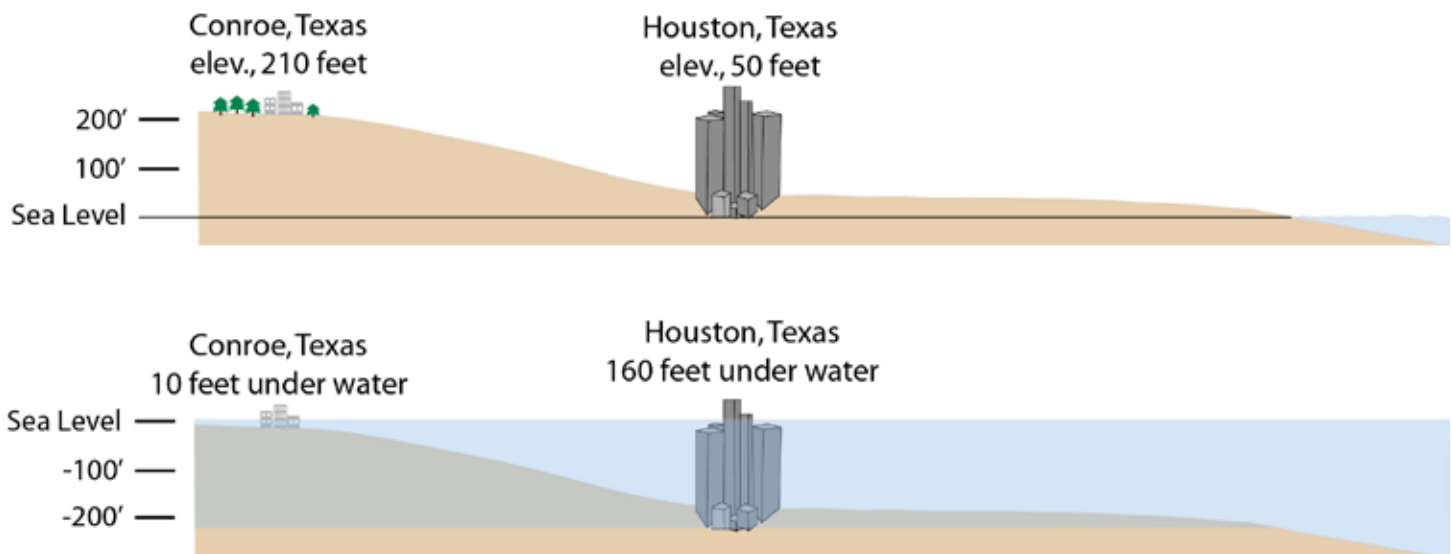


Figure 8.71. Effects of postulated 220-230 foot sea level rise in coastal Texas due to complete melting of land ice and thermal expansion of ocean water. While buildings exceeding approximately 25 stories would be above water, most of the built-up area would not be.



The global impact of a sea level rise of just a few feet would be severe. Damages and losses would run into the billions or trillions of dollars, and the ecological costs are impossible to calculate. Coastal ecosystems would be either translocated or destroyed. Much of the Everglades, for example, will cease to exist if sea level rises a mere two feet. Even a two-foot rise in sea level will eliminate between 17% and 43% of the wetlands of the United States. Coastal marshes are primary breeding grounds for crab, shrimp and other species, many of which we use as a food source. A 20-foot rise will submerge half of Florida and half of Louisiana. Sea level has already risen about a foot in the last 100 years, simply from the thermal expansion of water in response to warmer temperatures.

The major tropospheric greenhouse gases carbon dioxide (CO<sub>2</sub>), methane (CH<sub>4</sub>), and nitrous oxide (N<sub>2</sub>O) have all increased since the beginning of the Industrial Revolution. The concentrations of these greenhouse gases in early 2014 were 396 ppm, 1830 ppb, and 327 ppb, and exceeded the pre-industrial levels by about 40%, 150%, and 20%, respectively (Figures 8.72a, 8.72b and 8.72c). CH<sub>4</sub> and N<sub>2</sub>O are today greater than the highest concentrations recorded in ice cores during the past 800,000 years. Carbon dioxide concentrations have been increasing at an increasing rate for at least the past century. The 2013 IPCC report has included tropospheric ozone (O<sub>3</sub>) as an important greenhouse gas. Chlorofluorocarbons are only a very small component of greenhouse gases, but are very potent absorbers and have a long residence time (average length of time) in the atmosphere (Figure 8.73).

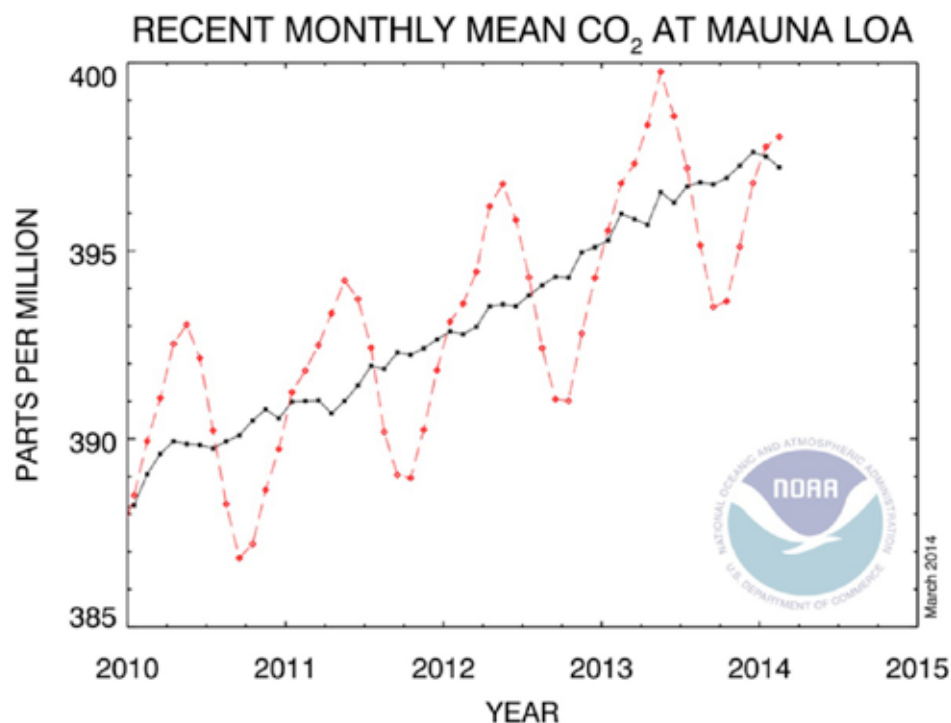


Figure 8.72a. Concentration of carbon dioxide from 2010-early 2014. Levels of carbon dioxide are increasing at an increasing rate and will soon eclipse the 400 ppm mark. Concentrations of carbon dioxide are higher now than at any time in the past 800,000 years, according to ice core analysis from Antarctica (Source/Credit: NOAA).

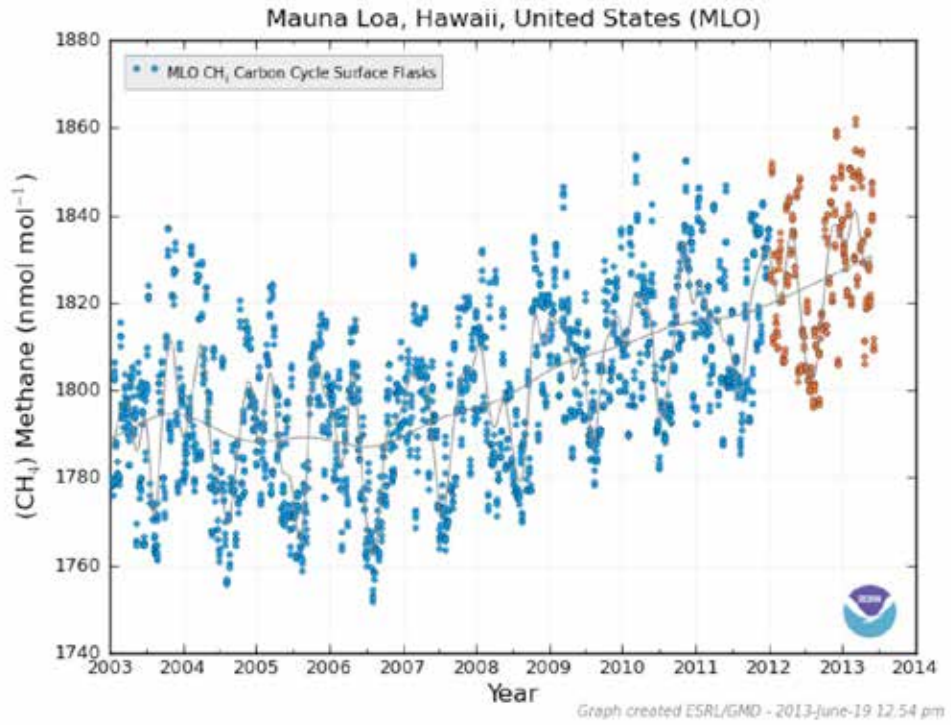


Figure 8.72b. Concentration of methane gas from 2003-2013 (Source/Credit: NOAA).

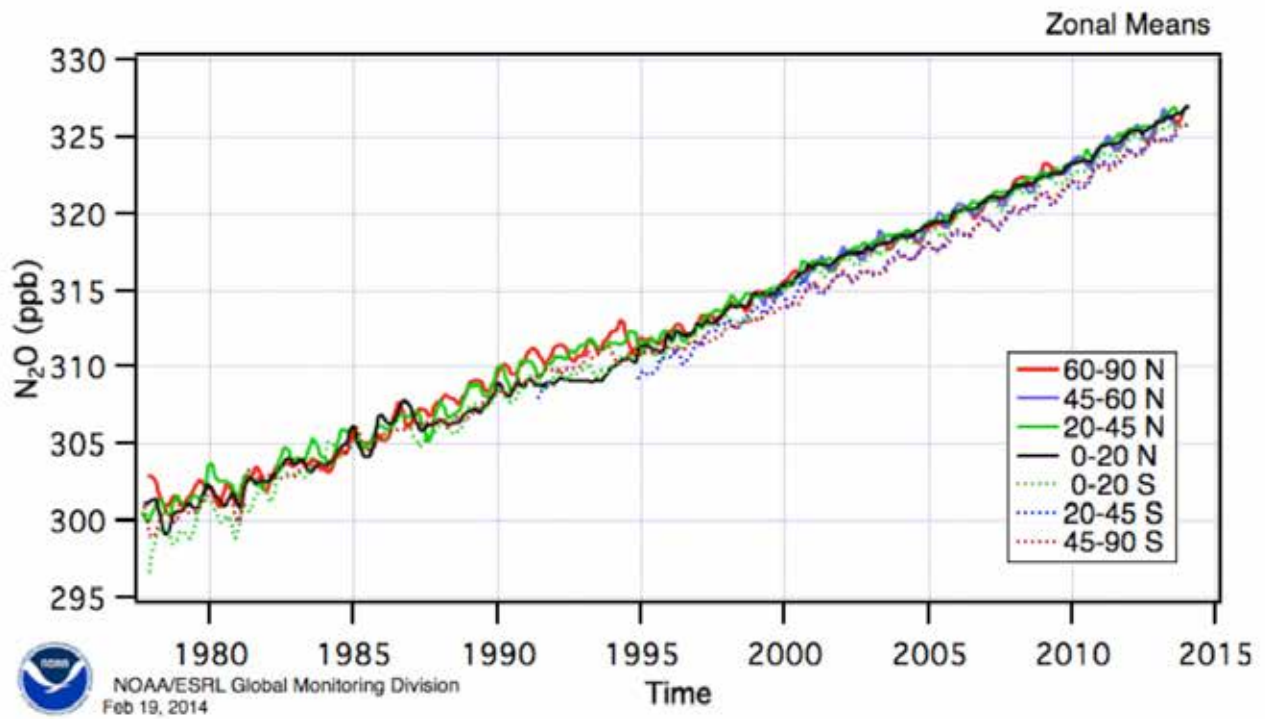


Figure 8.72c. Concentration of nitrous oxide from 1978-early 2014 (Source/Credit: NOAA).

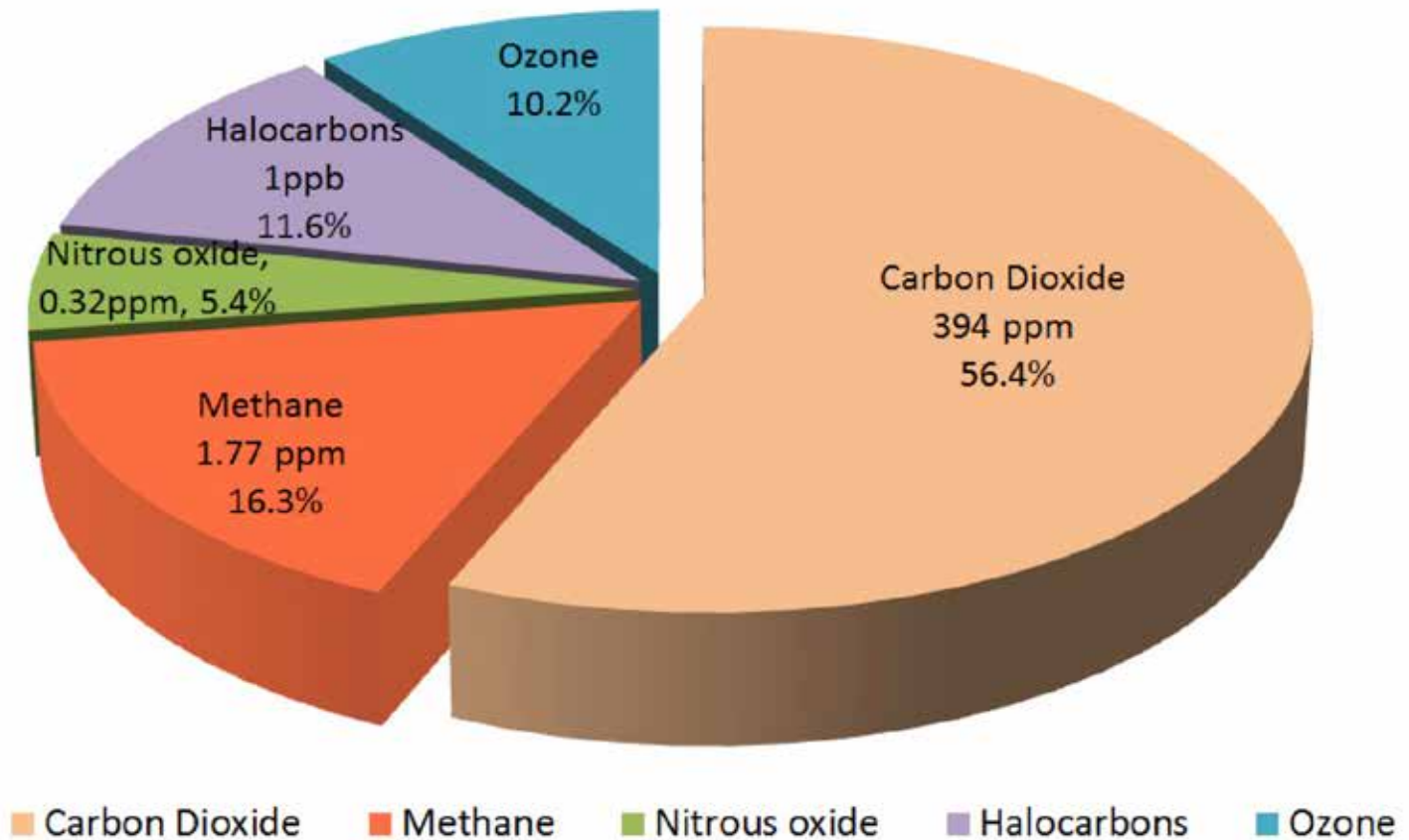


Figure 8.73. Relative importance of greenhouse gases to global warming after water vapor in 2013. Carbon dioxide dominates the number two position as a tropospheric greenhouse gas, even though some of the others are gaining in relative importance (Source/Credit: NASA).

The main causes of increases in carbon dioxide concentration are fossil fuel combustion changes in land cover, and cement production. The 2013 IPCC report estimates that fossil fuel emissions and cement production have added ~8.3 gigatons of carbon dioxide per year to the atmosphere over the period 2002-2011, and had jumped to 9.5 gigatons per year in 2011. Emissions were 54% above the 1990 level.

The oceans, the major sink of carbon dioxide, have absorbed about a third of what has been emitted by humans. In the process of absorbing added carbon dioxide, the oceans have become more acidic. Acidification and pollution of ocean waters are a major present and future threat to many marine ecosystems.

Continued global population growth, coupled with the trend toward increased global industrialization, will result in an even greater imbalance between greenhouse gas sources versus sinks (Figure 8.74a, 8.74b, and 8.74c). The amount of increase in concentrations of greenhouse gases depends on future emissions. The 2013 IPCC report contained several scenarios for increases in carbon dioxide projected to the year 2100. Estimates ranged from a low of 550 ppm to a high of >900 ppm. An average of these two extremes would put carbon dioxide levels at 788 ppm in 2100, almost a doubling of the 2014 level of 396 ppm. Other greenhouse gases are projected to increase in concentration throughout the 21<sup>st</sup> century. Switching to alternative energy sources, improved land use practices, and curbing population growth could dramatically reduce emissions, but concentrations will remain high throughout the century.

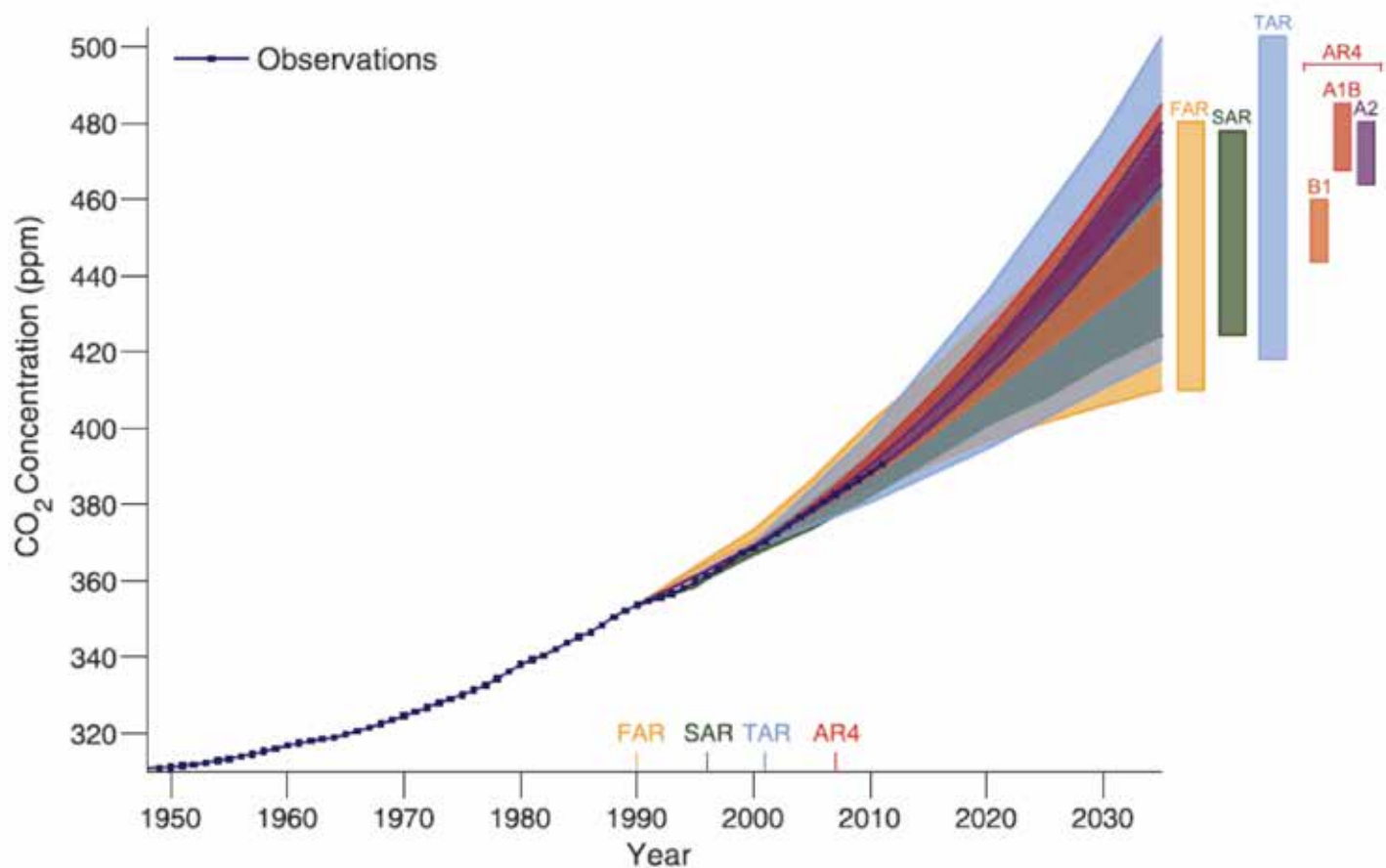


Figure 8.74a. Observed and projected carbon dioxide concentrations, 1950-2035. The different color bands for projected concentrations illustrate different models and emissions scenarios (IPCC, 2013).

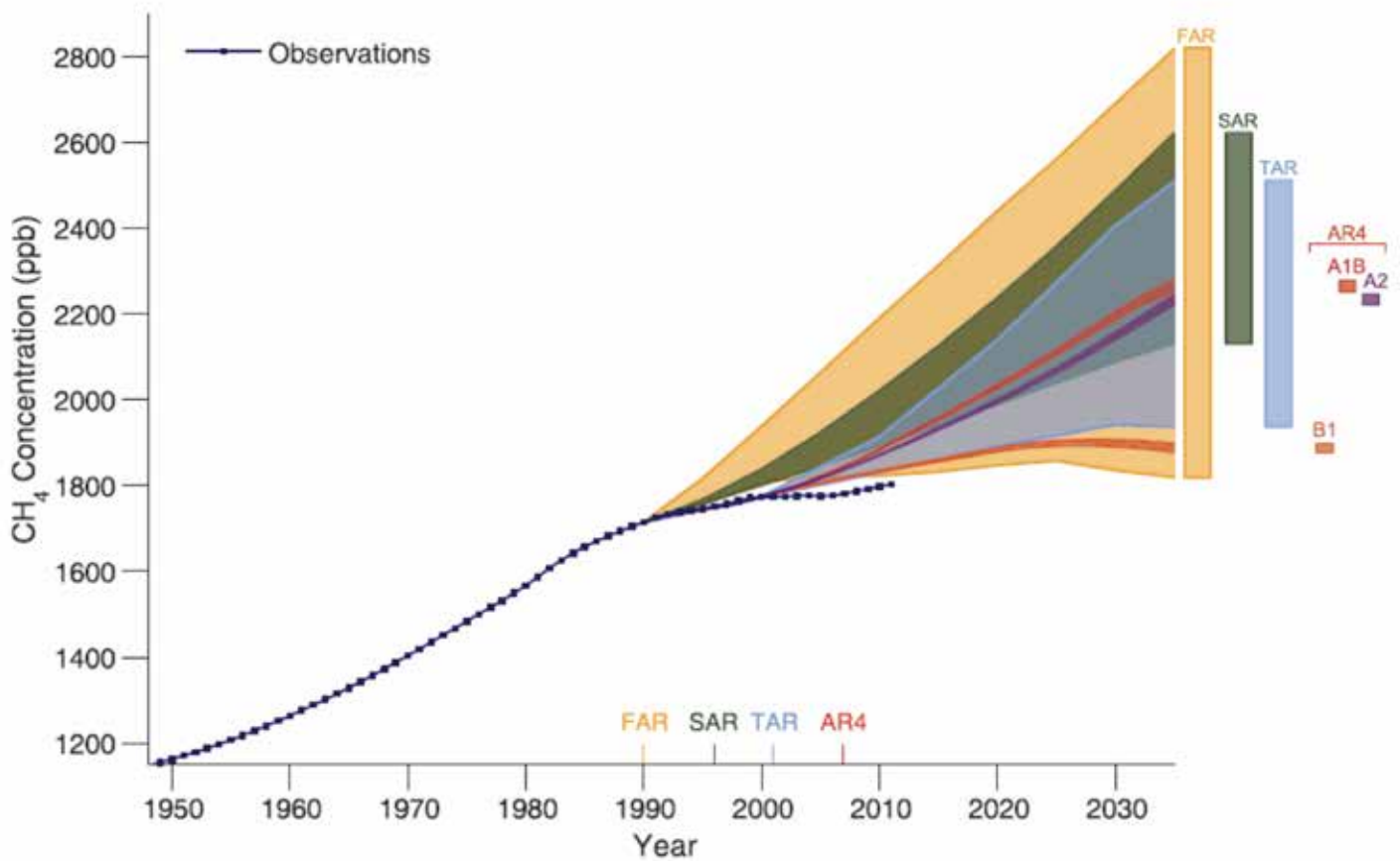


Figure 8.74b. Observed and projected methane concentrations, 1950-2035. The different color bands for projected concentrations illustrate different models and emissions scenarios. Note that some models project a leveling off of methane concentrations by about 2030 (IPCC, 2013).

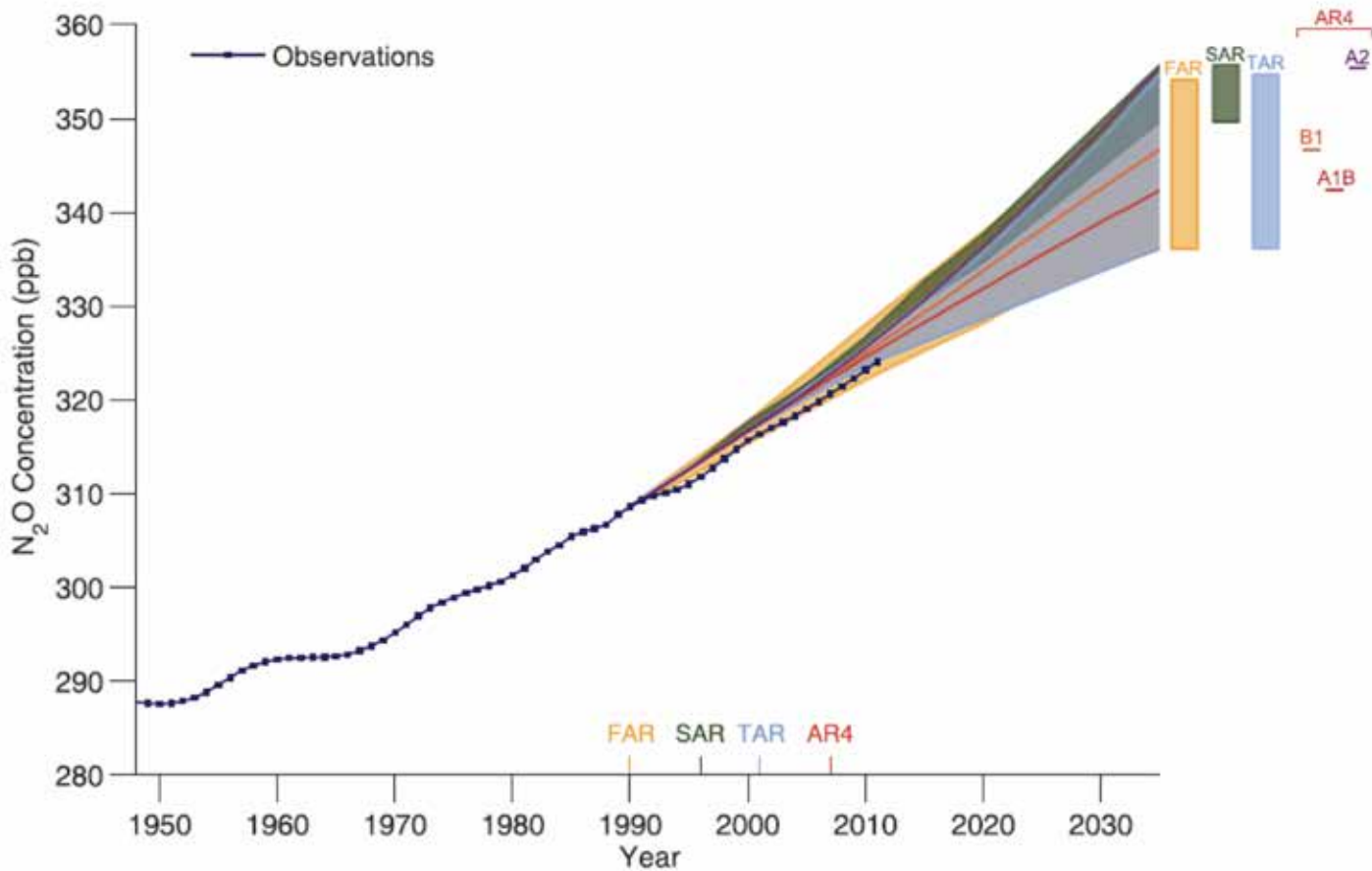


Figure 8.74c. Observed and projected nitrous oxide concentrations, 1950-2035. The different color bands for projected concentrations illustrate different models and emissions scenarios (IPCC, 2013).

Methane, nitrous oxide, and ozone are all expected to increase in concentration with increasing global industrialization and population growth. Anthropogenic sources of methane include rice fields, cattle, coal mining, and using natural gas. Natural sources of nitrous oxide include microbial processes in water and soil. Nitrogen-based fertilizers, fossil-fuel power plants, and vehicle emissions are major sources of anthropogenic nitrous oxide. Tropospheric ozone is largely anthropogenic and is in much higher concentrations in urban and industrial regions. Chlorofluorocarbons are exclusively anthropogenic. Although they occur in many different chemical combinations, collectively, they are now approximately of the same importance as tropospheric ozone as a greenhouse gas (Figure 8.75).

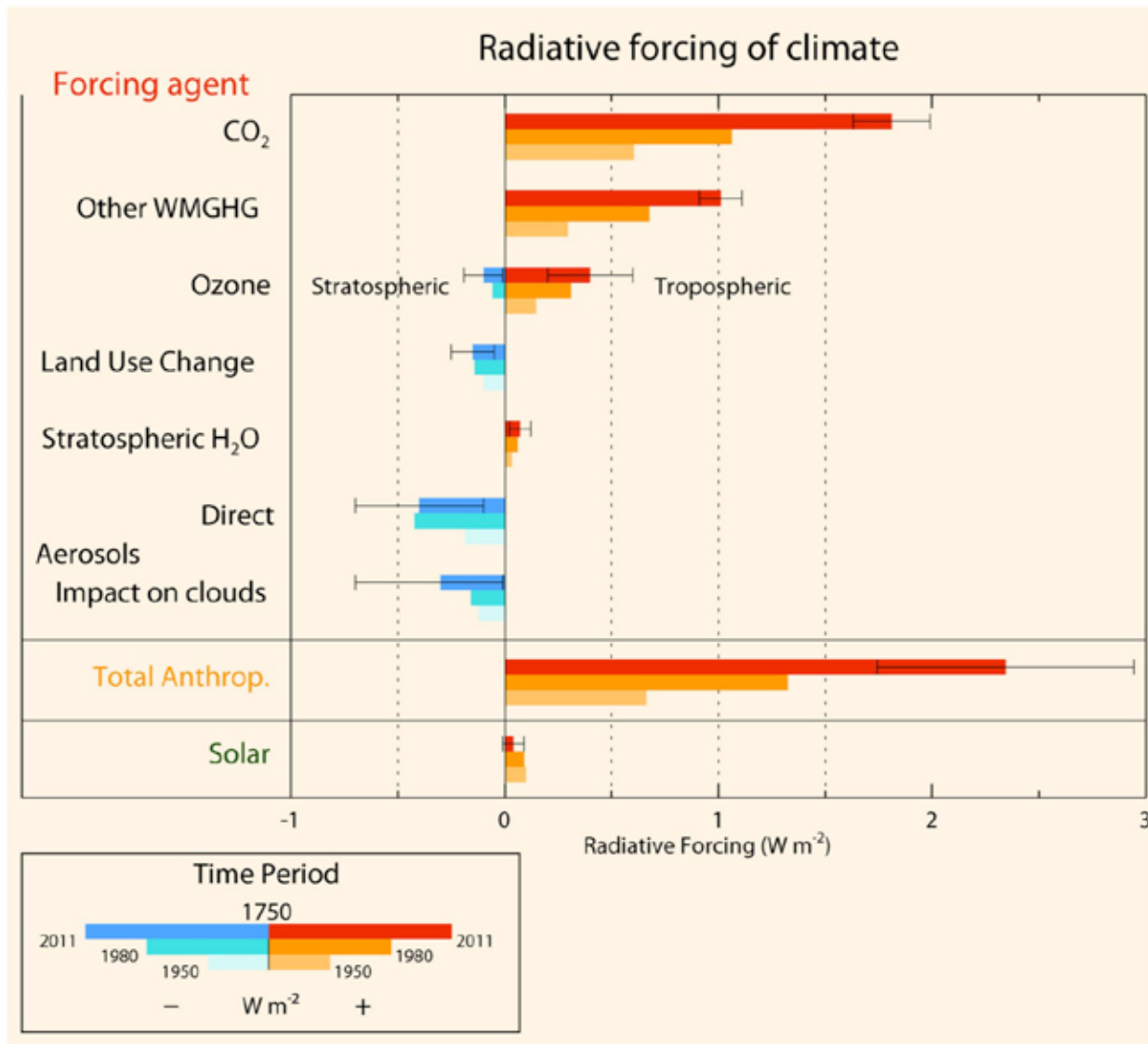


Figure 8.75. The bar graphs indicate a list of the principal gases, aerosols, and other influences that tend to warm the troposphere, called **positive radiative forcing** (bar graphs extending to the right of the solid vertical line, middle of graph), and **negative radiative forcing** (cooling effect, bar graphs to the left of the line). Radiative forcing estimates represent three time periods; 1750-1950, 1750-1980, and 1750-2011 (lower, middle, and upper bars). Values are global average radiative forcing. The radiative forcing of the Sun is also estimated. The bracketed horizontal black line represents the degree of uncertainty in the estimates. Total anthropogenic forcing is progressively greater for each of the time intervals (Source/Credit: IPCC 2013).

## Mitigation

What can be done to mitigate the problem of global warming? There is no single answer, but there are several things that, collectively, can help reduce the problem. Even if it cannot be stopped or reversed, the rate of change can be slowed, and this gives us more time to adjust to the changes and thereby lessens the impacts.

Since approximately half of greenhouse gas emissions stem from energy production and use, principally from the burning of fossil fuels, we can attempt to reduce these emissions. This can be done, in part, by creating more fuel-efficient automobiles. This would be a very important step because the burning of a single pound of gasoline generates several pounds of carbon dioxide.

More energy efficient machines and appliances can be developed. One study done in the early 1990s found that the application of known energy-efficiency improvements to seven types of home appliances would produce net savings in energy costs of \$50 billion over the next 20 years. By the same token, we can build more energy-efficient homes and use more energy efficient lighting. For example, the use of fluorescent light bulbs, instead of incandescent bulbs, could eliminate the need for about 30 coal-fired power plants.

We can create reforestation projects that will result in the removal of carbon dioxide from the air. However, a lot of reforestation would be required. To remove the carbon dioxide emitted in a single year requires planting an area the size of France. Nonetheless, it is a worthwhile effort and has many additional positive effects, such as reduction of soil erosion, increased habitat diversity and aesthetic appeal.

Eventually, there must be a switch to alternative sources of energy for the generation of electricity. Wind and solar energy will likely see a relative increase in energy production in the near future, particularly with the cost of crude oil fluctuating between \$75 and \$150 per barrel in the early 21<sup>st</sup> century. Technological advances in recent years have made these alternatives far more attractive from an economic standpoint. With time, and the increased environmental costs of fossil fuels, they will become economically viable and will play a major role in reducing fossil fuel consumption.



## Regional Trends and Impacts of Climate Change in the United States

The reality of global climate change is causing a major shift in attitude of many governmental and industrial institutions. The current climate change, and the prospect of accelerated change, has led to many studies of the impact of climate change, not just in a regional context, but within specific geographic regions. **With a better understanding of current and future climate change, and how these changes might impact various sectors such as energy production, water supply, human health, and agriculture, steps can be taken to better prepare for and cope with our climatic future.** Below are just a few examples of regional trends and impacts of climate change in selected regions of the United States. Three of the six regions of the United States are the focus of the commentary below. The Great Plains Region (including some of the Northern Rockies) and Southwest Region were chosen because both are in arid and semi-arid climates where water is relatively scarce and population growth is high. The third, the Pacific Northwest, was chosen because of its diverse climate and northerly latitude. Information for regional climate change in the United States was obtained from a variety of sources, many of which are available to the public at no charge on-line. These include, but are not restricted to, the following publications and agencies: (1) the National Oceanic and Atmospheric Administration (NOAA), (2) the National Aeronautics and Space Administration (NASA), (3) the National Center for Atmospheric Research (NCAR), (4) the Intergovernmental Panel on Climate Change (IPCC), (5) *Global Climate Change Impacts in the United States*, United States Global Change Research Program, 2009, (6) *Indicators of Climate Change in California*, California Environmental Protection Agency, Office of Environmental Health Hazard Assessment, 2009, (7) *Atlas of Health and Climate*, World Health Organization, 2012 (8) *State of the Climate in 2012*, Special supplement to the Bulletin of the American Meteorological Society, 2013, (9) *Developing Climate Change Environmental Public Health Indicators: Guidance to Local Health Departments*, Council of State and Territorial Epidemiologists (CSTE), 2013 and (10) *The Washington Climate Change Impacts Assessment*, University of Washington, Climate Impacts Group, June 2009.

## Great Plains

### Observations and Speculations about Climate Trends in the Great Plains

- Rising temperatures have increased the demand for energy and water and will likely continue to do so throughout the 21<sup>st</sup> century (Figure 8.76).
- Warmer temperatures and increasing drought will have an impact on ecosystems; deserts and grasslands will expand; forests and woodlands will shrink.
- The wind will become an increasingly important agent in semi-arid locations; in the Sand Hills, there may be massive re-activation of dune fields; in other places (north Texas and eastern Colorado) soil erosion will increase (Figure 8.77).
- Over-used aquifers, (e.g., the Edwards and Ogallala), will continue to be depleted, impacting the agricultural sector; irrigation agriculture will become more costly (Figure 8.78).
- Extreme weather events (e.g., heat waves, severe storms, dust storms, drought) will likely increase in frequency, if not in magnitude (Figure 8.79).
- Crop growth cycles will continue to be affected by warming temperatures and changes in the timing of precipitation; this may benefit the northern plains.
- An increase in temperature and aerosol content will increase health issues for people who are vulnerable.
- The Texas coastline will be progressively impacted by sea level rise, changing water salinity, fisheries, and vulnerability to tropical cyclones (e.g., storm surge).
- In the southern plains, warmer temperatures and more severe droughts will continue to increase the frequency and intensity of wildfires (e.g., Texas in 2011).

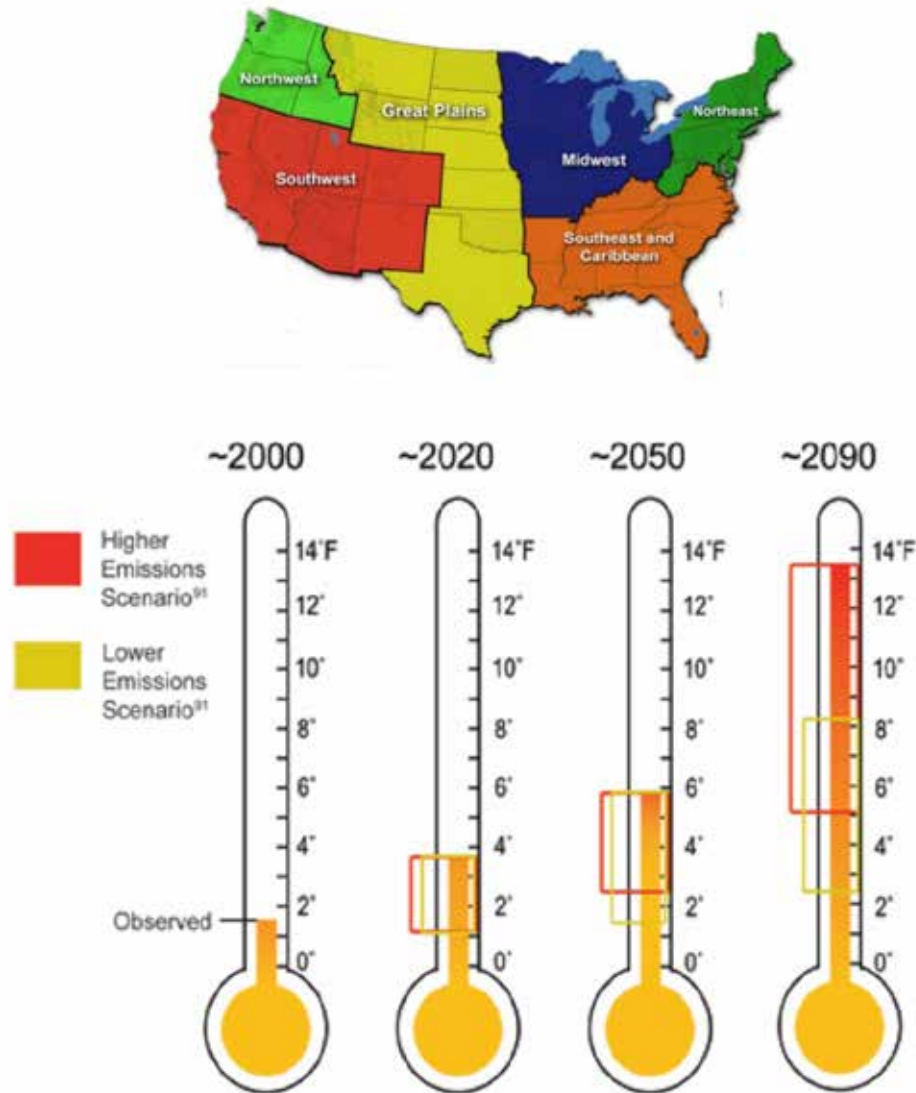


Figure 8.76. The average temperature in the Great Plains has risen about 1.5°F relative to the 1960s. Projections for the end of the century range from increases of 2.5°F to 13°F, depending on the model used and emissions scenario. Brackets indicate uncertainty (Source/Credit: Global Climate Change Impacts in the United States, United States Global Change Research Program, 2009).

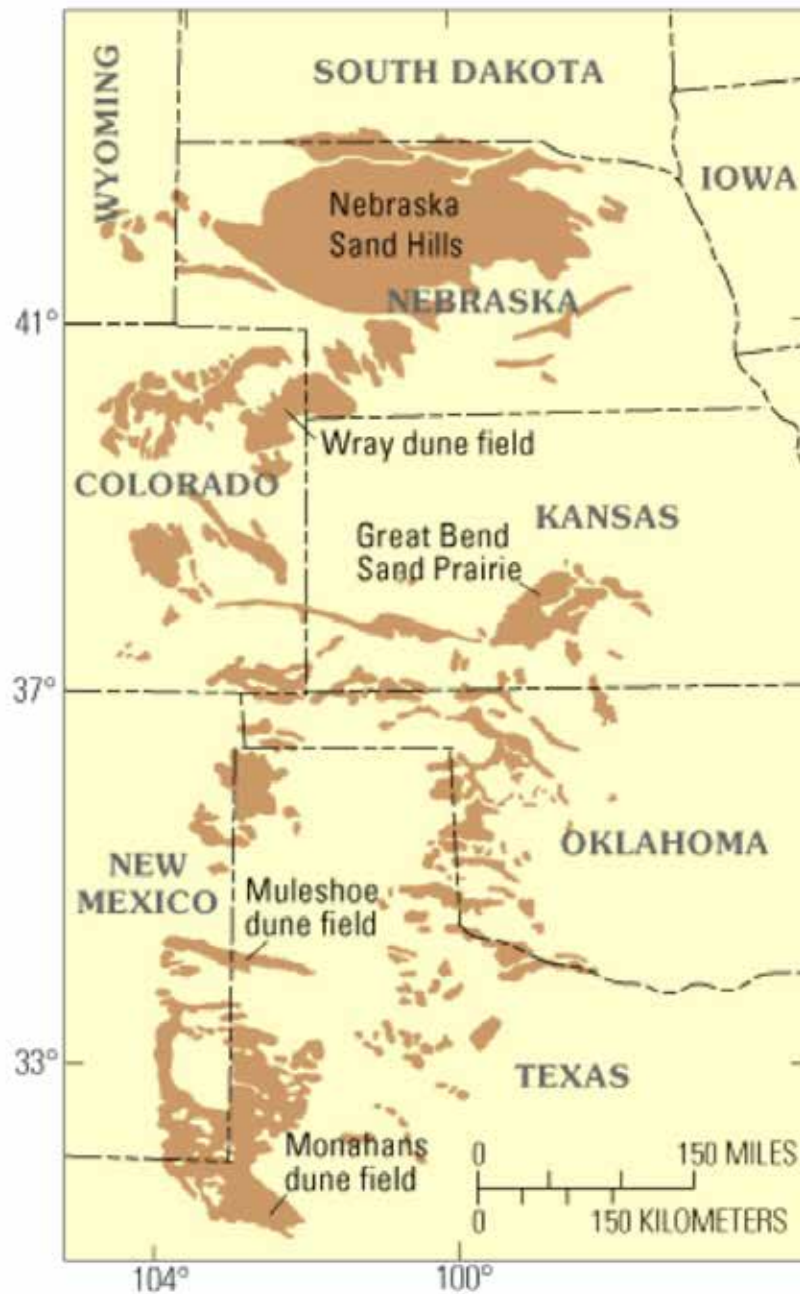


Figure 8.77. Map of stabilized dunes in the Great Plains. Many of these dune fields were initiated during the Late Wisconsin (last ice age), but have been re-activated several times in the past 10,000 years during the modern interglacial period. Some dune fields are active, such as Monahans in west Texas. Nebraska's Sand Hills are the largest fossil dune field in North America, covering about one-third of the state. Large portions of the Sand Hills were activated just 1000 years ago, presumably by a slight shift toward warmer and drier conditions (Source/Credit: USGS).

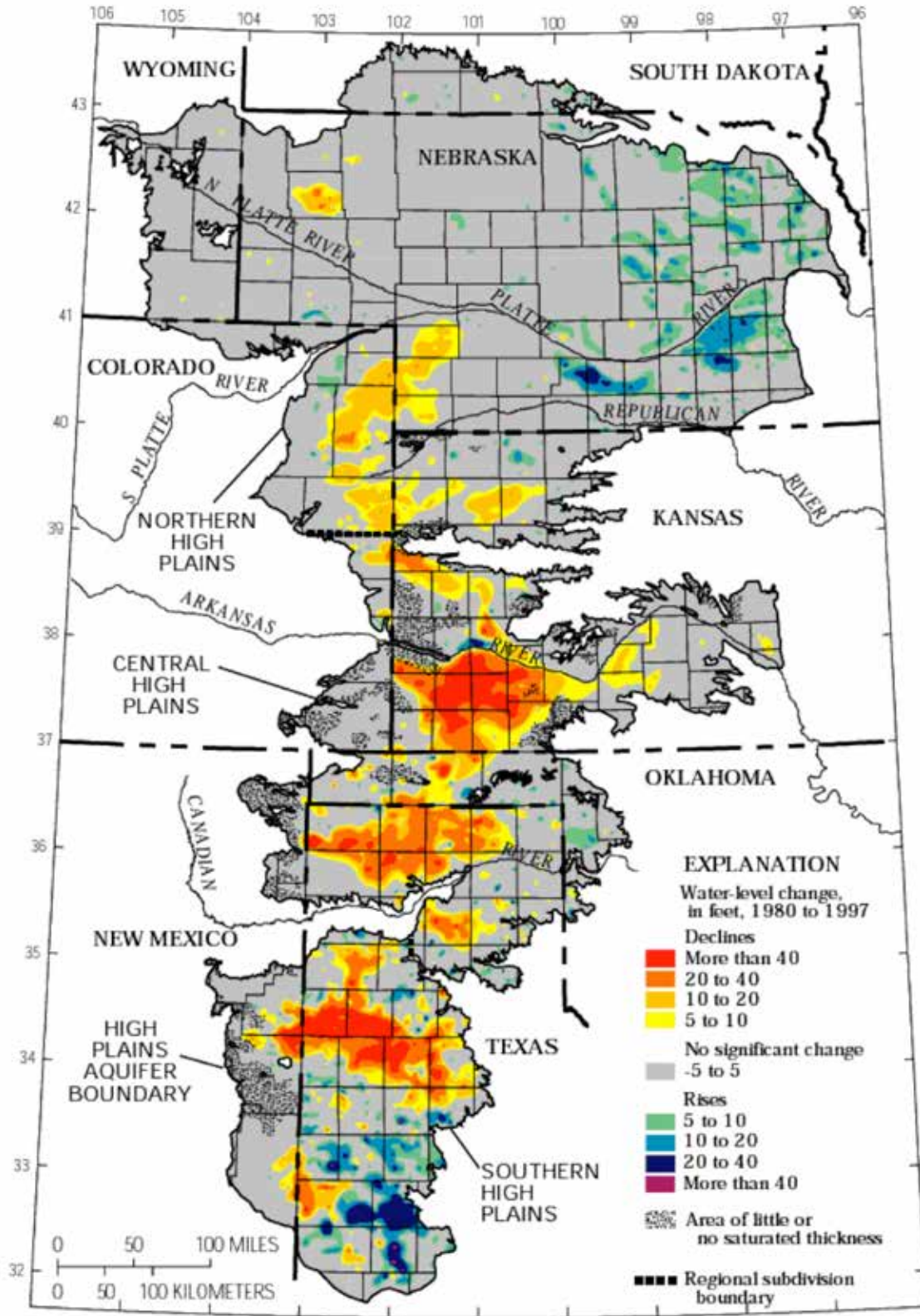


Figure 8.78. The map of the High Plains Aquifer, including the world-famous Ogallala Aquifer, shows the extent and changes in water level. Future depletion of water levels will require deeper wells and more costly irrigation. The Texas drought of 2011-2012 caused a decline in groundwater levels of over 2.5 feet in the Texas Panhandle, about three times the annual average (Source/Credit: USGS).

# U.S. Drought Monitor

March 25, 2014  
(Released Thursday, Mar. 27, 2014)  
Valid 8 a.m. EDT

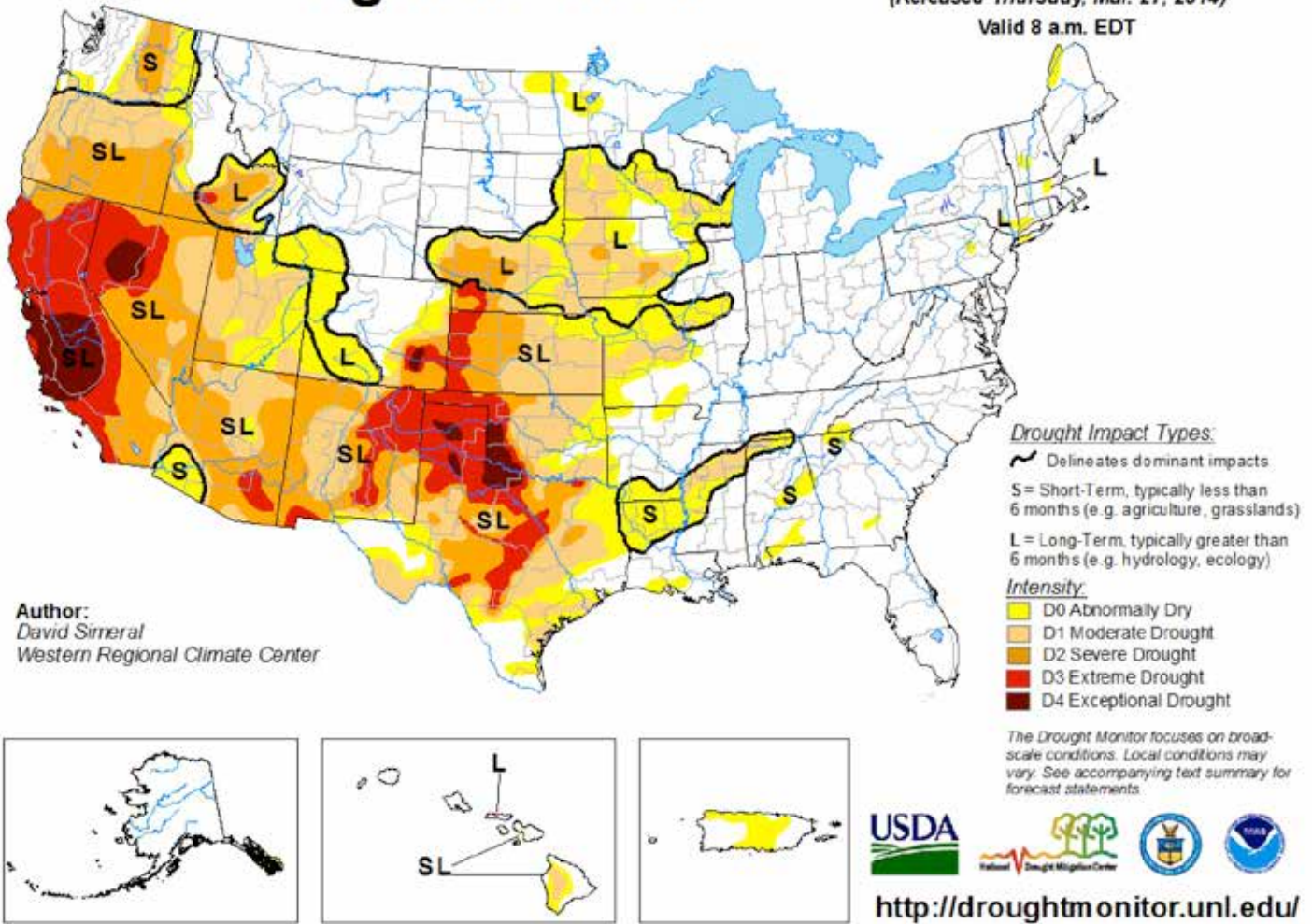


Figure 8.79. The United States Drought Monitor is one of several indices of drought severity. Most of the western United States, particularly the southern plains and Southwest, has been under drought for much of the 21<sup>st</sup> century. The cause is uncertain, but recent decadal warming makes the drought more severe (Source/Credit: Western Regional Climate Center).

## Southwest

### **Some interesting observations and speculations about climate trends:**

- Temperatures for 2001-2010 are 2°F warmer than average; it is likely that the period between 1950 and 2012 is hotter than any similar period in 600 years (Figure 8.80).
- Temperatures are projected to increase 2 to 10°F (1-5.5°C) by the end of the 21<sup>st</sup> century (Figure 8.81).
- Precipitation patterns are difficult to forecast; it is likely that precipitation will increase in the north, but decrease in the south (Figure 8.82).
- In higher elevations there will be earlier snowmelt, which will affect the timing of peak stream flow in most of the larger drainage basins (Colorado, Sacramento).
- There will be fewer cold snaps and longer, hotter summertime heat waves (Figure 8.83).
- There will be a decline in local forest health due to stress from increasing temperatures, pests, and wildfires.
- Increasing temperatures will cause altitudinal vegetation zones to shift toward higher elevations.
- Higher temperatures and decreased precipitation in many areas will cause more wildfires.
- Flood hazards will increase due to a higher frequency of heavy rainfall events.
- Natural droughts will be exacerbated by higher temperatures and land cover changes (Figure 8.84).
- Snowpack and stream flows from snowmelt will decline; water supply for agriculture, cities, and current ecosystems will be stressed.
- Sea-level rise will threaten low-lying coastal areas.
- Heat-related health problems will rise, including heat stroke, dehydration, respiratory problems, and heart health.
- Megadams such as Lake Powell and Lake Mead will experience periodic decline in water levels, reducing their use for recreation and power generation; reduced water availability will affect virtually every sector of the southwest (Figure 8.85).
- Extreme weather events, particularly haboobs (intense dust storms), will likely occur more frequently and be more destructive, generating local sporadic problems with visibility and health (Figure 8.86).
- Salinization, the increase in salt content of arid and semi-arid soils, will increasingly affect agriculture in low-lying areas such as desert basins, the Central Valley of California, and the Imperial Valley.

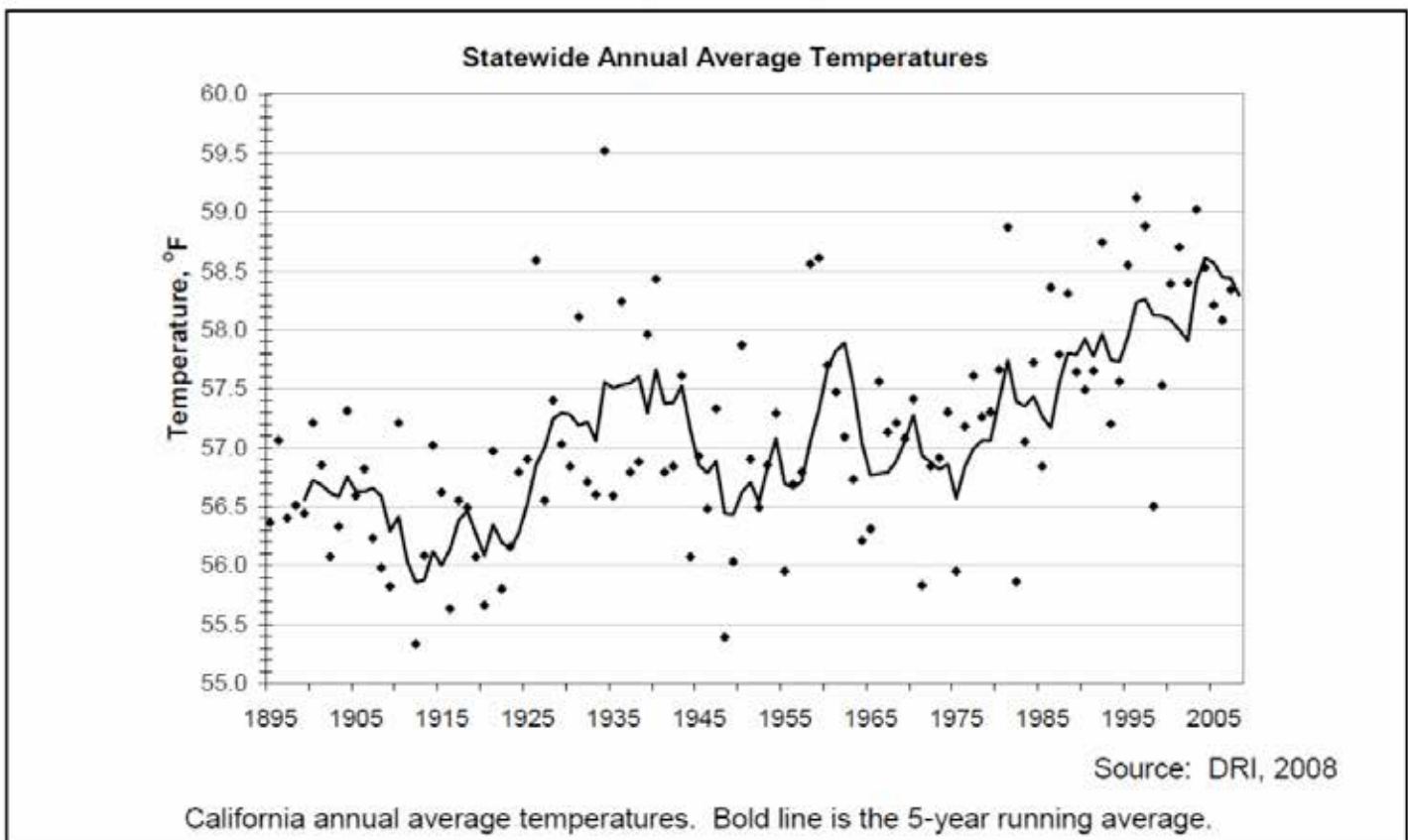


Figure 8.80. Average annual statewide temperature trends for California 1895-2007. Similar temperature increases have occurred at most locations in the Southwest (Source/Credit: Indicators of Climate Change in California, California Environmental Protection Agency, Office of Environmental Health Hazard Assessment).



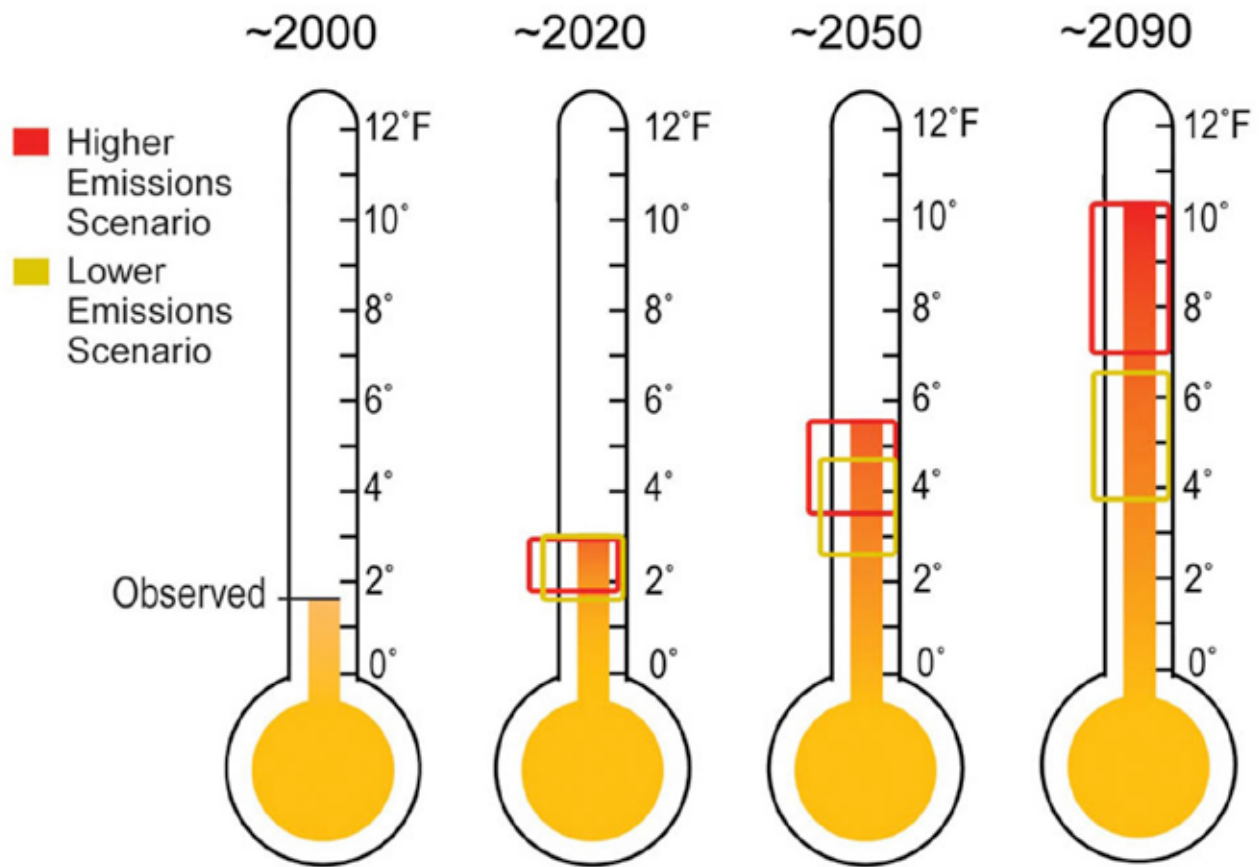


Figure 8.81. The average temperature in the Southwest has risen about 2°F (~1.1°C) relative to the 1960s. Projections for the end of the century range from increases of 2 to 10°F (1-5.5°C), depending on the model used, the emissions scenario, and location. Brackets indicate uncertainty (Source/Credit: Global Climate Change Impacts in the United States, United States Global Change Research Program, 2009).

**ANNUAL PRECIPITATION: STATEWIDE AND REGIONAL**  
*Little change is evident in precipitation trends.*

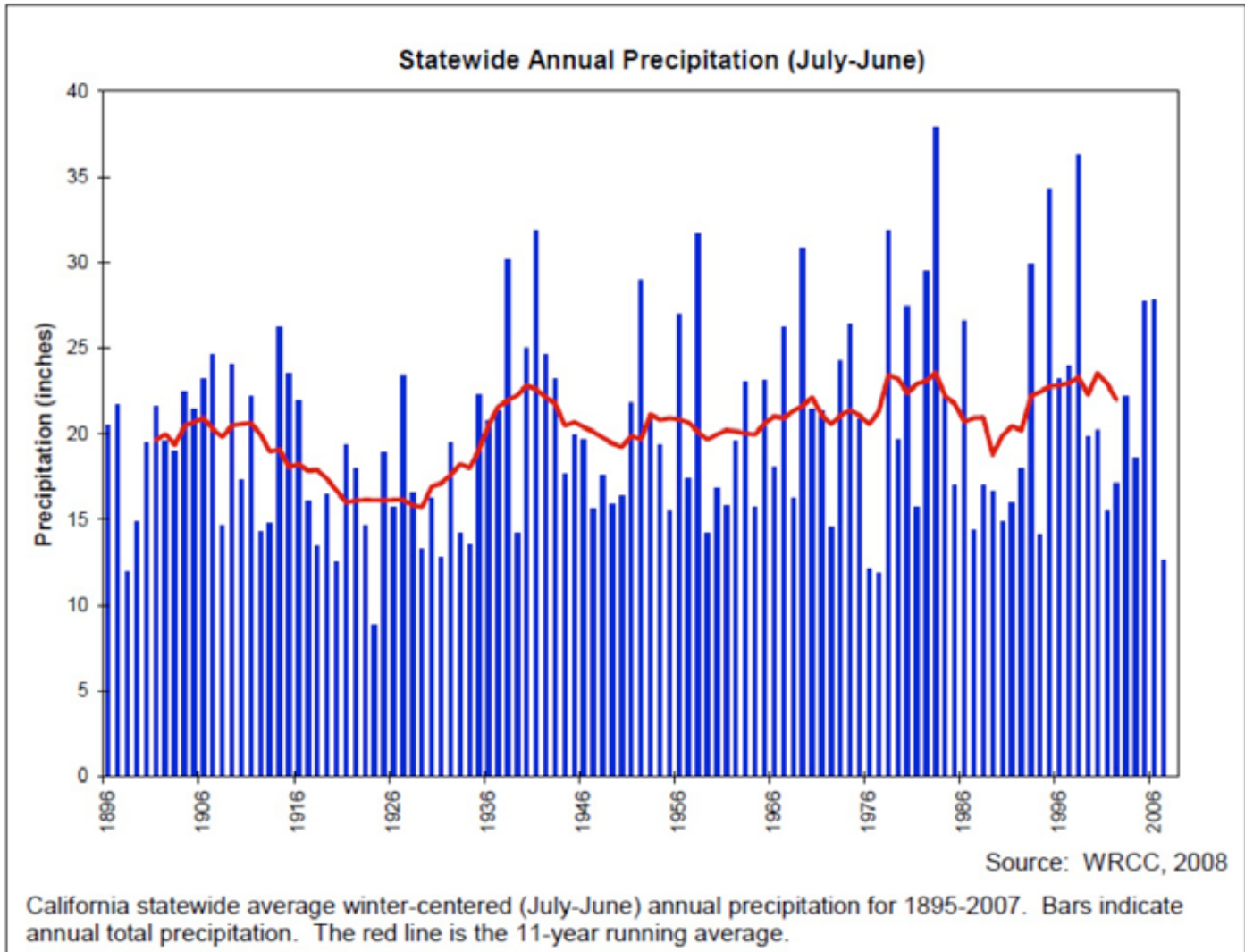


Figure 8.82. California precipitation shows a tendency toward decadal fluctuations, but very little overall trend in the past 100 years. The period beginning in 2011 and continuing through April 2014 (not shown on this graph) has been among the driest on record (Source/Credit: WRCC).

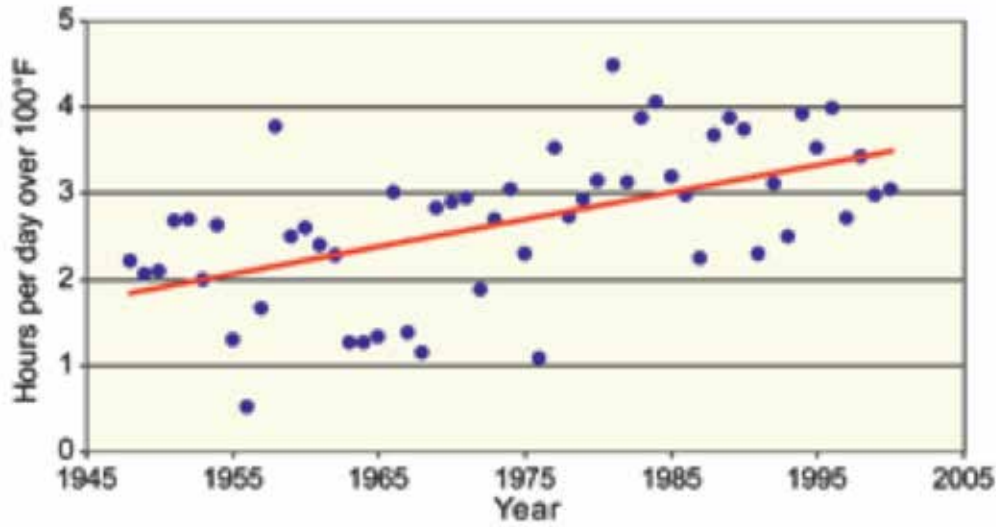


Figure 8.83. The graph indicated the increase in the number of hours per summer day that Phoenix has been over 100°F. The number has doubled over the past 50 years. Arizona’s heat-related deaths are the highest of any state (Source/Credit: Global Climate Change Impacts in the United States, United States Global Change Research Program, 2009).



Figure 8.84. As of early spring, 2014, California was suffering one of its worst droughts in history. The land-locked marina (above) at Folsom Lake, at the western base of the Sierra Nevada in California was unusable because the lake was at 17% capacity. The inset shows the marina under normal conditions. Sierran reservoirs provide most of the agricultural water for the Central Valley, one of the richest agricultural regions in the world (Source/Credit: California Department Water Resources).



Figure 8.85. The two largest megadams and reservoirs on the Colorado River are Lake Mead in Arizona and Lake Powell in Utah. Both reservoirs had an initial storage capacity of over 25 million acre-feet. From 1980 until 1999, both reservoirs were nearly full. Since 1999, the Upper Colorado River drainage basin has experienced drought. By 2007, both reservoirs had dropped to below 50% of their storage capacity. In late March 2014, Lake Mead and Powell were 46% and 39% of their storage capacity, respectively. The matching photos on the left show the results of the recent drop in lake level as well as the sedimentation at the head of Lake Powell. The images on the right show the abandonment of the Hite Marina due to declining lake levels. Red arrows indicate concrete launch ramp (Source/Credit: John Dohrenwend, left, Dennis I. Netoff, right).



Figure 8.86. A haboob (dust storm) in the Phoenix area on August 11, 2012 (Source/Credit: Andrew Pielage Photography, with permission).

## Northwest

### **Some interesting observations and speculations about climate trends:**

- Coastal areas, especially low-lying regions, are being threatened by inundation, erosion, shoreline habitats, and ocean acidification; some estimates of sea level rise in the Puget Sound are as much as 13 inches by the end of the 21<sup>st</sup> century (Figure 8.87).
- Average annual temperature is expected to increase 3 to 10°F (1.7-5.6°C) by the end of the century (Figure 8.88).
- Precipitation projections are less certain than temperature, but winter precipitation is expected to increase and summer precipitation is expected to decrease; fall precipitation may increase.
- Changes in temperature and precipitation will cause ecosystem change; boundaries between mountain ecosystems will rise in elevation and alpine tundra will shrink.
- Warmer temperatures will threaten some forest ecosystems, leaving them progressively more vulnerable to wildfire, pests and disease (Figure 8.89a and 8.89b).
- Some climate models predict enhanced wind velocities, which could increase coastal wave energy and erosion.
- Heavier winter rainfall will increase the risk of landslides, such as the catastrophic debris flow that killed more than 27 people in March 2014 (Figure 8.90).
- Higher winter temperatures will cause more rainfall and less snowfall.
- Snow melt timing will be earlier in the year affecting mountain stream flow.
- Winter flood risks will increase because of overall increase in precipitation and earlier snowmelt.
- Higher temperatures and increased rates of water loss through evapotranspiration are beginning to cause increases in the frequency of wildfires; areas burned by wildfires are projected to increase by a factor of 4 by 2080.
- April 1 snowpack decrease will continue to decrease throughout the century; 40% April 1 reduction in the Cascades by 2040s; 59% by 2080s.
- Puget Sound peak river flow will shift from spring (driven by snowmelt) to winter (driven by precipitation).
- The highly productive Yakima basin will have difficulty supplying adequate water to all users.
- Summer heating needs will rise due to population increase and temperature increase, but hydroelectric power may go down slightly.

- In the agricultural sector, apples, potatoes, wheat losses of ~25% by end of century.
- Decline in salmon habitat due to thermal stress and presence of physical barriers.



### Rising Sea Levels and Changing Flood Risks in Seattle

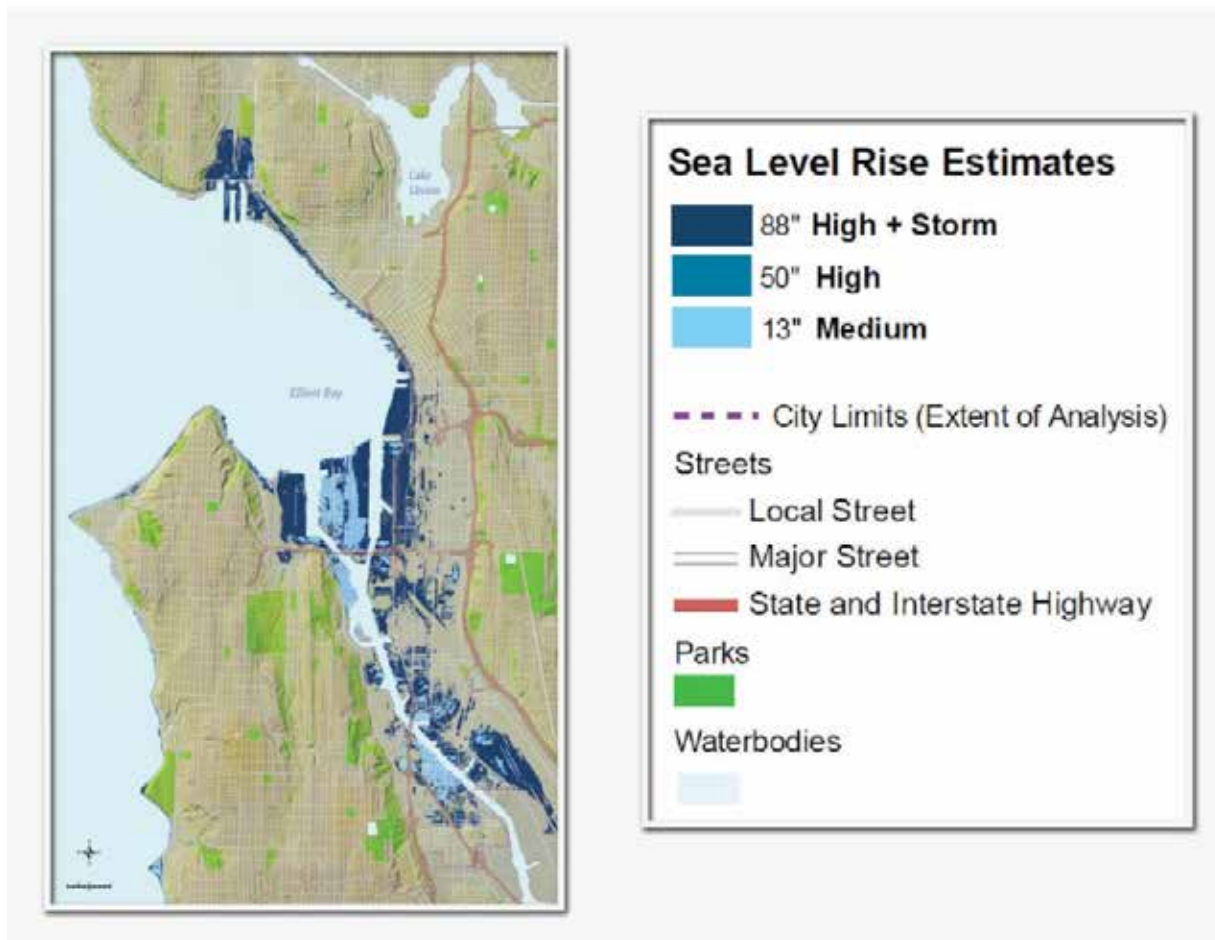


Figure 8.87. Area in the Puget Sound near Seattle at risk of future sea level rise and flood risks (Source/Credit: Seattle Public Utilities, from NCA report 2013 National Climate Assessment).

	Temperature Change (F°)	Precipitation Change (%)
2020s	+2.0 (+1.1 to +3.3)	+1.3 (-9 to +12)
2040s	+3.2 (+1.5 to +5.2)	+2.3 (-11 to +12)
2080s	+5.3 (+2.8 to +9.7)	+3.8 (-10 to +20)

Figure 8.88. Projected temperature and precipitation changes in the Northwest for the 2020s, 2040s, and 2080s relative to 1970-1999. Note the broad range in precipitation forecasts for each time interval (Source/Credit: The Washington Climate Change Impacts Assessment, University of Washington, Climate Impacts Group, June 2009).



Figure 8.89a. Increased fire and insect activity in the Northwest will lead to increased forest mortality in one of the densest forests outside the tropics. These impacts have already occurred and will continue to worsen throughout the century. Note the recent burn (left side) and insect damage (right side) by mountain pine and spruce beetles (Source/Credit: USGS, in NCA report 2013 National Climate Assessment).



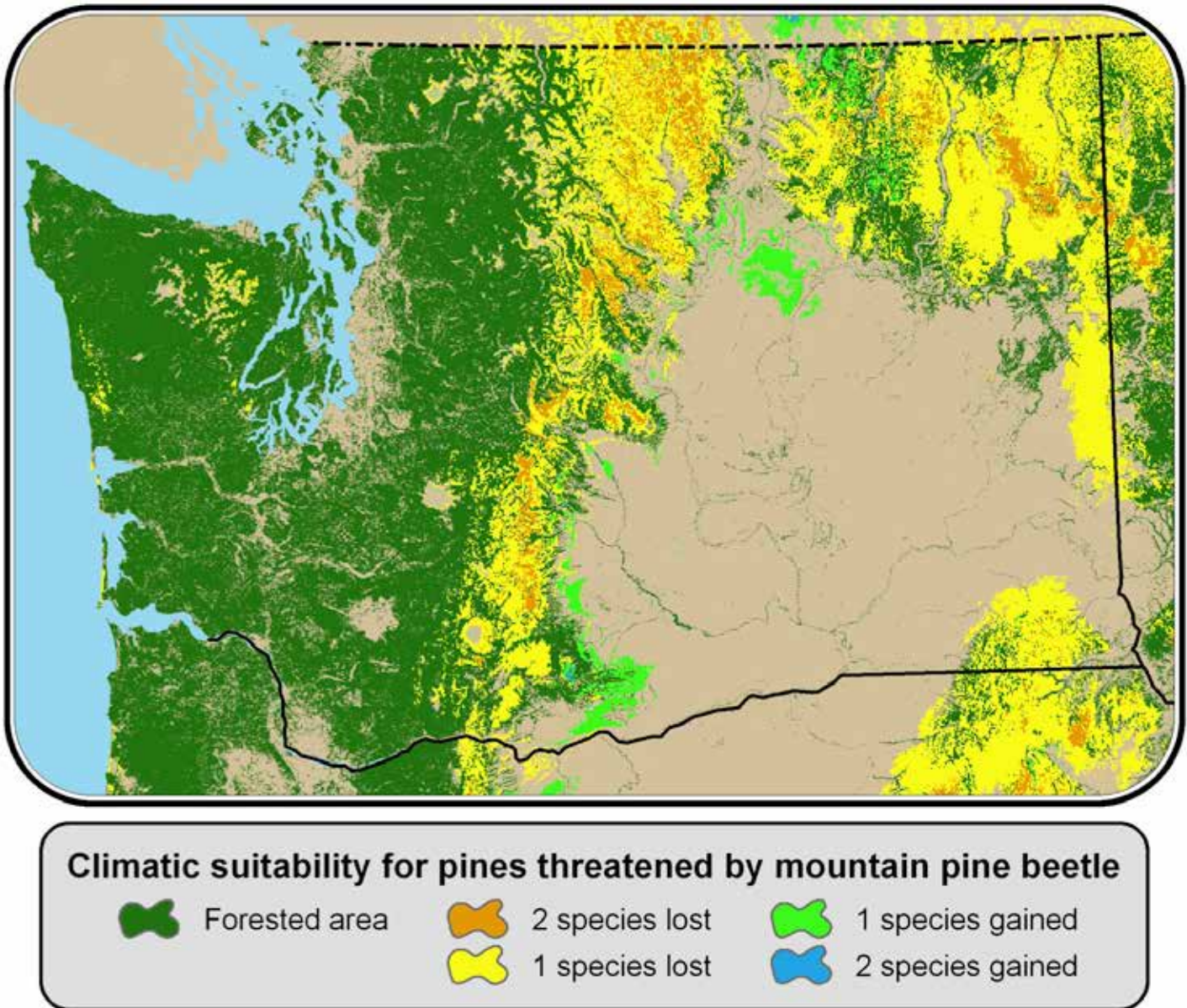


Figure 8.89b. Climate suitability for pines that will become progressively threatened by the mountain pine beetle. Areas of orange and yellow indicate places where one or more species of pines may have difficulty re-establishing after a disturbance because of future climate change (Source/Credit: The Washington Climate Change Impacts Assessment, University of Washington, Climate Impacts Group, June 2009).



Figure 8.90. Landslides in the mountains of the Pacific Northwest will become more frequent because of higher rainfall amounts and earlier snow melts. The devastating Oso landslide in Washington during March of 2014 killed more than 25 people (Source/Credit: Washington State Department of Transportation; Google map inset).



# Appendixes



## **Appendix 2**

### **Selected Useful Websites**

There are several websites that we found extremely useful in the writing of this ebook. They provide such things as current and archived weather maps (temperature, pressure, winds), satellite imagery, recent atmospheric research, atmospheric data and concepts, environmental data, planetary data, and more. If you have questions about specific atmospheric processes or events (e.g., Hurricane Katrina), start with a good search engine (e.g., Google) and type in your query. Or type in any of the following:

- Accuweather.com
- American Meteorological Society
- Blakey, Ron, Northern Arizona University
- California EPA, Office of Environmental Health Hazard Assessment
- Caltec (California Institute of Technology)
- CIRES (Cooperative Institute for Research in Environmental Sciences)
- Climate org
- CSTE (Council of State and Territorial Epidemiologists)
- DOE (Department of Energy)
- EPA (Environmental Protection Agency)
- European Southern Observatory
- FEMA (Federal Emergency Management Agency)
- Intellicast
- IPCC (Intergovernmental Panel on Climate Change)
- NASA (National Aeronautics and Space Administration)
- NCAR (National Center for Atmospheric Research)
- NCDC (National Climate Data Center)
- NOAA (National Oceanic and Atmospheric Administration)
- NRCS (Natural Resource Conservation Service)
- Ocean Prediction Center (under NOAA)

PIOMAS (Pan-Arctic Ice Ocean Modeling and Assimilation System)  
Special Supplement to the Bulletin of the American Meteorological Society, 2013  
SDO (Solar Dynamics Observatory)  
Texas Natural Resource Information System  
Texas Weather  
The Cloud Appreciation Society  
The National Weather Service (under NOAA)  
The Planets (NASA)  
The Weather Channel  
TWDB (Texas Water Development Board)  
UCAR (University Center for Atmospheric Research)  
University of Washington, Climate Impacts Group  
University of Texas Libraries, The University of Texas, Austin  
US Climate Normals (NOAA)  
USDA (United States Department of Agriculture)  
USGCR (United States Global Change Research Program)  
USGS (United States Geological Survey)  
Weather Underground  
Weatherspark.com  
World Resources Institute  
Western Regional Climate Center  
Wikimedia or Wikipedia  
World Health Organization